Biomechanics and Biomaterials in Orthopedics

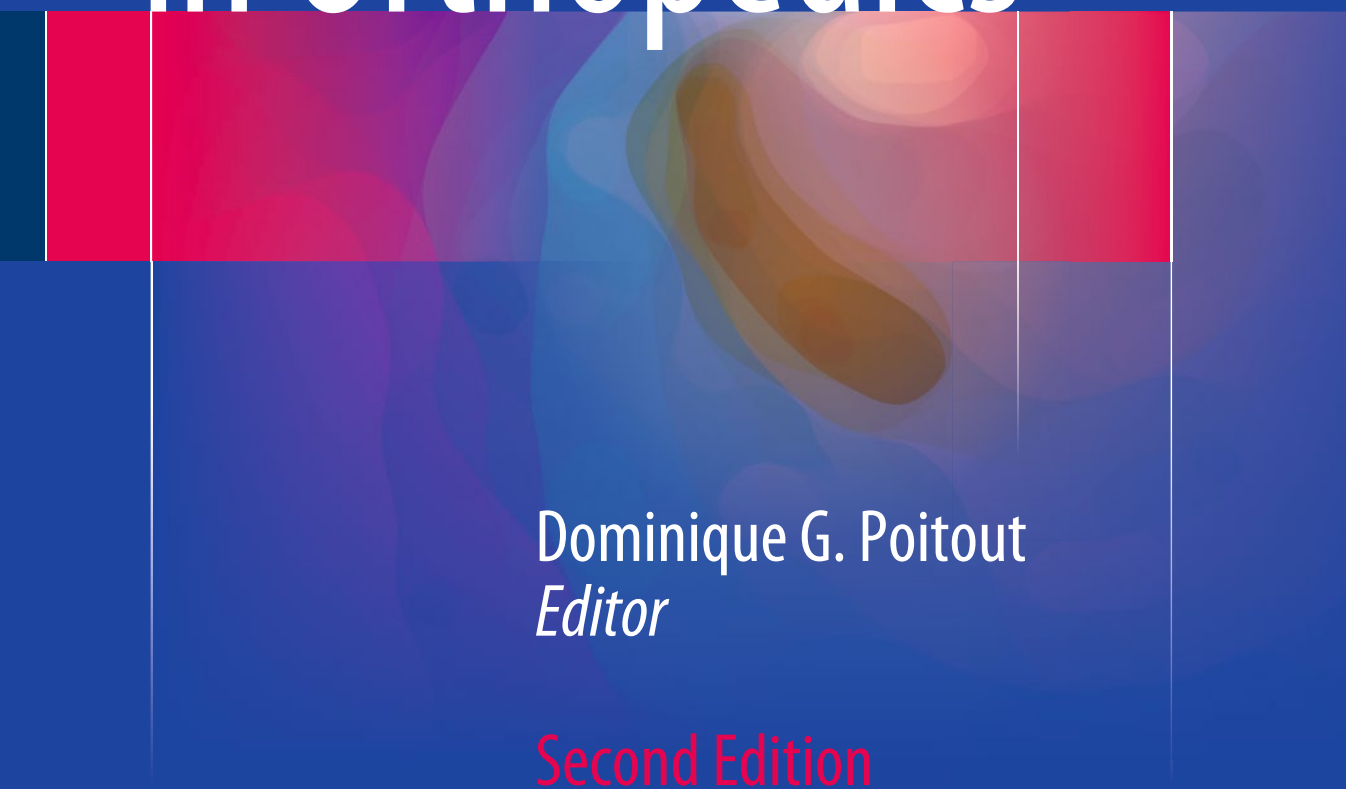

Dominique G. Poitout
Editor

Second Edition

Springer

Biomechanics and Biomaterials in Orthopedics

Dominique G. Poitout
Editor

Biomechanics and Biomaterials in Orthopedics

Second Edition

Springer

Editor
Dominique G. Poitout
Hôpital Nord
Aix-Marseille Université
Marseille CX 20
France

1st ed. published by Springer in 2004.
ISBN 978-1-84882-663-2 ISBN 978-1-84882-664-9 (eBook)
DOI 10.1007/978-1-84882-664-9

Library of Congress Control Number: 2016944146

Printed on acid-free paper

This Springer imprint is published by Springer Nature
The registered company is Springer-Verlag London Ltd.

Foreword

Even before biomechanics and biomaterials were recognised as specific scientific fields, they were a major concern of the earliest orthopaedic surgeons. The basic principles of biomechanics were first approached by Wolff in 1892. The design of implants and the selection of biocompatible materials became an essential field of research following the pioneering work on the first surgical fixation of fractures by Lambotte and Lane.

Since the recognition of these specific fields, it has become necessary to understand the complex multifactorial interaction of the musculoskeletal tissues. After the difficulties encountered in establishing a common language, these areas of research grew exponentially and involved many scientific disciplines. During the 1970s, the first Biomechanics and Biomaterials Societies were founded to meet this need.

From the study of the passive characteristics of the materials to improve mechanical resistance and the neutral biochemical behaviour of the implant, they gained an active role in controlling cell and tissue regeneration.

Smart implants ensure monitoring of bone healing and interactive regulation within biological parameters. Tissue and cell engineering is being constantly developed and appears to be a promising tool in the stabilisation of the degenerative process and repair of tissue defects.

In addition to the constant evolution of implant technology, the improvement in the production of allograft and bone substitutes significantly expands the armamentarium of the orthopaedic surgeon. The recent involvement of nanotechnologies opens up the possibilities of new approaches in the development of interactive interfaces of the implant.

These fields of science represent an essential part of the knowledge and experience of today's orthopaedic surgeons and it has to be mentioned that in this publication Dominique Poitout offers an informed contemporary insight into this fast expanding domain. In 1987, he achieved this objective by the publication of a first handbook "Biomécanique Orthopédique", which was a reference for many practitioners and scientists.

Currently, there is a need to summarise and update the advancements in the different specific topics to further new applications and initiate new researches. Dominique Poitout has been able to compile the most prominent active researches in the discipline to offer young orthopaedic surgeons a

summary of fundamental skills that they will need to apply in their day-to-day work, while also updating the knowledge of older surgeons in the most advanced fields. He has successfully fulfilled this goal with this book and we thank him for this fundamental contribution.

Maurice Hinsenkamp, MD, PhD
Free University of Brussels
Brussels, Belgium

Contents

Contributors

R. Aissaoui, PhD Génie de la production automatisée, École de Technologie Supérieure et CRCHUM, Montreal, QC, Canada

Jean-Noël Argenson, MD Department of Orthopaedic Surgery, Institute for Motion and Locomotion, Mediterannea University, Hôpital Sainte Marguerite, Marseille, France

Jean-Manuel Aubaniac, MD Department of Orthopaedic Surgery, Institute for Motion and Locomotion, Mediterannea University, Hôpital Sainte Marguerite, Marseille, France

Stéphane Aunoble, MD Department of Orthopedic and Traumatology Spine Surgery, Hopital Pellegrin, Bordeaux, France

Marcello Baricco, PhD Laboratory of Metallurgy, Chemistry Department, University of Turin, Torino, Italy

Stacey Berner, MD Hand Surgery Department, Sinai Hospital Orthopaedic, Baltimore, MD, USA

Louis Boissiere, MD Department of Orthopedic and Traumatology Spine Surgery, Hopital Pellegrin, Bordeaux, France

Todd M. Boyce, PhD Osteotech, Inc, Eatontown, NJ, USA

Elena M. Brach del Prever, MD 1st Orthopaedic Clinic University of Turin, Centro Traumatologico Ortopedico, Torino, Italy

Jiang Chang, PhD Biomaterials and Tissue Engineering Research Center, Shanghai Institute of Ceramics, Chinese Academy of Sciences, Shanghai, China

Philippe Chiron, MD, PhD Service d'Orthopédie-Traumatologie, CHU de Toulouse, Toulouse, France

Luigi Costa, PhD Molecular Imaging Center, Department of Molecular Biotechnology and Health Sciences, University of Turin, Torino, Italy

Guy Daculsi, PhD INSERM, University of Nantes, Nantes, France

Kerong Dai, MD Laboratory of Orthopaedics Cellular & Molecular Biology, Shanghai Institutes for Biological Sciences Chinese Academy of Sciences & Shanghai Jiao Tong University School of Medicine, Shanghai, China

Benoît de Germay, MD Department of Neurosurgery, Clinique de l'Union, Toulouse, France

Y. Nouaille de Gorce, MD Banque de Tissus EFS Alpes-Mediterranee, Marseille, France

J.A. de Guise, PhD Génie de la Production Automatisée, École de Technologie Supérieure et CRCHUM, Montreal, QC, Canada

J. Dubousset, MD Department of Orthopaedics, Académie Nationale de Médecine, Paris, France

N. Duval, MD Research Laboratory, Imaging and Orthopedic Research Center Hospital of the University of Montreal, Montréal, QC, Canada

J. Egan E-Tech, Ltd, Sheffield, England

Thierry Fabre, MD CIC IT, CHU of Bordeaux, Hôpital Xavier Larnozan, CHU de Bordeaux, Hôpital Pellegrin, service d'orthopédie, Bordeaux, France

Sybille Facca, MD, PhD Department of Hand Surgery, Strasbourg University Hospitals, Strasbourg, France

Antonio Faundez, MD Department of Orthopaedics, Geneva University Hospital, Geneva, Switzerland

J. Favre Aix-Marseille Université, Centre Hospitalo-Universitaire Marseille Nord, Marseille, France

Xavier Flecher, MD Department of Orthopaedic Surgery, Institute for Motion and Locomotion, Mediterannea University, Hôpital Sainte Marguerite, Marseille, France

A. Fuentes, PhD Research Laboratory, Imaging and Orthopedic Research, École Technologie Supérieure, Montreal, QC, Canada

Emanuel Gautier, MD Department of Orthopaedic Surgery and Traumatology, HFR – Cantonal Hospital Fribourg, Fribourg, Switzerland

Evgeny Grebenyuk, MD 3rd Orthopedic Department, Russian Ilizarov Scientific Center for Restorative Traumatology and Orthopaedics, Kurgan, Russia

Lyudmila Grebenyuk, PhD Department of Physiology, Russian Ilizarov Scientific Center for Restorative Traumatology and Orthopaedics, Kurgan, Russia

N. Hagemeister, PhD Génie de la production automatisée, École de Technologie Supérieure et, Montreal, QC, Canada

M.F. Harmand, MD LEMI, Martillac, Bordeaux, France

Philippe Hernigou, MD Orthopaedics Department, Hôpital Henri Mondor, Créteil, France

W.J. Kim, PhD Materials Science and Engineering, Hongik University, Seoul, South Korea

Meinhard Kuntz Oxide Development CeramTec GmbH, Plochingen, Germany

Atsushi Kusaba, MD, PhD Department of Rheumatology, Zama General Hospital, Zama, Kanagawa, Japan

D.R. Labbe, MD Research Laboratory, Imaging and Orthopedic Research Center Hospital of the University of Montreal, Montréal, QC, Canada

Jean-Charles Le Huec, MD, PhD Ortho-Spine Department, Surgical Research Laboratory, Bordeaux University Hospital, Bordeaux, France

J.C.Y. Leong, MD Department of Orthpaedics, The Open University of Hong Kong, Hong Kong, China

Ping-chung Leung, MBBS, MS, DSc, Hon DSocSc Department of Orthopaedics and Traumatology, Faculty of Medicine, Jockey Club Centre for Osteoporosis Care and Prevention, The Chinese University of Hong Kong, Shatin, Hong Kong, China

Philippe A. Liverneaux, MD, PhD Hand and MicroSurgery Department, Strasbourg University Hospital, Illkirch, France

Jianxi Lu, MD, PhD Department of Orthopaedic Sugery, Ninth People's Hospital, Shanghai Jiaotong University School of Medicine, Shanghai, China

W.W. Lu, PhD Department of Orthopaedics and Traumatology, The University of Hong Kong, Hong Kong, China

M. Mansat Department of Orthopedic Surgery and Traumatology, Pierre Paul RIQUET Hospital, CHU PURPAN, Toulouse Medical School, Paul Sabatier University, Toulouse, France

P. Mansat, MD Department of Orthopedic Surgery and Traumatology, Pierre Paul RIQUET Hospital, CHU PURPAN, Toulouse Medical School, Paul Sabatier University, Toulouse, France

Gustavo Mantovani, MD Department of Hand Surgery, Sao Paolo Hand Center, Ben Portuguesa Hospital, Sao Paolo, Brazil

Alessandro Massè, MD Department of Orthopaedics and Traumatology, University of Turin, Torino, Italy

Bernard Masson, MScPh Medical Division, BioConnect, Vieille-Toulouse, France

Hugues Pascal Mousselard, MD Orthopedic Service, CHU Pitié Salpétrière, Paris, France

Eric Nectoux, MD Department of Children's Surgery and Orthopedics, Lille University Hospital, Lille, France

G.X. Ni, MD, PhD Department of Orthopaedics and Traumatology, Nanfang Hospital, Southern Medical University, Guangzhou, China

Congqin Ning, PhD State Key Laboratory of High Performance Ceramics and Superfine Microstructure, Shanghai Institute of Ceramics, Chinese Academy of Sciences, Shanghai, China

Shanghai Institute of Ceramics, Chinese Academy of Sciences, Shanghai, China

Thomas Pandorf, Dr-Ing CeramTec AG, Plochingen, Baden-Württemberg, Germany

G. Parent, MD Research Laboratory, Imaging and Orthopedic Research Center, Hospital of the University of Montreal, – Hôpital Notre-Dame, Montréal, QC, Canada

Sebastien Parratte, MD Department of Orthopaedic Surgery, Institute for Motion and Locomotion, Mediterannea University, Hôpital Sainte Marguerite, Marseille, France

N. Pellet, MD Spine Unit, CHU Pellegrin, Universite Ségalen Bordeaux, Bordeaux, France

Corrado Piconi, MSc Department of Clinical Orthopedics, Catholic University, Roma, Italy

Dominique G. Poitout, MD Faculté de Médecine Nord, Sce Chirurgie Orthopédique et Traumatologie, Aix-Marseille Université, Centre Hospitalo-universitaire Marseille Nord, Marseille, France

Julien Rigal, MD Department of Orthopedics and Traumatology, CHU Hopitaux de Bordeaux, Bordeaux, France

B. Ripoll, MD Department of Orthopaedic Surgery and Trauma, Hopital Nord, Marseille, France

Nahum Rosenberg, MD Department of Orthopedic Surgery, Rambam Health Care Campus & The Rappaport Faculty of Medicine, Technion–Israel Institute of Technology, Haifa, Israel

Jean Louis Rouvillain, MD Orthopedic Service, CHU de Fort de France, Martinique, France

Rachid Sadikki, MD Spine Unit, CHU Pellegrin, Universite Ségalen Bordeaux, Bordeaux, France

Susumu Saito, MD, PhD Department of Orthopaedic Surgery, Showa University Fujigaoka Hospital, Yokohama, Kanagawa, Japan

Mamie Sancy, MD Escuela de Construcción Civil, Pontificia Unviersidad Católica de Chile, Santiango, Chile

V.A. Schurov, MD Laboratory for Deformity Correction and Limb Lengthening, Russian Ilizarov Scientific Center, Restorative Traumatology and Orthopaedics of the RF Ministry of Health, Kurgan, Russia

Moshe Solomonow, PhD, MD Department of Orthopedic Surgery, Bioengineering Division and Musculoskeletal Disorders Research Laboratory, University of Colorado, Denver, Health Sciences Center, Denver, CO, USA

Michael Soudry, MD Department of Orthopedic Surgery, Rambam Health Care Campus & The Rappaport Faculty of Medicine, Technion–Israel Institute of Technology, Haifa, Israel

Haim Stein, MD, DPhil (Oxon) Department of Orthopaedic Surgery A, Rambam Medical Center, Haifa, Israel

N. St-Onge, PhD Department of Exercise Science, Concordia University, Montreal, QC, Canada

S.I. Suk, MD, PhD Department of Orthopedic Surgery, Seoul Spine Institute, Inje Univ Sanggye Paik Hospital, Nowon-Ku, Seoul, South Korea

Karl-Goren Thorngren, MD, PhD, FRCSEd(Hon) Department of Orthopedics, Skane University Hospital, Lund, Sweden

M. Van de Putte, MSc Research Laboratory, Imaging and Orthopedic Research Center, Hospital of the University of Montreal, – Hôpital Notre-Dame, Montréal, QC, Canada

Magdalena Walczak, MD Department of Mechanical and Metallurgical Engineering, Escuela de Ingeniería, Pontificia Unviersidad Católica de Chile, Santiago, Chile

Youzhuan Xie, MD, PhD Department of Orthopaedic Surgery, Ninth People's Hospital, Shanghai Jiaotong University School of Medicine, Shanghai, China

L'H. Yahia, PhD Research Laboratory, Imaging and Orthopedic Research Center Hospital of the University of Montreal, – Hôpital Notre-Dame, Montreal, ON, Canada

Groupe de Recherche en Biomécanique/Biomatériaux, Ecole Polytechnique, Montreal, ON, Canada

Takao Yamamuro, MD, PhD Kyoto University, Kyoto, Japan

Research Institute for Production Development, Kyoto, Japan

B. Yu, MD, PhD Department of Orthopaedics and Traumatology, Nanfang Hospital, Southern Medical University, Guangzhou, Guangdong, China

Part I

Introduction

Bone as Biomaterial

1

Dominique G. Poitout

Since 30 years surgery has seen striking developments in the area of biomaterials and it is becoming increasingly necessary for surgeons from various specialisms to have an in-depth knowledge of the biomechanical properties of and what happens to foreign bodies implanted in the body, whether metallic or biological such as bone. Industrial researchers have to identify and then resolve the mechanical problems which arise when using inert (metallic or plastic) or biological materials to replace joints, ligaments, or even whole bones.

Using human or animal grafts (bone, cartilage, or ligament) in certain surgical, traumatological, or oncological indications requires a combination of various types of knowledge in the areas of immunology, biology, and biomechanics which are necessary for these allografts or these xenografts to be incorporated into the body.

Human bone, whether autologous and therefore bone-forming, allogenic, and simply bone-conducting or even animal bone (xenograft), behave biomechanically in a progressive fashion depending on the extent of the demands placed on it, the rate and degree of its revascularization, and of the procedures used to preserve and sterilize it. Bone substitutes are also currently being studied, whether in the area of hydroxya-patites, vitroceramics, tricalcium phosphates, corals, or even ceramized or heated allografts or xenografts. Mixed compounds combining a massive metallic prosthesis with bone from a bone bank surrounding it are composite biomaterials, the constituents of which each have their own advantages and disadvantages.

Introduction

Biomaterials can be defined as being "natural or synthetic substances, capable of being tolerated permanently or temporarily by the human body".

Indeed, although initially doctors chose mainly precious materials, as dentists still do, the development of new materials such as ceramics, polyethylene, carbon–carbon composites, or titanium have enabled the field of application which used to be limited to joint or dental prostheses to be extended to other areas such as ophthalmology and cardiology.

The use of allografts or xenografts is not recent but progress now being made in the areas of the sterilization and preservation of these products of human or animal origin mean that

D.G. Poitout, MD
Faculté de Médecine Nord,
Sce Chirurgie Orthopédique et Traumatologie,
Aix-Marseille Université, Centre Hospitalo-universitaire Marseille Nord, Bld Pierre Dramard,
Chemin des Bourrely, Marseille, France
e-mail: Dominique.POITOUT@ap-hm.fr

D.G. Poitout (ed.), *Biomechanics and Biomaterials in Orthopedics*,
DOI 10.1007/978-1-84882-664-9_1

there is fresh interest in the surgical techniques which use them.

Research in these areas focuses on three aspects:

First, the study of the mechanical, physical, and chemical behavior of the material in its biological environment, i.e., its resistance to fatigue, wear, its elasticity, its resistance to corrosion, its biomechanical behavior, and its possible incorporation into the structures of the human body.

Then the study of its biocompatibility, in particular the analysis and identification of the reactions which occur at the interface between the material and the live tissue (for example, at the interface between the receiving bone and the prosthesis or the graft which has been introduced).

The biochemical growth factors, the role of certain enzymes in the breakdown of the materials used, the problems inherent to rejection or even immunological phenomena in relation to the destruction of an implanted graft are currently the subjects of a great deal of research.

Finally, it is necessary to choose a method which makes it possible to decide on a product which can be implanted in the body and which is also relatively easy to manufacture industrially or, where bone is concerned, preserved and distributed under ideal sterile conditions and the biomechanical behavior of which is compatible with restoring satisfactory and long-lasting joint function.

The Materials Used in Orthopedics

In the field of biomaterials, research has to follow two different but complementary paths:

On the one hand the characteristics and performance alone of the material have to be studied in accordance with its role in the body,

On the other, its biocompatibility has to be studied.

The biomaterials used in orthopedic surgery have developed a great deal in recent years. We now have a better understanding of the advantages they bring and their limitations. We know that steels corrode (vitallium) and that cobalt-chromium alloys wear. The complications connected with intolerance to the debris of metallic wear have meant that metal–metal prostheses are no longer used. The combination of metal and polyethylene also produces wear debris which plays a decisive role in the physiopathology of the loosening of prostheses, and the ceramic–ceramic joint may become blocked if the slightest particle enters the interface.

Plastics, such as polyethylene, which cover the sliding surfaces of many joint prostheses, become deformed, creep, and break down, tending to limit the life of these prostheses.

Cements, made of methyl methacrylate, which are used to fix some joint prostheses in the bone, have a high polymerization temperature if they are used in large quantities (over 70 °C), and for this reason cause bone necrosis (proteins congeal at 54 °C). The salting-out product may be toxic to the heart and when first used caused peroperative cardiac arrest from which the patients did not recover.

In 10 % of cases allografts produce considerable immune reactions and are only slowly and incompletely assimilated by the skeleton. Bone substitutes are not necessarily successful in mechanical terms and at present can only be used to a limited extent.

Many materials have disappeared completely from our arsenal of therapeutic options and we may well ask ourselves what can be used in future to replace the biomaterials used at present.

Biodegradable Materials

The need to remove an osteosynthesis product which was implanted a few months or years earlier is inconvenient; it means that the patient has to be hospitalized and operated on again and leads to a search for products based on amino acid-based polymers which would break down and disappear spontaneously in the body within a few years.

Compounds made of polyglycolic or polylactic acid are currently used in the form of suture materials or parietal reinforcing plates and

produce reasonable results. Their mechanical strength and life have to be improved and the way they are implanted into the body has to be specified. However, as from now, there is hope that in future they will replace the metallic materials currently used for osteosynthesis.

Bone Replacement Materials

Bone grafts currently have a major role.

Autografts

Autografts (bone graft taken directly from the patient) cannot be used to replace large segments of bone or an osteocartilaginous segment forming part of a joint. Being bone-forming, they alone can induce the formation of new bone and help in the healing of a fracture or the assimilation of an allograft.

Allografts

Since 1979 we have turned our attention to Marseilles, to preservation in tissue banks of allogenic bone fragments (bone graft taken from another person) stored in liquid nitrogen at −196 °C with cryopreservatives.

Currently used in traumatology or in oncology, these allografts make it possible to reconstruct a bone segment which has been destroyed by a tumor or an accident. These allografts are well tolerated by the body and only in exceptional cases (10 % of cases) do immunological rejection phenomena occur. They can therefore be used easily in anybody requiring this type of operation.

Xenografts

Xenografts were used several decades ago by French teams (Judet-Sichard). The large number of rejection phenomena experienced with them (more than 50 %) led to people refusing to use them. Because of the current shortage of human grafts, new attempts using different sterilization, preparation, or treatment techniques (lyophilization, ceramization, irradiation, heating) try to mitigate the inadequacies of this type of graft.

Bone Substitutes

Derivatives of artificial hydroxyapatite (a combination of hydroxyapatite-collagen, hydroxyapatite cement, corals or madrepores, vitroceramics or bioglasses) are undergoing in-depth mechanical and experimental studies to see how well they are tolerated in-situ and how they can be used. Even if some bone substitutes really are "colonized" by the bone of the host, their mechanical properties are still inadequate and mean that large fragments cannot be used in human clinical medicine. Furthermore, these structures, which are uniquely bone-conducting, do not form new bone, and tend to break down rapidly.

Joint Replacement Materials

There are a great number of plastics including polyethylenes with mechanical properties which allow them to be used in human clinical medicine. Various treatments (irradiation of the grafts or the addition of other compounds, for example) are being used in an attempt to improve their properties and to prolong their life in the body.

Alumina ceramics have been used for more than 15 years and their mechanical properties are well known. As the manufacturing processes are now very well established, it is possible that this material has the best coefficient of friction and produces the least wear debris in the body.

Zirconia ceramics are currently being investigated. They are less hard than alumina ceramics, they are easier to shape, are extremely strong but in some cases can break. Biological tolerance studies are currently being carried out and their biomechanical behavior in use is being characterized.

Silicon carbides could be used as friction surfaces for joint prostheses because they seem to be well tolerated, as the experimental implants have shown, but their long-term fate is not yet completely understood.

The use of massive cartilaginous allografts is being proposed more and more frequently by some international teams producing surprisingly good clinical results. The assimilation of these

cartilaginous allografts is excellent as cartilage cells do not need vascularization to survive. They are sustained only by the components of synovial fluid. However, in order for the mechanical behavior of the graft to be adequate for the purpose, it is necessary for the cells contained in the cartilage, which ensure its trophicity in relation to the hydrophilia of the proteoglycans, to be protected during the freezing phase. Hence the advantages of using a cryopreservative when the temperature drops and the option of using secondary sterilization by heat, gas, or irradiation is absent. This has to be particularly rigorous when grafts are being taken and osteocartilaginous fragments are being stored so that the graft is definitely entirely sterile.

Capsuloligament and Joint Replacement Materials

The frequency with which tendons and ligaments tear directs world research towards these areas. Artificial ligaments are used more and more frequently in clinical practice but their long-term fate is unclear.

Carbon fibers sheathed in polylactic or polyglycolic acid, polyamide fibers, or high-density polyethylene threads are currently being tested for fatigue but they are already used in human surgery. Dacron or Teflon ligaments have not given good mechanical results in the medium term and have led to inflammation.

Preserving human ligaments in tissue banks is also an avenue of research which appears to be promising but comes up against the problem of how tissue banks obtain their supplies and of the mechanical behavior of the grafted ligaments while they are being revascularized.

Mineral Structure of Bone

Approximately 70 % of mature bone is made up of an inorganic substance: calcium phosphate, and 30 % of an organic matrix, the main component of which is a fibrous protein: collagen.

The exact nature of this mineral phase, which has been studied mainly by X-ray diffraction, remains unclear. Furthermore, it appears to be an established fact that the nature of this phase varies as the bone ages.

Several main components are frequently suggested:

brushite: $CaHPO_4 \cdot 2H_2O$
octacalcium phosphate: $Ca_8H_2(PO_4)_6 \cdot 5H_2O$
amorphous tricalcium phosphate: $Ca_3(PO_4)_2$
apatite, classically hydroxyapatite: $Ca_{10}(PO_4)_6(OH)_2$

The crystallites of bone apatite are small and often carry impurities. PO_4^{3-}, Ca^{2+}, and hydroxy-apatite hydroxide are replaced by carbonate, Mg^2, and fluoride respectively. Compared with mineral hydroxyapatite, these imperfect crystals are more soluble and easily dissolved during resorption in the acid environment of the brush border of the osteoclastic cells.

The smallest unit of crystalline structure of the apatites contains 18 ions and it appears probable that such a complex structure is formed de novo from ions in solution. Progression through simpler forms has been demonstrated in vitro. However, these forms are unstable and difficult to demonstrate in vivo. The fluid environments of the body are said to be metastable in terms of their calcium and inorganic phosphate concentration. More precisely, that this concentration is below that of the concentration necessary for spontaneous precipitation but well above the concentration needed for the growth of the crystal if apatite crystals are present in the solution.

This therefore leads us to consider two very different phenomena:

the initiation of mineralization or “nucleation”,
the growth of the first crystals formed.

Progression of Mineralization

It has been demonstrated in vivo that more than 90 % of mineralization takes place normally by the growth of pre-existing crystals. As far as the growth of the mineral phase is concerned, the problem here is how to control it. Indeed, once

mineralization has started in a metastable environment, it should continue until all the ions are used up. If this were the case, we would all be turned into a pillar of salt like Lot's wife. Mineral growth is therefore tightly controlled and regulated. Three factors play an important role: collagen, certain non-collagenic proteins, and proteoglycan.

Collagen

Initially considered to assist in nucleation, bone collagen essentially of type I helps in the formation of apatite in vitro and in particular organizes crystallization. The crystals are deposited parallel to the axis of the collagen fibrils and denaturing of the collagen disturbs this precipitation. Therefore, although in vivo studies tend to call into question the role of collagen in nucleation, it has an essential organizing role during the growth of the crystals.

Non-collagenic Proteins

Several non-collagenic proteins have been extracted from different calcified matrices. Two large groups have to be distinguished; the phosphoproteins and the GLA proteins (or proteins carrying gammacarboxyglutamic acid). The phosphoproteins have been isolated from bone, dentine, enamel, and calcified cartilage. Some phosphoproteins are more closely bound to collagen. Various roles have been suggested: orientation of the crystals, the control of their shape and size, or even a support role in particular in tissues which do not contain collagen, such as enamel. Osteonectin, a phosphorylated glycoprotein specific to bone tissue, is thought to help in binding calcium to collagen.

GLA proteins have been suggested as being the agent which regulates mineral growth but their role is still unclear and controversial. Their interest lies particularly in the possibility that a radioimmunological assay could be carried out on the serum, which would be a reliable and sensitive marker of bone remodeling activity.

Proteoglycans

These consist of a central protein of hyaluronic acid and of carbohydrate chains formed from the repetition of sulfated disaccharide units. Essential components of cartilage, proteoglycans have also been isolated from mineralized tissues.

Proteoglycans of bone are thought to be smaller and immunologically specific. It has been suggested that they play a role in calcification on account of the fact that there is a lower level of these in calcified tissues than in non-calcified tissues. Furthermore, in epiphyseal cartilage, the proteoglycans are thought to become smaller and fewer in number close to the calcification front. Moreover, proteoglycan aggregates inhibit the formation of apatite. The idea that proteoglycans indispensable to nucleation are transformed has therefore also been suggested. However Blumenthal has shown that the subunits, like the aggregates, inhibit mineralization. Poole et al., using immunofluorescence techniques, challenge the classical ideas of proteoglycans being reduced during endochondral ossification. In their view proteoglycans continue unchanged when mineralization starts and are only modified during immature primary bone modeling.

Bone Remodeling

Bone resorption and formation take place in a perfectly organized manner. The phenomena are most stereotypical in cortical bone. In old bone, and under influences which are currently little understood but which are certainly biochemical in nature, a population of osteoclasts appears which hollows out a resorption cavity which grows 7–9 microns a day up to a diameter comparable to that of a haversian osteon, and in particular advances into the bone, in a direction determined in particular by the mechanical constraints at a rate of 40–60 microns per day, thus producing a tunnel-like structure. After an intermediate phase (reversal phase), the osteoblasts appear on the walls of the cavity which initially deposit 8–10 lamellae of osteoid tissue and then, owing in particular to the osteoblastic alkaline phosphatases, cause the mineralization of this osteoid. Approximately 10 % of the osteoblasts remain in the bone tissue formed in this way and, when they mature they become osteocytes, reunited with each other and communicating with the cells remaining on the

surface of the residual canal by prolongations using a rich and anastomotic canalicular system. The end structure created in this way is the haversian osteon.

The resorption phase lasts approximately three weeks, the formation phenomena are spread over three months. In the trabeculae of the spongy bone the phenomena are the same but their spatial layout is different. Osteoclastic resorption takes places and advances on the surface of the bony trabeculae, forming Howship's lacuna, subsequently covered, there too, with osteoblasts transforming and then mineralizing the osteoid tissue. In this system, described by Frost, the site being remodeled is called the "basic multicellar unit" (BMU) and the cells which form it are called the "basic structural unit" (BSU), the end result of this remodeling is the haversian osteon.

Any pathological condition of the bone, and in particular diffuse conditions affecting the skeleton, is the result of an anomaly, varying in nature, of remodeling and of its elementary phenomena, with resorption always preceding its formation except in very specific cases (early stages of bony callus or ossifications of the soft tissues for example).

Morphology and Bone Mechanics in Hypodynamia

During its development each bone acquires a shape and a mass which is determined genetically in such a way that it has sufficient mechanical competence to perform the usual human activities. This acquisition requires the bone to be put into control, which allows it to be modeled during growth, followed by permanent remodeling throughout life. Physical activity therefore has a vital role to play in obtaining and then maintaining sufficient bone mass. A sedentary person will have a weaker bone mass and will be more likely to suffer fractures when making unaccustomed efforts. On the other hand, people who have been practicing a sport or an intense physical activity for a long time will have a higher bone mass or bone density than average (weight lifters, ballet dancers, tennis players) and may even thus be able to compensate for a diet which is extremely low in calcium, as is the case in some Equatorial areas.

The osteogenic stimulus therefore has a permanent effect on the bone, which continually adapts to this stimulus. Trabeculae of bone in children organize themselves in line with increasing functional activity, adopting an orthogonal arrangement according to the main force lines. This arrangement gives the system maximum strength with minimum bone tissue. On the other hand, cortical bone does not have the same mechanical requirements and its structural objectives are also different. There does not appear to be any clear relationship between the usual structure of the compact bones and the forces to which they are regularly subjected, but the ability of the bone cortices to react to a high local force is still possible (the end of a hip prosthesis, for example). Functional adaptation therefore affects the shape and mass of the bone from a basic level determined genetically, to a structurally adequate level. Nevertheless, each bone adapts itself independently; it is therefore the bone overall which adapts itself to the mechanical forces rather than specific tissue structures. The cell population of a bone is therefore able to assess the forces exerted on this bone.

Not only is the adaptation of the bone sensitive to the intensity and distribution of the force exerted, but in particular to the variations in this force. Static forces therefore appear only to have a moderate effect on bone remodeling and if they increase excessively, this can have a paradoxically negative effect.

It also seems that four daily compression cycles are sufficient to counterbalance the effect of immobilization, and that 36 daily cycles allow the maximum effect to be obtained.

Hypodynamia has a rapid and negative effect on the bone formed: the absence of forces exerted no longer allows the bone to adapt itself permanently, and opens the field to various biochemical and hormonal influences, of which adequate physical activity is the necessary counterpart. It has an identical effect on the

growing bone, which without adequate stimulation does not acquire the architecture or reach the bone mass critical for it to be compatible with normal functional activity (the sequelae of poliomyelitis, for example).

Epiphyseal Cartilage

Continuous axial compression slows down the growth of connecting cartilage. The clinical applications (epiphyseal agraffing when the length of the lower limbs is unequal) are evidence of this.

Increased axial compression leads not only to a resumption of the activity of the epiphyseal cartilage but to an even more rapid rate of growth than normal. (Bonnel's experience, growth spurts observed in children confined to bed). This hypothesis explains the apparently contradictory results for stresses on flexion. During the day, when under pressure, the part of the epiphyseal cartilage subjected to compression in the resolution of a stress on flexion grows at a reduced rate. At night, or when not under pressure, the growth rate of this same part is accelerated. The sum of these two phenomena is thought to have a positive effect on growth with, in all, a more rapid rate of growth than for the part of the cartilage subjected to traction, still in the context of flexion.

These considerations apply, of course, to stresses greater than those physiologically endured by epiphyseal cartilage but less than the pathological stresses for maintaining the biological competence of this cartilage. The effects observed combine to produce a biologically healthy epiphyseal cartilage.

Articular Surfaces and Friction

The types of friction of the articular surfaces can be of the limited type (or Coulomb's type) or of the viscous type. In the limited type, for a light load and a slow rate, friction occurs via a substance with remarkable sliding properties, absorbed in the articular surfaces.

In the viscous type, for a heavy load and a rapid rate, a continuous liquid film permanently separates the two articular surfaces. The thickness of this film depends on the stresses which are exerted normally on the surfaces and the rate at which they move in relation to each other.

These two types of friction occur in human joints. They were demonstrated experimentally by studying the way in which the oscillations of a pendulum decrease when attached to a joint: a linear decrease in the case of limited friction, an exponential decrease in the case of viscous friction.

Lubrication and Pathology

The synovial fluid of joints affected by rheumatoid arthritis has proved to be a slightly less-effective lubricant than normal fluid. The fluid taken from arthrosed joints is thought to be better, almost as good as normal fluid. In the opinion of Little et al. (1969), there is no significant difference between the coefficients of friction of normal hips and those of joints manifesting fibrillation phenomena. There is no evidence to date to suggest that a lubrication disorder is at the root of degenerative phenomena observed in clinical practice.

Finally: Tomorrow, Will Man Be Artificial?

If advances in technology continue at the current rate, it may be that many materials used today will be abandoned in years to come, but that, on the other hand, new products will appear on which the arthroplasties of the year 2000 will be based.

The reconstitution of joint cartilage by collagen, osteocartilaginous allografts, or artificial substances will allow huge strides to be made in the treatment of arthroses, the number of which increases as people live longer.

Methods of fixation for joint prostheses – biological fixation, new cements, so-called "intelligent" materials (nitinol and monocrystalline

aluminas), or even bone grafts sheathing a metallic prosthesis – will enable the prosthesis to be better tolerated by the body. However, no-one can predict how this area will develop as chemists and metallurgists will without a doubt discover some new materials which will turn the future of the science upside down.

Artificial organs are now part of the usual arsenal of medical solutions. But can we expect to see an artificial man tomorrow? The list of artificial organs which are currently available or are being created is so long that it is becoming increasingly difficult to draw up a comprehensive list of them. Artificial skin is currently being developed for very severe burns. Cell cultures of osteoblasts or chondrocytes could, in the near future, cover bone substitutes or recolonize them.

However, all these artificial organs are expensive. The cost of the worldwide use of artificial kidneys or renal dialysis, for example, is several billion dollars (and in the case of France alone, 1 % of the social security budget). It can well be imagined that the cost of creating very complex prostheses which can be used by only a small number of people could well be prohibitive, particularly for the most severely affected patients or the elderly who have relatively limited life expectancy.

Is it preferable to use grafts or artificial organs? In some cases it would be preferable to use prostheses and in others grafts. It would seem that the graft is the final element which would make it possible to save the patient, the prosthesis only allows him to wait until his graft can be implanted.

Combinations of prosthetic materials and biological materials are now used more and more frequently, whether it is a bone graft sheathing a prosthesis, or artificial skin made of human cells and cultured, or even live pancreatic cells developing within a synthetic structure.

In truth, it is worrying to think how far it could go, and whether one day it would be possible to create a wholly artificial man or carry out a succession of grafts aiming to replace the various components of the human body. For the moment it is still impossible to replace live organs with artificial organs which are as reliable, and in particular have the same capacity of self-repair as scar formation. Furthermore, their incorporation will without a doubt pose problems in the long term.

Nevertheless, the progress we are constantly making in the development of biocompatible implantable products – ever smaller circuits, ever more powerful software, and in particular live grafts assimilating perfectly into the body in which they are placed – give us real hope.

Part II

Biocompatible Materials

Biomaterials Used in Orthopedics

2

Dominique G. Poitout

The great advances in orthopedic surgery over the past few decades and the fact that it constantly out-performs itself are the result of a policy of rigor in various areas.

Rigor in the training of the surgeons in this discipline, which demands a long period of training in specialist departments.

Rigor in performing operating techniques as a result of which hazardous improvisation is excluded.

Rigor in the choice of materials, the use of which has opened up the way to progress but the quality of which determines the results.

Precision and reliability are therefore the key words of the orthopedic surgeon who is preparing and executing an osteotomy in the same way as an engineer approaches the bridges and road surfaces for the arch of a bridge. He needs a good knowledge of the laws of physics and of the rules of mechanics, but he also has to be able to apply this knowledge to living matter.

I also believe it to be important to stress that orthopedists are clinicians and care for patients and that, if clinical practices develop in a direction which is not in line with their wishes, even though the theory and the calculations are accurate, we should not try to understand how this should work but why it does not work. Indeed, there are so many parameters involved in human clinical medicine that it is often difficult, when trying to describe a movement or define the stresses on a particular material, to take all the normal physiological parameters into account.

Behavior of Biomaterials in Situ

Although the functional aspects of implanted materials can be anticipated fairly reliably, it is very often difficult to anticipate how well they will be tolerated clinically. For materials of any kind there are two aspects which have to be taken into account. They are:

on the one hand the *adhesion* between a biomaterial and the part of the human body with which it will be in contact,
on the other, the *aging* of the product implanted.

Adhesion involves all the problems of using cements and adhesives, the role of which is to transmit and distribute the stresses over the largest area of contact possible. This adhesion problem is far from being resolved satisfactorily from the practical point of view and there is still plenty of scope for the researchers to investigate. Should

D.G. Poitout, MD
Faculté de Médecine Nord, Sce Chirurgie Orthopédique et Traumatologie, Aix-Marseille Université, Centre Hospitalier et Universitaire Marseille North, Chemin des Bourrely, 13015 Marseille, France
e-mail: Dominique.POITOUT@ap-hm.fr

D.G. Poitout (ed.), *Biomechanics and Biomaterials in Orthopedics*,
DOI 10.1007/978-1-84882-664-9_2

a prosthesis be cemented, screwed, or introduced with force, hoping that its irregular surface will allow the bone to grow again and for the prosthesis to be fixed into the bone? More and more surgeons are currently abandoning these latter methods because of the frequency of painful failed fixations requiring surgery to be repeated (6–8 % on average after 12 months). Cement has its drawbacks but according to the current state of knowledge seems to be the best compromise for fixing material into bone.

Aging. As soon as it has been implanted in the body, the biomaterial finds itself in an environment which is more aggressive than sea water, not least on account of its higher temperature and its sodium chloride content. Furthermore, there are also the variations in pH which may lead to a rapid breakdown of plastics and may accelerate_metal corrosion.

I would like to dwell on this problem of metal corrosion for a few moments. Some metallic materials are very resistant to generalized corrosion. This is the case for Vitallium, stainless steels, or alloys based on titanium, but they are still vulnerable to corrosion if pitted, the risk of which increases with contact friction which leads to breaks in the protective passive layer. It is also necessary to take into account the simultaneous action of the corrosive environment on the prostheses and the mechanical stresses to which they are subjected. This results in the risk of corrosion under stress, and corrosion due to fatigue which can lead to the appearance of weak points with the risk of breakage. Another well-known case of corrosion is galvanic corrosion caused by placing two different metals in contact with each other in a conducting liquid which then behave like an electric battery.

When there is corrosion, metal ions pass into the body. Therefore, some studies have shown that for austenitic stainless steel osteosynthesis plates, 9.1 mg of the alloy passed into the body 2 years after having been implanted. That is to say that there is a release of iron, nickel, and chromium in an equal proportion to that of the composition of the alloy. For example, in an individual who had had intramedullary pinning of the tibia, after 18 years he was found to have a nickel concentration in his serum, urine, hair, and nails which was up to 18 times the normal concentration, almost the same level as is found in workers in the nickel industry.

More generally, the implantation of foreign material, and particularly a metallic material, always has consequences for the surrounding biological environment. It was even possible to demonstrate a transformation of the proteins left in contact with nickel, in particular by electron transfer at the metal–electrolyte interface.

The problems listed above therefore require the practitioner to know the mechanical and chemical properties of the materials to be implanted without, of course, forgetting the sterilization conditions which can alter certain materials (such as gamma rays on plastics, ethylene dioxide absorbed by certain materials then released producing toxic reactions).

If the surgeon cannot check all the properties of the material he uses by appropriate tests, he has to rely on the manufacturer's literature to make his choice. But if he knows the properties that he can expect for a given application, the dialog will be more to the point.

That is the current direction in the area of French orthopedics.

Biomaterials Used in Orthopedics

As it would be excessive to give an exhaustive list of all the biomaterials used in orthopedics, we will only take a few examples from each of the five main classes of orthopedic biomaterials;

metals and metal alloys,
ceramics and ceramo-metallic materials,
bone replacement materials and allografts
carbon materials and composites, polymers.

Metal Alloys and Metals

First, where steels are concerned, the introduction of alloys leads to a spectacular improvement in oxidation. Molybdenum plays an essential role in resistance to corrosion caused by pitting.

Chromium also plays an essential role from the point of view of corrosion. Indeed, exposed to

the air or to an oxidizing environment, chromium allows a very thin, invisible film of chromium oxide to form – this is called the passivation phenomenon. A minimum chromium content of 12 % is necessary to give steel its stainless properties.

Other elements can be added; this is true for nickel which, when in a proportion of 10–14 %, makes it possible to obtain an improvement in mechanical performance without leading to brittleness.

Steel with a high carbon content is therefore suitable for temporary surgical implants (osteosynthesis plates, intramedullary nails) because of its malleability and its stainless properties. But its poor prolonged resistance to corrosion means that it has to be removed after a few years.

Alloys based on cobalt–chromium are shaped by microfusion or casting, which is less good mechanically, and only very rarely has it been possible to make forgeable alloys, owing to considerable additions of molybdenum, tungsten, and nickel.

Although these materials have a resistance to corrosion and a breaking load which is better than stainless steel, their elastic limit is very close to the breaking load, which prevents any possibility of permanent deformation. And, as their resistance to fatigue is low, a significant breakage rate has been seen for femoral implants.

Their modulus of elasticity is high, at around 200,000 MPa, which poses the same problems as when using stainless steels (the modulus of elasticity of a bone being less than 20,000 MPAI). Due to their great hardness, alloys based on chromium and cobalt are the best compromise to date for making prosthetic femoral heads.

Titanium alloys have high resistance to all forms of corrosion and have good mechanical properties. Their modulus of elasticity is low, 110,000 MPa, which is half that of other alloys such as stainless steels. They have excellent biocompatibility, a high breaking load, and an elastic limit close to that of the breaking load, which eliminates any problems of permanent deformation in the case of high stresses, but also limits their use as a material in osteosynthesis. Owing to the passivation phenomenon, titanium covers itself spontaneously with a protective film of titanium oxide which renders it remarkably resistant to corrosion. This can be increased even further by the chemical process of anodization. There is one negative element that should be emphasized which is that titanium alloys have poor friction properties in that it is not possible to use them as prosthetic femoral heads or in the axis of a hinged prosthesis. Current trials, aiming to improve the friction characteristics by laying down deposits of titanium nitride or carbide, have not been very successful because these deposits are irregular and thin so that the layers abrade after a few thousand cycles.

Hydrogen or nitrogen ion inclusion techniques are still at the experimental stage.

Finally, the alloy most frequently used currently is an alloy containing a combination of aluminum and vanadium; Ti_6AP_4V, which has properties clearly superior to those of nickel–chromium–cobalt alloys. This is certainly the best solution today for all diaphyseal implants, particularly femoral hip implant which is subjected to high mechanical stresses.

Other metallic biomaterials could, in future, be useful in orthopedics; more specifically zirconium, tantalem, and nobium, all three of which display excellent biotolerance. However, progress still has to be made with alloys before they can rival titanium alloys.

Ceramics and Ceramic–Metal Compounds

Ever since man discovered that fire can modify the properties of clay (hydrated aluminum silicate), ceramics have never stopped developing. New ceramics have been developed and these materials take various forms:

oxides: aluminum oxide (Al_2O_3), zirconium oxide (ZrO_2),
carbides: silicon carbide (SiC),
nitrides, bromides, and fluorides.

The science of ceramics has also meant that new textures can be created such as ceramic composites with various fibers combining metals and ceramics, which are called ceramic–metals or

even cermets. There are also controlled crystallization glasses called vitroceramics.

The New Ceramics

Sintered oxides are either pure oxides such as alumina or mixtures of oxides. When high-purity alumina is used in the medical field, the specification is extremely precise. Alumina is a hydrophilic material (unlike polyethylene which is hydrophobic), it is very hard, slightly less so than diamond (which is, moreover, used to grind and polish it), and its modulus of elasticity is 380,088 MPa, which is practically twice that of the metal alloys. Its resistance to flexion, however, is low, which limits the indications in which it can be used as an osteosynthesis rod or plate. When alumina was first used as a prosthetic hip compound, there were many failures of the femoral head when used with an acetabulum also made of alumina.

The two pieces machined for each other:

tended to jam if the slightest particle of wear debris came between them.
produced very little wear debris, certainly, but as these were crystals they led to synovial reactions comparable to microcrystalline arthritis.
prevented any isolated change in one of the pieces of the prosthesis if only one became damaged.

The existence of a high modulus of elasticity, far higher than that of methyl methacrylate and that of cortical bone, led to problems when sealing an alumina acetabulum with methyl methacrylate because unsealing occurred more frequently and usually occurred between the cement and the acetabulum and not between the bone and cement, as is normally the case. On the other hand, if the alumina acetabulum is directly screwed into the bone, the quality of the fixation is exceptional and the mobility of the implant normal because of the almost inevitable appearance of a film of fibrous tissue between the implant and the bone. The use of alumina currently, therefore, seems to be restricted to femoral heads and sliding surfaces in contact with polyethylene.

Zirconia (ZrO_2) also has excellent mechanical properties, in particular flexion, together with satisfactory resistance to wear and friction, but in some cases it breaks! We hope that zirconias stabilized by yttrium oxide (Y_2O_3) and by alumina ($R_{12}O_3$) will be used routinely as friction components in total prostheses of the hip.

Carbides and Nitrides: These new materials include silicon carbide, which appears to have greater resistance to flexion than alumina as well as a higher modulus of elasticity, but its coefficient of friction is lower than that of alumina.

Ceramic–Ceramic and Ceramic–Metal Compounds

Fiber composites are a compromise between a deformable solid (for example, carbon fibers or alumina fibers) and a matrix which resists deformation (such as alumina or silicon carbide). To date, the first experiments with mixtures of aluminum oxide and iron have not produced useful results for improving the properties of the material. On the other hand, other combinations with molybdenum and its carbide, with tungsten and its carbide, or with titanium combined with zirconium oxide, seem to improve the resilience and toughness of the material considerably.

Glass and Vitroceramics

The mechanical strength of some glasses can be greatly improved by being transformed into vitroceramics. Direct anchoring, as for conventional ceramics, can, together with glasses and the vitroceramics, be performed by mechanical or chemical processes. In the case of vitroceramics anchored mechanically the dimensions of the interconnections between the pores are sufficiently large to allow colonization by bone tissue. Unfortunately, the mechanical properties of these vitroceramics are relatively poor. Resistance to breakage on flexion remains around 20 MPa, which is far too low for use in internal prostheses.

It seems that glasses and vitroceramics anchored chemically give better results. These materials initially have better mechanical strength than those of porous materials and are better than those of bone, but these criteria do not last. On

the other hand, adhesion only seems to occur if the implant is immediately placed into intimate contact with the bone tissue, which is not always easy to do in practice, because, as in the case of bio-inert materials, a fibrous capsule forms which isolates the material from the bone.

Natural, Biological, or Synthetic Bone Replacement Materials

Bone loss can be remedied today either by natural autologous or homologous bone grafts or with ceramic-like materials. This is particularly true for madreporic coral or synthetic coral which consist of calcium phosphates and fluoroapatites and are comparable to the vitroceramics we have been discussing.

Natural calcium carbonates are skeletons of madreporic corals with their organic part removed. They consist of virtually pure aragonite ($CaCO_3$). Used experimentally to replace bone substance losses or to fill cavities, it seems that the tendency is for the fragment of natural calcium carbonate to be resorbed, then for the carbonated skeleton to be replaced centripetally and gradually by bone. The structure of coral skeleton makes it possible to re-establish the intra-medullary circulation and its resorption releases calcium ions reused by the body for the precipitation of phosphocalcium apatite. However, the mechanical properties of the corals, which have a strength under flexion of the order of 3 MPa, and under compression of 16 MPa, are much inferior to those of bone and the clinical applications are comparable to bone autografts and allografts.

Materials Obtained by Synthesis

With comparable porosity, the mechanical properties of synthetic materials are generally superior to those of natural materials. Only the compressive strength of tricalcium phosphate, which is between 7 and 21 MPa, is of the order of magnitude of that of coral. As for the latter, there are ultimately extremely few clinical applications.

Allografts

Bone is a living tissue consisting of cells as well as of a prosthetic structure on which calcium and phosphorus have been precipitated. The introduction into the body of a bone graft of any kind will lead to the progressive destruction of its cells without modifying the supporting protein lattice. Indeed, although the cells are antigenically specific to any particular individual (various HLR groups), the collagen which forms the architecture of the bone is the same throughout the human race and will not give rise to rejection phenomena. Whether we use an autograft or an allograft, the clinical development of this tissue is approximately comparable and the cells will die. The protein structure on which the phosphocalcium raster is fixed will no longer exist and the bone cells of the host will recolonize the bone which serves as a mold. After several years, new bone will be reformed from the cells of the host.

As massive samples cannot be taken from the same person without running the risk of causing problems at the donor site, we turned to preservation by cryopreservation of the bone homografts in bone banks. In order for it to be preserved "indefinitely", it is necessary for the bone to be stored in very cold conditions below −80 °C. For these technical reasons, we chose to store the cryopreserved bone – preserved in 10 % DMSO in liquid nitrogen at −196 °C; which, subject to certain precautions, gives the most reliable results. Cryopreserved bone makes it possible to reconstruct a bone segment which had to be resected due to the existence of a bone tumor at that site and also to reconstruct the locomotor architecture after a considerable loss of bone substance due to trauma.

Massive osteocartilaginous fragments are used ever more frequently to reconstruct articular surfaces which have been damaged or removed as part of the excision of a tumor. Smaller, spongy fragments can also be used in addition to osteosynthesis to fill a bone cavity or to complete the fixation of an arthroplasty. The results we are obtaining currently are wholly encouraging and in many cases have made it possible to avoid amputation or the use of massive prostheses, the long-term mechanical future of which

is not guaranteed. Between 1978 and 2000, the Marseilles Bone Bank has supplied 1744 massive bone parts used for grafts.

Carbon Compounds

Since 1967, numerous procedures have been used to create biomedical carbon but so far none have given absolute biological stability. It cannot, therefore, yet be considered for use routinely in human biology, in spite of the very many suggestions which have been made (osteosynthesis plates, nails, joint prostheses) and in spite of its unrivalled endurance to fatigue (easily able to exceed ten million cycles). The natural communicating porosity of its structure allows colonization into the mass of the prosthesis by the surrounding biological tissues, and the structural flexibility of the composites harmonize with the elasticity of the host bone. The fact that they cannot be deformed means that they cannot be used as osteosynthesis plates and as the carbon fibers cannot tolerate lengthening, even to a very small extent, nor can they be bent to more than 30 ° without breaking. They cannot be used as a prosthetic ligament because fixing this ligament into bone is very difficult.

Finally, the many particles from wear found in the ganglions, and even in the spleen, mean that we have to be careful when using these composites. Owing to the hardness of the surfaces obtained by the ceramization treatment, it may be possible to consider using carbon as an articular surface, placing polyethylene in between the opposing surfaces.

Polymers

Numerous products have been suggested but, of course, they cannot all be considered.

As far as their common properties are concerned, it is important to stress the fact that they age physically and chemically.

The following will be discussed:

1. Silicones, which are chemically inert, have good biotolerance and a high hydrophobic capacity. They are used in plastic surgery or in orthopedics in the form of elastomer rubbers for joint prostheses of the fingers, for example.
2. Polyacrylics, and more specifically, methyl polymethacrylate, are well known in the area of orthopedics as they are used as a cement for fixing prostheses. The time that cements take to grip varies considerably depending on the type of used; also the polymerization reaction, which is very exothermic. If none of the heat were to be dissipated to the exterior while polymerizing, the mass of cement could reach more than 70 °C. It is thought that the maximum temperature should generally be no more than 40–50 °C in vitro, which is relatively close to the coagulation point for proteins (56 °C) and that of bone collagen (70 °C). It would therefore be desirable to find a new, weakly exothermic cement, which sets relatively slowly, but this is not yet available.

Currently, the cement penetrates the interstices of the bone more effectively and leads to even more secure anchorage if it is more fluid or less viscous. It is therefore preferable to use a cement with a viscosity of less than 100 Newton/s/m^2 after mixing.

Similarly, the porosity is a decisive factor in the mechanical behavior of the cement. For a particular cement, the size of the pores does not depend on the maximum temperature, but on the mixing and usage conditions. On the other hand, the number of bubbles per unit volume, for any particular cement, depends on the maximum polymerization temperature.

Finally, all acrylic cements show volume changes between the beginning of the mixing and the end of hardening. Currently, it appears that cement starts by contracting approximately 2.5–6.5 microns per 2 mm thickness. As far as the mechanical properties of cement are concerned, the Young's modulus is low (of the order of 3000 MPa) and traction strength and compressive strength are approximately a quarter of the strength of normal bone. It is therefore important to emphasize the preparation of the cement, the frequency of the movements, and the role of the additives. In this area, the addition of powders only very slightly changes their mechanical

properties. On the other hand, when a liquid, such as an antibiotic, is to be added, this leads to serious weak points appearing and causes fractures to start which will only spread under stress. Finally, irradiation does not cause any significant changes in the mechanical behavior of the cement.

3. Saturated polyesters, which are condensation polymers, are essentially represented by polyethylene terephthalate. This polymer has good resistance to chemical agents, good tolerance in solid form and good mechanical properties. However, its behavior in a humid environment is poor, with a sharp reduction of its mechanical properties. It is used in orthopedics in the form of plaited threads to make prosthetic ligaments (Dacron or Rodergon, for example). The poor elastic elongation properties (1.25 Y approximately) seem to be a very worrying factor for how this prosthesis behaves over time because the relative physiological elongation of the cruciate ligaments of the knee, for example, is 26–25 Y.
4. Polyolefins. In this group it is UHMW (Ultra-high-molecular-weight) polyethylene which is used for making friction components for prostheses of the hip, knee, and elbow because of its mechanical properties. A great deal of research is currently being carried out to improve its properties, and in particular its resistance to creep with, for example, the incorporation of carbon fibers. Polyethylene reticulated by ionizing radiation with grafting of polytetrafluoroethylene should also improve the resistance to wear and creep. The use of a metal backing for prosthetic cupulae also seems to limit the extent of creep. Polypropylene can be used for ligament use but here, too, its elastic elongation risks breaks in or detachment of the implant.

To conclude, how do these biomaterials behave in use? It should be borne in mind that the main reasons why these materials fail are due to an as yet inadequate understanding of the properties of the materials used. Detachment is due to a breakdown in the cements and requires research to be carried out into their properties together with research into the mechanics of the transfer of loads between the implant and the bone. The extent of wear on the polyethylene parts will mean that the properties of these products will have to be changed, while amending the design of the parts. The introduction of ceramics to reduce the extent of wear has not managed to stop it, and until these materials are made less brittle, there will still be the risk of accidents.

There is still insufficient experience with carbon composite materials and only rigorously controlled experiments will enable us to say whether the hoped for advantages of these new materials are accompanied by serious disadvantages linked to a possible fragmentation of the fibers.

Finally, in the case of metal alloys, an analysis of the behavior of the parts in use shows that the resistance to fatigue corrosion should be studied in experimental conditions to enable easier comparison of the advantages and disadvantages of the various alloys proposed.

Care should be taken not to reach too hasty a conclusion as to the risks of certain techniques and, perhaps even more importantly, the wholly beneficial effect of the new techniques where it is not possible to be entirely sure of the scientific objectivity of the measures. In practical terms, all the phenomena involved in the behavior of implantable materials start at the surface of the implants. It is therefore by studying the surfaces and their changes by physicochemical or mechanical treatment that advances can be made in the current techniques for manufacturing surgical implants. Reconstruction of joint cartilage with collagen, osteocartilaginous allografts, or artificial substances will allow enormous advances to be made in the treatment of arthroses, the number of cases of which rise as life expectancy increases.

Finally, many materials used today will probably be abandoned in the years to come. On the other hand, new products will appear which will be based on the arthroplasties of the year 2000. Today we are probably only aware of one third of the materials we will be using in 20 years time.

Bioceramics

3

Takao Yamamuro

Definition and Classification

Ceramic is defined as "synthesized inorganic, solid, crystalline materials, excluding metals". Ceramics used as biomaterials to fill up defects in tooth and bone, to fix bone graft, fracture or prosthesis to bone, and to replace diseased tissue, are called bioceramics. They must be highly biocompatible and antithrombogenic, and should not be toxic, allergenic, carcinogenic nor teratogenic. Bioceramics can be classified into three groups: (1) bioinert ceramics, (2) bioactive ceramics, and (3) bioresorbable ceramics. Bioinert ceramics have a high chemical stability in vivo as well as a high mechanical strength as a rule, and when they are implanted in living bone, they are incorporated into the bone tissue in accordance with the pattern of "contact osteogenesis". On the other hand, bioactive ceramics have a character of osteoconduction and a capability of chemical bonding with living bone tissue. In other words, when bioactive ceramics are implanted in living bone, they are incorporated into the bone tissue in accordance with the pattern of "bonding osteogenesis". Mechanical strength of bioactive ceramics is generally lower than that of bioinert ceramics. Bioresorbable ceramics have a character of being gradually absorbed in vivo and replaced by bone in the bone tissue. The pattern of their incorporation into the bone tissue is considered similar to bonding osteogenesis, although the interface between bioresorbable ceramics and bone is not stable as that observed with bioactive ceramics.

T. Yamamuro, MD, PhD
Department of Orthopaedic Surgery,
Faculty of Medicine, Kyoto University,
Kyoto, Japan

Research Institute for Production Development,
Shimogamo, Sakyo-ku, Kyoto, Japan
e-mail: mozume-takaoyama@sweet.odn.ne.jp

Bioinert Ceramics

In 1969, Benson [1] predicted that carbon ceramic will be brought into clinical application as a biomaterial in the near future, as it has an excellent biocompatibility, a high compressive strength, and a reasonable elastic modulus. When carbon fibers were used as an artificial ligament, however, it tended to undergo fragmentation. Recently such mechanically stronger carbons as low temperature isotropic carbon (LTI carbon) and carbon fiber reinforced carbon (CFRC) have been developed, but their clinical application has not yet been brought to realization.

Bionert ceramics such as alumina ceramic (Al_2O_3) and zirconia ceramic (ZrO_2) have a higher compressive and bending strength and better biocompatibility than stainless steel (SUS 316 L) or Co-Cr alloy. Alumina ceramic

D.G. Poitout (ed.), *Biomechanics and Biomaterials in Orthopedics*,
DOI 10.1007/978-1-84882-664-9_3

particularly, therefore, had been attempted to use as osteosynthetic devices (alumina monocrystal) or to fabricate bone and joint prostheses (alumina monocrystal + polycrystal) in 1980s [2]. Recently, however, due to their brittleness and too high elastic modulus as compared to those of human bone, they are used very little for above purposes. On the other hand, it has been known that a ball made of alumina or zirconia exhibits a wear resistant character when its surface is polished to an average surface roughness of 0.02 μm. At present, therefore, clinical application of alumina and zirconia is almost solely limited to the bearing surface of joint prosthesis.

It is well known that one of important factors causing loosening of joint prosthesis is the periprosthetic osteolysis which is due mainly to excessive macrophage activities against wear debris, particularly of polyethylene (PE), around the prosthesis. Even after the introduction of highly cross-linked polyethylene (XLPE) which is much wear resistant, there have been various attempts to reduce the number of wear debris by changing the bearing surface of prosthesis from PE-on-metal combination to metal-on-metal, ceramic-on-ceramic, or PE-on-ceramic combination. In 1970, Boutin [3] started to use an alumina-on-alumina combination for the bearing surface of hip prosthesis. According to Sedel [4], alumina ceramic used for the hip prosthesis between 1970 and 1979 had a mean crystal grain size of 7 μm and the linear wear of its bearing surface was 5 to 9 μm per year. While alumina ceramic currently used has a grain size of 2 μm that means less brittle than the old type, and the linear wear is in the order of 3 μm per year. Sedel further described that the overall wear of the currently used alumina-on-alumina hip prosthesis, calculated by the weight of debris generated, was approximately 1,000 times less than for metal-on-polyethylene and 40 times less than for metal-on-metal joint, if all requirements for alumina quality, sphericity, circularity, and clearance of the bearing components are met. Therefore, in spite of the fact that the alumina-on-alumina hip prosthesis used in 1970s did not show significantly better 10–15 year results as compared to those of Charnley hip prosthesis, the current alumina-on-alumina hip prosthesis is expected to bring about much better long-term results and less breakage than those used in 1970s.

On the other hand, it is a well known rule for hip prosthesis that the smaller the head size the less the volumetric wear of the bearing surface. This rule has been much accounted of the PE-on-ceramic hip prosthesis in attempts to reduce the volumetric wear of polyethylene. The diameter of most alumina femoral head of hip prosthesis has been limited to 26–32 mm even with new alumina ceramic, because it exhibits only moderate bending strength and toughness. If it is attempted to reduce the head size to 22 mm with absolute safety against breakage of the component, zirconia ceramic is naturally taken into consideration as a constituent material, as it has an advantage over alumina of higher bending, compressive, and impact strength, higher fracture toughness, and lower elastic modulus. The reasons why zirconia ceramic had not been brought into clinical application until recently were that the zirconia synthesized in 1980s was abnormally radioactive [5] and tended to biodegrade in vivo. Modern technology, however, made it possible to synthesize a new zirconia which is not abnormally radioactive and is stable in vivo. This has been accomplished mainly by developing a refining technique to obtain pure zirconium from a raw ore and by adding chemical stabilizers such as yttrium oxide or cerium oxide during the sintering process of zirconia. The estimated amount of radioactivity exhibited from the zirconia, prepared by us in Kobe Steel Company since 1993, was 1.152 μR, while normal background of radioactivity amounts to about 100 mR [6]. Thus, the radioactivity of new zirconia is considered negligible.

Concerning crystallographical stability, alumina ceramic (usually α-alumina) is entirely consisted of hexagonal crystals and hence it is chemically very stable in vivo. On the other hand, zirconia ceramic is usually consisted of three crystallographical phases; cubic, tetragonal, and monoclinic, and transformation of the phase

takes place under various conditions such as change of temperature, mechanical stress, and humidity. The phase transformation often results in self destruction of the ceramic. Until 1980s, such a crystallographical unstableness was one of reasons why zirconia had not been used as a constituent material for the bearing component of joint prosthesis in which high stress concentration may be created on the ceramic surface by repeated loading under wet condition. In 1990s, however, new sintering methods have been introduced to prepare crystallographically stable zirconia ceramics, by adding such chemical stabilizers as Y_2O_3, CeO_2, and MgO in the sintering process. They are called partially stabilized zirconia (PSZ). For example, to prepare a zirconia femoral head of 22 mm in outer diameter, zirconia powder with a grain size of less than 1 μm is mixed with chemical stabilizers (Table 3.1), and is moulded into a ball by rubber pressing at room temperature. The ball is then sintered for 2 h at 1,500 °C. The sintered zirconia ball undergoes machining to shape a precise spherical ball with an outer diameter of 22 mm and a tapering pit (Fig. 3.1). The ball is finally polished to obtain an average surface roughness of less than 0.02 μm. Thus made zirconia femoral head is consisted mainly of tetragonal phase and 1–2 % of monoclinic and cubic phase.

Mechanical properties of PSZs are compared with those of new alumina ceramic with grain size of less than 2 μm in Table 3.2. PSZs have significantly higher bending strength, compressive strength, fracture toughness, and impact strength, but have a lower Vickers hardness and elastic modulus than the alumina ceramic, although they are slightly different depending on the grain size and kind of chemical stabilizers used. Among them, yttrium oxide PSZ (Y-PSZ) has the highest bending strength and fracture toughness followed by cerium oxide PSZ (Ce-PSZ). Breaking tests for Y-PSZ and alumina femoral heads, 22 mm in outer diameter, were performed by static loading over a polyethylene liner which was set against the ceramic head. The alumina heads were broken by loads of 2,400–3,400 kg (average 2,800 kg), while Y-PSZ heads were broken by loads of 2,770–4,480 kg (average 3,700 kg). Thus, Y-PSZ head was significantly stronger than the alumina head against breakage [7]. Fatigue test was performed on eight Y-PSZ femoral heads on a hip simulator in physiological saline at 37 °C, by applying 10^7 cycles of repeated loading with 450 kg. This loading is considered to correspond approximately to 20 years of a person walking. After the test, no breakage was observed in all the eight Y-PSZ heads.

Wear tests for the polyethylene liner against the Y-PSZ, alumina and stainless steel head, all 22 mm in outer diameter, were performed using a hip simulator in physiological saline at 37 °C by applying a load of 450 kg at 1 Hz. After 5×10^5 cycles of loading, the polyethylene liner against the stainless steel head showed significant wear, while those against the Y-PSZ head and alumina head did not show any measurable wear, even after 2×10^6 loading [7].

Thus, alumina is chemically more stable than PSZ in vivo, while PSZ is mechanically stronger than alumina, and both of them exhibit much better wear-resistant character comparing the stainless steel or Co-Cr alloy as assessed in a form of bearing components of hip prosthesis. For these reasons, alumina is used to fabricate a ceramic-on-ceramic hip prosthesis where head size is not a key issue, while PSZ is used to fabricate a PE-on-ceramic hip prosthesis where the head size must be made reasonably small. One of reasons why the zirconia-on-zirconia or alumina-on-zirconia hip prosthesis is not yet brought to the market is that, even with the PSZ, its crystallographical stability in vivo in a long term has not been confirmed.

Table 3.1 Chemical composition of zirconia ceramic

	Weight %
SiO_2+M_20 (M_20:Na_20,K_20 etc)	0.1
Fe_20_3	0.1
Al_20_3	0.5
Y_20_3	4.8 ± 0.7
Zro_2	Remainder

On the other hand, recently a combined ceramic (Zirconia 20 % and Alunina 80 %) is brought into clinical use as a XLPE-on-Ceramic hip prosthesis. This combination of Zirconia and Alumina is to aim at covering the weak points each other. It is said, however, when a proportion of Zirconia exceeds 6 %, effect of phase transformation can not be neglected in vivo. Therefore,

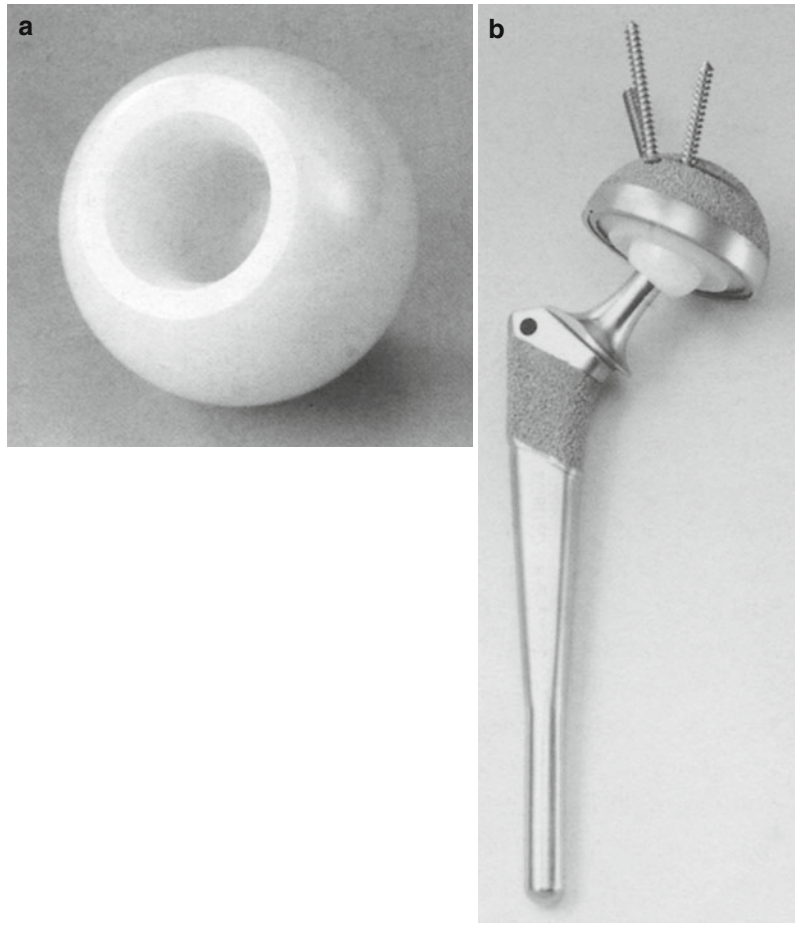

Fig. 3.1 (**a**) A zirconia made femoral head with an outer diameter of 22 mm. (**b**) A cementless hip prosthesis made of titanium alloy with a combination of zirconia head and polyethylene socket for the bearing component

Table 3.2 Mechanical properties of bioinert ceramics

		Zirconia	Alumina
Bending strength	(kgf/mm^2)	170	>40.8
Compressive strength	(kgf/mm^2)	500	408
Fracture toughness	($MPa,m^{1/2}$)	5.2	3.4
Impact strength	(kg/mm^2 or kJ/m^2)	14	4
Vickers hardness	(HV kg/mm^2)	1270	2300
Elastic modulus	(kgf/mm^2)	20500	>38800
Density	(g/cm^3)	6.05	>3.9
Crystal size	(μm)	0.2	<7

clinical follow-up longer than 10 years is required to confirm the long term results in this combination as well.

A new technology developed by Smith and Nephew Co. in 1998 using Zirconium-Niobium alloy made it possible to solve the problem of phase transformation of zirconia ceramic in vivo. When a high temperature is applied on Zr-Nb alloy, its surface transforms to a monoclinic zirconia layer in about 5 μm thick. The layer is called Oxinium. Thus made surface monoclinic zirconia layer (Oxinium) is a gradient material made from Zr-Nb alloy. When a femoral head of hip prosthesis is made by the use of the above technique, its surface is not affected by phase transformation in vivo as it is made of monoclinic zirconia, and, in addition, the femoral head is not broken as it is made of Zr-Nb alloy, a metal. For these reasons, Oxinium-on Oxinium hip prosthesis is considered reasonable theoretically.

Bioactive Ceramics

Bioactive ceramics include glasses, glass-ceramics, and ceramics that elicit a specific biological response at the interface between the material and the bone tissue which results in the formation of a bond between them. The first evidence of direct bone bonding to a glass implant was discovered by Hench et al. in 1970 [8]. Since then, some other glasses, glass-ceramics, and ceramics had been proved to have a bone bonding capability. Among them, Bioglass®, apatite-and wollastonite-containing glass-ceramic (AW-GC) and synthetic hydroxyapatite (HA) are representative materials currently used for clinical application.

In 1970, Hench et al. [8] synthesized a bioactive glass by a chemical composition of SiO_2 45, CaO 24.5, P_2O_5 6, Na_2O 24.5 (wt%). This glass is called 45S5 Bioglass® and known to exhibit the strongest bioactivity among hitherto developed bioactive ceramics. Wilson et al. [9] proved that when the implant-tissue interface was immobilized, collagen fibers of the soft tissue became embedded and bonded within the growing silica-rich and hydroxycarbonate apatite layer on the 45S5 Bioglass®. Such soft-tissue bonding has never been observed with other bioactive ceramics or glass-ceramics. However, as Bioglass® is mechanically much weaker than the human cortical bone, it cannot be used as a weight bearing bone prosthesis. In stead, it has been used as a bone void filler in a form of granule, coating material on metallic prostheses, and to fabricate a middle ear prosthesis.

Aoki et al. [10] in 1966 and Jarcho et al. [11] in 1976 separately developed a process for producing dense hydroxyapatite implants with considerably high mechanical strength. Synthetic hydroxyapatite ($Ca_{10}(PO_4)_6(OH)_2$) has a capability of chemical bonding with the living bone tissue, but it takes much longer time than Bioglass® for bone bonding. Its mechanical property is shown in Table 3.3 in comparison with that of the natural bone and AW-GC. The bending strength of HA is lower than that of the natural cortical bone, and hence HA cannot be used to fabricate a weight bearing bone prosthesis with absolute safety against breakage in vivo. It has been used as a bone void filler in a form of granule with various particle size (Fig. 3.2), coating material on metallic prostheses, and to fabricate an iliac crest prosthesis and a laminoplasty spacer in

Table 3.3 Mechanical property of natural bone and bioactive ceramics

	Bending strength (Mpa)	Compressive strength (Mpa)	Elastic modulus (Gpa)
Natural bone	30–190	90–230	3.8–17
Synthesized Hydroxyapatite	110–170	500–900	35–120
A-W Glass-Ceramic	220	1000	120

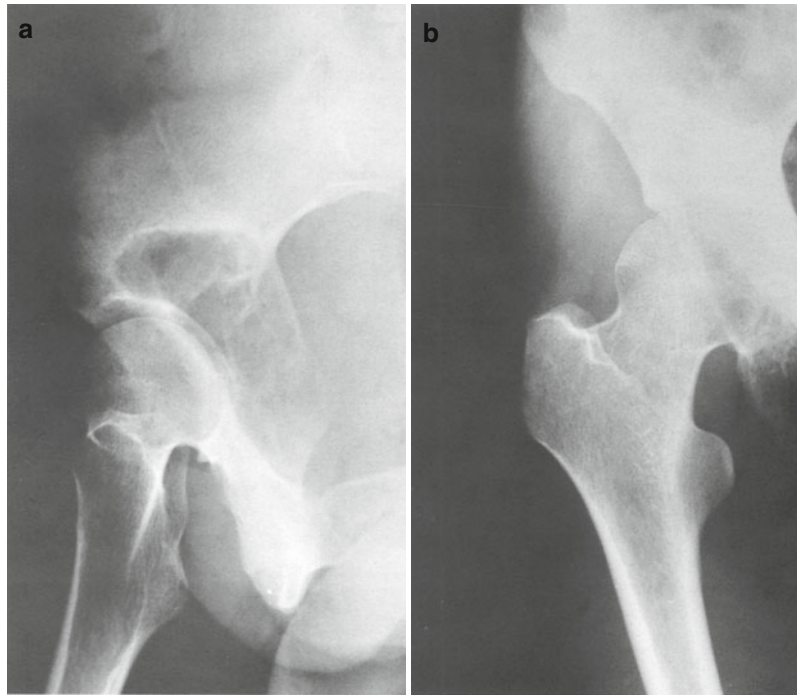

Fig. 3.2 (**a**) A giant cell tumor developed in the right ilium and ischium of a 27 year old female. The tumor was excised and the remaining large bone defect was filled with a mixture of autogenous bone chips, HA granules and fibrin glue. (**b**) 20 years postoperatively, HA has been well incorporated into the surrouding bone and the patient has no symptome

which high mechanical strength is not required. In 1987, Geesink et al. [12] developed a HA coated hip prosthesis and reported an excellent 10 year clinical result in a large number of patient (Fig. 3.3). At present, HA is the bioactive ceramic most widely used for clinical application as a bone void filler and a coating material for hip prostheses which are employed in cementless hip replacement.

The HA coating over the prosthesis is usually performed by plasma splay coating, and thus made HA coated layer is consisted of more than 50 % of amorphous apatite. As the amorphous apatite is absorbed by osteoclasts in a few years, HA coating only cannot maintain the firm connection between the prosthesis and bone for longer than 20 years. For this reason, modern cementless hip prosthesis has a HA coating over the porous Ti coating.

Aiming at producing a mechanically stronger bioactive material, Kokubo et al. [13] in 1982 developed apatite-and wollastonite-containing glass-ceramic (AW-GC or Cerabone AW®) by a chemical composition of SiO_2 34.0, CaO 44.7, P_2O_5 16.2, MgO 4.6, CaF_2 0.5(wt%). As shown in Table 3–3, AW-GC has a significantly greater bending and compressive strength than the human cortical bone and dense HA. Bioacitivity was compared among Bioglass®, HA and AW-GC by implanting them into the living bone tissue and carrying out detaching tests in different postimplantation periods. It was demonstrated that the bone bonding occurred earliest with Bioglass®

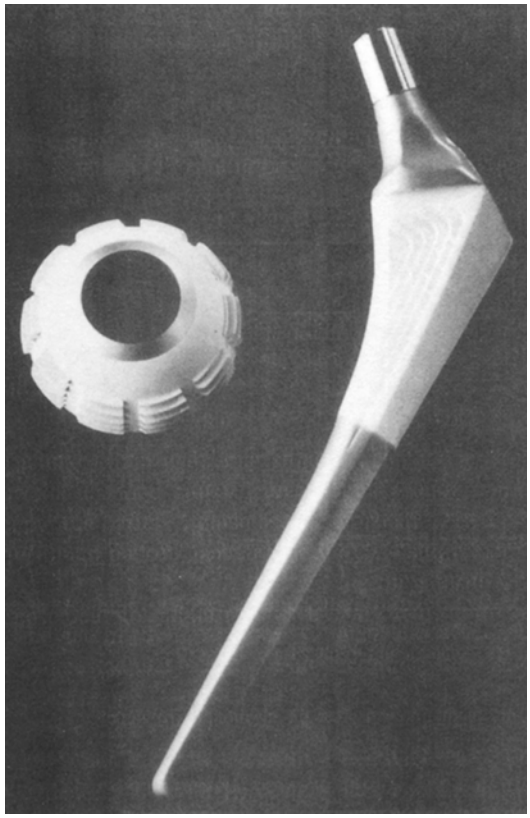

Fig. 3.3 HA coated hip prosthesis developed by Geesink et al.

followed by AW-GC and then HA. The essential mechanism of bone bonding for Bioglass® and AW-GC is considered similar, that is the formation of an apatite layer on the implant surface in the body environment. This surface apatite formation takes place by a chemical reaction of Ca^{2+} and $HSiO^{3-}$ ions dissolved from the implant surface. This apatite is called chemical apatite (Fig. 3.4). At the same time, on the cut surface of bone, an apatite layer accompanied by collagen fibers is formed by the activity of osteoblasts. This apatite layer is called biological apatite. Neo et al. [14] observed under transmission electron microscope that the chemical apatite and the biological apatite were intermingled at the bone bonding interface (Fig. 3.5). The HA implant also showed the similar bone bonding morphology under transmission electron microscope, but HA took longer time than Bioglass® or AW-GC for bone bonding. This may presumably be due to the fact that HA is solely consisted of crystals, while others contain the glass phase which is dissolved faster than the crystal and dissolved $HSiO_3^-$ ions might provide favorable sites for nucleation of the apatite [15].

Yamamuro et al. [16] replaced vertebral bodies of sheep with a vertebral prosthesis made of AW-GC and found that the prosthesis bonded directly to the adjacent vertebrae within about 1 year (Fig. 3.6). Then, by the use of AW-GC, various bone prostheses were fabricated such as iliac crest prosthesis, vertebral prosthesis, intervertebral spacer, and laminoplasty spacer (Fig. 3.7) [17]. The iliac crest spacer is used to substitute a bone defect remaining after harvesting a large bone graft from the iliac crest in various orthopaedic operations. The vertebral prosthesis is used to substitute for vertebral bodies suffering from benign and malignant tumors, compression fracture and burst fracture (Fig. 3.8). The intervertebral spacer is used for interbody fusion through either anterior or posterior approach (Fig. 3.9). The laminoplasty spacer is used to maintain bilateral laminae opened after surgical enlargement of the cervical spinal canal in degenerative spondylosis and ossification of the posterior longitudinal ligament (Fig. 3.10). AW-GC has also been used as a bone substitute in forms of either block (Fig. 3.11) or granule. When bioactive ceramic granule is used as a bone void filler together with fibrin glue, osteoconduction and bone bonding are accelerated. AW-GC is also widely used for bioactive coating of hip prosthesis. Its details are described in the Chapter of Ceramic Coating.

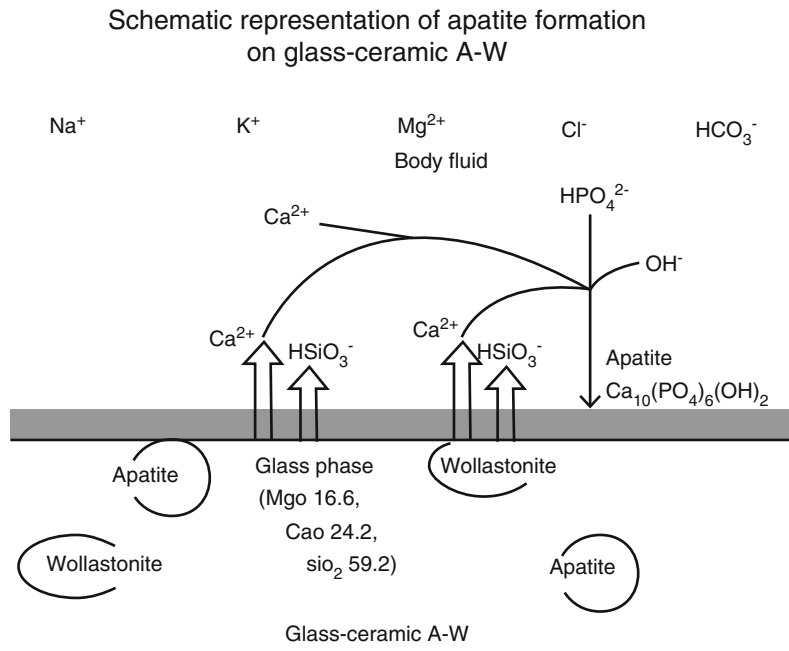

Fig. 3.4 Schematic representation of apatite formation on AW-GC

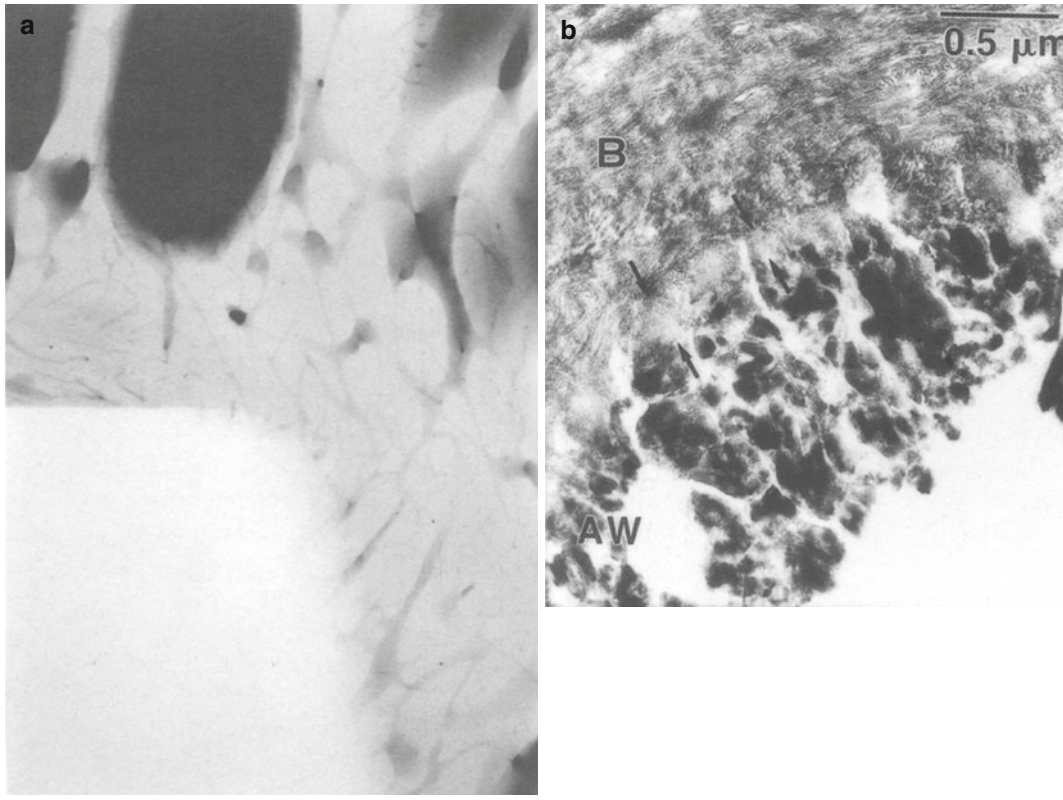

Fig. 3.5 (**a**) A contact micro-radiograph showing the bone bonding between AW-GC implant and newly formed bone. (**b**) A transmission electron micrograph showing the bonding interface between AW-GC (AW) and bone *B* (*arrows*). *AW* AW-GC crystals, *B* bone tissue

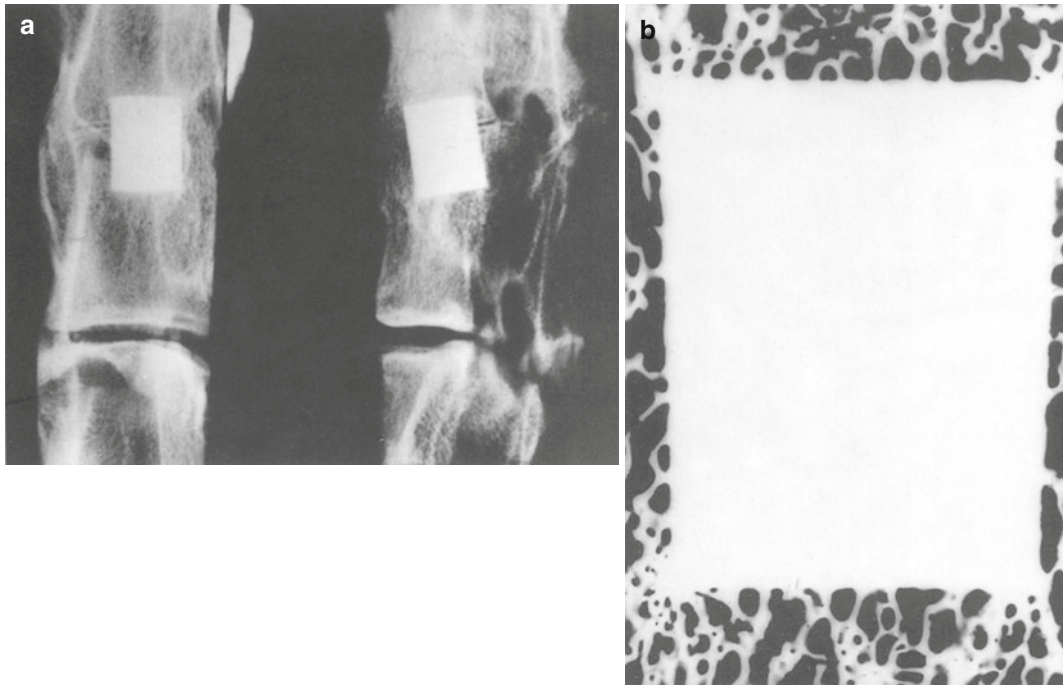

Fig. 3.6 (**a**) A X-ray picture showing an AW-GC implant used for interbody fusion of the lumbar vertebrae of a sheep. (**b**) A contact micro-radiograph demonstrating direct bonding between the AW-GC implant and bone trabeculae of the lumbar vertebrae, 1 year postimplantation

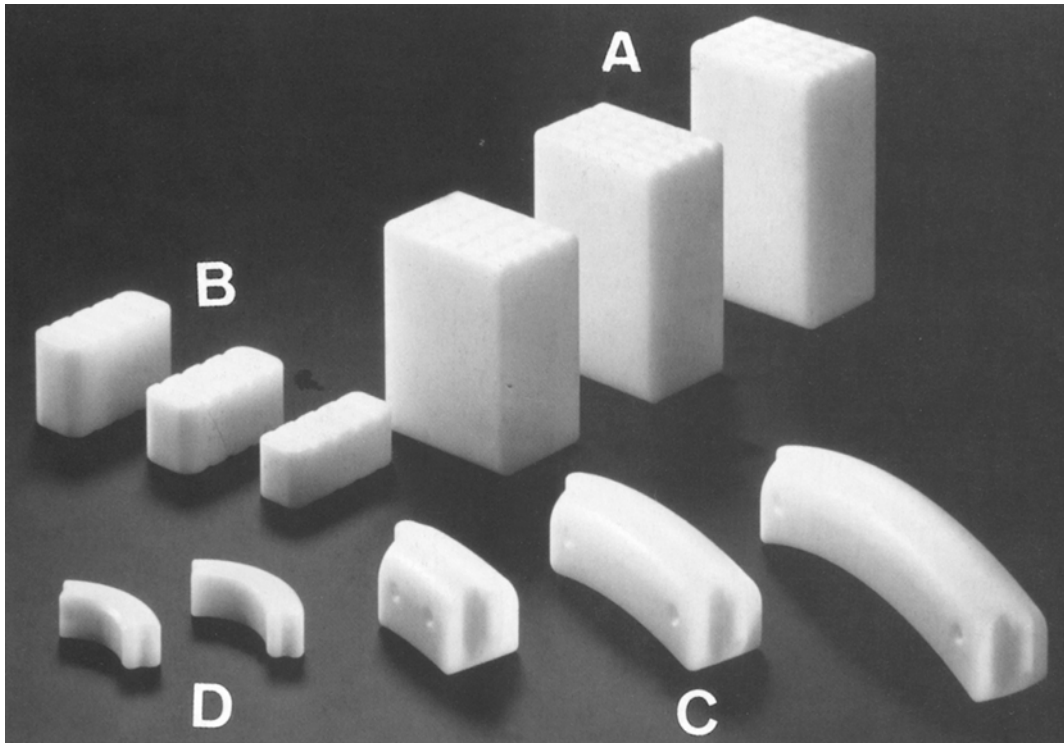

Fig. 3.7 Various bone prostheses. A: vertebral prosthesis, B:intervertebral spacer, C:iliac crest prosthesis, D:laminoplasty spacer

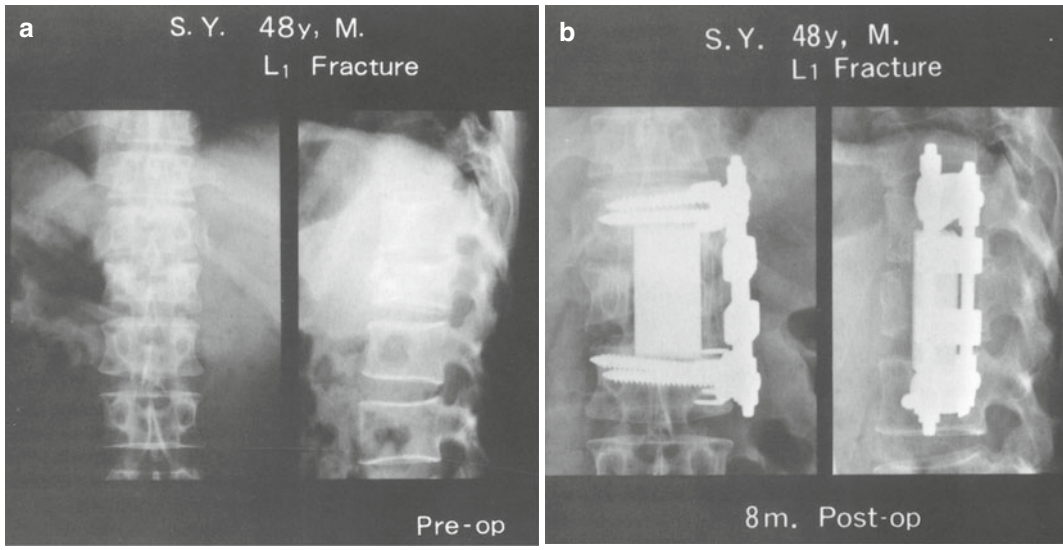

Fig. 3.8 (**a**) A x-ray picture demonstrating L_1 burst fracture associated with paraplegia developed in a 48 year old male. (**b**)**:** A postoperative X-ray picture showing a vertebral prosthesis used for the reconstruction of the lumbar spine

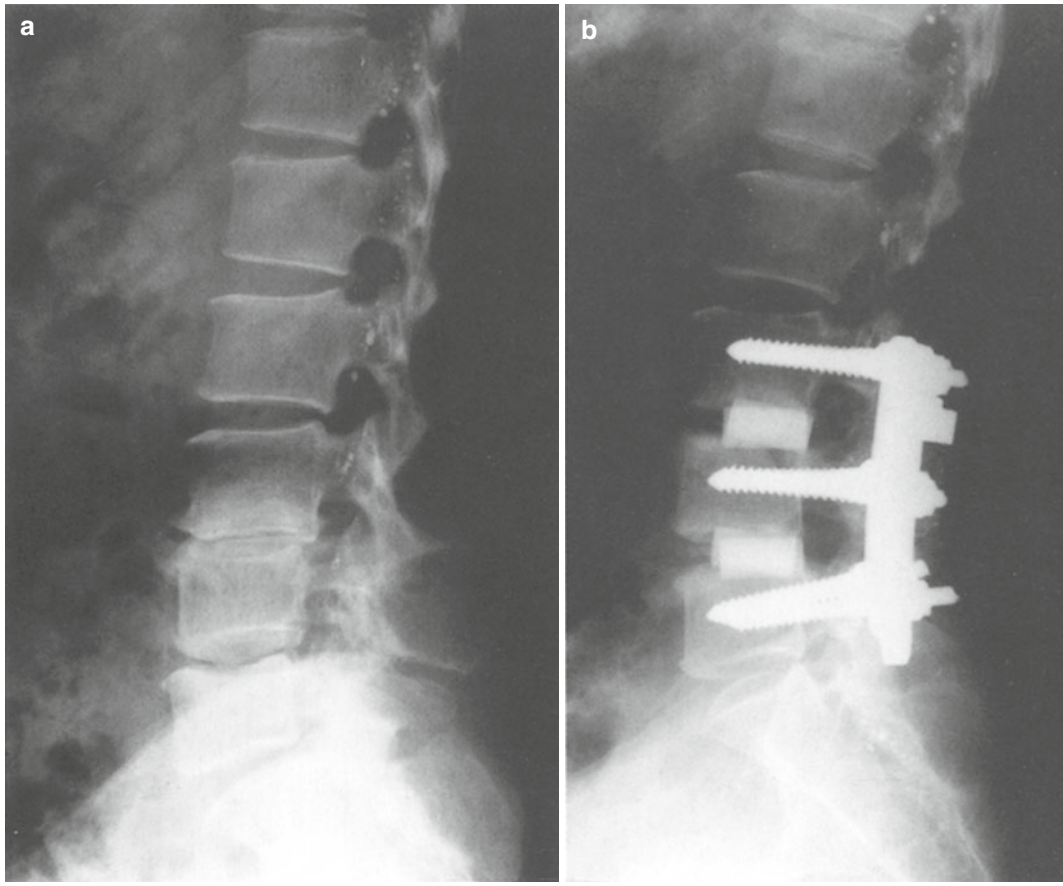

Fig. 3.9 (**a**) A case of multiple degenerative spondylosis of the lumbar spine developed in a 58 year old female. (**b**) A postoperative X-ray picture showing the results of postero-lateral interbody fusion using intervertebral spacers made of AW-GC

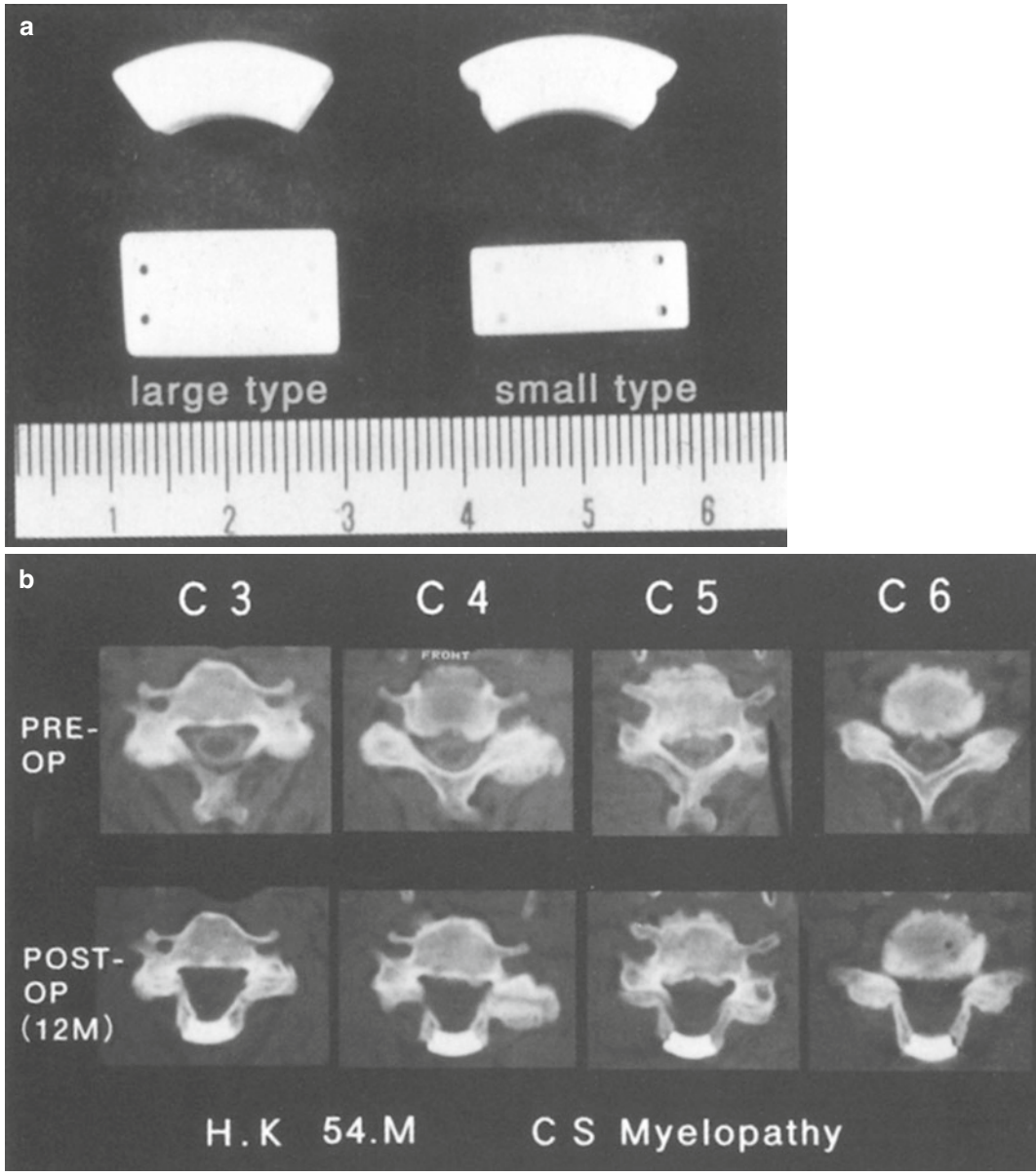

Fig. 3.10 (**a**) Laminoplasty spacers made of AW-GC. (**b**) CT images of a 54 year old male suffering from cervical myelopathy due to spondylosis (*upper row*). Enlargement and reconstruction of the spinal canal was performed by the use of laminoplasty spacers in four levels (*lower row*)

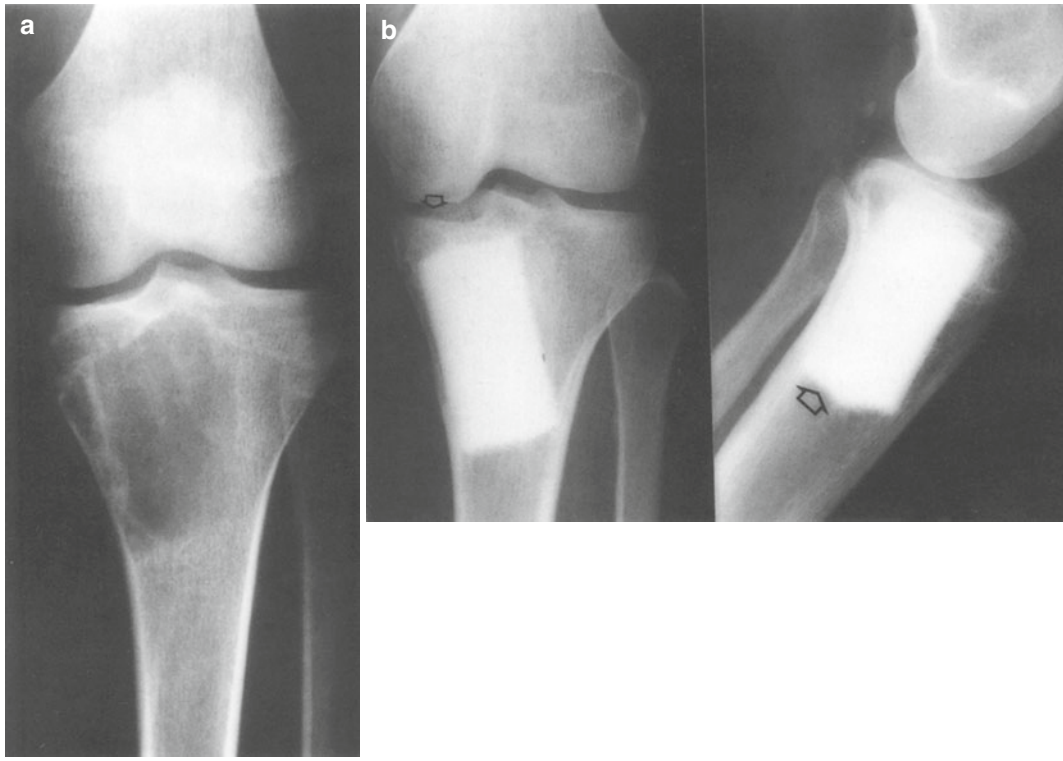

Fig. 3.11 (**a**) A giant cell tumor developed in the proximal tibia of a 15 year old female. (**b**) 10 years postimplantation of an AW-GC block that was used in combination of autogenous bone chips to replace the tumor. No clinical symptome postoperatively

References

1. Benson J. Presurvey on biomaterial application of carbons. North American Rockwell, Rocketdyne Report R-7855; 1969.
2. Yamamuro T, Kotoura Y, Kasahara K, Takahashi M, Abe M. Intraoprative radiotherapy and ceramic prosthesis replacement for osteosarcoma. In: Yamamuro T, editor. New development for limb salvage in musculoskeletal tumors. Tokyo: Springer; 1989. p. 327–36.
3. Boutin P, Blanquaert D. Le frottement alumine-alumine en chirurgie de la hanche 1205 arthoplasties totales: avril 1970- juin 1980. Rev Chir Orthop. 1981;67:279–87.
4. Sedel L. Evolution of alumina-on-alumina implants. Clin Orthop Relat Res. 2000;379:48–54.
5. Cales B, Peille CN. Radioactive properties of ceramic hip implants. Bioceramics. 1988;1:152–5.
6. Yamamuro T. Zirconia ceramic for the femoral head of a hip prosthesis. In: Sedel L, Cabanela ME, editors. Hip surgery, materials and development. London: Martin Duntz; 1998. p. 41–4.
7. Yamamuro T. A new model of bone-conserving cementless hip prosthesis made of high-tech materials: Kobelco H-5. In: Imu--ra S, Wada M, Omori H, editors. Joint arthroplasty. Tokyo: Springer; 1999. p. 213–24.
8. Hench LL, Greenlee TK Jr, Allen WC, Piotrowski G. U.S. Army Research and Development Command, Contract No. DADA 17-70-C-0001, University of Florida, Gainesville; 1970.
9. Wilson J, Pigott GH, Schoen FJ, Hench LL. Toxicology and biocompatibility of bioglasses. J Biomed Mater Res. 1981;15:805–17.
10. Aoki H, Shin Y, Akao M, Tsuji T, Togawa T, Ukegawa Y, Kikuchi R. Sintered hydroxyapatite for a percutaneous device. In: Christel P, Meunier A, Lee AJC, editors. Biological and biomechanical performances of biomaterials. Amsterdam: Elsevier; 1966. p. 1–3.
11. Jarcho M, Bolen CH, Thomas MB, Nobick J, Kay JF, Doremus RH. Hydroxyapatite synthesis and characterization in dense polycrystalline form. J Mater Sci. 1976;11:2027–34.
12. Geesink RGT, de Groot K, Klein CPAT. Chemical implant fixation using hydroxyl-apatite coatings: the development of a human total hip prosthesis for chemical fixation to bone using hydroxyl-apatite coating on titanium substrates. Clin Orthop Relat Res. 1987;225:147–70.

13. Kokubo T, Shigematsu M, Nagashima Y, Tashiro M, Nakamura T, Yamamuro T, Higashi S. Apatite-and wollastonite-containing glass-ceramic for prosthetic application. Bull Inst Chem Res Kyoto Univ. 1982;60:260–8.
14. Neo M, Kotani S, Nakamura T, Yamamuro T, Ohtsuki C, Kokubo T, Bando Y. A comparative study of ultrastrctures of the interface between four kinds of surface-active ceramic and bone. J Biomed Mater Res. 1992;26:1419–32.
15. Kokubo T. Bonding mechanism of bioactive glass-ceramic A-W to living bone. In: Yamamuro T, Hench LL, Wilson J, editors. Handbook of bioactive ceramic, vol I Bioactive glasses and glass-ceramics. Boca Raton: CRC Press; 1990. p. 41–9.
16. Yamamuro T, Shikata J, Okumura H, Kitsugi T, Kakutani Y, Matsui T, Kokubo T. Replacement of the lumbar vertebrae of sheep with ceramic prosthesis. J Bone Joint Surg. 1990;72-B:889–93.
17. Yamamuro T. A/W glass-ceramic: clinical applications. In: Hench LL, Wilson J, editors. An introduction to bioceramics. Singapore: World Scientific; 1993. p. 89–103.

Biomaterials for Bone Tissue Engineering

4

Congqin Ning

Bone tissue loss caused by various reasons including the accident trauma, tumor removal, or congenital deformity, etc., is a challenging problem in the clinic of orthopeadics, which brings the issue of bone grafting. Reconstructive surgery is based upon the principle of replacing these types of defective tissues with viable, functioning alternatives. It is reported that over 450,000 bone-grafting procedures are performed each year in the United States, and the number is expected to increase with the life expectancy increases [1]. Up to now, autologous transplantation is still considered as the golden standard procedure to orthopedic surgeons [2]. However, although autograft has good compatibility and no immunological response, the limited donor bone supply and additional trauma have limited its applications. Severe immunological problems and high risks of disease transmission have also limited the allograft applications, although a very careful screening process has eliminated most of the disease-carrying tissue [3]. Tissue engineering has emerged as a promising way to reconstruct and regenerate the lost or damaged bone tissues. Since the late 1980s, tissue engineering has been attracted much attentions in the fields of science, engineering, medicine and the society [4]. Tissue engineering has been defined by Laurencin et al. [5] as "the application of biological, chemical, and engineering principles towards the repair, restoration, or regeneration of tissues using cells, scaffolds and growth factor alone or in combination". There are two tissue-engineering approaches in regeneration of tissues or organs [6]. The initially described approach is that a small amount of cells harvested from the patients themselves are proliferated in vitro and then seeded into the appropriate three-dimensional scaffold in the presence of growth factors. The cells with growth factors under proper conditions will secret various extracellular matrix materials to create an actual living tissue in vitro, which will be implanted back to replace the damaged or defected tissues. Another approach is that the scaffold materials loaded with or without growth factors are implanted into the aim sites directly, which will guide the tissue formation in situ combining the degradation of scaffold materials. In the past several years, scaffolds, cells and growth factors have been considered as the three main factors for tissue engineering [1, 7]. Recently, with the development of materials science, it is controversial that growth factors are essential for bone tissue engineering. The new viewpoint is that the growth factor is not necessary for the bioactive material, which can induce

C. Ning, PhD
State Key Laboratory of High Performance Ceramics and Superfine Microstructure, Shanghai Institute of Ceramics, Chinese Academy of Sciences, 1295 Dingxi Road, Shanghai 200050, People's Republic of China
e-mail: cqning@mail.sic.ac.cn

D.G. Poitout (ed.), *Biomechanics and Biomaterials in Orthopedics*,
DOI 10.1007/978-1-84882-664-9_4

the tissue formation and enhance the secretion of growth factors from the host bone cells.

It is now generally accepted that one of the important issues for tissue engineering is the development of ideal scaffold materials. Since the human body is a complex and sensitive system, the requirements of the scaffold materials for tissue engineering are strict and extremely challenging. Up to now, the optimum material for tissue engineering scaffold has not yet been developed [8]. Nontoxicity and biocompatibility are the basic requirements for scaffold materials. The material should not have the potential to elicit an immunological or clinically detectable primary or secondary foreign body reaction [9, 10]. Suitable biodegradability is another essential requirement of the scaffold materials for tissue engineering; the resorption rate should match the tissue growth. Furthermore, the material should have proper mechanical properties matching those at the implant site, and can provide sufficient support to the new tissue during degradation until the new tissue is able to support itself [9]. In addition, the ideal scaffold materials for bone tissue engineering should also promote cell growth, cell differentiation and tissue regeneration. Synthetic materials for the bone tissue engineering have been studied extensively in the recent decades with the development of material sciences. Ceramics, polymers and their composites have all been investigated as scaffold materials for bone tissue engineering [1, 4, 8, 11–15].

Biodegradable Polymers

The biodegradable polymers used in bone tissue engineering can be classified into two categories. One is the natural-based polymers, such as starch, alginate, chitin/chitosan, collegen, silk, hyaluronic acid [16–23]. Another type is synthetic biodegradable polymers, like PLA, PGA, PLGA, PCL [24–26]. Most natural polymers are biocompatible, degradable and readily solubilized in physiological solution. However, they have some drawbacks, like immunogenecity, difficulty in processing, and a potential risk of transmitting animal-originated pathogens [2]. Among all the natural polymers, collagen is the most widely studied one. It is well known that collagen is the most abundant extra cellular matrix (ECM) protein and is originally secreted by osteoblasts, so it has a good biocompatibility with bone tissues [27]. However, the poor mechanical strength and rapid degradation rate greatly limited its applications as implantable porous scaffolds for bone tissue engineering.

Compared to natural polymers, synthetic polymers indeed have better chemical and mechanical properties. Moreover, synthetic polymers can eliminate the risk of disease transmission and immunogenecity. Synthetic polymers can provide versatile properties, since they can be synthesized under controlled conditions. The chemical and mechanical properties, degradation rate of synthetic polymers can be tailored by molecular weights, functional groups, configurations, and confirmations of polymer chains [2].

The most commonly used biodegradable synthetic polymers for bone tissue engineering are saturated poly-α-hydroxy esters such as poly lactic acid (PLA), poly glycolic acid (PGA), and their co-polymers (PLGA). The degradation of these polymers is through the procedure of de-esterification. The degradation products of these polymers are lactic and glycolic acids, which could be safely absorbed or derived by body metabolism. PLA, PGA and their copolymers have been approved by the US Food and Drug Administration to use as products and devices in clinic.

However, there are some drawbacks, which have limited their further applications [4, 25, 28, 29]. The hydrophobic characteristics of these polymers resulted in a poor cell attachment. The hydrophilicity of PLA and PGA scaffolds was effectively improved by Mikos et al. [25] using a two-step immersion in ethanol and water. Another problem of PLA, PGA and their co-polymers are aseptic inflammations, which is caused by the excessively low local pH value resulted from the accumulation of acidic degradation products. It is reported that aseptic inflammation occurred in a small but significant percentage (8 %) of patients [28]. In addition, PLA and PGA have no ability to induce apatite

formation in SBF, indicating a low bioactivity. Insufficient mechanical strength also inhibits their applications in bone tissue engineering

Poly (ε-caprolactone) (PCL) is another type of aliphatic polyester polymer for bone tissue engineering. It has been used to enhance bone ingrowth and regeneration in the treatment of bone defects. The degradation rate of PCL is much lower than that of PLA and PGA, which makes it less attractive for tissue engineering [30]. It has been reported that it took 3 years for PCL with a molecular weight of 50,000 to be completely removed from the host body [26, 31].

Polyhydroxyalkanoates (PHA) are also polyesters used in the field of bone tissue engineering, which are produced by microorganisms under unbalanced growth conditions. Up to date, only several polymers in the PHA family are available in sufficient quantity for applications in the bone tissue engineering, such as poly 3-hydroxybutyrate (PHB), copolymers of 3-hydroxybutyrate and 3-hydroxyvalerate (PHBV), poly 4-hydroxybutyrate (P4HB), copolymers of 3-hydroxybutyrate and 3-hydroxyhexanoate (PHBHHx) and poly3-hydroxyoctanoate [32]. This kind of polymers is also characterized with good biocompatibility and biodegradability and has been investigated as bone graft substitutes. The copolymerizing among the PHA polymers can dramatically change the properties of the material [33]. Among all the PHA polymers, PHB has been attracted the most attention as materials for bone tissue engineering, since it has been demonstrated that PHB showed a consistent favorable bone tissue adaptation response with no evidence of an undesirable chronic inflammatory response after implantation up to 12 months [34]. Doyle's work also showed that bone is rapidly formed close to the material and subsequently becomes highly organized, with up to 80 % of the implant surface lying in direct apposition to new bone [34]. However, pyrogens like endotoxin incorporated in the PHA polymers during the producing process may be a problem for its implantation uses. The investigations showed that pyrogens incorporated in the PHA polymers can be reduced by oxidizing agent, like hydrogen peroxide or benzoyl peroxide [35]. In addition, the limited availability and time-consumption extraction procedure are also the challenging issues for PHA polymers as bone tissue engineering materials [13].

In addition, copolymers of polyethylene glycol (PEG) and poly butylene terephathalate (PBT), commercially named as Polyactive™, are another type of polymers for bone tissue engineering [6, 36]. It seems the Polyactive™ is the only polymer which can form a bone bonding when implanted *in vivo* [37, 38]. It has been reported that the apatite layer formed on the surface of Polyactive™ is similar to that formed on the surface of bioactive ceramics [39]. Due to its bone bonding properties, Polyactive™ has been studied as bone tissue engineering material.

Three dimensional polymer scaffolds have been prepared by the following techniques.

Solvent Casting/Particulate Leaching

Solvent casting/particulate leaching is the most conventionally used methods to prepare porous polymer scaffold. In this technique, the polymer is first dissolved in an organic solvent, such as chloroform and methylene chloride. Salt particles with a desired particle size are then dispersed uniformly in the polymer solution. The polymer solution with salt particles is then cast in a glass container. After the evaporation of organic solvent, the polymer-salt particle composites were then immersed in water to leach out the salt particles to get a porous polymer structure [40]. The porous scaffold prepared by this technique could have a porosity ranging 87–91 %, which are predominated by the amount of salt particles. Moreover, the pore size of the scaffold could be controlled by the size of salt particles. Both porosity and pore size are undependent on the particle type. However, the solvent casting/particulate leaching technique only works for thin membranes or 3-D specimens with very thin wall sections. Otherwise, it is not possible to remove the soluble particles from within the polymer matrix [8, 41]. Mikos et al. [42] tried to fabricate 3-D structures by laminating the porous sheets using the technique. Another drawback of this technique is the extensive usage of highly-toxic solvents.

Emulsion Freeze-Drying/Thermally Induced Phase Separation

The emulsion freeze-drying technigue was first introduced to the field of tissue engineering by Whang and his colleagues [43, 44]. This technique consists of creating an emulsion by homogenization of a polymer solvent solution and water, rapidly cooling the emulsionto lock in the liquid-state structure, and removing the solvent and water by freeze-drying. Scaffolds with porosity greater than 90 %, pore size ranging from 15 to 200 μm were obtained using this method [44]. The scaffold also showed high volume of interconnected micropores and a high specific surface area (58–102 m^2/g) [45].

Gas Foaming

In the gas foaming technique, a small amount of gas (CO_2 or N_2) was dissolved into polymers under certain pressure and temperature levels. After the gas was released, a porous polymer scaffold formed. The concentration of CO_2 in the polymer, temperature, pressure, soaking time, depressurization, molecular weight and chemical composition of the polymer will all have significant effects on the pore structure [46, 47]. Barry et al. [48] reported that a rapid release of CO_2 gives smaller pores, while a slow release gives larger pores. This technique can get a pore size in a very wide range of 88–198 μm [49]. A porosity ranging 64.5–83.4 % are achieved in PLA scaffold [49]. The highlight of this technique is that it is a fully solvent-free technique.

Rapid Prototyping

Since the middle 1990s, rapid prototyping method (RP) has been introduced into the field of tissue engineering to fabricate scaffolds [50–52]. Rapid prototyping is a technique based on the advanced development of computer and manufacturing, which is also called solid free form fabrication (SFF) [53]. The potential to intimately control the microstructure of porous channels and the overall macroscopic shape of the scaffolds makes rapid prototyping an ideal process for fabricating scaffolds [54]. It can produce complex products rapidly from a designed model in the computer as well as digital data produced by an imaging source as computer tomography (CT) or magnetic resonance imaging (MRI) [55]. Another advantage of this technique is the structure of the scaffold is 100 % interconnected macropororous [8]. In addition, parameters, such as the porosity, interconnectivity, pore size and geometric stability of the scaffolds fabricated by the rapid prototyping can be controlled more precisely than conventional fabrication techniques [40, 56].

In addition, the polymer scaffolds have been also prepared by microsphere sintering, replication from natural materials, etc. Li et al. [57] prepared PDLLA scaffolds with a similar macroporous structure to natural cancellous bone using calcined bone as a negative mould. The scaffolds were fabricated by immersing the calcined bovine cancellous bone into PDLLA solution under repeated vacuum. The negative template was removed by a following treatment of the scaffolds in hydrochloric acid. The morphology and structure of the obtained scaffolds are similar to the organic matrix of natural concellous bone blocks. Moreover, the compressive strength and modulus of the obtained scaffolds could be adjusted by the concentration of polymer solution, which are significantly improved as compared to the scaffolds prepared by sovent casting/particulate leaching technique.

The most common problems for synthetic polymers are acute or chronic inflammatory response, which was due to the decreased local pH value caused by the acidic hydrolytic degradation products. No bioactivity is also a common problem for polymeric materials. Incorporation of basic ceramics into polymers could neutralize the local acidity effectively and could increase the bioactivity simultaneous.

Bioceramics

The use of ceramics in bone repair has a very long history, which can be traced back to thousands of years ago. The ceramics used at the early

stage are nearly bioinert in the biological environment, such as alumina (Al_2O_3) [58], zirconia (ZrO_2) [59], calcium sulphate ($CaSO_4$) [60] and calcium carbonate (coral) [61]. Compared with the bioinert ceramics, calcium phosphates and bioactive glasses and glass-ceramics can form a bonding interface with host tissues. Due to the good biocompatibility and bioactivity, they have been widely investigated as bone graft materials and some products have been successfully used in clinic.

Calcium Phosphates

It is well known that the inorganic components (over 60 wt%) of bone are hydroxyapatite ($Ca_{10}(PO_4)_6(OH)_2$, HA) [13]. Therefore, some calcium phosphates, like HA, tricalcium phosphates (α-TCP and β-TCP), octacalcium phosphate (OCP), calcium pyrophospates ($Ca_2P_2O_7$) have been intensively investigated as bone grafts [62–65]. The study of calcium phosphates as biomaterials for bone repair was started from the middle of 1970s, by Jarcho from the USA [66], de Groot from Europe [67], and Aoki from Japan [68], simultaneously. Calcium phosphate ceramics have been proved having good biocompatibility with bone and they can bond to bone without any fibrous capsule [69, 70]. Synthetic hydroxyapatite with a stoichiometric composition has been extensively studied as bone replacement material [63, 69]. It has been proved that porous HA has excellent biocompatibility and osteoconductivity, and some commercial products of HA have been used in clinic [69, 71, 72]. Porous hydroxyapatite (such as ProOsteon® and Interpore®) has been prepared by the hydrothermal conversion of corals, which caused a replacement of phosphate ions for the carbonate ions and changed the crystal structure to calcium phosphate [73–75]. The porous hydroxyapatite scaffolds prepared by this method have a uniformity of pore size ranging from 60 to 500 μm and have complete pore interconnection. However, the porosity of the HA scaffolds prepared by this method have a narrow porosity distribution ranging from 46 to 48 %, which is not good to the mechanical properties and biological applications. In addition, the final composition of the scaffold is hard to control, due to the impurities in the original corals [76].

The porous HA scaffolds can also be prepared by the demineralization of natural bone (Endobon®) [77], polymer foaming [78], H_2O_2 foaming [79], freezing casting [80], replicas of porous structures [81, 82], etc. The most simple and commonly used method to prepare porous ceramics is the polymer porosifier method. The parameters such as porosity, pore size and interconnectivity can be adjusted by the amount and size of porogen particles. It was reported that bone formation occurred in porous HA scaffolds mixed with fresh bone marrow cells after 3 weeks implantation, which was enhanced by a preculture process of bone marrow cells [83, 84].

However, it has been proved that the stoichiometric HA has limited ability to form chemical bonding with the host tissues and it also has limited ability to stimulate the bone formation [85]. Moreover, the stoichiometric HA has a very low degradation rate, and it almost remains as a permanent fixture susceptible to long-term failure [86]. The above drawbacks have limited its application in bone tissue engineering. Actually, the mineral phases of the natural bone differ from stoichiometric HA in composition, stoichiometry, and some properties, which are calcium deficient hydroxyaptite with some positive (Na^+, Mg^{2+}, K^+, etc.) and negative (CO_3^{2-}, F^-, Cl^-, etc.) ion substitutions. In particularly, the carbonate ion concentration in the bone apatite is up to 8 wt% [87]. These substitutions in the bone apatite structure play important roles in its biological activity. Recent years, substituted apatites have been attracted increasing interests [88–96]. The use of these substituted apatites in bone tissue engineering is still exploring. The substitution in the structure of HA indeed increased the bioactivity and bioresorbability of the material. In addition, Si incorporation in the calcium phosphates has been shown to increase osteogenesis of osteoblast-like cells [97]. Precipitation of a biological carbonated hydroxyapatite onto the surface of a scaffold by biomimetic method has also been extensively studied to improve the bioactivity of the scaffold [98–105].

Of all the substituted HA, Si-substituted HA have been investigated widely. Si has been found

to be essential for new bone formation, and it was found that Si localized at active calcification sites in the bones of young mice and rats [106]. A recent research has been found that a dietary Si intake was positively and significantly affecting the bone mineral density of humans [107]. Trace levels of Si in the structure of hydroxyaptite have remarkably increased the biological performance in comparison to stoichiometric HA [108]. The Si-HA has always been synthesized by wet chemical methods where Si is added through a silicon source, such as tetraethylorthosilicate (TEOS) and Si IV acetate ($Si(COOCH_3)_4$) [109–111]. Some research also added nanoparticulate silica during the precipitation and sintering of an amorphous calcium phosphate to fabricate silicon doped HA [112]. Si substituted hydroxyapatites have been proved to have the ability to induce biomimetic precipitation in a physiological solution due to the release of silicon [113]. The in vivo investigates have also shown that bone ingrowth into silicon-substituted HA granules was remarkably greater than that into pure HA [114]. Currently, two different Si-substituted calcium phosphates have been developed as bone substitute applications commercially [85]. Single phase Si-HA have been manufactured commercially by Apatech Ltd. under the trade name Actifuse™. Multiphase Si-stabilized calcium phosphates have been produced by Millenium Biologix Corporation under the trade name Skelite™.

β-TCP is another calcium phosphate material widely used for bone tissue engineering. Compared to stoichiometric hydroxyapatite, β-TCP has a much higher dissolution rate. Many researches have shown that the dissolution rates of β-TCP are much higher than that of HA, which is strongly dependent on the testing media [76, 115]. β-TCP has been accepted and used as a biocompatible, and resorbable material for bone repair. However, some studies have also showed that the high dissolution rate of β-TCP adversely accelerates material resorbability and elicits immunological response [116, 117]. There are some different reports about the degradation rate of β-TCP *in vivo*, which is dependent on the characteristics of the material used and the sites where the material is used. Similar to HA, substituted β-TCP have also been intensively investigated to pursue various properties [118–120]. It has been shown that magnesium substitution in the structure of β-TCP could decrease the biodegradation rate. The Si substitution enhanced the biological properties of β-TCP. The impurities in β-TCP may affect its sintering properties.

Parameters, like pore size and distribution, porosity and connectivity of porous β-TCP scaffolds prepared by the traditional methods are difficult to be controlled precisely. Recently, a new method has been developed to prepare porous β-TCP scaffolds, which can fully control the macroporosity, in terms of shape and size of pores and their interconnectivity [121, 122]. In this technique, β-TCP scaffolds were prepared by impregnating of an organic edifice with proper β-TCP suspension followed by sintering at elevated temperatures. The organic edifice served as the template, which was prepared by preheating polymer microspheres at a temperature higher than polymer glass transition point to make them bind together. The pore structure of the scaffolds can be controlled by the treatment parameters of polymer microspheres. Pore size, shape and porosity are controlled by the size, shape and amount of polymer spheres. The interconnection between the macropores depends on the amplitude bridging between polymer balls, which are controlled by the temperature and dwell time of the treatment of polymer frame. β-TCP scaffolds prepared by this method have good pore connectivity. Xie et al. [123] investigated the proliferation of stem cells inside the β-TCP scaffold prepared by the above described method, and showed that after a flow perfusion culture, the cells survived and proliferated through the whole scaffolds indicating its good connectivity and nutrition supply. The in vivo results also showed that these scaffolds had good osteoconductivity and good vascularization [124, 125]. In addition, parts with a gradient distribution of pore size, or interconnectivity to pursue specific properties can be easily handled by this technique. The β-TCP scaffolds prepared by this method have been commercialized by Shanghai Bio-Lu Biomaterial Corporation.

The poor mechanical property is the major problem of the porous bioceramic scaffold. Zhang et al. [126] prepared porous β-TCP scaffold inspired from the structure of natural bone, which is characterized by a macrostructure feature of porous cancellous bone inside with compact (or cortical) bone outside. The bioinspired structural β-TCP scaffolds were designed with a structure of porous cancellous structure (porosity: 70–95 %) inside and dense compact shell (porosity: 5–10 %) outside. The scaffold with this kind of bioinspired structure improved the mechanical properties.

Biphasic Calcium Phosphate

Biphasic calcium phosphates (BCP) are also important members of the calcium phosphates family. BCP are ceramics which containing both hydroxyapatite and TCP. It has shown that BCP exhibited prior bone repair and regeneration abilities than pure HA or β-TCP [127, 128]. The degradation rate as well as other properties can be controlled by the HA/TCP ratios to a certain degree [127–131]. It has been reported that BCP have osteoinductivity when implanted in muscle tissue [132, 133]. Grundel Ng et al. [134] seeded osteoprogenitor cells derived from periosteum onto HA/TCP scaffolds and then intramuscularly implanted them in nude mice after 4 weeks i*n vitro* culture, which indicated that HA/TCP showed superior in early bone formation than pure HA. BCP with 60 % HA and 40%TCP has been manufactured commercially under the trade name Triosite. Another BCP with 65%HA and 35%TCP has also been commercialized by Teknimed Limited Company under the name Ceraform.

Bioactive Glass and Glass-Ceramics

In 1969, Hench et al. found that some glasses with specific compositions had excellent biocompatibility with natural bone and they can form a chemical bonding with the host bone [135]. These glasses have been called as bioactive glasses, which contain SiO_2, Na_2O, CaO and P_2O_5 in specific proportions and have been commercially available as Bioglass®. The concept of "bioactive" has been aroused since then. The bioactive material was defined as "one that elicits a specific biological response at the interface of the material which results in the formation of a bond between the tissues and the material" [136]. The bioactive glasses have the ability to induce calcium-deficient, carbonated hydroxyapatite formation when in contact with physiological solutions or implanted in vivo [137, 138]. It has been accepted that the essential requirement for an artificial biomaterial to exhibit a bone bonding to living bone is the formation of a bone-like apatite layer on its surface in body environment and it has been used as a criteria to evaluate the bioactivity of biomaterials [135–138]. The mechanism of the bioactivity of bioactive glasses has been thoroughly investigated by Hench [137], which is due to complex ion exchanges occurred on the surface of bioactive glasses. Silicon is considered to play a key role in the bioactivity of bioactive glasses, which can induce the apatite nucleation. The ionic dissolution products from bioactive glasses were shown to enhance the proliferation of osteoblasts, upregulate seven families of genes that control osteogenesis and induce the synthesis of growth factors [114, 139–141]. The bioactive glasses have also been found to enhance enzyme activity, vascularization and the differentiation of mesenchymal cells into osteoblasts [13].

The bioactivity of the bioglass is composition dependent, which has been systematically summarized previously by Hench [140]. Only a limited range of bioactive glass compositions in the system SiO_2-Na_2O-CaO-P_2O_5, with less than 55 wt% SiO_2 exhibit Class A bioactivity [142], which are osteoproductive as well as osteoconductive, and can bond to both bone and soft connective tissues. Class B bioactive materials only exhibit osteoconductivity. In recent years, sol–gel technique has been used to prepare bioactive glasses [143–148]. The bioactive glasses produced by sol–gel method, also termed bioactive gel-glasses, have a higher bioactivity and resorb faster than the conventional glasses with the same composition [148]. The compositional range of Class A bioactive behaviour is considerable

extended for the sol–gel derived bioactive glasses over the conventional ones [142]. It is reported that P_2O_5-free bioglasses in the system SiO_2-Na_2O-CaO are also bioactive, which implies that P_2O_5 is not an essential component for bioactivity of the material. The great characteristics of the gel-glasses are the high specific surface area and fine porous structure [149–151]. In addition, the structure and chemistry of bioactive glasses can be tailored at a molecular level by sol–gel method [152]. The above features can further influence the biological activities, such as cell differentiation and proliferation, enzyme activity and tissue regeneration of the bioactive glasses [149, 150]. 45S5 Bioglass® has achieved much success in clinic as a treatment for periodontal disease (Perioglas) and as bone filling material (Novabone) [137, 140].

At the very beginning, the bioglass® were used in clinical applications only in the granule or bulk forms, since the bioglasses produced by high temperature melting have a poor machinability and are hard to be processed. Bioactive glasses have gained new attention recently as promising scaffold materials. Some works have attempted to introduce porous structure into melt-derived bioactive glasses. Yuan et al. [153] reported a method to prepare porous bioglass ceramic by H_2O_2 foaming method using ball-milled Melt-derived 45S5 Bioglass® powder. However, the porosity and pore interconnectivity of the porous scaffold prepared by the above method are not satisfied. Chen et al. [154] prepared porous bioactive glass scaffolds with porosity over 90 % by the replication method using polyurethane foam as a sacrificial template. The Melt-derived 45S5 Bioglass® powders were also mixed with polymer porogen to make porous scaffold using the traditional porosifier method [155, 156]. However, the scaffolds made by these method all had high-temperature treatment histories. It has been reported that crystallization of bioactive glasses will result in a decrease in bioactivity [157] and even turns a bioactive glass into bioinert material [158].

Hench group at Imperial College has produced scaffolds with hierarchical pore structure by foaming sol–gel derived bioactive glasses [10, 159–162]. In the first step of this method, a sol is prepared from a silica based alkoxide precursor, such as tetraethyloxysilane (TEOS). After complete hydrolysis, the sol is foamed using surfactants under vigorous agitation in air. The foamed sol with a high viscosity is then cast into sealable moulds, followed by aging, drying and thermal stabilization at 600–800 °C. To get a better mechanical property, the foamed scaffold can be further sintered at an elevated temperarure. Unary, binary and tertiary systems have all been successfully foamed as scaffolds [162]. The scaffold prepared by this method is comprised of large interconnected macropores (10–500 μm) and mesoporous pores (2–50 μm). The macropores with diameters over 100 μm, enable cells growing into 3D structures. The mesoporous structure is the inherent characteristic of sol–gel derived bioactive glasses, which can dissolve at a rate that releases the proper ionic concentration for osteogenesis. The pore interconnects in the foamed scaffolds are larger than 100 μm, which benefits to a 3D cellular structure formation and vascularization [142, 161]. Various parameters, including glass composition, surfactant concentration, gelling agent concentration, treating temperature, etc. all have an effects on the 3D structure of the foamed scaffolds [161].

In addition, many researchers are trying to prepare bone scaffolds with biomorphic structure to cancellous bone by using natural materials as templates [57, 82, 163]. However, most of the previous works just mimicked the macroporous structure of the natural materials. The fine microstructures of natural cancellous bone, such as ordered assembly of the nanoparticles on the pore wall, multimodal pore distribution on the micro- and nanometer scale, are challenging to mimic. The macroporous structure enables cell ingrowth, while the micro/nanoporosity improves fluid flow through the ceramics, providing nutrition for cells inside the scaffold [164]. In our lab, Xia et al. (unpublished data) produced porous bioactive glass scaffold with both similar macrostructure and microstructure to those of natural cancellous bone using a replication method. The obtained bioactive glass scaffold possessed a porosity of 89.3 %, which is similar

to the calcined bone (86.6 %). The compressive strength of the obtained scaffold is also similar to that of the calcined bone.

The degradability of these bioactive glasses is mainly based on dissolution process, which is influenced by the particle size, glass composition, etc. [165]. However, overall the biodegradation of these materials is considerably low [164].

Poor mechanical properties are the big drawbacks for bioactive glasses as scaffolds for tissue engineering. A glass can be converted to glass-ceramic by heat treatment. The crystallized glass-ceramic exhibits superior mechanical properties to the parent glass. In the early 1980s, Kokubo and co-workers developed a glass-ceramic, which contains crystalline phases of apatite and β-wollastonite and was termed A-W glass-ceramic [166, 167]. A-W glass-ceramic is prepared from the parent glass in the pseudoternary system $3CaO \cdot P_2O_5$-$CaO \cdot SiO_2$-$MgO \cdot CaO \cdot 2SiO_2$ with a composition of 38 wt% apatite, 34 wt% wollastonite and 28 % residual glass. This glass-ceramic material possesses both excellent mechnical properties and good bioactivity, and can be easily machined into various shapes, which has been used successfully in clinic as bone replacement under the trade name of Cerabone® [167]. The bending strength of A-W glass-ceramic is about 215 MPa, which is almost twice that of dense hydroxyapatite, and also much higher than that of bioglasses [11]. The fracture toughness is also much higher than that of hydroxyapatite and bioactive glasses [13]. The higher mechanical properties of A-W glass-ceramic are attributed to the precipitation of wollastonite. A-W glass-ceramic can form a bone bonding with natural bone through a thin layer of biologically active apatite and it can also induce apatite formation in an acellular simulated body fluid having ion concentrations nearly equal to those of human blood plasma (termed SBF). The mechanism of bioactivity of the A-W glass-ceramic is similar to that of bioactive glasses, which is attributed to the release of soluble Si, Ca and P ions into the physiological fluid. Dyson et al. [168] evaluated the behavior of mesenchymal stem cells on A-W glass-ceramic scaffolds produced by the layer manufacturing technique and selective laser sintering, showing that the expression of the osteogenic markers was significantly higher than that on the commercial calcium phosphate scaffold. However, it is definite that A-W glass-ceramic exhibits Class B bioactivity, which is lower than that of Bioglass® [169].

Ceravital® [170, 171] and BIOVERIT® [172, 173] are also commercially available glass-ceramics for bone replacement. However, there are very few reports on these two materials for applications in the field of bone tissue engineering. Recently, Vitale-Brovarone et al. [174–176] developed a series of K_2O-containing bioactive glass-ceramics. The glass with a molar composition of 50%SiO_2-44%CaO-6%K_2O (termed SCK) showed a crystalline phase of β-wollastonite (β-$CaSiO_3$), which exhibited good in vitro bioactivity. It is reported that a too higher pH can inhibit osteoblast activity and cause cell necrosis or apoptosis [177, 178]. To avoid the severe pH changes in the physiological solution, a new bioactive glass-ceramic, in the SiO_2-P_2O_5-CaO-MgO-K_2O-Na_2O system, was developed with a lower monovalent oxide content and a slightly higher P_2O_5 content compared to commercial bioactive glasses [175, 176]. $Ca_3Mg(SiO_4)_2$ and $Ca_2MgSi_2O_7$ were identified as crystalline phases of the above glass-ceramic. Macroporous scaffolds with a porosity over 70 % and pores in the range of 100–500 μm prepared from the above glass-ceramic showed high bioactivity and promoted a high cell differentiation. In addition, some researchers have also shown that some borate glasses can convert to hydroxyapatite and bond to bone chemically [179–181] like the silicate-based bioactive glass.

Silica-free calcium phosphate glass-ceramics have also been developed for bone tissue engineering [182–187]. Kasuga et al. [182–186] developed series calcium phosphate ceramics in CaO-P_2O_5-TiO_2 and CaO-P_2O_5-Na_2O-TiO_2 systems, which were initially used as coatings on titanium implants. The bioacvitity of these calcium phosphate glass-ceramics are composition dependent. The glasses with orthophosphate and pyrophosphate groups have the ability to induce apatite deposition, while the glass containing

no orthophosphate group does not deposit apatite. Moreover, the replacement of 7wt%TiO_2 by 7wt%Na_2O results in a significant increase in bioactivity. In addition, the apatite-forming ability of the above glass-ceramics is also strongly influenced by a small amount (3 %) of additive such as TiO_2 and MgO [186]. However, the mechanical properties of the calcium phosphate glass-ceramic are a little lower than those of silica-based A-W glass-ceramic [184].

Silicate Bioceramics

Inspired from the success of silicate –based bioactive glasses and glass-ceramics, some silicate ceramics have also been explored for bone tissue engineering applications, including wollastonite (low temperature calcium silicate, β-$CaSiO_3$) [188–193], pseudowollastonite (high temperature calcium silicate, α-$CaSiO_3$) [194–199], dicalcium silicate (Ca_2SiO_4) [200, 201], tricalcium silicate (Ca_3SiO_5)[202, 203], akermanite ($Ca_2MgSi_2O_7$) [204–206], bredigite ($Ca_7MgSi_4O_{16}$) [207, 208], diopside ($CaMgSi_2O_6$) [209–211], combeite ($Na_2Ca_2Si_3O_9$) [212], Silicocarnotite ($Ca_5(PO_4)_2SiO_4$) [213, 214] and silicate-based composites [215, 216].

As stated above, β-wollastonite is one of the crystalline phases of A-W glass-ceramic, which is mainly responsible for the bioactivity of A-W glass-ceramic. de Aza et al. [188] fabricated polycrystalline wollastonite by solid-state reactions at elevated temperature using solid calcium carbonate and silica with a CaO/SiO_2 molar ratio equal to one. The polycrystalline wollastonite showed a high "in vitro" bioactivity with the formation of apatite in the simulated body fluid. According to de Aza, the ionic interchange of Ca^{2+} for $2H^+$ between wollastonite and SBF resulted in an amorphous silica phase on the wollastonite surface and increased the calcium concentration and pH in the surrounding SBF, giving the conditions for HA precipitation.

The ex vivo cell culture studies have shown that β-wollastonite can enhance the attachment and proliferation of mesenchymal stem cells, and induce the differentiation of MSC to osteoblasts [217, 218]. In addition, the in vitro degradation rate of β-wollastonite scaffolds was substantially faster than that of the β-TCP [218]. In vivo evaluation of the plasma sprayed wollastonite coating showed that the wollastonite coating could form a tight bone-bonding with the surrounding bone tissue through a bone-like apatite layer [192]. Moreover, the wollastonite coating could also induce the apatite formation after 1-month implantation in muscle and could induce bone formation in marrow sites, indicating good bioactivity and osteoinductivity. Recently, the in vivo bone regenerative capacity and resorption of porous β-wollastonite scaffolds were investigated in a rabbit calvarial defect model using porous β-TCP scaffolds as a parallel by Xu et al. [219], showing that the β-wollastonite has a much higher resorption rate and more bone formation than β-TCP. After 16-week implantation, only 3.81 % of β-wollastonite remained (as shown in Fig. 4.1).

The pseudowollastonite (α-$CaSiO_3$), which is a high temperature form of calcium silicate, has also been found exhibiting good biocompatibility and bioactivity. Dufrane et al. [220] showed that the pseudowollastonite extract did not show significant cytotoxic effects confirming its biocompatibility. Lin et al. [221] also demonstrated good biocompatibility of α-$CaSiO_3$. The bioactivity of pseudowollastonite has been observed in vitro (in SBF) and in vivo (implanted in animals). Apatite formation on the surface of α-$CaSiO_3$ scaffold after soaking in SBF is shown in Fig. 4.2. Similar to wollastonite, pseudowollastonite also has the ability to induce apatite formation when immersed in SBF [197]. It can even induce apatite formation in human parotid saliva [195] and serum-containing media [10]. It has been reported that the rate of hydroxyaptite precipitation on the surface of pseudowollastonite surface are higher than those on all the reported bioglasses and glass-ceramics [222]. Sarmento et al. [198] found that osteoblasts could attach and proliferate well on the surface of pseudowollastonite. In addition, the cell attachment could be enhanced by preincubation of pseudowollastonite in serum or media containing fibronectin. The in vivo bioacticity of

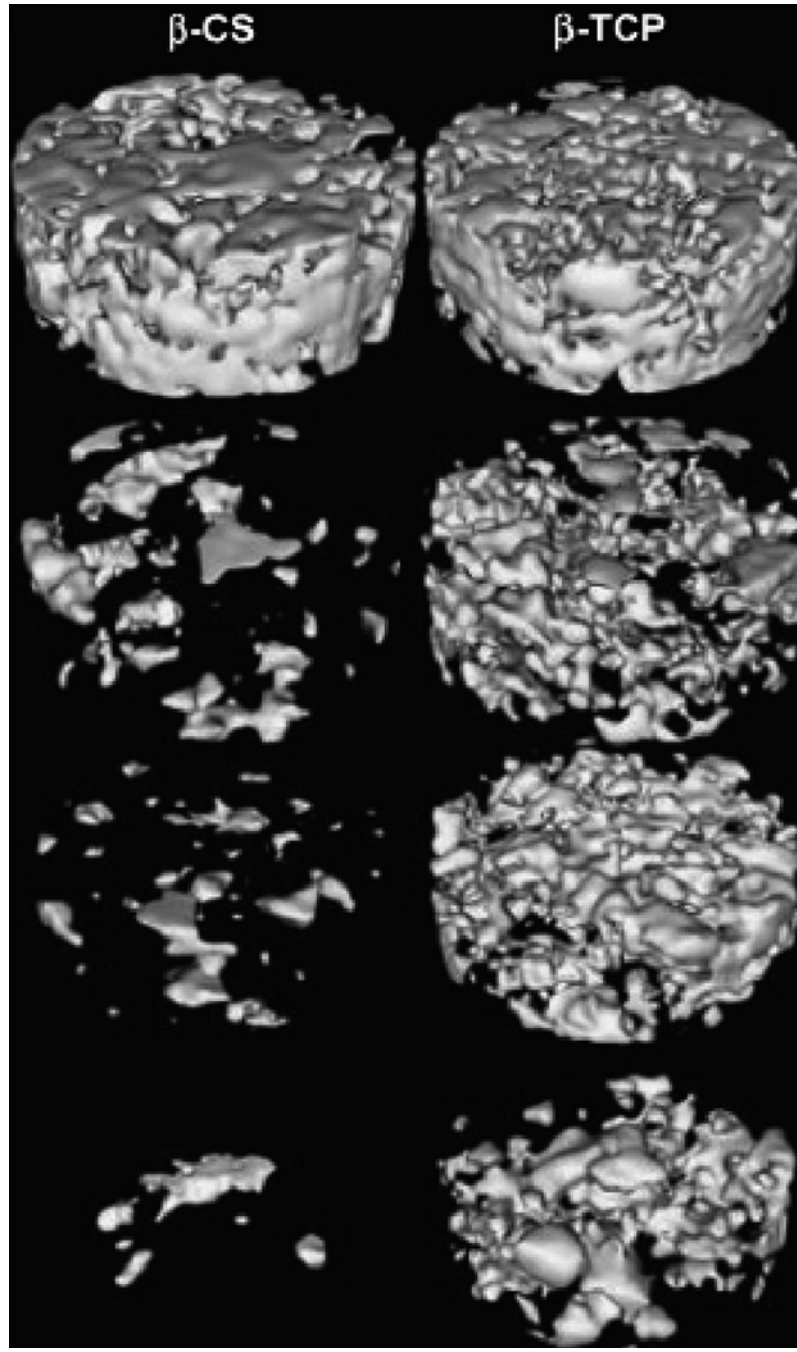

Fig. 4.1 3D reconstruction images of residual β-CS and β-TCP after implantation in the rabbit calvarial defects for different periods using Micro-CT analysis (From Xu et al. [219], with permission)

pseudowollastonite was evaluated by De Aza and co-workers through implantation into rat tibias [196, 199]. The SEM and EDS analyses showed that a calcium phosphate layer was formed at the implant interface, which had characteristics of new bone tissue. High resolution transmission electron microscopy observations confirmed the newly formed bone at the interface between the pseudowollastonite implant and the host bone as composed of hydroxyapatite-like nanocrystals growing epitaxially across the interface in the [002] direction [196]. It was shown that the rate of

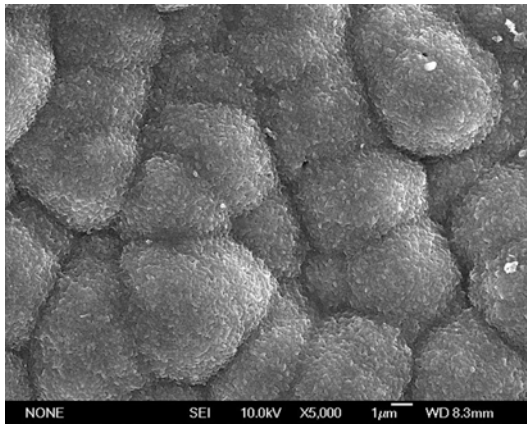

Fig. 4.2 Apatite formation on the surface of α-$CaSiO_3$ scaffold after soaking in SBF (From Lin et al. [221], with permission)

new bone formation around pseudowollastonite decreased after the first 3 weeks and reached constant value over the following 9 weeks, which coincided with the results of β-wollastonite reported by Xu and co-workers [219].

Sahai et al. [223] used crystallographic constraints with ab initio molecular orbital calculations to identify the active site and reaction mechanism for heterogeneous nucleation of calcium phosphate. It is proposed that the cyclic silicate trimer is the universal active site for heterogeneous, stereochemically promoted nucleation on silicate-based bioactive ceramics. A critical active site density and a less point of zero charge of the biomaterial than physiological pH are considered essential for bioactivity.

Chang and his colleagues find that dicalcium silicate and tricalcium silicate also show good bioactivity, and they can rapidly induce apatite formation in the SBF [201–203, 224]. Besides the binary calcium-silicates, some ternary calcium-silicate ceramics have also been attracted much attention in recent years. The investigation of diopside as implant material started by Nakajima in the late 1980s [225]. It was found that diopside can induce apatite formation in SBF and can form a bone bonding with surrounding bone tissues [209, 226, 227]. Calcium released from the material into SBF plays a key role in the apatite formation on the surface of diopside, which is initially released rapidly and eventually reaching steady-state. On the contrary, Mg and Si are released more slowly at similar rates to each other [12, 211, 228]. And Mg does not play a role for apatite nucleation on diopside [211]. It is proposed that the (100) plane of diopside epitaxially nucleates the (010) plane of octacalcium (OCP), which has a similar cell parameters to hydroxyapatite and has been considered as a precursor to hydroxyaptite in normal bone growth [12, 227]. The reported bending strength and fracture toughness of the diopside is 300 MPa and 3.5 $MPa \cdot m^{1/2}$, respectively [209]. These values are about two or three times higher than those of hydroxyapatite. However, the degradation rate of diopside is very poor, which is even lower than that of hydroxyaptite [209].

Besides diopside ceramics, akermanite and bredigite in the Ca-Si-Mg system have also been investigated for bone tissue engineering. Wu et al. [206, 229] synthesized pure akermanite and bredigite powders by sol–gel methods. Both akermanite and bredigite have the ability to induce apatite formation in SBF. The apatite formation ability decreases with the increase of Mg in the Ca-Si-Mg ceramics, i.e. bredigite has better apatite formation ability than akermanite, which is indicated by higher calcium content and lower phosphorus content in SBF after immersion. The increase in activation energy of Si release should be responsible for the reduced apatite formation ability [230]. In addition, activation energy of Si release also predominates the degradation rate of the Ca-Si-Mg ceramics. With the increase in Mg content, the degradation rate of the Ca-Si-Mg ceramics decreases. Considering the poor degradability of diopside, it may not be suitable as bone tissue engineering materials as the akermanite and bredigite. Akermanite prepared by two-step precipitation method has a higher bioactivity than that prepared by sol–gel method, due to its finer particle size. Akermanite and bredigite have all shown the ability to stimulate osteoblasts proliferation. The intensive investigation by Sun et al. showed that akermanite ceramics enhanced the expression of osteoblast-related genes, including alkaline phosphate (ALP), osteopontin (OPN), bone sialoprotein (BSP), and osteocalcin (OC) [231]. It also

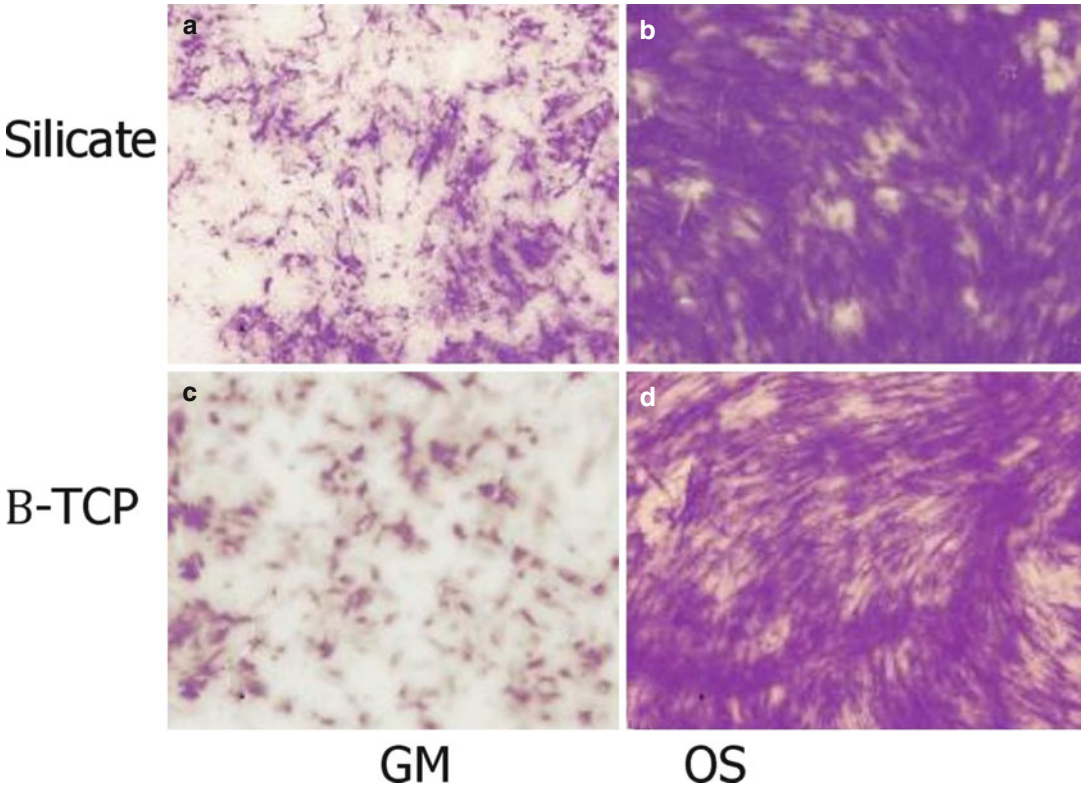

Fig. 4.3 ALP staining of differentiating hBMSC on the surface of different material. The hBMSC were cultured on akermanite disks (**a**, **b**) and β-TCP disks (**c**, **d**) for 7 days in growth medium (**a**, **c**) or osteogenic medium (**b**, **d**). ALP-positive cells are shown in purple. The bars in the pictures present 200 mm (From Sun et al. [231] with permission)

showed that akermanite could promote osteoblastic differentiation of human bone marrow stromal cells (hBMSC) in normal growth medium without osteogenic reagents, such as L-ascorbic acid, glycerophosphate and dexamethasone (as shown in Fig. 4.3). Highly connective porous akermanite and bredigite scaffolds, with porosity about 90 % and pore size ranging 300–500 μm, were prepared using polymer sponge as templates by Wu and his co-workers [208]. Both alkermanite and bredigite scaffolds could support osteoclasts-like cells growth, proliferation and differentiation. The biomimetic treatment of alkermanite and bredigite scaffolds in the SBF could enhance the cell proliferation and differentiation.

To combine the advantages of phosphates and silicates, Ning and her co-workers synthesized pure $Ca_5(PO_4)_2SiO_4$ (CPS) by a sol–gel method using triethyl phosphate (TEP), tetraethoxysilane (TEOS) and calcium nitrate tetrahydrate as original materials [213]. It is revealed that CPS has a greater in vitro apatite-forming ability than HA. In addition, the proliferation of rBMSC on CPS is significantly higher than that on HA. Moreover, the expression of alkaline phosphatase activity (ALP) and osteogenic-related genes, including Runx-2, osteopontin (OPN), bone sialoprotein (BSP) and osteocalcin (OC), demonstrated that CPS has enhanced the osteogenic differentiation of rBMSC and accelerated the differentiation process [214].

Silicate/Phosphate Based Composites

As stated above, silicate-based bioceramics exhibit excellent bioactivity, which can promote the osteoblast proliferation, induce the osteoblastic differentiation of marrow stem cells, and enhance the bone formation. On the other hand,

calcium phosphate ceramics have excellent biocompatibility due to their similar compositions to the bone minerals, while they have no obvious stimulatory effect on the proliferation and differentiation of osteoblasts. A composite strategy is applied to combine the advantages of silicates and phosphates, which is effective way to make materials with tailorable properties, such as mechanical property, bioactivity and biodegradation rate.

De Aza et al. [232, 233] developed a bioeutectic wollastonite-tricalcium phosphate ceramic, with a composition of 60 wt% wollastonite and 40 wt% TCP, by a specific high temperature treatment (termed W-TCP). The eutectic W-TCP material presented a high bioactivity in SBF [232] and human parotid saliva [233], with the formation of two well-differentiated zones of hydroxyapatite. The inner layer formed by pseudomorphic transformation of the tricalcium phosphate into hydroxyapatite after the dissolution of wollastonite into SBF, and the outer layer formed by the deposition of hydroxyapatite onto the surface of the material in the later stages of immersion.

Huang et al. [234] and Ni et al. [235] prepared β-$CaSiO_3$/β-$Ca_3(PO_4)_2$ composite materials by in-situ precipitation method. The mechanical properties of the CS-TCP composites increased with the increase in TCP content. A higher CS content also resulted in a higher dissolution rate. The CS-TCP composites exhibited good bioactivity. Compared with pure β-TCP, the CS-TCP composites, especially the composites with over 50 % wollastonite, enhanced the adhesion, growth and ALP activity of the osteoblast-like cells [235]. Zhang et al. [193] prepared nanocrystalline wollastonite/β-TCP composite powders by a two-step chemical precipitation method. Porous scaffolds were fabricated using these composite powders by porogen burnout technique. The mechanical properties of these scaffolds sintered from nano-scale composite powder were significantly improved, which were about twice as high as those of the scaffolds sintered from submicron powders. In addition, these scaffolds sintered from nano-powders showed less strength loss during the degradation process.

The silicate/phosphate composite ceramic with the composition of 32.9 mol% Na_2O, 32.9 mol% SiO_2, 22.8 mol% CaO and 11.4 mol% P_2O_5 were prepared by El-Ghannam and his co-workers [216], which showed main crystalline phases of Na_2CaSiO_4 and $NaCaPO_4$ (termed SCPC). This composite ceramic has compositional components similar to 45S5 bioglass. SCPC provided a superior release profile of biologically active rhBMP-2 compared to commercial porous hydroxyapatite. Moreover, cells attached to the SCPC produced mineralized extracellular matrix and bone-like tissue covered the entire material surface after 3 weeks culture in vitro, while the hydroxyapatite only produced limited amount of unmineralized ECM. Porous SCPC scaffold was prepared by rapid prototyping technique using a segment of a rabbit ulnar bone as prototype model [215]. After 4-weeks, CT scans showed that the defect filled by the above SCPC composite scaffold loaded with rh-BMP-2 had already been replaced by newly formed bone, indicating that SCPC are highly resorbable and have good bone formation ability.

Polymer/Inorganic Composites

The composite materials for bone tissue engineering have been pursued in the near decade, since the composites combine the advantages of the different components, which offered superiorities over single-phase materials.

Compared to the strengths of metals and ceramics, the strengths of biodegradable polymers are low. The porous structure of the scaffolds further decreases their strengths. Moreover, the synthetic polyesters are often non-osteoconductive. To enhance the strength and bioactivity of the polymer scaffolds, an inorganic component is always introduced to make polymer/inorganic composites. Studies have demonstrated that such composites could result in scaffolds with tailorable physical and biological properties for specific applications. The addition of an inorganic phase to a biodegradable polymer may also change the *in vitro* and *in vivo* polymer degradation behaviour.

Bioglass, glass-ceramics, calcium phosphates and silicates, etc. have all been used to reinforce polymers. The development of polymer/inorganic composites has been well reviewed in literatures [4, 13, 32]. In the recent years, the polymer/silicate ceramic composites have been intensively investigated. For example, wollastonite was incorporated into the PDLLA to prepare a bioactive PDLLA/wollastonite composite [236]. The composite scaffold was prepared using a solvent casting/particulate leaching method. With the same salt content, the porosity of the PDLLA deceased from 95 to 85 % as the wollastonite content increased from 0 to 40 %. The bioactivity of the PDLLA/wollastonite composite was confirmed by the formation of an apatite layer on its surface after immersing in SBF for seven days. The interesting and important advantage of the PDLLA/wollastonite composite is that the acidic degradation products of the PDLLA could be neutralized by the basic ions released from wollastonite due to its dissolution in the SBF solution. For the PHBV/wollastonite porous scaffolds, there were no significant differences in porosity between the samples with different wollastonite content [237]. However, the mechanical strength of the composite scaffolds was significantly enhanced by the incorporation of wollastonite. In addition, the incorporation of silicates into polymers will result in an improvement in hydrophilicity, expressed by a decrease in water contact angle [237, 238]. This implied that wollastonite could be used as a good candidate for preparation of bioactive polymer/ceramic composites for tissue engineering applications.

During the process of polymer/ceramic composites preparation, a common problematic issue is that it is difficult to get a uniform polymer/inorganic particle suspension, since the inorganic particles have the tendency to agglomerate. This problem makes it difficult to fabricate composites with a uniform microstructure [236, 237]. And it was found that some of the PDLLA/β-$CaSiO_3$ composites lost their strength rapidly under physiological environment, and failures mainly occurred at the interface between the β-$CaSiO_3$ agglomerates and the polymer matrix. Consequently, it is necessary to increase the compatibility between the inorganic component and the polymer matrix by improving the dispersion of inorganic particles in preparing polymer/inorganic composites.

Mechanical stirring [239] and ultrasonic energy [240] have been used to reduce agglomerate formation and provide some level of particle dispersion during the blend processing of composite. However, these effects are just temporary and particle agglomeration ensues once the mixing energy is removed.

It is supposed that chemical techniques can provide more permanent effect to solve this problem and various methods have been developed to match the surface properties between filler powders and a specific polymeric matrix [241–244]. Zhang et al. [241] used silane derivatives as modification molecules to shield hydroxyl groups (–OH) formed on the surface of HA to improve the interfacial property between the ceramic phase and the polymer phase, which resulted in a 27.8 % increase in maximum bending strength of the HA/PLA composites. Qiu et al. [242] modified the surface of HA with L-lactic acid oligomer, and the dispersion of HA particles in the polymer solution was improved significantly. The mechanical strength of the L-lactic modified HA/PLLA composite film was also increased [242, 243].β-$CaSiO_3$ particles treated with dodecyl alcohol can react with the Si-OH groups on the surface of β-$CaSiO_3$ particles in an aqueous solution by esterification reaction. This modification could make the β-$CaSiO_3$ particle hydrophobic and thus enhance its dispersion in the organic solvent (as shown in Fig. 4.4). The tensile strength of the modified β-$CaSiO_3$/PLLA composite film with 15 wt% ceramic phase increased 52.2 % compared to that of the unmodified one [244]. In addition, the modification had no effects on the bioactivity of the β-$CaSiO_3$/PLLA composite. Our experiments also showed that the dodecyl alcohol on the modified $CaSiO_3$ particles in the composite could be removed by hydrolysis in boiling water. The valuable results are that the esterification-hydrolysis process has improved the mechanical properties of β-$CaSiO_3$/PLLA composites, while without impairing their wettability and bioactivity. The same phenomenon was found for the 45S5/PLLA composites.

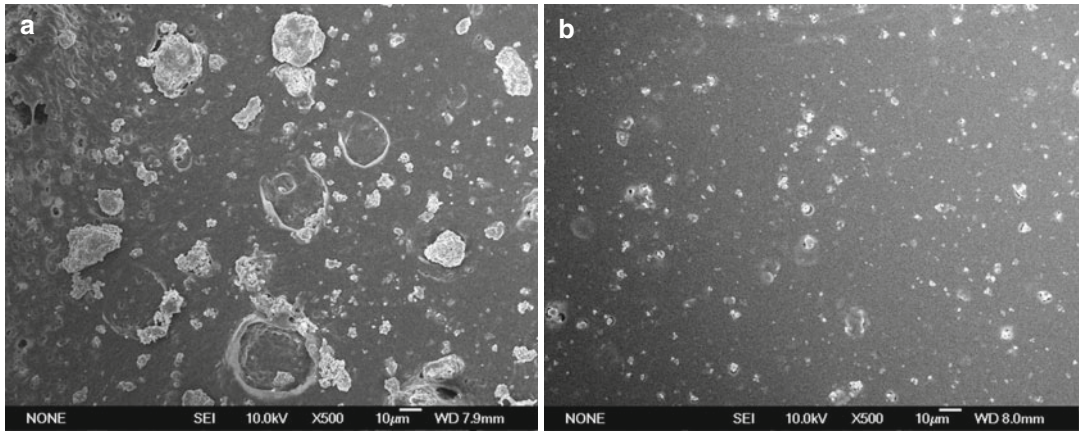

Fig. 4.4 SEM micrographs of the composite films. (**a**) composite film with 15wt%β-$CaSiO_3$ and (**b**) composite film with 15 wt% modified β-$CaSiO_3$ (From Ye et al. [244], with permission)

Concluding Remarks

The concept of replacement of tissues has been shifting to a new concept of regeneration of tissues in the new century [142]. Tissue engineering is an effective way to achieve the goal of tissue regeneration. From the perspective of materials science, the present challenge in tissue engineering is to develop bioactive and bioresorbable biomaterials, which should have the ability to activate the body's own repair mechanisms. An ideal biomaterial for bone tissue engineering should have favorite composition and structures which can facilitate cellular attachment, proliferation and stimulate osteoblastic differentiation of bone marrow stromal cells, and should initiatively participate in the activities of bone formation.

Generally speaking, silicate ceramics have superior bioactivity than phosphate ceramics. The former are considered as osteoconductive and may be considered as osteoinductive, while the latter are only considered as osteoconductive. Therefore, silicate ceramics have a more wide application perspective for bone tissue engineering than phosphate ceramics.

On the other hand, since the hard tissues in human body are natural composite materials, the composite strategy provides an effective way to fabricate scaffold biomaterial with tailorable physiochemical and/or mechanical properties. The composite scaffolds possessing both osteoconductivity and osteoinductivity appear to have great potential for bone tissue engineering applications.

In addition, the architecture of the scaffolds not only influences its mechanical properties and degradation behavior, but also strongly affects the cellular activities and nutrition supplies in the scaffold, which are also important factors for bone regeneration. Thus, the ideal scaffold material should also have highly connective porous structure.

References

1. Laurencin CT, et al. The ABJS Nicolas Andry award: tissue engineering of bone and ligament: a 15-year perspective. Clin Orthop Relat Res. 2006;447:221–36.
2. Lee SH, Shin H. Matrices and scaffolds for delivery of bioactive molecules in bone and cartilage tissue engineering. Adv Drug Deliv Rev. 2007;59(4–5):339–59.
3. Gazdag AR, et al. Alternatives to autogenous bone graft: efficacy and indications. J Am Acad Orthop Surg. 1995;3:1–8.
4. Wang M. Composites scaffolds for bone tissue engineering. Am J Biochem Biotech. 2006;2:80–4.
5. Laurencin CT, et al. Tissue engineering: orthopedic applications. Annu Rev Biomed Eng. 1999;1:19–46.
6. Liu Q. Tissue engineering. In: Shi D, editor. Biomaterials and tissue engineering. Beijing: Tsinghua University Press; 2004. p. 195–246.
7. Langer R, Vacanti JP. Tissue engineering. Science. 1993;260(5110):920–6.
8. Hutmacher DW. Scaffolds in tissue engineering bone and cartilage. Biomaterials. 2000;21(24):2529–43.

9. Simpson RL, et al. Development of a 95/5 poly(L-lactide-co-glycolide)/hydroxylapatite and beta-tricalcium phosphate scaffold as bone replacement material via selective laser sintering. J Biomed Mater Res B Appl Biomater. 2008;84(1):17–25.
10. Jones JR, Ehrenfried LM, Hench LL. Optimising bioactive glass scaffolds for bone tissue engineering. Biomaterials. 2006;27(7):964–73.
11. Shirtliff VJ, Hench LL. Bioactive materials for tissue engineering, regeneration and repair. J Mater Sci. 2003;38(23):4697–707.
12. Cerruti M, Sahai N. Silicate biomaterials for orthopaedic and dental implants. Med Mineraology Geochemistry. 2006;64:283–313.
13. Rezwan K, et al. Biodegradable and bioactive porous polymer/inorganic composite scaffolds for bone tissue engineering. Biomaterials. 2006;27(18):3413–31.
14. Wang M. Developing bioactive composite materials for tissue replacement. Biomaterials. 2003;24(13):2133–51.
15. Burg KJL, Porter S, Kellam JF. Biomaterial developments for bone tissue engineering. Biomaterials. 2000;21(23):2347–59.
16. Seeherman H, Wozney JM. Delivery of bone morphogenetic proteins for orthopedic tissue regeneration. Cytokine Growth Factor Rev. 2005;16(3):329–45.
17. Reis RL, et al. Mechanical behavior of injection-molded starch-based polymers. Poly Adv Technol. 1996;7(10):784–90.
18. Cai K, et al. Physical and biological properties of a novel hydrogel composite based on oxidized alginate, gelatin and tricalcium phosphate for bone tissue engineering. Adv Eng Mater. 2007;9(12):1082–8.
19. Di Martino A, Sittinger M, Risbud MV. Chitosan: a versatile biopolymer for orthopaedic tissue-engineering. Biomaterials. 2005;26(30):5983–90.
20. Damoulis PD, et al. Osteogenic differentiation of human mesenchymal bone marrow cells in silk scaffolds is regulated by nitric oxide. In: Zaidi M, editor. Skelet Biol Med Pt B. Oxford: Blackwell Publishing; 2007. p. 367–76.
21. Liu HF, et al. A comparison of rabbit mesenchymal stem cells and anterior cruciate ligament fibroblasts responses on combined silk scaffolds. Biomaterials. 2008;29(10):1443–53.
22. Cloyd JM, et al. Material properties in unconfined compression of human nucleus pulposus, injectable hyaluronic acid-based hydrogels and tissue engineering scaffolds. Eur Spine J. 2007;16(11):1892–8.
23. Lee SJ, Kim SY, Lee YM. Preparation of porous collagen/hyaluronic acid hybrid scaffolds for biomimetic functionalization through biochemical binding affinity. J Biomed Mater Res Part B Appl Biomater. 2007;82B(2):506–18.
24. Di Bella C, Farlie P, Penington AJ. Bone regeneration in a rabbit critical-sized skull defect using autologous adipose-derived cells. Tissue Eng Part A. 2008;14(4):483–90.
25. Mikos AG, et al. Wetting of poly(l-lactic acid) and poly(dl-lactic-co-glycolic acid) foams for tissue-culture. Biomaterials. 1994;15(1):55–8.
26. Pitt C, Gratzel M, Kimmel G. Aliphatic polyesters II. The degradation of poly(DL-lactide), poly(ε-caprolactone), and their copolymers in vivo. Biomaterials. 1981;2:215–20.
27. Toung JS, et al. Repair of a rodent nasal critical-size osseous defect with osteoblast augmented collagen gel. Laryngoscope. 1999;109(10):1580–4.
28. Peppas NA, Langer R. New challenges in biomaterials. Science. 1994;263(5154):1715–20.
29. Sims C, Butler P, Cao Y. Tissue engineered neocartilage using plasma derived polymer substrates and chondrocytes. Plast Reconstr Surg. 1998;101:1580–5.
30. Liu C, Xia Z, Czernuszka JT. Design and development of three-dimensional scaffolds for tissue engineering. Chem Eng Res Design. 2007;85(A7):1051–64.
31. Gabelnick H. Biodegradable implants: alternative approaches, in advanced in human fertility and reproductive endocrinology: vol. 2. In: Mishell D, editor. Long acting steroid contraception. New York: Raven Press; 1983. p. 149–73.
32. Chen GQ, Wu Q. The application of polyhydroxyalkanoates as tissue engineering materials. Biomaterials. 2005;26(33):6565–78.
33. Doi Y, Kitamura S, Abe H. Microbial synthesis and characterization of poly(3-hydroxybutyrate-co-3-hydroxyhexanoate). Macromolecules. 1995;28(14):4822–8.
34. Doyle C, Tanner ET, Bonfield W. Invitro and invivo evaluation of polyhydroxybutyrate and of polyhydroxybutyrate reinforced with hydroxyapatite. Biomaterials. 1991;12(9):841–7.
35. Williams SF, et al. Medical device containing polyhydroxyalkanoate treated with oxidizing agent to remove endotoxin: US, US 6623749 B2[P]. 2003.
36. Sakkers RJB, et al. Evaluation of copolymers of polyethylene oxide and polybutylene terephthalate (polyactive): mechanical behaviour. J Mater Sci Mater Med. 1998;9(7):375–9.
37. Radder AM, et al. The PEO/PBT copolymer-mineralized matrix interface in-vitro. Cells Mater. 1993;3(4):367–76.
38. Radder AM, Leenders H, Vanblitterswijk CA. Interface reactions to PEO/PBT copolymers (Polyactive(R)) after implantation in cortical bone. J Biomed Mater Res. 1994;28(2):141–51.
39. Radder AM, et al. Interfacial behavior of PEO/PBT copolymers (Polyactive(R)) in a calvarial system – an in-vitro study. J Biomed Mater Res. 1994;28(2):269–77.
40. Weigel T, Schinkel G, Lendlein A. Design and preparation of polymeric scaffolds for tissue engineering. Expert Rev Med Devices. 2006;3(6):835–51.
41. Mikos AG, et al. Preparation and characterization of poly(l-lactic acid) foams. Polymer. 1994;35(5):1068–77.
42. Mikos AG, et al. Laminated 3-dimensional biodegradable foams for use in tissue engineering. Biomaterials. 1993;14(5):323–30.

43. Whang K, Goldstick TK, Healy KE. A biodegradable polymer scaffold for delivery of osteotropic factors. Biomaterials. 2000;21(24):2545–51.
44. Whang K, et al. A novel method to fabricate bioabsorbable scaffolds. Polymer. 1995;36(4):837–42.
45. Wu L, Ding J. Advances in fabrication methodology and technology of three-dimensional porous scaffolds for tissue engineering. J Funct Polym. 2003;16(1): 91–6.
46. Pini R, et al. Sorption and swelling of poly(DL-lactic acid) and poly(lactic-co-glycolic acid) in supercritical CO2: an experimental and modeling study. J Polym Sci B Polym Phys. 2008;46(5):483–96.
47. Tai H, et al. Putting the fizz into chemistry: applications of supercritical carbon dioxide in tissue engineering, drug delivery and synthesis of novel block copolymers. Biochem Soc Trans. 2007;35:516–21.
48. Barry JJA, et al. Supercritical carbon dioxide: putting the fizz into biomaterials. Philos Transact R Soc A Math Phys Eng Sci. 2006;364(1838):249–61.
49. Collins NJ, et al. The influence of silica on pore diameter and distribution in PLA scaffolds produced using supercritical CO2. J Mater Sci Mater Med. 2008;19(4): 1497–502.
50. Liu L, et al. Porous morphology, porosity, mechanical properties of poly(alpha-hydroxy acid)-tricalcium phosphate composite scaffolds fabricated by low-temperature deposition. J Biomed Mater Res A. 2007;82A(3):618–29.
51. Park A, Wu B, Griffith LG. Integration of surface modification and 3D fabrication techniques to prepare patterned poly(L-lactide) substrates allowing regionally selective cell adhesion. J Biomater Sci Polym Ed. 1998;9(2):89–110.
52. Cima LG, et al. Tissue engineering by cell transplantation using degradation using degradable polymer substrates. J Biomech Eng Transact Asme. 1991; 113(2):143–51.
53. Beaman J. Bachround and definitions. In: Beaman J, et al., editors. Solid free-form fabrications: a new direction in manufacturing. Boston: Kluwer Academic Publishers; 1997. p. 1–20.
54. Yang S, et al. The design of scaffolds for use in tissue engineering. Part 2. Rapid prototyping techniques. Tissue Eng. 2002;8(1):1–11.
55. Agarwala M, et al. Structural quality of parts processed by fused deposition. Rapid Prototyping J. 1996;2(4):4–19.
56. Chua CK, et al. Development of a tissue engineering scaffold structure library for rapid prototyping. Part 1: Investigation and classification. Int J Adv Manuf Technol. 2003;21(4):291–301.
57. Li HY, Lin KL, Chang J. Preparation of macroporous polymer scaffolds using calcined cancellous bone as a template. J Biomater Sci Polym Ed. 2005;16(5): 575–84.
58. Yoon BH, et al. Aligned porous alumina ceramics with high compressive strengths for bone tissue engineering. Scr Mater. 2008;58(7):537–40.
59. Chevalier J. What future for zirconia as a biomaterial? Biomaterials. 2006;27(4):535–43.
60. Murashima Y, et al. Calcium sulphate as a bone substitute for various osseous defects in conjunction with apicectomy. Int Endod J. 2002;35(9):768–74.
61. Cui L, et al. Repair of cranial bone defects with adipose derived stem cells and coral scaffold in a canine model. Biomaterials. 2007;28(36):5477–86.
62. Pillar R, et al. Porous calcium pyrophosphate scaffolds for bone substitute applications – in vitro characterization. Biomaterials. 2001;22:963–72.
63. Yoon BH, et al. In-situ fabrication of porous hydroxyapatite (HA) scaffolds with dense shells by freezing HA/camphene slurry. Mater Lett. 2008;62(10–11): 1700–3.
64. Kumta PN, et al. Nanostructured calcium phosphates for biomedical applications: novel synthesis and characterization. Acta Biomater. 2005;1(1): 65–83.
65. Suzuki O, et al. Bone regeneration by synthetic octacalcium phosphate and its role in biological mineralization. Curr Med Chem. 2008;15(3):305–13.
66. Jarcho M, et al. Hydroxylapatite synthesis and characterization in dense polycrystalline form. J Mater Sci. 1976;11:2027–35.
67. de Groot K. Bioceramics consisting of calcium phosphate salts. Biomaterials. 1980;1(1):47–50.
68. Akao H, Aoki H, Kato K. Mechanical properties of sintered hydroxyapatite for prosthetic application. J Mater Sci. 1981;16:809–12.
69. Klein C, Patka P, den Hollander W. Macroporous calcium phosphate bioceramics in dog femora: a histological study of interface and biodegration. Biomaterials. 1989;10:59–62.
70. Walsh WR, et al. Beta-TCP bone graft substitutes in a bilateral rabbit tibial defect model. Biomaterials. 2008;29(3):266–71.
71. Ohgushi H, et al. Bone-formation process in porous calcium-carbonate and hydroxyapatite. J Biomed Mater Res. 1992;26(7):885–95.
72. Ripamonti U, et al. Osteogenin, a bone morphogenetic protein, adsorbed on porous hydroxyapatite substrata, induces rapid bone differentiation in calvarial defects of adult primates. Plast Reconstr Surg. 1992;90(3):382–93.
73. Bucholz R, Charlton A, Holmes R. Hydroxyaptite and tricalcium phosphate bone-graft substitutes. Orthop Clin North Am. 1987;18:323–34.
74. Jensen TB, et al. Bone allograft, Pro-osteon 200 (R) and osteogenic protein-1 device (R) around noncemented implants. Bone. 1999;24(4):428–428.
75. Okumura N, et al. Organ regeneration in porous hydroxyapatite. Bioceramics. 2006;18(Pts 1 and 2): 1017–20.
76. Wang M. Bioactive materials and processing. In: Shi D, editor. Biomaterials and tissue engineering. Beijing: Tsinghua University Press; 2004. p. 1–82.
77. Bareille R, et al. Various evaluation techniques of newly formed bone in porous hydroxyapatite loaded with human bone marrow cells implanted in an extraosseous site. Biomaterials. 2000;21(13):1345–52.
78. Fabbri M, Celotti GC, Ravaglioli A. Hydroxyapatite-based porous aggregates – physicochemical nature,

structure, texture and architecture. Biomaterials. 1995;16(3):225–8.
79. Almirall A, et al. Fabrication of low temperature macroporous hydroxyapatite scaffolds by foaming and hydrolysis of an alpha-TCP paste. Biomaterials. 2004;25(17):3671–80.
80. Deville S, Saiz E, Tomsia AP. Freeze casting of hydroxyapatite scaffolds for bone tissue engineering. Biomaterials. 2006;27(32):5480–9.
81. Tian JT, Tian JM. Preparation of porous hydroxyapatite. J Mater Sci. 2001;36(12):3061–6.
82. Tancred DC, McCormack BAO, Carr AJ. A synthetic bone implant macroscopically identical to cancellous bone. Biomaterials. 1998;19(24):2303–11.
83. Yoshikawa T. Bone reconstruction by cultured bone graft. Mater Sci Eng C. 2000;13:29–37.
84. Mendes SC, et al. Cultured living bone equivalents enhance bone formation when compared to a cell seeding approach. Bioceramics. 2002;14:227–31.
85. Pietak AM, et al. Silicon substitution in the calcium phosphate bioceramics. Biomaterials. 2007;28(28): 4023–32.
86. Mastrogiacomo M, et al. Tissue engineering of bone: search for a better scaffold. Orthod Craniofac Res. 2005;8(4):277–84.
87. Elliot J. Structure and chemistry of the apatites and other calcium orthophosphates. New York: Elsevier Science; 1994.
88. Lee Y, et al. Preparation and characterization of macroporous carbonate-substituted hydroxyapatite scaffold. Ind Eng Chem Res. 2008;47(8):2618–22.
89. Yasukawa A, et al. Ion-exchange of magnesium-calcium hydroxyapatite solid solution particles with Cd2+ ion. Colloids Surf A Physicochem Eng Aspects. 2008;317(1–3):123–8.
90. Barinov SM, et al. Stabilization of carbonate hydroxyapatite by isomorphic substitutions of sodium for calcium. Russ J Inorg Chem. 2008;53(2):164–8.
91. Kannan S, et al. Ionic substitutions in biphasic hydroxyapatite and beta-tricalcium phosphate mixtures: structural analysis by rietveld refinement. J Am Ceram Soc. 2008;91(1):1–12.
92. Kannan S, et al. Fluorine-substituted hydroxyapatite scaffolds hydrothermally grown from aragonitic cuttlefish bones. Acta Biomater. 2007;3(2): 243–9.
93. Li MO, et al. Structural characterization of zinc-substituted hydroxyapatite prepared by hydrothermal method. J Mater Sci Mater Med. 2008;19(2): 797–803.
94. Lin YG, Yang ZR, Jiang C. Preparation, characterization and antibacterial property of cerium substituted hydroxyapatite nanoparticles. J Rare Earths. 2007;25(4):452–6.
95. Wang XP, Ye JD. Variation of crystal structure of hydroxyapatite in calcium phosphate cement by the substitution of strontium ions. J Mater Sci Mater Med. 2008;19(3):1183–6.
96. Kim SR, et al. Synthesis of Si, Mg substituted hydroxyapatites and their sintering behaviors. Biomaterials. 2003;24(8):1389–98.
97. Langstaff S, et al. Resorbable bioceramics based on stabilized calcium phosphates. Part II: evaluation of biological response. Biomaterials. 2001;22(2):135–50.
98. Chen Y, et al. In vitro behavior of osteoblast-like cells on PLLA films with a biomimetic apatite or apatite/collagen composite coating. J Mater Sci Mater Med. 2008;19(6):2261–8.
99. Forsgren J, et al. Formation and adhesion of biomimetic hydroxyapatite deposited on titanium substrates. Acta Biomater. 2007;3(6):980–4.
100. Kamitakahara M, Ohtsuki C, Miyazaki T. Coating of bone-like apatite for development of bioactive materials for bone reconstruction. Biomed Mater. 2007;2(4):R17–23.
101. Klopcic SB, Kovac J, Kosmac T. Apatite-forming ability of alumina and zirconia ceramics in a supersaturated Ca/P solution. Biomol Eng. 2007;24(5):467–71.
102. Tuzlakoglu K, Reis RL. Formation of bone-like apatite layer on chitosan fiber mesh scaffolds by a biomimetic spraying process. J Mater Sci Mater Med. 2007;18(7):1279–86.
103. Yang F, Wolke JGC, Jansen JA. Biomimetic calcium phosphate coating on electrospun poly (epsilon-caprolactone) scaffolds for bone tissue engineering. Chem Eng J. 2008;137(1):154–61.
104. Leonor IB, et al. Biomimetic apatite formation on different polymeric microspheres modified with calcium silicate solutions. Bioceramics. 2006;18(Pts 1 and 2):279–82.
105. Zhang EL, Yang K. Biomimetic coating of calcium phosphate on biometallic materials. Transact Nonferrous Met Soc Chin. 2005;15(6):1199–205.
106. Carlise E. Si: a possible factor in bone calcification. Science. 1970;167:279–80.
107. Jugdaohsingh R, et al. Dietary silicon intake is positively associated with bone mineral density in men and premenopausal women of the Framingham Offspring cohort. J Bone Miner Res. 2004;19(2):297–307.
108. Vallet-Regi M, Arcos D. Silicon substituted hydroxyapatites. A method to upgrade calcium phosphate based implants. J Mater Chem. 2005;15(15):1509–16.
109. Ruys A. Silicon doped hydroxyapatite. J Aust Ceram Soc. 1993;29:71–80.
110. Gibson I, et al. Effect of Si content on the chemical and phase composition of novel Si substituted hydroxyaptites. In: LeGeros RaL J, editor. Bioceramics. Singapore: World Scientific Publishing; 1998. p. 105–8.
111. Gibson I, Best S, Bonfield W. Effect of silicon substitution on the sintering and microstructure of hydroxyaptite. J Am Ceram Soc. 2002;85:2771–7.
112. Li XW, Yasuda HY, Umakoshi Y. Bioactive ceramic composites sintered from hydroxyapatite and silica at 1200 degrees C: preparation, microstructures and in vitro bone-like layer growth. J Mater Sci Mater Med. 2006;17(6):573–81.
113. Porter AE, et al. Ultrastructural comparison of dissolution and apatite precipitation on hydroxyapatite

and silicon-substituted hydroxyapatite in vitro and in vivo. J Biomed Mater Res A. 2004;69A(4):670–9.
114. Xynos ID, et al. Bioglass (R) 45S5 stimulates osteoblast turnover and enhances bone formation in vitro: Implications and applications for bone tissue engineering. Calcif Tissue Int. 2000;67(4):321–9.
115. Black J, Hastings G. Handbook of biomaterials properties. London: Chapman & Hall; 1998.
116. Ducheyne P, Qiu Q. Bioactive ceramics: the effect of surface reactivity on bone formation and bone cell function. Biomaterials. 1999;20(23–24):2287–303.
117. Eggli P, Müller W, Schenk R. Porous hydroxyapatite and tricalcium phosphate cylinders with two different pore size ranges implanted in the cancellous bone of rabbits. Clin Orthop. 1988;232:127–38.
118. Kamitakahara M, et al. Control of the microstructure of porous tricalcium phosphate: effects of addition of Mg, Zn and Fe. J Japan Soc Powder Powder Metallurgy. 2005;52:256–359.
119. Ryu HS, et al. An improvement in sintering property of beta-tricalcium phosphate by addition of calcium pyrophosphate. Biomaterials. 2002;23(3):909–14.
120. Mastrogiacomo M, et al. Engineering of bone using bone marrow stromal cells and a silicon-stabilized tricalcium phosphate bioceramic: evidence for a coupling between bone formation and scaffold resorption. Biomaterials. 2007;28(7):1376–84.
121. Descamps M, et al. Synthesis of macroporous [beta]-tricalcium phosphate with controlled porous architectural. Ceram Int. 2008;34(5):1131–7.
122. Descamps M, et al. Manufacture of macroporous [beta]-tricalcium phosphate bioceramics. J Eur Ceram Soc. 2008;28(1):149–57.
123. Xie YZ, et al. Three-dimensional flow perfusion culture system for stem cell proliferation inside the critical-size beta-tricalcium phosphate scaffold. Tissue Eng. 2006;12(12):3535–43.
124. Guo XM, et al. Repair of large articular cartilage defects with implants of autologous mesenchymal stem cells seeded into beta-tricalcium phosphate in a sheep model. Tissue Eng. 2004;10(11–12):1818–29.
125. Guo XM, et al. Repair of osteochondral defects with autologous chondrocytes seeded onto bioceramic scaffold in sheep. Tissue Eng. 2004;10(11–12):1830–40.
126. Zhang F, et al. Bioinspired structure of bioceramics for bone regeneration in load-bearing sites. Acta Biomater. 2007;3(6):896–904.
127. Nery EB, et al. Tissue-response to biphasic calcium-phosphate ceramic with different ratios of ha/beta-tcp in periodontal osseous defects. J Periodontol. 1992;63(9):729–35.
128. Wang JX, et al. Biological evaluation of biphasic calcium phosphate ceramic vertebral laminae. Biomaterials. 1998;19(15):1387–92.
129. Ramay HRR, Zhang M. Biphasic calcium phosphate nanocomposite porous scaffolds for load-bearing bone tissue engineering. Biomaterials. 2004;25(21):5171–80.
130. Kwon SH, et al. Synthesis and dissolution behavior of beta-TCP and HA/beta-TCP composite powders. J Eur Ceram Soc. 2003;23(7):1039–45.
131. Kohri M, et al. Invitro stability of biphasic calcium-phosphate ceramics. Biomaterials. 1993;14(4):299–304.
132. Yuan HP, et al. Cross-species comparison of ectopic bone formation in biphasic calcium phosphate (BCP) and hydroxyapatite (HA) scaffolds. Tissue Eng. 2006;12(6):1607–15.
133. Yuan HP, et al. A comparison of the osteoinductive potential of two calcium phosphate ceramics implanted intramuscularly in goats. J Mater Sci Mater Med. 2002;13(12):1271–5.
134. Ng AMH, et al. Differential osteogenic activity of osteoprogenitor cells on HA and TCP/HA scaffold of tissue engineered bone. J Biomed Mater Res A. 2008;85A(2):301–12.
135. Hench LL, et al. Bonding mechanisms at the interface of ceramic prosthetic materials. J Biomed Mater Res Symp. 1971;2:117–41.
136. Cao WP, Hench LL. Bioactive materials. Ceram Int. 1996;22(6):493–507.
137. Hench LL. Bioceramics. J Am Ceram Soc. 1998;81(7):1705–28.
138. Hench LL, Wilson J. Surface-active biomaterials. Science. 1984;226:630–6.
139. Xynos ID, et al. Ionic products of bioactive glass dissolution increase proliferation of human osteoblasts and induce insulin-like growth factor II mRNA expression and protein synthesis. Biochem Biophys Res Commun. 2000;276(2):461–5.
140. Hench LL. Bioceramics – from concept to clinic. J Am Ceram Soc. 1991;74(7):1487–510.
141. Xynos ID, et al. Gene-expression profiling of human osteoblasts following treatment with the ionic products of Bioglass? 45S5 dissolution. J Biomed Mater Res. 2001;55(2):151–7.
142. Hench LL. The challenge of orthopaedic materials. Curr Orthop. 2000;14(1):7–15.
143. Balamurugan A, et al. Sol gel derived SiO2-CaO-MgO-P2O5 bioglass system-preparation and in vitro characterization. J Biomed Mater Res B Appl Biomater. 2007;83B(2):546–53.
144. Karpov M, et al. Sol–gel bioactive glasses support both osteoblast and osteoclast formation from human bone marrow cells. J Biomed Mater Res A. 2008;84A(3):718–26.
145. Yi J, et al. Sol–gel derived mesoporous bioactive glass fibers as tissue-engineering scaffolds. J Solgel Sci Technol. 2008;45(1):115–9.
146. Du RL, Chang J. The influence of Zn on the deposition of HA on sol–gel derived bioactive glass. Biomed Mater Eng. 2006;16(4):229–36.
147. Hamadouche M, et al. Absorbability of bulk sol–gel 1756 bioactive glasses. Bioceramics. 2000;192(1):593–96.
148. Zhong JP, Greenspan DC. Processing and properties of sol–gel bioactive glasses. J Biomed Mater Res. 2000;53(6):694–701.

149. Livage J. Sol–gel processes. Curr Opin Solid State Mater Sci. 1997;2(2):132–8.
150. Pereira MM, Clark AE, Hench LL. Calcium-phosphate formation on sol–gel-derived bioactive glasses in-vitro. J Biomed Mater Res. 1994;28(6):693–8.
151. Pereira MM, Clark AE, Hench LL. Homogeneity and bioactivity of sol–gel derived glasses. J Dent Res. 1994;73:276–276.
152. Ohura K, et al. Bioactivity of CaO•SiO2 glasses added with various ions. J Mater Sci Mater Med. 1992;3:95–100.
153. Yuan HP, et al. Bone induction by porous glass ceramic made from Bioglass (R) (45S5). J Biomed Mater Res. 2001;58(3):270–6.
154. Chen QZZ, Thompson ID, Boccaccini AR. 45S5 Bioglass (R)-derived glass-ceramic scaffolds for bone tissue engineering. Biomaterials. 2006;27(11):2414–25.
155. Kaufmann E, Ducheyne P, Shapiro IM. Effect of varying physical properties of porous, surface modified bioactive glass 45S5 on osteoblast proliferation and maturation. J Biomed Mater Res. 2000;52(4):783–96.
156. Livingston T, Ducheyne P, Garino J. In vivo evaluation of a bioactive scaffold for bone tissue engineering. J Biomed Mater Res. 2002;62(1):1–13.
157. Peitl O, LaTorre GP, Hench LL. Effect of crystallization on apatite-layer formation of bioactive glass 45S5. J Biomed Mater Res. 1996;30(4):509–14.
158. Li P, et al. The effect of residual glassy phase in a bioactive glass-ceramic on the formation of its surface apatite layer invitro. J Mater Sci Mater Med. 1992;3(6):452–6.
159. Jones JR, Hench LL. Effect of surfactant concentration and composition on the structure and properties of sol–gel-derived bioactive glass foam scaffolds for tissue engineering. J Mater Sci. 2003;38(18):3783–90.
160. Jones JR, Hench LL. Factors affecting the structure and properties of bioactive foam scaffolds for tissue engineering. J Biomed Mater Res B Appl Biomater. 2004;68B(1):36–44.
161. Jones JR, Lee PD, Hench LL. Hierarchical porous materials for tissue engineering. Philos Transact R Soc A Math Phys Eng Sci. 2006;364(1838):263–81.
162. Sepulveda P, Jones JR, Hench LL. Bioactive sol–gel foams for tissue repair. J Biomed Mater Res. 2002;59(2):340–8.
163. White RA, Weber JN, White EW. Replamineform: a new process for preparing porous ceramic, metal, and polymer prosthetic materials. Science. 1972;176(4037):922–4.
164. Habraken WJEM, Wolke JGC, Jansen JA. Ceramic composites as matrices and scaffolds for drug delivery in tissue engineering. Adv Drug Deliv Rev. 2007;59(4–5):234–48.
165. Sepulveda P, Jones JR, Hench LL. In vitro dissolution of melt-derived 45S5 and sol–gel derived 58S bioactive glasses. J Biomed Mater Res. 2002;61(2):301–11.
166. Kokubo T, et al. Apatite- and wollastonite-containing glass-ceramics for prosthetic application. Bull Inst Chem Res Kyoto Univ. 1982;60:260–68.
167. Kokubo T, et al. Ca, P-rich layer formed on high-strength bioactive glass-ceramic A-W. J Biomed Mater Res. 1990;24(3):331–43.
168. Dyson JA, et al. Development of custom-built bone scaffolds using mesenchymal stem cells and apatite-wollastonite glass-ceramics. Tissue Eng. 2007;13(12):2891–901.
169. Jones JR, Hench LL. Materials perspective – biomedical materials for new millennium: perspective on the future. Mater Sci Technol. 2001;17(8): 891–900.
170. Ohtsuki C, et al. Apatite formation on the surface of ceravital-type glass-ceramic in the body. J Biomed Mater Res. 1991;25(11):1363–70.
171. Reck R, Storkel S, Meyer A. Ceravital middle-ear prostheses – long-term follow-ups. Laryngologie Rhinologie Otologie Vereinigt Mit Monatsschrift Fur Ohrenheilkunde. 1987;66(7):373–6.
172. Dost P, et al. Reconstruction of the stapes superstructure with a combined glass-ceramic (Bioverit((R))) implant in guinea pigs. ORL J Otorhinolaryngol Relat Spec. 2002;64(6):429–32.
173. Jutte M, et al. Bioverit(R) enucleation protheses in rabbits. Klin Monatsbl Augenheilkd. 1992;200(6):674–7.
174. Vitale-Brovarone C, et al. Macroporous glass-ceramic materials with bioactive properties. J Mater Sci Mater Med. 2004;15(3):209–17.
175. Vitale-Brovarone C, et al. Development of glass-ceramic scaffolds for bone tissue engineering: characterisation, proliferation of human osteoblasts and nodule formation. Acta Biomater. 2007;3(2):199–208.
176. Vitale-Brovarone C, et al. Biocompatible glass-ceramic materials for bone substitution. J Mater Sci Mater Med. 2008;19(1):471–8.
177. Ramp WK, Lenz LG, Kaysinger KK. Medium pH modulates matrix, mineral, and energy-metabolism in cultured chick bones and osteoblast-like cells. Bone Miner. 1994;24(1):59–73.
178. Kaysinger KK, Ramp WK. Extracellular pH modulates the activity of cultured human osteoblasts. J Cell Biochem. 1998;68(1):83–9.
179. Conzone SD, et al. In vitro and in vivo dissolution behavior of a dysprosium lithium borate glass designed for the radiation synovectomy treatment of rheumatoid arthritis. J Biomed Mater Res. 2002;60(2):260–8.
180. Day DE, et al. Transformation of borate glasses into biologically useful materials. Glass Technol. 2003;44(2):75–81.
181. Liang W, et al. Bioactive borate glass scaffold for bone tissue engineering. J Non Cryst Solids. 2008;354(15–16):1690–6.
182. Kasuga T. Bioactive calcium pyrophosphate glasses and glass-ceramics. Acta Biomater. 2005;1(1):55–64.
183. Wang C, Kasuga T, Nogami M. Macroporous calcium phosphate glass-ceramic prepared by two-step pressing technique and using sucrose

as a pore former. J Mater Sci Mater Med. 2005;16(8):739–44.
184. Kasuga T, Abe Y. Novel calcium phosphate ceramics prepared by powder sintering and crystallization of glasses in the pyrophosphate region. J Mater Res. 1998;13(12):3357–60.
185. Kasuga T, Abe Y. Calcium phosphate invert glasses with soda and titania. J Non Cryst Solids. 1999;243(1):70–4.
186. Kasuga T, et al. Bioactive ceramics prepared by sintering and crystallization of calcium phosphate invert glasses. Biomaterials. 1999;20(15):1415–20.
187. Navarro M, et al. Development of a new calcium phosphate glass ceramic porous scaffold for guided bone regeneration. Bioceramics. 2004;16:945–8.
188. Deaza PN, Guitian F, Deaza S. Bioactivity of wollastonite ceramics – in-vitro evaluation. Scripta Metallurgica Et Materialia. 1994;31(8):1001–5.
189. Liu XY, Ding CX, Chu PK. Mechanism of apatite formation on wollastonite coatings in simulated body fluids. Biomaterials. 2004;25(10):1755–61.
190. Lin KL, et al. A simple method to synthesize single-crystalline beta-wollastonite nanowires. J Crystal Growth. 2007;300(2):267–71.
191. Liu XY, Ding CX. Reactivity of plasma-sprayed wollastonite coating in simulated body fluid. J Biomed Mater Res. 2002;59(2):259–64.
192. Xue WC, et al. In vivo evaluation of plasma-sprayed wollastonite coating. Biomaterials. 2005;26(17):3455–60.
193. Zhang FM, et al. Preparation, mechanical properties and in vitro degradability of wollastonite/tricalcium phosphate macroporous scaffolds from nanocomposite powders. J Mater Sci Mater Med. 2008;19(1):167–73.
194. De Aza PN, et al. Morphological studies of pseudowollastonite for biomedical application. J Microsc Oxford. 1996;182:24–31.
195. De Aza PN, et al. Bioactivity of pseudowollastonite in human saliva. J Dent. 1999;27(2):107–13.
196. De Aza PN, et al. Transmission electron microscopy of the interface between bone and pseudowollastonite implant. J Microsc Oxford. 2001;201:33–43.
197. Siriphannon P, et al. Influence of preparation conditions on the microstructure and bioactivity of alpha-CaSiO3 ceramics: formation of hydroxyapatite in simulated body fluid. J Biomed Mater Res. 2000;52(1):30–9.
198. Sarmento C, et al. In vitro behavior of osteoblastic cells cultured in the presence of pseudowollastonite ceramic. J Biomed Mater Res A. 2004;69A(2):351–8.
199. de Aza PN, et al. Morphological and structural study of pseudowollastonite implants in bone. J Microsc Oxford. 2000;197:60–7.
200. Gou ZR, et al. In vitro bioactivity and dissolution of Ca-2(SiO3)(OH)(2) and beta-Ca2SiO4 fibers. J Eur Ceram Soc. 2004;24(13):3491–7.
201. Gou ZR, Chang J, Zhai WY. Preparation and characterization of novel bioactive dicalcium silicate ceramics. J Eur Ceram Soc. 2005;25(9):1507–14.
202. Zhao WY, et al. In vitro bioactivity of novel tricalcium silicate ceramics. J Mater Sci Mater Med. 2007;18(5):917–23.
203. Zhao WY, Chang J. Sol–gel synthesis and in vitro bioactivity of tricalcium silicate powders. Mater Lett. 2004;58(19):2350–3.
204. Wu CT, Chang J. A novel akermanite bioceramic: preparation and characteristics. J Biomater Appl. 2006;21(2):119–29.
205. Wu CT, Chang J. Synthesis and apatite-formation ability of akermanite. Mater Lett. 2004;58(19):2415–7.
206. Wu CT, et al. In vitro bioactivity of akermanite ceramics. J Biomed Mater Res A. 2006;76A(1):73–80.
207. Wu CT, Chang J. Synthesis and in vitro bioactivity of bredigite powders. J Biomater Appl. 2007;21(3):251–63.
208. Wu CT, et al. A novel bioactive porous bredigite (Ca7MgSi4O16) scaffold with biomimetic apatite layer for bone tissue engineering. J Mater Sci Mater Med. 2007;18(5):857–64.
209. Nonami T, Tsutsumi S. Study of diopside ceramics for biomaterials. J Mater Sci Mater Med. 1999;10(8):475–9.
210. De Aza PN, Luklinska ZB, Anseau M. Bioactivity of diopside ceramic in human parotid saliva. J Biomed Mater Res B Appl Biomater. 2005;73B(1):54–60.
211. Iwata NY, et al. Sintering behavior and apatite formation of diopside prepared by coprecipitation process. Colloids Surf B Biointerfaces. 2004;34(4):239–45.
212. Du RL, Chang J. Preparation and characterization of bioactive sol–gel-derived Na2Ca2Si3O9. J Mater Sci Mater Med. 2004;15(12):1285–9.
213. Lu WH, Duan W, Guo YP, Ning CQ. Mechanical properties and in vitro bioactivity of $Ca_5(PO_4)_2SiO_4$ bioceramic. J Biomater Appl. 2012;26:637–50.
214. Duan W, Ning CQ, Tang TT. Cytocompatibility and osteogenic activity of a novel calcium phosphate silicate bioceramic: silicocarnotite. J Biomed Mater Res A. 2013;101A(7):1955–61.
215. El-Ghannam A, Cunningham L, Pienkowski D, Hart A. Bone engineering of the rabbit ulna. J Oral Maxillofac Surg. 2007;65:1495–502.
216. El-Ghannam A, Ning C, Mehta J. Cyclosilicate nanocomposite: A novel resorbable bioactive tissue engineering scaffold for BMP and bone marrow cell delivery. J Biomed Mater Res. 2004;71A:377–90.
217. Ni SY, Chang J, Chou L. A novel bioactive porous CaSiO3 scaffold for bone tissue engineering. J Biomed Mater Res A. 2006;76A(1):196–205.
218. Ni SY, et al. Comparison of osteoblast-like cell responses to calcium silicate and tricalcium phosphate ceramics in vitro. J Biomed Mater Res B Appl Biomater. 2007;80B(1):174–83.
219. Xu S, et al. Reconstruction of calvarial defect of rabbits using porous calcium silicate bioactive ceramics. Biomaterials. 2008;29(17):2588–96.
220. Dufrane D, et al. Indirect cytotoxicity evaluation of pseudowollastonite. J Mater Sci Mater Med. 2003;14(1):33–8.

221. Lin KL, et al. Study of the mechanical property and in vitro biocompatibility of CaSiO3 ceramics. Ceram Int. 2005;31(2):323–6.
222. Siriphannon P, et al. Preparation and sintering of CaSiO3 from coprecipitated powder using NaOH as precipitant and its apatite formation in simulated body fluid solution. J Mater Res. 1999;14(2):529–36.
223. Sahai N, Anseau M. Cyclic silicate active site and stereochemical match for apatite nucleation on pseudowollastonite bioceramic-bone interfaces. Biomaterials. 2005;26:5763–70.
224. Gou ZG, Chang J. Synthesis and in vitro bioactivity of dicalcium silicate powders. J Eur Ceram Soc. 2004;24(1):93–9.
225. Nakajima S, et al. Physicochemical characteristics of new reinforcement ceramic implant. Shikwa Gakuho. 1989;89:1709–17.
226. Nakajima S. Experimental studies of healing process on reinforcement ceramic implantation in rabbit mandible. Shikwa Gakuho. 1990;4:525–53.
227. Miake Y, et al. High resolution and analytical electron microscopic studies of new crystals induced by a bioactive ceramic (diopside). J Dent Res. 1995;74(11):1756–63.
228. Iwata NY, et al. Preparation of diopside with apatite-forming ability by sol–gel process using metal alkoxide and metal salts. Colloids Surf B Biointerfaces. 2004;33(1):1–6.
229. Wu CT, et al. Preparation and characteristics of a calcium magnesium silicate (bredigite) bioactive ceramic. Biomaterials. 2005;26(16):2925–31.
230. Arcos D, Greenspan DC, Vallet-Regi M. A new quantitative method to evaluate the in vitro bioactivity of melt and sol–gel-derived silicate glasses. J Biomed Mater Res A. 2003;65A(3):344–51.
231. Sun HL, et al. Proliferation and osteoblastic differentiation of human bone marrow-derived stromal cells on akermanite-bioactive ceramics. Biomaterials. 2006;27(33):5651–7.
232. De Aza PN, Guitian F, DeAza S. Bioeutectic: a new ceramic material for human bone replacement. Biomaterials. 1997;18(19):1285–91.
233. De Aza PN, et al. Reactivity of a wollastonite-tricalcium phosphate bioeutectic (R) ceramic in human parotid saliva. Biomaterials. 2000;21(17):1735–41.
234. Huang XA, Jiang DL, Tan SH. Apatite formation on the surface of wollastonite/tricalcium phosphate composite immersed in simulated body fluid. J Biomed Mater Res B Appl Biomater. 2004;69B(1):70–2.
235. Ni SY, et al. Beta-CaSiO3/beta-Ca-3(PO4)(2) composite materials for hard tissue repair: in vitro studies. J Biomed Mater Res A. 2008;85A(1):72–82.
236. Li HY, Chang J. Preparation and characterization of bioactive and biodegradable Wollastonite/poly(D, L-lactic acid) composite scaffolds. J Mater Sci Mater Med. 2004;15(10):1089–95.
237. Li HY, Chang J. Fabrication and characterization of bioactive wollastonite/PHBV composite scaffolds. Biomaterials. 2004;25(24):5473–80.
238. Cheng W, Li HY, Chang J. Fabrication and characterization of beta-dicalcium silicate/poly(D, L-lactic acid) composite scaffolds. Mater Lett. 2005;59(17):2214–8.
239. Sada E, Kumazawa H, Murakami Y. Hydrothermal synthesis of crystalline hydroxyapatite ultrafine particles. Chem Eng Commun. 1991;103:57–64.
240. Fang Y, et al. Ultrasonically accelerated synthesis of hydroxyapatite. J Mater Res. 1992;7(8):2294–8.
241. Zhang SM, et al. Interfacial fabrication and property of hydroxyapatite/polylactide resorbable bone fixation composites. Curr Appl Phys. 2005;5(5):516–8.
242. Qiu XY, et al. Hydroxyapatite surface modified by L-lactic acid and its subsequent grafting polymerization of L-lactide. Biomacromolecules. 2005;6(3):1193–9.
243. Qiu XY, et al. Surface-modified hydroxyapatite linked by L-lactic acid oligomer in the absence of catalyst. J Polym Sci A Polym Chem. 2005;43(21):5177–85.
244. Ye LZ, et al. Fabrication of poly-(DL-lactic acid)-wollastonite composite films with surface modified beta-CaSiO3 particles. J Biomater Appl. 2008;22(5):465–80.

Biomaterials for Total Joint Replacements

5

Elena M. Brach del Prever, Luigi Costa, Corrado Piconi, Marcello Baricco, and Alessandro Massè

The European Society for Biomaterials defines a *biomaterial* "a material that interacts with the biological systems to evaluate, treat, reinforce or replace a tissue, organ or function of the organism" and the *biocompatibility* "the ability of a material to perform with an appropriate host response in a specific application" [1]. Recently, a new concept of biocompatibility was suggested in relation with the new technologies [2] and the fourth generation of biomaterials, the so-called smart or biomimetic materials [3]. Biocompatibility of a biomaterials is tested by in vitro screening, in vivo testing and clinical monitoring; each step evaluates the biological response in different conditions. In vivo, few seconds after the implantation, the biomaterial is rapidly adsorbed by proteins, whose quantity and organisation depend on the characteristics of the biomaterial, such as chemical composition of the bulk and surface, surface geometry, chemical and physical properties and the properties of the proteins. The host cells contact the protein layer: in total joint replacements, bone cells ongrowing on the prosthetic surface determine an *osseointegration*, fibrous cells as *fibrous fixation.* The production of wear and degradation particles, inevitable in all TJR, determines a biological response defined as *bioreactivity*; its major determinants are the particle size, concentration, surface chemical composition, surface energy, surface charge, surface roughness, particle shape and nature of adsorbed proteins; genetics might be influent in determining the biological response. The wear particles activate macrophages and initiate the inflammatory cascade resulting in bone loss and reduced bone production, prosthetic loosening and eventual TJR failure. New therapeutic strategies try to diminish particle-associated periprosthetic inflammation modifying the monocyte/macrophages migration and activation [4].

Some wear metal particles are able to accumulate in the periprosthetic tissues and enter in the bloodstream, and can be responsible for chromosomal aberrations and DNA damage, which may promote cancerogenesis. Genotoxicity or mutagenicity, and/or carcinogenicity were demonstrated in experimental studies with CoCr

E.M. Brach del Prever, MD (✉)
1st Orthopaedic Clinic University of Turin, Centro Traumatologico Ortopedico, Torino, Italy
e-mail: elena.brach@unito.it

L. Costa, PhD
Molecular Imaging Center, Department of Molecular Biotechnology and Health Sciences, University of Turin, Torino, Italy

C. Piconi, MSc
Department of Clinical Orthopedics, Catholic University, Roma, Italy

M. Baricco, PhD
Laboratory of Metallurgy, Chemistry Department, University of Turin, Torino, Italy

A. Massè, MD
Department of Orthopaedics and Traumatology, University of Turin, Torino, Italy

D.G. Poitout (ed.), *Biomechanics and Biomaterials in Orthopedics*,
DOI 10.1007/978-1-84882-664-9_5

alloys, in accordance with epidemiological studies concerning the association of exposure to chromate particles and the incidence of nasal and lung cancer. Nickel is demonstrated to be genotoxic in vitro and carcinogenetic in vivo (lung and ethmoidal bone). However, after an average of 13 years and up to 25 years of follow-up, no increased cancer risk in patients with conventional total hip replacements was demonstrated [5–7].

In some previously sensitised patients, abrasion and corrosion products could behave like haptens, and the complex may stimulate memory-lymphocytes initiating an inflammatory process. In particular, metal particles can either act as haptens bindings to protein carriers, or as adjutants, forming insoluble complexes with the antigens, initiating an immune response. Hypersensitivity reactions have been reported to be more frequent with stainless-steel or cobalt alloy than with titanium alloy; hypersensitivity to polymethylmethacrylate was found to be 50 % in failed total hip implants.

The probability of developing a metal allergy seems to be higher post-operatively and the risk further increased when failed implants were compared with stable TJRs [8]

Ultra High Molecular Weight Polyethylene (UHMWPE)

A macromolecular chain of polyethylene (PE) can be represented by the following formula:

$\sim(CH_2\text{-}CH_2)_n\sim$

There are many types of PE, all characterised by the same structural unit, but with different lengths, different space arrangements and different chain imperfections. In total joint replacements, the Ultra High Molecular Weight Polyethylene (UHMWPE) is used because of its biocompatibility and excellent mechanical properties. UHMWPE is a high density PE (HDPE) with molecular mass more than 2.000.000 amu; it is a semi-crystalline polymer with a set of ordered regions (crystalline lamellae), where macromolecules are tightly packed and the density is at its highest, embedded in a disordered amorphous phase, where macromolecules are randomly arranged and orientated. Table 5.1 shows the required characteristics of orthopaedic UHMWPE according to ASTM 648-14. With an exception for the density (crystallinity degree is expressed as the percentage by weight of the crystalline regions present in the whole polymer), there are virtually no superior limits for the other characteristics. This means that UHMWPE can have different starting characteristics, whether chemical, physical or mechanical. It is worth mentioning that the determination of these characteristics is carried out on the original material, before processing and sterilisation [9–11].

Processing

The UHMWPE powder coming from the Ziegler-Natta polymerisation plant is processed by compression moulding and ram extrusion: both techniques use high pressure and controlled heating and cooling cycles, and do not significantly modify chemical, physical and structural characteristics of the starting polymer, with the exception of crystallinity (which is normally much higher in the pristine powder). Therefore all prosthetic components, ready to be sterilised, still retain all properties of the starting material.

Table 5.1 Requirements for UHMWPE fabricated forms, according to ASTM 648-14

Property (unit)	Test method	Requirement for type I (GUR 1020)	Requirement for type II (GUR 1050)
Density (g/cm^3)	ASTM D-792	0.927–0.944	0.927–0.944
Ash (mg/kg) (maximum)		125	125
Tensile strength (MPa)	ASTM D 638		
Ultimate (minimum)		40	40
Yield (minimum)		21	19
Elongation (%)	ASTM D 638	380	340
Izod impact strength (kJ/m^2) (min)	ASTM F 648–10 Annex A1	126	73
Charpy impact strength (kJ/m^2) (min)	ISO/CD 11542/2.3	180	90

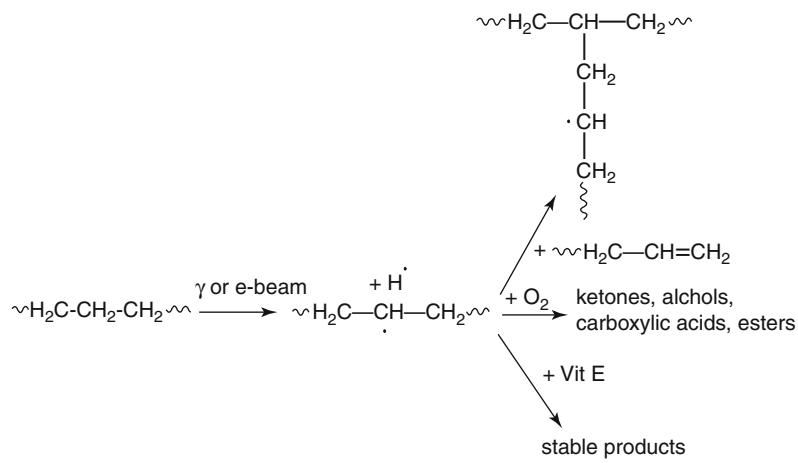

Fig. 5.1 The degradation of the UHMWPE induced by high energy radiation sterilization; in presence of oxygen, from the atmosphere, the process is called oxidation. Vitamin E is able to stabilize against oxidation

Sterilisation

The main sterilisation processes used nowadays employ ethylene oxide (EtO), gas-plasma (GP) and high-energy radiation (gamma radiation and electron beam) [9–11].

EtO and GP are surface sterilization methods and do not significantly affect the physical, chemical and mechanical properties of prosthetic components. GP is based on the action of ionized gas (i.e. hydrogen peroxide or peracetic acid).

Gamma radiations are emitted during decay of a ^{60}Co unstable nucleus. The dose absorbed by prosthetic components is about 25–30 kGy and depends upon the geometry of the sample and its position in relation with the source.

Electron beam is produced by thermally exciting a tungsten filament; the emitted electrons are accelerated by electric fields up to 10 MeV and then conveyed onto the material to be sterilised. The advantages of this method are the easy control of the apparatus and the very short period of treatment (seconds).

Degradation and Oxidation

Gamma radiation and electron beam have a mean energy some orders of magnitude higher than that of polymeric chemical bonds and therefore generate the scission of some chemical bonds of the UHMWPE and formation of free radicals. If even a single C-C bond of the UHMWPE chain is broken and 2° CH_2~radicals are formed, the length of the chain and consequently the molecular mass decrease, with worsening of some chemical and physical material characteristics. This process is called **degradation** and in presence of oxygen, **oxidation**, which involves free radicals (Fig. 5.1).

The oxidative process depends on the radicals (formed during sterilisation) and on the amount of oxygen diffused into the PE components from the atmosphere during processing, sterilisation if conducted in presence of air and storage [12].

The distribution of oxidative products in the prosthetic component depends from the following variables: rate at which radiations is supplied, temperature of the sterilisation chamber, amount of oxygen present in the polymer when irradiated and diffused afterwards. Both in new and retrieved component, a *crown effect* or *white band* was the macroscopic evidence of this oxidation, responsible for many severe failures (delamination and fracture) during service *in vivo* in years '90'. Unfortunately, the first dramatic failures of UHMWPE components in the mid 1980s were attributed to inadequate mechanical properties of the UHMWPE, despite the evidence that these properties were much better than those required by ASTM F648.

Packaging

An adequate packaging of the components is mandatory to assure the correct atmosphere in accordance with the chosen sterilization process; the packaging could be critical when high energy

radiation in vacuum or inert gases to reduce oxidation is used. Currently employed packaging can be included in three categories [13]:

- Gas-permeable packaging, adequate for EtO and GP sterilization: a polyethylene terephthalate (PET) blister with a Tyvek® cover;
- Polymer barrier packaging: multi-layer plastic bags with gas-barrier properties with limited but measurable permeability to oxygen;
- Aluminium barrier packaging: virtually impermeable to gases.

Ultimately, a complete absence of oxidation is obtained only by gas-sterilisation.

Debris and Diffusion

Polyethylene debris are particles loss due to friction, caused by the reciprocal movement of the loaded articular surfaces: for equal mechanical stress, material and interface, abrasion is function of time. Whereas dramatic failures due to anomalous wear of heavily oxidised polyethylene have become quite uncommon nowadays, the production of abraded particles remains a problem in young patients whose life expectancy and quality of life are very high. The debris initiate an inflammatory reaction, the formation of a loosening membrane and a secondary osteolysis. The junctional tissue depends from number, size and chemical structures of UHMWPE debris. While pointing out that this topic is in continuous development, it is important to realise that the debris is not just simple UHMWPE particles, but biologically active particles whose surface interact with the human tissues according with their macro and micromorphology, contact area, molecules adsorpted on their surface, superficial hydrophilic and hydrophobic character, release of free radicals and time [9–11].

A process of adsorption and deep diffusion into the UHMWPE prosthetic components of organic molecules present in the synovial liquid, such as cholesterol, ester of cholesterol, squalene, β-carotene, takes place in vivo. This diffusion explains the yellowish colour in some retrieved components [14].

Crosslinked UHMWPE

To increase the abrasion resistance, crosslinked UHMWPE (X-PE) appeared on the market in the late 1990s [9–11, 15]. Crosslinking of a polymer is the linking of two or more molecular chains by means of chemical covalent bonds: macro radical species, formed by treatment with high energy, react with vinyl double bonds, linking the polymer chains with a C-C stable chemical bond and giving Y-crosslink. The X-PE can be represented as one long, branched molecule with infinite molecular mass and consequent better wear resistance properties than standard UHMWPE, but also with some lower mechanical properties, owing to chemical and physical modifications induced by irradiation and heat treatment.

Commercially available X-PEs are obtained by different crosslinking processes, mainly based on gamma radiation or electron beam at doses ranging from 60 to 100 kGy at room temperature or in the molten state, depending on the manufacturer; the residual radicals are eliminated by thermal treatment, sometime at temperature below the melting point of the polymer (typically at 130 °C) (annealing). The final sterilization is obtained by EtO or gas-plasma or, in few cases, by gamma radiation in low oxygen environment [12].

Due to different crosslinking processes, the commercial X-PEs can be very different with variable properties, while standard UHMWPE has and maintain its properties if processed and sterilised in adequate ways.

Even if dramatic oxidation levels are not observed in newly produced UHMWPE components, it must be kept in mind that also very low oxidation levels can lead to significant variations in the mechanical properties of the polymer.

Vitamin E Stabilised UHMWPE

Vitamin E or, better, its synthetic derivative, alfa-tocopherol, is employed to stabilize UHMWPE against oxidation (ASTM F2695-12). As already pointed out, PE is easily subject to oxidation, which strongly compromises their mechanical properties. The oxidation is basically due to

the reaction between macroradicals and oxygen diffused into the polymer from the surrounding atmosphere; Vitamin E decreases the macro alkyl radicals available to react with the oxygen and thus to a significant slowdown of the oxidative cascade [9–11, 15–17]. Unfortunately, a decreased number of available alkyl radicals is also responsible for a lower efficiency of crosslinking at the same radiation dose, but a correct vitamin E concentration and radiation dose determine an oxidatively stable UHMWPE, without the need of a further thermal treatment, with enough crosslink density and consequent resistance to abrasion.

Polymethylmethacrylate, the Orthopaedic Cement

Orthopaedic cement is basically poly(methyl methacrylate) (PMMA) obtained by polymerising the methyl methacrylate monomer (MMA) [18, 19]. Usually it is supplied in two separate packages: a brown coloured vial (in order to avoid any negative influence of the light on the monomer) containing about 20 ml of transparent liquid, and one package or two containing 40 g of powder. The liquid contains: MMA, usually N,N dimethyl-p-toluidine (DMPT) to accelerate the polymerisation process in presence of radicals, and traces of hydroquinone to avoid premature polymerisation of the monomer. The powder is formed by pre-synthesised PMMA (at times polymethylmethacrylate-styrene as copolymers are used), dibenzoyl peroxide (DBP) and barium sulphate (or zirconium dioxide), the latter may be supplied in a separate package. PMMA is in the shape of spherical particles having a variable diameter between 30 and 250 μm; the size of the particles determines the viscosity of the cement. When the contents of the two packages are mixed, DBP initiates the radical process of polymerisation through polymerisation accelerator and the effect of polymerisation heat. Barium sulphate makes the cement radio-opaque.

Cements produced by different industrial companies have different chemical-physical characteristics and mechanical properties due various components and their relative concentrations.

Bone cement preparation is characterised by three phases: the wetting phase corresponds to mixing the solid part with the liquid, the setting phase (divided into ‘dough time’ and ‘working time’) corresponds to the initial polymerisation process (about 5 % of total), the curing phase corresponds to the final hardening phase and completion of the polymerisation process. During mixing, benzoyl peroxide, present on the surface of the PMMA powder, and DMPT present in the liquid, interact and the polymerisation process starts, mainly on the surface of the pre-synthesised poly(methyl methacrylate). Working time starts when a “dough” is obtained which no longer sticks to gloves and temperature increase of the cement is minimal, corresponding to minimal transformation of MMA to PMMA. The final polymerisation phase is characterised by the rapid increase of polymerisation rate and temperature. The time required for the various phases depend mainly on the temperature in the operating theatre: a 10 °C increase causes polymerisation to start twice as quickly, cutting mixing times by half. After polymerization, less than 5 % of MMA remains free and this percentage may slowly spread into the body. The MMA polymerization reaction is exothermic; the high temperature favours DBP decomposition leading to an increase in radical formation and consequently an increase in polymerization process. Therefore, polymerization speed is initially minimal and gradually increases. Where processing carried out in adiabatic conditions, the bone cement temperature would reach 160 °C. The actual temperature reached by the cement during the surgery depends on the balance between quantity and speed with which the heat is produced, and how easily the heat is dispersed from the surface into surrounding tissues. At the interface with spongy bone, due to vascularisation and the trabecular shape of the bone itself, temperatures of 60 °C can be reached, while in the centre of the mass of cement the temperature is higher than 100 °C. Schematically cement produces heat in function of the used amount, and the temperature at the interface increases with the higher quantity of cement. Based on this assumption, an adequate surgical technique can lower the temperature at the interface by using both

an adequate and not too thick layer of cement, and washing liquids in the final polymerization phase. Some cements are declared as "low temperature polymerization". They are characterised by a lower ratio monomer MMA/polymer that proportionally lowers the heat developed during transformation of monomer into polymer. High temperature is sought when the cement is used as adjuvant in bone tumours to ensure "sterilisation" of a bone surface from which the tumour has been removed; therefore in oncological surgery, standard PMMA is useful.

During polymerization reaction, a theoretical volumetric shrinking of the PMMA takes place proportional to the amount of MMA used; in the orthopaedic cement, the volumetric shrinking is 7 % of the initial volume. Another characteristic of cement is the porosity due to CO_2 formed during decomposition of the initiator, MMA monomer evaporation, air-bubble formed during hand preparation of the mixture, and the expansion due to temperature increase during polymerisation. In actual orthopaedic cements, the vacuum technique preparation decreases air-bubble formation; other factors cannot be eliminated.

Antibiotic-loaded cements are used in order to obtain a greater quantity of local antibiotic and to reduce the systemic quantity, thereby decreasing general toxicity; they are whether industrially packaged or prepared in the operating theatre according to the antibiogramme [20]. The state of the art on how the antibiotic manages to act is the following: the antibiotic, when soluble in water, dissolves from the surface of PMMA into the tissues; antibiotic molecules of notable size are physically blocked inside the bone cement and, therefore, cannot spread from inside the cement to the surface. The dissolution process depends on the type of antibiotic, on the characteristic of the surface of the cement and on the way the cement itself is prepared. When the antibiotic is added to the cement during preparation of the cement itself, that is in the operating room, only a small part of the antibiotic molecules are casually on the surface of the cement and will be able to dissolute. This process explains why the actual antibiotic-loaded cements have a limited antiseptical action.

Ceramic Biomaterials

Ceramics are solid materials, which have as their essential component inorganic non-metallic materials. In joint replacements oxide ceramics are used as components of the artificial joint (ball heads and inserts in hip replacements, femoral component in knee replacements, glenoid in shoulder replacements), while calcium phosphate ceramics (CPCs) are used as osteoconductive coatings on metal alloy components.

Oxide Ceramics

Two ceramic oxides are used in joint replacements: alumina and zirconia. Both are ionic solids, the high energy of the chemical bond giving them a high resistance to the corrosion, hardness, stiffness. The chemical stability of these oxides is the root of the excellent biological safety of their wear debris, a behaviour relevant for their intended use in arthroprostheses' bearings [21]. So far (end 2014) more that 80 % of Total Hip Replacements (THR) in Italy, France, Germany and Austria are making use of ceramic ball heads, as well as in Japan and Korea, while in the USA ceramic ball heads are used in about 20 % of THR only. The market leader CeramTec GmbH (Plochingen, Germany) declared to have sold by 2014 ten million of BIOLOX® ceramic bearing components. The behaviour of selected oxide ceramics is shown in Table 5.2.

Alumina

The development of alumina (aluminium oxide – Al_2O_3) as a biomaterial began in the mid-60s, the behaviour of alumina components (say total hip replacement – THR ball heads) were improved continuously over more than 40 years of clinical use, making alumina one of the better characterised biomaterials [22]. The material used in biomedical application is α-alumina, known as *corundum*, one of the most stable oxides, unaffected by corrosion (e.g. absence of ion release from bulk materials and from wear debris) in the most adverse conditions. The biocompatibility of alumina is a well-established property.

Table 5.2 Indicative values of selected properties of selected oxide bioceramics

Properties (unit)	Unit	BIOLOX®*forte*	Prozyr®	BIOLOX®delta
Usual name		Alumina	Zirconia Y-TZP	Alumina Matrix Composite (AMC)
Chemical composition	wt %	>99.8 Alpha-Alumina	ZrO_2 + 5,1 % Y_2O_3	Al_2O_3: 74 Y-TZP: 24 Other oxides: 2
Density	g/cm^3	3.97	6.08	4.37
Average grain size	µm	1.75	<0.5	0.56 (Al_2O_3) 0.15 (Y-TZP)
Bending strength	MPa	630	>1500	1390
Fracture toughness	MPa m^{½}	3.2	9	6.5
Elastic modulus	GPa	407	200	358
Hardness	HV	1975	1200	1760

Notwithstanding the improvements introduced in the processing of alumina ceramics for clinical applications, the weak point of this alumina remains its low toughness that limits the flexibility in design of alumina components. For this reason, alumina components today are used in about 15–20 % only of the ceramic implants, the balance being alumina-zirconia composites (see section on "Alumina-Zirconia Composites").

Zirconia

Zirconia (zirconium dioxide – ZrO_2) ceramics were developed and introduced in clinical use in the late 80s to overcome the toughness limitation of alumina. The early developments were oriented towards Magnesia-Partially Stabilised Zirconia (Mg-PSZ), in which the tetragonal phase is present within large cubic grains (Ø40 ÷ 50 µm) forming the matrix, a coarse structure that may negatively influence the wear properties of joints. Most of the developments were focused on Yttria stabilised Tetragonal Zirconia Polycrystal (YTZP), a ceramic constituted by tetragonal grains some hundreds of nanometer in size which has been a standard bearing material in orthopaedics up to the year 2000. The structural applications of zirconia ceramics are based on the constrained tetragonal-to-monoclinic (t-m) phase transformation, which acts as a dissipative mechanism for fracture energy. Briefly, the phase transformation is associated to the expansion of zirconia lattice (4 vol% in free grains) and to its change in shape of the crystal cells that have to overcome the constraint of the matrix grains. The process takes place at the expenses of the elastic energy field (tensile) associated to the developing crack, that to advance has in addition to win the compressive stress field due to grain t-m transformation. At a macroscopic level, this results in a toughened ceramic material, having bending strength twice the one of alumina (900–1100 MPa Vs. 500–600 MPa).

The t-m phase transformation that gives to zirconia its interesting behaviour is also its main drawback: zirconia is a metastable material, and its clinical outcomes were contradictory [23]. The worldwide recall of the zirconia Prozyr® ball heads made by Saint Gobain Advanced Ceramics Desmarquest (Evreux, France) led to the practical abandon of zirconia in arthroplasty, where thus far it is still used in some niche products only. On the other hand, zirconia has found recently a wide field of application as a biomaterial in dentistry, for the construction of dental implants, and of the structure of crowns, bridges, dentures by CAD-CAM processing of presintered blanks [21].

Zirconia is also used as a coating obtained by in-situ oxidation of zirconium-2,5Nb alloy (Oxinium®, Smith & Nephew, London, UK). In spite of many claims of good wear properties following total knee replacement either total hip replacement with OxZr femoral component, doubts have been recently raised about this technology in terms of wear reduction both in terms cost/benefits gains. Namely, due to its thickness

(5 μm) the surface zirconia scale can be easily scratched by third bodies, leading to the increased wear of the polyethylene counterface [24].

Alumina-Zirconia Composites

The abandon of zirconia opened a technological gap in arthroplasty. Then, manufacturers focused their attention of alumina zirconia composites, especially on two classes of materials called Zirconia-Toughened Alumina (ZTA) when alumina is the main component and zirconia the balance, either Alumina-Toughened Zirconia (ATZ) when the main component is zirconia.

The first material of this class used in clinics is BIOLOX®delta (Ceramtec GmbH, Plochingen, Germany), which is formed by a matrix of chromia-doped alumina containing 17 vol% Y-TZP and 1 vol% of strontium zirconate platelets. For its peculiar microstructure, this material do not belong to any of the formerly described classes, and was identified as AMC: Alumina Matrix Composite. The finely and homogenous distribution of Y-TZP both of the platelets is obtained by nucleation within the alumina matrix during the sintering cycle.

The high bending strength and toughness of BIOLOX®delta in comparison with alumina and Y-TZP is due to the constrained t-m transformation of the zirconia grains: the transformation imply the compressive deformation of the alumina matrix that has an elastic modulus (e.g. stiffness) twice the Y-TZP one (407 GPa Vs. 200 GPa). This increase the energy dissipated in the phase transformation. In addition, the platelets in BIOLOX®delta having width/length ratio 1:10 perform as a fibres reinforcing the material contributing to increase the material toughness. By December 2014 more than four million ball heads, inserts and condyles for knee replacements made out BIOLOX®delta have been sold worldwide, making this composite the standard "ceramic" in arthroplasty.

Nitride Ceramics

While titanium nitride (TiN) is clinical since a long while as a protective coating on metallic component of joint replacement bearings, bulk silicon nitride (Si_3N_4) has been tested for use in THR cups coupled to metallic either ceramic ball heads, but the future of this ceramic in arthroplasty remains still unclear [25].

Complications with Ceramic Bearings

Due to the improvements introduced in manufacturing, fractures of ceramic composites is today a very rare event. Arthroprostheses Registry data show that revision for fracture of ceramic component occurs with a frequency lower that the one of stem/neck fractures, either of collapse of the polyethylene inlays [26]. Fractures are typically associated to severe trauma either to technical errors in handling the ceramic components. Insert fractures are especially due to intraoperative mispositioning while the orientation of the cup is the reason of edge loading of the bearing components. Recently much attention was devoted to noises from THR bearings. Spectrum analysis demonstrated that the acoustical vibrations are depending on specific features of the implants. This explains also the prevalence of the problem in some Countries and its absence in others, likely due to the distribution of the devices [27].

Calcium Phosphate Ceramics

Calcium phosphate ceramics (CPCs) are since a long time used to give bone-bonding behaviour to the surfaces of metallic joint replacements (e.g. on THR stems) to enhance bony fixation. CPC osteoconductive coatings are a well established technology in joint replacements and long term follow-ups confirm the results obtained in early works [28]. CPC are a family of compound with different in vivo behaviour depending on a number of parameters especially on Ca/P ratio the most stable being Hydroxyapatite $Ca_{10}(PO_4)_6(OH)_2$ [29].

Osteoconductive CP coatings are made by plasma spray. A critical aspect in this technology is the Ca/P ratio of the starting powder and its crystallinity. Powder experience a severe

heating/cooling thermal cycle during this process. Formation of amorphous phases and of resorbable calcium phosphate ceramic (CPC) compounds, segregation of CaO and oxidation reactions must be carefully controlled. Namely, the rate of bone formation and the resorption of coating and its mechanical stability (shear strength, bond strength, fatigue life) are depending on a number of parameters, like e.g. presence of leachable phases, crystallinity, residual porosity [30].

Metallic Materials for Joint Prosthesis

Metallic materials with industrial relevance for joint prostheses belong to three main groups [31–36]: (i) stainless steel; (ii) alloys based on the Co-Cr system; (iii) Ti and its alloys. (i) The austenitic AISI 316 stainless steel was the first material used for orthopaedic implants. When it is specified as AISI 316 L, the carbon content is limited to 0.03 wt% for improving the corrosion resistance of this material. (ii) Co-Cr based alloys have been used for total joint prostheses since the early 1900s and are originating from modifications of dentistry alloy Vitallium (Haynes Stellite alloy N. 21). They combine good mechanical properties with a high biocompatibility, due to the presence of Cr, which forms spontaneously a protective oxide layer. The carbon content in the alloy must be carefully controlled, because the formation of carbide phases may be detrimental for mechanical properties. (iii) Ti and Ti-based alloys are widely used as biomaterials for their high biocompatibility, mainly due to a high corrosion resistance related to the formation of a passive oxide layer at the surface. Good mechanical properties and low density constitute an additional benefit for joint prostheses production. Commercially pure (cP) Ti is used in different grades, as a function of the oxygen content as impurity. Common Ti-based alloys contain aluminium (Al) and vanadium (V), the last often substituted by Niobium (Nb) in order to increase biocompatibility. The main components and physical properties of most widely used metallic biomaterials for joint prosthesis are collected in Table 5.3.

The industrial production of metallic components for joint prosthesis may be carried out in different steps. As a first step, raw metals and alloys are processed into stock shapes, such as bars, sheet, rods, plates, tubes, wires and powders. The second processing step is used to tailor the microstructure of the alloy, which is strongly related to the mechanical properties of the implant, by means of thermo-mechanical treatments. The transformation of stock materials into final products may be obtained by investment casting, machining, forging, and sintering. Techniques used to manufacture various alloys to produce metallic biomaterials for joint prostheses are collected in Table 5.4. Surface coatings aimed to improve functional properties of implant (i.e. biocompatibility, bone fixation) are often added as a final step. Functionality and duration of implants in a physiological environment are very sensitive to surface properties, which may be considered the most important and selective aspect for joint prosthesis selection. Surface treatments are mainly aimed to increase hardness and strength of the surface layer, in order to improve the resistance to wear and corrosion.

Even if metallic biomaterials show good static mechanical properties, they may suffer significantly for fatigue failures [37]. Fatigue strength is defined as the highest periodic stress that does not initiate a failure of the material after a given number of cycles. For hip prostheses, an average of $2 \cdot 10^6$ stress cycles per year can be estimated, so that more than 10^8 cycles may be applied during a lifetime. The applied stress for fatigue failures is in the elastic region of the static loading, so that fatigue strength is significantly lower than ultimate tensile strength. Metallic biomaterials have fatigue strengths in air generally well above the minimum required for joint prosthesis applications. Mechanical properties of most widely used metallic biomaterials for joint prostheses are collected in Table 5.3, together with those of cortical bones for comparison.

Total joint replacements are subjected to wear and abrasion so that the resistance against them is an important criterion for biomaterials.

Table 5.3 Typical composition (maximum amount allowed, wt%), physical and mechanical properties of metallic biomaterials

Materials	Main comp.	Other comp. (max wt%)	Density (g cm^{-3})	Yield strength (MPa)	Ultimate tensile strength (MPa)	Fatigue strength (10^7 cycles) MPa	Fracture toughness (MPa $m^{1/2}$)	Elastic modulus (GPa)	Elongation at fracture (%)
Stainless steels AISI 316	Fe	Ni (14), Cr (19), Mo (2.5), Mn (2)	7.5–8.0	170–790	480–1000	180–550	75–85	190–200	10–50
Co-Cr based alloys	Co	Cr (30), Ni (37), Mo (10.5), Mn (2.5)	8.2–9.1	250–1500	650–1800	300–950	50–60	210–240	8–50
cP-Ti	Ti	Fe (0.5), O (0.4)	4.5	170–485	240–550	200–330	65–75	110	15–25
Ti based alloys	Ti	Al (6.5), V (4.5), Nb (7.5), Fe (3), Mo (15), Zr (6)	4.4–5.3	800–1050	900–1100	450–650	50–55	75–115	8–20
Cortical bone					80–150	30	2–12	14–22	0–2

Table 5.4 Techniques used to produce metallic biomaterials for total joint replacements

Technique	Stainless steels	Co-Cr based alloys	cP-Ti	Ti based alloys
Casting	Not used	Investment casting	Difficult	Difficult
Machining	Possible	Difficult	Possible	Possible
Cold working	Rolling	Difficult	Rolling	Difficult
Hot working	Wrought, forged	Wrought, forged	Not used	Wrought, forged
Sintering	Possible	Hot isostatic pressing	Not used	Not used
Thermal treatments	Recrystallisation	Precipitation hardening	Recrystallisation	Precipitation hardening

High carbon Co-Cr based alloys (F75) improve significantly mechanical properties after working, so that small plastic deformations at the surface significantly increase the hardness of the alloy and, as a consequence, its wear resistance. In addition, the presence of fine dispersed hard carbides increases the wear resistance of these alloys. Oxide films formed by passivation at the surface of the Cr and Ti containing alloys are generally resistant to abrasion [38]. Load required to fracture the oxide surface film is lower for Ti-based alloys with respect to Co-Cr based alloy.

In conclusion, the ideal alloy should have the elastic modulus of bone, the strength of cobalt–chromium alloys, the corrosion resistance and biocompatibility of titanium alloys, and the fabrication cost of stainless steels [35, 36]. Each material has advantages and disadvantages, which drive applications. Stainless steels have good corrosion and fatigue resistance in short-term applications, have a low cost and they are easy to be machined, but tend to be corroded in long-term applications, have a high elastic modulus and can produce Ni and Cr allergy. Co-Cr based alloys show long-term corrosion resistance, a high fatigue and wear resistance and a good biocompatibility, but they are difficult to machine, and thus expensive to process, and, like stainless steel, they suffer for a high elastic modulus and Ni and Cr allergy. Ti-based alloys have a low density, joined with a relatively low elastic modulus, show the greatest corrosion resistance and have an excellent biocompatibility, but they have a relatively low shear strength and wear resistance and are quite expensive. As far as concern the total hip replacement, Table 5.5 reports the types of bearing types implanted in Italy on 2014 [39].

Table 5.5 Types of total hip replacement bearings implanted in Italy on 2014

Bearing type		
Head	Cup	Share (%)
Ceramic	Polyethylene	50.7
Ceramic	Ceramic	28.5
Metal	Polyethylene	16.7
Metal	Metal	2.8
Ceramic	Metal	0.7
Metal	Ceramic	0.5
Other		0.2

Data from Torre et al. [39]

References

1. Williams DF. Definition in biomaterials. Proceedings of the consensus conference of the European Society for Biomaterials, Chester, 1986. Amsterdam: Elsevier Ed.; 1987. p. 49–59.
2. Mertz L. What is biocompatibility? A new definition based on the latest technology. IEEE Pulse. 2013;4:14–5.
3. Holzapfel BM, Reichert JC, Schantz JT, Gbureck U, Rackwitz L, Nöth U, Jakob F, Rudert M, Groll J, Hutmacher DW. How smart do biomaterials need to be? A translational science and clinical point of view. Adv Drug Deliv Rev. 2013;65:581–603.
4. Yao Z, Keeney M, Lin TH, Pajarinen J, Barcay K, Waters H, Egashira K, Yang F, Goodman S. Mutant monocyte chemoattractant protein 1 protein attenuates migration of and inflammatory cytokine release by macrophages exposed to orthopedic implant wear particles. J Biomed Mater Res A. 2014;102:3291–7.
5. Visuri T, Pulkkinen P, Paavolainen P, Pukkala E. Cancer risk is not increased after conventional hip arthroplasty. Acta Orthop. 2010;81(1):77–81.
6. Visuri T, Borg H, Pulkkinen P, Paavolainen P, Pukkala E. A retrospective comparative study of mortality and causes of death among patients with metal-on-metal and metal-on-polyethylene total hip prostheses in primary osteoarthritis after a long-term follow-up. BMC Musculoskelet Disord. 2010;11:78.

7. Doherty AT, Howell RT, Bisbinas I, Learmonth ID, Newson R, Case CP. Increased chromosome translocations and aneuploidy in peripherial blood lymphocytes of patients having revision arthroplasty of the hip. J Bone Joint Surg Br. 2001;83B(7):1075–81.
8. Granchi D, Cenni E, Giunti A, Baldini N. Metal hypersensitivity testing in patients undergoing joint replacement: a systematic review. J Bone Joint Surg Br. 2012;94(8):1126–34.
9. Kurtz S. editor. UHMWPE biomaterials handbook. 3rd ed. Amsterdam: Elsevier; 2016.
10. http://www.uhmwpe.org
11. Brach del Prever EM, Bistolfi A, Bracco P, Costa L. UHMWPE for arthroplasty: past or future? J Orthop Traumatol. 2009;10:1–8.
12. Bracco P, Brach del Prever E, Cannas M, et al. Oxidation behaviour in prosthetic UHMWPE components sterilised with high energy radiation in a low oxygen environment. Polym Degrad Stab. 2006;91:2030–8.
13. Costa L, Bracco P, Brach del Prever E, et al. A survey of oxidation and oxidation potential in contemporary packaging for polyethylene total joint replacement components. J Biomed Mater Res. 2006;78B(1): 20–6.
14. Costa L, Bracco P, Brach del Prever E, et al. Analysis of products diffused into UHMWPE prosthetic components in vivo. Biomaterials. 2001;22(4):307–15.
15. Costa L, Bracco P. Chapter 26: Mechanism of cross-linking and oxidative degradation and antioxidant stabilization of UHMWPE. p. 467–487. In: Kurtz S., editor, UHMWPE biomaterials handbook. 3rd ed. Amsterdam: Elsevier; 2016
16. Wolf C, Lederer K, Bergmeister H, Losert U, Böck P. Animal experiments with ultra-high molecular weight polyethylene (UHMW-PE) stabilised with a-tocopherol used for articulating surfaces in joint endoprostheses. J Mater Sci Mater Med. 2006;17(12):1341–7.
17. Kurtz S, Bracco P, Costa L, Oral E, Muratoglu O. Chapter 17: Vitamin E-Blended UHMWPE Biomaterials, p. 293–306. In: Kurtz S. editor. UHMWPE biomaterials handbook. 3rd ed. Amsterdam: Elsevier; 2016.
18. Wixon RL, Lautenschlager EP. Methyl methacrylate. In: Callagan JJ, Rosenberg AG, Rubash HE, editors. The adult hip. Philadelphia: Lippincott-Raven Pub.; 1998. p. 187–200.
19. Brach del Prever EM, Costa L, Baricco M, Piconi C, Massè A. Biomaterials for joint prosthesis. In: EFORT (European Federation of National Associations of Orthopaedics and Traumatology), editor. Surgical techniques in orthopaedics and traumatology. Paris: Elsevier; 2004.
20. Trippel SB. Antibiotic- impregnated cement in total joint arthroplasty. J Bone Joint Surg (A). 1986;68A:1297–302.
21. Piconi C, Condò SG, Kosmac T. Alumina- and zirconia-based ceramics for load bearing applications. In: Shen JZ, Kosmac T, editors. Advanced ceramics for dentistry. 1st ed. Waltham: Butterworth-Heinemann; 2014. p. 220–53.
22. Piconi C. Alumina. In: Ducheyne P, Healey KE, Hutmacher DW, Grainger DW, Kirkpatrick CJ, editors. Comprehensive biomaterials, vol. 1. 1st ed. Amsterdam: Elsevier; 2011. p. 73–94.
23. Piconi C, Maccauro G, Angeloni M, Rossi B, Learmonth ID. Zirconia heads in perspective: a survey of zirconia outcomes in total hip replacement. Hip Int. 2007;17:119–30.
24. Piconi C, Porporati AA, Streicher RM. Ceramics in THR bearings: behavior in off-normal conditions. Key Eng Mater. 2015;631:1–7.
25. Piconi C. Non-oxide ceramics. Status quo in THR and future options. In: Cobb JP, editor. Modern trends in THA bearings. Berlin: Springer; 2010. p. 37–44.
26. Sadoghi P, Pawelka W, Liebensteiner MC, Williams A, Leithner A, Labek G. The incidence of implant fractures after total hip arthroplasty. Int Orthop. 2014;38:39–46.
27. Owen DH, Russell NC, Smith PN, Walter WL. An estimation of the incidence of squeaking and revision surgery for squeaking in ceramic-on-ceramic hip replacement. Bone Joint J. 2014;96-B:181–7.
28. Geesink RGT. Osteoconductive coatings for total joint arthroplasty. Clin Ortop. 2002;395:53–65.
29. Rey C, Combes C, Drouet C, Grossin D. Bioactive ceramics: physical chemistry. In: Ducheyne P, Healey KE, Hutmacher DW, Grainger DW, Kirkpatrick CJ, editors. Comprehensive biomaterials, vol. 1. 1st ed. Amsterdam: Elsevier; 2011. p. 187–221.
30. Sun L, Berndt C, Gross KA, Kukuc A. Material fundamentals and clinical performances of Plasma spray coatings: a review. J Biomed Mater Res (Appl Biomater). 2001;58:570–92.
31. Helsen JA, Breme HJ, editors. Metals as biomaterials. Chichester: Wiley; 1998.
32. Brunski JB. Metals. In: Biomaterials science, vol. 2. Academic Press: San Diego; 1996. p. 37.
33. Gilbert JL. Metals. In: Callaghan JJ, Rosenberg AG, Rubash HE, editors. The adult hip, vol. 8. Philadelphia: Lippincott-Raven Publishers; 1998. p. 134.
34. Ashby MF. Materials selection in mechanical design. Oxford: Butterworth-Heinemann; 1999.
35. Chen Q, Thouas AG. Metallic implant biomaterials. Mater Sci Eng R. 2015;87:1–57.
36. Davies JR, editor. Metallic materials. In: Handbook of materials for medical devices. Materials Park: ASM International; 2003. p. 21–50.
37. Teoh SH. Fatigue of biomaterials: a review. Int J Fatigue. 2000;22:825–37.
38. Bolton J, Hu X. In vitro corrosion testing of PVD coatings applied to a surgical grade Co-Cr-Mo alloy. J Mater Sci Mater Med. 2002;13:567–74.
39. Torre M, Luzi I, Carrani E, Leone L, Romanini E, Zanoli G. RIAP, Progetto Registro Italiano Artroprotesi – idea, sviluppo, avvio. Roma: Il Pensiero Scientifico; 2014. p. 144.

Bone Materials and Tissue Banks

6

Dominique G. Poitout

Introduction

When there is a considerable loss of bone substance after the excision of a large tumor in the pelvis, it is always difficult to reconstruct the cotyloid cavity. A massive metal prosthesis fixed on the remaining bone with a plate, screws, or cement is often unstable. Fixation of the greater trochanter on the remaining bone, whether the sacrum or the wing of the ilium or, as some authors suggest, the fact of leaving a swinging hip, makes it difficult for the limb operated on to bear weight. We are of the opinion that the best way to return relatively satisfactory function to the limb is to replace the head of the femur, using a massive allograft. Autografts are not sufficiently large to replace the loss of substance, even though they alone are osteo-forming and when incorporated into the skeleton have undeniable mechanical properties. Other types of grafts have to be used. Our decision to use a massive allograft is essentially linked to the rapid muscular refixation which it allows and the anatomical reconstruction of the pelvic ring on which a normal hip prosthesis has to be supported.

Since 1982, we have chosen to use massive cryopreserved and non-irradiated allografts because the experimental and clinical results seem to show that secondary irradiation of the allografts significantly reduces their mechanical strength in the short and medium term (and does not give complete safety from viruses). We prefer to use a bone removed under sterile and safe conditions at the fourth month rather than a bone removed under non-sterile conditions and irradiated later. The irradiation of tissue in the paste phase (as frozen bone is) requires doses of irradiation which are far higher than those usually used, or for the graft to be thawed. Freezing it again subsequently is not biologically satisfactory in our opinion. If the intention is to irradiate it before freezing, the waiting times are harmful to the mechanical quality of the bone, cartilage, or ligament allograft.

History

In 185 AD, Cosmas and Damian, the patron saints of surgeons, were canonized because they performed a posthumous miracle by grafting the limb of a person who had died onto the sacristan of their basilica in Rome, who had a tumor of the tibia. It was the first massive allograft reported

D.G. Poitout, MD
Faculté de Médecine Nord, Sce Chirurgie Orthopédique et Traumatologie, Aix-Marseille Université, Centre Hospitalier et Universitaire Marseille North, Chemin des Bourrely, 13015 Marseille, France
e-mail: Dominique.POITOUT@ap-hm.fr

D.G. Poitout (ed.), *Biomechanics and Biomaterials in Orthopedics*,
DOI 10.1007/978-1-84882-664-9_6

in history (grafting a human bone onto another human being).

Larrey tells the story of a Polish nobleman who had been struck by a Tartar's saber and had lost part of the top of his cranium. Seeing a large dog passing close by, he decided to graft the dog's cranium onto his head. He then noted that it bonded very well. This was the first xenograft (graft from an animal onto man).

As it is not possible to graft a large part of a bone or joint from one and the same subject onto a different site in the same person (autograft), it was necessary to develop bone preservation procedures and to create a tissue bank. Ollier [1] is the nineteenth-century author who most studied the various types of graft, whether autologous grafts, allografts, or xenografts. Many other cases where massive grafts were used have also been published by Albee [2], Abbot and et coll [3], Sicard and Binet [4], Sicard and Brièse [5], Sicard [6], Sicard and Gaudart d'Allaines [7], Sicard and Mouly [8], Judet [9], Judet and Arviset [10], Judet et al. [11], Ottolenghi [12], and Parrish (1972, 1973) [13, 14], but although in more than 50 % of cases these grafts gave results considered to be satisfactory, 15–20 years later, the problems posed by removing, sterilizing, and storing them deterred some surgeons, who turned towards other procedures for reconstructing the skeleton.

The progress made in cryopreservation, as well as in understanding the immunological and biological information provided by grafts, has meant that for 15 years now the use of preserved allografts has returned to popularity. In 1979 we saw the possibility of preserving large bone and cartilage fragments and set up a bone bank in Marseilles Poitout [15, 16] and Poitout and Novakovitch [17]. In 1978 we became interested in the problems posed by the removal, preservation, and use of bone from bone banks. Several preservation methods have been suggested since the use of allografts was considered. The techniques employed used:

Liquid Preservatives alcohol, phenol, ether, hydrochloric acid, or the sublimate among other things adversely alter the bone architecture more or less rapidly and destroy the cells inside. Furthermore they often have an inhibiting effect on osteogenesis, which in general led to their being abandoned [18].

Sterilization by Boiling studied by Gallie in 1912, was heavily used until 1920, in particular by Rouvillois' team. But problems with preparing the grafts and the many cases of resorption reported meant that this type of sterilization was abandoned; it appears to be becoming popular again.

Drying in a Vacuum or Lyophilization makes it easier to store products prepared by this method. However, as it destroys the rigidity of the bone structure, it makes them brittle. Bone crumbles under cutting forceps and is not mechanically adequate to withstand the usual mechanical stresses. Therefore, they cannot be used to replace massive diaphyseal bone segments or articular surfaces [19].

Ethylene Oxide would certainly be an excellent method for sterilizing bone grafts if the gas stayed inside the tissues during storage and if it did not lead to the formation of toxic and even carcinogenic products.

Irradiation has disadvantages as well as advantages. The legal dose is 2.5 megarads. At this dose we are going to destroy the bacteria as well as all the cells but it is not certain that all the viruses will be inactivated and destroyed. The irradiation dose needed to completely disorganize their DNA or RNA molecules would be very high and would at the same time lead to the destruction of the chains of protein molecules which form the architecture of the bone [20–23]. As far as osteocartilaginous parts are concerned, this method of preservation cannot be considered because it alters the cartilaginous structure of the graft profoundly. Therefore, in spite of certain undeniable advantages, such as that of allowing grafts to be removed in a nonsterile environment (which seems to us to be debatable), we have not used it [24].

Bone, cartilage, or ligament grafts are used more and more frequently for treating bone

tumors, performing reconstructive surgery after multiple operations such as, for example, on the hip and pelvis, or following traffic accidents. For the first time we are reconstructing the skeleton by bringing in new bone which will assimilate to the skeleton in a few months or years, whereas, to date, bone fragments were removed to be replaced by prostheses, which have a limited life. Currently 15–20 % of rejections can be solved by using anti-rejection drugs (Sandimmum®).

Cryopreservation Since 1876, Ollier recommended cryopreservation and had even published an experimental study on processes for preserving bone and periosteum grafts at −2 °C. In 1948 Jean and Robert Judet defined the broad lines of the cryopreservation processes. In Aix-les-Bains, Herbert organized the first reserve of frozen tissue and in 1951 at the Hôpital Beaujon in Paris, Sicard created the first bank of frozen bone tissue. Since 1979 we have been preserving massive osteocartilaginous grafts in liquid nitrogen at −196 °C [25, 26]. This method allows whole bones to be preserved indefinitely and preserves the viability of the cartilage cells. To prevent ice macrocrystals forming, it is necessary to impregnate the bone or cartilage tissues with a suitable cryoprotector (10 % DMSO). If we use relatively conservative storage temperatures (higher than −20 °C), the enzymes present in the tissues are not inactivated and will destroy the graft in a few weeks. At −80 °C (the limit for electric freezers), enzyme action, although being clearly reduced, is not totally prevented, because at this temperature only the collagenase is inactivated. On the other hand, DMSO has a prolonged efficacy limit of around −60 °C (eutectic point). Above this, the ice macrocrystals can combine again into macrocrystals and burst the cells and disrupt the architecture. At −196 °C, all enzyme activity is stopped and tissue preservation is unlimited. The temperature of the graft must not be lowered too wuickly and it will be necessary to vary the rate of the lowering in accordance with the temperature obtained. After studying the percentage of live cartilage cells after thawing, it seems to us that the optimum curve is 2 °C per minute down to −40 °C, then 5 °C per minute down to −140 °C, the temperature at which the graft is then plunged directly into a tank of liquid nitrogen where it will be stored.

Thawing, on the other hand, has to be quick so that the largest number of cells stay alive. Plasma or Ringer's lactate solution at 40/41 ° will be used to thaw out and wash the grafts, which will also eliminate the DMSO. Bone fragments are usable for a period of approximately 24–36 h approximately 2 h after having been removed from the liquid nitrogen tank, which allows them to be taken to any point in Europe. They cannot, of course, be refrozen after thawing.

From 1978 to 1983 studies were carried out in the Blood Transfusion Center where a tissue bank has been created in order to prepare bone for preservation. After various attempts, it was decided to use a programmed drop in temperature up to −140 °C, with preservation being in nitrogen vapor at −150 °C or in liquid nitrogen at −196 °C. It was then necessary to develop ways of removing the tissue. These discussions took place in the context of the national "France-Tissues" association, then with the collaboration of the French Graft Institute. Ever more stringent controls make it possible to guarantee the sterility of the fragments supplied and currently two successive controls, with an interval of 4 months between them, make it possible to deliver parts of various sizes 4 months after removal under wholly sterile conditions. In order to allow surgical teams from the private sector to benefit from the same safety when using tissue fragments, we gave them access to the bank, where they sent the femoral heads removed. The fragments they need are supplied to them after the usual sterility checks. In view of their number, femoral heads are sent by the Tissue Bank on a simple request, but where the massive removal of tissue is concerned (femur, tibia, pelvis, etc.) performed at the AP-HM (hospital), the consent of the referrer is required. These fragments, which are few in number, are delivered according to the instructions given by the surgeons. Grafts are sent throughout France. Owing to this chain of goodwill, we have been able to carry out more than 5,000 grafts.

A surgical world first was performed in 1985 by Professors Poitout and Trifaud, which consisted of replacing a complete femur with a bone from the bone bank sheathing a hip prosthesis and a knee prosthesis. However, in order to be able to perform these grafts, we should remember that they had to be removed and preserved. Informing the public and carers is therefore of prime importance if we are to collect as many grafts as possible which are going to give appreciable relief to patients for whom other surgical techniques would be far too incapacitating.

Bone Replacement Materials

Pride of place is currently reserved for bone grafts.

Autografts

Being osteo-forming, autografts alone can induce the formation of new bone and promote the healing of a fracture or the assimilation of an allograft.

Allografts

Immunology of Bone Allografts

The immune response is said to be *matrical* when there is a specific response to molecules isolated from collagen or from proteoglycans. It appears that this response is practically non-existent in the case of massive bone allografts. On the other hand, the *cellular* immune response caused by cells contained in the bone marrow (osteoblasts, osteocytes, fibroblasts, fat, vascular, nerve, or hematopoietic cells) is important provided, however, that all the cells are alive [27–30]. Clinically, rejection reactions occur infrequently (10 % delay in healing and 10 % true rejection with the graft having a lytic appearance), in spite of the use of massive diaphyso–metaphyso–epiphyseal grafts. When the osteosynthesis material is removed and a few years later a biopsy is carried out at the site of the graft, the HLA haplotype is always that of the host. And if a systematic study is carried out of the HLA groups of donors and hosts every month, after an allograft, if a monoclonal antibody specific to the HLA group of the donor is used, we can see that in 80 % of cases no immune HLA antibodies specific to the donor appear. The immune HLA groups which may appear after the graft are connected with the introduction into the body of leukocytes from the blood transfusions usually accompanying grafts. The preservation methods (lyophilization or freezing) do not significantly change the extent of the immunological responses:

Fate of the Grafted Tissue

The allograft does not assimilate with the host bone as it is; it undergoes resorption and then reconstruction phenomena which end in the formation of new bone which, in time, will replace the graft [31–33]. The mechanisms governing the assimilation of the graft are now well known and were already being mentioned by Sicard more than 30 years ago.

It is necessary to stress the importance of:

Age: the younger the graft, the better the assimilation of the allograft.

The fixing ability of the graft, which is essential if it is to be rehabilitated. Indeed, the precarious nature of the vascularization of the graft, particularly at the beginning of its recolonization, means that it must be particularly firmly fixed and attempts must be made to achieve optimum contact between the bone surfaces.

The site of the graft, which is decisive for its assimilation (muscular environment). If a cortical allograft is placed outside its usual location, far from a bone bed and an adequate muscular environment, it will most frequently be resorbed, which seems to indicate that there is a local stimulus promoting its incorporation. This promoting substance may be Urist's PBH (or even "osteogenin" already mentioned by Lacroix in 1950) which is thought to be a substance produced by live undifferentiated mesenchymatous cells [34–36]

The size of the graft.

Initially, the contours of the graft grow blurred, the bone becomes rarified and then fuses with the

adjacent bone. Secondly (around 12–18 months), there is densification of the allograft which indicates the new bone formation which surrounds the graft and consolidates it (Buchardt).

Biomechanics

The revascularization of the graft will only be superficial and only exceptionally and at a very late stage will it be possible to see deeper assimilation of the latter [37]. It also appears to be desirable for this bone lysis to only appear at as late a stage as possible because during the period of revascularization, the mechanical strength of the graft will fall by around 50 % between the 12th and the 18th month and it is therefore necessary to have attached it sufficiently firmly to be able to bear the stresses acting on the graft during this period. The mechanical properties of the allografts can be adversely changed by the preservation and storage processes. Low-dose irradiation (less than 2 megarads) only results in minor effects on the graft's strength. Cryo-preservation seems to improve the mechanical properties of the allografts, the strength of which is 110–120 % of that of fresh bone, but this method of preservation of the graft makes the diaphyseal cortical bone more brittle and liable to breakage. On the other hand, lyophilization or massive irradiation procedures on the bone parts (over 3 megarads) result in a clear reduction in the mechanical strength of the grafts (55 % in the case of lyophilization and 65–70 % in the case of massive irradiation of the strength of a fresh bone) [38]. When a further operation is performed to remove material a few years after a graft, the muscles are intimately fixed to the bone, through a tissue resembling periosteum, and the bone bleeds when this tissue is detached [39, 40].

Xenografts

Xenografts were used several decades ago by French teams (Judet-Sicard, Evre, Guilleminet). The large number of rejection phenomena they caused (more than 50 %) resulted in their no longer being used, hence the current shortage of human grafts. New attempts using different sterilization, preparation, or treatment techniques (lyophilization, ceramization, irradiation, heating, etc.) are being used in attempts to reduce the shortcomings of this type of graft.

Bone Substitutes

Artificial hydroxyapatite derivatives (hydroxyapatite collagen, hydroxyapatite cements, corals or madrepores, vitroceramics or bioglasses) are the subject of mechanical and experimental studies in order to define their tolerance in situ as well as the ways in which they are used. Even if some bone substitutes really are colonized by the host bone, their mechanical properties are currently still inadequate and do not allow the use of large fragments in human clinical medicine. Furthermore, these structures, which are often only osteo-conducting and sometimes osteo-inducing, do not form new bone (are not osteo-forming), and have a tendency to lyse rapidly or behave like a sequestrum.

Reconstructions with Massive Allografts

Bone reconstruction after surgery for excision of a tumor poses further problems, not all of which have been resolved. In the context of massive grafts we will study those used to replace diaphyseal fragments or articular surfaces. The use of prostheses sheathed by bone from a bone bank is an interim solution allowing joint solidity and stability to be combined, and muscular refixation on the periprosthetic bone. This technique should be used each time the loss of bone substance and soft tissue make revascularization of the graft hazardous.

Going beyond the indications of bone cavities being filled by spongy grafts, and beyond the reconstruction of the acetabulum by cortico-spongy allografts, it may be useful to have larger fragments in the bone bank (such as half-pelvises, for example) so that when the acetabulum is too

severely damaged or when there is a bone tumor, the half-pelvis can be replaced by an allograft into which a total hip prosthesis will be fixed.

Massive diaphyseal or epiphyso-metaphyseal grafts will allow the locomotor apparatus to be reconstructed after the excision of a tumor or if substance is lost after trauma. If the intention is to replace a diaphyseal fragment, we believe that it is preferable to use centro-medullary nailing, leaving the muscle masses in close contact with the graft allowing maximum peripheral vascularization. This nail may have to be locked if the upper and lower part of the bone segment of the host is small.

Osteocartilaginous grafts of different sizes may be used to replace articular surfaces destroyed by a tumor or trauma process.

Joint Replacement Options

The use of massive cartilaginous allografts is proposed more and more frequently. These cartilaginous allografts often become very well assimilated. As cartilage cells do not need to be vascularized to survive, they only obtain their nutrition from the constituents of the synovial fluid. However, in order for the mechanical behavior of the graft to be adequate, the cells – contained in the cartilage and ensuring that it is adequately nourished in relation to the hydrophilia of the proteoglycans – are protected during the freezing phase. Hence the advantages of using a cryopreservative when the temperature drops, and the absence of the option of using secondary sterilization by heat, gas, or irradiation. Particular rigor is required when taking and preserving osteocartilaginous parts so as to be certain that the graft is entirely sterile.

Immunogeneity of the Various Constituents of Cartilage

Cartilage is considered to be an immunologically favored tissue because the intact cartilaginous matrix constitutes a real barrier between the chondrocytes and the immunologically competent cells.

Chondrocytes have a histocompatibility system which is comparable to that of the autologous lymphocytes. Langer and Gross have, however, shown the development of cell-type immunity in the rat.

Collagen of human joint cartilage is a type II collagen, synthesized by the chondrocytes. All the collagens can induce an immunological, humoral, and cellular response but collagen II is the most immunogenic.

According to Hermann and Friedlander, the proteoglycans of cartilage are antigenic. An immune response to proteoglycans is possible in the case of cartilaginous lesions, whether they are inflammatory, infectious, or arthrotic. A response of this kind can play a role in the induction or maintenance of the inflammation and destruction of the cartilage.

In summary, the constituents of joint cartilage studied separately are antigenic and immunogenic, but immunogeneity does not manifest itself normally when the various cartilage constituents are intact. Healthy cartilage forms a barrier to their penetration [41, 42] (see Table 6.1).

As the joint graft requires capsuloligamentary coaptation, the collar of the capsule taken with the graft can be used, or the capsule and the ligaments of the host can be fixed directly onto the donor bone by trans-bone sutures. This latter method gives better stability to the limb. If

Table 6.1 Massive bone and osteochondral allografts: 1978–2000

Type	No. of cases
Spongy, cortical and osteocartilaginous allografts	871
Massive diaphyseal and cortico-spongy grafts	303
Hip reconstruction	356
Spongy (femoral heads)	286
Of which	
Acetabula	49
Five with the acetabular joint surface	
Half pelvis	21
Hip prostheses sheathed with associated bone from banks	29
Massive osteocartilaginous grafts	185
Total	1,744

articular necrosis were to occur, this would be painless because of the absence of innervation of the bone fragment and would only require partial replacement of the articular surface using a small prosthesis a few years later. The same problem also exists with the possible appearance of incapacitating ligament laxity, which could in the long-term justify stabilization with a prosthetic ligament or a preserved human ligament graft. Our current approach is the systematic insertion of a ligament support by doubling the ligaments grafted, in order to avoid excessive tension on those which are the source of the rupture or elongation.

The risks of secondary deterioration of the articular surface connected with ligament stability problems has led us to suggest the use of prostheses sheathed with bone from a bone bank which has the advantage of removing the cartilage viability problems with its risks of necrosis, and secondary ligament laxity with joint instability. The bone allograft which sheathes the metal core of a prosthesis allows the adjacent muscles to reattach themselves rapidly to the grafted area, which gives far less variable results in terms of function. Twenty-nine reconstructions using hip prostheses sheathed with bone from the bone bank have been used in association with acetabular grafts during the period 1988–2000.

Removal and Preservation of Grafts

All the allografts were removed during multiorgan removals. The grafts were repeatedly checked, i.e., checked when they were removed and at the fourth month, in the host after three successive bacteriological, urological, and immunological examinations had been carried out. The first on the donor, the second on the patients who had been given organs coming from the same donor. Any infection – general, viral, parasitic, or tumoral – or a systemic illness immediately leads to the destruction of all the grafts removed. The grafts are removed in an operating theater under surgically sterile conditions and preserved at −196 °C (in liquid nitrogen, after a progressive lowering of the temperature by 2 °C/min down to −40 °C, then by 5 °C/min down to −140 °C. The DMSO is used systematically at a dosage of 10 % and put into contact with the allograft after the latter has been refrigerated when its temperature reaches +4 °C. The allograft and the DMSO are cooled separately and are placed in contact with each other at this temperature (above +10 °C, DMSO is toxic to cells). Thawing has to be rapid, i.e., 1–2 h, with lavage of the DMSO in Ringer's lactate solution at +40 °C.

Clinical Experience

The first experimental joint transplants date from the beginning of the century, with the work of Henri Judet in 1908. The autologous and homologous osteochondral grafts performed then were complicated by progressive deterioration of the cartilaginous tissue with crumbling of the subchondral necrotic bone. The first massive osteochondral auto-transplants were performed by Reeves and Solmes (1966), Judet and Padovani (1973), and Goldberg et al. (1973 and 1980). Although the articular auto-transplants demonstrated excellent viability and are maintained in the long term, the allo-transplants produced acute rejection which took two forms:

on the one hand, massive necrosis of the transplant,
on the other, thrombosis of the supply vessels [43].

This was immunological rejection of the supply vessels. The transplant was invaded with lymphocytic cells. Necrosis progressed more rapidly when a homograft of skin or marrow preceded the transplant. Judet and Padovani are of the opinion that a purely immunological mechanism is involved due to the immediate revascularization which created the conditions for accelerated rejection by offering immediate contact between the antigen and the antibody. The delays in assimilation of the graft and its quality only appeared to be slightly altered by the use of cyclosporine A.

Immunosuppressant drugs, such as azathioprine, do not significantly increase the survival time of the transplants. According to Halloran, the anti-lymphocytic serum gives a survival time for the transplant of up to 5 months, but only in the semi-allogenic grafts, and retains identical growth potential to that of the contralateral limb. In our experience, which between 1978 and 2000 includes 185 massive osteocartilaginous transplants, it seems that the clinical result is all the more successful if satisfactory biomechanical conditions are restored to the best extent possible. Histological studies performed by drilling under arthroscopy, even 8 years after the graft, showed that the chondrocytes were alive in most cases and that although the superficial layers of the cartilage were sometimes changed and fissured, the deep layers were generally normal. The absence of painful symptoms in patients is a bonus and X-rays do not show any necrotic phenomena or crushing of the grafts. Some people fear the appearance of a tabes-like syndrome when the two parts of the joint are grafted jointly. It is true that the bone itself is no longer innervated and it is unlikely that a new proprioception will reappear during revascularization of the bone tissue. But the ligaments, muscles, and peripheral vasculonervous elements which have not been removed provide the medullary nerve centers with information and stabilize the bone and cartilage, which in fact behave like a metal prosthesis (also not innervated) [44, 45]. Clinical experience confirms this interpretation, as no tabes-like symptoms have been reported, even 15 years after these types of massive osteocartilaginous grafts were implanted [46, 47].

Capsuloligament and Articular Replacements by Massive Allografts

Preserving human ligaments in tissue banks is also an avenue of research which appears promising but which comes up against the problem of supplies from tissue banks and of the mechanical behavior of ligaments grafted during the period of their revascularization.

Ligament Allografts

These have to be removed from young donors, so that the force and stress values on breakage are close to those of a normal ligament (1,725 Newtons). The allograft which would best meet the morphological and structural criteria would, of course, be an anterior cruciate ligament allograft, however, choosing such an allograft would lead to considerable technical disadvantages and the revascularization of this ligament is risky. The patellar tendon can easily be removed with its two insertions on the patella and the tibia. It is sufficiently long and has mechanical properties which are clearly superior to those of the anterior cruciate ligament even if it is reduced to its central third.

Mechanical Studies

A graft consisting of the central third of the patellar tendon connected to its insertions was studied from a mechanical point of view. Creep tests as well as traction tests right up to rupture, show that:

freezing does not alter the appearance, color, or mechanical properties of grafts;
an irradiated tendon acquires a cardboard-like appearance;
the fibers of an irradiated and lyophilized tendon come apart and they acquire a fibrillary appearance.

The long-term mechanical behavior of these grafts in situ can be problematic when being revascularized. According to the first clinical results, it appears that a considerable percentage of residual articular laxity can be seen. The solution may be to combine a preserved allograft and a reinforcing ligament prostheses which would prevent the stresses being exerted directly on the allograft during its period of rehabilitation (2–3 years). The ligament prosthesis will rupture when the allograft will have regained satisfactory mechanical behavior. This is the technique we use currently but there is insufficient experience of it to be able to publish. Only the test of

time will confirm whether or not we were right to make this choice.

Surgical Technique for Reconstructing the Acetabulum and the Pelvis

The reconstruction of a half-pelvis requires a broad approach following in its middle part the iliac crest, in its anterior part the crural arcade curving in from the pubis along the pubioischiatic line, and in its posterior part, continuing horizontally up to the level of the spinous processes of the lumbar vertebrae. An extension upwards or downwards may make it possible to approach the last lumbar vertebrae or the sacrum. The initial locating of the external iliac vessels, the femoral vessels, and of the crural nerve makes it possible to perform a subperitoneal dissection of the tumor which generally pushes back the iliac muscle and only exceeds it at a late stage. This extension then often contra-indicates a carcinological surgical maneuver. The prosthesis is inserted and cemented in the half-pelvis allograft after fixing the latter by anterior and posterior plates screwed into the allograft on the remaining bone. When a whole half-pelvis is to be reconstructed, the gluteal muscles on the one hand and the adductors on the other have to be refixed to the bone by trans-bone sutures. In order to avoid the occurrence of an obturator hernia, the obturator is obstructed by a strip of silastic pressed on trans-bone sutures at the edge of the obturator.

The implantation of an acetabular graft may justify a simple transgluteal approach maintaining the continuity of the gluteus medius and of the external vastus muscle in a digastric form and retaining the continuity between the fibrous tendon and the bone in the greater trochanter. After having cut the graft as accurately as possible, filling precisely the resected bone, the anterior and posterior plates are screwed along the whole length of the allograft. The posterior plate rests on the ischium and the remaining iliac wing. The anterior plate rests on the pubis (if necessary the centrolateral pubis) and the remaining iliac wing. The prosthetic acetabulum is implanted after having synthesized the bony allograft. The anchorage holes are drilled right into the host bone, therefore allowing the cement to bridge the area of the allograft. We only insert metal pericotyloidian rings in very exceptional cases. Although in our first cases we did not routinely insert antidislocation rings, because of the occurrence of dislocations, we have now chosen to insert them routinely. One or two rings screwed into the rim of the acetabulum make it possible to obtain adequate mechanical setting of the prosthetic femoral head. In the case of operations involving mainly the acetabulum, it is generally useless to refix the gluteal muscles by trans-bone sutures. Only the digastric muscle is closed, and trans-bone sutures fix the part of this digastric muscle on the greater trochanter.

If there is infection, surgery should be carried out in two stages. The first stage is the ablation of all the foreign bodies, prostheses, material, cement, and bone as well as all the fistular courses and necrotic tissue. The limb is placed in traction (trans-femoral traction 1/10 of the body weight). A cement spacer containing antibiotics can be used to replace the part removed. In theory, this method allows the infected area to be sterilized locally and keeps the space free for the future graft. However, the local delivery of antibiotics by the cement spacer only reaches the area from its surface layers. The antibiotic contained inside the cement does not diffuse through this and only antibiotic particles at the surface of the cement enable antibiotics to be delivered at a bactericidal dose in situ. This cement is rapidly surrounded by a fibrous membrane which is impermeable to antibiotics, and in a few days the quantity of antibiotics in the bloodstream can be seen to drop. This technique is little used in the department. Irrigation and drainage may accompany this maneuver, delivering antibiotics in situ and carrying out mechanical cleansing of the infected area. This also makes it possible to carry out sampling on the exit drains, in the search for residual bacteria, making it easier to adapt general antibiotic therapy.

The second stage is that of reconstruction which may be carried out within 2 months of the

removal of the infected tissues, and if the sedimentation rate is less than 20 in the first hour and stable on several successive examinations, as should also be the case with the C-reactive protein level.

Results

Complications associated with the use of massive allografts are what currently determine the limits of this type of surgery, which should only be practiced if the excision of the tumor has the same carcinological value as an amputation, and if draconian precautions are taken when the grafts are removed to avoid these transmitting an iatrogenic pathology. Premature or secondary post-operative deaths were only seen in cases of major surgery of the pelvis for advanced tumoral lesions. The risks of sepsis are comparable in the various groups and are essentially linked to the quality of the cutaneous scarring under chemotherapy (approximately 6 %). Fractures of the graft occur when the osteosynthesis is inadequate or physiotherapy is too aggressive (areas unprotected by the osteosynthesis material). Non-healing of the ends of the bones is very much the exception if the junction between the allograft and the host bone is surrounded by autologous spongy tissue right from the first operation. Articular instability and arthrotic lesions depend on the stability of the reconstruction of the ligaments. The cartilage cells are present and, although reduced, the thickness of the cartilage guarantees correct joint function. No Charcot-type arthropathy has been demonstrated, periarticular innervation no doubt maintains articular trophicity.

Discussion

The revascularization of the graft, its assimilation to the skeleton, the fate of the grafted cartilage, and that of the ligament formations refixed to the graft or used as allografts still pose problems which have not been completely resolved. These massive grafts have to be studied over a longer period but the first results after 15 years are promising. The interim solution of the implantation of a prostheses sheathed with bone from a bone bank seems to be indicated in cases where resection of a tumor is large, removing bone, cartilage, ligaments, and muscles. By allowing the muscles to be refixed onto the graft, these sheathed prostheses limit the risks of the stem breaking or becoming detached. The use of a tibial graft including the patellar tendon makes reconstruction of the extensor apparatus easier. However, if physiotherapy is not started rapidly and continued regularly for several months, the graft will develop muscular adhesion, which sometimes considerably limits the freedom of movement of the joints.

Conclusion

Massive grafts are used more and more frequently in current surgical practice. The sterilization and preservation processes make it possible to make these bone and cartilage grafts easily usable and reliable [48].

In biological and clinical terms allografts assimilate perfectly to the skeleton but the complications associated with their use are what currently determine the limits of this type of surgery, which should only be practiced if the excision of the tumor has the same carcinological value as an amputation, and if draconian precautions are taken when the grafts are removed to avoid these transmitting an iatrogenic pathology [49].

Although the legislative problems have been alleviated since the Cavaillet law of 1976, there is still a great deal of opposition of an administrative, personal, and psychological nature from the public and also from some doctors, particularly if graft removals are to be performed on donors who are brain-dead.

On 11 July, 1950, during a meeting of the Academy of Medicine, Professor Moulonguet expressed the wish to see an organization set up to remove, preserve, and deliver human organs recognized as being necessary for therapy under the best possible moral, legal, and scientific conditions [50].

This discussion is entirely topical, as the Institut Français des Greffes (French Graft

Institute) is now being set up (35 years later, Decree of 10 October, 1994), and although the legal problems have been alleviated, there still remains a great deal of work to be done in this area because the use of human organs currently plays and will continue to play an ever greater role in our arsenal of therapy options. The use of cryopreserved massive allografts is an undeniable advance in our arsenal of therapies.

It is not reasonable, however, to ask of these grafts a result which could not be hoped for in the treatment of a simple fracture. They are often used in extreme conditions and often allow results to be obtained in otherwise hopeless cases. The last problem which has to be resolved is the one concerning the supplying of tissue banks with human grafts, because a great deal of opposition has to be overcome. Even if the legislative problems have been overcome, doctors and the public still do not have sufficient information, and efforts are required from everyone in order for the use of human grafts to be able to play an ever greater role in the future in our therapy.

References

1. Ollier L. Traité expérimental et clinique de la régénération des os et de la production artificielle du tissu osseux, vol. 2. Paris: Masson; 1887.
2. Albee FH. Principes du traitement des fractures non consolidées. SGO. 1930;51:289.
3. Abbot LC, et coll. La valeur de l'os compact et de l'os spongieux comme matériel de greffe. JBJS. 1947;29:381.
4. Sicard A, Binet JP. L'utilisation des greffons homogènes conservés. Congrès Fr de Chir Paris. 1949.
5. Sicard A, Brièse EG. Les applications chirurgicales de la réfrigération. Sem des Hôpitaux de Paris. 1949;25(76):3136.
6. Sicard A. Ce que l'on peut attendre d'une banque d'os. Prog Méd. 1951;65:17387–9.
7. Sicard A, Gaudart d'Allaines C. La fracture des greffes rachidiennes. Journ de Chir. 1952;68:N° 10.
8. Sicard A, Mouly R. Etude expérimentale des greffes osseuses conservées par le froid. Presse Med. 1953;61(N° 44):905–8.
9. Judet R. Hétérogreffes osseuses. Rev d'Orthop et de Chir de l'appar moteur, Oct Déc 1949;35:N° 6:532–4.
10. Judet R, Arviset A. Banque d'os et hétérogreffe. Presse méd. 1949;57:N° 68.
11. Judet R, Lagrange J, Dunoyer. Hétérotransplants osseux congelés. Acad de Chir. 3 Décembre 1952.
12. Ottolenghi CE. Massive osteo and osteo-articular bone grafts: technic and results of 62 cases. Clin Orthop. 1972;87:156–64.
13. Parrish FF. Homografts of bone. Clin Orthop. 1972;87:36–42.
14. Parrish FF. Allograft replacement of all or part of the end of a long bone following excision of a tumor: report of twenty-one cases. J Bone Joint Surg (Am). 1973;55-A:1–22.
15. Poitout D. Conservation et utilisation de l'os de banque Cahier d'enseignement de la SOFCOT. 1985;N° 23:157–77. Expansion Scientifique – Paris.
16. Poitout D. Greffes utilisées pour reconstruire l'appareil locomoteur. Paris: Masson; 1986.
17. Poitout D, Novakovitch G. Allogreffes et banque d'os, Encyclopédie médico-chirurgicale, Paris. Appareil Locomoteur 14015 A10–5. 1986. p. 6.
18. Herbert JJ. De l'utilisation des os conservés comme greffes. La banque d'os. Mém de l'Acad de Chir. 1949;75:60–8.
19. Fasquelle R, Barbier P. A propos de la dessication sous congélation. Sem des Hôpitaux de Paris. 1950; 26(N° 92):4762–6.
20. Roy-Camille R, Laugier A, Ruyssen S, Chenal C, Bisserie M, Pene F, Saillant G. Evolution des greffes osseuses cortico-spongieuses et radiothérapie. Rev Chir Orthop. 1981;67:599–608.
21. Hernigou P. Allogreffes massives cryopréservées et stérilisées par irradiation. Rev Chir Orthop. 1986;72:267–76.
22. Loty B. Irradiation des allogreffes osseuses. Rev Chir Orthop. 1988;74:116–7.
23. Loty B. Allogreffes osseuses massives. Rev Chir Orthop. 1988;74:127–31.
24. Kouvalchouk JF, Paszkowski A. Irradiation des homogreffes osseuses. Rev Chir Orthop. 1986;72:393–401.
25. Poitout D, Novakovitch G. Utilisation des allogreffes en oncologie et en traumatologie. Int Orthop. 1987;11:169–78. SICOT.
26. Poitout D. Indications classiques des allogreffes osseuses. Rev Chir Orthop. 1988;74:118–9.
27. Friedlaender GE. Bone allografts: the biological consequences of immunological events. J Bone Joint Surg (Am). 1991;8(73-A):1119–20.
28. Horowitz MC, Friedlaender GE. Induction of specific T-cell responsiveness to allogeneic bone. J Bone Joint Surg. 1991;73-A:1157–68.
29. Stevenson S, Li XQ, Martin B. The fate of cancellous and cortical bone after transplantation of fresh and frozen tissue-antigen-matched and mismatched osteochondral alografts in dogs. J Bone Joint Surg (Am). 1991;73-A:1143–56.
30. Stevenson S, Horowitz M. Current concepts review. The response to bone allografts. J Bone Joint Surg (Am). 1992;74-A:939–50.

31. Leriche P, Policard A. Le périoste et son rôle dans la formation de l'os. Presse Med. 1918;26:143–6.
32. Leriche R. De la valeur des signes tenus pour caractéristiques de la vie des greffons. Bull Soc Chir. 1919.
33. Policard A. Les phénomènes de la réparation des fractures étudiées par la méthode des cultures de tissu. C Acad Sci. 1927;184:117.
34. Urist MR. Calcification et ossification. JBJS. 1942; 24:47.
35. Urist MR, Silverman BF, Büring K, Dubuc FL, Rosenberg JM. The bone induction principle. Clin Orthop. 1967;53:243–83.
36. Urist MR, Delange R, Flnerman G. Bone cell differenciation and growth factors. Science. 1983;220:680–6.
37. Burchardt H. The biology of bone graft repair. Clin Orthop. 1983;174:28–42.
38. Fèvre, Judet J, Arviset A. Greffes osseuses hétérogènes. MAC. 1949.
39. Hernigou P. Conservation des allogreffes osseuses. Rev Chir Orthop. 1988;74:114–6.
40. Guilleminet, Stagnara, Dubost-Perret. Transplantations osseuses. Documentation expérimentale sur les hétérotransplants. Mém Acad de Chir. 1952.
41. Davis GB, Taylor AN. Greffes osseuses à pédicules musculaires. Arch of Surg Août. 1952;65(N° 2): 330–6.
42. Tomford WW, Thongphasuk J, Mankin HJ, Ferraro MJ. Frozen musculoskeletal allografts: a study of the clinical incidence and causes of infection associated with their use. J Bone Joint Surg (Am). 1990;72-A:1137–43.
43. Teot L. Les transferts osseux libres vascularisés avec cartilage de croissance. Rev Chir Orthop. 1982;68(Suppl II):40–2.
44. Poitout D, Gaujoux G, Lempidakis M. Reconstructions iliaques totales ou partielles à l'aide d'allogreffes de banque. Int Orthop. 1990;14:111–9.
45. Poitout D, Lempidakis M, Loncle X. Allogreffes otéocartilagineuses massives dans le traitement des nécroses ou des pertes de substance articulaires. Chirurgie. 1991;117:193–8.
46. Czitrom AA, Keating S, Gross AE. The viability of articular cartilage in fresh osteochondral allografts after clinical transplantation. J Bone Joint Surg (Am). 1990;72-A:574–81.
47. Enneking WF, Mindell ER. Observations on massive retrieved human allografts. J Bone Joint Surg (Am). 1991;73-A:1123–42.
48. Mankin HJ. Allograft transplantation in the management of bone tumors. In: Uhthoff HK, editor. London, England: Springer Verlag-USA; 1984. p. 147–62.
49. Gerard Y. Les Banques d'OS. Rev Chir Orthop. 1988;74:110–11.
50. Moulonguet P. De la nécessité d'un règlement touchant le prélèvement, la conservation et la délivrance des organes humains utilisés en thérapeutique. Bull de l'Acad Nat de Méd séance du 11 Juillet 1950. p. 494–6.

7 Bone Banks: Technical Aspects of the Preparation and Preservation of Articular Allografts

Dominique G. Poitout and Y. Nouaille de Gorce

For the technical aspects of this subject the Marseilles team collaborated with the Etablissement de Transfusion Sanguine Alpes-Provence (Alpes-Provence Blood Transfusion Service) to set up a bone bank on their premises because it has a competent cryobiology department equipped with storage tanks containing liquid nitrogen and a temperature-lowering programmer. This laboratory, which for a long time has been storing bone marrow, platelets, and various cryopreserved tissues, has the virology, bacteriology, quality control, and quality assurance laboratories of the Blood Transfusion Service and is accustomed to applying the transfusion safety standards. It was also one of the first in France to obtain the approval of the Microbiological Safety Committee of the Directorate General of Health in April 1996. Banks which were developed nationally have followed the same principles and currently more a hundred have been registered and some are awaiting authorization.

D.G. Poitout, MD
Faculté de Médecine Nord, Sce Chirurgie Orthopédique et Traumatologie, Aix-Marseille Université, Centre Hospitalier et Universitaire Marseille North, Chemin des Bourrely, 13015 Marseille, France
e-mail: dominique.poitout@univ-amu.fr

Y.N. de Gorce, MD (✉)
Brd Baille, Centre de Transfusion Sanguine, 13006 Marseille, France

The Removal of Articular and Osteocartilaginous Grafts

Because the bone and cartilage fragments which are removed are not subjected to secondary sterilization, it is imperative that therapeutic maneuvers are performed in wholly sterile conditions.

Selection of the Donors

Selection has to be rigorous so that there is no risk of the transmission of iatrogenic pathology to the host through the graft. This requires adequate knowledge of the history of the illness and the circumstances of the accident, as well as the medical history of the donor. There are many absolute contra-indications. Subjects with a cancerous condition, a systemic illness, collagenosis, an auto-immune disease, or bone dystrophy may not have tissue removed for grafts. We systematically eliminate from the list of donors those suffering from a viral, bacteriological, or parasitic infection, mycosis or tuberculosis as well as those with risk factors and those who have been on artificial ventilation for more than 72 h in intensive care, as they are potentially infected. As far as the validation of the grafting material is concerned, the banks have to conform to the legislation in force decreed by the French Graft Institute.

D.G. Poitout (ed.), *Biomechanics and Biomaterials in Orthopedics*,
DOI 10.1007/978-1-84882-664-9_7

Bacterial decontamination is performed using a solution of antibiotics consisting of rifocine and chloramphenicol.

Samples are taken from each graft before and after decontamination and after thawing. Positive bacteriological results will mean that the tissues will have to be destroyed.

Blood samples have to be taken from each donor (live or deceased) in order to perform the obligatory virological examinations.

In accordance with the decrees of 25 February, 1992, of 24 May, 1994, and of 24, July 1996, medical biological analyses are performed to test for infection:

by the hepatitis B virus (HBs antigen and anti-HBc antibodies),
by HIV (antigen P24 and anti-HIV 1 and 2 antibodies),
by HTLV (anti-HTLV 1 and 2 antibodies),
by hepatitis C (anti-HCV antibodies),
for detecting syphilis in two different tests (VDRL and TPHA),
for assaying for transaminases for the live donors.

Decree No. 97–928 of 9 October, 1997 removes the obligation to carry out a search for the agent responsible for toxoplasmosis, for infection by cytomegalovirus, and by the Epstein-Barr virus. The Decree of 1 April, 1997 requires that the results of the examinations performed are examined before the patients have been transfused, as any hemodilution could falsify the tests. Finally, the French Blood Agency and the French Graft Institute recommend that the tissues are placed into quarantine and that the virological tests are repeated 4–6 months after the tissue has been removed. These samplings are performed either on the live donor or on the host of organs coming from the same donor and are performed to reduce the risk in the event of the tissue having been removed during a seroconversion phase. However, placing these products into quarantine is only one of the possible ways of ensuring safety. A decree will specify the conditions under which it is to be performed in the various situations according to the other methods which could be used, in particular directly testing for the viruses by molecular biology techniques (PCR).

Removal Techniques

As the risk of infection is the main concern in this surgery, the various stages of surgery must be performed under the strictest aseptic conditions possible. The tissue therefore has to be removed in an operating theatre, according to the same principles as regulated orthopedic surgery, and it is considered that a maximum time lapse of 6 h from the circulation stopping can be reasonably accepted. For joint removals, the whole of the joint capsule is preserved as well as the intra-articular ligaments and the menisces or labra. In the case of the knee, and in order to keep the extensor apparatus intact, we retain the whole of the patellar tendon continuously with the posterior half of the patellar joint. This is also continuous with the quadricipital tendon, the upper part of which is cut into an inverted V. The muscular insertions are scraped and the surgeon removing the tissue cleans all the bone attachments of the ligaments allowing the capsule to be refixed firmly. The part is then placed in a bag which is resistant to very low temperatures (captonteflon bags). The reconstruction of the skeleton is one of the important stages of the removal. It is a legal obligation and it has to be as perfect as possible.

Coding and Measuring of the Parts

In order to find the desired bone fragment again easily in the bank, it is necessary to fill in the data sheet carefully and to perform X-rays without enlargement or with an enlargement control placed side-by-side with the bone part.

Quality Controls

All the bone banks have to be inspected periodically, and samplings are performed on a very regular basis (20 % of the grafts are rejected annually,

either immediately after having been removed on account of positive results being found in tests or subsequently at the 6-month checks).

Preservation Techniques

Preservation Methods

Many preservation methods have been suggested since the use of allografts was first considered. The techniques of irradiation and sterilization by moist heat will be described in detail subsequently. Cryopreservation is the only current procedure which makes it possible to preserve bone fragments and in particular cartilage cells safely.

Preserving fluids (antiseptics, 1 % sodium methyolate, β propriolactoses), as well as ethylene oxide are cytotoxic and the problems involved in handling them have meant that they have been abandoned. The same applies for the methods involving sterilization by boiling.

Drying under vacuum or lyophilization uses plasma preservation processes. These grafts, which are theoretically usable indefinitely at ordinary temperatures, are fragile and are not sufficiently strong in mechanical terms to withstand the usual mechanical stresses and, in particular, all the cells are destroyed preventing the use of friction surfaces.

Irradiation of bone fragments taken under conditions which are not sterile is recommended by some teams who see a practical advantage for taking grafts. However, not only does this irradiation, conventionally performed at 25 K Gray, not guarantee perfect viral sterility but it also causes the destruction of all the cells.

Since 1981 we have been using cryopreservation of massive osteocartilaginous grafts in liquid nitrogen at −196 °C. This method makes it possible to preserve whole bones and complete joints over an extended period as it preserves the viability of the cartilaginous cells, the fibers, and fibroblasts contained in the ligaments and capsules.

Without going into the technical details of cryopreservation and storage, we would like to underline the fact that tissue preservation has to obey two essential rules:

uppression of cadaveric disintegration phenomena, preservation for an extended period of the architecture of the bone and preservation of the viability of the cartilaginous cells.

To avoid the formation of ice macrocrystals, it is necessary to impregnate the bone, cartilage, and ligament tissues with a suitable cryoprotector. At Marseilles, we use a mixture of macro-molecules (4 % human albumin which is to be replaced by Héloes) and 10 % final DMSO. This solution is maintained at a temperature of 4 °C because DMSO is toxic. In theory, the "deep cold" should enable these objectives to be reached by stopping the action of the tissue enzymes. If relatively moderate freezing temperatures are used (higher than −20 °C), the enzymes present in the tissue are not inactivated and will destroy the architecture of the graft in a few weeks. At −80 °C (limit of electric freezers), although the enzymatic activity is clearly reduced, it is not totally stopped, only collagenase is inactivated at this temperature. At −196 °C all the enzymes are inactivated and the proteins can be preserved over an extended period. On the other hand, DMSO has a eutectic point around −60 °C, at this temperature, the microcrystals of ice can recombine into macro-crystals and make the cells burst. For the same reasons, the temperature of the graft cannot be lowered in an haphazard fashion, and it is necessary to vary the rate at which this takes place in accordance with the temperature obtained. The optimum curve seems to us to be 2 °C per minute down to −40 °C then 5 °C per minute down to −140 °C, the temperature at which the graft is then placed in nitrogen vapor, directly in the tank where it is stored.

Thawing, on the other hand, has to be rapid so that the largest number of cells remain alive. Physiological serum or Ringer's lactate solution at 40–41 °C will be used to thaw out and wash the grafts in order to eliminate the DMSO. Approximately 2 h after having removed the bone fragments from the liquid nitrogen tank, they are usable for a period of approximately 24–26 h, which means that they can be taken to any part of France and Europe. However, donors are becoming rarer and rarer and it is becoming increasingly difficult to obtain tissue.

Biomechanics and Immunology

The mechanical strength of the cortical allograft is only 50–60 % of the strength of normal bone during a period ranging from the 8th to the 18th month after the graft has been implanted (on account of the revascularization of the bone). Maximum fragility is at around the 12th month and it is only after 2–3 years after the graft has been implanted that the bone regains normal density and biomechanical strength. The fixation of the graft therefore has to be complete in order for this period of fragility to come to an end. The mechanical properties of the allografts can be changed by the preservation and storage processes. Lyophilization, massive irradiation of the grafts (in excess of three megarads), or moist heat used for more than 60 min at 120 °C adversely affect the mechanical behavior of the grafts considerably. Cryopreservation, on the other hand, seems to improve the mechanical properties of the allograft, the strength of which is 110–120 % that of fresh bone but the graft, although it is stronger, does in fact become more brittle (in the mechanical sense of the term) and therefore breakable. In the case of articular allografts, the crucial point is preservation of the ligament structures, of the synovial fluid, and of the menisces. The cells in these formations are preserved, as are their architectural and fundamental structure.

After having been reinstated, the vascularization is linked to the revascularization of the bone insertion area. It is inadequate for several months (or years) which means that they have to be doubled with an artificial ligament during this period to avoid excess stresses which would lead to their being stretched or even ruptured. The extent of the immunologically competent tissue (synovial, capsule, etc.) also risks leading to the occurrence of immunological rejection phenomena justifying the use of immunosuppressants (such as Sandimmum) in the event of the hyperproduction of fluid indicating an immune response.

Transport

Transporting bone parts over long distances will require the use of special containers, in which grafts will be preserved at low temperatures (liquid nitrogen or dry ice). When it is anticipated that these grafts will be used within 24 h following removal from the Bank, it is preferable to thaw the bone fragment and to dispatch it only after thawing. Once removed from liquid nitrogen, the graft has to be used within 24 h and it is not possible to refreeze it again if it is not used.

Use

The best indications for using these osteocartilaginous or complete joint grafts are in the knee, ankle, shoulder, elbow, and wrist.

Isolated Osteocartilaginous Grafts

Partial or total graft of the femoral condyle,
graft of the tibial plateau,
graft of the patella,
graft of the tibial pylon,
partial graft of the humeral head,
partial graft of the elbow,
graft of the inferior radius.

The graft is fixed by osteosynthesis material and the ligaments of the host are refixed onto the graft. The functional results are generally excellent.

Osteocartilaginous Graft Plus Ligaments from the Donor

The excision is larger and the donor ligaments remain attached to the graft and are refixed onto the host bone or over the ligaments of the host. They have to be protected during the period of revascularization by artificial ligaments.

This applies to:

massive grafts of the inferior extremity of the femur,
massive grafts of the superior or inferior extremity of the tibia,
grafts of the humeral head,
partial grafts of the elbow.

Complete Articular Grafts

A total joint graft with its capsule, its synovial membrane, its ligaments, and the fibrocartilages it contains (meniscus or labrum) is indicated in the case of an extensive tumoral lesion in the joint cavity justifying extensive excision in a single piece.

The problems posed are twofold:

Immunological: connected with the size of the immunologically competent material implanted with apparently an inflammatory reaction which could result in a cutaneous fistula giving rise to an infection.

Mechanical: the ligaments must not be strained during the period of their revascularization and have to be doubled up by artificial ligaments.

Reconstruction Prostheses Sheathed with Bone from a Bone Bank

The indications for using a prosthesis sheathed with bone from a bone bank are often present and have to be analyzed according to the extent of the loss of musculo-ligament and cutaneous substance which requires tumoral excision or which has been produced by the trauma.

Conclusion

It seems to us to be important to emphasize the fact that grafts have to be preserved without breaking the cold chain, without damaging the bags containing the graft, and under strictly technological conditions. The importance of the sterile environment for removing the graft has to be emphasized; for example, out of more than 5,000 parts preserved in the Blood Transfusion Center in Marseilles since 1981, we have had to destroy barely 2 % due to a super-infection being found. These encouraging results are due to extreme rigor in the ways in which the grafts are removed and the patients are selected. In our opinion, these preservation methods are the only ones which allow the bone, and particularly the cartilage, to still be guaranteed a normal structure and also good mechanical properties.

Appendix

Recommendations for Setting Up a Tissue Bank for the Locomotor Apparatus

These recommendations are those used by the Blood Transfusion Center of Marseilles to, among other things, preserve bone, cartilage, and ligament grafts.

The Organization of a Tissue Bank

General

The need for:

a tissue removal team approved by the Ministry, a geographical location for treating, storing, and making the tissue available.

Equipment

A preservation department equipped with storage tanks or apparatus, a temperature-lowering programmer indispensable for preserving bone, cartilage, and ligament tissue.Laboratories experienced in the following quality controls:

donor control,
tissue control,
validation of the preservation techniques.

Personnel

At the hospital:

the person in charge of tissue removal checks that removal from a subject in a state of brain death is in line with the regulations,
the surgical teams remove and treat the tissue.

At the tissue bank:

the bank receives the tissue,
the technical staff at the bank treats the tissue,
the laboratories perform viral serological tests on the donor and a bacteriological examination of the tissue removed,
the bank's medical supervisor oversees everything.

Techniques

For each tissue, all the technical aspects of the removal, treatment, storage, quality control, distribution, and results of examinations are recorded in a manual updated regularly.

Information

Information on the donor:

Identity, sex, age;
Radiography of the tissue if necessary;
Cause of death;
Medical history;
ABO blood group and HLA if known;
Operating protocol of removal, therapies used;
Results of any laboratory examinations;
Results of the control examinations;
Tissue removal center and department.

Information on the host:

Identity, sex, age;
Origin of the graft;
Attribution criteria;
Identification of the use of the graft, site and date;
Possible response to implantation of the graft;
ABO blood group and HLA if known;
Results of the culture at the time of the graft;
Note any departure from the guidelines for handling and reconstitution;
An estimate of the clinical results.

Quality Control

Each tissue preservation department has to take part in the development of the methods which make it possible to evaluate the indications of the tissue grafts preserved. Periodical monitoring of the bacteriological status has to be practiced, checking, before they are dispatched, at least 5 % of the grafts every 6 months and more if problems with bacterial contamination are suspected.

Tissue Removal

General Ethical and Legal Considerations

In general, acceptable sources of tissues are cadavers less than 6 h after circulation has stopped, patients in a state of brain death, and patients who

have had part of their tissue removed for therapeutic purposes (femoral head).The Caillavet law considers a donor to be any person who, during his lifetime, did not express any opposition to removal of his or her tissue. It is difficult, in practice, not to consider the pain suffered by those close to the person they have lost.

Selection Criteria

These vary depending on the tissue removed. Age may be a limiting factor following the use which will be made of the tissue taken. For cartilage in particular, it seems to be necessary to graft only normal joint surfaces which have been taken from healthy subjects.

Tissue may be removed from the cadaver for 5 h after his or her death if it is kept at ambient temperature and for approximately 12 h if the cadaver is stored at 4 °C immediately after death. The tissue removed from a live patient can be placed in a container, closed immediately and refrigerated at 4 °C. A valid preservation technique can be considered to be up to 12 h after the tissue has been removed and stored at the preservation temperature.

A medical history of the donor has to be sent. Potential donors will be excluded if their current medical history mentions:

developing septicemia,
a localized infection in the tissue to be removed,
a slowly developing viral episode
malignant neoplasia except for most of the cerebral tumors,
the existence of active hepatitis or unexplained jaundice,
systemic disease,
a patient belonging to the risk groups,
heavy irradiation on risk groups,
treatment with drugs which are toxic to the tissue to be removed.

Laboratory tests have to be performed on the blood of the cadaver or on the live donor:

a test for the hepatitis B virus,
a test for syphilis,
a test for HIV antibodies,
the transaminase levels,
a test for anti-HBc antibodies,
a test for anti-HCV antibodies,
a test for anti-HTL V1 and anti-HTL V2 antibodies
a test for anti-CMV antibodies.

The erythrocyte blood groups and tissue groups should be used and a serum bank should be set up.

Wherever possible, the tissue should be removed under sterile conditions in an operating theatre. If the allografts are removed in a non-sterile manner, it should be ensured that effective sterilization techniques can be used without damaging the tissue structure.

If a collecting medium is used, it has to be sterile and physiological.

If antibiotics are used, the bacterial cultures have to be grown before they are added and the type of antibiotics has to be clearly recorded. A final bacteriological check is recommended before the tissues are dispatched.

Fragments of tissues to be grafted have to undergo bacteriological and fungal studies using current methods and media. Cultures of the donor blood have to be carried out when the tissue is removed as well as a urine culture and possibly also a culture of a pleural effusion.

Secondary sterilization. If it is carried out, the biological and biochemical integrity of the graft has to be maintained. The methods used for decontaminating surfaces are acceptable if only the surface can be contaminated.

Preservation and Storage

The methods used to preserve and store tissue allografts vary according to the type of tissue and the clinical application in which they are included. Although the optimum methods have not been defined, the best for long-term preservation would appear to be preservation at very low temperatures (−80 °C). Continuous monitoring of the temperature may be necessary. Storage for 12 h at the most at 4 °C may be practiced from the time the tissue was removed. Only materials which are resistant to low temperatures are suitable for this type of preservation. They have to be sterile. The culture media may vary and have to

be defined for each type of cell. Precautions have to be taken to check the persistence of the activity of the cells being cultured and for the absence of contamination.

Bibliography

1. Babin SR, Katzner M, Vidal PH, Simon P, Kempf JF, Keiling R, Schvingt E. Résection – reconstruction diaphysaire fémorale par allogreffe massive fixée par clou médullaire vérouillé. Rev Chir Orthop Reparatrice Appar Mot. 1987;73:25–9.
2. Beaver RJ, Mahomed M, Bachstein D, Davis A, Zukor DJ, Gross AE. Fresh osteochondral allografts for post-traumatic defect in the knee. J Bone Joint Surg Br. 1992;74-B:105–10.
3. Brooks DB, Heiple KC, Herdon CH, Powell AE. Immunological factors in homogenous bone transplantation. IV The effect of various methods of preparation and irradiation on antigenicity. J Bone Joint Surg. 1969;45A:1617.
4. Brown K, Crues SR. Bone and cartilage transplantation, in orthopeadic surgery. J Bone Joint Surg Am. 1982;64:270–9.
5. Burchardt H. The biology of bone graft repair. Clin Orthop. 1983;174:121–35.
6. Burchardt H, Enneking WF. Transplantation of bone. Surg Clin North Am. 1978;58:409.
7. Burchardt H, Jones H, Gloweczewskie F, Rudner C, Enneking WF. Freeze-dried allogeneic segmental cortical bone grafts in dogs. J Bone Joint Surg. 1978;60A:1082.
8. Burwell RG. Studies in the transplantation of bone. V. The capacity of fresh and treated homografts of bone to evoke transplantation immunity. J Bone Joint Surg. 1963;45B:386.
9. Burwell RG. The fate of bone grafts. In: Apley AG, editor. Recent advances in orthopeadic. Baltimore: The Williams & Wilkins Co; 1969. p. 115.
10. Burwell RG. The fate of freeze-dried bone allografts. Transplant Proc. 1976;8 Suppl 1:95.
11. Burwell RG, Gowland G. Studies in the transplantation of bone. III. The immune responses of lymphnodes draining components of fresh homologous cancellous bone and homologous bone treated by different methods. J Bone Joint Surg. 1962;44B:131.
12. Burwell RG, Gowland G, Dexter F. Studies in the transplantation of bone. VI Further observations concerning the antigenicity of homologous cortical and cancellous bone. J Bone Joint Surg. 1963;41B:597.
13. Carr CR, Hyatt GW. Clinical evaluation of freeze-dried bone grafts. J Bone Joint Surg. 1955;37A:549.
14. Carrel A. La conservation des tissus et ses applications en chirurgie. J Am Med – Techniques chirurgicales orthopédique, Paris. 1984;44090:4–7–10.
15. Chalmers J. Transplantation immunity in bone grafting. J Bone Joint Surg. 1959;41B:160.
16. Charpentier B. Mécanisme du rejet des allogreffes. Presse Med. 1984;13:2697–700.
17. Chrisman OD, Fessel JM, Southwick WO. Experimental production of synovitis and marginal articular exostose in the knee joint of dogs. Yale J Biol Med. 1964;37:409.
18. Coutelier L, Delloye CH, De Nayer P, Vincent A. Aspects microradiographiques des allogreffes osseuses chez l'homme. Rev Chir Orthopédique. 1984;70:581–8.
19. Cracchiolo III A, Michaeli D, Goldberg LS, Fudenberg HH. The occurrence of antibodies to collagen in synovial fluids. Clin Immunol Immunopathol. 1975;3:567.
20. Curran WJ. The uniform anatomical gift act. N Engl J Med. 1969;280:36.
21. Darcy DA. Reaction of rabbits to frozen homografts. Pathol Bacteriol. 1955;70:143.
22. Devries PH, Badgley CE, Hartman JT. Radiation sterilization of homogenous-bone transplants utilizing radioactiv cobalt. Preliminary report. J Bone Joint Surg Am. 1958;40:187–203.
23. Duffy P, Wolf J, Collins G, De Voe AG, Streeten B, Cowen D. Possible person-to-person transmission of Creutzfeld-Jacob disease. N Engl J Med. 1974;290:692.
24. Duparc J, Nordin JY, Olivier H, Augereau B. Les résections-reconstructions dans les tumeurs osseuses des membres et du bassin. Encycl Méd Chir – Techniques Chirurgicales Orthopédie. 1984;44090:4–7–10.
25. Elves MW. Humoralimmune response to allografts of bone. Int Arch Allergy Appl Immunol. 1974; 47:708.
26. Elves MW. Newer knowledge of immunology of bone and cartilage. Clin Orthop. 1976;120:232.
27. Elves MW, Ford CHJ. A study of the humoral immunce response to osteoarticular allografts in the sheep. Clin Exp Immunol. 1974;17:497.
28. Friedlaender GE. Current concepts. Review: bone-banking. J Bone Joint Surg Am. 1982;64:307–11.
29. Friedlaender GE. Immune response to osteochondral allografts. Clin Orthop. 1983;174:58–67.
30. Friedlaender GE, Ladenbauer-Bellis I, Chrisman OD. Cartilage matrix components as antigenic agents in a osteoarthritis model. Trans Orthop Res Soc. 1980;5:170.
31. Friedlaender GE, Mankin HJ. Guidelines for the banking of musculoskeletal tissues. Am Assoc Tissues Banks Newsletter. 1980;4(suppl):30.
32. Friedlaender GE, Mankin HJ, Kenneth W. Osteochondral allografts (biology, banking and clinical applications). Boston Toronto: Little Brown; 1982.
33. Friedlaender GE, Strong DM, SELL KW. Studies on the antigenicity of bone. I. Freeze-dried and deep-frozen bone allografts in rabbits. J Bone Joint Surg. 1976;58A:854.
34. Friedlaender GE, Strong DM, Sell KW. Donor graft specific anti-HL-A antibodies following freeze-dried bone allografts. Trans Orthop Res Soc. 1977;2:87.

35. George CR, Chrisman OD. The role of cartilage polysaccharides in osteoarthritis. Clin Orthop. 1968;57:259.
36. Glant T, Hadas E, Nagry TJ. Cell-mediated and humoral immune responses to cartilage antigenic components. Scand J Immunol. 1979;9:29.
37. Golberg V, Heiple K. Experimental hemijoint and whole transplantation. Clin Orthop. 1983;174: 43–53.
38. Goldberg V, Bos G, Heiple K, Zita J, Powell A. Improved acceptance of frozen bone allografts in genetically mismatched dogs by immunosuppression. J Bone Joint Surg Am. 1984;66:937–50.
39. Greiff D, Milson TJ. Functional activities of isolated lymphocytes following drying by sublimation of ice *in vacus*. I. Rosette formation, stimulation by plant lectins (mitogens) and the mixed lymphocyte reaction. Cryobiology. 1980;17:319.
40. Gresham RB. The freeze-dried cortical bone homograft: a roentgenographic and histologic evaluation. Clin Orthop. 1964;37:194.
41. Gross AE, Langer F, Houpt J, Pritzker K, Friedlander CE. The allotransplantation of the partial joints in the treatment of osteoarthritis of the knee. Transplant Proc. 1976;8(Suppl I):129.
42. Gross AE, Langer F, Silverstein EA, Falk R, Falk J. The allotransplantation of the partial joints in the treatment of osteoarthritis of the knee. Clin Orthop. 1975;108:7–14.
43. Gross A, Mc Kee N, Pritzker K, Langer F. Reconstruction of skeletal deficit at the knee. Clin Orthop. 1983;174:96–106.
44. Guilleminet S, Dubost-Perret JA. Utilisation d'os hétérogènes réfrigérés en chirurgie humaine. Lyon Chir. 1952;47(1):57.
45. Hedde C, Postel M, Kerboul M, Courpied JP. La réparation du cotyle par homogreffe osseuse conservée au cours des révisions de prothèse totale de hanche. Rev Chir Orthop. 1986;72:267–76.
46. Heiple KG, Chase SW, Herndon CH. A comparative study of the healing process following different types of bone transplantation. J Bone Joint Surg. 1963;45A:1593.
47. Hiky V, Mankin HJ. Radical resection and allograft replacement in the treatment of bone tumors. J Jpn Orthop Assoc. 1980;54:475.
48. Houff SA, Burton RC, Wilson RW, et al. Human-to-human transmission of rabies virus by corneal transplant. N Engl J Med. 1979;300:603.
49. Huten D. Utilisation des allogreffes osseuses dans les reconstructions fémorales au cours des reprises de prothèse totale de hanche. Rev Chir Orthop. 1988;74:122–4.
50. Hyatt GW, Butler MC. Bone grafting. The procurement storage and clinical use of bone homograft. In: America Association of Orthopeadic Sugeons: Instructional courses lectures, vol. 14. Ann Arbor, Mich: J.W. Edwards Co; 1957. p. 343.
51. Inclan A. L'emploi des greffes osseuses conservées en Orthopédie. J Bone Joint Surg. 1942;26:81–96.
52. Inclan A. Use of preserved bone graft in orthopeadic surgery. J Bone Joint Surg. 1942;26:81.
53. James JIP. Tuberculosis transmitted by banked bone. J Bone Joint Surg. 1953;35B:578.
54. Judet J, Aviset A. Homogreffes provenants de la banque d'os. Mem Acad Chir N. 1948;27–8:671.
55. Judet H, Padovani JP. Transplantation d'articulation complète. Rev Chir Orthop. 1983;67:359–60.
56. Koskinen EV, Salenius P, Alho A. Allogeneic transplantation inlow-grade malignant bone tumors. Acta Orthop Scand. 1979;50:129.
57. Kossowska-Paul B. Studies on the regional lymph node plastic reaction evoked by allogeneic grafts of fresh and preserved bone tissue. Bull Acad Polon Sci. 1966;14:651.
58. Kruez FP, Hyatt GW, Turner TC, Basset al. The preservation and clinical use of freeze-dried bone. J Bone Joint Surg. 1951;33AA:863.
59. Langer F, Czitrom A, Pritzker KP, Gross AE. The immunogenicity of fresh and frozen allogeneic bone. J Bone Joint Surg. 1975;57A:216.
60. Lee EH, Langer F, Halloran P, Gross AE, Ziv I. The effect of major and minor histocompatibility differences on bone transplant healing in inbred mice. Trans Orthop Res Soc. 1979;4:60.
61. Lee EH, Langer F, Halloran P, Gross AE, Ziv I. The immunology of osteochondral and massive allografts. Trans Orthop Res Soc. 1979;4:61.
62. Lexter E. Die verwendung der freien knochenplastik nebst versuchen über gelenkversteifung und gelenktransplantation. Arch Klin Chir. 1908;86:939.
63. Lexter E. Joint transplantation and arthroplasty. Surg Gynecol Obstet. 1925;40:782.
64. Locht R, Gross A, Langer F. Late osteochondral allograft resurfacing for tibia plateau fractures. J Bone Joint Surg Am. 1984;66:328–35.
65. Macewen W. Observations concerning transplantation of bone. Illustrated by case of inter-human osseous transplantation, where by over two-thirds of shaft of a humerus was restored. Pro R Soc Lond. 1881;32:232.
66. Mankin HJ, Doppelt SH, Sullivan TR, Tomford WW. Osteoarticular and intercalary allograft transplantation in the management of malignant tumors of bone. Cancer. 1983;50:613.
67. Mankin HJ, Doppelt SH, Tomford WW. Clinical experience with allograft implantation. Clin Orthop. 1983;174:69–86.
68. Mankin HJ, Fogelson FS, Trasher AZ, Jaffer F. Massive resection and allograft transplantation in the treatment of malignant bone tumors. N Engl J Med. 1976;294:1247.
69. Marsh B, Flynn L, Enneking W. Immunologic aspects of osteosarcoma and their application to therapy, a preliminary report. J Bone Joint Surg. 1972;54A:1367.
70. Merle D'Aubigne R. A propos de la résection pour tumeurs du genou. Rev Chir Orthop. 1963;67:359–60.
71. Meyers MH, Chatterjee SN. Osteochondral transplantation. Surg Clin North Am. 1978;58:429.
72. Mnaymneh W, Emerson RH, Brajao F, Head WC, Malinin TI. Massive allografts in salvage revision

of failed total knee arthroplasties. Clin Orthop. 1990;269:144–53.
73. Musculo DL, Kawai S, Ray RD. Cellular and humoral immune response analysis of bone-allografted rats. J Bone Joint Surg. 1976;58A:826.
74. Nimelstein SH, Hotti AR, Homan HR. Transformation of a histocompatibility immunogen into a tolerogen. J Exp Med. 1973;128:723.
75. Ollier L. Traité expérimental et clinique de la régénération des os. Paris: Victor Masson & fils; 1867.
76. Ottolenghi CE. Massive osteo and osteo-articular bone grafts: technic and results of 62 cases. Clin Orthop. 1972;87:156.
77. Parrish FF. Allograft replacement of all part of the end of a long bone following excision of a tumor: report of twenty-one cases. J Bone Joint Surg. 1973;55A:1.
78. Pelkers R, Friedlander G, Markham T. Biomechanical properties of bone allografts. Clin Orthop. 1983;174:54–7.
79. Penn I. The incidence of malignancies in transplant recipients. Transplant Proc. 1975;7(2):323.
80. Poitout D. Greffes utilisées pour reconstruire l'appareil locomoteur. Paris: Masson; 1986.
81. Poitout D. Future of bone allografts in massive bone resection for tumor. Presse Med. 1996;25(11):527–30.
82. Poitout D. Reconstruction du cotyle et de l'hémibassin par allogreffe ou prothèse méttalique massive sur mesure. 73ème Réunion Annuelle de la S.O.F.C.O.T. – Paris les 10–13 novembre 1998. Revue de chirurgie Orthopédique. 1998;84(218):120–1.
83. Poitout D. Allografts of the patella and extensor apparatus. Atlas of open knee surgery. London/Paris: Edition Chapman & Hall; 1996. p. 42–9.
84. Poitout D. Allotraplanto della rotula e dell'apparato estensor. Atlante di technica chirurgica del ginocchio. Milan: Edition Masson; 1995. p. 42–9.
85. Poitout D. Banche d'osso: aspetti tecnici criopreservazione di allotraplanti osteocartilagineo. Atlante di technica chirurgica del ginocchio. Milan: Edition Masson; 1995. p. 178–9.
86. Poitout D. Bone bank: technical aspects of cryopreservation osteocartilaginous grafts. Atlas of open knee surgery. London/Paris: Edition Chapman & Hall; 1996. p. 178–9.
87. Poitout D. Conservation et utilisation de l'os de banque. Cahier d'enseignement de la S.O.F.C.O.T N°23. Expansion scientifique. Conférence 1985. p. 157–77.
88. Poitout D. Knee reconstruction prosthesis incorporating a large allograft. Atlas of open knee surgery. London/Paris: Edition Chapman & Hall; 1995. p. 145–51.
89. Poitout D. L'os biomateriaux. « Bulletin de l'Académie de Nationale de médecine ». Communication à l'Académie Nationale de Médecine. Paris, 14 mars 1995. 1995;179;3:517–36.
90. Poitout D. Les greffes de l'appareil locomoteur. Académie de Chirurgie (Paris, 10 avril 1996). « Mémoire de l'académie de Chirurgie ». 1996.
91. Poitout D. Les reconstructions de cotyle après chirurgie iterative de la hanche. (A propos de 37 cas). Académie Nationale de Médecine. Paris, 5 mars 1996. Bulletin de l'Académie de Nationale de médecine . 1996;180;3:515–31.
92. Poitout D. Protesi di ricostruzione di ginocchio con allotraplanto massivo. Atlante di technica chirurgica del ginocchio. Milan: Edition Masson; 1995. p. 145–51.
93. Poitout D, Bernat M, Martin G, Tropiano P. Indications des greffes osteocartilagineuses massives en traumatologie du genou. Acta Orthopedica Belgica. 1996;62(6):59–65.
94. Poitout D, Bernat M, Martin G, Tropiano P. Indications des greffes osteo-cartilagineuses massives en traumatologie du genou. Acta Orthopaedica Scandinavica. Edition Scandinavian University Press, vol. 62, 1997; suppl. 1.
95. Poitout D, Bernat M, Moulene JF, Tropiano P. Allogreffes de cotyle et d'hémi-bassin. A propos de 37 cas. 71ème Réunion Annuelle de la S.O.F.C.O.T. – Paris les 12–15 novembre 1996. Revue de chirurgie Orthopédique. 1996;87(152):100.
96. Poitout D, Bernat M, Moulene JF, Tropiano P. Devenir des fractures du col du fémur. 71ème Réunion Annuelle de la S.O.F.C.O.T. – Paris les 12–15 novembre 1996. Revue de chirurgie Orthopédique. 1996;87(153):100–1.
97. Poitout D, Bernat M, Moulene JF, Tropiano P. Indications for cryopreserved allografts in tumoral pathology. Eur J Orthop Surg Traumatol. 1997;7:100–4.
98. Poitout D, Bernat M, Moulene JF, Tropiano P. Massive HIP prothese ensheated by allografts. Eur J Orthop Surg Traumatol. 1997;7:123–6.
99. Poitout D, Bernat M, Moulene JF, Tropiano P. Allogreffes osteochondrales ou prothèses articulaires en chirurgie traumatologique ou oncologique du genou. 71ème Réunion Annuelle de la S.O.F.C.O.T. – Paris les 12–15 novembre 1996. Revue de chirurgie Orthopédique. 1996;69–70, 87–99.
100. Poitout D, Dubousset JF, Tomeno B. Arthrectomie monobloc du genou. Revue de Chirurgie Orthopédique. 1995;81–6:565, Paris.
101. Poitout D, Lempadakis M, Bernat M, Lecoq C, Martin G, Aswad R. Secondary internal osteosynthesis after fixation for recent or lower limb. Revue de chirurgie orthopédique Réparatrice. 1996;82(2):137–44.
102. Poitout D, Lempidakis M. Artificial ligament repairs. Atlas of open knee surgery. London/Paris: Edition Chapman & Hall; 1996. p. 76–85.
103. Poitout D, Lempidakis M. Legamentoplastiche artificiali. Atlante di technica chirurgica del ginocchio. Milan: Edition Masson; 1995. p. 76–85.
104. Poitout D, Lempidakis M, et Loncle X, Bernat M. Les sarcomes ostéogeniques de l'extrêmité inférieur du fémur. Techniques de reconstruction – L'avenir. « Revue de Chirurgie Orthopédique », Communication à l'Académie Nationale de Chirurgie, Paris le 29 mars 1995. 1995;566:81–6.
105. Poitout D, Lempidakis M, et Loncle X, Bernat M. Reconstructions massives du cotyle et du fémur proximal. Académie de Chirurgie (Paris, 1994). «

Mémoire de l'académie de Chirurgie » Tome N°5, 1994–5;120.
106. Poitout D, Lempidakis M, et Loncle X. Allotraplanto osteo-cartilagineo massive dell'estremita inferiore del femore. Atlante di technica chirurgica del ginocchio. Milan: Edition Masson; 1995. p. 164–9.
107. Poitout D, Lempidakis M, et Loncle X. Allotraplanto osteocartilagineo massivo dell'estremita superiore della tibia. Atlante di technica chirurgica del ginocchio. Milan: Edition Masson; 1995. p. 170–7.
108. Poitout D, Lempidakis M, et Loncle X. Osteocartilaginous graft of the lower extremity of the femur. Atlas of open knee surgery. London/Paris: Edition Chapman & Hall; 1996. p. 164–9.
109. Poitout D, Lempidakis M, et Loncle X. Osteocartilaginous graft of the upper tibia. Atlas of open knee surgery. London/Paris: Edition Chapman & Hall; 1996. p. 170–7.
110. Poitout D, Loncle X. Legamento crociato posteriore. Atlante di technica chirurgica del ginocchio. Milan: Edition Masson; 1995. p. 86–8.
111. Poitout D, Loncle X. Posterior cruciate ligament. Atlas of open knee surgery. London/Paris: Edition Chapman & Hall; 1996. p. 86–8.
112. Poitout D, Lu J, Huang ZW, Tropiano P, Clouet D'Orval B, Remusant M, Dejou J, Proust JP. Human biological reactions at the interface between bone tissues and poly-methylmethacryalate cement. J Mater Sci Mater Med. 2000;13:803–9.
113. Poitout D, Nandiegou Y, Lempidakis M. Artificial ligament repair. Atlas of open knee surgery. London/Paris: Edition Chapman & Hall; 1996. p. 89–93.
114. Poitout D, Nandiegou Y, Lempidakis M. Legamentoplatica artificiale. Atlante di technica chirurgica del ginocchio. Milan: Edition Masson; 1995. p. 89–93.
115. Poitout D, Novakovich G. Allogreffes et banque d'os. Encyclopédie Médico-chirurgicale (Paris-France), appareil locomoteur 14015AIO, 1986; 5–6.
116. Poitout D, Ozoux P. Intra-articular repair of the posterior cruciate ligament using either semitendinosus or gracilis tendons (Lindenmann's operation). Atlas of open knee surgery. Edition Chapman & Hall; 1996. p. 94–5.
117. Poitout D, Tropiano P. Les reconstitutions du cotyle après chirurgie iteractive de la hanche – A propos de 37 cas. Bull Acad Natl Med. 1996;180(3):515–31.
118. Poitout D, Tropiano P, Bernat M, Loncle X, Martin G. Greffes articulaires, mythe ou réalité? Entretiens de Bichat 1995. Paris 25–30 septembre 1995. Chirurgie-Spécialité. 1995;43–6.
119. Poitout D, Tropiano P, Bernat M, Moulene JF. Reconstruction massive de cotyle et du fémur proximal. Les Arcs, 20–25 janvier 1996. «Eur J Orthop Surg Traumatol». 1996;6:271–7.
120. Pool AR, Reiner A, Choi H, Rosenberg LC. Immunological studies of proteoglycan subunit from bovine and human cartilage. Trans Orthop Res Soc. 1979;4:55.
121. Pujet J, Utheza G. Reconstructionde l'os iliaque à l'aide du fémur homoilatéréal après résection pour tumeur pelvienne. Rev Chir Orthop. 1986;72:151–5.
122. Rodrigo JJ. Distal rat femur allografts: a surgical model for induction of humoral cytotoxic antibodies. Trans Orthop Res Soc. 1977;2:265.
123. Rodrigo JJ, Fuller TC, Mankin HJ. Cytotoxic HL-A, antibodies in patient with bone and cartilage allografts. Trans Orthop Res Soc. 1976;1:131.
124. Roy-Camille R, Laugier A, Ruyssen S, Chenal C, Bisserie M, Pene F, Saillant G. Evolution des greffes osseusescortico-spongieuses et radiothérapie. Rev Chir Orthop. 1981;67:599–608.
125. Sadler AM Jr, Sadler BL. Providing cadaver organs: three legal alternatives. Hastings Center Studies I. 1973;14.
126. Sadler Jr AM, Sadler BL, Stason EB, Stickel DL. Transplantation – A case for consent. N Engl J Med. 1969;280:862.
127. Sagi S, Turianskyj FH, Gyenes L. Immunogenicity of soluble murine histocomptabilicity antigens. Immunol Commun. 1974;3:85.
128. Salama R. Xenogeneic bone grafting in humans. Clin Orthop. 1983;174:113–21.
129. Schachar NS, Friedlander GE, Mankin HJ. Bone transplantation. In Slavin S, editor. Organ transplantation: present state, future goals. Amsterdam: Elsevier/North-Holland Biomedical Press B.V. 1978 (in press).
130. Schachar NS, Fuller TC, Wadsworth PL, Henry WB, Mankin HJ. A feline model for the study of frozen osteoarticular allografts. Development of lymphocytotoxic antibodies in allograft recipients. Trans Orthop Res Soc. 1978;3:131.
131. Schachar NS, Mankin HJ, Wadsworth PL, Henry WB, Castronovo FP. A feline model for the study of frozen osteoarticular allografts. I. Quantitative assessment of cartilage viability and bone healing. Trans Orthop Res Soc. 1978;3:130.
132. Sell KW, Friedlander GE, editors. Tissues banking for transplantation. New-York: Grune & Stratton, Inc; 1976.
133. Sell KW, Friedlander GE, Strong DM. Immunogenicity and freeze-drying. Cryoimmunology. 1976;17:187.
134. Shneider JR, Bright RW. Anterior cervical fusion using preserved bone allografts. Transplant Proc. 1976;8(suppl):73.
135. Shutkin NM. Homologous-serum hepatitis following use of refrigerated bone-bank bone: report of case. J Bone Joint Surg. 1954;36A:160.
136. Solomon L. Bone Grafts. J Bone Joint Surg Am. 1991;73-B:706–7.
137. Spence KF, Sell KW, Brown RH. Solitary bone cyst: treatment with freeze-dried cancellous bone allograft. J Bone Joint Surg. 1969;51A:87.
138. Stockley I, Mc Auley JP, Gross AE. Allograft reconstruction in total knee arthroplasty. J Bone Joint Surg Am. 1992;74-B:393–7.
139. Syftestad G, Urist M. Bone aging. Clin Orthop. 1982;162:288–97.

140. Takagi K, Urist M. The reaction of the dura to bone morphogenetic protein (BMP) in repair of skull defects. Ann Surg. 1982;196:100–9.
141. Takagi K, Urist M. The role of bone marrow in bone morphogenetic protein-induced repair of femoral massive diaphyseal defects. Clin Orthop. 1982;171:224–30.
142. Takami H, Doi T, Ninomiya S. Reconstruction of a large tibial defect with a free vascularized fibular graft. Arch Orthop Surg. 1984;102:203–5.
143. Tavernier. Sur les greffes d'os tué. Lyon Chir., 1922, séance du 17 novembre 1921. Utilisation d'os purum. Lyon Chir 1930.
144. Tomford WW, Fredricks GR, Mankin HJ. Cryopreservation of intact articular cartilage. Trans Orthop Res Soc. 1982;7:176.
145. Tomford WW, Fredricks GR, Mankin HJ. Cryopreservation of isolated chondrocytes. Trans Orthop Res Soc. 1982;6:100.
146. Tomford WW, Mankin HJ, Doppelt S. Bone bank procedures. Clin Orthop. 1983;174:15–21.
147. Tomford WW, Starkweather RJ, Golman MH. A study of the clinical incidence of infection in the use of banked allograft bone. J Bone Joint Surg. 1981;63A:244.
148. Trentham DE, Townes AS, Kang AH, David JR. Humoral and cellular sensitivity to collagen in type II. Collagen induced arthritis in rats. J Clin Invest. 1978;61:89.
149. Tuffier. Des greffes chirurgicales chez l'homme. Bull et Mém Soc Chir 36, 1983, Paris 1910.
150. Urist MR. Practical applications of basic research on bone graft physiology. In: AAOS: Instructional Course Lectures, vol. 25:1. St Louis: The C.V. Mosby Co; 1976.
151. Urist MR, Delange R, Finermann G. Bone cell differentiation and growth factors. Science. 1983;220:680–6.
152. Urist MR, Mikulski A, Boyd SD. A chemosterilized antigen-extracted autodigested alloimplant for bone banks. Arch Surg. 1975;110:416.
153. Urist MR, et al. Human bone morphogenetic protein. Proc Soc Exp Biol Med. 1983;173:194–9.
154. Volkov M. Allotransplantation of joints. J Bone Joint Surg Br. 1970;52B:49–53.
155. Volkov M, Imamaliyev AS. Use of allogenous articular bone implants as substitutes for autotransplants in adult patients. Clin Orthop. 1976;114:192.
156. Weiland A, Moore R, Daniel R. Vascularized bone autografts. Clin Orthop. 1983;174:87–95.
157. Weislander J, Heinegard D. Immunochemical analysis of cartilage proteoglycans: antigenic determinants of substructures. Biochem J. 1979;179:35.
158. Wilson PD. Follow-up study of the use of refrigerated homogenous bone transplants in orthopaedic operations. J Bone Joint Surg. 1951;33A:307.
159. Wilson RE, Penn I. Fate of tumors transplanted with a renal allograft. Transplant Proc. 1975;7(2):327.
160. Wittbjer J, Palmer B, Rohlin M, Thorngren K. Osteogenetic activity in composite grafts of demineralized compact bone and marrow. Clin Orthop. 1983;173:229–38.
161. Yablon I, Brandt KD, Delellis RA. The antigenic determinants of articular cartilage: their role in the homograft rejection. Trans Orthop Res Soc. 1977;2:90.
162. Yablon I, Copperband S, Covall D. Matrix antigens in allografts. Clin Orthop. 1982;168:243–51.
163. Yamane K, Nathenson SG. Biochemical similarity of papain-solubilized H-2d, alloantigens from tumor cells and from normal cells. Biochemistry. 1970;9:4743.
164. Zaleske D, Ehrlich M, Piliero C, May J, Mankin HJ. Growth plate behavior in whole joint replantation in the rabbit. J Bone Joint Surg Am. 1982;64: 249–57.

Formulated Demineralized Bone Grafts for Skeletal Applications

8

Todd M. Boyce

Demineralized bone matrix, is human allograft bone that is treated using acid to remove the mineral component, providing a cell-free, tissue-based biomaterial. In addition to acid treatment, the tissue receives other processes to decellularize the tissues and to inactivate any viruses, bacteria, or fungi that may be present. Demineralized bone is the extracellular matrix of human bone, treated to separate out the inorganic calcium phosphate portion and to retain the organic collagen and non-collagenous proteins.

Demineralized bone is osteoinductive, meaning that it is an active signaling component of bone healing rather than merely a passive scaffold. It is the extracellular matrix of human bone, including collagen and a variety of naturally-occurring growth factors and BMP's that are embedded in the tissue in physiological concentrations. But activity in demineralized bone is a function of the proteins in the matrix, and these proteins can be damaged by certain processes and excipients that may be applied to the tissues. This means that formulated demineralized bone products can vary in their activity, or ability to influence local cells to make bone tissue. Many clinical selections of a formulated demineralized bone matrix are based upon handling and packing characteristics, without an awareness of the importance of processing history and formulation on osteoinductive performance.

While demineralized bone without excipients had been used in some orthopaedic and dental applications for a number of years, it was only with the 1991 introduction [1] of Grafton® Gel, that surgeons began to find the combination of surgical handling characteristics and clinical efficacy that allowed them to routinely use demineralized bone as an off-the-shelf bone healing product. Before this time, such tissues had to be meticulously prepared by the hospital bone bank and delivered individually for a particular case – and then the surgeon was required to find a way to deliver dry, demineralized bone powders to the surgical site in an effective way. Many found that the handling characteristics of powdered demineralized bone were inadequate. Likewise, concerns about safety, and the limited processing capabilities of hospital-based bone banks had argued for a standardized, technology-based approach to the preparation of demineralized bone matrix. With the advent of the first Grafton® forms, demineralized bone matrix products have become consistent, allowing a surgeon to use any volume and any form that is appropriate to his/her particular procedure. The formulated demineralized bone graft contains natural inductive proteins, at physiological concentrations, to assist in bone healing.

At the time that this was written, the author was a Senior Principal Scientist at Osteotech. He is now a Senior Program Manager in Marketing at Medtronic.

T.M. Boyce, PhD
Osteotech, Inc., Eatontown, NJ, USA
e-mail: boyce@osteotech.com

D.G. Poitout (ed.), *Biomechanics and Biomaterials in Orthopedics*,
DOI 10.1007/978-1-84882-664-9_8

Since 1991, a number of additional forms have been developed that attempt to provide additional handling characteristics, offer improved osteoconduction, and are suited to specific procedures.

History of Demineralized Bone

Demineralized bone matrix is a primary source of naturally occurring bone morphogenetic proteins (BMP's) in the skeleton. It was the result of this experimental work on demineralized bone that led Urist to identify the process of osteoinduction [2]; in turn, it was the search for the proteins responsible for osteoinduction that led to the discovery of bone morphogenetic proteins (BMP's) in demineralized bone [3–7]. This work in demineralized bone [8] provided the research foundations both for today's formulated demineralized bone products and also the recombinant growth factor products [9] that have become available in recent years. It is the natural growth factors and BMP's that are present in bone, which are responsible for its osteoinductive activity.

Demineralization using acids has been well-known for centuries. There is convincing evidence that ivory, elephant dentin, was partly demineralized in vinegar in order to shape ivory sheets for statuary from the classical Greek and Roman times [10]. The acid of the vinegar demineralized the dentin, softening it and allowing it to be formed over a mold without cracking. It is generally accepted that the first surgical applications were developed by Senn [11] in 1889. Senn described several experiments with demineralized, perforated bone to support healing in the cranium of dogs, and then continued on to describe a series of ten osteomyelitis and tuberculosis cases using "antiseptic decalcified bone" at the Milwaukee Hospital from 1887 to 1889. He advocated the use of ox tibia, demineralized in muriatic (hydrochloric) acid, cut into pieces 1 mm thick and stored in a solution of sublimate in alcohol 1:500. The perforations in the demineralized bone were designed to permit early entrance of granulation tissues. In the following year, a colleague, Dr. Mackie, published a series of cases showing the broad applicability of "decalcified bone" [12]. By 1919, demineralized bone was being used in many areas of surgery. A general surgery text [13] listed uses for decalcified bone including Senn's application as a graft in voids and cranial defects, but also as a reinforcement for arterial anastamosis, treatment of joint ankylosis, non-unions (also attributed to Senn), nerve suturing, and as a form over which to suture the intestine. Thus, demineralized bone was used in surgery for nearly five decades before its osteoinductive potential was even discovered.

Osteoinduction, the creation of bone by inducing its formation in a heterotopic site, was described by Huggins in 1930 using urinary tract epithelium [14, 15]. Shortly after, Levander [16] performed a series of rabbit autograft experiments, which led him to the belief that

> (N)ew bone is formed directly out of the mesenchymal tissue which surrounds the graft. For such differentiation to take place in non-specific tissue, must necessarily show that the process is influenced in some way or another by some specific agent.

Levander then continued on in his experiments to seek the hypothetical osteoinductive "agent," by injecting aqueous and then alcohol extracts of bone and callus into the muscles of rabbits. He found osteochondral nodules at the sites of the injection in 22 % of the animals treated. In 1957, Ray and Holloway [17] showed histologically that demineralized bone had improved healing ability over both deproteinized bone and frozen autograft in a rat calvarial defect. They concluded that "*{T}he best substitute for fresh autogenous-bone grafts…..is the organic matrix devoid of its inorganic salt.*"

The concentrated research efforts of Urist in first demonstrating "autoinduction" of new bone and cartilage [2], and later, systematically assessing the "bone induction principle" using demineralized bone and its extracts, are the foundation of much of our understanding of formulated demineralized bone products used in skeletal healing applications. Urist then went on to extract, name and characterize the source of this osteoinductive activity – "Bone Morphogenetic Proteins" [3], which he obtained from demineralized bone by extraction. Since that time, researchers have gone

on to identify most of the growth factors and individual bone morphogenetic proteins that are present in the extracellular matrix of bone. These include BMP 1–7, TGF-β, IGF I and II, PDGF, Basic and Acidic FGF and Osteogenin, among others [18, 19].

Urist's papers provided the initial insights into processes that would be suited to making an inductive demineralized bone product. Urist performed a host of experiments on: effects of gamma irradiation [20, 21], tissue type [22], depth of the demineralization [23], response elicited by demineralized bone in ectopic sites throughout the body [24], functional characterization and localization of BMP's within demineralized bone [3, 4], effects of storage conditions on osteoinductivity of demineralized bone matrix [25], among other contributions. In the 1970s Reddi and Huggins worked to characterize the cellular events and sequence associated with the transformation of demineralized bone [26–28] into living bone tissue. One of the principal lessons of this body of work is that the biological performance of a demineralized bone is directly dependent upon the processing history of the tissue [3, 29]. Small changes in the process can denature the non-collagenous proteins that give the demineralized bone its osteoinductive character, lowering or eliminating activity.

For more than 100 years after Senn began using demineralized bone in a clinical setting, demineralized bone matrix was used in slabs, chips or powders prepared initially by the individual surgeon, and later by hospital bone banks, and then later still, by regional bone banks. With the introduction of Grafton gel in 1991, Osteotech offered the first formulated demineralized bone product. Since then, the Grafton products have been expanded to include such varied formulations as injectable gels, flexible sheets, moldable putties, combinations with radiopaque cancellous chips, and forms that expand upon rehydration to maintain congruity with the surgically prepared surface (Fig. 8.1).

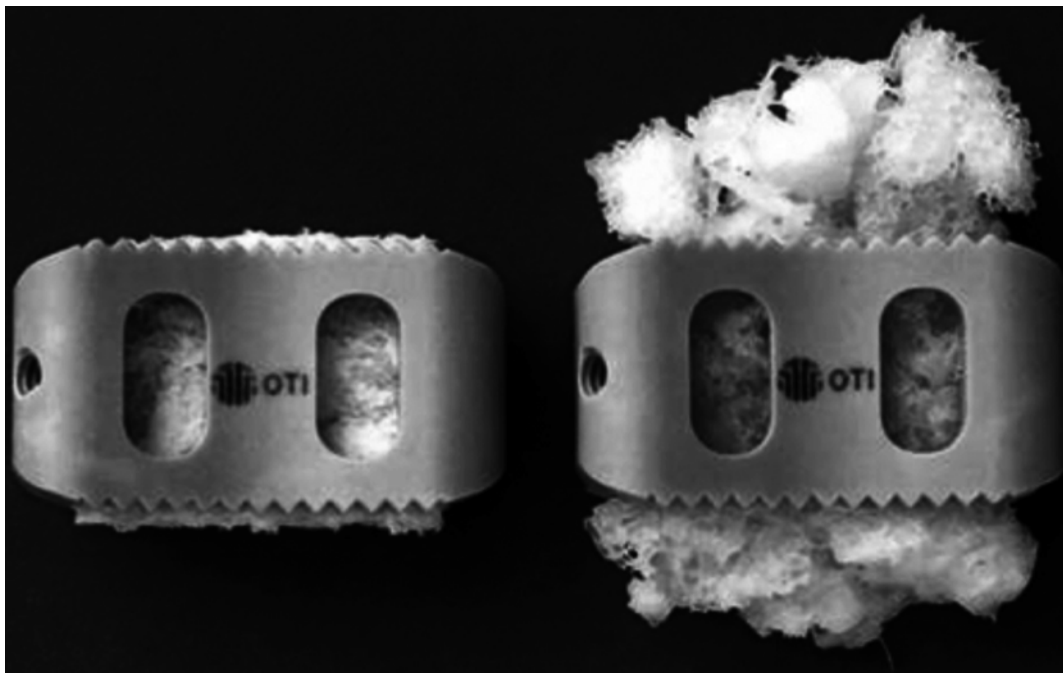

Fig. 8.1 A demineralized bone graft, Xpanse®, which expands when it is rehydrated. By expanding to create direct contact with the prepared host bone surface, it can assist osteogenic cells to travel into the graft

Beginning in the late 1990s a large number of other demineralized bone materials became available from tissue banking organizations, orthopaedic manufacturers, and alliances between the two. In an attempt to provide surgically-relevant handling characteristics using materials that were still outside of the prior patents, a host of carrier materials were introduced for the first time: carboxymethyl cellulose, hyaluronic acid, lipid-based carriers, reverse-phase polymers, among others –though all of these are not equivalent in their biological effects and may contribute to differences in performance. Around this time also, Osteotech developed and assessed various demineralized bone formulations that utilized fiber-based demineralized bone. It was shown that fibers offer distinct advantages in osteoconductivity for the formulation [30].

In the present time, there are a host of demineralized bone-based formulated grafting materials, each with its own group of claimed benefits, and each with significant differences in processing history, carrier materials, methods of achieving safety, and osteoinductive performance.

Demineralized Bone Safety

The safety profile for allograft bone is largely, but not completely, contributed by the process that it undergoes. Early development efforts on demineralized bone products [31–33] included viral, bacteriological and other safety considerations, and led to standardized techniques for demineralized bone processing and viral inactivation treatments. Tissues typically undergo processes that include cutting and shaping steps; milling; treatment with sterile water, alcohol, detergents and acid; freeze drying and packaging. The process is designed in such a way as to kill and remove bacteria, mold, fungi, virus and other potential adventitious agents, in accordance with government regulation and industry standards [34].

Demineralized bone comes from human cadaveric donors, who have made the choice, confirmed by a living family member, to donate tissue for the therapeutic use of an unrelated recipient. As with any human sourced-biologic product, a primary concern is the prevention of disease transmission from implanted tissues. This objective encompasses (1) Screening the donor population to exclude those with high risk; (2) Maintaining an aseptic processing environment that assures tissue sterility, as confirmed by bacteriologic testing; (3) Demonstrating process capabilities that inactivate virus, and (4) Prion considerations.

Screening and Initial Process

Initially, the donated human allograft bone tissue is screened [35] to exclude tissues that contain disease agents, and to exclude those donors that have lifestyle risks or a medical history that suggests risk of disease transmission. Donor selection (Fig. 8.2) starts with review of the medical history for the donor and an interview with a family member. Tissue is then procured aseptically, and stored in the frozen state. At the same time, the tissues are swabbed for bacterial contamination, and blood and tissue samples are obtained The samples go for detailed analysis and assessment for antibodies, antigens and NAT testing for HIV, HTLV, Hepatitis and Syphilis, in CLIA-certified testing laboratories, and using FDA-approved test kits. If an autopsy was performed, its results are obtained. Once the results become available, they are reviewed by the Medical Director (a board-certified physician with additional tissue banking credentials), and suitability is determined. There are many diseases and conditions which disqualify tissues from processing, including a host of diseases that could be transmitted by transplantation, evidence (e.g. recent tattoos) of an activity or lifestyle that increases risk, and conditions (e.g. Alzheimer's disease) that are sometimes mistaken for diseases that are communicable. Careful screening can dramatically reduced the potential for disease transmission – for HIV the risk is reduced to less than 1 in 1.6 million by the screening process [35].

These tissues undergo initial processing steps to remove soft tissues, and also to mill the bone into fibers or to grind it into particles. These particles or fibers then go through a series of solvent,

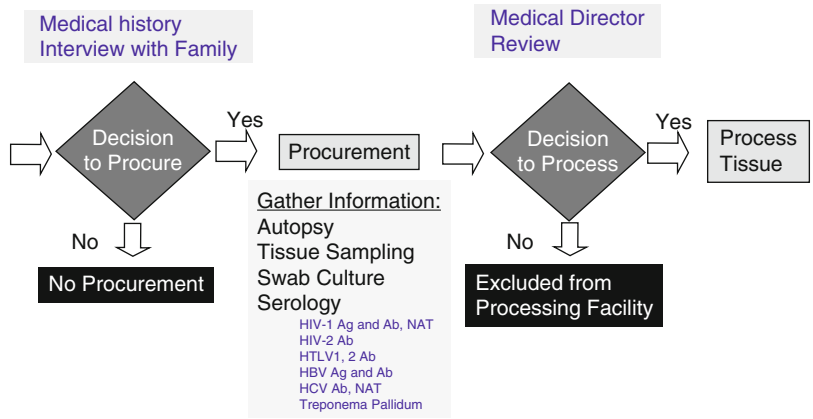

Fig. 8.2 Process for donor selection and suitability. At the first stage, a procurement decision is made, based upon the donor's medical history and an interview with a family member. Once tissue is procured, additional testing is performed, including serology. Prior to processing, all of the medical history, interview, and test results are reviewed and suitability is determined

detergent, and antibiotic treatments to remove remaining cells, and to assure viral inactivation [32, 33]. Hydrochloric acid, the same acid used by osteoclasts during the resorption phase of remodeling, is used to remove the mineral while retaining the protein elements. The result is processed demineralized bone, in a particulate form (fibers or powder, Fig. 8.3).

The processed demineralized bone is then combined with an excipient or carrier material to make the formulated demineralized bone product. As part of the regulatory filings required by governmental regulatory agencies, such excipients must demonstrate biocompatibility, usually including tests to demonstrate that the formulated demineralized bone matrix or its carrier is not cytotoxic, a sensitizer, an irritant, genotoxic, a pyrogen, or a hemolytic agent. They are also typically tested by implantation for acute systemic toxicity and subacute toxicity. Commonly, these are demonstrated by the appropriate tests of the ISO10993 [36].

Aseptic Processing

Aseptic processing is a system that is designed to process tissue without contaminating it. It differs from terminally sterilized processes in that the intermediate steps must be much more exacting to maintain sterility through the process, and to avoid the need to apply irradiation or other damaging treatments in the terminal step. In aseptic processing, there are two primary sources of contamination to avoid: contamination from the processing room environment, and contamination of the tissues of one donor by the tissues of another donor. These imperatives are achieved by careful processing controls (such as a rigid requirement that only the tissues of a single donor be allowed in a processing area at any given time), and bacteriological testing at multiple stages of the process. Aseptically processed tissue is prepared in a cleanroom environment. Cleanrooms are classified according to the number of particles that they allow, with smaller number classifications indicating a cleaner environment [37]. Aseptically processed tissues are typically processed in a very tightly controlled cleanrooms (e.g. class 100), and then only released after their sterility has been proven by bacteriological testing. Relatively few companies have chosen this approach, since it is more costly and labor intensive than a process with a less well-controlled environment that ends in terminal sterilization. However aseptic processing has the substantial advantage of eliminating protein damage in the graft, which is produced by the terminal sterilization step. The water and air that will come into contact with the tissues

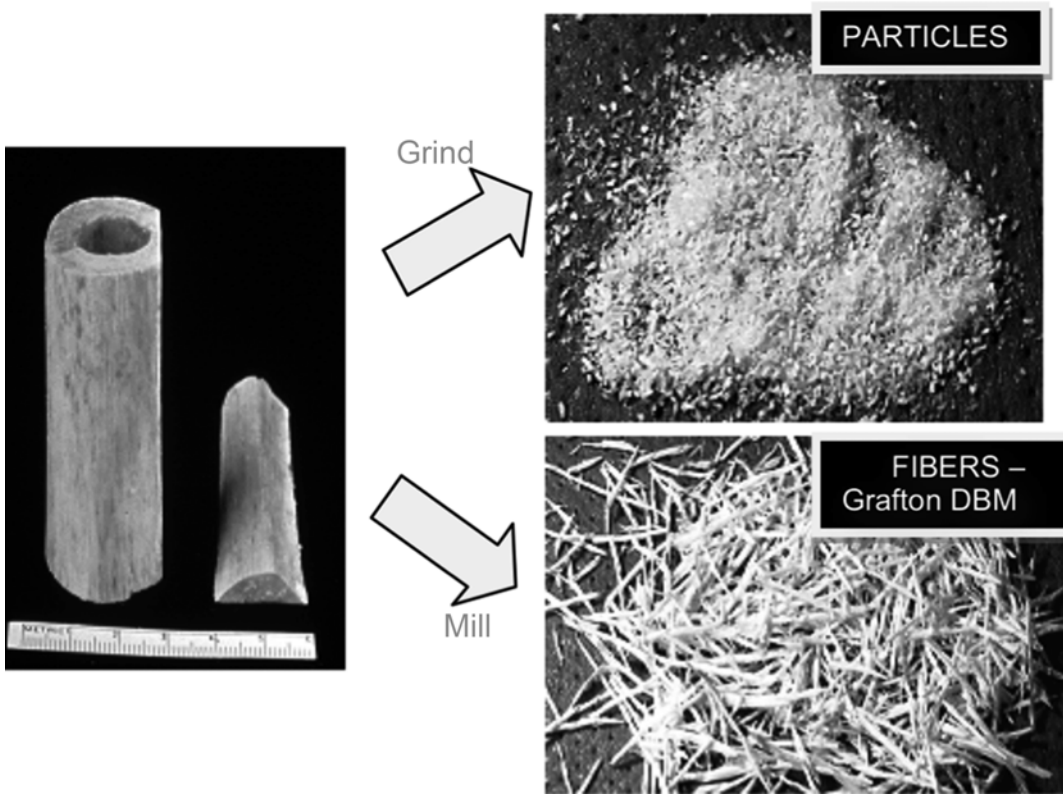

Fig. 8.3 Preparation of bone prior to making the formulated demineralized bone graft. Bone can be ground into particles, or it can be milled to provide rolled shavings, or fibers – which are exclusive to the Grafton® demineralized bone forms. Once prepared into this form, the particles or fibers continue on to be demineralized by treatment with hydrochloric acid and then are combined with the excipient to make the formulated demineralized bone matrix product

are filtered and purified. Electrical systems have fail-safe conditions, including backup generators in case of power failure. Workers involved in processing the tissue must be clad in specialized cleanroom gowns and must periodically demonstrate their ability to gown and function in the processing area without contaminating tissues. Validated cleaning procedures are used to clean each processing area between batches. Each batch represents the tissue of only one donor, with full traceability through the process and back to the procurement stage. All of this infrastructure relies extensively upon repeated and vigilant bacteriological testing, as the key to maintaining a sterile environment and a product that passes sterility testing at the end of the process.

Viral Inactivation

There is evidence that even "minimal processing", including marrow evacuation and lyophilization (which are always part of the process for demineralized bone), can cause a dramatic reduction to risks of viral transmission [38–40]. Demineralized bone undergoes these process steps and a number of others which each have the ability to kill virus. Taken together, they have the potential to achieve "viral inactivation". To call demineralized bone "virally inactivated", it is necessary to first estimate the maximum viral burden that could possibly be carried by the tissues, and then to calculate the capability of the process, established though validation testing, to kill or remove the virus. If the process capa-

bility provided by all process steps exceeds the maximal viral burden of the tissues by a sufficient magnitude (usually at least 3 logs, or 1000 times the theoretical maximum virus burden), then the process is a "viral inactivation process."

The first demonstration by a commercial manufacturer showing full viral inactivation in demineralized bone was the D-Min® process used in Grafton®, summarized in a 1995 publication [32], and was preceded by a research study demonstrating the removal of a virus from tissue that were known to be infected with HIV [31]. For HIV, the commercial process was shown to be capable of reducing virus by more than 2.8 billion times [32], or more than 400,000 times the highest estimated viral concentration of a tissue, should it be infected before processing. The process was likewise shown to be capable of killing more virus than could exist in the tissue for other clinically relevant virus types in addition to HIV, including Hepatitis B, Hepatitis C, CMV, and Poliovirus, and demonstrated to be effective at viral removal in tissues from systemically infected animals [41]. Since this time other manufacturers of formulated demineralized bone products have also developed viral inactivation methods, which differ dramatically in the mechanisms of inactivation, as well as the amount of damage caused to the tissue proteins by the process.

Demineralized human allograft bone is safer than is screened whole blood for any of the viruses where risks have been evaluated in both tissues [32, 33, 42, 43]. Currently, acellular blood components such as pooled plasma protein fractions receive viral inactivation treatment, but whole, or cell-containing blood fractions do not [44]. By contrast, demineralized bone is screened, and additionally it is *also* virally inactivated by the process. Using HIV as an example, the combination of these effects argues that demineralized bone is about 2.2 billion times *safer* than the screened blood that surgeons use every day, without concern [32, 35, 42].

TSE Agents/Prions

Prions [45], the causative agent for transmissible spongiform encephalopathies including Creutzfeldt-Jakob disease and Bovine Spongiform Encephalopathy, are a special issue for tissue processing. They are difficult to kill, resisting steam sterilization and other traditional methods of sterilization. Since prions are proteins, many of the processing steps that could be used to inactivate prions would also have the undesirable consequence of damaging the collagen, BMP's and other proteins that make demineralized bone function well in bone healing. However the potential for infectivity is not the same among all tissues of the body.

The infectious prion proteins (PrP) have been isolated in some (but not all) tissues, including muscle [46] and blood [47] in animal models of the infection. Different tissues have different levels of risk based upon the potential infectivity [48, 49]. According to the World Health Organization, neural tissues, pituitary and dura mater have the highest level of potential infectivity [48]. Blood is a tissue of intermediate infectivity which is categorized as a "Peripheral tissue{s} that have tested positive for infectivity and/or PrP in at least one form of TSE" [48]. By contrast, bone and tendon tissues are listed among those tissues with "no detected infectivity or PrP" by the World Health Organization.

Thus, the tissues being processed into demineralized bone have no known possibility of containing prions. Different processors take different approaches to establishing safety, and while no risk appears to be present, Osteotech has taken the additional steps of including screening steps that will exclude donors with any unexplained neurologic disorders, and will not collect tissues from sites near neural or other high infectivity tissues (e.g. vertebral bodies are not collected, due to their proximity to the spinal cord and nerve roots).

Composition

Many schoolchildren first become aware of demineralization by performing an experiment using a chicken bone, soaked for a time in a jar of vinegar, and then tying a knot in the bone after a sufficient portion of the inorganic mineral has been removed by the acid. The result is to

transform a mineral reinforced structural composite material into a collagen-based connective tissue with exposed non-collagenous proteins. If one takes this child's experiment, and modifies it by (1) Using *human* allograft tissue and hydrochloric acid, (2) separating the bone into sub-millimeter sized elements before treatment, (3) treating the tissue with detergents, antibiotics and alcohols to kill any potential pathogens and to remove cells, (4) processing, reacting and packaging in a cleanroom environment, and (5) encompassing the process with process validations, microbiological testing and a quality control system then the resulting processed demineralized bone matrix is the starting material for a formulated demineralized bone product.

Why Demineralize the Bone?

If demineralized bone is placed in a site without osteoblastic bone forming cells, but with access to the mesenchymal cells of surrounding tissues (as in a muscle bed) it will gradually transform into living mineralized cellular bone. This is ectopic bone formation. Why should demineralized bone produce such a dramatic response in tissues that do not have a direct mineralized tissue function? Early researchers compared the endochondral formation in ectopically implanted demineralized bone matrix to the events in embryological tissue formation [6], with the implication that the healing is tied in to remnant developmental pathways. This embryological context became the source of the concept of "induction" in association with demineralized bone matrix.

A more recent understanding comes from the osteoclastic events of bone remodeling that occur every day in the skeleton. The acid treatment used to prepare demineralized bone is actually a biomimetic process, since the osteoclasts that prepare the resorption site for new bone in remodeling also use hydrochloric acid to achieve demineralization of the interior surface of the resorption pit [50, 51], just as tissue processors do when they prepare demineralized bone. Thus, when allograft bone is demineralized in a processing facility, the entire surface of each bone element is treated with acid in the same manner as the interior surface of a resorption pit – a surface that the body recognizes as a location that requires a new layer of bone to refill. When demineralized bone is implanted, it provides many surfaces that are prepared, as osteoclasts would have prepared them, to receive osteogenic cells and to encourage bone formation.

The proteins that are responsible for the osteoinductive character of the demineralized bone are acid-stable, and can actually be damaged by neutral or basic conditions. In the early 1970s, Urist and his co-workers demonstrated that bone contains natural autolytic enzymes, which can degrade inductive proteins [25]. These autolytic enzymes have different activity, depending upon the temperature and the pH of the storage environment [25, 52, 53]. Urist showed that BMP's are preserved at acidic [25] pH (pH < 5.5) and degraded by autolysis at neutral pH (pH ~ 7.4). This is critical not only at the time of processing, but also during the period that the product is being stored prior to surgical use. Thus a demineralized bone formulation that contains a carrier or storage media maintaining it at neutral or basic pH, can cause the degradation of the proteins through autolysis [53], and thereby provide a demineralized bone that has lower inductive activity by the time that the package is opened in a surgical setting.

Basis of Healing

Acting Upon Cells to Influence Healing

Demineralized bone uses the natural growth factors and bone morphogenetic proteins (TGF-β, IGF, FGF, PDGF, and BMP's, among others [18]) that exist within the bone matrix to signal nearby cells and to influence them to become bone – forming cells and to make new bone. Even though they are present in mineralized bone, it takes the act of demineralization to expose them, making signaling possible [3]. These cell-signaling molecules inside demineralized bone have been successfully used in a host of applications for repair

or modification of skeletal tissues – in craniomaxillofacial, dental, spinal, trauma, joint arthroplasty, joint revision, and podiatry, among others. The reason for this widespread clinical use is the potential to positively influence the healing process through passive scaffolding (osteoconductive) and active signaling (osteoinductive) effects.

Osteoinduction: Signaling/ Recruitment/Differentiation

As a biomaterial for bone healing, demineralized bone matrix is unusual, in that it is not only osteoconductive, it is also *osteoinductive*. The term "osteoinductive" is widely used and extensively misused in the clinical and basic science literature, Einhorn [54] has provided a lucid definition which is in line with the original intent of Urist:

> Osteoinduction is a process that supports the mitogenesis of undifferentiated perivascular mesenchymal cells, leading to the formation of osteoprogenitor cells with the capacity to form new bone. Unlike osteoconductive materials, osteoinductive substances lead to the formation of bone at extraskeletal sites…..

The ability to form bone at an ectopic site, where no osteogenic cells were present at the time of implantation, is a hallmark of osteoinduction [2, 29, 55]. Even though cancellous iliac crest graft does promote bone formation in a *bony* site due to the osteogenic cells that it contains, it is not osteoinductive. It will resorb, rather than forming new bone when placed into an *ectopic* site [56, 57].

Similarly, pathological calcification in implanted tissue has been confused with osteoinduction [58–60]. Inert calcium phosphate materials [61, 62], have been advocated by some in the biomaterials community as "osteoinductive." This is a misuse of the term, however. These inorganic materials do not cause cells to differentiate or to divide – there is no active signaling. The behavior of these materials is analogous to that of natural mineral in pathological calcium deposits in the aorta and aortic valves [63–65] – rather than delivering a signaling substance such as bone morphogenetic protein, these materials co-opt molecules from the surrounding environment, in amounts too small to offer a clinical benefit.

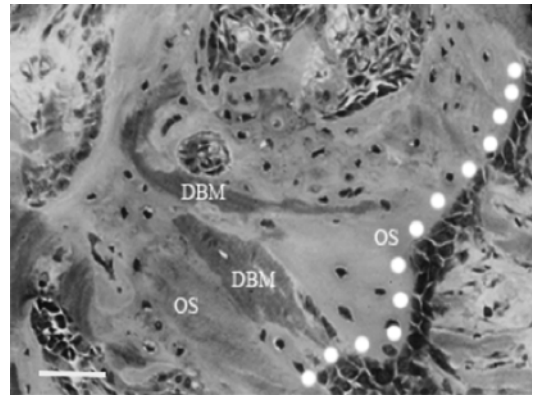

Fig. 8.4 Image of new bone formation in a rodent muscle site induced by demineralized bone. OS: regions of new osteoid created by a line of osteoblasts (*circles*). DBM: remnant fragments of demineralized bone. Bar = 100 μm

True osteoinduction is an active, protein-based signaling of cells, using the BMP's and associated growth factors that Marshall Urist identified in demineralized bone. In a rat muscle site, the implant follows an endochondral ossification pathway [7], by initially forming cartilage and then later replacing this scaffold with bone and marrow [7]. When explanted after 4 weeks, the demineralized bone which was originally implanted into a muscle with no existing osteoprogenitor cells, has been transformed to a nodule of hard mineralized bone. Histologically (Fig. 8.4), it shows evidence of active new bone formation, osteoblasts, osteoclasts, embedded osteocytes, and marrow elements. If the activity of the demineralized bone matrix has been maintained by careful processing to avoid deteriorating the embedded proteins, then the nodule should be filled with newly formed bone and marrow over more than 75 % of the nodule's volume [55].

Measurement of Osteoinductivity

Implantation studies and characterization of osteoinductivity are performed in living animals. Early work on osteoinductivity used a variety of animals and a variety of ectopic sites. Urist used

the rectus abdominus, quadriceps or erector spinae of rabbits, rats, mice, and guinea pigs [2]. Others used subcutaneous sites for evaluation [66, 67]. However, since vascularity and availability of mesenchymal cells will vary with the species of animal and the location of the implant, it is to be expected that osteoinduction results will not be comparable among them. Some have advocated using an in vitro test based upon either measured BMP content of the graft [68], or alternatively, on expression of osteoinductive markers [69] such as alkaline phosphatase, rather than in vivo testing in an animal model. However such tests have proven inconsistent their relationship to in vivo assessments – alkaline phosphatase expression in cell culture is not a reliable *quantitative* measure of osteoinductivity [70]. Likewise, the ELISA technique typically used to measure BMP content of the tissue is unreliable, due to variations in the ability to extract the BMP's and the fact that ELISA measures both active and inactive forms of BMP. This limitation was well-summarized by Bae et al [71]:

> The major disadvantage of ELISA is that its detection is based on an antibody that binds to only a small region of the complete protein structure. Therefore, it is possible that the protein detected by ELISA is just an inactive fragmented portion of the complete molecule. Even if the protein is indeed the complete molecule and not just a fragment, the protein may still not have any biologic activity (i.e., a dead protein).

Clearly the proper interpretation of ELISA results is critical, and conversely the misinterpretation – by equating all ELISA signal as *functional* inductive protein – is a major and common source of error. At this time, it is widely accepted that the only reliable quantitative measurement of osteoinductivity is a well characterized version of Urist's *in vivo* models in a muscle site. Edwards et al. [55], working at Osteotech, characterized and validated the model using an athymic rat and a hindlimb intermuscular in an athymic (rnu/rnu) rat. In his earliest work, Urist used *euthymic* animals [2, 29], but later as he worked with human demineralized bone, he began to use *athymic* rats and mice [72, 73]. Since athymic animals have no thymus gland, they allow the implantation of tissue from another species (human), without a cross-species incompatibility response.

Taking this lead from Urist, Edwards and colleagues utilized athymic rats, and a semi-quantitative scoring system based upon the proportion of newly formed bone and marrow within an implant, to quantify the amount of osteoinductivity present in demineralized bone [55]. They used a site between the semimembranous and adductor brevis muscles of the hindlimb. The implants remained in the site for 28 days, and then were removed and prepared for histological evaluation. Using a 0–4 scoring system in a controlled rnu/rnu strain of rats, Edwards and coworkers demonstrated selectivity (response only to active demineralized bone matrix), reproducibility (consistency of result from the same lot of demineralized bone matrix), and sensitivity (correlated increasing response to implants of higher activity) of the model. Such a model can then be used to assess a variety of factors that are thought to influence demineralized bone matrix activity, including age of the donor, source of the bone, processing variables and excipient.

Factors Influencing Osteoinductivity

Cortical and cancellous bone have different inherent capacities for osteoinductivity. When measured quantitatively using this method, cancellous bone is less osteoinductive than cortical bone, which is why formulated demineralized bone products are made of either particulated or milled cortical diaphyseal bone, rather than cancellous bone. In 1970, Urist and co-workers [22] performed an experiment in rabbits to quantify the amount of new bone that is formed from implants of either rabbit cortical bone or rabbit cancellous bone. They found that the amount of new bone induced by demineralized diaphyseal cortices implanted in a muscle site was four times that of an equivalent cancellous implant from the metaphysis. Others have later confirmed this in dogs [74].

In formulated demineralized bone products, the excipient is added to impart handling characteristics to the final formulation which are useful in its targeted surgical applications. However, the many materials that have been combined

with demineralized bone to make formulated products can also negatively influence the biological properties of the graft material [75] and contribute, along with the processing and sterilization method to substantial differences in performance among marketed demineralized bone products [58].

Likewise, sterilization procedures that can be used to effect sterility of the graft, including gamma irradiation [20, 76], ethylene oxide [76, 77], hydrogen peroxide treatment [78], steam sterilization [79, 80], gas-plasma sterilization [80] and some proprietary methods [81] used by various tissue banks can all damage the proteins responsible for osteoinductivity.

The American Association of Tissue Banks (AATB) established standards for moisture in demineralized bone products [34] of less than 6 % moisture content. Among other reasons for this, water can affect the storage stability of the demineralized bone [82] by damaging the inductive proteins present in the matrix. As a result, formulations that include water in the carrier can have a harmful effect on osteoinductivity, particularly as the product approaches its expiration date.

Process Effects on Osteoinductivity

As we have seen, the processing methods used in preparing demineralized bone directly define its safety characteristics. Less well understood, the processing history also defines the activity and inductive performance of the demineralized bone. Marshall Urist, and others after him, taught us that demineralized bone must be treated carefully during processing to assure osteoinductivity at the end. In processing demineralized bone, a host of factors can negatively impact biological activity [83], ranging from the form and temperature of tissue storage [25, 82, 84] to the pH, time and order of the demineralizing and antibacterial solutions [83] to the selection of a strategy for achieving sterility of the tissue [20, 76, 80, 83] to the choice of excipient added to offer handling characteristics of the graft [75, 85]. These can all dramatically affect the osteoinductive character of the demineralized bone [33]. Since the processing history cannot be identified by viewing the graft, the differences in product performance associated with processing history of one demineralized bone product versus another are often invisible to the surgeon.

Processing of allograft bone is a balance between providing process treatments that enhance the safety of the tissues, and conversely, minimizing the damage induced by these same treatments. This is because nearly all treatments so far devised in the name of enhanced safety carry some additional detrimental effects to the proteins and matrix that activate new bone formation. Gamma irradiation, often chosen as a sterilization method for metallic implants and medical supplies, will cause a decline in osteoinductive performance in demineralized bone [20, 76] as well as BMP's purified from demineralized bone [86]. The effect is dose-dependent, with greater declines corresponding to greater radiation doses [20, 87]. As a result, the most highly osteoinductive demineralized bone formulations are aseptically processed, rather than being terminally sterilized [33, 87].

Particle Shape

The shape of the demineralized bone particle has an impact on its performance. Martin et al. [30] used a posterolateral fusion model in rabbits to assess three different formulations of demineralized bone, one which contained particles that were nominally spherical and two that contained fibers. These materials used rabbit demineralized bone in gel, putty and flexible sheet forms, modeled after the Grafton Putty and Flex products. The fibers for the latter two forms were created by milling bone tissue into tubular shavings.

This rabbit model will demonstrate ~70 % fusion using rabbit autograft [88], leaving opportunity to perform better than autograft (>70 % fusion) and poorer than autograft (<70 % fusion), depending upon the overall healing characteristics of the formulations. Further, these formulations were assessed in both the autograft extender role (1:1 demineralized bone:Autograft), as well as the autograft replacement role (100 % demineralized bone), in two arms of the study. In the *extender*

application, the particles were able to reproduce the fusion rate of the autograft alone (70 %), while the two fiber formulations improved the fusion rate to 100 % (moldable Grafton® putty) and 100 % (flexible Grafton®sheet), respectively.

As a *replacement* for autograft, demineralized bone matrix in the particle form was a little less effective (58 %) than autograft. Yet even without the advantage of delivering cells with the graft, the fiber forms still demonstrated higher fusion rates than autograft: 83 % for the moldable putty and 100 % for the flexible sheet. This showed, at least in this animal model, that the shape of the individual elements of the demineralized bone do have an effect upon the bone healing capacity of the graft. But what was the basis?

To find out, Martin et al. ran a third arm of the study, in which they extracted the inductive proteins from each of the three forms. This isolated the particle shape effect on healing, without the effects of osteoinductivity on bone healing. The results showed that the particle formulation was unable to fuse any of the spines, while the fiber forms, without inductive proteins, managed to fuse 33 % and 36 % of the spines, respectively. In other words, when prepared in its most osteo*conductive* form (fibers), demineralized bone obtains ~50 % improvement in fusion rate in this animal model. This is largely due to the greater number of connected pathways that a fibrous matrix can provide for cells to enter and colonize the graft, relative to a particulate (Fig. 8.5).

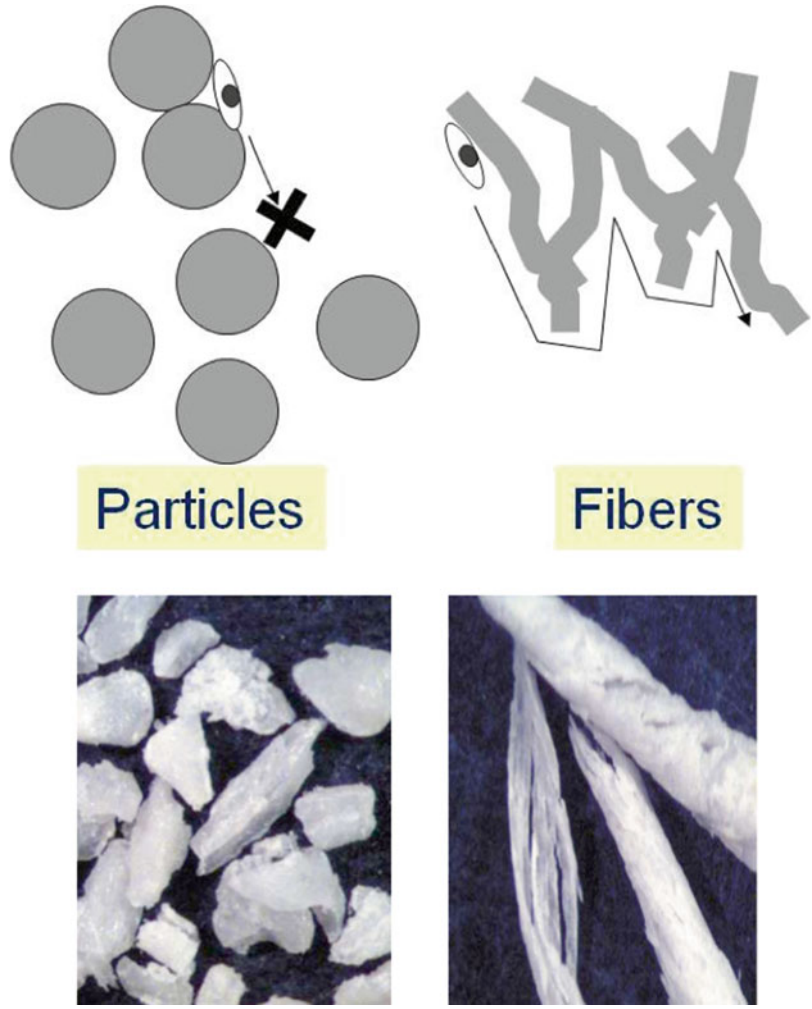

Fig. 8.5 Particles and Fibers permit different levels of osteoconductive cellular travel. Fibers offer connected pathways to the cells that allow them to move more freely in the graft matrix

Posterolateral fusion is an example of a procedure that actually needs both osteoinduction and osteoconduction. In situations such as this, or in a long bone segmental defect, the graft must perform several functions. It *may* deliver cells from autograft. It *must* provide an interconnected pathway for cells to pass from the source (the decorticated surfaces of the transverse processes) to bridge in the center. It *should* encourage cell growth – ideally by recruiting other cells from the surrounding tissues though osteoinduction. With these elements (cells, osteoconduction, osteoinduction), the graft has maximal opportunity to heal the site.

Grafting Strategy and Clinical Use

When considering the vast number of bone graft materials available for use, is it useful to remember that graft materials have different capabilities and different levels of proof for those capabilities. For instance, the majority of the grafting materials now on the market have proven their ability to heal a closed, metaphyseal defect. This is a site that often has excellent blood supply, is bathed in marrow, osteoprogenitors, and even osteoblastic cells on the cancellous surfaces. Success in such a site represents a modest level of performance, and one that is matched by many materials. In fact some of these are not even critical-sized defects, and bone would fill the defect with, or without, a graft. When the site is challenged by a poor blood supply, limited cell availability (due to systemic or local factors), or represents a substantial bridging distance – then the capabilities of the graft are challenged. Thus in surgical applications, a synthetic material made of one of the calcium phosphates, which could be perfectly suitable as an implant coating or as a filler for a closed defect, could be poorly suited for a posterolateral fusion, a long bone critical sized segmental defect, or other environments that are prone to delayed union, non-union or pseudoarthrosis. In rare reports where the same graft material is used in both closed metaphyseal defects and also a segmental defect or a posterolateral fusion, the differences in performance capacity are obvious [89]. On some occasions, such materials can also form particulates, generated and shed from the graft due to forces of surgical implantation or from loading activities of daily living. When in particulate form, such materials lose their ability to serve as a scaffold for bone formation, and instead initiate a sequence of detrimental inflammatory cellular and tissue responses [90–92], which are partly analogous to debris responses from other biomaterials [93].

In many countries, the performance requirements for a bone grafting product to enter the market are relatively low – demonstration of bone formation in a metaphyseal defect site, usually a rabbit or a dog. This means that surgeons are offered grafts that are designed for scaffolding functions (calcium phosphates, calcium sulfates, silicate-substituted apatites and silicate bioglasses), without an awareness that most of these products have never been evaluated in skeletal sites that have a limited blood supply and are not surrounded by osteoprogenitor and marrow cells. As a result, there is much confusion about product capabilities and which applications are suited to which products. Demineralized bone also has the ability to heal these relatively simple metaphyseal defects without difficulty, and may accelerate healing. In addition, if care is taken to maintain the protein activity during processing, then demineralized bone matrix can *also* heal defects that are significantly more challenging in humans. Fiber-based demineralized bone forms have shown efficacy in posterolateral fusions [30, 94–97], critical-sized segmental defects [98–102] and other extremely challenging conditions [103, 104] , where the graft must span a distance that has no existing osteoblastic cell source.

Likewise, the supporting levels of evidence [105, 106] can vary dramatically among different brands of formulated demineralized bone, with the poorest having only unpublished animal studies and no clinical support, and the strongest having level one prospective evidence, as well as other support. Given the dramatic effects of process history and influence from the formulation components described earlier, it does not seem unreasonable to demand substantiation of performance in *human* clinical studies.

The motivation for using demineralized bone in bone healing applications has come from two primary directions: Improving outcomes in skeletal healing; and avoiding autograft harvest morbidity. Proper selection of a graft material involves assessment by the clinician of the patient's systemic state, condition of the surgical site, and the surgical technique being chosen. Many clinically difficult situations [107, 108] can be interpreted as situations of poor availability or poor responsiveness of mesenchymal or osteoprogenitor cells. Consequently, strategies that increase the local concentration of cells that *are* osteoblastic or *can become* osteoblastic have a significant opportunity to improve outcomes [109].

Formulated demineralized bone materials offer the opportunity to influence outcomes by improving the available number of cells for healing in such compromised conditions, through their signaling function. Since osteoblastic cells do not "jump" across spaces, healing requires contact with the host bone where cells reside, as well as a pathway to conduct them into the central regions of the graft where they can create new tissues. Preparation of the surgical bed, by resecting to bleeding bone at the graft site and removing any intervening soft tissue can dramatically improve the grafting environment. Where possible, it is extremely helpful to retain the periosteum (a highly osteogenic tissue [110]), or to re-create a "periosteum" of sorts, as in the technique pioneered by Masquelet [111–113].

The bone graft can assist by ensuring congruity with the host bone surface [114, 115], or by using demineralized bone fibers, entangled in a matrix, to offer an improved osteoconductive pathway [30] that cells can use to enter and colonize the graft. They may also be delivered with a cell source, such as cancellous autograft or bone marrow, to increase the number of cells at the site that could potentially be influenced by the demineralized bone matrix signals.

At the risk of over-simplification, grafting can be distilled to two straightforward goals: (1) collecting cells to the graft site, and (2) influencing those cells to make bone. The cells can be either delivered with the graft (Autograft), or they can be collected from nearby tissues (Mesenchymal cells). They can also be either existing osteoprogenitor cells (osteoblasts), or they can be cells that have the potential to become osteoprogenitors. Demineralized bone, as a part of a composite bone graft, can be used in any of several ways in clinical practice, always with source in mind for the bone forming cells:

Provide viable osteoblastic cells along with the graft (Graft Including Morsellized Autograft, Fig. 8.6a). The surfaces of cancellous bone can provide cells that are already differentiated into the osteoblastic lineage. Thus, iliac crest autograft works as a grafting material, not because it is osteoinductive, but rather because it provides cells that are already suited to making new bone tissue. Demineralized bone can influence these cells in their osteoblastic role. It can also act as an extender in this application, when the quality or quantity of autograft available is limited [94, 95, 116]. Demineralized bone forms that include fibers can actually *enhance* the performance of the autograft in some applications [30, 96].

Provide a signaling (osteoinductive) graft that can influence undifferentiated cells of the surrounding environment (Demineralized Bone Matrix, Fig. 8.6b). When the graft includes osteoinductive demineralized bone, it can draw cells from adjacent tissues, and convert them to osteogenic forms, thereby inducing bone formation – providing that there are adequate nearby tissue sources of mesenchymal cells.

Provide viable undifferentiated cells with the graft, and then influence them to become bone forming cells [117] **(Demineralized Bone Matrix with Concentrated or Unconcentrated Bone Marrow**, Fig. 8.6c). This can be achieved by using demineralized bone along with autogenous bone marrow, or bone marrow concentrate. Marrow stem cells are delivered with the graft, and demineralized bone provides signals to induce differentiation and expansion of osteoprogenitors, as well as to draw cells from the surrounding tissues that can assist. The concentration and total number of viable cells delivered with the graft can affect the magnitude of the healing benefit [109].

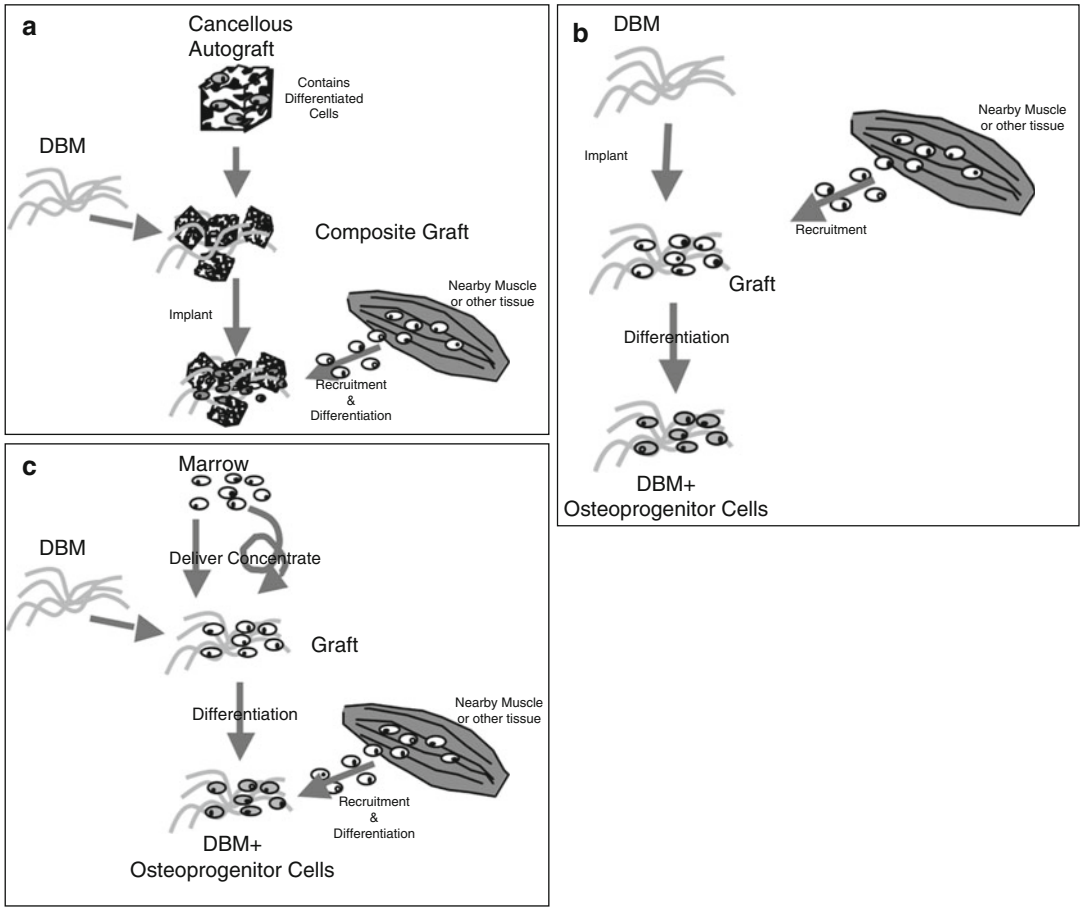

Fig. 8.6 Strategies for providing and/or influencing cells to make bone tissue. (**a**) Autograft + demineralized bone (DBM). (**b**) Demineralized bone alone, drawing cells from the environment. (**c**) Demineralized bone plus marrow, concentrated or unconcentrated

Conclusion

Demineralized bone, as a formulated, packaged product, is a little more than two decades old. In that time, we have learned much about the factors that contribute to efficacy, and have re-learned the lessons of Senn and Urist. We recognize the importance of establishing and demonstrating the safety of demineralized bone, but the approaches chosen vary substantially among processors and products, and are not equally efficacious. We now know that demineralized bone contains a variety of bone morphogenetic proteins and growth factors, and that processing can either expose and retain their function, or it can damage and inactivate them.

We know that demineralized bone, in clinical application can be very powerful. It has the ability to heal large critical sized defects that will not heal on their own or with non-inductive materials. It can provide functions specific to the application, such as holding autogenous graft or expanding to create congruency (Grafton® Matrix and Xpanse, respectively). It can be used in situations where recombinant growth factor products are contraindicated or have a history of significant complications.

In the field of tissue engineering, biomaterials scientists have expended great effort to build a biomaterial from the most basic building blocks, which can offer the characteristics necessary for bone regeneration. The evidence

shows that such a material already exists, and that it need not be synthesized in an intricate manufacturing process. Nature has already prepared such a material. We need only expose its potential (demineralization), preserve it (careful processing), formulate it with an understanding of its biological role (carrier selection and fibers), and fashion it into a form suited to a surgical procedure. We have yet to exhaust the possibilities for achieving these goals with demineralized allograft bone.

References

1. Borden M. The development of bone graft materials using various formulations of demineralized bone matrix. In: Laurencin CT, editor. Bone graft substitutes. West Conshohocken: ASTM International; 2003. p. 96–112.
2. Urist MR. Bone: formation by autoinduction. Science. 1965;150(698):893–9.
3. Urist MR, Strates BS. Bone morphogenetic protein. J Dent Res. 1971;50(6):1392–406.
4. Urist MR, Mikulski A, Lietze A. Solubilized and insolubilized bone morphogenetic protein. Proc Natl Acad Sci U S A. 1979;76(4):1828–32.
5. Riley EH, et al. Bone morphogenetic protein-2: biology and applications. Clin Orthop Relat Res. 1996;324:39–46.
6. Meikle MC. On the transplantation, regeneration and induction of bone: the path to bone morphogenetic proteins and other skeletal growth factors. Surgeon. 2007;5(4):232–43.
7. Glowacki J, Mulliken JB. Demineralized bone implants. Clin Plast Surg. 1985;12(2):233–41.
8. Harakas NK. Demineralized bone-matrix-induced osteogenesis. Clin Orthop Relat Res. 1984;188:239–51.
9. Rengachary SS. Bone morphogenetic proteins: basic concepts. Neurosurg Focus. 2002;13(6), e2.
10. Lapatin KDS. Pheidias ελεφαντουργοζ. Am J Archaeol. 1997;101:663–82.
11. Senn N. On the healing of aseptic bone cavities by implantation of antiseptic decalcified bone. Am J Med Sci. 1889;98:219–43.
12. Mackie W. Clinical observations of the healing of aseptic bone cavities by Senn's method of implantation of antiseptic decalcified bone. Med News. 1890;58:202–10.
13. Da Costa JC. Modern surgery: general and operative. 8th ed. Philadelphia: W.B. Saunders Co.; 1919.
14. Huggins CB. The formation of bone under the influence of epithelium of the urinary tract. Arch Surg. 1931;22(3):377–408.
15. Huggins CB. Influence of urinary tract mucosa on the experimental formation of bone. Proc Soc Exp Biol Med. 1930;27:249–51.
16. Levander G. A study of bone regeneration. Surg Gynecol Obstet. 1938;67(6):705–14.
17. Ray RD, Holloway JA. Bone implants; preliminary report of an experimental study. J Bone Joint Surg Am. 1957;39-A(5):1119–28.
18. Mohan S, Baylink DJ. Bone growth factors. Clin Orthop Relat Res. 1991;263:30–48.
19. Celeste AJ, et al. Identification of transforming growth factor beta family members present in bone-inductive protein purified from bovine bone. Proc Natl Acad Sci U S A. 1990;87(24):9843–7.
20. Buring K, Urist MR. Effects of ionizing radiation on the bone induction principle in the matrix of bone implants. Clin Orthop. 1967;55:225–34.
21. Buring K. Effects of ionizing radiation on the matrix of bone implants. Calcif Tissue Res. 1968;Suppl:8.
22. Urist MR, et al. Quantitation of new bone formation in intramuscular implants of bone matrix in rabbits. Clin Orthop. 1970;68:279–93.
23. Urist MR. Surface-decalcified allogeneic bone (SDAB) implants. A preliminary report of 10 cases and 25 comparable operations with undecalcified lyophilized bone implants. Clin Orthop Relat Res. 1968;56:37–50.
24. Urist MR, et al. Osteogenetic competence. Clin Orthop Relat Res. 1969;64:194–220.
25. Urist MR, Iwata H. Preservation and biodegradation of the morphogenetic property of bone matrix. J Theor Biol. 1973;38(1):155–67.
26. Huggins C, Wiseman S, Reddi AH. Transformation of fibroblasts by allogeneic and xenogeneic transplants of demineralized tooth and bone. J Exp Med. 1970;132(6):1250–8.
27. Reddi AH, Huggins C. Biochemical sequences in the transformation of normal fibroblasts in adolescent rats. Proc Natl Acad Sci U S A. 1972;69(6):1601–5.
28. Reddi AH, Huggins CB. Formation of bone marrow in fibroblast-transformation ossicles. Proc Natl Acad Sci U S A. 1975;72(6):2212–6.
29. Urist MR, et al. The bone induction principle. Clin Orthop. 1967;53:243–83.
30. Martin Jr GJ, et al. New formulations of demineralized bone matrix as a more effective graft alternative in experimental posterolateral lumbar spine arthrodesis. Spine. 1999;24(7):637–45.
31. Mellonig JT, Prewett AB, Moyer MP. HIV inactivation in a bone allograft. J Periodontol. 1992;63(12):979–83.
32. Scarborough NL, et al. Allograft safety: viral inactivation with bone demineralization. Contemp Orthop. 1995;31(4):257–61.
33. Boyce T, Edwards J, Scarborough N. Allograft bone: the influence of processing on safety and performance. Orthop Clin North Am. 1999;30(4):571–81.
34. Pearson K, Dock N, Brubaker S, editors. Standards for tissue banking. 12th ed. McLean: American Association of Tissue Banks (AATB); 2008. p. 208.

35. Buck BE, Malinin TI, Brown MD. Bone transplantation and human immunodeficiency virus. An estimate of risk of acquired immunodeficiency syndrome (AIDS). Clin Orthop Relat Res. 1989;240:129–36.
36. ISO 10993. Biological evaluation of medical devices, parts 1–20. Geneva: International Organization for Standardization; 1999–2008.
37. Institute of Environmental Sciences. Federal Standard 209E. Airborne particulate cleanliness classes in cleanrooms and clean zones. Institute of Environmental Sciences, Mount Prospect, IL, USA. 1992. p. 1–48.
38. Asselmeier MA, Caspari RB, Bottenfield S. A review of allograft processing and sterilization techniques and their role in transmission of the human immunodeficiency virus. Am J Sports Med. 1993;21(2):170–5.
39. Simonds RJ, et al. Transmission of human immunodeficiency virus type 1 from a seronegative organ and tissue donor. N Engl J Med. 1992;326(11):726–32.
40. Tugwell BD, et al. Transmission of hepatitis C virus to several organ and tissue recipients from an antibody-negative donor. Ann Intern Med. 2005;143(9):648–54.
41. Swenson CL, Arnoczky SP. Demineralization for inactivation of infectious retrovirus in systemically infected cortical bone: in vitro and in vivo experimental studies. J Bone Joint Surg Am. 2003;85-A(2):323–32.
42. Stramer SL. Current risks of transfusion-transmitted agents: a review. Arch Pathol Lab Med. 2007;131(5):702–7.
43. Dodd RY, Notari EP, Stramer SL. Current prevalence and incidence of infectious disease markers and estimated window-period risk in the American Red Cross blood donor population. Transfusion. 2002;42(8):975–9.
44. Klein HG. Pathogen inactivation technology: cleansing the blood supply. J Intern Med. 2005;257(3):224–37.
45. Prusiner SB. Prion diseases and the BSE crisis. Science. 1997;278:245–51.
46. Angers RC, et al. Prions in skeletal muscles of deer with chronic wasting disease. Science. 2006;311(5764):1117.
47. Saa P, Castilla J, Soto C. Presymptomatic detection of prions in blood. Science. 2006;313(5783):92–4.
48. Expert Committee on Biological Standardization. WHO guidelines on tissue infectivity distribution in transmissible spongiform encephalopathies (WHO/BS/07.2078, http://www.who.int/biologicals/BS%202078%20TSE.pdf). Geneva: World Health Organization; 2007. p. 17.
49. Sogal A, Tofe AJ. Risk assessment of bovine spongiform encephalopathy transmission through bone graft material derived from bovine bone used for dental applications. J Periodontol. 1999;70(9):1053–63.
50. Blair HC, et al. Osteoclastic bone resorption by a polarized vacuolar proton pump. Science. 1989;245(4920):855–7.
51. Vaananen HK, et al. The cell biology of osteoclast function. J Cell Sci. 2000;113(Pt 3):377–81.
52. Urist MR, et al. Observations implicating an extracellular enzymic mechanism of control of bone morphogenesis. J Histochem Cytochem. 1974;22(2):88–103.
53. Urist MR, et al. Bone morphogenesis in implants of insoluble bone gelatin. Proc Natl Acad Sci U S A. 1973;70(12):3511–5.
54. Einhorn TA. Enhancement of fracture-healing. J Bone Joint Surg Am. 1995;77(6):940–56.
55. Edwards JT, Diegmann MH, Scarborough NL. Osteoinduction of human demineralized bone: characterization in a rat model. Clin Orthop. 1998;357:219–28.
56. Persson PE, Sisask G, Nilsson O. Indomethacin inhibits bone formation in inductive allografts but not in autografts: studies in rat. Acta Orthop. 2005;76(4):465–9.
57. Finkemeier CG. Bone-grafting and bone-graft substitutes. J Bone Joint Surg Am. 2002;84-A(3):454–64.
58. Fox WC, Aufdemorte T, Sandhu HS. Comparative histologic and calcium content evaluation of Osteofil, Grafton and Dynagraft putty bone inductive materials in the nude rat at 28 days. North American Spine Society proceedings, New Orleans, LA, USA. 15th annual meeting; 2000.
59. Tsai CH, et al. A composite graft material containing bone particles and collagen in osteoinduction in mouse. J Biomed Mater Res. 2002;63(1):65–70.
60. Nimni ME, et al. Biochemical differences between dystrophic calcification of cross-linked collagen implants and mineralization during bone induction. Calcif Tissue Int. 1988;42(5):313–20.
61. Yuan H, et al. A preliminary study on osteoinduction of two kinds of calcium phosphate ceramics. Biomaterials. 1999;20(19):1799–806.
62. Samizadeh S, et al. Osseoinduction by calcium phosphate bone substitutes is a function of chemical composition and structure. 53rd Annual meeting of the orthopaedic research society, San Diego; 2007.
63. Liu K, Tripp S, Layfield LJ. Heterotopic ossification: review of histologic findings and tissue distribution in a 10-year experience. Pathol Res Pract. 2007;203(9):633–40.
64. Steiner I, et al. Bone formation in cardiac valves: a histopathological study of 128 cases. Virchows Arch. 2007;450(6):653–7.
65. Collett GD, Canfield AE. Angiogenesis and pericytes in the initiation of ectopic calcification. Circ Res. 2005;96(9):930–8.
66. Bernick S, et al. Cellular events associated with the induction of bone by demineralized bone. J Orthop Res. 1989;7(1):1–11.
67. Hamata MM, et al. A stereological analysis of the heterotopic osteogenesis induced by allogeneic bone matrix grafts in rat subcutaneous tissue. Braz J Morphol Sci. 2004;21(2):81–8.
68. Honsawek S, Powers RM, Wolfinbarger L. Extractable bone morphogenetic protein and correlation with induced new bone formation in an in vivo assay in the athymic mouse model. Cell Tissue Bank. 2005;6(1):13–23.
69. Zhang M, Powers Jr RM, Wolfinbarger Jr L. A quantitative assessment of osteoinductivity of human demineralized bone matrix. J Periodontol. 1997;68(11):1076–84.

70. Carnes Jr DL, et al. Evaluation of 2 novel approaches for assessing the ability of demineralized freeze-dried bone allograft to induce new bone formation. J Periodontol. 1999;70(4):353–63.
71. Bae HW, et al. Intervariability and intravariability of bone morphogenetic proteins in commercially available demineralized bone matrix products. Spine. 2006;31(12):1299–306; discussion 1307–8.
72. Urist MR, et al. Induction of new-bone formation in the host bed by human bone-tumor transplants in athymic nude mice. J Bone Joint Surg Am. 1979;61(8):1207–16.
73. Becker W, et al. Human demineralized freeze-dried bone: inadequate induced bone formation in athymic mice. A preliminary report. J Periodontol. 1995;66(9):822–8.
74. Schwarz N, et al. Decalcified and undecalcified cancellous bone block implants do not heal diaphyseal defects in dogs. Arch Orthop Trauma Surg. 1991;111(1):47–50.
75. Boyan BD, et al. Osteoinductive ability of human allograft formulations. J Periodontol. 2006;77(9):1555–63.
76. Munting E, et al. Effect of sterilization on osteoinduction. Comparison of five methods in demineralized rat bone. Acta Orthop Scand. 1988;59(1):34–8.
77. Pekkarinen T. Effect of sterilization and delivery systems on the osteoinductivity of reindeer bone morphogenetic protein extract. Faculty of Medicine, Division of Orthopaedic and Trauma Surgery, Department of Surgery. University of Oulu, Finland; 2005. p. 78.
78. Carpenter EM, et al. Effect of hydrogen peroxide on osteoinduction by demineralized bone. Am J Orthop. 2006;35(12):562–7.
79. Chakkalakal DA, et al. Demineralized bone matrix as a biological scaffold for bone repair. Tissue Eng. 2001;7(2):161–77.
80. Ferreira SD, et al. Effect of gas-plasma sterilization on the osteoinductive capacity of demineralized bone matrix. Clin Orthop. 2001;388:233–9.
81. Dunn MG, et al. Effect of allograft bone processing on structural cortical grafts: a comparison of three proprietary processing methods. Spine J/Proceedings of the NASS, Toronto, Ontario, Canada. 23rd annual meeting. 2008;8:138s.
82. Han B, Yang Z, Nimni M. Effects of moisture and temperature on the osteoinductivity of demineralized bone matrix. J Orthop Res. 2005;23(4):855–61.
83. Russell JL, Block JE. Clinical utility of demineralized bone matrix for osseous defects, arthrodesis, and reconstruction: impact of processing techniques and study methodology. Orthopedics. 1999;22(5):524–31; quiz 532–3.
84. Shimp L. Heat resistance of allograft tissue. Cell Tissue Bank. 2008;9(4):259–66.
85. Lee Y-P, Ghofrani H. Bone graft substitutes and extenders. Contemp Spine Surg. 2009;10(4):1.
86. Ijiri S, et al. Effect of sterilization on bone morphogenetic protein. J Orthop Res. 1994;12(5):628–36.
87. Han B, Yang Z, Nimni M. Effects of gamma irradiation on osteoinduction associated with demineralized bone matrix. J Orthop Res. 2008;26(1):75–82.
88. Boden SD, Schimandle JH, Hutton WC. An experimental lumbar intertransverse process spinal fusion model. Radiographic, histologic, and biomechanical healing characteristics. Spine. 1995;20(4): 412–20.
89. Turner TM, et al. Radiographic and histologic assessment of calcium sulfate in experimental animal models and clinical use as a resorbable bone-graft substitute, a bone-graft expander, and a method for local antibiotic delivery. One institution's experience. J Bone Joint Surg Am. 2001;83-A Suppl 2(Pt 1):8–18.
90. Harada Y, et al. Differential effects of different forms of hydroxyapatite and hydroxyapatite/tricalcium phosphate particulates on human monocyte/macrophages in vitro. J Biomed Mater Res. 1996; 31(1):19–26.
91. Bauer TW. An overview of the histology of skeletal substitute materials. Arch Pathol Lab Med. 2007;131(2):217–24.
92. Lee GH, et al. Adverse reactions to OsteoSet bone graft substitute, the incidence in a consecutive series. Iowa Orthop J. 2002;22:35–8.
93. Jacobs JJ, et al. Osteolysis: basic science. Clin Orthop Relat Res. 2001;393:71–7.
94. Cammisa Jr FP, et al. Two-year fusion rate equivalency between Grafton DBM gel and autograft in posterolateral spine fusion: a prospective controlled trial employing a side-by-side comparison in the same patient. Spine. 2004;29(6):660–6.
95. Kang J, et al. Grafton & local bone has comparable outcomes to iliac crest bone in single level lumbar fusions. American Academy of Orthopaedic Surgeons, 75th annual meeting, San Francisco; 2008.
96. Louis-Ugbo J, et al. Evidence of osteoinduction by Grafton demineralized bone matrix in nonhuman primate spinal fusion. Spine. 2004;29(4):360–6; discussion Z1.
97. Vaccaro AR, Stubbs HA, Block JE. Demineralized bone matrix composite grafting for posterolateral spinal fusion. Orthopedics. 2007;30(7):567–70.
98. Geesink RG, Hoefnagels NH, Bulstra SK. Osteogenic activity of OP-1 bone morphogenetic protein (BMP-7) in a human fibular defect. J Bone Joint Surg (Br). 1999;81(4):710–8.
99. Cobos JA, Lindsey RW, Gugala Z. The cylindrical titanium mesh cage for treatment of a long bone segmental defect: description of a new technique and report of two cases. J Orthop Trauma. 2000;14(1): 54–9.
100. Lane JM, Bostrom M. Grafton Crunch heals critical sized segmental ulna defects in the rabbit. Osteotech Whitepaper, Eatontown NJ, USA.
101. Attias N, et al. Surgical management of a long segmental defect of the humerus using a cylindrical titanium mesh cage and plates: a case report. J Orthop Trauma. 2005;19(3):211–6.
102. Attias N, Lindsey RW. Case reports: management of large segmental tibial defects using a cylindrical mesh cage. Clin Orthop Relat Res. 2006;450: 259–66.

103. Demircan MN, et al. Multilevel cervical fusion without plates, screws or autogenous iliac crest bone graft. J Clin Neurosci. 2007;14(8):723–8.
104. Radnay CS, Scuderi GR. Management of bone loss: augments, cones, offset stems. Clin Orthop Relat Res. 2006;446:83–92.
105. Brighton B, et al. Hierarchy of evidence: from case reports to randomized controlled trials. Clin Orthop. 2003;413:19–24.
106. Ebell MH, et al. Strength of recommendation taxonomy (SORT): a patient-centered approach to grading evidence in the medical literature. Am Fam Physician. 2004;69(3):548–56.
107. Kwong FN, Harris MB. Recent developments in the biology of fracture repair. J Am Acad Orthop Surg. 2008;16(11):619–25.
108. Gruber R, et al. Fracture healing in the elderly patient. Exp Gerontol. 2006;41(11):1080–93.
109. Hernigou P, et al. Percutaneous autologous bone-marrow grafting for nonunions. Influence of the number and concentration of progenitor cells. J Bone Joint Surg Am. 2005;87(7):1430–7.
110. Romana MC, Masquelet AC. Vascularized periosteum associated with cancellous bone graft: an experimental study. Plast Reconstr Surg. 1990;85(4):587–92.
111. Masquelet AC, et al. Reconstruction of the long bones by the induced membrane and spongy autograft. Ann Chir Plast Esthet. 2000;45(3):346–53.
112. Pelissier P, et al. Behaviour of cancellous bone graft placed in induced membranes. Br J Plast Surg. 2002;55(7):596–8.
113. Pelissier P, et al. Induced membranes secrete growth factors including vascular and osteoinductive factors and could stimulate bone regeneration. J Orthop Res. 2004;22(1):73–9.
114. Stevenson S, Emery SE, Goldberg VM. Factors affecting bone graft incorporation. Clin Orthop Relat Res. 1996;324:66–74.
115. Goldberg VM. Selection of bone grafts for revision total hip arthroplasty. Clin Orthop Relat Res. 2000;381:68–76.
116. Morone MA, Boden SD. Experimental posterolateral lumbar spinal fusion with a demineralized bone matrix gel. Spine. 1998;23(2):159–67.
117. Burwell RG. The function of bone marrow in the incorporation of a bone graft. Clin Orthop. 1985;200:125–41.

Bioreactors for Bone Tissue Engineering

9

Youzhuan Xie and Jianxi Lu

Large bone defect, which often results from the nonunion of the fracture, tumor resection, traumatology and revision reconstruction, is still a great challenge in the orthopaedic surgery. The ideal graft is autogenous bone which is limited in quantity and the harvest procedure is usually painful. The allogenous bone could be used as an alternative. However, the integration and replacement process are slow. And the potential viral and bacterial transmission and the immunoreactions draw back its application. In recent years, more and more biocompatible and biodegradable materials are used as bone substitutes. And tissue engineering provides a tool to create a living bone *in vitro*.

As we all known, tissue engineering has been defined as the application of principles and methods of engineering and life sciences for the development of biological substitutes, to restore, maintain or improve tissue function [1]. Cells, biomaterial scaffolds and external regulators (including biochemical and biophysical factors) are three elemental factors in bone tissue engineering. One of the typical strategies to construct tissue engineered bone is to use bone marrow mesenchymal stem cells (MSCs) associated with the 3-dimensional scaffold. The MSCs are multipotent but have the striking low quantity in the bone marrow (account for 0.001 % of nucleated bone marrow stromal cells in the adult) [2]. Therefore, the MSCs have to be expanded *in vitro* before its implantation into the body. Now the MSCs have been widely used to hybrid the small scaffold to generate new bone [3–6]. The scaffold used for bone tissue engineering should be biodegradable and has a porous structure for cell penetration and nutrition supply. During the bone development, the mechanical and biochemical signals play an important role on the cell differentiation. In order to create the functional tissue *in vitro*, it is necessary to mimic the *in vivo* environment during the engineering process. The bioreactor system is designed to culture tissue for this purpose. It provides not only the efficient nutrition supply to the cells but also the mechanical forces to direct cellular activity and phenotype. In this chapter, we focus on the several key roles of bioreactors in the bone tissue engineering processes including cell seeding of porous scaffolds, nutrition supply in the cell constructs, and mechanical stimulation of the developing tissues.

Bioreactor Design for Bone Tissue Engineering

Generally, the bioreactors are defined as devices in which biological and/or biochemical processes develop under closely monitored and tightly

Y. Xie, MD, PhD (✉) • J. Lu, MD, PhD
Department of Orthopaedic Surgery,
Ninth People's Hospital, Shanghai Jiaotong
University School of Medicine, Shanghai, China
e-mail: youzhuan.xie@gmail.com

D.G. Poitout (ed.), *Biomechanics and Biomaterials in Orthopedics*,
DOI 10.1007/978-1-84882-664-9_9

controlled environmental and operating conditions (e.g. pH, temperature, pressure, nutrient supply and waste removal). Bioreactors are classically used in industrial fermentation processing, wastewater treatment, food processing and production of pharmaceuticals and recombinant proteins (e.g. antibodies, growth factors, vaccines and antibiotics) [7]. Nowadays, three main kinds of bioreactors have been developed for bone tissue engineering: the spinner flask, the rotating wall vessel reactor and perfusion bioreactor. The main functions of these bioreactors include: (1) establish spatially uniform cell distribution on the 3-D scaffolds, (2) maintain desired concentrations of gases and nutrients in the culture system, (3) provide efficient mass transfer to the growing tissue, and (4) expose developing tissues to physical stimuli [8].

Spinner Flask

Although the spinner flask is often used for cartilage tissue engineering, it is one of the simplest bioreactor designs used in bone tissue engineering (Fig. 9.1a). In the spinner flask, a magnetic stirring bar at the bottom creates a dynamic fluid environment around the seeded scaffolds, which are attached to needles and suspended from the top cover of the flask [9]. Turbulent mixing created in a spinner flask bioreactor significantly improves the biochemical compositions and alteres morphologies of the cartilage constructs [10]. The flask system could culture up to 12 cell constructs at the same time. The nutrient mixed rate is controlled by the magnetic stirring bar. Medium is exchanged batchwise, while gas exchange is provided by surface aeration of culture medium via loosened side arm caps [8].

Rotating Bioreactor

The rotating bioreactor (Fig. 9.1b) is developed to engineer cartilage and bone. There are three kinds of geometries: the slow-turning lateral vessel (STLV), the high-aspect-ratio vessel (HARV) and the rotating-wall perfumed vessel (RWPV). They are composed of two concentric cylinders. The cell construct could float in the annular space between the two cylinders. The microgravity environment is produced by the dynamic laminar flow, which is created by the rotating of the cylinder. The gas exchange is performed via internal or external membrane. Medium is exchanged batchwise or by periodic medium recirculation. The rotating bioreactor provides a hydrodynamic environment which is suitable for bone [11, 12] and cartilage tissue growth and differentiation [13]. However, the environment in the spinner

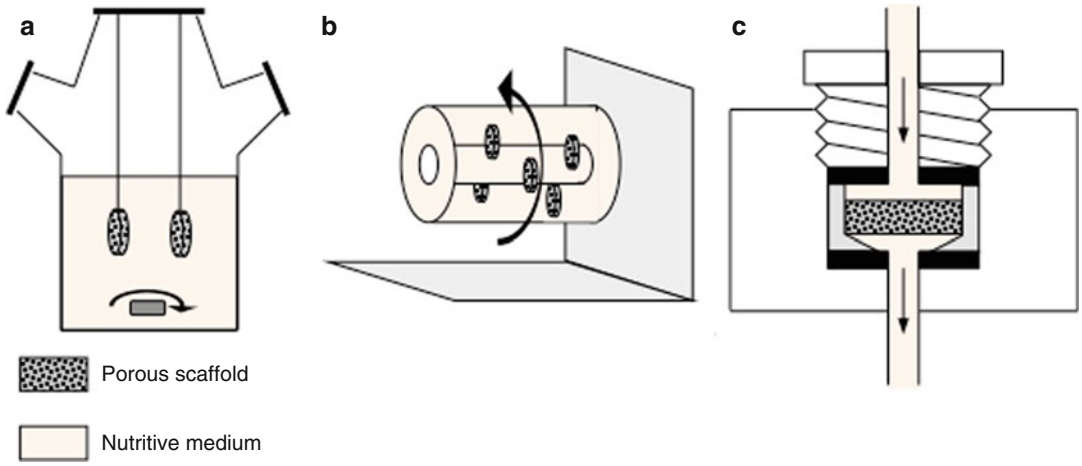

Fig. 9.1 Bioreactors diagram for bone tissue engineering. (**a**) Spinner flask; (**b**) Rotating wall bioreactor; (**c**) Flow perfusion bioreactor (From Olivier et al. [9], with permission)

flask bioreactor seems to favor the MSCs differentiation than in the RWV. Sikavitsas et al. [14] compared three different culturing conditions (spinner flask culture, static culture and rotating wall vessel culture) for their ability to promote the proliferation and differentiation of marrow stromal osteoblasts seeded on PLGA porous scaffolds. The results showed that the potential mitigation of external mass transport limitations in the spinner flask culture could have beneficial effects on the proliferation and differentiation of marrow stromal osteoblasts seeded on PLGA porous scaffolds.

Perfusion Bioreactor

The perfusion bioreactor is different from the above two bioreactors. It usually includes a pump, a reservoir, a chamber and the connecting tubes. The medium in the reservoir is pumped continuously into the chamber which contains the cell construct by a peristaltic pump [4]. Originally, the medium is passed around the edge of the scaffold and the bioreactor is called 'perfusion chamber'. However, the medium in the center of the scaffold could not be exchanged sufficiently in the perfusion chamber. In 2003, Bancroft et al. [15] introduced a new bioreactor (Fig. 9.1c) in order to confine the medium to pass through the interconnected porous network in the scaffold. The new system guaranteed an exchange of medium within the porous scaffold. The perfusion bioreactor could avoid the inappropriate shear stress created by the mechanical mixing in the rotating bioreactor or spinner bioreactor. Further study demonstrated that flow perfusion augmented the functionality of scaffold/cell constructs grown *in vitro* as it combined both biological and mechanical factors to enhance cell differentiation and cell organization within the construct [16]. The environment (e.g. pH, temperature, pressure, nutrient supply and waste removal) in the bioreactor can be precisely controlled and monitored. However, most perfusion systems are designed for culture small cell construct, which could not fulfill the need of large scale bone defect [17].

In 2006, Xie et al. [18] designed a simple novel perfusion bioreactor (Fig. 9.2) for engineering large scale cell construct. The system is composed of three parts: a peristaltic pump, a 75-cm^2 flask containing the perfusion medium and the tubes. One end of the silicone tubes penetrates through the plug cap into the flask as the inlet or outlet. Each cell construct is incubated separately and independently. The seeded scaffold is connected with the silicone inlet and is put into the flask and suspended in the perfusion medium which is over the top of scaffold. The perfusion bioreactor formed bionic circular system. The porous β-TCP scaffold has a central tunnel with blind end. The tunnel connects with the tubing system. The macropores open into this tunnel on the lateral wall. All the macropores are well interconnected mimicking the microcirculation system. The macropores also open into the medium through the lateral pore on the outer surface of the scaffold. Then the medium could be

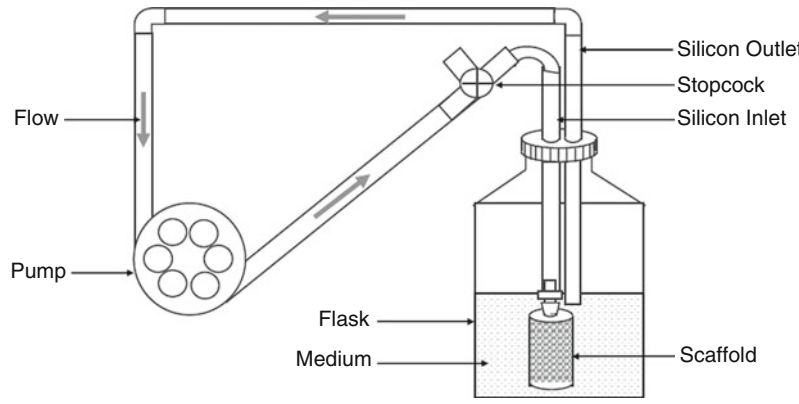

Fig. 9.2 Perfusion bioreactor diagram for large scale cell construct (From Xie et al. [18], with permission)

continually drawn from the reservoir and pumped into the scaffold through the central tunnel. Thus, the metabolic waste in the macropores is brought away. The fresh nutrition and oxygen are brought in. The medium is changed batchwise. The cells inside the scaffolds could survive and proliferate. This kind of built-in flow path not only assures the medium to be perfused into the scaffold, but also makes it possible to utilize the scaffolds with different size and shape. The latter is one of the prerequisites for using custom-made large scale scaffold, especially for reconstruction after bone tumor resection.

Roles of the Bioreactor in Bone Tissue Engineering

Cell Seeding

Cell seeding is the first step before engineering bone tissue. In this stage, the MSCs have to be loaded in the porous scaffold homogeneously. It is supposed that the greater number of cells loaded in the scaffold will increase bone mineralization [19]. Moreover, the spatial distribution of cells within the scaffold after seeding has an effect on the final engineered tissue [20, 21]. Hence, effort has been made to optimize the seeding method in order to achieve the initial construct with uniform and highly dense cells.

Static loading is the traditional way to seed the cells into the scaffold. In this fashion, the single cell suspension solution is prepared before loading. The solution is dropped into the scaffold. Or the porous scaffold is put in the solution directly. The vacuum is often produced by a pump to draw the air out of the scaffold and to make the cell solution penetrate into the scaffold. However, the resulting cell construct is not homogeneously, especially when the scaffold is large enough. The cell density on the surface of the scaffold is much higher than that in the center of the scaffold. Previous study showed that with the static loading, the seeding efficiencies are low and the cell distribution is not homogenous in the scaffold [19, 21–24].

Dynamic seeding is to seed the cell into the scaffold with dynamic flow. It has been reported that dynamic seeding yielded higher seeding efficiency and homogeneity than the static seeding. With the spinner bioreactor, the high and spatially uniform distribution of chondrocytes was achieved in highly porous, fibrous polyglycolic acid scaffolds for rapid and uniform tissue regeneration [25]. Du et al. [26] and Wendt et al. [27] developed an oscillatory perfusion bioreactor. The oscillating perfusion of cell suspensions through three-dimensional scaffolds yielded the higher seeding efficiency, and homogeneous scaffold cellularity throughout the scaffolds compared with either static seeding or the stirred-flask bioreactor. Li et al. [23] found that the dynamic depth-filtration seeding method was better in providing a higher initial seeding density and more uniform cell distribution and was easier to apply to large tissue scaffolds. A depth-filtration model was developed and could be used to simulate the seeding process and to predict the maximum initial seeding densities in matrices with different porosities. Nowadays, the perfusion seeding system has become part of a perfusion bioreactor system. This facilitates the seeding procedure and the subsequent culture procedure. Thus it reduces the possibility of contamination during the seeding and culture procedure.

Mass Transfer

After the seeding, the cell constructs have to be cultured *in vitro* for a period before the formation of the bone tissue. During this stage, the cells will proliferate and differentiate. The sufficient supply of oxygen and nutrient in the scaffold is the fundamental issue for cell survival and proliferation. Previous study on the tumor cellular spheroids showed that the spheroid larger than 600 μm in diameter generally contained a severe hypoxic center and the cells could only survive in the periphery [28]. The cells only survive and proliferate in the exterior pores of the 3-D scaffold under the static culture. Under static culture condition, the mass transfer depends on the gradient difference of mass concentration. The diffusion rate of mass transportation in the static culture was only sufficient to make the cells survive about 500–1500 μm under the scaffold surface

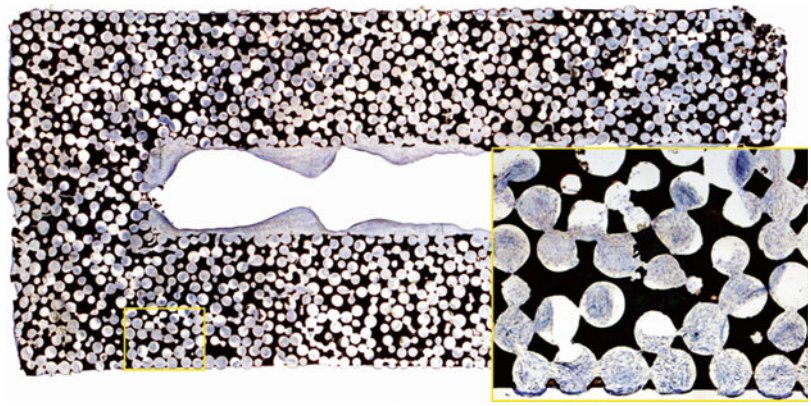

Fig. 9.3 Histological section of the cell/TCP composite stained with May-Grünwald Giemsa. After 28 days under three-dimensional dynamic perfusion culture, the MSCs survived and proliferated through the scaffolds (From Xie et al. [18], with permission)

[6, 29, 30]. Therefore, the cells proliferated sufficiently only in the macropores near the scaffold surface. Because the size of the engineered constructs is often too large to be cultured in a traditional way. The improvement of mass transfer is one of the challenges in the progress of bone tissue engineering.

Dynamic culture created by the bioreactor gives an answer to this problem. In the spinner flask, the oxygen and nutrients in the medium are mixed continuously. The concentration boundary layer at the construct surface also changes and the mass transfer is improved. It is supposed that the better mixing provided in the spinner flask, external to the outer surface of the scaffolds, enhances the proliferation and differentiation of marrow stromal osteoblasts [14].

In the rotating bioreactor, a dynamic laminar flow is generated and the mass transfer improved. It has been proved that the chondrocytes construct cultured in rotating bioreactor is superior to that cultured in the spinner flask or cultured statically [31]. The flow velocity around and through the scaffolds in rotating bioreactors can be manipulated and the 3D dynamic flow environment affects bone cell distribution in 3D cultures and enhances osteoblastic cell phenotypic expression and mineralized matrix synthesis within tissue-engineered constructs [11].

In the perfusion bioreactor, the medium is not only pumped into the reservoir but also perfused through the interior path in the scaffold. The interior passage for the fluid is composed of the macropores and the interconnections in the scaffold. This interior passage is also used for the cell adhesion and proliferation. Under dynamic perfusion culture the gas exchange and nutrition supply are improved in the center of the scaffold as well as in the peripheral part. The waste can be brought away directly [32]. Therefore, the cells survive and proliferate not only in the peripheral part but also in the center of the scaffold (Fig. 9.3). The early study demonstrated that the dynamic culture was superior to static culture for large scale cell construct cultivation [18]. Moreover, the MSCs can differentiate in to the osteogenic cells by the shear stress created by the perfusion flow. However, the different perfusion rate has a different effect on the cell proliferation and differentiation. It is important to tune the bioreactor in order to achieve a balance between the cell proliferation and differentiation.

Shear Stress

It is true that the mechanical stress will affect the MSCs differentiation. In the field of bone tissue engineering, shear stress created by the bioreactor will direct the MSCs to differentiate into osteogenic cells. It is reported that the cells in the scaffold increased in rotating wall vessel bioreactor (RWVB) were five times as that in T-flask and spinner flask. And with the stress stimulation

inside the fluid in the RWVB, the ALP expression was increased; the formation of mineralized nodules was accelerated [33]. The expression of selected bone marker proteins was also enhanced by the low shear stress under the 3D dynamic flow environment [11, 12]. The shear stress in the rotating bioreactor could be calculated and predicted according to the numerical model [34].

In the perfusion bioreactor, the shear stress produced by the bioreactor has more positive effect on the osteogenic differentiation. Datta et al. [35] found that the inherent osteoinductive potential of bone-like extracellular matrix (ECM) along with fluid shear stresses in the perfusion bioreactor synergistically enhanced the osteodifferentiation of MSCs. Leclerc et al. [36] demonstrated that osteoblastic cells could be successfully cultured inside the microdevices under dynamic conditions and their ALP activity was enhanced. Holtorf et al. [37] and Gomes et al. [38] found that under flow perfusion there was greater scaffold cellularity, alkaline phosphatase activity, osteopontin secretion, and calcium deposition compared with static culture even in the absence of dexamethasone. The results suggested that flow perfusion culture alone induced osteogenic differentiation of rat MSCs and that there was a synergistic effect of enhanced osteogenic differentiation when both chemical stimuli (dexamethasone) and mechanical stimuli (low shear stress) were applied. Further study showed that the effect was dose-dependent. In a study conducted by the Bancroft et al. [39], the marrow stromal osteoblasts were cultured on 3D scaffolds under flow perfusion with different rates of flow for an extended period to permit osteoblast differentiation and significant matrix production and mineralization. They found that with all flow conditions, mineralized matrix production was dramatically increased over statically cultured constructs with the total calcium content of the cultured scaffolds increasing with increasing flow rate. The signal transduction mechanism of shear stress in the osteogenic differentiation is complex and involves multiple extracellular signal-regulated kinases (ERK)-dependent and independent pathways [40].

Prospect

One of the goals in bone tissue engineering is to construct the large scale and patient specific tissue with computer-assisted design and computer-assisted engineering in the future. Because the large defect in some cases such as semi-pelvic reconstruction is patient specific and should be highly custom-designed and repaired. With some new technology such as rapid prototyping (RP) it is possible to fabricate a patient-specific scaffold [41]. The bioreactor can create an environment mimicking or replicating the *in vivo* condition. Moreover, the seeding procedure, the culture procedure and the mechanical stimuli could be assembled in one bioreactor. The osteogenic cells associated with the appreciate scaffolds could develop into bone tissue in the bioreactor. Thus, it is a promising technique to reconstruct the bone defect.

References

1. Langer R, Vacanti JP. Tissue engineering. Science. 1993;260(5110):920–6.
2. Pittenger MF, Mackay AM, Beck SC, Jaiswal RK, Douglas R, Mosca JD, Moorman MA, Simonetti DW, Craig S, Marshak DR. Multilineage potential of adult human mesenchymal stem cells. Science. 1999;284(5411):143–7.
3. Kruyt MC, de Bruijn JD, Wilson CE, Oner FC, van Blitterswijk CA, Verbout AJ, Dhert WJ. Viable osteogenic cells are obligatory for tissue-engineered ectopic bone formation in goats. Tissue Eng. 2003;9(2):327–36.
4. Wang Y, Uemura T, Dong J, Kojima H, Tanaka J, Tateishi T. Application of perfusion culture system improves in vitro and in vivo osteogenesis of bone marrow-derived osteoblastic cells in porous ceramic materials. Tissue Eng. 2003;9(6):1205–14.
5. Shin M, Yoshimoto H, Vacanti JP. In vivo bone tissue engineering using mesenchymal stem cells on a novel electrospun nanofibrous scaffold. Tissue Eng. 2004;10(1–2):33–41.
6. Mauney JR, Blumberg J, Pirun M, Volloch V, Vunjak-Novakovic G, Kaplan DL. Osteogenic differentiation of human bone marrow stromal cells on partially demineralized bone scaffolds in vitro. Tissue Eng. 2004;10(1–2):81–92.
7. Martin I, Wendt D, Heberer M. The role of bioreactors in tissue engineering. Trends Biotechnol. 2004;22(2):80–6.

8. Freed LE, Vunjak-Novakovic G. Tissue engineering bioreactors. In: Lanza RP, Langer R, Vacanti J, editors. Principles of tissue engineering. San Diego: Academic; 2000. p. 143–56.
9. Olivier V, Faucheux N, Hardouin P. Biomaterial challenges and approaches to stem cell use in bone reconstructive surgery. Drug Discov Today. 2004;9(18):803–11.
10. Vunjak-Novakovic G, Freed LE, Biron RJ, Langer R. Effects of mixing on the composition and morphology of tissue-engineered cartilage. AIChE J. 1996;42(3):850–60.
11. Yu X, Botchwey EA, Levine EM, Pollack SR, Laurencin CT. Bioreactor-based bone tissue engineering: the influence of dynamic flow on osteoblast phenotypic expression and matrix mineralization. Proc Natl Acad Sci U S A. 2004;101(31):11203–8.
12. Botchwey EA, Pollack SR, Levine EM, Laurencin CT. Bone tissue engineering in a rotating bioreactor using a microcarrier matrix system. J Biomed Mater Res. 2001;55(2):242–53.
13. Saini S, Wick TM. Concentric cylinder bioreactor for production of tissue engineered cartilage: effect of seeding density and hydrodynamic loading on construct development. Biotechnol Prog. 2003;19(2):510–21.
14. Sikavitsas VI, Bancroft GN, Mikos AG. Formation of three-dimensional cell/polymer constructs for bone tissue engineering in a spinner flask and a rotating wall vessel bioreactor. J Biomed Mater Res. 2002;62(1):136–48.
15. Bancroft GN, Sikavitsas VI, Mikos AG. Design of a flow perfusion bioreactor system for bone tissue-engineering applications. Tissue Eng. 2003;9(3):549–54.
16. Gomes ME, Bossano CM, Johnston CM, Reis RL, Mikos AG. In vitro localization of bone growth factors in constructs of biodegradable scaffolds seeded with marrow stromal cells and cultured in a flow perfusion bioreactor. Tissue Eng. 2006;12(1):177–88.
17. Janssen FW, Oostra J, Oorschot A, van Blitterswijk CA. A perfusion bioreactor system capable of producing clinically relevant volumes of tissue-engineered bone: in vivo bone formation showing proof of concept. Biomaterials. 2006;27(3):315–23.
18. Xie Y, Hardouin P, Zhu Z, Tang T, Dai K, Lu J. Three-dimensional flow perfusion culture system for stem cell proliferation inside the critical-size beta-tricalcium phosphate scaffold. Tissue Eng. 2006;12(12):3535–43.
19. Holy CE, Shoichet MS, Davies JE. Engineering three-dimensional bone tissue in vitro using biodegradable scaffolds: investigating initial cell-seeding density and culture period. J Biomed Mater Res. 2000;51(3):376–82.
20. Ishaug-Riley SL, Crane-Kruger GM, Yaszemski MJ, Mikos AG. Three-dimensional culture of rat calvarial osteoblasts in porous biodegradable polymers. Biomaterials. 1998;19(15):1405–12.
21. Kim BS, Putnam AJ, Kulik TJ, Mooney DJ. Optimizing seeding and culture methods to engineer smooth muscle tissue on biodegradable polymer matrices. Biotechnol Bioeng. 1998;57(1):46–54.
22. Xiao YL, Riesle J, Van Blitterswijk CA. Static and dynamic fibroblast seeding and cultivation in porous PEO/PBT scaffolds. J Mater Sci Mater Med. 1999;10(12):773–7.
23. Li Y, Ma T, Kniss DA, Lasky LC, Yang ST. Effects of filtration seeding on cell density, spatial distribution, and proliferation in nonwoven fibrous matrices. Biotechnol Prog. 2001;17(5):935–44.
24. Burg KJ, Holder Jr WD, Culberson CR, Beiler RJ, Greene KG, Loebsack AB, Roland WD, Eiselt P, Mooney DJ, Halberstadt CR. Comparative study of seeding methods for three-dimensional polymeric scaffolds. J Biomed Mater Res. 2000;51(4):642–9.
25. Vunjak-Novakovic G, Obradovic B, Martin I, Bursac PM, Langer R, Freed LE. Dynamic cell seeding of polymer scaffolds for cartilage tissue engineering. Biotechnol Prog. 1998;14(2):193–202.
26. Du D, Furukawa K, Ushida T. Oscillatory perfusion seeding and culturing of osteoblast-like cells on porous beta-tricalcium phosphate scaffolds. J Biomed Mater Res A. 2009;37(1):146–55.
27. Wendt D, Marsano A, Jakob M, Heberer M, Martin I. Oscillating perfusion of cell suspensions through three-dimensional scaffolds enhances cell seeding efficiency and uniformity. Biotechnol Bioeng. 2003;84(2):205–14.
28. Sutherland RM, Sordat B, Bamat J, Gabbert H, Bourrat B, Mueller-Klieser W. Oxygenation and differentiation in multicellular spheroids of human colon carcinoma. Cancer Res. 1986;46(10):5320–9.
29. Ishaug SL, Crane GM, Miller MJ, Yasko AW, Yaszemski MJ, Mikos AG. Bone formation by three-dimensional stromal osteoblast culture in biodegradable polymer scaffolds. J Biomed Mater Res. 1997;36(1):17–28.
30. Martin I, Padera RF, Vunjak-Novakovic G, Freed LE. In vitro differentiation of chick embryo bone marrow stromal cells into cartilaginous and bone-like tissues. J Orthop Res. 1998;16(2):181–9.
31. Vunjak-Novakovic G, Martin I, Obradovic B, Treppo S, Grodzinsky AJ, Langer R, Freed LE. Bioreactor cultivation conditions modulate the composition and mechanical properties of tissue-engineered cartilage. J Orthop Res. 1999;17(1):130–8.
32. Cartmell SH, Porter BD, García AJ, Guldberg RE. Effects of medium perfusion rate on cell-seeded three-dimensional bone constructs in vitro. Tissue Eng. 2003;9(6):1197–203.
33. Song K, Liu T, Cui Z, Li X, Ma X. Three-dimensional fabrication of engineered bone with human bioderived bone scaffolds in a rotating wall vessel bioreactor. J Biomed Mater Res A. 2008;86(2):323–32.
34. Botchwey EA, Pollack SR, Levine EM, Johnston ED, Laurencin CT. Quantitative analysis of three-dimensional fluid flow in rotating bioreactors for

tissue engineering. J Biomed Mater Res A. 2004;69(2):205–15.
35. Datta N, Pham QP, Sharma U, Sikavitsas VI, Jansen JA, Mikos AG. In vitro generated extracellular matrix and fluid shear stress synergistically enhance 3D osteoblastic differentiation. Proc Natl Acad Sci U S A. 2006;103(8):2488–93.
36. Leclerc E, David B, Griscom L, Lepioufle B, Fujii T, Layrolle P, Legallaisa C. Study of osteoblastic cells in a microfluidic environment. Biomaterials. 2006;27(4):586–95.
37. Holtorf HL, Jansen JA, Mikos AG. Flow perfusion culture induces the osteoblastic differentiation of marrow stroma cell-scaffold constructs in the absence of dexamethasone. J Biomed Mater Res A. 2005;72A(3):326–34.
38. Gomes ME, Sikavitsas VI, Behravesh E, Reis RL, Mikos AG. Effect of flow perfusion on the osteogenic differentiation of bone marrow stromal cells cultured on starch-based three-dimensional scaffolds. J Biomed Mater Res A. 2003;67(1):87–95.
39. Bancroft GN, Sikavitsas VI, van den Dolder J, Sheffield TL, Ambrose CG, Jansen JA, Mikos AG. Fluid flow increases mineralized matrix deposition in 3D perfusion culture of marrow stromal osteoblasts in a dose-dependent manner. Proc Natl Acad Sci U S A. 2002;99(20):12600–5.
40. Kapur S, Baylink DJ, Lau KH. Fluid flow shear stress stimulates human osteoblast proliferation and differentiation through multiple interacting and competing signal transduction pathways. Bone. 2003;32(3):241–51.
41. Detsch R, Uhl F, Deisinger U, Ziegler G. 3D-Cultivation of bone marrow stromal cells on hydroxyapatite scaffolds fabricated by dispense-plotting and negative mould technique. J Mater Sci Mater Med. 2008;19(4):1491–6.

Orthopedic Bone Cements

10

Jianxi Lu

"Cement", a word comes from the domain of architecture construction. It consists of a system of powder/liquid materials which, when mixed to a paste, set to a hard mass. "Bone cement" is to benefit this system for an application in medicine, for example: filling of bone defects and fixation of surgical prosthesis etc.

The history of the application of bone cement dates to more than 100 years. In 1890, Dr. Gluck described the use of the ivory ball-and-socket joints which were especially useful in the treatment of diseases of the hip joint. These joints were stabilised in the bone with a cement composed of colophony, pumice powder and plaster. He stated that the cement remained walled off in the marrow cavity in the same way as a bullet, the marrow cavity appearing to have almost unlimited tolerance to aseptic implantation [1]. In 1951, Dr. Haboush used self-curing acrylic dental cement to secure a total hip replacement [2]. Also at this time similar resins were being used to repair defects in the skull after brain surgery. Polymethylmethacrylate (PMMA) cement was used primarily in dentistry to fabricate partial dentures. orthodontic retainers, artificial teeth, denture repair resins, and an all-acrylic dental restorative. Dr. Charnely had used a cold-cured acrylic as a possible luting cement to retain the femoral shaft in total hip arthroplasty [3].

From 1950s to 1970s numerous studies and tong-term clinical trials exposed the biological disadvantages of PMMA cement: (1) the release of monomer toxicity; (2) the high temperature of the cement polymerisation; (3) osteonecrosis mediated by inflammatory reaction; (4) osteolysis caused by wear debris formation or (5) impairment of blood circulation in the bone caused by reaming, then, plug of cement [4]. Moreover, this cement is neither biodegradable nor colonisable by bone tissue. Therefore, surgeons sought to ameliorate the PMMA cement looking for new cement to replace it. Brown and Chow [5] were the first to develop and patent a calcium orthophosphate cement. Different formulations of the calcium phosphate cement have since been developed by various research groups [5–10]. The studies *in vitro* and *in vivo* have shown that the calcium phosphate cement (CPC) was an excellent biocompatibility, a good bioresorption, an osteoconducteur, and a less exothermic, but weaker mechanical properties than PMMA cement.

This paper provides a general regulatory background, chemical composition information, mechanical and biological properties as well as a discussion of the mechanisms of the risks and failures of bone cements. We present

J. Lu, MD, PhD
Department of Orthopaedic Surgery,
Ninth People's Hospital, Shanghai Jiaotong University School of Medicine, Shanghai, China
e-mail: 382139777@qq.com

D.G. Poitout (ed.), *Biomechanics and Biomaterials in Orthopedics*,
DOI 10.1007/978-1-84882-664-9_10

principally two bone cements; polymethylmethacrylate cement (PMMA) and calcium phosphate cement (CPC).

Polymethylmethacrylate Cement (PMMA)

Chemical Composition and Polymerisation of the PMMA

PMMA bone cement has remained largely unchanged over the years consisting of preformed PMMA beads mixed with methylmethacrylate (MMA) monomers. PMMA cements include: (1) the weight ratio of powder to the liquid monomer; (2) the use of PMMA or copolymers thereof; and (3) the use of benzoyl peroxide as initiator in the powder and MMA; (4) the use of MMA as the monomer in the liquid component; (5) the use of a radio-opaque filler (e.g. barium sulphate or zirconium dioxide). Differences include: (1) the amount of the initiator (benzoyl peroxide) in the powder; (2) the amount of accelerator (*N*,*N*-dimethyl-*p*-toluidine) in the liquid component; (3) the amount and type of stabilisers (e.g. hydroquinone) in the liquid component; and (4) the addition of chlorophyll used to colour the cement green. The chemical composition of the commercially available bone cements is similar, with the minor differences described in Table 10.1.

The polymerising process of the cement occurs as a result of the reaction between the initiator in the polymer powder and accelerator in the monomer. These act together to form a complex which produces benzoate and amine radicals. These two radicals then initiate polymerisation of the monomer [11]. A radiopacifier, added to the powder component, enables the surgeon to view the cement *in vivo*. This process transforms the initial thick liquid to a soft deformable material and finally to a rapidly hardening cement with an associated increase in temperature due the exothermic polymerisation which can exceed 80 °C. The cement sets through the polymerisation of the monomer, which concurrently dissolves and softens the polymer particles. The set mass consists of the polymer matrix uniting the undissolved but swollen original polymer granules. The degree of polymerisation is affected by the following: (1) the amount of accelerator and initiator in the powder and liquid monomer; (2) wetting caused by the monomer mixing with the powder; (3) the type of mixing used, (4) the pro-chilling of the monomer; and the presence of oxygen.

Table 10.1 General chemical compositions of various commercially available bone cements

	Brand 1	Brand 2	Brand 3	Brand 4
Powder components	***40 g***	***40 g***	***40 g***	***40 g***
PMMA (polymer)	88.85 %(w/w)		15.00 %(w/w)	89.25 %(w/w)
Polystyrene/MMA copolymer			75.00 %(w/w)	
MMA/PMMA copolymer		83.55 %(w/w)		
Benzoyl peroxide (initiator)	2.00 %(w/w)	0.5–1.6 %(w/w)		0.75 %(w/w)
Sulphate barium (radio-opacifier)	9.10 %(w/w)		10.00 %(w/w)	10.0 %(w/w)
Zirconium dioxide (radio-opacifier)		15.00 %(w/w)		
Liquid components	***18.37 g***	***20 ml***	***20 ml***	***20 ml***
MMA (monomer)	98.215 %(w/w)	99.26 %(w/w)	97.40 %(v/v)	97.25 %(v/v)
N,*N*-dimethyl-*p*-toluidine	0.816 %(w/w)	1.96 %(w/w)	2.62 %(v/v)	2.75 %(v/v)
(accelerator)	0.002 %(w/w)		75 ± 15 ppm	75 ± 10 ppm
Hydroquinone (stabilizer)	15–20 ppm			
Other monomeric additives				
Ethyl alcohol	0.945 %(w/w)			
Ascorbic acid	0.022 %(w/w)			
Chlorophyll (colour additive)		0.002 %(w/w)		

Table 10.2 Physical and mechanical properties

	ISO-5833
Dough time	5 ± 1.5 min
Setting time	3–15 min
Exothermic temperature	<90 °C
Compression strength	70 MPa
Tensile strength	50 MPa
Tensile modulus	1.8 GPa

Physical and Mechanical Properties of the PMMA

The physical and mechanical characteristics of the acrylic bone cement were determined by the ISO 5833–1992 standard [12] (Table 10.2). The liquid and powder mixing procedure should be influenced by various factors in order to modifier the properties. These factors include the amount of the ingredient, the temperature and humidity of the mixing environment, the type of sterilisation used and the type of mixing (hand, centrifugation, or vacuum mixing) used to prepare the cement; as well as the surgical installation used in the mixing process.

Physical Properties

Cement viscosity is increased by the addition of fibres, greater molecular weight of the polymer, solubility of the polymer in the monomer, variation in the powder composition or bead size distribution, and the temperature of the cement components. Pre-chilling the cement components increases the setting time and reduces the viscosity of the cement, as compared to cement components which are stored at room temperature prior to mixing. In contrast, mixing of bone cement under vacuum generally decreases the setting time. At the time mixing, the components are usually hand mixed in a bowl. However, with the use of vacuum mixing or centrifugation after mixing, the cement porosity and pore size can be reduced to improve the mechanical properties of the cured cement [13–16]. Greater monomer evaporation may occur if the applied vacuum is too great during vacuum mixing.

Poor monomer wetting in the powder can occur if: (1) the powder is insoluble or only partially soluble in the liquid MMA monomer; (2) an inadequate amount of MMA monomer is mixed into the powder; or (3) the free volume is lowered due to tighter packing of powder. On the other hand, styrene copolymers may have better wetting properties due to a higher free volume which allows for faster monomer diffusion rates [17].

High temperatures of the polymerisation process can cause evaporation of the monomer leading to microporosity in the curing cement. There are a number of factors that affect the maximum exothermic temperature. The following may contribute to a higher cement polymerisation temperature: (1) a large cement mass; (2) a cemented device with a low conduction heat;(3) a cemented device that is not cooled before implantation; (4) lack of irrigation at the implant site; (5) a greater amount of monomer mixed into the powder; or (6) increased levels of accelerators or initiators which may form radicals initiating rapid polymerisation [18].

Microporosity in the bulk cement may result form the following: (1) monomer evaporation during the exothermic reaction and/or leaching of the unreacted monomer [19]; (2) flow and wetting during mixing with the beads leading to air entrapment; (3) CO_2 formation due to a benzoyl peroxide reaction with the accelerator; (4) turbulent cement flow during the insertion of the implant into the cement; (5) the mixing method used to assemble the bone cement components.

Mechanical Properties

The implant-cement-bone interfacial strengths are also considered risk factors [20]. Implant-cement interfacial loosening may result from: (1) cement fracture or poor implant-cement bonding due to foreign matter; (2) inadequate coverage at the implant-cement interface [21]; (3) amount of mechanical interlocking; or (4) a lack of chemical bonding at this interface. More specifically, the inadequate cement coverage at the interface may be caused by: (1) shrinkage of the cement due to polymerisation; (2) poor mechanical interlocking strength between the implant and cured bone cement [22]; or (3) an increase in the bone cement viscosity over time leading to poor contact between the cement and implant.

Cement-bone loosening may result from: (1) cement fracture; (2) formation of gaps at the

interface; or (3) tissue failure. More specifically, the gaps may form due to: (1) bone resorption; (2) foreign material at the cement-bone interface such as bone particles or blood [23]; (3) shrinkage of the cement after implantation; (4) low cement pressurisation during implantation [24]; or (5) movement of the implant before hardening of the cement. For gaps caused by shrinkage, the shrinkage is greater as the porosity is decreased.

A fatigue fracture of the cement is a result of a cement stress which exceeds the fatigue limit of the bone cement. High cement stress may be due to an applied stress or a residual stress, cement modulus, implant loosening or poor cement bonding with the implant or with the bone. Other causes of cement fracture include; fibrous membrane formation between the bone and cement, improper cement mantle thickness (a layer too thin or too thick), lamination of the cement due to the presence of blood or other body fluids, poor canal preparation or areas of increased stress (e.g. the presence of a pore or a sharp corner of an implant). High stress applied to the bone cement may be caused by: (1) Increased patient weight or activity; (2) lack of constraint; (3) adverse implant size and orientation; or (4) inadequate bone cement mantle. The latter three are related to the quality of the tissue and the applied surgical technique. A weakness may also be caused by bone resorption or by disease.

Cement mechanical properties are affected by the level of stress at a specific site. This is influenced by: (1) irregular trabecular bone; (2) porous implant coatings; (3) sharp edges on the implant; or (4) a defect in the bulk cement such as a pore or additives. More specifically, localized stress caused by porosity and inclusions (e.g. additive agglomeration, redio-opacifiers and antibiotics) are perhaps the greatest factor affecting cement fatigue properties. The addition of agglomerates (e.g. redio-opacifiers) may also play a similar and significant role in cement fracture.

Biological Properties of the PMMA

All biomaterials must be biocompatible. PMMA cements are considered biocompatible despite the toxic potential of the bone cement monomer and the heat generated during the exothermic polymerisation.

Cellular Reactions

Initially, the major problems of PMMA bone cement are related to the temperature increase during the polymerisation and the release of residual monomer after polymerisation. PMMA is non toxic, but the residual monomer (MMA) can cause an irreversible deterioration of the cells [25, 26]. After 15 min of polymerisation, there is a residual monomer of approximately 3–5 %. This percentage may decrease up to 1–2 % with time [25]. Haas et al. [19] measured the residual MMA content to be 3.3 % after 1 h, 2.7 % after 24 h and 2.4 % after 215 days under storage in an ambient air environment. According to Schoenfeld et al. [27], the toxicity of the monomer disappears after 4 h. In our study of cement fragments which were harvested at the time of prosthetic revisions 48–78 months after implantation, there was no apparent toxic effect of the cement on the fibroblasts (L929) and human osteoblasts [28]. However, there may be variable reactions to PMMA depending of the cells involved.

PMMA is not cytotoxic with regard to human fibroblasts *in vitro*. However, it can stimulate proliferation and protein synthetic activity [29]. The increased proliferation of fibroblasts in response to PMMA exposure can be associated with an increased production of collagen and chemical mediators at the bone-cement interface [30, 31]. Chemical mediators, such as prostaglandin E2 (PGE2) and other cytokines (interleukine-1), have been shown to mediate inflammation, as well as induce cell division and differentiation [32, 33]. Fibroblasts have previously been implicated in the inflammatory response. Therefore, it is possible that they are responsible for the recruitment of inflammatory cells at the bone-cement interface via release of chemical mediators such as PGE2.

Monocytes and macrophages are significant agents of the inflammatory reaction. The principal function of the tissue macrophage is phagocytosis and the secretion of cytokines and

growth promoters. PMMA particles induce macrophages to secrete protein and to express mRNA of the proinflammatory cytokines, interleukin-1β (IL-1β), interleukin-6 (IL-6), tumour necrosis factor alpha (TNF-α), PGE2, proteinases, collagenases and oxygen metabolites. Other factors expressed include chemokines such as macrophage-activating and chemotactic protein 1 (MCP-1) as well as macrophage inflammatory protein (MIP) which may be linked to osteolysis [34–43]. Horowitz et al. described a dose-dependent release of arachidonic acid metabolites by murine macrophages induced by PMMA particles [44].

The osteoclast is a multinucleated cell which carries out the unique and highly specialized function of lacunar bone resorption. The osteoclast belongs to the mononuclear phagocyte system which consists of various cell types including monocytes, macrophages, Kupffer cells and microglia. A common feature of all these cells is their avid and efficient ability to carry out phagocytosis. Most studies have focused on the effect of biomaterial particle phagocytosis on the function of these cells and the observation that specific types of particle enhance the release of mediators thus stimulating osteoclastic bone resorption [45–47]. In addition, it has been shown that macrophages after having phagocytosed these particulates are capable of osteoclast differentiation [48]. Wang et al. [49] found that osteoclasts having phagocytosed PMMA wear particles exhibit normal lacunar bone resorption. As well, the phagocytosis of PMMA particles does not appear to compromise the response of osteoclasts to calcitonin or to the ability to carry out lacunar resorption, an observation that remains controversial. PMMA particles can inhibit osteoblast activities causing a decrease in cellular proliferation and collagen synthesis.

Local Tissue Reactions

PMMA bone cement is generally well tolerated and bony tissue, generally, flourishes on it's surface [29, 43]. However, there is evidence of the inflammatory potential of bone cement [50]. The tissue reaction around bone cement has several phases. Initially, there is a necrosis of the bone tissue and marrow to a depth of 5 mm depth related to the surgical wound and polymerisation. Next, there is a phase of cicatrisation lasting up to 6 months followed by a tissue granulation which develops over a period of 2 years. This tissue granulation is a characteristic of the chronic inflammation. The cement is then surrounded by a layer of fibrous tissue [51–54] and occasionally by a varying thickness of fibrocartilage [55, 56],.. Albrektsson [57] reported a 59 % reduction in the in growth of cortical bone into titanium bone chambers 1 month after cement application. Morberg et al. [58, 59] reported as well a decreased bone formation around cemented tibias, being 21 and 31 % lower than the non-cemented contralateral tibias after 3–11 and 32–55 weeks, respectively.

Osteonecrosis

Cell necrosis may occur because of the following: (1) monomer toxicity; (2) the high temperature of cement polymerisation; (3) pressure necrosis; (4) osteolysis caused by wear debris generation; or (5) the impairment of blood circulation in the bone caused by reaming and by the presence of cement [4]. Bone cement has been shown to decrease bone metabolism possibly causing a lower revascularisation [60, 61].

The production of heat at the bone-cement interface during the cement polymerisation *in vitro* is between 60 and 90 °C [62–64] and *in vivo* between 40 and 50 °C [65, 66], both depending on the thickness of the cement. The effect of this heat generation on bone was studied by Lundskog [67] who concluded that the exothermic polymerisation did not add to the surgical trauma and had no influence on bone generation. Lee et al. [68] found that the leakage of monomer was very low after the curing. Likewise, Sund and Rosensuist [69] stated "the effect of polymerisation heat and monomer toxicity are probably much less important than the trauma effected by blocking of the normal medullar blood supply". Rhinelander et al. [66] who noted a maximal temperature of 55 °C with the placement of thermometers at the bone-cement interface, concluded that thermal necrosis from cement polymerisation is not a

significant factor. Furthermore, after direct contact with acrylic cement, the delicate trabeculae of cancellous in the metaphysis contained healthy appearing osteocytes after 6 weeks.

Osteolysis

Bone surrounding an implant may undergo osteolysis leading to loosening and a decrease in cancellous bone strength. This may result in a weakening of the cement fixation or the formation of a gap between the cement and bone. Acrylic cement fragments are engulfed by eosinophilic histocytes which stimulated enzymatic release leading to bone resorption [70, 71]. In addition, bone cement particles could accelerate foreign body deterioration of articulating polyethylene inserts [72, 73]. The initial event can be either disintegration of bone cement or deterioration of the articulating surface. Phagocytosis and the development of foreign-body granulomas lead to osteolysis of the anchoring bone; thus disintegration or deterioration are enhanced accelerating the progress of osteolysis [51].

Formation of Fibrous Membrane

The formation of fibrous tissue is caused by the toxicity of the monomer release as well as the heat production of the polymerisation causing a chronic inflammation and eventual osteonecrosis and an osteolysis. It is a significant factor which induces the micromovements and the loosening of surgical implants. The thickness of the fibrous membrane around PMMA cement was of 40 μm and 60–70 μm after 1 and 4 weeks respectively in the tibiae diaphysis [53, 74]. In the human femur, the thickness was measured at 20–300 μm at 11 months to 7 years [55] and at 3–5 mm long-term. [54]

Implant Loosening

Revision of a cemented orthopaedic prosthesis may be necessary when pain occurs due to either the movement of the prosthesis, a bone fracture, bone cement fracture or prosthesis fracture. More specifically, these complications may result from prosthesis-cement, or cement-bone interfacial loosening or micromotion due to cement fracture or cement creep. Loosening of the prosthesis and fracture of the cement may lead to increased wear and bone cement particle formation. Those particles approximately less than 5 μm in size are phagocytosised by macrophages which become activated and directly or indirectly cause bone remodelling and osteolysis [14, 75–78]. However, PMMA particles ingested by macrophages cannot be degraded by lysosomal enzymes [45]. The final result is cell death leading to tissue necrosis and chronic inflammation [79]. For the femoral stem, the lower viscosity bone cement had a revision rate 2,5 times greater when compared to the use of higher viscosity cements. Additionally, a lower modulus cement had a revision rate that was 8.7 greater than the higher viscosity cements [80]. In general, revisions are required between 3.6 and 22.8 years following a total hip prosthesis. The most frequent periods of revision are either during the first 3 years or after 8 years postoperatively [81]. The aseptic loosening of the prosthesis is the principal cause of revision, implicated in: 73–74 % of the total cases [82, 83]. Subcritical debonding associated with mechanisms of cyclic fatigue crack growth are particularly relevant considering that these systems will experience over 1,000,000 physiological loading cycles per year, and are expected to survive a minimum of 10–15 years. In these terms, it is critical to understand the progressive debonding of prosthesis-PMMA cement interface [84].

Secondary Reactions

Systemic and Cardiovascular Reactions

Methylmethacrylate (MMA) is very volatile and is rapidly cleared from body through the lungs resulting in a local concentration that remains very low [85, 86]. MMA monomers escaping from the implanted polymerising cement have been associated with a decrease in both systolic blood pressure and arterial oxygen tension [87] and possibly cardiac arrest. [88] However, many studies have not confirmed this direct correlation between the concentration of MMA and blood pressure, heart depression or vasodilatation [86, 89, 90]. Circulatory disturbance during hip implantation may be primarily due to either the “implantation syndrome” or to the

blockage of pulmonary circulation by fat, bone marrow and entrapped air rather than MMA monomer. Release of MMA could cause a drop in the partial pressure of arterial oxygen leading to an increased heart rate [91, 92]. The possible metabolic pathway of MMA monomer is that the residual monomer is converted to methylacrylic acid rather than methylester. The methylacrylic acid, as a coenzyme A ester, is a normal intermediate in the catabolism of valine and the existence of an enzyme system would permit methylacrylic acid to enter a normal pathway, leading to carbon dioxide formation. Over 80 % of an administered dose of MMA is expired as carbon dioxide within 5–6 h [90].

Sensitising

While MMA is considered to be relatively immunologically inert, it can induce phagocytosis, the activation of macrophages and giant cells as well as the migration of inflammatory mononuclear cells [13, 14, 52, 74, 78]. Jensen et al. [52, 74] showed that MMA is extremely active in a guinea-pig maximisation test. The hospital personnel who repeatedly handle coring acrylic bone cement are potentially at risk of developing a delayed sensitivity [93]. Bengston et al. [94] reported that patients having received a cemented hip prosthesis had increased levels of anaphylatoxines which can contribute towards circulatory and respiratory disturbances. In contrast, Kanerva et al. [95] have found allergies to MMA to be rare in a study of patients between 1974 to 1992 (4 patients: a orthodontist, 3 dental technicians).

Improvement of the PMMA

The objective of the development of PMMA bone cement is to improve the biocompatibility, to diminish the temperature of polymerisation, to eliminate the generation of wear debris and fatigue fractures, as well as to increase the elastic modulus. Therefore, efforts to improve PMMA bone cement have proceeded in two main directions: (1) to change the composition and (2) to improve preparative techniques.

Tertiary aromatic amines are used as accelerators for the benzoyl peroxide (BPO) initiated MMA polymerisation. A complex series of reactions occurs between BPO and the amine, and free radicals are produced that initiate the polymerisation process [96, 97]. Several types of amine accelerators, such as dimethyl aniline and its derivatives, have been used in the polymerisation of MMA by the amines/BPO initiator system. Their relative efficiency as accelerators and their activating effects on the rate of polymerisation have been reported [96, 97]. Several workers have studied bone cement properties using a number of N,N-dimethyl-p-toluidine derivatives, such as, 4-dimethylaminobenzyl methacrylate, and 4-dimethylamino phenethyl alcohol [96–99]. Bone cement products containing residual monomer and amine have been reported in preparation where the amines/BPO molar ratio is outside the equimolar range [11]. Other study showed that MMA polymerisation in the presence of tir-*n*-butylborane used as the cure initiator does not occur too rapidly, and the high temperature during polymerisation is lower than that of conventional bone cement. The application time is short enough for clinical use, namely, within 10 min. As for the physical properties, it has a 3 % lower elastic modulus and greater ductility than the conventional cement [100].

Several workers have added particles or fibres to PMMA bone cement to improve the biocompatibility et the mechanical properties. The fibre reinforced bone cement possessed significantly greater stiffness and displayed poor intrusion characteristics [101–103]. A number of attempts have been made at filling a PMMA matrix with hydroxyapatite and tricalcium phosphate particles, and with bioactive glass [104–106]. The short-term results obtained are encouraging and suggest that the chemical nature of the bone/bioactive materials interface is very important relative to osteoconductivity [107]. For instant, PMMA bone cement can be used only to effectuate mechanical fixation for prosthesis or to physically fill bone defects. It however, does not exhibit the functions of osteointegration, biofixation, nor bioresorption.

Calcium Phosphate Cement (CPC)

Chemical Compositions and Crystallisation of the CPC

Calcium phosphate cements can be handled in paste form and set in a wet medium after precipitation of calcium phosphate crystals in the implantation site. Depending on the products involved in the chemical reaction leading to the precipitation of calcium phosphate, different phases can be obtained with different mechanical properties, setting times and injectability. Numerous components can enter the chemical reaction leading to calcium phosphate precipitation. More than 100 different of calcium orthophosphate cements were used to determine the compressive strength and the diametric tensile strength after storage. The setting was carried out on more than 15 formulations. These cements could be divided into four classes: dicalcium phosphate dihydrate, calcium and magnesium phosphates, octocalcium phosphate, and nonstoichiometric apatite cements [108, 109]. The calcium and phosphate compounds in Table 10.3 were often used to make the CPC. Moreover, adjuvants such as chitosan, lactic acid and glycerol are added to improve the injectability of the cement, and accelerators such as Na_2HPO_4, sodium phosphate, sodium succinate, and sodium chondroitin sulphate to accelerate its setting time.

The hardening process of CPC is complex and involves the dissolution of solid particles in the liquid, precipitation of HAP from the solution, and the reaction and diffusion on the particle surface. Under ideal conditions, continuing dissolution of the reactions supplies calcium and phosphate ions to the solution, while HAP formation depletes these ions. This process drives the solution composition to an invariant point, which is the intersection of the solubility curves for these two reactants. The pH is about 7.8, but this process is affected by many parameters, such as the component and the particle sizes of the solid phase, presence of HAP seed and properties, aqueous liquid, etc.

Physical and Mechanical Properties of the CPC

All CPC are formulated as solid and liquid components that, when mixed in predetermined proportions, react to form HAP. This final reactant is important because it determines whether the end product will be nonresorbable, minimally resorbable, or completely resorbable. The powder component usually consists of 2 or more calcium phosphate compounds, whereas the liquid component is either water, saline, or sodium phosphate (Table 10.4). Some of the calcium and phosphate compounds involved in bone and mineral formation, or as implants, are listed in Table 10.3. These materials have been well characterised chemically and have not been reported to cause foreign body reactions or other forms of chronic inflammatory response [110].

Table 10.3 Calcium and phosphate compounds

Name	Abbreviation	Formula	Ca/P	Solubility	Acidity	Stability
Monocalcium phosphate monohydrate	MCPM	$Ca(H_2PO_4)_2 \cdot H_2O$	0.5			
Dicalcium phosphate anhydrous	DCPA	$CaHPO_4$	1.0	+++++	+++++	+
Dicalcium phosphate dihydrate	DCPD	$CaHPO_4 \cdot 2H_2O$	1.0	+++++	+++++	+
Octacalcium phosphate	OCP	$Ca_4H(PO_4)_3$	1.33	++++	++++	++
Amorphous calcium phosphate	ACP	$Ca_9H(PO_4)_6$	1.3–1.5	+++	+++	+++
Tricalcium phosphate	TCP	$Ca_3(PO_4)_2$	1.5	++	++	++++
Hydroxyapatite	HAP	$Ca_{10}(PO_4)_6(OH)_2$	1.67	+	+	+++++
Tetracalcium phosphate	TTCP	$Ca_4(PO_4)_2O$	2.0			

Table 10.4 Properties of the CPC

Authors	Powders	Liquid	Setting (min)	Strength (MPa)	Resorption
Brown and Chow [5]	DCPD/DCP/TTCP/HA	H_2O	30–60	10	Minimally
Lemaitre et al. [6]	β-TCP/MCPM	H_3PO_4	10	25–35	Completely
BoneSource [110]	TTCP/DCPD	H_2O	10–15	36	Minimally
Norian [110]	MCPM/α-TCP/$CaCO_3$	$CaHPO_4$	10	55	Completely
Fernandez et al. [10]	DCPA/α-TCP	H_2O	–	30–40	Yes
Kurashina et al. [8]	α-TCP/DCPD/TTCP	Sodium succinate Sodium Chondroitin Sulphate	–	–	Yes
Liu et al. [9]	TTCP/DCPD/DCPA	H_2O	11	70	Yes
Ginebra et al. [7]	α-TCP/β-TCP	Na_2HPO_4	5–12	40	Yes

The physicochemical reaction that occurs during mixing of the solid and liquid compounds of CPC is complex. Briefly, when different calcium phosphate salts are mixed in an aqueous environment, dissolution of the solid compounds, then a precipitation or a nucleation, and finally a phase transformation occurs. The process leading to final phase transformation of the different forms of calcium phosphate salts is dependent on their solubility, product constant and pH. It is important to realise that water is not a reactant in the setting reaction of the cement, but it allows dissolution of the solids and precipitation of the products. The nature of the apatite makes the final form biocompatible and promotes a chemical bond to the host bone.

There is a possibility to transform the cement into an injectable paste by addition of adjuvants without fundamentally modifying the chemical reactions occurring during setting and hardening of the CPC. Leroux et al. [111] found that glycerol greatly improved the injectability and increased the setting time, but decreased the mechanical properties. Lactic acid reduced the setting time, increased the material toughness, but limited the dissolution rate. After injection, the cement did not present any disintegration. The effects of lactic acid were correlated with the formation of calcium complex. Its association with sodium glycerophosphate is particularly important. Chitosan alone improved the injectability, increased the setting time, and limited the evolution of the cement by maintaining the CPC phase.

The CPC have an inherent compressive strength at the final set that can govern their utility. Varying the crystallinity of the HAP or the particle size of materials used in the solid phase may alter the compressive strength. Because CPC are relatively insoluble at neutral and alkaline pHs, their porosity is related to the ratios of powder to liquid used in the starting mixture. Obviously, a cement with a high porosity would be expected to be of low compressive strength. Cements with a high compressive strength would be expected to find utility where they would stabilise nondisplaced bone fractures and comminutions, or repair large bone defects, or fixes surgical prosthesis. Cements with a low compressive strength would limit their utility and only fill small bone defects.

Biological Properties of the CPC

The calcium and phosphate compounds of the CPC have attracted considerable attention because they set like a dental cement and form hydroxyapatite as the end product which is the major mineral components of teeth and bone. A number of studies *in vitro* and *in vivo* have shown that CPC had no toxicity, negative mutagenicity and potential carcinogenicity [112, 113], no or slight inflammatory reactions, good osteoconductivity and bioresorption [114] as well as light exothermic temperature (<40 °C) during CPC hardening. However, CPC particles could be harmful for

osteoblasts with a decrease of viability, proliferation and production of extracellular matrix, especially when their size was smaller than 10 µm. A dose effect was present, ratio of 50 CPC particles per osteoblast could be considered as the maximum of what an osteoblast supported. The acidification of the medium due to the dissolution of the CPC could not be responsible for the decrease of osteoblast functions because the control of the pH value of the medium have shown that it did not change. It was then the direct interaction of osteoblasts with particles which was involved in the decrease of osteoblast functions [115]. Some adjuvants of the CPC can induce acidification and release some elements to modify the biological properties. We have cultivated osteoblasts on the CPC surface, cell proliferation increased after the first 7 days followed by a decrease afterwards and an absence of cells noted by the 21st day. This result indicated that the acidification of the medium and disaggregation of the CPC, are the two important factors: directly influencing cellular attachment and proliferation *in vitro* at cement surface. But, these cements are generally the product of an acid-base reaction which did not seem to induce any necrosis as no visible zone of dead tissue *in vivo* due to the system of the acid-base equilibrium in the organism.

The tissue reactions to the CPC are different in different tissues. When CPC was implanted in the cutaneous tissue, a slight inflammatory reaction with numerous macrophages and few foreign-body giant-cells were observed in the connective tissue adjacent to the cement implant. However, when CPC was implanted in the bone tissue, new bone was formed around the implant from 1 to 2 weeks, cements were resorbed and replaced by bone tissue from 4 to 8 weeks, then an bone remodelling occurred in the implanted zone, and no inflammatory reaction nor osteonecrosis at all phases [114, 116, 117]. From this difference, it could be hypothesised that micromovements persist in the materials implanted in the soft tissue which stimulate the tissue around implant to cause inflammatory reaction. On the contrary, the materials implanted in the bone tissue are immobilised by bone tissue which may explain the absence of this reaction.

There is controversy as to the resorption and replacement of CPC by bone tissue. Ikenaga et al. [118] reported that a CPC resorption was about 8 % at 2 weeks and 92 % at 12 weeks, and new bone formation was about 1 % at 2 weeks and 35 % at 12 weeks in the femoral condyle of rabbit. When CPC was implanted in same site, Frayssinet et al. [119] found a resorption of 54 %, 68 % and 89 %, and new bone formation of 25 %, 32 % and 23 % at 2, 6 and 18 weeks respectively. Our study have shown that the new bone formation increased from 2 to 24 weeks, and the material resorption was about 10 %, 15 %, 30 % and 60 % at 2, 4, 12, and 24 weeks respectively in the tibiae condyle of rabbit [114]. In contrast, Costantino et al. [120] made 2.5 cm in diameter full-thickness parietal skull defects in cats and reconstructed them with CPC. By 6 months, the CPC was replaced by new bone and soft tissue 7.2 mm in depth from the cement surface. Of the replacement tissue, 77.3 % was new bone and the remaining portion was soft tissue. Friedman et al. [121] found very little resorption of CPC or new bone deposition at months when the frontal sinus in the cat was obliterated and reconstructed with CPC. These differences are thought to be caused by many factors, including differences in species and age among the experimental animals, anatomical site, method and duration of implantation, composition of the CPC, etc.

CPC is only an osteoconductor without osteoinduction, and is in direct contact with osteoid or/and bone, but osteoblasts are rarely in direct contact with CPC surface. This maybe due to that the space formed rapidly by the material degradation at bone/cement interface, or/and products of the dissolution influence cellular adhesion. The biodegradation of the CPC respects the mechanisms of biomaterial which are resorption by phagocytic cells and dissolution by a physicochemical process. However, the degradation at the beginning is performed by the dissolution with the weak cellular process because of the presence of few osteoclasts, macrophages and foreign-body giant cells. From the 2nd week, numerous macrophages, few foreign-body giant cells and rare osteoclasts are found around cement, and CPC particles form at the interface and inside the cells.

We consider that the process of biodegradation is directly influenced by the type of crystallisation of the calcium phosphate material. For example, the sintered calcium phosphate bioceramics processed at a high temperature, exhibit good crystallisation and are primarily degraded by a process dependent on interstitial liquids. However, the phosphocalcic bone cement is formed by physicochemical crystallisation and is primarily degraded through a cellular process.

The mechanical properties of the CPC (compressive strength from 20 to 60 MPa) is less strong than that of PMMA cement (>70 MPa). Biodegrdation and new bone formation during implantation modify their properties. Yamamoto et al. [122] tested the CPC showed that a compressive strength increased at 3 days and 1 week, and decreased at 4 weeks *in vitro*; and *in vivo*, it increased at 3 days and 1, 2 weeks and decreased at 4 weeks *in vitro*. The values of these results *in vivo* was only 50–70 % of that *in vitro*. Our study revealed a strong decrease of the compressive strength after 2 weeks due to biodegradation, followed by a slight increase from 4 weeks due to new bone formation. There was a general decrease in the elastic modulus with time [114]. This change of the mechanical strength is supposed to be related to the kinetics of recrystallisation where the mechanical strength increased according to the progress of recrystallisation, but degradation of resorption subsequently starts after the crystallisation. This change also suggests that the calcium phosphate cement would be remodelled or resorbed in long term. This is the same as hydroxyapatite used as a bone substitute material, which is also the expected characteristic of calcium phosphate cement to be used for enhancing the initial fixation of implants and promote biological fixation in long term.

Clinical Application of the CPC

The CPC are a resorbable material with osteoconduction, which are not toxic, not exothermic and excellently biocompatible, but their mechanical properties are not ideal which limits their clinical utilisation. They are only used to fill small bone defect or to augment bone volume as bone substitute. Shindo et al. [123] reported that CPC has been used to augment the supraorbital ridge in dogs, as well as in a variety of skull base defects. It was also used in 24 patients, to augment or obliterate the frontal and ethmoid sinus regions and mastoid cavities. When these patients were observed for 2 years, it was necessary to remove the material in only a patient. Kveton et al. [124, 125] reported on the 2-year follow-up of 15 patients who underwent CPC reconstruction for translabyrinthine, middle cranial fosse, and suboccipital craniectomy; no complication were shown. Stankewich et al. [126] and Goodman et al. [127] showed augmentation of femoral neck fracture with CPC, which significantly improved the initial stability and failure strength of the fractures. The cement has also been used to stabilise distal radius fracture in 6 patients and appeared to promote healing and permit early mobilisation of the wrist. [128] Kopylov et al. [129] used an injectable calcium phosphate bone cement, with external fixation in the treatment of redisplaced distal radial fractures by a prospective randomised study in 40 patients. The chosen primary effect variable was grip strength at 7 weeks. Patients treated by injection of CPC had better grip strength, wrist extension and forearm supination at 7 weeks. There was no difference in functional parameters at 3 months or later. None of the methods could fully stabilise the fracture: radiographs showed a progressive redislocation over time.

Development of the CPC

The rational of using CPC is that this material will be completely resorbed and replaced by new bone. Two processes are simultaneously involved: (1) the degradation of CPC performed by osteoclasts and macrophagtes, and (2) the creation of new bone performed by osteoblasts. The presence of CPC particles could disturb the osteoblasts ability to make new bone. An unstable mechanical situation could result if the bone formation is delayed by the particles resulting from the CPC degradation. It would then be important

for future CPC development to minimise the generation of particles smaller than 10 μm.

Since the mechanical properties limit the clinical utilisation of the CPC, its composition or the adjuvants may be modified to maximise crystallisation to improved the mechanical properties. On the other hand, the equilibrium between osteogenesis and biodegradation is attentively thought. When CPC is rapidly resorbed during implantation and new bone formation is insufficient in the implanted site, or slowly resorbed to prevent the new bone formation and CPC loose its initial properties, the mechanical properties are decreased.

In orthopaedic surgery, PMMA cements are frequently used to fix prosthesis until today due to strong mechanical fixation, but this fixation presents loosening, especially in long term, because of the absence of biological fixation by bone tissue. For the fixation of surgical prosthesis, there is ideal to obtain the mechanical fixation in short time (during 1–3 months) and the biological fixation in long time (starting after 1 month). The mechanism of this fixation supposes that prosthesis are placed with a fixation by bone cement or by bone tissue, then the cement is resorbed and conducts new bone formation till the surface of prosthesis with excellent osteointegration to obtain the biological fixation. We think that when non-cemented prosthesis is combined with CPC, there is: (1) a mechanical fixation due to non-cemented prosthesis with a blockage between the prosthesis and bone tissue, and (2) the cement can fill the residual cavity around prosthesis. Ostoegenesis and an osteoconduction will lead to the fixation of the prosthesis by new bone formation.

References

1. Gluck T. Referat uber die durch das moderne chirurgische Exeriment gewonnenen positiven Resultate, betreffend die Naht und den Ersatz von Defecten hoherer Gewebe, sowie uber die Verwerthung resorbirbarer und lebendiger Tampons in der Chirurgie. Arch Klin Chir. 1891;41:187.
2. Haboush EJ. A new operation for arthroplasty of the hip based on biomechanics, photoelasticity, fast-setting dental acrylic, and other considerations. Bull Hosp Joint Dis. 1953;14:242.
3. Charnely J. The bonding of prostheses to bone by cement. J Bone Joint Surg [Br]. 1964;46:518.
4. Sorensen WG, Bloom JD, Kelly PJ. The effects of intramedullary methylmethacrylate and reaming on the circulation of the tibia after osteotomy and plate fixation in dogs. J Bone Joint Surg Am. 1979;61(3):417–24.
5. Brown WE, Chow LC. A new calcium phosphate, water-setting cement. Westerville: American Ceramic Society; 1986. p. 352.
6. Mirtchi AA, Lemaitre J, Munting E. Calcium phosphate cement: action of setting regulators on the properties of β-tricalcium phosphate-monocalcium phosphate cement. Biomaterial. 1989;10:634–8.
7. Ginebra MP, Fernandez E, Boltong MG, Bermudez O, Planell JA, Driessens FC. Compliance of an apatitic calcium phosphate cement with the short-term clinical requirements in bone surgery, orthopaedics and dentistry. Clin Mater. 1994;17(2):99–104.
8. Kurashina K, Kurita H, Kotani A, Kobayashi S, Kyoshima K, Hirano M. Experimental cranioplasty and skeletal augmentation using an alpha-tricalcium phosphate/dicalcium phosphate dibasic/tetracalcium phosphate monoxide cement: a preliminary short-term experiment in rabbits. Biomaterials. 1998;19:701–6.
9. Liu CS, Shen W, Gu YF, Hu LM. Mechanism of the hardening process for a hydroxyapatite cement. J Biomed Mater Res. 1997;35:75–80.
10. Fernandez E, Gil FJ, Best SM, Ginebra MP, Driessens FC, Planell JA. Improvement of the mechanical properties of new calcium phosphate bone cements in the $CaHPO_4$-alpha-$Ca_3(PO_4)_2$ system: compressive strength and microstructural development. J Biomed Mater Res. 1998;41(4):560–7.
11. Trap B, Wolff P, Jensen JS. Acrylic bone cement: residuals and extractability of methacrylate monomers and aromatic amines. J Appl Biomater. 1992;3:51–7.
12. ISO 5833. International standards for implants for surgery acrylic resin cement. International Standards Organisation. 1992.
13. Jasty M, Davies JP, O'Connor DO, Burke DW, Harrigan TP, Harris WH. Porosity of various preparations of acrylic bone cements. Clin Orthop. 1990;259:122–9.
14. Jasty M, Maloney WJ, Bragdon CR, Haire T, Harris WH. Histomorphological studies of the long-term skeletal responses to well fixed cemented femoral components. J Bone Joint Surg Am. 1990;72(8):1220–9.
15. Davies JP, O'Connor DO, Burke DW, Jasty M, Harris WH. The effect of centrifugation on the fatigue life of bone cement in the presence of surface irregularities. Clin Orthop. 1988;229:156–61.
16. Davies JP, Harris WH. Optimization and comparison of three vacuum mixing systems for porosity reduction of Simplex P cement. Clin Orthop. 1990;254:261–9.
17. Lautenschlager EP, Stupp SI, Keller JC. Structure and properties of acrylic bone cement. In: Ducheyne P, Hastings GW, editors. Functional behavior of orthopaedic biomaterials, Application, vol. II. Boca Raton: CPC Press; 1984. p. 87–119.

18. Ishidara K. Hard tissue compatible polymers. In: Tsuruta T et al., editors. Biomedical application of polymeric materials. Boca Raton: CPC Press; 1993. p. 143.
19. Haas SS, Brauer GM, Dickson G. A characterization of polymethylmethacrylate bone cement. J Bone Joint Surg Am. 1975;57:380–91.
20. Harrigan TP, Kareh JA, O'Connor DO, Burke DW, Harris WH. A finite element study of the initiation of failure of fixation in cemented femoral total hip components. J Orthop Res. 1992;10(1):134–44.
21. James SP, Schmalzried TP, McGarry FJ, Harris WH. Extensive porosity at the cement-femoral prosthesis interface: a preliminary study. J Biomed Mater Res. 1993;27(1):71–8.
22. Keller JC, Lautenschlager EP, Marshall Jr GW, Meyer Jr PR. Factors affecting surgical alloy/bone cement interface adhesion. J Biomed Mater Res. 1980;14(5):639–51.
23. Bannister GC, Miles AW, May PC. Properties of bone cement prepared under operating theatre conditions. Clin Mater. 1989;4:343–7.
24. Bean DJ, Hollis JM, Woo SL, Convery FR. Sustained pressurization of polymethylmethacrylate: a comparison of low- and moderate-viscosity bone cements. J Orthop Res. 1988;6(4):580–4.
25. Linder L. Reactions to bone cement. In: Williams DF, editor. Biocompatibility of orthopedic implants, vol. II. Boca Raton: CRC Press; 1982. p. 1–23.
26. De Waal Malefijt J, Sloof TJ, Huiskes R. The actual status of acrylic bone cement in total hip replacement. A review. Acta Orthop Belg. 1987;53(1):52–8.
27. Schoenfeld CM, Conard GJ, Lautenschlager EP. Monomer release from methacrylate bone cements during simulated *in vivo* polymerization. J Biomed Mater Res. 1979;13(1):135–47.
28. Lu JX, Huang ZW, Tropiano P, Clouet d'Orval B, Remusat M, Déjou J, Proust J-P, Poitout D: Human biological reactions at the interface between bone tissue and polymethylmethacrylate cement. J Mater Sci Mater Med. 2000 (accepted).
29. Frondoza CG, Tanner KT, Jones LC, Hungerford DS. Polymethylmethacrylate particles enhance DNA and protein synthesis of human fibroblasts *in vitro*. J Biomed Mater Res. 1993;27(5):611–7.
30. Golds EE, Mason P, Nyirkos P. Inflammatory cytokines induce synthesis and secretion of grow protein and a neutrophil chemotactic factor but not beta 2-microglobulin in human synovial cells and fibroblasts. Biochem J. 1989;259:585–8.
31. Dayer JM, Beutler B, Cerami A. Cachectin/tumor necrosis factor stimulates collagenase and prostaglandin E2 production by human synovial cells and dermal fibroblasts. J Exp Med. 1985;162:2163–8.
32. Akira S, Hirano T, Taga T, Kishimoto T. Biology of multifunctional cytokines: IL 6 and related molecules (IL 1 and TNF). FASEB J. 1990;4(11):2860–7.
33. Swan A, Dularay B, Dieppe P. A comparison of the effects of urate, hydroxyapatite and diamond crystals on polymorphonuclear cells: relationship of mediator release to the surface area and adsorptive capacity of different particles. J Rheumatol. 1990;17(10):1346–52.
34. Goldring MB, Goldring SR. Skeletal tissue response to cytokines. Clin Orthop. 1990;258:245–78.
35. Murray DW, Rushton N. Macrophages stimulate bone resorption when they phagocytose particles. J Bone Joint Surg [Br]. 1990;72(6):988–92.
36. Davis RG, Goodman SB, Smith RL, Lerman JA, Williams 3rd RJ. The effects of bone cement powder on human adherent monocytes/macrophages *in vitro*. J Biomed Mater Res. 1993;27(8):1039–46.
37. Glant TT, Jacobs JJ. Response of three murine macrophage populations to particulate debris: bone resorption in organ cultures. J Orthop Res. 1994;12(5):720–31.
38. Horowitz SM, Rapuano BP, Lane JM, Burstein AH. The interaction of the macrophage and the osteoblast in the pathophysiology of aseptic loosening of joint replacements. Calcif Tissue Int. 1994;54(4):320–4.
39. Herman JH, Sowder WG, Anderson D, Appel AM, Hopson CN. Polymethylmethacrylate-induced release of bone-resorbing factors. J Bone Joint Surg Am. 1989;71(10):1530–41.
40. Takagi M, Konttinen YT, Santavirta S, Sorsa T, Eisen AZ, Nordsletten L, Suda A. Extracellular matrix metalloproteinases around loose total hip prostheses. Acta Orthop Scand. 1994;65(3):281–6.
41. Horowitz SM, Gonzales JB. Effects of polyethylene on macrophages. J Orthop Res. 1997;15(1):50–6.
42. Lee SH, Brennan FR, Jacobs JJ, Urban RM, Ragasa DR, Glant TT. Human monocyte/ macrophage response to cobalt-chromium corrosion products and titanium particles in patients with total joint replacements. J Orthop Res. 1997;15(1):40–9.
43. Shanbhag AS, Jacobs JJ, Black J, Galante JO, Glant TT. Human monocyte response to particulate biomaterials generated *in vivo* and in vitro. J Orthop Res. 1995;13(5):792–801.
44. Horowitz SM, Gautsch TL, Frondoza CG, Riley Jr L. Macrophage exposure to polymethyl methacrylate leads to mediator release and injury. J Orthop Res. 1991;9(3):406–13.
45. Amstutz HC, Campbell P, Kossovsky N, Clarke IC. Mechanism and clinical significance of wear debris-induced osteolysis. Clin Orthop. 1992;276:7–18.
46. Harris WH. Osteolysis and particle disease in hip replacement. A review. Acta Orthop Scand. 1994;65(1):113–23.
47. Maloney WJ, Smith RL. Periprosthetic osteolysis in total hip arthroplasty: the role of particulate wear debris. Instr Course Lect. 1996;45:171–82.
48. Sabokbar A, Fujikawa Y, Murray DW, Athanasou NA. Radio-opaque agents in bone cement increase bone resorption. J Bone Joint Surg [Br]. 1997;79(1):129–34.
49. Wang W, Ferguson DJ, Quinn JM, Simpson AH, Athanasou NA. Biomaterial particle phagocytosis by bone-resorbing osteoclasts. J Bone Joint Surg [Br]. 1997;79(5):849–56.

50. Thomson LA, Law FC, James KH, Matthew CA, Rushton N. Biocompatibility of particulate polymethylmethacrylate bone cements: a comparative study *in vitro* and *in vivo*. Biomaterials. 1992;13(12):811–8.
51. Willert HG, Bertram H, Buchhorn GH. Osteolysis in alloarthroplasty of the hip. The role of bone cement fragmentation. Clin Orthop. 1990;258:108–21.
52. Jensen LN, Sturup J, Kramhoft M, Jensen JS. Histological evaluation of cortical bone reaction to PMMA cement. Acta Orthop Belg. 1991;57(3): 254–9.
53. Nimb L, Sturup J, Jensen JS. Improved cortical histology after cementation with a new MMA-DMA-IBMA bone cement: an animal study. J Biomed Mater Res. 1993;27(5):565–74.
54. Revell PA, Braden M, Freeman MA. Review of the biological response to a novel bone cement containing poly(ethyl methacrylate) and *n*-butyl methacrylate. Biomaterials. 1998;19(17):1579–86.
55. Charnley J. The reaction of bone to self-curing acrylic cement. A long-term histological study in man. J Bone Joint Surg [Br]. 1970;52(2):340–53.
56. Pizzoferrato A, Ciapetti G, Stea S, Toni A. Cellular events in the mechanisms of prosthesis loosening. Clin Mater. 1991;7(1):51–81.
57. Albrektsson T. Osseous penetration rate into implants pretreted with bone cement. Arch Orthop Trauma Surg. 1981;102:141.
58. Morberg P, Albrektsson T. Bone reactions to intramedullary insertion of methyl methacrylate. Eur J Muskuloskel Res. 1992;1:11.
59. Morberg P, et al. Impaired cortical bone formation after intramedullary insertion of bone cement. Clin Mater. 1992;10:139.
60. Christensen SB. Osteoarthrosis: changes of bone, cartilage and synovial membrane in relation to bone scintigraphy. Acta Orthop Scand Suppl. 1985;214:1–43.
61. Sturup J, Madsen J, Tondevold E, Jensen JS. Decreased blood perfusion in canine tibial diaphysis after filling with acrylic bone cement compared with inert bone wax. Acta Orthop Scand. 1990;61(2):143–7.
62. Mongiorgi R, Valdre G, Giardino R, Maggi G, Prati C, Bertocchi G. Thermodynamical aspects of the polymerization reaction of PMMA cement mixed with phosphatic mineral phases. Boll Soc Ital Biol Sper. 1993;69(6):365–72.
63. Berman AT, Reid JS, Yanicko Jr DR, Sih GC, Zimmerman MR. Thermally induced bone necrosis in rabbits. Relation to implant failure in humans. Clin Orthop. 1984;186:284–92.
64. Park JB, Turner RC, Atkins PE. EPR study of free radicals in PMMA bone cement: a feasibility study. Biomater Med Devices Artif Organs. 1980;8(1):23–33.
65. Biehl G, Harms J, Hanser U. Experimental studies on heat development in bone during polymerization of bone cement. Intraoperative measurement of temperature in normal blood circulation and in bloodlessness. Arch Orthop Unfallchir. 1974;78(1):62–9.
66. Rhinelander FW, Nelson CL, Stewart RD, Stewart CL. Experimental reaming of the proximal femur and acrylic cement implantation: vascular and histologic effects. Clin Orthop. 1979;141:74–89.
67. Lundskog J. Heat and bone tissue. An experimental investigation of the thermal properties of bone and threshold levels for thermal injury. Scand J Plast Reconstr Surg. 1972;9:1–80.
68. Lee AJ, Wrighton JD. Some properties of polymethylmethacrylate with reference to its use in orthopedic surgery. Clin Orthop. 1973;95:281–7.
69. Sund G, Rosenquist J. Morphological changes in bone following intramedullary implantation of methyl methacrylate. Effects of medullary occlusion: a morphometrical study. Acta Orthop Scand. 1983;54(2):148–56.
70. Williams RP, McQueen DA. A histopathologic study of late aseptic loosening of cemented total hip prostheses. Clin Orthop. 1992;275:174–9.
71. Harris WH. The problem is osteolysis. Clin Orthop. 1995;311:46–53.
72. Jasty M, Jiranek W, Harris WH. Acrylic fragmentation in total hip replacements and its biological consequences. Clin Orthop. 1992;285:116–28.
73. Jasty M, Bragdon CR, Lee K, Hanson A, Harris WH. Surface damage to cobalt-chrome femoral head prostheses. J Bone Joint Surg [Br]. 1994;76(1): 73–7.
74. Jensen LN, Jensen JS, Gotfredsen K. A method for histological preparation of undecalcified bone sections containing acrylic bone cement. Biotech Histochem. 1991;1(2):82–6.
75. Goodman SB, Fornasier VL, Kei J. The effects of bulk versus particulate polymethylmethacrylate on bone. Clin Orthop. 1988;232:255–62.
76. Renvall S. Bone cement and wound healing. An experimental study in the rat. Ann Chir Gynaecol. 1991;80(3):285–8.
77. Quinn J, Joyner C, Triffitt JT, Athanasou NA. Polymethylmethacrylate-induced inflammatory macrophages resorb bone. J Bone Joint Surg [Br]. 1992;74(5):652–8.
78. Santavirta S, Gristina A, Konttinen YT. Cemented versus cementless hip arthroplasty. A review of prosthetic biocompatibility. Acta Orthop Scand. 1992;63(2):225–32.
79. Horowitz SM, Frondoza CG, Lennox DW. Effects of polymethylmethacrylate exposure upon macrophages. J Orthop Res. 1988;6(6):827–32.
80. Havelin LI, Espehaug B, Vollset SE, Engesaeter LB. The effect of the type of cement on early revision of Charnley total hip prostheses. A review of eight thousand five hundred and seventy-nine primary arthroplasties from the Norwegian Arthroplasty Register. J Bone Joint Surg Am. 1995;77(10): 1543–50.
81. Hungerford DS, Jones LC. The rationale of cementless revision of cemented arthroplasty failures. Clin Orthop. 1988;235:12–24.

82. Herberts P, Ahnfelt L, Malchau H, Stromberg C, Andersson GB. Multicenter clinical trials and their value in assessing total joint arthroplasty. Clin Orthop. 1989;249:48–55.
83. Herberts P, Malchau H. How outcome studies have changed total hip arthroplasty practices in Sweden. Clin Orthop. 1997;344:44–60.
84. Ohashi KL, Dauskardt RH. Effects of fatigue loading and PMMA precoating on the adhesion and subcritical debonding of prosthetic-PMMA interfaces. J Biomed Mater Res. 2000;51(2):172–83.
85. Dahl OE, Johnsen H, Kierulf P, Molnar I, Ro JS, Vinje A, Mowinckel P. Intrapulmonary thrombin generation and its relation to monomethylmethacrylate plasma levels during hip arthroplasty. Acta Anaesthesiol Scand. 1992;36(4):331–5.
86. Gentil B, Paugam C, Wolf C, Lienhart A, Augereau B. Methylmethacrylate plasma levels during total hip arthroplasty. Clin Orthop. 1993;287:112–6.
87. Svartling N, Pfaffli P, Tarkkanen L. Methylmethacrylate blood levels in patients with femoral neck fracture. Arch Orthop Trauma Surg. 1985;104(4):242–6.
88. Patterson BM, Healey JH, Cornell CN, Sharrock NE. Cardiac arrest during hip arthroplasty with a cemented long-stem component. A report of seven cases. J Bone Joint Surg Am. 1991;73(2):271–7.
89. Wenda K, Scheuermann H, Weitzel E, Rudigier J. Pharmacokinetics of methylmethacrylate monomer during total hip replacement in man. Arch Orthop Trauma Surg. 1988;107(5):316–21.
90. Crout DH, Corkill JA, James ML, Ling RS. Methylmethacrylate metabolism in man. The hydrolysis of methylmethacrylate to methacrylic acid during total hip replacement. Clin Orthop. 1979;141:90–5.
91. Orsini EC, Byrick RJ, Mullen JB, Kay JC, Waddell JP. Cardiopulmonary function and pulmonary microemboli during arthroplasty using cemented or non-cemented components. The role of intramedullary pressure. J Bone Joint Surg Am. 1987;69(6):822–32.
92. Hofmann AA, Wyatt RW, Gilbertson AA, DeKoss L, Miller J. The effect of air embolization from the femoral canal on hemodynamic parameters during hip arthroplasty. Clin Orthop. 1987;218:290–6.
93. Fregert S. Occupational hazards of acrylate bone cement in orthopaedic surgery. Acta Orthop Scand. 1983;54(6):787–9.
94. Bengtson A, Larsson M, Gammer W, Heideman M. Anaphylatoxin release in association with methylmethacrylate fixation of hip prostheses. J Bone Joint Surg Am. 1987;69(1):46–9.
95. Kanerva L, Estlander T, Jolanki R, Tarvainen K. Occupational allergic contact dermatitis and contact urticaria caused by polyfunctional aziridine hardener. Contact Dermatitis. 1995;33(5):304–9.
96. Brauer GM, Davenport RM, Hansen WC. Accelerating effect of amines on polymerization of methyl methacrylate. Mod Plastic. 1956;34(11):154–256.
97. Lal J, Green RJ. Effect of amine accelerators on the polymerization of methacrylate with benzoyl peroxide. J Polym Sci. 1955;18:403.
98. Vazquez B, Elvira C, Levenfeld B, Pascual B, Goni I, Gurruchaga M, Ginebra MP, Gil FX, Planell JA, Liso PA, Rebuelta M, San Roman J. Application of tertiary amines with reduced toxicity to the curing process of acrylic bone cements. J Biomed Mater Res. 1997;34(1):129–36.
99. Fritsch EW. Static and fatigue properties of two new low-viscosity PMMA bone cements improved by vacuum mixing. J Biomed Mater Res. 1996;31(4):451–6.
100. Morita S, Kawachi S, Yamamoto H, Shinomiya K, Nakabayashi N, Ishihara K. Total hip arthroplasty using bone cement containing tri-*n*-butylborane as the initiator. J Biomed Mater Res. 1999;48(5):759–63.
101. Pourdeyhimi B, Wagner HD. Elastic and ultimate properties of acrylic bone cement reinforced with ultra-high-molecular-weight polyethylene fibers. J Biomed Mater Res. 1989;23(1):63–80.
102. Saha S, Pal S. Improvement of mechanical properties of acrylic bone cement by fiber reinforcement. J Biomech. 1984;17(7):467–78.
103. Topoleski LD, Ducheyne P, Cuckler JM. The fracture toughness of titanium-fiber-reinforced bone cement. J Biomed Mater Res. 1992;26(12):1599–617.
104. Ishihara K, Arai H, Nakabayashi N, Morita S, Furuya K. Adhesive bone cement containing hydroxyapatite particle as bone compatible filler. J Biomed Mater Res. 1992;26(7):937–45.
105. Beruto DT, Mezzasalma SA, Capurro M, Botter R, Cirillo P. Use of alpha-tricalcium phosphate (TCP) as powders and as an aqueous dispersion to modify processing, microstructure, and mechanical properties of polymethylmethacrylate (PMMA) bone cements and to produce bone-substitute compounds. J Biomed Mater Res. 2000;49(4):498–505.
106. Heikkila JT, Aho AJ, Kangasniemi I, Yli-Urpo A. Polymethylmethacrylate composites: disturbed bone formation at the surface of bioactive glass and hydroxyapatite. Biomaterials. 1996;17(18):1755–60.
107. Edwards JT, Brunski JB, Higuchi HW. Mechanical and morphologic investigation of the tensile strength of a bone-hydroxyapatite interface. J Biomed Mater Res. 1997;36(4):454–68.
108. Driessens FCM, Boltong MG, Bermudez O, Planell JA. Formulation and setting times of some calcium orthophosphate cements: a pilot study. J Mater Sci Mater Med. 1993;4:503–8.
109. Driessens FCM, Boltong MG, Bermudez O, Planell JA, Ginebra MP, Fernandez E. Effective formulations for the preparation of calcium phosphate bone cements. J Mater Sci Mater Med. 1994;5:164–70.
110. Schmitz JP, Hollinger JO, Milam SB. Reconstruction of bone using calcium phosphate bone cements: a critical review. J Oral Maxillofac Surg. 1999;57(9):1122–6.

111. Leroux L, Hatim Z, Freche M, Lacout JL. Effects of various adjuvants (lactic acid, glycerol, and chitosan) on the injectability of a calcium phosphate cement. Bone. 1999;25(2 Suppl):31S–4.
112. Liu CS, Wang W, Shen W, Chen TY, Hu LM, Chen ZW. Evaluation of the biocompatibility if a nonceramic hydroxyapatite. J Endodont. 1997;23(8):490–3.
113. Higashi S, Ohsumi T, Ozumi K, Kuroki K, Inokuchi Y, Terashita M. Evaluation of cytotoxicity of calcium phosphate cement consisting of alpha-tricalcium phosphate and dicalcium phosphate dihydrate. Dent Mater J. 1998;17(3):186–94.
114. Lu JX, About I, Stephan G, Van Landuyt P, Dejou J, Fiocchi M, Lemaitre J, Proust JP. Histological and biomechanical studies of two bone colonizable cements in rabbits. Bone. 1999;25(2 Suppl):41S–5.
115. Pioletti DP, Takei H, Lin T, Van Landuyt P, Ma QJ, Kwon SY, Sung KL. The effects of calcium phosphate cement particles on osteoblast functions. Biomaterials. 2000;21(11):1103–14.
116. Ohura K, Bohner M, Hardouin P, Lemaitre J, Pasquier G, Flautre B. Resorption of, and bone formation from, new beta-tricalcium phosphate-monocalcium phosphate cements: an *in vivo* study. J Biomed Mater Res. 1996;30(2):193–200.
117. Miyamoto Y, Ishikawa K, Takechi M, Toh T, Yoshida Y, Nagayama M, Kon M, Asaoka K. Tissue response to fast-setting calcium phosphate cement in bone. J Biomed Mater Res. 1997;37(4):457–64.
118. Ikenaga M, Hardouin P, Lemaitre J, Andrianjatovo H, Flautre B. Biomechanical characterization of a biodegradable calcium phosphate hydraulic cement: a comparison with porous biphasic calcium phosphate ceramics. J Biomed Mater Res. 1998;40(1):139–44.
119. Frayssinet P, Gineste L, Conte P, Fages J, Rouquet N. Short-term implantation effects of a DCPD-based calcium phosphate cement. Biomaterials. 1998;19(11–12):971–7.
120. Costantino PD, Friedman CD, Jones K, Chow LC, Sisson GA. Experimental hydroxyapatite cement cranioplasty. Plast Reconstr Surg. 1992;90(2):174–85.
121. Friedman CD, Costantino PD, Jones K, Chow LC, Pelzer HJ, Sisson Sr GA. Hydroxyapatite cement. II. Obliteration and reconstruction of the cat frontal sinus. Arch Otolaryngol Head Neck Surg. 1991;117(4):385–9.
122. Yamamoto H, Niwa S, Hori M, Hattori T, Sawai K, Aoki S, Hirano M, Takeuchi H. Mechanical strength of calcium phosphate cement *in vivo* and *in vitro*. Biomaterials. 1998;19(17):1587–91.
123. Shindo ML, Costantino PD, Friedman CD, Chow LC. Facial skeletal augmentation using hydroxyapatite cement. Arch Otolaryngol Head Neck Surg. 1993;119(2):185–90.
124. Kveton JF, Friedman CD, Piepmeier JM, Costantino PD. Reconstruction of suboccipital craniectomy defects with hydroxyapatite cement: a preliminary report. Laryngoscope. 1995;105(2):156–9.
125. Kveton JF, Friedman CD, Costantino PD. Indications for hydroxyapatite cement reconstruction in lateral skull base surgery. Am J Otol. 1995;16(4):465–9.
126. Stankewich CJ, Swiontkowski MF, Tencer AF, Yetkinler DN, Poser RD. Augmentation of femoral neck fracture fixation with an injectable calcium-phosphate bone mineral cement. J Orthop Res. 1996;14(5):786–93.
127. Goodman SB, Bauer TW, Carter D, Casteleyn PP, Goldstein SA, Kyle RF, Larsson S, Stankewich CJ, Swiontkowski MF, Tencer AF, Yetkinler DN, Poser RD. Norian SRS cement augmentation in hip fracture treatment. Laboratory and initial clinical results. Clin Orthop. 1998;348:42–50.
128. Kopylov P, Jonsson K, Thorngren KG, Aspenberg P. Injectable calcium phosphate in the treatment of distal radial fractures. J Hand Surg [Br]. 1996;21(6):768–71.
129. Kopylov P, Runnqvist K, Jonsson K, Aspenberg P. Norian SRS versus external fixation in redisplaced distal radial fractures. A randomized study in 40 patients. Acta Orthop Scand. 1999;70(1):1–5.

Cement with Antimitotics

11

Philippe Hernigou

There are two causes of failure in the surgical treatment of metastatic tumors : firstly, local recurrence of the tumour is not always prevented, even after extra-tumoral surgical exeresis and systemic chemotherapy, and secondly, failure of osteosynthesis after surgery. For these reasons, we thought that it would be helpful to provide local chemotherapy during and immediately after surgery, for instance, by adding an antimitotic to the acrylic cement used to replace the bone loss or to seal reconstruction prostheses. It was thought that the antimitotic would be likely to be released into the surrounding tissues in the same way as many antibiotics. Diffusion into the surrounding tissues is well established for numerous antibiotics [1–6].

We performed a number of experiments [7–9] to assess acrylic cement as a vehicle for local chemotherapy: (1) Diffusion of antimitotic drugs from acrylic cement was studied in vitro to determine that these drugs were released and were still biologically active after exposure to highly reactive monomer and the exothermic curing reaction. (2) Experiments in vivo were performed on two groups of animals. We tested the effect of such local chemotherapy on experimental osteosarcoma of the rat and on dogs with spontaneous osteosarcoma. General and local tolerance of the antimitotic-loaded cement was assessed.

Finally, we report our preliminary clinical investigations [10–12] with pharmacological data from patients. It was possible to envisage using cement/drug mixtures to treat orthopaedic complaints calling simultaneously for mechanical consolidation of the bone [13] and *in-situ* release of a drug: one example would be the strengthening of bone with cement after resection of a bone tumour [14] plus the local release of antimitotic drugs from the implant.

Cement was the first vehicle to be studied for the purpose of releasing local chemotherapy. Methyl polymethacrylate (P.M.M.A.) fulfils the two following criteria: it has good biocompatibility, since the system has to remain *in situ* throughout the rest of the patient's life; it is not biodegradable, so that it provides mechanical support for bone which has been weakened by the surgical exeresis of a neoplastic site.

Many antimitotic drugs are available; for our first investigations we used methotrexate and cisplatine. Methotrexate was chosen because its concentration is easy to determine by spectrophotometry, and because there is an antidote (citrovorum rescue) for adverse effects. We used the acrylic bone cement currently employed by the authors for clinical arthroplasty.

P. Hernigou, MD
Orthopaedics Department, Hôpital Henri Mondor, Créteil, France
e-mail: philippe.hernigou@wanadoo.fr

D.G. Poitout (ed.), *Biomechanics and Biomaterials in Orthopedics*,
DOI 10.1007/978-1-84882-664-9_11

Study of the Release of Methotrexate (MTX)

The first study investigated the *in-vitro* release of antimitotics included in acrylic cement. After confirming that this release does actually occur, starts rapidly and is maintained over a prolonged period, two further studies were then carried out *in vivo*: one in dogs suffering from spontaneous osteosarcoma, in order to investigate the release of the antimitotic from the cement into the plasma, the systemic safety and the local activity of the antimitotic-loaded cement following exeresis of the neoplasm.

The second study was conducted in laboratory rats with implanted osteosarcomas. This type of tumour was used so that a large number of animals with tumours could be studied and divided into uniform groups. Under these experimental conditions, it was possible to monitor the progress of the tumours left *in situ* as well as the histopathological changes brought about by the local action of antimitotics released from implants.

- Kinetic profile of the release of MTX from implants

To investigate the release of MTX from a block of acrylic cement implanted into the tissues, cubic test pieces were placed in 32 ml of physiological saline, which was changed every day. The concentration in the elution fluid was measured before each change. These test pieces were made from a mixture of 500 mg methotrexate powder, 46.5 g of polymer, and 20 ml of monomer, poured into 2 cm cubic moulds. Each cube weighed about 13 g and contained approximately 100 mg of methotrexate. Methotrexate elution was evaluated daily for 15 days and then weekly for 6 months for six specimens, the results being given as an average of the 6.

The release profiles from implants containing 1 % w/w have shown that methotrexate is released more rapidly during the first 2 h and 10 % of the load is released within the first 18 h. The rate of release then slows. Implants immersed in an extraction medium which is changed regularly, continue to release methotrexate for 6 months; the quantities released initially being greater the greater the initial load.

- The release of methotrexate from acrylic cement

This has been investigated *in vivo* in dogs with spontaneous sarcoma. We therefore chose an animal with a weight close to that of man, and a spontaneous tumour with an evolution like that of human osteosarcoma, similarly hypervascular because this may influence the diffusion of cisplatine. In experiments at the National Veterinary School of Maisons-Alfort, we used dogs with spontaneous osteosarcoma. This is a malignant tumour [15, 16] with the same aggressive properties as the human type. It affects the very large breeds of dog such as the Saint Bernard (mean weight 70 kg), the mastiff (55 kg) and the boxer (30 kg). It progresses rapidly in the absence of treatment, and death is the rule in a few months [17, 18]. Simple resection of the tumour rapidly leads to local relapse, and even after amputation 85 % of dogs die within 7 months of diagnosis [15, 19, 20]. The loss of substance resulting from the exeresis of the tumour was compensated using freshly prepared methotrexate-loaded cement. The dose of methotrexate received ranged from 1.6 to 16 mg/kg. Two hours after being implanted, plasma levels of methotrexate ranged from 0.08 to 0.02 µmol/l (1 µmol of methotrexate = 0.455 mg). After 24 h, the plasma levels were between 0.1 and 0.02 µmol/l and by the third day were no longer detectable. Toxic effects were observed on day 4 in the 3 animals which had received a dose of more than 200 mg of methotrexate. The other animals, which had received a dose of between 100 and 150 mg, did not display any signs of toxicity. The survival curve of the animals in this group seemed to be better than that of the animals which underwent surgery without adjuvant treatment, where 85 % of the animals had died within 7 months.

The Efficacy of Methotrexate-Loaded Implants

This was investigated using the experimental model of osteosarcoma in the rat [21, 22]. Using implants equivalent to 1.5 mg of active constituent, tumour

growth was temporarily slowed and the survival time of the animals significantly prolonged.

These experiments have shown that the rise in temperature which accompanies the polymerisation of the cement does not destroy MTX and, like antibiotics, MTX can be released from the cement. Migration probably occurs as a result of diffusion; the cement constitutes a network of pores and micro-fissures which makes it accessible to the liquid medium in which it is immersed. This liquid penetrates into the system and dissolves the crystals of MTX which then diffuse into the surrounding medium. This mechanism is certainly the dominant one at work during the early stages of MTX release. It probably accounts for the initial peak which characterises the kinetics of MTX release. It is logical to suppose that the outer layers of the cement are more accessible to the liquid medium than the inner layers.

Study of the Release of Cisplatin

Cisplatin is one of the antimitotics which would be suitable for mixing with cement and it has the following characteristics : it is often used to treat primary bone tumours; in the context of bone metastases from visceral tumours, it is generally used in multiple-drug therapy of tumours which are characterised particularly by being radioresistant and resistant to other antimitotics [23–27]: hence the appeal of a local cisplatin-based therapy, which has the advantage of being radiosensitising [28].

Cisplatin takes the form of a whitish-yellow crystalline powder. It has no melting point as it decomposes without melting at 270 °C. Cisplatin has a solubility in water at room temperature of 1 mg/ml.

In the solid state, cisplatin is relatively stable. In contrast, in solution it forms *mono-aquo* and *di-aquo* derivatives by the successive shedding of chloride ions. Cisplatin is most stable in solution at an acid pH and in the presence of chloride ions, which prevent a shift in the reaction equilibrium towards the formation of degradation products. It should also be noted that cisplatin has a chemically inert structure with few reactive groups. Differential thermal analysis did not provide further information in this regard, as cisplatin decomposes without melting at around 270 °C and parasite peaks from PMMA superimpose on the cisplatin peak at these temperatures. X-ray diffraction did however allow us to demonstrate that there is no difference between the spectrum of the physical mixture and that of the cisplatin implants. Moreover, this hypothesis was supported by a very simple experiment in which an accurately weighed 5 % cisplatin implant was dissolved in methylene chloride, a solvent for the polymer but not the cisplatin. The cisplatin crystals were sedimented and extracted by a 9 p. 1000 solution of sodium chloride in a separating funnel. Assay of this solution revealed that it contained all of the active ingredient present in the implant. The very slow release of cisplatin does not therefore appear to be due to a chemical bond with the polymer, but rather to the fact that a large proportion of cisplatin is trapped in the matrix.

The mixture was prepared as follows: during the first step, the active constituent, cisplatin, was mixed with the polymer. A predetermined weight of polymer was placed in a porcelain mortar. A known quantity of cisplatin was then added in small fractions. In the second step, the monomer was added, depending on the quantity of polymer taken, the volume of polymer being that recommended by the manufacturer. The constituents were then thoroughly mixed for 4 min to form a homogeneous paste.

This paste was then poured into the barrel of a stoppered syringe. The mixture was then expelled by the pressure of the piston into polyethylene moulds measuring 6.7 mm (inside diameter) by 10.3 mm in height (cylindrical mould, Prolabo, Paris [France]). The implants were left in the moulds for 24 h, to allow complete polymerisation to take place, and then tipped out and kept in darkness and at room temperature. The *in-vitro* release of cisplatin was investigated by placing the implants in a release medium with the following composition : sodium chloride: 9 g. distilled water, q.s.p.: 1000 ml; 1 N hydrochloric acid, q.s.p. pH = 4. After weighing, the implants were placed in the release medium at 37 °C and stirred in darkness. Samples were taken at regular intervals and an equal volume of fresh medium added to replace the reaction mixture removed. “Sink”

conditions were maintained, i.e. the concentration of cisplatin in the release medium was never more than one-tenth of the saturation concentration (i.e. 100 mg of cisplatin per litre).

The *in-vitro* release data obtained from implants containing various loads of cisplatin (from 1 to 20 % w/w) are shown as a function of time : the quantities released were related to the initial concentration of cisplatin in the implants. For instance, after 90 days, the implants with the highest load had released about 12 % of cisplatin, whereas implants containing 1 % had released only 3 % under these experimental conditions. It should also be noted that the release was incomplete from all the implants and never reached 100 % of the initial load.

In the case of pure PMMA films, diffusion experiments have shown that cisplatin in solution had great difficulty in crossing even a thin membrane. Cisplatin therefore appears to be unable to cross pure PMMA. In the case of PMMA/MMA films, we found that up to a certain thickness, cisplatin was readily able to diffuse across the membrane. This diffusion can be accounted for by the structure of the polymer, which is not a uniform matrix, but a layer of spheres of PMMA which are linked to one another by the polymerised monomer. In solution, cisplatin must be able to diffuse into the relatively less compact zone between the spheres, which may have defects of structure and cohesion. However at thicknesses from 133 µm, diffusion is slower, as if a thicker layer of spheres impedes the diffusion of the active constituent. These findings should be interpreted in the light of the structure of the cement viewed under electron microscopy, which reveals areas of regular polymer and defects, fissures which doubtless permit the diffusion cisplatin.

Clinical Experience

The clinical research was done at the Henri Mondor hospital and has confirmed the experimental data obtained in animal studies. It provided the basis of the protocol for clinical use. During surgery, a dose of 100 mg of MTX mixed with a complete dose of cement (46 g of polymer and 20 ml of monomer) was administered, followed by an intramuscular administration of folinic acid between 72 and 86 h later. This was well tolerated by the patient. The local concentration of MTX found in the drains within the first few hours may reach levels 10,000 times greater than the plasma concentration and remained 100 times greater than the plasma concentration for the next 3 days if the drain was kept in place. Systemic distribution of this local chemotherapy was observed, as can be seen from the blood levels of MTX. The release and diffusion of MTX from the cement was continued well beyond 10 days (when MTX could still be assayed in one patient), since urinary excretion continued for at least 3 weeks.

In the time of cisplatin, which has a lower rate of diffusion from the cement than methotrexate, a dose of 200 mg of cisplatin mixed with one packet of cement was used without any postoperative adverse haematological or renal effects being observed.

If further developments in the investigations we have initiated [7–9] confirm these early findings, this method of local neoplastic chemotherapy could offer an adjuvant therapy which is likely to be easier to handle. There is of course no question that this therapy could offer a substitute for systemic chemotherapy or radiotherapy when these therapies are indicated. Several other studies [29–32] have confirmed the experimental data of the diffusion of antimitotics from cement.

References

1. Buchholz HW, Engelbrecht H. Uber die Depotwirkung einiger Antibiotica bei Vermischung mit dem Kunstharz Palacos. Chirurg. 1970;41:511–5.
2. Carlsson AS, Josefsson G, Lindberg L. Revision with gentamicin impregnated cement for deep infections in total hip arthroplasties. J Bone Joint Surg Am. 1978;60-A:1059–64.
3. Elson RA, McGechie DB. Antibiotics and acrylic bone cement. J Bone Joint Surg [Br]. 1976;58-B:134.
4. Elson RA, Jephcott AE, McGechie DB, Verettes D. Antibiotics, loaded acrylic cement. J Bone Joint Surg [Br]. 1977;59-B:200–5.
5. Fischer L-P, Gonon G-P, Carret J-P, Vulliez Y, de Mourgues G. Association methacrylate de methyle (Ciment acrylique) et antibiotique: etude

bacteriologique et mecanique. Rev Chir Orthop. 1977;63:361–72 (Eng. abstr.).
6. Marks KE, Nelson CL, Lautenschlager EP. Antibiotic-impregnated acrylic bone cement. J Bone Joint Surg Am. 1976;58-A:358–64.
7. Hernigou P, Thiery JP, Benoit J, et al. Release of antimitotic drugs from acrylic cement and plaster. Eur Surg Res. 1987;19 Suppl 1:25.
8. Hernigou P, Thiery JP, Benoist M, et al. Etude experimentale sur l'osteosarcome d'une chimiotherapie locale diffusant a partir de ciment acrylique chirurgical et de platre. Rev Chir Orthop. 1987;73:517–25.
9. Hernigou P, Thiery JP, Benoit J, et al. Methotrexate diffusion from acrylic cement. Bone Joint Surg [Br]. 1989;71-B:804–11.
10. Hernigou P, Brun P, Thiery JP, et al. Antimitotic loaded acrylic cement. In: Langlais F, editor. Limb salvage. Berlin: Springer; 1991.
11. Hernigou P, Brun B, Autier A, et al. Osteosarcoma in adolescent and young adults. Boston: Kluwer Academic Publishers; 1993.
12. Hernigou P, Brun B, Astier A, et al. Diffusion of methotrexate from acrylic surgical cement. Cancer Treat Res. 1993;62:231–5.
13. Harrington KD, Sim FH, Enis JE, et al. Methylmethacrylate as an adjunct in internal fixation of pathological fractures: experience with three hundred and seventy-five cases. J Bone Joint Surg Am. 1976;58-A:1047–55.
14. Strube HD, Komitowski D. Experimental studies of the treatment of malignant tumors with bone cement. In: Enneking WF, editor. Limb salvage in musculoskeletal oncology. London: Churchill Livingstone; 1987. p. 459–69.
15. Brodey RS, Abt DA. Results of surgical treatment in 65 dogs with osteosarcoma. J Am Vet Med Assoc. 1976;168:1032–5.
16. Ling GV, Morgan JP, Pool RR. Primary bone tumors in the dog a combinated clinical, radiographic and histologic approach to early diagnosis. J Am Vet Med Assoc. 1974;165:55–67.
17. Misdorp W, Van der Heul RO. Tumours of bones and joints. Bull World Health Organ. 1976;53:265–82.
18. Owen LN. Cancer chemotherapy. Vet Ann. 1979;19:204–11.
19. Parodi AL. L'osteosarcome (sarcome osteogenigne) chez le chien. Chirurgie. 1970;96:75–80.
20. Pool RR. Bone and cartilage. In: Moulton JE, editor. Tumors in domestic animals. 2nd ed. Berkeley: University of California Press; 1978. p. 89–149.
21. Klein B, Pals S, Masse R, et al. Studies of bone and soft-tissue tumours induced in rats with radioactive cerium chloride. Int J Cancer. 1977;10:112–9.
22. Thiery JP, Perdereau B, Gongora R, Gongora G, Mazabraud A. Un modele experimental d'osteosarcome chez le rat: 11. L'osteosarcome greffable du rat. Sem Hop Paris. 1982;58:1686–9.
23. Baum ES, Gaynon P, Greenberg L, Krivit W, Hammond D. Phase II study of cis-dichlorodiammineplatinum (II) in childhood osteosarcoma: Children's cancer study group report. Cancer Treat Rep. 1979;63:9–10, 1621–1627.
24. Tsuchiya H, Tomita K, Yasutake H, Takagi Y, Katsuo S, et al. Intraarterial cisplatin and caffeine with/without doxorubicin for musculoskeletal high-grade spindle cell sarcoma. Oncol Rep. 1994;1:27–36.
25. Jaffe N, Keifer R, Robertson R, Cangir A, Wang A. Renal toxicity with cumulative doses of Cis-diamminedichloroplatinum-II in pediatric patients with osteosarcoma. Effect on creatinine clearance and methotrexate excretion. Cancer. 1987;59:1577–81.
26. Litterst CL, LeRoy AF, Guarino AM. Disposition and distribution of platinum following parenteral administration of cis-dichlorodiammineplatinum (II) to animals. Cancer Treat Rep. 1979;63(9–10):1485–92.
27. Straw RC, Withrow SJ, Douple EB, Brekke JH, Cooper MF, et al. Effects of Cis-diamminedichloroplatinum II released from D, L-polylactic acid implanted adjacent to cortical allografts in dogs. J Orthop Res. 1994;12:871–7.
28. Withrow SJ, Thrall DE, Straw RC, Powers BE, Wrigley RH, et al. Intra-arterial cisplatin with or without radiation in limb-sparing for canine osteosarcoma. Cancer. 1993;71:2484–90.
29. Janmin L. Experimental observations on acrylic bone cement containing antitumor drugs. Natl Med J China. 1989;69:143.
30. Marshall GJ, Kirchen ME, Lee JH, Menendez LA. The effect of methotrexate eluted from bone cement on giant cell tumour lines in vitro. Trans Orthop Res Soc. 1990;15:537.
31. Wang HM, Galasko CS, Crank S, Oliver G, Ward CA. Methotrexate loaded acrylic cement in the management of skeletal metastases. Clin Orthop. 1995;312:173–86.
32. Guan WY, Yi WT, Zhi MY, Zhen SS. Experimental research on the use of an antineoplastic drug with a bone implant. Int Orthop. 1990;14:387–91.

12 Striated Muscles, an Underestimated Natural Biomaterial: Their Essential Contribution to Healing and Reconstruction of Bone Defects

Haim Stein and Moshe Solomonow

Mechanical and Biological Factors

Surgery of the Musculoskeletal System is the most vibrant, quickly developing and enlarging reconstructive surgical specialty of this Century. The current 10 years are dedicated to this subject, and entitled "The bone and joint decade" which is a tribute to this subject's significance.

The past 35 years have been the stage for more significant developments and advances in reconstructive surgery of the Musculoskeletal System then all the previous decades from the time the name of "Ortho-Paeis" was cornered during the Industrial Revolution.

Studies into the mechanical properties of the thin wire hybrid three plane, circular external fixator, have opened and enlarged the understanding of biological processes stimulated and supported by the above mentioned mechanical environment. Thus, with time, the crucial role played by striated muscles in the physiology of bone growth and repair is attaining broader recognition and understanding.

H. Stein, MD, DPhil (Oxon)
Department of Orthopaedic Surgery A,
Rambam Medical Center, HaAliya HaShniya St 8,
Haifa 3109601, Israel

M. Solomonow, PhD, MD (✉)
Bioengineering Division and Musculoskeletal Disorders Research Laboratory, Department of Orthopedic Surgery, University of Colorado, Denver, Health Sciences Center, 12800 E 19th Ave, RC-1N, Mail Stop 8343, Box 6511, Denver, CO 80045, USA
e-mail: Moshe.Solomonow@ucdenver.edu

Mechanical Properties

Orthopaedic surgeons need to be updated on mechanical terminology.

1. Compliance is the inverse of stiffness.
2. Higher compliance allows higher deformation
3. Stiffness is the ratio between load and deformation. If measured in bending, it is expressed as the ration between the bending moment and the angular displacement is has caused. It is expressed in Newtonmeters by degree (Nm/degree). This modality is well accepted and used by engineers but less so by medical graduates. The latter, prefer the use of compliance.
4. Stiffness relates inversely to the angle of deformation. In-vivo, bones are surrounded by soft tissues. The latter create ligamentotaxis, which opposes bone displacement, provided bone integrity is preserved.
5. The ring fixation frame, introduced by Ilizarov into clinical practice, is minimally invasive. It is connected to bone by thin K-wires which create minimal damage to both muscle and

D.G. Poitout (ed.), *Biomechanics and Biomaterials in Orthopedics*,
DOI 10.1007/978-1-84882-664-9_12

bone. These wires, are the only means of osseous fixation for the frame and the varying degrees of tension applied to them, determine their frame's stiffness.

6. The ring configuration of the frame, resists torsion, shear and bending.
7. The factors which determine a ring fixators stiffness are:
   (a) the K-wire tension
   (b) the ring diameter
   (c) the centric or eccentric location of the bone within the ring.
8. In clinical practice, the ring diameter is often dependent on the circumference of the soft tissues present at the site. The larger the ring diameter, the lower the stiffness. The anatomical tissue topography, further dictates the location of the bone proper in the ring. The more eccentric the bone, the higher the stiffness. Hence, the only control over frame stiffness left to the surgeon, is the control of the tension applied to the transfixing K-wires.

The Biological Result

The mechanical properties of external fixation frames, have a direct influence on the rate of fracture healing [2–27]. In other words, the mechanical properties of external fixation frames have an unequivocal and direct influence on the biological conditions needed for successful (bone gap) fracture healing. This issue has been discussed also by Chao in his presentation to SICOT in Amsterdam [28]. Ring fixation frames harbour a "trampoline" effect which allows both axial compression and distraction during gait.

Intermittent distraction appears to be of crucial importance for physiological bone growth. The proof of this statement are tubercles, tuberosities and bone outgrowths wherever muscles are inserted into bone in the skeleton. Muscle tonus consists of intermittent contractions of muscle fibers. At the site of muscle tendon insertion, these physiological muscle contractions create intermittent distraction. The latter induce local bone growth the end result being a tubercle , a tuberosity or an outgrowth.

Frame stiffness of any ring fixation frame, is one of its more important mechanical properties. This stiffness depends upon the frame's K-wire tension. For how long does this tension persist in-vivo? Under continuous axial loading, it has been shown that the loading causes a decline in the tension of transverse positioned K-wires [29]. Continuous – in vivo – measurements of the residual tension present in such K-wires in experimental animals, has shown a rapid decline within 2 weeks of mounting the frame, the measured tension values disappearing altogether within 5 weeks of tensioning them in the rings.

Nevertheless, the first signs of intramembranous ossification in the fracture gap, were radiographically detectable 14 days after fracture stabilization by the ring frame, and the whole fracture gap, were radiographically detectable 14 days after fracture stabilization by the ring frame, and the whole fracture gap was filled by woven bone on day 35.

The bridging callus starts, and proliferates from the muscle bed of the fracture. In the tibia, where the significant muscle bed is always postero-medial, this is easy to observe and follow. In both clinical cases and in experimental fractures in the laboratory, the callus has been shown to start always in the posterior plane, next to the muscle bed, and progress from there anteriorly [30–32]. In these publications, the intimate relationship between the developing callus and the muscle bed, has been described.

Most of the load on weight bearing, is transmitted through the fixator [33]. In clinical practice, the choice of the fixator frame means choosing the mechanical configuration which will induce the optimal enhancement in callus formation and fracture healing [33].

A decline in frame stiffness, as initiated by a spontaneous decline in K-wire tension, appears to be an important stimulus for bone formation and healing [7]. Thus, it is very likely that bone mass is regulated by mechanical strain [5].

In fractures, or in the presence of bone gaps, this mechanical strain needs to be induced and maintained in the muscle tissue present in the fracture bed. Micromovements in the axial plane of the fracture stabilized by a ring fixator, induce

efficient medullary and periosted callus formation. This callus, undergoes early metaplasia into membranous bone, and thus stabilizes the fracture gap [34]. Similar observations have been reported by Wu [27] and by Younger [35].

The mechanical efficiency of the stabilizing fixation frame, can be evaluated by the amount of fracture callus formation, the stiffness of the latter being capable of early replacing the spontaneously declining stiffness of the ring fixation frame.

In conclusion, therefore, the preservation of the physiological function of striated muscles in the fracture bed appears to be the key biological factor for the efficient repair of a fracture with or without bone loss.

Muscle Assessments

The tools to assess the physiological function of striated muscles are either muscle charting or EMG. Muscle charting is a time honored manual semi-quantitative measurement, practiced by physiotherapists. This is a time consuming, not strictly s scientific method, the human factor being responsible for all variations in it. During the poliomyelitis epidemics, there was a whole generation of highly experienced physical therapists. Who by repeated muscle charting of the same patient, could provide reliable proof to the progress of the disease, or improvement of the patients due to active aggressive physiotherapy.

At the present, reliable, quantitative computerized muscle charting has become available with the aid of ARCON (http://www.arcon-rehab.com/dynamic.asp). This computerized assessment is particularly reliable in measuring the motor power of various muscle groups.

Electrophysiology and Biomechanics

The EMG is an important tool in the assessment of muscle activities in various occupational tasks, only if used properly. The recordings, processing and interpretation of the EMG should be done while considering the proper electrodes size, interelectrodes distance, muscle architecture, contraction rate, motor units recruitment pattern, muscle length, cross-talk from nearby muscles, sampling rate, filter bandwidths, and smoothing time constants. Each of the above factors, if not considered, can introduce substantial error and result in false or misleading interpretation.

The EMG is a by-product of muscle activity and therefore a dependent signal, influenced by various physiological and anatomical factors as well as the technical aspects of the recording/processing protocol.

The anatomical factors that have profound impact on the EMG are muscle fiber penation, and predominant fiber composition (fast or slow twitch types). Physiological factors that strongly impact the EMG are motor units firing rate and recruitment pattern, force generation rate (isometric), and muscle length changes (shortening or lengthening). Secondary anatomical/physiological issues are the size of the muscle, its depth (below the skin and other muscles), the presence of adipose tissue, nearby muscles and proximity to large blood vessels and bones.

The recording/processing hardware and software that influence the surface EMG are electrode size, material, interelectrode distance, electrode/skin interface, electrodes location relative to muscle shape and axis, differential recordings, recording frequency bandwidth, sampling rates, and smoothing time constant as the most important.

It becomes clear that the EMG is a complex dependent signal, and its recording and interpretation should not be taken lightly. In this paper, several of the most important factors affecting the EMG will be reviewed in the context of the EMG vs force relationship and finally, insights into the controversial issue of EMG cross-talk will be highlighted.

EMG vs Force Relations and Pre-dominant Fiber Type

Different muscles are composed of different proportions of fast and slow twitch fibers. The

soleus, for example is composed of 80 % slow twitch, fatigue resistant fibers of oxidative metabolism whereas its companion gastrocnemius muscle is composed of nearly 80 % fast twitch, fast to fatigue fibers activated by limited stored energy. In highly controlled studies in which both soleus and gastrocnemius were activated with the same contraction control, the EMG vs force relations of the two muscles were significantly different. The relations were linear for gastrocnemius but distinctly non-linear for the soleus [36].

While such findings explain, in part, the controversy of the linearity (or non-linearity) of the EMG-force relations, it issues a warning against the use of the relations without considering the predominant fiber composition of the tested muscle. Such data is available in the literature [37].

Investigators should, however, also consider that predominant fiber type of a muscle can change in individuals who acquired skill in a certain task.

EMG vs Force and Contraction Rate

It is known that the rate at which the muscle contracts and generates force may significantly influence the maximal force obtainable. How would such phenomena influence the EMG vs Force relations?

In highly controlled studies Solomonow et al, [38], recorded the EMG for a muscle increasing its force from 0 to 100 % (maximal force) at rates which varied from 36 to 360 % maximal force/sec. Calculations of the normalized EMG vs force curves did not yield any statistical difference. The maximal force obtained in the fast contraction, however, was 25 % larger than that of the slowest contraction.

Investigators are cautioned to compensate for the contraction rate when EMG is recorded as a measure of force, or risk up to 25 % error that can be associated with highly misleading conclusions. A proper approach is to define the EMG vs force curves at the contraction rate that is to be tested in the field.

EMG vs Force and Motor Units Recruitment

It is known that skeletal muscles utilize the size principle when recruiting motor units in order to increase the force. Small motor units are recruited initially, with gradually larger motor units as more force is required [39]. It is also known that motor units recruitment is completed by the time the initial 50–80 % MVC is generated. The remaining force segment up to 100 % MVC is accomplished by increasing the firing rate of the motor units. It is also known that a given muscle recruits all its motor unit pool in the initial 50 % MVC during fast contractions, and in the initial 80 % MVC in a slower, more accurate contraction.

Solomonow et al. [36], demonstrated that changing motor unit recruitment strategy has pronounced effect on the EMG vs Force relations. When all the motor units of gastrocnemius muscle were recruited in the initial 50 % maximal force segment, the EMG vs force was linear, however, when all the motor units were recruited over the initial 60 %, 70 % and 80 % of the maximal force, the relations were non-linear. Furthermore, the non-linearity was different at each of the three contractions, with the full recruitment completed at 80 % maximal force being the most non-linear.

The advise for proper use of the EMG vs force relations in ergonomics research, is to assess the recruitment pattern of the muscle in question [38–40] before attempting to relate EMG recording to force.

EMG Cross-Talk and Adipose Tissue

Many studies of static and dynamic movements of the extremities and spine demonstrate that co-activation of agonist and antagonist muscles takes place. However, the co-activation principle became controversial, as the low level EMG recorded from the antagonist muscles was considered by many to be cross-talk from the agonist muscles transmitted by volume conduction in the tissues. The sources of cross-talk could be

numerous, including; electrodes too large for the muscle under investigation, interelectrodes distance larger than necessary for the given muscles, proximity to large blood vessels, proximity to major bones, etc.

If one utilizes the correct electrodes size, interelectrodes distance and placement as delineated by Fugelvand et al, [41], such cross-talk can be fully eliminated.

Cross-talk EMG was reported despite proper utilization of electrodes, re-initiating the controversy. A more detailed study by Solomonow et al, [42], in a highly controlled experimental animals using surface and intramuscular wire electrodes gave a clear insight to the problem. Surface EMG recorded from muscles covered by adipose tissue gave as much as 36 % (of 100 % EMG from nearby muscles) cross-talk whereas wire electrodes from the same muscle yielded only 1–2 % cross-talk. Cutting the motor nerve of all the muscles in the leg, confirmed that the adipose tissue was indeed the source/cause of the cross-talk.

A warning is issued against the recording of surface EMG from muscles covered by adipose tissues, such as abdominal and buttocks muscles. Wire recordings should be employed in such cases. Otherwise, with the absence of adipose tissue, the cross-talk is at the noise level and should be of no concern for the investigator.

EMG Processing Issues

Several factors associated with the recording and processing of the EMG have pronounced impact on the validity of the data and its interpretation.

The raw EMG signal is commonly sampled into personal computers for later processing. One of the important aspects of such a procedure is the sampling rates used. The power spectrum of the surface EMG contains frequencies in the range of 0–350 Hz. Less than 5 % of the power is in frequencies above 350 Hz. Furthermore, movement artifacts associated with isometric or most free movements are associated with frequencies below 10 Hz. Therefore, in order to eliminate movement artifacts, a high pass filter with a frequency cut-off of 10 Hz is necessary. Also, in order to prevent any high frequencies (above 350 Hz) from contaminating the signal and to avoid aliasing, a low pass filter with a cut-off frequency of 350 Hz is required. Overall, a bandpass filter of 10–350 Hz will preserve all the important features of the surface EMG.

Sampling into the computer requires a rate of at least twice the highest frequency in the signal. In this case $350\ \text{Hz} \times 2 = 700\ \text{Hz}$. For better accuracy, sampling rates higher than 700 Hz should be used.

Sampling rates lower than 700 Hz will deform the EMG, cause loss of important features and will lead to wrong or misleading conclusions. Furthermore, utilization of a bandpass filter with a frequency cut-off above 350 Hz has very marginal improvement in signal content, but also requires higher sampling rates which in turn limit the number of channels that could be used, limit A/D capabilities and heavily tax storage space on a PC and time required to process the data.

Another important issue is the processing of the EMG into a smoothed curve that represent the changes in the level of activity of the muscle. Commonly, a low pass filter of a time constant ranging between 50 and 300 ms is used. If such a filter is constructed from hardware, one should assess the time delay imposed by the filter and compensate for such a delay when comparing EMG and force on the same time axis. Without applying the time compensation, and especially for fast movements, a discrepancy between force and EMG may lead to false conclusions.

EMG and Muscle Fatigue

When muscle fatigue is being studied via its EMG, the power spectra frequencies are commonly used. The Median Frequency (MF) of the power spectra represents the average conduction velocity of action potentials in the muscle. It is well known that the average conduction velocity decreases with muscle fatigue, giving rise to decrease in the MF. The assessment of muscle fatigue could be useful in ergonomics, especially

in optimizing task durations, work-rest time ratios, etc. Common pitfalls in using the MF of the surface EMG to study fatigue are especially in low level prolonged contractions in the presence of noise. Inherently, contractions producing low levels of force are producing low amplitude EMG. The assessment of fatigue, under such circumstances can become a grossly misleading procedure if the noise is not eliminated.

A method to eliminate such a problem was developed by Baratta et al. [43]. It consists of a noise subtraction step before the power spectra estimate is calculated. The results are much improved accuracy in the MF calculations and its proper and reliable interpretation.

MVC Determination

Determination of the Maximal Voluntary Contraction can introduce errors in the interpretation of EMG studies if not obtained correctly. In general, if an individual is asked to provide a maximal elbow flexion, for example, he will provide a strong contraction which is perceived by him as maximal. If the force output is displayed on a screen as a moving line, and the individual is asked to exceed the line location obtained from his perceived maximal contraction by 10 %, it is easily obtainable. Such feedback attempted normally result in final maximal force which is 25–35 % higher than the maximal force obtained in the first trial.

Such errors may have an impact on the interpretation of the EMG, and EMG vs force relations as well as MF calculations across the full force range. The error, however, is significantly amplified in the low force ranges, and especially in low level static contractions where the casually obtained MVC and the true MVC obtained by training could be miscalculated by 300 % at a 10 % MVC level.

It is difficult to give any advice to avoid or compensate this type of error. The true (e.g., trained) MVC is the most reliable baseline for all types of EMG work where relationships to force is made.

References

1. Calhoun JH, Li F, Bauford WL, Lehman T, Ledbetter FR, Lowery R. Rigidity of half-pins for the Ilizarov external fixator. Bull Hosp Jt Dis Orthop Inst. 1992;52(1):21–6.
2. Ilizarov GA. Clinical application of the tension stress effect for limb lengthening. Clin Orthop. 1990;250:8–26.
3. Ilizarov GA. Transosseous osteosynthesis. Heidelberg: Springer; 1991. p. 3–279.
4. Jorgens C, Schmidt HG, Schumann U, Fink B. Ilizarov ring fixation and its technical application. Unfallchirurg. 1992;95(11):529–33.
5. Paley D, Catangi M, Argnani F, Villa A, Benedetti GB, Cattaneo R. Ilizarov treatment of tibial nonunions with bone loss. Clin Orthop. 1989;141:146.
6. Gasser B, Bowman B, Wyder D, Schneider E. Stiffness characteristics of the circular Ilizarov device as opposed to conventional external fixator. J Biomech Eng. 1990;112:15.
7. Aronson IA, Harp JH. Mechanical considerations in using tensioned wires in a transosseous external fixation system. Clin Orthop. 1992;280:23–9.
8. Monticelli G, Spinelli R. Limb lengthening by closed metaphyseal corticotomy. Ital J Orthop Traumatol. 1983;4:139–50.
9. Hardy JM. Le fixateur externe monolateral "CAPUCINE". Presented at the 18th SICOT meeting. Montreal; 1990. Poster No. 94, p. 492.
10. Wasserstein I, Correl J, Niethard FU. Closed distraction epiphysiolysis for leg lengthening and axis correction of the leg in children. Z Orthop. 1986; 124(B):743–50.
11. Wagner R. Operative lengthening of femur. Clin Orthop. 1978;136:125–42.
12. Green SA, Harris NL, Wall DM, Iskanian J, Marinow H. The Rancho mounting technique for Ilizarov method. A preliminary report. Clin Orthop. 1992; 280:104–16.
13. DeBastiani G, Aldergheri R, Renzi-Brivio L, Trivella G. Limb lengthening by callus distraction (Callotasis). J Pediatr Orthop. 1987;7:129–34.
14. Kenwright J. The influence of cyclic loading upon fracture healing. J R Coll Surg Ed. 1989;34(3):160.
15. Fleming B, Paley D, Kristiansen T, Pope M. A biomechanical analysis of the Ilizarov external fixator. Clin Orthop. 1989;241:95–105.
16. Green SA. The use of wires and pins. Tech Orthop. 1990;5:19–25.
17. Alonso JE, Regazzoni P. The use of Ilizarov concept with the AO/ASIF tubular fixator in the treatment of segmental defects. Orthop Clin North Am. 1990; 21(4):655–65.
18. Uhli RL, Goldstock L, Carter AT, Lozman J. Hybrid external fixation for bicondylar tibial plateau fractures. Presented at the 61st American Academy of Orthopaedic Surgeons meeting, New Orleans; 26 Feb 1994. p. 192.

19. Weiner L. Fixation for complex tibial plateau fractures hybrid fixator. Presented at the orthopaedic trauma association specialty day symposium, 61st American Academy of Orthopaedic Surgeons meeting, New Orleans; , 26 Feb 1994.
20. Chamay A, Tschentz P. Mechanical influence in bone remodeling. Experimental research on Wolffs law. J Biomech. 1972;5:173.
21. Goodship AE, Kenwright J. The influence of induced micro-motion upon the healing of experimental tibia fractures. J Bone Joint Surg. 1985;67(b):650.
22. Kempson GE, Campbell D. The comparative stiffness of external fixation frames. Injury. 1981;12:297.
23. Kristiansen T, Fleming B, Neal G, Reinecke S, Pope MH. Comparative study of fracture gap motion in external fixation. Clin Biomech. 1987;2:191.
24. Panjoli MM, White AA, Wolf JW. A biomechanical cyclic compression of fracture healing in long bones. Acta Orthop Scand. 1979;50:653.
25. Rubin CT, Lonjon LE. Regulation of bone formation by applied dynamic loads. J Bone Joint Surg. 1987;66(A):397.
26. Sarmiento A, Schaeffer JF, Beckerman L, Latta L, Emis JE. Fracture healing in rat femur is affected by functional weight bearing. J Bone Joint Surg. 1977;59(A):367.
27. Wu JJ, Shyr HS, Chao EYS, Kelly PJ. Comparison of osteotomy healing under external fixation devices with different stiffness characteristics. J Bone Joint Surg. 1984;66(A):1258.
28. Chao EYS. Orthopaedic biomechanics. The past, present and future. Int Orthop. 1996;20:239–43.
29. Stein H, Perren SM, Moscheiff R, Baumgart F, Cordey J. The spontaneous decline in the transfixing K-wire's tension of the circular external fixator. Orthopedics. 2001 (in press).
30. Stein H, Cordey J, Perren SM. Segment transport for biological reconstruction of bone defects. Injury. 1993;Suppl 24(2):20–4.
31. Stein H, Coleman R, Mosheiff R, Cordey J, Rahn BA, Reznick A. Changes induced in limb muscles by distraction osteogenesis. Trans 43rd ORS meeting, San Francisco; 1997, p. 703.
32. Mosheiff R, Cordey J, Rahn BA, Perren SM, Stein H. The vascular supply to bone formed by distraction osteogenesis. An experimental study. J Bone Joint Surg. 1996;78-B:497–8.
33. Delprete C, Golo MM. Mechanical performance of external fixator with wires for the treatment of bone fractures. Part 1. Load displacement behavior. J Biomech Eng. 1993;115:29–36.
34. Stein H, Cordey J, Mosheiff R, Perren SM. Observation on the stiffness of neogenetic bone, produced by distraction or segment transport, and it's relationship to bone density. In: Wolter D, Hansis M, Havemann D, editors. 150 years Fixateursysteme. Berlin/Heidelberg/New York: Springer; 1995, p. 47–9.
35. Younger ASE, Mackenzie WG, Morrison JB. Femoral forces during limb lengthening in children. Clin Orthop. 1994;301:55–63.
36. Solomonow M, et al. EMG-force model: dependence on control strategy and fiber composition. IEEE Trans Biomed Eng. 1987;34:692–702.
37. Johnson M, et al. Data on the distribution of fiber types in thirty six human muscles. J Neurophysiol. 1965;28:85–99.
38. Solomonow M, et al. EMG-force of skeletal muscle: contraction rate and motor units control strategy. EMG Clin Neurophysiol. 1990;30:141–52.
39. Henneman E, et al. Functional significance of cell size in spinal motor neurons. J Neurophysiology. 1965; 28:560–80.
40. Bernardi M, et al. Motor unit recruitment strategy changes with skill acquisition. Eur J Appl Physiol. 1996;74:52–9.
41. Fugelvand A, et al. Detection of motor unit action potentials with surface electrodes: electrodes size and spacing. Biol Cybernetics. 1992;67:143–53.
42. Solomonow M, et al. Surface and wire EMG crosstalk in neighbouring muscles. J EMG Kinesiol. 1994;4:131–42.
43. Baratta RV, et al. Methods to reduce the variability of EMG power spectrum estimates. J EMG Kinesiol. 1998;8:279–85.

Clinical Application of Glass Ceramics

13

Takao Yamamuro

It is now widely known that bioactive ceramics such as Bioglass®, Ceravital®, synthetic hydroxyapatite (HA), apatite- and wollastonite-containing glass-ceramic (AW-GC) and ß-tricalcium phosphate (ß-TCP) have a character of osteoconduction and a capability of forming a direct bond to the living bone tissue [1, 2]. In other words, they are incorporated into the living bone tissue in accordance with the pattern of bonding osteogenesis. In their clinical use, however, the mechanical property and the grade of bioactivity required to each material differ depending on the case, i.e., size, shape and location of the bone defect, and the purpose of application. For example, when they are to be used for replacing a vertebral body, a high mechanical strength rather than a high bioactivity is required, if both are not available at the same time. On the contrary, when they are to be used as a coating material over the surface of joint prosthesis, a high bioactivity rather than a high mechanical strength is required. Generally in orthopaedic application of bioactive ceramics to substitute for a large bone defect, a high mechanical strength is always required. For this reason, Bioglass® and Ceravital® which have much lower mechanical strength than that of the human cortical bone have not been used in the field of orthopaedic surgery, although their bioactivity is higher than others. As ß-TCP is a biodegradable ceramic, its mechanical property after implantation can not be compared with those of others. The author's personal experience of their clinical use is, therefore, mostly limited to HA and AW-GC that were used in forms of either granular, porous or dense bone substitute in combination with autogenous bone, and also in forms of coating material for joint prosthesis or bioactive cement.

Why Glass Ceramic

At Kyoto University Hospital, in 1981, probably for the first time in the world as far as known from literatures and meetings, a large amount of synthetic HA granules was implanted into the human bone for a purpose to replace a large giant cell tumor which developed in the right ilium of a 27 year old female. At operation, the tumor was resected through a window made in the lateral wall of the ilium. The bone defect remained in the pelvic bone after the resection was too large to be completely filled in with autogenous bone chips, but bone allograft was not yet available in 1981. Then, a large amount of granular and porous HA was prepared mixed with fibrin glue and autogenous bone chips, and the mixture was

T. Yamamuro, MD, PhD
Kyoto University, Sakyo-ku, Kyoto 606-0805, Japan

Research Institute for Production Development, Shimogamo, Sakyo-ku, Kyoto, Japan
e-mail: mmozume-takaoyama@sweet.odn.ne.jp

D.G. Poitout (ed.), *Biomechanics and Biomaterials in Orthopedics*,
DOI 10.1007/978-1-84882-664-9_13

compactly filled into the bone defect. The clear line, which was demonstrated on the postoperative radiograph between the implanted mass and the pelvic bone, persisted for about 8 months after surgery suggesting that the implant had not yet united with the pelvic bone. At 10 months after surgery, a biopsy of the implanted mass was performed and it was confirmed histologically that the implanted HA granules have directly united with the newly formed bone in places. The radiograph taken 1 year postoperatively showed no clear line between the implanted mass and the pelvic bone. Then, the patient was allowed to bear the full body weight on the affected side. Thus, in this case, it took nearly 1 year after implantation to obtain complete gap filling and bone bonding with HA granule. The patient has been doing well up to now for 25 years after surgery with neither recurrence of the tumor nor limitation of movements of the hip joint of the affected side.

What we learned from this case a quarter of century ago were; firstly, that synthetic HA really bonded to the living bone tissue, but it took nearly 1 year after implantation for gap filling and bone bonding, indicating that HA has a relatively low osteoconductivity; and secondly, HA granule is mechanically too weak to be used under the situation where body weight should be loaded. Nevertheless, synthetic HA has widely been used thereafter in cases of bone tumors and hip revisions. In our surgical practice, however, often there is a need for a more bioactive and mechanically stronger bone substitute than synthetic HA, so that patients will be able to start the weight bearing much earlier after surgery.

At Kyoto University, the research group led by Yamamuro and Kokubo had attempted to synthesize such a biomaterial as that which has a stronger bioactivity and a higher mechanical strength than synthetic HA, and finally reached the synthesis of a new glass-ceramic in 1982 which was named apatite- and wollastonite-containing glass-ceramic (AW-GC) [3]. It was found that dense AW-GC has a bending strength and compressive strength both significantly higher than those of the human cortical bone, while the bending strength of dense HA is considerably lower than that of the human cortical bone. As for their bioactivity, when they were soaked in the simulated body fluid at body temperature, apatite formation was usually observed within 7 days over AW-GC, while it took 28 days for HA.

Application of AW-GC to the Spine

Vertebral Body Prosthesis

In February 1982, a vertebral body prosthesis made of AW-GC was first prepared for the purpose to replace the lumbar vertebra of a sheep [4, 5]. The prosthesis was implanted into the spinal column of a sheep to replace the 3rd and 4th vertebral bodies. A contact microradiograph of the specimen harvested 6 months after implantation demonstrated that the prosthesis had already bonded to the bone trabeculae all the way around. Thus, animal experiments performed on a number of sheep suggested that the vertebral body prosthesis made of AW-GC would be clinically better applicable, due to its stronger osteoconductivity as well as higher mechanical strength, than those made of HA . For these reasons, vertebral body prostheses made of AW-GC with different sizes were prepared for clinical application.

A 50 year old female who developed a breast cancer metastasis in the 10th thoracic vertebra with early sign of paraplegia. As the patient had multiple metastases in the bilateral ilia, it was difficult to harvest the autogenous bone graft. Therefore, in December 1982, the tumor in the spine was simply replaced with a vertebral body prosthesis made of AW-GC, and the body weight bearing was started 1 month after surgery. In spite of multiple metastases developed 5 years later in other organs, the patient survived 14 years after the first operation without paraplegia by the support of chemotherapy.

A 55 year old male developed a renal cancer metastasis in the 4th lumbar vertebra. The tumor was replaced with a vertebral body prosthesis made of AW-GC, and the patient had had no neurological problems until he died of lung metastasis 3 years after surgery. The radiograph of the operated spinal segment which was harvested

by autopsy demonstrated that the 8 cm long prosthesis had firmly bonded to bone and there observed no local recurrence of the tumor. Spinal instruments can be used to fix the vertebral body prosthesis to the adjacent vertebrae. This surgical technique by the use of a Kaneda device [6] is now completely established and applied to treat also burst fracture of vertebral bodies which is often associated with cauda equina lesion.

During the period from 1983 to 1994, when the author retired from Kyoto University, the vertebral body prosthesis made of AW-GC had been used in 1070 cases in Japan to treat bone tumors, burst fractures, and fracture dislocations of the spine, and now it reached about 3000 cases according to the manufacturer's survey. As far as the author has been informed either personally or by publications, there have been no serious complications such as infection, loosening, collapse, and breakage of prosthesis. The retarded bone bonding of the prosthesis in a few cases was virtually an only complication.

Intervertebral Spacer for the Lumbar Spine

Intervertebral spacers were also made of AW-GC to be used for lumbar interbody fusion. Usually, two spacers are implanted into one intervertebral space, and they are securely fixed to the adjacent vertebrae with Steffee's instruments [7, 8].

A case of isthmic spondylolisthesis developed between the 3rd and 4th lumbar vertebra in a 40 year old male, who complained of severe low back pain and neuralgia in both legs. At operation, reduction of the slipping was attempted after a wide laminectomy of the affected vertebrae, and two AW-GC spacers were implanted together with some autogenous bone chips into the intervertebral space. The spacers were securely fixed to the adjacent vertebral bodies above and below by the use of the spinal instruments.

Radiological follow-up studies of the patients, who underwent implantation of the intervertebral spacers, revealed that the spacer has an osteoconductive effect. No case showed late narrowing of the intervertebral space that is often observed when bone autograft or allograft is used for the interbody fusion.

During the period from 1989 to 1994, the intervertebral spacer made of AW-GC was used in 1005 cases in Japan, and, now it reached about 5000 cases. It is considered that the spacer is favorably indicated for lumbar interbody fusion in such conditions as lumbar spinal canal stenosis, degenerative spondylosis, degenerative spondylolisthesis, and postdiscotomy syndrome.

Laminoplasty Spacer for the Cervical Spine

In 1987, laminoplasty spacers were manufactured of AW-GC to be used for the purpose of laminoplastic enlargement in cases of multiple spinal canal stenosis of the cervical spine [9]. At operation, multi-level laminae of the cervical spine are first exposed, then spinous processes are split vertically, and the both split surfaces are opened with a spreader to enlarge the spinal canal. Usually, four to five laminae are enlarged, and bone defects remaining in each lamina are filled with the spacer, that is fixed to each spinous process with threads .

A 75 year old male suffered from tetraplegia due to ossification of the posterior longitudinal ligament from the 4th to the 7th cervical spine as demonstrated by the preoperative CT scanning images. In the postoperative CT images, significant enlargement of the spinal canal is observed, and all spacers seem to have united to the adjacent laminae 14 months postoperatively. In most cases, bone bonding of the spacer was observed on CT images within 6 months after surgery resulting in excellent stability of the spacer. Advantages of using the AW-GC spacer in laminoplastic enlargement are, firstly, no surgical intervention for harvesting bone graft is required, and secondly, late collapse of the implant never occurs because of its high mechanical strength.

During the period from 1988 to 1994, the laminoplasty spacer of AW-GC was used in 778 clinical cases in Japan, and now it reached about 12,000 cases. This operation is considered to be

best indicated for myelopathy caused by multilevel spinal canal stenosis of the cervical spine.

The Iliac Crest Prosthesis Made of AW-GC

A large bone defect remaining in the iliac crest after harvesting bone graft creates various cosmetic and neurological problems [10]. They must be prevented, if possible. For this purpose, the iliac crest prosthesis made of AW-GC was manufactured in different sizes. During the period from 1987 to 1994, the iliac crest prosthesis made of AW-GC was used in 4113 cases in Japan, and now it reached about 20,000 cases. It is reported that 97 % of the patients are satisfied with the iliac crest prosthesis made of AW-GC [11], while the similar prosthesis made of HA often breaks *in situ* after surgery by the accidental direct blow to the iliac crest. This is simply because the mechanical strength of HA is lower than that of AW-GC.

AW-GC to Replace Large Bone Tumors

The AW-GC made spacers have been used to replace large bone tumors that developed in the weight bearing location of long bones [12]. A giant cell tumor developed in the proximal epimetaphysis of the tibia of a 22 year old male. The tumor was removed by the use of a high speed burr and Argon beam coagulator, and the spacer was implanted together with some autogenous bone into the remaining bone defect.

In another case, a giant cell tumor developed in the proximal tibia of a 15 year old female. The same surgical procedure as above was performed. As some examples are demonstrated here, in many similar cases of large benign bone tumors developed in long bones, postoperative clinical and radiological results are quite satisfactory by using the AW-GC spacer. Thus, it was shown clinically that AW-GC can be used as a bone substitute even in locations where HA can not adequately be used.

AW-GC Coating on Hip Prosthesis

It is now widely believed that HA-coated hip prosthesis develops a stable fixation with the surrounding bone tissue due to osteoconductive property of the HA-coated layer. However, in foci of bone remodeling around the implant, osteoclast-mediated absorption of the HA-coated layer takes place constantly, as suggested by Bauer et al. in 1991 [13]. *In vivo*, the osteoclastic bone absorption is usually followed by the new bone formation by osteoblasts, but the newly formed bone which is generated over the prosthesis surface does not bond directly to the metal substrate. Therefore, in a hip prosthesis with a 50–100 μ thick HA-coated layer, it is anticipated that the major part of the prosthesis surface may become naked and biologically disconnected from the surrounding bone tissue in about 20–30 years. Based on the above assumption, the author designed a cementless hip prosthesis with two concepts that are (1) early bone ingrowth by AW-GC bottom coating and (2) persistent firm stability of the prosthesis by mechanical microanchoring with the ingrown bone. From our previous study [14], it was confirmed that AW-GC bottom coating accelerates bone ingrowth as well as implant fixation better than HA-coating or AW-GC full coating.

In 1992, the author's research group together with Kobelco Co. Ltd. (its biomaterials section is now converted to Japan Medical Materials Co.) developed a cementless hip prosthesis which has the AW-GC bottom coating over the whole surface of the socket back and a small circumferential area at the proximal part of the stem. Its bearing mechanism is consisted of Zirconia head and cross-linked polyethylene.

This hip prosthesis has been used in about 10,000 cases up to now in Japan. A follow-up study carried out 5–10 years after the hip replacement revealed an extremely low incidence of radiolucency at the porous coated area where the AW-GC bottom coating is applied. Characteristic of this hip prosthesis is an early osseointegration at the AW-GC bottom coated area.

Summary

Synthetic hydroxyapatite (HA) is now widely used as a bone substitute and as a coating material of joint prostheses, for the reason that HA has a character of osteoconduction and a capability of forming direct bond to the living bone tissue. In the clinical practice, however, often there is a need for a material which has both stronger bioactivity and higher mechanical strength than HA in order to obtain earlier bone bonding with bone substitute and to let patients put their body weight earlier on the affected site promoting their ambulatory life. Apatite- and wollastonite-containing glass-ceramic (AW-GC) synthesized at Kyoto University in 1982 has stronger bioactivity as well as higher mechanical strength than HA, and therefore, AW-GC has been used to fabricate various types of prostheses and spacers to be used in the spinal surgery and tumor surgery. Particularly, lumbar intervertebral spacers and cervical laminoplastic spacers have been used in thousands of clinical cases with excellent clinical, radiological and biomechanical results. AW-GC has also been used as a coating material of hip prosthesis by the technique of bottom coating over the porous surface. A mid-term follow-up study of several thousands of clinical cases of hip replacement demonstrated the significantly early osseointegration at the AW-GC bottom coated area comparing to the HA coated area. It is also anticipated based on animal experiments that the AW-GC bottom coating will ensure much longer stability of joint prosthesis than the AW-GC full coating or HA full coating. Thus, it was shown clinically that the AW-GC is useful as a bone substitute as well as a coating material even in locations where HA cannot adequately be used.

References

1. Oonishi H, Hench LL, Wilson J, Sugihara F, Tsuji E, Kushitani S, Iwaki H. Comparative bone growth behavior in granules of bioceramic materials of various sizes. J Biomed Mater Res. 1999;44:31–43.
2. Oonishi H, Hench LL, Wilson J, Sugihara F, Tsuji E, Matsuura M, Yamamoto T, Mizokawa S. Quantitative comparison of bone growth behavior in granules of Bioglass®, A-W glass-ceramic, and hydroxyapatite. J Biomed Mater Res. 2000;48:37–46.
3. Kokubo T, Shigematsu M, Nagashima Y, Tashiro M, Nakamura T, Yamamuro T, Higashi S. Apatite- and wollastonite-containing glass-ceramic for prosthetic application. Bull Inst Chem Res Kyoto Univ. 1982;60:260–8.
4. Yamamuro T, Shikata J, Okumura H, Kitsugi T, Kakutani Y, Matsui T, Kokubo T. Replacement of the lumbar vertebrae of sheep with ceramic prosthesis. J Bone Joint Surg. 1990;72-B:889–93.
5. Yamamuro T. Replacement of the spine with bioactive glass-ceramic prostheses. In: Yamamuro T, Hench LL, Wilson J, editors. Handbook of bioactive ceramics, vol 1. Boca Raton: CRC Press; 1990. p. 343–51.
6. Kaneda K, Taneichi H, Abumi K, Hashimoto T, Satoh S, Fujiya M. Anterior decompression and stabilization with the Kaneda device for thoracolumbar burst fractures. J Bone Joint Surg. 1997;79-A:69–83.
7. Shimizu K, Iwasaki R, Matsushita M, Yamamuro T. Posterior lumbar interbody fusion using AW-GC vertebral spacer. In: Yamamuro T, Kokubo T, Nakamura T, editors. Bioceramics 5. Kyoto: Kobunshi Kankoukai; 1992. p. 435–41.
8. Yamamuro T. A/W glass-ceramic: clinical applications. In: Hench LL, Wilson J, editors. An introduction to bioceramics. Singapore: World Scientific; 1993. p. 89–103.
9. Kamo Y, Takemitsu Y, Hamada O, Yamaga S. Cervical laminoplasty by splitting the spinous process using AW glass-ceramic lamina spacer (in Japanese). Clin Orthop Surg. 1992;27:1115–22.
10. Yamamuro T. Reconstruction of the iliac crest with bioactive glass-ceramic prostheses. In: Yamamuro T, Hench LL, Wilson J, editors. Handbook of bioactive ceramics vol 1. Boca Raton: CRC Press; 1990. p. 335–42.
11. Ito M, Abumi K, Moridaira H, Shono Y, Kotani Y, Minami A, Kaneda K. Iliac crest reconstruction with a bioactive ceramic spacer. Eur Spine J. 2005;14:99–102.
12. Kasahara K, Tuboyama N, Toguchida J, Nakamura T. Joint preserving surgical technique for giant cell tumor of bone by the use of surgical adjuncts and AW glass-ceramic (in Japanese). Clin Orthop Surg. 1996;31:1321–9.
13. Bauer TW, Geesink RGT, Zimmerman R, McMahon JT. Hydroxyapatite-coated femoral stems: histologic analysis of components retrieved at autopsy. J Bone Joint Surg. 1991;73-A:1439–52.
14. Yamamuro T, Takagi H. Bone bonding behavior of biomaterials with different surface characteristics under load-bearing conditions. In: Davies JE, editor. The bone-biomaterial interface. Toronto: University of Toronto Press; 1991. p. 406–13.

Alumina Composite: The Present Generation of Load Bearing Ceramics in Orthopedics

14

Bernard Masson and Meinhard Kuntz

It is now more than 40 years that commercially pure alumina is in clinical use for the production of heads and sockets for hip replacements [1]. So far more than six millions components have been implanted worldwide [2] and during the last two decades the use of alumina components has continuously increased in Europe and, more recently, in the USA.

The selection of alumina ceramic as a biomaterial was based on its unsurpassed biological safety and stability in the living environment and the first applications were based on pure alumina, which technology was continuously improved in order to increase the reliability and the performances of alumina components, an effort that has been very successful, as alumina in orthopedics is known as "The Ceramic".

Hip arthroplasty is among the most successful surgical procedures since ever. This has led to the widening of the eligibility of patients for this treatment. The Charnley's selection of metal-on-UHMWPE bearings for his low friction arthroplasty [3] is fully justified taking into account the age and the activity level of the early 1960s patients. Today hip arthroplasty patients are much more active, irrespectively of their age, and intended to save albeit improve their lifestyle after surgery. Ceramic components resulted especially suitable for these patients, and to fulfill the patients and surgeons demand the ceramists focused their efforts on the development of ceramic composites to obtain a ceramic with mechanical behavior suitable for the design of new and more challenging devices, joined to the high biological safety and wear behavior of pure alumina.

The first alumina and zirconia composite material introduced in clinic is a ZTA known under the trade name of BIOLOX® delta (CeramTec GmbH, Plochingen, Germany) [4]. So far, BIOLOX® delta has 10 years of clinical records in hip replacements and is opening its way also in the knee [5], while the development of other ceramic medical devices made out BIOLOX® delta is in progress.

Developments in Alumina Technology

As many ceramics, alumina shows very good performances in compression, but it is more sensitive to tensile stresses. The materials does not show (at room temperature) plastic deformation before fracture (e.g. no yield point in stress–strain curve before fracture), and once started

B. Masson, MScPh (✉)
Medical Division, BioConnect,
Vieille-Toulouse, France
e-mail: b.masson@wanadoo.fr

M. Kuntz, Dr-Ing
Oxide Development, CeramTec GmbH,
Plochingen, Germany

D.G. Poitout (ed.), *Biomechanics and Biomaterials in Orthopedics*,
DOI 10.1007/978-1-84882-664-9_14

fractures may propagate very fast (low toughness K_{IC}). As the tensile strength of alumina is improved the highest the density and the smaller the grain size, to maximize the density and to minimize the grain size were among the goals of the development process that was started soon after the introduction of alumina in clinical applications, aimed overall to improve the reliability of alumina components.

The first milestone in the development process may be set around 1980, when thanks to the introduction of high purity starting materials in ceramic production, to improvements in process control and to the definition of the standard ISO 6474, was obtained the so-called "second generation alumina". The experience gained led also to abandon some early design – e.g. skirted heads, due to the unacceptable complication rate [6].

The reliability of alumina balls and sockets was improved also by the use of the laser marking. The component identification marks in the first series were made by diamond engraving the components before firing, raising concerns about local stress concentrations. The application of the new laser marking technique demonstrated in clinical use its positive effects on the reliability of alumina ceramic components.

The most relevant development in improving the reliability of ceramic components was the introduction in the testing protocol of proof test, a nondestructive test aimed to discard all those components containing a critical size flaw that may shorten the expected lifetime.

A further contribution to the improvement of reliability of medical-grade alumina components was obtained by the introduction of Hot Isostatic Pressing (HIP). This thermal treatment – performed slightly below the sintering temperature under extremely high pressures (about 100 MPa) – allows to obtain high density limiting the development of the grain size.

All the process improvements in above led about 1995 to the introduction into the market of the present "third generation alumina" The average grain size decreased from 3.2 to 1.8 μm while bending strength in clinical grade alumina (e.g. BIOLOX® forte) is 650 MPa (Table 14.1).

Alumina Matrix Composites

Alumina-matrix composites represent the latest development in alumina technology, and are identified by some Authors as "the fourth generation alumina". Alumina-matrix composites had been developed to obtain a ceramic in which the biocompatibility and stability of alumina would be joined to enhanced toughness and mechanical properties with respect to pure alumina [7]. Materials with different microstructures may be achieved in these systems, as exhaustively reported by Claussen [8]. Zirconia-Toughened Aluminas (ZTAs) were investigated in France and Italy [9–11], in view of applications in orthopedics without leading to clinical applications up to now. It was in the 2000s that an in situ reacted Alumina Matrix Composite (BIOLOX® delta) had been qualified for clinical applications [4].

BIOLOX® delta is obtained by the following chemical-physical reactions taking place within the lattice during sintering [12]:

The basic transformation equations are known as follows:

$$2YCrO_3 \rightarrow Y_2O_3 + Cr_2O_3 \quad (14.1)$$

$$SrZrO_3 \rightarrow SrO + ZrO_2 \quad (14.2)$$

$$Al_2O_3 + Cr_2O_3 \rightarrow Al_2O_3 : Cr \quad (14.3)$$

$$SrO + 6Al_2O_3 : Cr \rightarrow SrAl_{12-x}Cr_2O_{19} \quad (14.4)$$

$$ZrO_2 + Y_2O_3 \rightarrow ZrO_2 : Y \quad (14.5)$$

The sub-micron particles of yttria-stabilized tetragonal zirconia (Y-TZP) are forming about 17 vol% of the material while strontium aluminate platelets are accounting for about 1 vol%, the balance being fine grained alumina containing in solid solution chromium dioxide, forming the matrix of the ceramic. toughened by phase

Table. 14.1 Required material properties according to the ISO standards 6474 – 1 (pure alumina), ISO 6474 – 2 (alumina – zirconia composite) and ISO 13 356 (zirconia)

ISO Standard		ISO 6474-1	ISO 13 356	ISO 6474-2
Material	Unit	Pure alumina	Zirconia	Alumina zirconia type X
Average bulk density		≥3.94 g/cm^3	≥6.00 g/cm^3	≥99 %
Chemical composition	wt %	$Al_2O_3 \geq 99.7$, $MgO \leq 0.2$, impurities ≤ 0.1	$ZrO_2 + HfO_2 + Y_2O_3 \geq 99.0$, Y_2O_3 4.5–6.0, $HfO_2 \leq 5$, $Al_2O_3 \leq 0.5$, Others ≤ 0.5	Al_2O_3 60–90, $ZrO_2 + HfO_2$ 10–30, additives ≤10, impurities ≤ 0.2
Grain size				
Mean value AI_2O_3	µm	≤2.5		≤1.5
Standard dev	%	≤40 %		≤25 %
Mean value ZrO_2	µm		≤0.4	≤0.6
Standard dev.	%			≤40 %
Strength	MPa	≥500	≥800	≥1000
Weilbull modulus (4 pt bending)		≥8		≥8
Young's modulus	GPa	≥380		≥320
Fracture toughness	MPa $\sqrt{m}$	≥2.5		≥4.0
Hardness HV1	GPa	≥18		≥16.0
Wear resistance		Info		For comparison before and after accelerated aging
Cyclic fatigue limit		No failure at 200 MPa	No failure at 320 MPa	No failure at 400 MPa
Upper limit of monoclinic phase	%		≤20	
Radioactivity zirconia raw material	Bq/kg		≤200	≤200
Accelerated aging			5 h authoclaving ≤ 25 % monocle phase	10 h autoclaving
Autoclave (0.2 MPa, 134° C)			Strength decrease not more than 20 %	

transformation in the Y-TZP grains and reinforced by the presence of platelets acting as a secondary, reinforcing structure in the composite.

Behavior of BIOLOX® Delta

Mechanical Properties

The bending strength and toughness values characteristic of BIOLOX® delta have been summarized in Table 14.1. These properties are based on the presence both of transformation toughening by zirconia and by the reinforcement due to the platelets within the alumina matrix.

Transformation Toughening by Zirconia

The presence of the Y-TZP phase is crucial for the reinforcement of BIOLOX® delta. These sub-micron particles evenly distributed within the microstructure are metastable in nature, and on their ability to transform their lattice from tetragonal to monoclinic relies their contribution to the mechanical properties of the composite. The tetragonal to monoclinic transformation in Y-TZP biomaterials had been already comprehensively described elsewhere [13]. In Alumina Matrix Composite when the constraint exerted onto the zirconia grains by the stiff alumina matrix is relieved, i.e. by a crack

advancing in the material, the zirconia grains near the crack tip shift simultaneously and in an ordered way into monoclinic phase The 3–4 % volume expansion and the shear strain associated to tetragonal-to-monoclinic transformation of grains absorbs energy. This dissipates the energy of the advancing crack at the crack tip due to the T-M transformation. The crack needs to overcome the compressive stress field created within the matrix by the volume expansion of the grains to progress further. These energy dissipating mechanisms are the basis of the toughening contribution of the YTZP phase to BIOLOX® delta.

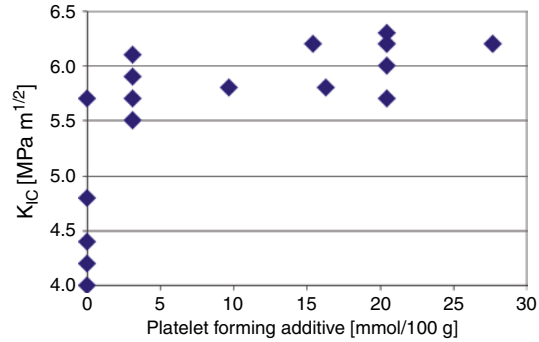

Fig. 14.1 Effect of platelet building ingredients on fracture toughness

New Experimental Evidence for the Impact of Platelets

Incorporation of fibres, whiskers or platelet shaped components into a ceramic composite material is a well-known concept for toughness improvement. The toughening mechanism of such components is usually described based on crack deflection and crack bridging. Crack deflection requires strong reinforcing elements and a relatively weak interface. Furthermore, the volume share of the reinforcing phase should cover at least 10 % or more.

Analysis of crack extension on the surface of a BIOLOX® delta specimen was conducted. It was found that the platelets visible on the surface do not provide any crack deflection nor crack bridging. While this analysis does not examine platelets in the bulk material, on the surface the cracks preferably cross the platelet crystals. It is suggested from this analysis that crack shielding and bridging may not be the only key mechanism in this material.

However, there is clear empirical evidence that presence of platelets leads to significant increase of fracture toughness. A large variety of experimental composites similar to BIOLOX® delta with and without platelet building ingredients was produced and the resulting fracture toughness was measured as it is shown in Fig. 14.1. Obviously, the average fracture toughness of composites with platelets is significantly higher than the variations without platelets. Currently the underlying mechanism of the toughening effect of the platelets is not fully clear. One theory is that the platelets support the extension of zirconia phase transformation in the vicinity of a crack tip.

Hardness

The final composition of BIOLOX delta also includes chromium. Some literature studies have indicated that the solid solution of chromium cations in the alumina lattice may increase the hardness of certain alumina materials [14]. However, the Bradt study suggests a measureable increase is only available at a Cr_2O_3/Al_2O_3 ratio around > 5 %. In BIOLOX® delta the Cr_2O_3/Al_2O_3 ratio is only 0.5 %. Consequently, this chromium content has no effect on the hardness of BIOLOX Delta. Taking into account measurement uncertainty and normal scatter of hardness, a material comparable to BIOLOX® delta, but without chromium, shows equivalent hardness. This is the result of a recent comprehensive study [15]. It should be considered that hardness of a ZTA ceramic can be influenced by several parameters, e.g. grain size, density or zirconia content. We assume today that early results of a chromium impact on hardness in BIOLOX® delta may be traced back to secondary effects. The only effect of chromium in BIOLOX® delta is the eye-catching pink color of the final material

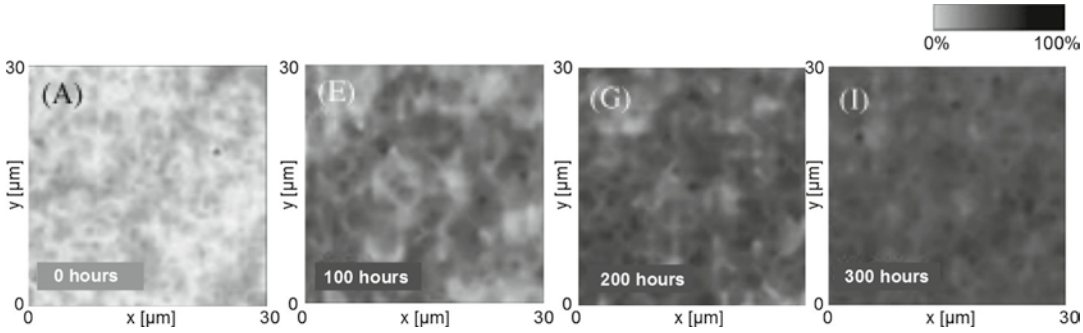

Aging duration	0 h	100 h	200 h	300 h
Monocl. Absolute	17,7 %	48,8 %	64,1 %	66,7 %
Monocl. Relative	3,0 %	8,3 %	10,9 %	11,3 %

Fig. 14.2 Increase of monoclinic phase content after very long term hydrothermal aging in an autoclave. Autoclaving conditions 121 °C, 1 bar. Quantitative monoclinic phase content obtained by direct communication to the author (Adapted from Pezzotti et al. [29])

Hydrothermal Aging

Phase transformation caused by hydrothermal aging is an undesired effect. However, as it has been shown in the previous chapters, monoclinic phase transformation is necessary for the reinforcement and the high strength and toughness of the material BIOLOX® delta. Thus, a certain amount of phase transformation in hydrothermal environment is not a matter of concern. It depends on the specific composition of the material if there is a critical level of phase transformation where the material can be damaged. In the years 2001–2002 some batches of the pure zirconia material Prozyr® of the company Desmarquest showed catastrophic failure in-vivo due to substantial monoclinic phase transformation at the surface [16]. It has to be emphasized that such a damage is impossible in BIOLOX® delta due to the fact that only 17 vol% consist of zirconia. Consequently, the ultimate upper limit of monoclinic zirconia is only a total of 17 % whereas 83 % of the material remains not affected by phase transformation and hydrothermal aging.

As mentioned above, hydrothermal aging is accelerated at elevated temperatures. For pure zirconia in biomedical applications a standardized accelerated aging test is recommended in ISO 13 356. Hydrothermal aging is evaluated using an accelerated aging test setup according to ISO 6474-2. The accelerated aging conditions are autoclaving at 134 °C, 2 bar steam for 10 h. As a rough estimate these conditions are equivalent to 40 year exposure in body fluid environment.

However, this transfer of aging kinetics depends on individual properties of a material.

The aging behavior of BIOLOX® delta has been extensively analyzed using accelerated hydrothermal aging by autoclaving. Moreover, the aging has been combined with severe mechanical static and dynamic testing in order to understand if any material degradation occurs during aging.

In fact, the monoclinic phase content in BIOLOX® delta is increased after long term aging. In Fig. 14.2 quantitative analysis of monoclinic phase transformation using Raman spectroscopy are shown. The aging conditions (121 °C, 1 bar) for this analysis were slightly different from the recommendation in the ISO standard. As in Fig. 14.2 the gray intensity indicates monoclinic phase distribution. As can be seen the monoclinic content is increased after extreme long exposure time. After 300 h the monoclinic phase content reaches a relative value of 66.7 %, i.e. 11.3 % of the total volume of the composite are monoclinic zirconia.

The autoclaving time used in this study is extremely long, much longer than recommended in the ISO standard. The monoclinic phase content seems to reach a saturation since the increase from 200 to 300 h is only marginal.

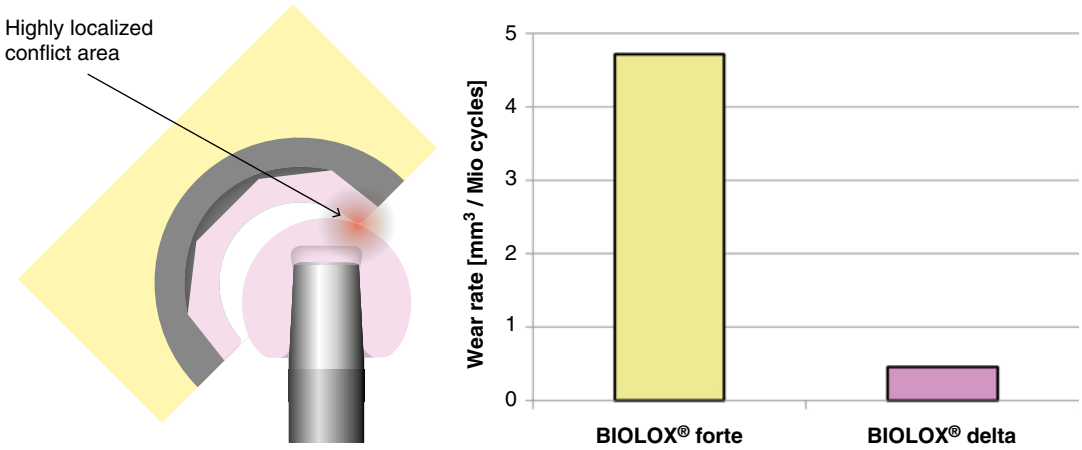

Fig. 14.3 Wear performance of BIOLOX® delta and BIOLOX® forte at simulated micro separation

Wear Behavior

At normal wear conditions (e.g. standard wear simulator) the wear of a hard-hard couple of BIOLOX® delta is very similar to the excellent performance of the well proven pure alumina BIOLOX® forte. The difference in hardness between these materials does not compromise the normal wear behavior.

However, a significant advantage of BIOLOX® delta is identified in the case of worst case wear simulation as shown in Fig. 14.3. In this experiment microseparation of ceramic ball head and insert during each load cycle has been simulated which leads to highly localized forces at the contact area. This experimental setup was supposed to simulate e.g. low tension of the soft tissue after surgery as it is discussed frequently by orthopedic experts. It was concluded from various retrievals that in some cases a well defined stripe-shaped area shows a more intense worn surface than the normal surface of the ball head. This phenomenon is known as "stripe wear".

In the experiment, heavy wear conditions are simulated due to the highly located contact area. It was found after five mio microseparation load cycles that the wear volume of BIOLOX® delta was ten times lower than that with the pure alumina BIOLOX® forte [17].

Obviously BIOLOX® delta shows an excellent "stripe wear tolerance". The analysis as given in [17] shows that in the stripe wear region the monoclinic phase content is strongly increased. This indicates the mechanism behind the excellent stripe wear tolerance of BIOLOX® delta. As a first approach it is assumed that at these special test conditions a very high localized stress acts in the contact area which may be able to introduce damage in the surface. In this case the reinforcing mechanism is activated in BIOLOX® delta. The toughness of the surface is increased by phase transformation which prevents surface damaging even under these extreme conditions. This assumption is supported by the Raman analysis of the worn surface. In the stripe wear region a high monoclinic phase content was found which indicates that phase transformation for reinforcement took place.

Applications in New Devices

On November 2014 more than five million BIOLOX® delta components had been implanted worldwide. Besides these devices the outstanding mechanical behavior of this composite have made possible the production of more challenging devices, like all-ceramic condylar component for Total Knee Replacements [18–20], Shoulder, inlays for pre-assembled big diameter (36 mm or more) THR bearings [21, 22] while other devices for application in the spine, small

Fig. 14.4 Ceramic components made out Alumina ceramics. One may note the TKR condylar component and the THR revision head both made out of the alumina matrix composite BIOLOX® delta

joints [23] or to achieve direct to bone fixation are under study [24].

A special mention has to be made of ball heads especially conceived for THR revision (BIOLOX® option system). It is known that since ever it was recommended to avoid the use of a ceramic head on a used taper, e.g. during a revision surgery of an implant with a well fixed stem (Fig. 14.4). By the composite ceramic BIOLOX® delta it was possible to manufacture ceramic ball heads with reduced thickness able to host a metallic sleeve which plastic deformation will accommodate the scratches and ridges of the taper, without inducing stress risers on the ceramic. Several sleeve design are available, that can provide different neck length (up to +7 mm) providing the way to assure intraoperatively the correct lateralization of the implant [25, 26].

Clinical Outcomes

The results of the prospective, randomized, multicenter IDE trial performed in the USA on BIOLOX® delta ceramic-on-ceramic (CoC) bearings have been recently reported [27]. This study was including 177 CoC bearings and 87 Ceramic-on-Cross Linked polyethylene (CoP – BIOLOX® delta on Marathon® , DePuy, J&J, Warsaw, IN). All the bearings were on 28 mm in diameter. The average duration of the follow-up was 31.3 months (range, 21–49 months). Overall the Harris Hip score of the CoC group was higher than the one of CoP group (94.4 Vs. 93.8) and the survivorship of both bearings was similar (CoC 97.6 % Vs. CoP 97.7 %).

No failures for early aseptic loosening nor dislocations were observed in the series of 386 THR with BIOLOX® delta ceramic-on-ceramic bearings reported by Oakley [28]. Implants had been performed between 2006 and 2008, the Oswestry Hip Score definitely improved postoperatively (OHS 43 Vs. 16 pre-op). No bearing-related complication were observed. Only in the radiograph performed at 1 year follow up it was noted one the chipping of the acetabular rim. It was presumably due to a patient fall, but being asymptomatic it required no action.

Conclusions

Alumina ceramics are still a valid option in THR bearings. The alumina matrix composite BIOLOX® delta represents the most advanced development of their technology which represents today the golden standard in hip arthroplasty. Namely, all the latest research now in progress are taking ceramic bearings as a reference. The excellent hydrothermal stability and aging behavior, joined to so far unsurpassed mechanical properties, high hardness, biological safety and excellent wear behavior also in off-normal conditions are making this ceramic a significant addition to the technology of arthroplasty both increasing the longevity of implants, both making possible the construction of reliable more challenging and innovative ceramic devices.

References

1. Boutin P. Arthroplastie totale de la hanche par prostheses en alumine fritté. Rev Chir Orthop. 1972;58:230–46.
2. Piconi C. Chapter 16 – alumina. In: Ducheyne P, editors. Comprehensive biomaterials. Elsevier; 2011. ISBN-978-008-055302-3 (in print).
3. Charnley J. Total prosthetic replacement of the hip. Physiotherapy. 1967;53:407–9.

4. Burger W, Richter HG. High strength and toughness alumina matrix composites by transformation toughening and "in situ" platelet reinforcement (ZPTA). Key Eng Mater. 2001;192–195:545–8.
5. Heimke G, Leyen S, Willmann G. Knee arthroplasty: recently developed ceramics offer new solutions. Biomaterials. 2002;23:1539–51.
6. Piconi C, Maccauro G. Zirconia as a ceramic biomaterial. Biomaterials. 1999;20:1–25.
7. Rieu J, Goeuriot P. Ceramic composites for biomedical applications. Clin Mater. 1993;12:211–7.
8. Claussen N. Microstructural design of zirconia-toughened ceramics. In: Claussen N, Ruhle M, Heuer AH, editors. Science and technology of zirconia II. Columbus: American Ceramic Society; 1984. p. 325–51.
9. Mandrino A, Eloy R, Moyen B, Lerat J-L, Treheux D. Base alumina ceramics with dispersoids: mechanical behaviour and tissue response after in-vivo implantation. J Mater Sci Mater Med. 1992;3:457–63.
10. Salomoni A, Tucci A, Esposito L, Stamenkovich I. Forming and sintering of multiphase bioceramics. J Mater Sci Mater Med. 1994;5:651–3.
11. Affatato S, Testoni M, Cacciari GL, Toni A. Mixed-oxide prosthetic ceramic ball heads. Biomaterials. 1999;20:1925–9.
12. Burger W. Umwandlungs- und plateletverstärkte Aluminiumoxid-Matrixwerkstoffe (Teil 1). Keram Z. 1997;49:1067–70.
13. Hannink RHJ, Kelly PY, Muddle BY. Transformation toughening in zirconia-containing ceramics. J Am Ceram Soc. 2000;83:461–87.
14. Bradt RC. Cr2O3 solid solution hardening of Al2O3. J Am Ceram Soc. 1967;50(1):54–5.
15. Kuntz M. The effect of chromia content on hardness of zirconia platelet toughened alumina composites. https://www.ceramtec.com/files/.
16. Chevalier J. What future for zirconia as a biomaterial. Biomaterials. 2006;27:535–43.
17. Clarke IC, Pezzotti G, Green DD, Shirasu H, Donaldson T. Severe simulation test for run-in wear of all-alumina compared to alumina composite THR. Proceedings 10th BIOLOX symposium, 11–20; 2005.
18. Dalla Pria P, Giorgini L, Kuntz M, Pandorf T. Ceramic knee design. In: Benazzo F, Falez F, Dietrich M, editors. Bioceramics and alternative bearings in joint arthroplasty. Springer. 2006; p. 115–24..
19. Mittelmeier W, Ansorge S, Kluess D, Kircher J, Bader R. Ceramic knee endoprostheses: reality or future? In: Benazzo F, Falez F, Dietrich M, editors. Bioceramics and alternative bearings in joint arthroplasty. Springer; 2006. p. 125–32.
20. Bergschmidt P, Lohmann C, Bader R, et al. A national prospective duocenter study on the clinical and radiological outcome of the multigen plus total knee system with a alumina matrix composite femoral component. In: Cobb JP, editor. Modern trends in THA bearings. Heidelberg: Springer; 2010. p. 245–50.
21. Scholes SC, Unsworth A. Tribological testing of pre-assembled alumina matrix composite hip prostheses. In: Cobb JP, editors. Modern trends in THA bearings. Springer; 2010. p. 139–44.
22. Wilson K, Roques A, Dickinson A, Mathias R, Taylor A, Holland J. Initial fixation of a pre-assembled cup system. In: Cobb JP, editors. Modern trends in THA bearings. Springer; 2010. p. 233–7.
23. Graessel M. Spine: ceramic disc – what you should know. In: Chang JD, Billau K, editors. Bioceramics and alternative bearings in joint arthroplasty. Springer; 2007. p. 261–8.
24. Burgkart R, Eichhorn S, Kershbaumer S, et al. Mechanical and histological results of a porous coating based on alumina matrix composite. In: Cobb JP, editor. Modern trends in THA bearings. Springer; 2010. p. 245–50.
25. Chang J-D, Kamdar R, Yoo J-H, Hur M, Lee S-S. Third generation ceramic-on-ceramic bearing surfaces in revision total hip arthroplasty. J Arthroplasty. 2010;24:1231–5.
26. Lazennec JY, Boyer P, Rousseau MA, et al. Revision strategy and clinical results with alumina matrix composite revision ball heads: a 2 years follow up preliminary results. In: Cobb JP, editors. Modern trends in THA bearings. Springer; 2010. p. 103–6.
27. Hamilton WG, McAuley JP, Dennis DA, Murphy JA, Blumenfeld TJ, Politi J. THA with delta ceramic on ceramic. Clin Orthop. 2010;468:358–66.
28. Oakley J. The early clinical results of alumina matrix composite ceramics in primary cementless total hip arthroplasty. In: Cobb JP, editor. Modern trends in THA bearings. Berlin/Heidelberg: Springer; 2010. p. 179–82.
29. Pezzotti G, Yamada K, Sakakura S, Pitto RP. Raman spectroscopic analysis of advanced ceramic composite for hip prosthesis. J Am Ceram Soc. 2008;91(4):1199–206.

Validation of a High Performance Alumina Matrix Composite for Use in Total Joint Replacement

15

Bernard Masson and Meinhard Kuntz

Since 200. more than 3.8 million femoral head and 1.5 million inserts of the new high performance ceramic composite BIOLOX®*delta* have been successfully implanted. Due to the unique strength and toughness of this material the risk of fracture has been substantially reduced when compared to conventional ceramic materials.

However, one should keep in mind that the outstanding properties of BIOLOX®*delta* rely on complex reinforcing mechanisms. Therefore, it is necessary to assess if reinforcement is maintained throughout the live-time of the artificial joint which is anticipated to exceed more than 20 years.

Like any other material which is intended for surgical applications, the suitability must be evaluated based on multiple approaches, like intrinsic mechanical material properties, biocompatibility, system compatibility and finally in-vivo scoring of the surgical outcome

The basis of all progress in material development for surgical applications are the intrinsic material properties. When the surgeon decides to replace a known material by a new one, there must be sufficient indication for a substantial benefit. The most challenging question is to predict the reliability of the material after many years of service life.

Within the scope of this paper, the intrinsic material properties of the composite ceramic BIOLOX®*delta* are analysed. Life time can be traced back to basic principles, i.e. how can a material be damaged after many years of service. Every material degrades after many years loading in an aggressive environment. It is the challenge to create a material which preserves sufficient residual reliability even under worst case conditions for many years.

Due to the chemical stability ceramics obviously provide an intrinsic advantage in comparison to other materials like metals and polymers. Ceramics are produced in the state of a fully saturated chemical bonding. There is no driving power left for further chemical interaction with the environment. Thus, typical life time limiting problems like corrosion or water adsorption are not relevant for high performance and high purity ceramics.

It must be considered if there are other mechanisms which may limit the life time of ceramics. It is well known that like all other materials also ceramics may suffer degradation from following distinguished events:

Fatigue	Resistance against long time static and alternating load
Ageing	Resistance against hydrothermal or other chemical attack
Wear	Durability under abrasive conditions

B. Masson, MScPh (✉)
Medical Division, BioConnect,
Vieille-Toulouse, France
e-mail: b.masson@wanadoo.fr

M. Kuntz, Dr-Ing
Oxide Development, CeramTec GmbH,
Plochingen, Germany

D.G. Poitout (ed.), *Biomechanics and Biomaterials in Orthopedics*,
DOI 10.1007/978-1-84882-664-9_15

In this chapter, the life time limiting mechanisms and the relevance for the application as a surgical implant are discussed. It is shown how life time of the ceramic material BIOLOX®*delta* can be described and evaluated. The unique microstructure and reinforcing mechanisms of the material not only support the short term performance like fracture toughness and strength but also improve substantially the long term reliability.

Description of Biolox®*Delta*

BIOLOX®*delta* is an alumina based composite ceramic. 80 vol % of the matrix consist of fine grained high purity alumina which is very similar to the well known material BIOLOX®*forte*. As it is the case in any other composite material, the basic physical properties like stiffness, hardness, thermal conductivity etc. are mainly predetermined from the dominating phase. It was the basic idea for the development of the new material to preserve all the desirable properties of BIOLOX®*forte* which has millions of components in service but to increase its strength and toughness. These properties are rigorously improved by implementation of reinforcing elements. Figure 15.1 shows the microstructure of BIOLOX®*delta*.

Two reinforcing components are integrated in BIOLOX®*delta*. 17 vol % of the matrix consist of tetragonal zirconia particles. The average grain size of the zirconia is around 0.2 µm. As a further reinforcing element, apprx. 3 vol % of the matrix are built by platelet shaped crystals of the ceramic composition strontiumaluminate. The platelets stretch to a maximum length of apprx. 3 µm with an aspect ratio of 5–10

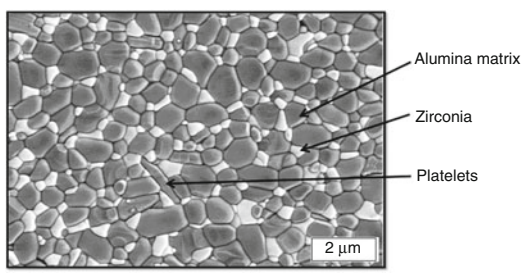

Fig. 15.1 Microstructure of BIOLOX®*delta*

Additionally to the reinforcing components, there are other elements doped to the material. The composite contains yttrium which is solved in the zirconia and which supports the stabilization of the tetragonal phase. The material contains Chromium, this element is known to be soluble in the alumina matrix, similar to the gemstone ruby which is an alumina single crystal with certain chromium content. The only effect of chromium in BIOLOX®delta is the eye-catching pink color of the final material

The reinforcing elements, in particular the zirconia, substantially increase fracture toughness and strength of the material [1, 2]. Fracture toughness (K_{IC}) is a measure for the ability of the material to withstand crack extension. Strength (s_c) is defined as the maximum stress within a structure that causes failure of the component. Consequently, when the fracture toughness of the alumina is increased also the strength is directly improved. This basic principle is the concept of the development of BIOLOX®*delta*. The microstructure is designed in order to provide a maximum of resistance against crack extension.

The benefit in crack resistance which is obtained from incorporating zirconia into an alumina matrix are well known in the science of high performance ceramics, as it is shown in Fig. 15.2.

The figure represents a realistic part of the microstructure. In the case of severe overloading crack initiation and crack extension will occur. High tensile stresses in the vicinity of the crack tip trigger the tetragonal – monoclinic phase transformation of the zirconia particles. The accompanied volume expansion leads to the formation of compressive stresses which are very efficient for blocking the crack extension.

As it is shown this reinforcing mechanism is fully activated within a region of a few micrometers. For the macroscopic performance of the material it is extremely important that immediately at the beginning of crack initiation also the reinforcing mechanisms are activated. Regarding Fig. 15.2 one should keep in mind that the

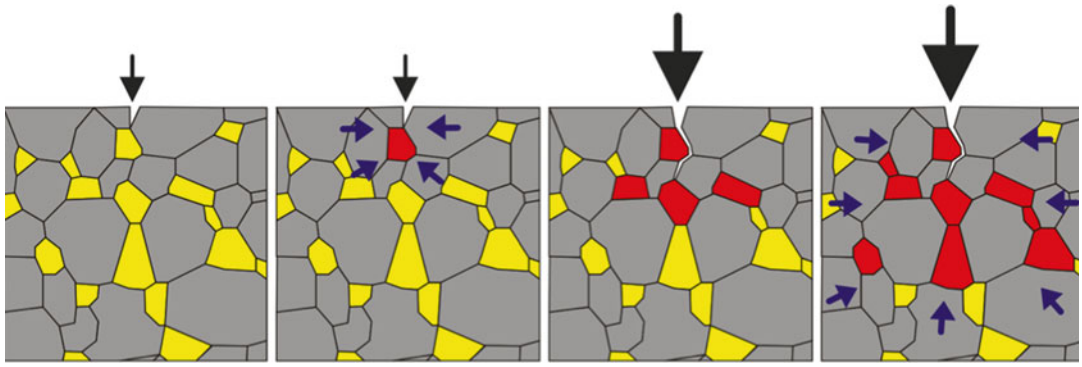

Fig. 15.2 Reinforcing mechanism in BIOLOX®*delta* at crack initiation and propagation

average distance between the reinforcing zirconia particles is apprx. 0.2 µm, i.e. similar to the grain size. Thus, the reinforcement is activated immediately when any microcrack is initiated.

The reinforcing ability of zirconia particles is a consequence of the phase transformation, i.e. the spontaneous change from the tetragonal to the monoclinic phase. The phase transformation is accompanied by a volume change of 4 % of the zirconia particle, i.e. a linear expansion of 1.3 %. Spontaneous phase transformation is a well known principle in material science. For example, the properties of high performance steels also rely on spontaneous phase transformation from austenite to martensite.

It should be emphasized that the ability of phase transformation is the precondition for any benefit of the zirconia within the material. The composite is designed such that phase transformation occurs when it is needed, i.e. in the case of microcrack initiation. In contrast to pure zirconia (which draws its high strength from the same principle) the main source of the stability of the tetragonal phase is the embedding of the zirconia particles in the alumina matrix. In contrast, the stability of pure zirconia only relies on the chemical stabilisation (i.e. doping with yttria) and the grain size, which should not exceed a certain range. This is the most important distinction of the composite material BIOLOX®*delta* to pure zirconia. In particular, the mechanical stabilization of the stiff alumina matrix is not sensitive to any ageing effect.

Correlation of Material and Component Properties

Material properties are determined to ISO 6474-2 which is applicable for zirconia toughened alumina composite ceramics. In comparison to a pure alumina material, these composites are distinguished by a significantly improved strength and toughness. It should be noticed that the high strength limit in ISO 6474-2 of 1000 MPa is outperformed by BIOLOX delta by almost + 40 % ! In this chapter it is intended to discuss shortly how these materials data correlate to component properties, e.g. the strength of ball heads and inserts.

In general, the performance of any system depends on the intrinsic material properties, the design and manufacturing quality of the components and the system, the external load and the particular environment, and finally the quality of mounting and installation. The use of high performance materials inevitably promotes the performance of a system – however, the other factors may be even more decisive for the success of a system. These complex correlations must be necessarily evaluated by design analysis, modeling, simulations, risk analysis and many other tools. In order to eliminate any influences of design features most of the material testing has been performed using 4-point bending bars.

In Fig. 15.3 the setup of the regular 4-point bending test as recommended in ISO 6474-2 and

the burst test according to ISO 7206 are shown. The bending test reveals the intrinsic strength of the material whereas the burst test is designed in order to simulate the in-vivo load of ceramic ball heads.

The strength measured with the bending test is – to a first approach – an intrinsic material parameter, whereas the burst load as obtained from the burst test depends on the materials strength and the design of the ball head and the taper. This is directly shown by comparison of strength and burst load of different ball heads made of BIOLOX®forte and BIOLOX®delta, see Table 15.1.

Effect of Hydrothermal Aging on Strength of Biolox®Delta

It is necessary to examine if the phase transformation reveals any damage or loss in strength of the material. For this purpose experiments were designed in order to combine accelerated aging and mechanical loading at a very high stress level. The specimens were prepared according to the 4-point bending configuration as it is shown in Fig. 15.3 (left). These bend bars were exposed to accelerated aging and then to loading-unloading cycles at high stresses. After aging and cyclic loading the residual strength was determined.

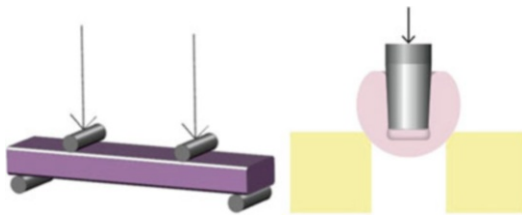

Fig. 15.3 Schematic set-up of 4 point bending test and ball head burst test

Two stress levels (300 MPa and 600 MPa) were chosen for the cyclic loading tests. The lower stress level was applied for 20 Mio cycles, the higher stress level for 5 Mio cycles. All tests were performed in Ringer's solution. The accelerated aging was simulated by 5 h and 100 h treatment in standard autoclaving conditions (134 °C, 2 bar water steam). It should be noted that again an aging time much longer than required from the standard was used. For each step of the experiments (as received, after aging, after aging and cycling) the monoclinic phase content was measured using X-ray diffraction.

As the most amazing result the yield of specimens surviving all the tests was 100 % in all cases. Even most severe conditions (i.e. 100 h autoclaving, 600 MPa cyclic load) did not reveal any premature failure. It should be recalled that this stress level represents four times the highest load level at worst case conditions in-vivo. We can thus conclude that the reliability of BIOLOX®delta exceeds by far the necessary requirements for reliable surgical components.

Table 15.2 shows the results of the post – test analysis including residual strength and monoclinic phase content. There is –as expected – a marginal natural scatter in residual strength. However, statistical analysis using Student's *t*-test did not reveal any significant deviation of all strength results.

In contrast, there is a clear tendency of an increase in monoclinic phase content both, after autoclaving and after cyclic loading, which is

Table 15.1 Comparison of strength and burst load of BIOLOX®forte and BIOLOX®delta

Parameter	Test/design	Unit	BIOLOX forte	BIOLOX delta	Ratio delta/forte
Strength	Bend bar 3×4×45	MPa	620	1370	2.2
Burst load	28–12/14 L	kN	54	85	1.6
Burst load	36–12/14 M	kN	110	131	1.2

Due to the statistical nature the strength also slightly depends on the specimen size and the stress distribution. Size effects can be mathematically balanced. In order to obtain results which can be directly compared to each other the standardized set-up of the bending test should be used

Table 15.2 Residual strength and monoclinic phase content after diverse treatments

Autoclaving duration		No cyclic load	300 MPa, 20×10^6 cycles	600 MPa, 5×10^6 cycles
0 h	Strength (MPa)	1346	1433	1284
	Monoclinic phase content (%)	18	33	43
5 h	Strength (MPa)	1332	1248	1361
	Monoclinic phase content (%)	22	35	42
100 h	Strength (MPa)	1234	1308	1300
	Monoclinic phase content (%)	30	33	47

Monoclinic phase is given relative to the total volume of the material

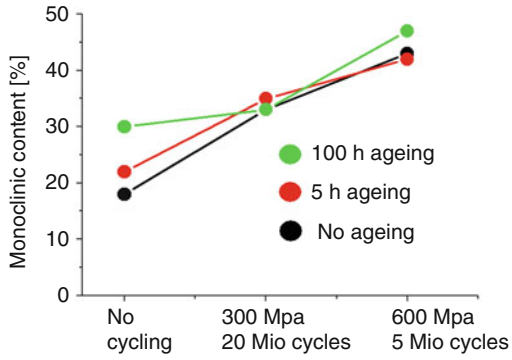

Fig. 15.4 Increase of monoclinic phase content at cyclic loading

illustrated in Fig. 15.4. For example, the test series without autoclaving shows an increase of monoclinic phase content from 18 % in the initial state to 47 % after 5 Mio cycles at 600 MPa. It must be concluded that the cyclic mechanical loading at a high stress level (600 MPa) which represents already the strength of pure alumina activated the reinforcing ability of the material. As discussed under Fig. 15.2, a high mechanical stress triggers localized phase transformation which prevents any further crack propagation. Obviously the increased amount of monoclinic phase content does not deteriorate the strength of the material. This important conclusion is independent from the source of the phase transformation. In other words, when the phase transformation is activated either by accelerated aging, cyclic fatigue or a combination of both, the residual strength remains at the initial level.

Conclusions

The material BIOLOX®*delta* has been exposed to extreme conditions (accelerated ageing and cyclic loading in Ringer's solution). It has been shown that even a combination of worst case conditions does not reveal any premature failure. Furthermore, it was shown that the residual strength remains on the initial level. A certain amount of phase transformation was observed during the tests. The highest amount of monoclinic phase relative to the total volume of the specimen was 47 %. The residual strength was not affected by the phase transformation.

In other studies it was shown that BIOLOX®*delta* performs extremely well in severe wear tests [6]. These results are also attributed to the reinforcing mechanism in the material. These exciting results promote the confidence that BIOLOX®*delta* offers the highest probability of long term durability in well designed artificial joint systems.

References

1. Hannink RHJ, Kelly PM, Muddle BC. Transformation toughening in zirconia-containing ceramics. J Am Ceram Soc. 2000;83(3):461–87.
2. De Aza AH, Chevalier J, Fantozzi G, Schehl M, Torrecillas R. Crack growth resistance of alumina, zirconia and zirconia toughened alumina ceramics for joint prostheses. Biomaterials. 2002;23:937–45.

3. Pezzotti G. Environmental phase stability of next generation ceramic composite for hip prostheses. Key Eng Mater. 2006;309–311:1223–6.
4. Ohmichi N, Kamioka K, Ueda K, Matsui K, Ohgai M. Phase transformation of zirconia ceramics by annealing in hot water. J Ceram Soc Jpn. 1999;107(2):128–33.
5. Gremillard L, Chevalier J, Epicier T, Deville S, Fantozzi G. Modeling the ageing kinetics of zirconia ceramics. J Eur Ceram Soc. 2004;24:3483–9.
6. Clarke IC, Pezzotti G, Green DD, Shirasu H, Donaldson T. Severe simulation test for run-in ear of all-alumina compared to alumina composite THR. Proceedings 10th BIOLOX symposium, 11–20 (2005).

16 New Composite Material: PLLA and Tricalcium Phosphate for Orthopaedic Applications-In Vitro and In Vivo Studies (Part 1)

Jean Charles Le Huec, Antonio Faundez, Stephane Aunoble, Rachid Sadikki, and Julien Rigal

β-tricalcium phosphate (β-TCP) is an osteoconductive, absorbable material, which, in porous ceramic form, is highly suitable for implants used in bone reconstruction, or as bone substitutes. Tricalcium phosphate, used for many years to replace or complement autologous bone in bone grafts, has proved its clinical effectiveness in many indications [1–7]. Like any ceramic material, however, these implants have a brittle fracture behaviour. They break suddenly, without any prior plastic strain, which restricts the clinical applications for these materials to surgery with low stress levels.

J.C. Le Huec, MD, PhD (✉)
Ortho-Spine Department, Surgical Research Laboratory, Bordeaux University Hospital, Bordeaux, France
e-mail: j-c.lehuec@u-bordeaux2.fr

A. Faundez, MD
Department of Orthopaedics, Geneva University Hospital, Geneva, Switzerland
e-mail: Antonio.Faundez@hcuge.ch

S. Aunoble, MD
Department of Orthopedic and Traumatology Spine Surgery, Hopital Pellegrin, Bordeaux, France

R. Sadikki, MD
Spine Unit, CHU Pellegrin, Universite Ségalen Bordeaux, Bordeaux, France

J. Rigal, MD
Department of Orthopedics and Traumatology, CHU Hopitaux de Bordeaux, Bordeaux, France

On the other hand, biodegradable polymers from aliphatic polyesters of alpha-hydroxy acid derivatives, such as polylactic acid (PLA), evidence a modulus of elasticity closer to that of natural cortical bone and can retain high strength over time [8]. But these materials can induce unspecific inflammatory tissue response [9–15] resulting in delayed bone healing / fusion or osteolytic reactions [9–21].

To overcome the disadvantages of these different materials, composite materials of calcium phosphates and polyesters have been developed and evaluated in-vitro or in-vivo [22–32]. Such composite materials tend to increase phenotypic expression of osteogenic cells, reduce foreign-body reaction and improve bone healing in a dose-dependent manner as compared to pure polymer materials. Various calcium phosphate (HA or β-TCP) contents have been evaluated, ranging 5–60 % (w/w) depending on the study. A low mineral content (10 % w/w) seems to induce a moderate inflammatory reaction and does not evidence significant improvement of bone response in the sheep femur as compared to pure PLLA [33] since higher HA ratios improves bone healing and lowers inflammatory response of bone tissue in the same model. Similar results are reported concerning PLLA/TCP composites (70/30 w/w) in the dog mandible and tibia [34]; such implants are progressively replaced by normal bone tissue without adverse reaction. Significant improvements of in the extend and

D.G. Poitout (ed.), *Biomechanics and Biomaterials in Orthopedics*,
DOI 10.1007/978-1-84882-664-9_16

quality of bone healing are also reported about composite materials containing up to 60 % (w/w) of calcium phosphate mineral in the rabbit or rat [35, 36].

The objective of this research was to carry out an *in vitro* and *in vivo* study of the biological performance of PLLA/TCP composite materials with increasing mineral contents (0–60 % w/w) in order to estimate the influence of the β-TCP ratio on human osteogenic cells behavior and bone tissue response, then further to evaluate the scope of potential applications in bone surgery.

Material and Methods

Samples

The β-TCP granules were prepared by granulation and sintering at 1000 °C in air of a β-TCP powder free of HA or calcium pyrophosphate by infrared spectrometry and X-Ray diffraction, then further sieved to <125 µm particles. Appropriate w/w mixtures of β-TCP and PLLA (Purac Biochem, Gorinchem, The Netherlands) were prepared by mixing in air at 60 °C ± 5 °c for 24 h then processed by injection molding in the desired shape and size. Resulting composite samples were sterilized by gamma irradiation (25 KGr).

The pure β-TCP ceramic samples (SBM, Lourdes, France) had a total porous volume of 50 % (±5 %) with pore size ranging 5–400 µm, and were free of HA or calcium pyrophosphate by infrared spectrometry and X-Ray diffraction.

In Vitro Study

The *in vitro* study consisted of an evaluation of inflammatory potential by assaying the IL-1α secreted by monocytes, then cell proliferation (counting) and phenotype expression (PAL and I collagen) in human osteogenous cells in contact with samples of PLLA/TCP composite materials (e = 2 mm / ϕ = 10 mm) containing 0 %, 30 %, and 60 % (w/w) β-TCP, respectively.

In brief, the cell proliferation tests were carried out using human osteogenous cells from bone marrow, as these composite materials are destined for use in bone implants. Cells were seeded at an initial density of 5000 cells.cm^{-2} in slide wells (Iscove's modified Dubelco medium + fetal calf serum at 10 % v/v) containing material samples (36 wells per material) then incubated for increasing periods, up to 27 days. Cells were counted in Malassez cells following trypsinization of the cell layers. Alkaline phosphatase (PAL) was assayed by colorimetry, using p-nitrophenyl phosphate substrate, after centrifuging the suspensions and freezing the cell pellet. To study collagen synthesis, the wells containing the samples were seeded at an initial density of 40.10^3 cells.cm^{-2} then the slides were incubated for 48 h, changing the medium (IMDM + 1 % SVF) after 24 h. Extra- and intracellular collagen was assayed separately by colorimetry (Kit Biocolor S2000). Monocyte-macrophages from human peripheral blood were put in contact with the various materials to study their inflammatory potential (3.4.10^6 cells/well, HAM F12 + 10 % v/v SVF and antibiotics). This cell/material contact may induce cell activation, causing them to synthesize and secrete cytokines, particularly IL-1α, indicative of an inflammatory reaction. The density of cells in contact with the material was assessed after 24–72 h in culture, using the protocol described above. The quantity of extra- and intracellular IL-1α secreted by the cells was also assayed (ELISA, Cayman chemical Interleukin 1-α kit). The culture well was the negative control and the culture medium containing 10 µg.ml^{-1} lypopolysaccharides was the positive control.

In Vivo Study

The *in vivo* study was carried out using cylindrical implants de composite materials (l = 8 mm / ϕ = 6 mm) composed of composite materials containing 0 % or 60 % β-TCP and pure β-TCP, respectively. The implants were inserted in femoral sites in rabbits, using the Kathagen protocol.

Each animal received a 60 % implant and either a 0 % or a 100 % implant in the contralateral femur so that the materials could be compared with one another. Five animals were examined for each material and implantation period, giving a total of 30 animals. They were sacrificed by an overdose of anesthetic 1, 3, and 6 months after implantation. The rabbit femurs were fixed in a 4 % formaldehyde solution for several weeks. Each femur was cut transversally above and between the condyles so that the implant could be cut transversally. The fragments were then washed in tap water and demineralized in a 5 % EDTA diNa solution. The implants containing PLA were dehydrated in increasingly concentrated ethanol solutions then dissolved in chloroform for a few hours. The femur fragments were then put into absolute ethanol for 24 h. They were immersed in HEMA solution for 48 h, then in HEMA solution containing the activator for 24 h. Once the blocks had set, 5 µm slices were cut and colored using Giemsa solution.

Results

In Vitro Study

The results showed, first of all, that the composition of the materials tested had no significant impact (Mann & Whitney) on IL-1α secretion in the intra- or extracellular compartments. The values measured for each material were comparable to those of the negative control and ten times less than those of the positive control, irrespective of the incubation period. Similar results were obtained for monocyte proliferation. None of the materials studied had any cytotoxic effects.

The results of the proliferation of the osteogenous cells from bone marrow (CO) are shown in Fig. 16.1, which represents the variation in the number of CO depending on the culture time for the different materials studied.

Cell density increased not only over time, but also with the percentage β-TCP in the composite material, which had a significant impact (Mann & Whitney) after 3 days in culture. For example, at the end of the test (27 days), the number of osteogenous cells present on the 60 % material ($61{,}000 \pm 3500$ cells.cm^{-2}) was 220 % higher than on the 0 % ($27{,}300 \pm 300$ cells.cm^{-2}) and 120 % higher than on the 30 % material ($42{,}500 \pm 3600$ cells.cm^{-2}). The PAL activity was comparable for all the materials, but the percentage β–TCP in the composite had a significant impact on type I collagen synthesis. The quantity of collagen fixed in the extracellular matrix, assessed per well (Fig. 16.2a) or per 10^6 cells (Fig. 16.2b), increased with tricalcium phosphate content, reaching a maximum at 60 % mineral content.

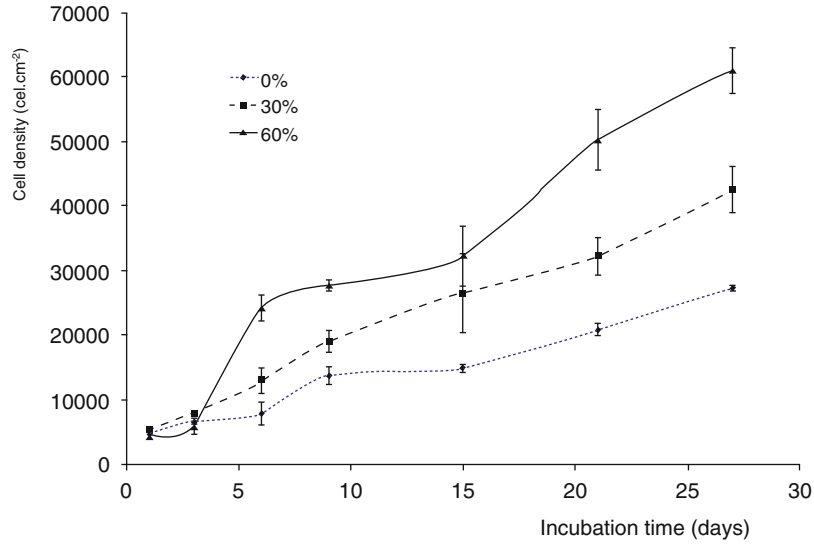

Fig. 16.1 Variations in the density of human osteogenous cells on the surface of various composite materials in function of the incubation period

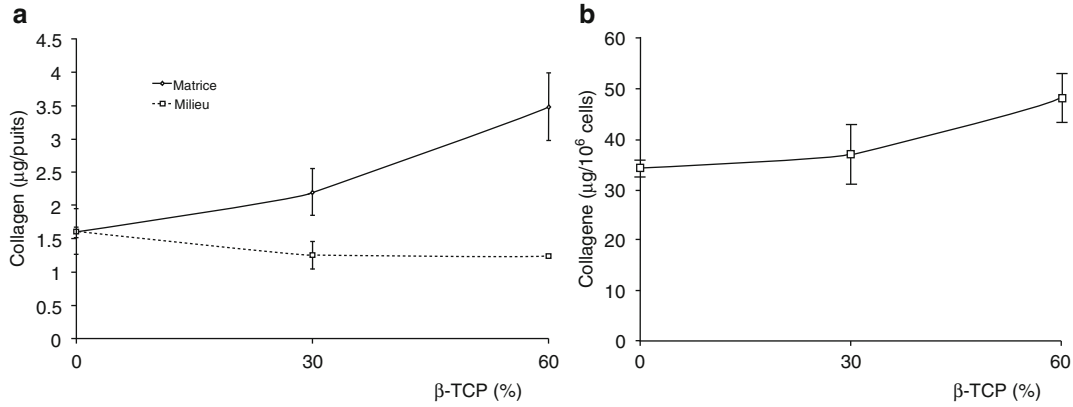

Fig. 16.2 (**a**) Assay of type I collagen per well as a function of the β–TCP content of the materials studied. (**b**) Assay of type I collagen in the extracellular matrix on the basis of 10^6 cells, as a function of the β–TCP content in the materials studied

In Vivo Study

The pure PLLA implants did not appear degraded, even after the longest implantation time. They were surrounded by conjunctival tissue containing large numbers of macrophages. After 6 months, some of the macrophages had phagocytized particles that appeared crystalline, but the implant maintained its structure. There were few bone trabeculae in direct contact with the implants, although, after 6 months, there was some ossification in contact with the material, separated by a fine layer of a few µm of metachromatic material. There were still some macrophage cells and collagen at the material interface.

Very soon after implantation, bone tissue was detected in direct contact with the composite implants. This tissue showed residues of cartilaginous matrix and was probably formed by chondroid ossification (Fig. 16.3).

At 6 months, the implant showed signs of degradation. Loose conjunctival tissue containing bone trabeculae infiltrated the implant, breaking it up in certain cases. It should be noted that these areas contained few macrophages. Their appearance was no different to that observed with porous ceramics of pure β-TCP. The bone tissue was in direct contact with the implant. After 6 months, some implants had broken up. The fragments were relatively homogeneous in size, i.e. a few hundred µm. A web of bone trabeculae had formed between the fragments (Fig. 16.4).

A few macrophages containing polymer debris were observed, but in a very limited number. More generally, the surface had been eroded, with widespread pits several hundred microns deep. Ceramics particles had been released and were trapped in the trabeculae or medullary cavities.

Discussion

The results of the *in vitro* tests indicate that adding increasing quantities of tricalcium phosphate to the lactic acid polymer stimulates both the proliferation of human osteogenous cells and the synthesis of the extracellular matrix. Cell density increased with the percentage of β–TCP in the composite, showing that cell proliferation was promoted by the presence of β–TCP. The results of the collagen assays in the extracellular matrix showed clearly that the quantity of collagen per cell increased in the same way, indicating that the β–TCP in the polymer matrix stimulated cell activity. The composite material with the highest mineral content (60 % by mass) showed the best behavior. We know that healing and consolidation of the bone by endochondral ossification are directly linked to the recruitment and phenotype expression of osteogenous cells at the site.

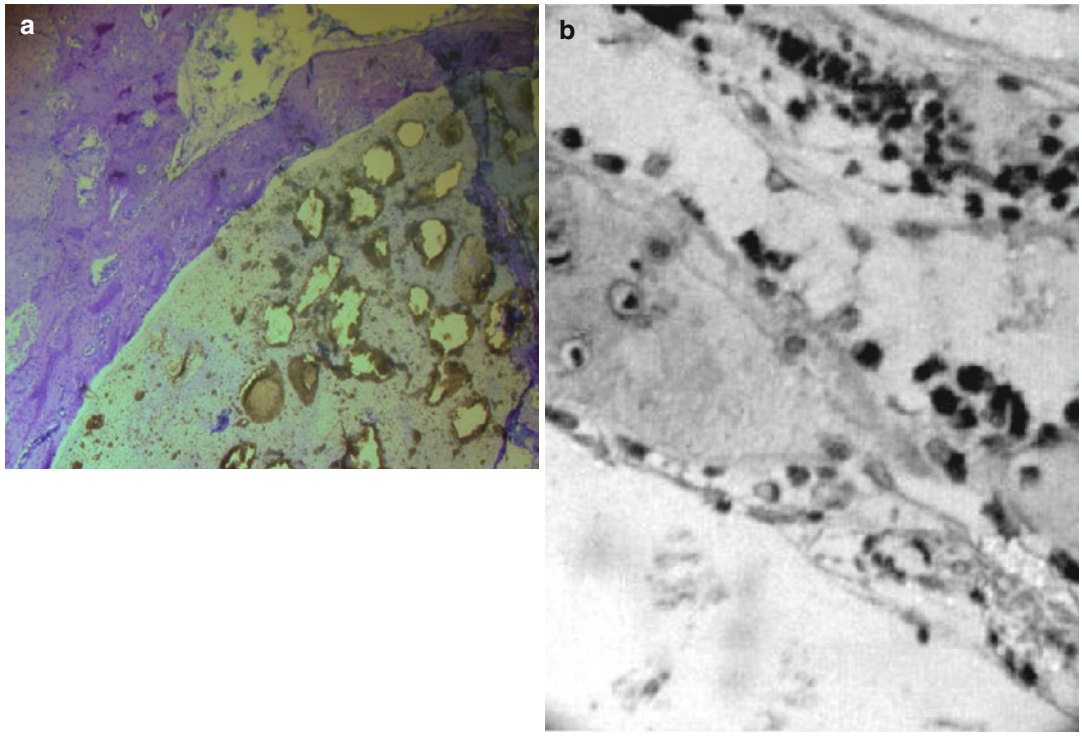

Fig. 16.3 (**a**) Beginning of the composite degradation process. Many implants still have the same texture as PLLA. Toluidine blue. (**b**) Detail of bone trabeculae in contact with the composite. There is no sign of a reaction to a foreign body. Toluidine blue × 40

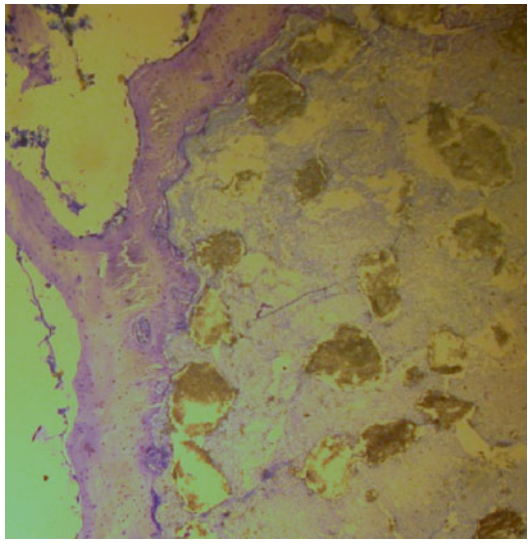

Fig. 16.4 Irregular composite surface after 3 months. There are even calcium phosphate particles released from the matrix and integrated into the bone tissue. Toluidine blue × 300

Composite materials thus seem more favorable for bone consolidation than pure polymer materials and have been shown *in vitro* to improve biological behavior. These results confirm hypotheses on PLA/TCP [26–28, 37] materials and, more generally, the absorbable polyester/calcium phosphate composites presented in the literature [22–25, 29–32, 38], where the presence of minerals in the polymer matrix promoted the proliferation and phenotype expression of osteogenous cells *in vitro*. These findings were also corroborated by the histological examinations, which indicated clearly that pure PLA implants were systematically surrounded by a layer of conjunctival tissue containing large numbers of macrophages, irrespective of the length of implantation, whereas bone tissue grew in direct contact with composite implants during the first few months and matured gradually until the end of the study period with no marked macrophage activation. The composite material under

investigation is thus more favorable for bone consolidation *in vivo* than pure PLA and has identical properties to those of pure β–TCP ceramics.

This result is not particularly surprising if we consider the properties of the materials in the composite separately. We know that pure lactic acid-based polymers are not cytotoxic or inflammatory *in vitro* [10–13, 39, 40] but are capable of causing an inflammatory reaction *in vivo* [9–13, 15], as confirmed by clinical observations [16–21]. Pure β–TCP, on the contrary, promotes bone healing by osteoconduction, becoming surrounded by healthy bone tissue containing active osteogenous cells, with no intermediate fibrous layer. It is, thus, conceivable that composite materials such as those we studied have a "hybrid" biological behavior that becomes closer to that of pure tricalcium phosphate as the mineral content increases. What mechanisms are involved?

Pure lactic acid polymer implants are absorbed slowly, over several years, depending on the volume of the implant [19, 41]. The main mechanism is internal hydrolysis [42], resulting in the sudden release of partially degraded polymer and monomer particles [9] at the end of the resorption process, which acidifies the peri-implant region [43]. During this phase, large numbers of active macrophages, containing particles resulting from hydrolytic degradation, are found within fibrous inflammatory tissue on the implant surface [10–15, 19]. If no macrophage activation mechanism is established it may be assumed that the monomer concentration [9, 43] (drop in pH) and the number of fine "phagocytizable" [44] particles contribute to this reaction. We observed significant resorption of composite material implants, and thus of polymer, without any inflammation. At 6 months, the surface was eroded to a depth of several hundred micrometers but there were only very few macrophages, some of which contained polymer particles. It cannot, therefore, be considered that activation of the cells during resorption of the polymer matrix was solely due to the presence of these particles. We know that the acidification that accompanies the degradation of lactic acid polymers may also set off an inflammatory reaction [43]. In a systematic *in vitro* study, Lin [28] measured the pH of solutions containing a variety of PDLLA/TCP composite materials. The pH stabilized at 2.3 for a pure polymer material and 5 for all the materials containing mineral, which shows the effect of β–TCP on the acidity of the solution. This observation was interpreted by the author as a result of the slower degradation kinetics of composite materials as compared to pure polymers. However, other authors have confirmed our histological finding that degradation kinetics increased with a higher mineral content [23, 26, 38], which leads us to observe that β–TCP causes an increase in both the degradation kinetics of the composite material and the pH of the solution. This may be interpreted by noting that the TCP particles increase the permeability of the material, resulting in a more homogeneous hydrolysis of the polymer matrix in a liquid medium, whereas hydrolysis of pure polymer materials starts from the surface. β–TCP is alkaline in solution and may neutralize the acid functions of the hydrolyzed polymer chains. It is also soluble in an acid medium and dissolves in the hydrolyzed polymer, thus buffering the acidification of the medium. This may also account for the high level of osteoblast activity observed, as human osteogenous cells are stimulated by the dissolution products of materials containing calcium and phosphate ions, like β–TCP [13, 30]. More generally, osteoblast cells activity and healing time may be linked to the concentration of dissolved calcium and phosphate ions and, thus, the dissolution kinetics of ionic materials. This interpretation accounts for our observations and is in agreement with widespread findings in the literature.

Conclusion

This study showed that adding increasing percentages of β–TCP to a lactic acid polymer matrix stimulated the proliferation of human osteogenous cells and synthesis of the extracellular bone matrix in a dose-dependent manner.

In vivo results indicate that, in comparison with pure PLA, tricalcium phosphate-containing composite materials had faster degradation kinetics, caused less inflammatory reaction, and promoted contact osteogenesis.

The composite material containing 60 % β-□TCP demonstrated a similar performance to pure tricalcium phosphate bone grafts in terms of osteogenesis and is apparently compatible with the production of intra-osseous implants for obtaining bone fusion or healing. Further studies are necessary to evaluate the ability of such a composite material to retain sufficient mechanical strength overtime for providing safe correction or stabilization of the implanted bone fragments.

References

1. Bonnevialle P, Abid A, Mansat P, Verhaeghe L, Clément D, Mansat M. Ostéotomie tibiale de valgisation par addition médiale d'un coin de phosphate tricalcique. Revue de chirurgie orthopédique. 2002;88:486–92.
2. Galois L, Mainard D, Cohen P, Delagoutte J-P. 23 cas d'utilisation du phosphate tricalcique β pour le comblement des pertes de substance osseuse au pied. Med Chir Pied. 2001;17:44–53.
3. Galois L, Mainard D, Cohen P, Pfeffer F, Traversari R, Delagoutte J-P. Comblement des pertes de substance osseuse par le phosphate triCalcique β en traumatologie. Ann Chir. 2000;125:972–81.
4. Galois L, Mainard D, Pfeffer F, Traversari R, Delagoutte J-P. Use of β -triCalcium phosphate in foot and ankle surgery : a report of 20 cases. Foot Ankle Surg. 2001;7:217–27.
5. Galois L, Mainard D, Delagoutte J-P. β -triCalcium phosphate ceramic as a bone substitute in orthopaedic surgery. Int Orthop (SICOT). 2002;26:109–15.
6. Le Huec J-C, Langlois V, Liquois F, Lesprit E, Clément D. Arthrodèse intersomatique cervicale par greffon en phosphate tricalcique- etude rétrospective de 33 cas. 1 à 3 ans de recul. Rachis. 2001;13 / 3:197–202.
7. Le Huec J-C, Lesprit E, Delavigne C, Clément D, Chauveaux D, Le Rebeller A. Tricalcium phosphate ceramics and allografts as bone substitutes for postero-lateral spine fusion in idiopathic scoliosis: comparative clinical results at 4 years. Acta Orthop Belg. 1997;63 / 3:202–11.
8. Daniels AU, Chang MK, Andriano KP. Mechanical properties of biodegradable polymers and composites proposed for internal fixation of bone. J Appl Biomater. 1990;1(1):57–78.
9. Bergsma JE, de Bruijn WC, Rozema FR, Bos RR, Boering G. Late degradation tissue response to poly(L-lactide) bone plates and screws. Biomaterials. 1995;16(1):25–31.
10. Bos RR, Rozema FR, Boering G, Nijenhuis AJ, Pennings AJ, Verwey AB, Nieuwenhuis P, Jansen HW. Degradation of and tissue reaction to biodegradable poly(L-lactide) for use as internal fixation of fractures: a study in rats. Biomaterials. 1991;12(1):32–6.
11. Fuchs M, Koster G, Krause T, Merten HA, Schmid A. Degradation of and intraosseous reactions to biodegradable poly-L-lactide screws: a study in minipigs. Arch Orthop Trauma Surg. 1998;118(3):140–4.
12. Paivarinta U, Bostman O, Majola A, Toivonen T, Tormala P, Rokkanen P. Intraosseous cellular response to biodegradable fracture fixation screws made of polyglycolide or polylactide. Arch Orthop Trauma Surg. 1993;112(2):71–4.
13. Peltoniemi HH, Hallikainen D, Toivonen T, Helevirta P, Waris T. SR-PLLA and SR-PGA miniscrews: biodegradation and tissue reactions in the calvarium and dura mater. J Craniomaxillofac Surg. 1999;27(1):42–50.
14. Schakenraad JM, Hardonk MJ, Feijen J, Molenaar I, Nieuwenhuis P. Enzymatic activity towards poly-(L-lactic acid) implants. J Biomed Mater Res. 1990;24:529–45.
15. Van der Elst M, Klein CPAT, De Blieck-Hogervorst JM, Patka P, Haarman HJTM. Bone tissue response to biodegradable polymers used for intra medullary fracture fixation : a long term in vivo study in the sheep femora. Biomaterials. 1999;20:121–8.
16. Bergsma EJ, Rozema FR, Bos RR, de Bruijn WC. Foreign body reactions to resorbable poly(L-lactide) bone plates and screws used for the fixation of unstable zygomatic fractures. J Oral Maxillofac Surg. 1993;51(6):666–70.
17. Bostman OM. Osteoarthritis of the ankle after foreign-body reaction to absorbable pins and screws: a three- to nine-year follow-up study. J Bone Joint Surg Br. 1998;80(2):333–8.
18. Bostman OM, Philajamaki HK. Adverse tissue reactions to bioabsorbable fixation devices. Clin Orthop. 2000;371:216–27.
19. Lajtai G, Noszian I, Humer K, Unger F, Aitzetmuller G, Orthner E. Serial magnetic resonance imaging evaluation of operative site after fixation of patellar tendon graft with bioabsorbable interference screws in anterior cruciate ligament reconstruction. Arthroscopy. 1999;15(7):709–18.
20. Martinek V, Friederich NF. Tibial and pretibial cyst formation after anterior cruciate ligament reconstruction with bioabsorbable interference screw fixation. Arthroscopy. 1999;15(3):317–20.
21. Takizawa T, Akizuki S, Horiuchi H, Yasukawa Y. Foreign body gonitis caused by a broken poly-L-lactic acid screw. Arthroscopy. 1998;14(3):329–30.
22. Furukawa T, Matsusue Y, Yasunaga T, Nakagawa Y, Okada Y, Shikinami Y, Okuno M, Nakamura T. Histomorphometric study on high-strength hydroxyapatite/poly(L-lactide)composite rods for internal fixation of bone fractures. J Biomed Mater Res. 2000;50(3):410–9.
23. Higashi S, Yamamuro T, Nakamura T, Ikada Y, Hyon SH, Jamshidi K. Polymer-hydroxyapatite composites

for biodegradable bone fillers. Biomaterials. 1986; 7(3):183–7.
24. Ignjatovic N, Savic V, Najman S, Plavgic M, Uskokovic D. A study of HAp/PLLA composite as a substitute for bone powder, using FT-IR spectroscopy. Biomaterials. 2001;22(6):571–5.
25. Ignjatovic N, Tomic S, Dakic M, Miljkovic M, Plavsic M, Uskokovic D. Synthesis and properties of hydroxyapatite/poly-L-lactide composite biomaterials. Biomaterials. 1999;20(9):809–16.
26. Imai Y, Fukuzawa A, Watanabé M. Effect of blending tricalcium phosphate on hydrolytic degradation of a block polyester containing poly(L-lactic acid) segment. J Biomater Sci Polym Ed. 1999;10(7):773–86.
27. Kikuchi M, Tanaka J, Koyama Y, Takakuda K. Cell culture test of TCP/CPLA composite. J Biomed Mater Res. 1999;48(2):108–10.
28. Lin FH, Chen TM, Lin CP, Lee CJ. The merit of sintered PDLLA/TCP composites in management of bone fracture internal fixation. Artif Organs. 1999;23(2):186–94.
29. Ma PX, Zhang R, Xiao G, Franceschi R. Engineering new bone tissue in vitro on highly porous poly(alpha-hydroxylacids)/hydroxyapatite composite scaffolds. J Biomed Mater Res. 2001;54(2):284–93.
30. Rizzi SC, Heath DJ, Coombes AG, Bock N, Textor M, Downes S. Biodegradable polymer/hydroxyapatite composites: surface analysis and initial attachment of human osteoblasts. J Biomed Mater Res. 2001;55(4):475–86.
31. Verheyen CCPM, de Wijn JR, van Blitterswijk CA, de Groot K, Rozing PM. Évaluation of hydroxylapatite/poly(l-lactide) composites : an animal study on push-out strength and interface histology. J Biomed Mater Res. 1993;27:433–44.
32. Yasunaga T, Matsusue Y, Furukawa T, Shikinami Y, Okuno M, Nakamura T. Bonding behavior of ultra-high strength unsintered hydroxyapatiteparticles/poly(L-lactide) composites to surface of tibial cortex in rabbits. J Biomed Mater Res. 1999;47(3):412–9.
33. Prokop A, Chmielnicki M. Management of dislocated radial head fractures with biodegradable implants. Article in German. Z Orthop Unfall. 2013;151(6):565–8. doi:10.1055/s-0033-1351079. Epub 2013 Dec 17.
34. Kikuchi M, Koyama Y, Yamada T, et al. Development of guided bone regeneration membrane composed of beta-tricalcium phosphate and poly (L-lactide-co-glycolide-co-epsilon-caprolactone) composites. Biomaterials. 2004;25(28):5979–86.
35. Meretoja VV, Tirri T, Malin M, et al. Enhanced osteogenicity of bioactive composites with biomimetic treatment. Biomed Res Int. 2014;2014:207676. doi:10.1155/2014/207676. Epub 2014 Apr 9.
36. Balçik C, Tokdemir T, Senköylü A, et al. Early weight bearing of porous HA/TCP (60/40) ceramics in vivo: a longitudinal study in a segmental bone defect model of rabbit. Acta Biomater. 2007;3(6):985–96. Epub 2007 Jun 15.
37. Flahiff CM, Blackwell AS, Hollis JM, Feldman DS. Analysis of a biodegradable composite for bone healing. J Biomed Mater Res. 1996;32(3):419–24.
38. Furukawa T, Matsusue Y, Yasunaga T, Shikinami Y, Okuno M, Nakamura T. Biodegradation behavior of ultra-high-strength hydroxyapatite/poly (L-lactide) composite rods for internal fixation of bone fractures. Biomaterials. 2000;21(9):889–98.
39. Hollinger JO. Preliminary report on the osteogenic potential of a biodegradable copolymer of polyactide (PLA) and polyglycolide (PGA). J Biomed Mater Res. 1983;17(1):71–82.
40. Murphy WL, Kohn DH, Mooney DJ. Growth of continuous bone like mineral within porous poly(lactide-co-glycolide)scaffolds in vitro. J Biomed Mater Res. 2000;50(1):50–8.
41. Stroman PW, Dorvil JC, Marois Y, Poddevin N, Guidoin R. In vivo time course studies of the tissue responses to resorbable polylactic acid implants by means of MRI. Magn Reson Med. 1999;42(1): 210–4.
42. Williams DF. Enzimatic hydrolysis of polylactic acid. Eng Med. 1981;10:5–7.
43. Agrawal CM, Athanasiou KA. Technique to control pH in vicinity of biodegrading PLA-PGA implants. J Biomed Mater Res. 1997;38(2):105–14.
44. Lam KH, Schakenraad JM, Esselbrugge H, Feijen J, Nieuwenhuis P. The effect of phagocytosis of poly(L-lactic acid) fragments on cellular morphology and viability. J Biomed Mater Res. 1993;27(12): 1569–77.

17 Clinical Results of a New Resorbable Composite Material for Cervical Cage: 6 Years' Follow-up (Part 2)

Jean Charles Le Huec, Antonio Faundez, Stephane Aunoble, Rachid Sadikki, and Julien Rigal

Efficiency of corticocancellous autologous bone grafts in cervical interbody fusion has been widely reported since Smith and Robinson [1] or Cloward [2]. Depending on the studies, 70–96 % of the patients develop good or excellent results. However, the use of autologous grafts induces a second operation, generally on the iliac crest, and may be associated with an important morbidity [3]. Moreover, such complications as long term pain syndrome, femorocutaneus nerve damage, infection or secondary fracture has been reported [4–6]. In order to prevent such risks, different bone substitutes are nowadays available. Natural ones like allografts or xenografts [7, 8] have been studied since decades. With a cancellous-like architecture, their macroscopical structure can help bone ingrowth and lead to satisfying results with regards to bone fusion, both on animal models or humans. But these natural bone grafts still represent a microbiological risk, like AIDS, hepatitis or non-conventional disease transmission. For these reasons, we preferred synthetic materials when choosing a bone substitute. Elaborated from pure chemical compounds, such materials seemed safer to us. Among the family of synthetic materials, calcium phosphate compounds like hydroxylapatite (HA) are probably better known. Intensively studied over the last 20 years [9], such compounds are biocompatible. In a porous form, they facilitate bone cells penetration and lead, as well as allografts or heterografts, to bone healing and fusion with surrounding bone [10–18]. HA is reported to be poorly – or non – resorbable and capable of achieving a long-term correction if sufficient mechanical strength and stability can be obtained. Clinical studies recently confirmed these theorical findings, in the filling of non load-bearing bone defects or in spinal surgery [16, 19–25]. Tricalcium phosphate (TCP) is completely resorbable in a variable period depending on the porosity and the mass. The advantage of this ceramic is that the resorption occurs in the same time of bone healing and this leads to a complete fusion with at the end only bone in the same way as a Cloward procedure. However, pure HA or TCP ceramic materials are brittle

J.C. Le Huec, MD, PhD (✉)
Ortho-Spine Department, Surgical Research Laboratory, Bordeaux University Hospital, Bordeaux, France
e-mail: j-c.lehuec@u-bordeaux2.fr

A. Faundez, MD
Department of Orthopaedics, Geneva University Hospital, Geneva, Switzerland
e-mail: Antonio.Faundez@hcuge.ch

S. Aunoble, MD
Department of Orthopedic and Traumatology Spine Surgery, Hospital Pellegrin, Bordeaux, France

R. Sadikki, MD
Spine Unit, CHU Pellegrin, Universite Ségalen Bordeaux, Bordeaux, France

J. Rigal, MD
Department of Orthopedics and Traumatology, CHU Hopitaux de Bordeaux, Bordeaux, France

D.G. Poitout (ed.), *Biomechanics and Biomaterials in Orthopedics*,
DOI 10.1007/978-1-84882-664-9_17

and can fracture without prior elastic deformation, leading to the formation of hard debris presenting a risk of spinal cord or nerve root lesion. We have recently developed a composite material composed of b-TCP and lactic acid polymer (PLLA), which has a high breaking strength and a real capacity to withstand plastic and elastic strain. It thus has the major advantage that it can be used under conditions of high biomechanical stress with a low risk of rupture. This could be a serious advantage but there is no study at time to know if this fusion occurs without loss of correction and there is no study to evaluate the rate of complications of such a resorbable material. The objective of this study was to carry out a clinical study to evaluate radiological and clinical results of this new composite cervical interbody cage.

Materials and Methods

Patients were operated with Implants provided by SBM (SBM, Lourdes, France). The cage was made of composite material (material containing 60 % PLA and 40 % TCP) and inside was impacted a tricalcium phosphate ceramic block (porosity: 60 %) that matched the cage size (Fig. 17.1). These material was previously tested and evaluated in an in vitro and in vivo study (see Chap. 19).

Fourty patients, suffering of cervical nevralgia in relation with soft disc herniation, were operated according to the Smith and Robinson technique [1], Clinical evaluation at pre-op, post-op and each follow-up visit included JOA scoring, neurological evaluation, AP and lateral Xrays with bending films. At 2 years follow-up a CT scan evaluation of the fusion was performed to evaluate the fusion quality and the resorption of the cage and X rays at 4 and 6 years.

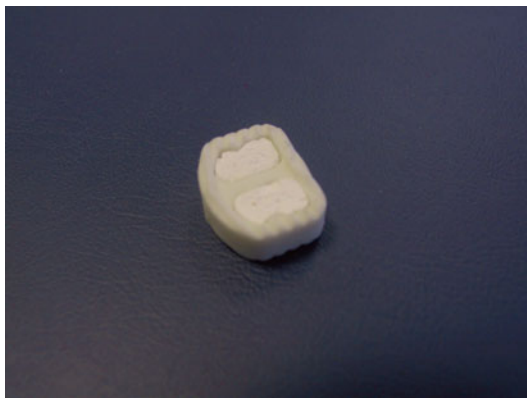

Fig. 17.1 Cervical Cage "Duosorb" ™ (SBM, Lourdes, France)

Preoperatively templates were used to determine the right size of the implant, and the cages were softly introduced in the disc space. Further insertion was carefully performed with a polyethylene bone impactor. Doing so, the implants were located at the center of the disc, ensuring vertebral end-plates parallelism, which was confirmed via peri-operative radiographic controls. All the patients were stabilized by an anterior titanium plate fixed by four screws and locking mechanism (Zephyr plate, Medtronic, Memphis, USA).

Verticalization was allowed the day after surgery, with no particular care except a soft collar, further maintained during 10 days. A 24 h postoperative radiographic control was performed. Data were collected from a homogenous consecutive series of patients, operated between 2004 and 2005. The same surgeon assumed reviews 1, 3 and 6, 12 months and each year after surgery, then at latest follow-up.

For each of the patients, we have postoperatively evaluated the clinical benefits of surgery and possible sequels : dysphagia, radicular or cervical residual pain. Correction (disc height and kyphotic/lordotic deformation), displacement and/or fracture of the implant, radiolucent line, dynamic mobility of the vertebrae (flexion/extension X-Rays) were radiologically assessed at each examination. The resorption of the material was evaluated radiographically by an independent radiologist in four stade: no resorption, partial resorption (inferior to 50 %); major resorption (more than 50 %); complete resorption. Finally, twenty patients got a CT evaluation of the fusion at 2 years follow up.

Results

Twenty patients included in the study were all followed at 2 years, mean age 48 years, average follow-up 28 months (Min 18/Max 47). The main

syndrome at first examination was cervical pain (30 %), radicular syndrome (60 %), myelopathic syndrome (15 %). A single level fusion was performed in all the patients.

From a clinical point of view, we observed one dysphagia. Improvement in initial pain syndrome was noted for 80 % of the patients. Radicular pain syndrome is present at latest follow-up for 15 % of the patients, as residual cervical syndrome is noted for 40 % of the patients. Complete disappearance of pain occurred for 80 % of the patients who initially presented radicular syndrome and for 50 % of the patients who presented preoperative cervical pain.

Radiological findings evidenced that 95 % of the patients conserved initial correction, with neither measurable (<1 mm) loss of disc height nor kyphotic lordotic evolution of the curve. One patient showed impaction of the implant inside the lower vertebra with a 3 mm loss of disc height. In 100 % of our observations, no measurable (<1 mm) implant displacement was observed at latest follow-up. Flexion/extension X-ray showed no mobility of the grafted level(s) for all the patients, for whom fusion was considered to be acquired. A moderate radiolucent dark line was observed in two of our observation in contact with one vertebral end plates. Its thickness decreased over time, and becomes invisible at 6 months and at latest follow-up. No visible signs of implant resorption was noticed using routine x rays at 6 months follow up.

No cyst or lysis where detected on CT scan analyzis. The quantity of new bone formation at the cage level was evaluated as 62.6 % (12.4 sd) of the volume of the cage at 2 years. No infection, no neurological complications were reported.

Discussion

In animal studies histological examinations indicated clearly that pure PLLA implants were systematically surrounded by a layer of conjunctival tissue containing large numbers of macrophages, irrespective of the length of implantation, whereas bone tissue grew in direct contact with composite implants during the first few months and matured gradually until the end of the study period with no marked macrophage activation. The composite material under investigation is thus more favorable for bone consolidation *in vivo* than pure PLA and has identical properties to those of pure b-TCP ceramics. This result is not particularly surprising if we consider the properties of the materials in the composite separately. We know that pure lactic acid-based polymers are not cytotoxic or inflammatory *in vitro* [4, 8, 24, 26–30] but are capable of causing an inflammatory reaction *in vivo* [4, 8, 26, 30–33], as confirmed by clinical observations [10, 18, 19, 34–36]. Pure b-TCP, on the contrary, promotes bone healing by osteoconduction, becoming surrounded by healthy bone tissue containing active osteogenous cells, with no intermediate fibrous layer. It is, thus, conceivable that composite materials such as those we studied have a "hybrid" biological behavior that becomes closer to that of pure tricalcium phosphate as the mineral content increases.

This clinical series showed that fusion occurred within regular time period. No inflammatory reaction was noted confirming in vivo study. Radiolucent line in two cases disappeared quickly which might the sign of progressive bone healing process around the implant. No loss of disc height was noted at latest follow up assessing the good behaviour of the implant when an anterior plating is performed. This preliminary results needs further studies to confirm strength retention properties of the implant and its resorption rate over time. We haven't observed radiological resorption of the cage during the time of the study despite significant resorption was seen in animal study. This could be attributed to the neutralization effect of the anterior plate decreasing the stresses applied on the cage. Since no loss of correction was observed we can admit that the mechanical properties of the cage was maintained during this period otherwise screw mobilization would probably have appeared.

Conclusion

This new composite material eliminates the inflammation reaction induced by the use of PLA alone and promotes new bone formation. The ceramic block guarantees the maintenance of the disc height and its slow resorption

allows long term fusion and stability. At the end this combination provides the same results as tri-cortical iliac crest graft without the disadvantages of the bone harvesting site. Further clinical studies are requested to confirm these results.

References

1. Smith GW, Robinson RA. The treatment of certain cervical-spine disorders by anterior removal of the intervertebral disc and interbody fusion. J Bone Joint Surg Am. 1958;40-A:3. Williams DF. Enzimatic hydrolysis of polylactic acid. Eng Med. 1981;10:5–7.
2. Cloward RB. The anterior approach for removal of ruptured cervical disks. J Neurosurg. 1958;15:602–17.
3. Younger EM, Chapman MW. Morbidity at bone graft donor sites. J Orthop Trauma. 1989;3:192–5.
4. Fuchs M, Koster G, Krause T, Merten HA, Schmid A. Degradation of and intraosseous reactions to biodegradable poly-L-lactide screws: a study in minipigs. Arch Orthop Trauma Surg. 1998;118(3):140–4.
5. Fielding WJ. Complications of anterior cervical disc removal and fusion. Clin Orthop. 1992;284:10–3.
6. Bos RR, Rozema FR, Boering G, Nijenhuis AJ, Pennings AJ, Verwey AB, Nieuwenhuis P, Jansen HW. Degradation of and tissue reaction to biodegradable poly(L-lactide) for use as internal fixation of fractures: a study in rats. Biomaterials. 1991;12(1):32–6.
7. Sasso R, Le Huec JC, Shaffrey C. Iliac crest graft donor site pain after anteriorlumbar interbody fusion: a prospective patient satisfaction outcome assessment. J Spinal Disord Tech. 2005;18(Suppl):S77–81.
8. Le Huec J-C, Langlois V, Liquois F, Lesprit E, Clément D. Arthrodèse intersomatique cervicale par greffon en phosphate tricalcique- etude rétrospective de 33 cas. 1 à 3 ans de recul. Rachis. 2001;13 / 3:197–202.
9. Paivarinta U, Bostman O, Majola A, Toivonen T, Tormala P, Rokkanen P. Intraosseous cellular response to biodegradable fracture fixation screws made of polyglycolide or polylactide. Arch Orthop Trauma Surg. 1993;112(2):71–4.
10. Mainard D, Galois L, Bordji H, Membre H, Clément D, Delagoutte JP. Comparative study of bone growth into porous hydroxylapatite and tricalcium phosphate ceramics with four different pore size ranges". Presented at the second congress of the European Federation of National Associations of Orthopaedics and Traumatology, Munich; 1995.
11. Bostman OM, Philajamaki HK. Adverse tissue reactions to bioabsorbable fixation devices. Clin Orthop. 2000;371:216–27.
12. Furukawa T, Matsusue Y, Yasunaga T, Shikinami Y, Okuno M, Nakamura T. Biodegradation behavior of ultra-high-strength hydroxyapatite/poly (L-lactide) composite rods for internal fixation of bone fractures. Biomaterials. 2000;21(9):889–98.
13. Galois L, Mainard D, Cohen P, Delagoutte J-P. 23 cas d'utilisation du phosphate tricalcique β pour le comblement des pertes de substance osseuse au pied. Med Chir Pied. 2001;17:44–53.
14. Galois L, Mainard D, Pfeffer F, Traversari R, Delagoutte J-P. Use of β -tricalcium phosphate in foot and ankle surgery : a report of 20 cases. Foot Ankle Surg. 2001;7:217–27.
15. Higashi S, Yamamuro T, Nakamura T, Ikada Y, Hyon SH, Jamshidi K. Polymer-hydroxyapatite composites for biodegradable bone fillers. Biomaterials. 1986;7(3):183–7.
16. Ignjatovic N, Savic V, Najman S, Plavgic M, Uskokovic D. A study of HAp/PLLA composite as a substitute for bone powder, using FT-IR spectroscopy. Biomaterials. 2001;22(6):571–5.
17. Ignjatovic N, Tomic S, Dakic M, Miljkovic M, Plavsic M, Uskokovic D. Synthesis and properties of hydroxyapatite/poly-L-lactide composite biomaterials. Biomaterials. 1999;20(9):809–16.
18. Imai Y, Fukuzawa A, Watanabé M. Effect of blending tricalcium phosphate on hydrolytic degradation of a block polyester containing poly(L-lactic acid) segment. J Biomater Sci Polym Ed. 1999;10(7): 773–86.
19. Martinek V, Friederich NF. Tibial and pretibial cyst formation after anterior cruciate ligament reconstruction with bioabsorbable interference screw fixation. Arthroscopy. 1999;15(3):317–20.
20. Bergsma EJ, Rozema FR, Bos RR, de Bruijn WC. Foreign body reactions to resorbable poly(L-lactide) bone plates and screws used for the fixation of unstable zygomatic fractures. J Oral Maxillofac Surg. 1993;51(6):666–70.
21. Galois L, Mainard D, Cohen P, Pfeffer F, Traversari R, Delagoutte J-P. Comblement des pertes de substance osseuse par le phosphate tricalcique β en traumatologie. Ann Chir. 2000;125:972–81.
22. Galois L, Mainard D, Delagoutte J-P. β -tricalcium phosphate ceramic as a bone substitute in orthopaedic surgery. Int Orthop (SICOT). 2002;26:109–15.
23. Le Huec J-C, Clément D, Brouillaud B, Barthe N, Dupuy B, Foliguet B, Basse-Carthalinat B. Evolution of the local calcium content around irradiated β -TCP ceramics implants : In-Vivo study in the rabbit. Biomaterials. 1998;18:733–8.
24. Le Huec J-C, Lesprit E, Delavigne C, Clément D, Chauveaux D, Le Rebeller A. Tricalcium phosphate ceramics and allografts as bone substitutes for postero-lateral spine fusion in Idiopathic scoliosis : comparative clinical results at 4 years. Acta Orthop Belg. 1997;63 / 3:202–11.
25. Murphy WL, Kohn DH, Mooney DJ. Growth of continuous bone like mineral within porous poly(lactide-co-glycolide)scaffolds in vitro. J Biomed Mater Res. 2000;50(1):50–8.
26. Oonishi H, Hench LL, Wilson J, Sugihara F, Tsuji E, Matsuura M, Kin S, Yamamoto T, Mizokawa S.

Quantitative comparison of bone growth behavior in granules of bioglass, A-W glass-ceramic, and hydroxyapatite. J Biomed Mater Res. 2000;51(1):37–46.
27. Hollinger JO. Preliminary report on the osteogenic potential of a biodegradable copolymer of polyactide (PLA) and polyglycolide (PGA). J Biomed Mater Res. 1983;17(1):71–82.
28. Kikuchi M, Tanaka J, Koyama Y, Takakuda K. Cell culture test of TCP/CPLA composite. J Biomed Mater Res. 1999;48(2):108–10.
29. Martins AN. Anterior cervical discetomy with and without interbody bone graft. J Neurosurg. 1976;44:290–5.
30. Peltoniemi HH, Hallikainen D, Toivonen T, Helevirta P, Waris T. SR-PLLA and SR-PGA miniscrews: biodegradation and tissue reactions in the calvarium and dura mater. J Craniomaxillofac Surg. 1999;27(1):42–50.
31. Bergsma JE, de Bruijn WC, Rozema FR, Bos RR, Boering G. Late degradation tissue response to poly(L-lactide) bone plates and screws. Biomaterials. 1995;16(1):25–31.
32. Schakenraad JM, Hardonk MJ, Feijen J, Molenaar I, Nieuwenhuis P. Enzymatic activity towards poly-(L-lactic acid) implants. J Biomed Mater Res. 1990;24:529–45.
33. Van der Elst M, Klein CPAT, De Blieck-Hogervorst JM, Patka P, Haarman HJTM. Bone tissue response to biodegradable polymers used for intra medullary fracture fixation : a long term in vivo study in the sheep femora. Biomaterials. 1999;20:121–8.
34. Bostman OM. Osteoarthritis of the ankle after foreign-body reaction to absorbable pins and screws: a three- to nine-year follow-up study. J Bone Joint Surg Br. 1998;80(2):333–8.
35. Lajtai G, Noszian I, Humer K, Unger F, Aitzetmuller G, Orthner E. Serial magnetic resonance imaging evaluation of operative site after fixation of patellar tendon graft with bioabsorbable interference screws in anterior cruciate ligament reconstruction. Arthroscopy. 1999;15(7):709–18.
36. Takizawa T, Akizuki S, Horiuchi H, Yasukawa Y. Foreign body gonitis caused by a broken poly-L-lactic acid screw. Arthroscopy. 1998;14(3):329–30.

Shape Memory Alloys and Their Medical Applications

18

Kerong Dai and Congqin Ning

Shape memory alloys (SMA) are a kind of metallic materials with the characteristics of returning to the previously defined shapes when subjected to some appropriate thermal procedure. Just because of its particular functional properties, especially the shape memory effect (SME) and superelasticity (SE), shape memory alloys have attracted wide attention. It was Chang and Read who first observed the unique memory effect of shape memory alloys in Au 47.5 at % Cd alloy early in 1951 [1]. But it was not until 1963 when Buehler and his co-workers [2] rediscovered the SME in equiatomic Ni-Ti that SMAs actually began to cause a great deal of commercial interest, especially after they were widely put into use in the field of medicine [3–5]. Although quite a number of alloys are known to show shape memory behavior, only those that could generate substantial amounts of strain or could generate significant force upon the changing shape so as to make it recover are of commercial value. In the medical field, the family of Ni-Ti alloys is the most popular one that gets wide clinical application, owing to its good biocompatibility, substantial resistance to corrosion and fatigue, and the fact that its elastic modulus is quite close to that of human bone. In some cases, Ni or Ti (only a few per cent) in Ni-Ti alloys can be partially replaced by Cu, Co, Fe, Nb, or Mo to improve the hysteresis (stress and/or temperature hysteresis), corrosion behavior, control of transformation temperatures, fatigue behavior, etc. [6].

K. Dai, MD (✉)
Laboratory of Orthopaedics Cellular & Molecular Biology, Shanghai Institutes for Biological Sciences Chinese Academy of Sciences & Shanghai Jiao Tong University School of Medicine, Shanghai, China
e-mail: krdai@163.com

C. Ning, PhD
State Key Laboratory of High Performance Ceramics and Superfine Microstructure, Shanghai Institute of Ceramics, Chinese Academy of Sciences, Shanghai, China
e-mail: cqning@mail.sic.ac.cn

Martensitic Transformation

The functional properties of shape memory alloys are closely related to a solid-solid phase transformation named Martensitic transformation. For many metallic materials, as their cooling speed reaches a certain extent, they will undergo a phase transformation in their crystal structure while cooled from a high temperature form (Austenite) to a low temperature form (Martensite). This procedure is known as Martensitic transformation, which is a nondiffusion phase transformation. The transformation from Martensite to Austenite upon heating is known as the reverse transformation. The

D.G. Poitout (ed.), *Biomechanics and Biomaterials in Orthopedics*,
DOI 10.1007/978-1-84882-664-9_18

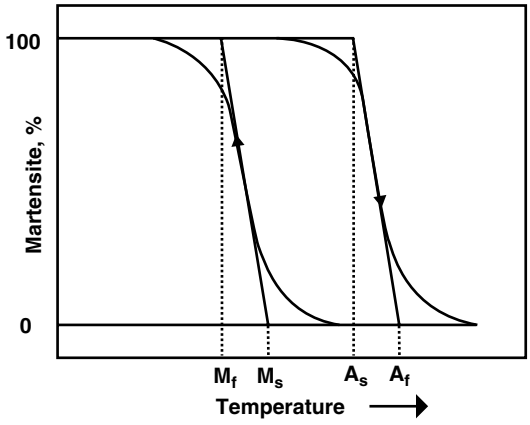

Fig. 18.1 Schematic representation of the volume transformed as a function of the temperature

characteristic transformation temperatures are defined as follows [7]:

M_s Temperature: The temperature at which a shape memory alloy starts transforming to Martensite upon cooling.

M_p Temperature: The temperature at which a shape memory alloy is about 50 % transformed to Martensite upon cooling.

M_f Temperature: The temperature at which a shape memory alloy finishes transforming to Martensite upon cooling.

A_s Temperature: The temperature at which a shape memory alloy starts transforming to Austenite upon heating.

A_p Temperature: The temperature at which a shape memory alloy is about 50 % transformed to Austenite upon heating.

A_f Temperature: The temperature at which a shape memory alloy finishes transforming to Austenite upon heating.

Transformation temperatures of the SMA can be adjusted by slightly changing the alloy compositions or by thermo-mechanical treatment. Usually, the illustration of the Martensitic transformation and its reverse transformation is shown as Fig. 18.1.

According to its characteristics, Martensite transformation can be classified into two types- thermoelastic Martensite transformation and non-thermoelastic Martensite transformation. What distinguishes shape memory alloys from conventional materials is their ability to form thermoelastic Martensite. During the process of thermoelastic Martensite transformation, while below the transformation temperature, the deformation of the shape memory alloy is caused by simply adjusting the orientation of the crystal structure through the movement of twin boundaries (a twinning mechanism), instead of slipping and dislocation movement. In other words, the shape change resulting from Martensitic transformation can be accommodated by a crystal lattice distortion, and the boundary between Martensite and the parent phase can be driven by slight changes of the temperature or stress. That is to say, thermoelastic Martensite is completely crystallographically reversible. Whereas on the contrary, the growth rate of the non-thermoelastic Martensite is so quick because of the larger driving force from Martensite transformation that the boundary between Martensite and the parent phase is destroyed during the transformation, which results in an irreversible parent- Martensite boundary.

The Martensite transformation occurs not at a single temperature but within a range of temperatures (as shown in Fig. 18.1), which varies according to different alloy composition and microstructure constitution, the latter being determined mainly by the thermomechanical treatments. Since the phase transformation temperatures during heating and cooling do not overlap, a temperature hysteresis appears, which also varies according to different alloy systems. This temperature hysteresis is generally illustrated as the difference between A_f and M_s (i.e., $\mathbf{\Delta}T = A_f - M_s$) or the difference between A_p and M_p (i.e., $\mathbf{\Delta}T = A_p - M_p$).

Functional Properties

Shape Memory Effect

Usually, under external forces, a common metallic material deforms elastically first, then plastic deformation occurs after its yield point, and finally, even if the force is removed, the permanent deformation will be reserved. But for some other alloys, even when a plastic

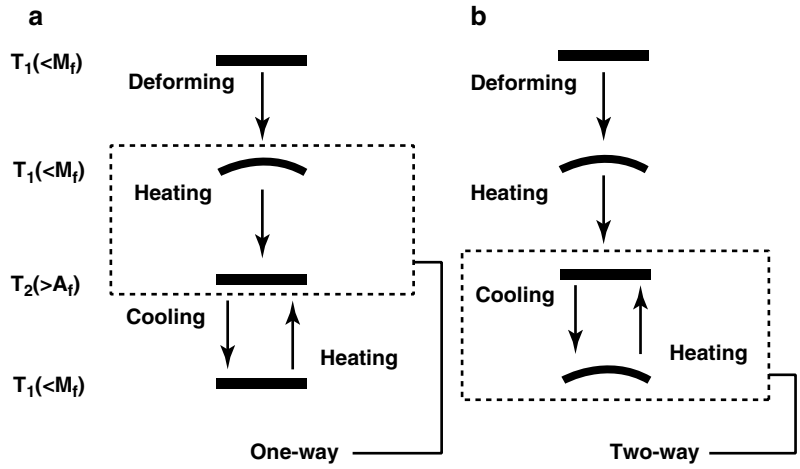

Fig. 18.2 Schematic representation of one-way (**a**) and two-way (**b**) memory effects

deformation occurs, they can still return to their original shapes after being heated up to a certain temperature. Such a shape recovery phenomenon is called the Shape Memory Effect (SME), which is due to the Martensitic transformation in these alloys. When an alloy with a given shape cools from the Austenite form to the Martensite form, it is easily deformed to a new shape (the restriction is that the deformations must not exceed a certain level), but if the same alloy is heated up to its transformation temperature, it will recover its previous shape due to the reversible reverse transformation.

After being deformed, Martensite can recover its parent shape via reverse transformation. This effect is called the one-way memory effect (Fig. 18.2a). After given proper training, some alloys can memorize to return to not only the parent shape during heating, but also the deformed Martensite shape during re-cooling. This effect is called the two-way memory effect (Fig. 18.2b). The latter can be obtained only after a specific thermomechanical treatment, which is usually called "training". The amount of shape change that can be obtained by the two-way memory effect is always significantly less than that by the one-way memory effect.

Generally, the shape memory effect can be expressed by the shape recovery ratio (i.e., η). If the initial shape of the alloy in Austenite form is l_0 (expressed as length), the shape of deformed Martensite (e.g., tension) is l_1, and the shape after reverse transformation at high temperature is l_2, the η can be expressed as [8].

$$\eta(\%) = (l_1 - l_2)/(l_1 - l_0) \times 100\%$$

Superelasticity

Superelasticity, as the name implies, refers to a phenomenon that the alloy can exhibit strain far beyond its elastic limit upon loading, whereas once the stress is removed, the original strain will be returned completely. According to the characteristics of the stress–strain curves, the superelasticity can be classified into two types: linear and non-linear superelasticity. The latter is caused by a stress that occurs during a loading and unloading process, which leads to Martensitic transformation and its reverse transformation at a temperature range above A_f. The former is probably related to the contribution of microtwins to the deformation. The two kinds of superelastic behavior are shown in Fig. 18.3. As for the non-linear superelasticity, when the stress reaches a critical level, the alloy will start to transform into Martensite, accompanied by an increasing strain at constant stress until the alloy is fully transformed into Martensite (see Segment A–B in Fig. 18.3). When the stress is removed, the reverse transformation will occur at a lower stress level (see Segment C–D in Fig. 18.3). The SME described above depends on temperature changes. In contrast, the superelastic effect of shape memory alloys is a kind of isothermal

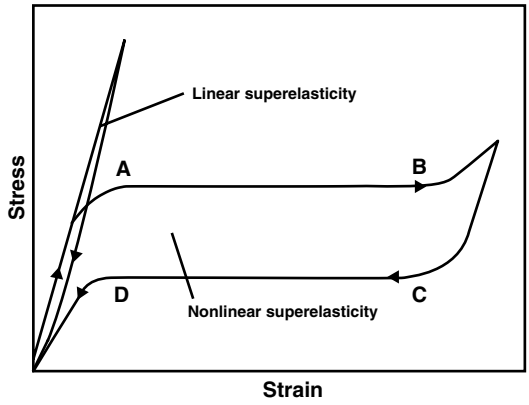

Fig. 18.3 Two kinds of superelastic behavior at constant temperature

phenomenon and the temperature changes are not necessary. The critical stresses can be adjusted by alloy composition, treatment and temperature. In general, the stress levels increase linearly with increasing temperatures [6]. Reversible strain obtained by the superelastic effect is always up to 8 %, which is 10–20 times higher than the normal elastic strain of conventional metallic materials. As shown in Fig. 18.3, the stress upon loading and unloading does not overlap and shows a hysteresis as well.

High Damping Capacity

The shape memory alloys have a high damping capacity in the Martensite state or two-phase state. The high damping capacity of SMA is related to the hysteretic movement on interfaces (Martensite variants interfaces, twin planes, parent-Martensite interfaces) whereas a contribution of dislocations is not excluded [5].

Applications

Shape memory alloys have now been widely used in many fields of industry such as fasteners, actuators, satellite antenna, and decorations, etc. This chapter only introduces several examples of shape memory alloy products applied in medical fields.

Application of the Shape Memory Effect

Free Recovery

This refers to the memory effect that after an SMA component is deformed in the Martensitic state, the component can recover its previous shape upon heating without any restrictions. A prime application of this kind of SME is the blood-clot filter developed by Simon [9]. It is made from Ni-Ti wire. After being chilled to make it collapse, the filter is inserted into the vein, and the temperature of body heat is high enough to help it return to its previous functional shape, enabling it to anchor itself in a vein and catch passing clots.

Constrained Recovery

If a deformed shape memory alloy or its components is subjected to an external constraint during the heating process, it will induce a recovery force, which is a function of the temperature, and varies with the constraint strain. The larger the constraint strain becomes, the greater the recovery force will be. This recovery force can be used for the purpose of clamping, fixation, or stiffening. In biomedical fields, there are many such products: dental root implants, stents, and fixators for bone fractures. The shape memory compression staple will be described as an example here: the staple was designed by Dai and it is the first SMA device used inside the human body [10, 11]. It is U-shaped, having two straight legs connected by a transverse wave-like segment with angles of 70° (Fig. 18.4a). At low temperature, i.e., below 4 °C, the wavy segment is expanded to increase the length. At the same time, the included angles are expanded from 70 to 90° to elongate the span between the ends of the legs (Fig. 18.4b). After the fracture is reduced, the expanded staple is placed across the fracture line by inserting the two legs into the holes prepared in the proximal and distal fracture fragments respectively. When the local temperature is raised by hot compresses with hot saline gauze, the staple(s) will tend to restore its original shape but at the same time being constrained

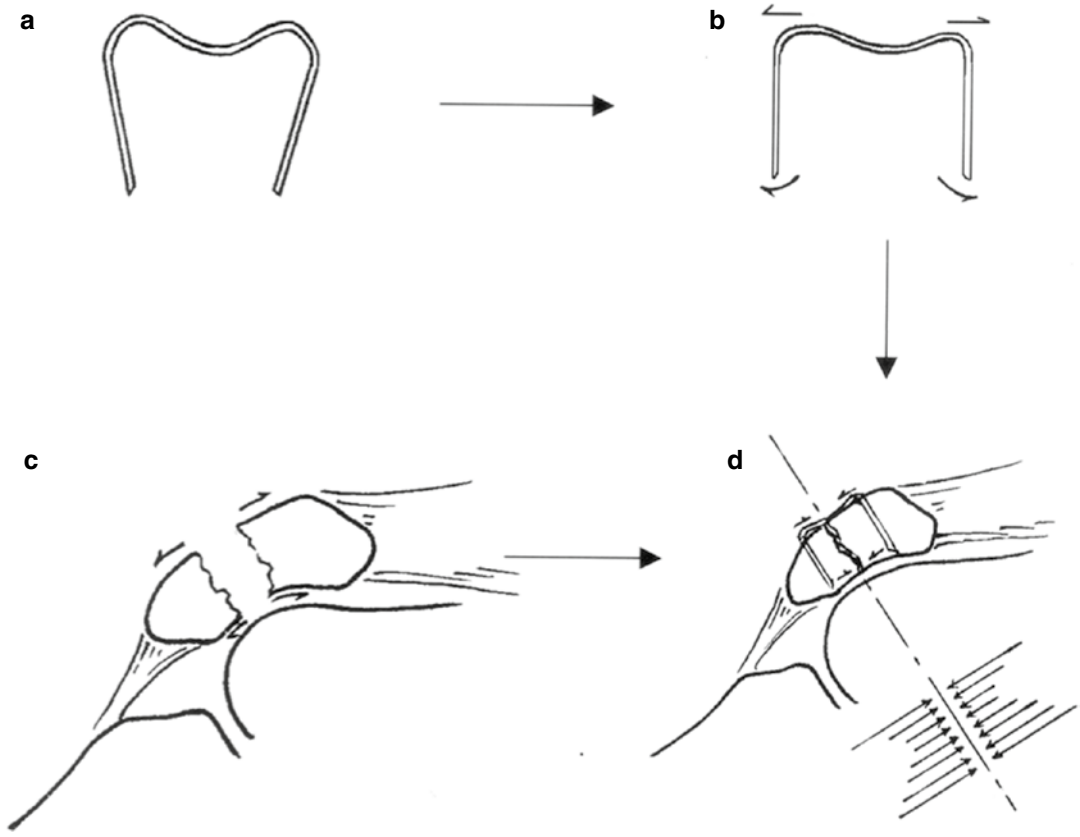

Fig. 18.4 (**a**) Schematic diagram of the shape memory compression staple. (**b**) The staple distracted at the wavy segment and the included angle are expanded from 70 to 90 °C. (**c**) Patella fracture with a separated tendency. (**d**) After fracture reduction and staple fixation, the staple can not restore to its original shape and a large recovery force is created at both sides of the fracture to fix the fracture against the distraction forces produced by the muscle and joint flexion. *Arrows* in each diagram indicate the stress direction, and in diagram (**d**) also indicate the magnitude of stress

by the walls of the holes so that they will generate a constrained recovery force on both side of the fracture line to hold the fracture fragments in place, exerting sustained compression on the fracture and resisting muscular pull (Figs. 18.4c, d and 18.5). The compression force will be significantly decreased if the distance between the two holes is not wide enough.

The embracing fixator is made of Ni-Ti Shape memory saw-tooth arm finator (Fig. 18.6) has also been used clinically to treat fractures of the shaft of the femur, humerus, tibia, and other long bones, and is particularly good for the fixation of periprosthetic fractures of the femur (Fig. 18.7) [12–14]. Its strength is adequate to meet the requirements for internal fixation of a long bone shaft, and the elastic modulus at 37 °C is only 54.18 Gpa (200 Gpa for 316 L stainless steel), means it have a rather low stress-shielding rate. In vitro mechanical analyses and in vivo animal experiments have been done to evaluate the embracing fixator. In vitro experiments found that the difference in bending strength of the embracing fixator and the bone plate is not significant, but the compressive stress-shielding rate of the embracing fixator is markedly lower than that of the bone plate. While the torsion strength of the fixator is significantly higher than that of the intramedullary nail, no harm is done to the medullary blood vessels. Torsion experiments showed that they yielding torsional moment of the fixator is

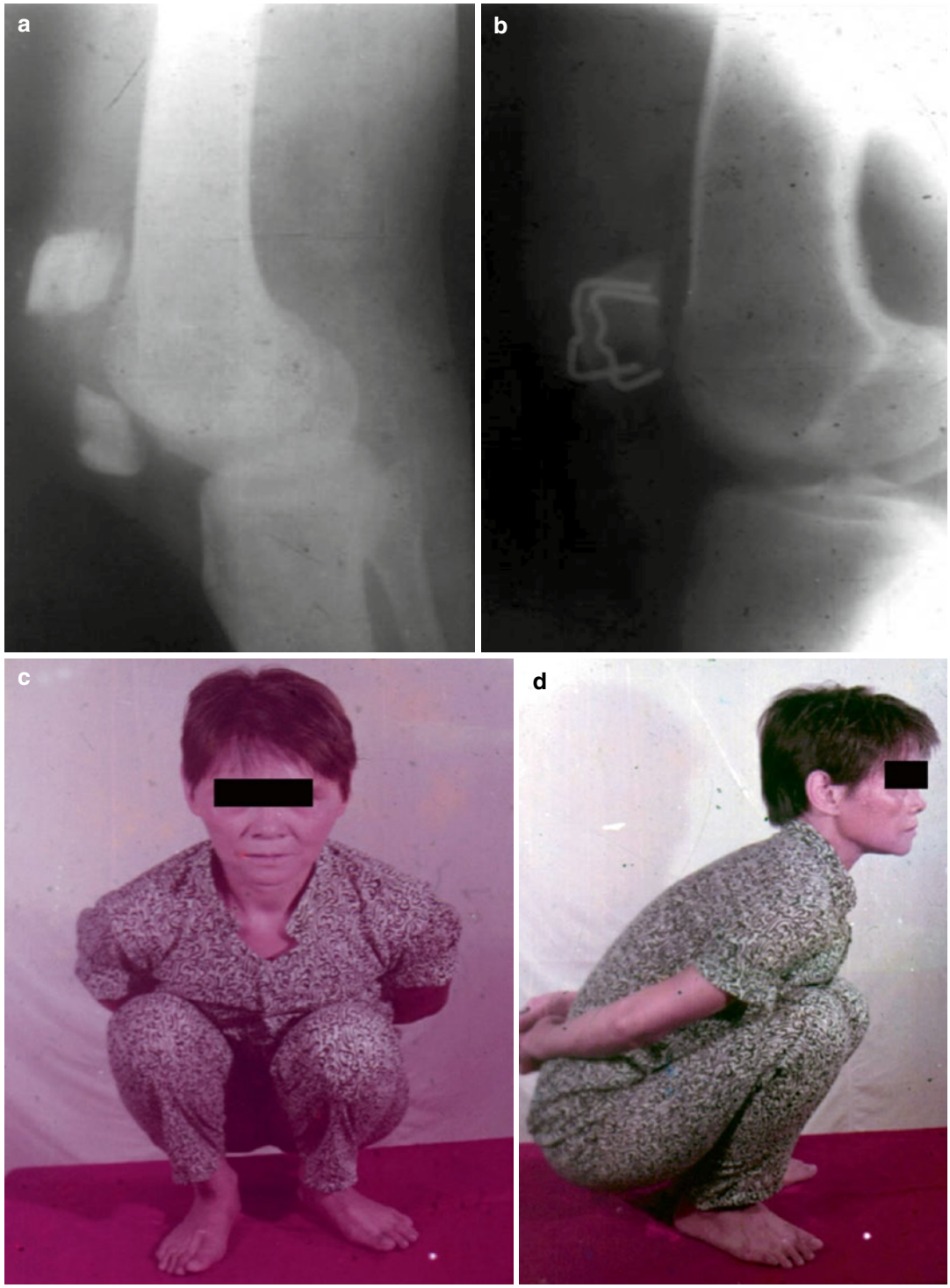

Fig. 18.5 A shape memory staple was use for the first time inside the human body. (**a**) Patellar fracture, preoperative. (**b**) Staple fixation, postoperative. (**c**, **d**) Recovery of function

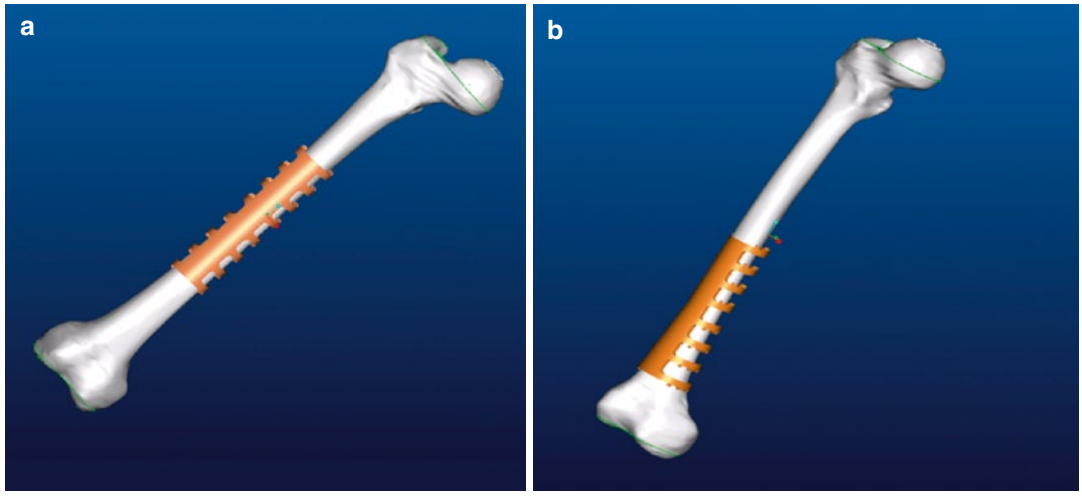

Fig. 18.6 Sawtooth-arm embracing fixator for treatment of fracture of long bone shaft. (**a**) Cylinder type and (**b**) Cone type used in mid and near end parts of the shaft respectively

markedly higher than that of the intramedullary nail group, the ratio of the averages being 6.85:1; but lower than that of the bone plate group, the ratio of the averages being 1:1.28, not much different. Animal experiments demonstrated that when fixed with an embracing fixator, the fracture shows satisfactory secondary union with the formation of a certain amount of outer callus. In addition, the disorganization of collagen fiber and the degree of bone resorption are lower than in the rigid bone plate group. Its shape memory effect make the placement of the fixator during operation quite simple and ensures the maintenance of sawtooth arms firmly embracing the fracture segment after surgery.

The inner diameter of the shape memory sawtooth arm fixator, should be less than the outer diameter of the fracture bone in order to constrain the recovery of the fixator so that a reliable stability of the fracture can be obtained.

Up to now, nickel-titanium shape memory alloy has been used for the manufacture of several kinds of fracture fixators, scoliosis correction devices, prostheses for hip resurfacing, intervertebral prostheses, arteriobembolizators, dental root implants, and stents of hollow organs and vessels [3, 4].

Superelastic Applications

Arch wires made of Ni-Ti for orthodontic correction have been used for many years, especially beneficial for the correction of tooth deformation.

Self-Expanding Stent

The self-expanding stent is already widely used in the treatment of stenosis of certain hollow structures such as vessels, trachea-bronchus, urethra, biliary tract, esophagus, etc. Within the catheter, the compressed stent made of shape memory alloy is inserted into the duct by interventional techniques and is left in the stenosis area. In this way it will not only constantly expand the duct or vessel with its superelastic property or shape memory effect but it will also avoid the shifting of the self-expanding stent [3, 4].

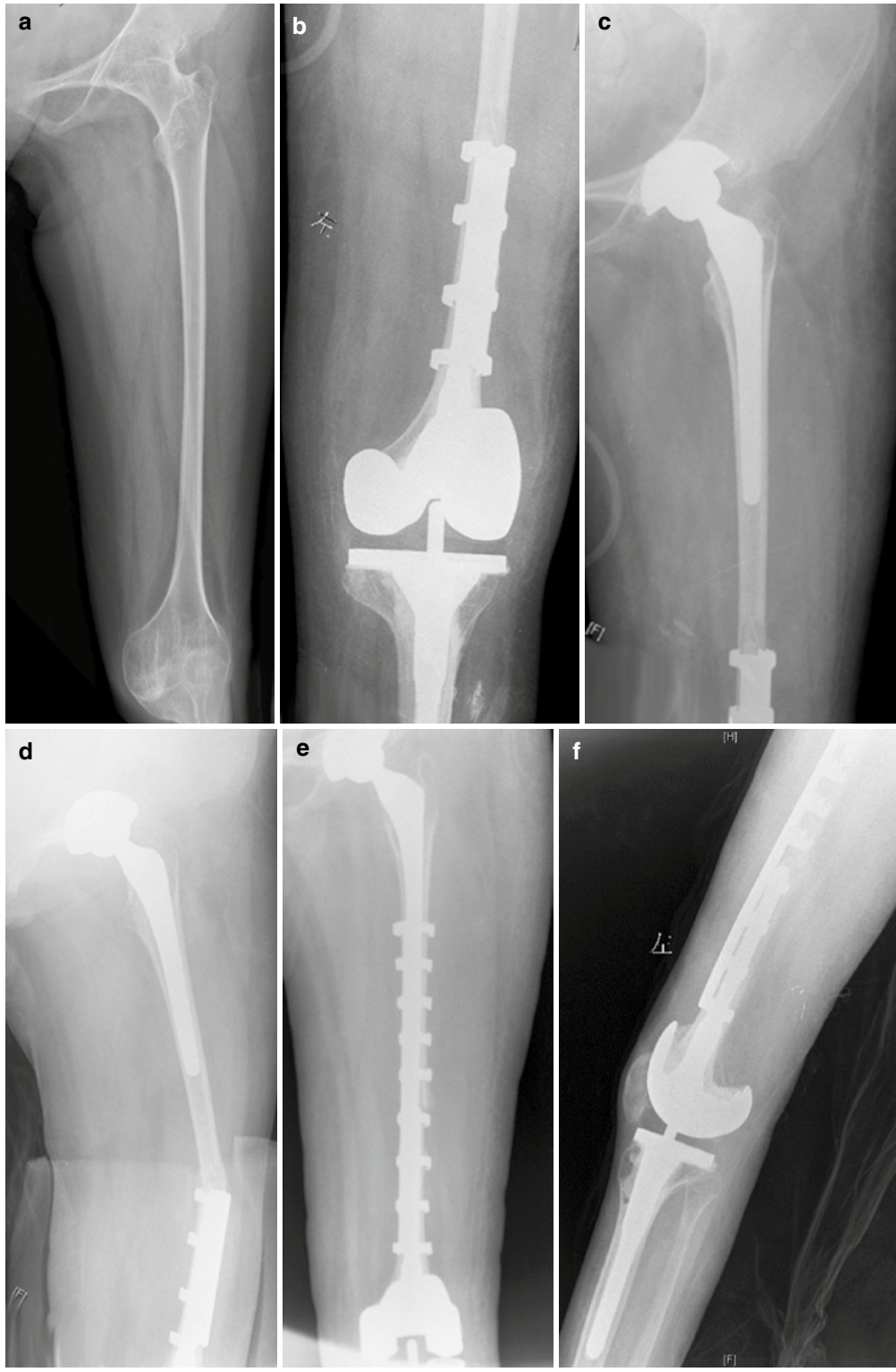

Fig. 18.7 (**a**) Rheumatoid arthritis, bong ankylosis of hip and knee joint, with severe osteoporosis. (**b**, **c**) After total hip and total knee arthroplasty, sawtooth-arm embracing fixator was used in distal femur for preventing fracture. (**d**) 3 months after operation, fracture occurred at the proximal level of embracing fixator. (**e**, **f**) Fracture treated with a custom-made embracing fixator

References

1. Chang LC, Read TA. Plastic deformation and diffusionless phase changes in metals – the gold – cadmium beat phase. Trans AIME. 1951;189:47–52.
2. Buehler WJ, Gilfrich JW, Wiley RC. Effect of low-temperature phase changes on mechanical properties of alloys near composition TiNi. J Appl Phys. 1963;34:1475–7.
3. Dai KR, Chu YY. Studies and applications of NiTi shape memory alloys in the medical field in China. Biomed Mater Eng. 1996;6:233–40.
4. Chu YY, Dai KR, Zhu M, Mi X. Medical Application of NiTi shape memory alloys in China. Mater Sci Forum. 2000;327:55–62.
5. Van Humbeeck J. Non-medical applications of shape memory alloys. Mater Sci Eng. 1999;(A)273–5:134–48.
6. Van Humbeeck J, Stalmans R, Besselink PA. Shape memory alloys. In: Helsen JA, Breme HJ, editors. Metals as biomaterials. 1st ed. Chichester: Wiley & Sons; 1998. p. 73–100.
7. Otsuka K, Ren X. Recent development in the research of shape memory alloys. Intermetallics. 1999;7:511–28.
8. Zuyao X. Shape memory materials. 1st ed. Shanghai: Shanghai Jiaotong University Press; 2000. p. 2–5.
9. Simon M, Athanasoulis CA, Kim D. Simon nitionol inferior vena cava filter: initial clinical experience. Radiology. 1989;172:99–103.
10. Dai KR, Hou XK, Sun YH Tang RG, Qiu SJ, Ni C. Treatment of intra-articular fractures with shape memory compression staples. Injury. 1993;24:651–5.
11. Dai KR, Zhang XF, Yu CT. Orthopaedic application of shape memory compression staple. Chin J Surg. 1983;21:343–5.
12. Dai KR, Ni G, Wu XT, Qiu SJ, Xu XL, Zhu XS. An experimental study and preliminary clinical report of shape memory sawtooth-arm embracing internal fixator. Chin J Surg. 1994;32:629–32.
13. Dai KR, Wu XT, Zu XS. An investigation of the selective stress-shielding effect of shape-memory sawtooth-arm embracing fixator. Mater Sci Forum. 2002;394–395:17–24.
14. Zhao X, Zhu ZA, Sun YH, Wang Y, Zhao J, Zhang YJ, Dai KR. Nickel-titanium shape-memory sawtooth-arm embracing fixator for periprosthetic femoral fractures. Int Orthop. 2012;36(3):619–26.

Part III

Tissue Biomechanics and Histomorphology

Biotribocorrosion of Implants

19

Magdalena Walczak and Mamie Sancy

Biotribocorrosion can be broadly defined as all the aspects of tribocorrosion, i.e. the degradation of surfaces by the combined effect of corrosion and wear, related to biological systems. Whereas tribology alone, also known as friction-corrosion, corrosion-wear, wear-corrosion or (micro) abrasion-corrosion, is concerned with the phenomena occurring at the interface of surfaces in mutual motion (friction, lubrication and wear), corrosion is the science and engineering of chemical and electrochemical reactions at the interface between a material and the environment it is exposed to. In the case of biotribocorrosion, the environment is necessarily that of a living organism or a combination of living organisms (biofilm). Although all materials may suffer biotribocorrosion it is especially pronounced in case of metallic alloys due to the electrochemical nature of their interaction with aqueous media such as the interior of a human body. Both corrosion and wear result in the weight loss over the exposed surface; however, the total weight loss of a tribosystem immersed in a corrosive environment is larger than a simple sum of the losses caused by corrosion and wear alone.

In this chapter the principles of biotribocorrosion are presented and discussed for the specific case of alloys typically used in replacement of large joints. Since all the involved processes occur at the surface of the metal, first, the description of technical and natural surfaces is provided. The various interactions with environment and third bodies are then discussed, followed by a review of the methods of testing and mitigation of surface damage applicable for medical implants.

Interface Between Metal and a Biologic Environment

Both corrosion and wear are defined as detrimental processes of loss of mass through progressive removal of matter at the surface. Whereas corrosion is caused by (electro)chemical interactions with the environment, wear involves damage by localized mechanical forces. Surface properties are of special interest because they determine the way the material interacts with the environment, including corrosion resistance and wear durability of the entire element. The physical surface that experiences tribocorrosion, such as that of an implant, can be represented as a general delineation between the solid domain and the neighboring phase, such as body liquid or bone tissue,

M. Walczak, MD (✉)
Department of Mechanical and Metallurgical Engineering, Escuela de Ingeniería, Pontificia Unviersidad Católica de Chile,
Vicuna Mackenna, Santiago, Chile
e-mail: mwalczak@ing.puc.cl

M. Sancy, MD
Escuela de Construcción Civil, Pontificia Unviersidad Católica de Chile, Santiango, Chile
e-mail: mamiesancy@uc.cl

D.G. Poitout (ed.), *Biomechanics and Biomaterials in Orthopedics*,
DOI 10.1007/978-1-84882-664-9_19

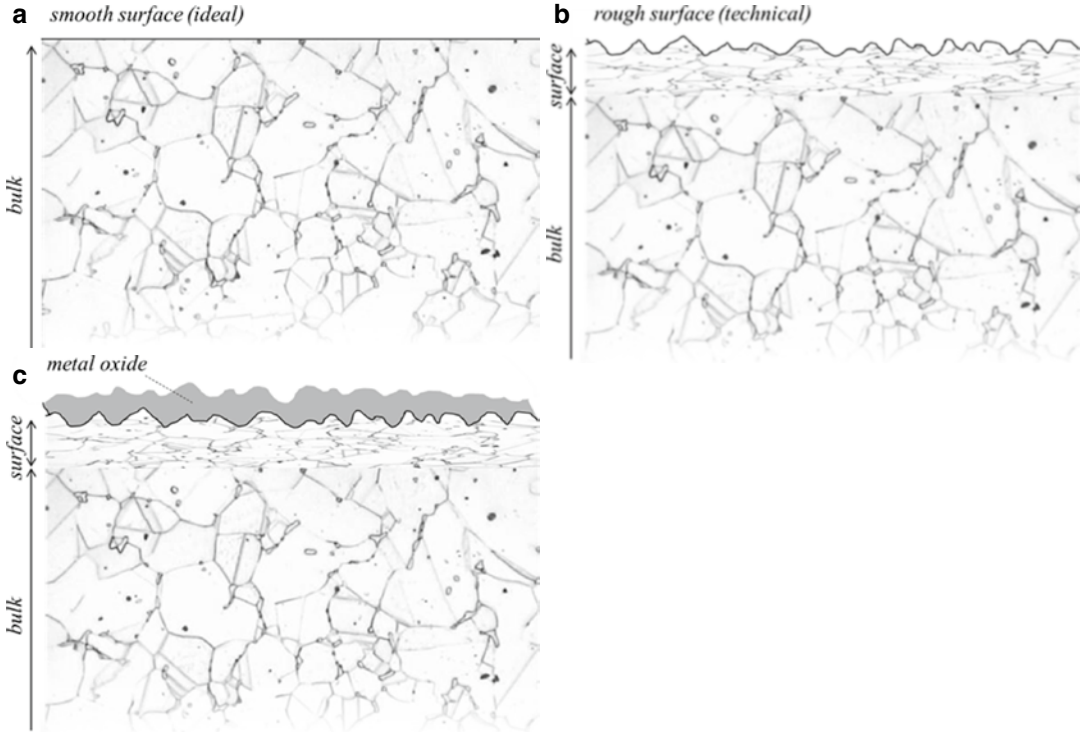

Fig. 19.1 Schematic representation of a metallic surface: (**a**) ideal surface, (**b**) technical surface obtained by metal processing, (**c**) technical surface with oxide layer. The miscrostructure (grains) is typical for AISI 316 L stainless steel observed at 500×

including a layer within which the properties of the solid differ from those of the bulk. The extent of this surface layer depends on the considered characteristics (geometric, energetic, chemical, physical or mechanical properties) as well as their gradients. Thickness of the surface layer is the dimension perpendicular to the geometrical surface of an object described by two boundaries: (*i*) external, separating the surface layer from the surrounding environment (biological tissue), and (*ii*) internal, separating the surface layer from the bulk (implant). The actual thickness of surface layer is difficult to determine experimentally because the interface is not a geometrical surface; it resembles a thick woolen textile rather than silk.

The first feature of a real (technical) surface as compared with a perfect one shown in Fig. 19.1a is its roughness, i.e. deviation of surface normal from its nominal direction distributed over the surface as shown in Fig. 19.1b. The arithmetic average of the absolute height (difference between peaks and valleys) is referred to as R_a, the most common measure of roughness. The performance of a biotribological system relies on the roughness of involved surfaces due to its effect over both friction and wear. Whereas both quantity and quality of surface roughness evolve while an articulation is active [1], corrosion processes of rough surfaces are generally enhanced due to larger effective surface area. Also, mechanical properties of fracture and fatigue are compromised because surface imperfections contribute to the initiation and propagation of cracks. When the distance between peaks and valleys of a surface is significantly longer than its height, the surface profile is said to be wavy and assigned a waviness parameter analogous with roughness. Although waviness is a valid surface characteristic it is mostly irrelevant for biomedical implants where the general matching in topography of the involved surfaces is of interest.

Another difference between the ideal and technical surfaces is the deformation of microstructure. Whereas the microstructure just under the ideal surface is identical with that of the bulk, technical surface is associated with a layer in which the microstructure is deformed. In the example shown in Fig. 19.1, the grains of the bulk steel are of regular shape, whereas technical surface is terminated by a layer of deformed grains in which mechanical properties and electrochemical potentials may deviate from those of bulk values. The deformation results from manufacturing processes such as cutting, grinding or polishing typically employed in the fabrication of metallic implants. It may also arise as product of friction and wear. The microstructure of the subsurface layer has been discussed as crucial in the biomedical applicability of CoCrMo alloys [2].

Further attribute of a technical surface is its interaction with the environment. Especially gasses and liquids (electrolytes) tend to react with metallic surfaces producing adsorbed or passive layers. In the example of Fig. 19.1c a passive layer corresponding with metal oxides typically formed by intereaction with an aqueous environment is shown. This layer might be porous consisting in submicron- or nanocrystals or be a continuous film. The later efficiently separates the base metal from further interaction with the environment. It should be noted that biological environment of a living organism is not constant in time. The variation of temperature, chemical composition and condition of flow may affect the structure of the passive film. Also, mechanical properties of both the film as well as the bulk material might be compromised through the Rehbinder (or Rebinder) effect [3], which considers the role of adsorbed surface active molecules in the propagation of cracks.

The interface described above is further modified when the surface is set in motion, especially when both shear and normal forces are involved. In this case, the surface layer can be compromised and the elements of the environment –small molecules, debris particles, etc. – be included to the solid interface. Such a condition is referred to as tribolayer and is a commonplace in metal on metal hip replacements. It has been shown to be organometallic in nature and containing a number of embedded particles, which are smoother and smaller than the initial debris, e.g. [4]. The electrochemical nature of the tribolayer, and thus its contribution to overall surface degradation, also varies in function of the actual surface condition as shown on the example of CoCrMo alloys [5].

Corrosion Damage of Implants

Unlike mechanical damage, damage through (electro)chemical interaction with the environment cannot be avoided by removing the primary cause. In case of metals the contribution of electrons is significant and the entire process, necessarily detrimental in nature, is referred to as corrosion.

Corrosion takes place at the interface with external medium and involves exchange of both charge and mass. The metal is said to be an anode when electrons are being extracted from it, whereas it becomes a cathode by accepting electrons. At the kinetic equilibrium, i.e. with no external source of current applied, the loss of electrons by a metal (anode) is essentially accompanied by loss of metal ions (metallic dissolution). On the other hand, the cathodic reaction can involve electro-active species present in the environment, such as the oxygen reduction reaction in neutral and alkaline media as well as hydrogen ion reduction or hydrogen evolution ion of acid environments. In principle, metal ion reduction and metal deposition can be also take place on the surface [6]. Thus, corrosion can be viewed as a spontaneous process of returning metal to its mineral (oxidized) state, which is given by the laws of thermodynamics, in particular, expressed by free Gibbs energy (Eq. 19.1). Since, by definition, electrons are involved in the reaction, it is convenient to express the energy of each ion in terms of electric potential (Eq. 19.2):

$$\Delta G = \Delta G^{\otimes} + RT\sum_{i=1}^{k} \ln a_i^{\nu_i} \tag{19.1}$$

$$\Delta G = -zF\Delta E \tag{19.2}$$

where ΔG, $\Delta G^{\otimes}$, R, T, a_i, ν_i, z, F and ΔE are the free Gibbs energy, free Gibbs energy at

standard conditions, gas constant, temperature, activity coefficient of species *i*, stoichiometric coefficient of species *i*, charge number, Faraday constant and the electric potential, respectively. Although the free Gibbs energy associated with an electrochemical reaction is determinant for its occurrence, in practice, it is the rate of the reaction rather than shear energy differences that determine the feasibility of a metal for particular environment. In practice, thermodynamics predicts the likelihood of corrosion process, which can be determined by the corrosion potential (E_{corr}) using electrochemical techniques such as the variation of potential as a function of immersion time with no current applied, i.e. at open circuit potential (OCP). However, it does not provide information about corrosion rate [7]. In general, an electrochemical system is given by the Butler-Volmer equation, which corresponds to a relationship between the potential and current, as is shown in the Eq. 19.3

$$j = j_o\left[\exp\left(-\frac{\alpha z F\eta}{RT}\right) - \exp\left(\frac{(1-\alpha)zF\eta}{RT}\right)\right] \tag{19.3}$$

where j, j_o, α, and η are current density, exchange current density, symmetry factor and overpotential, respectively. Figure 19.2 shows the behavior predicted by Eq. 19.3. The solid curve shows the actual total current for a large overpotential, which is the sum of the cathodic (j_c) and anodic (j_a) current densities. For large negative overpotentials, the anodic component is negligible and the total current is essentially cathodic current. On the other hand, at large positive overpotentials, the cathodic component is negligible and the total current is essentially anodic. In practice, the corrosion process occurs when total current is zero. A typical polarization diagram of an implant metal (316L, Co-alloy or Ti-alloy) is shown schematically in Fig. 19.2.

Stability of the passive layer is a valid concern because corrosion resistance of the majority of implant alloys relies on the formation of a passive layer on the surface that provide an effective barrier to electron and ion transport, playing a very important role in the long-term clinical success of implants. However, a depassivation process can also take place producing increase in the corrosion rate. In particular, in crevices or other types of occluded such as local environments due to cell activity, where local pH changes due to chemical reactions may also occur [8].

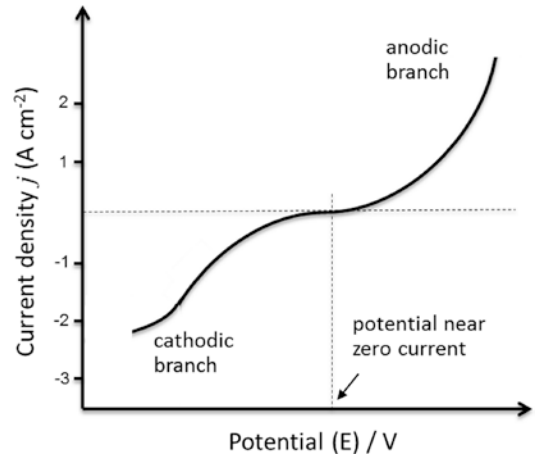

Fig. 19.2 Schematic current density versus potential curve of an electrochemical system

The fraction of the stable and unstable oxide species determines the overall stability and dissolution behavior of the passive film. For instance, the presence of TiO_2 on the surface of CP-Ti provides the resistance to activation upon acidification. However, all aluminum oxides are soluble in acidic solution so that Al-containing Ti-alloys are less corrosion resistant.

The composition of the oxide film formed in air usually differs from that of a passive film formed in a solution. This fact is used in improving corrosion resistance by growing the passive layer of desired composition (see later discussion).

The greatest concern for clinical praxis (apart from biomechanical compatibility) is the release of metal ions and corrosion products that may cause inflammation, allergic reactions and other not desired effects. Although corrosion is mostly associated with materials damage and high corrosion resistance is generally aspired, corrosion-related degradation can also be exploited. An example are biodegradable Mg-alloys which are currently evaluated for biomedical applications [8].

The typical materials used for surgical implants are 316L stainless steels, CoCr alloys, CoCrMo alloys, commercially pure Ti (CP-Ti) and Ti-based alloys. The 316L, CoCr and CoCrMo alloys have an elastic modulus close to 200 GPa, which is much higher than that of compact bone tissue being in the range from 2 to 30 GPa [9–11]. On the other hand, CP-Ti and Ti-based alloys have been readily employed due to their lower elastic modulus, lower density, good biocompatibility and, above all, corrosion resistance [9–11]. The excellent corrosion resistance that CP-Ti and Ti-alloys demonstrate in a variety of media is attributed to the passive behavior associated with formation of Ti-oxide on the surface and owed to their thermodynamic properties described by Eq. 19.1. However, the passive layer might be compromised by depassivation which immediately results in increase of the corrosion rate. Should this occur within the human body, local changes of pH due to hydrolysis of metal ions may result in inflammation of the nearby tissues. One of the most common causes of depassivation in absence of motion is the formation of crevices or other, areas of differential aeration. Crevice corrosion of Ti-alloy implant might be associated with cementation and the local changes of pH along the corroded stem were suggested to induce aseptic loosening [9]. It should be noted that the Ti-alloys of first generation implants employed Al, V, Ni and Co as alloying elements in order to improve the mechanical properties. However, corrosion of the alloys can also produce metallic dissolution of the alloying elements, which can cause an undesirable toxic effect in the human body. The alloys of the second generation were developed to contain only the least toxic elements [9, 11–18], although the TiAlV and TiAlNb are still used. In general, these alloys have demonstrated high corrosion resistance in different media, such as artificial saliva (Ringer's solution) or physiological saline solution (0.9 % NaCl) [19, 20].

Wear Damage of Implants

The phenomena occurring between two surfaces in relative motion are the domain of tribology and can be roughly classified as friction, lubrication or wear. Whereas friction is the force resisting the motion, lubrication and wear affect friction by preservation and destruction of the surface layer, respectively. The individual processes can be of mechanical, thermal and physiochemical type or their combinations as summarized in Fig. 19.3. In

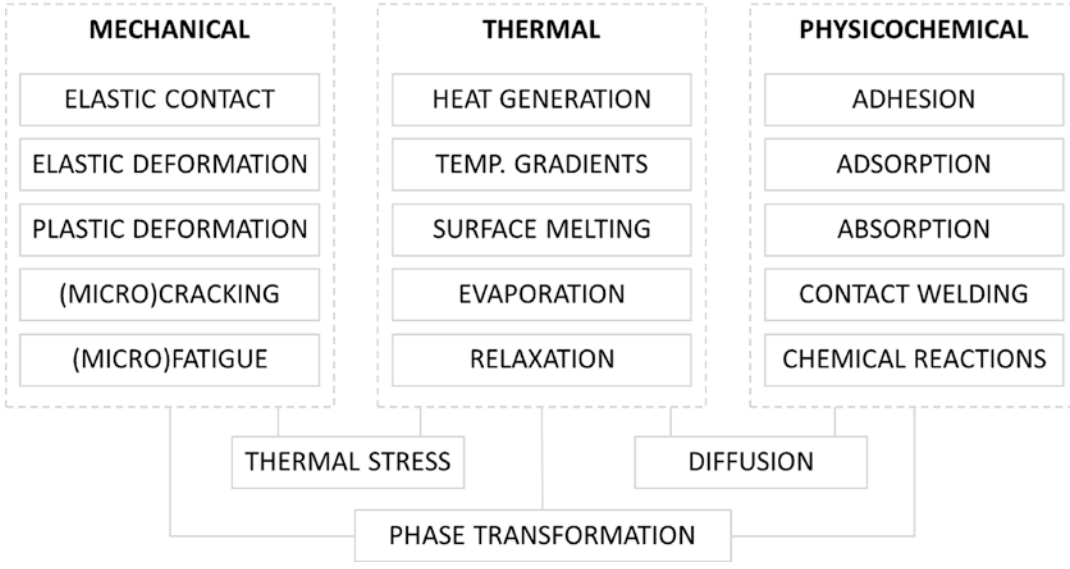

Fig. 19.3 Processes that may take place in surface layer when in relative motion aganist a counter surface

a medical implant under normal conditions of use the following processes are of little importance:

- Temperature gradients,– although local generation of heat is unavoidable and has been shown to produce temperatures above 46°C [21] possibly leading to apoptosis of osteoblasts [22], these temperatures are unlikely to affect other processes through gradients;
- Surface melting,– the melting temperature of all the biomedical alloys is above 1000°C, which is unlikely to be reached;
- Evaporation,– evaporation would require even higher temperatures and/or lower pressures, which are unexpected within human body;
- Contact welding,– this process requires localized temperatures and/or high pressures, which are impossibly reached through friction of an articulation.

The intensity of all the remaining processes is lower than that observed during manufacturing, where surface is removed intentionally; however unlike manufacturing there is a high degree of inhomogeneity associated with their spatial distribution, thus local concentration of forces may indeed lead to catastrophic effects. A review of all the mechanisms with regard to natural and artificial joints can be found in Ref. [23], whereas here only the primary concepts, necessary for introducing the corrosion enhanced damage, are mentioned.

Friction and Lubrication

Friction being the force resisting motion of two bodies in contact is a straightforward consequence of the tribological contact. Depending on the presence of a liquid between the surfaces and the extent of the normal force dry friction, lubricated friction and mixed friction can be distinguished. Of course, dry friction is not expected in a functioning articulation but might be the case in adverse conditions of disease when too little of the synovial fluid is provided as well as under high loads. The dissipation of energy between sliding bodies have been known for centuries and the classic work of Da Vinci and Amonton provided the four basic laws: (*i*) there is a proportionality between the maximum tangential force before sliding and the normal force when a static body is subjected to increasing tangential load; (*ii*) the tangential friction force is proportional to the normal force in sliding; (*iii*) friction force is independent of the apparent contact area; (*iv*) friction force is independent of the sliding speed.

The quantity of friction is determined as proportion between the force of friction and the force acting normal the sliding interface. The proportion is the coefficient of friction and it is said to be static (μ_s) when the force of friction is measured just before sliding begins or kinetic (μ_k) when the force of friction is measured during sliding. Although the definition is simple and straightforward for sliding in one direction, the complex geometry of natural joints requires taking into account 3-axis cyclic forces acting along with 3-axis cyclic frictional moments [24–26].

The friction coefficient in natural joints varies between 0.001 and 0.03 [25] depending on the actual loading conditions and type of lubrication. Artificial joints can fairly reproduce these values [26], however at compromised lubrication conditions the increase of friction might lead to considerable wear [27–30]. Association of friction coefficient with squeaking in ceramic-on-ceramic couplings have also been reported [28].

The actual thickness of the lubrication film during motion is predicted by a hydrodynamic theory which takes into account the effect of normal force acting on the element. In addition, viscosity of the lubricant changes in these dynamic conditions making the prediction of friction coefficient a matter of elastohydrodynamic lubrication theory (EHL). In healthy natural articulations tens of microns of synovial fluid separates the opposing surfaces and the predominant type of friction is lubricated friction. Only in extreme cases of overload boundary friction may occur, however, it is typically of short duration and causes no damage. A similar situation has been reported for artificial joints, where high friction coefficients typically associated with dry friction have been found in-vivo [29]. The thickness of lubricating film has been shown to be sensitive to

the load to a greater extent than predicted by the EHL models [30].

It should be noted, that low friction is typically sought after for the moving surfaces of artificial joints but large friction is also desired for the surfaces that are not supposed to move respectively, e.g. interface between an implant and bone or implant and bone cement. Low amplitude motion at these surfaces leads to a tribological damage referred to as fretting corrosion. The damage itself results from destruction of the passive oxide layer that brings enhanced corrosion through direct exposure of the metallic surface to a corrosive environment. In addition, particles of polymer and metal oxide form debris that my further accelerate the process. Evolution of fretting damage in a stainless steel/PMMA couple at different electrochemical potential has been shown to be accompanied by the increase of friction coefficient [27]. The root cause of fretting might be related with the micro-damage that bone tissue experiences under cyclic compressive loads associated with physical activities [31], although the cement itself is typically more at risk of fatigue failure than bone [32].

Wear

All bodies subject to friction are susceptible to wear, including the natural healthy articulation, where the loss of mass is quickly replenished and the products of wear, the debris, are resorbed by the body with no side-effect. This autoregulation system is evidently missing in artificial joints and to provide an efficient method of prevention and/or mitigation requires understanding of the involved wear mechanisms. These mechanisms can be classified as abrasive, adhesive and fatigue, according to ASTM terminology [33].

Abrasive wear is due to hard particles or hard protuberances forced against and moving along a solid surface. Within this category it is commonly distinguished between the mode of three-body and the mode of two-body wear (Fig. 19.4). In the first case, the all the three elements: surface of the implant, counter surface and debris particles act in way that debris particles are allowed both to slide and roll. Whereas, although two-body wear also includes the three here the debris particles are only allowed to slide. The two-body case can also be thought of as debris particles fixed to the counter surfaces and thus mimicking its sliding motion. Due to limited distance between a typical sliding surface of and implant and the counter surface two-body wear mechanism is mostly the case; however, evidence of the three-body mechanism has also been reported [34].

Adhesive wear is due to localized bonding between contacting solid surfaces leading to material transfer between the two surfaces or

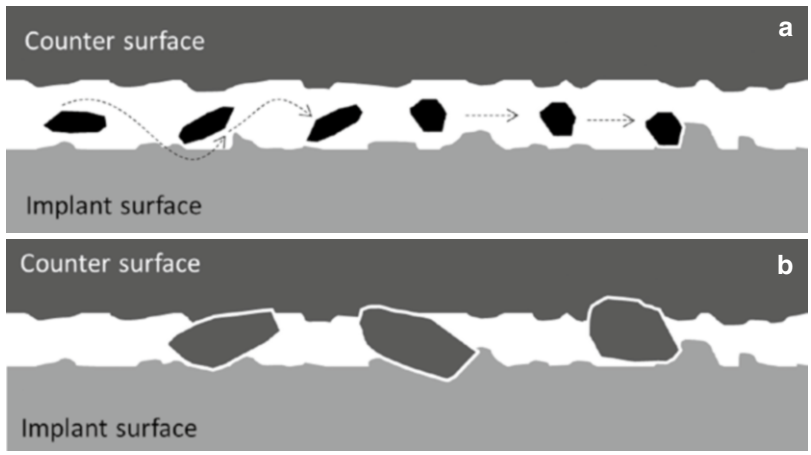

Fig. 19.4 Schematic representation of abrasive wear: (**a**) three-body mode of wear with debris particles sliding and rolling, (**b**) two-body mode of wear with debris particles allowed only to slide

loss from either surface. Unlike abrasive wear, the material removed from the worn surface is transferred to the counter surface rather than to the medium, thus, no debris is formed. The mass transfer takes place from softer to the harder surface, example from polyethylene to CoCrMo [35], or between surfaces of the same hardness, example metal-on-metal [36] or ceramic-on-ceramic [37].

Fatigue wear is due to (micro)fracture arising from material fatigue. Repetitive loads, normal to the surface, that in no cycle exceed yield strength of the material, do cause cumulative microscopic damage that eventually sums up to a fracture. Because this damage is localized near surface, the cracks are generally parallel with surface resulting in flake-like debris rather that bulk failure associated with propagation of a vertical crack. Plastic deformation of surface layer as well as presence of the micro-scale cracks have been shown in HC CoCr femoral heads [38].

Independent of the actual damage mechanism, the amount of wear experienced by the material can be quantified by Archards equation (Eq. 19.4) in terms of wear volume V_W, i.e. loss of mass occurring under specific load L on a specific sliding distance S:

$$V_W = k_w \frac{LS}{H} \tag{19.4}$$

where k_w and H are dimensionless wear coefficient and measure of hardness of the surface, respectively. The equation expresses the proportionality of wear volume to the work done by friction forces and may have different variants depending on how volume and sliding distance are expressed. The wear volume is typically expressed in the units of volume, e.g. [mm^3], or mass [g] determined for specified sliding path or number of cycles. It can be also normalized and expressed as wear rate, for instance [mm^3/year], or as a linear wear rate (depth of penetration), in [μm/year]. In case of adhesive wear, the coefficient k_w can be interpreted as the proportion of asperity contacts resulting in wear, thus never exceeding the value of one. An example wear rate of CoCr MoM determined from retrieved implants is in the order of 5 μm/year [39]. Due to variability of the wear coefficient associated with the changing physiological conditions numerical prediction of implant wear is difficult even when complex geometry of the triboelement is accounted for [40].

A straightforward consequence of Eq. 19.4 is that an optimum material for a biotribological application must be both hard and produce low friction coefficient in the system. The use of material couplings of low friction coefficient has been introduced already in the beginnings of joint replacement technology; however, these tend to fail in the long run due to wear of the softer material.

Corrosion and Wear Combined

A tribological element working in a corrosive environment inevitably experiences tribocorrosion. The term is sometimes restricted to situations when synergy between corrosion and wear damage takes place, i.e. the total degradation rate is larger (or less often smaller) than a simple sum of the two individual effects. Although the individual phenomena of corrosion and wear are relatively well described a detailed understanding of tribocorrosion is still missing because of the experimental difficulties in following the multitude of simultaneously undergoing reactions in which metastable products and reactants are often included. Tribocorrosive degradation affects a number of engineering systems like pumps, propellers, impellers, valves, mill liners etc. and is commonly described phenomenologically by the total material loss V expressed by Eq. 19.5:

$$V = V_W + V_C + S_{WC} \tag{19.5}$$

where V_W, V_C and S_{WC} are the mass loss due to wear in the absence of corrosion, mass loss due to corrosion in the absence of wear and the synergistic interaction term, respectively. Guidelines for experimental determination of S_{WC} are given by the ASTM standard [41].

The synergy between corrosion and wear (S_{WC}) can be generally separated into wear enhanced corrosion, i.e. the increase of corrosion rate than

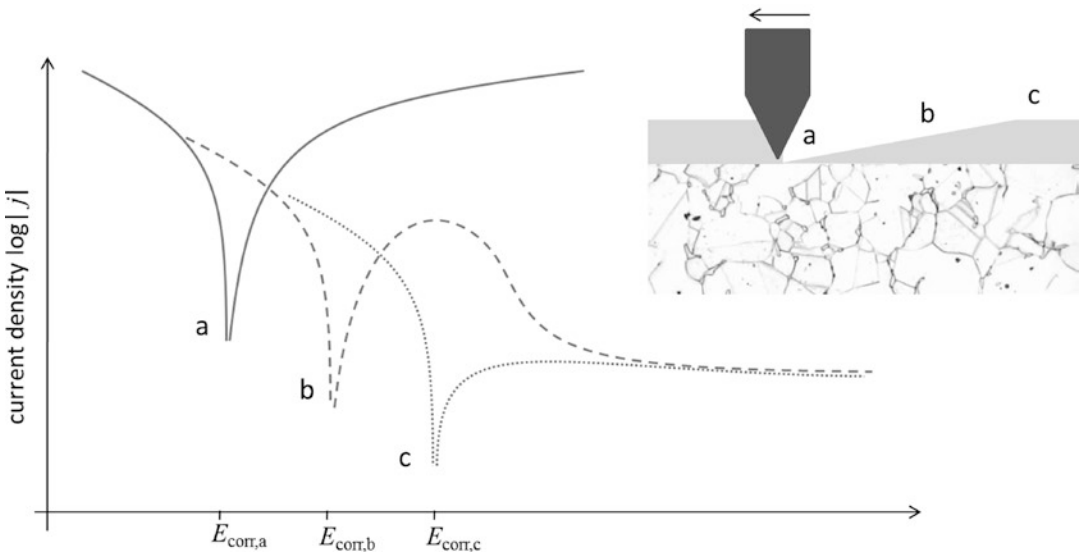

Fig. 19.5 Schematic explanation of the effect of removing passive layer on the polarization curve of the metal. The letters indicate curves associated with particular instance during recovery of the passive layer after scratching

can be attributed to wear, and corrosion enhanced wear, i.e. the increase of wear that can be attributed to corrosion.

Wear enhanced corrosion is most pronounced in the active-passive material. Since corrosion resistance of these materials relies on the presence of a thin passive layer (1–10 nm) any instance of its discontinuity results in an immediate onset of localized corrosion. Because all the wear mechanisms involve damage of the passive layer high current corrosion following the Bulter-Volmer kinetics (Eq. 19.3) is the immediate consequence at the places where bare metal is exposed to the environment. This situation is depicted schematically in Fig. 19.5 as case "a". Although the layer might recover relatively fast in the process of repassivation there exists a time in which the metal follows an accelerated corrosion kinetics prior establishing its steady-state passive behavior depicted in Fig. 19.5 as case "c". In case of CoCrMo alloys repassivation takes about 5 s in 0.9 % NaCl solution [42] and it seems to be much slower in case of Ti-alloys [43]. Both kinetics of oxide growth and mechanical as well as topological properties of the debris present in lubricant both have an effect in this wear accelerated corrosion. In consequence, changing friction conditions during different stages of the walking cycle results in varying rate of corrosion [38]. Further, adsorption of organic molecules such as serum albumin may reduce the repassivation kinetics as shown for Ti-alloys [44], whereas osteoblastic cells seeded over Ti6Al4V alloy was shown to prevent damage to the passive film [45]. It should be noted that in absence of a passive film, the localized deformation of asperities induced by wear may also accelerate the rate of corrosion. In this case, the shape of curve "a" in Fig. 19.5 would not change while wear damage progresses. Rather the entire curve would be shifted towards higher values of electric current.

In case of coated alloys, for instance CrN-coated stainless steel, the galvanic interaction between the different alloys may further contribute to corrosion-wear [46]. Galvanic interaction between the sliding/rolling surfaces may lead to increase of roughness and thus increase of friction. Also, the plastic deformation of coating resulting in micro-cracks or other coating defects may enable the galvanic coupling between the coating material and the substrate. An example of this mechanism is the blistering of TiN coated Ti-alloys [47].

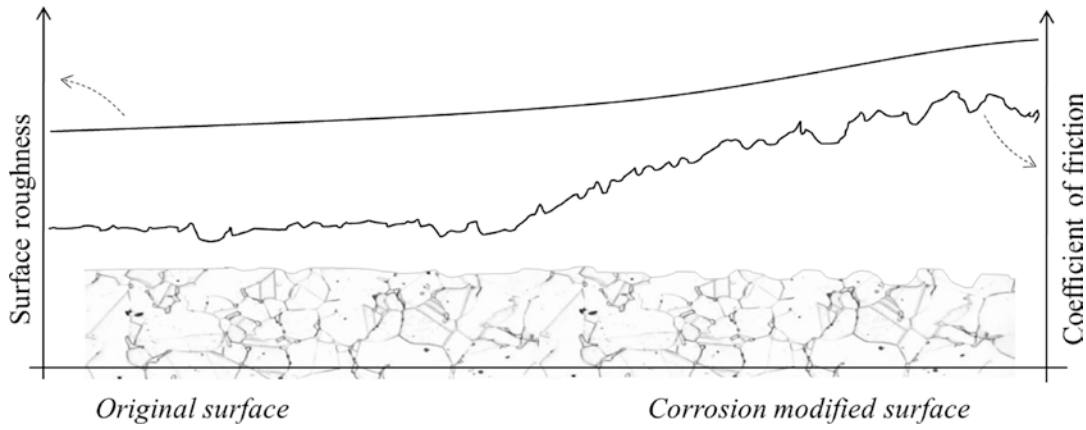

Fig. 19.6 Schematic representation of the relationship between corrosion, surface roughness and the coefficient of friction

Corrosion enhanced wear is the product of several alterations that corrosion may introduce to the triboelement. The most direct is the change of surface topology associated with dissolution and oxidation of the metallic surface. Since free corrosion (with no external potential applied) distributes anodic and cathodic processes over the same surface, inhomogeneity arises that in general results in increased roughness, which in turn increases the coefficient of friction (Fig. 19.6). A related mechanism is that of localized modification of material properties of the substrate that results in increased wear rate. The amount of corrosion enhanced wear can be determined by polarizing the metal cathodically, which disables the anodic dissolution by providing the electrons externally. Using this method an example of 22–32 % contribution of corrosion to wear enhancement has been shown for a CoCrMo alloy [48].

Further, when the oxide formed by corrosion is much harder than the metal itself, there might be a significant acceleration of wear, even when sliding against a much softer counterface. The soft counterface can provide a resilient bed for abrasive particles of oxide, leading to rapid wear of the metallic surface through the two-body abrasion mechanism (Fig. 19.4b). An example of this corrosion-abrasion mechanism are the Ti-Al-V alloys experiencing rapid wear even in contact with a soft UHMWPE counterface [49].

In order to estimate apriori the rate of surface degradation various mechanisms and combination thereof must be taken into account. An example of such combined model considering mechanical wear by plastic deformation at asperities, wear accelerated corrosion in addition to the hydrodynamic lubrication theory was shown to work for a CoCrMo sliding tribocorrosion contact [50]. The contribution of wear enhanced corrosion to the total material loss measured in a hip simulator for a CoCrMo MoM couple is about 13 % [51]. However, the relative importance of different wear mechanisms may vary when the tribological conditions change.

One possibility of visualizing the interdependence of tribocorrosion mechanism on the distinct environmental parameters is through mapping [52]. The idea of a tribocorrosion map, first introduced for technical problems and then adapted to biological systems [53], is that of representing the intensity of material waste in function of two process parameters. The analogy with a topographic map is that the contour lines of the terrain (constant elevation over the sea level) are the analogy of constant rate of waste, whereas the spatial coordinates correspond with variables modifying the waste mechanism. The variables that are relevant to consider for biotribocorrosion

are velocity of sliding, applied load as well as composition of the lubricating film [54].

In order to construct the map, the contribution of each variable to the total material loss (Eq. 19.5) must be determined separately. The total mass loss rate (K), hereafter considered in the normalized units of mass per area per time, i.e. $kg \cdot m^{-2}s^{-1}$, is separated the individual contributions considering the interactions between corrosion and wear:

$$K = K_W + K_C + K_{W-C} + K_{C-W} \qquad (19.6)$$

where K_W, K_C, K_{W-C}, K_{C-W} are the mass loss rates due to wear only, corrosion only, wear enhanced corrosion and corrosion enhanced wear, respectively. The experimental determination of each contribution relies on suppressing the contribution of one of the mechanisms. For instance, cathodic polarization of the metal surface (application of potential negative with respect to the corrosion potential E_{corr}) disables the anodic dissolution of the metal and thus prevents corrosion. With the mass loss rates determined experimentally, two basic types of map can be constructed.

Intensity map, where each contour line corresponds with a constant mass loss rate. The regions of high, medium and low wastage can be defined arbitrary, depending on the utility of the map. In the example shown in Fig. 19.7a, the regimes of mass loss rate are the following:

Low: $K \leq 10^{-7}$ $[g \cdot cm^{-2}min^{-1}]$
Medium: $10^{-7} < K \leq 20 \times 10^{-7}$ $[g \cdot cm^{-2}min^{-1}]$
High: $20 \times 10^{-7} < K$ $[g \cdot cm^{-2}min^{-1}]$

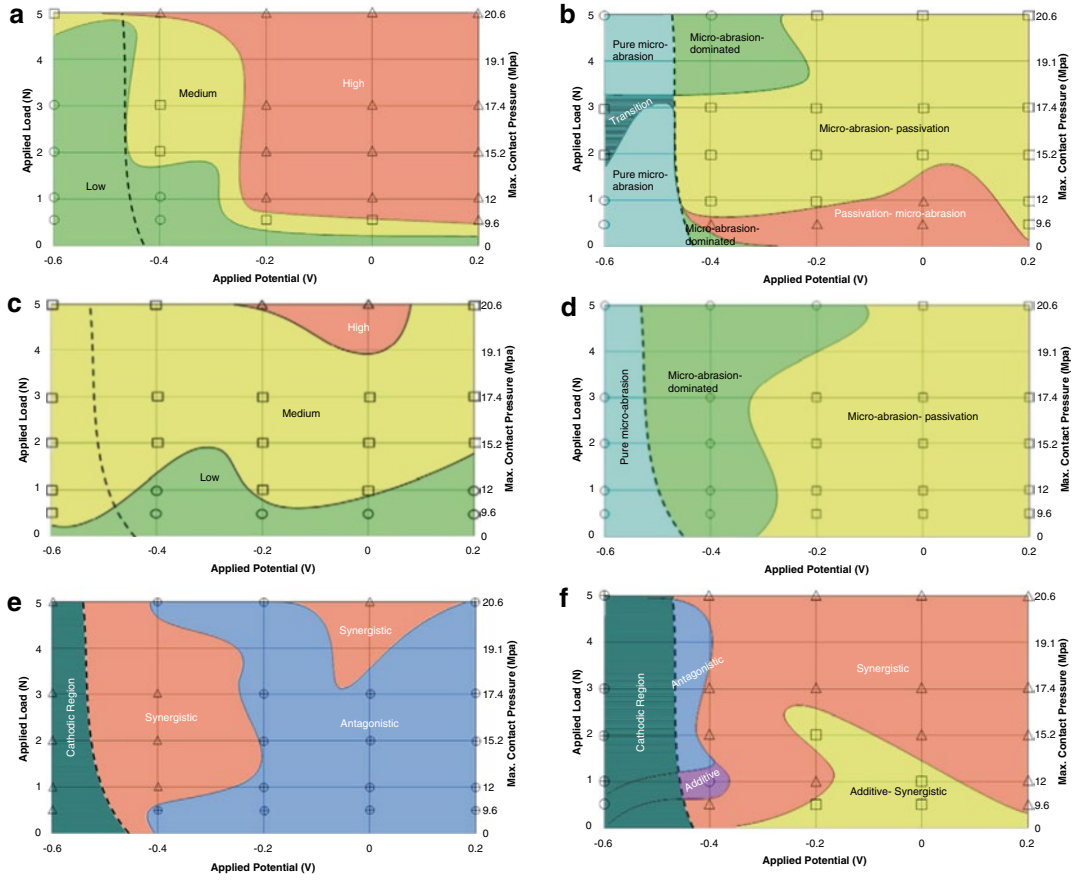

Fig. 19.7 An example of tribocorrosion map obtained by micro-abrasion of flat CoCrMo alloy sliding against a rotating UHMWPE ball in an FCS solution: (**a**) intensity view, and (**b**) mechanistic view. (Adapted from K. Sadiq, M. M. Stack, and R. a. Black, "Wear mapping of CoCrMo alloy in simulated bio-tribocorrosion conditions of a hip prosthesis bearing in calf serum solution," Mater. Sci. Eng. C, vol. 49, pp. 452–462, 2015, with permission.)

Mechanistic map, where each contour line correspond with transition from one dominant corrosion-wear mechanism to another. In the example shown in Fig. 19.7b, the following regimes were defined:

Micro-abrasion dominated:

$$\frac{K_C + K_{W-C}}{K_W + K_{C-W}} \leq 0.1$$

Micro-abrasion/Passivation:

$$0.1 < \frac{K_C + K_{W-C}}{K_W + K_{C-W}} \leq 1$$

Passivation/Micro-abrasion:

$$1 < \frac{K_C + K_{W-C}}{K_W + K_{C-W}} \leq 10$$

Passivation dominated: $10 < \frac{K_C + K_{W-C}}{K_W + K_{C-W}}$

In this example, the term wear was replaced with a more specific term abrasion and the term corrosion was replaced with passivation which is the specific corrosive mechanism interacting with abrasion.

Although mapping corrosion-wear makes a significant contribution to understanding the dynamic changes between the dominating mechanisms, comparison of literature data on rates of mass loss is difficult because loading and kinematic conditions are taken from different sources or do no necessary correspond with those of a real articulation in motion. The limitations underline the difficulty of a realistic theoretical description of the hip implant tribological behavior, increased by the complex model solution.

Clinical Implications of Biotribocorrosion

All the possible adverse effects of tribocorrosion on the functioning of the biological system can attributed to the very processes associated with a working triboelement (Fig. 19.3). Although the wear rate of most implant bearings is fairly low as compared with technical systems, the amount of metal and other tribocorrosion products released to the body can be considerable and the side effects associated with wear debris are considered a limiting factor in introducing MoM bearings in disc arthroplasty [55]. Although, the wear volume alone is often insufficient as an indicator of potential danger because biological reactions may also be sensitive to the number, size as well as size distribution of the wear debris. For instance, nanoscale metallic particles are less likely to produce a reaction than less numerous but larger particles of polyethylene.

Due to complex nature of the processes taking place in a functioning articulation, no integrated model of the effect of tribocorrosion is yet available. From the mechanistic point of view, the adverse reactions can be attributed to either wear enhanced corrosion (including corrosion alone) and/or corrosion enhanced wear (including wear alone). In the first case, the effects are analogous with the previously described effects of corrosion alone. In the second case, the root cause of undesired reactions is the presence of debris. Motion of debris particles can be described by employing the EHL theory of lubrication as shown for an artificial hip joint [56]. However, the particles do not necessary remain encapsulated and may affect other organs.

The adverse effects attributed to tribocorrosion debris where shown to include:

- Increased levels of metal ions in blood due to further corrosion of the metallic debris. Just like in case of corrosion alone, these metal ions may be distributed and accumulated in various organs. The accumulation might also take place for metallic particles, for instance in the para-aortic lymph nodes, the liver and spleen leading to granulomas [57].
- Hypersensitivity reaction, which may be immediate, e.g. [58], or delayed, e.g. [59], and which used to be associated with aseptic lymphocytic vasculitis-associated lesions [59].
- Pseudotumors, soft-tissue mass associated with the implant neither, however mostly resulting in pain [60]. The prevalence of pseudotumors does not necessarily correlate with elevated metal ion levels after MoM [61].

- Osteolysis resulting from the biological reaction to wear debris [62, 63].
- Lymphocyte proliferation due to contact with nanoparticle debris [64].
- Aseptic loosening due to adverse response to wear debris, e.g. [29, 57].
- Mechanical fracture of the implant due to surface generated cracks, e.g. [65].
- Infection due to interference of wear debris with the immune system and or inhibition or acceleration of bacterial growth [66].

The collection of variety of symptoms including inflammatory masses (pseudo-tumor), fluid collections, localized soft tissue necrosis, and histological evidence of a dense lymphocytic chronic inflammatory infiltrate is often referred to as adverse local tissue response (ALTR) and has been identified as one of the four failure modes in modular femoral stems by the review of Esposito et al. [67]. However, the local tissue reaction is generally mild and the effect of continued elevated levels of metal ions not known [57].

It should be kept in mind that the tissue reaction around implant surface is multifactorial in nature, whereas the parameters associated with functioning of the triboelement are not necessarily the most important. Factors like individual patient immunoreactivity [68] or even gender [69] should also be taken into account for predicting the long term outcome of a arthroplasty because the correlation between the necessity of revision, metal release, and material category is not straightforward [70–72].

Methods of Testing

Tribocorrosion of biological systems is difficult to test due to complexity of surface structure and large number of the involved processes. The most accurate prediction of triboelement performance is obtained from testing the element itself; however, laboratory testing is unavoidable for the obvious reason of limiting experiments on living organisms.

Due to the corrosion and wear synergy, experimental separation as well as combination of corrosion and wear is necessary in order to determine how each system parameter affects the tribological performance. A typical sequence of testing goes from laboratory, through simulated joints to in-vivo test, whereas the complexity of testing conditions increases. In general, when a new material is developed it should first meet certain standard in a corrosion test before being considered for tribological testing.

The summary of the testing methods is shown in Table 19.1 gives the overview of applicability with respect to the mechanism considered

Table 19.1 Summary of testing methodologies for mechanistic studies of tribocorrosion of biomedical systems

	Corrosion	Wear-enhanced corrosion	Wear	Corrosion-enhanced wear	Total tribocorrosion
Laboratory	Electrochemical testing Weight-loss testing	Additional corrosion current caused by sliding/abrasion	Wear test under cathodic polarization	Wear test under anodic polarization Difference between total weight-loss and data for corrosion, wear and wear-enhanced corrosion	Total weight-loss
Joint similator	Not applicable	Additional corrosion current when in motion	Weight-loss under cathodic polarization	Wear test under anodic polarization Difference between total weight-loss and data for corrosion, wear and wear-enhanced corrosion	Total weight-loss
In-vivo	Not applicable	Not applicable	Not applicable	Not applicable	Testing retrieved implants Imaging techniques of implants in use

and type of test. In the following, each method is explained briefly.

Laboratory Testing

Testing in laboratory offers the most variety of techniques for testing the individual contributions to tribocorrosion.

Electrochemical testing is one of the methods of evaluating the risk of corrosion. The other alternative is determination of weight loss and evaluation of possible occurrence of localized corrosion in a long-term exposition. Electrochemical testing relies on the analysis of electric potential and electric currents that flow through the interface between an electronic conductor (metal) and ionic conductor (electrolyte). The metal is the coated or uncoated implant, whereas the choice of electrolyte depends on the environment that is to be simulated. Typically, it is a buffered aqueous solution with a physiological content of salts used at body-specific temperature, but proteins are often added in order to account for the possible interference of adsorbed molecules. Table 19.2 summarizes the composition of electrolytes customarily used in biotribocorrosion testing. All solutions are obtained by dissolving chemicals of high purity grade in deionized water [73].

Prior electrochemical testing, surface treatment must be employed in order to clean the surface. Unlike wear testing, setting this initial condition of metal is crucial for accuracy of the results. The most common method is polishing (chemical and/or mechanical depending of type of metal) followed by removing debris in ultrasonic bath and degreasing with acetone.

The weight-loss due to corrosion is estimated by determining the rate of corrosion (V_{corr}), which in turn is determined from the amount of charge exchanged per unit of area in a unit of time, i.e. corrosion current. It should be kept in mind that corrosion current is sensitive to the composition of the electrolyte, temperature, movement of the solution, metal history, and other parameters [74]. In this context, an electrochemical cell is employed, in general, with a three electrodes configuration shown in Fig. 19.8. Reference electrode provides a reference potential in order to determine the potential of the polarized surface. Typical electrodes are Ag/AgCl and saturated calomel electrode (SCE). Counter electrode, also referred to as auxiliary electrode, provides additional surface for completing intensively undergoing reactions and also serves for precise measurement of electric current. Typical materials are Pt gauze electrode and graphite. Working electrode, i.e. the element being tested, can be of any form, for instance a rod (Fig. 19.8a) or flat surface (Fig. 19.8b), but must be of known surface area. The electrochemical measurements are completed using a potentiostat/galvanostat controlled by a computer. In practice, the kinetics of a corroding metal is characterized by determining parameters such as corrosion current density (j_{corr}), Tafel slopes (b_a, b_c), polarization resistance (R_p), oxide resistance (R_{ox}), film resistance (R_f), etc. [7, 8]. These electrochemical parameters can also be obtained by electrochemical impedance

Table 19.2 Composition of typical electrolytes used in biotribocorrosion testing

Solution	NaCl (g/L)	KCl (g/L)	$NaHCO_3$ (g/L)	$CaCl_2$ (g/L)	NaH_2PO_4 (g/L)	Na_2S (g/L)	Urea (g/L)	KH_2PO_4 (g/L)	Others (g/L)	pH
Ringer's	9.00	0.43	0.20	0.24	–	–	–	–		7.4
Hank's	8.00	0.40	0–0.35	0–0.19	0.050	–	–	–	1.00–10.00[a]	7.2–7.6
Fusuyama's	0.40	0.40	–	0.91	0.69	0.005	1.00	–	–	5.3
PBS[c]	8.00	0.20	–	0–0.13	1.42	–	–	0.24	–	7.4
SBF[d]	8.04	0.23	0.35	0.29	0	–	–	0.23	7.094[b]	7.4

[a]d-glucose, phenol red, $MgSO_4$
[b]$MgCl_2 \cdot H_2O$, HCl, Na_2SO_4, tris (hydroxylmethyl) aminomethane
[c]Phosphate buffered saline
[d]Simulated body fluids

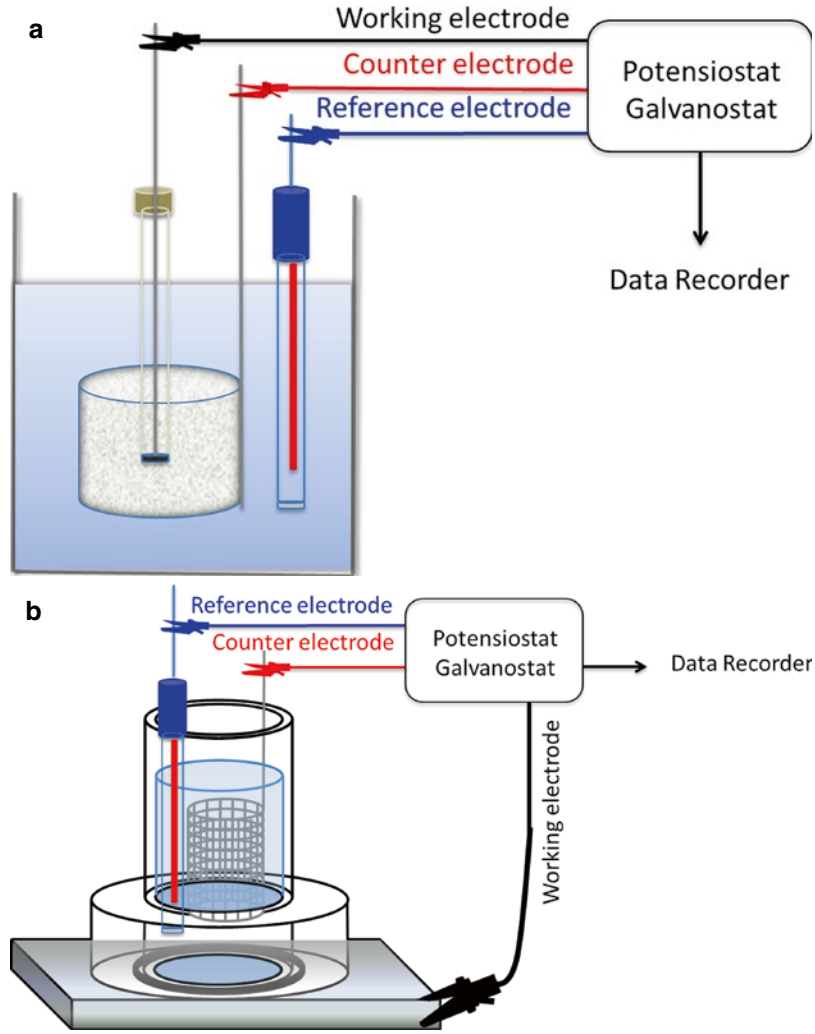

Fig. 19.8 Schematic drawing of an electrochemical cell: (**a**) working electrode (test sample) consists of a metal rod of known area; (**b**) working electrode consists of a plate of known area

spectroscopy (EIS) [75]. The technique can be employed at E_{corr} or under polarization using a sinusoidal signal over a range of frequencies, which provides a frequency specific response that can be interpreted through application of a circuit model to determine the above mentioned quantities as well as parameters charactering the interface between electron and ionic conductivity [9, 75–77]. On the other hand, Tafel slopes and corrosion potential (E_{corr}) are determined through a polarization experiment (Fig. 19.2) or simply by monitoring the value of OCP [77]. Figure 19.9 shows schematically a typical polarization curve which is plotted in a logarithmic scale for the range of potentials near OCP.

It should be noted that the significance of temperature is given by Eqs. 19.1 and 19.2, which describe its impact on electrochemical equilibrium and kinetics of corrosion that allows determine E_{corr} and j_{corr}, respectively.

Whereas so formulated simulation of body fluid serves for the electrochemical characterization it does not necessarily provide necessary condition for the testing of wear. The structure of the adsorbed layer is very sensitive to the presence of surface active agents and other potentially chemisorbing molecules. Finally, to approach the real case of implanted metal the influence of living cells should also be considered. The presence of living cells is similar to biologically

induced corrosion associated with the presence of bacteria. The formation of local concentration cells and obstruction of diffusion can have both accelerating and inhibiting effect on materials degradation.

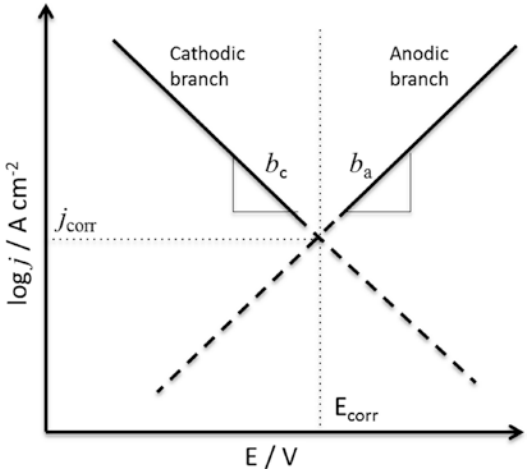

Fig. 19.9 Schematic representation of a polarization curve near corrosion potential. Dashed lines correspond with Tafel slopes b_a, b_c

Tribological testing relies on the use of a tribometer in which two bodies are set in mutual motion under controlled conditions. Typical configurations are those of a flat surface (disc or plate) being scrubbed by a counter-body shaped as a pin, ball or a ring (Fig. 19.10). The test body can be either the pin, the ring, the ball, the disc, or the plate depending on which one is controlled for the loss of weight/volume and/or inspected for surface chemistry and topology after the test. Due to limitations of common surface characterization techniques, the test sample is typically chosen to be the flat one; however, inverse configurations are also used in cases when characterization of weight loss is sufficient for evaluation. The effect of body weight is simulated by applying mechanical force perpendicular to the test surface.

The wear scar can be obtained in a continuous (Fig. 19.10b, d, f) or intermittent manner

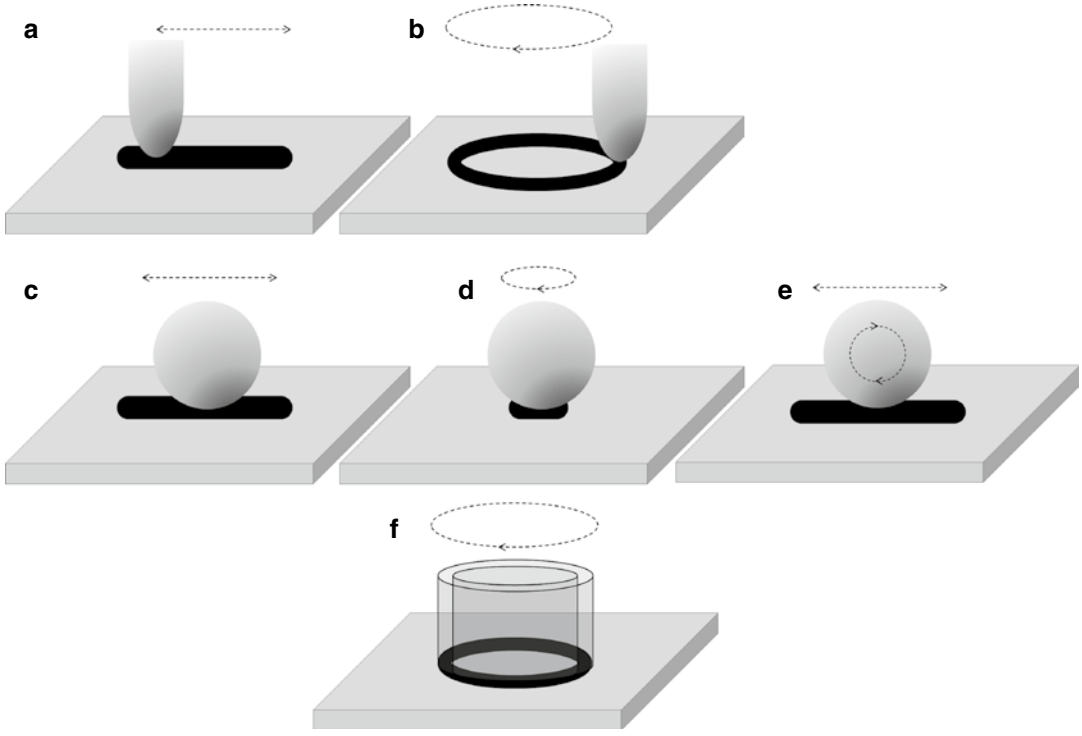

Fig. 19.10 Possible configurations of tribometers employed in tribological testing of biomedical materials: (**a**, **b**) fin on disc, (**c**–**e**) ball on disc, (**f**) ring on disc. The dashed lines indicate the direction in which the counter-body moves (or rotates). The resulting wear scar is indicated in black

(Fig. 19.10a, c). Unlike the continuous mode, the intermittent one involves the change in direction of motion and is therefore referred to as reciprocal. Rotation of the counter-body (Fig. 19.10e) allows for including the effect of rolling wear associated with surface fatigue.

Tribological testing of biomaterials is often conducted in an aqueous lubricant (electrolyte), thus the effect of corrosion is accounted for but cannot be separated nor quantified. Both constant volume and flow-through of the electrolyte are feasible. In the first case, corrosion and wear products accumulate simulating the physiological condition; however debris particles may undergo attrition. Testing in the flow-through condition allows exploring the effect of debris particle shape and size. In order to facilitate continuous flow of the lubricant, the arrangement is rotated so that the flat surface is vertical and the lubricant can flow down freely.

Tribocorrosion testing allows for the mechanistic separation of corrosion and wear in a single testing apparatus. A typical set-up consists in one of the configurations presented in Fig. 19.10 arranged in the modality of electrochemical testing by adding reference and counter electrodes to be in ionic contact with the lubricating electrolyte and connecting the entire system to a computer controlled potentiostat/galvanostat with the test body being the working electrode. The contribution of corrosion can be suppressed by cathodic polarization of the working electrode, which provides electrons externally to sustain the cathodic reaction while the anodic metal dissolution and possible oxidation remain suppressed.

In contrast to technical components such as automobile transmission shafts, the mechanical conditions in biotribocorrosion are much more varied considering the periods of increased mechanical load during walking or running followed by practically no tribological contribution during sleep. In the periods of rest free corrosion is expected, whereas mobility would enhance the contribution of wear depending on the combination of normal and shear stresses imposed during physical activity. It is also known that the wear rate of a tribocorrosion element stabilizes only after several test cycles with initial wear rate being at least one order of magnitude faster as comparted with the wear rate of the steady-state [78]. In order to address these constraints, a typical testing protocol consists in a combination of phases distinctive by the applied load, normal and shear components considered separately. Although several norms have been developed, e.g. [79], that prescribe the test sequence there is no protocol that would provide because of the multitude of human gait conditions and activities performed by individuals [80].

Joint simulators are a special type of tribometers that allow for testing the complex geometries of actual implants in simulated dynamic physiological conditions. The main purpose is to predict the clinical performance of prospective materials, which has been shown feasible in some aspects [81, 82]. A simulator can be programmed to simulate loading cycles of walking or running, including a daily cycle of its intensity. By now, the use of hip joint simulators is a well-established method providing good prediction of the long-term clinical performance, a reason for which it is routinely used in quality control as well as the development of new material concepts. However, severe conditions such as presence of unexpected third body, edge wear or ageing of the materials may results in wear patterns that are impossibly reproduced by standardized testing [83].

In Vivo Testing

Testing and evaluating an implanted material is the only accurate indicator of its performance in use. In-vivo studies are of outmost importance for the understanding of real case but uncovering the mechanistic corrosion-wear relationships is rather unlikely because of the variety of implant systems and uniqueness of every patient.

Examination of retrieved implants permits the evaluation of weight loss by the gravimetric method, however the mass gain due to adsorbed tribofilm as well as possible fluid absorption should be taken into account [83–85]. Surface of the retrieved implant can be further analyzed to determine its composition, topography

and morphology. An alternative to the gravimetric method is the use of coordinate measuring machine, which allows a three dimensional comparison of the worn surface with its original geometry. The method has been shown applicable to both hip [86] and knee implants [87], although its accuracy depends on the number of points and the mathematical algorithm used for reconstructing the surface.

Imagining techniques rely on stereometric analysis of the implanted device. Both X-ray as well as MRI images can be used and the basic idea is the geometrical reconstruction of the implant and its comparison with known initial dimension or and image obtained shortly after implantation.

Instrumented hip joint is a recent development based on the idea of equipping the implant with an electronic system collecting data and sending them wirelessly to a receiver. So far, only systems for measuring mechanical forces were developed allowing the determination of contact forces and friction moments in vivo during walking [29, 88]. However, measuring corrosion currents or wear rates in-vivo is for now a distant perspective.

Mitigation of Biotribocorrosion

Degradation of implants by tribocorrosion is unavoidable due to physical nature of the involved processes. The best option of mitigation is an intervention aiming at reducing and/or controlling the rate of corrosion and wear. However, the methods of cathodic protection, application of corrosion inhibitors and modification of the lubricant known to be efficient in technical applications are not viable for arthroplasty and the options are limited to materials selection, surface modification and mitigation through design. Whereas materials selection permits the most efficient reduction of tribocorrosion damage, the choices for implants are limited due to the laborious and demanding process of clinical trials and market admission. Modification of surface and design are the in fact the only practical options for improving performance of implants.

The function of a surface modification is to lower the coefficient of friction and to prevent the release of ions and debris particles. An additional function might be considered in preventing bacterial attack or improving general biocompatibility. A distinction is made between surface coating and surface treatment. Both types of modification may involve relative shift of the surface level (thickening/thinning) as well as change in chemical composition of the surface layer, but only surface coating results in the formation of a clear interface between the base material and the additional surface layer. Whereas coating always implies deposition of a new material, surface treatment may be completed without any chemical change. Typical ranges of thickness for the various types of surface modifications applicable to implants are summarized in Fig. 19.11.

Surface Coating

Modification of materials functionality through coating is one of the oldest approaches to improving durability of materials but only the newest developments are applicable to implants due the requirements of biocompatibility. The prospective coating must produce excellent adherence with the substrate in order to prevent its delamination. Further requirements include hardness slightly lower than that of the counter-body to prevent excessive wear of the counter-body, elastic modulus similar to the substrate material to assure synchronous deformation in the elastic range and sufficiently high fracture toughness to avoid fracture. Surface chemistry should also be such as to produce soft tribofilms on both counter parts in order to prevent formation of hard debris. In order to meet all the requirements only advanced fabrication techniques are feasible.

Physical vapor deposition (PVD) allows condensing coatings from the vapor phase. The process is completed in a vacuum chamber in which the native oxide can be removed at the atomic level assuring good adhesion of the coating. Modification of the process by including plasma in the ionization of coating's precursor allows completing the deposition at lower temperatures and thus preventing alterations of the substrate

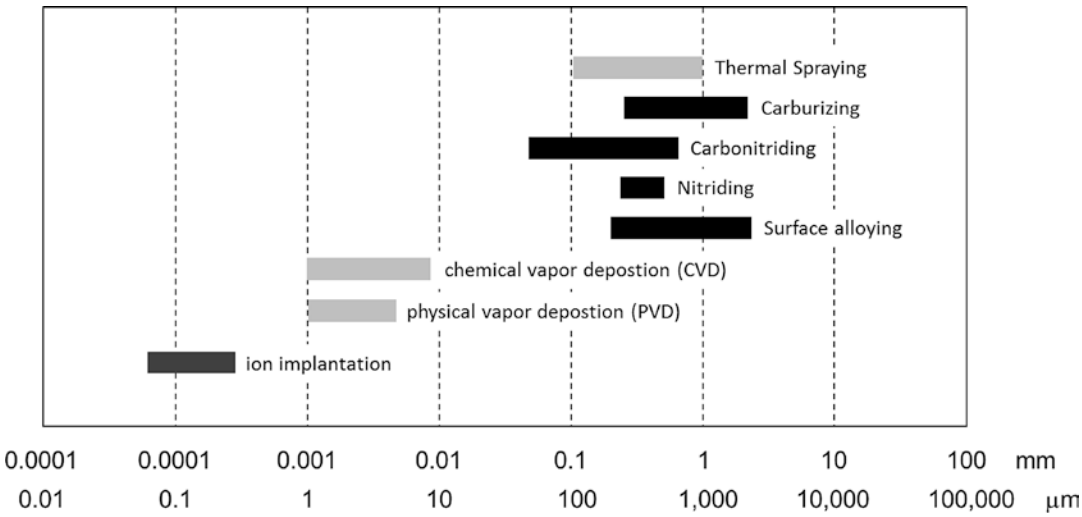

Fig. 19.11 Thickness surface layer affected by surface modification techniques employed or studied for biomedical applications

microstructure. This process is known as plasma enhanced (PE-PVD), sometimes referred to as plasma assisted (PA-PVD). An alternative of vapor deposition is chemical vapor deposition (CVD) where the precursor is introduced in the gaseous form and the coating is completed by chemical reaction between the precursor and substrate. When the occurrence of chemical reactions is promoted by creation of plasma, the method is referred to as plasma enhanced CVD or PE-CVD. Thermal spraying consists in projecting heated or molten particles with high velocity onto the substrate. The kinetic energy acquired by acceleration promotes melting and formation of a continuous coating. Molten salts produce coating by metallurgical reaction between the substrate and metal ions present in the salt, analogous to hot dip galvanizing.

The classification of coatings considers either their chemical composition, distinguishing between metallic and inorganic coatings, or their microstructure, distinguishing between single, multilayer coatings and gradient coatings. A multilayer coating containing only few interlayers is referred to as sandwich. Gradient coatings are characterized by a gradual change of chemical composition with no interface between areas of distinctive chemical composition.

Table 19.3 summarizes examples of coatings that have been considered for metallic implants. All of them show improved tirbocorrosion performance as compared with the bare metal alloy. Amorphous carbon (a-C) and diamond-like coatings (DLC) are sometimes considered synonymous due to lack of crystallinity and similarity in chemical composition. Although, the amorphous structure is not necessarily the same (polyamorphism) and some authors distinguish DLC due to similarity of some of its properties to those of diamond. In general, all the a-C coatings seem to provide a fair reduction of corrosion-wear damage. Its been reported that DLC coating on a Ti-alloy produce bigger particles in lower number which could reduce the risk of pseudotumors and necrosis [89].

The current research frontiers focus on multilayer and gradient coatings which provide more flexibility in combining corrosion and wear properties, whereas the mechanical properties are tuned by adjusting the sequence of layers or intensity of gradients.

Surface Treatment

Metallic surface can be modified by treatments aiming at changing its chemical composition, microstructure, topography or combination thereof. Table 19.4 summarizes examples of treatments that have been considered for modification of implants.

Table 19.3 Summary of surface coatings considered for mitigation of biotribocorrosion

Method	Coating thickness	Metal alloy	Counter body	Lubricant	Test method	Reported results	Ref
PA-PVD	a-C/a-C:Ti (multilayer) ~1.8 µm	Ti6Al4V	Al_2O_3 (ball)	Pure water	Ball-on-flat (reciprocating)	Good adherence. Resist $5 \cdot 10^6$ cycles without failure	[90]
PVD (magnetron sputtering)	a-C/a-C:Ti (multilayer) ~2.1 µm	Ti6Al4V	Si_3N_4 (ball)	Hank's solution	Ball-on-disk	Excellent mechanical properties and extremely improved tribological properties compared with a-C single layer films Low friction coefficient	[91]
PA-PVD	DLC 2 µm	ASTM F1537-08 (CoCr)	ASTM F75/98	Fetal bovine serum solution at 25 %	Hip joint simulator (multi-station)	DLC reduces wear up to 5 times.	[92]
PVD	DLC (multilayer) 2–3 µm	Ti6Al4V	WC (ball)	Not specified	Ball-on-flat (reciprocating)	Decreases the wear rate Produce debris with bigger size	[89]
PE-CVD	a_SiN_x/DLC (sandwich) 350/650 nm	316 L	Al_2O_3 (ball)	NaCl 1 wt % solution	Ball-on-flat (reciprocating)	Increased the corrosion resistance, and assures high wear resistance and low friction	[93]
PA-PVD	CrN 3.75 µm	ASTM F1537-08 (CoCr)	ASTM F75/98	Fetal bovine serum solution 25 vol %	Hip joint simulator	CrN reduces wear up to 55 times.	[92]
PVD	CrNi <10 µm	CoCrMo	CoCrMo	25 %vol newborn bovine serum with 0.1 % (w/v) sodium azide	Hip joint simulator	Wear reduced by 80 % Ion release reduced by 73 % and 98 % Reduced ion release of Cr and Co	[94]
PVD	CrTi 2.4–4.2 µm	Ti6Al4V	Al_2O_3 (ball)	0.9 % NaCl solution	Ball-on-flat (reciprocating)	Reduction in corrosion–wear by up to 40 times	[95]
PVD	FeCrNi 2.3–3.0 µm	AISI 316 L	Al_2O_3 (ball)	0.89 % NaCl solution	Pin-on-plate (reciprocating)	Increasing the Cr content of the surface cause a significant reduction in the total area material loss under potentiostatic conditions.	[96]
Thermal treatment in molten salts	Ta/TaC/Ta_2C (sandwich) 0.3–1 µm	CoCrMo	Al_2O_3 (ball) Polyethylene (pin)	calf bovine serum 25 vol%	Ball on disk (continuous sliding) Pin-on-disk (continuous sliding)	Hardness increased more than double with respect to the untreated alloys. Prominently improve in wear resistance; it reduces the wear volume and rate of about one order of magnitude.	[97]

Thermal treatment in molten salts	Ta_xC_{1-x} (single and multilayer, 500–600 nm)	Co–Cr–Mo	Al_2O_3 (ball) Polyethylene (pin)	Bovine serum 25 vol%	Ball on disk (continuous sliding) Pin-on-disk (continuous sliding)	Lower friction coefficient Higher wear resistance and adhesion	[98]
PVD	Ta_xC_{1-x} (1.2 µm)	316 L	WC + 6 %Co (ball)	Phosphate buffered saline (PBS)	Pin on disk test	Excellent wear resistance Improve corrosion resistance	[99]
PVD	TiN TiNbN TiCN	316 L	UHMWPE (pin)	Bovine serum albumin Hank's solution	Pin-on-disk (rotating)	Good biocompatibility Wear reduced in the presence of bovine serum albumine	[100]
PA-PVD	TiN/CrN (multilayer) 3.25 µm	ASTM F1537-08 (CoCr)	ASTM F75/98	Fetal bovine serum solution 25 vol%	Hip joint simulator	(TiN/CrN)×3 reduces wear up to 8 times	[92]

Table 19.4 Summary of surface treatments considered for mitigation of biotribocorrosion

Method	Modification Affected thickness	Metal alloy	Counter body	Lubricant	Test method	Results	Ref
Thermal oxidation	Artificial oxide 7.5 µm	Ti6Al4V	UHMWPE	Bovine serum 25 vol%	Pin-on-flat (reciprocating)	Coefficient of friction decreased 77.6 % while wear volumes decreased 68 %	[101]
Thermal oxidation	Artificial oxide 0.8–2.4 µm	CP-Ti Ti6Al4V	Al_2O_3 (ball)	0.89 wt % NaCl solution	Ball-on-flat (reciprocating)	Improves corrosion–wear resistance	[102]
PIII (oxygen)	Artificial oxide (10–15 nm)	Co28Cr6Mo	CoCr (ball) UHMWPE (ball)	Hank's solution	Ball-on-disk (reciprocating)	Friction coefficient reduced from 0.36 to below 0.1 Wear results showed important decreases in wear rate	[103]
Plasma surface alloying	Artificial oxide 5 µm	CP-Ti	GCr15 (ball)	dry	Ball-on-disk	Excellent mechanical and wear resistant properties.	[104]
Plasma oxidation	Artificial oxide 2–15 µm	CoCrMo	Al_2O_3 (ball)	Simulated Body Fluid (SBF)	Pin-on-disc	Increases wear resistance and microhardness.	[105]
PIII (carbon)	Carburizing 110–190 nm	Ti6Al4V	Al_2O_3 (ball)	Dry	Ball-on-disk (reciprocating)	Tribological properties improvement between 44 and 65 % of carbon concentration Enhancement in sliding performance	[106]
Plasma carburizing	carburizing <20 µm	ASTM F2581-07	WC (ball)	Ringer's solution	Ball-on-disk (reciprocating)	Improve wear resistance in 140 % during the Reciprocating ball test, improve the fretting wear resistance and considerably reduces the friction coefficient.	[107]
PIII (nitrogen)	Nitriding 5 µm	CoCr	Al_2O_3 (ball)	Simulated body fluid (SBF)	Ball-on-disk (continuous sliding)	Below 400°C to achieve an optimal interplay between low wear rates and high corrosion resistance	[108]
Plasma nitriding	Nitriding 2–8 µm	CoCrMo	CoCrMo	25 % bovine serum solution	Pin-on-disc	Lower wear rate and higher wear resistance. Typical hardness values are Increased almost two times	[109]
PIII (nitrogen)	CrN precipitation	CoCrMo	Si_3N_4 (ball)	Simulated body fluid (NBS)	Ball-on-flat	Enhances hardness, corrosion and tribocorrosion properties. Reduces the friction coefficient from 0.35 to 0.15.	[110]
Laser surface melting (LSM)	Surface melting <1199 µm	Ti6Al4V	100Cr6 steel (ball)	Simulated body fluids (SBF)	Ball-on-disk (reciprocating)	Lower in vitro wear than untreated surfaces.	[111]
Laser patterning	Surface patterning 0.02–0.04 µm	CoCrMo	Al_2O_3 (ring)	Calf serum solution 25 vol%	Ring-on-disc (ISO 6474)	Better performance than flat polished surfaces. The volume of free wear debris could be decreased by about eight times.	[112]

Plasma carburizing	S-phase 8 µm	Co–28Cr–10Mo ASTM F1537	Al_2O_3 (ball)	Ringer's solution	Pin-on-disc	High hardness, excellent repassivation ability and good corrosion and wear resistance.	[113]
Plasma surface alloying	S-phase 50 nm	316 (ball)	ASTM F138 ASTM F1586 (steel plate)	Ringer's solution	Ball-on-disk (reciprocating)	Improve wear resistance due an increase of surface hardness Makes it possible for austenitic stainless steel to slide against austenitic stainless steel without causing scuffing or seizure	[114]
Micro-machining	Surface texturing (honing) 3.4–4.2 µm	CoCrMo	CoCrMo	Synthetic lubricant (5 W/30)	Hip joint simulator	Reductions in static friction coefficient by 50 % Reduction in dynamic friction coefficient by 38 %	[115]

Change of chemical composition can be obtained through thermal treatment or implantation of foreign ions. Thermal treatment consists in exposition to oxidizing atmosphere in which a protective oxide layer is formed and its properties are superior to the native oxide. Because the layer attains structure and composition different to the one formed in typical conditions of use, the oxide is referred to as artificial. Implantation of ions is a general description to several processes that result in insertion of individual atoms, mostly in ionized form, into the surface layer. In case of carbon and nitrogen, the process is referred to as carburizing and nitriding, respectively. Both are well-known metallurgical methods of improving hardness of alloys through microstructure modificiation. All the processes of ion implantation can be followed by thermal treatment (superficial or entire piece) in which the foreign atoms spread towards the bulk increasing the depth of modification and possibly resulting in the formation of precipitates. A special case of ion implantation is the formation of carbon supersaturated solid solution, so called S-phase, characterized by superior hardness and corrosion resistance.

The techniques explored for modification of surface topology involve laser surface melting and laser patterning. Laser surface melting (LSM) is achieved by focusing laser beam on the surface of a metal and thus transferring sufficient energy produce solid to liquid phase transformation. The beam is then scanned over the surface to cover the desired area of treatment. Due to short interaction time, bulk of the material does not increase its temperature and the microstructure of the molten and solidified metal is distinctive through its metastable character. On the other hand, laser surface patterning requires the use of two or more beams which are brought into interference and the interference pattern is then imprinted in the surface layer by the same principle of energy transfer as used in LSM.

Design Aspects

Much of the corrosion-wear damage can be reduced considering the possible degradation already when designing the device. Both material choice as well as definition of the geometry may improve the tribocorrosion life of the implant.

The straightforward focus in selecting material are the options that have proven promising the laboratory testing. However, it should be kept in mind that bringing two metals in contact in the same volume of an electrolyte, which is the case in modular design of dissimilar metals, might produce the effect of galvanic corrosion. In this case, the metal characterized by low corrosion current may accelerate the rate of corrosion by an order of magnitude or more when in contact with a more noble metal; i.e. metal that has a higher corrosion potential when immersed alone. An example of this type of accelerated corrosion was reported on retrieved MoM THR where corrosion of CoCr was accelerated by contact with a Ti-alloy [116].

The choice of geometry and topology also affects biotribocorrosion performance of implant. In THR, 36-mm metal femoral heads were shown to produce increased corrosion as compared with 28-mm heads [117]. Hip simulator studies indicate that smaller clearance allows reducing running-in wear [118]. Esposito et al. provided a review of the design features associated with tribocorrosion of taper junctions [67]. Trunnion length, trunnion diameter, and taper angle are parameters thought to contribute to tribocorrosion; however, there is disagreement as to whether a thinner and shorter taper is more beneficial than a longer, thicker one.

The more we know about the parameters determining biotribocorrosion the more reliable models can be constructed that would allow predicting the risk of particular corrosion-wear problem to occur at given mechanical and chemical conditions. An example of employing numerical modeling to predict corrosion at the head-neck contact indicate that limiting angular mismatch and centering offset could be helpful [119].

Acknowledgement This work has been supported by Fondo Nacional de Desarollo Cientifico y Technologico Chile (FONDECYT), project N°1121085 and project N°1141107.

References

1. Ryu JJ, Letchuman S, Shrotriya P. Roughness evolution of metallic implant surfaces under contact loading and nanometer-scale chemical etching. J Mech Behav Biomed Mater. 2012;14:55–66.

2. Fischer A, Weiß S, Wimmer MA. The tribological difference between biomedical steels and CoCrMo-alloys. J Mech Behav Biomed Mater. 2012;9:50–62.
3. Malkin AI. Regularities and mechanisms of the Rehbinder's effect. Colloid J. 2012;74(2):223–38.
4. Hesketh J, Ward M, Dowson D, Neville A. The composition of tribofilms produced on metal-on-metal hip bearings. Biomaterials. 2014;35(7):2113–9.
5. Mathew MT, Nagelli C, Pourzal R, Fischer A, Laurent MP, Jacobs JJ, Wimmer MA. Tribolayer formation in a metal-on-metal (MoM) hip joint: an electrochemical investigation. J Mech Behav Biomed Mater. 2014;29:199–212.
6. Perez N. Electrochemistry and corrosion science. Springer Science & Business Media, Springer US. 2004.
7. Marcus P. Corrosion mechanisms in theory and practice. 2nd ed. New York: Marcel Dekker Inc; 2002.
8. Chen Y, Xu Z, Smith C, Sankar J. Recent advances on the development of magnesium alloys for biodegradable implants. Acta Biomater. 2014;10(11):4561–73.
9. Ruzickova M, Hildebrand H, Virtanen S. On the stability of passivity of Ti-Al alloys in acidic environment. Z Phys Chem. 2005;219(11):1447–59.
10. Geetha M, Singh AK, Asokamani R, Gogia AK. Ti based biomaterials, the ultimate choice for orthopaedic implants – A review. Prog Mater Sci. 2009;54(3):397–425.
11. Silva-Bermudez P, Rodil SE. An overview of protein adsorption on metal oxide coatings for biomedical implants. Surf Coat Technol. 2013;233:147–58.
12. Cruz HV, Souza JCM, Henriques M, Rocha LA, Tribocorrosion and bio- tribocorrosion in the oral environment : the case of dental implants, In: J. Paulo Davim, editor. Biomedical Tribology. Nova Science Publishers, Inc. no. July 2015. 2011.
13. Williams DF. On the mechanisms of biocompatibility. Biomaterials. 2008;29(20):2941–53.
14. Wang X, Li Y, Xiong J, Hodgson PD, Wen C. Porous TiNbZr alloy scaffolds for biomedical applications. Acta Biomater. 2009;5(9):3616–24.
15. Wen CE, Yamada Y, Shimojima K, Chino Y, Hosokawa H, Mabuchi M. Novel titanium foam for bone tissue engineering. J Mater Res. 2002;17(10):2633–9.
16. Variola F, Brunski JB, Orsini G, Tambasco de Oliveira P, Wazen R, Nanci A. Nanoscale surface modifications of medically relevant metals: state-of-the art and perspectives. Nanoscale. 2011;3(2):335–53.
17. Dohan Ehrenfest DM, Coelho PG, Kang BS, Sul YT, Albrektsson T. Classification of osseointegrated implant surfaces: materials, chemistry and topography. Trends Biotechnol. 2010;28(4):198–206.
18. Eisenbarth E, Velten D, Müller M, Thull R, Breme J. Biocompatibility of β-stabilizing elements of titanium alloys. Biomaterials. 2004;25(26):5705–13.
19. Han M-J, Choe H-C, Chung C-H. Surface characteristics of clinically used dental implant screws. Met Mater Int. 2005;11(6):449–56.
20. Schiff N, Grosgogeat B, Lissac M, Dalard F. Influence of fluoride content and pH on the corrosion resistance of titanium and its alloys. Biomaterials. 2002;23(9):1995–2002.
21. Bergmann G, Graichen F, Rohlmann A, Verdonschot N, Van Lenthe GH. Frictional heating of total hip implants. Part 2: finite element study. J Biomech. 2001;34(4):429–35.
22. Li S, Chien S, Brånemark PI. Heat shock-induced necrosis and apoptosis in osteoblasts. J Orthop Res. 1999;17(6):891–9.
23. Wang C, Wang Y. Tribology of endoprostheses. In: Poitout D, editor. Biomechanics and biomaterials in orthopedics SE – 16. London: Springer; 2004. p. 168–78.
24. Farhoudi H, Oskouei RH, Jones CF, Taylor M. A novel analytical approach for determining the frictional moments and torques acting on modular femoral components in total hip replacements. J Biomech. 2015;48(6):976–83.
25. Dumbleton JH. Tribology of natural and artificial joints. New York: Elsevier; 1981.
26. Brockett C, Williams S, Zhongmin J, Isaac G, Fisher J. Friction of total hip replacements with different bearings and loading conditions. J Biomed Mater Res B Appl Biomater. 2007;81B(2):508–15.
27. Kim K, Geringer J, Pellier J, MacDonald DD. Fretting corrosion damage of total hip prosthesis: friction coefficient and damage rate constant approach. Tribol Int. 2013;60:10–8.
28. Fan N, Morlock MM, Bishop NE, Huber G, Hoffmann N, Ciavarella M, Chen GX, Hothan A, Witt F. The influence of stem design on critical squeaking friction with ceramic bearings. J Orthop Res. 2013;31(10):1627–32.
29. Damm P, Dymke J, Ackermann R, Bender A, Graichen F, Halder A, Beier A, Bergmann G. Friction in total hip joint prosthesis measured in vivo during walking. PLoS One. 2013;8(11):1–8.
30. Myant C, Underwood R, Fan J, Cann PM. Lubrication of metal-on-metal hip joints: the effect of protein content and load on film formation and wear. J Mech Behav Biomed Mater. 2012;6:30–40.
31. Tozzi G, Zhang Q, Tong J. Microdamage assessment of bone-cement interfaces under monotonic and cyclic compression. J Biomech. 2014;47(14):3466–74.
32. Janssen D, Mann KA, Verdonschot N. Finite element simulation of cement-bone interface micromechanics: a comparison to experimental results. J Orthop Res. 2009;27(10):1312–8.
33. ASTM International G40-13. Standard terminology relating to wear and erosion. ASTM B. Stand. Vol. 03.02; 2013.
34. Alonso Gil R, Igual Muñoz A. Influence of the sliding velocity and the applied potential on the corrosion and wear behavior of HC CoCrMo biomedical alloy in simulated body fluids. J Mech Behav Biomed Mater. 2011;4(8):2090–102.
35. Galetz MC, Seiferth SH, Theile B, Glatzel U. Potential for adhesive wear in friction couples of UHMWPE running against oxidized zirconium, titanium nitride coatings, and cobalt-chromium alloys. J Biomed Mater Res – Part B Appl Biomater. 2010;93(2):468–75.

36. Lee Y-S, Niinomi M, Nakai M, Narita K, Cho K. Predominant factor determining wear properties of β-type and (α+β)-type titanium alloys in metal-to-metal contact for biomedical applications. J Mech Behav Biomed Mater. 2015;41:208–20.
37. Brandt J-M, Gascoyne TC, Guenther LE, Allen A, Hedden DR, Turgeon TR, Bohm ER. Clinical failure analysis of contemporary ceramic-on-ceramic total hip replacements. Proc Inst Mech Eng H. 2013;227(8):833–46.
38. Hesketh J, Hu X, Yan Y, Dowson D, Neville A. Biotribocorrosion: some electrochemical observations from an instrumented hip joint simulator. Tribol Int. 2013;59:332–8.
39. Rieker CB, Koettig P, Schoen R, Windier M, Wyss UP. Clinical wear performance of metal-on-metal hip arthroplasties. In: Jacobs J, Craig T, editors. Alternative bearing surfaces in total joint replacement, ASTM STP 1346. 1998; p. 144–56.
40. Mattei L, Di Puccio F. Wear simulation of metal-on-metal hip replacements with frictional contact. J Tribol. 2013;135(2):021402.
41. ASTM International G119-09. Standard guide for determining amount of synergism between wear and corrosion. ASTM B. Stand. Vol. 03.02, 2009.
42. Sun D, Wharton JA, Wood RJK. Micro- and nano-scale tribo-corrosion of cast CoCrMo. Tribol Lett. 2011;41(3):525–33.
43. Diomidis N, Mischler S, More NS, Roy M. Tribo-electrochemical characterization of metallic biomaterials for total joint replacement. Acta Biomater. 2012;8(2):852–9.
44. Dimah MK, Devesa Albeza F, Amigó Borrás V, Igual Muñoz A. Study of the biotribocorrosion behaviour of titanium biomedical alloys in simulated body fluids by electrochemical techniques. Wear. 2012;294–295:409–18.
45. Runa MJ, Mathew MT, Fernandes MH, Rocha LA. First insight on the impact of an osteoblastic layer on the bio-tribocorrosion performance of Ti6Al4V hip implants. Acta Biomater. 2015;12:341–51.
46. Dearnley PA, Aldrich-Smith G. Corrosion-wear mechanisms of hard coated austenitic 316L stainless steels. Wear. 2004;256(5):491–9.
47. Komotori J, Lee B, Dong H, Dearnley P. Corrosion response of surface engineered titanium alloys damaged by prior abrasion. Wear. 2001;251(1–12):1239–49.
48. Yan Y, Neville A, Hesketh J, Dowson D. Real-time corrosion measurements to assess biotribocorrosion mechanisms with a hip simulator. Tribol Int. 2013;63:115–22.
49. Shi W, Dong H, Bell T. Tribological behaviour and microscopic wear mechanisms of UHMWPE sliding against thermal oxidation-treated Ti6A14V. Mater Sci Eng A. 2000;291(1–2):27–36.
50. Cao S, Guadalupe Maldonado S, Mischler S. Tribocorrosion of passive metals in the mixed lubrication regime: theoretical model and application to metal-on-metal artificial hip joints. Wear. 2015;324–325:55–63.
51. Hesketh J, Meng Q, Dowson D, Neville A. Biotribocorrosion of metal-on-metal hip replacements: How surface degradation can influence metal ion formation. Tribol Int. 2013;65:128–37.
52. Stack MM. Bridging the gap between tribology and corrosion: from wear maps to Pourbaix diagrams – Runner-up for the Guy Bengough Award, IoM3, 2007. Int Mater Rev. 2005;50(1):1–18.
53. Stack MM, Jawan H, Mathew MT, On the construction of micro-abrasion maps for a steel/polymer couple in corrosive environments. Tribol Int. 2005;38(9 SPEC. ISS):848–56.
54. Sadiq K, Stack MM, Black RA. Wear mapping of CoCrMo alloy in simulated bio-tribocorrosion conditions of a hip prosthesis bearing in calf serum solution. Mater Sci Eng C. 2015;49:452–62.
55. Golish SR, Anderson PA. Bearing surfaces for total disc arthroplasty: metal-on-metal versus metal-on-polyethylene and other biomaterials. Spine J. 2012;12(8):693–701.
56. Jhurani SM, Fred Higgs C. An elastohydrodynamic lubrication (EHL) model of wear particle migration in an artificial hip joint. Tribol Int. 2010;43(8):1326–38.
57. Dumbleton JH, Manley MT. Metal-on-metal total hip replacement: What does the literature say? J Arthroplasty. 2005;20(2):174–88.
58. Grosse S, Haugland HK, Lilleng P, Ellison P, Hallan G, Høl PJ. Wear particles and ions from cemented and uncemented titanium-based hip prostheses-A histological and chemical analysis of retrieval material. J Biomed Mater Res Part B Appl Biomater. 2015;103(3):709–17.
59. Willert H-G, Buchhorn GH, Fayyazi A, Flury R, Windler M, Köster G, Lohmann CH. Metal-on-metal bearings and hypersensitivity in patients with artificial hip joints. A clinical and histomorphological study. J Bone Joint Surg Am. 2005;87(1):28–36.
60. Pandit H, Whitwell D, Gibbons CLM, Athanasou N, Gill HS, Murray DW. Pseudotumours associated with metal-on- metal hip resurfacings. J Bone Joint Surg. 2008;90(7):847–51.
61. Bayley N, Khan H, Grosso P, Hupel T, Stevens D, Snider M, Schemitsch E, Kuzyk P. What are the predictors and prevalence of pseudotumor and elevated metal ions after large-diameter metal-on-metal THA? Clin Orthop Relat Res. 2014;473(2):477–84.
62. Magone K, Luckenbill D, Goswami T. Metal ions as inflammatory initiators of osteolysis. Arch Orthop Trauma Surg. 2015;135(5):683–95.
63. Gustafson K, Jakobsen SS, Lorenzen ND, Thyssen JP, Johansen JD, Bonefeld CM, Stilling M, Baad-Hansen T, Søballe K. Metal release and metal allergy after total hip replacement with resurfacing versus conventional hybrid prosthesis. Acta Orthop. 2014;85(4):348–54.
64. osada OM, Tate RJ, Grant MH. Toxicity of cobalt-chromium nanoparticles released from a resurfacing hip implant and cobalt ions on primary human lymphocytes in vitro. J Appl Toxicol. 2015;35(6):614–22.
65. Gilbert JL, Mali S, Urban RM, Silverton CD, Jacobs JJ. In vivo oxide-induced stress corrosion cracking

of Ti-6Al-4V in a neck-stem modular taper: emergent behavior in a new mechanism of in vivo corrosion. J Biomed Mater Res – Part B Appl Biomater. 2012;100(2):584–94.
66. Hosman AH, van der Mei HC, Bulstra SK, Busscher HJ, Neut D. Effects of metal-on-metal wear on the host immune system and infection in hip arthroplasty. Acta Orthop. 2010;81(5):526–34.
67. Esposito CI, Wright TM, Goodman SB, Berry DJ. What is the trouble with trunnions? Clin Orthop Relat Res. 2014;472:3652–8.
68. Ebramzadeh E, Campbell P, Tan TL, Nelson SD, Sangiorgio SN. Can wear explain the histological variation around metal-on-metal total hips? Clin Orthop Relat Res. 2014;473(2):487–94.
69. Latteier MJ, Berend KR, Lombardi AV, Ajluni AF, Seng BE, Adams JB. Gender is a significant factor for failure of metal-on-metal total hip arthroplasty. J Arthroplasty. 2011;26 Suppl 6:19–23.
70. Jakobsen SS, Lidén C, Søballe K, Johansen JD, Menné T, Lundgren L, Bregnbak D, Møller P, Jellesen MS, Thyssen JP. Failure of total hip implants: metals and metal release in 52 cases. Contact Dermatitis. 2014;71(6):319–25.
71. Mattei L, Di Puccio F, Piccigallo B, Ciulli E. Lubrication and wear modelling of artificial hip joints: a review. Tribol Int. 2011;44(5):532–49.
72. Mattei L, Di Puccio F, Ciulli E. A comparative study of wear laws for soft-on-hard hip implants using a mathematical wear model. Tribol Int. 2013;63:66–77.
73. ASTM International G31-12a/NACE TM0169. Standard guide for laboratory immersion corrosion testing of metals. ASTM B. Stand. Vol. 03.02. 2012.
74. Bard AJ, Faulkner LR. Electrochemical methods: fundamentals and applications. 2nd ed. New York: Wiley; 2001.
75. Orazem ME, Tribollet B. Electrochemical impedance spectroscopy, vol. 48. Hoboken: Wiley; 2008.
76. Barão VA, Mathew MT, Assunção WG, Yuan JC, Wimmer MA, Sukotjo C. The role of lipopolysaccharide on the electrochemical behavior of titanium. J Dent Res. 2011;90(5):613–8.
77. Perez N. Electrochemistry and corrosion science. Dordrecht: Springer Science & Business Media, Springer US. 2004.
78. Dowson D, Hardaker C, Flett M, Isaac GH. A hip joint simulator study of the performance of metal-on-metal joints: part I: the role of materials. J Arthroplasty. 2004;19(8 Suppl):118–23.
79. ISO 14242-1:2014 – Implants for surgery – Wear of total hip-joint prostheses – Part 1: Loading and displacement parameters for wear-testing machines and corresponding environmental conditions for test. [Online]. Available: http://www.iso.org/iso/home/store/catalogue_ics/catalogue_detail_ics.htm?csnumber=63073. Accessed 29 July 2015.
80. Oliveira ALL, Trigo FC, Martins FPR. Quantitative evaluation of parameters used in wear testing simulators of total hip arthroplasty components. Wear. 2014;313(1–2):1–10.
81. Affatato S, Spinelli M, Zavalloni M, Mazzega-Fabbro C, Viceconti M. Tribology and total hip joint replacement: current concepts in mechanical simulation. Med Eng Phys. 2008;30(10):1305–17.
82. Asseman F. Comments on 'tribology and total hip joint replacement: current concepts in mechanical simulation' [Med. Eng. Phys. 2008;30:1305–17]. Med Eng Phys. 2009;31(6):730.
83. Zietz C, Fabry C, Reinders J, Dammer R, Kretzer JP, Bader R, Sonntag R. Wear testing of total hip replacements under severe conditions. Expert Rev Med Devices. 2015;12(4):393–410.
84. Grillini L, Affatato S. How to measure wear following total hip arthroplasty. Hip Int. 2013;23(3):233–42.
85. Krismer M, Biedermann R. How to measure wear following total hip arthroplasty – EBRA not mentioned! Letter to the Editor and Authors' response. Hip Int. 2014;24(6):664–5.
86. Lu Z, McKellop HA. Accuracy of methods for calculating volumetric wear from coordinate measuring machine data of retrieved metal-on-metal hip joint implants. Proc Inst Mech Eng Part H J Eng Med. 2014;228(3):237–49.
87. Knowlton CB, Wimmer MA. An autonomous mathematical reconstruction to effectively measure volume loss on retrieved polyethylene tibial inserts. J Biomed Mater Res – Part B Appl Biomater. 2013;101 B(3):449–57.
88. Damm P, Bender A, Bergmann G. Postoperative changes in in vivo measured friction in total hip joint prosthesis during walking. PLoS One. 2015;10(3):e0120438.
89. Oliveira LYS, Kuromoto NK, Siqueira CJM. Treating orthopedic prosthesis with diamond-like carbon: minimizing debris in Ti6Al4V. J Mater Sci Mater Med. 2014;25(10):2347–55.
90. Österle W, Klaffke D, Griepentrog M, Gross U, Kranz I, Knabe C. Potential of wear resistant coatings on Ti-6Al-4V for artificial hip joint bearing surfaces. Wear. 2008;264(7–8):505–17.
91. Cai JB, Wang XL, Bai WQ, Wang DH, Gu CD, Tu JP. Microstructure, mechanical and tribological properties Of A-C/A-C:Ti nanomultilayer film. Surf Coat Technol. 2013;232:403–11.
92. Ortega-Saenz JA, Alvarez-Vera M, Hernandez-Rodriguez MAL. Biotribological study of multilayer coated metal-on-metal hip prostheses in a hip joint simulator. Wear. 2013;301(1–2):234–42.
93. Azzi M, Paquette M, Szpunar JA, Klemberg-Sapieha JE, Martinu L. Tribocorrosion behaviour of DLC-coated 316L stainless steel. Wear. 2009;267(5–8):860–6.
94. Leslie IJ, Williams S, Brown C, Anderson J, Isaac G, Hatto P, Ingham E, Fisher J. Surface engineering: a low wearing solution for metal-on-metal hip surface replacements. J Biomed Mater Res – Part B Appl Biomater. 2009;90(2):558–65.
95. Mallia B, Dearnley PA. The corrosion – wear response of Cr – Ti coatings. Wear. 2007;263:679–90.

96. Dearnley PA, Mallia B. The chemical wear (corrosion-wear) of novel Cr based hard coated 316L austenitic stainless steels in aqueous saline solution. Wear. 2012;306(1–2):263–75.
97. Balagna C, Faga MG, Spriano S. Tantalum-based multilayer coating on cobalt alloys in total hip and knee replacement. Mater Sci Eng C. 2012;32(4): 887–95.
98. Balagna C, Faga MG, Spriano S. Tribological behavior of a Ta-based coating on a Co-Cr-Mo alloy. Surf Coat Technol. 2014;258:1159–70.
99. Ding MH, Wang BL, Li L, Zheng YF. A study of TaxC1-x coatings deposited on biomedical 316L stainless steel by radio-frequency magnetron sputtering. Appl Surf Sci. 2010;257(3):696–703.
100. Serro AP, Completo C, Colaço R, dos Santos F, da Silva CL, Cabral JMS, Araújo H, Pires E, Saramago B. A comparative study of titanium nitrides, TiN, TiNbN and TiCN, as coatings for biomedical applications. Surf Coat Technol. 2009;203(24): 3701–7.
101. Wang S, Liu Y, Zhang C, Liao Z, Liu W. The improvement of wettability, biotribological behavior and corrosion resistance of titanium alloy pretreated by thermal oxidation. Tribol Int. 2014;79: 174–82.
102. Dearnley PA, Dahm KL, Çimenoğlu H. The corrosion-wear behaviour of thermally oxidised CP-Ti and Ti-6Al-4V. Wear. 2004;256(5):469–79.
103. García JA, Díaz C, Mändl S, Lutz J, Martínez R, Rodríguez RJ. Tribological improvements of plasma immersion implanted CoCr alloys. Surf Coat Technol. 2010;204(18–19):2928–32.
104. Qi H, Wu HY. Effect of surface modification of pure Ti on tribological and biological properties of bone tissue. Surf Eng. 2013;29(4):300–5.
105. Çelik A, Aslan M, Yetim AF, Bayrak Ö. Wear behavior of plasma oxidized cocrmo alloy under dry and simulated body fluid conditions. J Bionic Eng. 2014;11(2):303–10.
106. Pierret C, Maunoury L, Monnet I, Bouffard S, Benyagoub A, Grygiel C, Busardo D, Muller D, Höche D. Friction and wear properties modification of Ti-6Al-4V alloy surfaces by implantation of multicharged carbon ions. Wear. 2014;319(1–2):19–26.
107. Buhagiar J, Qian L, Dong H. Surface property enhancement of Ni-free medical grade austenitic stainless steel by low-temperature plasma carburising. Surf Coat Technol. 2010;205(2):388–95.
108. Lutz J, Mändl S. Reduced tribocorrosion of CoCr alloys in simulated body fluid after nitrogen insertion. Surf Coatings Technol. 2010;204(18–19):3043–6.
109. Wang Q, Zhang L, Dong J. Effects of plasma nitriding on microstructure and tribological properties of CoCrMo alloy implant materials. J Bionic Eng. 2010;7(4):337–44.
110. Guo Z, Pang X, Yan Y, Gao K, Volinsky AA, Zhang T-Y. CoCrMo alloy for orthopedic implant application enhanced corrosion and tribocorrosion properties by nitrogen ion implantation. Appl Surf Sci. 2015;347:23–34.
111. Balla VK, Soderlind J, Bose S, Bandyopadhyay A. Microstructure, mechanical and wear properties of laser surface melted Ti6Al4V alloy. J Mech Behav Biomed Mater. 2014;32:335–44.
112. Tarabolsi M, Klassen T, Mantwill F, Gärtner F, Siegel F, Schulz AP. Patterned CoCrMo and Al2O3 surfaces for reduced free wear debris in artificial joint arthroplasty. J Biomed Mater Res – Part A. 2013;101(12):3447–56.
113. Luo X, Li X, Sun Y, Dong H. Tribocorrosion behavior of S-phase surface engineered medical grade Co-Cr alloy. Wear. 2013;302(1–2):1615–23.
114. Buhagiar J, Jung A, Gouriou D, Mallia B, Dong H. S-phase against S-phase tribopairs for biomedical applications. Wear. 2013;301(1–2):280–9.
115. Choudhury D, Walker R, Roy T, Paul S, Mootanah R. Performance of honed surface profiles to artificial hip joints: an experimental investigation. Int J Precis Eng Man. 2013;14(10):1847–53.
116. Gascoyne TC, Dyrkacz RM, Turgeon TR, Burnell CD, Wyss UP, Brandt J-M. Corrosion on the acetabular liner taper from retrieved modular metal-on-metal total hip replacements. J Arthroplasty. 2014;29(10):2049–52.
117. Dyrkacz RMR, Brandt JM, Ojo OA, Turgeon TR, Wyss UP. The influence of head size on corrosion and fretting behaviour at the head-neck interface of artificial hip joints. J Arthroplasty. 2013;28(6):1036–40.
118. Kretzer JP, Kleinhans JA, Jakubowitz E, Thomsen M, Heisel C. A meta-analysis of design- and manufacturing-related parameters influencing the wear behavior of metal-on-metal hip joint replacements. J Orthop Res. 2009;27(11):1473–80.
119. Donaldson FE, Coburn JC, Siegel KL. Total hip arthroplasty head-neck contact mechanics: a stochastic investigation of key parameters. J Biomech. 2014;47(7):1634–41.

Massive Allografts: Techniques and Results with 30 Years' Follow-Up

20

Dominique G. Poitout

The use of preserved bone and cartilage is not a recent technique and since 1879 fresh and frozen grafts has been used in numerous cases. Since 1980 we have been using massive grafts preserved in the Bone Bank of Marseille created in 1978.

Reconstructive metal mega hip prosthesis are commonly used, but they might be responsible of mechanical failures or stability due to muscle non fixation. Autologous grafts, unlike allogenic grafts, have an important osteogenic potentie. But in as much as the procurement volume is limited, they do not permit massive bone or joint reconstruction when there has been partial or total resection as a result of either a bone tumor or a post-traumatic lack of substance.

For this reasons, we have elected since 1981 to use deep-frozen allogenic grafts to rebuild the skeleton. We have used since 1979 fresh allogenic bone grafts and, since 1981 deep-frozen, allogenic grafts to rebuild the skeleton:

1979–2015: 11.532 cases of spongious and massive allografts have been conserved in deep frozen liquid nitrogen

1981–2015: 835 massive bone allografts
1983–2015: 423 hip reconstructions
1985–2015: 278 massive osteochondral allografts.

Deep-freezing alone allows the preservation of voluminous bone pieces in satisfactory conditions of conservation.

This type of preservation keeps the bone architecture in an optimal biological and biomechanical state. Allografts allowing vascular recolonization and rapid muscle tightening give good functional results. We think that in some indications, it is better to use an osteochondral allograft or a mega prosthesis surrounded by allograft.

Allograft Biology

Immunology

Allografts are well incorporated by the skeleton. If osteoid or blood cells (mostly leukocytes) as well as blood vessels and nerves have an inner antigenic potenty, leading to immune reaction, the proteinic matrix and the minerals fixed on it are either non-antigenic or less antigenic.

Spongious bone of the donor is injected in the receiver when we make a multi tissue grafting (face or upper arms total grafting) to decrease the antigenetic reactions. Clinically speaking, the immunological reactions are almost non existent with the use of massive allografts (8 %).

D.G. Poitout, MD
Faculté de Médecine Nord, Sce Chirurgie Orthopédique et Traumatologie, Aix-Marseille Université, Centre Hospitalier et Universitaire Marseille North, Chemin des Bourrely, 13015 Marseille, France
e-mail: Dominique.POITOUT@ap-hm.fr

D.G. Poitout (ed.), *Biomechanics and Biomaterials in Orthopedics*,
DOI 10.1007/978-1-84882-664-9_20

Biological Integration

Spongious Allografts

Spongious allografts are evoluating in two successive phases. For about 3 weeks after the grafting, an osteogenic phase induced by the grafted cells may be observed. Then followed by a stop of several months (Burchardt 1983; Burchardt et al. 1978; Burwell & Gowland 1962) and a coming back of the osteogenesis under the dependence, at this time, of the guest's cells.

The spongious allografts are different form the cortical grafts, principally through the fact that the mechanism of their revascularization is effectuated by "creeping-substitution" and that the integration of this graft will be complete.

The time will be much shorter (about 3 weeks) for the vessels to penetrate into a spongious graft than to recolonize a cortical graft. The complete revascularization needs about 2 months.

Cortical Allograft

The rehabitation or cortical allografts begins with at first a phase of active resorption, which is quite normal during the first 2 weeks, intense for the following 4 weeks, and it is only about the 9th week that the osteoblasts will appear, inducing the beginning of the regeneration.

During this period the biomechanical behaviour of the graft decrease (50 % less at the 18th month) the stem orl the plate has to be strong enough by itself and well fixed in the receiver bone to support the body weight.

When we compare on the cat the evolution of massive autologous and osteochondral allografts, we see that they are evoluating quite similarly but the duration of the revascularization process is different.

The two types of grafting are revascularized and the dead bone replaced by a new bone through creeping apposition. The intensity of the reconstruction is more important between the sixth and the ninth months in the case of allografts, and between the third and the sixth months for the autografts. The material can be removed after 5 years.

Bone Allograft Technology

The Marseilles team collaborated with the Transfusional center to set up a bone bank on their premises because it has a competent cryobiology department equipped with storage tanks containing liquid nitrogen and a temperature-lowering programmer.

This laboratory, which for a long time has been storing bone marrow, platelets, and various cryopreserved tissues, has the virology, bacteriology, quality control, and quality assurance laboratories of the Blood Transfusion Service and is accustomed to applying the transfusion safety standards

It is also the first in France to obtain the approval of the Microbiological safety Committee of the Directorate General of Health in April 1996. Banks which were developed nationally have followed the same principles

Because the bone and cartilage fragments which are removed are not subjected to secondary sterilization, it is imperative that the therapeutic maneuvers are performed in wholly sterile conditions.

Selection of Donors

Has to be rigorous so that there is no risk of the transmission of iatrogenic pathology to the host through the graft. We have to know:

- History of the illness
- Circumstances of the accident
- Medical history of the donor*

They are absolute contra-indications:

- Cancerous conditions
- Systemic illness
- Collagenosis
- Auto-immune disease
- Bone dystrophy
- Viral, bacteriological, parasitic infection, mycosis or tuberculosis
- Artificial ventilation for more than 72 h

Bacterial decontamination using solution of antibiotics

Samples taken after decontamination and after thawing

Blood Samples taken to perform virological examinations

- Hepatitis B and C
- HIV
- HTLV
- Syphilis
- Transaminases
- Toxoplasmose
- Cytomegalovirus
- Epstein-Barr virus

Tissue are placed into quarantine and the virological tests repeated 4–6 month after the tissue has been removed. These samplings are performed either on the live donor or on the host of organs coming from the same donor.

Removal Techniques

Are made under the strictest aseptic conditions possible in an Orthopedic Operating theatre. The whole bone with cartilage, the ligaments and capsule, tendons and meniscus are put in sterile Capton-Teflon bags with antibiotics (Figs. 20.1 and 20.2). The reconstruction of the skeleton has to be perfect. Coding and Measuring of the Parts are made by X-Rays. Quality Controls are made every 6 months. 20 % of the grafts are rejected annually.

Preservation Techniques

Preservation Methods

Cryopreservation in liquid Nitrogen at – 196 °C is used to avoid the formation of ice macrocrystals, we used cryoprotector (10 % DMSO), but the DMSO is toxic at a temperature higher than 8 °C. So, we have to decrease les temperatures to 6° before been in contact with the graft.

We have determined an optimal curve for decreasing the temperature (2°/′ from 6° initial

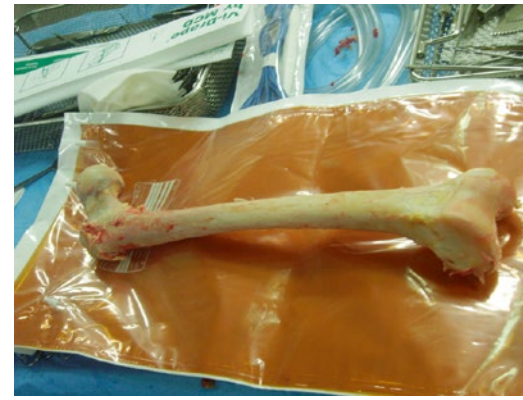

Fig. 20.1 Femur extracted

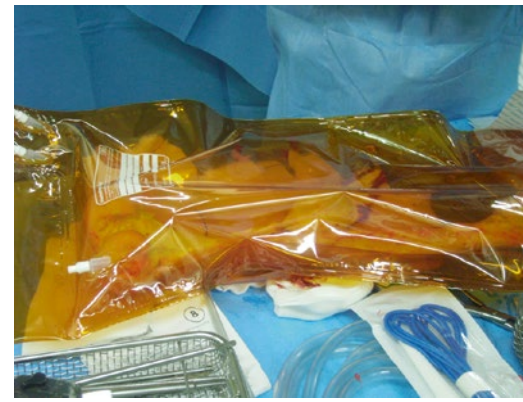

Fig. 20.2 Femur in the containing, sterile bag

–40 °C, then 5°/′ from –40 °C, –140 °C then put in liquid nitrogen at –196 °C) and rapid thawing in physiological à 41 °C permit the use of the graft after 30 min

Biomechanics and Immunology

Mechanical strength of the cortical allograft is only 50–60 % of the strength of normal bone during a period ranging from the 8th to the 18th month after the graft has been implanted. The fixation of the graft has to be perfect with a perfect contact between the recipient bone and the allograft.

Mechanical properties of the allograft can be changed by the preservation and storage processes (no irradiation – no heat – no ethylenoxyde – no acetone)

The preservation of the ligament structures, the capsule, and the meniscus is very important and the immunological response of the bone, the cartilaginous cells and ligament cells are very low. We can use immuno suppressants (like SANDIMMUM) if there is an immunological response (serosity surrounding the graft) (8 %) at the graft.

Transport

Can be made in liquid nitrogen or dry ice. If we use the graft with 12 h

We can thaw the fragment directly in the bone bank laboratory or in the operating room. We put it in sterile Liquid heated at 41 °C. It will also wash the DMSO from the tissue. After having thawed the graft we can use it for reconstruction of the skeleton in oncology, traumatology or loss of substance.

Massive Osteochondral Allografts

What is new is the knowledge of the Mechanism of Conservation and the behavior of Chondral Deep-Frozen Allografts:

- The chondrocytes has to be protected to be able to fix the water molecules on the glyco-amino-glycans present in the cartilage
- We cannot use a sterilisation by irradiation which would destroy all the cells and we have to use very carefully DMSO 10 % to stop massive ice cristal formation , not to impare the cartilaginous cellular function
- The cartilaginous tissue is deep frozen and conserved in Liquid nitrogen at – 196 °C
- The Cartilaginous Matrix has to have a normal tightness to protect the Chondrocytes
- The sub-chondral bone has to be vascularized to survive, but the Cartilaginous cells only needs synovial fluid imbibition
- The Cartilaginous cells are not replaced, and the one seen some years after grafting are those initially present in the graft
- The Cartilage is a special tissue which don't give immune response
- If we have an immune response it is because of the surrounding tissue
- Taken apart each component of the cartilage give an immunological response but when we graft the whole cartilage, there is no réaction

Material and Methods

1983–2012: 278 Patients had Massives Ostéochondral Allografts 197 Females/81 Males

- 27 Cases of Massive Osteochondral Acetabulum
- 3 total femoral reconstruction with osteochondrome femoral licard?? placed in the osteochondral acetabulum of the recipient
- 173 Patients with Knee reconstructions
  - Trochlea (29 cases)
  - Condyle (68 cases)
  - Patella (7 cases)
  - Tibial plateau (46 cases)
  - Total Lower part of Femur (14 cases)
  - Total upper part of Tibia (9 cases)

Some (specially in traumatologic cases) had different diseases

- 7 Cases of Wrist reconstruction
- 48 Cases of Shoulder reconstruction
- 16 Cases of Total Elbow reconstruction
- 7 Cases of Radius reconstruction

Used for

- especially Oncologic diseases (73 % of the cases)
- but also Traumatic Surgery (21 % of the cases)
- and Iterative surgery (6 % of the cases)

Oncology

Most of the time we use Conservative treatment in oncologic surgery

Technical problems can lead to amputation

But the final Aim is to save the patient life and to make him have a good function (Lumbo salvage surgery)

The absolute contra-indications are:

- Voluminous Tumor
- Infected Tumor
- Skin Recoverage Problems
- Malpositioned Biopsy

The relative Contra-indications are:

- Irradiated Tumor
- Very young patient

The result depends on the quality of the resection of the Tumor (Contaminated, Marginal, Large or Radical)

Traumatology

Most of our cases are surrounding the Knee but also at the upper arm.

- Osteonecrosis
- Lack of substance
- Destruction of the Condyle, Trochlea or Tibial Plateau but also Elbow, and Schoulder

Iterative Operations

Specially at the Hip Joint and Knee

Results

Globally

The analysis of the function of the graft is made during the time of survival in Oncologic diseases. For the survival cases and the other nononcologic cases the Follow-up is of 28 Years: Good muscular and Ligamentary fixation in 76 % of the cases. Good healing at the junction. Allograft-Recipient Bone in 92 % of the cases. Good integration of the graft in 88 % of the cases. Immunological reactions occurred in 12 % of the cases.

Arthrosis and articular destruction occurred in 14 % of the cases due to ligamentary instability.

No more infections (4 %) occurred than occur in massive reconstructions especially when we use chemotherapy. Joint function was excellent in 131 Cases (76 %), Good in 17 Cases (10 %) Bad in 24 Cases (14 %).

In the hip, We obtained good function and no arthrosis with the Acétabulum reconstruction; even the size of the grafted cotyle is not exactly the same as the recipient femoral head.

In the knee joint, The function dépend of the stability of the graft and specially the ligamentary refixation.

In the shoulder, we have had some Necrosis of the Humeral head (4 cases) so that we use now more often Metal prosthesis surrounded by allograft . We have also to take care of the holes made in the upper part of the graft to fix the tendons on it. It can frgilize the graft and make it brake (3 Cases).

In the elbow, the initial function is satisfactoring but after some years (Brooks et al. 1969; Brown & Crues 1982; Burchardt & Enneking 1978; Burchardt 1983; Burchardt et al. 1978; Burwell & Gowland 1962; Burwell 1963; Burwell 1969; Burwell 1976; Burwell et al. 1963; Carr & Hyatt 1955; Carrel A. La conservation des tissus et ses applications en chirurgie. J Am Med- Techniques chirurgicales orthopédique 1984; Chalmers 1959) most of the joint become instable due to loosening of the ligaments fixing the elbow and the articular component destroy themselves but without pain.

Discussion: Global Follow-Up of 30 Years

- We see tumoral reccurrencies when the tumor is not well taken off or specially aggressive
- Infection can be seen, in the same percentage of cases (3 %) than the one we have when we use massive métallic prostheses. Some times when there is serum collection surrounding the graft, it can be seen as an infection. But when we make a biopsy or a procurement their are no germs. This liquid is an immunological response to the graft (8 % of the cases)

- The Cartilaginous cells are still alive in the cartilage 10 or 20 years after grafting, they produce new Amino-glycans and fix Blue Colorants
- If the thickness of the cartilage decrease , it is not clinically followed by pain because the cartilaginous tissue is not innevaled and we have very exceptionnally used a prosthesis
- Most of the time the destruction of the joint, after grafting is due to ligamentary instability so we have to use primarily artificial ligaments or refix on the graft the ligaments of the recipient patient

Acetabulum and Pelvic Reconstructions with Massive Allografts

Revision arthroplasty of the hip and large-scale excision due to tumors are reasons for large losses of bone. Massive allografts make muscle refixation easier and provide the volume of bone needed for reconstruction of the loss of substance which is why we prefer them to massive metal prostheses. However their biological characteristics , their fragility on exposure to fatigue stresses and their immunological properties are subjects for discussion. Since 1982 we have been using 423 massives grafts preserved in the Bone Bank in Marseille for hip reconstruction (Acetabulum, Iliac wing, obturateur ring, whole hemi pelvis)

Etiologies

Tumoral Etiologies

- Chondrosarcomas (57 % of the cases)
- Fibrosarcomas
- Ewing's Tumors (21 % of the cases)
- Plasmocytomas
- Rhabdomyosarcomas
- Giant cell tumor (18 % of the cases)

Infectious Etiologies

- Echinococcosis
- Sepsis

Hip Reconstruction after Revision Surgery

- Acetabulum

Allografts

The graft is taken under very strict aseptic conditions in operating theatre

The graft is deep frozen and conserved in liquid nitrogen at – 196 °C with antibiotics. We can use it within 2 h after having thawed it

Surgical Techniques

Reconstruction of the Pelvis

The Patient is laid in ¾ dorsal decubitus position. The homolateral leg is left free to be mobilized. We have described a wide approach allowing the whole hemi-pelvis to be excised; The incision was started in the inguinal region taking the vessels into account, then extended downwards, towards the homolateral ischium, and upwards up to the antéro-supérior iliac spine.

Dissection of the Iliac and femoral vessels, spermatic cord, crural nerve, psoas, iliac muscles, pubis, bladder, obturator ring, lumbar and sacral roots, sacrum, iliac wing, femoral neck.

Osteotomies are performed at the end of the dissection when everything is under control (nerves and vessels, bladder and uretere, muscles and Bowel Loop).

Reconstruction of the hemi pelvis when an acetabular cup has been cemented directly on the bone allograft before it, is fastened. Fixation of the sacroiliac joint or of the sacrum.

One or Two plates are used after having been modulated inside the pubis and on the posterior wall. Refixation of the muscles on the bone. The femoral prosthesis is cemented in the desired position in the diaphyseal shaft of the femur after the canal has been prepared.

For 2 days the patient will remain in the intensive care unit. Walking and weight-bearing are permitted from the 8th day after operation. Total Weight –bearing is possible by 15–21 days postoperatively.

For Isolated Reconstructions of the Acétabulum

The approach used in revision surgery of the hip is a lateral external transgluteal route , creating a digastric muscle from the gluteus medius and with the vastus externus left connected to each other by trochanteric attachments. The femur is dislocated and freed from its acetabular attachments.

Then freeing of the acetabulum : ablation of the implant, of all the cement, and of any fibrosis, removing of the necrotic bone.

The femoral allograft(s) is (are) remodelled in such a way as to reconstruct the acetabulum perfectly after screwing them directly into the spongy bone. Further drilling is performed.

Anchorage points are drilled into the roof of the acetabulum, the pubis, and the ischium, through the allograft direct into the patient's bone. The cement is applied when it is in its pasty phase.

Clinical Applications and Results

From the Carcinological point of view, the chondrosarcomas which were the main reasons for performing our pelvic grafts were always resected on a large scale.

There are very few relapses within the 10–15 years after operation but we see some after this period of time. On the other hand, the others sarcomas all resulted in the death of the patients after a longer or shorter interval.

Septic Loosening of prosthesis appear to us to be a good indication for surgery in two stages. A fracture of the allograft may heal completely. The allograft-host union has to be fastened by stable osteosynthesis and surrounded by spongy autograft.

The shafts of the prosthesis have to be cemented into the host femur as well as into the allograft. The number of septic complications is comparable in our series to that of the series using massive metal prosthesis. A number of serous effusions led us to review the immunology of the bone allografts

The Mega-Hip Prosthesis Surrounded By Allografts

Reconstructive metal mega hip prosthesis are commonly used, but they might be responsible of mechanical failures or instability due to muscle non fixation. One of the actual problems concerning articular allografting is the biomechanical behavior of the ligaments and the revascularization of the cartilage.

Autologous grafts, unlike allogenic grafts, have an important osteogenic potentie. But in as much as the procurement volume is limited, they do not permit massive bone or joint reconstruction when there as been partial or total resection as a result of either a bone tumor or a post-traumatic lack of substance.

Computerized Custom Made Mega Hip Prosthesis

Shape

To rebuilt the upper part of the femur destroyed by a tumor of after numerous operations. We have had, to study first the inner shape of the femur. The prosthesis has to have the same anatomical shape than the medullar bone. The form that has been given by C.A.O. is an italic S with a long inferior curve.

It is important to rebuilt exactly the inside anatomical aspect of the bone, for the prosthesis to be directly in contact with the cortical bone. If you use a straight stem you cannot obtain every where a good contact and you have stress schilding in some places of the bone and also you cannot use a massive allograft because you cannot introduce the stem in it.

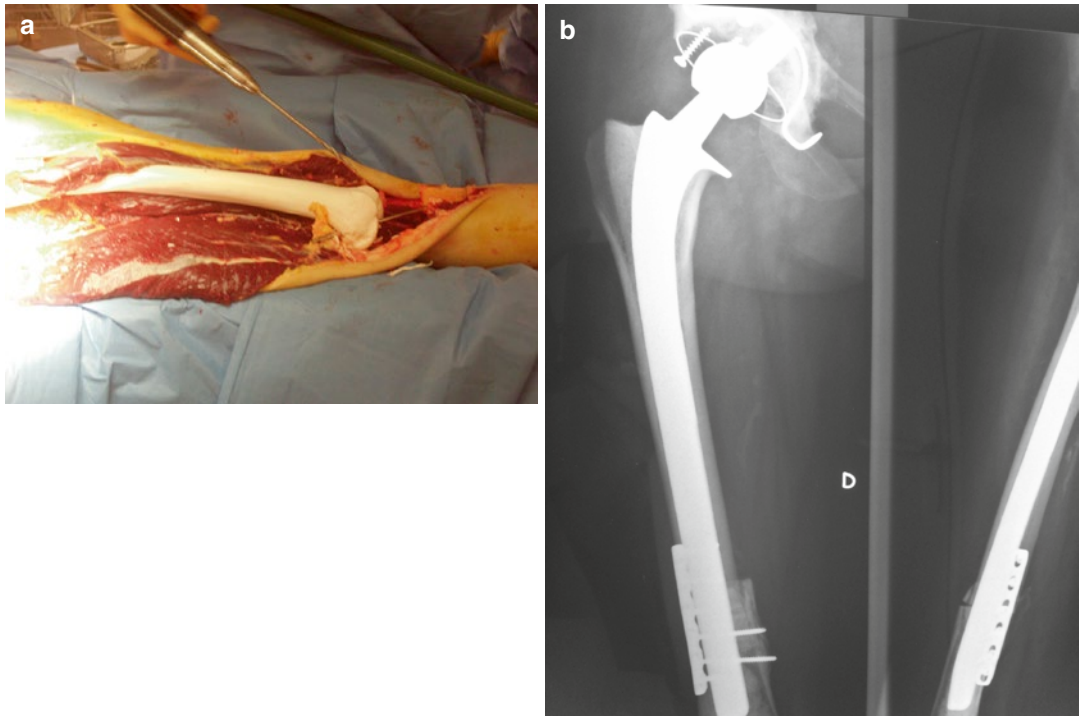

Fig. 20.3 (**a**) Implementation of bone substitution. (**b**) Prosthesis in place

Fixations

The Mega prosthesis has to be introduced very easily in a massive diaphyseal allograft without risks of breakage. We can use it with or without cement, but we think that the best utilisation is with cement in the upper part next to the allograft and also with cement in the lower part of the stem which is fixed in the receiver bone. The muscles surrounding the allograft will fix themselves directly on it. Some special fixation can also be used for the trochanteric muscles.

Clinical Applications

In reconstructive surgery, it is the first time that we increase the bone in using a prosthesis surrounded by allograft. In bone tumors when muscles and ligaments have to be removed, like in some traumatological cases, the use of massive osteocartilaginous allografts is not indicated because of the poor vascular surrounding of the graft and problems linked to articular instability. We think the best we can do in those cases, is to propose the use of massive metallic articular prosthesis surrounded by one allograft.

Prosthesis brings an immediate stability and allows the patient to walk a few days later, while the graft will permit the remaining muscles to fix themselves on it. This solution is the one choosen each time there is a reconstruction of the upper part of the femur (Fig. 20.3).

Conclusion

The use of a megahip prosthesis surrounded by allograft has a lot of advantages. It allows muscular or ligamentary fixation and better biomechanical behaviour which decrease the risks of articular instability; no risk of articular necrosis means we can authorize a early loading; and especially we increase the volume of skeletal bone instead of decreasing it and that is a very new and important point.

Suggested Reading

Babin SR, Katzner M, Vidal PH, Simon P, Kempf JF, Keiling R, Schvingt E. Résection – reconstruction diaphysaire fémorale par allogreffe massive fixée par clou médullaire vérouillé. RCO. 1987;73:25–9.

Beaver RJ, Mahomed M, Bachstein D, Davis A, Zukor DJ, Gross AE. Fresh osteochondral allografts for post-traumatic defect in the knee. J Bone Joint Surg BR. 1992;74-B:105–10.

Brooks DB, Heiple KC, Herdon CH, Powell AE. Immunological factors in homogenous bone transplantation. IV. The effect of various methods of preparation and irradiation on antigenicity. J Bone Joint Surg. 1969;45A:1617.

Brown K, Crues SR. Bone and cartilage transplantation, in orthopeadic surgery. J Bone Joint Surg Am. 1982;64:270–9.

Burchardt H, Enneking WF. Transplantation of bone. Surg Clin North Am. 1978;58:409.

Burchardt H. The biology of bone graft repair. Clin Orthop. 1983;174:121–35.

Burchardt H, Jones H, Gloweczewskie F, Rudner C, Enneking WF. Freeze-dried allogeneic segmental cortical bone grafts in dogs. J Bone Joint Surg. 1978;60A:1082.

Burwell RG, Gowland G. Studies in the transplantation of bone. III. The immune responses of lymphnodes draining components of fresh homologous cancellous bone and homologous bone treated by different methods. J Bone Joint Surg. 1962;44B:131.

Burwell RG. Studies in the transplantation of bone. V. The capacity of fresh and treated homografts of bone to evoke transplantation immunity. J Bone Joint Surg. 1963;45B:386.

Burwell RG. The fate of bone grafts. In: Apley AG, editor. Recent advances in orthopeadic. Baltimore: The Williams & wilkins Co; 1969. p. 115.

Burwell RG. The fate of freeze-dried bone allografts. Transplant Proc. 1976;8(Suppl1):95.

Burwell RG, Gowland G, Dexter F. Studies in the transplantation of bone. VI. Further observations concerning the antigenicity of homologous cortical and cancellous bone. J Bone Joint Surg. 1963;41B:597.

Carr CR, Hyatt GW. Clinical evaluation of freeze-dried bone grafts. J Bone Joint Surg. 1955;37A:549.

Carrel A. La conservation des tissus et ses applications en chirurgie. J Am Med- Techniques chirurgicales orthopédique. 1984;44090:4-7-10, Paris.

Chalmers J. Transplantation immunity in bone grafting. J Bone Joint Surg. 1959;41B:160.

Charpentier B. Mécanisme du rejet des allogreffes. Presse Med. 1984;13:2697–700.

Chrisman OD, Fessel JM, Southwick WO. Experimental production of synovitis and marginal articular exostose in the knee joint of dogs. Yale J Biol Med. 1964;37:409.

Coutelier L, Delloye CH, De Nayer P, Vincent A. Aspects microradiographiques des allogreffes osseuses chez l'homme. Rev Chir Orthop. 1984;70:581–8.

Cracchiolo III A, Michaeli D, Goldberg LS, Fudenberg HH. The occurrence of antibodies to collagen in synovial fluids. Clin Immunol Immunopathol. 1975;3:567.

Curran WJ. The uniform anatomical gift act. N Engl J Med. 1969;280:36.

Darcy DA. Reaction of rabbits to frozen homografts. J Pathol Bacteriol. 1955;70:143.

Devries PH, Badgley CE, Hartman JT. Radiation sterilization of homogenous-bone transplants utilizing radioactiv cobalt. Preliminary report. J Bone Joint Surg Am. 1958;40:187–203.

Duffy P, Wolf J, Collins G, De Voe AG, Streeten B, Cowen D. Possible person-to-person transmission of Creutzfeld-Jacob disease. N Engl J Med. 1974;290:692.

Duparc J, Nordin JY, Olivier H, Augereau B. Les résections-reconstructions dans les tumeurs osseuses des membres et du bassin. Encycl Méd Chir-Techniques Chirurgicales Orthopédie. 1984; 44090:4-7-10.

Elves MW. Humoralimmune response to allografts of bone. Int Arch Allergy Appl Immunol. 1974;47:708.

Elves MW. Newer knowledge of immunology of bone and cartilage. Clin Orthop. 1976;120:232.

Elves MW, Ford CHJ. A study of the humoral immune response to osteoarticular allografts in the sheep. Clin Exp Immunol. 1974;17:497.

Friedlaender GE, Mankin HJ. Guidelines for the banking of musculoskeletal tissues. Am Assoc Tissue Banks Newslett. 1980;4(suppl):30.

Friedlaender GE. Current concepts. Review: bone-banking. J Bone Joint Surg Am. 1982;64:307–11.

Friedlaender GE. Immune response to osteochondral allografts. Clin Orthop. 1983;174:58–67.

Friedlaender GE, Ladenbauer-Bellis I, Chrisman OD. Cartilage matrix components as antigenic agents in a osteoarthritis model. Trans Orthop Res Soc. 1980;5:170.

Friedlaender GE, Mankin HJ, Kenneth W. Osteochondral allografts (biology, banking and clinical applications). Boston/Toronto: Little Brown; 1982.

Friedlaender GE, Strong DM, Sell KW. Donor graft specific anti-HL- A antibodies following freeze-dried bone allografts. Trans Orthop Res Soc. 1977;2:87.

Friedlaender GE, Strong DM, Sell KW. Studies on the antigenicity of bone. I. Freeze-dried and deep-frozen bone allografts in rabbits. J Bone Joint Surg. 1976;58A:854.

George CR, Chrisman OD. The role of cartilage polysaccharides in osteoarthritis. Clin Orthop. 1968;57:259.

Glant T, Hadas E, Nagry TJ. Cell-mediated and humoral immune responses to cartilage antigenic components. Scand J Immunol. 1979;9:29.

Golberg V, Heiple K. Experimental hemi joint and whole transplantation. Clin Orthop. 1983;174:43–53.

Goldberg V, Bos G, Heiple K, Zita J, Powell A. Improved acceptance of frozen bone allografts in genetically mismatched dogs by immunosuppression. J Bone Joint Surg Am. 1984;66:937–50.

Greiff D, Milson TJ. Functional activities of isolated lymphocytess following drying by sublimation of ice

in vacus. I. Rosette formation, stimulation by plant lectins (mitogens) and the mixed lymphocyte reaction. Cryobiology. 1980;17:319.

Gresham RB. The freeze-dried cortical bone homograft: a roentgenographic and histologic evaluation. Clin Orthop. 1964;37:194.

Gross A, Mc Kee N, Pritzker K, Langer F. Reconstruction of skeletal deficit at the knee. Clin Orthop. 1983;174:96–106.

Gross AE, Langer F, Houpt J, Pritzker K, Friedlander CE. The allotransplantation of the partial joints in the treatment of osteoarthritis of the knee. Transplant Proc. 1976;8(suppl I):129.

Gross AE, Langer F, Silverstein EA, Falk R, Falk J. The allotransplantation of the partial joints in the treatment of osteoarthritis of the knee. Clin Orthop. 1975; 108:7–14.

Guilleminet, Stagnara, Dubost-Perret, Jarret, Audry. Utilisation d'os hétérogènes réfrigérés en chirurgie humaine. Lyon Chir. 1952;47 N°1, Janvier.

Hedde C, Postel M, Kerboul M, Courpied JP. La réparation du cotyle par homogreffe osseuse conservée au cours des révisions de prothèse totale de hanche. Rev Chir Orthop. 1986;72:267–76.

Heiple KG, Chase SW, Herndon CH. A comparativ study of the healing process following different types of bone transplantation. J Bone Joint Surg. 1963;45A:1593.

Hiky V, Mankin HJ. Radical resection and allograft replacement in the treatment of bone tumors. J Jpn Orthop Assoc. 1980;54:475.

Houff SA, Burton RC, Wilson RW, et al. Human-to-human transmission of rabies virus by corneal transplant. N Engl J Med. 1979;300:603.

Huten D. Utilisation des allogreffes osseuses dans les reconstructions fémorales au cours des reprises de prothèse totale de hanche. Rev Chir Orthop. 1988;74:122–4.

Hyatt GW, Butler MC. Bone grafting. The procurement storage and clinical use of bone homograft. In: America Association of Orthopeadic Sugeons. Instructional courses lectures 14:343. Ann Arbor: J.W. Edwards Co; 1957.

Inclan A. L'emploi des greffes osseuses conservées en Orthopédie. J Bone Joint Surg. 1942a;26:81–96. Janvier.

Inclan A. Use of preserved bone graft in orthopeadic surgery. J Bone Joint Surg. 1942b;26:81.

James JIP. Tuberculosis transmitted by banked bone. J Bone Joint Surg. 1953;35B:578.

Judet H, Padovani JP. Transplantation d'articulation complète. Rev Chir Orthop. 1983;67:359–60.

Judet J, Aviset A. Homogreffes provenants de la banque d'os. Mem Acad Chir N. 1948;671:27–8.

Koskinen EV, Salenius P, Alho A. Allogeneic transplantation in low-grade malignant bone tumors. Acta Orthop Scand. 1979;50:129.

Kossowska-Paul B. Studies on the regional lymph node plastic reaction evoked by allogeneic grafts of fresh and preserved bone tissue. Bull Acad Polon Sci. 1966;14:651.

Kruez FP, Hyatt GW, Turner TC, Basset al. The preservation and clinical use of freeze-dried bone. J Bone Joint Surg. 1951;33AA:863.

Langer F, Czitrom A, Pritzker KP, Gross AE. The immunogenicity of fresh and frozen allogeneic bone. J Bone Joint Surg. 1975;57A:216.

Lee EH, Langer F, Halloran P, Gross AE, Ziv I. The effect of major and minor histocompatibility differences on bone transplant bealing in inbred mice. Trans Orthop Res Soc. 1979a;4:60.

Lee EH, Langer F, Halloran P, Gross AE, Ziv I. The immunology of osteochondral and massive allografts. Trans Orthop Res Soc. 1979b;4:61.

Lexter E. Die verwendung der freien knochenplastik nebst versuchen über gelenkversteifung und gelenktransplantation. Arch Klin Chir. 1908;86:939.

Lexter E. Joint transplantation and arthrosplasty. Sug Gynecol Obstet. 1925;40:782.

Locht R, Gross A, Langer F. Late osteochondral allograft resurfacing for tibia plateau fractures. J Bone Joint Surg Am. 1984;66:328–35.

Macewen W. Observations concerning transplantation of bone. Illustrated by case of inter-human osseous transplantation, where by over two-thirds of shaft of a humerus was restored. Pro R Soc Lond. 1881;32:232.

Mankin HJ, Doppelt SH, Tomford WW. Clinical experience with allograft implantation. Clin Orthop. 1983a;174:69–86.

Mankin HJ, Doppelt SH, Sullivan TR, Tomford WW. Osteoarticular and intercalary allograft transplantation in the management of malignant tumors of bone. Cancer. 1983b;50:613.

Mankin HJ, Fogelson FS, Trasher AZ, Jaffer F. Massive resection and allograft transplantation in the treatment of malignant bone tumors. N Engl J Med. 1976;294:1247.

Marsh B, Flynn L, Enneking W. Immunologic aspects of osteosarcoma and their application to therapy, a preliminary report. J Bone Joint Surg. 1972;54A:1367.

Merle D'aubigne R. A propos de la résection pour tumeurs du genou. Rev Chir Orthop. 1963;67:359–60.

Meyers MH, Chatterjee SN. Osteochondral transplantation. Surg Clin North Am. 1978;58:429.

Mnaymneh W, Emerson RH, Brajao F, Head WC, Malinin TI. Massive allografts in slavage revision of failed total knee arthroplasties. Clin Orthop. 1990;269:144–53.

Musculo DL, Kawai S, Ray RD. Cellular and humoral immune response analysis of bone-allografted rats. J Bone Joint Surg. 1976;58A:826.

Nimelstein SH, Hotti AR, Homan HR. Transformation of a histocompatibility immunogen into a tolerogen. J Exp Med. 1973;128:723.

Ollier L. Traité expérimental et clinique de la régénération des os. Paris: Victor Masson & fils; 1867.

Ottolenghi CE. Massive osteo and osteo-articular bone grafts: technic and results of 62 cases. Clin Orthop. 1972;87:156.

Parrish FF. Allograft replacement of all part of the end of a long bone following excision of a tumor: report of twenty– one cases. J Bone Joint Surg. 1973;55A:1.

Penn I. The incidence of malignancies in transplant recipients. Transplant Proc. 1975;7(2):323.

Pelkers R, Friedlander G, Markham T. Biomechanical properties of bone allografts. Clin Orthop. 1983;174:54–7.

Poitout D, et Tropiano P. Les reconstitutions du cotyle après chirurgie iteractive de la hanche – A propos de 37 cas. Bulletin de l'Académie Nationale de Médecine. 1996;180-N°3:515–31.

Poitout D. Allografts of the patella and extensor apparatus. Atlas of open knee surgery. Edition Chapman & Hall; 1996. p. 42–9.

Poitout D. Allotraplanto della rotula e dell'apparato estensor. Atlante di technica chirurgica del ginocchio. Milan: Edition Masson; 1995. p. 42–9.

Poitout D. Banche d'osso: aspetti tecnici criopreservazione di allotraplanti osteocartilagineo. Atlante di technica chirurgica del ginocchio. Milan: Edition Masson; 1995. p. 178–9.

Poitout D. Bone bank: technical aspects of cryopreservation osteocartilaginous grafts. Atlas of open knee surgery. Edition Chapman & Hall; 1996. p. 178–9.

Poitout D. Conservation et utilisation de l'os de banque. Cahier d'enseignement de la S.O.F.C.O.T N° 23. Expansion scientifique. Conférence. 1985. p. 157–77.

Poitout D. Future of bone allografts in massive bone resection for tumor. Presse Médicale. 1996;30;25(11): 570–30.

Poitout D. Greffes utilisées pour reconstruire l'appareil locomoteur. Paris: Masson; 1986.

Poitout D. Knee reconstruction prosthesis incorporating a large allograft. Atlas of open knee surgery. Edition Chapman & Hall; 1995. p. 145–51.

Poitout D. L'os biomateriaux. "Bulletin de l'Académie de Nationale de médecine". 179, 3, 517–536, 1995. Communication à l'Académie Nationale de Médecine. Paris, 14 mars 1995.

Poitout D. Les greffes de l'appareil locomoteur. Académie de Chirurgie (Paris, 10 avril 1996). "Mémoire de l'académie de Chirurgie", 1996.

Poitout D. Les reconstructions de cotyle après chirurgie iterative de la hanche. (A propos de 37 cas). Académie Nationale de Médecine. Paris, 5 mars 1996. "Bulletin de l'Académie de Nationale de médecine". 180(3):515–31.

Poitout D. Protesi di ricostruzione di ginocchio con allotraplanto massivo. Atlante di technica chirurgica del ginocchio. Milan: Edition Masson; 1995. p .145–51.

Poitout D. Reconstruction du cotyle et de l'hémibassin par allogreffe ou prothèse méttalique massive sur mesure. 73ème Réunion Annuelle de la S.O.F.C.O.T.- Paris les 10–13 novembre 1998. Revue de chirurgie Orthopédique. 1998;84, N°218:120–1.

Poitout D, Bernat M, Martin G, Tropiano P. Indications des greffes osteocartilagineuses massives en traumatologie du genou. Acta Orthop Belg. 1996a;62(6):59–65.

Poitout D, Bernat M, Martin G, Tropiano P. Indications des greffes osteo-cartilagineuses massives en traumatologie du genou. "Acta Orthopaedica Scandinavica", Edition Scandinavian University Press; vol. 62, suppl. 1, 1997.

Poitout D, Bernat M, Moulene JF, Tropiano P. Allogreffes de cotyle et d'hémi-bassin. A propos de 37 cas. 71ème Réunion Annuelle de la S.O.F.C.O.T.- Paris les 12–15 novembre 1996. Revue de chirurgie Orthopédique. 1996;87, 152:100.

Poitout D, Bernat M, Moulene JF, Tropiano P. Allogreffes osteochondrales ou prothèses articulaires en chirurgie traumatologique ou oncologique du genou. 71ème Réunion Annuelle de la S.O.F.C.O.T.- Paris les 12–15 novembre 1996. Revue de chirurgie Orthopédique, 87–99, 69–70, 1996.

Poitout D, Bernat M, Moulene JF, Tropiano P. Devenir des fractures du col du fémur. 71ème Réunion Annuelle de la S.O.F.C.O.T.- Paris les 12–15 novembre 1996. Revue de chirurgie Orthopédique, 87,153, 100–101, 1996.

Poitout D, Bernat M, Moulene JF, Tropiano P. Indications for cryopreserved allografts in tumoral pathology. Eur J Orthop Surg Traumatol. 1997b;7:100–4.

Poitout D, Bernat M, Moulene JF, Tropiano P. Massive HIP prothese ensheated by allografts. Eur J Orthop Surg Traumatol. 1997c;7:123–6.

Poitout D, Dubousset JF, Tomeno B. Arthrectomie monobloc du genou. "Revue de Chirurgie Orthopédique". 1995;81–6, 565, Paris.

Poitout D, Lempadakis M, Bernat M, Lecoq C, Martin G, Aswad R. Secondary internal osteosynthesis after fixation for recent or lower limb. "Revue de chirurgie orthopédique Réparatrice ». 1996;82(2):137–44.

Poitout D, Lempidakis M, et Loncle X. Osteocartilaginous graft of the upper tibia. Atlas of open knee surgery. Edition Chapman & Hall; 1996. p. 170–7.

Poitout D, Lempidakis M, et Loncle X. Allotraplanto osteocartilagineo massivo dell'estremita superiore della tibia .Atlante di technica chirurgica del ginocchio. Milan: Edition Masson; 1995. p. 170–7.

Poitout D, Lempidakis M, et Loncle X. Allotraplanto osteocartilagineo massive dell'estremita inferiore del femore. Atlante di technica chirurgica del ginocchio. Milan: Edition Masson; 1995. p. 164–9.

Poitout D, Lempidakis M, et Loncle X. Osteocartilaginous graft of the lower extremity of the femur. Atlas of open knee surgery. Edition Chapman & Hall; 1996. p. 164–9.

Poitout D, Lempidakis M, et Loncle X, Bernat M. Les sarcomes ostéogeniques de l'extrêmité inférieur du fémur. Techniques de reconstruction – L'avenir. "Revue de Chirurgie Orthopédique", 81-6, 566, 1995. Communication à l'Académie Nationale de Chirurgie, Paris le 29 mars 1995.

Poitout D, Lempidakis M, et Loncle X, Bernat M. Reconstructions massives du cotyle et du fémur proximal. Académie de Chirurgie (Paris, 1994). "Mémoire de l'académie de Chirurgie" Tome 120, 1994–1995 – N°5.

Poitout D, Lempidakis M. Artificial ligament repairs. Atlas of open knee surgery. Edition Chapman & Hall; 1996. p. 76–85.

Poitout D, Lempidakis M. Legamentoplastiche artificiali. Atlante di technica chirurgica del ginocchio. Milan: Edition Masson; 1995. p. 76–85.

Poitout D, Loncle X. Legamento crociato posteriore. Atlante di technica chirurgica del ginocchio. Milan: Edition Masson; 1995. p. 86–8.

Poitout D, Loncle X. Posterior cruciate ligament. Atlas of open knee surgery. Edition Chapman & Hall; 1996. p. 86–8.

Poitout D, Lu J, Huang ZW, Tropiano P, Clouet D'orval B, Remusant M, Dejou J, Proust JP. Human biological reactions at the interface between bone tissues and polymethylmethacryalate cement. J Mater Sci Mater Med. 2002;13:803–9.

Poitout D, Nandiegou Y, Lempidakis M. Legamentoplatica artificiale. Atlante di technica chirurgica del ginocchio. Milan: Edition Masson; 1995. p. 89–93.

Poitout D, Nandiegou Y, Lempidakis M. Artificial ligament repair. Atlas of open knee surgery. Edition Chapman & Hall; 1996. p. 89–93.

Poitout D, Novakovich G. Allogreffes et banque d'os. Encyclopédie Médico-chirurgicale (Paris-France), appareil locomoteur 14015AIO, 5-1986 6P, 1986.

Poitout D, Ozoux P. Intra-articular repair of the posterior cruciate ligament using either semitendinosus or gracilis tendons (Lindenmann's operation). Atlas of open knee surgery. Edition Chapman & Hall; 1996. p. 94–5.

Poitout D, Tropiano P, Bernat M, Loncle X, Martin G. Greffes articulaires, mythe ou réalité ? Entretiens de Bichat 1995. Paris 25–30 septembre 1995. "Chirurgie-Spécialité", 43–46, 1995.

Poitout D, Tropiano P, Bernat M, Moulene JF. Reconstruction massive de cotyle et du fémur proximal. Les Arcs, 20–25 janvier 1996. "European Journal of Orthopaedic surgery and traumatology." 1996;6:271–7.

Pool AR, Reiner A, Choi H, Rosenberg LC. Immunological studies of proteoglycan subunit from bovine and human cartilage. Trans Orthop Res Soc. 1979;4:55.

Pujet J, Utheza G. Reconstructionde l'os iliaque à l'aide du fémur homoilatéréal après résection pour tumeur pelvienne. Rev Chir Orthop. 1986;72:151–5.

Rodrigo JJ. Distal rat femur allografts: a surgical model for induction of humoral cytotoxic antibodies. Trans Orthop Res Soc. 1977;2:265.

Rodrigo JJ, Fuller TC, Mankin HJ. Cytotoxic HL-A, antibodies in patient with bone and cartilage allografts. Trans Orthop Res Soc. 1976;1:131.

Roy-Camille R, Laugier A, Ruyssen S, Chenal C, Bisserie M, Pene F, Saillant G. Evolution des greffes osseusescortico-spongieuses et radiothérapie. Rev Chir Orthop. 1981;67:599–608.

Sadler AM Jr, Sadler BL. Providing cadaver organs: three legal alternatives. Hastings Center Studies I. 14, 1973.

Sadler Jr AM, Sadler BL, Stason EB, Stickel DL. Transplantation – a case for consent. N Engl J Med. 1969;280:862.

Sagi S, Turianskyj FH, Gyenes L. Immunogenicity of soluble murine histocomptabilicity antigens. Immunol Commun. 1974;3:85.

Salama R. Xenogeneic bone grafting in humans. Clin Orthop. 1983;174:113–21.

Schachar NS, Friedlander GE, Mankin HJ. Bone transplantation. In: Slavin S, editor. Organ transplantation: present state, future goals. Amsterdam: Elsevier/North-Holland biomedical Press B.V. (in press).

Schachar NS, Fuller TC, Wadsworth PL, Henry WB, Mankin HJ. A feline model for the study of frozen osteoarticular allografts. Development of lymphocytotoxic antibodies in allograft recipients. Trans Orthop Res Soc. 1978a;3:131.

Schachar NS, Mankin HJ, Wadsworth PL, Henry WB, Castronovo FP. A feline model for the study of frozen osteoarticular allografts. I. Quantitative assessment of cartilage viability and bone healing. Trans Orthop Res Soc. 1978b;3:130.

Sell KW, Friedlander GE, editors. Tissues banking for transplantation. New-York: Grune & Stratton, Inc; 1976.

Sell KW, Friedlander GE, Strong DM. Immunogenicity and freeze-drying. Cryoimmunology. 1976;17:187.

Shneider JR, Bright RW. Anterior cervical fusion using preserved bone allografts. Transplant Proc. 1976;8(suppl):73.

Shutkin NM. Homologous-serum hepatitis following use of refrigerated bone-bank bone: report of case. J Bone Joint Surg. 1954;36A:160.

Solomon L. Bone grafts. J Bone Joint Surg Am. 1991;73-B:706–7.

Spence KF, Sell KW, Brown RH. Solitary bone cyst: treatment with freeze-dried cancellous bone allograft. J Bone Joint Surg. 1969;51A:87.

Stockley I, Mc Auley JP, Gross AE. Allograft reconstruction in total knee arthroplasty. J Bone Joint Surg Am. 1992;74-B:393–7.

Syftestad G, Urist M. Bone aging. Clin Orthop. 1982;162:288–97.

Takagi K, Urist M. The reaction of the dura to bone morphogenetic protein (BMP) in repair of skull defects. Ann Surg. 1982a;196:100–9.

Takagi K, Urist M. The role of bone marrow in bone morphogenetic protein-induced repair of femoral massive diaphyseal defects. Clin Orthop. 1982b;171: 224–30.

Takami H, Doi T, Ninomiya S. Reconstruction of a large tibial defect with a free vascularized fibular graft. Arch Orthop Surg. 1984;102:203–5.

Tavernier. Sur les greffes d'os tué. Lyon Chir., 1922, séance du 17 novembre 1921. Utilisation d'os purum. Lyon Chir. 1930.

Tomford WW, Fredricks GR, Mankin HJ. Cryopreservation of intact articular cartilage. Trans Orthop Res Soc. 1982a;7:176.

Tomford WW, Fredricks GR, Mankin HJ. Cryopreservation of isolated chondrocytes. Trans Orthop Res Soc. 1982b;6:100.

Tomford WW, Mankin HJ, Doppelt S. Bone bank procedures. Clin Orthop. 1983;174:15–21.

Tomford WW, Starkweather RJ, Golman MH. A study of the clinical incidence of infection in the use of banked allograft bone. J Bone Joint Surg. 1981;63A:244.

Trentham DE, Townes AS, Kang AH, David JR. Humoral and cellular sensitivity to collagen in type II. Collagen induced arthritis in rats. J Clin Invest. 1978;61:89.

Tuffier. Des greffes chirurgicales chez l'homme. Bull. et Mém. Soc. Chir. 1910;36:1983, Paris.

Urist MR. Human bone morphogenetic protein. Proc Soc Exp Biol Med. 1983;173:194–9.

Urist MR. Practical applications of basic research on bone graft physiology. In: AAOS. Instructional Course Lectures, 25: 1. St Louis: The C.V. Mosby Co; 1976.

Urist MR, Delange R, Finermann G. Bone cell differentiation and growth factors. Science. 1983;220:680–6.

Urist MR, Mikulski A, Boyd SD. A chemosterilized antigen-extracted autodigested alloimplant for bone banks. Arch Surg. 1975;110:416.

Volkov M, Imamaliyev AS. Use of allogenous articular bone implants as substitutes for autotransplants in adult patients. Clin Orthop. 1976;114:192.

Volkov M. Allotransplantation of joints. J Bone Joint Surg Br. 1970;52B:49–53.

Weiland A, Moore R, Daniel R. Vascularized bone autografts. Clin Orthop. 1983;174.

Weislander J, Heinegard D. Immunochemical analysis of cartilage proteoglycans: antigenic determinants of substructures. Biochem J. 1979;179:35.

Wilson PD. Follow-up study of the use of refrigerated homogenous bone transplants in orthopaedic operations. J Bone Joint Surg. 1951;33A:307.

Wilson RE, Penn I. Fate of tumors transplanted with a renal allograft. Transplant Proc. 1975;7(2):327.

Wittbjer J, Palmer B, Rohlin M, Thorngren K. Osteogenetic activity in composite grafts of demineralized compact bone and marrow. Clin Orthop. 1983;173:229–38.

Yablon I, Brandt KD, Delellis RA. The antigenic determinants of articular cartilage: their role in the homograft rejection. Trans Orthop Res Soc. 1977;2:90.

Yablon I, Copperband S, Covall D. Matrix antigens in allografts. Clin Orthop. 1982;168:243–51.

Yamane K, Nathenson SG. Biochemical similarity of papain-solubilized H-2d, alloantigens from tumor cells and from normal cells. Biochemistry. 1970;9:4743.

Zaleske D, Ehrlich M, Piliero C, May J, Mankin HJ. Growth plate behavior in whole joint replantation in the rabbit. J Bone Joint Surg Am. 1982;64:249–57.

Express Diagnosis of Mechano-Biological Limb Skin Condition During Prolonged Dosed Stretching in Orthopedics

21

Lyudmila Grebenyuk and Evgeny Grebenyuk

Non-invasive express estimation of skin quantitative parameters has remained a current task for plastic surgery, orthopedics, oncology and skin cosmetology [1, 2]. An express analysis of mechano-acoustic condition of the skin in the conditions that are close to extreme, in particular during lengthening of congenitally short limbs, forearm or lower leg stumps, also appears to be a topical problem. Despite the fact that the skin has a high potential for stretching, hyperextension signs can develop by reconstructive and restorative treatment of the patients with congenital limb anomalies accompanied by large discrepancies in limb length and deficit of soft tissue components. The diagnostic value of acoustic testing was studied by many researchers and mainly in clinical settings [3–5]. The obtained results show that mechano-acoustic properties of the skin can be used for evaluating the efficiency of various treatment methods, as well as for prediction of disadaptive shifts in the tissue such as overstretching (striae) that impair the cosmetic effect of operative limb segment lengthening.

Reconstructive and restorative treatment with the method of Ilizarov provides the objective control of bone and soft tissues condition of the involved limb in order to correct the treatment tactics for each patient. The systemic observations of skin integument response to prolonged dosed stretching have proven the necessity to perform biomechanical monitoring of soft tissues, including the skin. It has been noted that a number of patients that underwent large amounts of limb lengthening developed the signs of tissue overstretching (striae) while the level of regenerative process during the period of distraction was satisfactory. Therefore, we have developed and introduced the technique for studying the acoustic properties of the skin in the patients with orthopaedic pathologies that enables us to measure the velocity of the sound in the skin in the on line mode, non-invasively and considering the structural heterogeneity of the tissue.

Technique

An acoustic skin analyzer ASA-4 [6–8] was used to perform the study. Methods are considered based on the measurements of acoustic impedance, the shear and surface wave speeds (SWS), as well as of static moduli. SWS range – 10–300 m/s. Measurements in the longitudinal

L. Grebenyuk, PhD (✉)
Department of Physiology, Russian Ilizarov Scientific Center for Restorative Traumatology and Orthopaedics, Kurgan, Russia
e-mail: gla2000@yandex.ru

E. Grebenyuk, MD
3rd Orthopedic Department, Russian Ilizarov Scientific Center for Restorative Traumatology and Orthopaedics, M. Ulianova St., 6, Kurgan 640014, Russia

D.G. Poitout (ed.), *Biomechanics and Biomaterials in Orthopedics*,
DOI 10.1007/978-1-84882-664-9_21

(in parallel with anatomical limb axis), transverse and diagonal directions (45° and 135° by Cartesian coordination system) was performed before treatment start, during distraction by method of Ilizarov, fixation and at different time intervals after the Ilizarov fixator removal. The anterior surface of segmental middle third was an area to be studied for all limb segments. A patient was in horizontal position, his (her) elbow, knee and hip joints were extended (angle in the joints amounted to about 180°). Statistical analysis consisted in checking the parameters obtained for following normal distribution law, calculation of mean value, standard error and standard deviation. Provided the normal distribution law of sampled population the authenticity of differences was estimated with Student *t*-test.

In the process of analyzing the effect of distraction on skin integument biomechanical behaviour in the segment being lengthened the following characteristic features of integument tissue mechanics-and-acoustic state were determined.

Analysis of Forearm Skin Mechanics-and-Acoustic Properties for Graduated Distraction in Patients with Congenital Anomalies of the Upper Limb

A dynamic study was performed in the group of patients (n = 39) with congenital growth and development anomaly of forearm (CGAF) on the basis of measuring the spreading velocity of surface acoustic wave in the forearm being lengthened. The main part of patients was represented by children and adolescents with congenital radial or ulnar club hand at the age of 3–18 years, who were subjected to forearm lengthening. The mean value of lengthening amounted to 6.4 ± 1.0 cm (range: 5.5–8 cm).

As it rises from Table 21.1, the gain in sound velocity in patients at the age of 3–11 years was observed for transverse C(x) and longitudinal C(z) orientations, as well as for diagonal one C(135). Specifically, by 30 and 60 days of distraction C(x) parameter 31.1 % and 37.5 % exceeded the values of intact segment, respectively. Similarly to this, C(135) parameter also was 34.6 % and 32.5 % higher, than that of contralateral forearm. The value studied registered for longitudinal orientation 32.3 % increased by 30 day of lengthening and 36.9 % increased – by 60 day of distraction.

Changes in acoustics properties in the age group of 12–18 years occurred similarly to those in the younger age group (3–11 years, Table 21.2). As it rises from Tables 21.1 and 21.2, the character of increasing the SWS value in integument tissue of the forearm involved for the group of patients at the age of 12–18 years by 30 day of distraction was identical to that in age group of patients of 3–11 years. As far as graduated distraction continued, the gain in SWS for longitudinal, transverse and diagonal (135°) directions amounted to 32.9 %, 38.3 % and 39.2 %. This indirectly evidences the development of comparable by value tension state in skin in the three directions mentioned, though the SWS parameter in absolute values in the longitudinal orientation reaches maximum – 87.9 %.

On the basis of the scalars of SWS vectors there are reasons to draw a conclusion about the transfer of operated forearm skin integument to stressed-and-deformed state [3].

It should be noted that in case of surgical treatment of patients with upper limb CGAF the necessity of repeated segment lengthening arises due to the fact that lengthening of segments starts from the age of 5–7 years. This creates favourable conditions for patients' social adaptation and motor development. That is why in case of soft-tissue component deficit the appearance of the signs of skin integument overstretching in the forearm involved (striae) may be noted in single cases. Quite by the end of fixation period the signs of skin overdistension were reduced essentially, and in the first days after the fixator removal the striae in skin of the forearm lengthened were significantly reduced as a result of successful adaptation to new biomechanical conditions, as well as owing to tissue growth in response to graduated distraction.

Table 21.1 Dynamics of sound velocity values in forearm skin for surgical lengthening in patients at the age of 3–11 years with forearm congenital malformation upper limb, M ± m (m/s)

	Forearm involved				The contralateral (intact) forearm			
Distraction – 30 days (n = 22)								
Parameter	C(z)	C(x)	C(45)	C(135)	C(z)	C(x)	C(45)	C(135)
M ± m	74.0 ± 2.7[a]	62.8 ± 3.6[a]	70.8 ± 2.6[a]	70.9 ± 3.0[a]	56.6 ± 1.93	43.3 ± 3.91	52.4 ± 2.18	46.4 ± 1.52
Coefficient of variation	15.8	24.9	15.9	18.4	13.2	34.9	16.1	12.7
% of intact	+23.5	+31.1	+26.0	+34.6				
Distraction – 60 days (n = 21)								
Parame-ter	C(z)	C(x)	C(45)	C(135)	C(z)	C(x)	C(45)	C(135)
M ± m	86.1 ± 3.28[a]	61.4 ± 2.59[a]	75.8 ± 3.01[a]	79.3 ± 2.96[a]	62.3 ± 2.38[a]	38.4 ± 1.07[a]	54.1 ± 2.69[a]	53.5 ± 1.84[a]
Coefficient of variation	17.4	18.8	17.3	16.7	16.0	12.0	21.0	15.0
% of intact	+27.4	+37.5	+28.6	+32.5				

Note: M ± m, *M* mean value, *m* standard error

[a]Statistical significance of differences by Student *t*-test with authenticity P < 0.01

Table 21.2 Changes in the value of sound velocity in forearm skin for surgical lengthening in patients at the age of 12–18 years with forearm CGA, M ± m (m/s)

	Forearm involved				The contralateral (intact) forearm			
Distraction – 30 days (n = 23)								
Parameter	C(z)	C(x)	C(45)	C(135)	C(z)	C(x)	C(45)	C(135)
M ± m	82.8 ± 3.14[a]	63.3 ± 2.14[a]	75.8 ± 2.99[a]	77.3 ± 2.48[a]	63.0 ± 3.32	39.6 ± 2.27	57.9 ± 3.32	54.8 ± 2.93
Coefficient of variation	17.0	16.0	17.0	16.0	18.0	20.0	20.0	18.0
% of intact	23.9	37.4	23.6	29.1				
Distraction – 60 days (n = 21)								
M ± m	87.9 ± 3.61[a]	68.3 ± 0.19[a]	78.0 ± 3.57[a]	81.2 ± 2.79[a]	57.0 ± 4.97	42.2 ± 2.49	58.7 ± 4.57	49.4 ± 3.25
Coefficient of variation	18.0	21.0	20.0	16.0	26.0	18.0	23.0	19.0
% of intact	32.9	38.3	24.9	39.2				

M mean value, *m* standard error

[a]Authenticity of differences by Student *t*-test $P < 0.01$

Thigh Skin Response to Dosed Lengthening in the Patients with Congenital Lower Limb Shortening

Analysis of Mechano-acoustic Skin Properties in Healthy Subjects and Its Practical Value

In order to reveal the acoustic properties of the limb skin, we examined a group of practically healthy subjects that conducted the usual way of life but did not participate in sport activities. There were 9 control males aged 18–23 years (n = 18, n – number of segments).

An acoustic analyzer ASA, which sensor provides to realize the tests with its various orientations in reference to the anatomical limb axis (angular orientation) was used in the study. Measuring of surface wave speed (SWS) was parallel [C(z)], transversal [C(z)], at 45° [C(45)] and at 135° [C(135)] relative the anatomical axis of the limb. The life-time skin tests were conducted with the hip and knee joints in extension (180°) or their flexion at 90°. The examined person was in supine position with the angle in knee joint approximately 180°; the foot was in its physiological position at 80–90° of flexion in the ankle joint. The studied area was the anterior surface of the thigh and shin in their middle thirds.

The analysis of the obtained acoustic parameters in the thigh skin showed the following (Table 21.3). The SWS use to measure in the longitudinal direction in the skin of the thigh with the limb positioned in the maximal extension of the knee and hip joints (position A) made 64.8 ± 1.3 m/s. Lower limb flexion in the knee joint at 90° did not result in significant changes of the velocity in the longitudinal direction. Sound properties of the thigh skin in the control male group had no significant changes in other applied orientations such as transverse, at angles of 45 or 135° relative the longitudinal limb axis either.

The comparison of the obtained skin acoustic testing results of the shin with the adjacent joints in extension and flexion (180° and 90° respectively) did not reveal significant differences for all four applied orientations (Table 21.4).

When testing the mechano-acoustic parameters of the shin in the same group of healthy subjects, the analysis of the SWS in the integument tissue of the shin in four directions with the limb adjacent joints in extension revealed significantly higher values of this parameter as compared with the values in the thigh (Table 21.4). Those differences reflect, first of all, the presence of denser integument tissue in the shin. The structural basis of this fact is different types of collagen weave in the thigh and shin, as well as the thickness of collagen bundles. These differences can have an important applied significance for predicting the skin response to plastic surgery and reconstructive/restorative treatment of patients with congenital and acquired pathology of the locomotor system.

Table 21.3 Sound velocity in thigh skin of males aged 18–23 years (control group) by flexion and extension in the adjacent joints, M ± m, m/s

n = 18	Thigh, extension 180° (pos. A)				Thigh, flexion 90° (pos. B)			
Parameter	zTh-180[a]	xTh-180	45Th-180	135Th-180	zTh-90	xTh-90	45Th-90	135Th-90
M ± m	64.8 ± 1.3	57.5 ± 1.1	63.6 ± 1.7	62.1 ± 1.6	66.2 ± 1.7	55 ± 1.3	63.7 ± 1.6	62.4 ± 1.1
Standard deviation	5.7	4.5	7.2	7.0	6.9	5.0	6.2	4.2
Shapiro-Wilk test	Normal	Normal	Normal	Deviation from normal	Deviation from normal	Normal	Normal	Normal
Wilcoxon test	p > 0.05	p > 0.05	p > 0.05	p > 0.05	p > 0.05	p > 0.05	p > 0.05	p > 0.05

M mean value, *m* standard error

[a]Notes: zTh-180 – skin sound velocity in the longitudinal direction, xTh-180 – transverse direction, 45Th-180 and 135Th-180 – at 45° and 135° relative the anatomical limb axis

Table 21.4 Differences in acoustic parameters of the thigh and shin skin when tested in four directions in healthy subjects aged 18–23 years in the physiological position of extension in the adjacent joints, M ± m, m/s

n = 18	Thigh (180° extension)				Shin (180° extension)			
Parameter	zTh-180[a]	xTh-180	45Th-180	135Be-180	zSh-180	xSh-180	45Sh-180	135Sh-180
M ± m	64.8 ± 1.3	57.5 ± 1.1	63.6 ± 1.7	62.1 ± 1.6	81.4 ± 2.6	79.4 ± 2.4	77.3 ± 2.3	83.3 ± 3.7
Standard deviation	5.7	4.5	7.2	7.0	10.9	10.1	9.8	15.3
Shapiro-Wilk test	Normal	Normal	Normal	Deviation from normal	Deviation from normal	Normal	Normal	Normal
Student *t*-test	$p < 0.001$	$p < 0.001$	$p < 0.001$	$p < 0.001$	–	–	–	–

M mean value, *m* standard error

[a]Notes: zTh-180 – skin sound velocity in the longitudinal direction, xTh-180 – transverse direction, 45Th-180 and 135Th-180 – at 45° and 135° relative the anatomical limb axis

Table 21.5 Sound velocity in shin skin of males aged 18–23 years (control group) by flexion (90°) and extension (180°) in the adjacent joints

n = 18	Shin, extension, 180° (pos. B)				Shin, flexion (90°) (pos. G)			
Direction	zSh-180*	xSh-180	45Sh-180	135Sh-180	zSh-90	xSh-90	45Sh-90	135Sh-90
M ± m	81.4 ± 2.6	79.4 ± 2.4	77.3 ± 2.3	83.3 ± 3.7	78.5 ± 2.1	78.2 ± 2.3	80.5 ± 2.0	79.9 ± 2.2
Stand. deviation	10.9	10.1	9.8	15.3	9.0	9.6	8.4	9.5
Shapiro –Wilk test	Deviation from normal	Normal	Normal	Normal	Normal	Normal	Normal	Normal
Student's *t*-test	$p > 0.05$	$p > 0.05$	$p > 0.05$	$p > 0.05$	$p > 0.05$	$p > 0.05$	$p > 0.05$	$p > 0.05$

M mean value, *m* standard error

*Notes: zSh-180 or zSh-90 – shin skin sound velocity in the longitudinal direction, xSh-180 or xSh-90 – transverse direction, 45Sh-90 and 135Sh-90 at 45° and 135° direction accordingly relative the anatomical limb axis

The analysis of acoustic skin properties in the shin of healthy subjects by the change of the position in the adjacent joints did not reveal significant difference in the mechano-acoustic condition of the tissue in two mentioned positions. It proves the fact that a small range change in the flexion-extension angle (not more than 90°) does not result in noticeable changes in the biomechanical skin condition of the shin. The issue of the influence of a greater amount of change of the range of motion in the joints that are adjacent to the femur and tibia on the mechano-acoustic properties of the skin requires further studying (Table 21.5).

Twenty-one patients with the orthopedic pathology were subjected to mechano-acoustic testing for analyzing the dynamics of the acoustic skin properties of the shortened thigh during prolonged dosed stretching in the conditions of Ilizarov distraction osteosynthesis. Each patient had growth disturbances and malformation of one lower limb. Their age ranged from 16 to 21 years (mean: 18.7 ± 0.7). The amount of congenital shortening of the femur was between 3 and 7 cm (4.2 ± 04 см). On line tracking of the dynamics of the SWS in the skin of the lengthened thigh revealed a gradual growth of this parameter as compared to preoperative values, and moreover, this growth was noted in all four tested directions. It was established that the SWS in the skin of the lengthened thigh in the longitudinal direction by the end of the second distraction month made 96.6 ± 5.4 m/s (53.1 % higher than preoperative values, $p < 0.001$ Student's *t*-test), in the transverse direction was 67.8 ± 4.9 m/s (23.5 % increase, $p < 0.05$ Student's test), at 45° direction – 90. ±5.4 m/s (45.4 % increase, $p < 0.001$ Student's *t*-test) and at 135° – 86.0 ± 5.7 m/s (46.8 % increase, $p < 0.01$ Student's *t*-test). A significant rise of

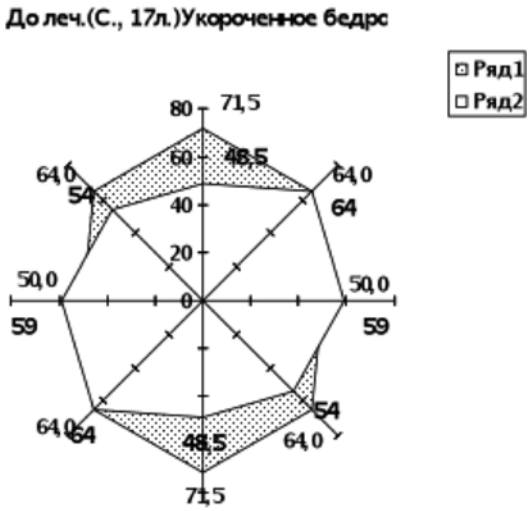

Fig. 21.1 The shape of the circumferential curve that is built at the ends of sound velocity vectors in the skin of the shortened thigh before lengthening (*shaded area*) in extension of the adjacent joints (180°). The white acoustic field with a similar circumferential curve in the skin of the same thigh in maximal flexion of the adjacent joints. Female patient, 17 y.o. Congenital shortening of the right femur; before lengthening. Ordinate – C(z), abscissa – C(x), C(45) and C(135) in the Cartesian system of coordinates correspond to quadrants I and IY

the studied SWS in the skin of the lengthened thigh was preserved during the fixation period, and in the short-term period after frame removal it practically did not differ from the preoperative values. So, by the end of leg fixation this parameter in the longitudinal direction was 87.6 ± 4.7 (38.8 %) m/s versus 63.1 ± 3.8 m/s in the preoperative period. In the short-term period after treatment, the SWS distribution reached 60.5 ± 2.9 m/s and did not differ from the initial preoperative values. The same correlation of the speed indices was preserved also in long-term periods after fixator removal, exceeding 12 months.

Taking into account the fact that flexion and extension take place in the joints of the lower limb during movements and locomotor activity, seven patients were tested functionally and the test results were compared for acoustic skin properties of the thigh in extension (180°) and of the maximally flexed knee and hip joints.

The differences in SWS in the shortened thigh integument by the change of the spatial position of the limb were more marked in the preoperative period. As it is shown in Fig. 21.1, the shape of the acoustic field changed from the longitudinally extended ellipse to a transversally extended ellipse, that is the SWS in the skin decreased by 47.4 % in the longitudinal direction and by 18.5 % in angular orientation at 135° during functional tests (extension-maximal flexion in the hip and knee joints) before lengthening of the femur. In the same situation, the SWS in the transverse direction increased by 18 %. Once the discrepancy of the femur had been equalized the speed grew in all used orientations of the sensor by maximal flexion in the knee joint, and the increment ranged between 3 and 18.5 m/s.

The group of patients that underwent treatment with monofocal distraction osteogenesis had no signs of skin overstretching (striae) as mechano-acoustic tests showed. However, skin overstretching was noted in a number of patients with congenital lower limb shortening accompanied by more marked disproportion of the longitudinal femur size that required operative lengthening exceeding 6–7 cm (more frequently it refers to the age 14–15 years).

Overstretching signs in the skin of the lengthened thigh were located in different areas (Figs. 21.2 and 21.3). According to our observations, the striae developed more frequently in the patients with congenital lower limb shortening in the conditions of bifocal distraction osteogenesis. They were located on the *anteromedial surface of the thigh* or the *posterior popliteal area*, and rarely were noted on the *anterior surface of the lengthened thigh*. One of the possible causes of the phenomenon is thinner skin layers in the mentioned areas and the decreased skin plasticity potential during dosed lengthening of the segment.

It is not always a solvable task to follow the dynamics of acoustic skin properties on the basis of predicting the appearance of overstretching in integument tissue for each patient. Nevertheless, the possible location of overstretching was empirically established.

The quantitative analysis of mechano-acoustic skin properties dynamics in cases of the congenitally short femur that is lengthened

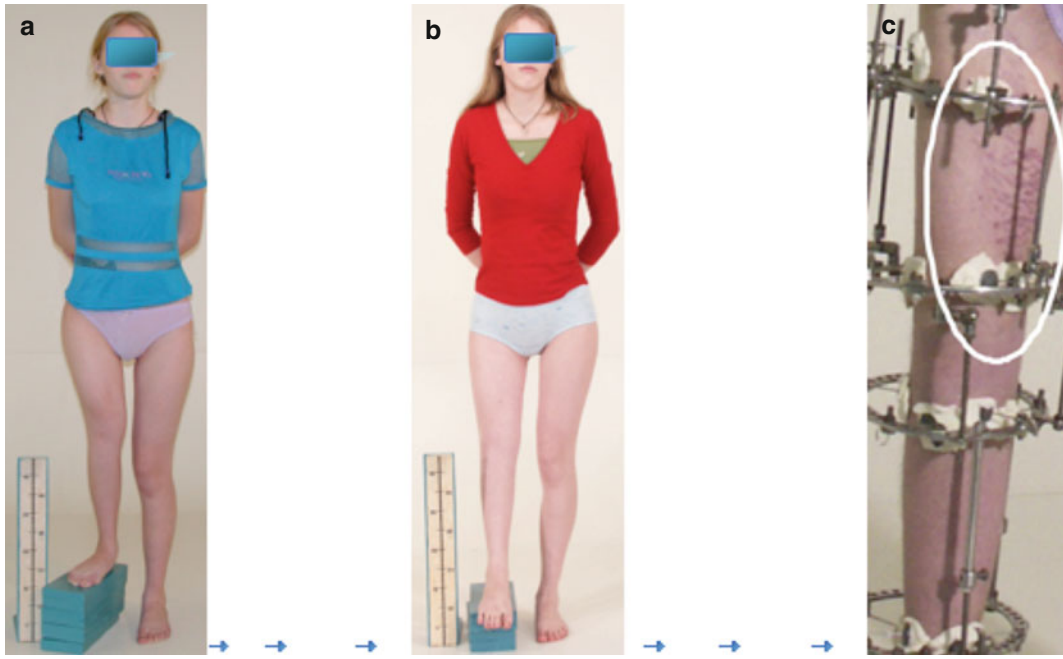

Fig. 21.2 Case of thigh skin overstretching (striae) in the conditions of Iliarov bifocal distraction osteosynthesis (stiae are shown with the white circle). (**a**) Before lengthening (**b**) 12-months after lengthening of the right femur (**c**) Fixation period (48 days). Bifocal lengthening of the right femur by 10 cm

with the method of bifocal distraction osteosynthesis demonstrated the following. The measurements of SWS in the skin of the lengthened thigh in the areas adjacent to the osteotomy line during distraction enabled to estimate its acoustic heterogeneity. The coefficient of heterogeneity (ratio of the SWS in the longitudinal direction to the value in the transverse direction) for the upper third of the thigh (A_B) was 1.5, while for the lower third it was (A_H) – 1.4. Before application of the fixator to the limb, they were as follows, $A_B = 1.1$ and $A_H = 1.0$. It is associated with the growth of the SWS both in the upper and lower thirds of the lengthened thigh, moreover during the first distraction month the SWS grew by the longitudinal orientation of the sensor (Fig. 21.4).

The SWS in the skin of the upper third of the thigh continued growing already in the transverse direction by further lengthening. A more increased coefficient of anisotropy was detected in one patient whose age was 6 years (patient C, 6 y.o). The lengthened amount achieved 7 cm, and the coefficients A_B and A_H reached 1.7, though the increased SWS in the longitudinal direction in this patient was compatible with the speed values in the whole group and was equal 118.5 ± 4.0 m/s in the upper third of the thigh and 127.8 ± 3.2 m/s in the lower one.

On the whole, the coefficients A_B and A_H were 1.4 и 1.3 by 1 month of fixation, and by 2.5–3 months they were 1.1 и 1.0 respectively in the group of patients who underwent bifocal osteosynthesis. As far as the distraction forces in the system fixator-limb continued to decrease by the end treatment, a gradual recovery of anisotropy character to the initial one was noted by the end of fixation period. It proves that rapid restoration of acoustic skin properties of a congenitally short thigh takes place at the stages of lengthening by the Ilizarov method and testifies the transition of the skin, being a biological tissue-composite, in the biomechanical system “fixator-limb” from a stressed deformed state into the state of relaxation.

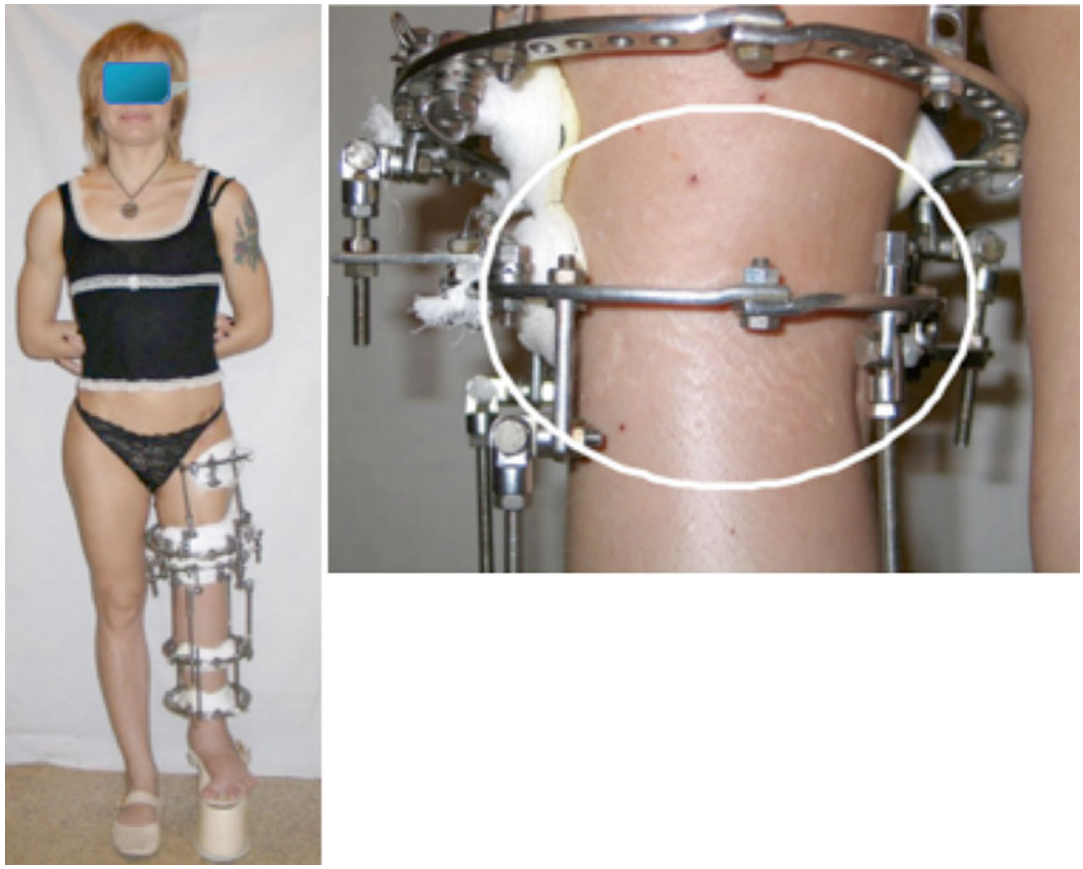

Fig. 21.3 Another case of thigh skin overstretching (striae) in the conditions of Iliarov bifocal distraction osteosynthesis (stiae are shown with the *white circle*). Female patient, 35 y.o. Bifocal lengthening of the left femur by 8 cm. 45 days of fixation

Conclusion

Skin integument has a high potential to stretching. Anisotropy, both structural and biomechanical properties of the skin are the most important properties [1, 3, 5, 8, 9]. Skin as a composite material in response to dosed stretching (distraction) during operative lengthening shortened limb is moving into an oriented stress-strain state. However, skin overstretching is possible and appears like striae, can be painful and impairs the appearance of the lengthened limb in cases of reconstructive and restorative treatment of patients with congenital malformations with a relatively large amount of bone shortening and soft tissue deficit. The overstretched areas can be located in various sites and develop with a higher probability in the skin regions that have lower thickness. The clinical observations have shown:

1. Multistaged lengthening of congenitally short femurs with the technique of bifocal distraction osteosynthesis have a higher probability to cause the development of striae as compared to other Ilizarov techniques;
2. The signs of skin overstretching of the lengthened thigh skin in lower limb congenital anomalies in adults can develop more frequently than in children and adolescents. One of the explanations is a lower plasticity and regeneration potential of integument tissue in adults.

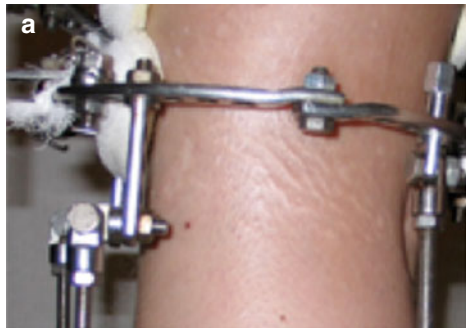

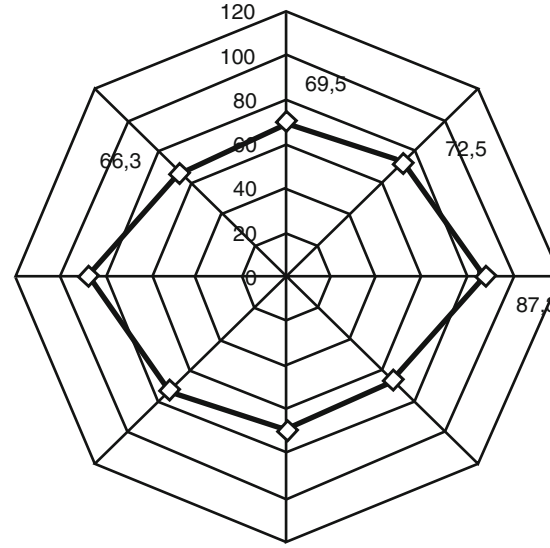

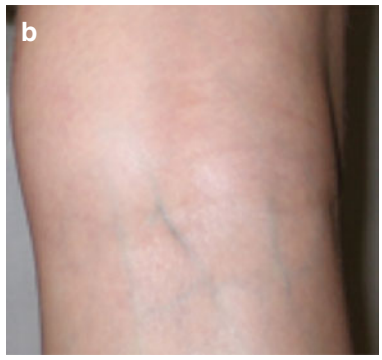

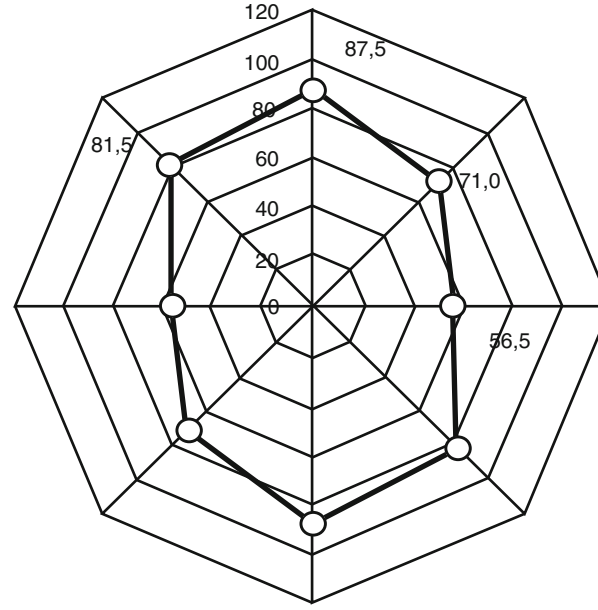

Fig. 21.4 (**a**) Same patient. On the right. The shape of the circumferential curve that is built at the ends of sound velocity vectors in the skin of the shortened t lengthening thigh. (**b**) Same female patient. Symmetrical area in the intact limb. The shape of the circumferential curve that is built at the ends of sound velocity vectors in the skin of the intact thigh

3. The sings of skin overstretching during distraction in cases of congenital growth disturbance and malformations of the upper limb occur much more rarely than in cases of lower limb malformations. The lower limb skin striae can be preserved from 12 to 24 months, but gradually become less noticeable. The prediction of striae development in the skin for management of big amounts of limb segment shortening requires further study. It is important to reduce the period of fixation in the system "Ilizarov apparatus – limb" for the earlier rehabilitation after reconstructive and restorative treatment by Ilizarov.

References

1. Vexler A, Polyansky I, Gorodetsky R. Evaluation of skin viscoelasticity and anisotropy by measurement of speed of shear wave propagation with viscoelasticity skin analyzer. J Invest Dermatol. 1999;113(5): 732–9.
2. Thacker JG, et al. Practical application of skin biomechanics. Clin Plast Surg. 1977;4(2):167–71.
3. Shevtsov VI, Grebenyuk LA, Popkov AV, Grebenyuk EB. Dynamics of acoustic properties of skin integument and hydroxyproline content during surgical treatment of congenital limb malformation. Vestn Ross Akad Med Nauk. 2009;(6):37–43.
4. Grebenyuk LA, Kobyzev AE, Grebenyuk EB, Ivliev DS. The technique for skin plasticity reserve assessment in patient with orthopedic pathology. Med Sci Educ Urals. 2013;(4):11–8.
5. Grebenyuk LA. Analyzing the impact of increased physical loads on the microcirculation and mechanical–acoustic properties of human limb skin. Hum Physiol. 2014;40(4):470–3.
6. Sarvazyan A, Ponomarjev V, Vucelic D, Popovic G, Veksler A. Method and device for acoustic testing of elasticity of biological tissues. USA Patent No 4,947,851, 14 Aug 1990.
7. Popovic G, Sarvazyan AP, Ponomarev VP, Vucelic D. Method and device for non-invasive acoustic testing of elasticity of soft biological tissues. USA Patent No 5,115,808, 26 May 1992.
8. Sarvazyan AP. Chapter 5, Elastic properties of soft tissues. In: Levy M, Bass HE, Stern RR, editors. Handbook of elastic properties of solids, liquids and gases, vol. III. New York: Academic; 2001. p. 107–27.
9. Ruvolo EC, Stamatas GN, Kollias N. Skin vescoelasticity displays site- and age- dependent angular anisotropy. Skin Pharmacol Physiol. 2007;20(6):313–21.

Part IV

Biomechanics of Bone Growth

Biomechanics of the Spine During Growth

22

J. Dubousset

Biomechanism of the spine start as soon as the conception of one individual start as soon as the primary gamets meet together because their DNA bring with them all the genes necessary to determine the unique aspect static and dynamic of this spinal organ so important for the erect bipedal posture which is the basic characteristic of the human.

Each person is unique, even if we find some general characters common to many, it is always with a large range of variations that define so the normality.

The growth of the spine start before birth, then continue all along the infancy and childhood until the end of adolescence with the so called growth spurt making the final touch to the entire program. Each phase of this growing time is different from the previous one because of the size of the elements but also because of the physical and biological characters of the tissues involved.

Finally according to all the genetics, the young adult produced by the end of growth will have the harmony in the space, not only for cosmesis, but mainly for function as well as rest or during the effort and protection of the nervous system a major role of this spinal organ.

J. Dubousset, MD
Department of Orthopaedics, Académie Nationale de Médecine, Paris, France
e-mail: Jean.dubousset@wanadoo.fr

The spinal organ is from an anatomical point of view made of bone structures, the vertebrae, linked by intervertebral disc and ligamentous and muscular formations. Its goals are double : first is to give static and dynamic conditions for the trunk considering that the first vertebra from a biomechanical point of view is the entire head with its proper weight and location (remember that the occipital bone is coming from the first 3 cephalad somites), so we can call it cephalic vertebra. Doing so we must consider also that the entire pelvis is the last vertebra (pelvic vertebra) intercalary bone between trunk and lower limbs with a strategic role as well for standing as for sitting position. Second as we already know, it is all the structures surrounding and protecting the nervous central structures and especially the spinal cord.

Embryology

It is important to remember the various embryologic stages during the first month of life because as soon as the 15th day after conception, the embryo (1,5 mm length) look like an embryonic disc with its 3 leaves ectoblast, mesoblast, endoblast, and from that 15th day the neural gutter starts and is perfectly established upon the ectoblast and at day 20th start also to close at the middle part giving the neural tube. Closure of this neural tube occurs more quickly on the cephalad

D.G. Poitout (ed.), *Biomechanics and Biomaterials in Orthopedics*,
DOI 10.1007/978-1-84882-664-9_22

side (26th day) than on the caudal (28th day). It is during this time that (under the influence of the notochord) the mesoblast will organize. This notochord realize the longitudinal axis and around it vertebral bodies will organize the mesoblast paraxial will became segmented giving the first somites at the middle part of the embryo. In reality because of the important development of the cephalic and brain part of the embryo this level fit with the occiput. Then segmentation continue in direction of the caudal region and the human embryo at the end of the 5th week after gestation counts 42 pairs of somites half on the right, half on the left. These somites will give the future vertebrae and the muscles (myotome).

At the beginning of the 4th week, it is easy to see cells from the medial border of these somites that migrate around the notochord to built the outline of the vertebra, the remaining cells spreading out laterally to give the muscles, especially the paravertebral muscles. So as soon as the 28th day when the caudal neuropore is closed, spinal segmentation is already perfectly achieved. At this purely mesenchymal stage, all the vertebrae are perfectly organized and from anatomical point of view everything is already done. At the same time, coming from intermediate position of the mesoblast, the future nephrotome so kidney organ will develop as well as the cardiac and great vessels structures.

Then from mesenchymal appearance, it will happen chondrification and finally ossification is starting as soon as 2d month of in utero life to end in adulthood around 18–20 years old.

Biomechanical Consequences

So it is clearly understandable that any trouble during this embryologic phase will disturb future biomechanics. For example congenital malformations leading to instability by missing levels of bone, cartilage, or soft tissues, or because malalignment with kyphosis or lateral curvature with related consequences as failure of segmentation, bars, exist at that age and will disturb such growth during the following phase.

Vertebral Growth in Space and Time

Vertebral Growth from Enchondral Ossification

Figure 22.1 The model from cartilage starts to ossify as soon as the 2 months of IU life. The ossification points exist at the level of vertebral bodies, posterior arches, laminae spinous and transverse processes. They determine real growth plate already perfectly visible at birth where only 30 % of spinal ossification is achieved.

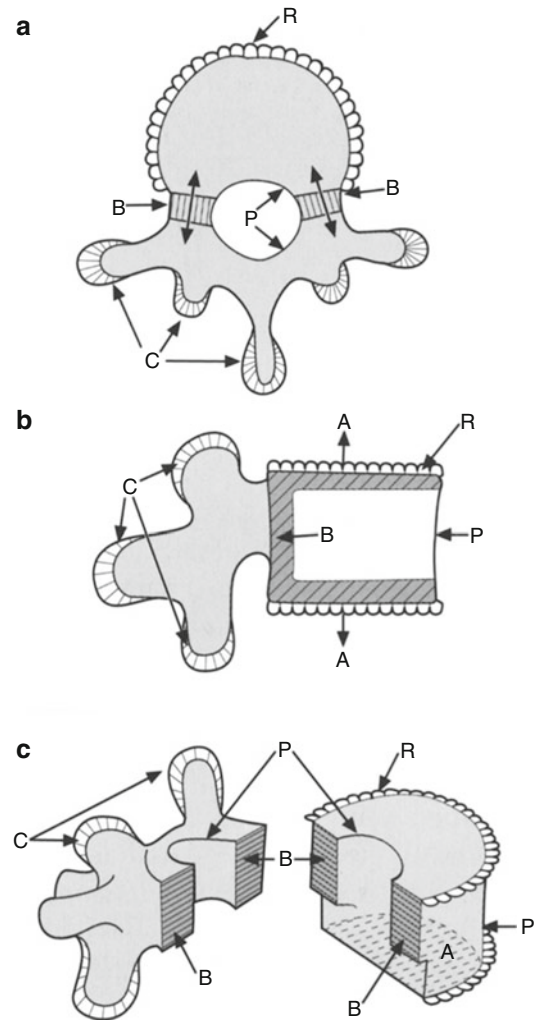

Fig. 22.1 Growing cartilage of a vertebra. (**a**) Vertebral plateau. (**b**) Bipolar cartilage = neurocenral cartilage. (**c**) Posterior elements apophyseal cartilage. *P* periosteum, *R* ring apophysis

Vertebral Growth Plates

Each vertebra has many growth plate levels, but these are harmoniously located and coordinated, so that growth is realized in 3D and is perfectly harmonious.

Each vertebral plateau has its own growth plate, so one superior, one inferior, for each vertebra, giving vertebral growth in length with the rate of 1.2 mm/vertebra/year for lumbar region and 0.9–1 mm for thoracic region.

The neurocentral cartilage is a very important one that allows the junction between anterior body part with the posterior elements. It is a bipolar cartilage giving AP growth as well horizontal growth. They are located vertically, one right, one left, from the neural canal between the two plateau. The junction between vertebral plateau, cartilage and neurocentral cartilage, it is really an unique region when 3D growth is perfectly determined.

They will close between 8 and 12 years even more. It is clear that the unilateral closure of these cartilage lead to horizontal deformity giving typically a scoliosis.

The growth around posterior arch has a proper growth really linked to the neural tube evolution. Secondary ossification centers appears at the tip of spinous process transverse, facets joints and work under the influence of ligaments and muscles insertions. It is important to notice that pars inter articularis is already ossified at birth.

Generally fusion of spinous process on the middle line occurs at age 1, first in the thoracic area, then progress to lumbar and sacrum. Reversely ossification is active for atlas at age 2 and axis at age 4.

The size of the spinal canal remodel through construction – destruction process and has reached adult age size at age 5. This is an essential point for pathology allowing to perform for example circumferencial fusion on a small child without fear [1–3].

Finally as soon as age 10 appears at the superior and inferior plateau border a ring apophysis that ossify slowly according an apophysis front to back and fuse with the vertebral body between 18 and 25 years old.

Vertebral Growth Over Time

Figure 22.2: As it very well represented in the excellent book of Alain Dimeglio [4], spinal growth is exponencial from 0 to 5 years old. At that age, we must remember that 70 % of sitting height as achieved in girls and 66 % in boys. The gain is 27 cm for upper segment in 5 years (12 cm for the first year, 5 cm for second year, 4 cm for third year and 3 cm for 4th and 5th years). Between 5 and 10 years old, growth is more quiet 2–3 cm/year. At 10 years old 80 % of final height is acquired. Then growth spurt occurs with a 4.5 cm/year of growth in mean for the upper segment, then a deceleration more slow and variable from one patient to the other. Notice that the amplitude of such growth spurt is higher in boys (2 cm/year more) than in girls. But growth spurt is always delayed 2 years in boys according chronological age.

We must remember also that at the time of growth spurt, the speed for each vertebra is 1.2 mm for thoracic and 1.6 mm for lumbar between 13 and 16 years for example.

Another item about T1 S1 size is important for biomechanics : Thoracic segment represent 2/3

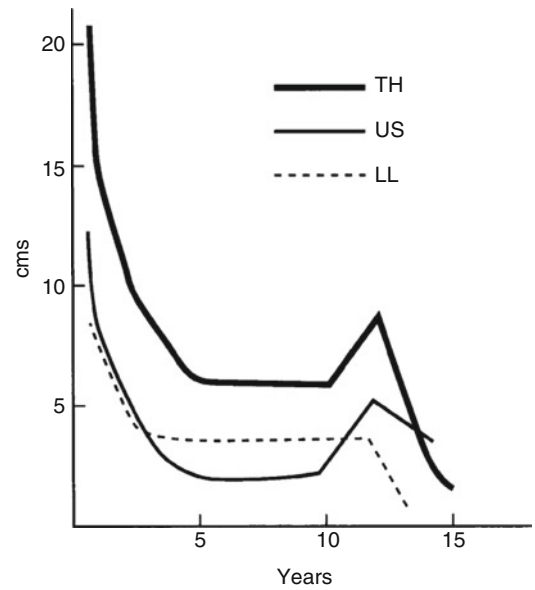

Fig. 22.2 Growth in time (speed). *TH* total height, *US* upper segment height (sitting height), *LL* lower limbs height

and lumbar segment 1/3. But T1 S1 represent 50 % of sitting height. It is why it is important to know the maturation of bone and cartilage for spinal growth. Bone age of the hand is less helpful than Risser sign that remain an important marker; linked with the closure of triradiate cartilage (corresponding more or less to Risser +), linked and correlated to closure of the cartilage of the elbow, but also correlated to sexual maturation (pubic hair, breast in girls, testis volume and beard in boys). All this give an idea of the status of the patient at the time of examination allowing to approach the real vertebral age because none of these sign is absolute by itself, large variation may exist from one individual to another and if we multiply the signs we can reach more close measurement.

Finally it is very important to remember thoracic cage growth very much related to spine : From new born to adulthood, thoracic cage volume is multiply by 14 and 50 % of the final volume is achieved by age 10.

Notice that growth of the thorax in volume continue to increase during 2 years after end of spinal growth.

Biomechanical Consequences

We have many growth tables, charts, to help to control development of the spine and the thorax according age.

This help a lot to decide for example what is the good time to perform fusion when deformity and it is important to recognize the loss of height we can accept by doing so fusion, especially if it is extended to the thoracic area. For example, if we fuse the entire thoracic area in a boy of 10 years old, we remove 6 cm of thoracic height and if we do the same at the lumbar area, we remove 3.6 cm.

A typical consequence for biomechanics of the spinal growth in space as well in time is the crankshaft phenomenon (Fig. 22.3). That is the phenomenon complicating some treatment in the pediatric spine. It is seen when isolated posterior fusion is realized on a scoliotic immature spine. In spite of a solid posterior fusion, we can observe a progressive bending of the fusion mass because of the continuation of the anterior growth. This is explain clearly biomechanically because the growth plate on the front are deviated laterally but continue to grow and make progression of the

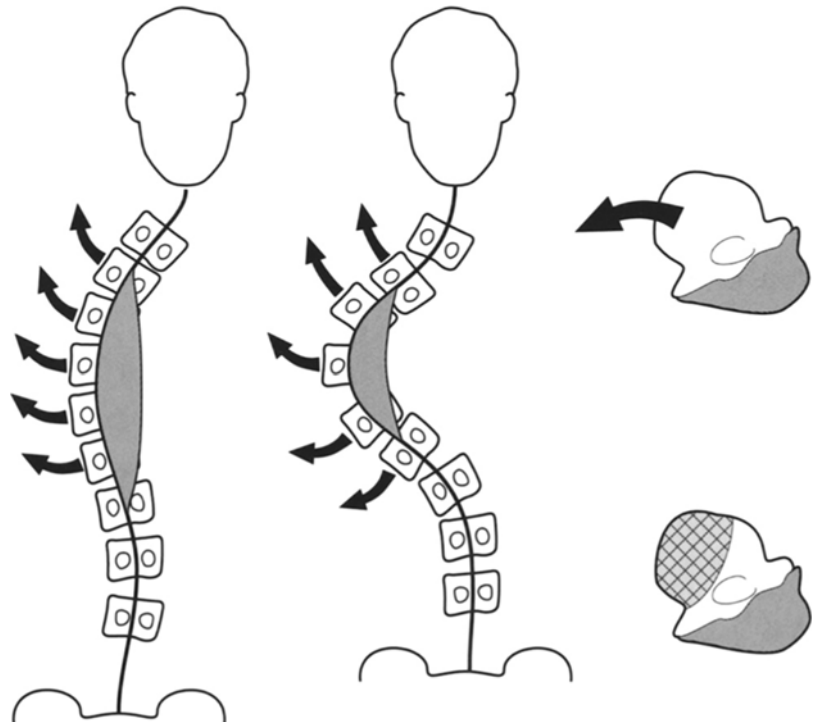

Fig. 22.3 Crankshaft phenomenon. A solid posterior fusion on a growing scoliotic spine play a role of posterior tether on a distorted element and the continuation of anterior growth (*arrow*) increase the rotational deformity. Prevention is of course anterior convex epiphysiodesis (at the opposite side of the posterior fusion)

deformity until growth is completed. It is why the treatment come really from biomechanics : it is a preventive anterior epiphysiodesis done at the same time as the posterior fusion and on the same levels [5–7].

Importance of the Soft Tissues Component of the Spinal Organ

Even if soft tissues (discs, ligaments, muscles) are almost half part of the anatomic structures of the spinal organ, their study is less developed than the one on the bone and cartilage side.

Nevertheless their quality appears very important about flexibility or stiffness even in some case laxity and instability.

The definition of instability is still controversial and involve as the bone and cartilage part coming from the joints facets and disc space structures as well as the soft tissue part coming from disc space structures, capsules, ligaments and muscles. The quality of these tissues depends mainly of genetic aspects of their basic molecular structures, especially connective tissues, collagen, as well as elastic tissues.

From early childhood, one can recognize the elastic component of the tissues with hyperextension of the thumb or hyperlaxity of the joints. This may contrast to joint stiffness with a decrease of normal motion. It is the same on muscles displacement and range of motion, everything is individual.

It is clear that with age maturation of the soft tissues occurs but are much less studied and known than bone and cartilage maturation. For example hypermobility Is more frequent in early age allowing from time to time hypermotion, making discussion with instability like C2 C3 flexion extension test where we can find such over alignment considered physiological.

On the other hand one can have large amount of displacement in severe neck injury in infants giving spinal cord injury without any bone fracture.

Of course the relative higher weight of the head in an infant related to the entire body can play a role in these problem. But it is also sure that with time this hypermobility decrease unless a real pathological connective tissue pattern remain such as in Ehlers Danlos or Marfan disease.

The biomechanical importance of the stability of the spine and the permanent mixture between bone and cartilage and soft tissue conditions is well demonstrated by the consequence of laminectomy in growing child. A biomechanical study has been made in spinal columns of neonate and children by measuring intradiscal pressure of the specimen submitted to constant load in the normal specimen first then after removal one by one of the posterior structures. Starting with only removal of the interspinous ligament the pressure start to increase then one side ligamentum flavum then both side then one facet joint then second facet. This demonstrate clearly that the pressure inside the disc space was increasing constantly as we produce increasing posterior destruction of the stabilizing elements with subsequent increase in kyphosis (Fig. 22.4) [8–11].

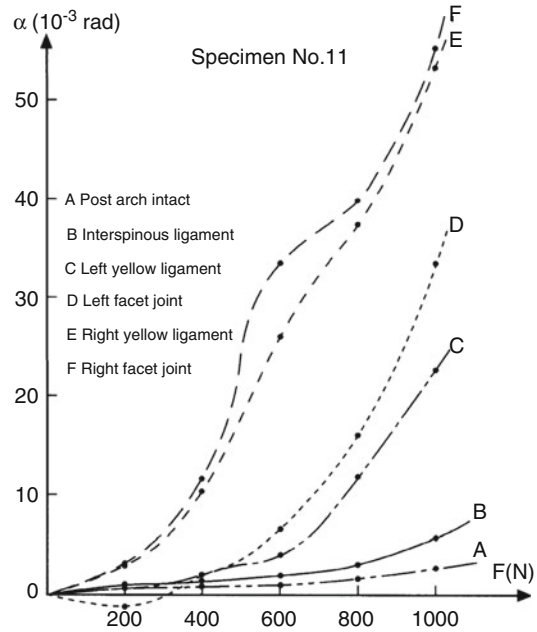

Fig. 22.4 Evolution of kyphosis after experimental removal of the successive elements of the posterior arch in a spinal specimen. α sagittal angle, F force applied (D'après H. Robert. *J Biophys Med Nucl.* 1984;8(4):243–9)

This experiment corroborate perfectly with our observation in pathology in children with instability and kyphosis increasing also constantly. Finally the hyper pressure on the disc space transmit to the growth plate of the bodies and delay growth potential because of the hyper pressure and change completely the aspect of the body becoming cuneiform with decrease of anterior growth and progressing kyphosis.

Prevention by laminoplasty instead of laminectomy when possible consisting to replace the posterior elements removed "en bloc" after the neurosurgical intra spinal work associated with proper immobilization giving proper healing prevent kyphosis and secondary growth disorders.

The importance of the soft tissue maturation is also well demonstrated by a group of scoliotic curves where non surgical treatment was started after end of most vertebral growth done (Risser +++ or ++++) and continued over 1 year after completion of bone maturation. In the group of patients in spite of complete bone maturation improvement of the curve was maintained after removal of the brace : so the only explanation can come from maturation and stiffness that occurred on the soft tissues of such scoliotic spines [12].

The importance of soft tissue factor in the growing spine with a combination of ligamentous, muscular, and nervous components simultaneously injured during the treatment of some tumoral disease of the chest in paraspinal area like neuroblastoma is also easy to demonstrate.

In a child when such removal on intercostal space including from time to time one or two ribs and subsequent intercostal neurovascular bundle is done, the result is invariably a spinal deformity convex toward the side of the injury.

It is not a question of bone, but only a question of soft tissue defect giving slight instability on the ligament linking 2 or 3 spinal segments and localized difference on bone pressure of the growth plate secondary to paralysis of posterior muscles leading to deformity. Even if radiation therapy is given with the disastrous effect well known on the growth plate, the deformity is still convex to the side of the soft tissue injury. Reversely for Wilms tumor in a child treated with surgery and radiation, the deformity is secondary to asymetrical radiation because there is no involvement of paraspinal muscles and the effect of asymetrical radiation on growth plate give a deformity concave to the side of the injury. These two examples demonstrate well biomechanics of the bone as well as biomechanics of soft tissue on a growing spine [5, 10].

Setting Up of the Erect Posture and Its Consequences

Getting the Erect Posture in Humans

As we know at birth the sagittal spine shape looks like a gentle C arcuature [13]. When the child start to be on his prone position the heavy head start to be lifted up and the cervical lordosis develops. The next step is walking on the upper limbs and knees ("crawling four feet") and cervical lordosis increase as well as lumbar lordosis initiates. Then when he stops, he starts to lift up the upper limbs and raise his back on the knee flexed, but hip extended and so lumbar lordosis progress to be established. Then he stand up with proper cervical lordosis, thoracic kyphosis and lumbar lordosis. The erect posture is so acquired and will develop all along childhood and adolescence to the adult age.

Maturation of the Central Nervous System

It is during that phase of setting up the erect posture that the maturation of the nervous system take place. At birth it is well known that the nervous system is not completely developed and still immature especially about the myelinisation of the central nervous area.

The coordination and achievement of balance continue to extend during a large part of childhood. The postural balance integrate sensori stimuli coming from eyes, ears, vestibular and proprioception is established with proper automatic function coming from the motor reaction of muscles surrounding joints themselves getting information from receptors inside the capsules or tendons.

We still don't known exactly what are the neurohormonal transmitters working on the postural balance at the level of the relationship between right and left brain and the function of hypothalamus.

This is a way of research developing around the etiopathogeny of idiopathic scoliosis with the experiment done with the pineal gland, neurotransmitters function, as well in bipedal animal where scoliosis exist and can be reproduced and quadrupedal animals where scoliosis don't exist and cannot be reproduced experimentally with neurological lesion done distant from the spine itself [14].

The maturation of this nervous system play probably a great role in the idiopathic scoliosis and may explain why some real infantile severe curves can regress completely with a pure non surgical treatment (brace or cast for example) and some even spontaneously, even with some remnent of the deformity with wedged vertebrae included in a straight spine. And also explain in case of persistent immaturity of the nervous system why some other malignant cases cannot correct with the same kind of treatment.

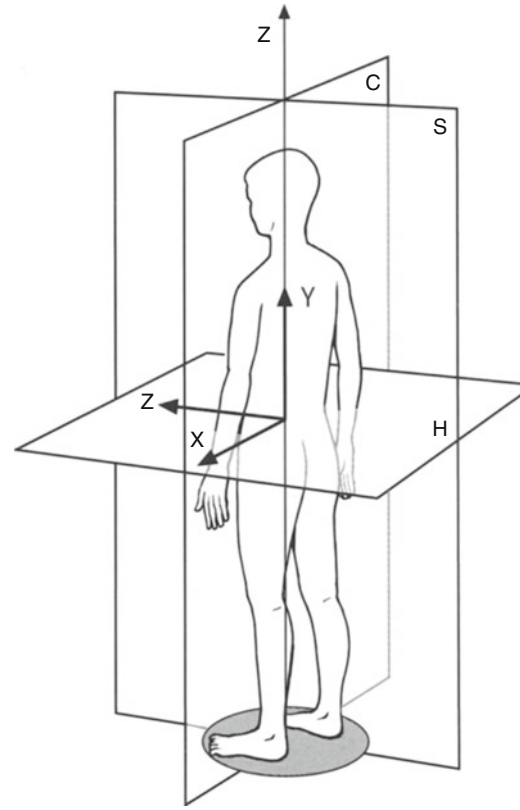

Fig. 22.5 Standing posture planes of reference and polygon of sustentation. (1) Polygon of sustentation. (2) Orthogonal gravity line. *R* sagittal plane, *H* horizontal plane, *C* coronal plane

Biomechanical Consequences of the Erect Posture in Children and Adolescents

Of course the concepts recognized and developed here for the growing spine by the author are easily adaptable for adult spine.

Static and Dynamic 3D Balance

If we consider the erect posture in a human (as in a young or an older child or an adult), we know that in a standing position, both feet are pushing on the ground and delineate a surface ellipsoidal called the polygon of sustentation (Fig. 22.5). If you consider the same human at any age seated, you have the same polygon of sustentation now looking like a frame done with both thighs and ischial tuberosities.

Either standing or sitting from the center of this polygon of sustentation, if you draw the orthogonal line, you have all your body including the head aligned harmoniously within this line realizing such gravity line with a patient in a good 3 dimensional balance. Anatomically on the sagittal plane this line goes from tragus to the center of this polygon and the spine is harmoniously aligned with cervical lordosis, thoracic kyphosis, lumbar lordosis, sufficient pelvic tilt, hips extended and knee extended with the ankle joints at more or less 90° from the ground. This is defined like a balanced spine where the spinal curvatures balance themselves in opposite direction to achieve harmony and function with the head projecting inside this polygon of sustentation.

When the patient is seated, it is the same with the head entirely balanced to the center of the sitting frame and the spinal curves adapting to the

proper pelvic tilt necessary to compensate the absence of lumbar lordosis or the kyphotic lumbar deformity. This balance is defined static when no motion at all is observed but in human there are constant motion within this surface of polygon in a 3D manner.

Cephalic and Pelvic Vertebra Concept

Resulting from the previous 3D balance, we consider the entire head with its own mass and weight (# 4.5 or 5 Kg) like the first vertebra (Figs. 22.6 and 22.7). This weight lying at the top of the spinal construct is almost always moving and realize like a gyroscope to maintain the balance [13, 15, 16].

Simultaneously the entire pelvis (because of the minimal movement inside the sacro-iliac joint less than 1.5° motion unless pregnancy where it can reach 3.5° of motion) can be considered like one unique vertebra, the last of the spine and like an intercalary bone between trunk and lower limbs.

Doing so when a global thoracic kyphotic deformity occurs, the pelvic vertebra can compensate by anterior tilt realizing a compensation, lordosis at the lumbar level, etc. This pelvis vertebra has 6° of freedom for each hip joint and the same for lumbo-sacral junction.

It is interesting to notice here various work about this pelvic vertebra because it has been proven that the proper anatomy of this pelvic vertebra play a great role in the amount of lordosis necessary to achieve balance, especially in the sagittal plane. The angle between the center of femoral head and the orthogonal projection to the center of S1 superior plateau determine the Incidence. The variation of this angle is observed generally between various patients with no more than 12–15° variation. It is also remarkably stable during life and very few or almost no change after age 5. This angle determine the amount of lordosis necessary to get a good sagittal balance. The incidence represent in reality the positioning of the SI joint in the space regarding the one of the femoral heads. This explain the wide variation we can get between male and female and morphotype of patients (thin and tall or short and wide).

Concept of the Conus of Economical Consumption and Economical Function

If we consider the human body in a standing (or sitting) posture, the feet are located within the polygon of sustentation, the body under the influence of muscle function can move in a conical fashion without moving the feet (Fig. 22.8). The maximum variable amplitude are at the pelvic and the head levels, we can determine a maximum cone when muscles are working at their maximum of excursion and strength to maintain balance. But also we can determine a smooth cone when muscles are working at their minimum in some cases almost nothing to maintain balance mainly achieved by the passive balanced stretching of discs, ligaments and soft tissue structures with the minimum of muscle action. This is obtained when the body is well balanced within this smooth cone, the muscle function is economial. When the body is out of balance, we must anticipate a permanent curd costly muscle function [13, 15, 16].

Biomechanics of Ligaments, Aponevrosis and Muscles Surrounding the Spine for Static and Dynamic Function During Erect Posture

One must distinguish two groups of soft tissues structures:

- Ligaments and aponevrosis (not only within the spine itself, but also concerning the entire body of the trunk) will determine like a net of more or less rigidity within the large thoracolumbar fascia. When all these fibers are stretched then the net is rigid and stable. When these fibers are relaxed then everything can occurs, especially when speaking about motion and passive motion is only limited by the passive tension of these structures [16, 17].
- Muscles : the muscles of the trunk around the spine are of two types, the ones very close to the spinal body structures like interspinous, paraspinous, multifidus, transverse, and the ones relatively away from the spine like abdominal muscles, ilio-costalis, longissimus dorsi, longissimus lumborum…Each one of these muscles may have two main functions.

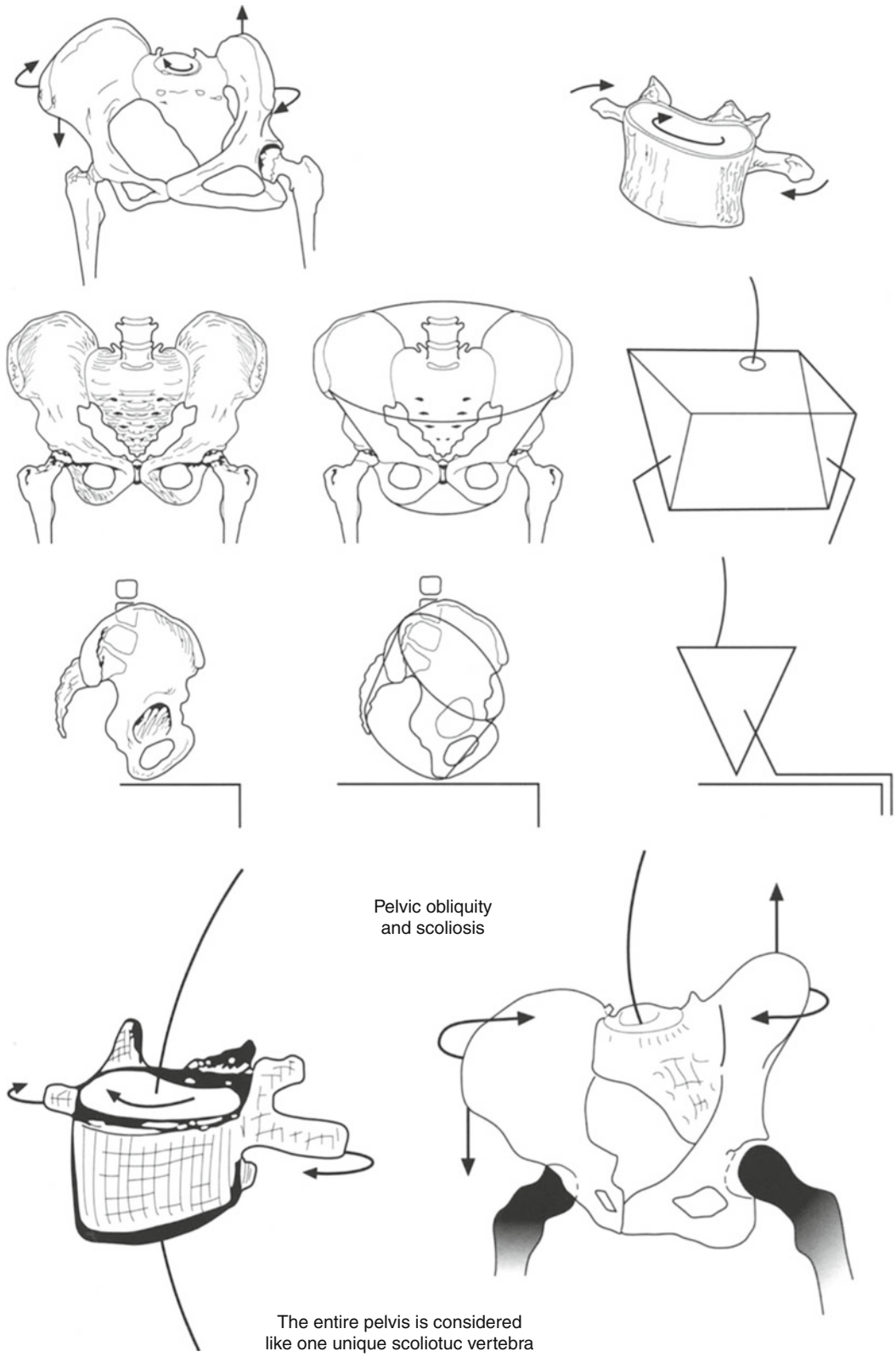

Fig. 22.6 Coming from the study of pelvic obliquity and scoliosis, the entire pelvis must be considered like one unique vertebra

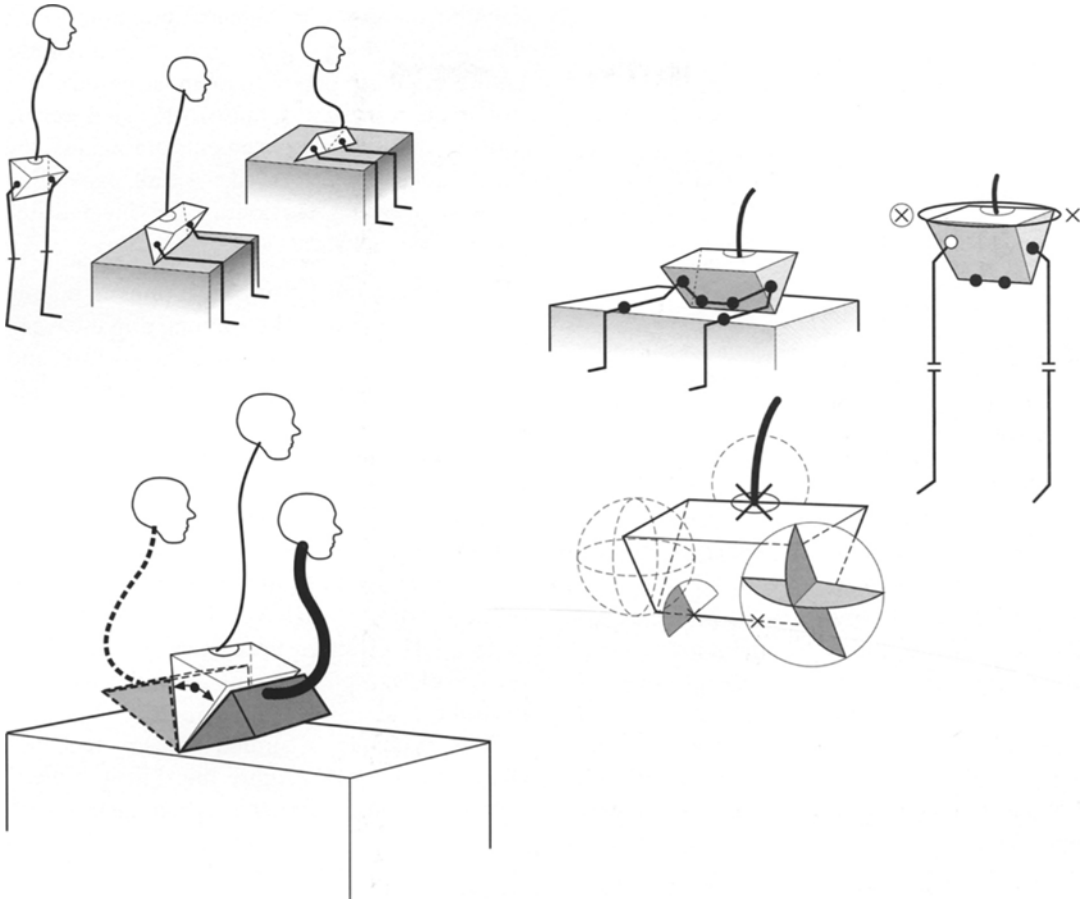

Fig. 22.7 The entire head must be considered as the cephalic vertebra and the pelvis as the pelvic vertebra acting as an intercalary bone to achieve balance

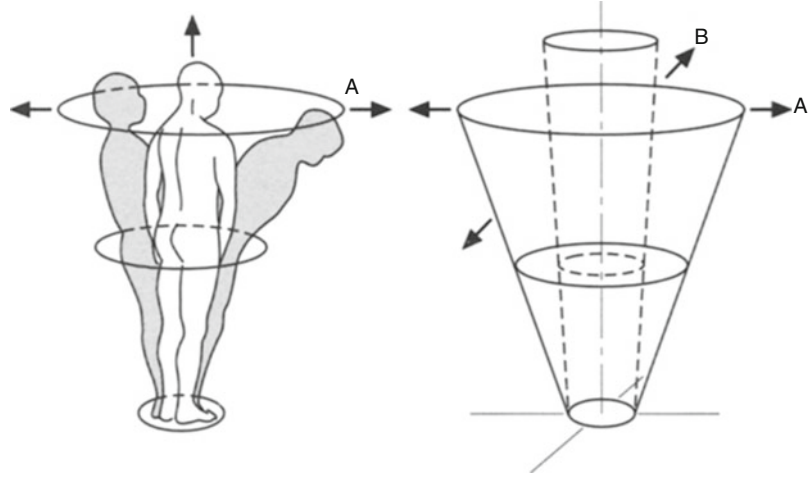

Fig. 22.8 Concept of the conus of economical function in standing position. (*A*) Maximum of function before falling down. (*B*) Economical function where the spine is balanced with almost no muscle action

Some are working like a string pushing pulling two elements one against the other. Some are working like a ball expanding inside the net and tensioning strongly the inextensible fibers of the network.

The first function (string or pump) is mainly devoted for motion and mainly voluntary, but the second one (ball type) is mainly devoted for posture and especially economical posture and they are mainly automatically working (Fig. 22.9).

One can understand why the automatic system is of importance with short reflex coming from this erect posture where the human want always to get or recover the horizontal gaze whatever the spinal deformity. There are a complex automatic net of short reflexes from visual vestibular as well as mechanical extensor flexor muscle and ligaments receptors origin to achieve erect posture.

It is probably very close system that allow to acquire walking. Because walking is a permanent search of balance after the instability induced by the first step. It is why patient that are not able to stay seated in an erect posture on the side of a table are not able to walk because the muscles function of their erect posture giving stability as well as motion of their spine is not achieved. It is the same reason for some diplegia cerebral palsied patients are not able to stop during walking in the middle of the room without help of upper limbs on a stable support.

Development of the EOS System

All these previous concepts were at the basis of the development of the EOS machine.

Thanks to the invention of Georges Charpak (Nobel Price of Physics 1991) who designed the detectors to use the x-ray with a very significant reduction dose eight to ten times less than conventional x-ray for 2D imaging, we were able to purpose in conjunction with E.N.S.A.M. engineers in biomechanics in Paris and L.I.O. engineers in biomechanics in Montreal, to built a device able to scan the human head to feet in standing position simultaneously AP and lateral [18].

This is the EOS machine where scanning is done for the whole skeleton in about 15–20 s. From this thanks to a proper software a surfacic 3D reconstruction of the whole skeleton is done. Accuracy was compared for similar patients and various specimen to the 3D reconstruction obtained from CT scan conventional 1 mm slices. Accuracy was measurement as good as the one

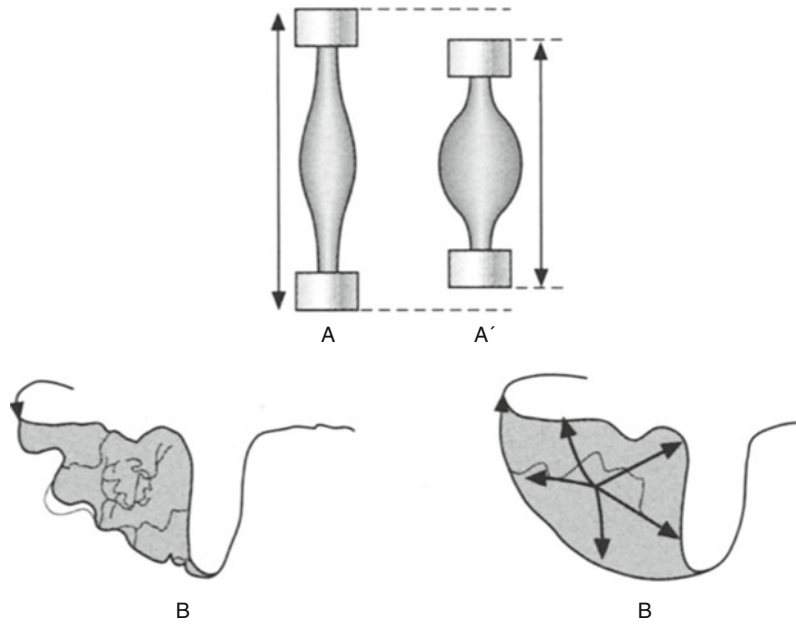

Fig. 22.9 Concept of "string" and "pump" function of the muscles surrounding the spine. (*A*, *A′*) String function moving the bone. (*B*, *B′*) Pump function expanding and tensioning the net of aponevrosis of the postero-lateral spinal muscles

coming from CT, but the reduction dose was enormous from 800 to 1000 less.

Thanks also to the introduction in the machine of a force plate the real functional study of the patient was possible in 3D. This was not only to study the spinal structures alignment, deformities, correction of them after surgery or worsening, but also to study balance and compensation from one part of the skeleton to the other one. The view from the top is unique to measure all the horizontal plane phenomenon that is rotational deformities of the lower links, of the pelvis, of the spine, of the head.

The very powerful role of the pelvic vertebra in the compensation of lumbar or thoracic spinal deformities become evident and really seen and measured. For example, in the aging spine the role of the pelvis which is often a starting point in the beginning of the decompensation is clearly demonstrated.

The only limitation of use of this device is the very young age of the patient, when he is unable to remain still and quiet for the time of the scan (20 s for an adult 1.70 m, 10 s for a child 1.00).

Application to the Common Pathology of the Growing Spine

Pure sagittal deformity is easy to understand because there are no deviation in the horizontal plane neither in the coronal plane.

Deformity may be regular in kyphosis or lordosis that is variation from normal but occurs at every level and determine an apical zone that is the most deviated from the gravity axis that is smooth because very little change from one vertebra to the other one and junctional zone that is the zone of transition from one direction (for example kyphosis) to the other (for example lordosis). This regular kyphosis with smooth apical zone generally don't create apical compression at the level of spinal canal.

The main pathology for this is Scheuermann kyphosis with various apex, thoracic or thoracolumbar, very seldom lumbar where hyper kyphosis has a subsequent above and below hyper lordosis in order to maintain the sagittal balance. In contrast for example thoracic hypo kyphosis leads to a decrease of normal cervical and lumbar lordosis and create a flat back. From a 3D point of view, thoracic hyper kyphosis is generally associated with an increase of antero-posterior diameter of the chest and vertical orientation of the ribs and very few respiratory consequence. In contrast, thoracic hyper lordosis is associated with a decrease of the AP diameter, horizontal ribs and more respiratory compromise leading in some cases to intermittent compression of the airway and in major cases atelectasia. This allowed us to describe the spinal penetration index (Fig. 22.10) that is the amount of protrusion of a real vertebral intra thoracic hump that in normal spine is around 10 % of the surface or thoracic volume and can reach 50 % in some severe lordotic cases (Fig. 22.10). This allow to know the useful thoracic volume devoted to the lungs and mediastinum structures.

The sagittal deformity may be angular: that is the deformity lies still in the sagittal plane only, but on a few levels sometimes only one and create

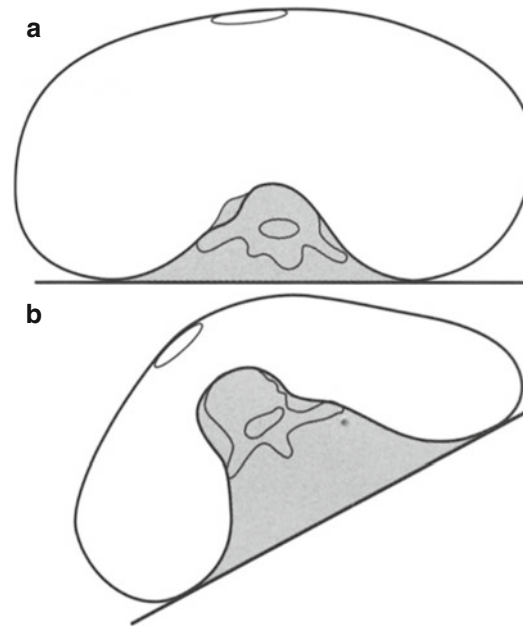

Fig. 22.10 Spinal penetration index. Surface or volume occupied by the spinal structures inside the thoracic cage. Normally around 10 % (**a**). it can reach 50 % in severe cases (**b**)

a sudden change in the alignment of the apical zone with subsequent possible compression of the spinal canal. Especially the angular kyphosis may be associated to instability that may be immediate when the posterior alignment of the vertebral bodies are demonstrating a sudden abnormal motion when dynamic imaging is done. It may be potential when dynamic imaging don't demonstrate abnormal motion but where malalignment exist from the beginning. In such cases either progression of the deformity with growth or sudden mild injury can create a spinal cord traumatic lesion [1–3, 19, 20].

The biomechanics consequence for surgery of such angular kyphotic spine is that when an anterior empty space exist in the front of the spine, it is mandatory to supplement the anterior pillar by anterior fusion to fill the gap and stabilize the spine. The stability can be achieved if there is a large kyphosis by anterior strut "palissade" graft inserted from the bottom of the apex going ideally to the gravity line and so suppressing the kyphosing forces (Fig. 22.11).

Scoliotic Deformities

The basic structural scoliotic segment [12, 16] is represented by a succession of vertebral units that are always located in extension or lordosis from one to the next with axial rotation of each vertebra always in the same direction. This begins with one neutral vertebra (without axial rotation) and continue with a successive increase in axial rotation achieving maximum axial rotation at the apical vertebra of this segment. Then runs down with decreasing axial rotation in the same direction to the end at the next neutral vertebra. This movement is called torsion (Fig. 22.12), the real basis deformity, that cannot be located in one plane, but has an infinity of planes. This phenomenon is secondary to a rotatory movement which is thwarted by the orientation of the pelvis, shoulder, and head and involving subsequently all bone and soft tissue structures of the spine and perhaps each molecule. The 3 dimensional computerized reconstruction demonstrates very well the anatomy and also the progression in space of

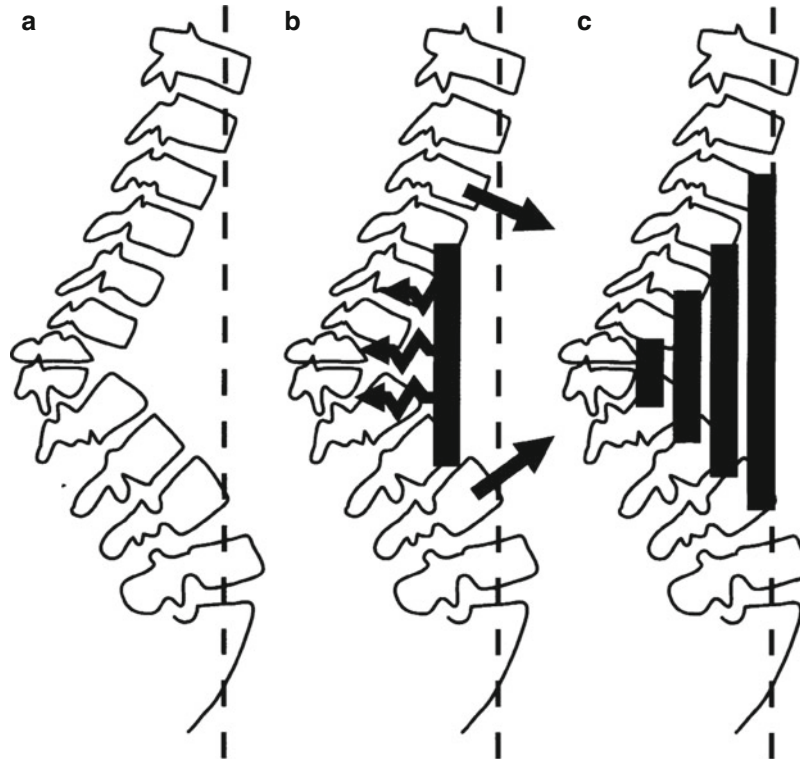

Fig. 22.11 (**a**) Angular rigid kyphosis. When by pass strut graft (*dotted line*). (**b**) It remain kyphosis forces (*straight arrows*) and a gap toward the apex (*z arrows*). (**c**) To suppress it, it's necessary to realize a palissade strut graft

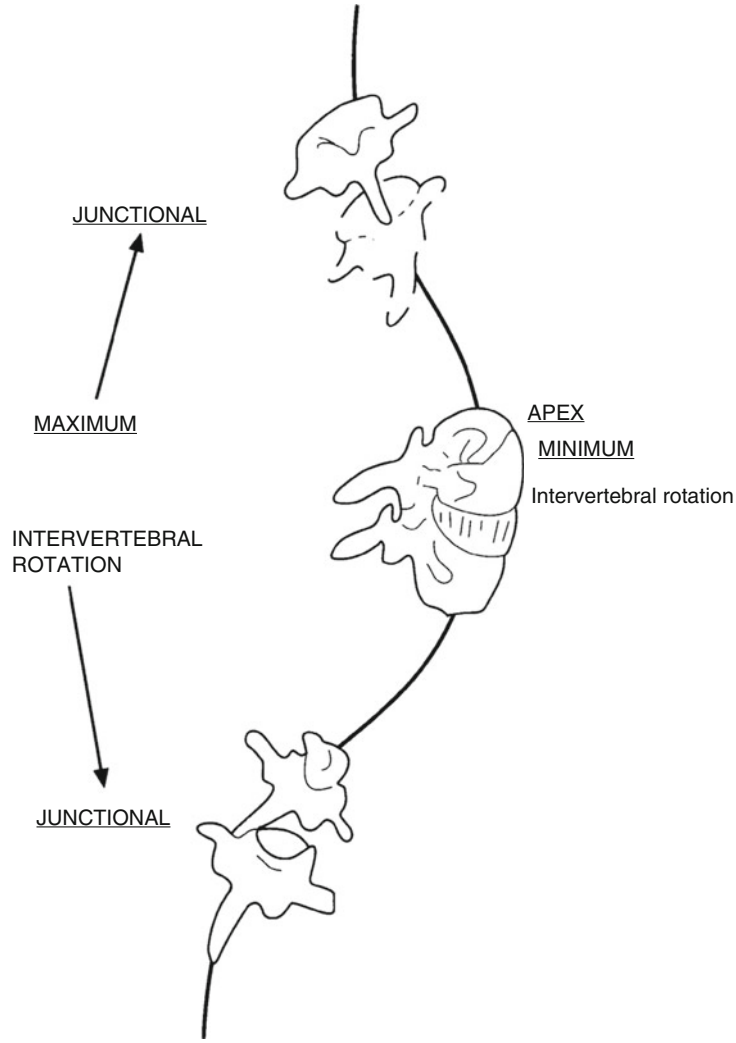

Fig. 22.12 The basic structural scoliotic segment where anterior length is greater than posterior one at the level of 2 consecutive vertebral units

the deformity with time. This also demonstrate that the Cobb angle so widely use measure in fact only the collapsing of the spine and not the real 3D deformity (Figs. 22.12, 22.13, and 22.14).

So a scoliotic spine is made by either multiple scoliotic structural segments or by only one scoliotic structural segment followed above and below by a compensatory (not structural) segment in order to achieve alignment and balance either for standing or sitting posture. That is the characteristic of human bipedal status. So each one of these segments is linked with the other with a junctional zone representing either one disc space only or the zone of one disc and the vertebra above and the vertebra below or at maximum a group of two consecutive vertebrae, the middle element has a neutral axial rotation while the adjacent has an opposite side axial rotation from the above to the below. This realize a balanced spine in the 3D (Fig. 22.14). It is why the maximum of axial rotation in a scoliotic spine is located at the apex, but with the minimum of the intervertebral rotation (that is the axial rotation of two adjacent vertebrae), so apex is the stiffest part. Reversely junctional zone is the one with minimum of axial rotation, but maximum of intervertebral rotation so the most mobile one [16] (Figs. 22.12, 22.15, and 22.16).

This concept was very important in the biomechanical design and use of the spinal instrumentation, especially for C.D. instrumentation of the many multiples hooks, screws and rods

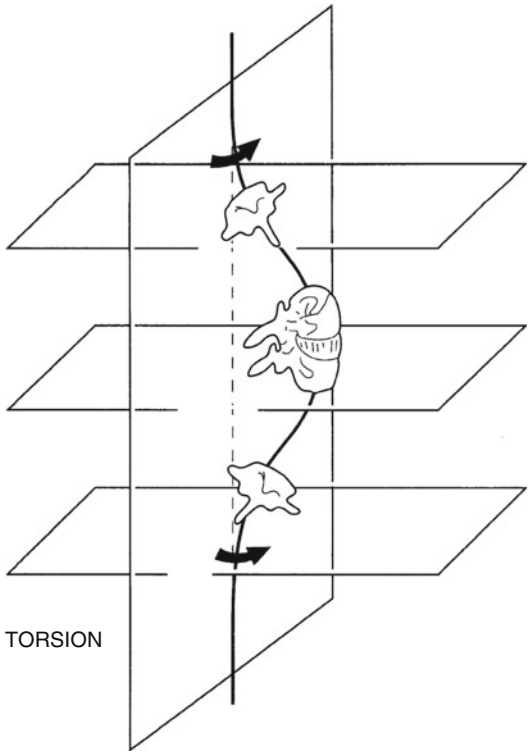

Fig. 22.13 Torsion is the 3D characteristic deformity of a structural scoliosis

systems actually widely used all around the world. It is why in reality for correction with these systems we always use compression, distraction, rotation, translation, for any correction of a scoliotic curve and all the discussions about that problem of one using more rotation than translation or compression are sterile because all mechanisms of correction are used obligatory due to the 3D shape of the scoliotic curve. These must be analyzed simultaneously AP and lateral, each segment replaced in the entire spine (Figs. 22.15 and 22.16).

Two consequences of this three D analysis came from these concepts :

The rotatory dislocation of the spine concept (Fig. 22.17) [21] that we described already in 1972 for some dystrophic, congenital or idiopathic conditions [22]. This is realized by the junctional zone in between two scoliotic segments occurring on a weak bone tissue. The basic mechanism is at the level of the most dysplastic area when located at the junction of two lordotic segments, a rotational movement in an opposite direction occurs in front of the spinal canal and initiates the deformity. As the deformity increase

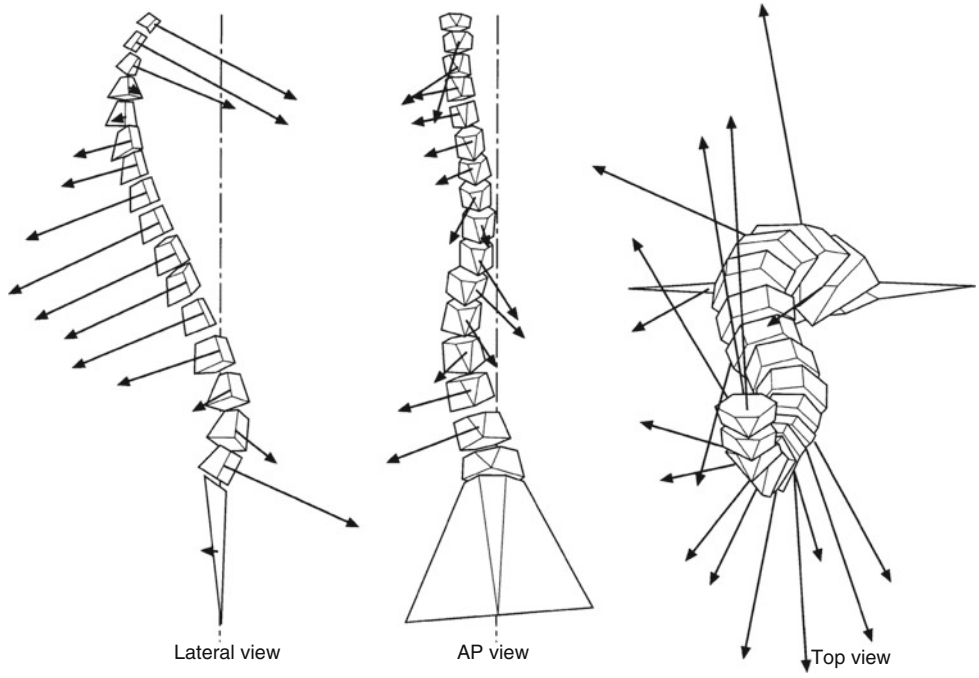

Fig. 22.14 3D computerized reconstruction of a scoliotic curve. The top view is particularly well suggestive of the real deformity not always recognized from x-rays

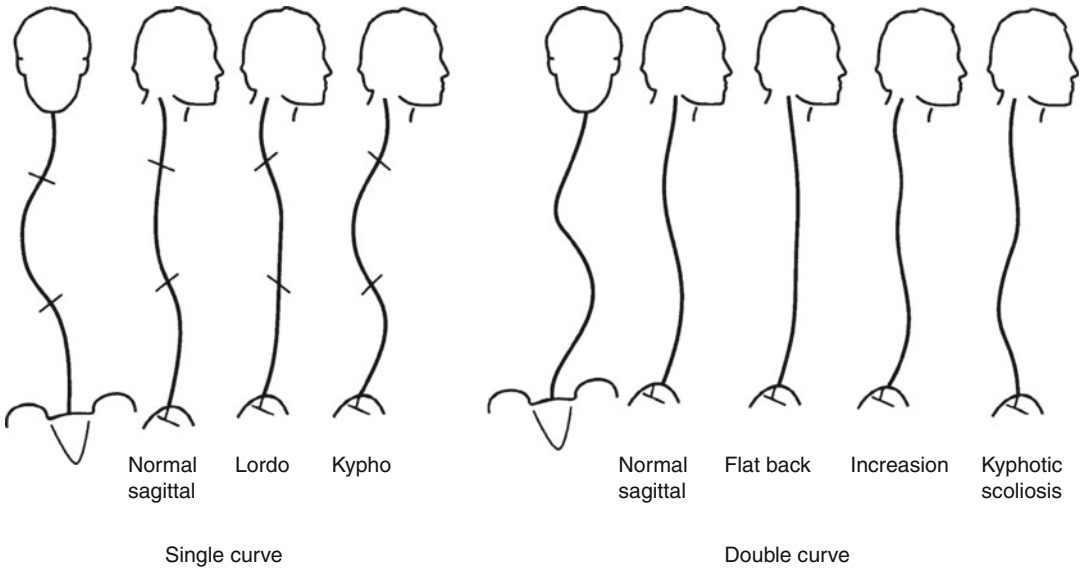

Fig. 22.15 Practical approach to the surgical treatment of a scoliotic spine either for simple curve or double curve. Global analysis demonstrate well for a similar AP view various sagittal possible alignment. So to realize the proper fitting of instrument, it is mentally necessary to match AP and lateral aspect globally as well as for each segment of the spine and determine apical zone and junctional zone

an expulsive force generated by the rotational movement lead to increase deformity in the three planes and in some case may compromise the spinal cord. But in most of the cases the canal is still in continuity without any dislocation, especially if the dystrophy exists on multiple successive levels (2, 3 or 4). Then because the canal is in continuity and rotating deformity progressively increased, it is obvious that we can use the flexibility of the spine in the other way and if we submit traction progressive but constant, we can reduce the deformity in a great amount. In addition when progressive neurological troubles appeared subsequent to the progression of this kyphosis, they can reverse completely with this traction because of the relaxation of the tension of the neural structures. Subsequently also stabilization of the spine must be achieved by circumferencial front and back fusion. The anterior fusion must be done from the concavity (Fig. 22.18) of the coronal deformity in order to be in alignment with the gravity line that cannot be reached if the approach is done from the convex side. This convex approach in addition bring more instability because remove the convex ligaments working in tension and disrupt the tension band given by the ligaments. Here the concave struts grafts will work in compression and stabilize the spine.

For idiopathic conditions (Fig. 22.16) it is exactly the same mechanism occurring on good bone vertebrae and the deformities are not so important, but just a little and allow to determine the junctional zone especially critical to avoid the so called junctional kyphosis factor of poor balance result after instrumentation or for spontaneous evolution whatever the level in the spine but mainly in upper thoracic or thoraco-lumbar areas [12, 16].

It is easy to recognize on AP and sagittal x-rays because the apex of the kyphosis lies at the junction of two scoliosis curves anatomically lordotic.

The hyper rotatory kyphosis (Fig. 22.19): this deformity is still another basic deformity of the scoliotic spine especially in the infantile group. It is in reality a paradoxical kyphosis. It corresponds to intervertebral lordosis, but with an axial rotation so marked that the lateral scoliotic collapse appears on the sagittal plane and the

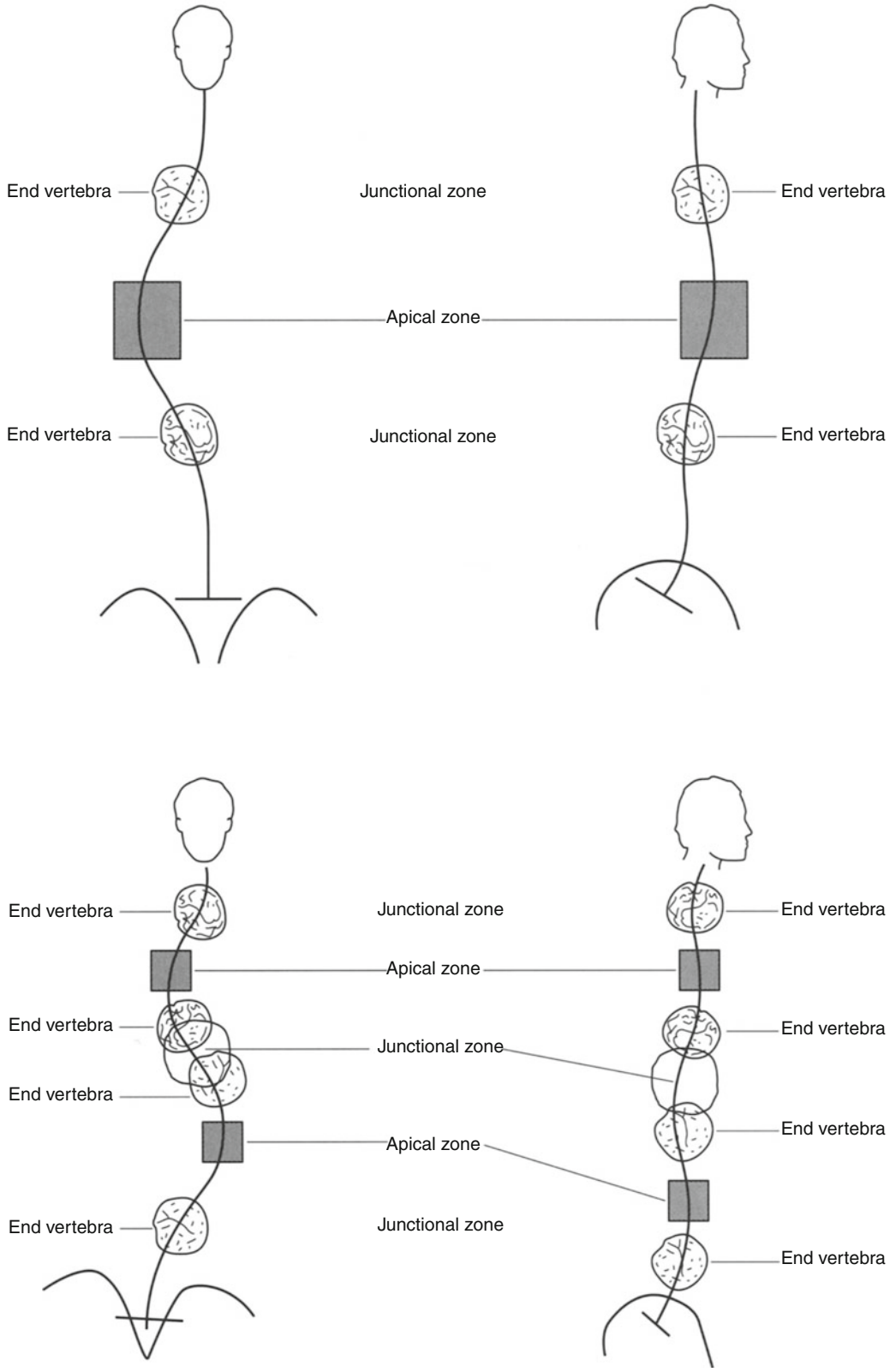

Fig. 22.16 Analysis to determine the apical zone and junctional zone for idiopathic curves

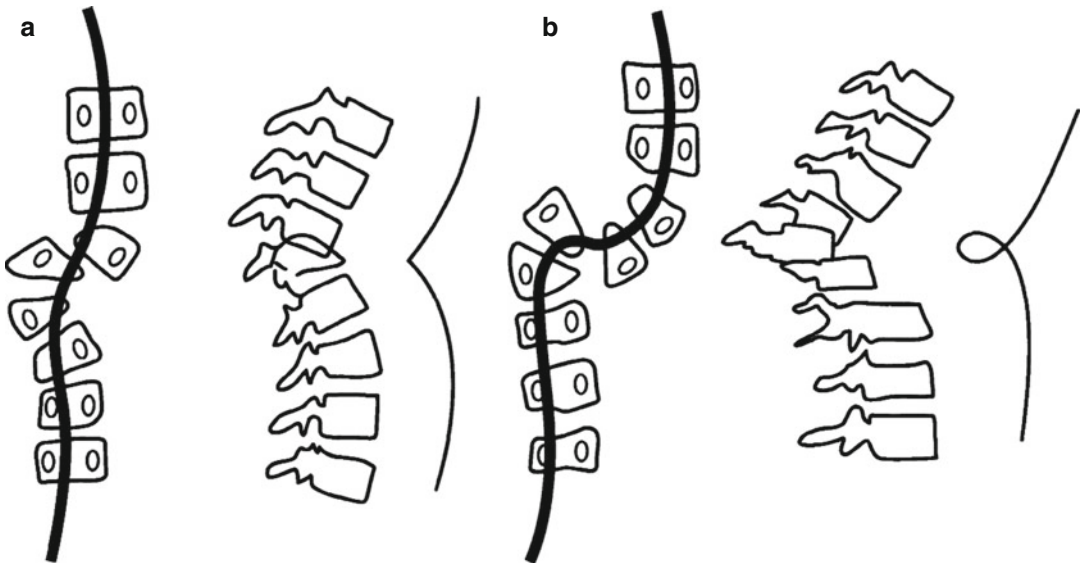

Fig. 22.17 (**a**) The rotatory dislocation of the spine concept. The apex of the kyphosis coincide with the junction of the 2 curves on the coronal plane (first dessin left). (**b**) Increase of the angle of both curves in the coronal plane means increase of the kyphosis (second dessin right)

patient looks kyphotic. It is specially apparent when viewed from the top in 3D computerized reconstruction and easy to recognize on AP and sagittal view because the apex of the kyphosis is exactly at the same level as the apex of the scoliotic curve (Fig. 22.19a, b).

This deformity is common for infantile and very progressive juvenile scoliosis idiopathic curves. But also it is the same in lumbar kyphosing scoliosis in adult and elderly spines. There it is mixed with degenerative change in capsules, discs and ligaments. For these hyper-rotatory kyphoscoliosis the three columns horizontal concept is very important because if the anterior column disappears or was ejected laterally and backward from the gravity line, nothing hold the spine in the front and the collapse looks kyphotic. So this type of hyper rotatory curve can be corrected through an anterior convex approach with detorsion devices following anterior real release and instrumentation. The realignment of the spine is obtained by correction of axial rotation and lateral ejection, this automatically correct the sagittal plane [12, 16].

Remember finally that this hyper rotatory kyphoscoliosis is exactly what we can observe in the crankshaft phenomenon already described because introduce to the 3D concept, with addition in the 4th dimension that is time (Fig. 22.19b, c).

Paralytic pelvic obliquity is also a great application of spinal biomechanics in a growing spine (Fig. 22.20) comes directly from the pelvic vertebra concept. This pelvic vertebra intercalary between spine and lower limbs will be displaced in 3D according to the imbalance created by the paralysis. It is why obliquity of the pelvis must be considered in 3 dimensions and displaced from the physiological anatomical positioning in relation not only with the amount and quality of the paralysis, but also from the subsequent contractures more or less symmetrical or asymetrical coming from the paralysis. Obliquity of the pelvis must be considered on the coronal sagittal and horizontal plane. Each displacement in one direction results change in the two others. We must distinguish three levels of disorders and deformities able to move the pelvic posture: they can exist above the pelvis, below the pelvis and event inside the pelvis itself [7, 16, 23, 24].

Above the pelvis reasons lies in the evolution of the lumbar spine with big difference between the pelvis continuing the deformity in the same

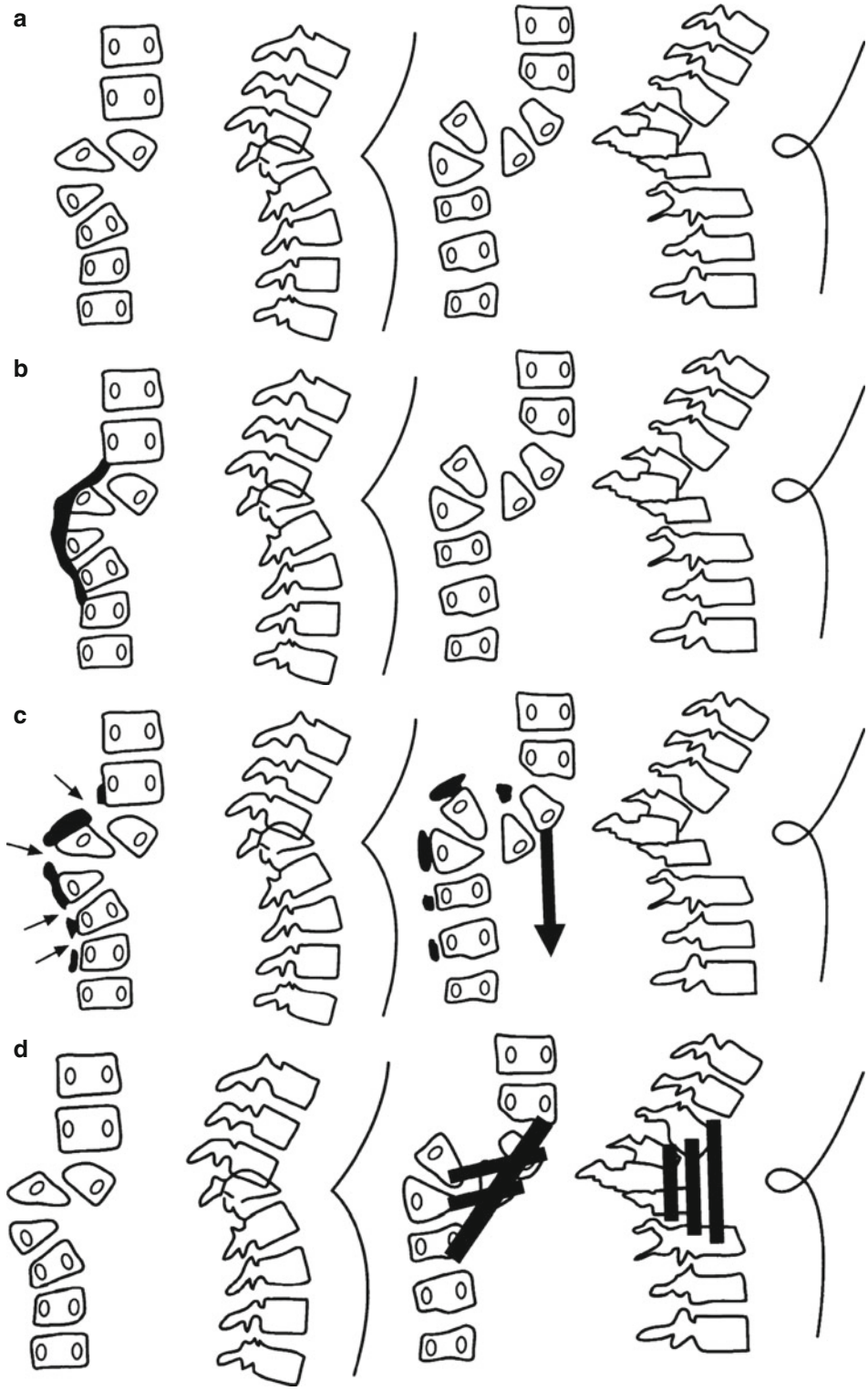

Fig. 22.18 (**a**) Rotatory dislocation pattern. (**b**) Notice the tension band on the convexity. (**c**) When convex approach is realized, the tension band of ligaments on the anterior part of the spine is disrupted and instability is increased, curve must worsen (*arrow*). (**d**) The concave side approach with strut grafts stabilize. Notice that they are always oblique in the coronal plane

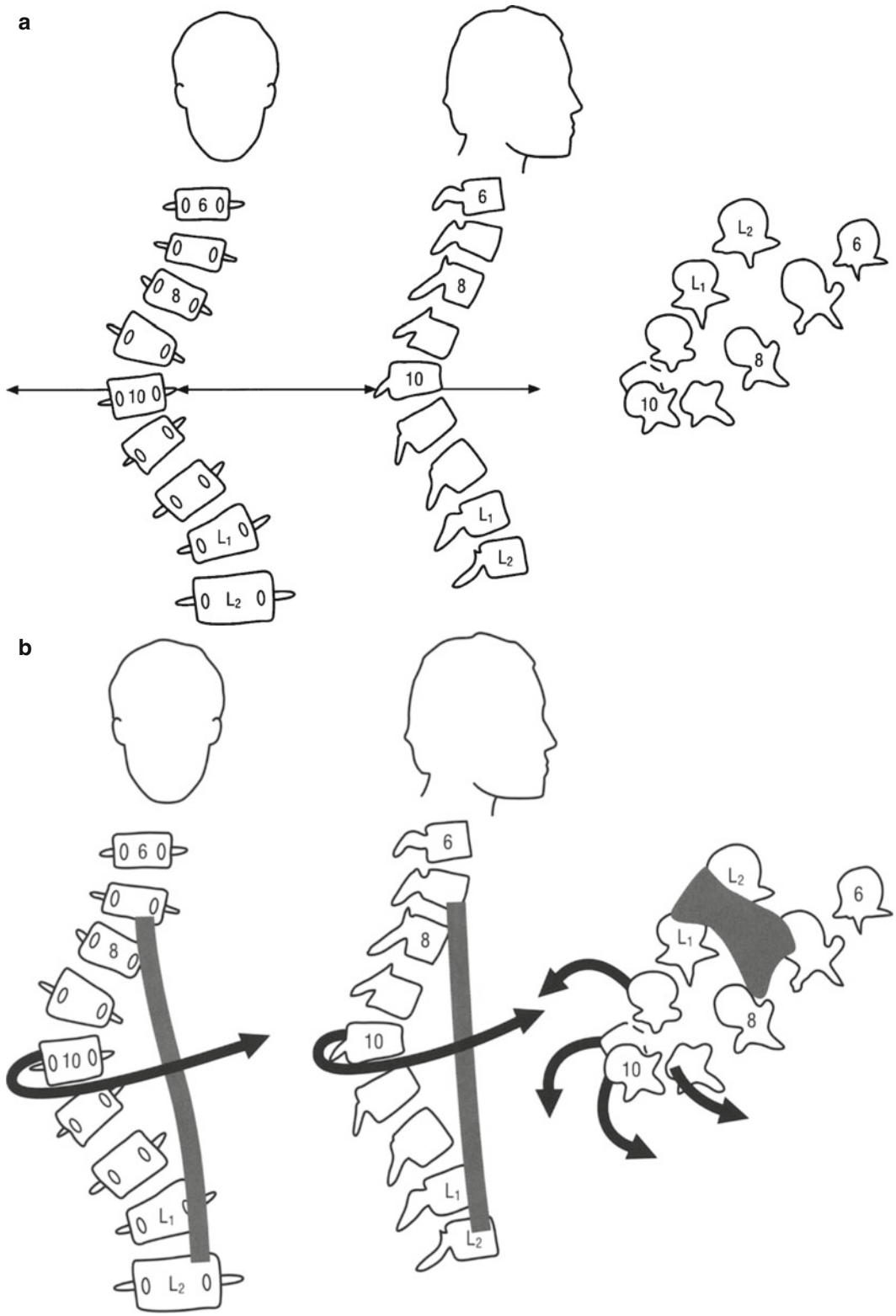

Fig. 22.19 Apparent kyphoscoliosis. (**a**) Hyper rotatory type. Apex in sagittal and coronal projection coincide. (**b**) If anterior fusion from concavity with by pass anterior growth continue. (**c**) Or if posterior convex, the anterior growth will continue and create progression (crankshaft)

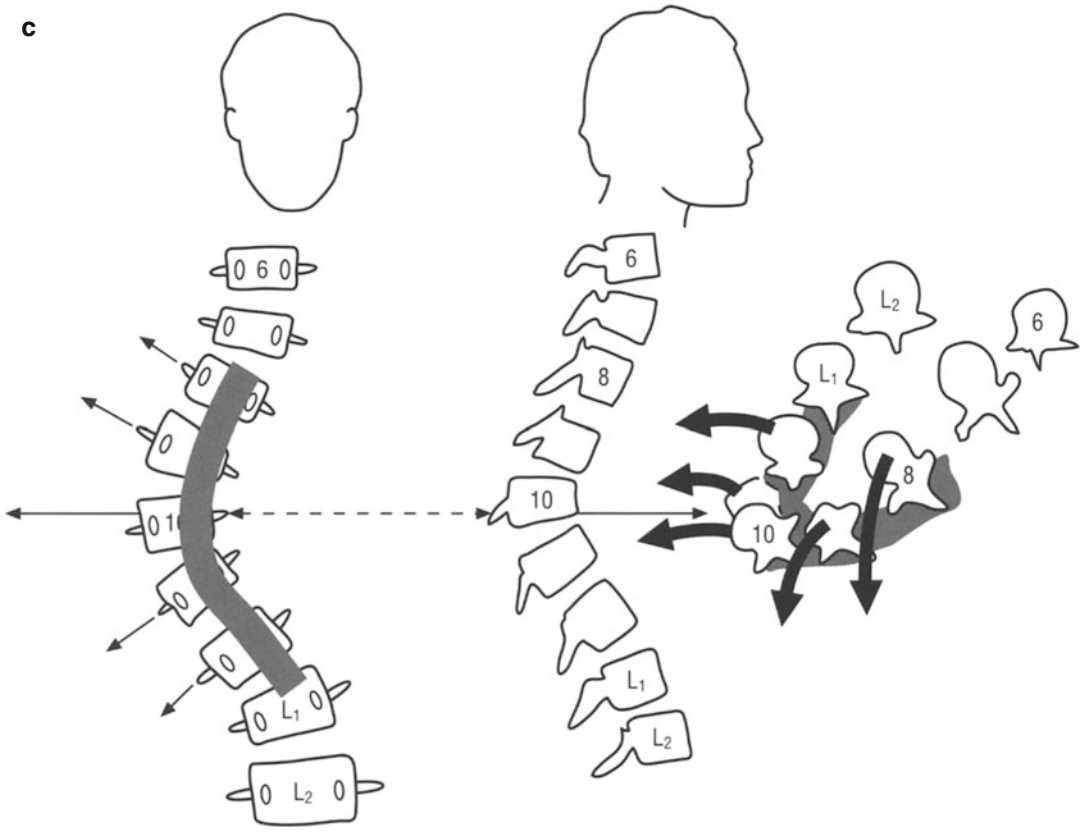

Fig. 22.19 (continued)

direction as the lumbar spine whatever the plane of study. It is the regular pelvic obliquity. Reversely the pelvis can be displaced in the opposite direction (whatever plane) and we call that opposite pelvic obliquity.

Below the pelvis reasons are given by contractures and paralysis more or less symmetrical or asymetrical giving displacement of the pelvic vertebra due to these contractures (for example hip flexor contractures giving hyperlordosis and pelvic anteversion or adductum or abductum) giving displacement in the coronal plane of the pelvis.

Finally if the paralysis have occurred in a young growing child, exactly the same thing as in other joint or bone, appears and the deformity occurs inside the pelvis itself and one can produce bone twisting of the pelvis itself one side from the other. Correction of the above reason can be achieved with correction of the spine itself, correction of the below reason come from surgery around the hips, correction inside the pelvis can only come from more or less sophisticated pelvic osteotomies. This lead also to case of paralytic scoliosis where fusion to the sacrum is recommended. This for us has to be done every time the pelvis is displaced in the same direction as the lumbar curve, or when this displacement is even more pronounced, but also when permanent asymetrical contractures or paralysis remain at the lumbo-pelvic junction. On the opposite, not necessary to fuse if L5 is perfectly aligned with the pelvis and when no asymmetry exist at the lumbo-pelvic junction on the 3D muscle balance. These concepts must be remembered when surgical treatment is achieved in a logical manner (Fig. 22.19b) [15].

Post laminectomy disorder (Fig. 22.21a, b): At it was already demonstrated when the resulting kyphosis lies at only one or two successive levels,

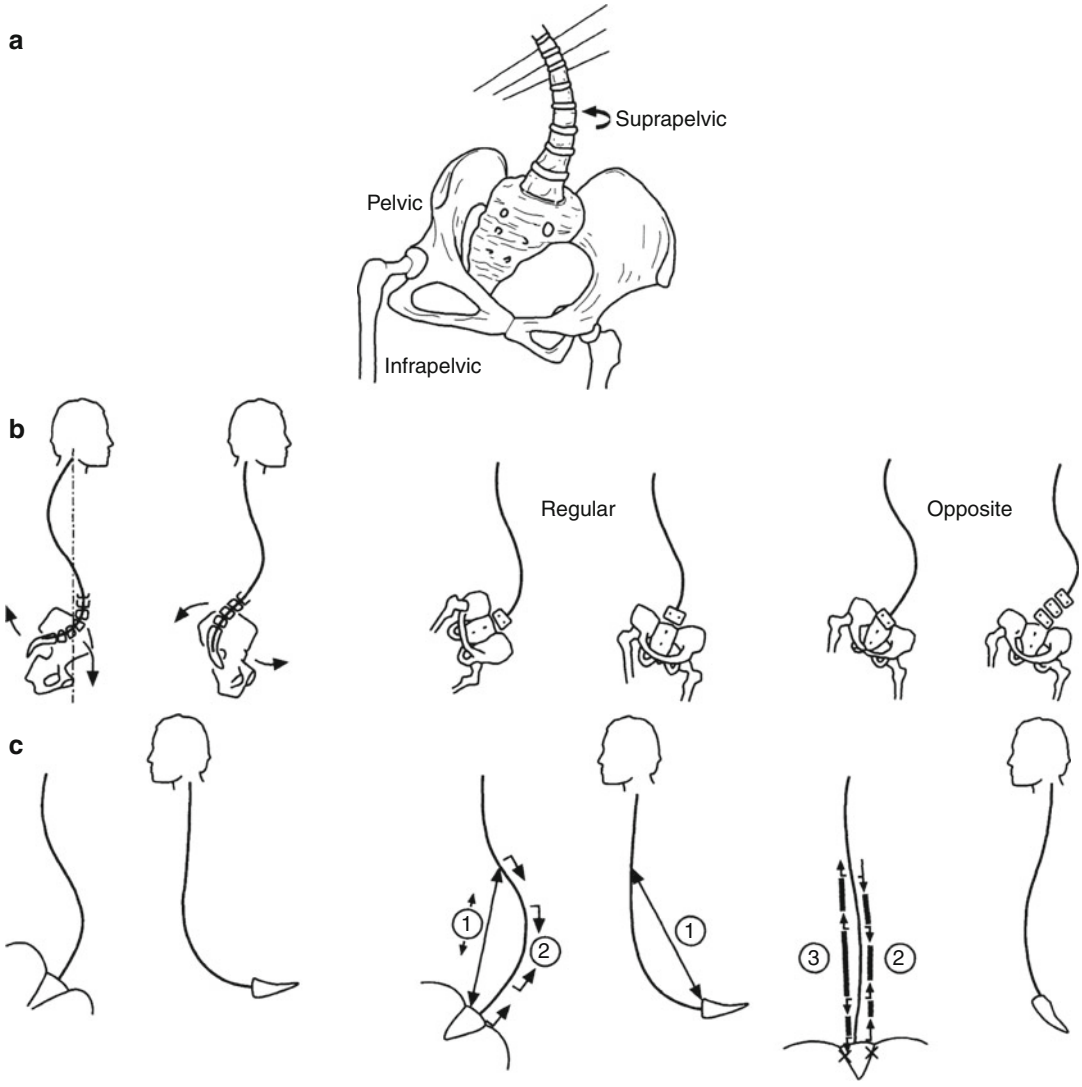

Fig. 22.20 (**a**) In paralytic pelvis obliquity, the reasons of distorsion are coming from 3 levels : – above (supra pelvic) = spine deformity/Below (infra pelvic) = lower limb contracture/Inside (pelvic) = proper distorsion of the pelvic unit. (**b**) We must think as well on sagittal plane with lumbosacral lordosis or kyphosis as in the coronal plane. This allows to have regular pelvic obliquity where lumbar spine and pelvis are going in the same direction or opposite when pelvis is displaced in the opposite direction of the lumbar spine. (**c**) Logical manner to analysis and treat pelvic obliquity

this gives an angular kyphosis. When existing on a long segment many levels involved for example the entire thoracic spine, this result with a long smooth regular kyphosis. But if the location is cervico-thoracic for example laminectomy C5 D5, then because of the failure of the stabilization start to develop kyphosis especially just after the junction with normal spine the combination weight of the entire head + necessity of the horizontal gaze lead to the well-known swan neck deformity progressing all along growth if not treated and protected by brace and cast [8–10].

Pathological Examples of Biomechanics Related to Spinal Balance in Childhood and Adolescence

Fusion to the sacrum [15] can give balance and favour walking in paralytics, it is the example of a paralytic post polio spine fixed to L4 for scoliosis on a patient with complete paralysis of both lower limbs. In spite of two lower limbs calippers standing posture was not achieved without support of two crutches. It appears a progressive flexion of the L5 and pelvic vertebra to the front. Extending the fusion in a lordotic manner to the sacrum allow the patient to get balance and standing position with the two below hip calippers without any support from the upper limbs.

Fusion to the sacrum without sufficient lumbar lordosis (flat back) [15, 17] can destroy standing possibility in some muscular dystrophy patient. This realizing a flat back give anterior tilting of the trunk and instability. The gravity axis runs in front of the femoral head instead of going behind. Correction can be made by osteotomy of the lumbar fusion giving lordosis or by bilateral anterior opening pelvis osteotomy giving posterior translation of the gravity line (until lying just behind the center of femoral heads) and achieving sagittal balance.

L5 S1 spondylolisthesis is a perfect example of genetic and traumatic growing spine disorder . For spondylolisthesis in children two types can be recognized: (Fig. 22.22a, b).

One is secondary to repeated traumatic stress fracture of pars interarticularis coming from overuse, often seen in gymnastics and other repetition sports in young children. The lysis may remain without slippage and when the slippage start the sacrum is still horizontal and remain almost always horizontal. This occurs in reality with a genetic factor probably on the shape of the pelvis and lumbo-sacral area as we can find examples on one or both parents.

The other one called sometimes congenital, even if spondylolisthesis generally don't exist at birth, has not the same aspect, very quickly a congenital kyphosis occurs at the lumbo-sacral area and create a vertical sacrum with very often seen local congenital anomalies like spina bifida occulta as well as very short posterior lever arm for soft tissues and ligamentous structures insertions.

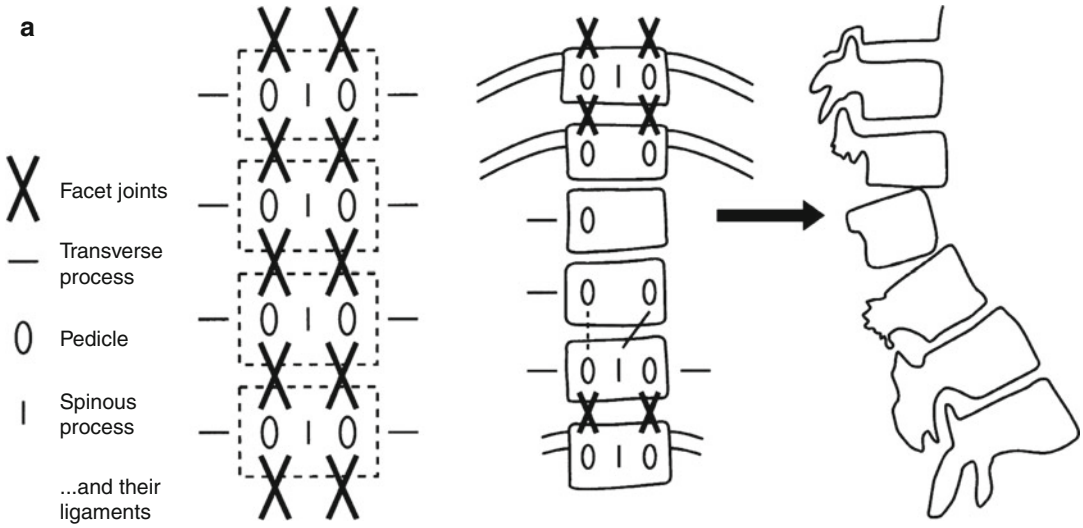

Fig. 22.21 Post laminectomy disorders. (**a**) Analysis of removal of stabilizing structures and consequences. (**b**) 2 types of post laminectomy kyphosis. Acute cervical kyphosis after short laminectomy. Swan neck deformity after long cervico-thoracic laminectomy

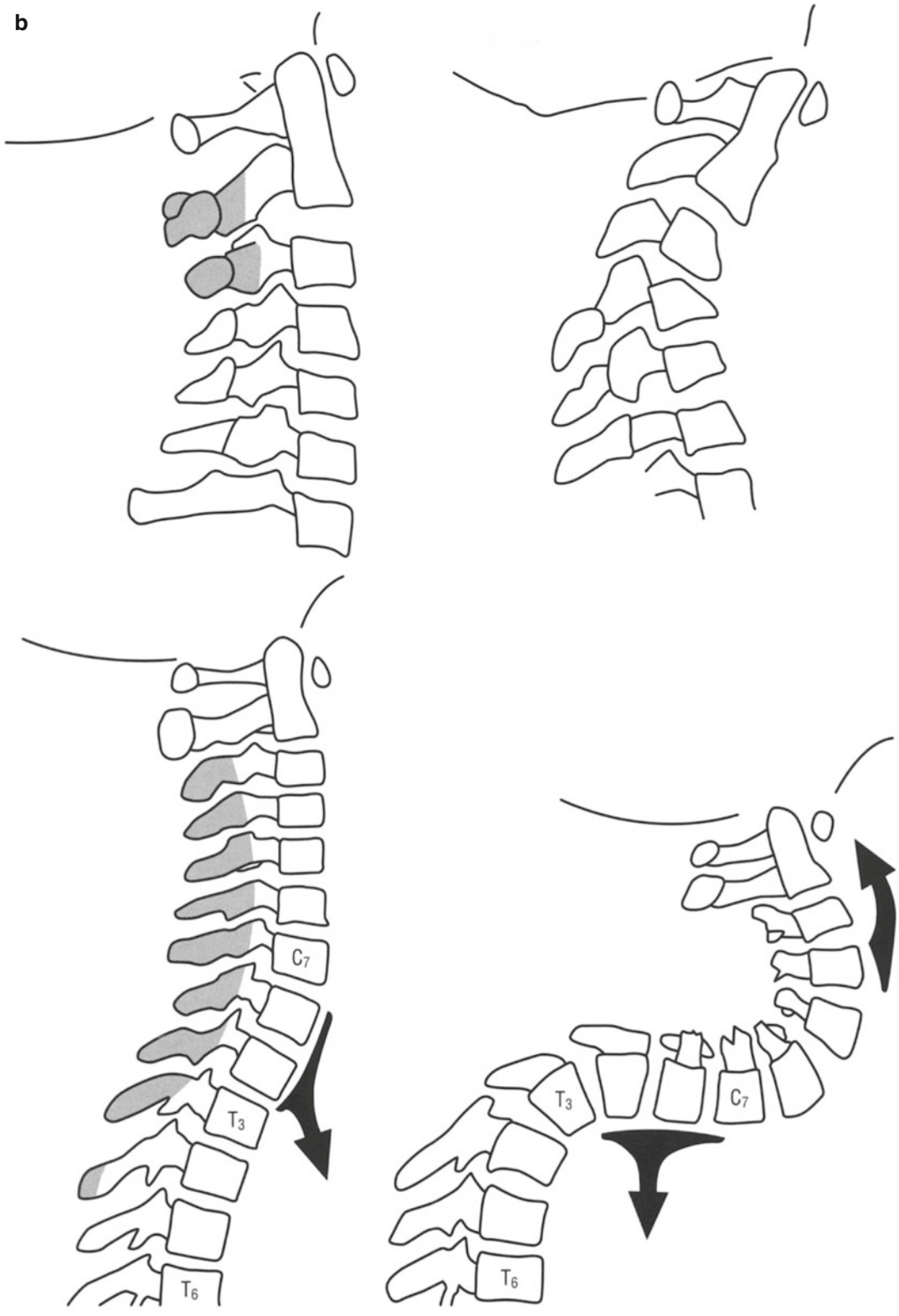

Fig. 22.21 (continued)

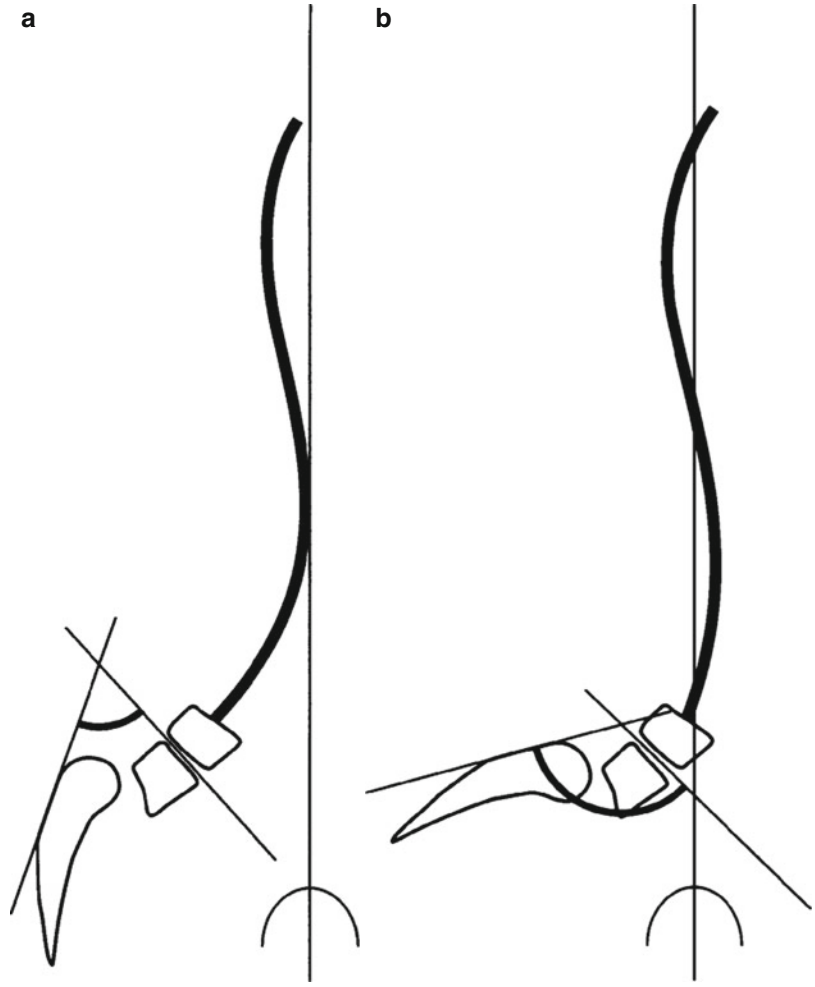

Fig. 22.22 Spondylolisthesis in children. The difference between the horizontal (**b**) and vertical sacrum (**a**) is very important for prognosis

The one with horizontal sacrum where the sagittal angle constructed by upper part of L5 and posterior part of S1 is above 110° and generally don't progress and very rarely require surgical treatment, and the one with vertical sacrum where the angle is below 90° realizing a true lumbo-sacral kyphosis always progressing and requiring most of the time surgical treatment to prevent progression and mostly to correct the kyphosis to lordosis and fuse the lumbo-sacral junction in a correct position of the angle (≥110°) sign of permanent stability when fusion is achieved in that good position [25].

In vivo dynamic evaluation of scoliosis before and after surgery and spinal fusion is another demonstration of spinal biomechanics [26, 27]. This is done with 3D Vicon camera and studying posture as well as motion in the three directions for various levels of fusion in idiopathic scoliosis. This study has demonstrated that:

- Pelvic and head posture in a thoracic scoliotic curve is very different from control group of children same age without spinal deformities.
- After surgery the 3D position of the pelvis and the head is very different of the posture preoperative showing that compensation of the change of the spinal contour in a segmental region (thoracic) develop change in head and pelvic positioning to achieve balance. It is why motion of the hip joints especially for

possible hyper extension is so important to allow motion of the pelvic vertebra in the sagittal plan to get this compensatory tilt of the intercalary bone in the sagittal balance chain.

This is why EOS machine help a lot in the vision and can match the 3D reconstruction of the entire skeleton in the functional standing posture, with the measurements done with the external markers like with the VICON system. This already gave very new information in the relationship of the hip joint with the spine [18].

Genetic Factors

Genetic factors involve all previous characteristic of the growing spine. It is well known on the bone and cartilage structures and very much confirmed in the quality of the soft tissues (hyperlaxity, borderline chondrodystrophy, very seldom short stature parents give their genes for giant in children). Even maturation of the nervous system is probably genetically predicted. But we must remember that each person is unique because the amount of characteristics has been delivered genetically with some changes resulting of interaction of adjacent genes.

This realize some specific factors to the growing spine and differentiate it from adult and from other children same age giving them their own originality about growth potential, hyper mobility, adaptation to malleability of the spinal organ.

The changing of mechanical properties of the structures with age depends also very much from genetics as well as the shape of the sagittal contour that determine the thoracic kyphosis and subsequent lumbar lordosis, or the expansion of the shoulders and upper limbs full span. Some children grow and develop quickly, other more slowly . It is amazing to realize that Mediterranean girl has menarches around 11 years chronological age and Scandinavian around 15 years. The variation is individual but genetically predicted. It is the same for the quality of regeneration after injury of bone, or articular cartilage and finally also the same for maturation of neuromuscular control.

It is why better than comparing one child to another to give difficult table and reference for normality, we must understand that normality covers a wide range of variations and that each child must be analyzed individually for all the items entering in the definition of spinal biomechanics.

Conclusion

Biomechanics of the spinal organ during the growth period is of importance for the function of the spine during adulthood because it is the time when the volume, morphology, levers arms of the skeletal structures are getting completely achieved before aging. But also it is the time when maturation of neuromuscular system occurs giving the best possible adaptation to the genetic morphotype of the person of the function for erect posture as well for standing or sitting or moving performance.

Before the end of growth aging starts giving other pathological changes that will influence the spinal organ and subsequent posture and function and as usual the influence of genetic factor for aging is great and we can say that for biomechanics in orthopaedic and especially for spine, genetic factors and traumatic factors are the only reasons for developmental growing as well as for degenerative aging spine.

Finally orthopaedics in general but especially seen with the scope of spinal physiopathology is really a 3 dimensional science and must be understood theoretically but also practically in that dimension.

References

1. Dubousset J, Gonon GP. Les cyphoses et cyphoscolioses angulaires. Rev Chir Orthop. 1983;69(supp II).
2. Dubousset J. Congenital kyphosis. The pediatric spine, Bradforf Hensinger. 1986;1
3. Dubousset J. Congenital kyphosis and lordosis. The pediatric spine. Weinstein Raven Press, 2 vol, Ch. 10.
4. Dimeglio A. Le rachis en croissance. Sauramp 1, 1 vol.
5. Dubousset J. Déformations rachidiennes post-radiothérapiques après traitement du néphroblastome chez l'enfant. Rev Chir Orthop. 1980;7(66):441–51.
6. Dubousset J, Herring T, Shufflebarger H. The crankshaft phenomenon. J Ped Orthop. 1989;5:541–50.

7. Dubousset J, Katti E, Seringe R. Epiphysiodesis of the spine in young children for congenital spinal malformation. J Pediatr Orthop B vol. 1993;1:123–30.
8. Dubousset J, Guillaumat M, Mechin JF. Cyphoscoliose après laminectomie chez l'enfant. Réunion commune GES-SRS Lyon, Bosq, 1 vol. 1963. p. 67.
9. Dubousset J, Guillaumat M, Mechin JF. Séquelles des laminectomies de l'enfant. Les compressions médullaires non traumatiques chez l'enfant. Sous la direction de J. Rougerie, 1 vol, Masson ed. Paris; 1973.
10. Dubousset J. Instability of the spine secondary to the treatment of intra spinal tumors in children: diagnosis, cure and prevention. Spinal instability, 1 vol. Springer; 1991.
11. Dubousset J. Spinal deformities secondary to traumatic lesions involving the spine and spinal cord in children. Thoracolumbar spine fracture, 1 vol; Ch. 245. Raven Press; 1993.
12. Dubousset J. La scoliose idiopathique – Perspectives actuelles et futures. In: Kohler R, Berard J, editors. La scoliose idiopathique. Sauramps; 1997.
13. Dubousset J, D'Amico M, et al. Three dimensional analysis of spinal deformities. Ios Press; 1992. p. 232–3.
14. Dubousset J. La scoliose idiopathique est originaire d'un désordre du système nerveux. Minerva Ortopedica e Traumatologiia. 1991;11:875–80.
15. Dubousset J. Treatment of paralytic scoliosis with special reference for pelvic obliquity. In: Dewald B, editor. Surgery of the spine. Vol 1 et 2, Ch. 54. Lippincott First Edition 1992, Second Edition 1997.
16. Dubousset J. Three dimensional analysis of the scoliotic deformity. The pediatric spine, 2 vol, Ch. 22. Weinstein Raven Press; 1994.
17. Dubousset J. Balance – considerations in revisions in children. Revision spine surgery 1 vol, Ch 6. Mosby; 1999.
18. Dubousset J, Charpak G, Dorion I, Skalli W, Lavaste F, de Guise J, Kalifa G, Ferey S. Une nouvelle imagerie ostéo-articulaire basse dose en fonction debout: le système EOS. Bull Acad Nationale Med. 2005;189(2):287–300.
19. Dubousset J, Duval-Beaupère G, Anquez L. Déformations vertébrales et paralysie – le rachis luxé congénital. Les compressions médullaires non traumatiques de l'enfant; Sous la direction de J. Rougerie. 1 Vol. Masson ed. Paris; 1973.
20. Zeller R, Ghanem I, Dubousset J. The congenital dislocated spine. Spine. 1996;21:1235–40.
21. Zeller R, Dubousset J. Progressive rotational dislocation in kyphoscoliotic deformities – presentation and treatment. Spine. 2000;25(9):1092–7.
22. Duval-Beaupere G, Dubousset J. La dislocation rotatoire progressive du rachis. Rev Chir Orthop. 1972;4:323.
23. Dubousset J. CD instrumentation, pelvic obliquity. Orthopade. 1990;19:5.
24. Dubousset J. Pelvic obliquity correction. Lumbosacral and spino-pelvic fixation, 1 vol, Ch. 4. Lippincott Raven; 1996.
25. Dubousset J. Treatment of sondylolysis and spondylolisthesis in children and adolescents. Clin Orthop. 1997;337:77–85.
26. Ployon A, Lavaste F, Maurel N, Skalli W, Roland Gosselin A, Dubousset J, Zeller R. In vivo experimental research in the pre and post operative behavior of the scoliotic spine. Hum Mov Sci. 1997;16, 2, 3:299–308.
27. Ployon A, Lavaste F, Maurel N, Skalli W, Dubousset J, Zeller R, Roland Gosselin A. Protocole pour l'évaluation expérimentale 3D in vivo de la posture et de la cinématique globale du rachis. Rev Chir Orthop. 1997;83:719–29.

23 Effect of Tension Stress by Surgical Lengthening of Limbs with Growth Retardation on Biomechanical and Functional Properties of Tissues

V.A. Schurov

Surgical lengthening of limbs with growth retardation performed according to Ilizarov has allowed to recover disproportions of limb growth, to achieve 20-cm and more increase of the height of patients with achondroplasia, to make cosmetic correction of body longitudinal sizes for subjectively small height. The theoretical substantiation of lengthening of limbs using the values comparable to their initial sizes is demonstrated in G.A. Ilizarov's discovery of the law concerning stimulating effect of distraction-related tension stress of tissues on their regeneration and growth [1].

The increase of limb length in patients contributes to their transfer from the category of patients with dwarfish height (below 140 cm) or subjects of low height (2δ below mean standard values) to the category of people with normal body height (Fig. 23.1). Besides, in spite of some decrease of muscle functional potentials, step length in patients increases (Fig. 23.2), thereby giving the possibility to preserve or raise 24-hourly locomotor activity.

Bone injury is an indispensable starting moment for bone regeneration. The time constant of regenerative process start in soft tissues adapted to the action of axial mechanical loads is far greater. In addition, an orthopedist must have a clear idea of the fact, what's the difference between natural longitudinal growth of children's limbs and growth of limbs in case of their surgical lengthening; what biomechanical conditions contribute to such a growth, and how much the limbs lengthened are functionally proper.

We analyzed the contemporary records of treatment of 235 patients with achondroplasia at different age when the patients were admitted for treatment within the period of 1975–1990 and when other institutions had no sufficient experience of treating such patients, while in the clinic of our scientific center optimal conditions for treatment were being searched for the purpose of achieving maximal lengthening of limbs. Age-related distribution of patients' sample can be considered as a quite objective value. Most often limb lengthening started at the age of 8–16 years (Fig. 23.3).

The analysis of the dependence of maximally obtained values of leg lengthening (L, см) on the age of treatment start (in patients above 10 years) has revealed that these values decrease every year (t): $L = 20 - 0.36 * t$, $r = -0.950$ ($p < 0.001$). As far as the age of treatment start in patients 1 year increases, the possibility of relative leg lengthening is 2 % limited [2].

Average daily rate of leg lengthening at two levels simultaneously also decreased as far as

V.A. Schurov, MD
Laboratory for Deformity Correction and Limb Lengthening, Russian Ilizarov Scientific Center, Restorative Traumatology and Orthopaedics of the RF Ministry of Health, Kurgan, Russia
e-mail: shchurovland@mail.ru

D.G. Poitout (ed.), *Biomechanics and Biomaterials in Orthopedics*,
DOI 10.1007/978-1-84882-664-9_23

patients' age 0.9 % increased. Fixation period duration of the leg being lengthened reflects bone tissue regenerative potential and increases as far as patients' age increases (Fig. 23.4).

The facts revealed became a stimulating reason for studying the age-related dynamics of biomechanical properties of different leg tissues, determined by changes in structure and volume of soft-tissue elements.

In the process of leg lengthening the amount of distraction forces is known to reach from 170 to 400 N depending on tissue mass [3, 4]. Preferable character of «lengthening-strength» dependence consists in continuous increase of tissue resistance that conforms to their elastic deformity preservation. Time periods of treatment for such patients are shorter. The fall of strengths occurs in case of tissue transfer from elastic deformity state to plastic one. In this case cavities appear in regenerated bone, and muscle contractility after treatment remains substantially decreased.

Techniques to Study Elasticity of Skin Integuments and Arterial Walls

Study of skin elastic properties was performed with a device worked out by us. The technique of biomechanical testing proposed allows to measure the state of leg skin integuments in the process of patients' treatment. The principle of operation of the device for studying biomechanical

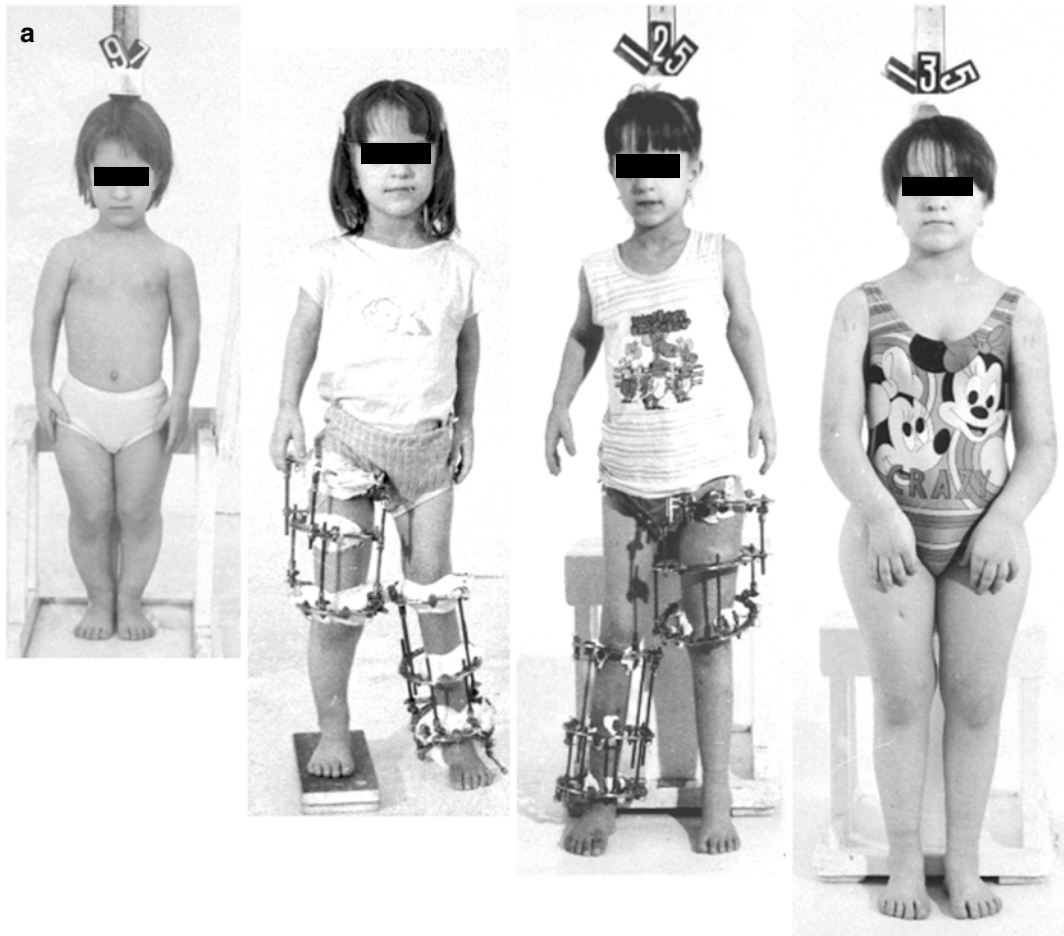

Fig. 23.1 (**a**) Scheme of successive stages of treatment of patients with achondroplasia. (**b**) Chart of the simultaneous removal of the tibia and femur

Fig. 23.1 (continued)

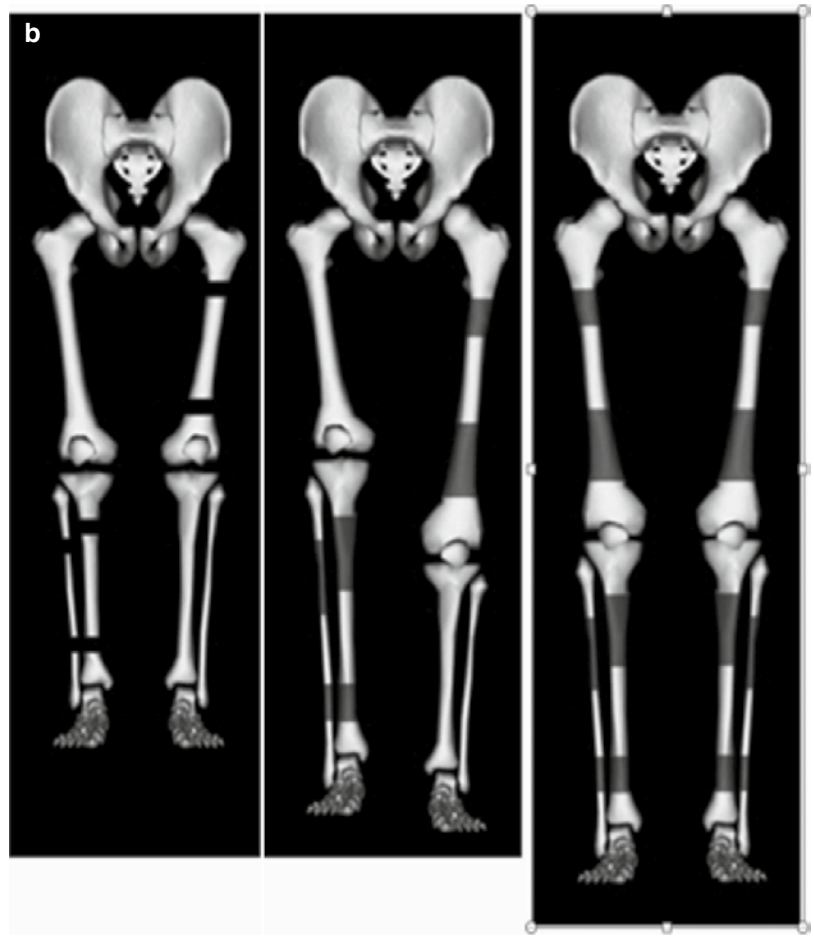

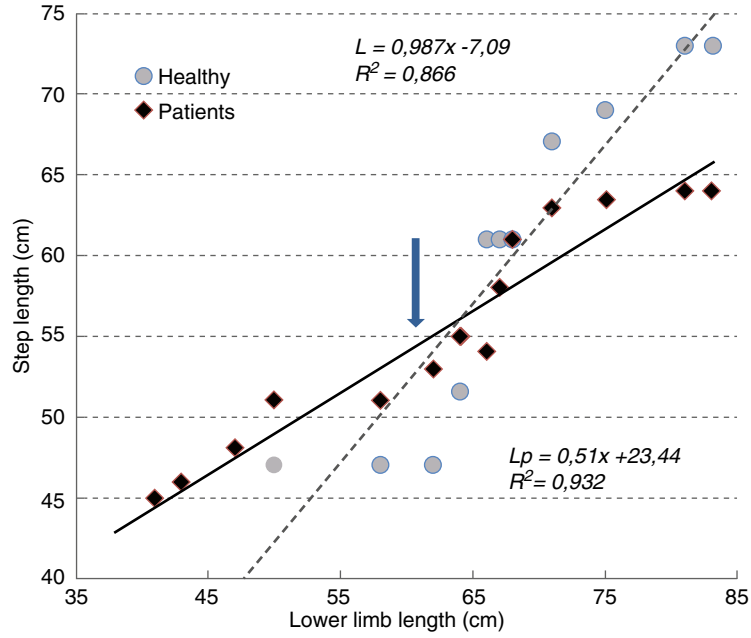

Fig. 23.2 Dependence of step length on lower limb length of normal subjects and patients with achondroplasia before and after lengthening performance

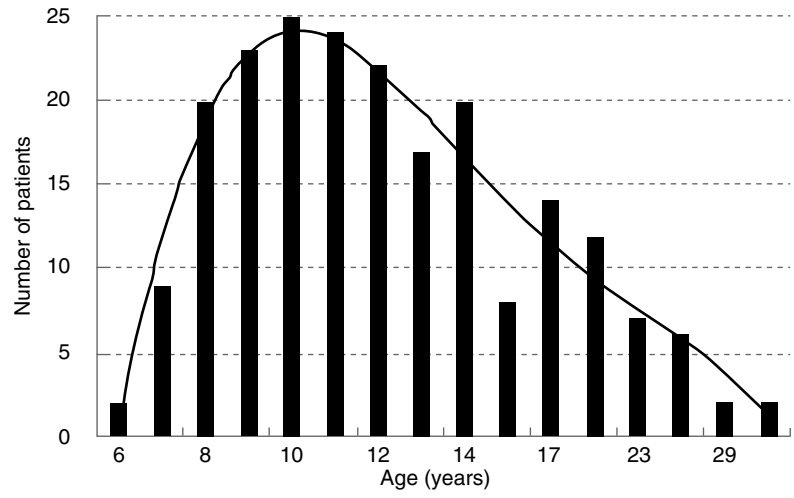

Fig. 23.3 Age-related distribution among 235 patients with achondroplasia admitted for treatment

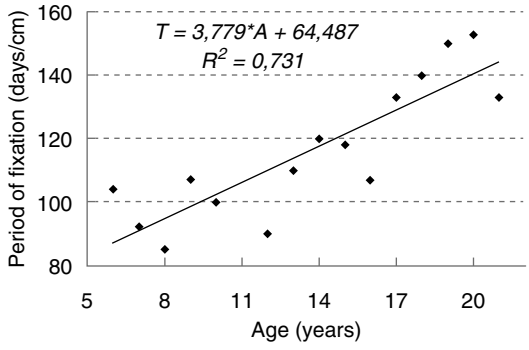

Fig. 23.4 Age-related dynamics of relative duration of fixation period

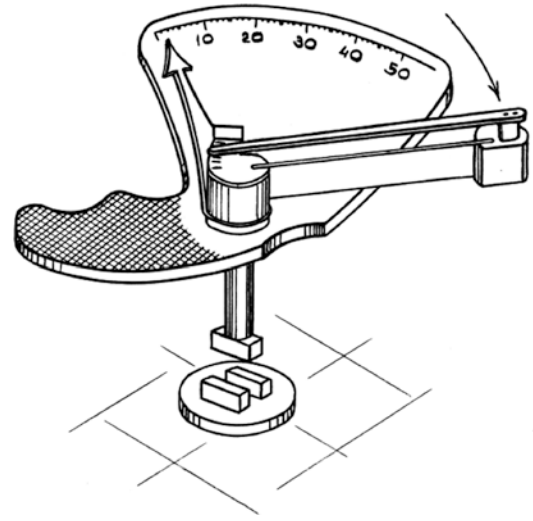

Fig. 23.5 The principle of the device to study the elastic properties of human skin

properties of human common integuments is based on measuring degree of skin rotation, produced by application of tangentially directed rotational moment of force. In the simplest design of elastometer the moment of force is applied to skin surface through a supporting disk precovered with adhesive material (Fig. 23.5).

The device consists of a rod, being an axis, at one end of which the supporting disk is attached in a stationary way, and a metal plate is attached at its other end. A scale is marked in degrees on the sector. A pointer serves to read the angle of superimposed disk rotation under the influence of the force moment applied. A flat spring is connected with the rod free of motion. The scale and another pointer are intended for controlling the rotational moment required. The disk diameter is 20 mm, the amount of working rotational moment – 6 N*cm.

During testing of skin integuments using moments of force over the range of 5–10 N*cm the connection between the moments of force, the superimposed disk area and the angle of skin rotation can be described to an accuracy of ±5 % using the following approximate dependence:

$$\mathbf{E} = \mathbf{M} / (\mathbf{a} * \mathbf{S}),$$

where E – indicator of skin elasticity, M – moment of force, a – angle of skin rotation, S – area of supporting disk.

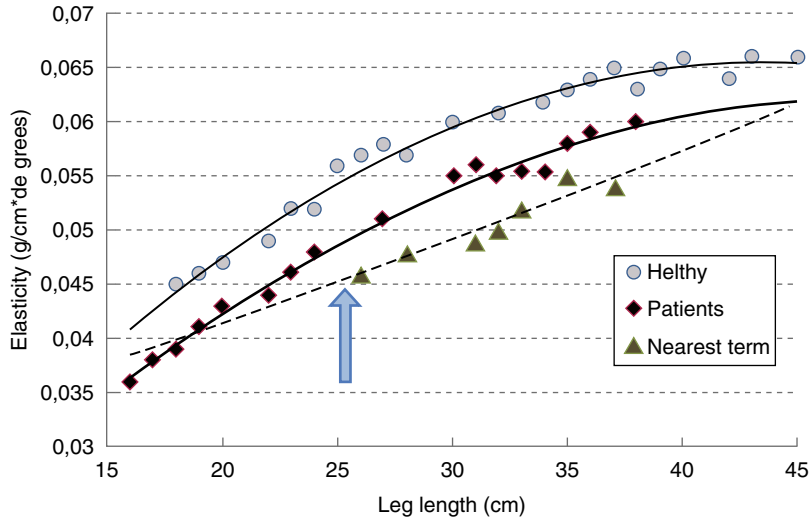

Fig. 23.6 Elasticity values of leg skin integuments normally and in patients before treatment, in the immediate and long-term periods after leg lengthening

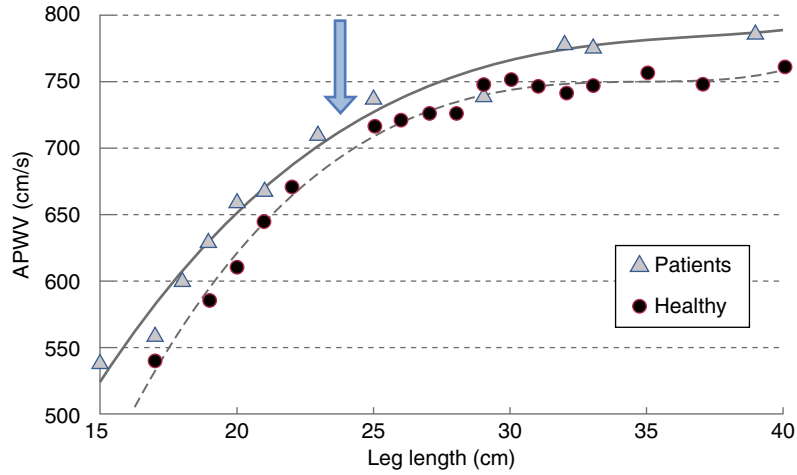

Fig. 23.7 The dependence of the velocity of arterial pulse wave from the length of the legs

In the limits of acting forces the angle of skin rotation is proportional to the moment of force applied and inversely proportional to the area of superimposed disk and the elastic properties of skin integuments. Indicator dimensions are expressed in N/(cm*degrees). E indicator is inversely proportional to skin rotation angle provided that both moment of force and superimposed disk area are constant.

Elastic properties of leg back surface skin integument were studied under the condition of physical rest in supine position of the subject examined.

It has been revealed that the value of skin integument elasticity in normal children below 10 years increases in proportion to leg length increase. In patients with achondroplasia this value is below normal one and it increases after limb length surgical gain, reaching estimated values in the long-term periods (above 1 year) after treatment (Fig. 23.6).

Elasticity of leg arterial walls was judged by the value of arterial pulse wave velocity (APWV) in the region from popliteal fossa to foot. In children below 6 years the value traces changes in leg length. Subsequently its increase rate is determined by the number of life years elapsed. In patients with achondroplasia APWV increases after operative changes in longitudinal leg size (Fig. 23.7). During distraction, unlike biomechanical parameters of other tissues, APWV value shouldn't increase substantially, contributing to maintain the lumens of blood carrying arteries.

Dynamics of Tissue Biomechanical Properties in the Process of Natural Growth and Under Surgical Leg Lengthening

The increase of limb longitudinal sizes leads to quantitative and qualitative changes in developing muscles. Specifically, the values of contractility increase, as well as transverse hardness of muscles [5]. Unlike skin integuments and arterial walls the muscle biomechanical properties of lower limbs are determined by their longitudinal sizes up to the end of natural longitudinal growth period (to 18 years) and in case of leg length increase up to 60 cm.

Myotonometry

Measurements of the transverse hardness of muscles, which is caused by their tone and muscle structure itself, were performed using the simplest but highly sensitive mechanical myotonometer (Fig. 23.8) made on the basis of transfer indicator of dial type with 0.01-mm least graduation, and on its stem a support cylinder with 20-mm outside diameter is fastened, inside of which a movable rod is set with a supporting heel of 5-mm diameter. The depth of the rod descending is 4.35 mm.

The myotonometer was lowered strictly vertically on the leg part examined (the belly of m. gastrocnemius lateral head). The myotonometer's own mass (250 g) was traded off for the constant value of tissue squeezing cup pressure. The transverse hardness of muscles was estimated in arbitrary units under the condition of physical rest in supine position of the subject examined. In normal women at the age of 20–40 years this value amounts to 75–100 arbitrary units, in men of the same age – 100–150 arbitrary units.

Besides, there is correlation between the value of m. gastrocnemius transverse hardness and the value of intramuscular pressure determined by modified Henderson method [6] (Fig. 23.9), which increases as far as leg longitudinal sizes increase. 50 mmHg is a critical value of intramuscular pressure at which blood flow in

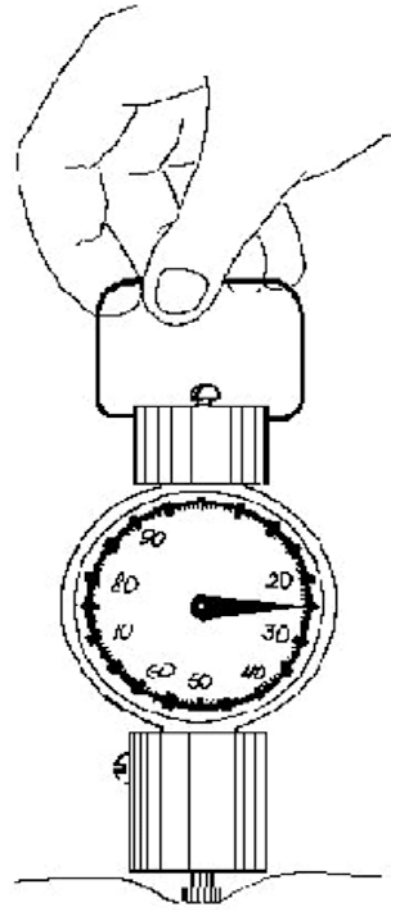

Fig. 23.8 A system illustrating the procedure for determining the hardness of transverse gastrocnemius

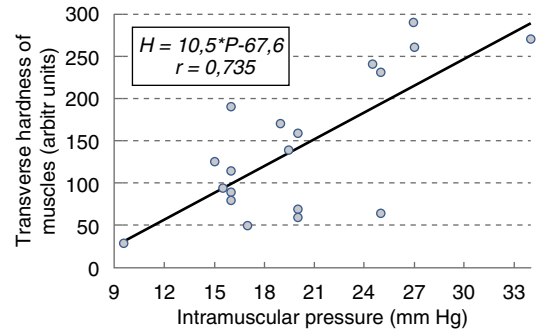

Fig. 23.9 Correlation between the values of m. gastrocnemius transverse hardness and those of intramuscular pressure in human subjects of different age normally and for leg lengthening

arterioles is blocked. During leg lengthening in the first 20 days of distraction elasticity value of the posterior group of leg muscles 346 % increased in comparison with initial level. In addition, leg circumference became 3 cm more. Probably, elasticity increase is associated with change in soft tissue hydration. Further increase of segment length led to the fact, that the increment of elasticity value reached 400 % in comparison with initial level.

After the end of leg lengthening throughout fixation period the value of muscle elasticity decreased, being preserved substantially higher than initial values (183 ± 8 arbitrary units) due to remaining increased hydration of tissues. Subsequently, in the long-term periods (above 1 year) after fixator removal the value approaches the level conforming to that of normal subjects of the same age with the analogous sizes of the lower limbs (Fig. 23.10). In the process of limb natural longitudinal growth in children not only bone length increases spontaneously, but the contractile part of muscles as well [7].

That is why the value of their transverse hardness remains comparatively low. In adolescents the tendinous part of muscles increases under the influence of their traction by actively growing bone. Moreover, tension stress of tissues increases. The same is observed for surgical limb lengthening as well, but the rate of size increase in this case is about 30-fold higher, and tension stress is two to three-fold more, respectively. Plastic potentials of soft-tissue elements are significantly lower, that is why the complete compensation of the increased values of muscle elasticity at the expense of longitudinal growth of muscle tendinous part occurs in the immediate months after the end of distraction period and manifests itself in increasing the change range of muscle contractile part length. In this situation it's important to avoid the increase of intramuscular pressure during distraction up to the values of arteriolar bed blocking, that leads to ischemia and irreversible damage of tissues.

There are some ways to prevent ischemic involvement of muscles: creation of the initial reserve of muscle free motion during the fixator application and insertion of wires beyond the belly of the most important muscles, pharmacological increase of the value of muscle tension stress; high-divisional distraction (1 mm for 60 times per 24 h) throughout 24 h; control of the state of the muscles being lengthened, that of limb blood supply, as well as patient's general condition and his or her arterial pressure level.

If these measures are observed, contractility of muscles after treatment should be recovered completely. When lengthening gain is more than 10 % of the initial length of limb, its reduction should not exceed 25 % of the initial level. Muscle contractility should be controlled using dynamometric stands.

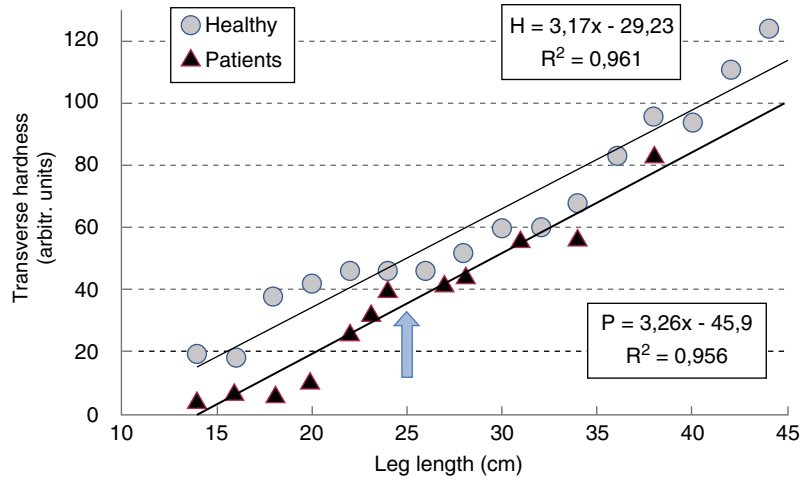

Fig. 23.10 Dependence of transverse hardness value on leg longitudinal sizes in normal subjects examined and in patients before and after leg lengthening

Effect of Muscle Biomechanical Properties on Blood Supply of the Leg Being Lengthened

Volumetric rate of leg circulation has been studied by the technique of occlusion plethysmography. After osteotomy and the Ilizarov fixator application this value two-fold increases in comparison with initial level and remains at increased level all over the period of distraction, being normalized not at once after lengthening cessation in the period of fixation (Table 23.1). At the end of lengthening period the values of peak blood flow decreases evidencing the reduction of vascular bed reserve potentials. The blood flow at rest decreases up to 1.53 ± 0.19 ml/min.*100 cm^3 in the immediate months after the fixator removal.

In general, during treatment the value of circulation volumetric rate (CVR) отслеживает traces the gain of muscle elasticity up to the moment when intramuscular pressure starts to interfere with blood passing through capillary bed:

$$\mathbf{OCK = 0.23 + 0.0162 * D; r = 0.930, p \leq 0.001}$$

Physiological mechanism of the event revealed – blood flow acceleration for pressure increase in the surrounding tissues – is known. This is Ostroumov-Beilis reaction – relaxation of arteriole walls under the influence of transmural pressure decrease.

In the first days of distraction start systemic arterial pressure 37 % increases ($p \leq 0.05$). After 1 month of distraction the levels of systolic and diastolic pressures reached 160 ± 9 and 113 ± 7 mmHg, respectively, and remained high up to the start of fixation period. In the period of fixation hypertension amounted to 23 % of the initial level on the average. Such hypertension may be caused by the increase of afferent impulse flow from tension receptors of muscles and other tissues and it is of protective-and-adaptive character because it keeps tissues away from ischemia, increasing the critical level of arteriolar bed blocking.

While comparing natural growth and limb lengthening it's necessary to pay attention to the fact, that in the first case the higher its rate, the faster blood flow and the lower muscle elasticity, and in the second case – the faster blood flow and the more tension stress of tissues (Fig. 23.11).

Muscle Contractility Recovery in the Limb Lengthened

It's the most easiest to judge the recovery of muscle functional properties after limb lengthening by range of motion restoration in the knee and ankle. During treatment the joints are beyond the zone of surgical intervention/that is why their mobility is mainly determined by the ability of muscle contractile part to change its length. In the process of limb lengthening the decrease of length change amplitude in muscles occurs due their tension. The longitudinal growth of muscle tendinous part in adults and that of the whole

Table 23.1 Dynamics of blood supply of the leg being lengthened in patients with achondroplasia (M ± m)

Stage of treatment	Number of observa-tions	Muscle elasticity (arbitr. units)	Volumetric blood flow (ml/min.*100 cm^3)	
			VBF at rest	Peak VBF
Before treatment	29	16 ± 2	1.24 ± 0.09	4.9 ± 0.4
Distraction: 0.2 month	8	53 ± 8	2.42 ± 0.49	4.3 ± 0.6
0.5 month	6	84 ± 1	2.42 ± 0.26	3.4 ± 0.8
1 month	8	93 ± 12	2.42 ± 0.29	5.9 ± 1.3
2 months	8	125 ± 9	2.59 ± 0.27	7.5 ± 1.8
3 months	2	172 ± 29	2.40 ± 0.76	3.0 ± 0.4
Fixation: 0.2 months	6	211 ± 9	2.13 ± 0.42	3.2 ± 0.5
0.5 months	6	231 ± 7	1.48 ± 0.31	3.3 ± 0.1
1 month	6	213 ± 11	1.51 ± 0.33	2.7 ± 0.4

muscle in children contributes to the recovery of joints' mobility under the conditions of the muscle length changed after treatment. Range of motions in adjacent joints restores gradually throughout several months.

Two factors mainly influenced the rate of mobility recovery in the knee after femoral lengthening: limb lengthening amount and patients' age. The results of the studies performed in a group of patients (63 patients at the age of 6–54 years with 2–23 cm growth retardation of one of their limbs) confirm the effects of lengthening amount on the state of muscles and joints both during distraction and after the end of treatment.

The range of motion decreased steadily as far as femoral length increased during distraction (Fig. 23.12).

After the end of distraction period the range turned out to be four to five-fold decreased in all the patients. At the end of fixation period it 1.5-2-fold increased (Fig. 23.13).

The most substantial differences in the range values were revealed in patients with different amount of lengthening in the first 2 months after the fixator removal. In 12 months after the end of treatment the knee function was practically the same as before treatment.

Provided that the amount of femoral lengthening was the same, the younger patients,

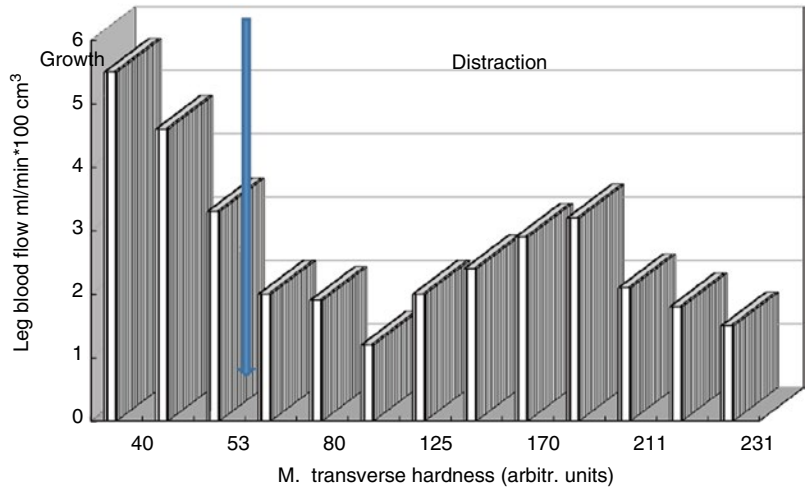

Fig. 23.11 Correlation of the values of leg circulation rate and m. gastrocnemius transverse hardness under the conditions of natural growth and limb lengthening

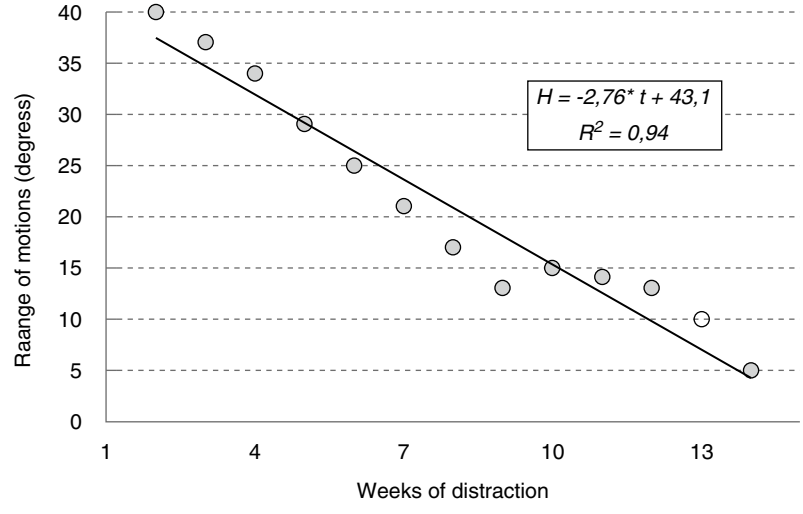

Fig. 23.12 Dynamics of the knee range of motions in patients during femoral lengthening

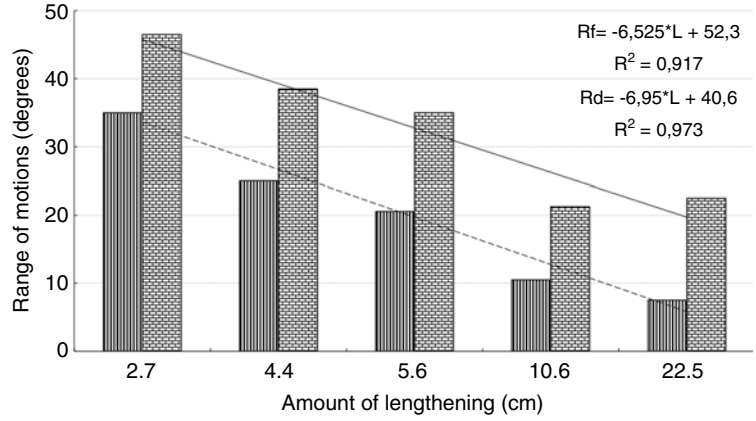

Fig. 23.13 Dependence of the knee range of motions after the end of distraction and fixation periods on femoral lengthening amount

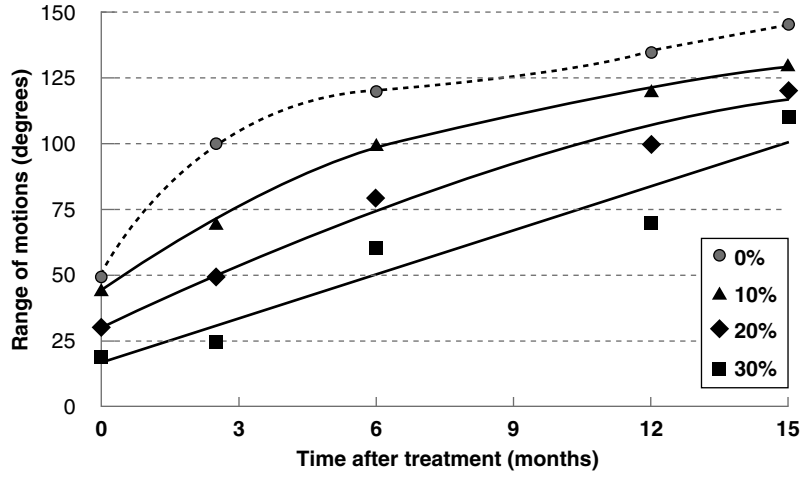

Fig. 23.14 Dynamics of the knee range of motion recovery after limb lengthening of different amount in patients

the faster and of the greater extent was the knee range of motion recovery. Age was of great importance for the rates of range of motion recovery as well. Thus, by the end of 1-year period after the Ilizarov fixator removal the dependence of the knee range of motions on patients' age is described by regression equation: $H = 148 - 3.40^{*} t$; $r = 0.720$; $p \leq 0.05$.

The rates of the knee range of motion recovery depended on the amount of lower limb lengthening significantly. Provided that the values of joint function at different stages of rehabilitation were known for 30 %–, 20 %- and 10 %-lengthening of a limb, the corresponding values were calculated using the method of linear extrapolation, as well as the «ideal» curve of range recovery was plotted which would have been observed without limb lengthening (Fig. 23.14).

For the purpose of muscle function recovery active movements are necessary, which usually can be trained in adult patients during treatment only under the supervision of exercise therapy specialist.

Determination of the maximal moment of foot flexors and extensors was performed using dynamometric stands [8, 9]. Constructional details of the stands allow to make measurements irrespective of age-related features and distraction fixator's presence or absence. In the stand for leg muscle strength measuring the possibility is provided for positioning foot in the ankle at different angles within the range of 70–120° with 5° spacing, that allows to assess the contractility preservation degree in muscles for change in their longitudinal size.

All the measurements are made for voluntary maximal isometric contraction of muscles. The

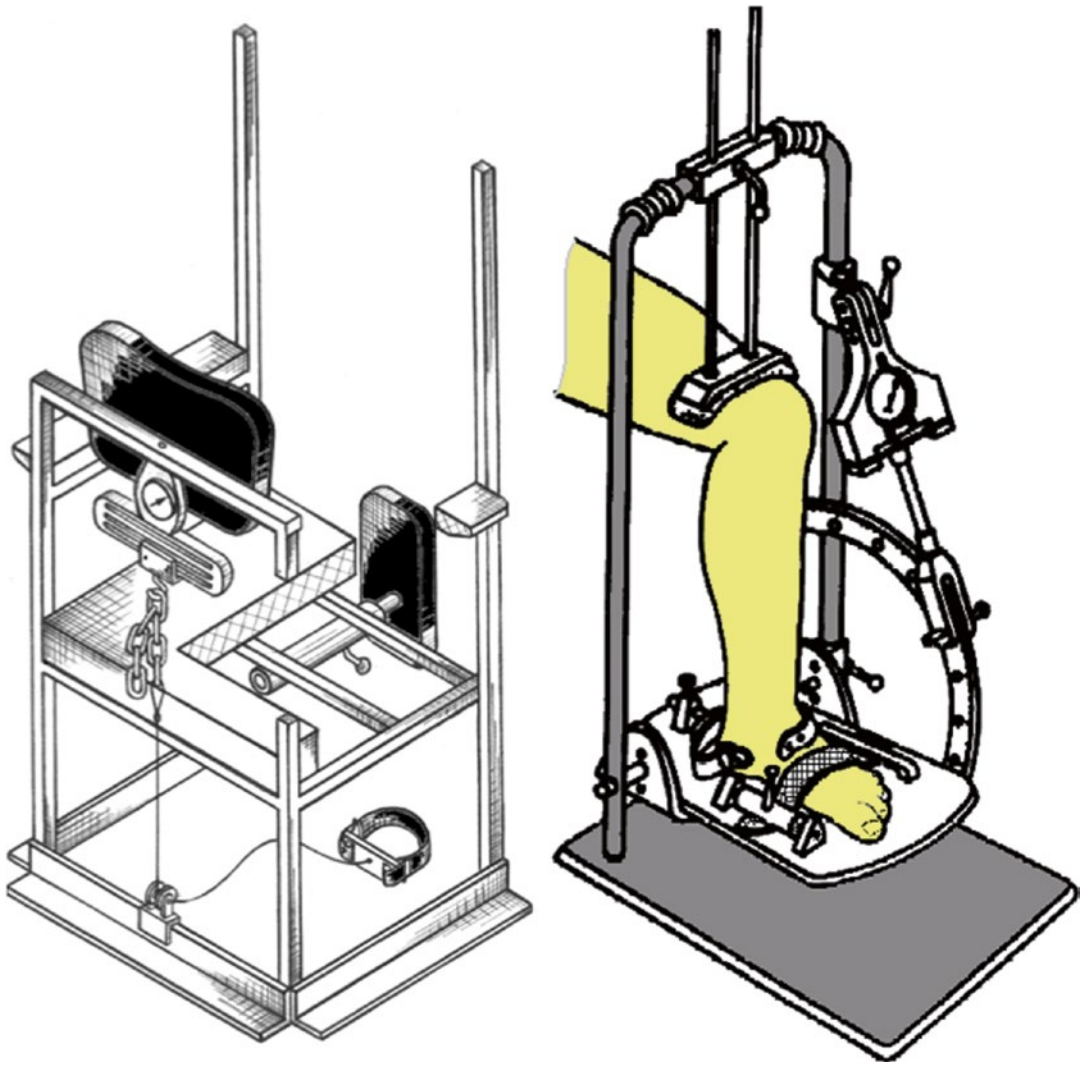

Fig. 23.15 System of dynamometric units for determination of femur and leg muscle strength

stands provide for standard position and fixation of lower limb owing to special attachments and stops (Fig. 23.15).

To rule out the influence on the values of increasing with age body mass we used the relative values of muscle strength moment (RSM), expressed in N*m per 1 kg of body mass.

In normal people (450 subjects at the age from 7 to 18 years) muscle strength in the anterior femoral group of muscles is more than that in the posterior one, that is to a great extent explained by prolonged staying of schoolchildren in sitting position. In males the strength is more than in females, and the difference increases with age (Fig. 23.16). In sportsmen anterior/posterior muscle group strength ratio depends on specialized training. The anterior group of muscles is significantly stronger in weight-lifters. In track and field athletes the posterior group of muscles is relatively stronger.

Sex of the persons examined is of great importance as well (Fig. 23.16). The moment of muscle strength in girls increases faster at the age of 11, in boys – at the age of 12. Correlation of between the strength moment values of foot plantar muscle flexors and maximal circumference (p, cm),

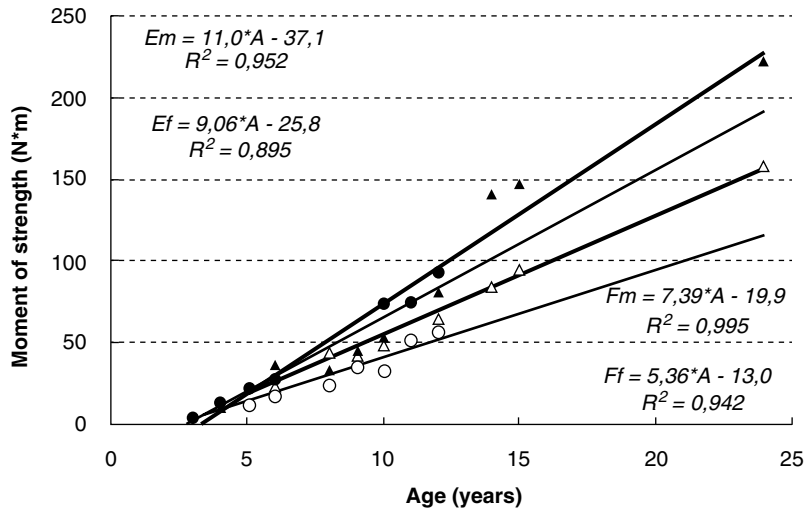

Fig. 23.16 Age-related dynamics of the moment of strength of the anterior and posterior groups of femoral muscles (shin extensors and flexors) in the normal male and female subjects examined

leg length (L, cm) and age (T, years) in normal girls and boys can be described by regression equation:

$$\mathbf{MC}_{\text{Де}\text{В}} \frac{\mathbf{p^2 * L * (0.719 * T + 10.71) * 10^{-2}}}{\mathbf{4 * \eta}}$$

$$\mathbf{MC}_{\text{Ма}\text{Л}} \frac{\mathbf{p^2 * L * (0.916 * T + 12.93) * 10^{-2}}}{\mathbf{4 * \eta}}$$

Contractility of lower limb muscles is an important value of functional state of the locomotor system. Under the conditions of natural growth in children and adolescents the strength of femur and leg muscles increases in proportion to changes in longitudinal sizes of these limb segments. However, in femur and leg surgical lengthening muscle dynamometric characteristics fall practically up to zero and recover in the immediate months after treatment completion, not reaching initial values usually. To approximate the conditions of distraction to the conditions of natural growth the special sparing techniques of osteotomy at two levels are used, as well as automatic mode of distraction with twisting rate up to 60 times per day. Distraction rate doesn't exceed 2 mm per day [10, 11].

Hundred and three patients with congenital and acquired shortenings of one of their lower limbs were examined before treatment. Hundred and nineteen patients at the age of 7–23 years were examined in the immediate 6 months and in the long-term periods after the end of 5–9-cm gaining in length using the technique of transosseous osteosynthesis of the lower limb with growth retardation at the expense of femur and leg lengthening. Moreover, in 54 cases the leg was lengthened using automatic distraction by 60 times per day. Mean age of patients for examination in the immediate 6 months after treatment was 13.2 ± 0.8 years.

Absolute values of muscle strength in normal children and adolescents increased in proportion to their age. Relative moment of muscle strength (RSM) increased up to 30 years. Subsequently, body mass increase, especially in females, didn't accompanied by the adequate gain of dynamometric value. In normal subjects close correlation between limb longitudinal sizes and muscle contractility was revealed. In patients before treatment the correlation coefficient between these values in intact limb was decreased up to 0.46 and was absent in the limb with growth retardation.

We have revealed the craniocaudal gradient of reparative potentials of different body parts. As far as moving towards periphery, postnatal increment of body parts increases, as well as growth rate and regenerative potentials of tissues [9, 12]. That is why the maximally acceptable amounts for lengthening of leg, which don't lead

Table 23.2 Relative moment of femoral muscle strength before and after lengthening (N*m/kg)

Examined group	Number of observations	Leg extensors		Leg flexors	
		Intact leg	Involved leg	Intact leg	Involved leg
Before treatment	103	1.63 ± 0.08	1.15 ± 0.07	1.27 ± 0.06	1.01 ± 0.05
Immediate periods after treatment	27	1.50 ± 0.16	0.73 ± 0.16	1.25 ± 0.12	0.81 ± 0.15
Long-term periods after treatment	27	1.65 ± 0.13	1.09 ± 0.10	1.37 ± 0.12	1.02 ± 09.08

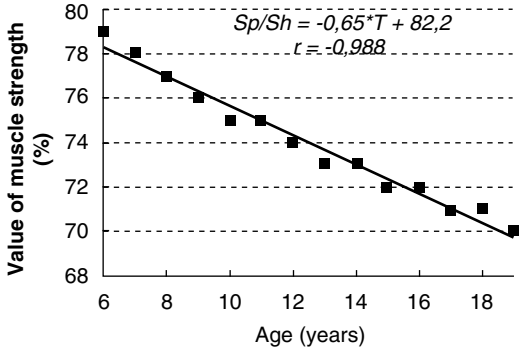

Fig. 23.17 RSM dynamics in the anterior group of muscles of the femur lengthened after the end of treatment

to muscle contractility loss, are comparably more than those for femur.

Before treatment the strength of femoral muscles in the limb involved amounted to 70–80 % ($p \leq 0.001$) of normal limb level. In the immediate periods after treatment of patients using automatic mode of distraction it was 49–65 % and in the long-term periods – 66–75 % (Table 23.2), that means, it approximated to the initial level.

The relative moment of strength in the anterior and posterior muscle groups of the leg with growth retardation before treatment amounted, respectively, to 73 and 78 % ($p \leq 0.001$) of normal leg level. In the immediate periods after treatment – 70 and 55 %, in the long-term periods – 71 and 81 % (Fig. 23.17 and Table 23.3).

It should be noted that muscle strength recovery occurs vigorously in the first year after treatment, after that the value level can decrease temporarily and after 4–5 years it can increase again (Fig. 23.17). Such curve character is associated with the phenomenon of muscle compensatory hypertrophy after injury. Subsequently, the recovery occurs only under the influence of restoration of patients' functional motor activity.

In our opinion, rapid recovery of muscle strength during the first year after the end of treatment is connected with the fact that the recovery occurs through compensatory hypertrophy of muscles. After completion of distraction regenerated bone reorganization this hypertrophy probably disappears, and further increase of contractility occurs only under the influence of motor activity increase. The stationary level of muscle strength value for intact femur – 1.2–1.6 N*m/kg and for the femur lengthened – 0.9 N*m/kg.

As far as patients' age increased the level of muscle strength recovery in the limb lengthened became lesser (Fig. 23.18). That is why the limb lengthening at early age (below 10 years), despite difficulties of service to patients, is justified, because the processes of natural growth and tissue adaptation to new biomechanical conditions continue after treatment.

It has been established that the more growth retardation of limb, the lower values of its strength. The ratio between the amount of leg longitudinal size retardation (L, cm) and the relative strength moment of foot plantar flexor muscles (F, N*m/kg) can be described by equation of linear regression: $\mathbf{F = 1.7 - 0.096 * L; R^2 = 0.26}$. In addition, the more amount of leg lengthening, the lower level of muscle strength recovery. Complete recovery of muscle contractility was noted for 45–70 % (8–12 cm) increment of leg length. Lesser lengthening amounts are associated with problems during distraction.

The performed studies of femur and leg muscle contractility after limb segment lengthening have demonstrated that under automatic distraction the recovery of muscle contractility attains high level. Thus, the most important group of leg extensor muscles after

Table 23.3 Relative moment leg muscles before and after treatment (N*m/kg)

Examined groups	Number of observa-tions	Foot dorsal flexors		Foot plantar flexors	
		Intact leg	Involved leg	Involved leg	Intact leg
Before treatment	103	0.70 ± 0.04	0.51 ± 0.04	1.10 ± 0.07	1.41 ± 0.05
Immediate periods	27	0.58 ± 0.05	0.41 ± 0.04	0.70 ± 0.10	1.26 ± 0.09
Long-term periods	27	0.68 ± 0.06	0.48 ± 0.05	1.26 ± 0.18	1.56 ± 0.16

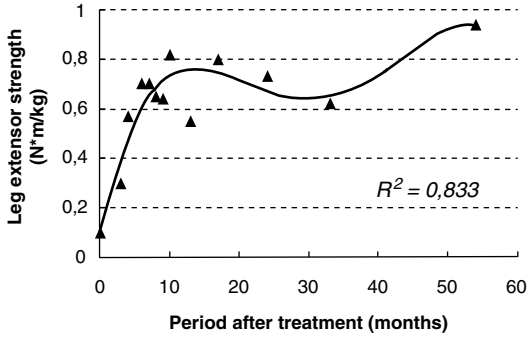

Fig. 23.18 Age-related dynamics of ratio between the relative strength moment of leg muscle posterior group in the limb lengthened and that in intact limb

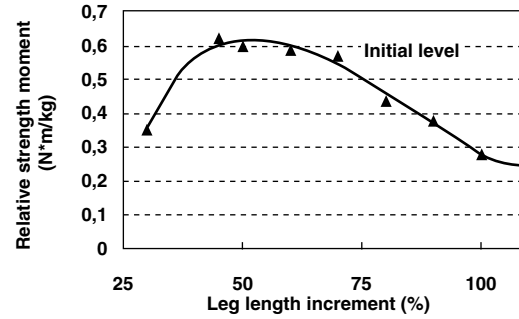

Fig. 23.19 Dependence of the strength recovery level of leg muscle posterior group on the amount of leg lengthening with reference to initial sizes

treatment with manual twisting the fixator in the long-term periods reaches 58 % ($p \leq 0.001$) of the initial level, while in patients with automatic distraction – 95 %. The strength of leg muscle posterior group amounts to 65 % ($p \leq 0.02$) and 114 %, respectively.

Our observations show, that searching the conditions under which muscle strength in children and adolescents after limb size increase will gain in the same way as under natural longitudinal growth, is not unfounded (Fig. 23.19). There are only isolated observations of such effect, which have been taken in adolescent patients and which are hardly explained. For achieving such effect it's necessary to improve treatment technique and to determine optimal biological conditions of treatment (age, lengthening amounts).

It has been found by us, that in normal women and men the excess of leg length by 44 and 46.5 cm, respectively, contributes to the decrease of relative strength moment of limb muscles. For patients the optimal biological value of leg length is significantly lesser, it is achieved in puberty and should amount to 36 and 38 cm (conforms to mean leg sizes of human subjects before starting the period of growth acceleration).

It should be mentioned that steady rise of arterial elasticity for up to 8-cm leg lengthening with signs of ischemic disorders and hypertension was observed in a girl of asthenic constitution at the age of 11 years, and the gain of muscle strength after lengthening, equivalent to the gain for natural growth, – in an adolescent of hypersthenic constitution.

Constitution Type Effect on Surgical Lengthening Outcomes of a Limb with Growth Retardation

Limb growth in girls at the age of 10–11 years is intensive. In case of distraction in this very period the greatest amounts of limb length increase can be achieved with good functional outcomes. That means, this is a period when the limits of genetically laid program of natural growth allow the most complete adaptation to changing environmental conditions. Girls' puberty is an uneven process, it doesn't come simultaneously in female representatives of different constitution type.

We examined normal girls at the age of 11–12.5 years (46 female subjects). Three main

Table 23.4 Description of groups of the subjects examined (M ± m)

Groups of the subjects examined	n	Height (cm)	Weight (kg)	Length of intact leg (cm)	Limb shortening (cm)
Normal subjects at the age of 11–12	46	153 ± 1.3	41.6 ± 1.5	37 ± 0.5	–
Patients at the age of 11–13	26	154 ± 4.6	43.8 ± 4.0	38 ± 2.6	7 ± 1.4
Patients at the age of 15–26	28	168 ± 4.3	58.1 ± 5.6	40 ± 0.8	6 ± 0.8

somatic types were singled out in those examined subjects based on their data of the shape of chest, abdomen, back, lower limbs, as well as on anthropometric measurements, allowing to estimate quantitatively the state of bone, muscular and fatty components; they were as follows: normosthenic (11), hypersthenic (17) and asthenoid (18).

The main group consisted of 26 children at the age of 10–16 years and 28 adult female patients with congenital growth retardation of lower limb segments (Table 23.4). In patients lower limb segments were lengthened by the amounts from 3 to 7 cm using the technique of distraction osteosynthesis according to Ilizarov. The amount of distraction forces was determined with tensometric sensors [7] on 15, 30 days of treatment and at the end of leg lengthening period. The fixation index was determined by correlation between the duration of this period and the height of distraction regenerated bone.

It has been revealed that in normal girls of asthenoid constitution later coming of puberty is observed, as well as their anthropometrical values are in retard of the values in examined subjects of normosthenic constitution. Leg longitudinal sizes are the least in female representatives of asthenoid somatic type (37 ± 0.7 cm), and they are the greatest – in those of normosthenic one (38 ± 0.4 cm). The greatest transverse diameter of femoral distal end was also determined in female representatives of normosthenic somatic type (8 ± 0.17 cm), while in those of asthenic somatic type it was the least (7 ± 0.18 cm).

At the same time, in patients of normosthenic constitution all over limb lengthening the value of distraction forces was significantly lower, than in those of hypersthenic constitution and especially in those of asthenic one (Fig. 23.20). The duration of fixation period, estimated by the fixation index, was 8.4 day/cm for normosthenic subjects, 9.9 – for hypersthenic subjects and 12.7 day/cm – for asthenic ones. Range of motions in the knee at 3 months after the end of treatment in patients with normosthenic type 2.5-fold increased, in those with hypersthenic type 3.3-fold increased and in patients with asthenic type – 1.8-fold.

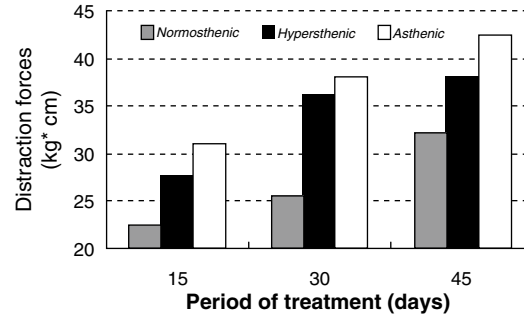

Fig. 23.20 The amount of distraction forces in treatment of patients with normosthenic, hypersthenic and asthenic type of constitution

The cause of relatively more rise of distraction forces and increased fixation duration in female patients (women and girls) of asthenoid constitution is not quite clear. Structural differences in forming regenerated bone may take place in representatives of different somatic types. At any rate, it's known that the mineral density of limb long tubular bones is higher in subjects of asthenoid constitution type [5].

Some suppositions can be made concerning the cause of the differences revealed in examined subjects with different constitution type. First, there are relatively more red muscular fibers of lesser diameter and lesser angle of bundle departure in muscles of asthenic subjects. In this case muscles of hypersthenic subjects will be in more favourable position. Secondly, the rates of range-of-motion recovery are determined by the rate of rest muscle length recovery, which depends on the rate of tendon longitudinal growth. Muscle

tendinous part in asthenic subjects have slower rates of natural growth, because their rates of puberty are lower.

In any case, the approach to determine distraction rates and to predict the rates of functional rehabilitation in patients of different somatic types should be individual. In patients if asthenoid constitution type the rates of distraction should be lower.

Conclusion

As far as natural longitudinal growth occurs, as well as age-related development, the gain of limb soft tissue elastic properties takes place in patients, which evidences the decrease of the reserves of their functional recovery after surgical increasing the limb length. During distraction the tension gain in muscles plays a key role in limitation of the scale of patients' body growth increase – the extension of muscle contractile part doesn't lead to adequate growth and is accompanied by worsening of capillary blood supply conditions. Ischemic involvement of muscles leads to their structure disorder and subsequently – to fail to proper contractility recover. That is why while predicting functional outcomes of treatment not only the aesthetic effect of length gain of limbs with growth retardation and that of step length increase should be taken into consideration, but also the degree of muscle contractility decrease, which grows as far as distraction continues and patients' age increases. The best effect is observed for treatment of subjects with normosthenic and hypersthenic types of constitution, in children in the period of limb natural growth acceleration, when distraction of high-division is used.

References

1. Ilizarov GA. General biological property of tissues to response to graduated distraction by growth and regeneration (the Ilizarov effect). Diploma No 255. Application No 11271 of 25.12.85. (in Russian) Bull. No 15. 1989:1.
2. Schurov WA, Muradisinov SO. The second rule of regeneration and leg elongation by Ilizarov. Chir Narz Ruchu Ortop Pol LIX. 1994;4(Suppl):32–8.
3. Pfluger G, Wolner C, Thoma H, et al. Objektivirung des Gesamtwiderstandes bei der Beinverlängerung. Orthop Prax. 1976;2:160–4.
4. Shevtsov VI, Schurov VA. Gradient cranio-caudal des resources de regeneration des members inferieurs. Rev Chir Orthop. 2003;89(10):3S43.
5. Ilizarov GA, Schurov VA. Effect of tension stress on biomechanical properties of muscles, their blood supply and leg growth (in Russian). Hum Physiol. 1988;14(1):26–32.
6. Henderson Y, Oughterson AW, Greenburg LA. Muscle Tonus? Intramuscular pressure and venopressor mechanism. Am J Physiol. 1936;114:261–8
7. Stewart DM. The regulation of organ and tissue growth. Chapter 5: role of tension in muscle growth. Academic Press; 1972. p. 77–100.
8. Schurov VA. A device for angulodynamometry. Patent 2029536 RU. IPC[3] A 61 H 1/00, No 5042260/14; Zayavleno 15.05.1992. Publ. 27.02.1995. Bull. No 6. 1995:1–4.
9. Schurov VA, Dolganova TI, Dolganov DV. Femoral muscle Dynamometr. Biomedical Engeneering (in Russian). 2014;48(1):30–2.
10. Paley D. Current techniques of limb lengthening. Review article. J Pediatr Orthop. 1988;8(1):73–91.
11. Popkov AV, Diachkova GV, Shchurov VA, et al. Automatic lengthening of the lower limbs (in Russian). Tezisy dokl. Mezhdunarodn. konf. posviashchon. pamiati akademika G.A. Ilizarova (Heads of Reports of the International Conference in memory of Academician GA Ilizarov). Kurgan, 1993. p. 168–70.
12. Shevtsov VI, Popkov AV. Surgical lengthening of the lower limbs (in Russian). Moskwa: Meditsina; 1998. 190 p.

Biomechanics of Pediatric Hip

24

Susumu Saito and Atsushi Kusaba

Congenital Dislocation of the Hip Joint

Congenital dislocation of the hip joint includes prenatal, acquired, and developmental dislocation (*i.e.,* femoral head dislocates from the acetabulum gradually after birth). Most of this disease occurs while this disease is named as "congenital". True congenital dislocation is often intractable, as it has severe dislocation and is accompanied by considerable anomalies. In true congenital dislocation, the acetabulum is extra remarkably shallow and steep, and anterosion of the femur is severe. In acquired or developmental dislocation, environmental factors have more influence on the occurrence of the dislocation than congenital ones. The kind of diaper is one of the most important factors. The prevalence of dislocation is high in some cold areas. In such area, diaper or clothes is set to fix the knee and the hip in the extended position to keep the children from the coldness. In hemilateral dislocation after birth, lying position has influence on its occurrence. Joint instability, which is caused by hormone around birth, and contracture due to the position may cause dislocation. In left wryneck position (*i.e.,* the face rotates in the right and the neck flexes in the left), the trunk often takes right lateral position. In such position, the left hip joint takes adducted position and tends to have adduction contracture, and dislocation may occur in the left hip. The degree of the dislocation varies from children. Hamstring muscles have strong influence on the occurrence of the dislocation. These muscles push the femoral head proximally. When secondary dysplasia of the acetabulum exists besides the dislocation, spontaneous rectification hardly occurs and the hip is still unstable even after the manual reduction. After the occurrence of the dislocation, contracture of the iliopsoas muscles and varus position of the labrum are inhibitors against the reduction.

Posture or motion of the fetus in the uterus also has strong influence on the occurrence. According to Vartan [1] and Tompkins [2], 56–75 % of breech delivery fetuses have extended knee posture in the uterus while only 3 % of cephalic delivery fetuses have such posture. Wilkinson [3] studied 866 cephalic delivery children and 123 breech delivery children. Fully flexed knee posture was observed in 83 % of cephalic delivery children while it was in 35 % in breech delivery children. The fully flexed knee posture was observed only in 20 % of children with hip dislocation. From these results, he concluded that disturbance of the leg holding mechanism is an important factor to the dislocation. Vartan [1] reported that disturbance of leg holding

S. Saito, MD, PhD
Department of Orthopaedic Surgery,
Showa University Fujigaoka Hospital,
Yokohama, Kanagawa, Japan

A. Kusaba, MD, PhD (✉)
Department of Rheumatology,
Zama General Hospital, Kanagawa, Japan
e-mail: weardebris@AOL.com

D.G. Poitout (ed.), *Biomechanics and Biomaterials in Orthopedics*,
DOI 10.1007/978-1-84882-664-9_24

mechanism causes extended knee posture, which disturbs posture change in the uterus, and causes breech birth. Michelson and Lamgenskiold [4] made an experimental study using juvenile rabbits. They fixed the knee joints of the rabbits and succeeded in making artificial dislocation or subluxation. In their experiment, no dislocation or subluxation occurred in the rabbits after hamstring myotomy. They suspected that continuous spasm of the hamstrings was the main cause of the dislocation. The hamstring is a diarthric muscle that affects the hip and the knee joint. Thus when the hip joint is forced to flex with the knee joint extended, severe axial load is given to the femur. Michele [5] reported that contracture or shortening of iliopsoas muscle may cause anthropologic dislocation. He emphasized that the iliopsoas muscle is the most important etiologic factor of congenital dislocation of the hip joint. Mckibbin [6] made a postmortal examination of neonates. According to his report, extended position of the hip caused a tendency of hip dislocation in the neonates with iliopsoas contracture. After myotomy of iliopsoas, such phenomenon went off. Yamamuro [7] made an experimental study and reported that hip dislocation was caused by reciprocal force of the hamstring and the iliopsoas. According to his report, when the knee is fixed in the extended position, the hip is extended due to the excessive tension of the hamstring. Extended hip position cause the excessive tension of the iliopsoas and the tension forces the hip to be flexed against the tension of the hamstring. In such a situation, the iliopsoas acts to rotate the femur externally and to cause the dislocation. From these reports, both the hamstring and the iliopsoas seem to influence on the hip dislocation. In prenatal period, the hamstring has more influence than the iliopsoas, as most fetuses have flexed posture. After birth, the iliopsoas has more influence than the hamstring, as most neonates have extended posture.

Treatment for Congenital Hip Dislocation

Taking frog (flexed-abducted-externally rotated) position, preventing the hip from the dislocation is possible in neonates before the dislocation, even if the hip is unstable and the joint laxity exists. Some methods exist to take such position. The most common method is Riemenbügel. Taking frog position, dislocated femoral head is brought near to the acetabulum. The weight of the lower extremity reduces the tension and contracture of the adductor muscles. Consequently the femoral head gets over the acetabular rim and is reduced into the acetabulum. This reduction force is given not by the motion of the lower extremity through the stirrup but by the weight of it. The authors made an above-knee Riemenbügel (without the stirrup) and succeeded in the reduction. Generally the success rate of reduction is around 80 % of dislocation in infancy. Riemenbügel is effective for mild dislocation. Traction, manual reposition, or open reduction is necessary for dislocation that is irreducible in both in extended and in frog position. Such treatment is also necessary for dislocation accompanied by varus labrum.

Overhead traction method diminishes the spasm of surrounding muscles and capsular ligaments to enlarge the acetabular inlet, and expands the spasm of obstructive muscles. First, horizontal traction reduces contracture of the iliopsoas and rectus femoris and expands the capsular ligament inferiorly. Next, gradual flexion of the hip with extended knee position reduces the contracture of the hamstring. As the iliopsoas, which suppresses the acetabular inlet anteriorly, becomes loose, the inlet spreads. Finally, traction in fully abducted position reduces contracture of the adductor muscles to reduce the femoral head into the acetabulum without pressing the head to the labrum.

Configuration of the Hip Joint and Alignment of Lower Extremity

The femur in congenital hip dislocation has more antetorsion angle and neck schaft angle than anatomical one. The acetabulum in congenital hip dislocation is steep and shallow. Because of such configuration, the hip is unstable just after the reduction. The steep and shallow acetabulum is

improved gradually. When the improvement is insufficient, arthrosis may occur after the residual subluxation. For residual subluxation, pelvic osteotomy and/or derotation-varus osteotomy is necessary. Today, pelvic osteotomy is preferable. Pelvic osteotomy brings about better containment and stability of the hip. However, some pelvic osteotomy that enlarges the ilium superoinferiorly causes hemodynamic change of the femur and increased growth of the femur. As the result, functional dysplasia may occur in standing position. Recurrence of valgus sometimes occurs after the derotation-varus osteotomy of the femur. Atrophy of abductor muscles, residual dysplasia of the acetabulum, or damage of trochanteric apophysis is conjectured for this recurrence of valgus. Excessive recurrent valgus causes recurrence of subluxation and instability of the hip. Degree of recurrent valgus is more in younger children. Thus, more varus angle of the osteotomy is necessary for younger children. Pelvic osteotomy combined with varus-derotation osteotomy is adopted when simple pelvic osteotomy does not bring about sufficient containment. Generally, the combined osteotomy is necessary for the femur with 60° or more antetorsion angle. Otani [8] made an experimental study using three-dimensional elasto-optic method to support such indication. The authors made a study over alignment after the osteotomy. FTA increased just after the surgery [9]. However, because of recurrent valgus and the remodeling in the distal femur, FTA decreased in the postoperative course. The functional axis of the lower extremity (Mikulicz Line) returned to go through the midpoint of the knee 1 year after the surgery.

Femoral Antetorsion and Cooperated Factors of Torsion

The angle of the femoral antetorsion angle is the angle between the mediolateral femoral condyle line and the axis of the femoral neck in a horizontal plane. Many measuring methods of the antetorsion angle have existed [10–19]. Femoral antetorsion angle in prenatal period has individual difference and varies from reports [20–22]. During the early prenatal period, femoral neck has retrotorsion. From the middle stage in the prenatal period, femoral neck begins to have antetorsion. The position of legs in the uterus and tension of muscle attach to the trochanters have a strong influence on this phenomenon. According to Michele, from the sixth to ninth month of intrauterine life, the lower extremities rotate internally and this phenomenon brings about the femoral antetorsion [5]. Some authors pointed out the relation between congenital hip dislocation and the antetorsion angle in this stage [20, 23, 24]. In this stage, contracture of the iliopsoas muscle can cause excessive antetorsion or superior displacement of the femoral head. The antetorsion angle is 30° or more at perinatal period. The angle at 1 year old is around 50° and decreases with growth [24–26]. Such a phenomenon seems to have a relation to walk in erect posture. According to Lanz, the angle is 15–57 (average, 32) degrees in neonates, 20–50 (average, 34) degrees in 1–3 year-old-children, 12–38 (average, 25) degrees in 4 to 6-year-old children, and −25–37 (average, 12) degrees in adults [22].

The femur antetorsion angle can increase in patients with some diseases such as congenital dislocation of the hip or Perthes' disease. The increased antetorsion angle may influence on the congruency or stability of hip joint. In residual subluxation after the treatment for congenital dislocation, increased antetorsion angle of the femoral neck is often observed. Better congruency in abduction-inner rotation position aids to diagnose the existence of the increased antetorsion angle. As far as no contracture of the iliopsoas muscle exists, the increased antetorsion angle can be improved in the natural course after virgin gait [27, 28].

Experimental Study of Femoral Antetorsion

The authors made an experimental study concerning the femoral antetorsion in congenital dislocation of the hip joint [29, 30]. Twenty young mongrel dogs with experimental complete

dislocation of the hip joint were studied. Seven or eight Kirschner wires were inserted vertically to the longitudinal axis of the femur. They were inserted taking care not to injure the growth plate. They were inserted so that each wire was just parallel and has an equal interval. The most distal wire was inserted in the distal epiphysis. The wire second to the most distal one was inserted in the distal portion of the femoral metaphysis. Thus, the distal epiphyseal line existed between the two distal wires. They were cut and buried in the femur. Increased antetorsion was observed even 1 week after the surgery. Another Kirschner wire was inserted along the axis of the femoral neck. The femurs were examined after the retrieval. From the position of each wire, the rotation of the femur was evaluated. The most distal wire rotated internally against the next wire. At this time, all wires in the metaphysis, physis, and the wire in the neck kept parallel each other. This phenomenon indicates the distal epiphyseal line brings about that antetorsion. When this distal rotation was excessive, compensative retrotorsion occurred between the proximal two wires (in the portion between the wire in the neck and the next wire) after the occurrence of the antetorsion. This indicates that the proximal portion of the femur (proximal epiphyseal line or the neck) (Table 24.1, Figs. 24.1, 24.2, 24.3, 24.4, 24.5, and 24.6). In conclusion, the femoral torsion is mainly brought about by the distal epiphyseal line and additionally by proximal portion of the femur. Adequate load seems necessary to get this proximal retroversion so that the antetorsion angle will be excess in congenital hip dislocation [29, 30].

Slipped Capital Femoral Epiphysis

Slipped capital femoral epiphysis is divided into three types. Acute type is a fracture in proximal femoral growth plate. This type is generally caused by significant trauma. In chronic type, the femoral head slips gradually because of the brittleness of the growth plate. Chronic type is the most common. Slip progresses acutely during the chronic course in acute on chronic type. The most direction of the slip is posteroinferior. The direction has close relation to neck-shaft angle. Wilson [31] reported that 85 % of posteroinferior slip had 140°\\ of neck-shaft angle, According to Inhäuser [32], the head slips posterolateralinferiorly when severe coxa valga such as 160° of neck-shaft angle exists. In such coxa valga, growth plate in the standing position is almost parallel to the floor. Ordinal anteroposterior radiograph of the hip shows as if the head slips posteromedialinferiorly because of the externally rotated femur. Posteroinferior slip is obvious on the radiograph taken without rotation of the femur. Three-dimensional CT scan study supports this fact. Lateral view radiograph is thus essential to measure the slip-angle. Imhäuser's method is quite useful to measure the angle [32]. The anatomical angle in his method is 10 or less degrees. In his criteria, 30 or less degrees is slight slip, 30–70 is moderate, and 70 or more is severe.

According to Harris [33], growth hormone accelerates the mitosis of the proliferating layer and causes the hypertrophy of the hypertrophied cartilage layer. Growth hormone decreases the yield strength of the growth plate while sexual hormone increases the strength. His report suggests that insufficient sexual hormone or excessive growth hormone may cause the slip. Relative excessive growth hormone can occur when secretion of the growth hormone continues after the growth period.

The growth-plate has three-dimensional unevenness, which has been confirmed by scanning electron microscopic studies. This unevenness gives the growth-plate a multidirectional endurance against compression, strain, and shear stress. The yield strength of a growth-plate depends on the degree of this three-dimensional unevenness [34, 35]. Acute slip is a kind of fracture and thus complete rupture occurs in the growth plate, or Salter-Harris Type II injury occurs. In chronic slip, repetition of stress causes gradual disruption and after that slip occurs when the stress exceeds the yielding strength. External rotation contracture occurs when the slip angle is 30 or more. Gait in externally rotated position due to the pain and bearing weight accelerates the

Table 24.1 Summary of wire in the femur, time elapsed from dislocation and relative increase or decrease of antetorsion

Postoperative (weeks)	Condylen-upracondylen	Distal third of femoral shaft	Proximal third of femoral shaft	Subtrochanter	Femoral neck-femoral head
1–3	→	→	→	→	
4	↑	→	→	→	
6	↑	→	→	→	→
8	↑	↑	→	↓	
9	↑	↑	→	→	
10	↑	↑	→	↓	
13			→	↓	
14	↑	↑	→	→	↓↓
16	↓	↑	→	↓	↑
21	↑	↑	→	↓	↓

Dark arrows indicate an increase of antetorsion Light arrows indicate a decrease of antetorsion. The thicker arrows mark greater changes

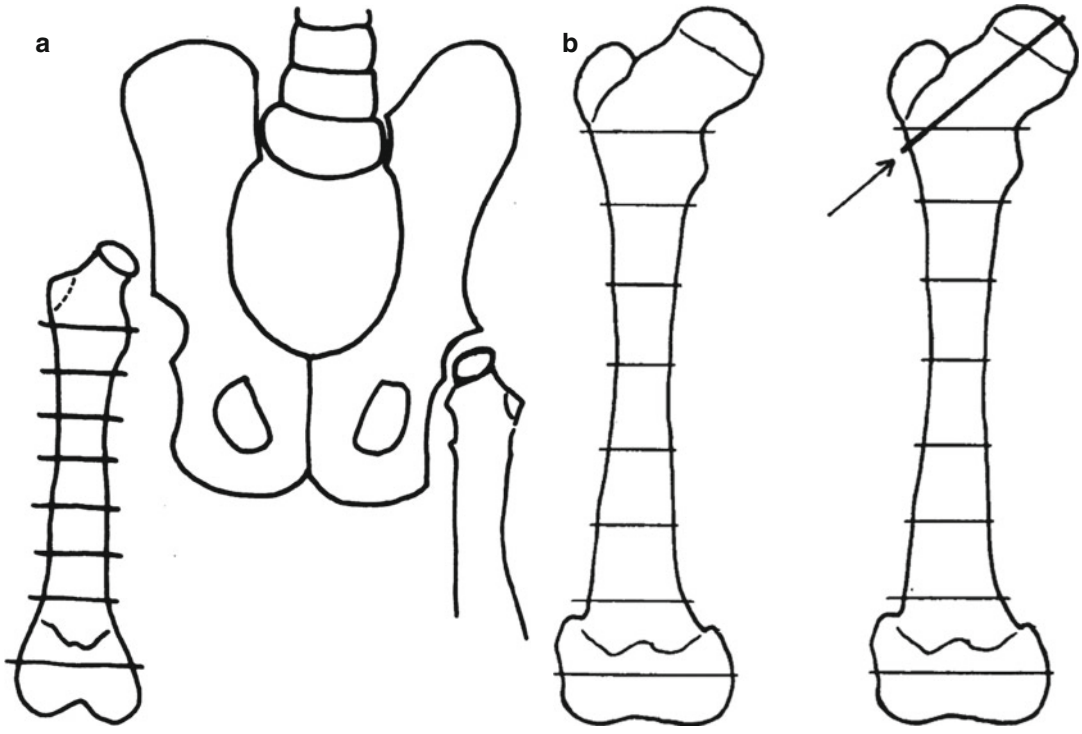

Fig. 24.1 (**a**) The method of experiment. The right femoral head of the dog was dislocated surgically. And Kirschner wires were inserted parallel into the femur. (**b**) Parallel wires were inserted into the femur. Right: One extra wire was inserted through the proximal neck and head still in the same plane as that of the parallel wires along the femur

disruption. According to Morscher [36], analyzed the posterior tilting angle and concluded that posterior stress force in internally rotated position is the main cause of slip. In slipped capital femoral epiphysis, motion range of the hip increases in external rotation and decreases in internal rotation. Flexion range is also limited. Drehmann's phenomenon is obvious in slipped capital femoral epiphysis; as the thigh is flexed, it tends to roll into external rotation and abduction. After progress of the slip, varus deformity of the hip occurs and both Trendelenburg's phenomenon and gait become obvious.

Reported yield strength of the growth-plate has been various as it depends on the material of the experiment [37]. According to Bright, the strength of the force, which made a crack in the growth-plate was one-half of the yield strength of the growth-plate. On the other

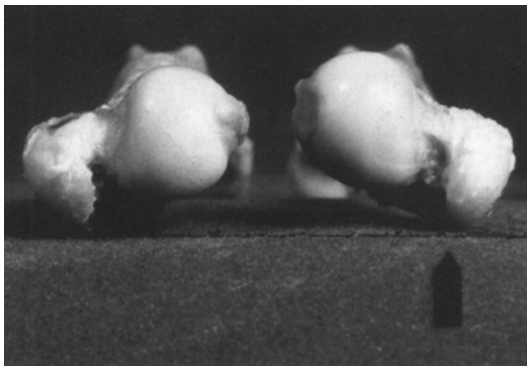

Fig. 24.2 One week after dislocation. More antetorsion existed on the right femur. Arrow shows dislocated femur

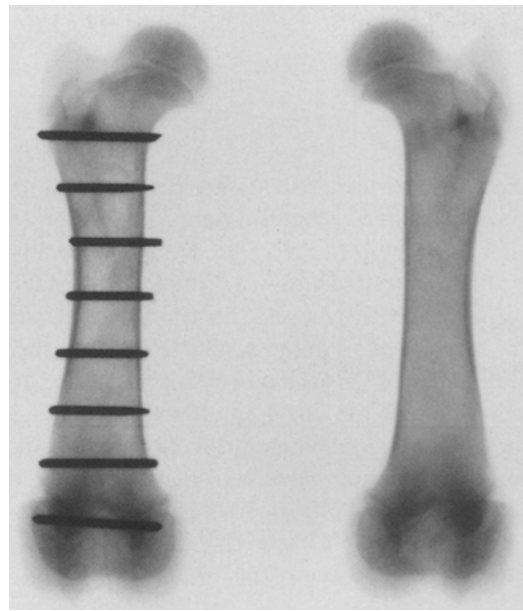

Fig. 24.3 Radiograph taken 1 week after dislocation. All wires were still parallel

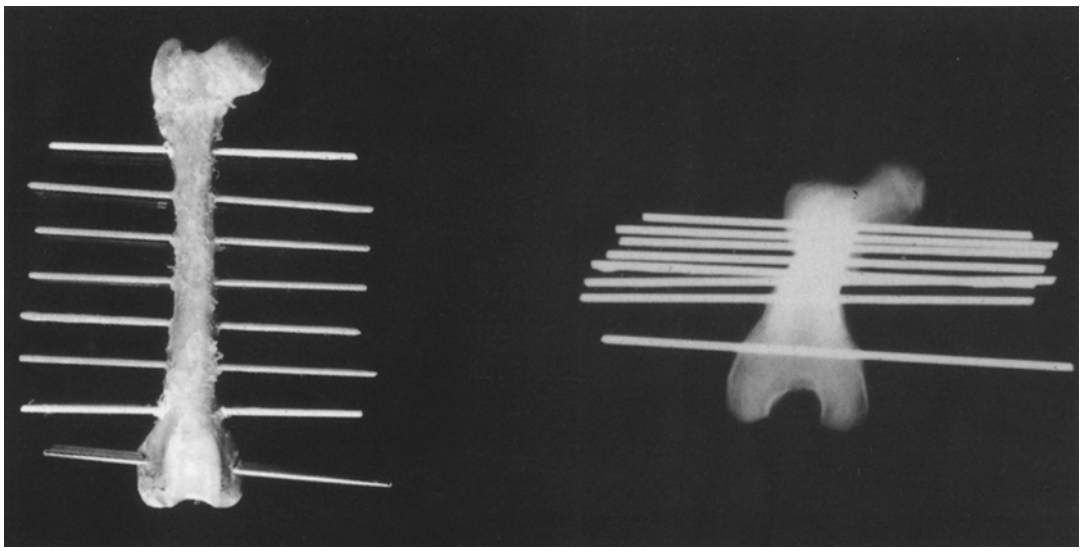

Fig. 24.4 Four week after dislocation. All wires but the most distal were still parallel

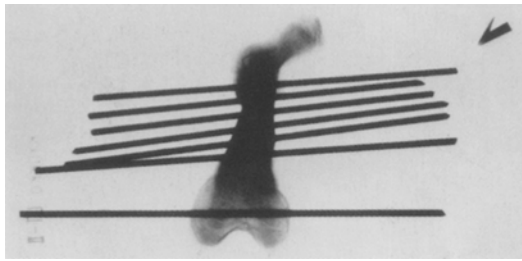

Fig. 24.5 Eight weeks after dislocation. The wire inserted into the upper most part of the femur rotated slightly inwards (*arrow*)

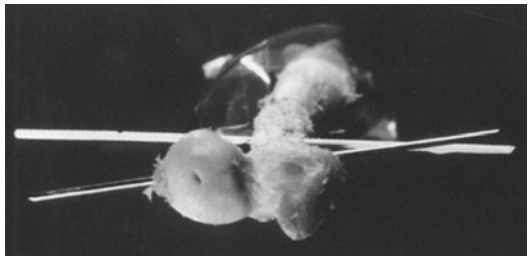

Fig. 24.6 The wire inserted through the femoral neck and head rotated inward. This indicated decrease of antetorsion

hand, Bright and Nakada reported that there was no relation between these two strengths [35, 38]. Chung reported that force within the strength of physiological range was enough to cause the epiphyseal slipping in overweight children and suggested that purely mechanical factors may play a major role in the etiology of slipped capital femoral epiphysis [39]. Williams made an experimental study and found that the shear strength of the physis varies with anatomic location. According to this experiment, the posterior region of tibia physis had the greatest strength and stiffness, lowest physeal thickness, and steepest inclination [37]. Kim pointed out that the strength depends on the existence of the membrane of cartilage [34]. The membrane seems to reinforce the growth-plate in cooperation with the three-dimensional structure of the growth-plate. In his report, the ratio of fracture strain between the growth-plate without / with cartilage membrane was 61 % (tensile strength) and 37 % (strain strength). Chung made post-mortem studies of hips in children to determine the shear strength and modes of failure of the capital femoral growth-plates [39]. In this experiment, the shear strength of the human growth-plate varied with age and was greatly dependent on the surrounding perichondrial complex in infancy and early childhood, but less so in adolescence. When this complex was excised, the strength of the epiphyseal plate was diminished, especially in younger children. In acute slip, such membrane is disrupted while it is preserved in chronic slip.

The velocity of stress is also an important factor in growth-plate injury, as the growth-plate has viscoelastic property. Kim reported that Salter-Harris type I injury is caused by the stress of relatively slow velocity and II and III by high velocity [34]. Histological study performed concurrently with the yield-strength test, varies among the authors. This may be brought about mainly by the difference in the method of experiment. According to Salter and Amailo, the epiphyseolysis occurred in the hypertrophying layer [40, 41]. Bright reported it occurred with a stairway form in the hypertrophying layer and palisading layer [42]. According to Nakada and Brasher, epiphyseolysis occurred in different layers depending on the portion of the growth-plate [35, 42]. From the point of clinical view, epiphyseolysis mainly occurs in the hypertrophying layer or transient portion to the metaphysis in slipped capital femoral epiphysis [33, 37, 43].

References

1. Vartan CK. The behaviour of the foetus in utero with special reference to the incidence of breech presentation at term. J Obstet Gynec Brit Emp. 1945;52:417–34.
2. Tompkins P. An inquiry into the cause of breech presentation. Am J Obstet Gynec. 1946;51:595–606.
3. Wilkinson JA. A postnatal survey for congenital dislocation of the hip. J Bone Joint Surg. 1972;54B:40–9.
4. Michelson JE, Langenskiöld A. Dislocation or subluxation of the hip, regular sequels of immobilization of the knee in extension in young rabbits. J Bone Joint Surg. 1972;54A:1177–86.
5. Michele AA. Iliopsoas. Springfield: Charles C Thomas; 1962.

6. McKibbin B. Anatomical factors in the stability of the hip joint in the newborn. J Bone Joint Surg. 1970;52B:148–59.
7. Yamamuro T, Hama H, Takeda T, Shikata J, Sanada H. Sexual hormone in the experimental hip dislocation. Cent Jpn J Orthop Traumat. 1976;19:770–1.
8. Otani T. Studies on photoelastic stress analysis of congenital dislocation of the hip. J Jpn Orthop Assoc. 1964;37:1001–26.
9. Saito S. Change in the alignment of the lower extremities in children- A study of the cases with fractures of the femur and congenital hip dislocation of the hip. J Jpn Paed Orthop Assoc. 1993;3:148–56.
10. Schneider B, Laubenberger J, Jemlich S, Groene K, Weber HM, Langer M. Measurement of femoral antetorsion and tibial torsion by magnetic resonance imaging. Br J Radiol. 1997;70:575–9.
11. Drehmann F, Becker W. A simple clinical investigation method for the approximative rapid determination of the antetorsional angle of the neck of femur. Z Orthop. 1980;118:236–40.
12. Grote R, Elgeti H, Saure D. Determination of the antetorsional angle at the femur with axial computer tomography. Rontgenblatter. 1980;33:31–42.
13. Tomczak RJ, Guenther KP, Rieber A, Mergo P, Ros PR, Brambs HJ. MR imaging measurement of the femoral antetorsional angle as a new technique: comparison with CT in children and adults. AJR Am J Roentgenol. 1997;168:791–4.
14. Haspl M, Bilic R. Assessment of femoral neck-shaft and antetorsion angles. Int Orthop. 1996;1996(20):363–6.
15. Bruckl R, Grunert S, Rosemeyer B. Roentgenologic determination of the actual femoral neck-shaft and antetorsion angle. 2: Alternatives to the Rippstein and Muller procedure. Radiologe. 1986;26:305–9.
16. Wissing H, Spira G. Determination of rotational defects of the femur by computer tomographic determination of the antetorsion angle of the femoral neck. Unfallchirurgie. 1986;12:1–11.
17. Gunther KP, Kessler S, Tomczak R, Pfeifer P, Puhl W. Femoral anteversion: significance of clinical methods and imaging techniques in the diagnosis in children and adolescents. Z Orthop Ihre Grenzgeb. 1996;134:295–301.
18. Gormand E, Barral F, Roussille M, Bochu M, Fournet-Fayard J, Kholer R. Comparison between ultrasonic and x-ray computed tomographic measurements of femoral antetorsion in children. J Radiol. 1985;66:789–92.
19. Clarac JP, Pries P, Laine M, Richer JP, Freychet H, Goubault F, Barret D, Hurmic A, Vandermarcq P, Drouineau J. Measurement of antetorsion of the femoral neck by ultrasonics. Comparison with x-ray computed tomography. Rev Chir Orthop. 1985;71:365–8.
20. Badgley CE. Correction of clinical and anatomical facts leading to a conception of the etiology of congenital hip dysplasias. J Bone Joint Surg. 1943;25:503.
21. Badgley CE. Etiology of congenital dislocation of the hip. J Bone Joint Surg. 1949;31A:341.
22. Lanz T, Mayet A. Die Gelenkkorper des menschlichen Huftgelenks in der progredienten phase ihrer umwegigen Ausformung. Z Anat. 1953;117:317.
23. Le Damany P. Die angeborene Hüftgelenkverrenkung. Ihre Ursachen: ihre Mechanismus: ihre arthropologische Bedeutung. Z Orthop Chir. 1908;21:129.
24. Somerville EW. Development of congenital dislocation of the hip. J Bone Joint Surg. 1953;40A:803.
25. Chandler F. Anatomical study of congenital dislocation of the hip. J Bone Joint Surg. 1929;11:546.
26. Shands Jr AR, Steele MK. Torsion of the femur. A follow-up report on the use of the Dunlop method for its determination. J Bone Joint Surg. 1958;40A:1147.
27. Sylkin NN. Developmental tendency of the femur head following femoral head necrosis due to conservative treatment of a dislocated hip (2nd report). Z Orthop Ihre Grenzgeb. 1995;133:367–73.
28. Lingg G, Nebel G, Thomas W, Hering L. Value of computed tomography in congenital hip dysplasia and hip luxation. Rontgenblatter. 1983;36:407–13.
29. Saito S, Kuroki Y, Uchida T, Mori Y. Experimentelle Untersuchungen uber die Entstehung der Antetorsion am Femur. Z Orthop. 1980;118:612.
30. Saito S, Kuroki Y, Uchida T. An experimental study on the change of the femoral antetorsion. J Jpn Orthop Assoc. 1978;52:1185.
31. Wilson PD, Jacob B, Schecter L. Slipped capital femoral epiphysis. J Bone Joint Surg. 1965;47A:1128–45.
32. Imhäuser G. Die jugendliche Hüftkopflösung bei steilem Schenkelhals. Z Orthop. 1959;91:403–13.
33. Harris R, Hobson KW. The endocrine basis for slipping of the upper femoral epiphysis. J Bone Joint Surg. 1950;32B:5–11.
34. Kim WC. Biomechanical properties of growth plate. J Jpn Paed Orthop Assoc. 1996;6:128–32.
35. Nakada D. Torsional strength of the epiphyseal plate and fracture patterns with aging, three-dimensional analysis with SEM. J Jpn Orthop Assoc. 1993;67:1045–54.
36. Morscher E. Zur Pathogenese der Epiphyseolysis capitis femoris. Arch Orthop Unfallchir. 1961;53: 331–43.
37. Yoshida M, Kim WC, Arai Y, Inoue N, Watabe K, Takai N, Kusaka Y, Hirasawa Y. The effect of maturation on dynamic visco-elastic properties of epiphyseal plate in rabbit. J Jpn Clin Biomech. 1994;15: 147–50.
38. Bright RW, Virginia R, Burstein AH. Epiphyseal-plate cartilage. J Bone Joint Surg. 1974;56A:688–703.
39. Chung SM, Batterman SC, Brighton CT. Shear strength of the human femoral capital epiphyseal plate. J Bone Joint Surg. 1976;58A:94–103. 1989.
40. Amadio P, Ehrlich MG, Mankin HJ. Matrix synthesis in high density cultures of bovine epiphyseal chondrocytes. Connect Tissue Res. 1983;11:11–9.
41. Salter RB, Harris WR. Injuries involving the epiphyseal plate. J Bone Joint Surg. 1963;45A:587–622.
42. Brasher Jr HR. Epiphyseal fractures. A microscopic study of the healing process in rat. J Bone Joint Surg. 1959;41A:1055–4064.
43. Hurley JM, Betz RR, Loder RT, Davidson RS, Alburger PD, Steel HH. Slipped capital femoral epiphysis. The prevalence of late contralateral slip. J Bone Joint Surg. 1996;78A:226–30.

Biomechanics of Fracture in Growth Period

25

Atsushi Kusaba and Susumu Saito

Characteristics of Fractures in Children

Management of fractures in children is completely different from that of adults. Biological reaction for fracture is characteristic in children because of the anatomic, physiological, and biomechanical property of skeletal structure [1]. Comprehension of the properties of children's bone is essential to treat fractures in children. Some properties act favorably for the bone union and some make it difficult to treat fractures.

The Role of Periosteum

The detailed biomechanics of periosteum are described in Chap. 31. Periosteum in children's bone is far thicker than that of adults and thus much callus would appear early after the injury. This is one of the reasons why union of fracture is obtained easily in children. High activity and rich blood supply in the thick periosteum affect new bone formation. The new bone formation in children occurs so immediately after the injury that reduction of the displacement, if necessary, should be achieved in early stages. The periosteum in children's bone is stronger than that of adults [1]. It is well known that the connection between metaphysis and epiphysis is very strong. This strong connection is brought about by the strength of the periosteum. When bending stress is applied to the pediatric bone, the periosteum would be ruptured only in the convex side but not in the concave side. The periosteum in the concave side could act as "intact hinge". This intact hinge is helpful to reduce the position and to maintain the reduced position. On the other hand, if the displacement is not reduced in the early stage, the gap between the exfoliated periosteum and the bone would be filled by new bone and severe deformity would remain [2]. This phenomenon is often observed in unreduced supracondylar fracture of the humerus or the radius distal fracture.

Characteristics of Children's Bone

Bone density of children is lower than that of adults [3]. Bone porosity of children is higher than that of adults. Most of the bone cortex in children is occupied by Haversian canals [4]. Because of both the structural properties of bone and the thick periosteum, the whole bone unit in

A. Kusaba, MD, PhD (✉)
Department of Rheumatology,
Zama General Hospital,
Zama, Kanagawa, Japan
e-mail: weardebris@AOL.com

S. Saito, MD, PhD
Department of Orthopaedic Surgery,
Showa University Fujigaoka Hospital, Yokohama,
Kanagawa, Yokohama, Japan

D.G. Poitout (ed.), *Biomechanics and Biomaterials in Orthopedics*,
DOI 10.1007/978-1-84882-664-9_25

children has more endurance against stress (*e.g.,* compressive stress, tensile stress, bending stress) than that of adults. Currey made an experimental study concerning the strength of the femur in children. Compared with adults, children had a lower modulus of elasticity, a lower bending strength, and a lower ash content. However, the children's bone deflected more and absorbed more energy before breaking. It absorbed more energy also after fracture had started. The typical greenstick fracture surface of many specimens of children's bone requires more energy for its production than the smooth surface of adult specimens [5]. Even when a fracture occurs in child bone, the fracture line is simple and is rarely accompanied by severe displacement. Most fractures in children are incomplete fractures in which the partial continuity of bone remains (*i.e.,* subperiosteal fracture). When bending stress beyond the physiological tolerance is given to a bone, angular deformity of fracture occurs less often in children than in adults. In such cases, greenstick fracture more likely occurs in children. This fracture is often observed especially in distal third of the radius. When axial compressive stress is given to the bone, bamboo or buckle fracture often occurs at metaphysis, where the maximum porosity exists. Otherwise, a plastic deformation may occur [6]. The plastic deformation often observed in pediatric long bone fracture which is due largely to the complex nature of the molecular and histologic aspects of pediatric bone. Pediatric cortical bone has a lower mineral content than adult bone, accounting in part for its different material properties. Although plasticity allows children's long bones to absorb more energy before fracture, a significant deformity may persist after injury [7, 8].

Epiphyseal Injury

Fracture of the growth plate is an injury unique to childhood. The prevalence of this injury in the whole fractures in children is 10–30 % [9]. Salter classified this injury into five groups by the verosity of stress on the epiphyseal plate and direction stress distribution at the plate, and the prognosis: type I, fracture through the growth plate; type II, fracture through the growth plate and metaphysis; type III, fracture through the growth plate and epiphysis; type IV, fracture through the growth plate, epiphysis and metaphysis, and type V, crush or compression injury of the growth plate [2]. Ogden proposed a new classification scheme of physeal and epiphyseal injuries to allow better estimation of prognosis for normal or abnormal growth. This classification based partially on the Salter-Harris system, but additionally detail subclassifications that relate to specific injury patterns [10]. Epiphyseal fracture often occurs in the metaphyseal side of the epiphysis and most of the epiphyseal cartilage cells remain in the epiphyseal side. Most such fractures heal without permanent deformity. A small percentage, however, has subsequent complications such as aseptic necrosis of epiphysis, non-union, premature epiphyseal closure (*i.e.,* growth arrest), joint deformity (angulation, rotation) due to partial epiphyseal closure, and unequal length of leg or arm. The growth-plate has three-dimensional unevenness, which has been confirmed by scanning electron microscopic studies. This unevenness gives the growth-plate a multi directional endurance against compression, strain, and shear stress. The yield strength of a growth-plate depends on the degree of this three-dimensional unevenness [11, 12]. Reported yield strength of the growth-plate has varied as it depends on the material of the experiment [13]. According to Bright, the strength of the force which made a crack in the growth plate was one-half of the yield strength of the growth-plate. On the other hand, Bright and Nakada reported that no relation existed between these two strengths [12, 14]. Kim pointed out that the strength depends on the existence of the membrane of cartilage [11]. The membrane seems to reinforce the growth-plate in cooperation with the three-dimensional structure of the growth-plate. In his report, the ratio of fracture strain between the growth-plate without / with cartilage membrane was 61 % (tensile strength) and 37 % (strain strength). Amamilo reported that the periosteum contributed significantly to the stiffness of the

epiphyseal plate [15]. The hypertrophying and calcifying layer is more fragile than the resting and proliferative layer. However, the section where the crack in the epiphyseal injury existed varies between authors. Bright reported that the crack was not observed only in the hypertrophying layer but also in the resting and the proliferative layer [14]. Nakada reported that crack existed mainly between the proliferative and hypertrophying layer [12]. Amamilo reported that the crack existed in the calcifying layer [15].

Remodeling After Fractures in Children

When malunion occurs after fracture in children, spontaneous correction of deformity is produced by bone remodeling during growth [16–21]. A good example of remodeling can be observed in birth fracture. Malunion in children is often observed in supracondylar fracture of the humerus, lateral condylar fracture of the humerus, Monteggia fracture, distal radius fracture, proximal femoral fracture, and femoral shaft fracture. The remodeling is brought about by Wolff's law and law of Heuter-Volkmann. Both have been recognized as the bone reaction against the stress such as weight bearing, muscle tension, and joint movement. Wollf's law is both periosteal absorption in convex side and periosteal bone formation in the concave side in the diaphysis. Treharne regarded this law as an effect of piezoelectricity of bone [22]. Abraham made a detailed experimental study concerning this law [23]. According to the study, the bone absorption at the convex side did not occur so much as the bone formation at the concave side. Weight bearing did not have as much influence on remodeling; no significant difference was observed between remodeling after fracture of upper extremity and that of lower extremity. The Law of Heuter-Volkmann is asymmetrical epiphyseal growth. Karaharju *et al*. made an experimental study to find out in which phase and to what extent asymmetrical epiphyseal growth participated in the correction of an experimentally produced deformity. According to their experiment, epiphyseal growth played an important role in the remodeling process. The greatest correction occurred during the first weeks. Correction of the epiphyseal angle took place with acceleration of growth [24]. The remodeling potential of angular deformities in the coronal and sagittal planes in children is well known. According to Wallace and Hoffman, in children less than 13 years of age, malunion of as much as 25° in such planes will remodel enough to give normal alignment of the joint surfaces. They also pointed out that 74 % of correction occurred at the physes and only 26 % at the fracture site. On the other hand, poor remodeling potential of significant posttraumatic torsional deformity of the femur in children [25]. The authors made a clinical study concerning three-dimensional remodeling against malunion after femoral shaft fracture [26, 27]. Valgus deformity was more often than varus deformity when the primary union was achieved. This may have been an influence of traction direction. On the other hand, the angle of deformity at the final follow-up was more in varus deformity than that of valgus deformity. The convex angle of deformity had no significant difference between the anterior and posterior convex deformity at the final follow-up. Rotational malunion was also compensated in some extent. The antetorsion angle of femoral neck against femoral condyle became around 30° at the final follow-up either in external or internal rotational malunion cases. In any kind of deformity, the younger the child, the more angle of spontaneous correction is observed. Also, the motion and flexibility of joints compensated the deformity. Mikulics line shifted from the medial side to near the center of the knee joint in children with valgus convex and shifted from the lateral side to near the center of the knee joint children with varus convex. Such compensation occurred earlier than the compensation by the remodeling. Considering these compensations, the deformity within following angles does not cause problems over activity of daily living. The maximum angle of acceptable deformity after the primary union is 30° in children one or less than 1, 20° in 1–5 year old children, 15° in 6–10 years old children, and 10° in 11 or older children [26].

Shortening of bone length can be also compensated in children's fractures to some extent. Excessive compensation is often observed especially in femoral shaft fractures. Excessive growth of bone length occurs more likely in surgically treated fractures than conservatively treated fractures. The average difference of length discrepancy in conservatively treated femoral shaft fractures was around 10 mm in the authors' study. Shortening of the femur showed almost no compensation in most children 10 years old or older. In most children younger than 10 years old, excessive growth of bone length continued until 2 years after the injury. Excessive bone growth of two or more centimeters, compared with the other side, occurs during the growth period and may be treated by epiphyseodesis (*e.g.,* stapling) or elongation of leg using external skeletal fixation [28].

References

1. Canale ST. Fractures and dislocation in children. In: Canale ST, Beaty JH, editors. Campbell's operative orthopaedics. 11th ed. Philaderphia: Elsevier Inc; 2006. p. 1533–6.
2. Salter RB, Harris WR. Injuries involving the epiphyseal plate. J Bone Joint Surg. 1963;45A:587–622.
3. Boot AM, de Ridder MA, Pols HA, Krenning EP, de Muinck Keizer-Schrama SM. Bone mineral density in children and adolescents: relation to puberty, calcium intake, and physical activity. J Clin Endocrinol Metab. 1997;82:57–62.
4. Rang M. Children's fractures. 2nd ed. Philadelphia/Toronto: Lippincott; 1983.
5. Currey JD, Butler G. The mechanical properties of bone tissue in children. J Bone Joint Surg Am. 1975;57A:810–4.
6. Mabrey JD, Fitch RD. Plastic deformation in pediatric fractures: mechanism and treatment. J Pediatr Orthop. 1989;9:310–4.
7. Connolly JF. Torsional fractures and the third dimension of fracture management. South Med J. 1980;73:884–91.
8. Borden 4th S. Roentgen recognition of acute plastic bowing of the forearm in children. Am J Roentgenol Radium Ther Nucl Med. 1975;125:524–30.
9. Wilkins KE. The incidence of fractures in children. In: Rockwood CA, Wilkins KE, Beaty JH, editors. Fractures in children. 4th ed. Philadelphi/New York: Lippincott-Raven; 1996. p. 3–15.
10. Ogden JA. Injury to the growth mechanisms of the immature skeleton. Skeletal Radiol. 1981;6:237–53.
11. Kim WC. Biomechanical properties of growth plate. J Jpn Paed Orthop Ass. 1996;6(128–132):1996.
12. Milz S, Boszczyk A, Putz R. Development and functional structure of the epiphyseal plate. Orthopade. 2002;31:835–40.
13. Fishkin Z, Armstrong DG, Shah H, Patra A, Mihalko WM. Proximal femoral physis shear in slipped capital femoral epiphysis-a finite element study. J Pediatr Orthop. 2006;26:291–4.
14. Bright RW, Virginia R, Burstein AH. Epiphyseal-plate cartilage. J BoneJoint Surg. 1974;56A:688–703.
15. Amamilo SC, Bader DL, Houghton GR. The periosteum in growth plate failure. Clin Orthop. 1985;194:293–305.
16. Saito S, et al. Experimentelle Untersuchungen ueber Entstehung der Antetorsion am Femur. Z Orthop. 1980;118:612.
17. Husby OS. Spontaneous correction of femoral torsion. Acta Orthop Scand. 1987;58:113–6.
18. Oberhammer J. Degree and frequency of rotational deformities after infant femoral fractures and their spontaneous correction. Arch Orthop Traum Surg. 1980;97:249–55.
19. Dobbs MB, Luhmann SL, Gordon JE, Strecker WB, Schoenecker PL. Severely displaced proximal humeral epiphyseal fractures. J Pediatr Orthop. 2003;23:208–15.
20. Shiohara K, Saito S, Kusaba A Experimentalle Untersuchungen über die Entstellung der Antetorsion am Femur. In: Herausgegeben von Kirschner P, Stürmer K.M, Hefte Zu, editors. "Der Unfallchirurg". Springer-Verlag GMBH & Co. KG; 2001.
21. Wakita M. Fundamental and clinical studies of the projection method of the femur. Showa Univ J Med Sci. 1996;56:140–52.
22. Treharne RW. Review of Wolff's law and its proposed mean of operations. Orthop Rev. 1981;10:35.
23. Abraham E. Remodeling potential of long bones following angular osteotomies. J Pediatr Orthop. 1989;9:37–43.
24. Karaharju EO, Ryoppy SA, Makinen RJ. Remodelling by asymmetrical epiphysial growth. An experimental study in dogs. J Bone Joint Surg. 1976;58B:122–6.
25. Davids JR, Maguire MF, Mubarak SJ, Wenger DR. Lateral condylar fracture of the humerus following posttraumatic cubitus varus. J Pediatr Orthop. 1994;14:466–70.
26. Saito S, et al. Changes in the alignment of the lower extremities in children – a study of the cases with fractures of the femur and congenital dislocation of the hip. J Jpn Paed Orthop Ass. 1993;3:148–56.
27. Saito S, Kurisaki K, Omata T. A study of fractures among children less than 5 years. Showa Univ J Med Sci. 1997;9:11–5.
28. Glorion C, Pouliquen JC, Langlais J, Ceolin JL, Kassis B. Femoral lengthening by callotasis. A study of a series of 79 cases in children and adolescents (Alongement de femur par callotasis. Etude d'une serie de 79 cas chez l'enfant et l'adolescent). Rev Chir Orthop Reparatrice Appar Mot. 1975;81:147–56.

Experimental *In Vitro* Methods for Research of Mechanotransduction in Human Osteoblasts

26

Nahum Rosenberg and Michael Soudry

Bone matrix is generated and organized according to the direction of mechanical force, e.g., following muscular contraction, impact with supporting surface and gravity. Cellular mechanotransduction from outer milieu, which is a biochemical expression of the external mechanical force via cellular pathways, determines the three dimensional structure of bone following interactions between its generation and resorption, i.e., remodeling and repair process by interaction between osteoblast and osteoclast activities. Of the latter two type of cells the osteoblast governs this complex process, partially following the external mechanical effect. Therefore understanding and recognizing of the nature of the cellular pathways in osteoblast mechnotransduction might reveal new therapeutic methods in numerous disabling bone pathologies due to the loss of bone mass or the loss of its structural integrity [1, 2].

N. Rosenberg, MD • M. Soudry, MD (✉)
Department of Orthopedic Surgery,
Rambam Health Care Campus & The Rappaport Faculty of Medicine, Technion–Israel Institute of Technology, Haifa, Israel

Experimental Methods

The experimental methods for studying the mechanotransduction in osteoblasts in two dimensional culture in vitro are based on controlled propagation of external force upon the culture plate via induced intra- and extracellular fluid flow in cells which are adherent to plastic surface of the culture plate. The ability of osteoblast to adhere to plastic surfaces (Fig. 26.1), which is also common in other cells of mesenchumal origin, is indespensible characteristic that enables to induce cellular deformation with subsequential activation of the cytoskeleton indirectly by controlling the fluid flow by external mechanical means [3, 4]. Accordingly many of the experimental methods which are related to mechanotransduction in osteoblasts utilize two dimensional cultures with cells adherent to plastic surfaces and exposed to external mechanical force. This type of experimental model is easily reproducible and relatively easy for maintenance (Fig. 26.2).

Osteoblasts in the two dimensional cultures adhere to the plastic surface of the culture container by protein extracellular extensions of the cytoskeleton. These extensions through the cell membrane are proteins from the groups of cadhedrins, integrins and selectines. The magnitude of anchorage energy that they generate with the plastic surface is in the scale of 10^{-16} J, which is two orders higher than the total cellular membrane

D.G. Poitout (ed.), *Biomechanics and Biomaterials in Orthopedics*,
DOI 10.1007/978-1-84882-664-9_26

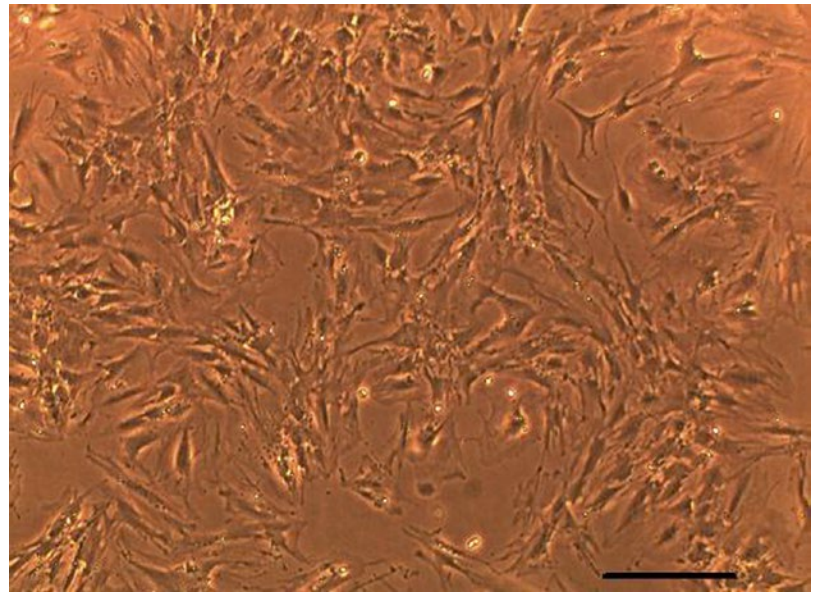

Fig. 26.1 Micrograph of human osteoblast-like cells in monolyer explant culture. The cells are adherent to a plastic surface (scale – 20 μ)

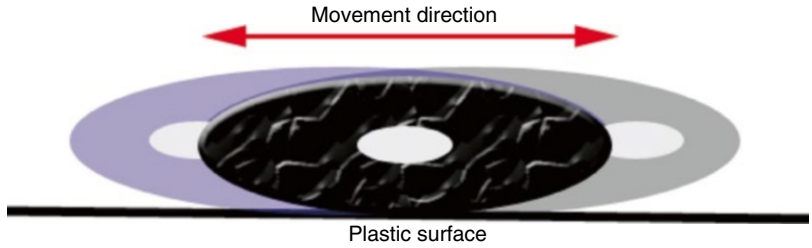

Fig. 26.2 A schematic representation of a cell adherent to a plastic surface and deformed in two dimensional plane due to interaction between stretchable cellular membrane and its cytoskeletal anchorage with externally induced fluid flow, extracellular and intracellular. The resting cell is presented in the central position. The *arrow* shows the direction of the surface alternating movement

bending energy of 10^{-18} J [5]. Therefore a significant deformation of the whole cell can occur without disrupting the cellular membrane integrity and without disconnecting of the cellular adhesion to the container surface. This difference in the strength of anchorage and of the membrane integrity allows a safe 4–5 % strain application to a pure vesicle bound by a lipid bilayer membrane when it is adherent to a surface [5]. Since the mechanical structure of osteoblast is reinforced by a cytoskeleton, much higher mechanical deformation is possible without its disconnection from the surface and without distraction of the cellular membrane.

Accordingly in most of the methods of evaluation of mechanotransduction in adherent osteoblast in two dimensional culture, a similar concept of mechanical movements of the surface and/or of the culture media over the adherent cells are utilized. By these methods a deformation of the cellular membrane on its free, not adherent, edge is generated following flow of the surrounding media and cyclic movement of the adherent to the surface cellular part (Fig. 26.2).

Although the basic principle of mechanical stimulation of osteoblasts in monolayer culture is similar in different studies there is a high range of mechanical parameters that was applied by the different authors, e.g., cellular displacement between 0.0003 and 0.025 mm (estimated from strains applied to cells and assuming that the

diameters of the osteoblasts are in the range of 20–40 μm), acceleration of mechanical force in the range of 0.0009–500 mm/s^2, if a close to the sine shaped alternating force was used at frequencies between 0.05 and 20 Hz [6–10]. Currently there is no uniform experimental setup for mechanotransduction studies of the cells in a monolayer culture and therefore a comparison between different studies is sometimes difficult or even impossible.

The most popular research model for the *in vitro* study of mechanotransduction in osteoblasts utilizes a controlled cyclic stretching of an artificial silicon membrane, when the cells are adherent to its surface [11]. The membrane is stretched radially or bended with subsequent change in its surface. This process generates a mechanical strain on the adherent cells. This method does not allow generating uniform stretching forces on all the adherent cells because the strain magnitude changes radially when the highest strain is generated on the bending axis or on the periphery of two dimensional stretchable membrane, while on the center of the membrane the strain is almost negligible. By using this experimental setup strains of cells up to 20 % can be generated [11, 12]. The generated strains on cells are also dependent on the material properties of the membrane surface or on the geometrics of the bending curvature.

Additional widely used experimental method for mechanotransuction research is by exposure of a monolayer of cultured osteblasts, which are adherent to a plastic surface, to a controlled flow of culture media. By this method an alternating or continuous cell deformation can be achieved by controlled inflow of media from an external pump into the culture container in a closed circuit [13]. The flow can be continuous, pulsatile or oscillatory.

In the two methods described above, i.e., stretchable surfaces and fluid flow application, there is a limitation in providing controlled oscillating strain in frequencies up to 5 Hz. Therefore in most studies the range of alternating mechanical stimulation is 0.1–2 Hz [12, 14–16]. The basic design of these devices does not allow investigating mechanical frequencies that exceed 10 Hz, therefore mechanical stimulation of osteoblasts in the infrasonic range of frequencies is impossible if these types of mechanical sources for inducing cellular strain are used. The reasoning to investigate the low frequency stimulation in experiments on mechanotransduction in cultured osteoblasts is related to the human body locomotion, which is usually in the range of 0.5–1.5 Hz of frequencies. This basic assumption can be challenged by the fact that the osteocytes, which are embedded in the canaliculi in the bone matrix, are exposed also to the higher frequencies of mechanical stimulation, up to 60 Hz, by normally stretching of muscles, even at rest, as can be detected by a normal vibromyogram [17, 18]. Therefore this higher range of frequencies might affect different mechanotransduction pathways but cannot be investigated by the previously described experimental methods due to the limitation of their design, as described above.

In order to overcome these basic design limitations another more versatile experimental setup for activation of osteoblasts in monolayer culture was developed. This method allows the use of higher range of mechanical stimulation frequencies without interfering with cells adherence to a culture surface, i.e., up to frequency of 60 Hz [6]. The method utilizes application of external controlled and tunable mechanical vibration directly to the supportive surface with adherent cultures of osteoblasts and the vibration movement of the surface causes deformation of the adherent cells. The vibration force is uniformly transferred to all cultured cells, regardless to their topographic position on the culture surface. Subsequentially the intracellular mechanotransduction pathways should respond via the excitation of cytoskeletal components following cell deformation induced by the interaction of external fluid flow and external surface movement [13]. This experimental approach overcomes the problem of the non-uniform strains provided by the use of elastic membranes and reduces the number of mechanical parameters since the applied vibration movement is uniaxial. Therefore a similar, in magnitude and direction, deformation force is applied to a large number of cultured cells. The generic design of this method utilized a horizontal surface with mounted and firmly fixed plastic

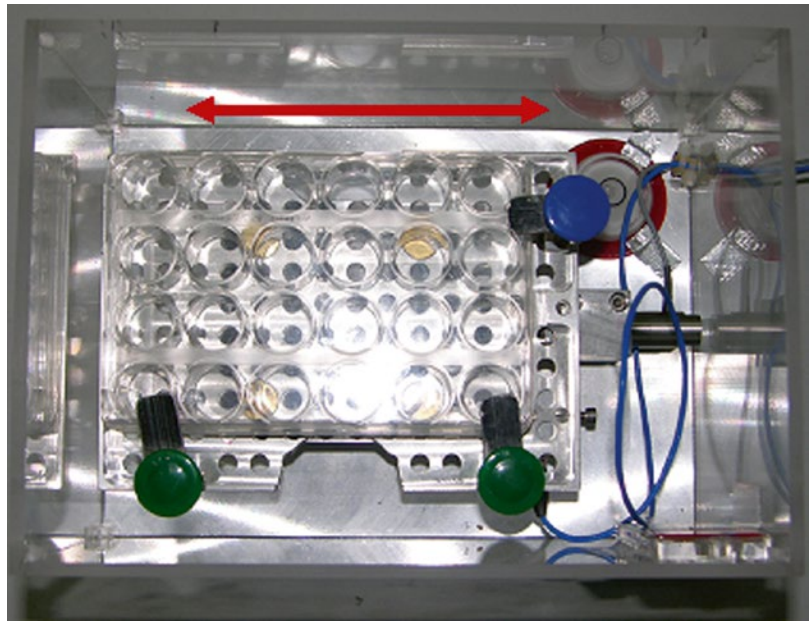

Fig. 26.3
Experimental setup for vibration of cultured osteoblasts. A 24-well plate with cultured cells is mounted on a horizontally oriented shaker – view from above. The horizontal vibrating movement of the shaker is controlled (direction of the movement is indicated by the *double arrow*). The acceleration and displacement are measured by a piezoelectric accelerometer

culture container with adherent cells. The plastic surface vibrates in the horizontal plane by a mechanical actuator. The vibration movement is tunable in the range of frequencies between 0 and 60 Hz. The surface acceleration, frequency and displacement are measured by a piezoelectric accelerometer (Fig. 26.3).

By this method not only the delivered mechanical parameters are recordable but rather the actual data of the supporting surface movement, which reflects the actual movement of cells, can be measured.

The existing difference between the "delivered" by different types of inducible movements and the "actual" movement of cells in the presented above methods is due to the "fatigue" factor of the stretchable surface [11] or due to the to the friction between the moving parts of the supporting platform in the vibration model. But in the vibration model only the "actual" cellular movement parameters can be recorded and a more precise data on cellular strains can be calculated according to these measurements.

If the friction between the moving parts is reduced in the vibration model the difference between the "excitation" and the "actual" mechanical parameters can be reduced to the minimum (Fig. 26.4).

It is very important to emphasize that the differences in the experimental setups in the research in cellular mechanotransduction cause undesirable uncertainties in comparing the results from different experiments. In order to compare data from different studies, the mechanical stimulation parameters should be uniformly characterized, e.g., the resultant displacement, frequency, acceleration, wave shape of the applied force and resultant cellular strain. In the most of the studies this comprehensive data is not provided or provided only partially with difficulty to compare to other studies. Therefore more efforts should be directed upon research protocols' standardization, regardless to the experimental method used. This effort might provide all the essential biomechanical data, such as exact profile of the resultant mechanical force applied to the cells. Having this information available, the optimal parameters of the mechanical stimulation of osteoblasts in monolayer culture can be determined and the cellular mechanotransduction pathways will be detected at the optimum of their activity.

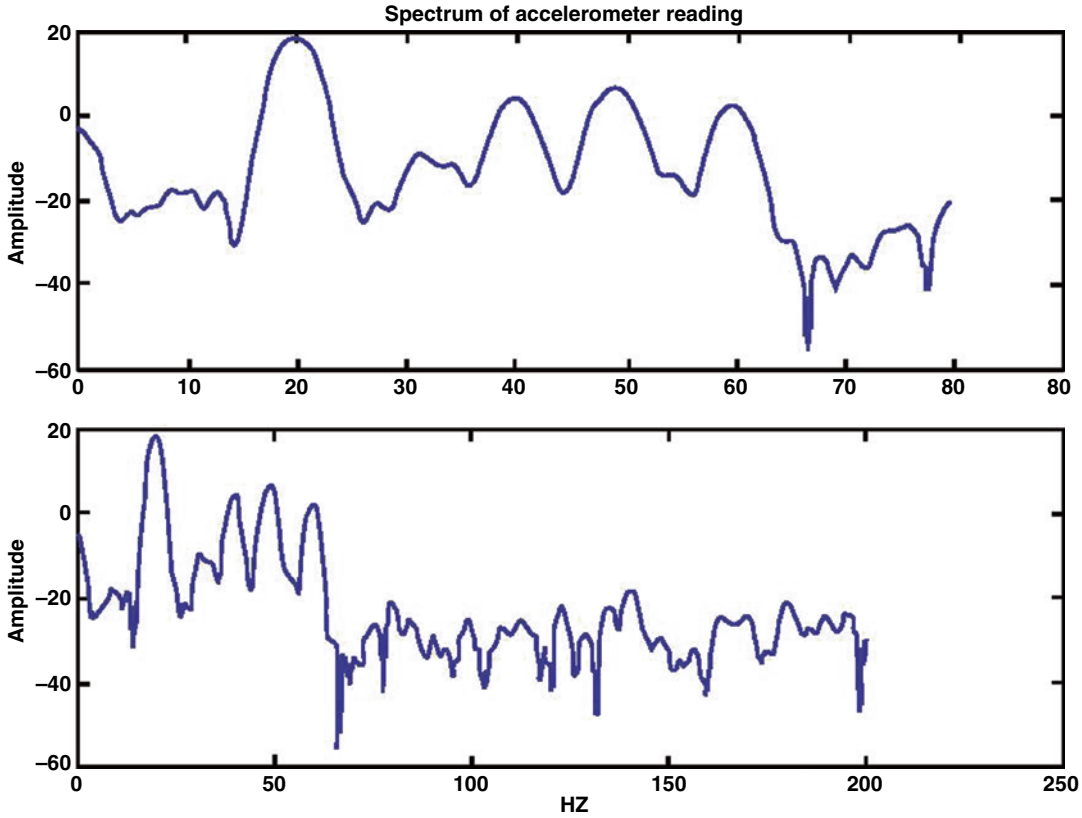

Fig. 26.4 An example of a spectrum of frequencies of the resultant vibration movements of culture plate (*lower profile*) following the excitation of 20 Hz (*upper profile*) showing that the high proportion of the generated vibration with frequency of 20 Hz is actually delivered to the vibrating surface and the adherent to it cells. Therefore most of the excitation parameters were expressed in the resultant vibration movement

Conclusion

We gave an overview of the existing generic concepts that are used in the research of mechanical stimulation of cultured osteoblasts. It is apparent that the optimal method for a particular experiment, which should be designed according to the research hypothesis, can be chosen according to the principles that we described above.

References

1. Rubin CT, Hausman MR. The cellular basis of Wolff's law. Transduction of physical stimuli to skeletal adaptation. Rheum Dis Clin North Am. 1988;14(3): 503–17.
2. Rosenberg N, Rosenberg O, Soudry M. Osteoblasts in bone physiology – mini review. Rambam Maimonides Med J. 2012;3:1–7.
3. Burger EH, Klein-Nulend J. Microgravity and bone cell mechanosensitivity. Bone. 1998;22:127S–30.
4. Rosenberg N. The role of the cytoskeleton in mechanotransduction in human osteoblast-like cells. Hum Exp Toxicol. 2003;22:271–4.
5. Boal D. Chapter 8. Intermembrane forces. In: Boal D editor. Mechanics of cell. Cambridge: Cambridge University Press; 2002. p. 274–79.
6. Rosenberg N, Levy M, Francis M. Experimental model for stimulation of cultured human osteoblast-like cells by high frequency vibration. Cytotechnology. 2002;39(3):125–30.
7. Buckley MJ, Banes AJ, Levin LG, Sumpio BE, Sato M, Jordan R, Gilbert J, Link GW, Tran Son Tay R. Osteoblasts increase their rate of division and align in response to cyclic, mechanical tension in vitro. Bone Miner. 1988;4:225–36.

8. Neidlinger-Wilke C, Wilke HJ, Claes L. Cyclic stretching of human osteoblasts affects proliferation and metabolism: a new experimental method and its application. J Orthop Res. 1994;12:70–8.
9. Jones DB, Nolte H, Scholubbers JG, Turner E, Veltel D. Biochemical signal transduction of mechanical strain in osteoblast-like cells. Biomaterials. 1991;12: 101–10.
10. Stanford CM, Morcuende JA, Brand RA. Proliferative and phenotypic responses of bone-like cells to mechanical deformation. J Orth Res. 1995;13:664–70.
11. Banes AJ, Link GW, Gilbert JW, Tran Son Tay R, Monbureau O. Culturing cells in a mechanically active environment. Am Biotechnol Lab. 1990;8:12–22.
12. Colombo A, Cahill PA, Lally C. An analysis of the strain field in biaxial Flexcell membranes for different waveforms and frequencies. Proc Inst Mech Eng H. 2008;222:1235–45.
13. Pitsillides AA, Das-Gupta V, Simon D, Rawlinson SCF. In: Helfrich MH, Ralston SH, editors. Methods for analyzing bone cell responses to mechanical loading using in vitro monolayer and organ culture models. Bone research protocols. Totowa: Humana Press; 2003. p. 399–422.
14. Donanhue SW, Jacobs CR, Donanhue HJ. Flow-induced calcium oscillations in rat osteoblasts are age, loading frequency, and shear stress dependent. Am J Physiol. 2001;281:C1635–41.
15. Jacobs CR, Yellowley CE, Davis BR, Zhou Z, Cimbala JM, Donanhue HJ. Differential effect of steady versus oscillating flow on bone cells. J Biomech. 1998;31:969–76.
16. Partap S, Plunkett NA, O'Brien FJ. Bioreactors. In: Eberli D, editor. Tissue engineering. Tech – Open Access Publisher, Rijeka, Crotia. 2010. p. 323–33.
17. Rubin C, Li C, Sun Y, Fritton C, McLeod K. Non-invasive stimulation of trabecular bone formation via low magnitude, high frequency strain. Trans ORS. 1995;20:548.
18. Nigg BM. Acceleration. In: Nigg BM, Herzog W, editors. Biomechanics of the musculo-skeletal system. Secondth ed. Chichester: Wiley; 1998. p. 300–1.

Part V

Applications of Biomechanical Principles to Orthopedics and Traumatology

Computer-Assisted Designed Hip Arthroplasty

27

Xavier Flecher, Sebastien Parratte,
Jean-Manuel Aubaniac, and Jean-Noël Argenson

Restoration of hip biomechanic during the arthroplasty is one of the prerequites to a full function recovery and a good longevity. The general use of computer technology in the operating room to assist the surgeon during the surgery underlines our strong believe of a global concept which starts at the time of the stem conception, or at the time of computerized preoperative planning in case of individual stem solution. The purpose of this chapter is to describe the elements which will lead to the use of computer assisted hip arthroplasty according to the 20 years experience obtained in computer assisted preoperative planning of total hip arthroplasty and computer assisted designed of custom hip stem.

X. Flecher, MD (✉) • S. Parratte, MD
J.-M. Aubaniac, MD • J.-N. Argenson, MD
Department of Orthopaedic surgery,
Institute for Motion and Locomotion,
Mediterannea University, Hôpital Sainte Marguerite,
Marseille, France
e-mail: Xavier.FLECHER@ap-hm.fr

The Concept of Computer Assisted Hip Arthroplasty

The concept of individual computer assisted design (CAD) has been the consequence of the natural evolution of the authors in the field of total hip arthroplasty (THA), facing the unacceptable failure rate of conventional stems as reported in the literature for young and active patients [1–10].

The cementless fixation presented as an alternative to cement fixation has gained a global acceptance on the acetabular side but is still facing some controversies on the femoral side partly due to the poor designs proposed in the early days [9, 11]. Quickly basic studies showed that successful fixation without the use of cement on the femoral side may be possible but requires some principles which include proximal adaptation and avoidance of micromovements in order to obtain an optimal load transmission to the femur [12]. These principles are advocated in order to avoid stress shielding and thigh pain, the two complications often reported with cementless stems [13, 14]. This adaptation to the proximal femur is only possible when the stem can match the patient femoral anatomy. Several anatomical studies have shown the wide range of proximal femoral anatomy faced in either conventional osteoarthritis or more frequently in congenital or traumatic etiology leading to a narrow,

D.G. Poitout (ed.), *Biomechanics and Biomaterials in Orthopedics*,
DOI 10.1007/978-1-84882-664-9_27

curved and excessively ante or retroverted upperfemur [15–17].

The logic answer to the necessary adaptation to the proximal intramedullary femur combined to the obligatory corrections in the prosthetic neck for solving extramedullary deformities was CAD of individual stem geometry. In the authors perception the three-dimensional design of the neck is at least of equal importance than the intramedullary part in order to restore a correct hip function.

The design of a three-dimensional custom neck allows correction in length, lever arm and anteversion. The clinical consequence of such design is the restoration of leg length, abductor function and proper lower limb rotation. Among all factors involved in acetabular cup or stem positioning, femoral lateralization (femoral offset) is well known to influence the results of total hip arthroplasty [18, 19]. It represents the femoral lateralization and has been defined by the distance from the center of the femoral head and the femoral diaphysis axis [20]. Adequate femoral lateralization has been shown to enhance hip stability [21], improve the range of motion and abductor strength [22] as well as decrease contact force and thus polyethylene wear [23]. The amount of offset of the femoral prosthesis theoretically influences the mechanics of the hip after a total hip arthroplasty. An increased offset increases the moment arm of the abductor muscles. This reduces the abductor force required for normal gait and consequently reduces the force across the hip. Of course, this is a simplified interpretation of gait because other muscles about the hip in addition to the abductors are active during walking. Recent clinical studies demonstrated that an increase of femoral offset could significantly decrease wear [22–24], while this increase could also be a cause for early aseptic loosening of the femoral stem by increasing the bending moment [25, 26]. It is though unclear how the surgeon should decide of the proper postoperative femoral offset value in THA, from a strict preoperative reproduction to an 'ideal' value, based on clinical or biomechanical considerations.

The appropriate anteversion of the neck may also contribute to reduce dislocation rate. The mechanical consequence of such neck design is also to optimize load transmission to bone stem interface and finite element analysis have shown the influence of the extramedullary parameters on the stem stability and stress transfer [26].

The intramedullary stem design is a combination of CT-based reconstruction of the proximal femoral anatomy and priority areas of contact to obtain stability in rotation. The distal diameter of the stem is reduced to avoid any cortical impingement distally, possible source of thigh pain with maximal canal filling stems. It is thus of high importance to preserve all the cancellous bone around the whole stem from proximal to distal by the use of a smooth compactor of identical shape than the final prostheses.

This concept of computer assisted hip arthroplasty leading to individual custom neck and stem design was addressed by Aubaniac and Essinger in 1987 and lead to the development of softwares for cancellous bone density evaluation and three-dimensional custom neck design, which is the rationale of the Symbios® custom concept (Symbios Inc, Yverdon, Switzerland). The global concept of computerized preoperative planning and the first applications for osteoarthritis following high congenital dislocation of the hip have been originally published close to 20 years ago [27–29].

The Computer Assisted Planning of Total Hip Arthroplasty

Preoperative Data

X-Ray Data

The radiographic analysis is based on several x-ray views. A full view of the two limbs using scanography is needed to assess the global pelvis and limb anatomical status, and to evaluate the extent of disturbance of the pelvic balance by assessing bilaterally the position of the hip rotation centers (in the vertical axis). A *frontal pelvis view* is used to determine the extent of

lever arms between the rotation centers and the corresponding femoral axes. Discrepancies are recorded and will be used later in the pre-operative planning to correct the anatomy of the diseased joint such that full restoration of the pelvic balance can be achieved. Eventually, *frontal and lateral x-ray views* of the diseased joint are necessary to complete the x-ray data set.

CT Data

Data obtained from computerized tomography scanner are necessary both for the design of the intramedullary femoral stem and for the planning of the extramedullary part of the joint reconstruction. Except in special cases, the CT data acquisition must follow an established protocol elaborated by Symbios. However, in special cases such as for instance very severe congenital dislocations, the radiologist may have to select a modified protocol based on the x-ray status.

The intramedullary femoral anatomy is assessed by CT views taken every 5 mm from the acetabular summit down to the bottom of the lesser trochanter, then every 10 mm until the femoral isthmus.

The extramedullary planning requires CT views taken at three different levels: *(1)* at the base of the femoral neck (assessment of helitorsion axis), *(2)* at the knee level, across the femoral condyles (assessment of posterior bicondylar axis), *(3)* at the foot level, by the second metatarsus axis (assessment of foot axis).

Pre-operative Planning

Acetabular Cup

If the contralateral hip is healthy, planning the rotation center of the replaced joint and the socket size is performed by reproducing the contralateral geometry on the x-ray frontal pelvis view. In presence of a bilateral lesion and in most high dislocation cases, the position of the rotation center and the size of the acetabular socket are decided together with the surgeon. In certain cases, the size is determined using the CT view

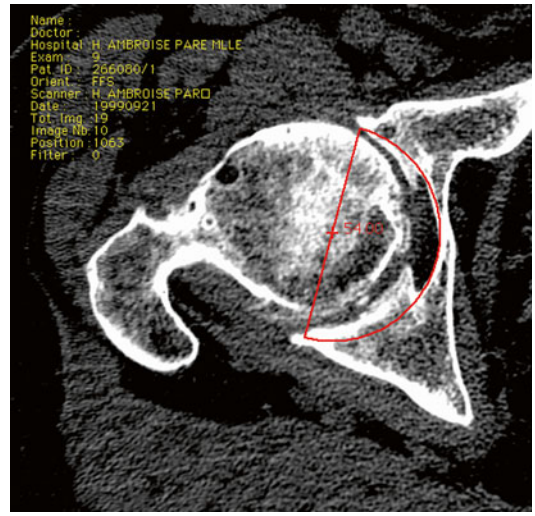

Fig. 27.1 Planning of the acetabular socket using CT image

passing through the center of the true acetabulum (which allows furthermore assessment of bone stock) (Fig. 27.1), then by reporting the result on the x-ray pelvic view.

According Position of the Femur

The future position of the femur (as determined for instance by the location of the greater trochanter) is determined on the frontal view based on the position of the acetabular socket, on the desired lengthening as determined from the scanogram, and on the neck lever arm (femoral offset). This position will determine the level of the femoral cut and assess the correct neck lever arm on the frontal view. However, osteotomy of the greater trochanter may be necessary in cases where extensive lengthening is required, associated to a wrong anteroposterior position of the greater trochanter due to excessive anteversion.

The anteversion angle of the prosthesis neck must be set such that normal gait anatomy can be restored. The normal gait anatomy requires three conditions: *(1)* foot axis showing 10–20° of external rotation, *(2)* posterior bicondylar axis perpendicular to the gait direction, *(3)* anteversion of the femoral neck between 15 and 20° with respect to the bicondylar axis. It has been shown that in most cases of congenital dysmorphism,

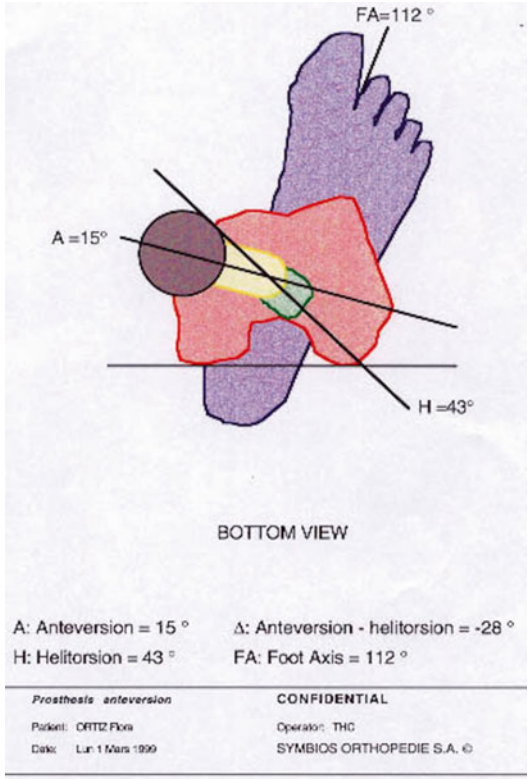

Fig. 27.2 Restoration of normal gait anatomy based on the correction of the helitorsion angle (*H*); *AV* desired prosthetic neck anteversion, *BPA* bicondylar posterior axis, *alpha* correction made in the prosthetic neck between H and AV

the upper femur axis, also called helitorsion axis and defined as the axis passing across the longer diameter at the level of osteotomy, is not aligned with the neck axis [30]. This phenomenon is usually not taken into account in standard prostheses. This results in such cases most frequently in an over- or under-correction of the prosthetic anteversion angle, thus preventing from full restoration of the normal gait. By superimposing the three CT views of the osteotomy level (usually above the lesser trochanter), and of the knee and foot levels, it is possible to calculate the correction angle to add (or subtract) to the helitorsion angle such that a final prosthetic anteversion angle of 15–20° is achieved (Fig. 27.2).

The Computer Assisted Design of Custom Hip Stem

The Design of the Intramedullary Section

Contouring

Upon their reception, raw CT data is processed by numerical thresholding such that non bony structures are excluded from the images. Following this "image filtering" step, the design engineer runs an image analysis program to select both the internal and external contours of the bone section on each femoral CT slice. This *contouring* process is normally performed fully automatically, except in the area of the femoral neck and in cases of important artefacts on CT images for which manual intervention is needed.

Matching CT and X-Ray Data

Anatomical landmarks on the diseased joint must be first registered. These landmarks will be used later for the definition of the osteotomy. The summits of the greater and lesser trochanters and the femoral head summit are localized and indicated on the x-ray frontal view.

The next step in the design process consists in superimposing the CT and x-ray data on the same image file. For this, frontal and lateral radiographic views of the diseased hip are first digitalized using an x-ray compatible image scanner. The contouring data obtained during the previous step is numerically added to the digitalized x-ray views. A manual fitting of the two types of images is then performed independently on the frontal and lateral view.

Definition of Osteotomy Orientation

Once merging of CT and x-ray data is completed, osteotomy directions are calculated and added to the image file. The level of the osteotomy is defined such that neck length, optimized stability in rotation and optimized bone stock preservation are taken into account.

Generation of the Initial Stem and Extraction

Based on the internal contouring data, the design software uses then numerical interpolation procedures to generate a first stem shape limited to the intramedullary zone. However, the very precise reproduction of the femoral internal contour on this first draft makes it most often useless without modifications, as local protrusions and depressions at the bone surface would prevent any movement of the stem within the femur. It is therefore necessary to simulate numerically the extraction of the stem from the femur. This is done by successive iteration steps during which the stem is extracted incrementally by rotations and translations in the three main orthogonal axes. During each iterative step, incremental stem shape modifications are performed by the software in order to allow the extraction while maintaining the contact zones necessary for an optimized mechanical support of the stem in the femur. Optimized support is sought in medial, lateral, and anterior metaphyseal areas. At the end of the simulation, a new, modified version of the stem is obtained that can be implanted into the femur with a very restricted degree of freedom for the insertion path.

Final Adaptations

At the end of the extraction process, numerical integration of the new stem shape in the CT data is performed. It enables the design engineer to view each CT section together with the corresponding stem section ("composite" view, Fig. 27.3). By switching to the editor mode of the software, the engineer can also perform a final design "tune up", during which he can still implement slight modifications on each stem section to further optimize bone-prosthesis adjustment.

Stem Insertion and Resistance Simulation

The final step in the design of the intramedullary part of the femoral stem consists in simulating a subsidence of the stem in the femoral canal in order to be sure that the stem is at worst in contact with the cortical bone in this shifted position.

A numerical 3-point bending simulation test is then performed to validate the mechanical resistance of the stem.

The Design of the Extramedullary Section

The design of the extramedullary part of the stem is performed as well in the frontal and lateral as in the sagittal plane. The determination of the anteversion angle of the prosthesis neck taking into account the correction for helitorsion, has already been explained earlier. With the intramedullary stem integrated in the x-ray frontal view, the design engineer calculates the optimized combination of CCD angle, neck length and head offset such that the planned rotation center and lever arm are respected (Fig. 27.4).

The Prosthesis Validation

The pre-operative planning of a custom made prosthesis is performed together by the surgeon and the design engineer at Symbios. Following the planning, the design of the stem is done entirely by the design engineer. Therefore the final design must be validated by the surgeon before the fabrication of the prosthesis can be launched. A complete patient file is provided to the surgeon including the CT composite view, the normal gait restoration scheme, and the x-ray frontal (with osteotomy parameters, Fig. 27.5) and lateral view with the designed stem.

The Stem Manufacturing

Stem Machining

Upon validation of the stem design and pre-operative planning by the surgeon, the fabrication

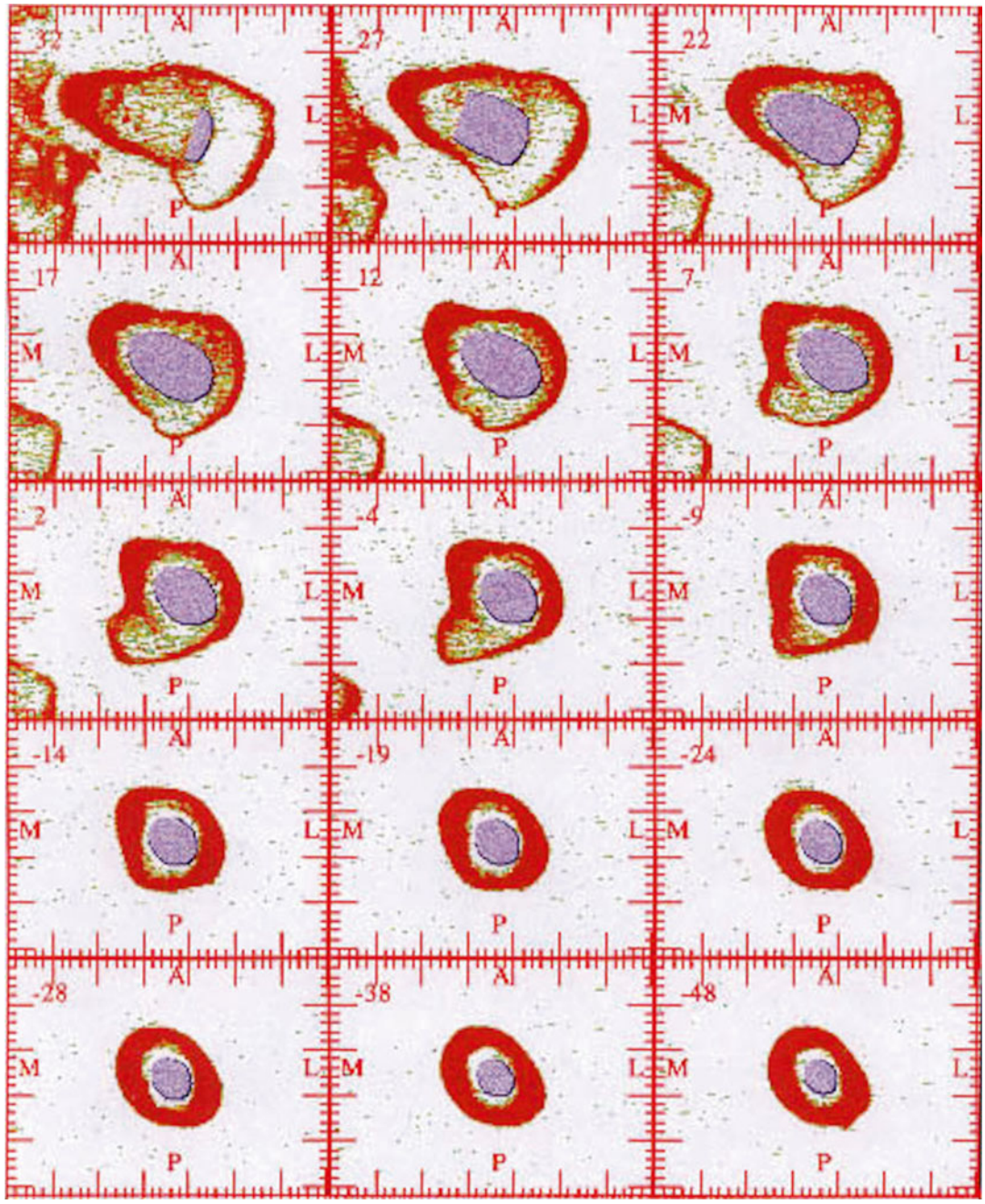

Fig. 27.3 Composite CT views with integration of stem sections

of the prosthesis can proceed. For this, the stem CAD data is transferred into a Computer Assisted Machining (CAM) software that pilots a 5-axis milling machine. In parallel, a compactor with a smooth surface is machined with the same design as the stem itself. It is used for compaction of the cancellous bone before the stem itself is introduced (Fig. 27.6).

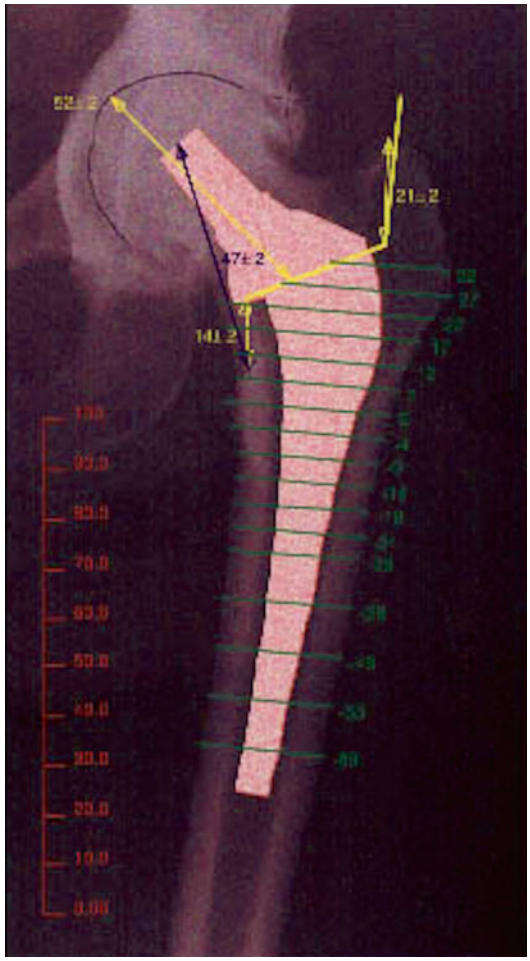

Fig. 27.4 Composite x-ray frontal view with integration of intra- and extramedullary stem sections

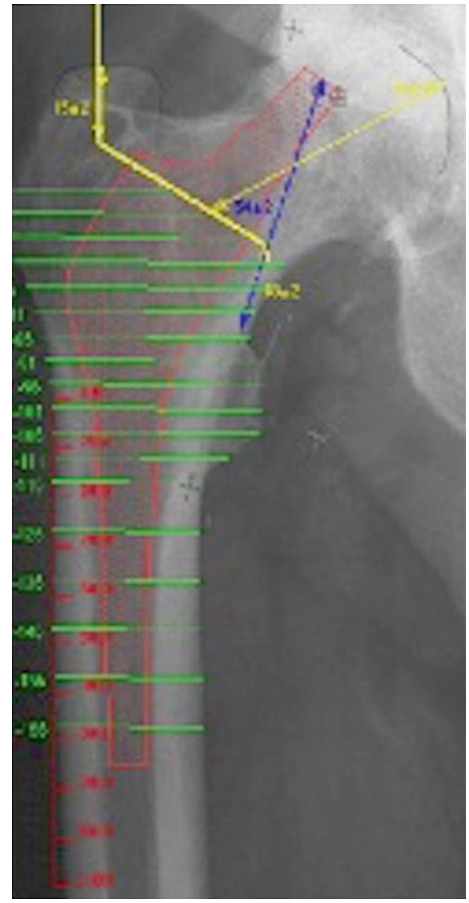

Fig. 27.5 The x-ray frontal view with osteotomy parameters

Materials and Coatings

Wrought Ti6Al4V titanium alloy is used most of the time for the fabrication of the stem. In very few cases, stainless steel stems are produced upon request of the surgeon. The rasp itself is made out of wrought stainless steel. After machining, the prosthesis stem undergoes a surface plasma spray coating procedure which can vary from one stem to the other, depending again on the surgeon's request. In most cases a first layer of ~300 μm of porous titanium followed by a ~80 μm layer of porous hydroyapatite (HA) are coated on the intramedullary section of the stem, from the osteotomy level down to the distal level at which the transition from an elliptic to a circular section takes place.

Sterilization and Packaging

The final steps in the production of the prosthesis are the gamma sterilization and the final packaging procedure which is performed in clean room conditions.

The Twenty-Years Clinical Use of Individual Cad for Cementless Hip Arthroplasty

The Rationale for the Use of Custom CAD for Hip Arthroplasty

The self-preservation of the dense cancellous bone compacted towards the inner cortical femur is obtained by the use of a smooth compactor of

Fig. 27.6 Example of porous coated custom made prosthesis together with the corresponding "rasp" for compaction of cancellous bone and implant preparation

identical intra and extramedullary shape than the final prostheses. The preservation of this cancellous bone is mandatory for secondary biologic fixation to the hydroxyapatite (HA) covering the final prosthesis. Both the clinical and the radiological evaluation of different stem coatings lead us to move from a proximal HA to a full HA coating [31].

The solution provided by three-dimensional designed custom neck to face excessevely anteverted upper femur often encountered in dysmorphic or dysplasic hips was a retroversion of the custom neck to restore an appropriate anteversion of 15–20° on the knee condylar plane [32, 33]. In such situations some authors have described the association of a derotational osteotomy to a conventional stem or the use of modular necks [13].

We studied by X-rays and CT the morphology of 83 hips from 69 European adults with osteoarthritis following developmental dysplasia of the hip (DDH) [17]. A cohort of 310 primary osteoarthritic hips was used as a control group. According to the classification [34] of dysplastic hips were graded as class I, 27 as class II and 23 as class III or IV. The intramedullary femoral canal had reduced mediolateral and anteroposterior dimensions for all groups compared to primary osteoarthritis control group. The individual variability was important when measuring the CT-scan canal flare index, despite the subluxation class considered. The femoral neck shaft angle was increased only for femora of class II. The proximal femur had more anteversion in all the DDH groups, ranging from 2 to 80°. The mean anteroposterior diameter of the true acetabulum for classes III/IV was smaller compared to primary osteoarthritis. The severity of the dysplasia may influence the difficulty of achieving hip center location in the true acetabulum but does not correlate with the degree of individual femoral anteversion.

This study provides additional information to one already available for the Japanese population and may be of value for femoral hip stem design and for planning total hip arthroplasty in hip dysplasia.

The Authors' Indications for Custom CAD in Cementless Hip Arthroplasty

- The dysmorphic and dysplasic hips in which conditions of normal hip anatomy cannot be restored by a standard neck and a standard stem
- The young and active patients for whom full and quick recovery of hip function is required. In the future the increasing lifetime expectancy will emphazise this need of long standing solution for highly sollicited hips [35].

The Clinical Results of Computer Assisted Designed Stems in THA

We reported several publications in the population of dysmorphic hips [36] or young patients [37, 38]. The study [36] relates the results of 257 custom uncemented stem for osteoarthritis due to

developmental dysplasia of the hip at 2–12 years follow up study. The average age was 55 years. There were 174 dysplasias and 83 luxations (39 % stage 1, 30 % stage 2, 14 % stage 3, 17 % of stage 4). Average lengthening to realize was of 39 mm. The average anteversion angle was 28 ± 16° and the average anteroposterior diameter of the acetabulum of 51 mm. The clinical score of Harris reached from 58 to 93 points. We found a good stem integration in 88 % of the cases, an osteolysis in 5 % and 1 case of depression of the stem. Six hips required a change: three sepsis, one dislocation and two for no stem integration. The survival rate was 97 % at 11 years.

We thus perfomed a retrospective study including 116 custom THA for congenital dislocation of the hip (96 women and 20 men) at a mean follow up of 6.6 years (3–12 years) [39]. Two patients were died of causes unrelated to the total hip arthroplasty, before a minimum duration of follow-up of 5 years and 17 were lost to follow-up. The study consist then in 79 patients (97 hips). The mean age was 51 (17–82 years). According to the Crowe classification, there were 35 class 1, 29 class 2, 13 class 3 and 20 class 4. The average lengthening to be realized was 25 mm (5–58 mm). The helitorsion angle was 33° (−22 to 72°). The average Harris hip improved from 57 to 91. No patient had revision, loosening, luxation or migration of the components. Radiographic analysis has shown a good osteointegration of the stem in 80 % and radiographic radiolucient line in 8 % without any progression.

We also asked whether a three-dimensional custom cementless stem could restore hip function, decrease osteolysis and wear, and enhance stem survival in young patients [37]. We retrospectively reviewed 212 patients (233 hips) younger than 50 years (mean, 40 years) at a followup of 5–16 years (mean, 10 years). The Merle D'Aubigne′-Postel and Harris hip scores improved at last followup. No thigh pain was recorded for any of the patients; 187 of the 212 patients (88 %) had full activity recovery, 206 had full range of motion, and 151 had a score greater than 80 points for all five categories of the Hip disability and Osteoarthritis Outcome score. Five patients had femoral osteolysis not associated with pain. With revision for any reason as an end point, the survivorship was 87 % (range, 77–97 %) at 15 years, and considering stem revision only, the survi- vorship was 93 % (confidence interval, 90–97 %) at 15 years. Our data compared favorably with those from series using standard cementless stems at the same follow-up with a high percentage of patients achieving functional restoration and a low rate of complications.

The Basis for Computer Assisted Hip Arthroplasty

This global concept of computer assisted preoperative planning and CAD for THA represents in the authors perception the ideal basis for the use of computer assisted surgery in THA. The clinical results obtained at 20 years are encouraging, and are at least similar or better to the one previously reported with conventional cemented implants in young age groups using modern cementing technique [3, 7, 40–47], or with standard cementless prosthesis [13, 14]. The goals fixed in 1990 seem to be reached in 2010 with an increased stem longevity for patients under 65 years old, a reduced dislocation rate regarding the 0.6–15 % reported in the literature [48], and a return to full social and sport activities.

However the remaining problems for the current use of CAD custom stems are : higher price, delay for conception, and surgeon adaptation. The price difference regarding conventional implant moved from a factor to five to a factor to two during the ten last years and this process must continue in the coming years. The 5 weeks delay for stem fabrication may be significantly reduced to 3 weeks in the short future with the regular use of teleradiology. Finally, the orthopaedic surgeon used to have a large number of size in the operating room has to deal with one compactor and one final prosthesis with the CAD concept. This requires a learning curve, quickly achieved by the full computerized preoperative planning helpful during surgery and

once this adaptation is achieved this custom concept may be able to solve a number of surgical difficulties previously encountered with conventional implants.

Finally, the logical following step is the use of computer assisted technology for improving the positioning of the implants, specially on the femoral side since the optimal final position of the stem has been determined by the computerized preoperative planning. Indeed the simulation of penetration –extraction realized during the stem conception will be highly helpful to provide the correct informations for guiding the CADesigned custom rasp. This will ideally prepare the intramedullary femoral cavity ready to receive the final implant. Since the rotational stability will have been determined during the proximal femur reconstruction based on density data this step will be much more precised than the usual manual rasping. Additionally the three-dimensional design of the custom neck combined to the possibilities offered by the computer assisted technologies will allow the surgeon to evaluate intraoperatively the global range of motion achieved with such socket location and neck offset orientation.

Conclusion

Computer assisted hip arthroplasty is certainly a step forward in the future of hip arthroplasty for restoring function and improve implant longevity for patients with high activity and/or modified anatomy. The experience obtained after 20 years of computer assisted planning and CAD for custom stem will logically provide the natural basis for the use of the computer in the operating room since all the previous steps will have been managed in the planning and during stem conception.

Further research in the biomechanical field including the expected bone remodeling around the stems by finite element analysis and the evaluation of the patient hip function after total hip arthroplasty using gait analysis, fluoroscopy, or accelerometry during everyday activities will be also necessary in order to assess step by step such emerging technology.

References

1. Chandler HP, Reineck FT, Wixson RL, McCarthy JC. Total hip replacement in patients younger than thirty years old. A five-year follow-up study. J Bone Joint Surg Am. 1981;63(9):1426–34.
2. Collis DK. Cemented total hip replacement in patients who are less than fifty years old. J Bone Joint Surg Am. 1984;66(3):353–9.
3. Dorr LD, Luckett M, Conaty JP. Total hip arthroplasties in patients younger than 45 years. A nine- to ten-year follow-up study. Clin Orthop Relat Res. 1990; 260:215–9.
4. Dorr LD, Takei GK, Conaty JP. Total hip arthroplasties in patients less than forty-five years old. J Bone Joint Surg Am. 1983;65(4):474–9.
5. Halley DK, Wroblewski BM. Long-term results of low-friction arthroplasty in patients 30 years of age or younger. Clin Orthop Relat Res. 1986;211:43–50.
6. Sharp DJ, Porter KM. The Charnley total hip arthroplasty in patients under age 40. Clin Orthop Relat Res. 1985;201:51–6.
7. Stauffer RN. Ten year follow-up study of total hip replacement. J Bone Joint Surg Am. 1982;7: 983–90.
8. White SH. The fate of cemented total hip arthroplasty in young patients. Clin Orthop Relat Res. 1988;231: 29–34.
9. Malchau H, Herberts P. Prognosis of total hip replacement in Sweden. Proceedings of the 65th annual meeting of the American Academy of Orthopaedic Surgeons. New Orleans, Louisiana. 1998.
10. Boeree NR, Bannister GC. Cemented total hip arthroplasty in patients younger than 50 years of age. Ten-to 18-year results. Clin Orthop Relat Res. 1993;287: 153–9.
11. Judet R, Siguier M, Brumpt B, Judet T. A noncemented total hip prosthesis. Clin Orthop Relat Res. 1978;137:76–84.
12. Robertson DD, Walker PS, Hirano SK, et al. Improving the fit of press-fit hip stems. Clin Orthop Relat Res. 1988;228:134–40.
13. Mont MA, Maar DC, Krackow KA, et al. Total hip replacement without cement for non-inflammatory osteoarthrosis in patients who are less than forty-five years old. J Bone Joint Surg Am. 1993;75(5): 740–51.
14. Glassman AH. Porous coated total hip replacement in young patients. Read at the annual meeting of the American Academy of Orthopaedic Surgeons. New Orleans, Louisiana. 1990.
15. Rubin PJ, Leyvraz PF, Aubaniac JM, et al. The morphology of the proximal femur. A three-dimensional radiographic analysis. J Bone Joint Surg Br. 1992;74(1):28–32.
16. Noble PC, Alexander JW, Lindahl LJ, et al. The anatomic basis of femoral component design. Clin Orthop Relat Res. 1988;235:148–65.

17. Argenson J-N, Ryembault E, Flecher X, et al. Three-dimensional anatomy of the hip in osteoarthritis after developmental dysplasia. J Bone Joint Surg Br. 2005;87(9):1192–6.
18. Bennett D, Humphreys L, O'Brien S, et al. Activity levels and polyethylene wear of patients 10 years post hip replacement. Clin Biomech (Bristol, Avon). 2008;23(5):571–6.
19. Bontrager KC. Proximal femur and pelvic girdle. In: Radiographic positioning and related anatomy. 5th ed. London: Mosby; 2001.
20. Bourne RB, Rorabeck CH. Soft tissue balancing: the hip. J Arthroplasty. 2002;17(4 Suppl 1):17–22.
21. Fackler CD, Poss R. Dislocation in total hip arthoplasties. Clin Orthop Relat Res. 1980;151:169–78.
22. Breathnach AS. Frazer's anatomy of the human skeleton. London: Churchill; 1965. p. 120.
23. Davidson JA. Characteristics of metal and ceramic total hip bearing surfaces and their effect on long-term ultra high molecular weight polyethylene wear. Clin Orthop Relat Res. 1993;294:361–78.
24. DeLee JG, Charnley J. Radiological demarcation of cemented sockets in total hip replacement. Clin Orthop Relat Res. 1976;121:20–32.
25. Devane PA, Horne JG, Martin K, Coldham G, Krause B. Three-dimensional polyethylene wear of a press-fit titanium prosthesis. Factors influencing generation of polyethylene debris. J Arthroplasty. 1997;12(3): 256–66.
26. Ramaniraka N, Rakotomanana L, Rubin PJ, Leyvraz PF. Influence of the extramedullary parameters on the stem stability and the stress transfer. Proceedings of the 11th annual symposium of the International Society for Technology in Arthroplasty, Marseille, France. 1998.
27. Argenson JN, Pizzetta M, Essinger JR, Aubaniac JM. Symbios custom hip prosthesis : concept, realization and early results. J Bone Joint Surg [Br]. 1992;74-B(Supp 2):167.
28. Argenson JN, Simonet JY, Aubaniac JM. The indications for cementless custom prostheses in congenital hip dislocation. J Bone Joint Surg [Br]. 1993;75-B(Supp 1):113.
29. Argenson JN. Preoperative planning of total hip reconstruction for congenital dislocation of the hip using custom cementless implants. J South Orthop Assoc. 1994;3:11–8.
30. Husmann O, Rubin PJ, Leyvraz PF, de Roguin B, Argenson JN. Three-dimensional morphology of the proximal femur. J Arthroplasty. 1997;12(4):444–50.
31. Argenson JN, Ettore PP, Aubaniac JM. Revêtement des tiges fémorales non cimentées. Etude comparative clinique et radiographique. Revue de Chirurgie Orthopédique. 1997;83(Supp 2):44–5.
32. Argenson JN, Hostalrich FX, Essinger JR, Aubaniac JM. Preoperative planning in designing custom made hip prosthesis. J South Orthop Assoc. 1992;74-B Suppl 2:180.
33. Aubaniac JM, Argenson JN, Pizzetta M. Addressing the anteversion problem in severe CDH and primary or secondary dismorphic, with Egoform and Symbios custom made prosthesis, Marseille, France. 1990.
34. Crowe JF, Mani VJ, Ranawat CS. Total hip replacement in congenital dislocation and dysplasia of the hip. J Bone Joint Surg Am. 1979;61(1):15–23.
35. Kerjosse R, Tamby I. La situation démographique en 1999. Mouvement de la population. Démographie société in INSEE. Résultats; 1999.
36. Flecher X, Argenson JN, Parratte S, Ryembault E, Aubaniac JM. Custom cementless stem for osteoarthritis following developmental hip dysplasia. Rev Chir Orthop Reparatrice Appar Mot. 2006;92(4):332–42.
37. Flecher X, Pearce O, Parratte S, Aubaniac J-M, Argenson J-N. Custom cementless stem improves hip function in young patients at 15-year followup. Clin Orthop Relat Res. 2010;468(3):747–55.
38. Wettstein M, Mouhsine E, Argenson J-N, et al. Three-dimensional computed cementless custom femoral stems in young patients: midterm followup. Clin Orthop Relat Res. 2005;437:169–75.
39. Flecher X, Parratte S, Aubaniac J-M, Argenson J-N. Three-dimensional custom-designed cementless femoral stem for osteoarthritis secondary to congenital dislocation of the hip. J Bone Joint Surg Br. 2007;89(12):1586–91.
40. Collis DK. Long-term (twelve to eighteen-year) follow-up of cemented total hip replacements in patients who were less than fifty years old. A follow-up note. J Bone Joint Surg Am. 1991;73(4):593–7.
41. Amstutz HC, Markolf KL, McNeice GM, Gruen TA. Loosening of total hip components : cause and prevention. The hip : Proceedings of the 4th Open Scientific Meebog of the Hip Society, St Louis, Missouri. 1976. p. 102–16.
42. Ballard WT, Callaghan JJ, Sullivan PM, Johnston RC. The results of improved cementing techniques for total hip arthroplasty in patients less than fifty years old. A ten-year follow-up study. J Bone Joint Surg Am. 1994;76(7):959–64.
43. Harris WH, McCarthy Jr JC, O'Neill DA. Femoral component loosening using contemporary techniques of femoral cement fixation. J Bone Joint Surg Am. 1982;64(7):1063–7.
44. Joshi AB, Porter ML, Trail IA, et al. Long-term results of Charnley low-friction arthroplasty in young patients. J Bone Joint Surg Br. 1993;75(4):616–23.
45. Mulroy Jr RD, Harris WH. The effect of improved cementing techniques on component loosening in total hip replacement. An 11-year radiographic review. J Bone Joint Surg Br. 1990;72(5):757–60.
46. Oh I, Carlson CE, Tomford WW, Harris WH. Improved fixation of the femoral component after total hip replacement using a methacrylate intramedullary plug. J Bone Joint Surg Am. 1978;60(5):608–13.
47. Solomon MI, Dall DM, Learmonth ID, Davenport JM. Survivorship of cemented total hip arthroplasty in patients 50 years of age or younger. J Arthroplasty. 1992;7(Suppl):347–52.
48. Huten D. Luxation et subluxation des prothèses totales de hanche. Dans: Cahiers d'Enseignement de la SOFCOT. Paris: Expansion Scientifique Française; 1996. p. 19–46.

28 Hip Resurfacing Guided by Fluoroscopy and Minimal Invasive Anterolateral Approach: Technique and Results

Philippe Chiron

We offer since 2003, a technique for guiding the positioning of the femoral resurfacing cup guided by a pin positioned under image intensifier before the incision [1]. Later this technique has been adopted and published with satisfaction by Wirth and Hurst [2, 3]. You can then use all possible approaches. For our part we have developed a minimally invasive antero lateral approach type Rottïnger for hip resurfacing [4, 5]. We will successively describe these two techniques and report results of a series of 129 consecutive hips included in a prospective study between 2003 and 2009.

Targeting of the Pin-Guided Femoral Component Under Fluoroscopic Control

Using the pin technique does not change the use of the following:

- Equipment for implanting the femoral component and preparing the femoral head,
- Type of prosthesis used for the head and the cup,
- Surgical indications, which remain absolutely the same,
- The approach, which remains the surgeon's choice.

Which Particular Equipment Must Be Used?

- A long pin must be used, but this is already available as part of the initial equipment.
- A long drill of the same diameter but longer than the one available: these drills are already available commercially.
- The only specific tool is a special scissor for the dislocation, which is an adaptation of Moore's scissor. Smith and Nephew have made the adaptation, drawings exist and the equipment has already been made after several tests.
- However, the full targeting box for the femoral component is no longer necessary.

Technique

We take for example a patient aged 42 years, practicing a combat sport since childhood, who has bilateral Tönnis stage IV osteoarthritis, following the aftermath of slipped epiphysis (Fig. 28.1a, b) [6].

P. Chiron, MD, PhD
Service d'Orthopédie-Traumatologie, CHU de Toulouse, Toulouse, France
e-mail: descorthopedie@free.fr

D.G. Poitout (ed.), *Biomechanics and Biomaterials in Orthopedics*,
DOI 10.1007/978-1-84882-664-9_28

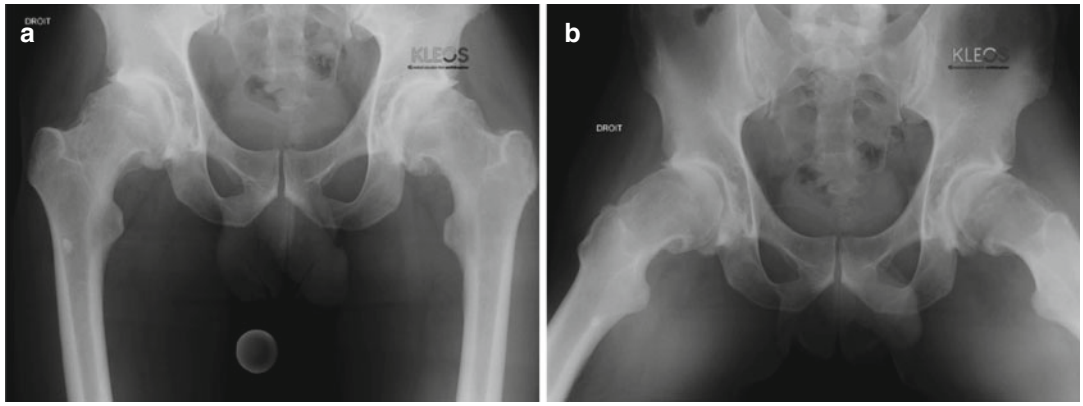

Fig. 28.1 (**a**, **b**) Bilateral osteoarthritis stage Tonnïs IV due to sequelae of slipped epiphysis. (**a**) Antero posterior view, (**b**) lateral view

Preparation

The patient is moved into the lateral decubitus for anterior or posterior approach; Postero lower arm of the table was removed to facilitate the movement of forward dislocation of the femoral head. After positioning the sheets, an image intensifier protected by sterile sheets is set up to above the patient to obtain an anteroposterior incidence of the hip to replace.

Targeting the Pin

Without changing the position of the image intensifier, it is possible to obtain a front view of the neck of the femur by rotating the lower limb in internal rotation by 10° and profile view by positioning the limb in flexion at 45°, with external rotation and abduction. The guide pin penetrates through a 1 cm small incision in the lateral sub-trochanteric zone opposite the low part of the lesser trochanter, medially in the antero posterior direction. It is oriented in the required direction according to the front and profile incidences, along the axis of the neck or in slight valgus in the frontal plane, and at the centre of the neck in the sagittal plane. When the right direction is obtained, the pin is pushed toward the subchondral bone of the femoral head. The long perforated drill, guided by the pin, passes through the group comprising the femur neck, the head and the cortical bone of the femur head. All the material is then withdrawn. The image intensifier is removed. It is then possible to perform the chosen approach – the posterior, Hardinge, anterolateral or anterior approach.

Minimally Invasive Antero Lateral Approach for Hip Resurfacing: Technique

Preparation

The anterolateral approach of the hip goes behind the sheath of the fascia lata tensor muscle and in front of the gluteal muscles. This is a minimally invasive approach that enables no muscles to be desinserted. The installation is performed in the lateral decubitus position, with the posterior half-table section moved out of the way to facilitate the dislocation movement.

Incision

The incision is made extending from a point located 2 cm below the trochanteric ridge to a point on the anterosuperior iliac spine (ASIS). It starts, along this line, from the anterior edge of the greater trochanter, moving toward the ASIS over a length of 8–10 cm, without going past a point located two fingers below the ASIS to preserve the vascular and nerve pedicle of the tensor fascia lata (Fig. 28.2a–c).

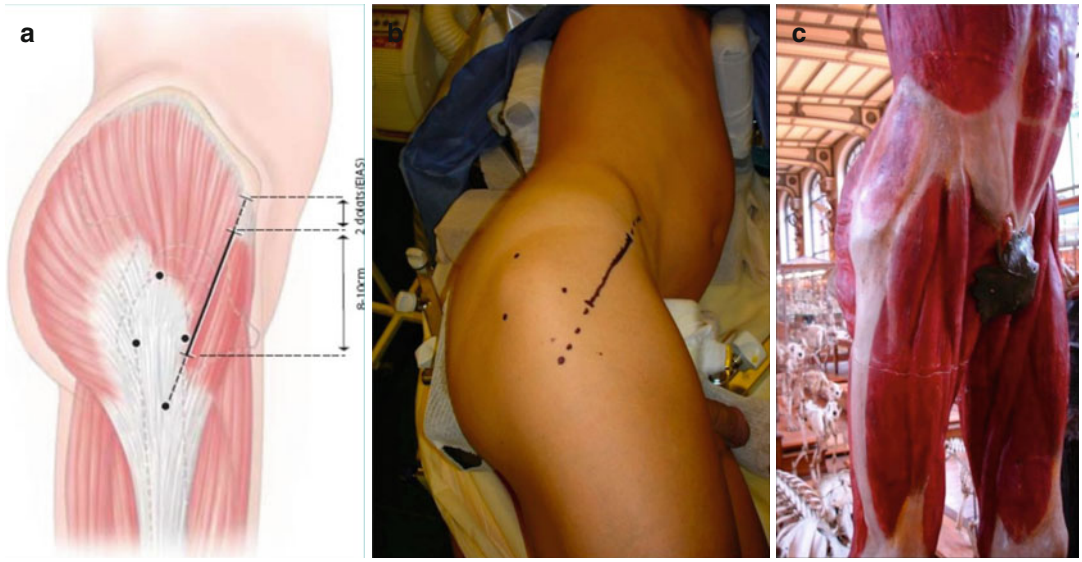

Fig. 28.2 (**a**–**c**) On a line from the pinhole to ASIS, the incision is performed from the anterior ridge of the trochanter to 2 cm before ASIS (**a**, **b**). It passes between tensor facia lata and medius and minus glutei

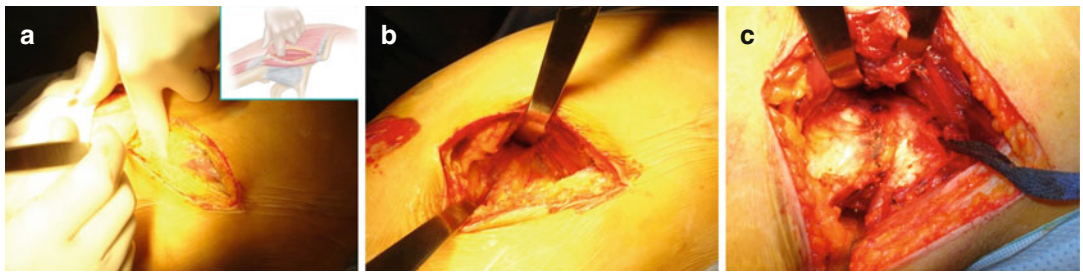

Fig. 28.3 (**a**–**c**) The ilio tibial band is opened behind the facia lata aponevrosis (**a**); the space between glutei and facia lata tensor are dissociated (**b**); the capsule is widely exposed (**c**)

Hip Approach

After careful sectioning and haemostasis of the adipose tissue, the iliotibial band is identified, tissue with strong resistance that is incised along the entire length of the approach. The limb is positioned in flexion and external rotation. A gentle dissection with scissors and by hand (Fig. 28.3a) carried out at the distal part of the wound near the trochanter enables the space between the front of the fascia lata tensor muscle and behind the medium and small gluteal muscles (gluteus medius and minus). This space leads to the plane of the capsule (Fig. 28.3b). The traps to avoid are basically perforating the aponevrosis of the fascia lata tensor muscle if the approach is too anterior, and crossing the anterior fasciculus of the gluteus medius muscle if the approach is too lateral. Generally, this space must be sought at the bottom of the incision and forwards by bypassing the fibres of the gluteus medius muscle (Fig. 28.3a).

Capsule Dissection

The capsular plane can be recognised by palpating the anterior face of the neck and by exposing the capsule by means of angled retractors in an extra-capsular position above and below the neck (Fig. 28.3a, b). The capsule must have a thick, fatty and yellow appearance. If there are muscles remaining after placing a retractor, these are

likely to be the fibres of the gluteus minus. Another search must be made to find the correct plane. The dissociation of the space upwards must stop above the reflected ligament of the anterior link, without reaching the anterosuperior iliac spine, to prevent a lesion of the tensor of fascia lata nerve that comes from the gluteal pedicle in the plane between the small and medium gluteal muscle. For an ideal exposure of the elements between the joint and sufficient clearance of the capsule, the capsule must be cleared correctly in the extra-capsular position before the incision is performed. The medial clearance is obtained by dissociating the capsule of the tendon of the rectus femoris muscle and by replacing the angled retractor between the capsule and the tendon (Fig. 28.3c). Towards the top, it is necessary to create a space with a raspatory between the capsule, the iliac bone and the small gluteal muscle to expose the reflected tendon of the rectus femoris muscle (Fig. 28.3c). An abdominal sheet is pushed between the space between the wing of Ilium and the gluteal muscles, to make a special space for the femoral head when exposing the acetabulum, at the top and rear above the sciatic notch.

Capsule Incision

The capsule is incised along the axis of the neck, from the intertrochanteric line up to the acetabulum, then by the longest possible medial and lateral counter incision, at the level of the intertrochanteric line and periacetabular region, to open up the capsule like a book. The very thick capsule can be suspended on a wire and sutured at the end of the procedure. The retractors are then positioned in the intra-capsular position (Fig. 28.4a, b).

Hip Dislocation

The hip is dislocated in extension –external rotation – adduction. However, dislocation is difficult as long as the ligamentum Teres is intact. In the aforementioned position, the curved scissor is passed under the femoral head and impacted over the entire length (Fig. 28.5a–d). It is also necessary to remove the osteophytes from the anterior wall of the acetabulum, notably with regard to the anteroinferior iliac spine. A Lambotte's hook is passed under the femoral neck. While assistance is given to make the adduction movement – external rotation of the lower limb, the surgeon lifts the neck of the femur upwards (Fig. 28.5e, f).

Acetabulum Preparation

When the hip is dislocated, the lower limb is positioned in flexion – external rotation. To do this, the leg passes from the back to the front of the table. The femoral pusher is used to help pass the femoral head under the gluteal muscles, below the acetabulum. A compression movement in the axis of the femur is used to move the femoral head backwards. The lower limb is then positioned in flexion – external rotation (Fig. 28.6a).

Exposure of the Acetabulum

A long angled retractor is positioned on the posterior wall of the acetabulum in the convexity of the neck; another retractor is positioned at the level of the lower part of the anterior wall (Fig. 28.6b–d). The capsule is sectioned at the bottom, opposite the transverse ligament of the acetabulum, over its entire length, in order to facilitate the posterior translation of the femoral head.

Reaming the Acetabulum

The acetabulum exposed in this manner can be prepared. The acetabulum is reamed by using the drill guide handle. An angled handle is recommended for minimally invasive approaches. The milling tools are first positioned in the acetabulum, then the support attaches to the milling tool which makes it easier to set up the equipment. A useful piece of advice is to lock the

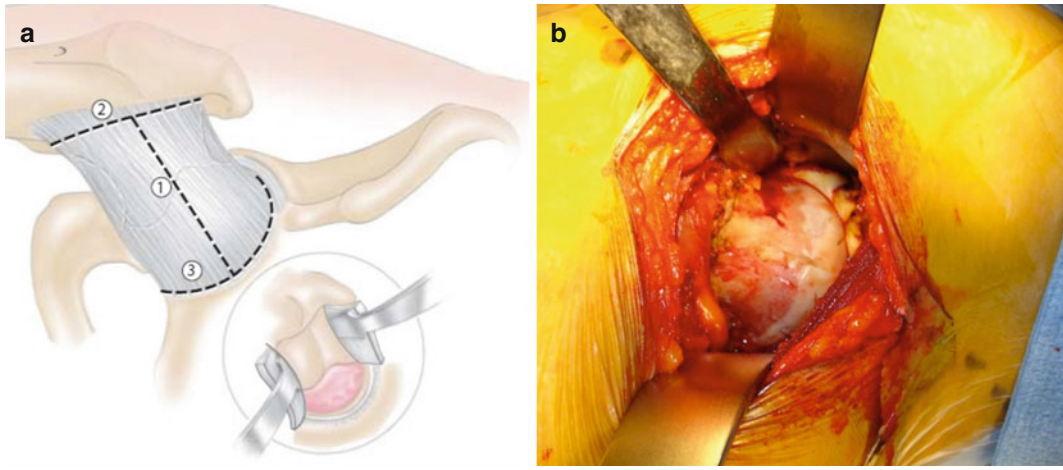

Fig. 28.4 (**a**, **b**) The capsule is opened like a book (**a**); the capsule is widely released in the tidal acetabulum and along the intertrochanteric line (**b**). Incision:*1* along the neck, *2* distal, *3* Periacetabular

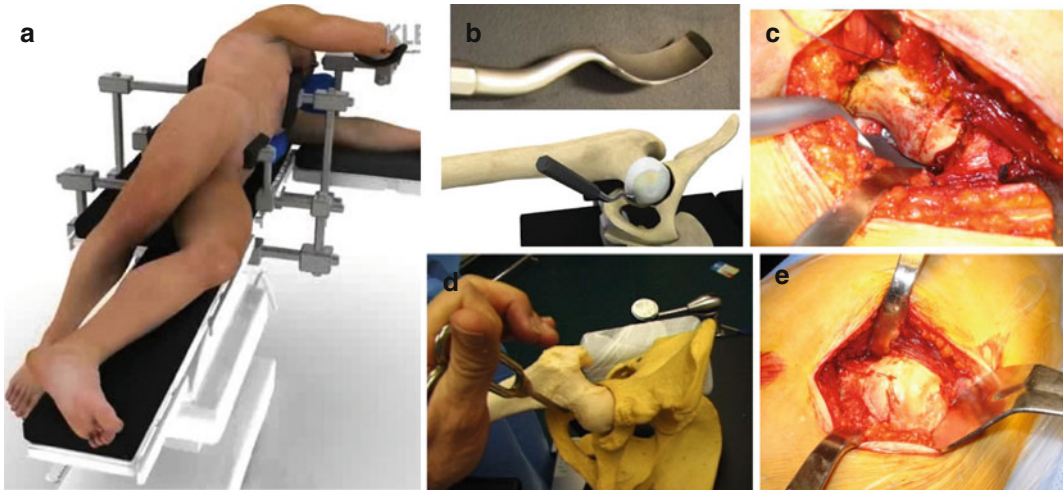

Fig. 28.5 (**a**–**e**) The hip is dislocated in extension, adduction and external rotation (**a**); a special long curve chisel introduced in the lower space of the head cuts the ligamentum Teres (**b, c**); A hook allow to tract up (**d**); the dislocated head (**e**)

ring, in open position, with a piece of a drain so as to be able to attach and remove the handle of the reamer easily (Fig. 28.6e).

Acetabular Implantation

Implantation of the acetabular component through the usual technique according to the component that is used. The acetabular component has to be orientated less than 45° in a frontal plane. The cup is protected by a compress or plaque of guidance for the remainder of the procedure.

Exposure of the Femur

The lower limb is again positioned in extension – rotation External – adduction supplied by redoing pass leg from the front to the back of the table. The head is well presented in incision

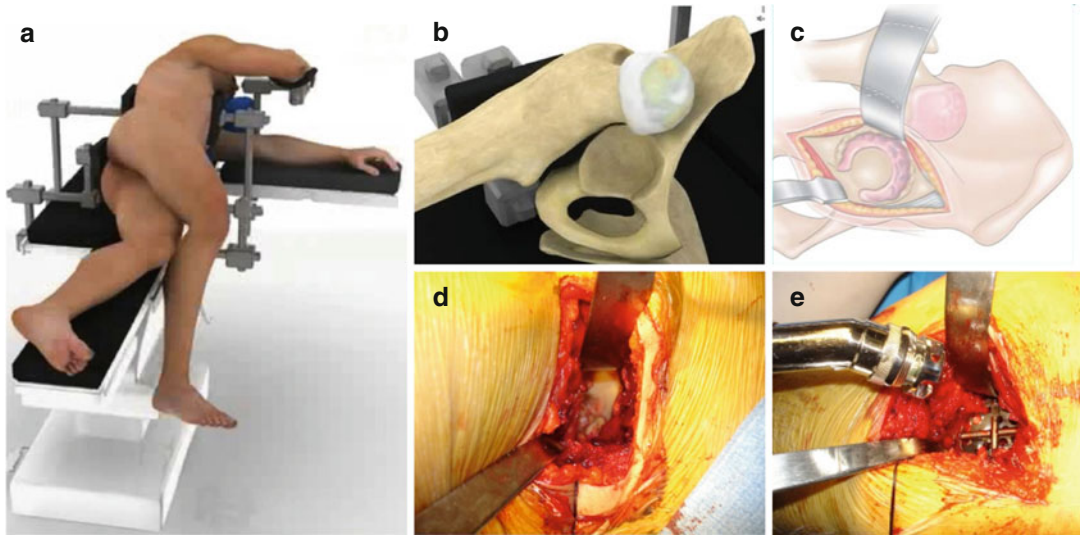

Fig. 28.6 (**a**–**e**) The acetabulum is exposed in flexion, abduction internal rotation (**a**); the head is pushed posteriorly (**b**) and is stabilised by a retractor (**c, d**); It is reamed with an angled handle introduce separately from the milling tools (**e**)

between the tensor fascia lata and buttocks. Spacers against bent can be exposed.

Femoral Preparation

Cylindrical Reaming of the Femoral Head

After impaction of the acetabular component, the femoral component is positioned in the direction provided by the perforation channel. Position the guide rod in this channel. The cylindrical reamer corresponding to the size of the cup chosen is positioned along this axis. The femur head is reamed up to the cylinder reamer guard.

Leg Length Determination

Surgeon has to determine the thickness of the base of the femoral component and removes it from the top of the head perpendicularly to the femoral guide. Different techniques can be performed, using the trial component or a spacer of the thickness of the base of the femoral cup. A mark is made on the femoral head corresponding to the thickness of the base of the femoral component if the lower limbs are not unequal in length.

Final Milling

The flat cutting tool is fitted and the femoral head reamed up to the mark made.

- Use the chamfer-cutting tool matching the size of the femoral component. The central canal is reamed to the diameter of the final stem. The preparation of the head is now complete.
- Trials.
- Femoral component cementation: A notch, made at the front or rear of the femoral head depending on the approach, prevents the cement from causing too much pressure between the cup and the bone, and prevents as well impaction failure.

Reduction and Closure

Before reduction, similarly to any resurfacing, it is necessary to remove all the foreign bodies (cement and bone) to prevent any risk of conflict and third-body wear. This cleaning must be extremely thorough. The reduction is made with the hip in flexion while avoiding an abduction movement. After reduction, the correct orientation of the acetabular component must be checked, together with the absence of any cam effect when positioning the

limb in neutral position and by making, in extension of the knee, outward rotation movements. If a subdislocation of the head occurs, this means that either the acetabular part is positioned too far forward, or there is a foreign body. Closure of the capsule. Fitting a drain, preferably low pressure. Closure of the iliotrochanteric band and the skin. Post operative Xrays.

Postoperative

The patient is lifted on the first day with partial weight bearing. Rehabilitation of joint mobility in the second day. The canes are dropped at the end of the first month.

A Series of 129 Cases Between 2003 and 2009

Method

A prospective study was performed in a consecutive series of 129 patients during 6 years. This study reflects the learning curve of the technique. All the patients were operated on under general anaesthesia, by a single senior surgeon in our Department, using the technique described above. The first 86 patients received the same metal-on-metal device Durom™(Zimmer, Warsaw, Indiana, USA) and the last 43 patients received Birmingham (Smith et nephew, UK) with an uncemented press-fit acetabular component and a femoral component inserted with Palacos™ gentamicin-containing cement.

All the radiographs had the same magnification factor (1.15), and were evaluated by a single independent reviewer. The features assessed were the centring of the femoral component with regard to the femoral neck, in the coronal plane on the AP views and in the sagittal plane on the frog lateral views. Centring was rated as excellent, good, fair, or poor. The angle between the stem of the femoral component and the axis of the femoral neck was measured on the AP and the lateral views. An angle of between −3° (AP: varus; lateral: retroversion) and +3° (AP: valgus; lateral: anteversion) was judged satisfactory. The angle between the femoral component stem and the femoral shaft was measured and compared with the pre-operative neck-shaft angle. Femoral offset was measured pre- and postoperatively. Centring of the acetabular component was assessed with the technique described by Pierchon et al. Centring was considered good if the difference between the desired value and the measured value was < 5 mm; fair, if it was between 5 and 10 mm; and poor if it was > 10 mm. A check was also made to see whether the component was too high, too low, too far to medial, or too far to lateral.

The main results to assess the value of a technique described by acetabular pin guided amplifier are summarized in Fig. 28.7a, b.

The mean operative time was 111 min (75–100), with markedly shorter times towards the end of the series. The mean duration of fluoroscopy was 24 s corresponding to an average of six views of 2 s by intervention. There were three intra-operative complications: one guide pin breakage, one tilting of the acetabular component during reduction (Durom), and one anterior dislocation of the femoral head. The first two complications were noted intra-operatively; the third was seen on the immediate postoperative film, and necessitated immediate operative correction under the same anaesthetic. There were no intra-operative fractures. Postoperatively, one patient had a painful haematoma, as a result of a blocked suction drain.

The mean in-patient stay was 6.7 days (6–14 days); two thirds of the patients were discharged home.

The calculated mean RBC loss was 611 ml (147–1087). Given a mean pre-operative haematocrit of 44 %, this meant a mean blood loss of 1388 ml.

Cement leaks were found in four cases; all the leaks were along the underside of the neck. The positioning of the femoral component stem was excellent or good in over 96 % of the cases on the AP radiographs, and in over 90 % on the lateral radiographs. None patient had varus of the femoral component comparatively to the CCD angle of the pre operative hip. An excellent femoral offset had been restored or preserved.

Centring of the stem 129 hips
Method of Parker.

a

	A.P. View	Lateral view
Excellent	112 / 129	110/129
Good	7 / 129	8/129
Middle	8/ 129	11/129
Bad	0/129	0/129

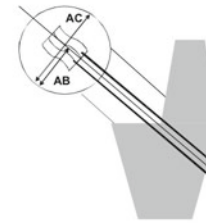

CCD Angle: native angle / femoral component angle

0° / + 10 °	Excellent/good	126
Varus less than 3°	Middle	3
VARUS > 3°	Bad	0

129 Hips

b

Anterior Offset
Average + 7,74 mm

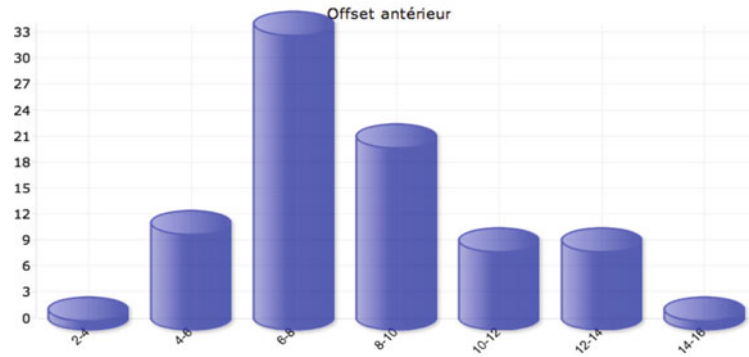

2-4	4-6	6-8	8-10	10-12	12-14	14-16	total
1	11	34	21	9	9	1	86

Fig. 28.7 (**a, b**) Main results of assessing the value of a technique described by acetabular pin guided amplifier are summarized

Discussion

Advantages and Disadvantages of the Use of a Guide Pin

Advantages

- Simple, safe positioning of the cup in the frontal and sagittal plane. Currently, positioning errors are basically made with the targeting guide available in the sagittal plane.
- Conservation of the neck vascularisation: it is unnecessary to dissect the soft tissues around the neck to be able to palpate and carry out the targeting, so the arrival of the retinacular arteries that vascularise the head is maintained.
- As the milling is performed along the good axis, this avoids creating a notch on the upper part, which is a source of fractures.
- The choice of length, after fitting the femoral component, can be adapted since the upper

part of the head has not been removed to position the equipment.
- The learning curve is fast: all orthopaedic surgeons are able to place a front and profile pin in a femur neck or at the centre of a head.
- There are few specific instruments: Actually this reduces the quantity of equipment for this seemingly complex operation.
- All approaches are enabled with the pin technique, both posterior and anterior.
- The pin technique enables a minimally invasive approach to be used more easily, as it is no longer necessary to make large femur neck incisions to expose it. An available exit hole is all that is required.
- Hess et al. [7, 8] advocate the use of navigation to obtain a well-centred femoral component. We feel that this would add to the time required and to the cost of the procedure; above all, navigation provides a computer image of the femoral *head* as an aid to the determination of the head centre, while what is actually required is a correct assessment of the femoral *neck* axis. In order to obtain a computer image of that axis, one would need to gauge around the neck, which would entail the exposure and, hence, the devascularisation, of the neck. It is, in fact, simpler, safer, and very much less expensive to insert a guide pin with fluoroscopy.

Disadvantages
- This technique requires the use of an image intensifier. The average time for a trained surgeon is 20–40 s. This is the typical time used for fitting a pin in a neck for a dynamic screw-plate or a gamma nail or any other technique that requires targeting the femur neck.
- The surgeon must plan the right direction he wants to give the femoral cup, taking into account initial architectural distortion and good management constraints which most often leads to position the cup valgus parallel to the spur of Merckel.
- For the right direction of the pin, he may need to reposition it.
- It is important to change the pin for each operation, as there is a risk of the pin breaking if such a pin is used.

To summarise, the pin technique is simple, within the reach of all surgeons and can be used for any approach. It makes the placement of the femoral component safer.

Advantages and Risks of the Anterolateral Approach

Advantages
- The glutei muscle may be mobilised by rotating the hip, where as the tensor fascia lata and the Sartorius are biarticular muscles that do not lend themselves to mobilisation.
- The posterior part of the capsule and the short external rotators are preserved.
- This ensures maintenance of the femoral neck blood supply [9–13], which is a major consideration in resurfacing arthroplasty.
- Also, a strong posterior capsule and intact muscles will ensure that the hip is better stabilised, both actively and passively, to resist forces that may produce posterior dislocation [14, 15].
- The anterolateral approach provides good exposure of the anteverted femoral neck, and facilitates resurfacing. The acetabulum is seen head-on, which reduces the risk of a cam effect on the reamers.
- This is a direct approach on the capsule. It is unnecessary to use an orthopaedic table. The patient is in the lateral decubitus position and the dislocation is carried out at the front, which enables the femur head to be presented in the approach.
- Dislocating the head backwards exposes the acetabulum, which is the usual position for traumatic hip dislocations. The head is located above the sciatic notch and the sciatic nerve is slack. Moreover, paralysis of the sciatic nerve after pure dislocation is rare in traumatology.
- Rehabilitation is faster. Subsequent surgery is made easier in the event of wear or a fracture of the neck. It is possible to take an anterolateral approach or use a new posterior approach.

Disadvantages
- The learning curve can be evaluate around 20 cases including the learning of the cups' positioning.

- This approach is hard to perform when the shape of the femur is retroversion and varus. The ideal is to master the posterior approach also.
- This surgical approach leads to the surgeon too anteverted acetabular cup.
- The haemostasis should be careful to avoid a postoperative hematoma.
- Two assistants are required.

Conclusion

Resurfacing has made a major contribution to hip arthroplasty in young subjects. It permits patients to be physically active, preserves bone stock, and allows revision to a standard THR, usually with the acetabular resurfacing component left *in situ* [16].

The use of an anterolateral approach and a guide pin makes this a minimal-incision procedure like the one proposed for THR. The postoperative management is simplified. Above all, the vascularity of the neck is preserved, and the femoral component can be correctly placed even in badly deformed heads whose centre is out of line with the neck axis.

Mastery of the technique involves a learning curve. Surgeons may not initially be familiar with the anterolateral approach, the fitting of the femoral component, or the insertion of the acetabular component for a large-diameter head. Consciously, this paper includes the results of a learning curve to be sure that this new technique does not induct severe or mild complications. Learning may advantageously start with doing a THR using a large-diameter femoral head, through the anterolateral approach. It should of course take into account the complications resurfacing, fractures of the femur neck, but also reactions to metal debris released by the couple (ALVAL and solid tumors).

References

1. Chiron P. Use of a guide wire in hip resurfacing arthroplasty. Osteologie. 2005;14:65–8.
2. Hurst JM, Millett PJ. A simple and reliable technique for placing the femoral neck guide pin in hip resurfacing arthroplasty. J Arthroplasty. 2010;25:832–4.
3. Wirth CJ, Gosse F. Improved implantation technique for resurfacing arthroplasty of the hip. Oper Orthop Traumatol. 2006;18:214–24.
4. Bertin KC, Rottinger H. Anterolateral mini-incision hip replacement surgery: a modified Watson-Jones approach. Clin Orthop Relat Res. 2004;429: 248–55.
5. Chiron P, Pailhe R, Reina N, Ancelin D, Sharma A, Maubisson L, et al. Radiological validation of a fluoroscopic guided technique for femoral implant positioning during hip resurfacing. Int Orthop. 2013;37(3):361–8.
6. Murgier J, Espie A, Bayle-Iniguez X, Cavaignac E, Chiron P. Frequency of radiographic signs of slipped capital femoral epiphysiolysis sequelae in hip arthroplasty candidates for coxarthrosis. Orthop Traumatol Surg Res. 2013;99(7):791–7.
7. Hess T, Gampe T, Kottgen C, Szawlowski B. Intraoperative navigation for hip resurfacing. Methods and first results. Orthopade. 2004;33:1183–93.
8. Schnurr C, Michael JW, Eysel P, Konig DP. Imageless navigation of hip resurfacing arthroplasty increases the implant accuracy. Int Orthop. 2010;22(3): 307–16.
9. Beaule PE, Campbell P, Lu Z, Leunig-Ganz K, Beck M, Leunig M, Ganz R. Vascularity of the arthritic femoral head and hip resurfacing. J Bone Joint Surg Am. 2006;88 Suppl 4:85–96.
10. Beaule PE, Campbell P, Shim P. Femoral head blood flow during hip resurfacing. Clin Orthop Relat Res. 2007;456:148–52.
11. Leunig M, Ganz R. Vascularity of the femoral head after birmingham hip resurfacing. A technetium tc 99m bone scan/single photon emission computed tomography study. J Arthroplasty. 2007;22:784–5; author reply 785–6.
12. McMahon SJ, Young D, Ballok Z, Badaruddin BS, Larbpaiboonpong V, Hawdon G. Vascularity of the femoral head after birmingham hip resurfacing. A technetium tc 99m bone scan/single photon emission computed tomography study. J Arthroplasty. 2006;21:514–21.
13. Steffen R, O'Rourke K, Gill HS, Murray DW. The anterolateral approach leads to less disruption of the femoral head-neck blood supply than the posterior approach during hip resurfacing. J Bone Joint Surg Br. 2007;89:1293–8.
14. Mont MA, Ragland PS, Marker D. Resurfacing hip arthroplasty: comparison of a minimally invasive versus standard approach. Clin Orthop Relat Res. 2005;441:125–31.
15. Nork SE, Schar M, Pfander G, Beck M, Djonov V, Ganz R, Leunig M. Anatomic considerations for the choice of surgical approach for hip resurfacing arthroplasty. Orthop Clin North Am. 2005;36: 163–70.
16. Pailhe R, Sharma A, Reina N, Cavaignac E, Chiron P, Laffosse JM. Hip resurfacing: a systematic review of literature. Int Orthop. 2012;36(12):2399–410.

Biomechanics of Osteosynthesis by Screwed Plates

29

Emanuel Gautier

Internal fixation of fractures using plates developed more than 100 years ago following the widespread use of radiographs. Hansmann reported the technique of plating lower limb shaft fractures as early as in 1886 and presented a plate design allowing subcutaneous insertion of the plate and percutaneous insertion of the plate screws [1]. Lambotte, Lane and Sherman experimented in the first decades of the twentieth century with new implant materials and improved the plate and screw designs to decrease the risk of corrosion and mechanical failure of the implants [2–4]. Danis, Bagby and Müller introduced the concept of compression plating to improve the stability of fixation and to protect the implant from mechanical overload [5–7].

Since then, conventional plating techniques and plate designs have evolved constantly. This evolution is based on an improved understanding of the biology of fracture healing, of the biomechanics of fracture fixation, and on experience analyzing previous failures - such as fatigue failure of the implants, deep infection, and delayed union or non-union. It has involved the implants, the technique of its application, and the surgical technique with bone and soft tissue care or reconstruction [8–32] (Table 29.1).

E. Gautier, MD
Department of Orthopaedic Surgery and Traumatology,
HFR – Cantonal Hospital Fribourg,
Fribourg, Switzerland
e-mail: gautiere@hopcantfr.ch

Biological Aspects of Plate Fixation

Blood Supply of Cortical Bone

The three primary components of the afferent vascular system to bone tissue are the principal nutrient artery, the metaphyseal arteries, and the periosteal arterioles. The nutrient and metaphyseal arteries together compose the medullary arterial system which is the major afferent supply nourishing about the inner two thirds of the bone cortex. The periosteal vessels enter the cortex mainly at sites of fascial and muscle attachment and appear to supply the outer third of the bone diaphysis [33–38]. Cortical circulation usually flows in a centrifugal direction. In the diaphysis the inner cortical layers are drained through venous channels, the periosteal layers directly by periosteal capillaries. In case of damage to the medullary system following trauma or operation a compensatory flow reversal occurs to some extent [33, 38–42].

Vascular Disturbance Due to Trauma, Surgery, and Implant

As a result of bone fragmentation and displacement of fragments, periosteal, intracortical and endosteal vessels are ruptured [13, 35–37, 41, 43]. At each fracture line all intracortical vessels are disrupted due to the direct damaging of

D.G. Poitout (ed.), *Biomechanics and Biomaterials in Orthopedics*,
DOI 10.1007/978-1-84882-664-9_29

Table 29.1 Common mechanical terms and formula

Brittle material	Material with no or low capacity of plastic deformation.
Ductile material	Material with large capacity of plastic deformation.
Elasticity	Reversible deformation of a material. The material regains its original dimensions and shape after unloading.
Elastic modulus E	Constant of proportionality between stress and strain. Slope of the initial curve of a stress–strain diagram. Represent the stiffness of a material to an imposed load. Also called modulus of elasticity, Young's modulus.
	$E = \delta\sigma/\delta\varepsilon = \tan\varphi$
Friction	Friction force at an interface. Product of a force perpendicular to a surface and a proportional constant (friction coefficient).
	$F_f = \rho\ F_a$
Plasticity	Irreversible deformation of a material. Materials capable of withstanding large strains are referred to as ductile materials; the converse applies to brittle materials.
Stability	Degree of relative movement between fragments. Absolute stability means no motion between fragments under given load. Relative stability means that the fragments displace under load, but go back to the initial position with unloading.
Stiffness	The resistance of a material to deformation under load. The higher the stiffness of a material the smaller its deformation under a given load.
	The product of the cross-sectional area and the elastic modulus expresses axial stiffness:
	$R_{ax} = A\ E$
	Bending stiffness is defined as the product of the axial area moment of inertia (with respect to the individual bending axis) and the elastic modulus:
	$R_{be} = I_{ax}\ E$
Strain ε	Deformation of a material under a given load. It is expressed as elongation per unit of original length and is a dimensionless quantity.
	$\varepsilon = \Delta l/l_0$
Strength	Ability of a material to withstand load without structural failure. It can be reported as ultimate tensile strength, as bending strength or torsional strength. It is expressed in units of force per unit of area (stress) or elongation at rupture (strain).
Stress σ	Force per unit cross-sectional area. Stress is directly proportional to strain with the elastic modulus (E) as constant of proportionality. Unit of stress is Newton/m^2 (Pa). Normal stress means that the force is acting perpendicular to the surface, shear stress that the force acts parallel to a surface.
	$\sigma = F/A$
	$\sigma = E\ \varepsilon$

its surrounding osteons. Major displacement of the fracture fragments may disrupt larger vessels like the nutrient artery, the central artery or its intramedullary branches. This disruption of the medullary blood supply in turn leads to avascularity and devitalization of a large amount of the bone cortex. The stripping of the periosteum with its vascular network during injury is of particular importance, because disruption of the periosteum may be severe or total between fragments leaving smaller fragments completely devascularized.

The surgical approach to the fracture leads to an additional considerable vascular damage to the bone tissue by the soft tissue retraction. Additional damage is added by subperiosteal exposure that leads to more damage compared to careful epiperiosteal exposure [44]. Fragment manipulation by reduction clamps and the plates itself result in further damage to the blood supply of bone. Complete visualization of the fracture area is needed neither for fracture reduction nor for positioning of the plate and insertion of the screws [15, 45, 46].

In conventional plating technique some amount of contact between plate and bone is needed for stability reasons to allow load

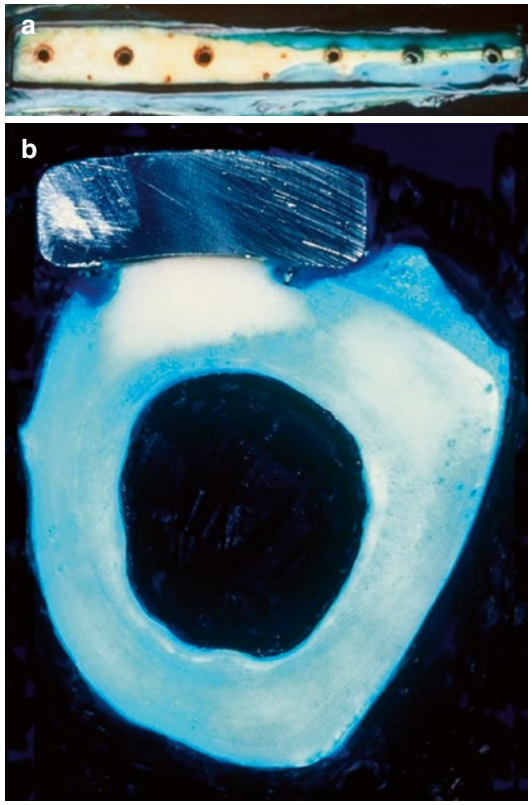

Fig. 29.1 Vascular disturbance underneath a conventional plate**.** The compression of the periosteal vessels results in an avascular area underneath a conventional plate (**a**). The bone section at 4 weeks reveals the importance of the disturbance of the blood supply under the plate, which is mainly due to impairment of the venous efflux (**b**)

transmission by friction at the interface. The axial screw force generated by tightening the screws and the compressive strength of cortical bone gives the minimum area required for load transfer. Shaping the plate to the bone surface as exactly as possible is mandatory not to be faced with the problem of secondary fracture dislocation when the fragment is pulled towards the plate by tightening the screws. The biological disadvantage of the conventional contact plating concept is the appearance of a relatively large zone of blood supply disturbance directly underneath the implant (Fig. 29.1a, b). This deficiency of perfusion is caused by direct compression of the periosteal vascular network under the plate and leads to necrosis of cortex adjacent to the plate [47–55]. Dead bone can only be revitalized by removal and replacement (creeping substitution), a biological process which takes a long time to be completed. During the recovery of the blood supply, a temporary porosis of the bone is observed as a result of the tremendous intracortical remodeling. The remodeling activity starts at the boundary between vital and initially devascularized bone and is usually directed towards the implant (Fig. 29.2a, b). It is accepted that necrotic tissue disposes to and sustains infection [56]. The recovery of the original bone structure and vitality generally takes more than one year. In the past, many authors have tried to explain this temporary

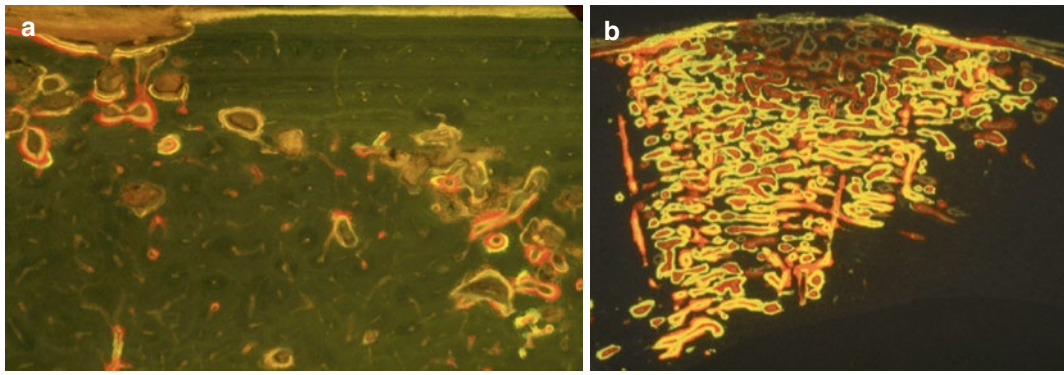

Fig. 29.2 Bone remodelling after plating. At ten weeks after plating, fluorescent labelling of cortical bone shows that the remodelling activity starts at the boundary between the zone of avascular bone and viable bone (**a**). The remodelling front reaches the periosteum at about 20 weeks resulting in complete revascularization of the formerly avital bone cortex. This creeping substitution of bone results in a temporary porosity (**b**)

bone porosity as a functional adaptation of the bone structure to the unloading effect of the plate according to Wolff's law [57–69]. The newer generations of plates (limited contact, no contact implants) decrease the amount of devascularization of cortical bone due to a reduction or the complete absence of implant-bone contact.

Fracture Healing and Stability of Fixation

Fracture healing is the recovery of the biological and mechanical integrity of the osseous tissue, i.e., return of the prefracture tissue vitality and structure as well as the prefracture stiffness and strength of the injured bone segment [70]. The amount of stability achieved by implants is the mechanical input for the biological response of bone healing. Beside the injury itself, the healing process additionally is modulated by the additional surgical damage to the bone and surrounding soft tissue envelope during the process of reduction and fixation [9, 25, 71, 72]. In plate osteosynthesis the importance of the amount of mechanical stability to achieve direct bone healing was overestimated for a long time. Forcing precise reduction to improve the postoperative radiological appearance was likely to be linked to additional and sometimes extensive surgical trauma with stripping and denuding of bone fragments. Because dead bone is unable to heal some of the possible complications such as deep infection, non-union, delayed union, and refracture have to be attributed to the iatrogenic surgical tissue damage during the operative procedure. Radiographically and histologically different healing patterns can be differentiated depending on the local mechanical environment [3, 6, 73].

Absolute stability is present when the fracture is stabilized by a stiff implant which maintains the fracture reduction with no or minimal displacements occurring under functional loading. As a biological consequence primary bone healing without radiographically visible callus formation occurs. It can be assumed that fragment end necrosis induces internal remodeling of the bone which repairs the fracture by the effect of crossing osteons.

Flexible fixation allows the fracture fragments to displace in relation to each other when load is applied. The external load results only in reversible deformation of the splint. After unloading, the fracture fragments move back into their former relative position. When the load results in an irreversible deformation of the splint, the fragments remain permanently displaced. Such a situation with plastic deformation of the implant is called unstable fixation. All fracture fixation devices possess different degrees of implant stiffness and lead to fixations of gradually differing flexibility depending on how they are applied and loaded. It appears likely that some flexibility of fixation is the most important mechanism triggering and inducing callus [74].

Table 29.2 Stability of fixation, strain of interfragmentary tissues and biological bone reaction

	Stability of fixation	
Gap width	Rigid	Flexible
Small or no gap	Direct bone healing	Delayed union, non-union
Large	No stimulus for bone formation	Callus healing

With no gap and stable fixation primary bone healing occurs. A small gap with some motion results in high tissue strain and therefore in delayed union or non-union. A large gap with some motion between the fragments stimulates callus formation. A large gap rigidly fixed by implant shows no healing tendency because no mechanical stimulus for bone formation is present

In bone healing, the strain conditions of the involved tissues have to be taken into account when judging under which condition bridging by bone formation will occur or a non-union develops (Table 29.2). The comminution reduces the strain magnitude of the interfragmentary tissues in each gap for a given amount of overall displacement, thus allowing its safe differentiation and ossification. On the other side, a small gap with some instability still present increases the strain of the interfragmentary repair tissue with inherent risk for non-union [75].

Mechanical Aspects of Plate Fixation

Basic Mechanical Principles of Internal Fixation

There are two basic mechanical principles how a fractured bone can be stabilized: interfragmentary

compression and splinting. Interfragmentary compression functions by the elastic preload of both, the bone and the implant. Thereby, the plate is loaded in tension and the bone in compression creating high amounts of friction between the bone fragments. Interfragmentary compression can either be static, i.e., induced as a result of a pretensioned implant, or dynamic, i.e., generated by means of the functional load allowing coaptation of the fragments along a non locked internal or external splint. Static interfragmentary compression can be accomplished only in case of at least a partial bony contact between the main fragments. Additionally, interfragmentary compression is very sensitive to minimum amounts of motion-induced bone resorption, diminishing the preload of both, the implant and the bone, with consecutive loss of stability [76, 77].

Splinting consists of the connection of an implant to a broken bone. The stability of this composite system depends on the stiffness of the splint itself, the quality of coupling between the splint and the bone, and the presence or absence of fracture comminution and bone defects. Depending on the localization of the implant, splinting can either be external or internal. Internal splints can be positioned inside or outside the medullary cavity. Depending on the mechanical use of the implant, a splint can be either gliding (nonlocked or dynamically locked) or nongliding (statically locked). The plate design itself does not define its later mechanical function; it can be used for splinting and/or for compression osteosynthesis.

Plate Designs and New Plate Developments

The Dynamic Compression Plate (DCP) was introduced in 1969 [8]. The idea of this plate was to enhance stability of fixation by interfragmentary compression and load transfer by friction (Fig. 29.3a-c). To improve periosteal vascularity underneath a plate, in a first step the plates were undercut as far as safe application of the plate screws would allow without exceeding the compressive strength of the underlying cortical bone. The Limited Contact Dynamic Compression Plate (LC-DCP) which is still in clinical use was the first implant modified to preserve the bone circulation [12, 78, 79]. Nevertheless, some contact between bone and implant is still needed to allow load transfer by a friction force at the interface created by tightening the screws.

The next step consisted in minimizing the plate-bone contact to isolated points only. With the Point Contact Fixator (PC-Fix) the plate is not compressed towards the bone. The isolated contact points between the plate holes serve only to hold the plate at a distinct distance from the bone surface as soon as the screw heads engage in a conical non-threaded plate hole [80]. With the PC-Fix the load transmission is based on the partial interlocking of the screw heads in the plate holes. Thus, the amount of contact of the implant remains very small and without any adverse biological or mechanical effects to the underlying bone (Fig. 29.4).

Nowadays, conventional plating is increasingly replaced by using internal fixators. Internal fixators are "plates" (splints) with completely locked screw heads. These implants are not pressed onto the bone and do not need any contact between implant and bone. Further advantages are the possible reduction of the screw length to monocortical dimension with the advantage not to need screw length measurements and the possibility of using self-drilling and self-tapping screws.

The Less Invasive Stabilization System (LISS) was the first internal fixator of the AO-ASIF conceived for the meta- and epiphyseal regions of the distal femur and proximal tibia (Fig. 29.5). Its shape conforms to the anatomical contours of the specific area of the bone and is designed for application via a minimally invasive submuscular approach. First step is the anatomic reconstruction of the articular component followed by the restoration of the correct bone axis in all planes using the femoral distractor [81, 82].

A further development is the Locking Compression Plate System (LCP) which offers the advantage that the surgeon can choose during the operation whether to use it with conventional (non-locked) screws, with locked screws, or with a combination of both [83]. The specific design of the plate hole shows two functional elements:

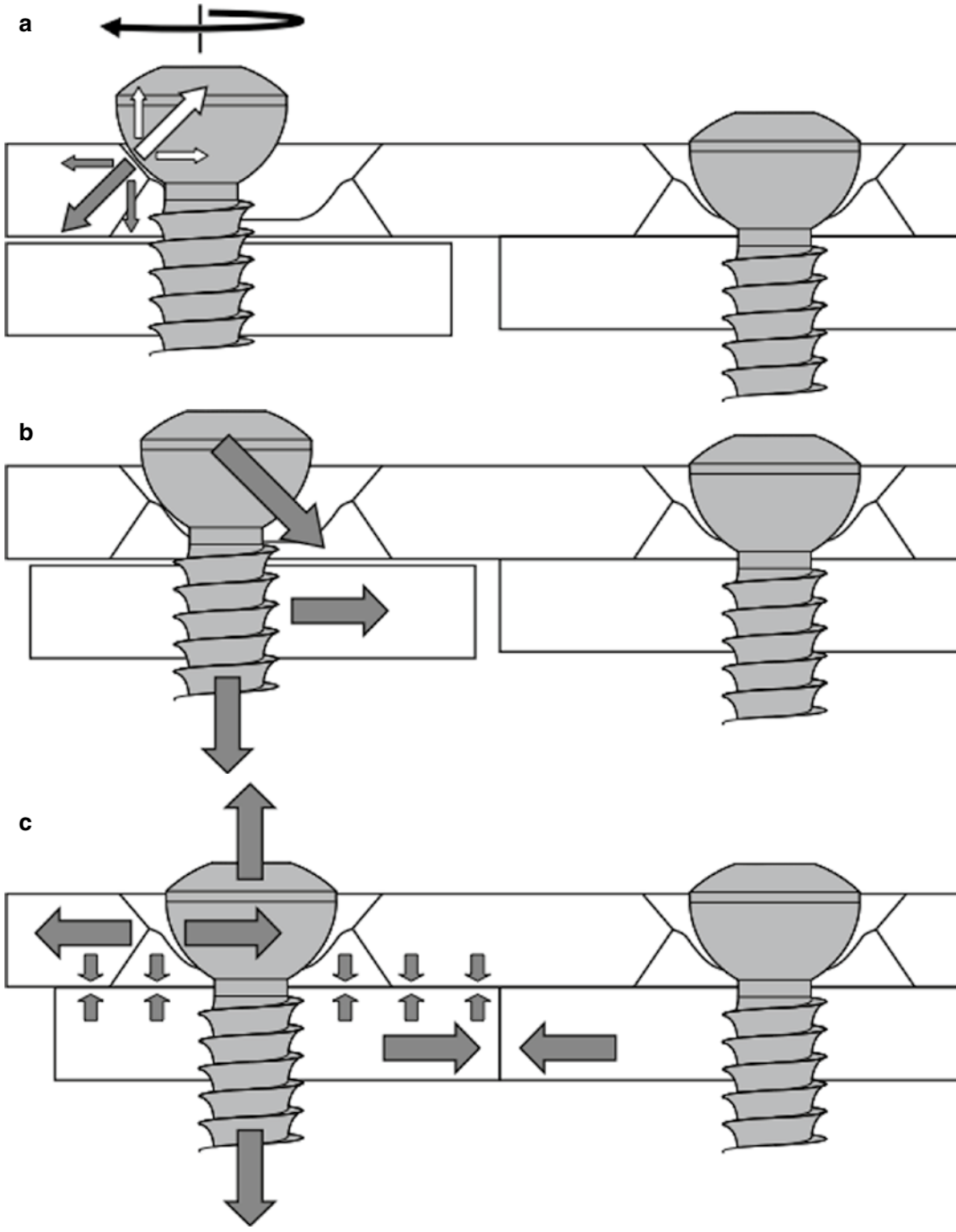

Fig. 29.3 Mechanism of dynamic compression. When a plate screw is inserted eccentrically (**a**) the screw head slips down along the oblique part of the CD-hole (**b**). By tightening the screw compression in the fracture plane and friction at the interface bone-implant is created (**c**)

The first half of the hole comprises a dynamic compression unit that is intended for a standard cortical or cancellous bone screw. As in standard DC-plating technique the eccentric screw insertion allows an axial compression at the fracture site to be achieved. Additionally, the screw can be angulated with respect to the longitudinal and transverse plate axis. The second half of the

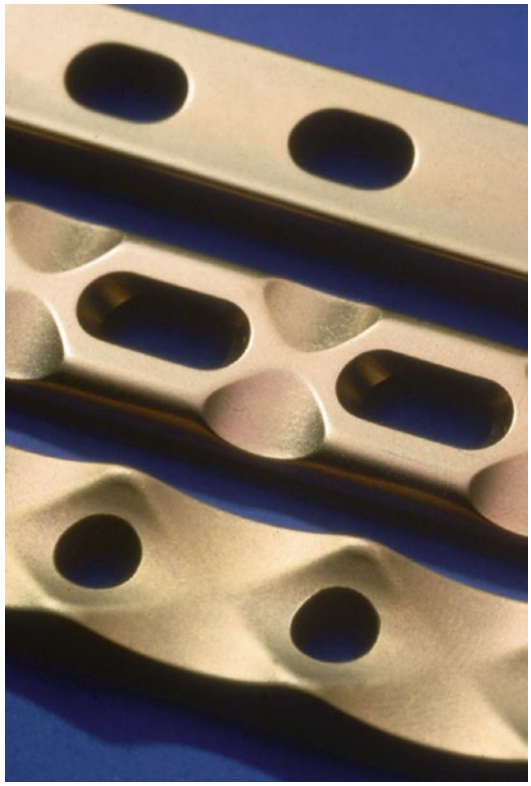

Fig. 29.4 Undersurface of different plates. The undersurface of a conventional dynamic compression plate (DCP), the limited contact dynamic compression plate (LC-DCP), and the point contact fixator (PC-Fix) is shown

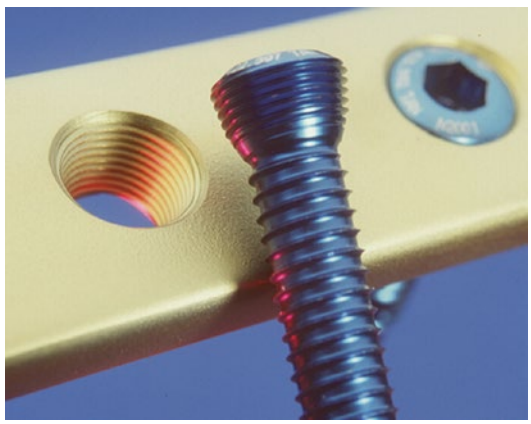

Fig. 29.5 Less invasive stabilization system (LISS). The screw head and the plate hole have a conical thread. This construction composes a tight and fix angle connection between plate and screw

hole is threaded and conically shaped permitting the locking of the special locking head screws (Fig. 29.6a-c). The conical shape of the threaded screw head stops the tightening well before the thread within bone sustains critical loads. This in addition eliminates plastic deformation of the screw while tightening and equally excludes the reported high incidence of screw failures during insertion of conventional screws. No contact between bone and implant is needed for load transmission. The angular stability of the screws results in a lower incidence of screw loosening and secondary displacement of the fracture fragments. In addition, the protection of the periosteal blood supply is superior and in subcutaneous and submuscular plating techniques there is no need for accurate contouring of the plate [84–86].

Due to the surgical needs for plate-screw systems allowing locking of the screws in different directions other systems were developed. The plate hole of the Variable Angle Locking Compression Plate has four columns of threads providing four points of locking between the Variable Angle LCP and the variable angle screw, forming a fixed-angle construct at the desired screw angle (Fig. 29.7a, b). Screws can be angulated anywhere within a 30° cone around the central axis of the plate hole (Fig. 29.8a, b). The variable angle LCP combi hole combines a dynamic compression hole with a variable angle locking screw hole and provides flexibility of selecting either axial compression or variable angle locking in the same plate hole.

Another technical solution is found with the noncontact bridging plate (NCB) technology allowing polyaxial screw placement with screw locking achieved through the use of locking caps that are threaded into the plate holes. Nevertheless, due to the fact that the locking of screw with the locking cap is performed after screw tightening the biological advantage of a no contact system can be abolished (Fig. 29.9). On the biomechanical side all this variable angle screw locking system are as safe as the plate systems with fixed angle locking screws [87–89].

Load Transfer in Conventional Plating

In a conventional plating technique, insertion and tightening of the plate screw generates an axial screw force (F_a), which compresses the plate onto

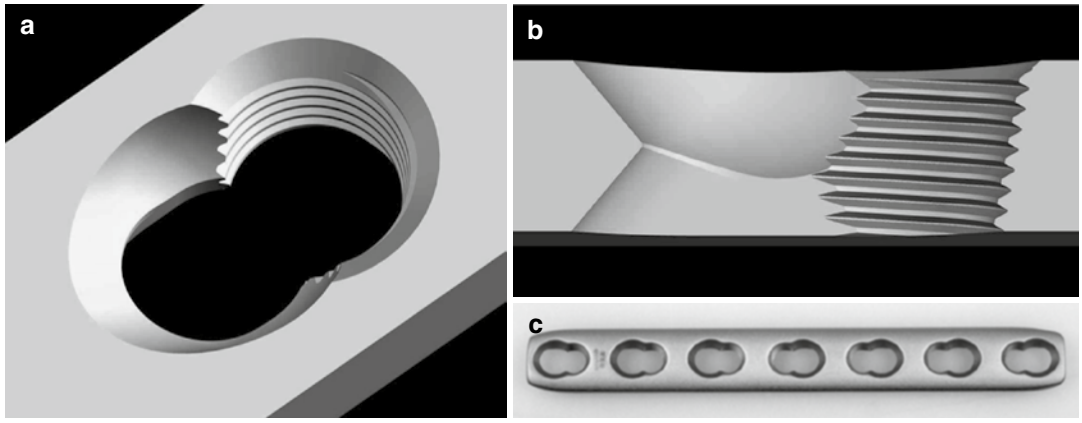

Fig. 29.6 Locking compression plate (LCP). The locking compression plate is a further modification of the dynamic compression hole. The one half consists of a regular dynamic compression hole; the other half is conical and threaded (**a**, **b**). Standard cortical or cancellous bone screws as well as locked head bone screws can be inserted according to the surgeon's preference and the mechanical demands of the fixation. The LCP is an asymmetrical plate with a defined middle section of the plate (**c**)

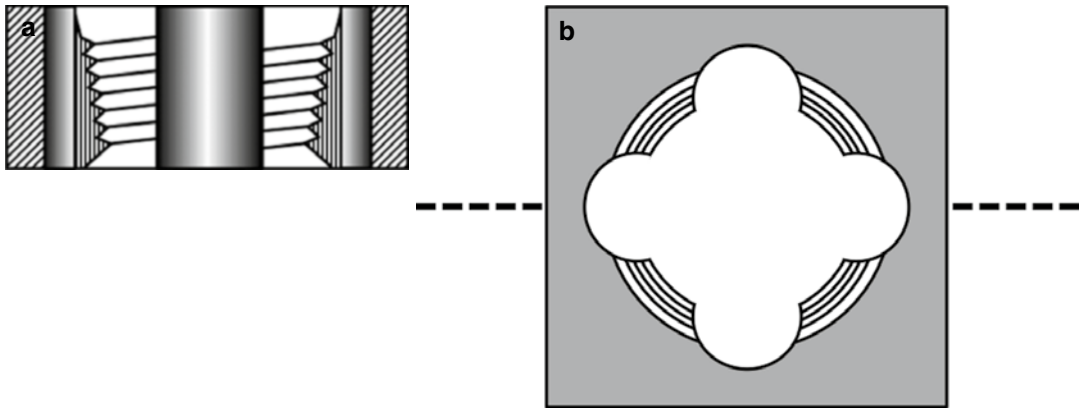

Fig. 29.7 Variable Angle Locking Compression Plate. The section through the plate hole shows that the plate hole is partially threaded (**a**). The view from above shows the four columns of threads providing corresponding four points of locking between the screw head and the plate (**b**)

the bone surface. This compression leads to a friction force (F_f) at the interface bone-implant. The friction force is proportional to the amount of compression with the specific bone-implant coefficient of friction (ρ) as a constant of proportionality. Under functional loading, a plate osteosynthesis is loaded mainly in bending and in axial load. These loading patterns tend to displace the plate with regard to the bone. As soon as the external load (F_e) exceeds the amount of friction force installed at the plate-bone interface, the plate will slip on the bone (Fig. 29.10). Under stable conditions, the screw is mainly loaded in tension. Once the plate starts slipping on the bone surface an additional bending moment at the screw head-screw shaft junction is present [77]. The advantage of the conventional plating is the possibility to angulate the screws with respect to the plate surface (Fig. 29.11). The disadvantage is that with time the axial screw force is diminished due to bone remodelling around the screw threads leading to a corresponding decrease of the friction force at the bone-implant interface. In addition, in osteoporotic bone the maximum screw force that can be obtained by screw tightening can be very low from the beginning resulting in a low friction force and later instability.

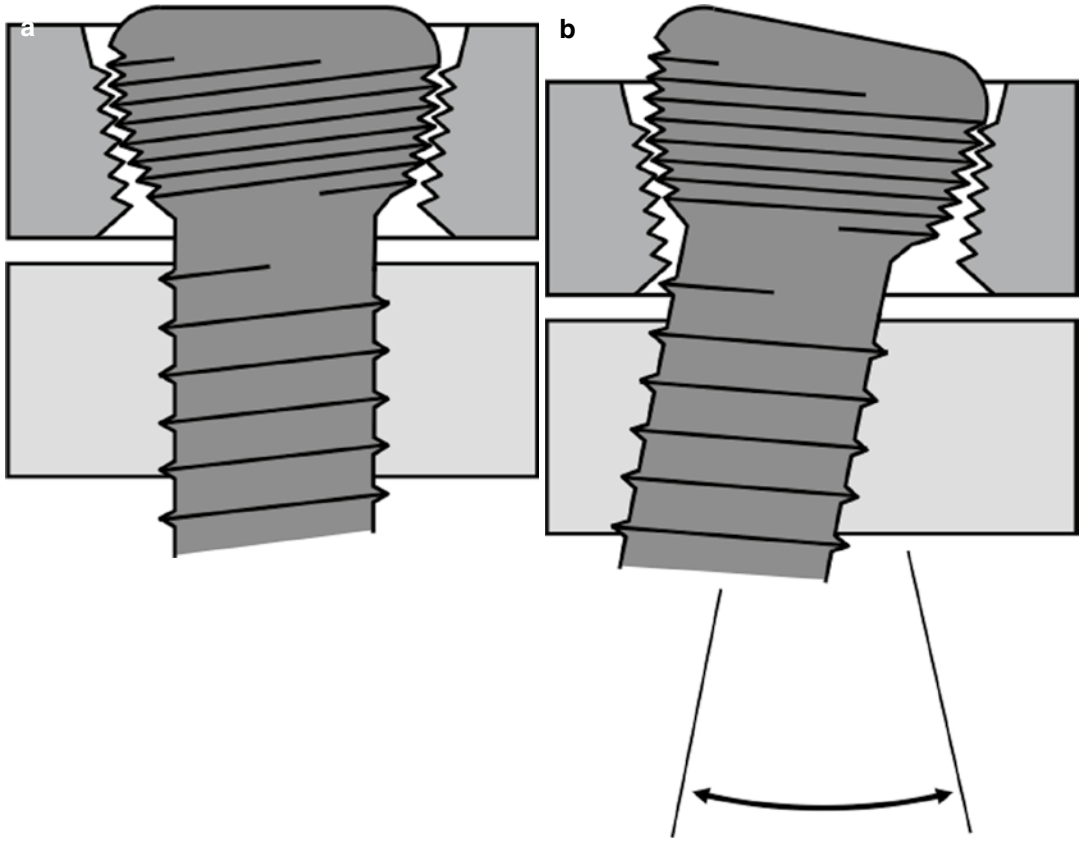

Fig. 29.8 Variable Angle Locking Compression Plate. The section through the plate hole shows that with screw insertion perpendicular (**a**) or oblique (**b**) to the plate surface only small part of the threaded spherically shaped screw head and the conically shaped threaded plate hole are kept in contact assuring on the the tight locking and allowing angulation of the screw with respect to the plate surface

Load Transfer in Locked Screw Head Plating

In contrast to the conventional plating technique, in "locked screw head" plating no contact between implant and bone is needed for load transfer from one main fragment to the other. Therefore, no friction force is generated by axial screw force at the interface bone-implant to withstand the displacement forces. Mechanically this so-called internal fixator is defined as a construct in which the screws are the principal load-transferring elements from the main bone fragments to the implant. In such a construct the screws are firmly locked to the internal fixator to allow for moment and force transfer (Fig. 29.12). Thus, the longitudinal displacement forces acting on the construct are directly transferred from the bone to the implant by bending and shear across the screw neck [45, 80]. The advantage of the locked screw head is the change of the mechanical loading condition of the screw, which now is mainly in bending and less in axial pull-out. The disadvantage is the complete loss of the surgical feeling of screw tightening. Even in weak bone, the threaded screw head engages firmly inside the plate giving false information about the holding of the screw inside the bone. The former disadvantage of the fixed angle screw direction inside the LCP is resolved with the newer generation of Variable Angle Locking Compression Plates.

Plate Fixation in Osteoporotic Bone

In osteoporotic bone the commonly recommended fixation concepts fail, because bone quality is poor. Holding power of each screw in conventional plate osteosynthesis is decreased leading to the problem of early pullout of screws and secondary fracture displacement. A possibility to enhance the quality of fixation is the use of bone cement. Bone cement can be used around blade plates to diminish the danger for cut-out and around the intramedullary part of the screws to enhance the holding power. In such a case, two screws should be angulated to each other and the intramedullary space in between should be filled with bone cement (Fig. 29.13). After polymerization the screws are tightened. The pairwise obliquely inserted screws give a very stable fixation of the plate.

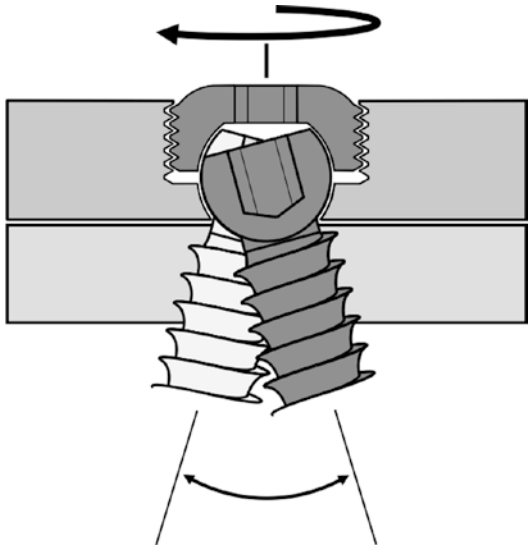

Fig. 29.9 Noncontact Bridging Plate (NBC). Plate screws can be inserted with some angulation with respect to the plate surface. Locking in the final screw position is achieved by tightening locking caps creating high friction force between the cap and the spherically shaped unthreaded screw head

In osteoporotic bone fracture fixation using the internal fixator concept seems to be advantageous, because stability of fixation does not rely on an axial screw force creating a friction force at the implant-bone interface, but on locked screws loaded mainly in bending during functional loading.

Another possibility to increase the holding of screws in osteoporotic bone is the use of "schuhli nuts". Schuhli nuts are placed underneath the plate and have an identical thread like the conventional cortical screws. Tightening the screw locks it within a plate hole creating an angular stability of the screw-plate-schuhli construct with

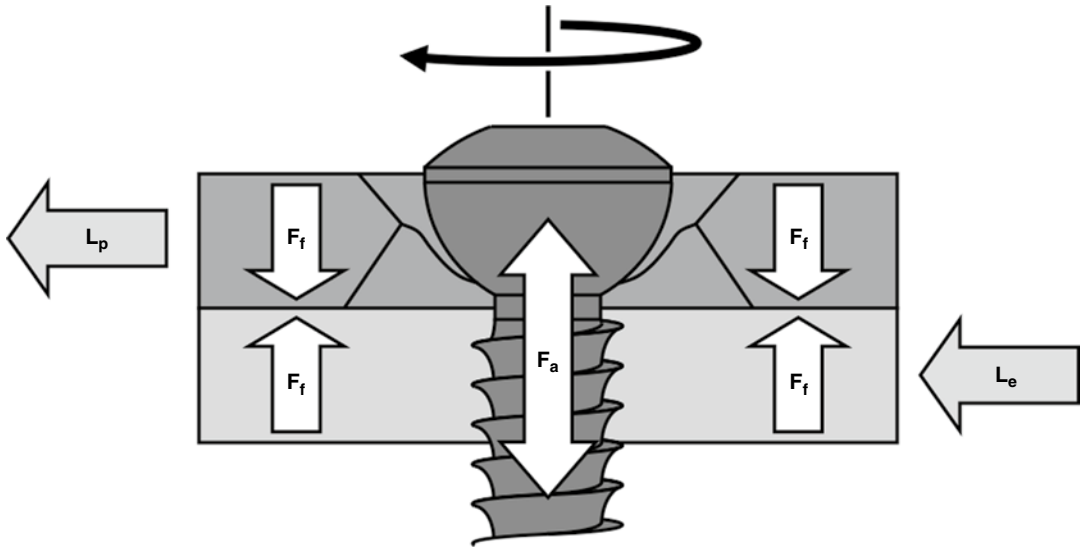

Fig. 29.10 Load transfer in conventional plating. Tightening of a conventional plate screw results in tensile load of the screw and in compression at the interface bone-implant. This in turn creates friction at the interface able to withstand external loads tending to displace the plate on the bone surface

enhanced holding power (Fig. 29.14). The advantage of the schuhli nuts is avoiding the potential adverse effects of bone cement on fracture healing with extravasation and thermal necrosis [90–92]. But, the fiddling factor of the schuhli nuts is more important than with the use of a locking screw head system (LCP, LISS).

Mechanical Characteristics of Plates

Most plates used for osteosynthesis are still metallic implants (stainless steel or titanium). The availability of the material and more important the excellent mechanical and biological properties of metals are the main reasons for its widespread use in internal fixation. Metals offer on the mechanical side high stiffness and strength to withstand deformation or fatigue failure, sufficient ductility to allow shaping of the implant, corrosion resistance and on the biological side good tissue compatibility without localized toxic reactions [93–96].

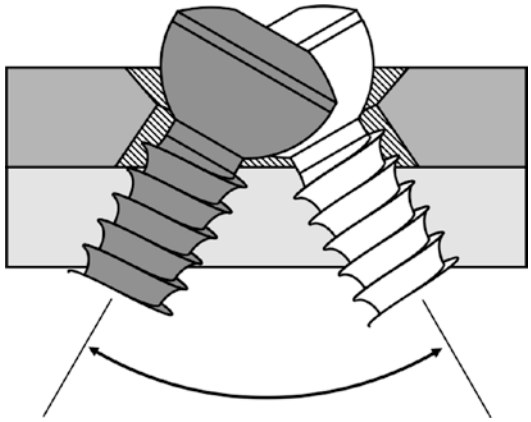

Fig. 29.11 Adjustment of plate screws in conventional plating. The advantage of conventional plate screws is the potential to be angulated with respect to the longitudinal and transverse axis of the plate

According to Hooke's law the relationship between stress and strain is linear for all materials up to the proportional limit ("ut tensio sic vis" Robert Hooke 1676). The slope of the curve is a measure for the stiffness of the material; it is high in rigid implants and low in flexible implants. In the following short part of the stress–strain diagram deformation of the material is still elastic, but disproportional until the elastic limit is reached. At the yield point plastic deformation (creeping) of the material occurs without a substantial change of the stress magnitude. Elasticity means that the material regains completely its original dimensions upon removal of the applied forces. With further loading a plastic and irreversible deformation of the material occurs. Materials capable of withstanding large strains are referred to as ductile materials; the opposite applies for brittle materials. In osteosynthesis ductile materials are needed to allow shaping and contouring the implants. The highest point of the diagram is called the ultimate strength of the material. The endpoint of the diagram is given by the failure of

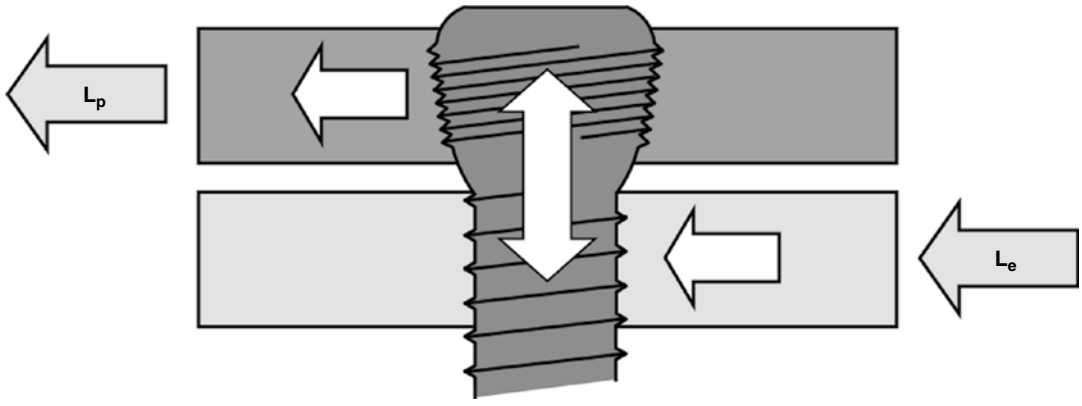

Fig. 29.12 Load transfer in locked screw head plating. When the locking screw is tightened, the thread of the screw head engages in the conical threaded hole of the plate providing a stable construct between the plate and the screw. The external load is not transferred by a friction force at the interface but by interlocking. This in turn results in a bending moment at the screw-head-screw-shaft junction

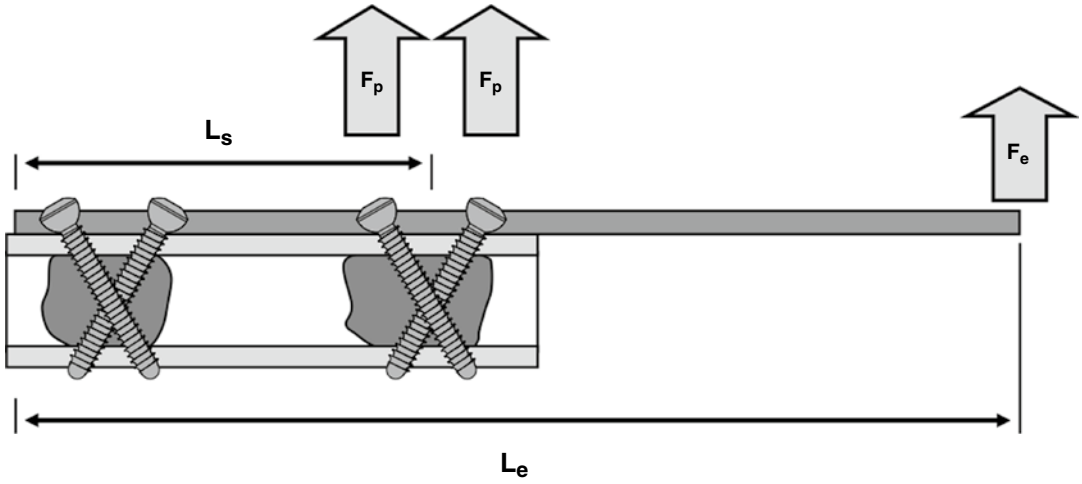

Fig. 29.13 Screw fixation in osteoporotic bone. In osteoporotic bone the holding power of conventional screws is weak leading to only small friction at the interface with later risk of secondary displacement and screw pullout. To enhance the holding power of the screws, two paired screws should be angulated and the intramedullary cavity in between filled off with bone cement

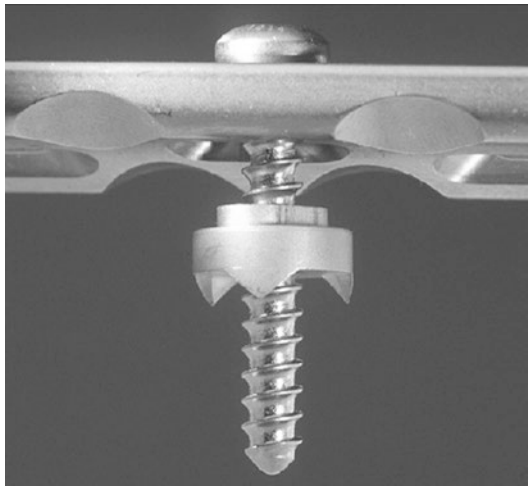

Fig. 29.14 Schuhli nut. The schuhli nut is some sort of a threaded washer, which is positioned underneath conventional DC-plate. By tightening of the screw the nut is pulled towards the plate creating an angular stable system with enhanced holding

the material where the elongation at rupture can be defined. The term strength defines the limit of stress that a material can withstand without rupture; it determines the level of load up to which the implant remains intact (Fig. 29.15).

Regularly, all implants are repetitively loaded well below the ultimate strength of the material. Thus, much more important than the ultimate strength of the material is the fatigue behaviour of the implants. The relationship between stress magnitude and number of loading cycles is described by Wöhler's curve (Fig. 29.16).

Beside the pure mechanical characteristics of implants its surface structure is important in respect to tissue adherence which may prevent formation of a fluid-filled dead space surrounding the implant promoting growth of bacteria [95, 97–99].

Mechanics of Osteosynthesis Using Plates or Internal Fixators

Loading of the screw

In conventional plating technique the screw is regularly loaded under tension. The pullout force depends on bone quality, cortical thickness and outer diameter of the screw. Neither the depth nor the pitch of the thread has an important influence on the holding power of a screw. Pullout of a screw is characterized by the avulsion of a bony

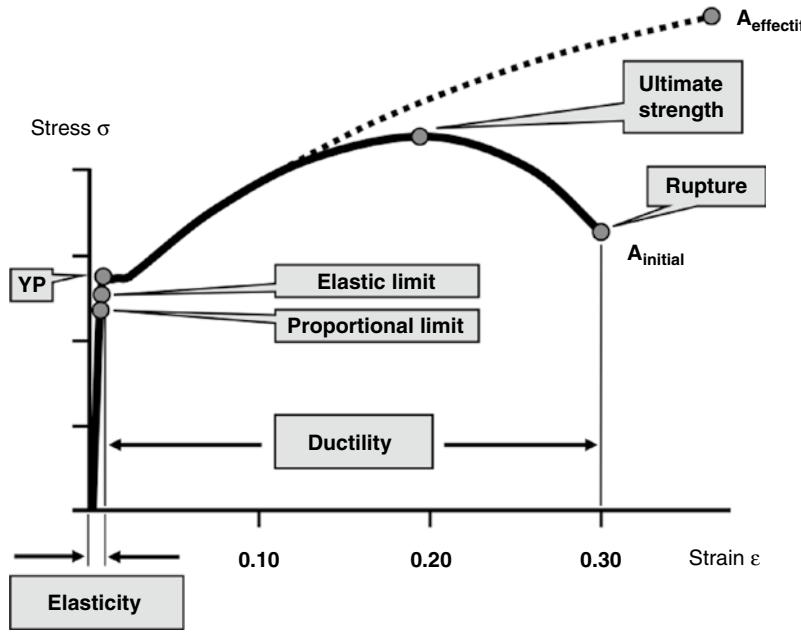

Fig. 29.15 Stress–strain diagram. The diagram describes the behaviour of a material under tensile load. Stress and strain are proportional up the proportional limit. The elastic modulus of the material is the constant of proportionality. Up to the elastic limit, a short part of further elastic, but disproportional deformation of the material is observed. With further loading plastic and irreversible deformation occurs. The yield point is characterized by a creeping of the material, i.e., elongation without an increase of the stress. The ultimate strength is defined as the highest stress tolerated by the material without failure (calculated for the initial cross-section). Failure occurs after further plastic deformation; at that point the elongation at rupture can be determined

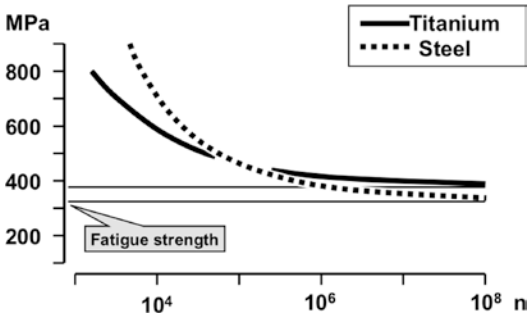

Fig. 29.16 Fatigue strength of materials. The fatigue behaviour of an implant is much more important in internal fixation than the ultimate strength. During functional rehabilitation until the bone has healed cyclic loading of the implant occurs with the risk of fatigue failure of the implant. The higher the stress the less loading cycles are tolerated by a given implant. The fatigue strength is defined as the asymptotic line of the so-called Wöhler curves (stress-loading cycle diagram). For high stresses a steel plate withstands more loading cycles than a titanium plate. For low stresses the resistance of titanium against fatigue failure is higher

cylinder around the screw due to shear forces at the interface bone implant (Fig. 29.17a, b).

Locking head screws need no contact between plate and bone for load transfer. Using this technique the screw is mainly loaded in bending (a). Thus, with an increasing distance between the bone surface and the plate underface (b) the bending moment as well as the screw loading increase (Fig. 29.18a, b).

The holding power of unicortical screws can be critical in bone segments loaded mainly under torque (e.g., humeral shaft). With a thick bone cortex (a) the tendency for rational displacement of the fragments is low, whereas a thin cortical thickness (b) increases the risk for rotational displacement. This phenomenon is explained by the different working length of a thick (c) and a thin (d) cortex. In case of a thin bone cortex or when plating bone segments loaded mainly in torque the use of bicortical screw is recommended

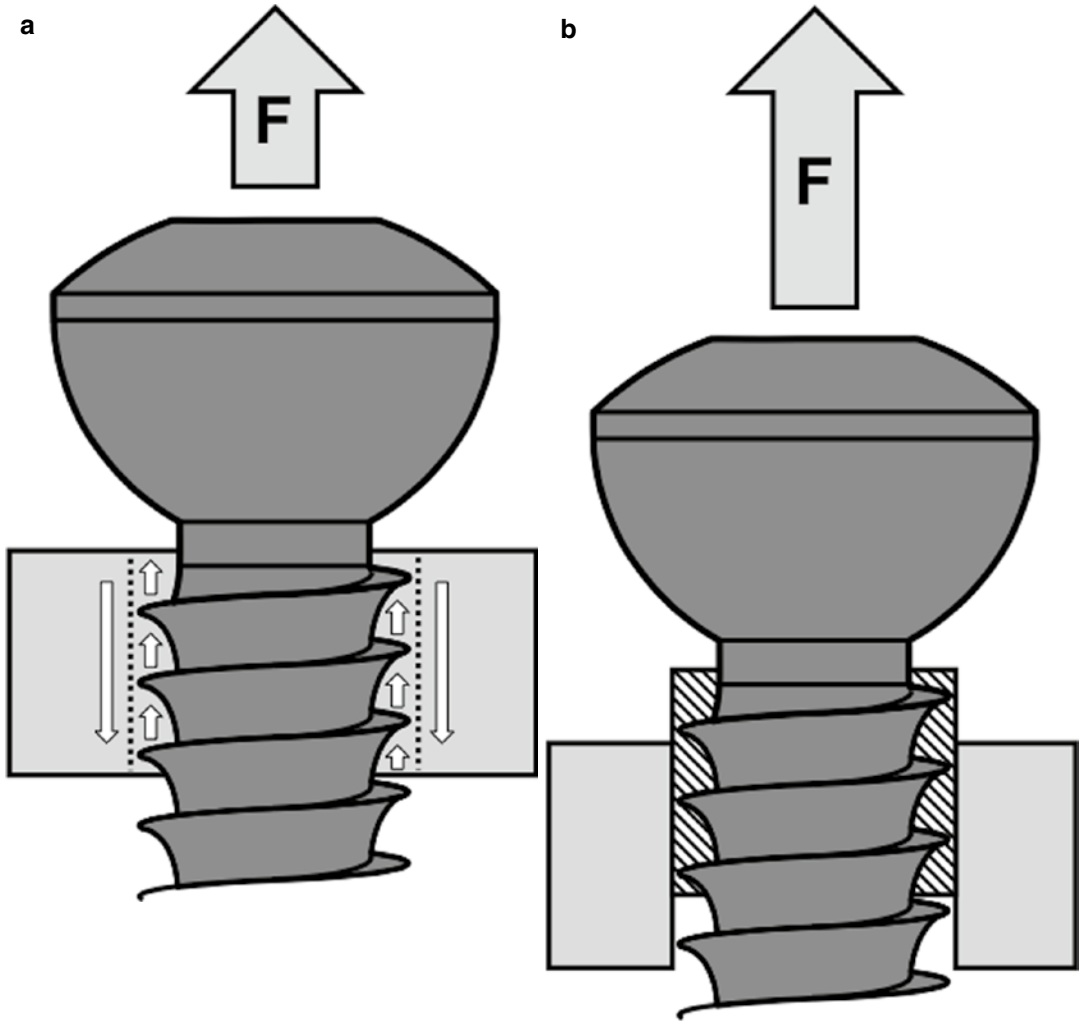

Fig. 29.17 (**a**) Pullout of a screw. Under tension the interface between bone and outer screw diameter is loaded in shear. (**b**) Thus, the pullout force is proportional to the bone quality, the thickness of the bone cortex and outer circumference of the screw

to increase the working length of the screws (Fig. 29.19a-e).

Effect of Plate Length on Screw Loading

In plate osteosynthesis the length of the plate and the position of the plate screws play an important role with respect to plate and screw loading conditions. The longer the splint is, the less pull-out force is created on the screws due to improvement of the working leverage of the screws (Fig. 29.20a-d). Thus, when using a plate as a splint the use of a very long plate is important from the mechanical point of view [26, 100, 101]. With the newer subcutaneous and submuscular plating techniques the surgical dissection to insert long plates is not increased, thus the mechanical advantage of the use of longer plates has no biological disadvantage [11, 15, 18, 21, 26, 30, 32, 102]. Using an internal fixator with locked screw heads, the screw loading is mainly in bending and not in pullout. With an external bending moment all the screws are loaded at the same time and thus, failure is less frequent (Fig. 29.21a, b). Nevertheless, the working leverage of an internal fixator should also be kept long and spacious.

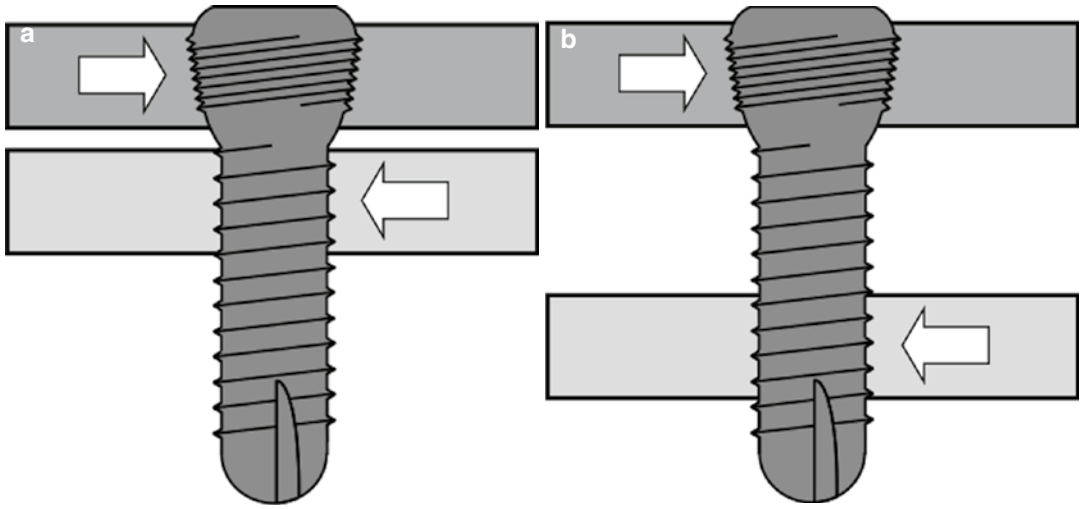

Fig. 29.18 (**a**) Loading of a locking head screw. The locked screw is mainly loaded in bending. (**b**) The higher the distance between plate and bone the higher is the bending moment and thus, the screw loading

Effect of Screw Position on Plate Loading

Bridging a longer bone segment in the middle of the plate over the fracture area reduces the implant strain due to bending. Bending a plate over a short segment enhances the local strain inside the implant. Bending over a longer segment reduces the local strain that results in a protection effect against fatigue failure of the implant. But, this beneficial effect only holds true under the condition that there is a distance limitation at the opposite cortex due to interference with bone fragments. When this is not the case the plate deforms according to the externally applied bending moment and the plate loading is not influenced by the gap width (Fig. 29.22a-e). Thus, in compression plating with the load sharing condition of plate and bone the inner plate screws can be inserted as close as possible to the fracture, the peripheral screws are inserted at each plate end. With locked screw head plating and the mechanical condition of splinting, a longer distance between the two screws adjacent to the fracture is needed to obtain a longer distance and a lower elastic plate deformation [28, 101, 103, 104].

When the stress of the plate due to external loads is small, more loading cycles are tolerated without fatigue failure of the implant. The fatigue strength of the implant is more important than the pure ultimate strength and the stress at rupture of the implant [94].

Effect of Plate Position on Rigidity of Fixation

The concept of load sharing is important for the loading condition and endurance of a plate. When bony contact between the main fragments is achieved after fracture reduction, even broken bone is able to withstand compressive loads leading to partial unloading of the plate. In the composite mechanical system of plate osteosynthesis the plate is firmly connected to bone either by a friction force at the interface or by locked plate screws. Composite structures, such as a composite bone-metal beam, show a different mechanical behaviour compared to individual beams. The rigidity of such a system is much greater than the sum of the rigidity of the individual beams. The composite structure bends in a new common neutral axis lying in between the neutral axes of the two individual beams (Fig. 29.23a, b). In case of different modules of elasticity and different cross-sections of the beams, the new neutral axis is found where the products formed by the axial stiffness and the distance to the new neutral axis of each beam is equalized [93, 105, 106]:

$$(EA)_{plate}(h-z) = (EA)_{bone}\, z$$

E Elastic modulus
A Area of the cross-section
h Distance between the two area centres of gravity
z Shift of the neutral axis of the bone
h-z Shift of the neutral axis of the plate

The composite beam theory determines the mechanical behaviour of two beams under pure bending or eccentric axial load. The axial rigidity of a beam is the product of its modulus of elasticity and the cross-section (EA). The bending rigidity of a beam is the product of its modulus of elasticity and the area moment of inertia with respect to the specific bending direction (EI). The

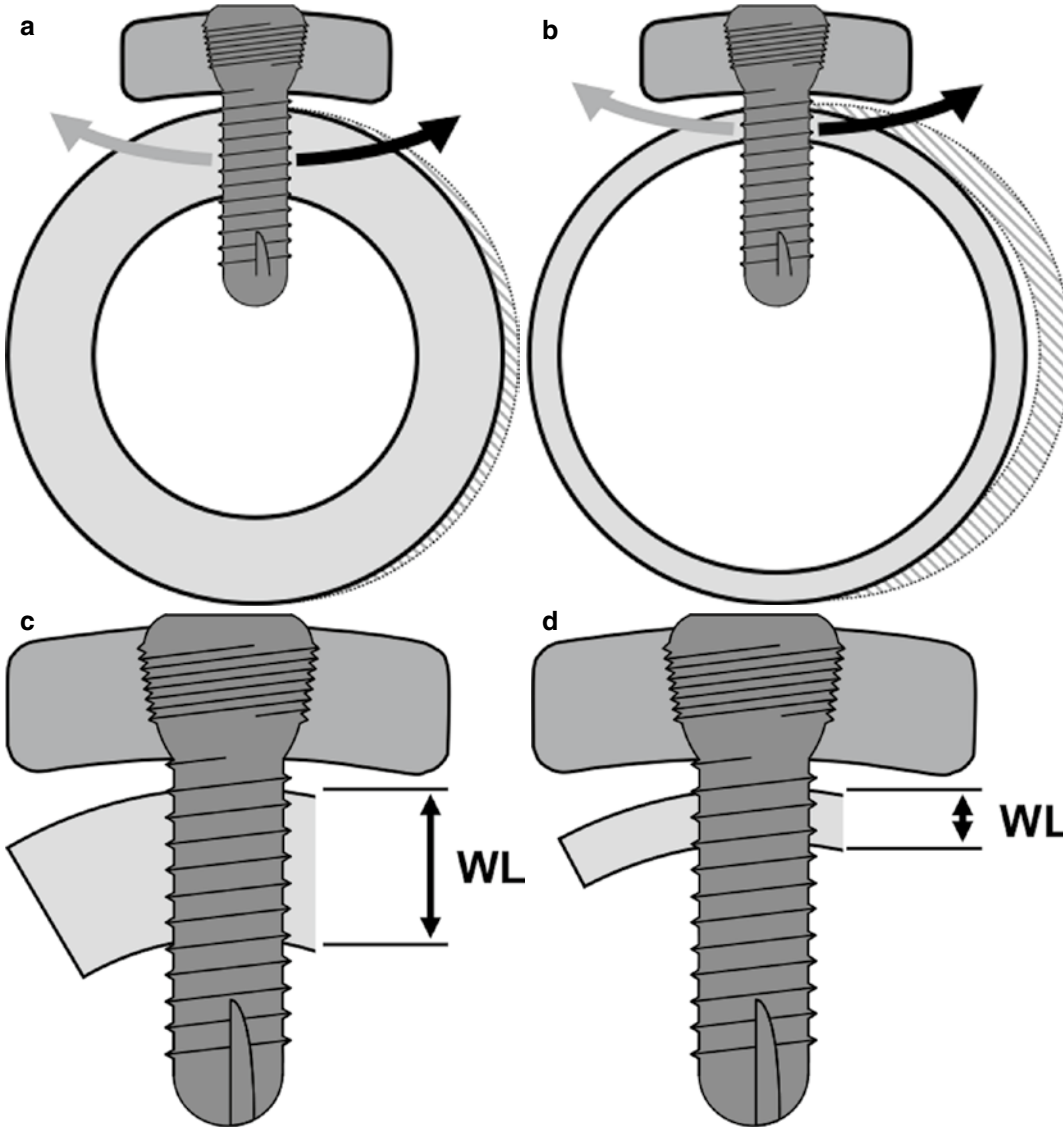

Fig. 29.19 Unicortical versus bicortical screw. The use of unicortical screws should be limited to bone segments loaded in bending or in axial load. Bones mainly loaded in torque create high stresses at the interface between screw and bone with a tendency for rotational displacement (**a**, **b**). Unicortical screws have a relatively short working length which is even reduced in osteoporotic bone having a thin bone cortex (**c**, **d**). Thus, to increase the working length of the screw bicortical screw insertion is recommended in bones loaded in torque or with osteoporotic thin bone cortices (**e**)

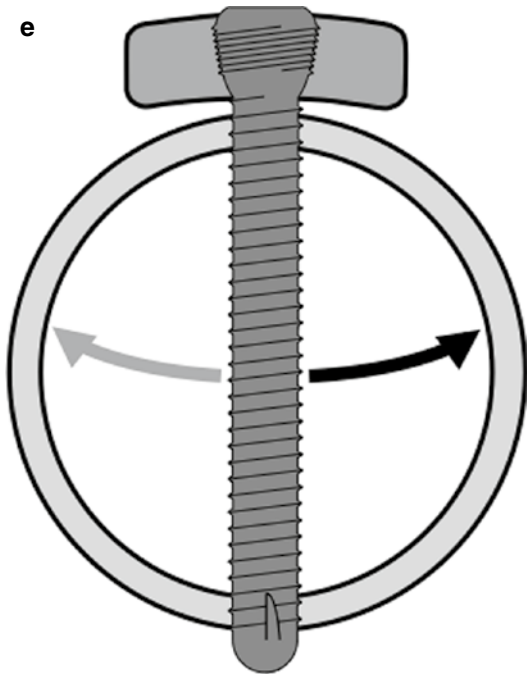

Fig. 29.19 (continued)

stiffness of a composite beam can be calculated using the following formula:

$$EI_{composite} = (EI)_{bone} + (EI)_{plate} + (EA)_{bone} z^2 + (EA)_{plate} (h - z)^2$$

According to the Steiner's principle, the increase in the bending stiffness of the composite beam with respect to the bending stiffness of the individual unconnected beams is mainly caused by the shift of the neutral axis with dramatic enhancement of the area moment of inertia of both, the bone and the implant [93, 96].

A plate has a different bending rigidity according to the individual bending direction (Fig. 29.24). Thus, plate position and bending direction influence the overall stiffness of a plate osteosynthesis. Fig. 29.25 shows the bending rigidity of an intact tubular bone (taken as 100 %), steel and titanium plates and osteosynthesis using steel or titanium plates under different bending direction [106]. It is remarkable that the stiffness of the plate itself is relatively small compared to the bending stiffness of the bone alone. Using either steel or titanium plate, the differences in the modulus of elasticity of the plates are unimportant with regard to the changes in the overall rigidity due to different bending directions. It is evident that a rigid composite system leads to unloading of the plated bone segment with the unloading being highest in the cortex directly underneath the implant [107].

The shift of the common neutral axis in bending can even be more important in wave plate osteosynthesis where the bending stiffness is higher than in conventional plating technique when the cortex opposite the wave plate is in tight contact and loaded in compression. Biologically, the wave plate osteosynthesis is advantageous in case of disturbed vascularity of the bone cortex underneath the plate to allow revascularization of the bone despite a bone plate in situ [19, 108–110].

Effect of Plate Position and Plate Contouring on Plate Loading

The position of a plate influences the amount of plate loading. This is essential when plating is performed in a diaphysis, which is eccentrically loaded such as in the femur. Each eccentric axial load on a beam results in a bending moment of the beam with tensile stress on the one and compressive stress on the other side. For anatomic and mechanical reasons, in the femur the plate is positioned regularly on the lateral side. In case of contact between the main fracture fragments the bone is loaded in compression and the plate in tension. In such a load-sharing situation the load on the plate is low and mainly in tension which is well tolerated by the implant (Fig. 29.26). In case of a comminution without bony contact between the main fragments the laterally positioned plate is the only load carrier and undergoes high tensile and compressive stress due to pure bending (load-bearing situation). Only the rapid formation of callus with integration of the bony fragments opposite to the plate (biobuttress) protects the implant from mechanical overload and fatigue failure. Theoretically, in such a case the loading of the plate can be decreased when positioning the plate on the medial aspect of the femoral diaphysis. In this position the plate is close to the weight bearing axis of the leg and

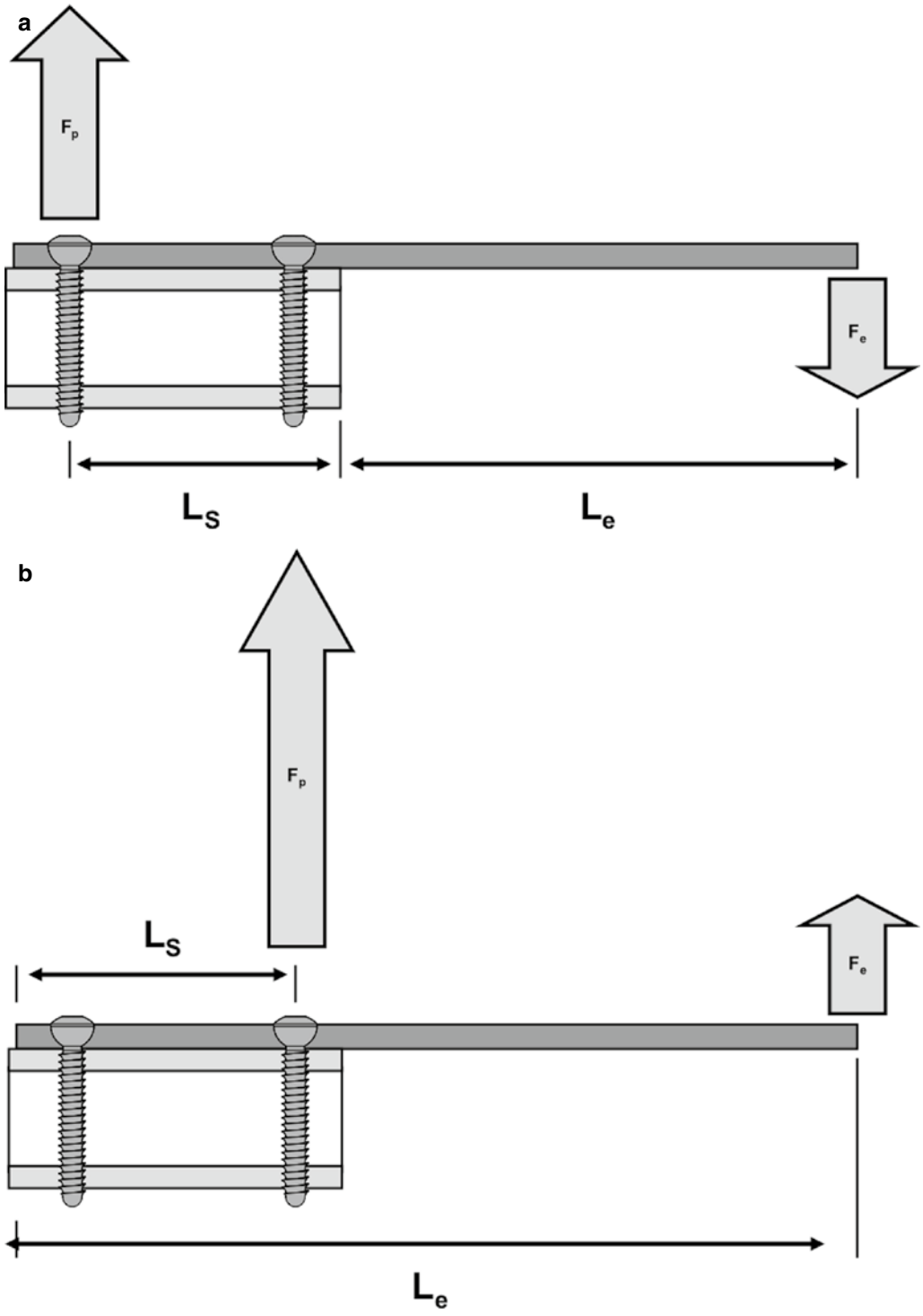

Fig. 29.20 Effect of plate length on screw loading. Bending moment acting on a plate osteosynthesis tends to pullout the plate screws. With a short plate the screw loading is relatively high due to a short working lever arm of the screws (**a**, **b**) for both directions of bending moment (force acting towards the plate or away from the plate). The use of a long plate increases the working lever arm of each screw. Thus, under a given bending moment the pullout force of the screws is decreased (**c**, **d**)

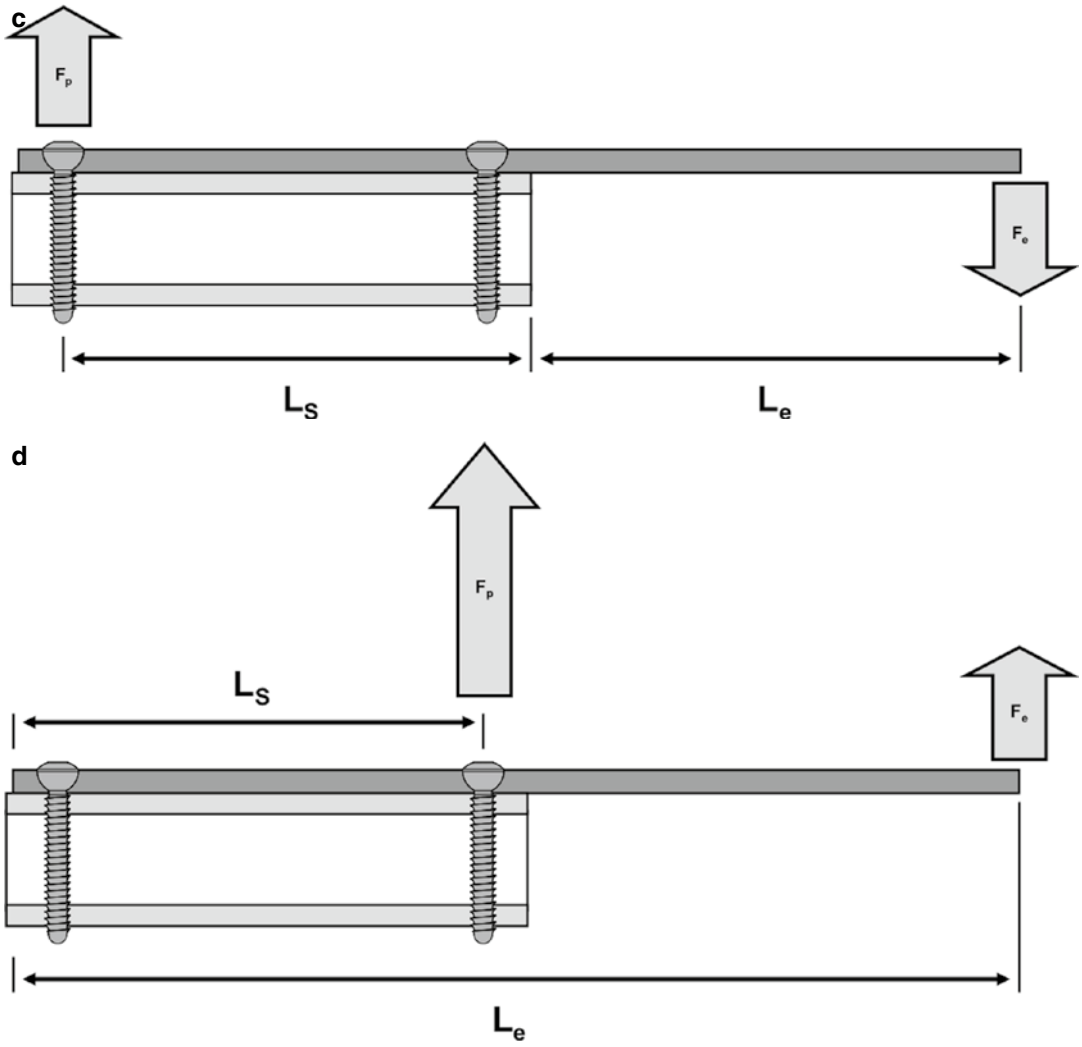

Fig. 29.20 (continued)

therefore, the load on the implant is mainly axial (compressive) and less bending (Fig. 29.27). But, clinically the medial approach to the femur and a medial plating technique is used only when the fracture is associated to a vascular injury needing repair. In osteosynthesis using a wave plate load sharing between implant and bone is even more important than with a regular straight plate. When there is no osseous contact between the main fragments only the lever arm of the externally applied axial load is increased creating even a higher bending moment of the plate than with the use of straight plate. In case of at least partial osseous contact, in addition the lever arm of the wave plate is increased which leads to a reduction of the implant loading (Fig. 29.28).

Clinical Aspects of Plate Fixation

Plate Functions

In clinical practice, plates can be used with different mechanical functions. But, often a combination of different mechanical functions is possible in plate osteosynthesis. Plate functions include:

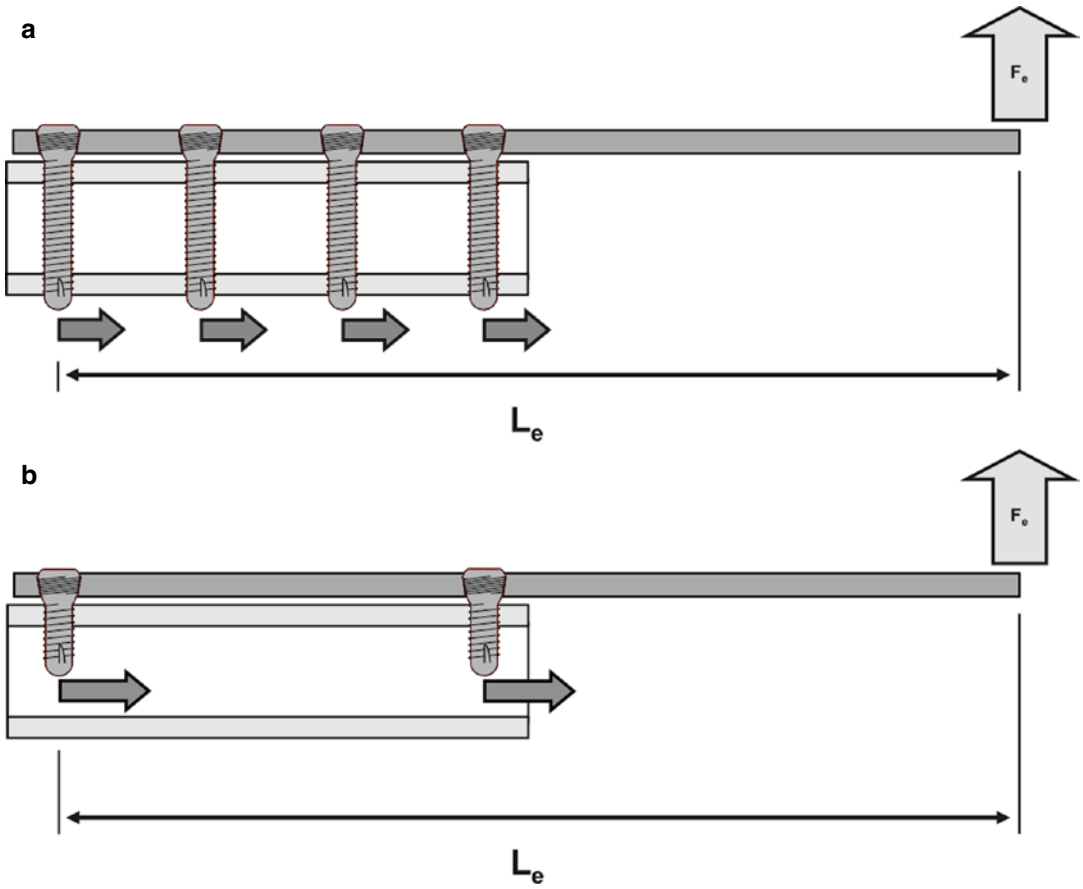

Fig. 29.21 Screw loading in locked head screws. Bending moment acting on an internal fixator with locked plate screws leads to simultaneous bending of all the screws and not to an isolated pullout force on each individual screw (**a**). Thus, resistance against screw failure is improved. This holds true also in case of the use of monocortical selfdrilling screws (**b**)

- Plate as an internal splint
- This is the main function of each plate. It is each time present when a plate is used for internal fixation of a fracture. The efficacy of the splint function depends on the mechanical properties of the splint and the quality of anchorage of the splint to the bone.
- Bridge plate
- The plate spans a comminuted fracture area and provides elastic fixation with the mechanical function of a pure splint.
- Tension band plate
- The plate is applied on the tension side of the bone (e.g., lateral side of the femoral shaft) and must be prestressed in tension in order to create a reversed bending moment which neutralizes the bending moment due to physiological loading. The bone is loaded in static and/or dynamic compression. Thus, load sharing between the plate and the bone is present.
- Compression plate
- Compression can be exerted by the use of the eccentric screw holes, the tension device, or by overbending of the plate.

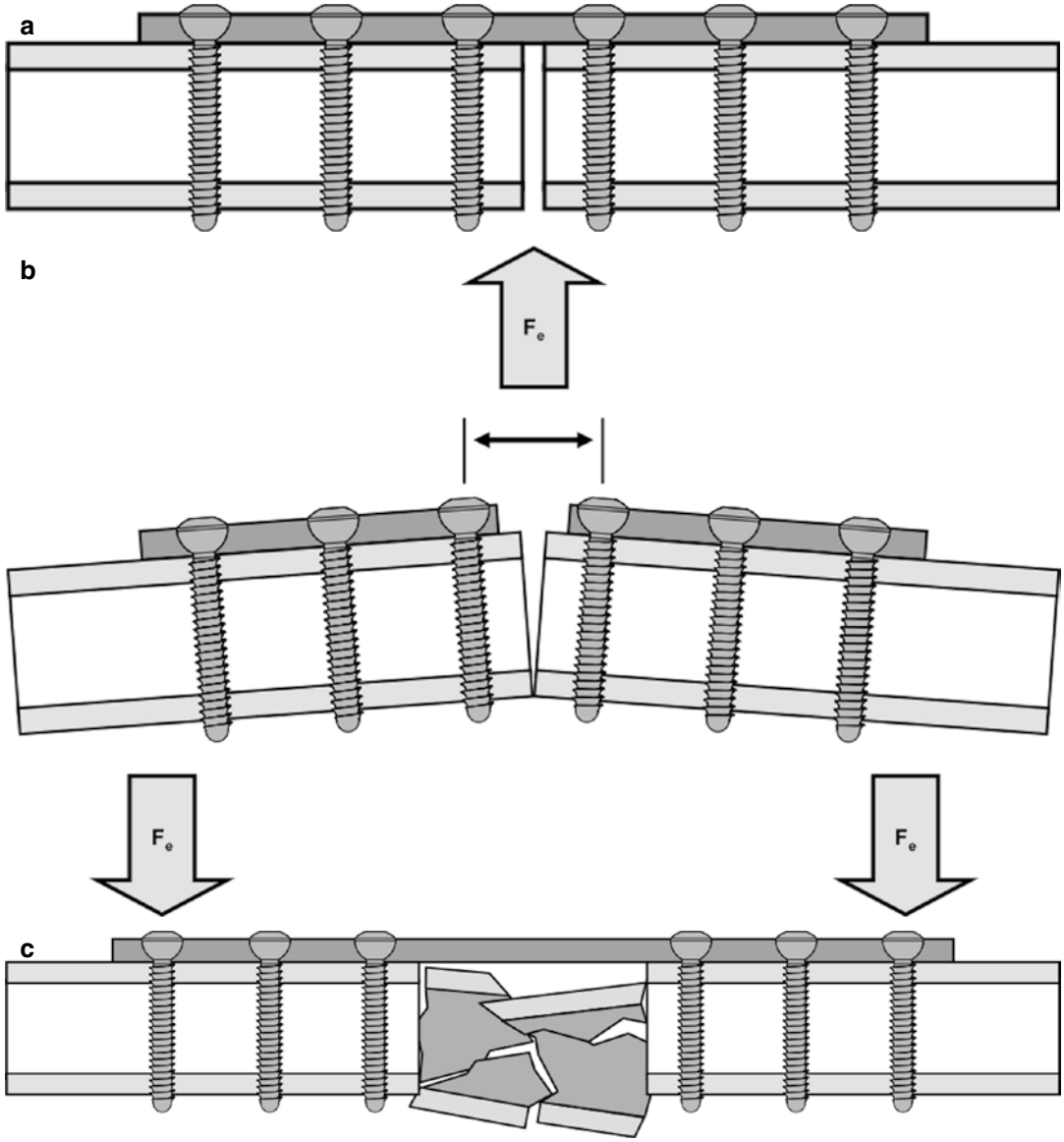

Fig. 29.22 Effect of screw position on plate loading. A small gap after internal fixation using a plate leads to a stress concentration of the implant at the gap site when the plate screws are inserted closely to the gap (**a**, **b**). When a larger gap is present after osteosynthesis the external load results in a stress distribution over a longer segment of the plate with concomitant decrease of the plate loading. This beneficial effect only holds true under the condition that there is a distance limitation at the opposite cortex due to interference with bone fragments (**c**, **d**). When there is no distance limitation the plate deforms according to the external loading and deformation is not influenced by the width of the gap (**e**)

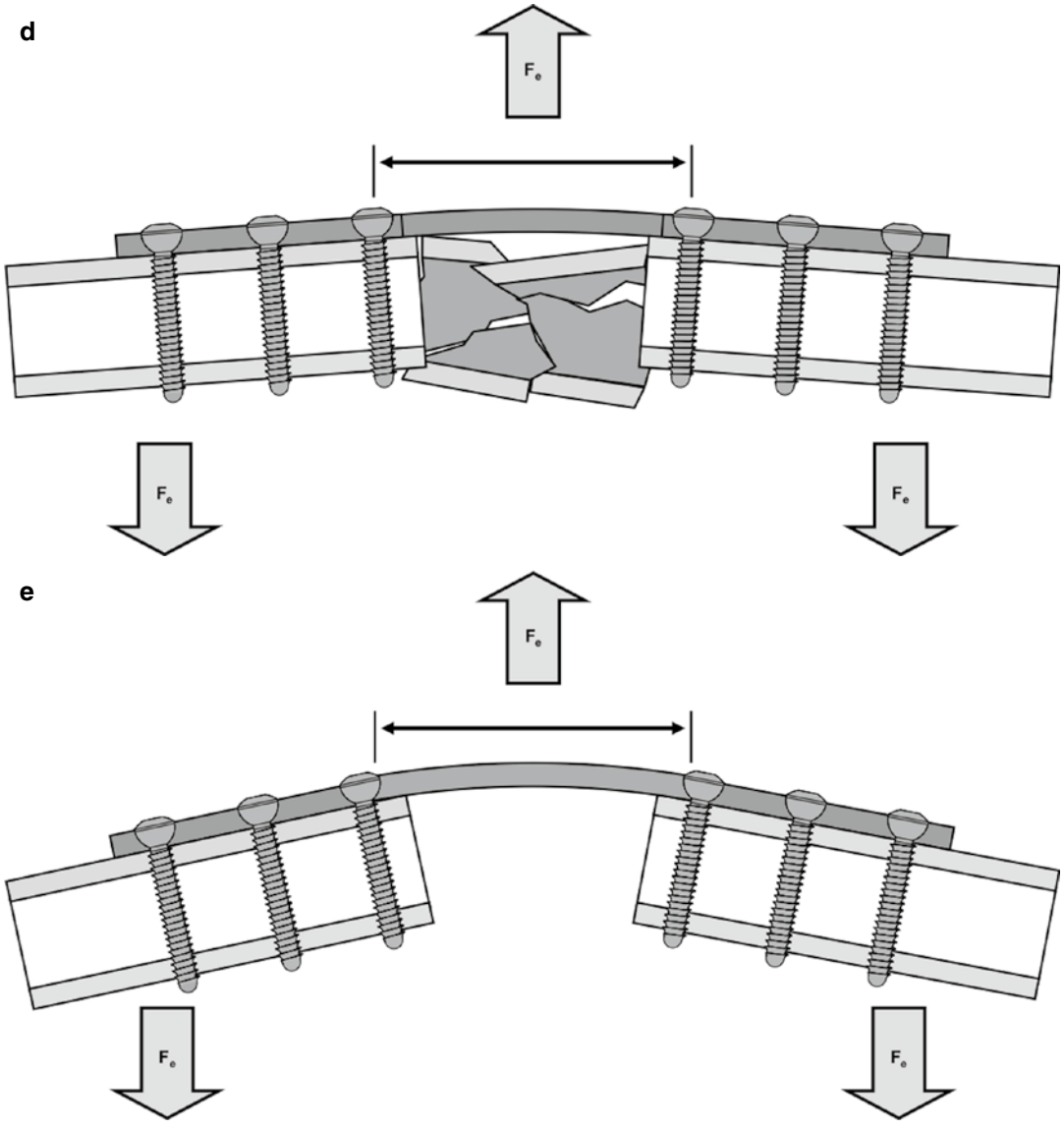

Fig. 29.22 (continued)

- Neutralization or protection plate
- In case of a lag screw fixation of a simple fracture, the additional neutralization of the fracture area by means of a protection plate is recommended. The technique of lag screw fixation and compression osteosynthesis is more and more abandoned due to its inherent risk for surgically induced vascular damage to bone and soft tissues.
- Buttress plate
- The plate supports a piece of bone mainly in the meta- or epiphyseal area.
- Antiglide plate
- The plate is positioned in a way to push a fragment into its anatomical position and to inhibit secondary displacement by a direct interference with a meta- or diaphyseal bone fragment.

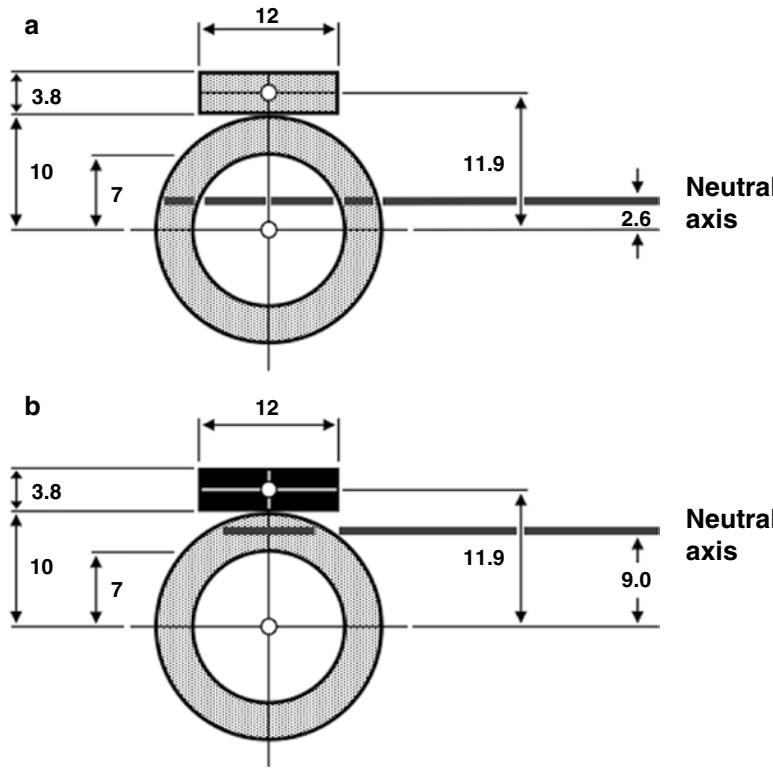

Fig. 29.23 Shift of the neutral axis of a composite beam. The tight connection of two beams (plate and bone) results in a shift of the neutral axis of the composite structure. Using a plate with an elastic modulus of bone leads only to a small shift (**a**). A steel plate with high elastic modulus increases the shift of the new common neutral axis. This shift enhances the area moment of inertia – and with that also the stiffness - of both the plate and the bone (**b**)

Reduction Technique

The technique of direct reduction of a fracture by visualization of the fragments is an invasive and devitalizing way to achieve "anatomical" reduction of a fracture. In diaphyseal fractures today's reduction technique is indirect with a minimal exposure of the fracture and the fragments [46].

Any relatively straight portion of any bone may be reduced by the application of a straight plate. The plate application precedes reduction; it acts as a splint to restore alignment. Distraction of the fracture increases the tension in the soft tissues. This tends to recentralize the fragments, causing them to approximate their previous location in the fractured bone [23]. The disadvantage of this technique is the potential for incorrect reduction when the plate used for reduction onto the implant was initially not shaped accurately to the bone surface (Fig. 29.29a-d). Another mechanism is the reduction through interference along the external surfaces of bone and plate. This principle can be demonstrated during reduction and fixation of a malleolar fracture using the antiglide function of the plate [111]. In case of an oblique fracture, the application of the plate to the proximal fragment results in interference with the distal fragment. As the plate pushes against the displaced distal fragment, it forces the reduction along the oblique fracture surfaces. When using the locked screw head system no reduction of bone fragments onto the implant is possible. The fracture needs to be reduced properly before the internal fixator is inserted to maintain the achieved reduction. In such a procedure, it is advantageous that fracture fragments do not tend to redisplace during screw tightening because the screws engage inside the threaded plate hole without pulling the fragment towards the plate.

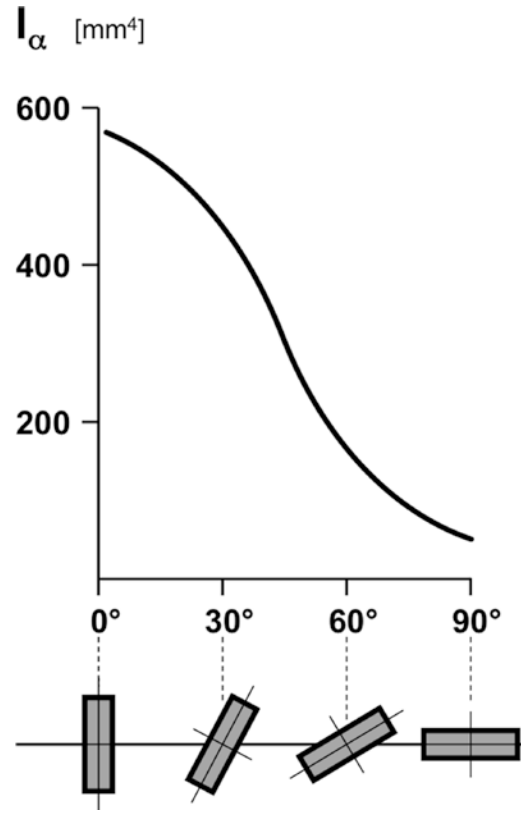

Fig. 29.24 Bending stiffness of plate under different bending direction. The bending stiffness of a plate depends on the direction of the bending moment. Bending towards the highest dimension or bending towards the smallest dimension makes about a factor 8 difference in bending stiffness of the plate

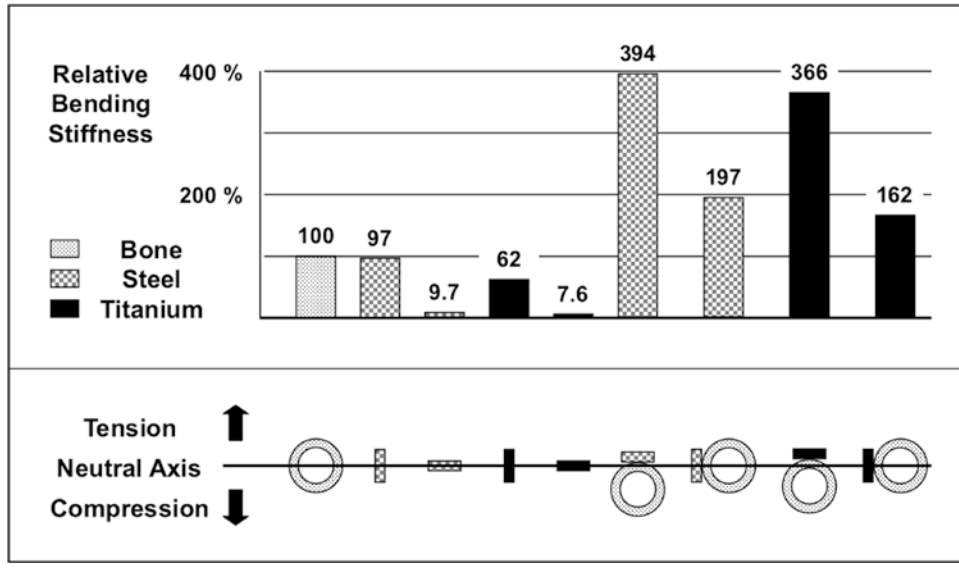

Fig. 29.25 Bending stiffness of plate osteosynthesis. The bending stiffness of a plate osteosynthesis depends mainly on the position of the plate with regard to the bending direction. When the bone can withstand compressive loads the highest stiffness of the composite beam is reached when the implant is positioned on the tension side. The elastic modulus of the plate is unimportant when comparing steel and titanium plates (elastic modulus of steel 190 GPa, of titanium 110 GPa)

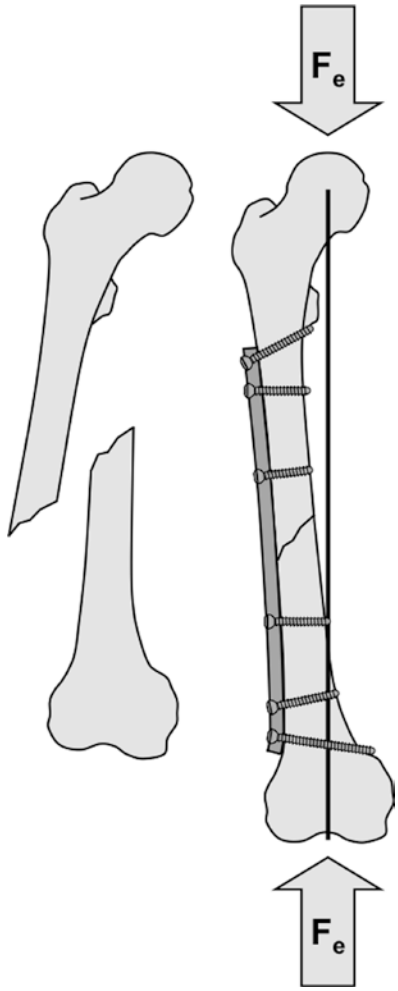

Fig. 29.26 Load sharing situation after femoral plating. In plate osteosynthesis the plate loading due to an eccentric axial load is comparably small when the main fracture fragments are in contact and the bone able to withstand compressive loading (tension band plating)

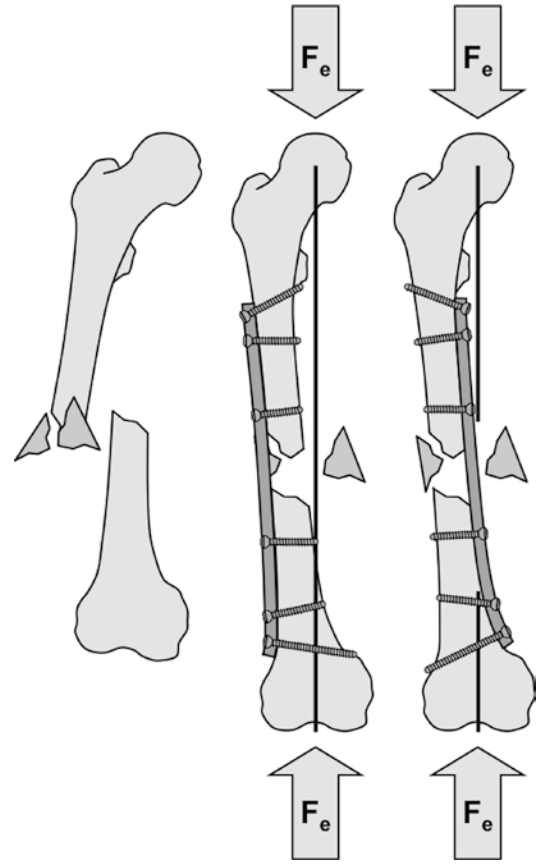

Fig. 29.27 Load bearing situation after femoral plating. In a comminuted fracture pattern the plate is the only load carrier of the osteosynthesis. Due to the distance between the plate and the weight-bearing axis a high bending moment is present resulting in high bending stress of the plate. In such a situation the plate loading can be substantially decreased, when the plate is positioned as closely to the weight-bearing axis as possible. This decreases the eccentricity of the axial load and the plate is mainly loaded in compression

Fixation Technique

Today fixation technique uses principles to be minimal, but optimal. That means longer splints acting with optimal lever arms for the screws are preferable [14, 16, 26]. The main fragments are held in place using balanced fixation on both sides of the fracture. In case of a simple fracture, the use of interfragmentary compression is still safe from the mechanical point of view. A small fracture gap in a simple fracture configuration combined with elastic fixation leads to high interfragmentary tissue strain, which sometimes can inhibit fracture consolidation. In such short fractures, repetitive bending stresses will be concentrated and centred on a short segment of the plate, which thereby can break more easily due to fatigue. The risk of mechanical implant failure can be considerably reduced if longer plates are used despite a short fracture zone, so that stresses are distributed over a longer section of the plate.

In multifragmentary fractures a bridge plate technique is advantageous. The implant spans over a longer bone segment decreasing the

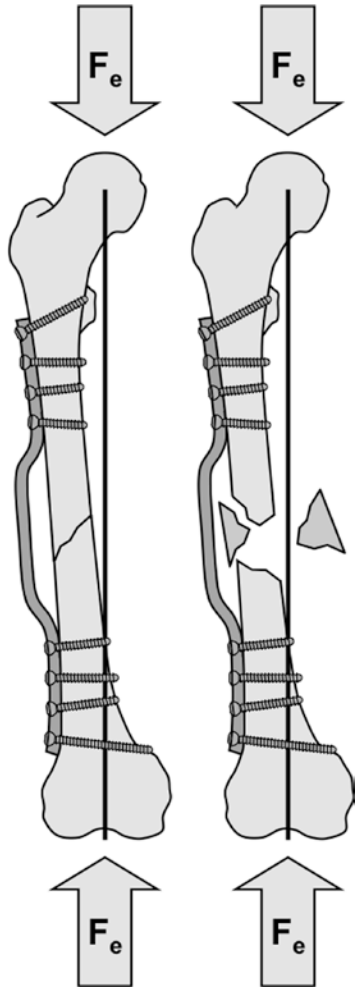

Fig. 29.28 Stiffness of a wave plate osteosynthesis. With at least unicortical contact between the main fracture fragments a wave plate osteosynthesis is a very stiff composite construct. In a comminuted fracture the wave plate is critical from the mechanical point of view, because the distance between the plate cross-section under load and the external axial load is increased. This enhances the bending moment and the plate loading

strain of the granulation tissue, which is going to be formed between the fracture fragments allowing its safe differentiation into bone tissue. Additionally, the plate itself undergoes low deformation during functional aftercare as bending stresses are distributed over a long segment of the plate with reduced risk of plate failure - this all under the condition that overall deformation of the implant is limited by bony fragments.

Conclusions and Outlook

Within the last three decades new thinking of operative fracture treatment using plates has been established. Using plates for internal fixation the advantages of operative and conservative treatment have to be combined: proper alignment of the injured bone segment and sufficient stability of fixation allowing functional aftercare and an undisturbed natural course of bone healing. Thus, in shaft fractures, the exact reduction of each bone fragment is no longer a goal in itself. Rather, the overall restoration of length, axial alignment, and rotation are the goals.

Plate osteosynthesis keeps its important and well-established place in the treatment of certain fractures. Classical indications for an osteosynthesis using plates or internal fixators are articular fractures, metaphyseal fractures, and some diaphyseal fractures, such as forearm fractures, diaphyseal fractures with associated articular fractures, diaphyseal fractures in polyfractured or polytraumatized patients, narrow medullary canal not suitable for intramedullary rodding, and some diaphyseal fractures in children.

The understanding of bone biology caused not only a change in the surgical tactic when performing internal fixation, but it stimulated research to modify and improve the existent implants aiming to reduce vascular damage to the bone tissue caused by the implant. Internal fixators with locked plate screws mechanically used as pure splints and inserted in a minimally invasive subcutaneous or submuscular way replace more and more the older conventional plating concepts. The new technique minimizes the surgical devascularization and the implant-inherent vascular insult to the bone tissue. Preserving the viability of all fracture fragments by protecting the soft tissue envelope is more important than the primary stability of an osteosynthesis. Healing by means of callus formation is potentially faster than the one based on inherently slow cortical remodeling. The good healing capacity of viable fragments results in stable conditions after a short time period protecting the implant from fatigue failure. The surgeon's task is to make the

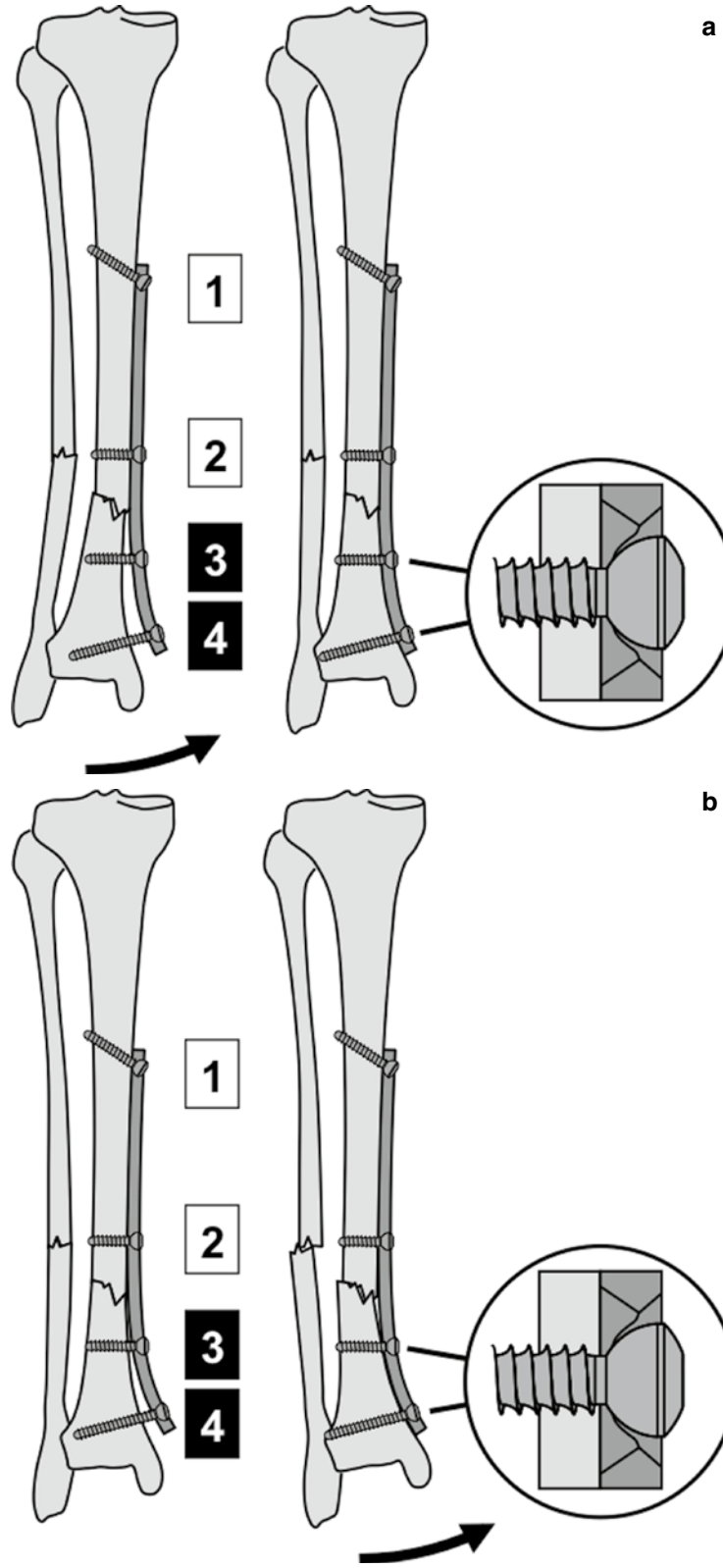

Fig. 29.29 Reduction in plate osteosynthesis. In conventional plating the plate should be contoured exactly to the shape of the surface of the bone. After having fixed the plate to the one main fragment, the other fragment can be pulled towards the plate by inserting screws leading to proper reduction and fixation (**a**). When the plate is not properly contoured, reduction on the plate results in an axial malalignment (**b**, **c**). Using an internal fixator with locked screw heads no risk for loss of reduction exists during screw tightening, because the screws engage inside the threaded plate hole before pulling the bone fragment towards the plate (**d**)

Fig. 29.29 (continued)

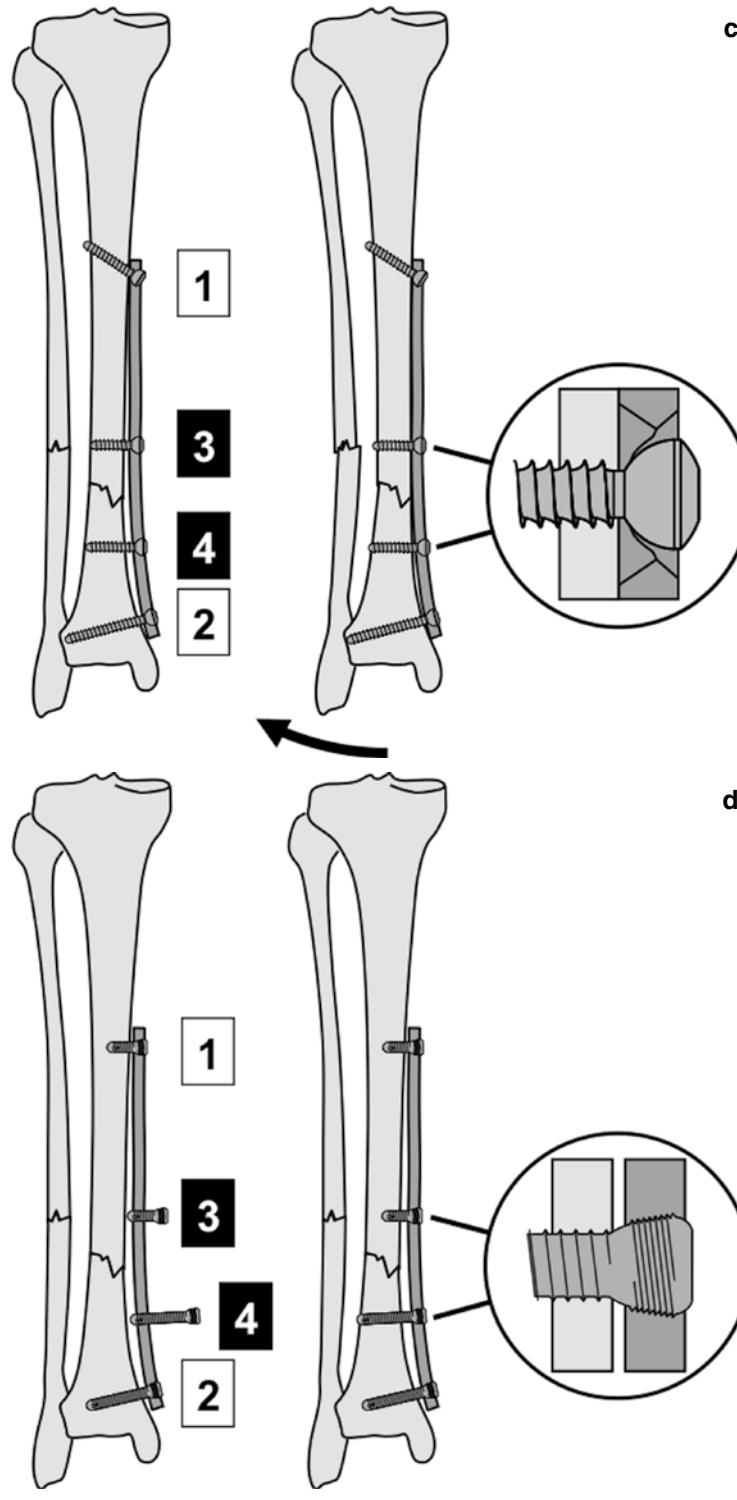

sound synthesis between mechanical demands of the fracture and biological competence of the involved tissues.

References

1. Hansmann M. Eine neue Methode der Fixation der Fragmente bei complicirten Fracturen. Verhandlungen der Deutschen Gesellschaft für Chirurgie. 1886;15:134–7.
2. Lambotte A. L'intervention opératoire dans les fractures récentes et anciennes. Paris: Maloine; 1907.
3. Lane WA. The operative treatment of fractures. London: Medical Publishing; 1913.
4. Sherman OWN. Vanadium steel bone plates and screws. Surg Gynecol Obstet. 1912;14:629–34.
5. Bagby GW. Compression bone-plating. Historical considerations. J Bone Joint Surg. 1977;59-A:625–31.
6. Danis R. Théorie et pratique de l'ostéosynthèse. Paris: Masson; 1949.
7. Müller ME, Allgöwer M, Willenegger H. Technik der operativen Frakturenbehandlung. Berlin/Heidelberg/New York: Springer; 1963.
8. Allgöwer M, Ehrsam R, Ganz R, Matter P, Perren SM. Klinische Erfahrungen mit der neuen Kompressionsplatte "DCP". Acta Orthop Scand Suppl. 1969;125:1–20.
9. Baumgaertel F, Buhl M, Rahn BA. Fracture healing in biological plate osteosynthesis. Injury. 1998; 29(Suppl):3–6.
10. Chrisovitsinos JP, Xenakis T, Papakostides KG, Skaltsoyannis N, Grestas A, Soucacos PN. Bridge plating osteosynthesis of 20 comminuted fractures of the femur. Acta Orthop Scand Suppl. 1997;275:72–6.
11. Farouk O, Krettek C, Miclau T, Schandelmaier P, Tscherne H. Effects of percutaneous and conventional plating techniques on the blood supply to the femur. Arch Orthop Trauma Surg. 1998;117:438–41.
12. Gautier E, Perren SM. Die "Limited Contact Dynamic Compression Plate" (LC-DCP–Biomechanische Forschung als Grundlage des neuen Plattendesigns. Orthopade. 1992;21:11–23.
13. Gautier E, Perren SM, Ganz R. Principles of internal fixation. Curr Orthop. 1992;6:220–32.
14. Gautier E, Ganz R. Die biologische Plattenosteosynthese. Zentralbl Chir. 1994;119: 564–72.
15. Gautier E, Marti CB, Schuster AJ, Wachtl SW, Jakob RP. Die eingeschobene Femur- und Tibiaplatte. OP-J. 2000;16:260–7.
16. Gerber C, Mast JW, Ganz R. Biological internal fixation of fractures. Arch Orthop Trauma Surg. 1990;109:295–303.
17. Heitemeyer U, Hierholzer G, Terhorst J. Der Stellenwert der überbrückenden Plattenosteosynthese bei Mehrfragmentbruchschädigung des Femur im klinischen Vergleich. Unfallchirurg. 1986;89: 533–8.
18. Helfet DL, Shonnard PY, Levine D, Borelli J. Minimally invasive plate osteosynthesis of distal fractures of the tibia. Injury. 1997;28 Suppl 1: 42–8.
19. Karnezis IA. Biomechanical considerations in 'biological' femoral osteosynthesis: an experimental study of the 'bridging' and 'wave' plating techniques. Arch Orthop Trauma Surg. 2000;120:272–5.
20. Kinast C, Bolhofner BR, Mast JW, Ganz R. Subtrochanteric fractures of the femur. results of treatment with the 95 degree condylar plate. Clin Orthop. 1989;238:122–30.
21. Krettek C, Schandelmaier P, Miclau T, Tscherne H. Minimally invasive percutaneous plate osteosynthesis (MIPPO) using the DCS in proximal and distal femoral fractures. Injury. 1997;28 Suppl 1:20–30.
22. Krettek C, Schandelmaier P, Miclau T, Bertram R, Holmes W, Tscherne H. Transarticular joint reconstruction and indirect plate osteosynthesis for complex distal supracondylar femoral fractures. Injury. 1997;28 Suppl 1:S31–41.
23. Mast J, Jakob R, Ganz R. Planning and reduction technique in fracture surgery. Berlin/Heidelberg/New York: Springer; 1989.
24. Miclau T, Martin RE. The evolution of modern plate osteosynthesis. Injury. 1997;28 Suppl 1:3–6.
25. Perren SM. The concept of biological plating using the limited contact dynamic compression plate (LC-DCP). Injury. 1991;22 Suppl 1:1–41.
26. Rozbruch RS, Müller U, Gautier E, Ganz R. The evolution of femoral shaft plating technique. Clin Orthop. 1998;354:195–208.
27. Rüedi TP, Murphy WM. AO principles of fracture management. Stuttgart/New York: Thieme; 2000.
28. Schmidtmann U, Knopp W, Wolff C, Stürmer KM. Results of elastic plate osteosynthesis of simple femoral shaft fractures in polytraumatized patients. An Altern Proced Unfallchir. 1997;100:949–56.
29. Siebenrock KA, Müller U, Ganz R. Indirect reduction with a condylar blade plate for osteosynthesis of subtrochanteric femoral fractures. Injury. 1998;29 Suppl 3:7–15.
30. van Riet YE, van der Werken C, Marti RK. Subfascial plate fixation of comminuted diaphyseal femoral fractures: a report of three cases utilizing biological osteosynthesis. J Orthop Trauma. 1997;11:57–60.
31. Wenda K, Runkel M, Degreif J, Rudig L. Minimally invasive plate fixation in femoral shaft fractures. Injury. 1997;28 Suppl 1:13–9.
32. Weller S, Höntzsch D, Frigg R. Die epiperostale, perkutane Plattenosteosynthese. Eine minimalinvasive Technik unter dem Aspekt der “biologischen Osteosynthese”. Unfallchirurg. 1998;101:115–21.
33. Brookes M. The blood supply of bone. an approach to bone biology. London: Butterworth; 1971.
34. Ficat P, Arlet J. Ischémie et nécrose osseuses. L’exploration fonctionelle de la circulation

intra-osseuse et ses applications. Paris/New York/Barcelone/Milan: Masson; 1977.
35. Göthman L. Vascular reactions in experimental fractures. Acta Orthop Scand Suppl. 1961;284:1–34.
36. Macnab I, de Haas WG. The role of periosteal blood supply in the healing of fractures of the tibia. Clin Orthop. 1974;105:27–33.
37. Rhinelander FW. The normal microcirculation of diaphyseal cortex and its response to fracture. J Bone Joint Surg. 1968;50-A:784–800.
38. Trueta J. Blood supply and the rate of healing of tibial fractures. Clin Orthop. 1974;105:11–26.
39. Kelly PJ. Anatomy, physiology and pathology of the blood supply of bones. J Bone Joint Surg. 1968;50-A:766–83.
40. Nelson GE, Kelly PE, Peterson LFA, Janes JM. Blood supply of the human tibia. J Bone Joint Surg. 1960;42-A:625–36.
41. Rhinelander FW. Tibial blood supply in relation to fracture healing. Clin Orthop. 1974;105:34–81.
42. Rhinelander FW, Wilson JW. Blood supply to developing, mature, and healing bone. In: Sumner-Smith G, editor. Bone in clinical orthopaedics. A study in comparative osteology. Philadelphia/London/Toronto: Saunders; 1982. p. 81–158.
43. Moor R, Tepic S, Perren SM. Hochgeschwindigkeits-Film-Analyse des Knochenbruchs. Z Unfallchir Versicherungsmed. 1989;82:128–32.
44. Alexander AH, Cabaud HE, Johnston JO, Lichtman DM. Compression plate position. Extraperiosteal or subperiosteal? Clin Orthop. 1983;175:280–5.
45. Fernandez Dell'Orca A, Regazzoni P. Internal fixation: a new technology. In: Rüedi T, Murphy WM, editors. AO principles of fracture management. Berlin/Heidelberg/New York: Thieme; 2000. p. 249–53.
46. Gautier E, Pesantez RF. Surgical reduction. In: Rüedi T, Buckley RE, Moran CG, editors. AO principles of fracture management. Stuttgart/New York: Thieme; 2007. p. 165–86.
47. Gautier E, Cordey J, Mathys R, Rahn BA, Perren SM. Porosity and remodelling of plated bone after internal fixation: result of stress shielding or vascular damage? In: Ducheyne P, van der Perre G, AE Aubert AE, editors. Biomaterials and biomechanics. Amsterdam: Elsevier Science Publishers BV; 1984. p. 195–200.
48. Gautier E, Perren SM. Die Reaktion der Kortikalis nach Verplattung - eine Folge der Belastungsveränderung des Knochens oder ein Vaskularitätsproblem? In: Wolter D, Zimmer W, editors. Die Plattenosteosynthese und ihre Konkurrenzverfahren. Berlin/Heidelberg/New York: Springer; 1991. p. 21–37.
49. Gautier E, Rahn BA, Perren SM. Vascular remodelling. Injury. 1995;26 Suppl 2:11–9.
50. Gunst MA, Suter C, Rahn BA. Die Knochendurchblutung nach Plattenosteosynthese. Helv Chir Acta. 1979;46:171–5.
51. Jacobs RR, Rahn BA, Perren SM. Effect of plates on cortical bone perfusion. J Trauma. 1981;21:91–5.
52. Jörger KA (1987) Akute intrakortikale Durchblutungsstörung unter Osteosyntheseplatten mit unterschiedlichen Auflageflächen. MD thesis, University of Bern.
53. Lippuner K, Vogel R, Tepic S, Rahn BA, Cordey J, Perren SM. Effect of animal species and age on plate-induced vascular damage in cortical bone. Arch Orthop Trauma Surg. 1992;111:78–84.
54. Lüthi UK (1980) Auflageflächen von Osteosyntheseplatten und intrakortikale Durchblutungsstörungen. MD thesis, University of Basel.
55. Perren SM, Cordey J, Rahn BA, Gautier E, Schneider E. Early temporary porosis of bone induced by internal fixation implants. a reaction to necrosis, not to stress protection? Clin Orthop. 1988;232:139–51.
56. Arens S, Kraft C, Schlegel U, Printzen G, Perren SM, Hansis M. Susceptibility to local infection in biological internal fixation. experimental study of open vs minimally invasive plate osteosynthesis in rabbits. Arch Orthop Trauma Surg. 1999;119:82–5.
57. Akeson WH, Woo SL-Y, Rutherford L, Coutts RD, Gonsalves M, Amiel D. The effects of rigidity of internal fixation plates on long bone remodeling. Acta Orthop Scand. 1976;47:241–9.
58. Claes L. The mechanical and morphological properties of bone beneath internal fixation plates of differing rigidity. J Orthop Res. 1989;7:170–7.
59. Cochran GVB. Effects of internal fixation plates on mechanical deformation of bone. Surg Forum Orthop Surg. 1969;20:469–71.
60. Cordey J, Schwyzer HK, Brun S, Matter P, Perren SM. Bone loss following plate fixation of fractures? Helv Chir Acta. 1985;52:181–4.
61. Gördes W, Kossyk W, Holländer H. Histologische und histomorphometrische Veränderungen bei Plattenosteosynthesen nach Osteotomien an der Tibia des Kaninchens. Arch Orthop Unfallchir. 1975;82:123–33.
62. Matter P, Brennwald J, Perren SM. Biologische Reaktion des Knochens auf Osteosyntheseplatten. Helv Chir Acta. 1974;12(Suppl):1–44.
63. Moyen BJ-L, Lahey PJ, Weinberg EH, Rumelhart C, Harris WH. Effects of application of metal plates to bone. Acta Orthop Belg. 1980;46:806–15.
64. Strömberg L, Dalen N. Atrophy of cortical bone caused by rigid internal fixation plates. Acta Orthop Scand. 1978;49:448–56.
65. Terjesen T, Benum P. The stress-protection effect of metal plates on the intact rabbit tibia. Acta Orthop Scand. 1983;54:810–8.
66. Uhthoff HK, Dubuc FL. Bone structure changes in the dog under rigid internal fixation. Clin Orthop. 1971;81:165–70.
67. Uhthoff HK, Bardos DI, Liskova-Kiar M. The advantages of titanium alloy over stainless steel plates for the internal fixation of fractures. J Bone Joint Surg. 1981;63-B:427–34.
68. Uhthoff HK, Finnegan M. The effects of metal plates on post-traumatic remodelling and bone mass. J Bone Joint Surg. 1983;65-B:66–71.
69. Wolff J. Das Gesetz der Transformation der inneren Architektur der Knochen bei pathologischen

Veränderungen der äusseren Knochenform. Berlin: Berliner Akademie der Wissenschaften Reichsdruckerei; 1884.
70. Chidgey L, Chakkalakal D, Blotcky A, Connolly JF. Vascular reorganization and return of rigidity in fracture healing. J Orthop Res. 1986;4:173–9.
71. Claes L, Heitemeyer U, Krischak G, Braun H, Hierholzer G. Fixation technique influences osteogenesis of comminuted fractures. Clin Orthop. 1999;365:221–9.
72. Tepic S, Remiger AR, Morikawa K, Predieri M, Perren SM. Strength recovery in fractured sheep tibia treated with a plate or an internal fixator: an experimental study with a two-year follow-up. J Orthop Trauma. 1997;11:14–23.
73. Schenk RK, Willenegger H. Zum histologischen Bild der sogenannten Primärheilung der Knochenkompakta nach experimentellen Osteotomien am Hund. Experientia. 1963;19:593.
74. Terjesen T, Apalset K. The influence of different degrees of stiffness of fixation plates on experimental bone healing. J Orthop Res. 1988;6:293–9.
75. Perren SM, Boitzy A. Cellular differentiation and bone biomechanics during the consolidation of a fracture. Anat Clin. 1978;1:13–28.
76. Müller ME, Allgöwer M, Schneider R, Willenegger H. Manual of internal fixation. Berlin/Heidelberg/New York: Springer; 1990.
77. Ito K, Perren SM. Biology and biomechanics in fracture management. In: Rüedi T, Buckley RE, Moran CG, editors. AO principles of fracture management. Stuttgart/New York: Thieme; 2007. p. 9–31.
78. Perren SM, Klaue K, Pohler O, Predieri M, Steinemann S, Gautier E. The limited contact dynamic compression plate (LC-DCP). Arch Orthop Trauma Surg. 1990;109:304–10.
79. Vattolo M (1987) Der Einfluss von Rillen in Osteosyntheseplatten auf den Umbau der Kortikalis. MD thesis, University of Bern.
80. Tepic S, Perren SM. The biomechanics of the PC-Fix internal fixator. Injury. 1995;26(Suppl):5–10.
81. Babst R, Hehli M, Regazzoni P. LISS-Traktor, Kombination des "less invasive stabilization systems" (LISS) mit dem AO-Distraktor für distale Femur- und proximale Tibiafrakturen. Unfallchirurg. 2001;104:503–5.
82. Krettek C, Gerich T, Miclau T. A minimally invasive medial approach for proximale tibial fractures. Injury. 2001;32(Suppl):4–13.
83. Frigg R, Frenk A, Haas NP, Regazzoni P. LCP: the locking compression plate system. AO Dialogue. 2001;14:8–9.
84. Sommer C, Gautier E, Müller M, Helfet DL, Wagner M. First clinical results of the locking compression plate (LCP). Injury. 2003;34 Suppl 2:43–54.
85. Gautier E, Sommer C. Guidelines for the clinical application of the LCP. Injury. 2003;34 Suppl 2: 63–76.
86. Wagner M, Frigg R, Buckley R, Gautier E, Schütz M, Sommer C (2006) Internal fixators. Concepts and cases using LCP and LISS. In: AO manual of fracture management. Stuttgart/New York: Thieme.
87. Otto RJ, Moed BR, Bledsoe JG. Biomechanical comparison of polyaxial-type locking plates and a fixed-angle locking plate for internal fixation of distal femur fractures. J Orthop Trauma. 2009;23:645–52.
88. Rausch S, Schlonski O, Klos K, Gras F, Gueorguiev B, Hofmann GO, Mückley T. Volar versus dorsal latest-generation variable-angle locking plates for the fixation of AO type 23C 2.1 distal radius fractures: a biomechanical study in cadavers. Injury. 2013;44:523–6.
89. Wilkens KJ, Curtiss S, Lee MA. Polyaxial locking plate fixation in distal femur fractures: a biomechanical comparison. J Orthop Trauma. 2008;22:624–8.
90. Jazrawi LM, Bai B, Simon JA, Kummer FJ, Birdzell LT, Koval KJ. A biomechanical comparison of Schuhli nuts or cement augmented screws for plating of humeral fractures. Clin Orthop. 2000;377:235–40.
91. Kolodziej P, Lee FS, Patel A, Kassab SS, Shen KL, Yang KH, Mast JW. Biomechanical evaluation of the schuhli nut. Clin Orthop. 1998;347:79–85.
92. Simon JA, Dennis MG, Kummer FJ, Koval KJ. Schuhli augmentation of plate and screw fixation for humeral shaft fractures: a laboratory study. J Orthop Trauma. 1999;13:196–9.
93. Müller H. Festigkeits- und Elastizitätslehre. München: Carl Hanser; 1970.
94. Richards GR, Perren SM. Implants and materials in fracture fixation. In: Rüedi T, Buckley RE, Moran CG, editors. AO Principles of fracture management. Stuttgart/New York: Thieme; 2007. p. 33–44.
95. Perren SM, Pohler OEM, Schneider E. Titanium as implant material for osteosynthesis applications. In: Brunette DM, Tengvall P, Textor M, Thomson P, editors. Titanium in medicine. Berlin/Heidelberg/New York/Barcelona/Hongkong/London/Milan/Paris/Singapore/Tokyo: Springer; 2001. p. 771–825.
96. Popov EP. Mechanics of materials. Englewood: Prentice-Hall; 1976.
97. Arens S, Schlegel U, Printzen G, Ziegler WJ, Perren SM, Hansis M. Influence of the materials for fixation implants on local infection. An experimental study of steel versus titanium DC-Plates in rabbits. J Bone Joint Surg. 1996;78-B:647–51.
98. Johansson A, Lindgren JU, Nord CE, Svensson O. Local plate infections in a rabbit model. Injury. 1999;30:587–90.
99. Johansson A, Lindgren JU, Nord CE, Svensson O. Material and design in haematogenous implant-associated infections in a rabbit model. Injury. 1999;30:651–7.
100. Burstein AH, Wright TM. Fundamentals of orthopaedic biomechanics. Baltimore/Philadelphia/Hongkong/London/Munich/Sydney/Tokyo: Williams & Wilkins; 1994.
101. Stürmer KM. Elastic plate osteosynthesis, biomechanics, indications and technique in comparison with rigid osteosynthesis. Unfallchirurg. 1996;99:816–29.
102. Farouk O, Krettek C, Miclau T, Schandelmaier P, Guy P, Tscherne H. Minimally invasive plate osteosynthesis: does percutaneous plating disrupt femoral

blood supply less than the traditional technique? J Orthop Trauma. 1999;13:401–6.
103. Ellis T, Bourgeault CA, Kyle RF. Screw position affects dynamic compression plate strain in an in vitro fracture model. J Orthop Trauma. 2001;15:333–7.
104. Field JR, Tornkvist H, Hearn TC, Sumner-Smith G, Woodside TD. The influence of screw omission on construction stiffness and bone surface strain in the application of bone plates to cadaveric bone. Injury. 1999;30:591–8.
105. Cordey J, Gautier E. Strain gauges used in the mechanical testing of bones. Part III: strain analysis, graphic determination of the neutral axis. Injury. 1999;30(Suppl):21–5.
106. Gautier E, Perren SM, Cordey J. Influence of the plate position relative to the bending direction onto the rigidity of a plate osteosynthesis - a theoretical analysis. Injury. 2000;31 Suppl 3:14–20.
107. Gautier E, Perren SM, Cordey J. Strain distribution in plated and unplated sheep tibia. An Vivo Exp Injury. 2000;31(Suppl):37–44.
108. Blatter G, Weber BG. Wave plate osteosynthesis as a salvage procedure. Arch Orthop Trauma Surg. 1990;109:330–3.
109. Ring D, Jupiter JB, Sanders RA, Quintero J, Santoro VM, Ganz R, Marti RK. Complex nonunion of fractures of the femoral shaft treated by wave-plate osteosynthesis. J Bone Joint Surg. 1997;79-B:289–94.
110. Ring D, Jupiter JB, Quintero J, Sanders RA, Marti RK. Atrophic ununited diaphyseal fractures of the humerus with a bony defect: treatment by wave-plate osteosynthesis. J Bone Joint Surg. 2000;82-B:867–71.
111. Brunner CF, Weber BG. Special techniques in internal fixation. Berlin/Heidelberg/New York: Springer; 1982.

Part VI

Applications of Biomechanics Principles to Oncology

Malignant Bone Tumors: From Ewing's Sarcoma to Osteosarcoma

30

Dominique G. Poitout and J. Favre

Introduction

Primitive malignant bone tumors are rare as they represent less than *1 % of all cancers*. Osteosarcoma and Ewing's sarcoma occur the most frequently. They affect, in particular, older children, adolescents, and young adults. For many years these tumors could be controlled locally (often involving an amputation) by radical surgery accompanied or not by radiotherapy, depending on the histological type. Unfortunately, most of the patients died within 2 years from secondary lesions in the lung.

Only recently has it been possible to improve the survival rate. Indeed, the prognosis of these tumors, until then complicated by the occurrence of pulmonary metastases in almost 90 % of cases, has been revolutionized by the advent of "heavy" chemotherapies, capable of eradicating infraclinical metastases. At the same time, the progress made in surgical techniques has enabled the number of limbs saved to be increased and therefore an improvement in the future of these young patients in terms of function. First of all we should stress the importance of close multidisciplinary collaboration, from diagnosis to post-therapeutic monitoring through all the stages of treatment, a collaboration upon which the prognosis of the survival of the patient for whom we are responsible depends.

Epidemiology

Frequency

There are approximately 100 new cases of osteosarcoma per year in France. The incidence of Ewing's sarcoma is estimated at two to three new cases per year and per million children under 15 years of age in the USA and in the United Kingdom. There is a slight preponderance of males suffering from these two tumors with a gender ratio of approximately 1:5. Osteosarcoma can occur at any age but is found mainly in young people with an average age of 17 years.

Ewing's sarcoma most often occurs during the second decade of life with an average age of 11. It is exceptional before 5 years of age and after 30. Finally, it should be noted that Ewing's sarcoma is very rare in people of black African descent.

D.G. Poitout, MD (✉)
Faculté de Médecine Nord, Sce Chirurgie Orthopédique et Traumatologie, Aix-Marseille Université, Centre Hospitalier et Universitaire Marseille North, Chemin des Bourrely, 13015 Marseille, France
e-mail: Dominique.POITOUT@ap-hm.fr

J. Favre
Aix-Marseille Université,
Centre Hospitalo-Universitaire Marseille Nord, Marseille, France

D.G. Poitout (ed.), *Biomechanics and Biomaterials in Orthopedics*,
DOI 10.1007/978-1-84882-664-9_30

Risk Factors

There is often a history of trauma in the weeks preceding the discovery of the tumor, but whether this factor is responsible is still being discussed and it could be no more than a factor which makes clinical discovery more likely. Both types of tumor seem to occur more frequently in tall patients. This, no doubt, is related to the hormone changes of rapid growth.

Osteosarcoma

In the child, osteosarcoma may be accompanied by familial retinoblastoma in 4 % of cases. Then the same cytogenetic anomalies are found for bone tumors as for the retinal tumors. One percent of Paget's disease of the bone can degenerate into osteosarcoma. A radiation-induced etiology is also possible for this disease (osteosarcomas have been described in particular after anti-inflammatory radiotherapy for aneurysmal bone cysts). In these two latter cases, adults beyond the quarantine period are most often involved.

Tumors of the ethmoid in people exposed to wood dust are classical, with the most frequent histology being adenocarcinomas, of course, but osteosarcomas can also be present.

Ewing's Sarcoma

Few specific risk factors have been described for Ewing's sarcomas. They may occur on pre-existing benign bone lesions.

Pathological Anatomy

Varieties

Osteosarcomas

Osteosarcomas start in the center of the medulla, most frequently in the metaphysis of the long bones. The lower extremity of the femur, and the upper extremity of the tibia or of the humerus are the most frequent sites (80 % of cases). At a microscopic level, these tumors are characterized by osteoid production. Osteoblastic and chondroblastic varieties (characterized by the presence of chondroid tissue) have been described. Due to cell differentiation and the quality of the stroma, distinctions can be drawn between the fibrous osteosarcomas (with an abundance of collagen), telangectasic osteosarcomas (considerable vascularization), and anaplastic osteosarcomas (very non-differentiated). These last two varieties have the worst prognosis. Parosteal sarcoma, a highly ossifying variety of osteosarcoma, has a better prognosis.

Anatomical pathological examination can also pinpoint the fusiform or small cell nature of the tumor (the latter have a poorer prognosis). Some authors also suggest a cytological scale of 1–4 in order of increasing malignancy. Indeed, the introduction of intensive chemotherapy has removed the role of these prognostic factors. The histological variety of the tumor no longer affects the course of the disease.

Ewing's Sarcoma

Unlike osteosarcoma, in more than half of cases, Ewing's sarcoma develops in the axial skeleton starting from the pelvic girdle. This fact was first described by J. Ewing in 1921 as a bone tumor with small round cells, distinct from osteosarcoma. The origin of the tumor has long been discussed. An endothelial, neural, mesenchymatous starting point has been suggested. It would currently appear, owing to the immunohistochemical and cytogenetic data, that it is one of the tumors deriving from the neurectodermis, of which it would be the least differentiated form, and of which the neuroepithelioma would be the differentiated form.

From an anatomical pathological point of view, it is a monomorphous proliferation of small round cells with fine chromatin, positive PAS, with a fine network of intercellular reticulin. Immunohistochemistry and, in particular, cytogenetics make it possible to differentiate Ewing's sarcoma from other small round cell tumors in the child and in the adolescent. In more than 80 % of cases of Ewing's sarcoma, there is specific translocation (11, 22 q24; q12). In the absence

of specific translocation, chromosome 22 derives from translocation in 9 % of cases.

Spread

Osteosarcomas

It is customary to say that "osteosarcoma is a lung disease starting in the bone". This brief description straight away emphasizes the early and extreme frequency of the pulmonary micrometastases which do, of course, determine the prognosis in terms of survival. Locally, the tumor develops centrifugally, invading and destroying the normal bone up to the cortex and to the adjacent soft tissue. There is often a pseudo-capsule which really consists of inflammatory tissue at the interface between the tumor and normal tissue.

The very frequent presence of satellite tumoral nodules situated on the same bone as the main tumor but not continuous with it has also been described. These are, in fact, "local metastases" which have developed from tumoral emboli via the medullary sinuses. These have to be taken into account when determining the extent of the surgical excision. Ganglionic involvement is unusual for this histological type since it only appears in less than 10 % of cases in autopsy series. On the other hand, hematogenic metastases are extremely frequent and develop at an early stage. They occur predominantly in the lungs, and it is estimated that approximately three-quarters of patients have microscopic pulmonary metastases at the time of diagnosis.

The second site for metastases in order of frequency is the bone but it is rare that bone metastases are present if earlier pulmonary lesions are absent. Other types of metastases only occur very exceptionally.

Ewing's Sarcoma

The local development of Ewing's sarcoma is slightly different. There is often complete invasion of the medullary cavity of the bone concerned as well as involvement of the cortex and of the soft tissue. Ganglionic metastases seem to be a little more frequent than for osteosarcomas, but here, too, it is the hematogenous metastases which tend to occur with a frequency of 15–40 % at the time of diagnosis. Pulmonary secondaries still arrive there first, followed by bone metastases and invasion of the medulla.

Diagnosis

Circumstances in Which It Is Discovered

Pain is often the first symptom; it may be intense and accompanied by serious functional infirmity or, on the other hand, not intense and only felt if pressure is applied. Sometimes there is a nocturnal recrudescence. This pain, caused by intraosseous hypertension, is considerable in the forms which start centrally. It may also be accompanied by limping in lesions of the leg.

Its site varies depending on the type of tumor:

In the case of osteosarcoma, it is most frequently found in the metaphysis of the long bones, "close to the knee and far from the elbow". Lower extremity of the femur (50 %), upper extremity of the tibia (15 %), upper extremity of the humerus (15 %).

Ewing's sarcoma tends to develop in the axial skeleton and in shoulder and pelvic girdles. Involvement of the flat bones, although exceptional for osteosarcomas, is very common in Ewing's sarcoma.

The tumor can also be palpated. A careful examination shows that it is one with the bone, with the neighboring joints rarely being affected. It varies in consistency, being hard, firm, or sometimes softer. The tumor may be pulsating. Classically there may be crepitus on pressure but this sign is, in fact, rare. The tumor increases rapidly in size, deforming the bone concerned; the skin has a smooth and stretched appearance, with dilated veins.

The disease may also be manifested by a pseudo-infectious syndrome. Indeed, hemorrhaging and intra-tumoral necrosis may make the tumor fluctuant, with an increase in temperature

locally and cutaneous erythema, mimicking an abscess.

The diagnosis may also be made in the presence of a spontaneous fracture or secondary to minimal trauma.

When the tumor is large, the mass can lead to vascular, nervous, and medullary compression of a hollow organ; this rarely reveals the disease except for pelvic or vertebral lesions.

Finally, the diagnosis may be made when prevalent, mainly pulmonary, metastases appear or even when the patient's general condition deteriorates and may be accompanied by fever.

The Components Involved in the Diagnosis

History-Taking and Clinical Examination

The person taking the history will look for any risk factors, and the existence of functional or general signs and their development over time. The examination will establish the extent of the lesion, its clinical appearance and the presence of complications. Ganglionic metastases are rare and secondary visceral lesions are usually asymptomatic.

Biology

There are no specific markers of these tumors. At most there may be an inflammatory syndrome without any specific features. Ewing's syndrome may be accompanied by an increase in the LDHs.

Radiological Examinations

X-rays without preparation classically show different images according to the histological type but only an anatomical–pathological study will provide diagnostic proof. The osteosarcomas may be non-ossifying. The X-ray picture then displays non-homogeneous lysis and is poorly defined. On the surface, there is sub-periosteal osteophytosis forming spicules and it is responsible for a "sun ray" appearance. Ossifying osteosarcomas give the same radiological signs, accompanied by intra-tumoral opacities which are sometimes very dense. These ossification images may also exist in extraosseous tumoral zones when the soft tissues are invaded.

The radiological signs of Ewing's sarcoma, such as simple gumming of the bone framework, are sometimes very difficult to see. The typical appearance is that of osteolysis bordered by a considerable periosteal reaction, resulting in the so-called "onion-skin appearance".

Specific incidences may be useful for sites such as the sacrum and the vertebrae.

Whatever type of tumor is involved, bone scintigraphy using Technetium 99 will reveal intense hyperfixation.

Computerized tomography has to be carried out, adhering to certain quality criteria and dual window examination to allow a detailed examination of the bone and soft tissue, before and after injection of the contrast medium. The lesion is irregular, poorly defined, invading the adjacent soft tissue with *often* heterogeneous uptake of the contrast medium.

MRI, used in addition to the scanner and allowing a tri-dimensional study of the tumor, seems to be more successful in evaluating whether it has spread to the soft tissue and to the bone medulla, and establishes its relationship with the vasculonervous bundles.

Angiography reveals anarchical vascularization of the tumoral mass. It is particularly useful for establishing the lesion's relationship to the large vessels and for guiding the surgeon in his maneuvers.

Pathological Anatomy

Only an anatomical–pathological examination will make it possible to make a formal diagnosis. Therefore, a biopsy has to be performed as a matter of surgical urgency but it does involve some risk of hematogenic dissemination and local release of growth factors. It involves a real surgical operation and therefore has to be performed by a qualified surgeon who is a member of the multidisciplinary team which will be taking care of the patient.

This procedure has to performed under general anesthetic, with a tourniquet at the base of the limb and before any treatment. The technique has to be performed correctly, with surgical opening of the tumor to enable removal accompanied by rigorous hemostasis and careful suturing. Needle or trocar biopsies are only indicated for sites which are difficult to access such as the vertebral bodies. The surgical approach and course of the drains will ultimately have to be removed with the tumor in order to limit the risk of a local relapse.

Differential Diagnosis

There is more than one infection-related problem which may be particularly reminiscent of Ewing's sarcomas, all the other benign bone tumors will also have to be eliminated (osteoma, chondroma, fibroma, angioma, giant-cell tumor, solitary or aneurysmal cyst. But it is, in particular, the other malignant bone tumors which can sometimes pose a problem in differential diagnosis: chondrosarcoma (the prognosis of which is poor because at present there is no treatment apart from radical surgical excision), Parker and Jackson's lymphoma (which really belong to the group of non-Hodgkin's malignant lymphoma and therefore must be treated as such), fibrosarcoma and angiosarcoma (forming part of the group of sarcoma of the soft tissue), and adamantinoma of the long bones (a variety of tumor which does not metastasize much but has a marked tendency to recur locally).

Although the various X-ray examinations may point in the right direction, only a biopsy together with a cytogenetic study allows a reliable diagnosis to be made and therefore to guide the treatment.

Pre-therapeutic Inventory

Inventory

Loco-Regional

Clinical examination only allows a rough evaluation of the tumor. Standard X-rays underestimate the extent of the lesion, not only in the bone but also its spread to the soft tissue. Bone scintigraphy is sometimes more precise; it also reveals any satellite tumoral nodules. However, computerized tomography and magnetic resonance imaging in particular clarify the extent of the tumor. Both inside and outside the bone these two examinations are useful because they often provide additional information. The aim of other investigations, and in particular angiography, is to provide us with information on the vascularization of the lesion and on how it relates to the main vessels, therefore enabling the surgeon to select the most suitable operating technique.

Metastatic Spread

There is no point in systematically searching for ganglionic metastases because they rarely occur. On the other hand, secondary pulmonary and bone lesions must be searched for. The standard chest X-ray is insufficient, and a CT scan therefore has to be performed in order to diagnose small lesions. Bone scintigraphy with Technetium allows any bone metastases to be found. For Ewing's sarcomas, myelograms are carried out systematically to look for any medullary invasion. Other visceral lesions only occur in exceptional cases and therefore do not require systematic paraclinical examination.

Classification

The TNM classification is not suitable for primitive malignant bone tumors. At present there is no satisfactory prognostic classification which can be used routinely. However, it is possible to define a number of prognostic factors:

the size of the tumor linked to the prognosis, with a worse prognosis for tumors 10 cm in diameter or larger.

Soft-tissue involvement would also have a worse prognosis but this is so frequent that such a criterion would be of little value.

Osteosarcomas secondary to Paget's disease or radiation-induced have a less favorable course than others.

For Ewing's sarcomas the LDH levels would have a prognostic value.

However, the main factor determining survival is, of course, the response to the treatment.

Treatment

Method

Surgery

Radical Surgery

This is, in fact, amputation of a limb. This has to be performed leaving a safety margin of a few centimeters. Sometimes, in cases where the proximal part of the limb is affected, the only possible procedure is the complete disarticulation of the limb concerned, which of course makes the functional prognosis even worse. Nowadays, with the progress made in surgical techniques and the contribution made by induction chemotherapy, the indications for these methods are becoming fewer and fewer.

Conservative Surgery

This technique has been used successfully in 40–80 % of cases depending on the series. Its success depends on close interdisciplinary coordination and strict pre-therapeutic evaluation. This surgery takes place in three stages:

resection of the tumor has to adhere strictly to the rules of oncological surgery in order to limit the risks of a relapse: excision of the whole of the lesion takes place in a single piece with a safety margin of 6–7 cm above the scanographical limit of the involvement in the bone. This resection also includes the muscles adjacent to the extraosseous spread. The part operated on has to include the earlier biopsy sites as well as all the potentially contaminated tissues. The joint and the adjacent articular capsule are also resected.

It is then necessary to reconstruct the bone defect, the average length of which often reaches 15–20 cm. Three main methods can be used:
the implantation of a prosthesis,
bone "graft" from a bone bank,
arthrodesis.

The choice of technique is decided on a case-by-case basis by the surgeon. The operation ends by transposing the muscles and soft tissue. Indeed, adequate muscle and skin cover of the operating area significantly reduces postoperative morbidity.

Radiotherapy

The indications for radiotherapy vary considerably according to the histological type. Osteosarcomas are tumors which respond very little to radiotherapy. The doses needed to obtain an acceptable level of sterilization are greater than or equal to 80 Gy and are the source of major complications. This is why radiotherapy is only used in totally exceptional or palliative cases.

On the other hand, 80–90 % of cases of Ewing's sarcoma can be cured by radiotherapy if a dose of 60–65 Gy can be delivered to the whole of the primary tumor. Lower doses (40–45 Gy) are adequate for sterilizing micrometastases or very small postoperative residual lesions.

A rigorous technique with anticipatory dosimetry is necessary in order to limit the risk of complications.

Chemotherapy

There is no doubt that, by enabling the disease in general to be treated, chemotherapy has improved the prognosis of these tumors. Indeed, before this treatment was available, the vast majority of these patients (80–90 %) died from metastases in the 2 years following satisfactory local treatment.

The methods are to be adapted according to the following histological types.

Osteosarcoma

The products used in the treatment of osteosarcomas are the following:

high-dose methotrexate (MTX HD): combines hyperhydration with alkalination followed by injections of folinic acid. At standard doses, methotrexate is not at all effective. Very high doses (of the order of 8–10 g/m^2) are necessary. These doses are potentially lethal or likely to lead to major and, in particular, renal complications. Ideally, "drugs have to be

prescribed at plasma doses making it possible to adapt their dosages". In all cases, very strict rules of hydration and alkalination have to be adhered to.

"BCD" combination (Bleomycin - Cyclophosphamid - Actinomycin D) – adriamycin and other anthracyclines.

Iphosphamide, in association with uromitexan and sufficient hydration to limit the risk of hemorrhaging.

CDDP.

Ewing's Sarcoma

Drugs which are effective in the treatment of Ewing's sarcomas are:

anthracyclines,

VAC-type combinations (vincristine, actinomycin O, endoxan),

Bleomycin,

Methotrexate,

IVA combinations (Iphosphamide, vincristine, actinomycin), IVAD combinations (iphosphamide, vincristine, adriamycin). This type of protocol is nevertheless responsible for considerable toxicity which limits the indications for it.

Indications

Osteosarcomas

The first phase of the treatment consists of preoperative chemotherapy, starting as soon as the result of the biopsy is obtained, and consists of courses of treatment with high-dose methotrexate. The patient is then operated on. Whenever possible, conservative surgery is performed. Nevertheless, there are certain contra-indications to this maneuver: major neuro-muscular invasion, pathological fracture, poor diagnostic biopsy technique, local infection.

The subsequent chemotherapy methods are decided according to the response to the treatment, evaluated on clinical, radiographic, and particularly anatomopathological criteria. When the response is good, the same type of treatment is continued. If not, the prescription is changed to other potentially effective drugs. Chemotherapy lasts approximately 9 months in all. Any delay in the progress of the treatment has to be avoided as much as possible, in particular by prescribing hematopoietic growth factors.

Special Case

Pulmonary metastases, whether they appear first or particularly late, can justify an aggressive approach if the primary tumor is under control: heavy chemotherapy followed by metastasectomy and resuming chemotherapy according to the response to the treatment. This is often necessary if survival is to be prolonged.

Tumors which cannot be eradicated; the treatment combines chemotherapy with irradiation, the dose of which takes account of the adjacent critical organs (50–75 Gy according to the case).

Tumors in elderly subjects are often osteosarcomas for which a risk factor is found (Paget's disease, irradiation, professional exposure, etc.). The treatment, in particular chemotherapy, has to be adjusted according to age, the patient's general condition and predisposition.

Ewing's Sarcoma

In terms of the treatment plan, the treatment resembles that for osteosarcoma: the local treatment is incorporated into the overall strategy, which starts with induction chemotherapy, generally including an anthracycline and a VAC-type combination administered with the dual aim of reducing the tumoral mass and eradicating the micrometastases.

Surgery and radiotherapy are generally accompanied by local treatment. Indeed, surgery alone is often not enough to guarantee satisfactory local control. On the other hand, irradiation alone requires doses of the order of 60–65 Gy, which is sometimes a source of major complications, particularly in children on account of the growth problems that it causes. Furthermore, the level of local recurrence after irradiation remains high (approximately 20 %) in spite of chemotherapy. These considerations lead to proposing a combination of radiotherapy and surgery in a number of cases.

Local treatment is followed by a resumption of chemotherapy. Other chemotherapy protocols based on taking cyclophosphamide orally together with other active drugs make it possible to obtain equivalent survival at the price of often less toxicity. The place of intensive chemotherapy with bone marrow autografts is not clearly defined. Metastatic Ewing's sarcomas are caused by systemic chemotherapy. There are fewer indications for metastasectomy than there are for the osteosarcomas. In cases of complete remission, the subsequent therapeutic strategy is the same as in non-metastatic patients.

Course and Monitoring

Osteosarcoma

Nowadays, owing to chemotherapy, the survival rate from osteosarcomas is approximately 50 % at 5 years. Most of the relapses occur within 2 years but just as survival is being prolonged, there are also cases of late relapses sometimes after 8–10 years.

Metastatic tumors are *mostly fatal* even if prolonged remissions can sometimes be obtained. Monitoring therefore has to be particularly close in the first years but also has to be prolonged. Apart from a careful clinical examination, it also has to include X-rays and a CT scan or MRI examination of the affected region as well as bone scintigraphy and a chest scan to detect secondary lesions.

Ewing's Sarcoma

In spite of all these improvements in therapeutic techniques, the overall results have hardly progressed these last few years. Survival without a relapse is estimated at 60 % at 3 years and overall survival at 70 % at 3 years. The course can be complicated by the occurrence of an osteosarcoma in the area irradiated. In metastatic patients survival rates of more than 50 % have been reported after remission and rigorous locoregional treatment. The practical methods of chemical and paraclinical monitoring are comparable to those for osteosarcoma.

Conclusion

Primitive bone tumors are rare conditions but mainly affect young people. Up until the 1970s, their prognosis was complicated by the appearance of metastases in the vast majority of cases, but they have largely benefited from advances in chemotherapy. However, only close multi-disciplinary collaboration makes it possible to define a suitable therapeutic strategy for each patient, to optimize the diagnosis, the treatment, and the subsequent monitoring and hence to increase the chances of a cure.

Therapeutic Orientation in Osteogenic Sarcomas

For a long time the treatment of osteogenic sarcoma has been concerned solely with the local bone lesion which has either been immediately surgically excised, or has been irradiated following an amputation which has been delayed in principle or due to necessity. A successful outcome at 5 years of 20 % is equivalent with these two methods of treatment and, from the functional point of view, although local irradiation allows unnecessary mutilations to be avoided in subjects who are going to die due to the development of pulmonary metastases, it should be recognized that its insufficiencies and sequelae lead, except in rare exceptional cases, to patients who have been cured nevertheless having to undergo an amputation at a later stage.

A better understanding of the factors which affect the prognosis of osteogenic sarcomas has to guide the treatment. From this point of view, the problem of pulmonary metastases dominates that of the bone lesion, and osteogenic sarcoma could be considered to be a lung disorder, in the history of which there is a bone lesion, since death is due to the development of the metastases even though the bone lesion has been removed or could be if its existence had not become contingent from the prognostic point of view.

Lung metastases are present in 98 % of patients followed up until their death. The date

they appear is known exactly due to the observations made in important series:

eighty-five percent appear in the first 2 years,
after 18 months only 30 % of the patients are clear.

But it is necessary to distinguish the development of the metastases linked to an anatomical development which makes it possible to diagnose them and their much earlier presence since the calculation, according to the time of duplication, leads us to think that they already exist in 60–80 % of cases at the time when the bone lesion is diagnosed. This idea of an imperceptible disease, upon which the prognosis ultimately depends, is the main element in deciding which of the current treatments to adopt. It allows us to target the treatment in a logical and effective way since it is here that the right or wrong decision is taken. All the more so as many arguments lead us to believe that these lung metastases always occur in osteogenic sarcoma and that even the cures seen with traditional treatments limited to local action on the bone lesion, are only due to the "failure" of these metastases because of the spontaneous role of the natural immune defenses.

The role played by immune reactions, which Tavernier suspected without naming them, is based today on the knowledge acquired in the area of virology, cyto-carcinogenesis, and immunology. We know that osteogenic sarcomas, and certainly other conjunctive sarcomas, are viral in origin (but also that other associated conditions are necessary for oncogenesis). We know that it is the integration or transcription of the viral genome in the tumor cells which is the foreign antigenic element responsible for immune responses involving rejection, due to the involvement of specific tumor or cell-mediated antibodies. We also know that the cytolytic potency of these immune reactions is weak, without possible action on a large bone tumor or large metastasis but that it is perhaps decisive at the stage when lung metastases cannot be seen.

After a long, disappointing time, chemotherapy for osteogenic sarcomas seems to have entered a phase of spectacular progress owing to the products used (high-dose methotrexate, adriamycin).

Part VII

Articular Biomechanics

31 The Biomechanics of the Glenohumeral Articulation and Implications for Prosthetic Design

P. Mansat, M. Mansat, and J. Egan

Introduction

To undertake normal activities of daily living the shoulder joint must allow a quite considerable range of motion [22]. The maximum elevation of the shoulder in the scapular plane generally lies between 170 and 180° (Freedman et al.) [3, 5]. To achieve this motion requires contributions from four shoulder components, namely the glenohumeral, acromioclavicular, sternoclavicular, and scapulothoracic articulations.

Muscle forces act across the glenohumeral joint to balance externally applied loads and the large motion at the shoulder involves changes of muscle moment arms. In an analysis of these forces across the shoulder it is convenient to divide the muscles into three groups: thoracoscapular, scapulohumeral, and thoracohumeral muscles. However, the motion is complex, as is the relationship between the muscle actions and the joint movement. Three-dimensional analyses that approximate the real complexity of the shoulder [1, 12, 23, 24] cannot be solved uniquely due to the large number of active muscle elements. Therefore, some numerical optimization method is required to provide estimates of the applied forces. Electromyography has been used for assessing muscle function, but this technique is limited to a small number of superficial muscles and the signal is not directly related to the muscle force magnitudes.

This paper will follow the two-dimensional analysis used by Poppen and Walker in 1976 and 1978 [17]. This considers elevation of the shoulder as a combination of the movement of the scapula across the thorax together with the articulation of the glenohumeral joint. In the normal shoulder the ratio of scapulothoracic to glenohumeral motion is 1:2, though this may reverse to 2:1 in the diseased shoulder, as glenohumeral motion becomes restricted [6].

This two-dimensional analysis is able to establish some quite fundamental biomechanical principles that can be applied to understand the stability of the shoulder in the plane of the scapula. It is justified since it has been shown that the predominant motion of the scapula during the humeral elevation is upward rotation [10]. Biomechanical stability implies that the glenohumeral articulating surfaces should remain in contact throughout the ranges of motion that the joint might naturally encounter.

The analysis presented herein also considers what this requirement for biomechanical stability implies for the design of shoulder prostheses. The first step is to set out some quite fundamental biomechanical principles that can be applied to understand the stability of the shoulder.

P. Mansat, MD (✉) • M. Mansat
Department of Orthopedic Surgery and Traumatology, Pierre Paul RIQUET Hospital, CHU Purpan, Toulouse Medical School, Paul Sabatier University, Toulouse, France
e-mail: mansat@cict.fr

J. Egan
E-Tech Ltd, Sheffield, England

D.G. Poitout (ed.), *Biomechanics and Biomaterials in Orthopedics*,
DOI 10.1007/978-1-84882-664-9_31

Basic Biomechanical Principles

To articulate a shoulder joint, muscle forces must act some distance away from the center of rotation to create a turning moment. As well as rotating the joint, these muscle forces have a tendency to cause the joint surfaces to translate if they are not balanced by an equal opposing force. In particular, the action of the deltoid muscle at the shoulder gives this combination of the abduction rotation of the glenohumeral joint with a tendency for the upward translation of the humeral head across the glenoid surface as shown in Fig. 31.1. Excessive translation must be resisted for the joint to remain stable [19].

When a force is applied to the proximal humerus, the direction of this force determines whether the shoulder will remain stable or whether subluxation will occur. If we assume in the first instance that the effects of friction are negligible, then the glenohumeral joint force must be exactly perpendicular to the articular surfaces at their point of contact. That is, the position of the humeral head will move across the glenoid surface until the point of glenohumeral contact directly opposes the applied force. If no such point of contact exists then the joint will not be stable as indicated in Fig. 31.2. This is the fundamental geometrical contact requirement for joint stability. Indeed, many of the experimental observations on shoulder behavior are a direct consequence of this fundamental principle.

Under the action of the deltoid muscle alone, the shoulder joint would tend to be unstable. The large range of motion requires that joint ligaments remain slack and only apply their passive constraints at extremes of motion. Active stabilization is needed and this is provided by the additional contraction of the rotator cuff muscles. To understand this combined effect of deltoid and rotator cuff contraction we must consider how their forces can be combined into a single "resultant" force. To combine the effects of two or more forces that act in different directions we can use the parallelogram of forces as shown in Fig. 31.3.

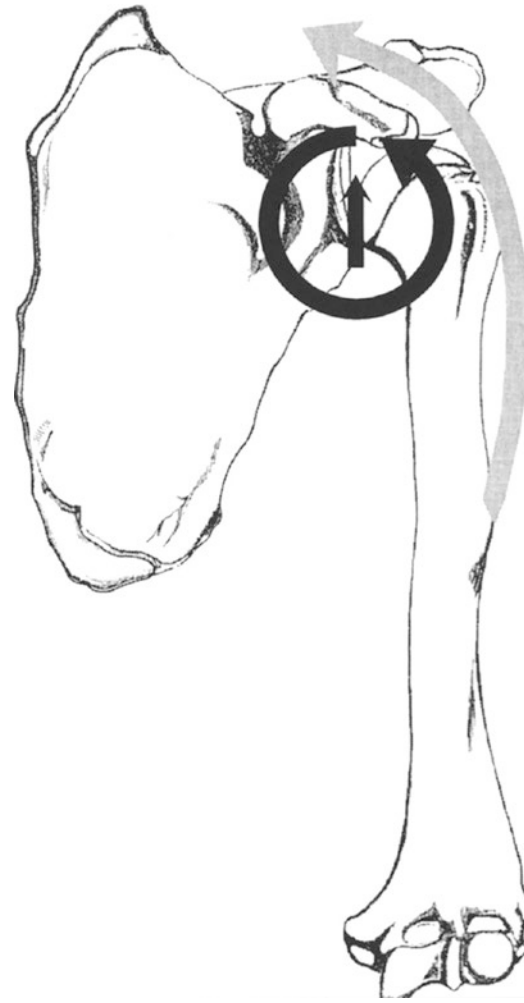

Fig. 31.1 The force from deltoid contraction (*gray*) acts some distance from the center of glenohumeral rotation and therefore acts both to rotate the joint and to translate this superiorly

Note that the muscles that give rise to these force do not have to be attached physically to the same point, the parallelogram represents only their directions and not their physical location.

Also, the parallelogram of forces can be used to uncouple a single force R into its horizontal and vertical components, R_x and R_y respectively, as shown in Fig. 31.4.

When performing any of the activities of daily living, numerous forces act upon the humerus.

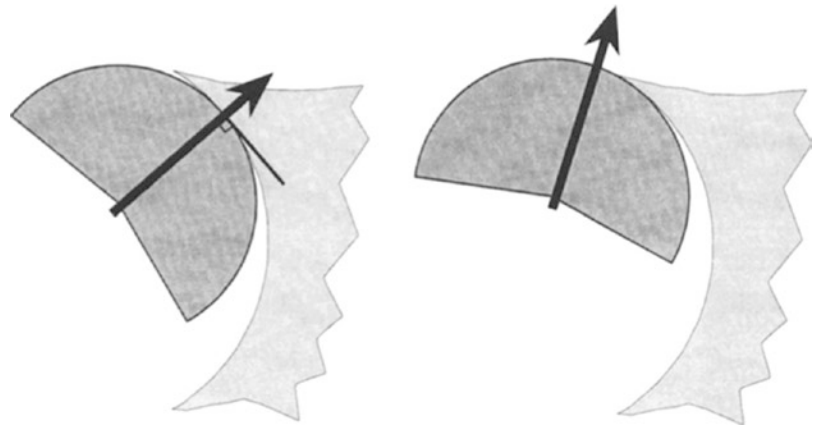

Fig. 31.2 Under conditions of zero friction stability of the glenohumeral joint depends on whether the humeral head can slide over the glenoid surface to find a contact that is perpendicular to the applied force. The condition on the left is stable; that on the right is not

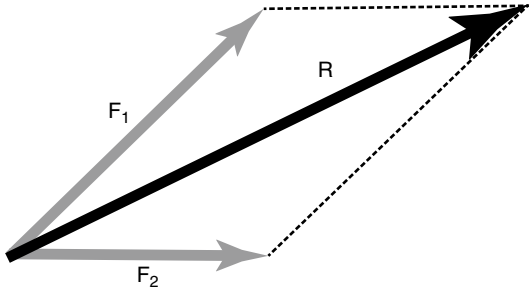

Fig. 31.3 The length of the two connecting sides of the parallelogram F1 and F2 represents the magnitude of two forces. The resultant force R is represented in both magnitude and direction by the diagonal across the parallelogram of forces

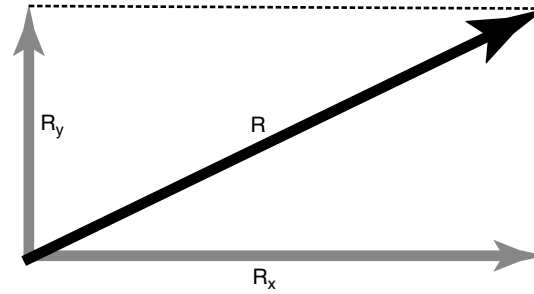

Fig. 31.4 A single force R can be separated into its horizontal and vertical components, R_x and R_y using the parallelogram of forces concept. The two forces R_x and R_y will thus produce exactly the same effect as R

These forces are derived from muscle actions, ligament constraints, and any supported weights. If at such a time the arm is held in a steady position, then the humerus itself is said to be in a state of mechanical "equilibrium" in which all applied moments (forces multiplied by the distance to the center of rotation) balance, so the net turning effect is zero. Also, all the applied forces similarly balance, so that all the horizontal and vertical components sum to zero, and consequently the net resultant force on the humerus is zero.

Armed with these three basic concepts of (i) the geometric contact requirements for joint stability, (ii) the parallelogram of forces, and (iii) the balance of turning moments and forces for mechanical equilibrium, we now have the tools necessary for a mechanical analysis of the glenohumeral joint.

Glenohumeral Force and Joint Stability

Before considering the forces that act across the shoulder, let us first examine the stability of the anatomical glenohumeral joint. Any glenohumeral joint force *R* can be uncoupled using the parallelogram of forces into a force R_x directed centrally into the glenoid and a

second shearing force R_y component that is perpendicular to this as shown in Fig. 31.4. R_x tends to stabilize the joint whilst the component R_y tends to cause the joint to dislocate. The dominate effect depends on the curvature of the glenoid.

Iannotti et al. [9] have conducted a detailed study into the geometry of the glenohumeral joint and have found the geometry of the anatomical humeral and glenoid surfaces to be approximately spherical. The average radius of curvature of the normal glenoid surface is 27 mm with an average supero-inferior dimension of 39 mm. Therefore, in the scapular plane, this average glenoid surface will subtend an arc of ±46° about the center of the glenoid as shown in Fig. 31.5. In the absence of other factors, the requirement for joint stability is that the direction of the joint force R must be within this arc. That is:

$$R_y / R_x < \tan 46°$$

$$R_y / R_x < 1.04$$

Therefore, whilst this R_y/R_x ratio value will normally vary as the shoulder moves, it must always be less than unity for the shoulder joint to remain stable in the supero-inferior direction. A consequence is that a high R_x force component will increase glenohumeral stability. Subluxation forces will therefore be directly proportional to the applied joint load, as has been observed experimentally by both Fukuda et al. [7] and Severt et al. [8]. Lippit et al. [15] referred to this effect as "concavity compression", noting that increased stability correlated with the depth of the glenoid concavity and indicated that scapular movement may also help centralize the glenohumeral articulation.

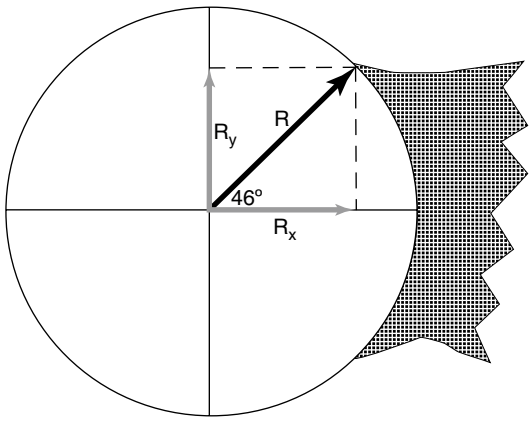

Fig. 31.5 This scale drawing shows the mean anatomical supero-inferior dimension of the glenoid and the maximum angle of the joint resultant force R for joint stability. To maintain R within this maximum limit the ratio of R_x:R_y must be less than 1:1.04. The angle 46° determines the "constraint," the higher this angle is the more constrained is the joint

Other factors will also play a role in augmenting the stability of the glenohumeral joint. The periphery of the joint is surrounded by a fibrous tissue labrum that further resists joint subluxation by effectively extending the glenoid surface through a greater arc than is shown in Fig. 31.5. The labrum consequently increases resistance to subluxation by between 18 and 52 % around the glenoid [15]. However, on the other hand, the deformation of the humeral and glenoid articular cartilage will modify surface curvature under loading so that subluxation may begin inside the glenoid periphery. The above theoretical maximum R_y/R_x ratio for the normal glenoid therefore probably overestimates the limit to glenoid stability.

The humeral head radius of curvature is found typically to be 2 mm smaller than the radius of the glenoid [9, 15]. Although the deformation of the articular cartilage that covers the opposing surfaces will accommodate some of this mismatch, the curvature difference will give the humeral head the capacity to slide across the face of the glenoid somewhat to find a position of mechanical equilibrium as shown in Fig. 31.2.

Constraint and Conformity of the Glenoid Surface

The angle subtended by the glenoid, as shown in Fig. 31.5, determines the *constraint* of the glenohumeral joint. The more the glenoid surface wraps around the humeral head, the greater is the joint stability, but this increased constraint reduces the available range of motion. Therefore, a compromise is needed. In the shoulder, the need for a great range of motion requires a significantly reduced constraint than, for example, in the hip where a greater stability and reduced motion is more suitable.

A second feature that defines the glenohumeral articulation is the *conformity* that is given by the mismatch between the radii of curvature of the opposing contact surfaces. As noted above, the glenoid radius of curvature may typically be 2 mm larger than that of the opposing humeral surface, enabling some degree of translation of the humeral head across the glenoid surface [11]. Therefore, one would expect any increase in conformity to reduce range of motion to some degree, as this sliding motion is more limited, although Harryman et al. [8] found this effect to be small. Reduced conformity does lead to reduced contact areas and thus increased contact stresses, so that again some form of compromise is required.

From the analysis given above, the maximum R_y/R_x ratio defining the limit for the stable shoulder will increase as the constraint increases, varying with the tangent of the glenoid angle as shown in Fig. 31.6. Conformity would not be expected to affect the stability in the same way.

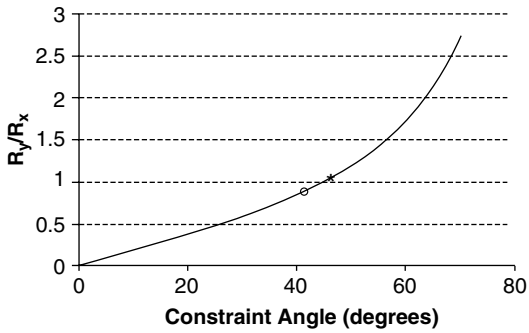

Fig. 31.6 Variation of the maximum R_y/R_x value with the geometric constraint of the glenoid. The mark (*) shows the constraint of the average anatomical glenoid and (*o*) shows the comparable position of the Neer prosthetic glenoid

Forces in the Abducted Shoulder

Analysis of the kinematics of the shoulder is complex in three dimensions. The joint itself is a mechanically indeterminate system so that, for instance, the same amount of glenohumeral movement can be achieved though different muscle actions [24]. However, an insight into the basic mechanics and the stabilizing action of the rotator cuff can be gained from a simple two-dimensional mechanical analysis. The first such analysis was conducted by Poppen et al. [16] and the analysis presented here is a derivation of this approach.

Here we will consider the situation shown in Fig. 31.1, in which the deltoid muscle alone is acting to abduct the humerus in the scapular plane [1]. The major effect of the rotator cuff musculature in this two-dimensional analysis is to pull the humeral head into the face of the glenoid, though supraspinatus is also able to abduct the shoulder [1]. The role of the rotator cuff musculature in other planes, such as for humeral internal and external rotation, cannot be considered in this two-dimensional analysis.

A first example considers a horizontally outstretched arm of 10 % body weight (0.1 W) supporting a further 0.1 W weight in the hand. In this arrangement, the force exerted by the deltoid muscle in order to maintain equilibrium with a horizontal abduction is shown in Fig. 31.7. For equilibrium, the clockwise turning moment of the loaded arm must be matched by the anti-clockwise turning moment generated by the deltoid. That is:

$$0.1\mathrm{W} \times \mathrm{L} + 0.1\mathrm{W} \times 2\mathrm{L} = 0.1 \times \mathrm{L} \times \mathrm{F}_{\mathrm{deltoid}}$$

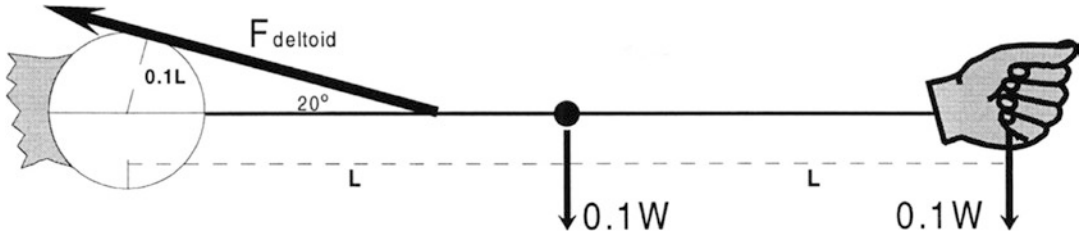

Fig. 31.7 Loading example of the horizontal arm. The hand is carrying a weight of 10 % body weight (0.1 W) and the weight of the arm itself (0.1 W) acts through the center of the limb. The two loads provide a clockwise turning moment that must be balanced by the anticlockwise moment of the deltoid force for the arm to remain abducted in equilibrium

$$F_{deltoid} = 3W$$

So that despite a fairly low physical loading (0.2 W), a deltoid force of three times body weight is needed to maintain equilibrium. This is simply because the deltoid acts through a small moment arm of only 5 % of the limb length (2 L), and thus a much higher force is needed to create an equivalent turning moment.

The parallelogram of forces can be used to combine the forces that are now acting on the humerus into a single resultant force *R* as shown in Fig. 31.8. To maintain equilibrium this joint force is counteracted by an equal opposing reaction force from the glenoid onto the humerus. The single joint force *R* can be uncoupled using the same technique to give its horizontal and vertical components that are R_x and R_y. In this way R_x is simply the combined horizontal effect of the two original forces and R_y is likewise their combined vertical effect. Therefore, for the mechanical equilibrium shown in Fig. 31.8:

$$R_x = 3W\cos 20° = 2.82W$$

$$R_y = 3W\sin 20° = -0.2W = 0.83W$$

The parallelogram of forces can be used to calculate the single joint force *R* where:

$$R^2 = R_x^2 + R_y^2$$

In this case the value of *R* is 2.9 W and the R_y/R_x ratio value of this resultant force is 0.29. Remember that the shoulder will be unstable if this ratio exceeds a theoretical value of unity. Thus, one may conclude that equilibrium is likely be maintained by the arrangement of forces shown in Fig. 31.8.

Now, in a second example, consider the same loading situation with the arm hoisted to only 30° of abduction as shown in Fig. 31.9. In this case the balance of rotational moments gives:

$$0.1W \times L \times \sin 30° + 0.1W \times 2L \times \sin 30°$$
$$= 0.1 \times L \times F_{deltoid}$$
$$F_{deltoid} = 1.5W$$

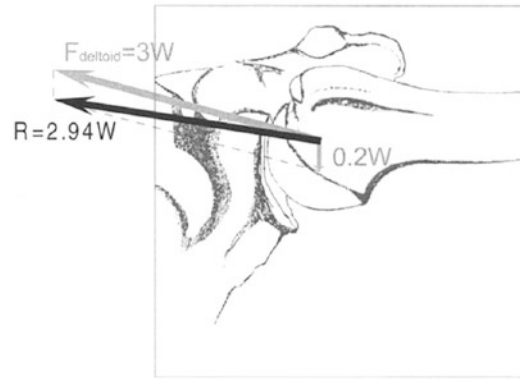

Fig. 31.8 The forces applied to the humerus in Fig. 31.7 can be collected into a single resultant force that has a magnitude of 2.94 times body weight and acts at 16.3° to the horizontal. Under this loading the shoulder is stable

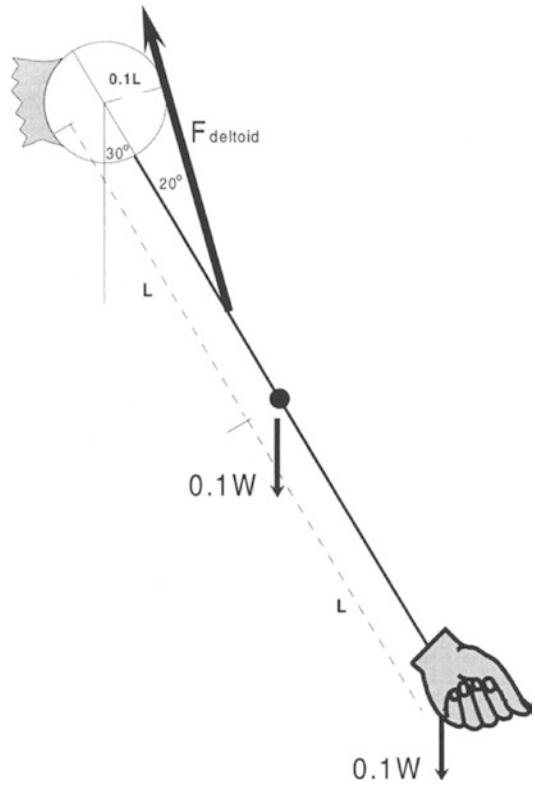

Fig. 31.9 Loading example with the arm abducted to 30°. The perpendicular distance of the 10 % body weight in the hand and the weight of the arm from the center of rotation is smaller than in Fig. 31.7 being 2 L sin 30 and L sin 30 respectively. Therefore, the clockwise turning moments is reduced compared to that in Fig. 31.7 and the opposing deltoid force is smaller

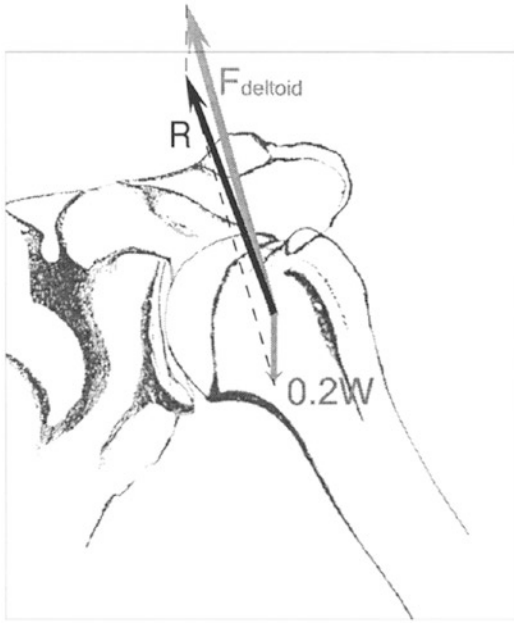

Fig. 31.10 The forces applied to the humerus in Fig. 31.9 can be collected into a single resultant force that has a magnitude of 1.3 times body weight and acts at 78.5° to the horizontal. Under this loading the shoulder is unstable

So now a lesser deltoid force of 1.5 times body weight is required to maintain the equilibrium. However, the direction of this deltoid force is much more vertical, so that the parallelogram of force creates a more vertical resultant glenohumeral force as shown in Fig. 31.10. The horizontal and vertical components of this resultant force are now:

$$R_x = 1.5\text{W}\cos 80° = 0.26\text{W}$$

$$R_y = 1.5\text{W}\sin 80° - 0.2\text{W} = 1.28\text{W}$$

Here the resultant joint force R magnitude is 1.3 W but the R_y/R_x ratio takes a value of 4.92. Under this resultant force, the shoulder would be expected to be unstable in this case and would certainly dislocate superiorly.

Now the action of the rotator cuff musculature can be superimposed onto the resultant joint force calculated using Fig. 31.10. Here we will assume that this rotator cuff force acts perfectly horizontally. In combination with the joint force, a new parallelogram can be formed to calculate a new

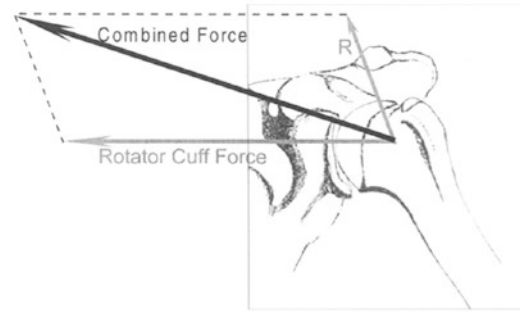

Fig. 31.11 The rotator cuff muscles effectively increase the horizontal force component R_x so that the R_y/R_x ratio is reduced to a point where the shoulder can be stable. However, to achieve this with the forces shown requires a rotator cuff force of 3.24 times body weight

final resultant single force. In Fig. 31.11 the R_y/R_x ratio value is brought down to 0.36 (tan 20°), at which point the shoulder may be expected to be stable. Effectively, the rotator cuff is reducing this ratio by increasing the denominator R_x value. However, this stabilization requires a large cuff force of 3.24 times body weight and the resultant combined joint reaction force in now 3.72 W. In this case, rotator cuff activity from supraspinatus will be most effective to protect the joint from superior subluxation, although an intact "transverse force couple" (subscapularis, infraspinatus, teres minor) may itself ensure normal glenohumeral motion [19, 20].

In a modification of the above scenario, Fig. 31.12 shows the effect when the rotator cuff force is displaced downwards by 10°. With this fairly minor adjustment, the rotator cuff force needed to maintain stability is reduced by 31 %.

Because the shoulder system is mechanically indeterminate, it is not possible to be sure that the above picture presents an accurate view of reality, as the same shoulder positions can be achieved through the actions of different muscles. Indeed, supraspinatus may have a role in the initiation of abduction [20]. However, the analysis does demonstrate that high loads can be created at the glenohumeral joint as the rotator cuff contracts to increase the normal force (R_x) to ensure joint stability. The effect of the rotator cuff is required

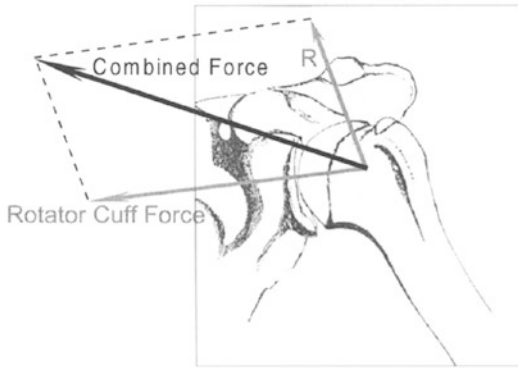

Fig. 31.12 Displacing the rotator cuff force downwards somewhat has the effect of reducing the muscle forces and the combined joint reaction force appreciably compared to those in Fig. 31.11

more in early abduction when the direction of the deltoid force is more tangential to the glenoid fossa.

Anterior–Posterior Considerations

The whole of above analysis concerns the abduction of the glenohumeral joint in the scapular plane and movement is entirely supero-inferior. However, the same considerations apply in the antero-posterior (a–p) direction with activities requiring internal and external rotation. In this plane the glenoid fossa is a more complex pear shape with an average superior dimension of 23 mm and a larger inferior dimension of 29 mm [9]. Note that these sizes are smaller than the equivalent supero-inferior dimension, so that the glenoid is less constrained in the antero-posterior direction. The 1:0.8 ratio in the superior and inferior a–p dimension observed by Iannotti exactly matches the 1:0.8 ratio in superior and inferior a–p subluxation forces measured by Lippit et al. [15], once again showing how the glenoid concave geometry is a major determinant of shoulder stability.

In fact, using the theoretical techniques described above, inferior a–p subluxation should require a maximum R_z/R_x ratio value of 0.64. This will again probably be less in practise due to a flattening of the curvature of the articulating surfaces under load. Rotator cuff activity from subscapularis and infraspinatus will be effective in preventing anterior and posterior instability respectively.

The Effect of Joint Friction

The above analysis has been conducted under the assumption that the effect of friction at the glenohumeral articulation is negligible. The coefficient of friction of the cartilage surface of the anatomical joint is about 0.003, which contributes a friction force of only 3 thousandths of the resultant force calculated above. This may accurately be described as negligible. In the case of the prosthetic joint, the coefficient of friction for metal on polyethylene reaches approximately 0.08 so that again the friction force will comprise less than 10 % of the joint reaction force. This friction will act in a direction to resist dislocation so that the joint will consequently be more stable by this same amount. Experimental measurement of frictional torque by Severt et al. [18] presents low values of 0.1–0.3 Nm, with the lowest values in this range associated with prostheses with the lowest conformity.

Glenohumeral conformity will have a greater frictional effect with rotation in the plane of the glenoid, as may occur in humeral elevation perpendicular to the scapular plane. Whilst the friction forces will be the same, the frictional torque will then depend on the radius of the joint contact area, which can be much smaller in the less conforming geometry.

The most significant effect of joint friction is likely to occur in hemi-arthroplasty where friction of the metal-on-bone articulation has been estimated to reach 0.3. Therefore, an additional frictional force 30 % of the joint reaction force will enter the analysis and make the joint more stable against dislocation. However, the cost of this higher joint friction may be to increase the wear damage of the glenoid cavity which will change its geometry, possibly reducing the constraint and eventually leading to reduced joint stability. This behavior [14] appears in the posterior glenoid wear that may accompany

hemi-arthroplasty [14]. This loss of glenoid constraint may be restored with the use of a prosthetic glenoid.

Implications for Shoulder Prosthesis Design

The typical share of scapulothoracic to glenohumeral motion is 1:1.3 after shoulder arthroplasty rather than the normal 1:2 [6], and also the range of motion is often less that the normal shoulder. Therefore, one may expect that normal shoulder kinematics are not usually restored by this surgery. The anatomical position of the glenohumeral articulation is clearly important for rotator cuff function [13]. The balance of moments in Figs. 31.7 and 31.9 demonstrates the importance of the deltoid moment arm which must be restored with sufficient lateral offset in a humeral prosthesis, otherwise even larger deltoid forces and joint reaction forces must be generated around the joint to achieve equilibrium.

In their cadaver study, Severt et al. [18] revealed that the lateral humeral offset that determines the deltoid moment arm increases with humeral head thickness. This anatomical feature is reflected in the design of the Neer 3 humeral component (Fig. 31.13) in which the larger humeral head positions are adjusted medially to increase their effective deltoid moment arm.

As discussed above, the constraint and the conformity of the glenohumeral articulation are two principle features that determine shoulder motion and stability. On Fig. 31.6 the supero-inferior constraint produced by the standard Neer II prosthetic glenoid component is indicated alongside that of the average anatomical glenoid. From the theoretical calculation as conducted above, the expected maximum R_y/R_x ration at subluxation for the standard Neer II glenoid prosthesis would be 0.89. This is 14 % lower than the normal glenoid, although the smaller supero-inferior dimension of the Neer glenoid prosthesis (33.3 mm) is somewhat compensated by a reduced radius of curvature of 25 mm.

In fact, Severt et al. [18] experimentally measured a R_y/R_x ratio of 0.6 at subluxation with the Neer glenoid and this same figure varied from 0.2 to 0.8 with different types of glenoid prostheses depending on the prosthetic design and the direction of loading. Fukuda [7] similarly measured this ratio for the Neer II glenoid at 0.87 decreasing to 0.53 as the central loading (R_x) approaches body weight. These figures are close to the theoretical value shown in Fig. 31.6. A difference between these experimental estimates and the theoretical calculation of the maximum R_y/R_x ratio is due to the effects of the deformation of the polyethylene prosthesis under load that reduces its effective curvature and hence its constraint. Indeed, this indicates the importance of achieving the full seating of the all-polyethylene glenoid prosthesis against a prepared glenoid cavity to protect against instability. A ratio value of 0.43 occurs when an all-polyethylene prosthesis is not fully supported on its bone-contacting surface.

Karduna et al. [11] have demonstrated that variation of conformity in a total shoulder prosthesis has a negligible effect on stability as indicated by the maximum R_y/R_x ratio. Therefore, a reduction in conformity with some radical mismatch between the humeral and glenoid

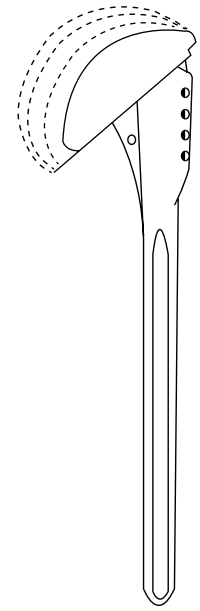

Fig. 31.13 In the Neer 3 humeral stem design, the articulation of the larger head sizes is medialized to increase the deltoid moment arm

articulating surfaces may provide for a more physiological motion with some glenohumeral translation without a penalty of a loss of stability. Severt et al. [18] found that reducing conformity increases the translation to reach the maximum subluxation force. This is to be expected from the analysis presented above (Fig. 31.2). In fact, in the absence of polyethylene deformation, a perfectly conforming articulation would not translate at all prior to dislocation.

An increased conformity will increase the frictional torque in elevation rotation in the plane of the glenoid. This will inevitably increase the demands on the fixation of a glenoid prosthesis. On the other hand, a reduced conformity will increase the glenohumeral contact stresses that may take these values beyond the yield stress for the polyethylene and result in an increased wearing of this material [21].

All factors that have the virtue of increasing the stability of the shoulder by increasing the subluxation forces inevitably have the consequence that the higher forces will also place greater demands on the implant fixation. Therefore, it is important to consider how the changes of glenohumeral articulation may affect the stresses transferred from the implant to the bone, which may determine the durability of the fixation of the glenoid prosthesis.

Couteau et al. [2] have used a three-dimensional finite element model to examine the changes in scapular stresses with off-center loading. Figure (plate section) shows that a principle effect of the off-center loading is a modification of the bending of the scapula in the vicinity of the posterior notch. One may expect that whilst this bending may normally serve a useful physiological shock-absorbing function, an exaggerated bending may challenge implant fixation. One may conjecture that central glenoid loading is likely to be most conservative for the implant fixation, with a reduction of a so-called "rocking-horse" effect [4]. Following on from the analysis given above, central glenoid loading is dependent on a proper functioning of the rotator cuff musculature. Indeed, rotator cuff dysfunction has been associated with glenoid implant loosening [4].

A second and surprising effect uncovered in the finite-element study of Couteau et al. [2] is the increase of implant bone interface stresses as the conformity of the glenohumeral articulation is reduced.

The scapular bone stock available for glenoid fixation and the condition of the rotator cuff musculature are two factors that must influence prosthesis selection and operative procedure. If the rotator cuff cannot be expected to aid joint stability, then a more conforming articulation that is inherently more stable may be preferred, even though this may place increased demands on glenoid fixation.

Summary

Although the shoulder is a non-weight-bearing joint, high loads can nevertheless be generated across the glenohumeral articulation.

The stability of the glenohumeral articulation, both anatomical and prosthetic, is dependent on the humeral and glenoid articulating geometry, the adequate bony support for a glenoid prosthesis, and also on the function of the rotator cuff musculature.

The mechanical demands placed on glenoid prosthesis fixation are also appreciably affected by the characteristics of the glenohumeral articulation, but the effects here are complex and require a full three-dimensional mechanical analysis to comprehend.

Acknowledgements Dr Beatrice Couteau of INSERM U305, Toulouse, for biomechanical discussions and permission to use the graphic.

References

1. Bassett RW, Browne AO, Morrey BF, An KN. Glenohumeral muscle force and moment mechanics in a position of shoulder instability. J Biomech. 1990;23:405–15.
2. Couteau B, Hobatho MC, Darmana R, Mansat P. Finite element model of the scapula with an anatomically shaped glenoid implant – analysis of the joint contact. Proc. XVIIth ISB congress (Calgary); 1999. p. 181.

3. Doody SG, Freedman L, Waterland JC. Shoulder movements during abduction in the scapular plane. Arch Phys Med Rehabil. 1970;51:595–604.
4. Franklin JL, Barrett WP, Jackins SE, Matsen III FA. Glenoid loosening in total shoulder arthroplasty. Association with rotator cuff deficiency. J Arthroplasty. 1998;3:39–46.
5. Freedman L, Munro RR. Abduction of the arm in the scapular plane: scapular and glenohumeral movements. J Bone Joint Surg Am. 1966;48:1503–10.
6. Friedman RJ. Prospective analysis of total shoulder arthroplasty biomechanics. Am J Orthop. 1997;26:265–70.
7. Fukuda K, Chen CM, Cofield RH, Chao EY. Biomechanical analysis of stability and fixation strength of total shoulder prostheses. Orthopedics. 1988;11:141–9.
8. Harryman DT, Sidles JA, Harris SL, Lippitt SB, Matsen III FA. The effect of articular conformity and the size of the humeral head component on laxity and motion after glenohumeral arthroplasty. A study in cadavera. J Bone Joint Surg. 1995;77(A):555–63.
9. Iannotti JP, Gabriel JP, Schneck SL, Evans BG, Misra S. The normal glenohumeral relationships. An anatomical study of one hundred and forty shoulders. J Bone Joint Surg. 1992;74A:491–500.
10. Karduna AR, Williams GR, Williams JL, Iannotti JP. Glenohumeral joint translations before and after total shoulder arthroplasty. A study in cadavera. J Bone Joint Surg. 1997;79A:1166–74.
11. Karduna AR, Williams GR, Williams JL, Iannotti JP. Joint stability after total shoulder arthroplasty in a cadaver model. J Shoulder Elbow Surg. 1997;6:6–511.
12. Karlsson D, Peterson B. Towards a model for force predictions in the human shoulder. J Biomech. 1992;25/2:189–99.
13. de Leest O, Rozing PM, Rozendaal LA, van der Helm FC. Influence of glenohumeral prosthesis geometry and placement on shoulder muscle forces. Clin Orthop. 1996;330:222–33.
14. Levine WN, Djurasovic M, Glasson JM, Pollock RG, Flatow EL, Bigliani LU. Hemiarthroplasty for glenohumeral osteoarthritis: results correlated to degree of glenoid wear. J Shoulder Elbow Surg. 1997;6:449–54.
15. Lippitt S, Matsen F. Mechanisms of glenohumeral joint stability. Clin Orthop. 1993;291:20–8.
16. Poppen NK, Walker PS. Normal and abnormal motion of the shoulder. J Bone Joint Surg Am. 1976;58A:195–201.
17. Poppen NK, Walker PS. Forces at the glenohumeral joint in abduction. Clin Orthop. 1978;135:165–70.
18. Severt R, Thomas BJ, Tsenter MJ, Amstutz HC, Kabo JM. The influence of conformity and constraint on translational forces and frictional torque in total shoulder arthroplasty. Clin Orthop. 1993;292:151–8.
19. Soslowsky LJ, Carpenter JE, Bucchieri JS, Flatow EL. Biomechanics of the rotator cuff. Orthop Clin North Am. 1997;28:17–30.
20. Thompson WO, Debski RE, Boardman III ND, Taskiran E, Warner JJ, Fu FH, et al. A biomechanical analysis of rotator cuff deficiency in a cadaveric model. Am J Sports Med. 1996;24:286–92.
21. Tomaszewski PR, Ondria JM. Incongruency and its relation to stress in prosthetic shoulder components. Orthopaedic Research Society; 1992.
22. Triffitt PD. The relationship between motion of the shoulder and the stated ability to perform activities of daily living. J Bone Joint Surg. 1998;80A:41–6.
23. van der Helm FC. A finite element musculoskeletal model of the shoulder mechanism. J Biomech. 1994;27:551–69.
24. van der Helm FC. Analysis of the kinematic and dynamic behavior of the shoulder mechanism. J Biomech. 1994;27:527–50.

Robotic Surgery of the Scapulo-Clavicular Girdle

32

Eric Nectoux, Sybille Facca, Gustavo Mantovani, Stacey Berner, and Philippe A. Liverneaux

Surgery of the scapulo-clavicular girdle underwent several developmental steps tending towards utilization of both lesser invasive surgical approaches and ever more precise technical procedures. At the beginning, from the advent of modern anaesthesia until the end of the first half of the twentieth century, numerous so-called "open" surgical approaches had been described. Each responded to a precise goal, that is to reach a deeply situated tissue in order to perform the repair of a given lesion, while avoiding any harm to every other noble anatomical structures. However, during this period, surgeons did not usually care about the size of the residual scarring or the extension of the underlying dissection. "Great surgeon, large incision" as the popular saying used to underline. Nowadays, such surgeons have lost a great deal of their panache, and these large incisions (i.e., the Martini approach) have been progressively abandoned because they are too invasive. Some open approaches are still in use in prosthetics surgery or in traumatology when there is a need to extract bony fragments and /or introduce large prosthetics components or large osteosynthesis devices.

"Open" surgery up until the 80s was the only way to approach the scapulo-clavicular girdle, despite the publication of the first arthroscopic gleno-humeral studies in a human cadaver in the 1950s [1, 2]. The main goal of arthroscopy is to reach deep tissues in order to repair several types of lesions with limited harm to other structures thanks to punctiform approaches. It wasn't until the 90s that routine gleno-humeral arthroscopy was performed in clinical practice [3–5]. In fact, scapulo-clavicular girdle arthroscopy itself needed several steps to develop [6]. The first step was represented by a dramatic improvement in diagnosis, with comparison to previous low-quality paraclinical examinations and regarding difficult if not damaging surgical approaches. The second step consisted in proposing various surgical techniques equivalent to their "open" homologues [7] (repair of gleno-humeral ligaments, acromioplasty, acromio-clavicular joint resection, rotator cuff suture…). The third step was to propose new and previously undescribed

E. Nectoux, MD
Department of Children's Surgery and Orthopedics, Lille University Hospital, Lille, France

S. Facca, MD, PhD
Department of Hand Surgery, Strasbourg University Hospitals, Strasbourg, France

G. Mantovani, MD
Department of Hand Surgery, Sao Paolo Hand Center, Ben Portuguesa Hospital, Sao Paolo, Brazil

S. Berner, MD
Hand Surgery Department, Sinai Hospital Orthopaedic, Baltimore, MD, USA

P.A. Liverneaux, MD, PhD (✉)
Hand and MicroSurgery Department, Strasbourg University Hospitals, Illkirch, France
e-mail: liverneaux@chru-strasbourg.fr

D.G. Poitout (ed.), *Biomechanics and Biomaterials in Orthopedics*,
DOI 10.1007/978-1-84882-664-9_32

techniques (cure of SLAP lesions, chondroplasty, joint washing, partial debridements, shrinkage, mini-open cuff repair…). The fourth step arrived when arthroscopy left the sole gleno-humeral joint to explore other joints such as the acromio-clavicular [8–11], the sterno-clavicular [12] or the scapulo-thoracic joints [13]. The fifth and still actually developed step to date is to extend the use of endoscopic means to the exploration of peripheral nervous tissue. Supra-clavicular neurolysis has already been described [14–16], and some recent reports propose an endoscopic approach of the brachial plexus [17, 18], and its surgical repair [19].

In this context, we think it possible to take a step further by developing robotically assisted surgery of the scapulo-clavicular girdle. Theoretical assets of robotics versus endoscopy are the suppression of physiological tremor, three-dimensional high definition view of the surgical field, optical magnification and comfortable ergonomics. However, since surgical robots available on the market to date have been designed for soft tissue surgery, it seems logical in the first place to focus on robotically-assisted surgery of the nervous tissue of the scapulo-humeral girdle. We will firstly expose our experimental studies before reporting our preliminary clinical experience.

Experimental Surgery

Regarding surgical management of scapulo-clavicular girdle palsies, recent development of neurotizations should not make us forget that direct exploration of nervous lesions has still got many indications, especially in total brachial plexus palsies. Of course, surgical approach of the supra-clavicular plexus, often performed 3 months after the initial trauma, is rendered difficult with soft tissue sclerosis. In this context however, development of minimally-invasive techniques should allow early intervention, within the 8 following days after injury. The main goal would be both an assessment and early surgical repair in semi-emergency of any graftable root, without breaking all ties with possible secondary complementary neurotizations.

This study was conducted at the experimental robotic surgery lab at Intuitive Surgical™ (Sunnyvale, CA, USA). In a fresh cadaver were prepared three 8 mm approaches next to the external half of the right clavicular region, starting from the lateral tip of the clavicle and further on separated from each other by 6 cm gaps, all of them being distant of at least 9 cm from the cervical region. Then was installed a DaVinci® robot (Intuitive Surgical™, Sunnyvale, CA,USA) next to the right shoulder. Using the two most lateral and medial approaches were introduced 2 arms holding detachable surgical instruments, and by the in-between approach was inserted a double endoscopic 3D HD camera. A dissection chamber was created using forceps and bipolar scissors, furthermore maintained during the procedure by CO_2 insufflation 4 mmHg pressure (Fig. 32.1).

The supra-clavicular brachial plexus and adjacent anatomical structures were dissected: jugular vein, phrenic nerve, scaleni muscles, C4–C7 nerve roots. Haemostasis was obtained by using both electrocoagulation and surgical clips. An artificial lesion was performed by cutting a 2 cm gap in the C5 root. This "substance loss" was auto-grafted by matching both extremities with epiperineural 10/0 nylon stitches performed via the instrumental port. The entire procedure was filmed and recorded. No technical difficulties were noted (Fig. 32.2).

Our results show that an endoscopic treatment of supra-clavicular palsies seems possible. Low pressure CO_2 insufflation not only avoided both tissular coadaptation of the dissection and subcutaneous gaseous emphysema, but also provided comfortable working chamber. Using a surgical robot facilitated the dissection step, and allowed performance of microsurgical sutures in very comfortable conditions. Ideally, one should have available smaller instruments and instruments more adapted to nervous surgery such as fibrine glue or electrostimulation in order to perform

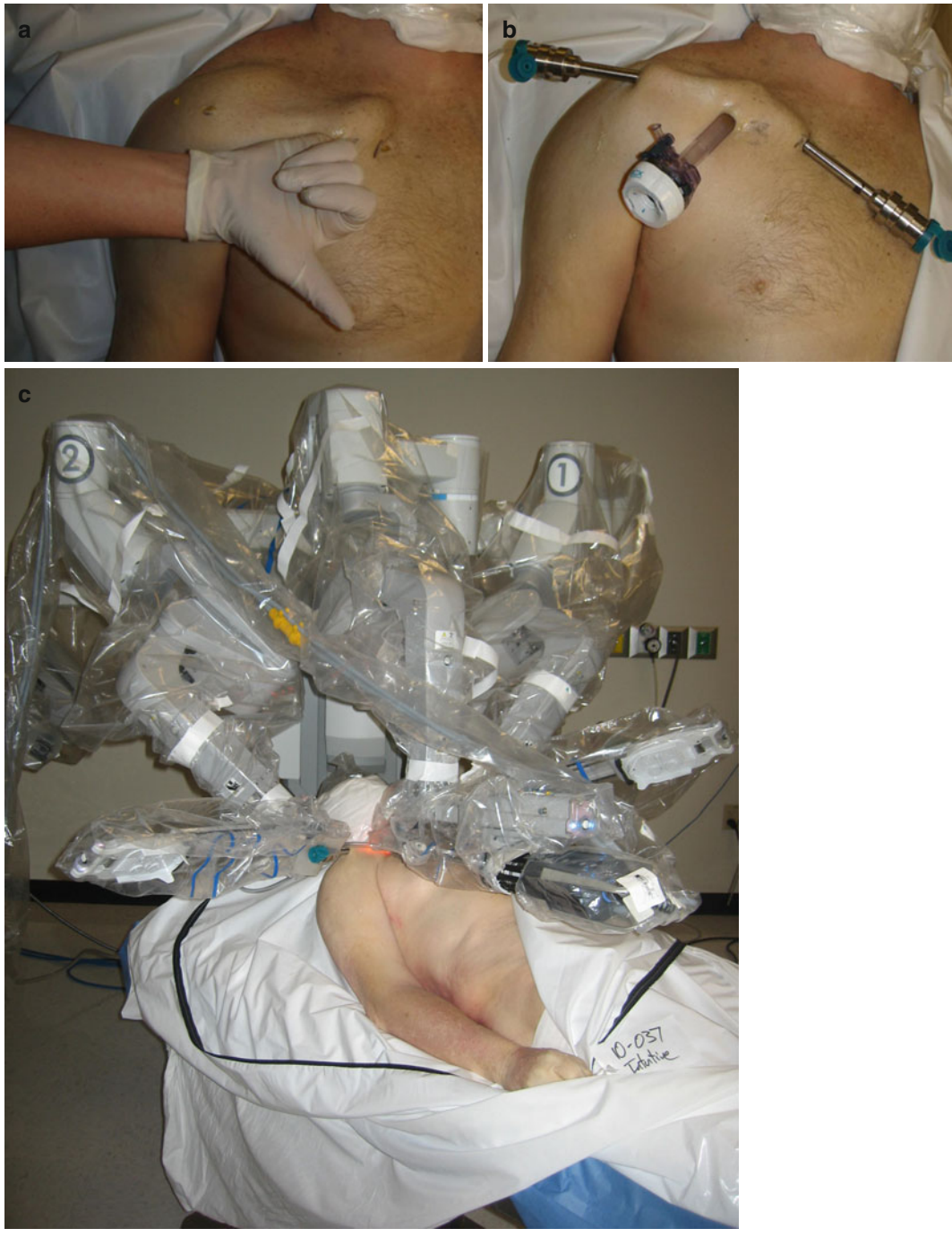

Fig. 32.1 Preparation of arobotically-asisted endoscopic repair of a right supraclavicular brachial plexus: (**a**) finger introduction into one of the instrumental approaches in order to perform a subcutaneous dissection preparing the working chamber. (**b**) The 3 trocars are set in place. (**c**) The robot ready to operate. Note that the "slave" base of the robot is situated at the cranial extremity on the opposite side

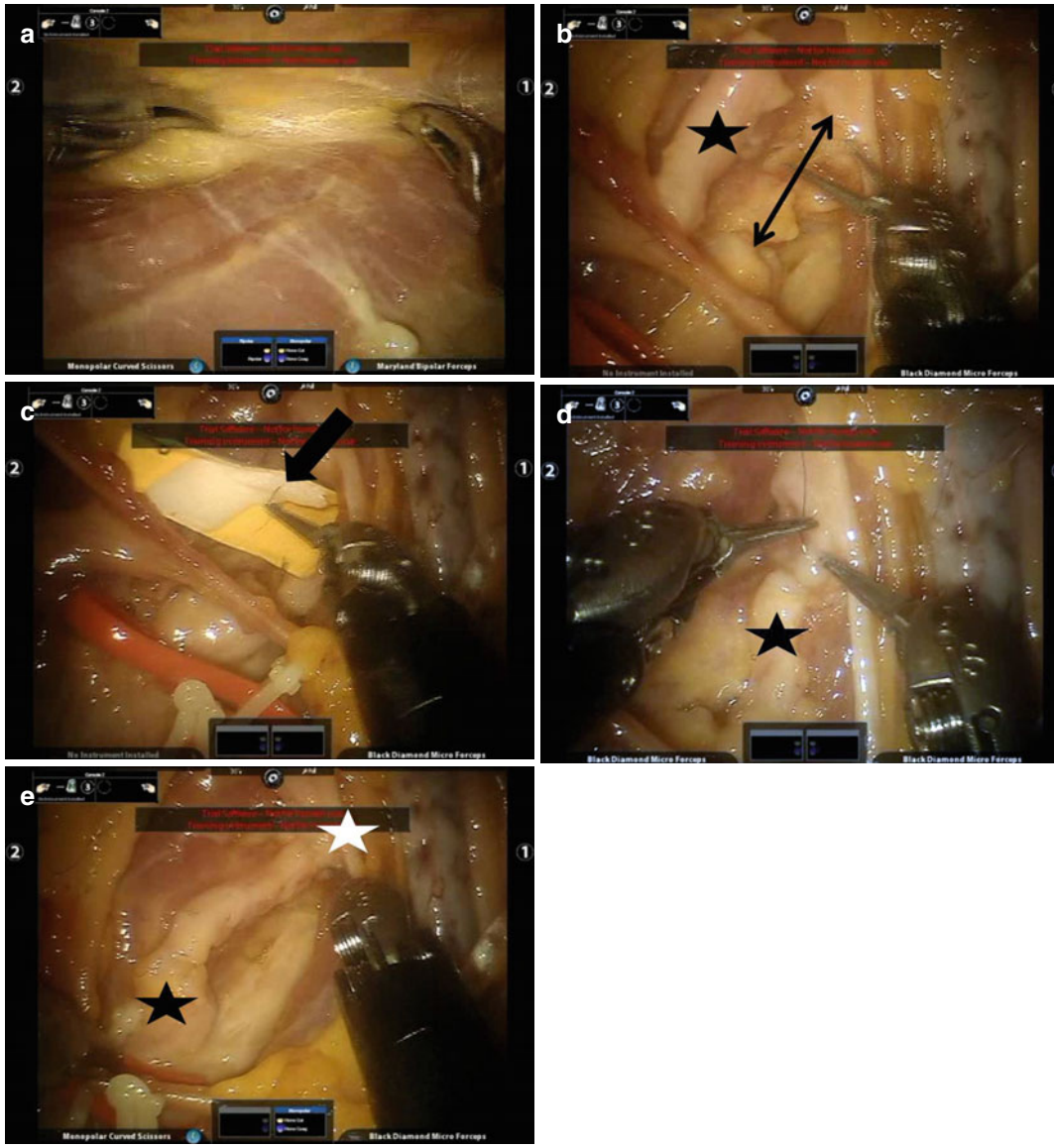

Fig. 32.2 Endoscopic view from the master console of a robotically-assisted repair of a right supraclavicular brachial plexus: (**a**) View of the working chamber, progressively widened by an instrumental dissection. Note on both sides of the operating field bipolar "Maryland" forceps. (**b**) View of the working chamber. The C5 root with its 2 cm gap section as an experimental graft model (black star). The black arrow points towards the substance loss. (**c**) View of the working chamber. Introduction of a 10/0 nylon thread with its support using one of the two instrumental trocars. The needle is held by a "Black diamond®" forceps (**d**) View of the working chamber. Note the needle through the proximal stump of the C5 root. The black star points the graft model described in G. (**e**) View of the working chamber. Final view of the graft. The white star shows the C5 root upstream of the graft and the black star the C5 root following the graft

such a procedure in routine clinical practice. Nonetheless, the perspective of having such minimally-invasive techniques coming in handy and available should allow surgical management in semi-emergency of traumatic brachial plexus palsies with maximal reliability.

Table 32.1 Our clinical series of 8 scapulo-clavicular girdle palsies

Patient	Gender	Age	Side (R-L)	Lesion	Procedure	Follow-up (months)	BMRC score
1	M	35	L	Total brachial plexus	C5-Musculocutaneous graft	22	0
2	M	23	R	Total brachial plexus	XI- musculocutaneous graft	18	2+
3	M	33	L	Axillary nerve	Neurolysis	12	5
4	M	20	L	Axillary nerve	Neurolysis	10	5
5	M	22	R	C5-C6 roots	Oberlin procedure	8	4
6	M	31	L	C5-C6 roots	Oberlin procedure	7	4+
7	M	24	R	C5-C6 roots	Oberlin procedure	10	4+
8	M	26	L	Axillary nerve Musculocutaneous nerve	Somsak procedure Oberlin procedure	12	4 4+

BMRC British Medical research council score for muscular force, *R* right, *L* left, *M* male

Clinical Experience

Since the 90s, telesurgery has been routinely performed in cardiac, urologic, gynaecologic and digestive surgery. It has brought major progress in these fields: reduction of total procedure duration, enhancement of both precision and accuracy of the surgical gesture, decrease in blood loss, better surgical ergonomics. For all these reasons, we developed the concept of telemicrosurgery [20] and tried to apply the latter to surgical indications belonging to nervous microsurgery [21]. We report a series of 8 cases of nervous lesions at the scapulo-clavicular girdle operated with a DaVinci S® robot since 2009.

All patients were operated at the Hôpitaux Universitaires de Strasbourg (Strasbourg University Hospital) (Table 32.1). Our series comprised eight patients, all men, aged a mean 27 year (20–35). There were 2 complete brachial plexus palsies, 3 partial C5–C6 brachial plexus palsies and 2 in-continuity axillary nerve lesions, and at last one associated palsy of the axillary nerve and musculo-cutaneous nerve.

All patients were operated by telemicrosurgery using a DaVinci S® robot. The robot was equipped with 3 arms, one bearing Potts scissors and the two other microsurgical Black Diamond® forceps. All sutures were performed with 9/10 and 10/0 nylon in addition to biological glue.

Both complete brachial plexus palsies underwent sural nerve grafting between the C5 root or the spinal nerve and the musculo-cutaneous nerve at the arm. The latter procedures were performed after subcutaneous dissection of the supraclavicular region up to the cervical region. The 3 incisions each measured 8 mm but an "open" conversion had to be done in both cases because dissection of the area was too difficult. C5–C6 avulsions were managed by neurotisation of an ulnar nerve fascicle onto the motor branch of the musculo-cutaneous nerve (Oberlin technique). In both cases of axillary nerve exploration, using the robot failed because it was found impossible to reach the lesion with the microsurgical instruments. An "open" conversion was needed in these two cases. Concerning the combined palsy of the axillary nerve and the musculo-cutaneous nerve, a neurotisation of the axillary nerve by the nerve of the long head of the triceps brachii (Somsak technique) and a neurotisation of an ulnar nerve fascicle onto the motor branch of the musculo-cutaneous nerve (Oberlin technique) were performed.

This small series with a very short follow-up nonetheless highlights new perspectives regarding indications of telemicrosurgery in peripheral nerve surgery, depending on the lesional level.

At the cervical level, contribution of telemicrosurgery might well prove capital, by allowing minimally-invasive approach of the brachial plexus. Beyond the cervical level, indications for telemicrosurgery are quite similar to those in conventional microsurgery. However, its main

features greatly facilitate the surgical gesture. At the axillary level, moreover in lateral decubitus, the combined anterior and posterior approach of the axillary nerve is impossible in telemicrosurgery, since DaVinci S® ergonomics are not designed for "horizontal surgery".

We think that it will be possible, hopefully in a near future, to define specific indications for telemicrosurgery [22], thanks to its outstanding features (suppression of physiological tremor, simultaneous utilization of several microinstruments, enhancement of the surgeon's gestures, three-dimensional HD vision) [23].

Conclusion

Robotically-assisted surgery of the scapuloclavicular girdle is at its birth. In comparison with endoscopy, development of this technique follows the opposite direction, since endoscopy started with the articular exploration and further steps led to exploration of the soft tissues. Robotically-assisted surgery starts to the contrary with the exploration of peripheral nerve structures, and will hopefully find new indications in the future.

References

1. Burman MS. Arthroscopy, a direct visualization of joints: an experimental cadaver study. J Bone Joint Surg. 1931;13A:669.
2. Watanabe M. Atlas of arthroscopy. 2nd ed. Tokyo: Igakui-Shoin; 1969.
3. Caspari RB. Shoulder arthroscopy: a review of the present state of the art. Contemp Orthop. 1982;4:523.
4. Johnson LL. Arthroscopy of the shoulder. Orthop Clin North Am. 1980;11:197.
5. Poehling GG, Whipple TL. Elbow arthroscopy: a new technique. Arthroscopy. 1989;5:222.
6. Fontes D. Chirurgie arthroscopique du membre supérieur. Chir Main. 2006;25:S4–7.
7. Rockwood CA. Shoulder arthroscopy. J Bone Joint Surg. 1988;70A:639.
8. Boileau P, Old J, Gastaud O, Brassart N, Roussanne Y. All-arthroscopic Weaver-Dunn-Chuinard procedure with double-button fixation for chronic acromioclavicular joint dislocation. Arthroscopy. 2010;26:149–60.
9. Nourissat G, Kakuda C, Dumontier C, Sautet A, Doursounian L. Arthroscopic stabilization of Neer type 2 fracture of the distal part of the clavicle. Arthroscopy. 2007;23:674.
10. Lafosse L, Baier GP, Leuzinger J. Arthroscopic treatment of acute and chronic acromioclavicular joint dislocation. Arthroscopy. 2005;21:1017.
11. Pujol N, Philippeau JM, Richou J, Lespagnol F, Graveleau N, Hardy P. Arthroscopic treatment of distal clavicle fractures: a technical note. Knee Surg Sports Traumatol Arthrosc. 2008;16:884–6.
12. Tavakkolizadeh A, Hales PF, Janes GC. Arthroscopic excision of sternoclavicular joint. Knee Surg Sports Traumatol Arthrosc. 2009;17:405–8.
13. Clavert P. L'arthroscopie de la scapulo-thoracique. In: Allieu Y, Roux JL, Zu Reckendorf GM, et al., editors. La ceinture claviculo-scapulaire – actualités thérapeutiques. Montpellier: Sauramps; 2010.
14. Barber FA. Percutaneous arthroscopic release of the suprascapular nerve. Arthroscopy. 2008;24:236.
15. Ghodadra N, Nho SJ, Verma NN, Reiff S, Piasecki DP, Provencher MT, Romeo AA. Arthroscopic decompression of the suprascapular nerve at the spinoglenoid notch and suprascapular notch through the subacromial space. Arthroscopy. 2009;25:439–45.
16. Lafosse L, Tomasi A, Corbett S, Baier G, Willems K, Gobezie R. Arthroscopic release of suprascapular nerve entrapment at the suprascapular notch: technique and preliminary results. Arthroscopy. 2007;23:34–42.
17. Garcia Jr JC, Mantovani G, Liverneaux PA. Brachial plexus endoscopy: feasibility study on cadavers. Chir Main. 2012;31:7–12.
18. Pan WJ, Teo YS, Chang HC, Chong KC, Karim SA. The relationship of the lateral cord of the brachial plexus to the coracoid process during arthroscopic coracoid surgery: a dynamic cadaveric study. Am J Sports Med. 2008;36:1998–2001.
19. Xu WD, Lu JZ, Qiu YQ, Jiang S, Xu L, Xu JG, Gu YD. Hand prehension recovery after brachial plexus avulsion injury by performing a full-length phrenic nerve transfer via endoscopic thoracic surgery. J Neurosurg. 2008;108:1215–9.
20. Taleb C, Nectoux E, Liverneaux P. Telemicrosurgery: a feasability study in a rat model. Chir Main. 2008;27:104–8.
21. Nectoux E, Taleb C, Liverneaux P. Nerve repair in telemicrosurgery: an experimental study. J Reconstr Microsurg. 2009;4(25):261–5.
22. Germain M, Liverneaux P, Missana MC. Microchirurgie avec le robot Da Vinci S. La télémicrochirurgie: l'essor imminent. E-mémoires de l'Académie Nationale de Chirurgie, Paris; 2010:9. p. 74–77.
23. Liverneaux P, Nectoux E, Taleb C. The future of robotics in hand surgery. Chir Main. 2009;28:278–85.

Pedicle Screw Fixation in Thoracic or Thoracolumbar Burst Fractures

33

S.I. Suk and W.J. Kim

When the decision is made to perform a posterior stabilization procedure for a thoracic or thoracolumbar burst fracture, pedicle screw fixation is a valuable assistance. Pedicle screw fixation of the spine, first described by Boucher [1] in 195Y and popularized by Roy Camille [2, 3] in the 1960s, has evolved through an era of pedicle screw and plate to today's modern pedicle screw and rod system. As it offers rigid fixation unparalleled by other fixation methods enabling a reliable fixation even in a vertebra with posterior element defects or severe osteoporosis, it has now become one of the most widely employed fixation devices in the field of spinal surgery, including spine fractures [4–6]

In surgeries for thoracic or thoracolumbar burst fractures pedicle screw fixation has proven itself to be extremely effective and useful, offering the advantages of rigid fixation, improved segmental control, enhanced deformity correction, and reduction of the fusion extent in both fresh fractures and old fractures with deformity [7, 8]. The purpose of this chapter is to introduce the biomechanical, anatomical basis and techniques of treating thoracic or thoracolumbar burst fractures with pedicle screw fixation.

Anatomy and Biomechanics

For a safe and reliable pedicle screw fixation of a thoracic and thoracolumbar burst fracture, a thorough understanding of the pedicle anatomy throughout the thoracic and the lumbar spine and of the biomechanical basis of the pedicle screw fixation is an absolute prerequisite.

Pedicle Anatomy

The pedicles in the thoracic and lumbar vertebrae are two short, thick processes that project dorsally, one on either side from the cranial part of the vertebra body at the j unction of its dorsa and lateral surfaces. Medially, they border the spinal dura. Laterally, they are in proximity to the exiting nerve roots and the segmental vessels. Superior and inferior, they form the intervertebral foramina with the pedicles of the adjacent vertebrae, through which the spinal nerve roots exit. The roots traverse the foramina just inferior to the pedicles. This anatomic relationship puts the structures in proximity to dangers of injury in malpositioning of the screws.

S.I. Suk, MD, PhD (✉)
Seoul Spine Institute, Inje Univ Sanggye Paik Hospital, Nowon-Ku, Seoul, South Korea
e-mail: seilsuk@unitel.co.kr

W.J. Kim, PhD
Materials Science and Engineering, Hongik University, Seoul, South Korea

D.G. Poitout (ed.), *Biomechanics and Biomaterials in Orthopedics*,
DOI 10.1007/978-1-84882-664-9_33

The pedicle is an oval-shaped cylinder of cortical bone filled with some cancellous bone in the center. The medial wall of the pedicle is thicker than the lateral wall and for this anatomical reason, the transpedicular screws are more apt to be out of the pedicle laterally than medially.

The pedicle shape, dimensions, and orientations vary from region to region [9–11]. in adults, the vertical diameter of the pedicle increase steadily from 7 to 15 mm going down from Tl to L5. The horizontal diameter decreases gradually from 7 in Tl to 5 mm in T5 and then gradually increases to 16 mm in L5. The transverse angle of the pedicles, which is the angle formed by the axis of the pedicle and the vertical line, gradually decreases from a mean of 30° in Tl to −5° in T12 and then increases to 30° in L5. The horizontal angle, which is the angle formed by the axis of the pedicle and the horizontal line paralleling the lower vertebral end plate, shows the greatest negative value in 19 and 10 (Fig. 33.1a–d). These facts are important guidelines for an appropriate choice of the screw sizes and directions of screw insertion in the intended instrumentation levels, especially in deformed spines where radiographic guide is made more obscure by the rotational or angular deformity of the spinal column.

In children, the pedicles are smaller, but their relative dimensions and orientations are similar to those found in adults. As the spinal canal reaches YU% of adult size at the time of birth and reaches the adult size by the age of 2 [12], pedicle screw fixation may be carried out without dangers of causing iatrogenic spinal stenosis after this age. Though the pedicles are very small in pediatric patients, their bone is very plastic and the pedicles usually receive a screw larger than the outer diameter of the specific pedicle by plastic deformation of the pedicle cortex when the screw is inserted slowly through the center of the pedicle provided that the pedicular cortex is not violated [13, 14].

Biomechanics

Among the many advantages the greatest offered by the pedicle screw is rigid fixation, far superior to non-pedicle fixations [4–6] However, obtaining such a reliable, rigid fixation is possible only through a sound technique, with a thorough understanding of the variables which may affect the strength of the fixation. The influence of various screw related and insertion technique related parameters on the rigidity of the fixation offered by a pedicle screw has been extensively studied by nondestructive biomechanical studies and studies measuring the pullout strength of pedicle screws.

Pedicle Screw Diameter

Generally, the pullout strength of a pedicle screw increase with increasing major diameter of the screw as long as the integrity of the pedicle is not violated [15, 16]. The pedicles usually accepted screws with diameters less than 86 % of the isthmic outer diameter of the pedicle without significant structural alterations [10]. A screw of a larger diameter may cause a linear fracture of the pedicles, but the pullout strength is not significantly affected. The pedicles are capable of receiving a screw up to 116 % of the isthmic diameter without significant change in the pullout strength. Though some speculate that a screw with a diameter of 3.5–4 s is sufficient to resist any pullout force generated in the human body, we believe it is much more reliable to use a screw with a diameter of approximately 80 % of the pedicle diameter; this offers maximum pullout strength.

Screw Length

Theoretically, the pullout strength of a pedicle screw increases with increasing depth of insertion as the surface area of contact increases. Some even advocate penetration of the anterior vertebral cortex to obtain a bicortical fixation to increase the pullout strength [17]. However, there have been contradictory studies stating that the pullout strength is not significantly affected by the depth of insertion when the screw passes deeper than the posterior one half of the vertebral

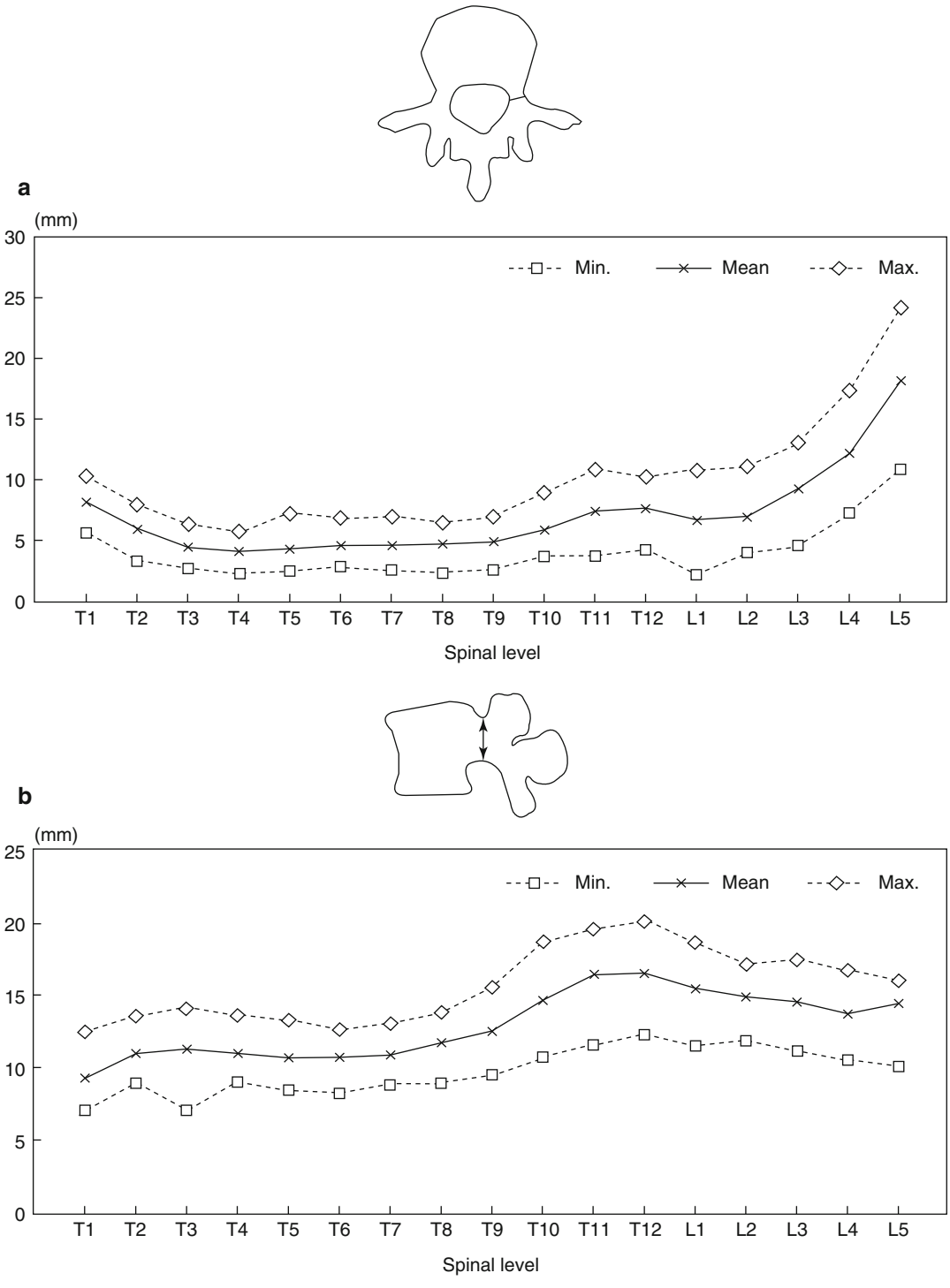

Fig. 33.1 (**a**) Transverse pedicle diameters. (**b**) Superoinferior pedicle diameters. (**c**) Anteroposterior pedicle angles. (**d**) Horizontal pedicle angles

Anteroposterior pedicle angle (α) and depth to the anterior cortex through line parallel to midline axis (◂- - - -▸) and pedicle axis(◂——▸) a: midpoint of transverse pedicle diameter.

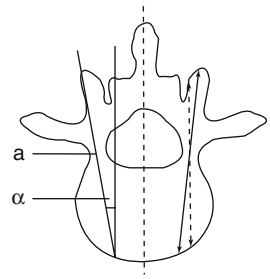

c

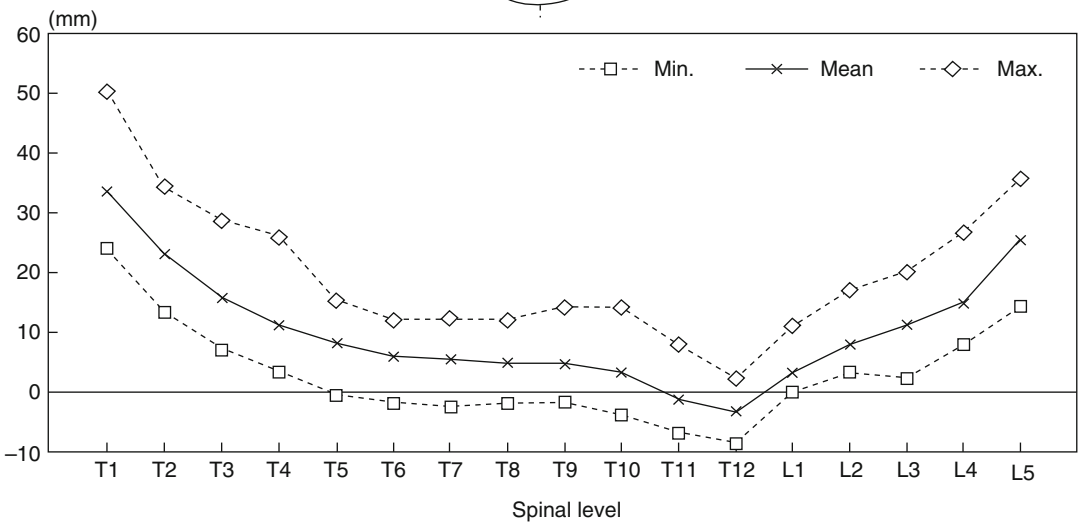

Horizontal pedicle angle (β) b : midpoint of superoinferior pedicle diameter.

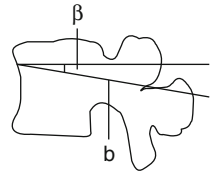

d

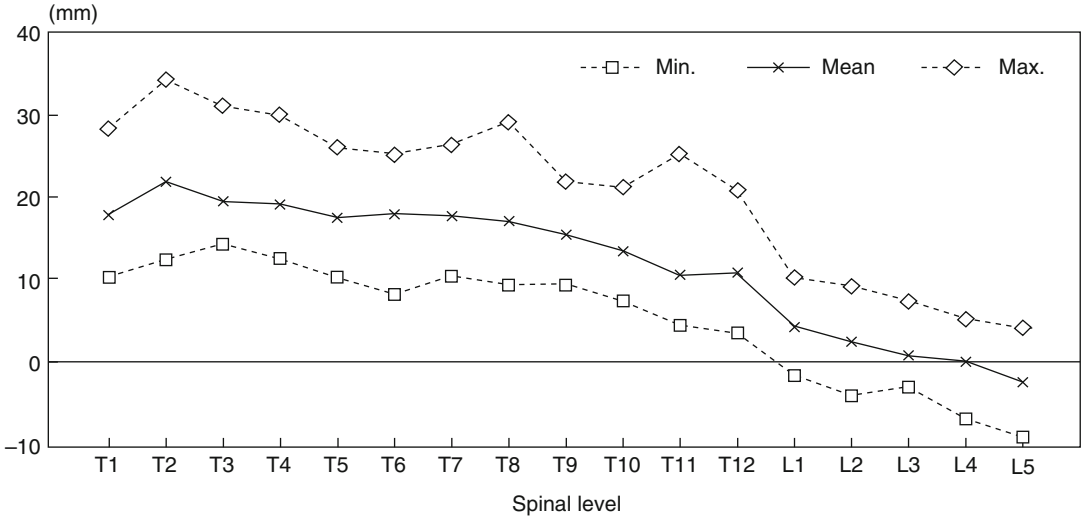

Fig. 33.1 (continued)

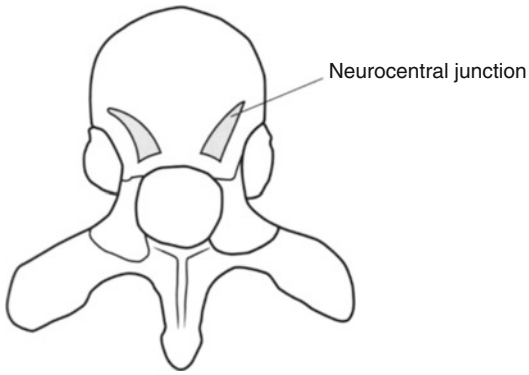

Fig. 33.2 Neurocentral junction

body [16, 18, 19]. The authors agree with the latter view and advocate using screws that penetrate .0-.030 of the anteroposterior vertebral diameter. This apparent paradox is attributed to the presence of a dense sheet of cortical bone, the so called neurocentral junction [19], situated in the posterior one third of the vertebral body at the site of former neurocentral synchondrosis, that makes biomechanical bicortical fixation possible (Fig. 33.2). The neurocentral junction marks the site of union between the centrum and the two neural arches which develop from separate primary ossification centers and unite at the age of 3–6 years.

Screw Direction

Except in the sacrum where the pedicles are large enough to allow a significant alteration in the directions of the pedicle screws to engage the medial anterior cortex, the upper sacral end plate or the ala, the optimal direction of a pedicle screw seems to be along the axis of the pedicle. Though this does not significantly affect the screw pullout strength in most situations, it reduces the chance of pedicular cortical perforations.

Screw Hole Preparations

Pedicle screws offer greatest pullout strength when the diameter of the screw holes are as large as the minor diameter of the screws inserted, approximately 60 % of the pedicular isthmic outer diameter [14]. When the diameter of the holes are smaller, screw insertion is not only difficult but may also cause pedicle fractures. Making a hole of a larger diameter in the pedicle may cause breakage of the pedicle cortex during the hole preparation procedure and reduces the pullout strength [14, 20]. As to the method of making the screw holes, there was no significant difference in the pullout strength between holes prepared by drilling and probing [20, 21]. However, probing seems to reduce the chance of damage to the pedicular cortex.

Number of Screws

The rigidity of fixation increases with increasing number of screws, thus being most rigid in segmental instrumentation where screws are inserted in every segment fused [5, 22]. In a nondestructive study using porcine vertebral columns, the segmental screw fixation construct was significantly stiffer than the nonsegmental screw construct in all the parameters of flexion, extension, lateral bending, and torsion [23] Though there had been enthusiasm to reduce the instrumentation to one side (unilateral instrumentation technique), the authors advocate bilateral instrumentation to enhance resistance to torsional forces.

Transverse Links

The audition of transverse links to bilateral segmental constructs significantly increases the stability in axial rotation [24–26]. A transverse link is more effective if placed in the proximal part of the construct than if placed distally. Two transverse links show increased torsional stiffness than one transverse link especially in longer constructs.

Methods of Increasing the Stiffness of the Pedicle Screw Construct

When posterior instrumentation with pedicle screws is performed on an unstable spine with

an anterior column defect, the lack of normal anterior support significantly reduces the flexion/extension and torsional stiffness of the pedicle screw construct even when a very rigid implant is used [27, 28]. In this situation the stability of the pedicle screw construct may be enhanced by restoration of the anterior defect, by expanding the level of instrumentation, or by the use of more rigid external immobilization postoperatively

Treatment Considerations and Indications

The ultimate goals of treatment for a spinal fracture are restoration of the neurologic and the mechanical stability of the injured spine with minimal sacrifice of motion segments. This same principle applies to the pedicle screw fixation. When restoration of the spinal stability with pedicle screw fixation is contemplated for a thoracic or thoracolumbar burst fracture, both the neurologic and the mechanical aspects need to be considered before finally deciding on the combination of available surgical techniques to successfully accomplish the goals.

As regards biomechanical aspects, the degree of vertebral body comminution and the magnitude of local kyphotic deformity are the major determinants. Though modern biomechanics understand the intact spine as a tricolumnar structure composed of anterior, middle, and the posterior column, the biomechanics concerning the surgical reconstruction of a burst fracture considers the spine basically as a bicolumnar structure, composed of an anterior weight-bearing column and the posterior tension column, whose stability is essentially dependent on the competence of the anterior column. This means that when there is residual, unattended incompetence of the anterior column, the spine will continue to be unstable and is ultimately doomed to fail under repeated loading. This fact is to be always kept in mind in all posterior instrumentation and fusions for thoracic and thoracolumbar burst fractures, including pedicle screw fixation, which inherent y restores or reinforces the posterior column but leaves the essential anterior column untouched, relying for its restoration on the bony healing of the fractured vertebral body The essence of the advantage offered by rigid fixation with pedicle screw fixation lies in the fact that the fractured vertebral body is more effectively protected from the detrimental forces until the fracture union occurs and becomes stable under physiologic loads. By the same token, when the anterior column incompetence is so severe that it is not expected to become a competent weight-bearing structure by itself, a deliberate restoration of the anterior column is warranted. When a significant local kyphosis or comminution of the vertebral body is present, a mere posterior reduction and stabilization with pedicle screw fixation will create an anterior unsupported gap. In the presence of such a gap, the posterior constructs are destined to fail, however stiff they may be, not being able to withstand the flexion moment concentrated at the fracture site devoid of the anterior load sharing structural support [27, 28]. in these situations, elimination of the anterior defect either by restoration of the anterior column or by shortening of the posterior column is warranted. Anterior column reconstruction may be done by an interbody fusion via an anterior or a posterior route, or transpedicular bone grafts.

Posterior Pedicle Screw Fixation

Pedicle screw fixation is applicable and is indicated in all thoracic and thoracolumbar burst fractures in which a posterior fixation and fusion is under consideration. Since it offers a rigid fixation with enhanced segmental control, it is more advantageous than hooks and other nonpedicle fixation devices in the aspect that it offers a better restoration of the spinal sagittal contour and makes a shorter fusion feasible, saving more motion segments [29]. Moreover, as pedicle screw fixation offers a more reliable fixation in the osteoporotic spine and in vertebra with previous laminectomy, they are particularly advantageous in these situations.

Though there are still questions about the safety of pedicle screws in the thoracic and thoracolumbar region, when correctly placed in the pedicles, the screws stay out of the spinal canal and remain insulated from the neural elements by the surrounding pedicular bone, precluding neurologic derangement by the device. The authors have been using pedicle screws in the thoracic spine since 1988 in thousands of patients with various conditions including the most severe deformities and revision surgeries, inserting probably more than 20,000 screws. Yet, there was not a single major neurologic or visceral complication attributable to the pedicle screw fixation per se and the authors believe the procedure to be perfectly safe when performed with a sound technique [5, 30–32]

The indications of a simple posterior stabilization with pedicle screw fixations in thoracic and thoracolumbar burst fractures are:

Cord level fractures with complete paraplegia: Since saving the motion segments is not a crucial problem in this situation, a lengthy fusion with pedicle screws which increases the stiffness of the construct is a suitable choice as it allows an early mobilization without an external support.

Unstable burst fractures without neurologic compromise when they satisfy all of the following

Spinal canal encroachment <60 % on axial CT or MRI.
Local kyphosis <5O degrees.
Without significant comminution of the vertebral body
Fracture less than 72 h old.

As these fractures will heal eventually to offer an anterior support, a mere posterior ligamentotaxis and protection from the detrimental forces will suffice (Fig. 33.3a–g).

Fractures with neurologic compromise when they satisfy all of the following.

Spinal canal encroachment <40 % on axial CT or MRI.
Local kyphosis <50°.
Without significant comminution of the vertebral body.
Fracture less than 72 h old.

In these fractures, a posterior ligamentotaxis may be tried. When there is no neurologic improvement, an additional direct decompression of the neural element is necessary (Fig. 33.4a–h).

Established post-burst fracture kyphosis of less than 50°without significant neurologic compromise: Though the correction of kyphotic deformity is negligible, most patients do well without further progression of the deformity.

Senile burst fractures with pain and progressive deformity without significant neurologic compromise: These osteoporotic burst fractures are best stabilized with a pedicle screw fixation as the pedicles are affected less by the osteoporosis than the laminae. As most of these fractures are without significant canal compromise, an in situ stabilization is usually sufficient.

Posterior Pedicle Screw Fixation with an Anterior Column Reconstruction

In pedicle screw fixation, an additional anterior column reconstruction is indicated when there is significant anterior column incompetence which is not expected to heal sufficiently to function as a stable, weight-bearing structure as in fractures with significant kyphosis, severe vertebral body comminution, and following a corpectomy procedure for direct decompression of the neural elements. Though some favor an anterior stabilization and fusion in these situations, we believe a combined anterior and posterior column reconstruction with posterior pedicle screw fixation has several advantages over the anterior instrumentation/fusion only [33]. They are: 1) Better restoration of spinal alignment. When the kyphosis is severe, it is easier to restore a physiologic sagittal profile with a posterior pedicle screw fixation than with an anterior instrument. 2) More reliable rigid fixation. In osteoporotic

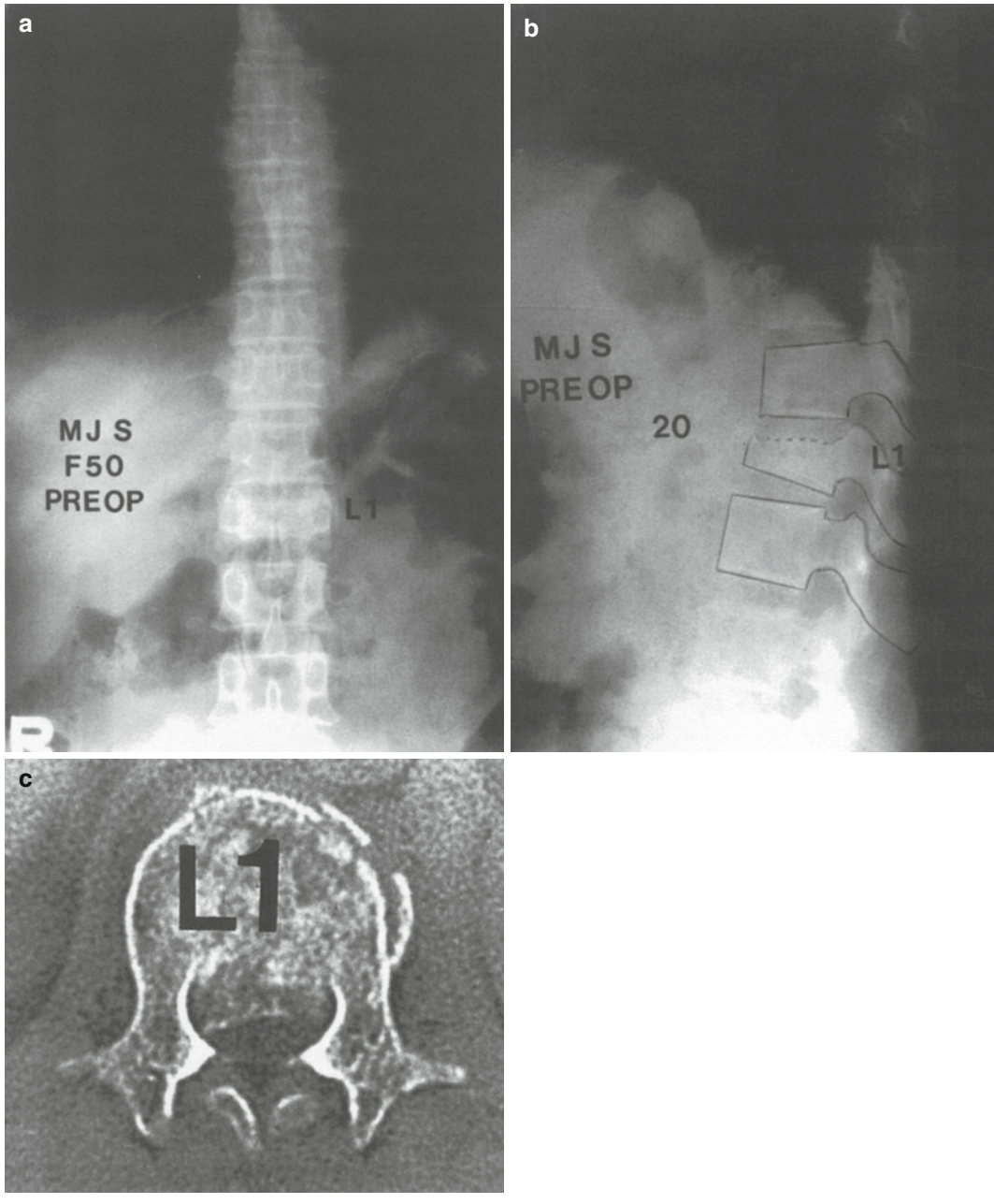

Fig. 33.3 (**a, b**) A 50-year-old female with L1 unstable burst fracture. There was a 20° kyphotic deformity at the thoracolumbar junction. (**c**) Preoperative CT show 40 % canal encroachment. (**d, e**) She was treated by posterior fusion with pedicle screw fixation from T11 to L2. Postoperatively kyphosis was corrected to 10°. (**f**) Postoperative CT show canal encroachment reduced to 10 %. (**g**) Ligamentotaxis

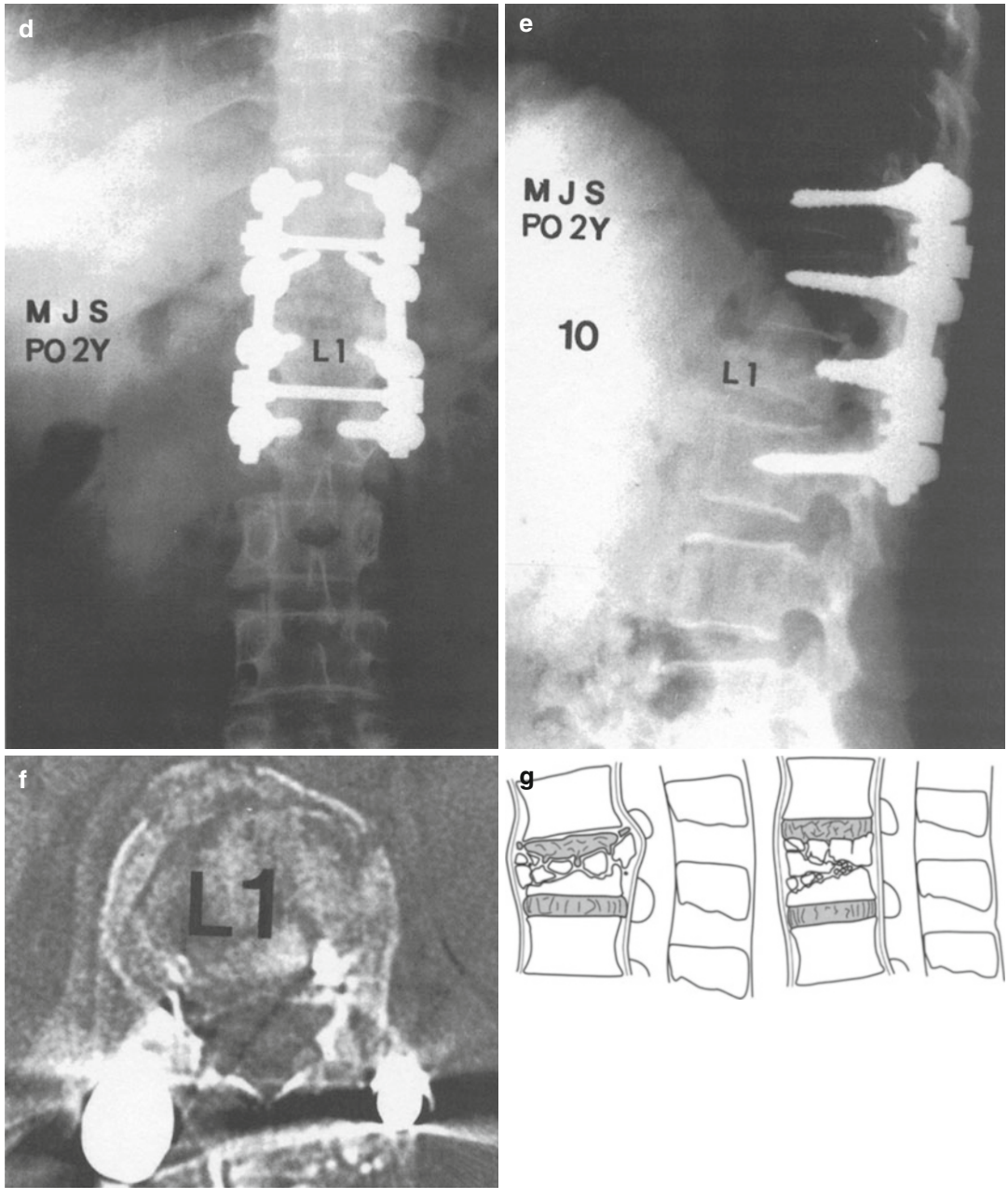

Fig. 33.3 (continued)

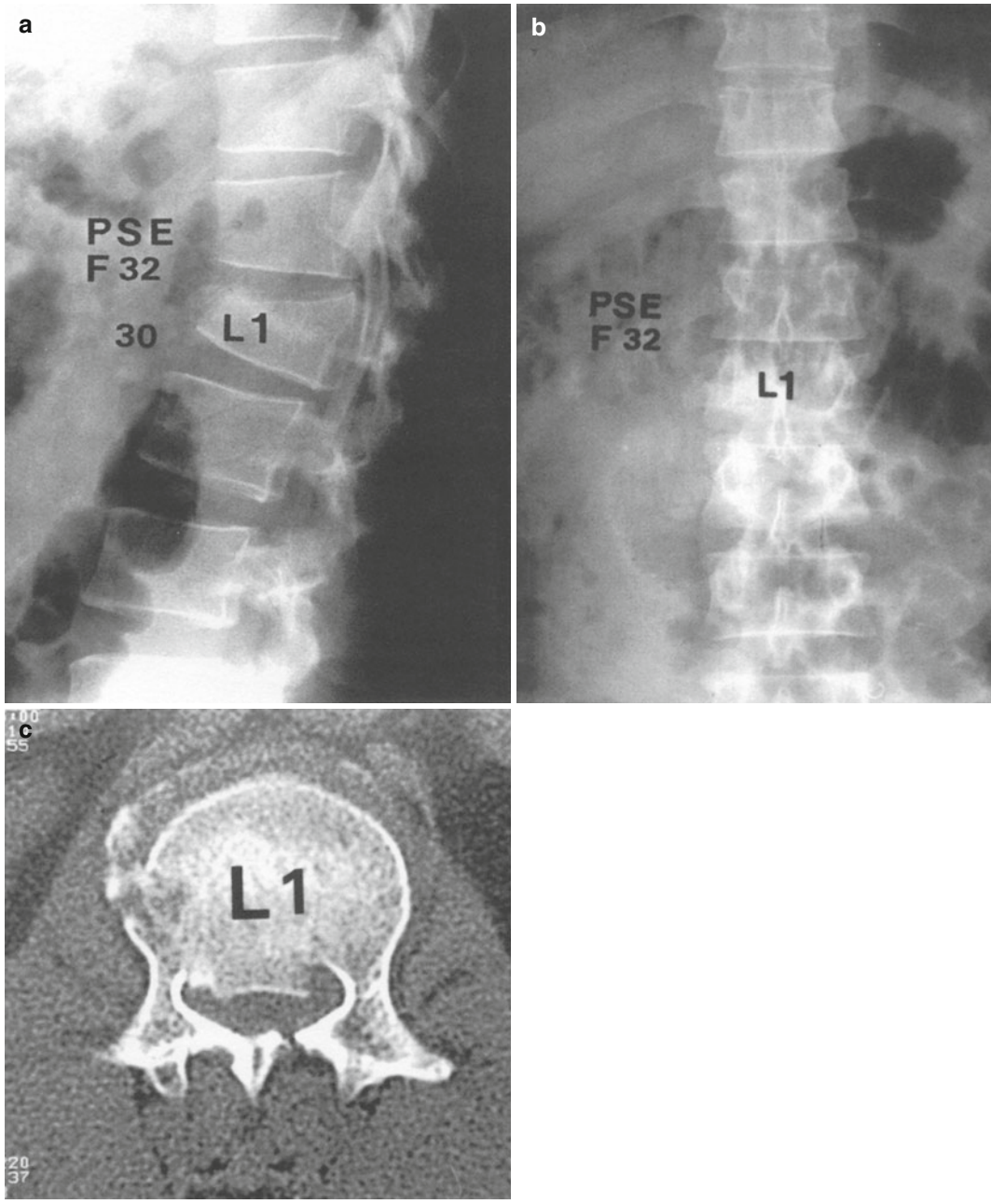

Fig. 33.4 (**a, b**) A 32-year-old female with L1 unstable burst fracture at vertebra. Preoperative neurology was intact except for bowel and bladder control. There was a 30° kyphotic deformity at the thoracolumbar junction. (**c**) Preoperative CT show 60 % canal encroachment. (**d**, **e**) She was treated by the posterior fusion with pedicle screw fixation from T11 to L2. Following surgery, kyphosis was corrected to 12°. (**f**) Postoperative CT show canal encroachment reduced to 20 %, but she had no neurologic improvement. (**g–h**) One week later after the posterior surgery, anterior decompression was carried out. Following the anterior surgery, her bladder control improved. Postoperative 1-year-follow-up radiographs show satisfactory maintenance of reduction

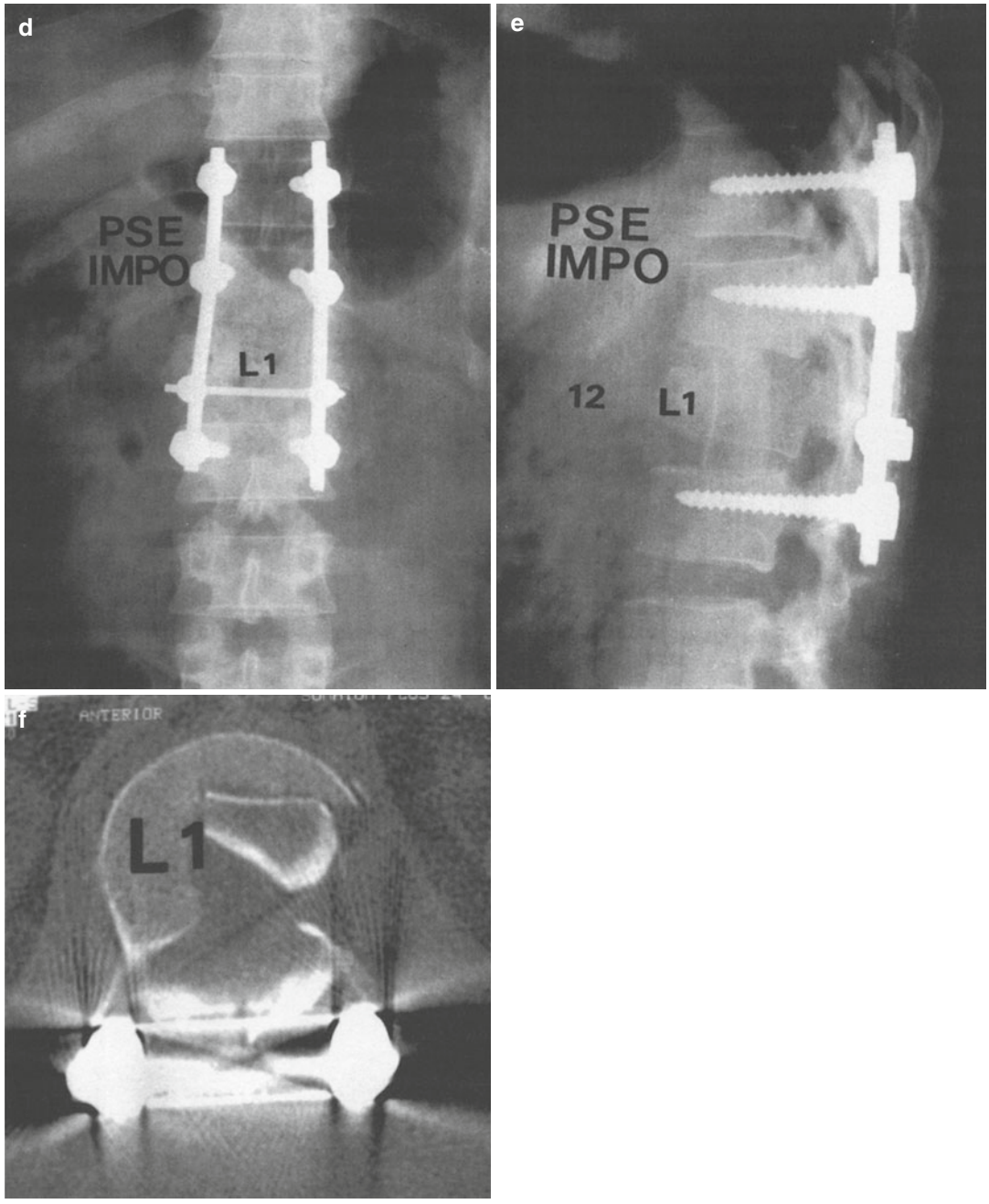

Fig. 33.4 (continued)

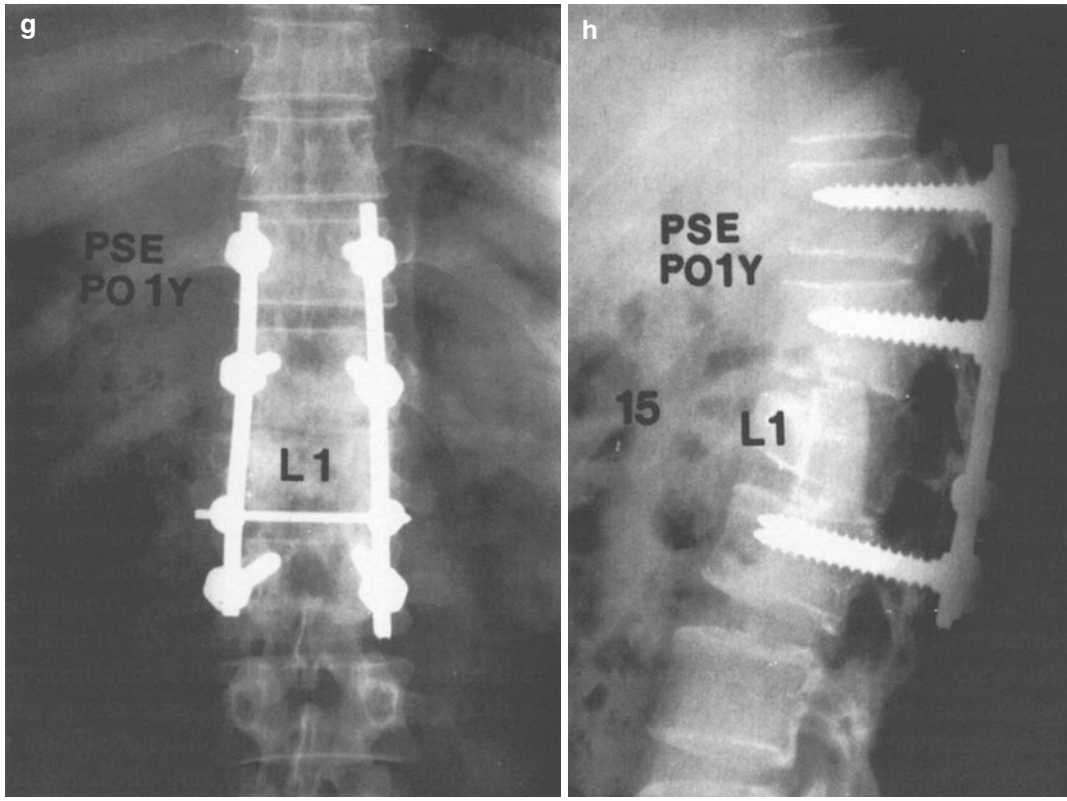

Fig. 33.4 (continued)

patients, the pedicle screw fixation offers more reliable fixation than the anterior instruments holding the osteoporotic vertebral bodies. 3) increased versatility Pedicle screw fixation offers a rigid fixation in locations where anterior instrumentation is difficult or needs extensive dissection (e.g., cervicothoracic junction). Though an anterior column reconstruction is more commonly performed through an anterior approach, a reliable anterior column reconstruction is also feasible from the posterior, by transpedicular bone grafting [34], by interbody fusion using the costotransversectomy approach [35], or using a modified egg-shell procedure [36]. In the former, cancellous chip grafts are added into the fractured vertebral body and the damaged disc space through the pedicles of the fractured vertebra using a narrow funnel. In the latter, the anterior column may be supported by a structural graft or by autogenous cancellous graft tightly packed into the void in the anterior column. When local kyphosis is severe, a type of posterior closing wedge osteotomy may be performed through the posterior approach to obliterate the anterior unsupported gap. The advantage of the anterior column reconstruction front the posterior in conjunction with pedicle screw fixation is the feasibility of a global fusion through a single approach, saving the operative time and reducing the morbidity of an anterior thoracotomy or thoracolumbotomy [33]. It also permits a direct exploration and repair of the associated dural tear or nerve root entrapment. Its disadvantage is destruction of the relatively intact posterior column, reducing the posterior fusion base. However, this drawback may be overcome by one of the following methods; 1) Saving the lamina and pedicle on one side. 2)

By adding a bridging bone graft. 3) By shortening the entire posterior column to achieve a bony contact between the two laminae above and below the laminectomy.

The indications for posterior stabilization with anterior column reconstruction are;

Presence of a neurologic deficit necessitating a formal decompression of the neural tissue:

Spinal canal encroachment more than 60 %.
Failure of the indirect decompression by ligamentotaxis
Fractures more these 72 h old.
Local kyphosis greater than 50°
Significant comminution of the vertebral body.

Established post-burst fracture kyphosis greater than 50° (Posterior or anterior fusion alone in this situation is more prone to failure and should be treated by a global fusion.) (Fig. 33.5a–f).

Surgical Techniques

Presurgical Considerations

Anesthesia

For a posterior stabilization with pedicle screw fixation, a general anesthesia with a full monitoring of vital signs including the arterial and the central venous pressure is prefreed. As an anterior column reconstruction is often accompanied by a substantial amount of bleeding from the epidural vein and the cancellous bone of the fractured vertebral body, securing a large-bore central venous channel is highly recommended. Hypotensive anesthesia is especially helpful in cases where anterior column reconstruction is considered. When intraoperative-evoked potential monitoring is contemplated, intravenous anesthesia with fentanyl and propopol is preferable to inhalation anesthesia as they affect monitoring less severely than the latter: However intravenous anesthetics require a substantially longer time for recovery than inhalation anesthetics and may even require several hours of ventilator care in the recovery room.

Intraoperative Monitoring

As we have never had a major neurologic complication related to the pedicle screw placement and are perfectly confident of the safety, we do mat use intraoperative neurophysiologic monitoring except in cases in which the spinal cord is directly exposed. However, intraoperative monitoring of the neurologic function r5 a valuable aid to ensure the safety of the procedure and for keeping a record for possible medicolegal problems [37, 38]. Although the wake-up test is a reliable monitoring method, we prefer motor-evoked potential or somatosensary-evoked potential, which can be more conveniently performed without extending the operative time [39].

Positioning

The ideal position for a pedicle screw fixation is the standard prone position with the abdomen hung free by means of a pad, four posters, or a special surgical frame to reduce venous bleeding. The operating table should be X-ray penetrable to allow the intraoperative postero-anterior roentgenogram. When posterior column shortening is contemplated, care should to taken to place the osteotomy site over the hinge of the operating table so that closure of the posterior gap created by the osteotomy may be aided by extension of the operating table. For this procedure, we prefer to use roll pads which are flexible enough to allow extension of the spinal column with the table extension.

Fusion/Instrumentation Extent

The instrumentation and fusion should be long enough to offer adequate rigidity of the internal fixation but should be minimized to that absolutely necessary to save as many motion segments as possible especially when the fusion is extended into the lumbar spine. Pedicle screws, which enable rigid fixation, are especially helpful for this purpose. We prefer to fuse all the levels instrumented as the “rod-long, fuse-short” technique of long instrumentation and short fusion not only inflicts more extensive soft tissue damage and increases the risk of damaging healthy joints but also causes degeneration of the articu-

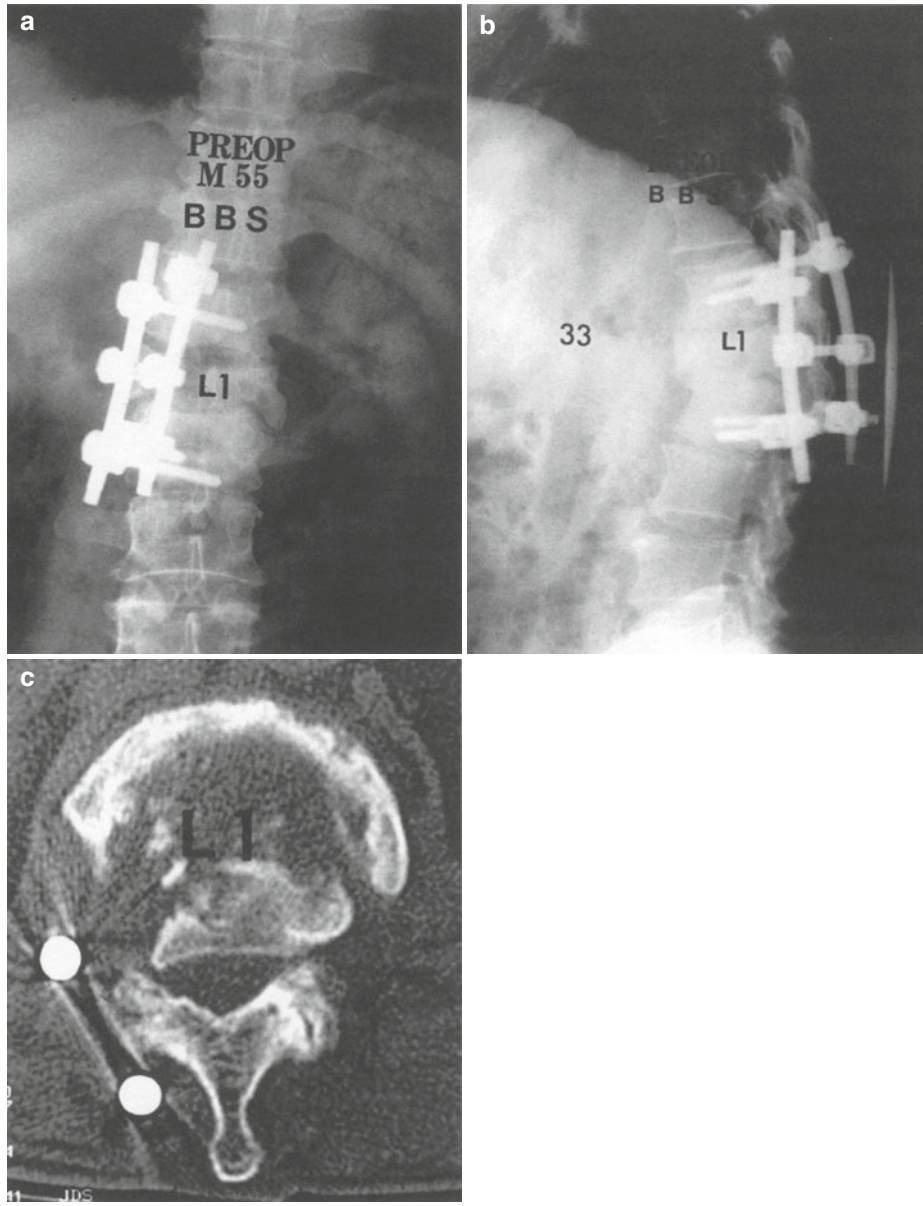

Fig. 33.5 (**a**, **b**) A 68-year-old male with a post-traumatic kyphosis and cauda equina syndrome. One and half years prior to the visit, he sustained a burst fracture which was treated by posterior decompression and fusion. (**c**) Preoperative MRI show local kyphosis with canal encroachment. (**d**, **e**) He was treated by the posterior vertebral column resection at L1 and fused from T11 to L2. Postoperative one-year-follow-up radiographs show satisfactory maintenance of sagittal balance. (**f**) Posterior vertebral column resection

lar cartilage of the unfused, immobilized facet joints within the instrumented extent. In thoracolmrbar burst fractures, we prefer to fuse two levels proximal and one level distal to the fractured vertebra, securing four and two fixation points proximal and distal to the fracture both for a simple posterior stabilization and posterior stabilization with anterior column reconstruction. The reason

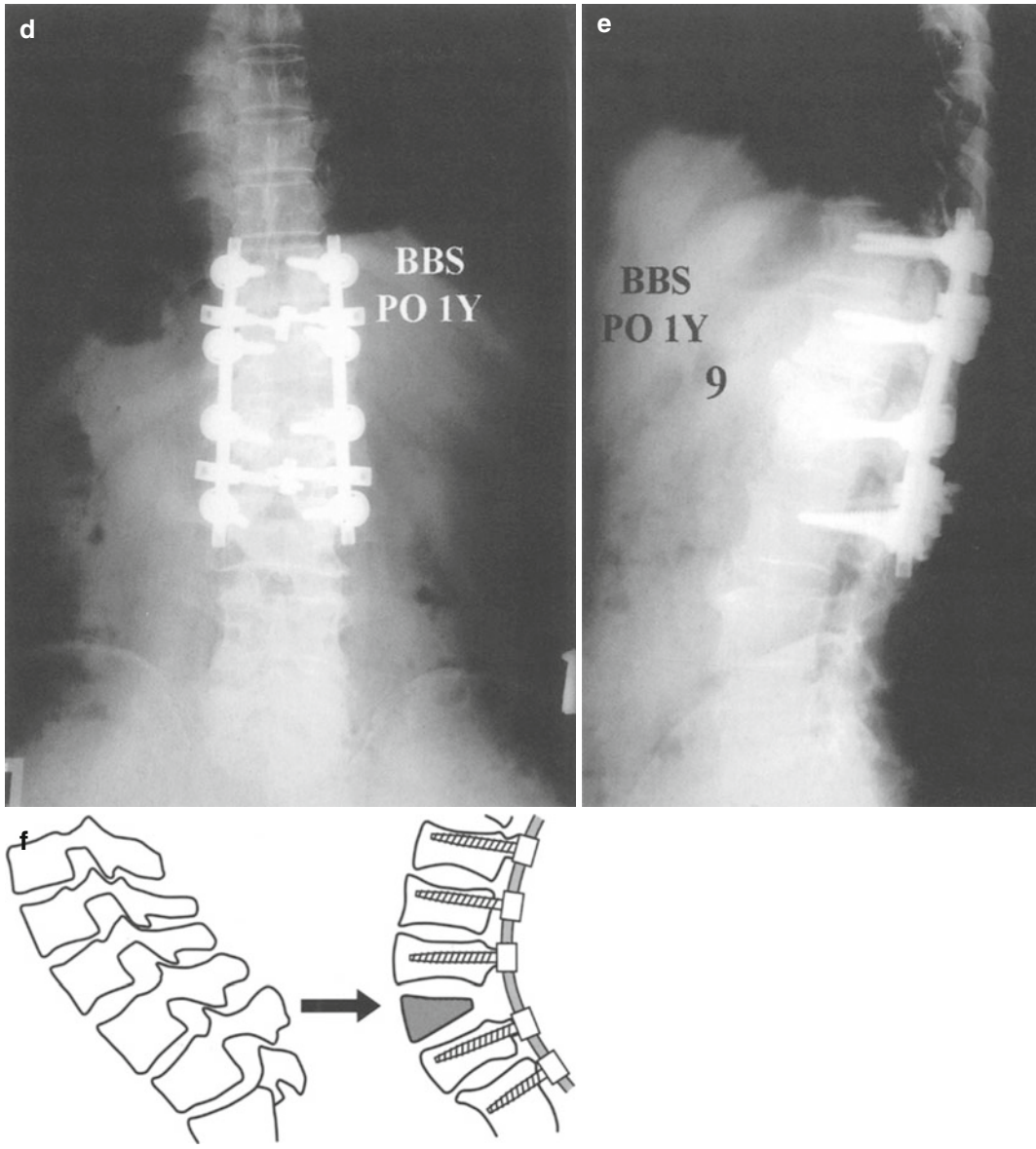

Fig. 33.5 (continued)

for extending two levels higher into the thoracic spine is to increase the stiffness of the construct with minimum sacrifice of the valuable lumbar motion segments.

Choice of Implants

For pedicle screw instrumentation of the thoracic spine, pedicle screws of smaller diameter than the usual lumbar screws may be necessary. For average-sized adults, 6 mm screws are usually sufficient as the thoracic pedicles are large enough. For children and smaller-sized adults whose pedicles are smaller, 4.0 mm screws are advisable in the upper thoracic spine (T 4, 5, 6) where the pedicles are smallest. Concerning the shape of the screws, cylindrical screws are as

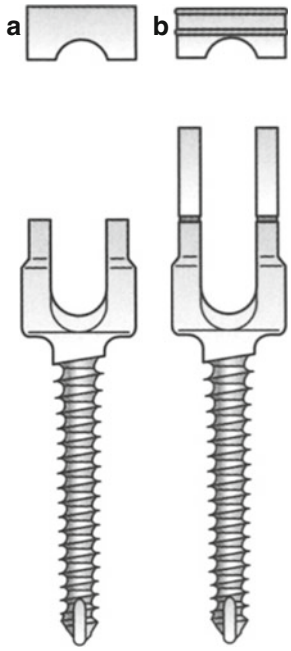

Fig. 33.6 (**a**) Ordinary screw. (**b**) Long arm screw

effective as conical screws in patients with normal bone quality [40]. However, as the fixation strength of conical screws is affected by the mass of the cancellous bone, cylindrical screws may be better for internal fixation of the osteoporotic spine. In patients with a significant local kyphotic deformity or when posterior column shortening is contemplated, use of long-arm or reduction screws may be helpful in gradually correcting the deformity [41, 42] (Fig. 33.6a, b).

Between the pedicle screw-plate and pedicle screw-rod systems, we prefer the rod system as they are easier to contour to the normal sagittal contour and allow more room for insertion of the bone grafts [43]. Among the many designs of pedicle screw-rod systems, we prefer the top open design similar to the Cotrel-Doubousset, Synergy, and the Diapason system as it is easier to connect the rod to the top open screws than to a side-attaching system. However, we believe the training and the experience of the surgeons are the most important factors in the choice of implants and strongly recommend using the instruments most familiar to the operating staff.

Though there is little difference in the clinical performance as to the metallurgy of the implants, we recommend the use of implants made of titanium in case a postoperative imaging of the spinal canal is needed.

Posterior Pedicle Screw Fixation

Incision and Exposure

As the pedicle screw instrumentation needs a wide exposure to the tip of the transverse process, the incision should be large enough to avoid excessive retraction on the paraspinal muscles to prevent myonecrosis. For a thoracic fracture, the usual incision spans from the upper end of the spinous process two levels above the uppermost pedicle instrumented in the thoracic spine to the lower end of the lamina of the lowest instrumented vertebra. It is advisable to take an intraoperative roentgenogram to confirm the spinal levels in the course of the exposure to prevent errors of operating on wrong levels.

The spine is exposed in a standard fashion with an electric knife, staying strictly subperiosteal to reduce bleeding. The vertebrae instrumented are exposed to the tip of the transverse processes bilaterally. Care should be taken not to disturb the facets adjacent to the uppermost pedicles instrumented during the exposure as damage to the facets may result in postoperative pain and late instability. On completion of the exposure, the facets within the intended fusion extent are destroyed by inferior facetectomy with thorough removal of the articular cartilage to promote intra-articular arthrodesis. After the facet preparation, pedicle fixation is begun by preparation of the pedicle entry sites. In the thoracic spine, the pedicle entry point is at the junction of the superior margin of the transverse process and the lamina (Fig. 33.7a, b). In the lumbar spine, the point is at the junction of a line drawn through the middle of the transverse process and the lateral margin of the facet joint (Fig. 33.8a, b). The presumed entry sites are decorticated with a rongeur to expose the cancellous bone overlying the pedicles to facilitate insertion of the guide pins for the pedicle screws. In the lumbar spine, in addition to the entry sites, transverse processes and the lateral

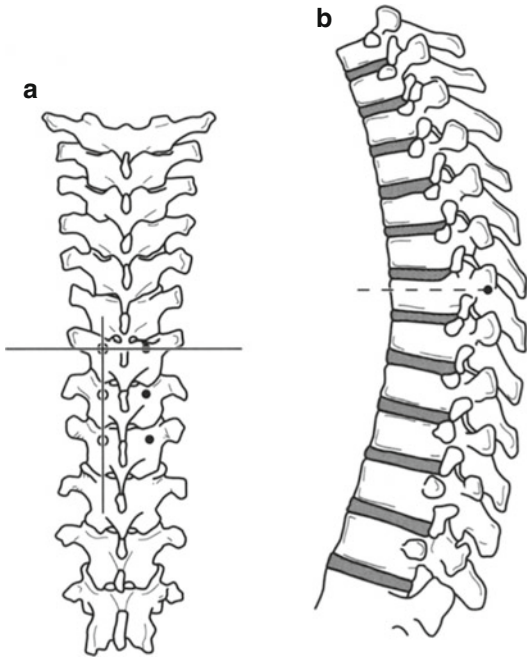

Fig. 33.7 Pedicle entrance point in thoracic spine (**a**) Antero-posterior view. (**b**) Lateral view (Redrawn from Roy-Camille et al. [28])

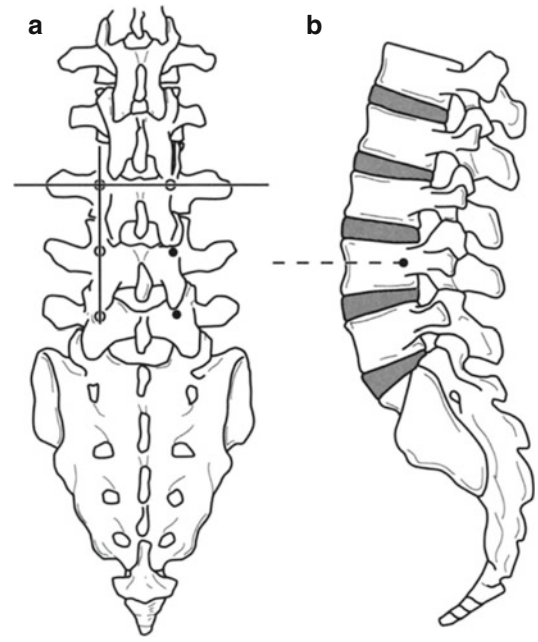

Fig. 33.8 Pedicle entrance point in lumbar spine (**a**) Antero-posterior view. (**b**) Lateral view (Redrawn from Roy-Camille et al. [28])

aspect of the facet joints are decorticated at the same time. They are to be decorticated before the insertion of the pedicle screws as it is difficult to perform a reliable decortication in these bone bases with the screws in place. Decortication of the lumbar transverse processes should be started from the tip towards the base as decortication weakens this very weak bony process. Taking the reverse direction often results in fracture of the transverse process, reducing the bone base available for lateral intertransverse fusion. We prefer to insert pedicle screws even in the fractured vertebra for a simple posterior fusion as such segmental instrumentation increases the stiffness of the pedicle screw construct. However, as there is always a possibility of residual neurologic compromise that might need a direct decompression of the neural elements, we put a short screw that passes just a few screw turns into the pedicle on one side of the fractured vertebra so that the pedicle screws do not become an obstacle for an anterior decompression and reconstruction. For fractures subjected to an anterior column reconstruction from the posterior, we do not put pedicle screws in the fractured vertebra as corpectomy and reconstruction becomes very difficult with the screws in the pedicles.

Pedicle Screw Insertion

Following the preparation of the entry sites the pedicle screws are inserted segmentally into the vertebrae within the fusion extent in the following manner.

Step 1: Insertion of the guide pins Guide pins, about 15 cm long, made from K-wires are inserted shallowly into the exposed cancellous bone at the presumed pedicle entry point by means of a mallet. To facilitate interpretation of the relative position of the guide pin tips on the intraoperative roentgenograms, the guide pins are directed along the axis of the pedicle in the frontal and the sagittal planes. Following insertion of guide pins on one side, guide pins of a different diameter are inserted on the opposite side pedicles to avoid confusion in reading the intraoperative roentgenogram.

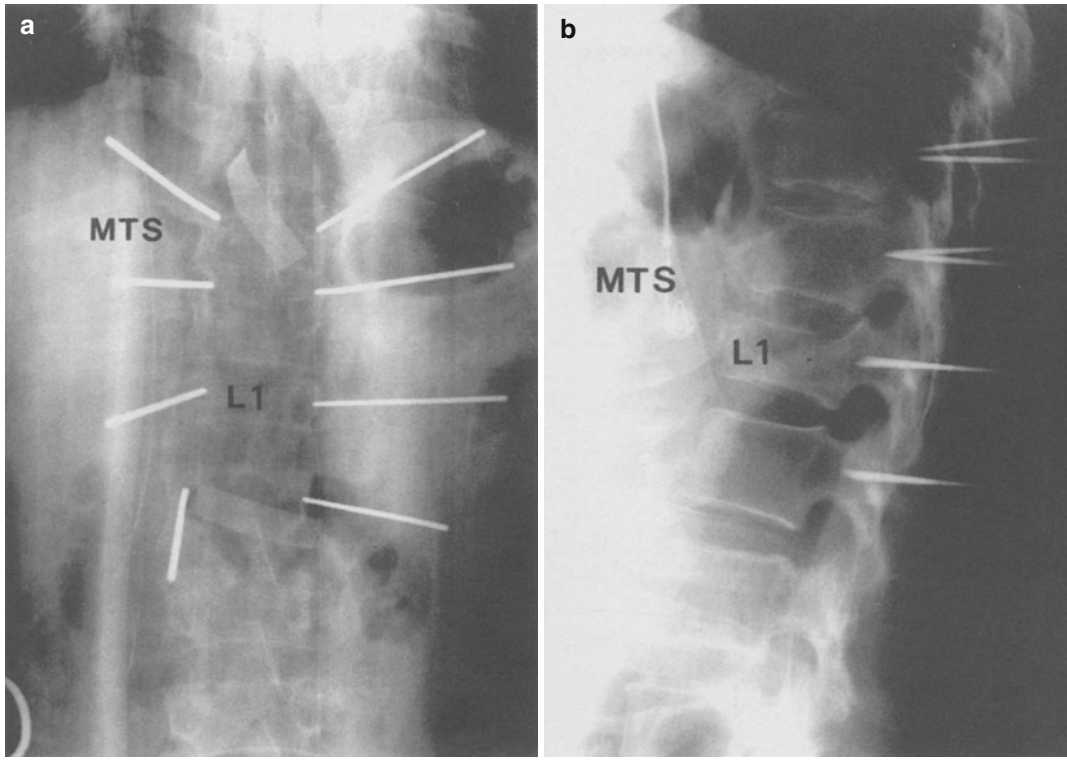

Fig. 33.9 Intraoperative roentgenogram. (**a**) PA roentgenogram. (**b**) Lateral roentgenogram

Step 2: Confirming the entry point and screw direction With the guide pins placed in the presumed entry points, intraoperative PA and lateral roentgenograms are taken to determine the relationship between the presumed entry point and the ideal entry point identifiable on the X-ray, and to determine the direction of the screws. Considering the transverse angle of the pedicles in the thoracic and thoracolumbar spine, the ideal pedicle entry point (IPEP) in a neutrally rotated vertebra is at the junction of the line parallel to the lower or upper end plate bisecting the pedicle and the lateral margin of the pedicle ring shadow on a PA film (Fig. 33.9a, b). In rotated vertebrae, as found in scoliosis, the pedicle on the side of the rotation assumes a more medial position than neutrally rotated vertebra relative to the lateral border of the vertebra, whilst the opposite side pedicle becomes relatively more laterally situated. Naturally, the IPEP on the rotated side (convex side in scoliosis) moves more medially while the IPEP of the opposite side (concave side in scoliosis) moves more laterally with increasing amount of rotation.

On the lateral view, the IPEP is situated at the junction of the line passing through the axis of the pedicle and the posterior border of the facet joints. Screw direction is determined on the lateral X-ray. Ideally, it should be along the axis of the pedicle, sloping about 10° cranially in the thoracic and the upper lumbar spine. However, in clinical practice, insertion of the screws parallel to the superior end plate of the vertebra is preferable to prevent possible penetration of the pedicle screws into the disc space superior to the instrumented vertebra.

Step 3: Pedicle entry After determining the ideal pedicle entry point and the direction, the entry hole is made with an awl, and the hole is deepened with a small diameter drill or a small curette, taking into considerations the normal transverse angle of the pedicles for the particular level. After passing the pedicle, the drill or curette meets some resistance as it traverses the dense sheet of bone in the neurocentral junction. Over the past several years, various methods of

confirming a safe passage through the pedicles have been introduced. Probing, arthroscopic examination of the hole by inserting a narrow scope into the hole [44], measuring the electrical resistance by means of an electrode placed in the hole [45], and measuring the electrical resistance of the inserted screws are among many methods. We use probing to check the entry as a minor pedicular cortical breakage that might occur during pedicle entry does not significantly affect the safety or the strength of fixation of a pedicle screw. A safe entry is confirmed when the probe hole is globally surrounded by bone and meets resistance in all directions, especially when there is a feeling of the spongy cancellous bone giving way to the pressure exerted by the probe at the far end of the hole.

Step 4: Hole preparation Deep drilling is per formed following the probe path using a drill bit with a diameter the same as the minor diameter of the screw used. When there is a large discrepancy between the sizes of the pilot drill/curette and the final drill, the hole is enlarged by using larger diameter drills sequentially. We do not usually tap the hole, but for some implants, tapping of the hole prior to insertion of the screws may be necessary.

Step 5: Screw insertion The screw is inserted after reconfirming the bony containment of the drilled screw hole with a blunt probe. When starting to insert the screw, it is absolutely necessary to turn the screw with a very gentle force so that the screw follows the predrilled path. Undue force at the beginning may misdirect the screws in the wrong direction especially in the osteoporotic spine where cortical bone is very weak and offers little resistance. When inserting the screws, the general alignment and depth of the screws should be taken into consideration as misaligned screws make rod attachment extremely difficult. When a screw seems strangely out of alignment compared to other screws, most probably the screw is not in the pedicle properly. When the screws are not in the pedicles, they are not only useless as reliable anchors but also very dangerous, being in proximity with the neural elements medially and inferiorly and the great vessels anteriorly. This requires re-placing the mispositioned screw exactly in the pedicles. If this is not possible, it is much safer to remove the screws than accept a potentially hazardous screw without any function. The depth of the screws are also very important as it is extremely difficult to attach a rod to the screws when there is a large discrepancy. As turning the screw backwards increases the risk of screw loosening, the screws should be inserted a little shallowly at first and then adjusted after completion of screw insertion on the particular side.

Rod Insertion

Following the segmental screw insertion, the rods are attached to the screws. The rod should be long enough to allow reliable locking with the screws at both ends of the construct but not long enough to touch the unfused adjacent facet joints or hinder the motion of the unfused segments. The rod is contoured to the normal sagittal contour of the segments instrumented. Though the thoracolumbar junction is relatively flat, we prefer to add a slightly exaggerated sagittal curve to prevent potential junctional kyphosis.

Ligamentotaxis

After placing the rods on both sides, ligamentotaxis is routinely performed to reduce the fracture fragments. In patients without a significant facet joint instability, the facet joints act as a fulcrum and the compression force over the fracture site via the pedicle screws attached to the normal sagittal contoured rod generates distractive force on the anterior column, effecting some reduction of the fractured fragments by tension in the longitudinal ligaments and the outer annulus. When there is significant facet joint destruction, the facet joints are unable to act as a fulcrum to the posterior compression force and the whole fractured vertebra may collapse under a compressive force, with risk of worsening the canal encroachment. In this situation, the pedicle screws are locked in situ over the fractured segment with some compression over the relatively intact segments. Though some advocate distraction over the fracture site for reduction of the fracture fragments in this situation, we believe

distraction in the presence of a significant facet instability will lengthen the spinal column, producing an unsupported gap which increases the risk of implant failure: we are strongly against this idea.

With all the screws tightened, an intraoperative lateral roentgenogram is taken to confirm the restoration of the normal sagittal contour. When the result is acceptable, the rods are connected by cross links. On completion of the instrumentation, posterior fusion is carried out after a wide decortication of the laminae and addition of the local bone gained during the operative procedure. When the amount of the local bone is not sufficient, allograft is added to expand the graft volume. The wooed is then closed tightly in the usual manner after careful hemostasis. Suction drains are not used as they only increase postoperative bleeding.

Posterior Pedicle Screw Fixation with Anterior Column Reconstruction

Posterior Pedicle Screw Fixation with Anterior Decompression/ Stabilization

For cases for anterior decompression and fusion through an additional anterior approach, the posterior procedure is identical to the simple posterior stabilization. On completion of the posterior procedure, the anterior procedure is carried out. It may be done in the same anesthesia or later as a staged surgery in the usual patient, we prefer to do the anterior surgery in the same anesthesia as it reduces the morbidity of repeated anesthesia and the duration of the hospital stay.

Posterior Pedicle Screw Fixation with Transpedicular Bone Graft

When transpediular bone graft is chosen for the anterior reconstruction, a pedicle in the fractured vertebral body is used to place the autogenous cancellous bone graft into the fractured vertebral body and the damaged disk space. After placing the bone grafts, a pedicle screw is inserted into the hole used for the bone graft and posterior fixation procedure is carried out in the usual manner.

Posterior Pedicle Screw Fixation with Corpectomy/Anterior Column Reconstruction via the Posterior Approach (Posterior Vertebral Column Resection)

The procedure [42] is identical to the posterior pedicle screw fixation until the pedicle screw insertion stage except that pedicle screws are not inserted into the fractured vertebral body. Then the procedure is carried out as described below.

Step 1: Laminectomy A total laminectomy of the fractured vertebra is performed using a small-bore Kerrison punch. The laminectomy should be very careful especially in patients with a lamina fracture as there might be entrapment of the neural elements between the fracture fragments. When dural laceration is present it is repaired primarily or with a dural graft. The ligamentum flavum beneath the adjacent superior and inferior laminae also removed during the procedure to prevent compression of the neural elements which might occur with shortening of the vertebral column.

Step 2: Foraminotomy The bony roof of neural foramina suoperior and inferior to the pedicles of the fractured vertebra is removed totally with a Kerrison punch to fully expose the exiting nerve roots. In the thoracic spine, opening up the superior foramina should be accompanied by complete removal of the superior articular facet that.lies deep to the lamina of the superior adjacent vertebra as leaving a loose bony fragment in the spinal canal may increase the risk of neurologic compromise with shortening of the vertebral column.

Step 3: Transverse process/rib resection To isolate the pedicles, an osteotomy is performed at the bases of the transverse process of the fractured vertebra. With a blunt elevator in the osteotomy site and dissecting downward, the lateral aspect of the pedicle and the vertebral body is readily exposed in the lumbar spine. In the thoracic spine,

the osteotomy leads to the costotransverse joint. To expose the lateral aspect of the vertebral body, the rib head is removed totally by an osteotomy at the costotrarsverse junction and disarticulation of the costovertebral joint. In removing the rib, care should be taken not to injure the pleura. When the pleura is inadvertently opened, it is to be closed.

Step 4: Pedicle resection With the pedicles isolated, the pedicles are resected with a narrow osteotome making a circumferential osteotomy around the base of the pedicles taking care not to injure the exiting nerve roots above and below. The resected pedicles are taken gently out, releasing the soft tissue attachments with a Penfield freer.

Step 5: Corpectomy Corpectomy is begun by removing the cancellous bone of the fractured vertebra body through the base of the resected pedicles with an angled curette. When enough cancellous bone is removed through the pedicles from both sides, the channel created will meet at the center forming a tunnel with the posterior wall of the vertebral body as the roof. The tunnel is enlarged by removing more cancellous bone anterior and laterally, leaving only the cortical portion of the vertebral body like an eggshell. At this point, a short rod is connected to the screws spanning the fracture site to endow temporary stability to the vertebral column. This temporary stabilization is extremely important as the spine becomes very unstable after the destruction of the cortical shell and inadvertent translation of the vertebral column may occur. Following this temporary stabilization, the remaining posterior wall is imploded into the void created in the vertebral body by means of a downward curette and removed by means of a pituitary forcep. After removing the posterior wall, the damaged endplate and the intervertebral disc is resected with an osteotome and pituitary forceps until the endplate of the adjacent vertebral is exposed. It is crucial to excise the damaged disk as the fractured fragments usually have some attachment to the annulus fibrosus and cannot be completely removed without a formal discectomy. When superior and inferior endplates are both damaged, both endplates and the disks are resected to expose a reliable bone base for fusion. In patients with significant kyphosis in whom posterior column shortening osteotomy is planned, the remaining lateral walls of the subject vertebra are resected by means of a narrow osteotome.

Step 6: Anterior column reconstruction The anterior column reconstruction may be done by tightly packing the autogenous iliac cancellous chip grafts or by insertion of a structural graft such as an autogenous iliac strut graft or a titanium mesh cylinder. When the anterior gap is small as in posterior column shortening osteotomy,we just pack the gap tightly with cancellous chips. When the gap between the superior and inferior bone base is substantial, we prefer a titanium mesh filled with morcellized autogenous bone from the vertebral body and the iliac crest as taking a strut from the posterior iliac crest is more difficult than from the anterior. After measuring the size of the bone defect, an appropriate-sized titanium mesh is inserted into the gap. When the nerve roots are in the way, in the thoracic spine we choose to sacrifice a nerve root rather than retracting it as a thoracic root is not crucial and retraction of a nerve root may exert tension on the spinal cord. However, in the lumbar spine, as all roots are very important, they are retracted gently to provide room for the mesh. The mesh is impacted deeply into the gap, ideally to rest in the anterior and middle third of the vertebral body. It is important to place the structural support anterior to the vertebral axis of rotation to effectively resist the flexion moment. On completion of the procedure, rods contoured to the desired sagittal contour of the instrumented segments are inserted into the opposite side screws. Then the screws are locked with compression over the mesh. With the rod locked in position, the temporary stabilizing rod is changed to a contoured longer rod and is inserted onto the screws. These are also locked in position with compression over the mesh cylinder.

When anterior reconstruction is complete, an intraoperative PA and lateral roentgenogram is taken to confirm the position of the mesh cylinder. With an acceptable spinal realignment and mesh position, cancellous chips are added beside the mesh cylinder and are tightly packed in position.

Following decortication of the posterior elements, a posterior fusion is performed using a broad sheet of cortical bone from the iliac crest to bridge the posterior defect. Then the wound is closed in the usual manner over double suction drains.

Posterior Pedicle Screw Fixation with Augmentation Vertebroplasty

In severely osteoporotic fractures, polymethylmethacrylate vertebroplasty may be used to restore the deranged anterior column. The vertebroplasty is performed exactly like the procedure performed for an osteoporotic compression fracture, through the pedicles of the fractured vertebrae before the pedicle screw instrumentation procedure. Care should be taken for posterior leakage of the bone cement as posterior wall is often incompetent in osteoporotic burst fractures. Pedicle screw instrumentation is commenced after full consolidation of the bone cement. Pedicle screws are not inserted into the fractured vertebrae subject to vertebroplasty at least on one side, to secure the access to the spinal canal should there be a necessity to perform an anterior neural decompression. Anterior decompression may be necessary for situations such as posterior leakage of bone cement causing neurologic compromise, retropulsion of the bony fragment or bone cement fragments. The retropulsion of the cement is caused by collapse of the fractured vertebrae and is invariably associated with failure of fracture stabilization[46].

Aftertreatment

For both the sample posterior stabilization and the posterior stabilization with an anterior column reconstruction, the patient is allowed to sit with bed elevation on the first postoperative day. Ambulation is started on the second or third postoperative day with a custom-made TLSO, which is to be kept for 3 months. The patients are allowed to perform daily activities with the brace and are sent back to work by the first postoperative month.

Complications

Pedicle screw fixation is a safe procedure with very few complications when performed properly [32]. However, potential complications such as the following may occur.

Neurologic complications; may be caused by misplaced pedicle screws. However, complications related to pedicle screws may be prevented by strictly adhering to the proper technique previously described. Of more than 10,000 pedicle screw placed in the thoracic spine, we did not have a single major complication attributable to the pedicle screw placement.

Bleeding; vascular injury due to misplaced screws are extremely rare and are preventable by strictly adhering to the proper screw insertion technique.

References

1. Boos N, Webb JK. Pedicle screw fixation in spinal disorders: a European view. Eur Spine J. 1997;6:2.
2. Boucher HH. A method of spinal fusion. J Bone Joint Surg. 1959;41B:248.
3. Darden 2nd BV, Owen JH, Hatley MK, Kostuik J, Tooke SM. A comparison of impedance and electromyogram measurements in detecting the presence of pedicle wall breakthrough. Spine. 1998;23:256.
4. Darden 2nd BV, Wood KE, Hatley MK, Owen JH, Kostuik J. Evaluation of pedicle screw insertion monitored by intraoperative evoked electromyography. J Spinal Disord. 1996;9:8.
5. Dick JC, Zdeblick TA, Bartel BD, Kunz DN. Mechanical evaluation of cross-link designs in rigid pedicle screw systems. Spine. 1997;22:370.
6. Dickson RA. Deacon p. spinal growth. J Bone koint Surg Br. 1987;69:690.
7. George DC, Krag MH, Johnson CC, Van Hal ME, Haugh LD, Grobler LJ. Hole preparation techniques for transpedicle screws. effect on pull-out strength from human cadaveric vertebrae. Spine. 1991;16:181.
8. Heinig CF, Boyd BM. One-stage vertebrectomy or eggshell procedure. Orthop Trans. 1985;9:130.
9. Hirano T, Hasegawa K, Takahashi HE, Uchiyama S, Hara T, Washio T, Sugiura T, Yokaichiya M, Ikeda M. Structural characteristics of the pedicle and its role in screw stability. Spine. 1997;22:2504.
10. Kim C, Suk SI, Hong KH, Kim JH, Kim WJ, Lee CH, Kim CH. Intraoperative monitoring Using somatosensory evoked potential during spinal deformity surgery. J Koren Acad Rehab Med. 1999;23:581.
11. Krag MH, Weaver DL, Beynnon BD, Haugh LD. Morphometry of the thoracic and lumbar spine

related to transpedicular screw placement for surgical spinal fixation. Spine. 1988;13:27.
12. Kuner EH, Kuner A, Schlickewei W, Mullaji AB. Ligamentotaxis with an internal spinal fixator for thoracolumbar fractures. J Bone Joint Surg Br. 1994;76:107–12.
13. Kwok AW, Finkelstein JA, Woodside T, Hearn TC, Hu RW. Insertional torque and pull-out strengths of conical and cylindrical pedicle screws in cadaveric bone. Spine. 1996;21:2429.
14. Lee CS, Suk SI, Sung KS. Biomechanical study on multiple hooks and screws fixation in the long posterior spinal instrumentation. J Korean Spine Surg. 1997;4:212.
15. Levy Jr WJ, York DH. Evoked potentials from the motor tracts in humans. Neurosurgery. 1983;12:422.
16. Lim TH, Eck JC, An HS, Hong JH, Ahn JY, You JW. Biomechanics of transfixation in pedicle screw instrumentation. Spine. 1996;21:2224.
17. Maat GJ, Matricali B, van Persijn van Meerten EL. Postnatal development and structure of the neurocentral junction. its relevance for spinal surgery. Spine. 1996;21:661.
18. Magerl FP. Stabilization of the lower thoracic and lumbar spine with external skeletal fixation. Clin Orthop. 1984;189:125.
19. Maiman DJ, Larson SJ, Luck E, El-Ghatit A. Lateral extracavitary approach to the spine for thoracic disc herniation: report of 23 cases. Neurosurgery. 1984;14:178.
20. McCormack T, Karaikovic E, Gaines RW. The load sharing classification of spine fractures. Spine. 1994;19:1741.
21. McLain RF, Sparling E, Benson DR. Early failure of short-segment pedicle instrumentation for thoracolumbar fractures. a preliminary report. J Bone Joint Surg Am. 1993;75:162.
22. Misenhimer GR, Peek RD, Wiltse LL, Rothman SL, Widell Jr EH. Anatomic analysis of pedicle cortical and cancellous diameter as related to screw size. Spine. 1989;14:367.
23. Nash Jr CL, Lorig RA, Schatzinger LA, Brown RH. Spinal cord monitoring during operative treatment of the spine. Clin Orthop. 1977;126:100.
24. Olerud S, Karlstrom G, Sjostrom L. Transpedicular fixation of thoracolumbar vertebral fractures. Clin Orthop. 1988;227:44.
25. Puno RM, Bechtold JE. Biomechanical analysis of transpedicular rod systems. a preliminary report. Spine. 1991;16:973.
26. Resina J, Alves AF. A technique of correction and internal fixation for scoliosis. J Bone Joint Surg Br. 1977;59:159.
27. Roy-Camille R, Saillant G, Mazel C. Internal fixation of the lumbar spine with pedicle screw plating. Clin Orthop. 1986;203:7.
28. Roy-Camille R, Saillant G, Mazel C. Plating of thoracic, thoracolumbar, and lumbar injuries with pedicle screw plates. Orthop Clin North Am. 1986;17(1):147.
29. Cheffer MM, Currier BL. Thoracolumbar burst fractures. In: Levine AM, Eismont FJ, Garfin SR, Zigler JE, editors. Spine trauma. Philadelphia: WB Saunders; 1998.
30. Skinner R, Maybee J, Transfeldt E, Venter R, Chalmers W. Experimental pullout testing and comparison of variables in transpedicular screw fixation. a biomechanical study. Spine. 1990;15:195.
31. Stauber MH, Bassett GS. Pedicle screw placement with intraosseous endoscopy. Spine. 1994;19:57.
32. Suk SI. Application of Diapason reduction screws. Presented in Stryker Spinal Invitational Symposium. Cheju; 1998.
33. Suk SI, Cha SI, Lee CK, Kim WJ. A study on the pullout strength of pedicle screws in relation to the size of the drill holes and inserted screws. Presented at the 30th Annual Meeting of the Scoliosis Rearch Society. Asheville; 1995.
34. Suk SI, Kim JH, Kim WJ, Lee SM, Chung ER. Treatment of congenital scoliosis with pedicle screw fixation. Presented at the 33rd Annual Meeting of the Scoliosis Research Society, New York; 1998.
35. Suk SI, Kim MD, Shin JW, Lee SJ, Kim WJ. A numerical investigation of the axial rotational stability of transfixation in pedicle screw instrumentation. Presented at 8th international congress of SIROT. Sydney; 1999.
36. Suk SI, Kim WJ. Treatment of fixed lumbosacral kyphosis by all posterior vertebral column resection. Presented at the 5th IMAST meeting. Sorrento; 1998.
37. Suk SI, Kim WJ, Kim JH, Lee SM. Restoration of thoracic kyphosis in the hypokyphotic spine: a comparison between multiple-hook and segmental pedicle screw fixation in adolescent idiopathic scoliosis. J Spinal Disord. 1999;12:489.
38. Suk SI, Lee CK, Kim WJ, Chung YJ, Park YB. Segmental pedicle screw fixation in the treatment of thoracic idiopathic scoliosis. Spine. 1995;20:1399.
39. Suk SI, Lee JH. A study of the diameter and change of the vertebral pedicle after screw insertion. Boston, Massachusetts: Presented at third intermeeting SIROT; 1994.
40. Suk SI, Shin BJ, Lee CS, Lee MC. Cotrel-dubousset pedicular screw in the treatment of unstable dorsolumbar fracture. comparison with harrington SSI. J Korean Society Fracture. 1989;2:91.
41. Vaccaro AR, Garfin SR. Internal fixation (pedicle screw fixation) for fusions of the lumbar spine. Spine. 1995;20:157S.
42. Weidenbaum M, Farcy JPC. Surgical management of thoracic and lumbar burst fracture. In: Bridwell KH, DeWald RL, editors. The textbook of spinal surgery. 2nd ed. Philadelphia: Lippincott-Raven; 1997.
43. Zdeblick TA, Kunz DN, Cooke ME, McCabe R. Pedicle screw pullout strength. correlation with insertional torque. Spine. 1993;18:1673.
44. Zindrick MR, Wiltse LL, Doornik A. Field BT. analysis of the morphometric characteristics of the thoracic and lumbar pedicles. Spine. 1987;12:160.
45. Zindrick MR, Wiltse LL, Widell EH, Thomas JC, Holland WR, Field BT, Spencer CW. A biomechanical study of intrapeduncular screw fixation in the lumbosacral spine. Clin Orthop. 1986;203:99.
46. Kim WJ, Lee ES, Jeon SH, Yalug I. Correction of osteoporotic fracture deformities with global sagittal imbalance. Clin Orthop Relat Res. 2006;443:75–93.

34 Efficacy and Safety of an Absorbable Cervical Cage with and Without Plating: A Multicenter Case Study

Louis Boissiere, Benoît de Germay, Stephane Aunoble, and Jean-Charles Le Huec

Traumatic lesions and degenerative diseases of the cervical spine can efficiently be treated by means of anterior interbody fusion for restoring stability and preventing neurological lesions [1–5]. Spinal angulation, recurrent ipsilateral or contralateral compression of the nerve root caused by collapse of the disc space or increased postoperative neck and scapular pain, can be observed with anterior cervical discectomy without fusion [3, 4].

On the other hand, fusion with autograft is associated with significant morbidity at the iliac crest donor site, and increases the duration and risk of surgery [6]. Cages filled or not with a block of synthetic calcium phosphate ceramic material, have proven to be a safe alternative to the use of autograft, providing reliable fusion and preservation of the initial vertebral alignment [6–13].

Implanting such a device leads to let a foreign body in place, and the idea was to develop an absorbable cage that would allow for facilitating further explorations [15–31]. We have recently developed an absorbable interbody fusion cage with promising preliminary clinical results [32]. The objective of the present study is to evaluate the results of an absorbable composite cervical cage (TCP/PLLA) in anterior cervical discectomy and fusion (ACDF) on a larger series.

Methods

Participants

We undertook a prospective case study at two sites between February 2007, and June 2010. Patients were eligible for enrolment if they had traumatic or degenerative soft disc herniation from C2 to T1, foraminal stenosis, cervical spinal stenosis or spondylosis of the lower cervical spine (C2-T1). There were 59.6 % of males and 40.4 % of female patients. Mean age was 48.0 years (range, 18–83 years).

Surgery concerned one level in 78.7 % of the patients, two levels in 19.1 % and three levels in 2.2 %. 110 levels were involved, and all of the patients with multiple levels were operated on at adjacent vertebrae levels. The clinical data of the

L. Boissiere, MD • S. Aunoble, MD
Department of Orthopedic and Traumatology
Spine Surgery, Hopital Pellegrin, Bordeaux, France

B. de Germay, MD
Department of Neurosurgery, Clinique de l'Union, Toulouse, France

J.-C. Le Huec, MD, PhD (✉)
Ortho-Spine Department, Surgical Research Laboratory, Bordeaux University Hospital, Bordeaux, France
e-mail: j-c.lehuec@u-bordeaux2.fr

D.G. Poitout (ed.), *Biomechanics and Biomaterials in Orthopedics*,
DOI 10.1007/978-1-84882-664-9_34

operated patients are summarized in (Tables 34.1 and 34.2). There were 17.6 % of the patients operated on at two levels for which additional plating was not used.

Table 34.1 Baseline characteristics of the patients operated on using Duocage® cages

Patient number	89
Age (years)	48.0 (range, 18–83)
Male/Female	53 / 36

Table 34.2 Operated level

	With plating	Without plating	All patients
One level	**31**	**39**	**70**
C2-3	1	0	1
C3-4	3	1	4
C4-5	5	4	9
C5-6	14	9	23
C6-7	6	19	25
C7-T1	1	5	6
Missing data	1	1	2
Two levels	**14**	**3**	**17**
C3-4, 4-5	2	0	2
C4-5, 5-6	4	2	6
C5-6, 6-7	7	1	8
C6-7, 7-T1	1	0	1
Three levels	**2**	**0**	**2**
C5-6, 6-7, 7-T1	2	0	2

Surgical Technique

The operative procedure was performed by an antero-lateral approach following epi and lateral X-rays. After discectomy, curettage of the disc space with preparation of the cortical structures of the vertebral endplates and a decompression of neural structures, a synthetic composite (TCP/PLLA) ceramic cervical cage (Duocage®, SBM, Lourdes, France) with suitable height and width was introduced. The cages have been placed into the interbody space, at the center of the vertebral end plates, under careful impaction. The additional plating used was a Zephir® (Medtronic, Memphis, TN, USA) in all cases.

A soft collar was used during 3 weeks after the surgery.

Procedures

The primary endpoints were the resorption (over 75 %, 25–75 %, or under 25 %) as evaluated by comparing the initial density of the implant to that of adjacent cancellous bone, and the fusion of the cervical interbody cage (Fig. 34.1). Fusion was evaluated by means of dynamic flexion extension X-rays (less than 3°), displacement (none, 1–5 mm, or over 5 mm) and loss of disc height (none, 1–3 mm, or over

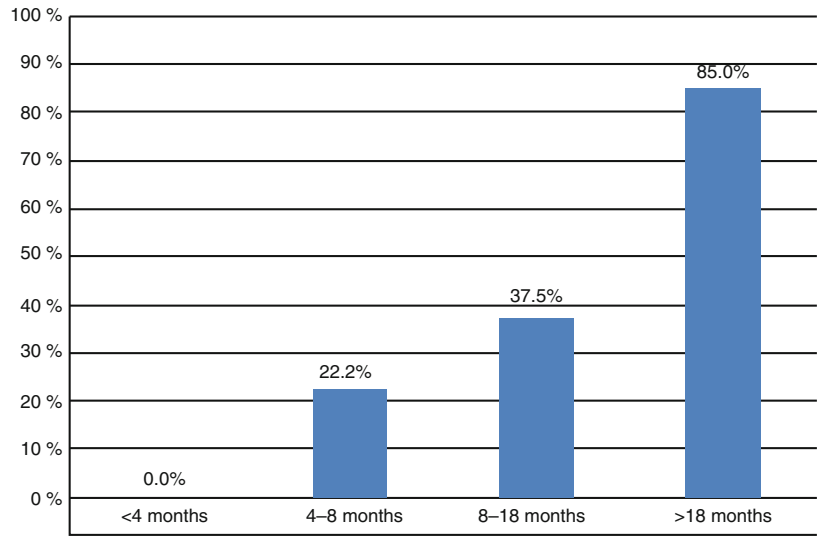

Fig. 34.1 Resorption higher than 25 %

3 mm) by measuring the distance of the two adjacent intact vertebral plateau to eliminate the imprecision of measure at the treated level. Prespecified secondary outcomes were clinical inflammatory reactions (no or yes), functional result (good, fair, or poor), pain (none, moderate, or acute) using VAS scale and return to physical activities, sportive and professionals (good, fair, or poor). Radiological evaluation also included the presence of a radiolucent line (none, 0–1 mm, or over 1 mm). Data were measured at 3, 6 and 12 months after the surgery and at the latest follow-up available, at least 18 months where the overall result was estimated (excellent, good, fair, or bad). All adverse events were reported.

Migration was defined as a displacement of the cage superior to 5 mm, and subsidence was defined as a more than 3 mm loss of initial implant height. Migration, subsidence or fracture of the implant, non-union and fusion, were evaluated by means of standing lateral spinal radiographs including flexion-extension radiographs and CT scan evaluation at 1 year or latest follow up. They were taken at each follow-up, except at the first to prevent risks of non-union during bone healing.

Statistical Analysis

89 patients were enrolled, and 110 cages were implanted. The number of patients required was not based on statistical considerations. Analysis of difference between the groups with or without a plate, with separated analysis for the one-level and the multi-level operated patients, were conducted using descriptive statistics and the t-test or the Wilcoxon test to compare the calculated means at every endpoint, depending of the normality of the observed distribution. Patient's proportions were compared by the χ [2] or the Fisher's exact test, depending on the computed theoretical effectives. The approach was two-sided and a type I error of 5 % was chosen for declaration of statistical significance. SAS version 8.2 (Inst; Cary, NC, USA) was used for all statistical analyses.

Results

The average follow-up is 19 months (range, 1–36 months). Ten subjects were lost to follow-up: 2 died, 1 moved, 5 withdrawn their consent and 2 files were lost.

Radiological Results and Adverse Events

The radiological data of the operated patients are summarized in Table 34.3 (Fig. 34.2 and 34.3). Cervical interbody fusion with Duocage® cage was uneventful in all patients. There were no early or late implant-related complications. There were two patients with pseudarthrosis. No late inflammation was noticed. We did not observe any problems such as cage fracture.

A bony bridge was observed between the two vertebrae with no mobility in every except the patients who presented a pseudarthrosis. One of these patients, operated on two levels without plate fixation, evidenced non union only on one of the two levels since fusion was achieved at the upper level.

A slight hypo density at the periphery of the cage was still present at the last follow-up in 26.9 % of the operated levels, without relation to the number of operated levels. No radiolucent line around the implant was observed for 97.0 % of the operated levels at the last follow-up. Three patients (3.8 %) had a radiolucency, all without a plate fixation. In one case there was a massive osteolysis. Another patient had previously undergone a posterior cervical foraminotomy. For the

Table 34.3 Radiological results at last follow-up

(%)	With plating	Without plating	All levels
Stable dynamic X-rays	100.0	93.8	98.0
Radiolucent line under 1 mm	100.0	88.9	97.0*
Migration under 5 mm	100.0	88.2	97.0*
Loss of disc height under 3 mm	100.0	88.9	97.0*

*$P < 0.05$, *Fisher's exact test, between with or without plating groups*

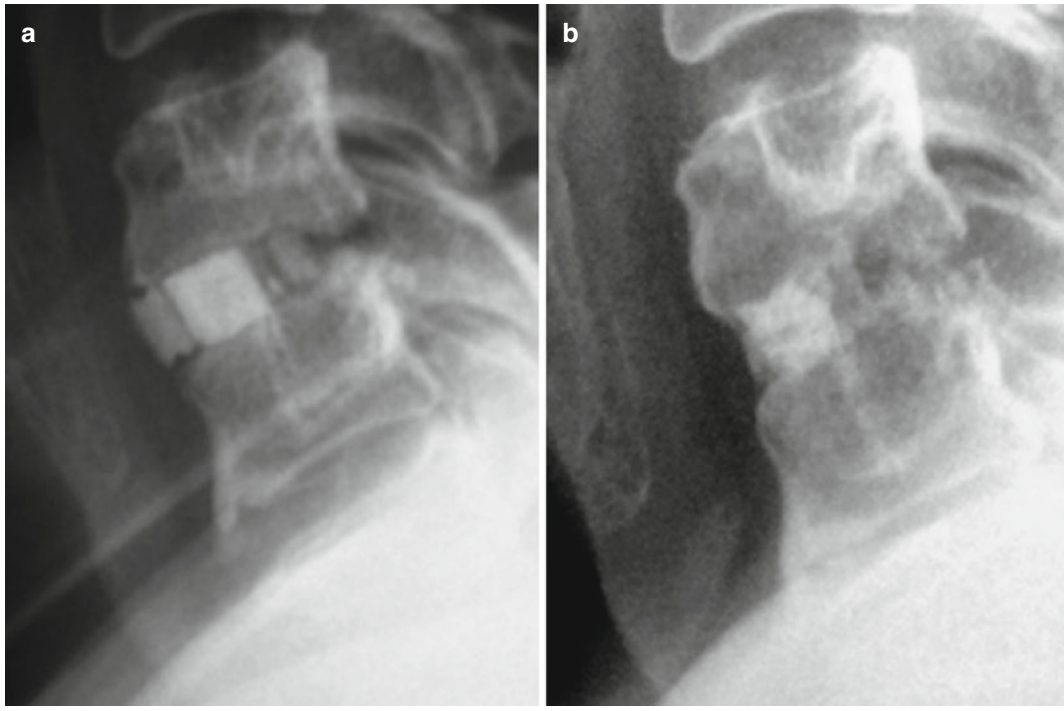

Fig. 34.2 Fusion and resorption of the Duocage®: extension X-rays at (**a**) 4 months and (**b**) 32 months after surgery without plate

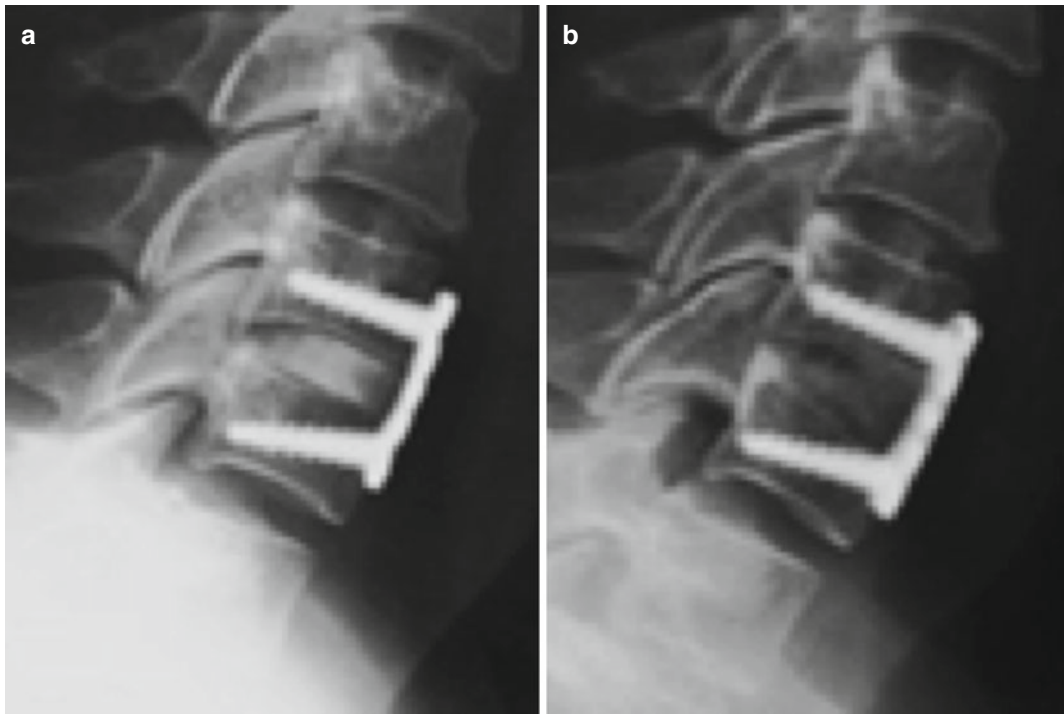

Fig. 34.3 Fusion and resorption of the Duocage®: patient with a fixation plate at (**a**) immediate post-operative visit and (**b**) 24 months after surgery

last case, the cage was inserted at the anterior third of the disc plate opening the anterior space. The rate of radiolucency were significantly different in the groups with or without a fixation plate for the subjects operated on one level at the first follow-up ($p \leq 0.001$, Fisher's exact test), and for the subjects operated on two levels at the last follow-up ($p = 0.016$, Fisher's exact test).

In 38.5 % of the patients without plate fixation, a slight migration, between 1 and 5 mm, was observed at the last follow-up. A strong migration, over 5 mm, was observed in 2 patients without plate fixation (15.4 %). None of the patients with additional plating had any cage migration at any of the follow-up.

Two patients had a loss of disc height greater than 3 mm at their last follow-up: in one case it was a massive osteolysis, in the other two cases there was a pseudarthrosis. No patient with additional plating had any loss of disc height at any of the follow-up.

There is a statistically significant difference between the groups with or without a plate fixation regarding the migration ($p \leq 0.001$, Fisher's exact test) and the loss of disc height ($p \leq 0.001$, Fisher's exact test) at the last follow up. These findings confirm that the fixation plate has a key role regarding the migration and the subsidence of the cage.

The resorption rate was over 25 % in 66.2 % of the cases at the last follow up, and in 85.0 % of the cases after 18 months. It was over 75 % in 30.0 % of the cases after 18 months. The resorption rate was not related neither to the number of operated levels, nor to the presence of additional plating.

Clinical Outcome

There were two patients with important cervicalgia at first follow-up, which completely disappeared thereafter. Functional results were never poor in any case but one. These outcomes are equivalent in both groups, except when considering the multi-levels implanted patients, where the functional results were good in all cases with a plate and only in one patient without a plate at the last follow-up ($p = 0.032$, Fisher's exact test, for the patients operated on two levels) (Table 34.4).

Table 34.4 Clinical outcome at last follow-up

(%)	With plating	Without plating	All levels
Inflammatory reaction	2.3	0.0	1.2
Good or fair functional result	100.0	97.4	98.8
Good or fair return to activities	100.0	86.9	94.0*
None or moderate pain	100.0	97.4	98.8

$P < 0.05$, Fisher's exact test, between with or without plating groups

Return to activities was good for 83.3 % of the studied population, nearly equivalent for all the patients with or without a fixation plate, at the last follow-up. No patient with a fixation plate had bad results, whereas it concerned 13.2 % of the operated levels in the group without a fixation plate ($p = 0.031$, Fisher's exact test). At the first follow-up, all patients with a plate and 65.7 % of the patients without a plate, had returned to normal activities. The conclusions are identical at the last follow-up, for all the patients followed at least 18 months. It seems that a plate can be helpful for obtaining a faster and long-lasting return to sport and professional activities. No relation was shown with the number of operated levels.

There was no pain for 61.2 % of the operated levels at the last follow-up, and no significant difference between the plating and the non-plating patients at any follow-up was found. When considering the multi-level operated patients, all of the patients without a plating fixation felt moderate pain, whereas 38.1 % of the patients fixed with a plate felt pain at the last follow-up. Only one patient, without a fixation plate, showed accurate pain from the 6 months follow-up.

Discussion

The overall result was good or excellent for 88.9 % of the patients with one operated level, and for 75.0 % of the patients with two operated levels. This overall result was equivalent for the patients with or without a fixation plate if they were operated on one level. The result is even

excellent for 70.0 % of the patients operated on two levels with a fixation plate.

Only one patient had a bad overall outcome, caused by a pseudoarthrosis, and one patient, who had a previous cervical foraminotomy and was previously operated on two levels by a posterior approach, had poor radiological and clinical results.

This case study shows that the fusion of the Duocage® is excellent, with stables X-rays for 98.0 % of the operated levels, and with no real radiolucent line, under 1 mm, for 97.0 % of the operated levels. These rates could be compared to the best of those seen in the literature, where fusion rates range from 79–98 % with the Smith-Robinson technique [26, 29, 31]. Furthermore, our results are in accordance to approve that the multi-level fusion rates are increased with the adjunction of a fixation plate [26, 33].

The loss of disc height due to subsidence can only be noticed here in 3.0 % of the total of the studied population, at the last follow-up. The few published studies range the subsidence from 18–79 % [22–31], where the best case can be correlated with the 14.9 % of operated levels with an insignificant, under 3 mm, loss of disc height noticed in this case study.

As regards to the risk of migration, the current series noticed 3.0 % of patients with a migration over 5 mm. In this series, 14.9 % of the patients had, at worst, a minor displacement, less than 5 mm, where the conclusions found in the literature shown 4–54 % of patients with migration of the cage [24].

The Duocage® cage also provided a good resorption, with 85.0 % of cages over 25 % after 18 months which confirms previous animal and clinical studies [20].

The functional results and the return to activities are also good even excellent.

As well, this study confirms that patients with a fixation plate have better outcomes in terms of functional results and pain when operated on several levels. These differences are significant, for all patients without considering the number of operated level, for the migration and the loss of disc height.

These finding will help to inform decisions about the use of a plating fixation device when several levels are involved.

The potential of TCP ceramics in spinal fusion has been evidenced on animal models in both postero-lateral [13] and interbody grafting [32]. Clinical results have confirmed these data in various clinical situations like post-traumatic reconstruction, thoracic or lumbar postero-lateral fusion [34]. During resorption, dissolved calcium and phosphate ions participate to new bone matrix formation and are physiologically involved in the local bone metabolism [20].

This study confirms that the Duocage® composite cage is capable of achieving complete fusion without inflammatory reaction during resorption. This new composite material reduces the inflammatory reaction induced by PLLA alone and promotes new bone formation. The ceramic block guarantees the maintenance of the disk height and its slow resorption which allows long term fusion and stability. At the end, this combination provides the same results as tricortical iliac crest graft without the disadvantage of the bone harvesting site.

References

1. Robinson RA, Smith GW. Anterolateral cervical disc removal and interbody fusion for cervical disc syndrome. Bull Johns Hopkins Hosp. 1955;96:223–4.
2. Smith GW, Robinson RA. The treatment of certain cervical-spine disorders by anterior removal of the intervertebral disc and interbody fusion. J Bone Joint Surg Am. 1958;40–A:3.
3. Cloward RB. The anterior approach for removal of ruptured cervical disks. J Neurosurg. 1958;15: 602–17.
4. Bailey RW, Badgley CE. Stabilization of the cervical spine by anterior fusion. J Bone Joint Surg Am. 1960;42–A:565–94.
5. Verbiest H. La chirurgie antérieure et latérale du rachis cervical. Neurochirurgie. 16(Suppl 2):1–212.
6. Flately TJ, Lynch KL, Benson M. Tissues responses to implants of calcium phosphate ceramic in the rabbit spine. Clin Orthop. 1983;179.
7. Nasca RJ, Lemons JE, Montgomery R. Evaluation of cryoconserved bone and synthetic biomaterials in promoting spinal fusion. Spine. 1991;16:330.
8. Bucholz RW, Carlton A, Holmes RE. Hydroxyapatite and Tricalcium Phosphate bone graft substitutes. Orthop Clin North Am. 1987;18(2):323–34.
9. Cazeau C, Doursounian L, Touzard RC. Utilisation de céramique de phosphate tricalcique dans la réparation des fractures du plateau tibial: résultats sur 10 cas revus à 2 ans. Enseignement de la SOFCOT; 1994.

10. Le Huec JC. Fractures articulaires récentes de l'extrémité supérieure du tibia de l'adulte. Conférences d'enseignement de la SOFCOT; 1996. p. 97–117.
11. Husson JL, Poncer R, Chatellier P, Morel G, Polar JL, Missoury F, Lancien G, Phosphates tricalciques et arthrodèses lombaires : résultats cliniques, radiographiques et histologiques. Enseignement de la SOFCOT; 1994.
12. Lantuejoul JP, Cambuzat A, Ray O, Clement D, Merloz P, Faure C, et Plaweski S. Utilisation du phosphate tricalcique comme substitut osseux: A propos d'une série de 55 cas. Compte-rendu du G.R.E.C.O. Rev de Chir Orthop. 1995;82:175.
13. Le Huec JC, Lesprit E, Delavigne D, Clement D, Chauveaux D, Le Rebeller A. Tri-calcium phosphate ceramics and allografts as bone substitutes for spinal fusion in idiopathic scioliosis : comparative clinical results at four years. Acta Orthop Belg. 1997;63:3.
14. Robert R, Faure A, Bord E, Delecrin J, Szapiro J, Passuti N, Cervical interbody fusion by xenograft and ceramics in traumatology. 1996, 3rd European GICD Forum: problems of the cervical spine surgery. Barcelone, ESPAGNE. 21–23 avril. 1996, Communication orale.
15. Faure A, Raoul S, Bord E, Rebai R, Delecrin J, Passuti N, Robert R. Intérêt des xénogreffes et des céramiques dans la chirurgie du rachis cervical. Journée sur les substituts osseux synthétiques en chirurgie orthopédique, Clinique U.C.L. Mont-Godinne – Namur, BELGIQUE, 14 juin.1997 Communication orale.
16. Robert R, Raoul S, Bord E, Faure A, Delecrin J, Passuti N. Evaluation of xenograft and ceramics in cervical corporectomy and discectomy. International Forum on New Technologies in Advanced Spine Surgery, State of the Art 199, Bad Fussing, ALLEMAGNE. 23–25 mai 1997; Communication orale.
17. Robert R, Faure A, Bord E, Raoul S, Delecrin J, Passuti N. Surgical anatomy and techniques used in cervical spine surgery at the cervicothoracic junction. Advanced Spine Course. Kruger Park, AFRIQUE DU SUD. 19–22 juin 1997; Communication orale.
18. Faure A, Bord E, Delecrin J, Perrouin-Verbe B, Richard I, Mathe JF, Robert R, Utilisation de greffons hétérologues et céramiques dans le rachis cervical traumatique. XI ème Congrès National de la SOFFMERR. Limoges, 12–14 septembre 1996, Communication orale.
19. Robert R, Raoul S, Delecrin J, Bord E, Faure A, Passuti N. Anterior cervical surgery and fusion by Tricalcicphosphate (Biosorb). Preliminary study on 25 cases. 6th European Forum of GICD, Segmental Instrumentation in Spine Surgery: Long Term Follow-up and New Techniques, Nantes, 19–20 janvier 1998, Communication orale.
20. Aunoble S, Clement D, Frayssinet P, Harmand M-F, Le Huec J-C. Biological performance of a new β-TCP/PLLA composite material for applications in spine surgery : In vitro and in vivo studies. J Biomed Mater Res A. 2006;30749:1–7.
21. Pascal-Mousselard H, Daculsi G, Lazennec J-Y, Catonné Y, Saillant G. Les cages intervertébrales cervicales: analyse critique de la littérature. Maîtrise Orthopédique n°147 – octobre 2005.
22. Barsa P, Suchomel P. Factors affecting sagittal malalignment due to cage subsidence in standalone cage assisted anterior cervical fusion. Eur Spine J. 2007;16(9):1395–400. Epub 2007 Jan 13.
23. Bartels RH, Donk RD, Feuth T. Subsidence of standalone cervical carbon fiber cages. Neurosurgery. 2006;58(3):502–8; discussion 502 – 8.
24. Chen Y, Chen D, Guo Y, Wang X, Lu X, He Z, Yuan W. Subsidence of titanium mesh cage: a study based on 300 cases. J Spinal Disord Tech. 2008;21(7): 489–92.
25. Cho DY, Lee WY, Sheu PC. Treatment of multilevel cervical fusion with cages. Surg Neurol. 2004;62(5):378–85; discussion 385 – 6.
26. Dai LY, Jiang LS. Anterior cervical fusion with interbody cage containing beta-tricalcium phosphateaugmented with plate fixation: a prospective randomized study with 2-year follow-up. Eur Spine J. 2008;17(5):698–705. Epub 2008 Feb 27.
27. De Germay B, Dubois G, Clément D. Clinical results of cervical interbody fusion with hydroxylapatite. A retrospective study about 67 cases. Rachis. 2001:13(3).
28. Kast E, Derakhshani S, Bothmann M, Oberle J. Subsidence after anterior cervical inter-body fusion. A randomized prospective clinical trial. Neurosurg Rev. 2009;32(2):207–14; discussion 214. Epub 2008 Sep 17.
29. Kulkarni AG, Hee HT, Wong HK. Solis cage (PEEK) for anterior cervical fusion: preliminary radiological results with emphasis on fusion and subsidence. Spine J. 2007;7(2):205–9. Epub 2006 Nov 17.
30. Matgé G. Cervical cage fusion with 5 different implants: 250 cases. Acta Neurochir (Wien). 2002;144(6):539–49; discussion 550.
31. Song KJ, Taghavi CE, Lee KB, Song JH, Eun JP. The Efficacy of Plate Construct Augmentation Versus Cage Alone in Anterior Cervical Fusion. Spine (Phila Pa 1976). 2009;34(26):2886–92.
32. Debusscher F, Aunoble S, Alsawad Y, Clément D, Le Huec JC. Anterior cervical fusion with a bioresorbable composite cage (beta TCP – PLLA): clinical and radiological results from a prospective study on 20 patients. Eur Spine J. 2009;18(9):1314–20.
33. Song KJ, Taghavi CE, Hsu MS, Lee KB, Kim GH, Song JH. Plate augmentation in anterior cervical discectomy and fusion with cage for degenerative cervical spinal disorders. Eur Spine J. 2010;19(10): 1677–83.
34. Bansal S, Chauhan V, Sharma S, Maheshwari R, Juyal A, Raghuvanshi S. Evaluation of hydroxyapatite and beta-tricalcium phosphate mixed with bone marrow aspirate as a bone graft substitute for posterolateral spinal fusion. Indian J Orthop. 2009;43(3): 234–9.

35 Biomechanics of Posterior Instrumentation for Spinal Arthrodesis

S.I. Suk and W.J. Kim

The main purposes of spinal instrumentation are restoration of stability in an inherently unstable or surgically destabilized spine, and correction and maintenance of spinal deformities via forces effected by the instrumentation [1–6]. Spinal instrumentation may be, at large, divided into anterior instrumentation and posterior instrumentation by the element of the vertebral body utilized to fix the implant to the vertebral column. Those fixing the anterior column (usually the vertebra body proper) are considered anterior instrumentation while those fixing the structures of the posterior column (lamina, facets, pedicles) are considered posterior instrumentation.

Though there are many factors which may affect the choice of the instrumentation method for a specific spinal problem, the two most important factors seems to be the location of the pathology causing the instability or the deformity and the experience of the treating surgeon.

An anterior instrumentation is indicated when the spinal pathology or the instability is located predominantly in the anterior column. However, anterior instrumentation may be difficult to apply when it is necessary to incorporate a large number of spinal segments or when the instrumentation needs to span across the cervicothoracic, the thoracolumbar, or the lumbosacral junction due to the complex anatomy of the junctional regions.

By the same token, a posterior instrumentation is indicated when the spinal pathology or the instability is located predominantly in the posterior column. Though a pathology or instability arising from the posterior column is rare, posterior instrumentation is more commonly used than anterior instrumentation. This is due to the fact that the posterior approach is more often employed than the anterior approach in the practice of spinal surgery due to its relative ease, extensibility, and lower risk of a major visceral injury, which subsequently makes the instrumentations in the posterior column more frequent [7].

The purpose of this chapter is to introduce the biomechanical basis of posterior instrumentation techniques and to offer a guideline for an appropriate choice of technique or techniques for various spinal conditions subject to stabilization or correction by posterior instrumentation.

Implant Characteristics

Materials

The biomechanical characteristic of a spinal implant is often governed by the material properties of the implant. Modern spinal posterior

S.I. Suk, MD, PhD (✉)
Department of Orthopedic Surgery,
Seoul Spine Institute, Inje Univ Sanggye Paik Hospital,
Nowon-Ku, Seoul, South Korea
e-mail: seilsuk@unitel.co.kr

W.J. Kim, PhD
Materials Science and Engineering,
Hongik University, Seoul, South Korea

D.G. Poitout (ed.), *Biomechanics and Biomaterials in Orthopedics*,
DOI 10.1007/978-1-84882-664-9_35

implants are usually made of metal, either in pure or in alloyed forms. Metal is superior to other materials as spinal implants in the aspects of its mechanical strength, relative ease of shaping, possibility of obtaining uniform material property throughout the whole implant, and for mass production.

Metals commonly used for spinal implants are pure unalloyed titanium, Ti-6AI-4 V, 316 L stainless steel, 22-13-5 stainless steel, cast Co-Cr-Mo, and Vitallium, which is also a Co-Cr alloy [8]. Though pure titanium and the titanium alloys have a lower modulus of elasticity (less stiffness) than the stainless steel or other Co-Cr alloys, they have the advantage of producing less distortion of CT or MR images [9]. As they allow improved postoperative radiological examination of the spinal canal, they are presently increasing in use as spinal implants (Fig. 35.1).

Design

The usual posterior spinal implant is composed of anchoring members, longitudinal members, a kind of component-component connecting mechanism to connect the anchoring members to longitudinal members, and the transverse members to cross-link the longitudinal members.

Anchoring Members

The anchoring member is the part of implant system that grips the bony structure of the spinal column and transmits the force effected by the instrumentation to the spinal column. As this component comes directly in contact with the bone, there forms a bone-component interface. Anchoring members for the posterior spinal

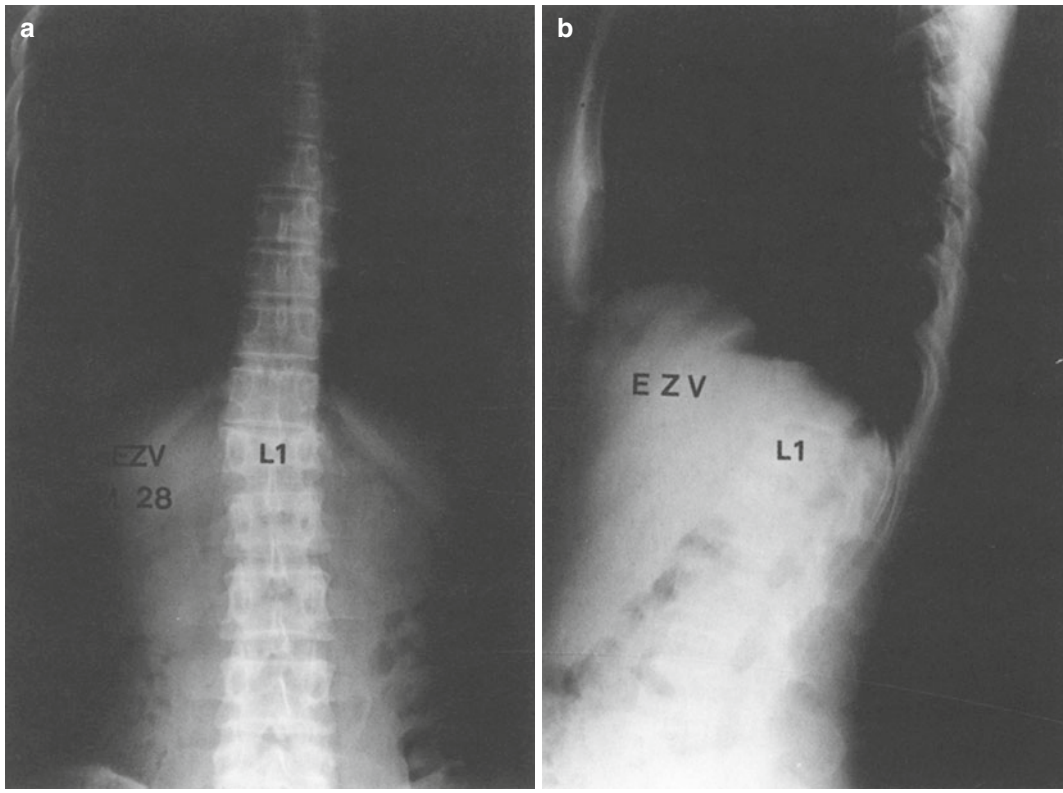

Fig. 35.1 (**a**, **b**) A 28-year-old male with an unstable bursting fracture of ll. (**c**, **d**) He was treated by posterior instrumentation with pedicle screws made of titanium alloy. (**e**, **f**) Postoperative sagittal and axial MRI show little metallurgic artifact, allowing view of spinal canal (Continued next page)

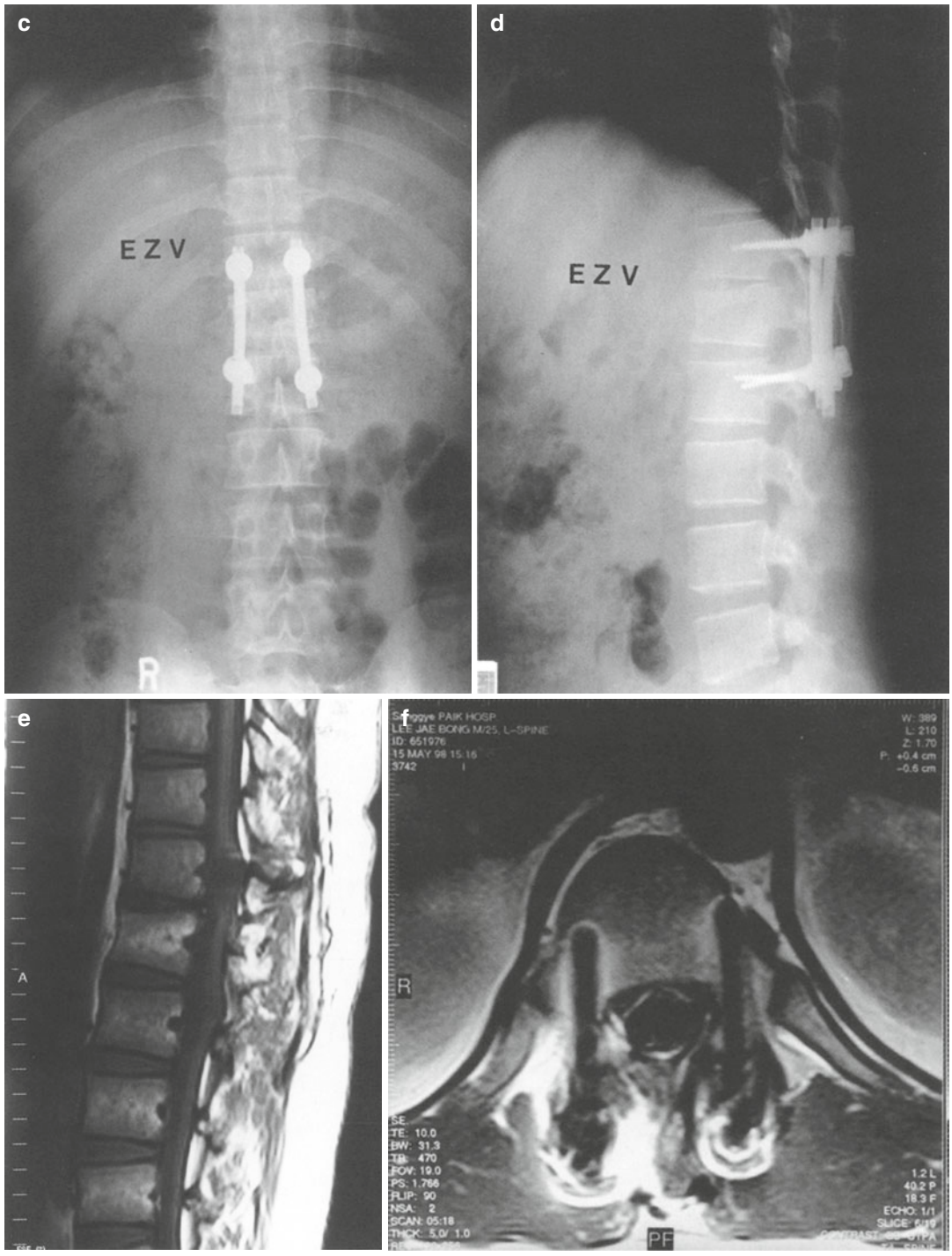

Fig. 35.1 (continued)

instrumentation may be divided into a penetrating type and a gripping type by the form of their bone-component interface.

Penetrating-type anchoring members are those engaging the bone by penetration into the bony structure. They make an important component

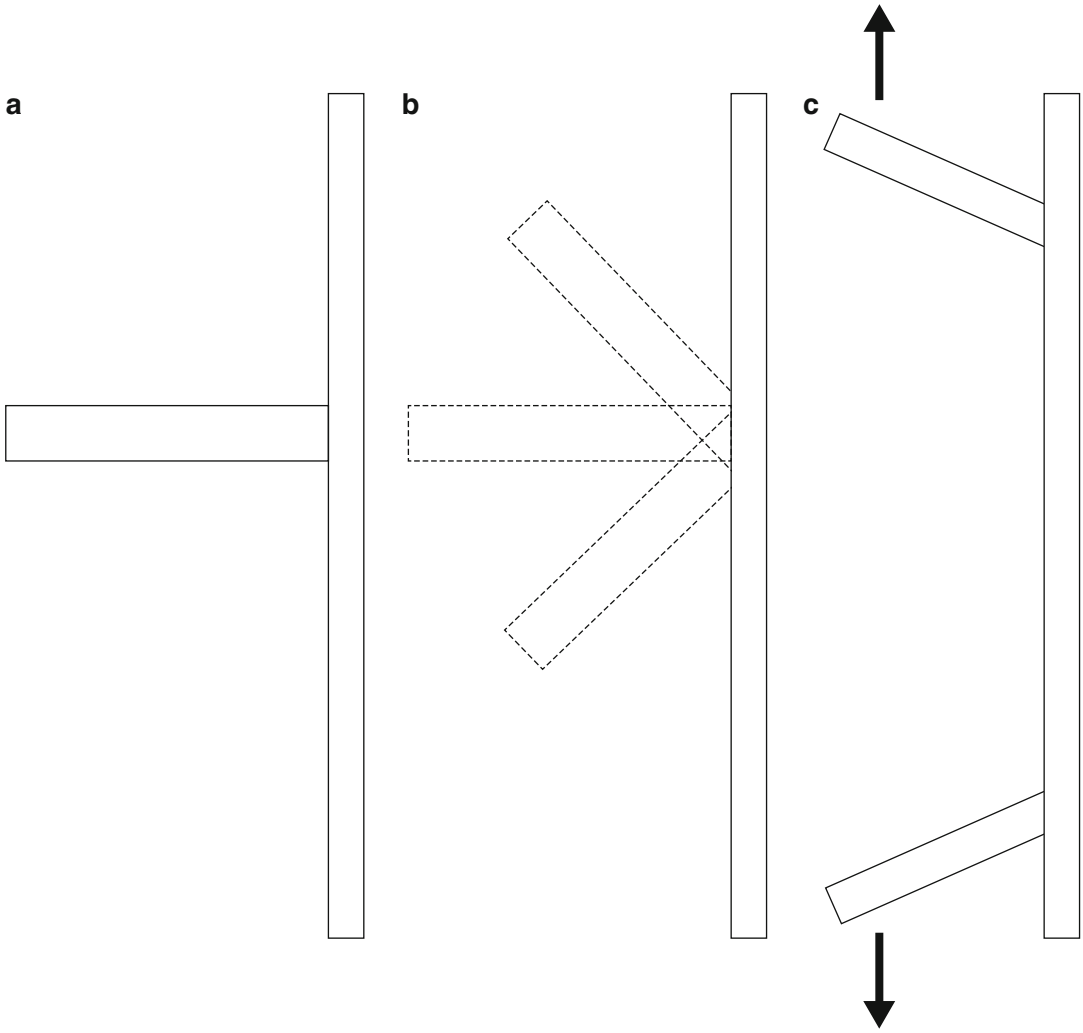

Fig. 35.2 Cantilever beam constructs. (**a**) Fixed moment arm cantilever beam construct. (**b**) Non-fixed moment arm cantilever beam construct. (**c**) Applied moment arm cantilever beam construct

of the cantilever constructs. By the alternation of the component-component connecting mechanism, they may act as a fixed moment arm, non-fixed moment arm, or an applied moment arm cantilever beam (Fig. 35.2). Penetrating anchors are divided into two groups; those with pullout resistance and those without pullout resistance. However, penetrating anchors without pullout resistance, called the "post", are seldom, if ever, used alone in posterior implant systems [8]. Penetrating anchors with pullout strength comprise screws and smooth posts that change shape to offer pullout resistance after penetration into the bone. In present practice, screws are the most commonly employed penetrating anchors in posterior instrumentation [10].

Screws are presently used in the posterior instrumentation system for fixation in the pedicle [6, 11], cervical lateral mass [12], sacral ala [13], and iliac wings [14]. They have gained more popularity in recent years as they offer a rigid vertebral grip which is stable immediately after the insertion without need of a force loading and enable reliable fixation in the presence of posterior element defects which preclude the use of gripping types of anchors. But in some

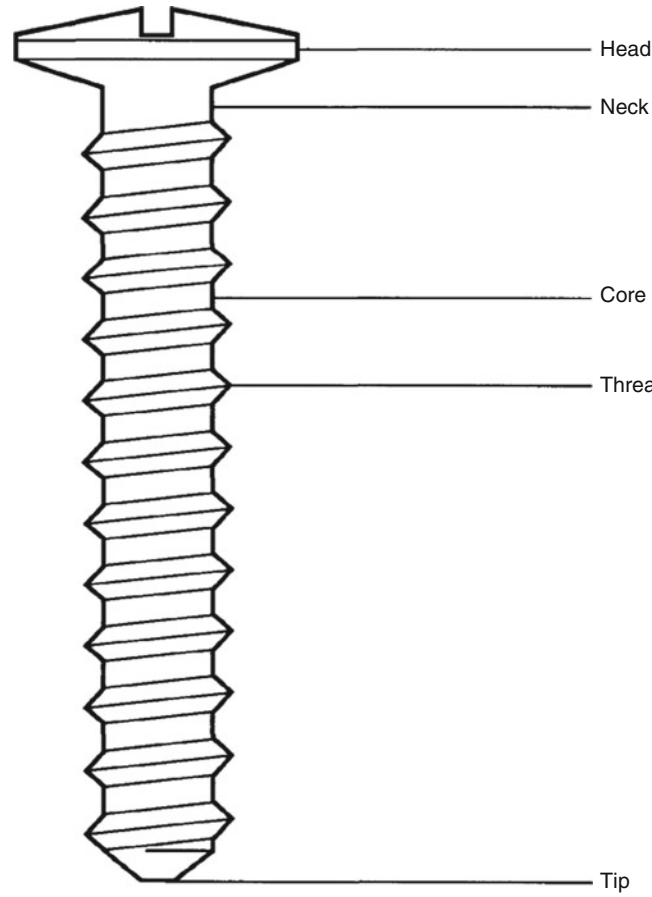

Fig. 35.3 A screw and its five parts. The screw is composed of head, core, thread, tip, and neck

situations, employing a penetrating-type anchor may be difficult due to the complex anatomy of the region and risks of causing a major neural element or vascular damage [11, 15].

Screws used for posterior instrumentation may be a cortical or a cancellous type. However, the fact that the parts of the vertebra which engage the screws, including the pedicles, are composed of cancellous bone, the use of cancellous-type screws is more common [16]. A screw is made up of five parts: head, core, thread, tip, and the neck that connects the screw head to the core (Fig. 35.3). The screw head is the part of the screw opposite the tip and functions as the receiving port to the inserting device. Its main biomechanical function is to resist the inward translation force generated by the rotation of the screw at the terminal phase of screw tightening. When the screw is designed to tighten against a metallic implant, for example a plate, the implant will offer a substantial resistance to pull-through and the screw head needs to be just so big so as not to pass through the screw hole. On the other hand, if the screw is designed

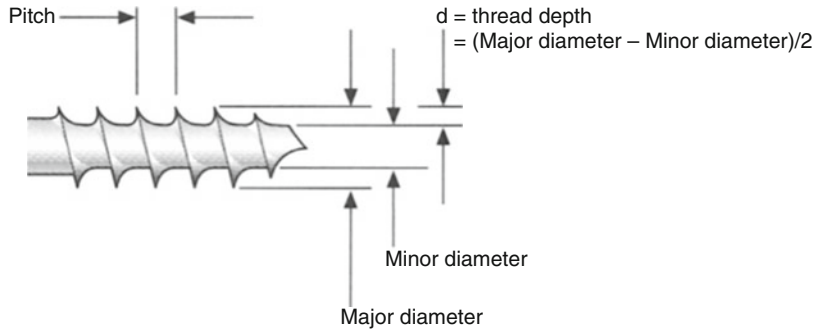

Fig. 35.4 Thread depth and pitch

to tighten against the bone, the screw head must be substantially larger to offer an effective resistance to pull-through.

The screw core is the part of the screw from which the threads arise. Biomechanically, it provides the strength of the screw per se and resists bending and torsion moments acting on the screw. Since screws are frequently subject to bending moments in posterior instrumentation, the bending strengths of screws have significant clinical importance. The bending strength of a screw is proportional to the section modulus (Z) that is calculated as $Z = \pi D^3/32$, in which D is the core diameter of the screw. As the section modulus changes by the cube of the change in the core diameter, even a slight alternation in the core diameter greatly affects the bending strength of the screw. This implies the importance of using a screw of the largest permissible diameter when using screws as anchoring members [17].

The screw thread is the part of the screw that provides the pullout resistance against a force directed along the long axis of the screw. As the pullout strength of the screw is proportional to the volume of the bone between the threads, the pullout strength is affected by the major diameter of the screw, thread depth, and pitch, which is the distance between two threads (Fig. 35.4). The cancellous-type screws used in posterior instrumentation causes compression of the soft cancellous bone during insertion and increases the density, and hence the amount of bone held within the threads, and are effective in enhancing the pull-out strength of the screws [18]. Screws used in posterior instrumentation have various designs to increase the pull-out strength (Fig. 35.5).

The screw tip is the part of the screw that first enters the bone. Though most of the screws used in posterior instrumentation are cancellous-type screws that do not need pre-tapping, some screws have leading-edge flutes like self-tapping screws to facilitate insertion (Fig. 35.6).

The neck of the screw is the part connecting the head of the screw to the core. As screws are frequently subject to cantilever bending moments, the neck portion receives most of the bending moment acting on the screw and is the most frequent site of fracture [19]. Some screws are designed to have a reinforced neck to offer more effective resistance to the cantilever bending moments concentrated here.

Gripping-type anchors are the components which "grip" the vertebra without penetrating into the bone. Hooks and wires are gripping type anchors most commonly employed in posterior instrumentation. The common sites for application of the gripping-type anchor are lamina, pedicle, spinous process, and the transverse process. The pull-out strength of the gripping-type anchors may be substantial as they contact the hard cortical shell of the vertebra. Biomechanically, the pull-out strength of the gripping-type anchor depends on the surface area under the component and the structural integrity of the bony element to which the anchor is attached. Since the bone has to resist the pull-out force by its inherent mechanical strength, even a minor fracture that weakens the part of the posterior element receiving the anchor substantially decreases the pull-out strength. This fact also limits the use of gripping-type anchors in the osteoporotic spine where cortical bone fails

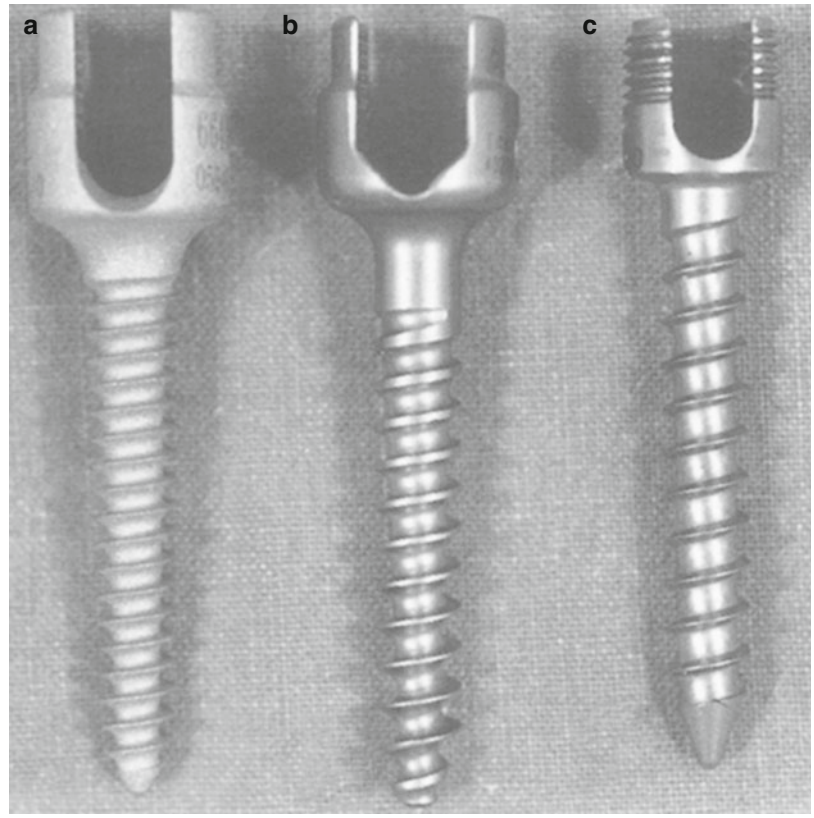

Fig. 35.5 Screws of various design. (**a**) Conical cancellous type screw. (**b**) Cylindrical screw with tapered conical core. (**c**) Cylindrical screw

to provide enough resistance to the cut through of the components.

Recently, gripping-type anchors have been decreasing in use and are being replaced by penetrating anchors. The main reason for this substitution is the inferiority of holding power when compared to the screws. Additional reasons are prerequisite of an intact posterior element for a reliable fixation, necessity of preloading that inhibits the unconstrained motion of the spinal column under force, and the necessity of intruding the spinal canal that may increase the risk of neurologic injury.

In today's modern posterior spinal instrumentation, implants are designed in such a way that several types of anchoring members may be used in the same instrumentation procedure, allowing the surgeon to choose the anchoring component according to the situation. Gripping-type anchors may be used with penetrating-type anchors in the same instrumentation to share the pull-out strength and hence protect the penetrating-type anchors from excessive pull-out stress.

Longitudinal Members

The longitudinal members are the part of the implant to which the anchoring members are attached. The biomechanical function of the longitudinal member is to resist the principle force applied to the instrument. The longitudinal member of the distraction instrumentation has to resist the bending moment created by the weight of the body above the instrument while the longitudinal member of the compression instrumentation has to resist the tension stress.

Longitudinal members in a posterior implant may be a plate or a rod. Plates are very strong and offer a rigid fixation when combined with a constrained bolt. However, they are gradually becoming less popular as contouring of a plate to conform to the curvature of the spine is difficult and is fraught with technical problems. Additional reasons for this trend are lack of versatility that limits the available anchoring component to screws and the relative bulk of

Fig. 35.6 A pedicle screw with leading edge flute to act as a self-tapping screw

the implant that causes greater extent of soft tissue damage during implantation and takes up room for placement of bone graft.

The rod is presently the most common form of longitudinal member employed in the posterior instrumentation. They are easy to contour and allow attachment of both the gripping and the penetrating-type anchoring members. Similar to screws, their strength is proportional to the section modulus (Z). As $Z=\pi D^3/32$, the strength of the rod is greatly influenced by the diameter. However, as increasing the diameter of the rod also increases the bulk of the implant causing many untoward problems, the manufacturers are trying more and more to produce thinner rods with increased strength which allow the implant to have a low profile [20]. Some are trying to use rods of higher elasticity to prevent mechanical failures, but the ultimate result is still to be clarified. Rods may be sliding types with or without a surface finish, a threaded or a rachetted type (Fig. 35.7).

The sliding type of rod is the most common type used presently. It allows free sliding of the anchoring members along the length of the rod enabling distraction and compression along the rod. It is suitable tar both distraction and compression constructs. While some of these rods are smooth, some have surface alterations to increase the friction between the rod and the component attaching mechanism.

Threaded rods allow powerful, controlled distraction or compression of the anchoring

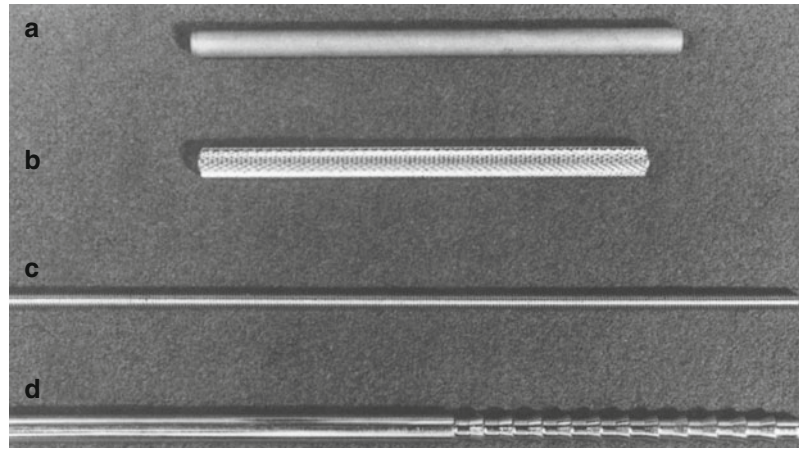

Fig. 35.7 Various rods. (**a**) A smooth rod. (**b**) A knurled rod to increase surface friction. (**c**) A threaded rod. (**d**) A rachetted rod

members along the rod. However, as bending of the rod with mechanical benders often results in damage to the threads causing difficulty in tightening of the nuts, they are usually more malleable than the sliding-type rods. This limits their use in posterior instrumentation to compression (tension band) constructs.

Rachetted rods like the one used in the Harrington distraction device are primarily used in distraction constructs. As the rackets act as stress risers, often leading to mechanical failure of the rod, this type of rod is rapidly falling out of favor.

Component-Component Connecting Mechanism

The longitudinal member of the posterior implant is connected to the anchoring members by a component-component connecting mechanism Except for a wire which is tightened around the longitudinal member to offer a grip, all the connection between the components of posterior implants are one or combinations of the following six fundamental locking mechanisms; (1) three-point shear clamp, (2) lock screw, (3) circumferential grip, (4) constrained screw-plate, (5) semiconstrained screw-plate, (6) semiconstrained anchoring component-rod.

The three-point shear clamp is the mechanism of locking employed in the screws in the synergy (Cross Medical, USA) system and the new type DDT of the Cotrel-Dubousset system (Sofamor-Danek, USA). The locking is provided by the force applied at the interface and the friction between the components.

The lock screw mechanism uses the set screw to push the rod to abut the other part of the component and is presently the most common type of locking mechanism used in posterior instrumentation. Examples are the screws and hooks of the Cotrel-Dubousset system (Sofamor-Danek, USA) and the Diapason system (Stryker, USA).

Circumferential grip offers connection between the components by friction effected by two halves of the pincer. An example is the old type DTT in the Cotrel-Dubousset system and the closed clamps in the Colorado system (Sofamor-Danek, USA).

The constrained bolt plate is the type of locking mechanism used in the VSP (Acromed, USA) and connection of the closed clamp with the anchoring components in the Colorado system (Sofamor-Danek, USA). It is very rigid and offers the strongest component-component connection available. However as it needs a perfect contact between the undersurface of the plate with the upper surface of the screw for optimal function constrained bolt plate connections directly between the anchoring member and the longitudinal member pose many problems in practice and are also falling out of favor. Newly developed implants employing this component-component interface usually use this mechanism to connect the anchoring member to a clamp that is again connected to the longitudinal member to facilitate the instrumentation procedure.

The semiconstrained screw plate is the type of connection employed in most of the screw plate systems. As the screws are not rigidly fixed to the plates, this connection allows toggling of the screws on the plate and is unable to achieve a true rigid fixation. Although bicortical fixation of the screws increases the rigidity of this kind of connection, obtaining a bicortical fixation from the posterior side of the spine is often difficult and dangerous. In posterior instrumentation, Roy-Camille plates and the cervical lateral mass plates use this component-component interface.

The semiconstrained component-rod is the type of connection that allows toggling of the anchoring member on the rod. A typical example is the Harrington distraction device. As they do not achieve a true rigid fixation and are prone to mechanical failure at the component-rod interface, they are also gradually fading away.

Transverse Members

The transverse member, commonly known as the cross link, is the component that transversely connects two or more longitudinal members of posterior implants to convert the construct into a quadrilateral frame. Its biomechanical function

is to enhance the torsion resistance and to resist parallelogram deformation of the construct [21, 22]. Transverse members do not increase mechanical resistance to other stresses (e.g., flexion-extension, lateral bending) [21, 22].

The optimal number of cross linking is at two sites, as adding more transverse connections does not significantly increase the torsion resistance.

Classification of Posterior Instrumentation

The posterior instrumentation maybe classified by the nature of the force imparted by the instrumentation on the spinal column. Though it is sometimes very difficult to define the principle acting force due to the complex three-dimensional nature of the spinal anatomy, the principle forces effected by the posterior instrumentation are distraction, compression, three-point bending, and translation. By the degree of freedom allowed by the instrumentation, they are further divided into rigid and dynamic types. The rigid type is the construct that does not allow motion between the instrumented spinal segments whereas the dynamic types allow some motion in the instrumented segments either by motion at the component-component interface or component-bone interface.

Posterior Distraction Instrumentation

This type of instrumentation exerts a distraction force on the spinal column and is biomechanically characterized by bearing of the axial load created by the weight of the body cranial to the proximal anchoring member by the implant when the patient is in an upright position. It comprises instrumentation applied under active distraction in the operating room and those fixed in so-called "neutral fixation" without any active compression or distraction. Neutral fixation has to be considered a distraction type of instrumentation since the implant has to maintain the length of the instrumented segment per se and has to bear the axial load when the patient assumes an upright position even though there has been no active distraction in its application.

Although many constructs may be used for posterior distraction instrumentation, simple distraction, fixed moment arm cantilever beam fixation, and applied moment arm cantilever beam fixation are the most common forms used for this purpose.

Simple Distraction Construct

This construct applies distraction in a short spinal segment and is typified by the Knodt rod. It is usually a hook-rod system. The characteristic of this type of instrumentation is that the fixation becomes stable only with active distraction by the implant. As distraction is applied posterior to the spinal instantaneous axis of rotation (IAR), the posterior column is lengthened, and a kyphosis is created. This instrumentation system is not employed frequently in present-day posterior instrumentation due to its biomechanical and biological disadvantages of the inability to offer a reliable resistance to the flexion moment and engagement of spinal sagittal contour. However, it may be used in special situations which need correction of local lordotic deformity. When employing this instrumentation, the structural integrity of the anterior column is an absolute prerequisite as elongation of the posterior column in the face of an anterior column incompetence would result in serious exaggeration of kyphosis and ultimate failure of instrumentation.

When simple distraction is applied to a segment longer than four or five spinal segments, the resulting kyphosis from elongation of the posterior column creates abutment of the longitudinal members on the apex of the kyphosis and exerts a three-point bending force.

Fixed Moment Arm Cantilever Beam Fixation Construct

A fixed moment arm cantilever beam construct exerts a distraction force on the spinal column and bears the axial load when applied in an active

distraction or in a neutral fixation. However, as active distraction of the spinal column is more effective with the applied moment arm cantilever beam fixation, it is usually used in neutral fixation mode.

As the bending moment is resisted by the fixed moment arm which projects into the vertebral body in front of the IAR, it offers greater resistance to flexion moment even with a shorter-length construct and is much less prone to failure than the simple distraction construct. Constrained screw-plate and most of the pedicle screw-rod systems are typical examples of this type of instrumentation.

As the axial load is borne on the cantilever beam, mechanical failure occurs at the junction of the beam and the longitudinal members [23]. To reduce mechanical failure, adequate reconstruction of the anterior load-bearing ability to share the axial load is advisable.

Contrary to the simple distraction instrumentation that creates a local kyphosis and causes anterior rotatory displacement when applied in a short segment, distraction by the fixed moment arm cantilever results in simple elongation of the segments under distraction along the longitudinal member. This is because of the short effective distance between the point of force application and the component-component interface which acts as the fulcrum and the inherent buttressing effect of the instrumentation reducing resistance to the bending moment.

Applied Moment Arm Cantilever Beam Fixation Construct

The applied moment arm cantilever beam fixation is a variation of the fixed moment arm cantilever beam system and differs only in the sense that an effective torque may be generated posterior to the IAR to offer a flexion or an extension moment to the subject spinal segments. Effective flexion or extension moment is applied by increasing the distance between the point of application of the desired force and the fulcrum located on the longitudinal member and by adopting a component-component locking system which allows connection of the anchoring member and the longitudinal member at various positions. When the components are rigidly locked in the desired position, the construct assumes the biomechanical characteristics of a fixed moment arm cantilever beam construct. The AO internal fixator (AO, Swiss) and the Socon system (Aesculap, Germany) are typical examples of this type of instrumentation.

Posterior Compression Instrumentation

This type of instrumentation exerts a compression force on the posterior spinal column and acts as a tension band resisting the flexion moment generated by application of an axial load. As its primary function is compression, the implant per se is biomechanically unstable in compression and ineffective in bearing the axial load. So, for the posterior compression system to function adequately, a structure that effectively resists the axial compression force is absolutely necessary [24].

In posterior spinal surgery, the posterior compression system is applied when the anterior weight-bearing column is intact or reconstructed to provide effective load bearing. As application of the compression results in close abutment of weight-bearing structures, the axial load is borne mainly by these structures and little is conveyed to the implant. This a lows posterior compression implants to be of smaller bulk than the distraction devices. Posterior compression instrumentation may be applied by a variety of constructs. The most common forms are simple compression fixation fluxed moment arm cantilever beam fixation and non-fixed moment arm cantilever beam fixation.

Simple Posterior Compression Construct

Typical examples of this type of construct are the Harrington compression system and the Halifax system. As they apply compression force

posterior to the IAR, lordosis is created within the instrumented segment. When the structural integrity of the anterior weight-bearing structure is compromised active application of posterior compression may result in exaggerated lordosis and excessive shortening of the vertebral column until competent anterior structures abut to offer effective resistance to the compression.

As simple compression instrumentation offers little resistance to translational deformation its present use is practically limited to the cervical spine where the orientation of the facets effectively blocks the anterior translation deformation.

Fixed Moment Arm Cantilever Beam Construct

A fixed moment arm cantilever beam fixation may be used as a posterior compression system by an active application of compression over the instrumented segments. As the compression brings the weight-bearing anterior structures to abut tightly there will be little axial load conveyed to the implants and the implants will function biomechanically just as a tension band.

Using the fixed moment arm cantilever beam fixation for posterior compression instrumentation offers an advantage over the simple posterior compression construct in that it offers a substantial resistance to the translational deformation and has the ability to resist over-compressive axial load, reducing the risk of mechanical failure.

Non-fixed Moment Arm Cantilever Beam Construct

Though this system does not offer a rigid fixation, it may be used to impart stability to the spinal column as a tension band when axial load-bearing structures are competent. Bio-mechanically, it offers no advantage over the fixed moment arm cantilever beam construct and is fading away. The only advantage of the system is that the bulk of the implant is significantly less than the fixed moment arm type as it does not a need special component-component interface. Its clinical use is primarily in the cervical spine as lateral mass plates.

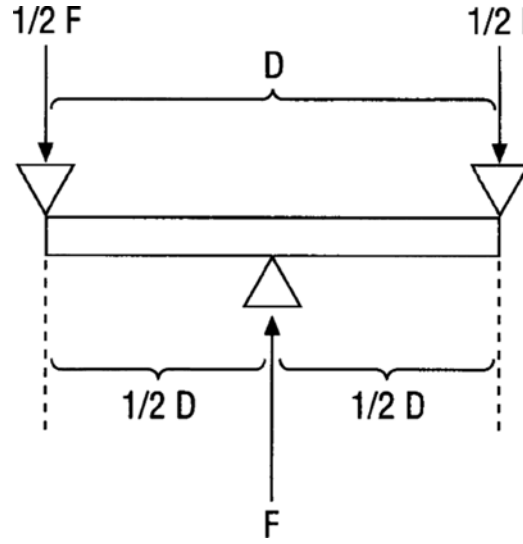

Fig. 35.8 If a three-point bending construct is symmetrically placed, the sum of the two terminal forces is of equal magnitude to the force acting on the fulcrum but in opposite directions

Posterior Three-Point Bending Instrumentation

The three-point bending force is one of the most commonly employed forces in posterior spine instrumentation. It is the principle force in many situations where translational deformity is reduced. Application of a three-point bending force needs two points onto which forces in same direction are applied, with a fulcrum between the two points. When the construct is stable, the force acting at the fulcrum will be in the opposite direction to the two terminal forces with a magnitude equal to the sum of two terminal forces (Fig. 35.8). Three-point bending may be applied by various posterior spinal constructs.

Posterior Distraction Construct

The simple posterior distraction construct may be used to effect a three-point bending force on the spinal column. This is attributed to their ability to generate torque posterior to the IAR and create a kyphosis, which will gradually come into contact with the longitudinal member to act as a fulcrum. However, for the simple distraction construct to

effect a three-point bending force, a considerable length of instrumentation is necessary and when used in –the lumbar spine, due to the length of the spinal segment subject to distraction, a flat back deformity results. Addition of reduction sleeves in the mid-portion of the longitudinal member may hasten the contact of kyphosis to the longitudinal member and also effectively restores lordosis. The use of a simple distraction construct for the attainment of three-point bending force is decreasing due to the necessity of a lengthy instrumentation sacrificing the motion segments.

Cantilever Beam Constructs

As forms of cantilever beam construct may be applied to generate a three-point bending force on the spinal column. This is attributed to their ability to create a posterior-directed pull up force on the displaced vertebra by means of screws. They have the advantages over the simple distraction constructs when used in this mode of application as they do not need a lengthy instrumentation and do not cause flattening of the lordosis [25]. Some instrument systems offer specially modified implants to facilitate application of three-point bending force (Fig. 35.9).

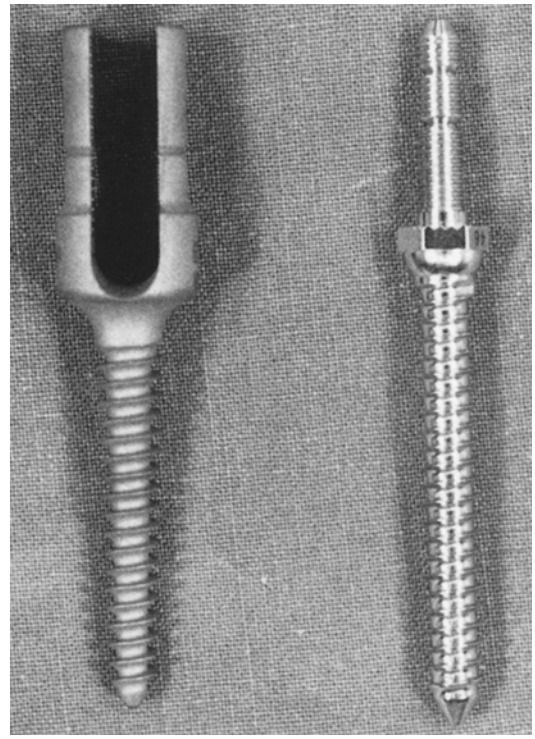

Fig. 35.9 Screws with modification to facilitate application of three-point bending force. Extended arms make force application more effective

Posterior Translation Instrumentation

This type of instrumentation effects translation of the vertebra as the primary force of action and is used mainly for correction of spinal deformities. There are two modes of applying translation to the vertebral column by these instruments. The first is the translation of the vertebra by bringing the anchoring members to the longitudinal members and is called the vertebra-to-rod method [20]. The second is by changing the shape or alignment of the longitudinal member to which the anchoring members have been already attached and may be called the longitudinal member maneuvering method. The rod decoration maneuver and in situ rod bending [26, 27] are principle longitudinal member maneuvering methods. Recent investigations suggest possible future employment of shape memory alloys for the latter purpose [28]. There are two construct forms in this category.

Dynamic Translation Construct

This is typified by the Luque segmental sublaminar wiring and is applied in a vertebra-to-rod method. As there is no rigid fixation between the anchoring member and the longitudinal member, some movement will occur between the instrumented spinal segments. Though this is a disadvantage that leads to loss of correction by settling of the spinal column under gravity, it may be exploited in the maintenance of deformity correction in young children as the sliding of the wires on the rods will allow growth of the spinal column.

Rigid Translation Construct

Most of the implants used for spinal deformity fall into this category. As they offer a rigid component-component interface, they, in theory, do not allow intersegmental motion and result in better maintenance of the deformity correction.

The effectiveness of the rigid translation construct is greatly influenced by the position and the fixation strength of the anchoring members and the relative stiffness between the longitudinal member and the spine deformity. To increase the correction of the deformity, employment of segmental anchors, preferably screws and a stiff rod [6] is advantageous. When the deformity is rigid, increasing the flexibility of the deformity by an adequate releasing procedure is helpful in attaining a better correction. They may be applied in the vertebra to rod method or the longitudinal member maneuvering method.

Clinical Applications

In practice, the forces applied by the posterior spinal instrumentation is much more complex than those described in the preceding sections due to the three-dimensional nature of the anatomy and coupling actions which inevitably accompany application of forces on a three-dimensional structure. The presence of a multiple number of movable joints acting as hinges and the difference in the mechanical characters between the structures comprising the vertebral column further complicates clear delineation of the forces acting on the instrumented spinal column. This mandates careful preoperative consideration and meticulous planning for every case under consideration for spinal instrumentation.

Fractures and Dislocations

In stabilization of traumatic instabilities of the spine, the degree of structural compromise in the injured vertebral column and the experience of the treating surgeon are the main factors that determine the choice of instrumentation method. When a decision is made to apply a posterior instrumentation for stabilization, the following should be taken into consideration.

Degree of Anterior Column Destruction

When there is severe anterior column destruction, the spinal column is devoid of axial load-bearing ability Though a posterior rigid distraction instrumentation may be performed, it is not sound biomechanically as the axial load is borne solely by the instrument and often results in mechanical failure of the implant or the bone-implant interface [23]. To resist the bending moment at the fracture site effectively, the instrumentation has to be of considerable length, sacrificing multiple non injured motion segments. In this situation, adequate reconstruction of the anterior column and application of posterior compression instrumentation with a fixed moment arm cantilever beam construct is preferable (Fig. 35.10).

When anterior column destruction is mild or moderate, healing of the fracture effectively restores the axial load-bearing ability of the spinal column. The role of instrumentation here is to prevent further deformation of the spinal column and protect the injured vertebra until healing occurs. In this situation, rigid distraction instrumentation by the fixed moment arm cantilever beam construct or applied moment arm cantilever beam construct is indicated (Fig. 35.11).

When the bony structures of the anterior column are relatively intact as in seatbelt type injury the disks may be brought together to reestablish a competent weight-bearing column using posterior compression instrumentation [29, 30]. In the cervical spine, spinous process wiring or the Halifax clamp may be used. In the thoracic and lumbar spine, posterior compression instrumentation with a type of cantilever beam construct is preferable (Fig. 35.12).

Translational Deformity

In the presence of a translational deformity, posterior instrumentation is better than anterior instrumentation as reduction of the facet dislocation is much easier from the posterior side. When

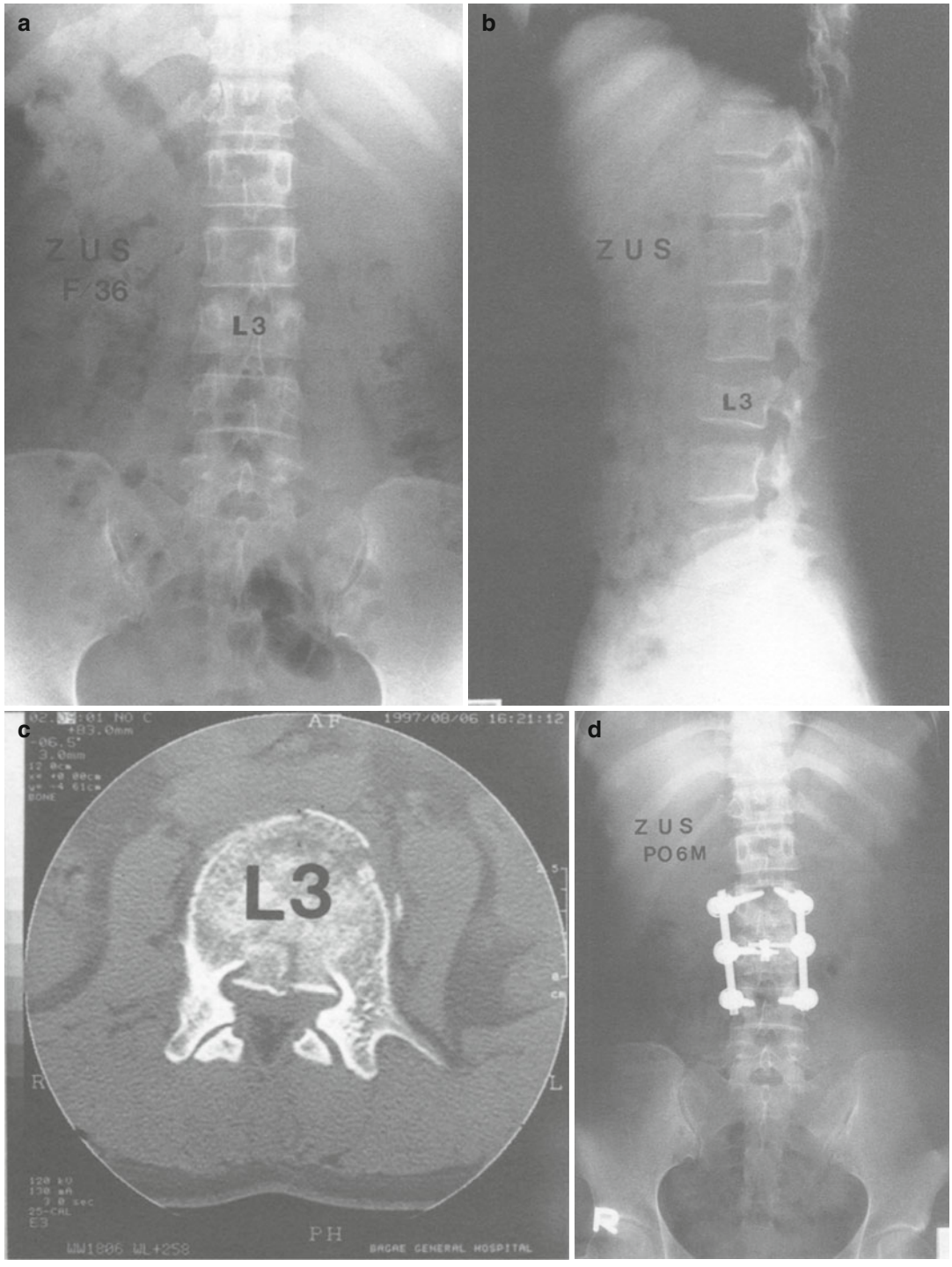

Fig. 35.10 (**a, b**) A 36-year-old female with L3 unstable burst fracture. (**c**) Preoperative CT shows 50 % canal encroachment with severe destruc-tion of vertebral body. (**d, e**) Treatment consisted of posterior fixed moment arm cantilever fixation. The anterior column was reconstructed with strut bone graft

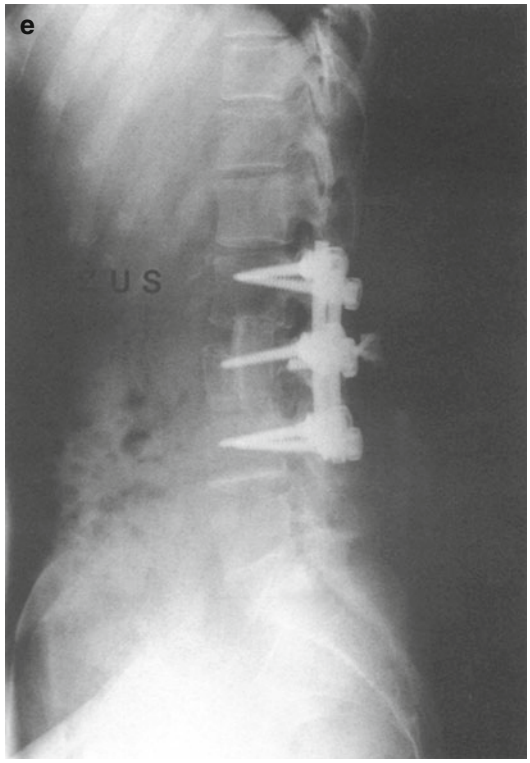

Fig. 35.10 (continued)

translation is significant, three-point bending instrumentation or rigid translation instrumentation is indicated. This is preferably done with a fixed moment arm cantilever or applied moment arm cantilever beam construct. When there is severe destruction of the anterior column reconstruction of the anterior column after the reduction of translation is indicated (Fig. 35.13).

Degenerative Diseases

As most degenerative instabilities have competent anterior weight-bearing columns, posterior compression instrumentation will do the job. For this purpose a fixed moment arm cantilever beam construct is most suitable. When discectomy is performed simultaneously, posterior compression instrumentation with restoration of the anterior column by anterior or posterior interbody fusion is preferable (Fig. 35.14).

Deformities

The ideal instrumentation depends on the type, location, and severity of the deformity.

Scoliosis

Historically, correction of scoliosis by posterior instrumentation started in the early 1960s with the Harrington device, a type of rigid posterior distraction instrumentation [4]. Although a fair amount of correction could be obtained in the coronal plane from elongation of the concave side and associated media translation of the apex, numerous drawbacks pertinent to the biomechanical characteristics of simple distraction instrumentation were observed including lack of rigidity of fixation necessitating prolonged postoperative external immobilization, high frequency of proximal hook dislodging, mechanical failure at the rackets, and derangement of spinal sagittal contour resulting in loss of normal thoracic kyphosis or flat back syndrome.

Then came the Luque segmental spinal instrumentation in the early 1980s, a type of dynamic translation instrument [5]. This corrected scoliosis employing the vertebra-to-rod method, pulling the vertebra up to the contoured rod by means of wires with a gripping-type anchor holding the lamina. This system solved many of the problems posed by the simple distraction instrumentation. The fixation of the vertebra was more rigid, precluding the necessity of prolonged external immobilization, the derangement of the sagittal contour was much less due to absence of the distraction effect of the instrumentation, and mechanical failures were much less frequent. However, there were also drawbacks pertinent to the biomechanical characteristics of the instrumentation and the anchoring member. As the fixation was dynamic, the vertebral column settling under gravity could not be effectively resisted. The necessity of intruding the canal to pass the sublaminar wires was also a significant problem, increasing the risk of neurologic injury.

Then, in 1983, shortly after popularization of the Luque instrumentation, came the Cotrel-Dubousset system, a rigid translation instrument with multiple anchors that became the prototype for numerous other similar instrumentation systems [3]. It corrected scoliosis deformity by translocation of the curve from the coronal plane to the sagittal plane by a rod derotation maneuver, a form of longitudinal member maneuvering method. After the derotation, the system became a combined simple distraction-simple compression instrument

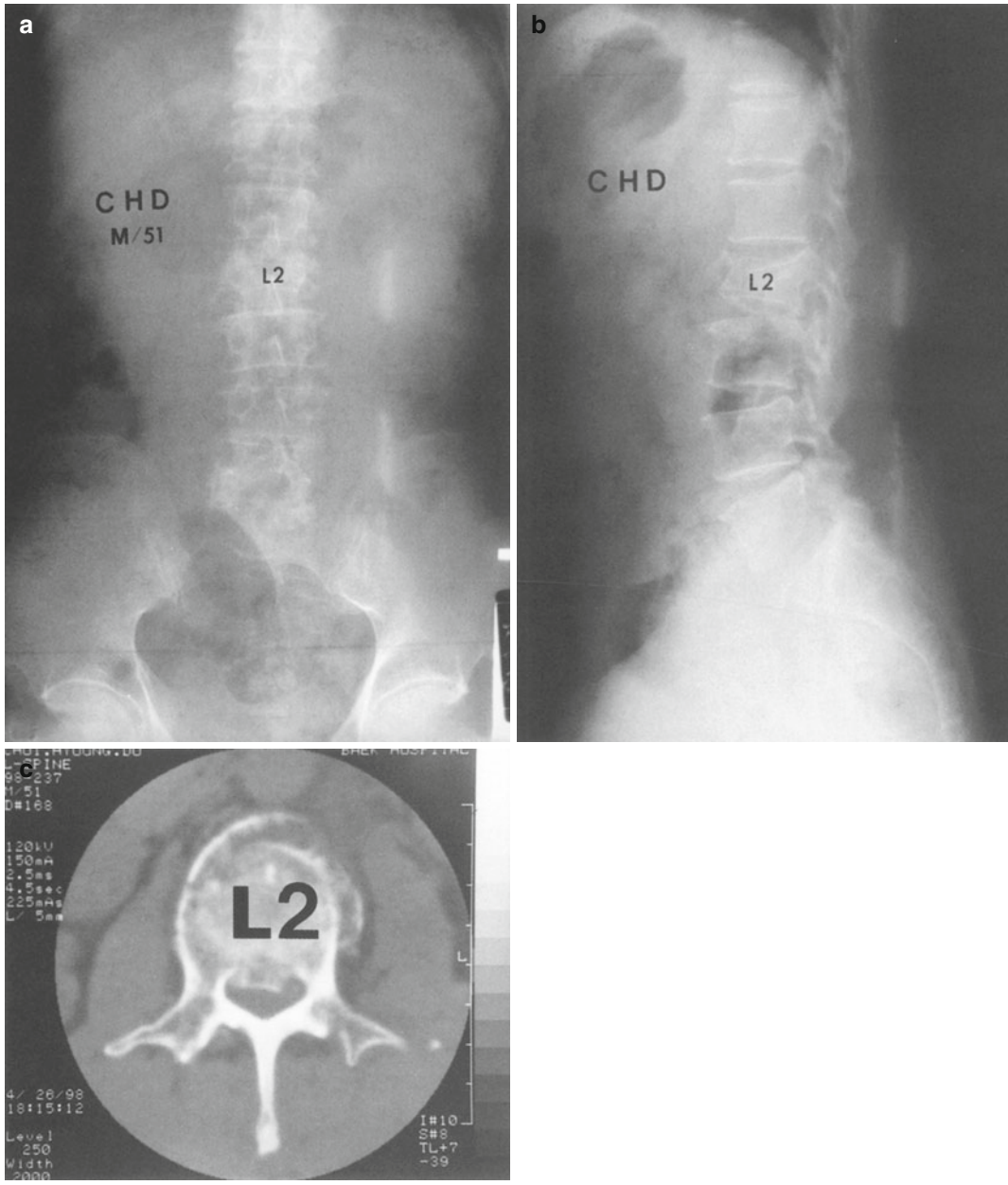

Fig. 35.11 (**a**, **b**) A 51-year-old male with L2 unstable burst fracture. (**c**) Preoperative CT shows 40 % canal encroachment. (**d**, **e**) He was treated by posterior fixed moment arm cantilever fixation

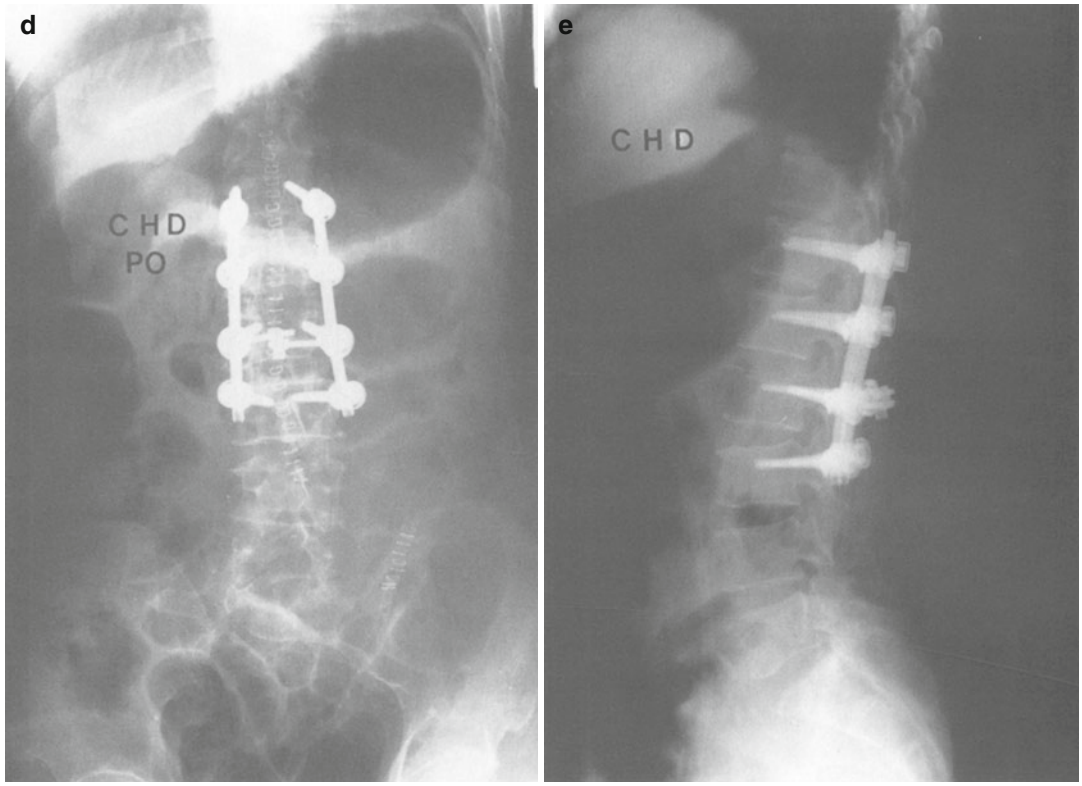

Fig. 35.11 (continued)

by the nature of the anchoring members, generating forces behind the IAR. By their biomechanical characteristics application of compression produced lordosis. However, application of distraction did not restore as much thoracic kyphosis as desired due to generation of a three-point bending force acting on the apex of developing kyphosis. Inadequate restoration of kyphosis in turn produced very little rotational correction in the horizontal plane. Despite these drawbacks, the system offered a rigid fixation, improved coronal plane correction, and true three-dimensional correction of the scoliosis deformity (Fig. 35.15).

In 1992, a major breakthrough in rigid translation instrument was developed by Suk, introducing the use of segmental pedicle screws as anchoring members for the system [6]. The use of penetrating anchors converted the system into a fixed moment arm cantilever beam construct after the decoration maneuver, solving many problems of simple compression-distraction instrumentation.

The increased holding power of the implant using segmental penetrating anchors enhanced the correction of coronal plane deformity and at same lime reduced failure at the bone-implant interface. Being converted into a fixed moment arm cantilever beam construct, it did not need any distraction to stabilize the anchoring members. It prevented generation of a ventral three-point bending force, at the same time permitting unconstrained spinal motion, allowing the spinal column to conform more easily to the rod contoured to the normal sagittal contour. In thoracic scoliosis, use of top open screws with a lock screw component-component interface also played a role in restoration of thoracic kyphosis, combining the vertebra-to-rod translation to the rod derotation. This restoration of kyphosis in turn improved rotational correction in the horizontal plane, thus truly improving the deformity three dimensionally (Fig. 35.16).

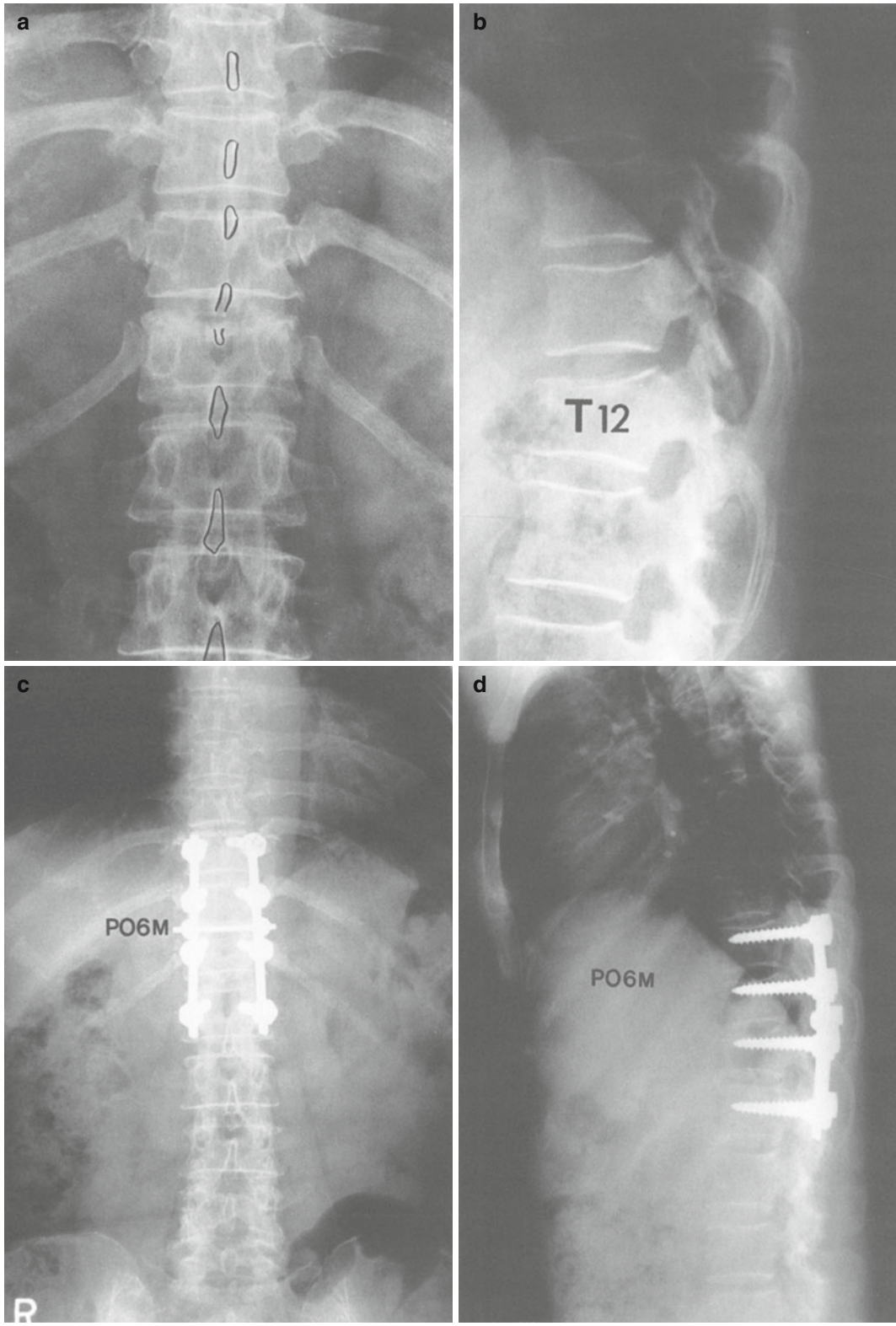

Fig. 35.12 (**a**, **b**) A 40-year-old female with T11 chance fracture. (**c**, **d**) She was treated by posterior compression instrumentation with pedicle screws

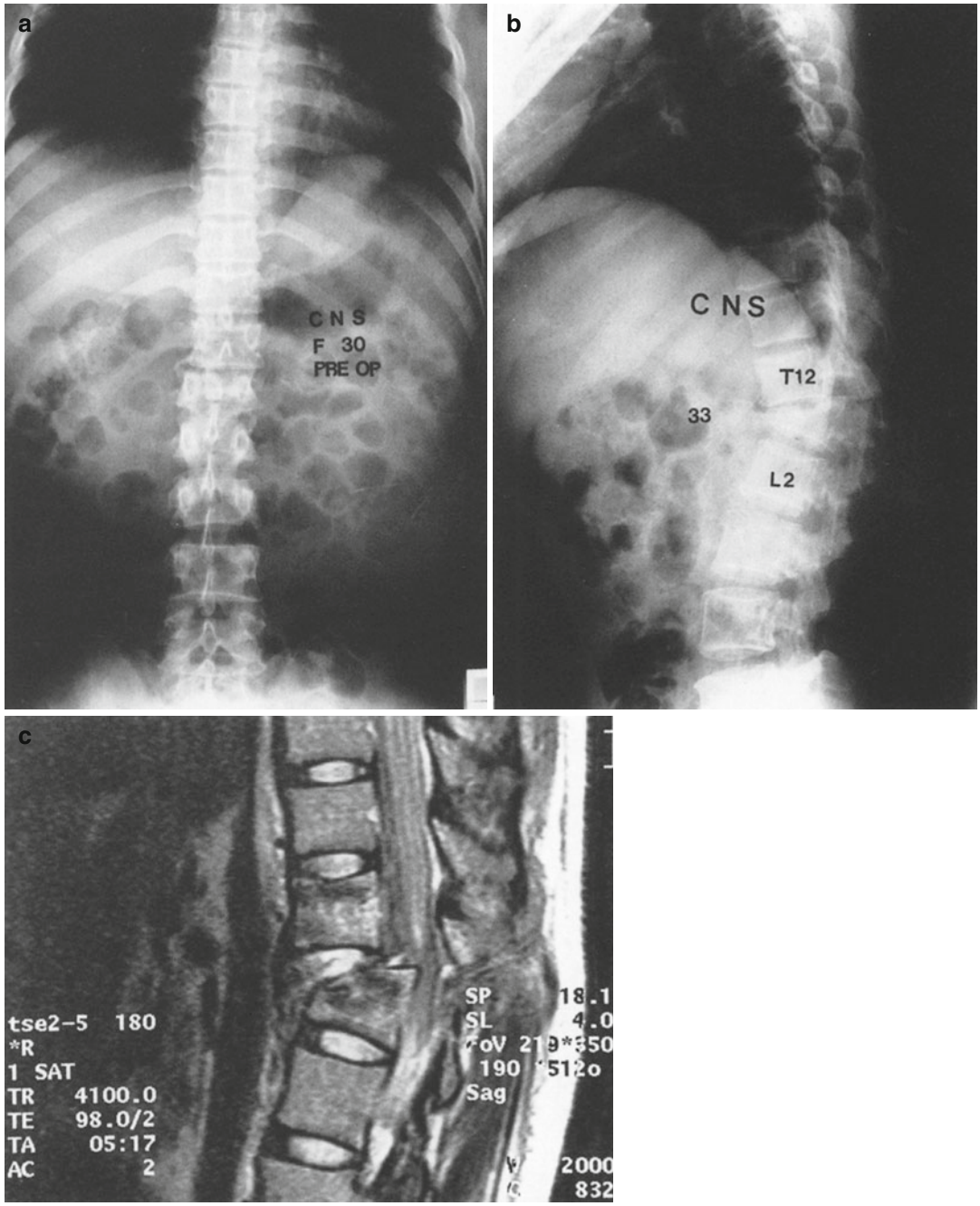

Fig. 35.13 (**a**, **b**) A 30-year-old female with T12 L1 fracture dislocation. C MRI shows gross displacement. (**d**, **e**) She was treated by posterior instru-mentation in neutral mode and then anterior column reconstruction

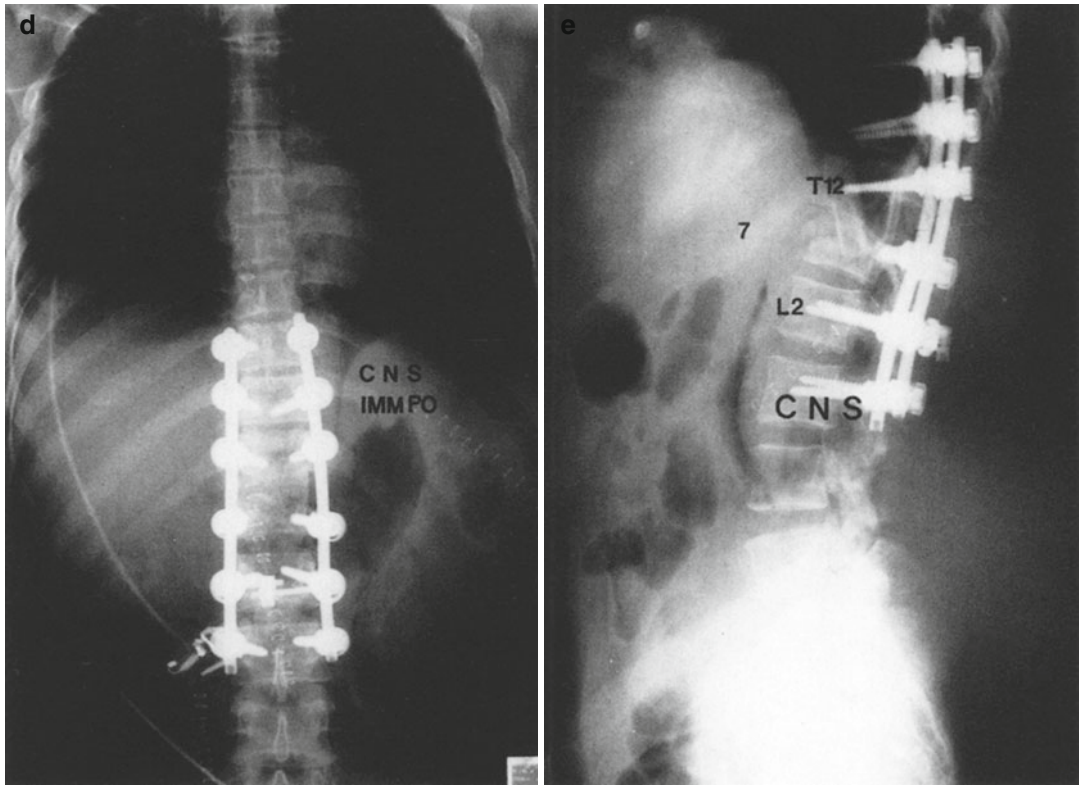

Fig. 35.13 (continued)

In posterior instrumentation for scoliosis, the risk of mechanical failure of the instrument is greatly affected by the flexibility of the deformity and the quality of bone to which the anchoring members are attached regardless of the types of instrumentation used. In rigid deformities, increasing the flexibility of the deformity by an adequate release or an osteotomy prior to posterior correction is advisable to reduce mechanical failures [31, 32]. Increasing the number of the anchoring members by segmental application disperses the stress put on each anchoring member and reduces the risk of failure at the bone component interface especially in the osteoporotic spine.

Kyphosis

The choice of instrumentation method for kyphosis is primarily governed by the flexibility of the deformity. In flexible kyphosis, three-point bending instrumentation offers a satisfactory correction. Although three-point bending forces for correction of kyphosis may be applied by several types of construct, the most commonly used is translation instrumentation. Translation instrumentation generates three-point bending on the apex of the kyphosis by exerting a posterior displacement force on the vertebra subject to translation (Fig. 35.17). In flexible deformity, both dynamic and rigid translation instrumentation may yield satisfactory results.

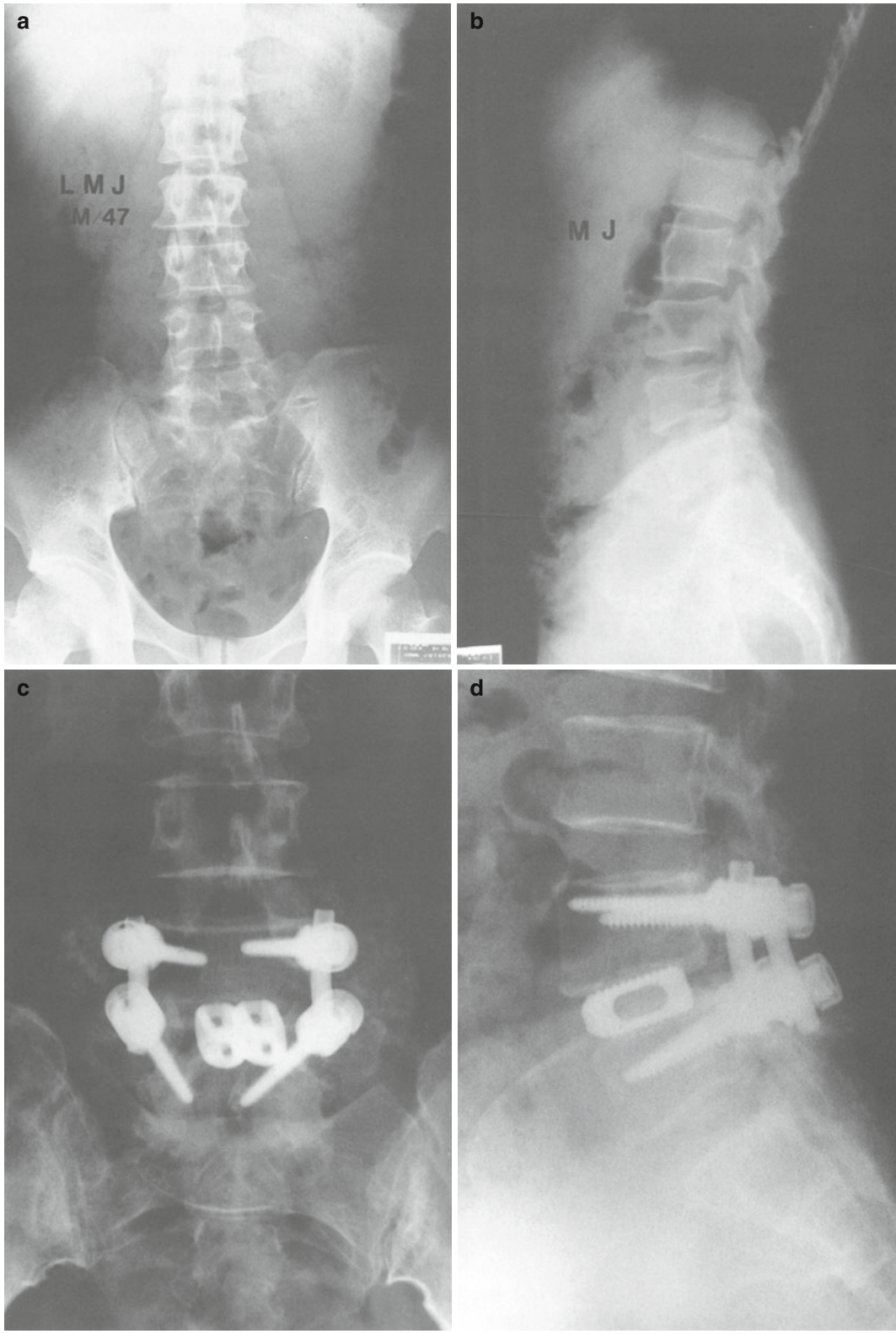

Fig. 35.14 (**a**, **b**) A 47-year-old male with l4-5 spinal stenosis. (**c**, **d**) He was treated by posterior decompression and posterior compression instru-mentation with anterior support

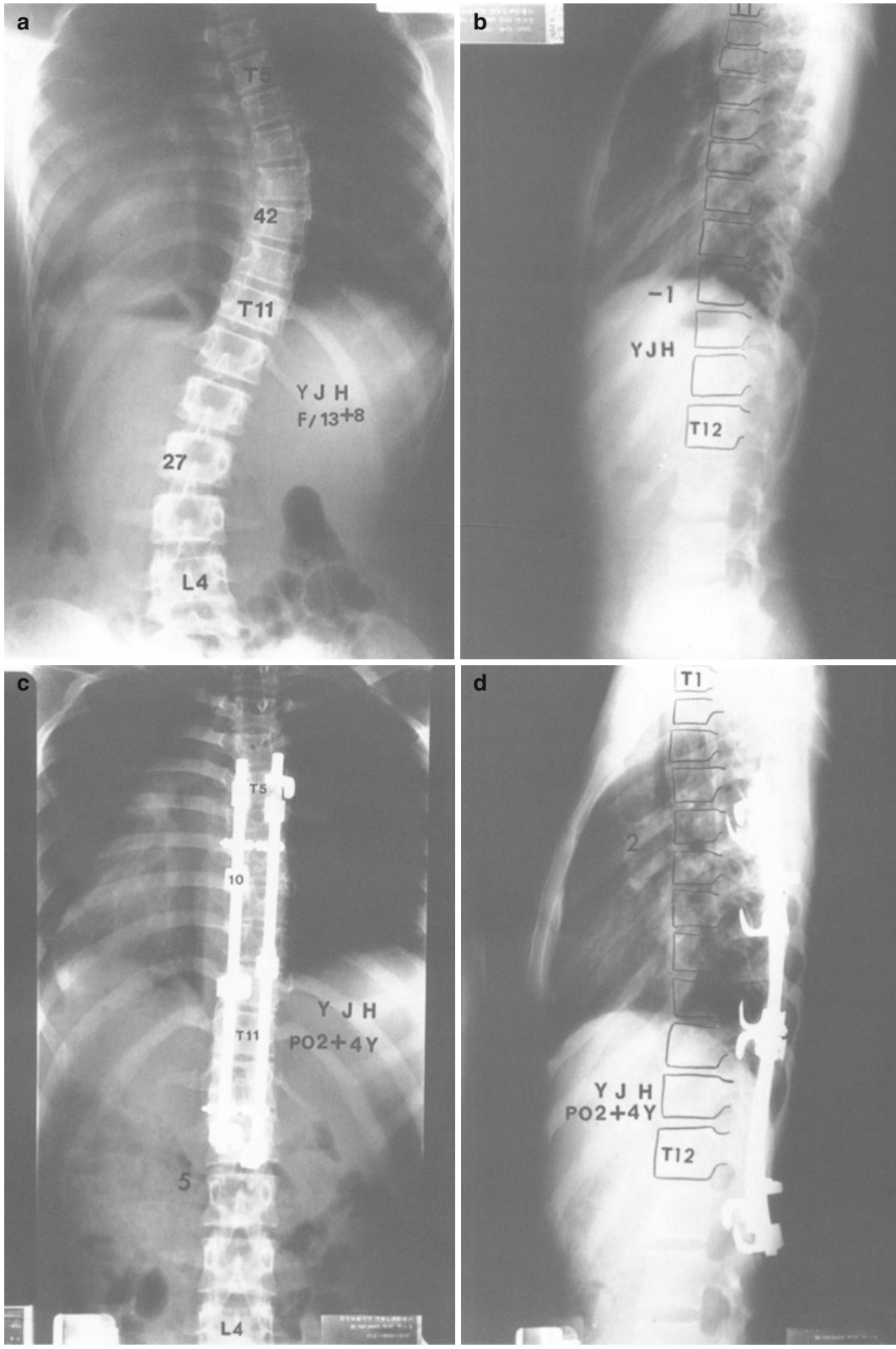

Fig. 35.15 (**a**,**b**) A 13.7-year-old female with adolescent idiopathic scoliosis. (**c**, **d**) She was treated by rigid translation instrumentation using mul-tiple hooks

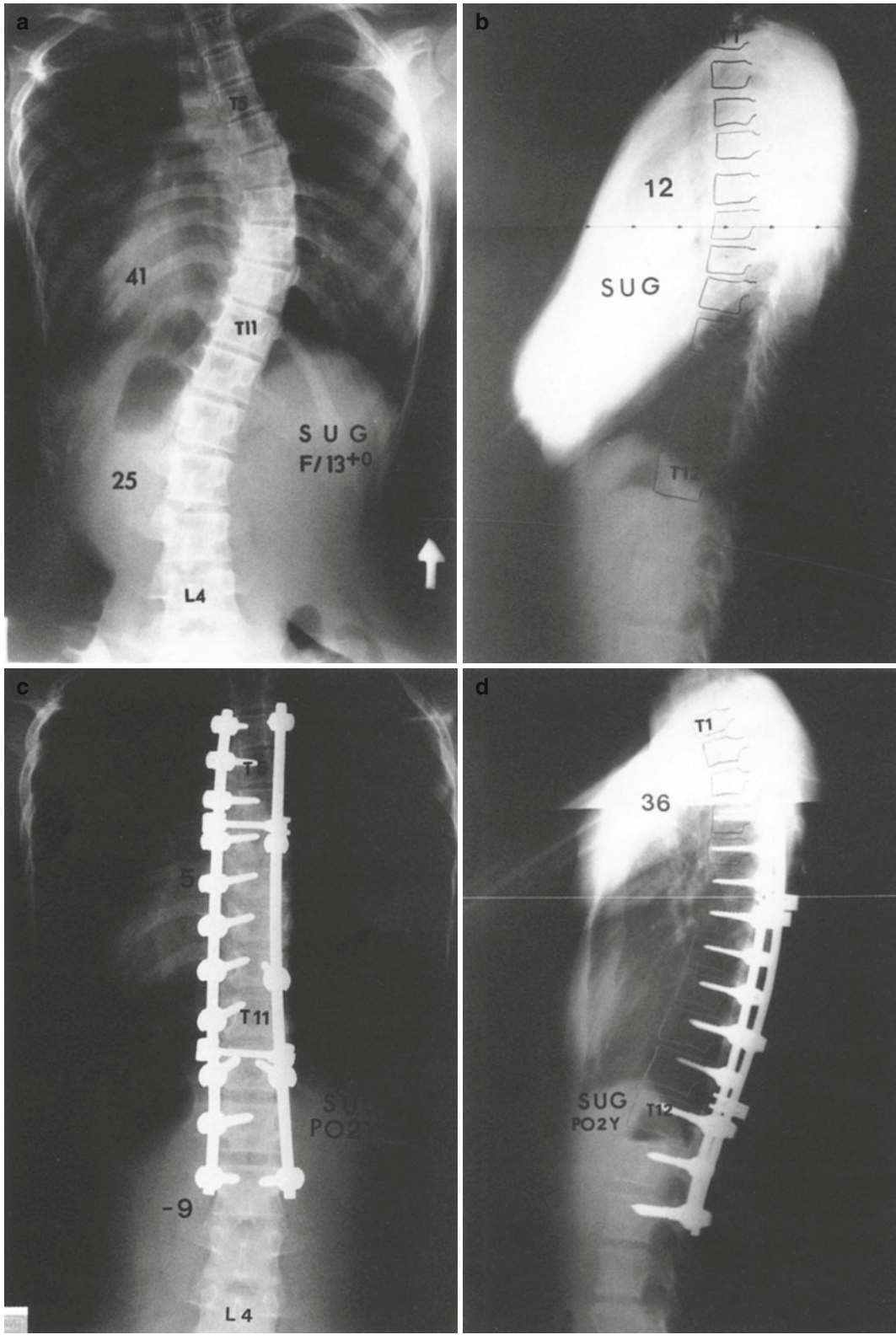

Fig. 35.16 (**a**, **b**) A 13-year-old female with adolescent idiopathic scoliosis. (**c**, **d**) She was treated by rigid translation instrumentation using segmental pedicle screws. Note the improvement of the sagittal contour

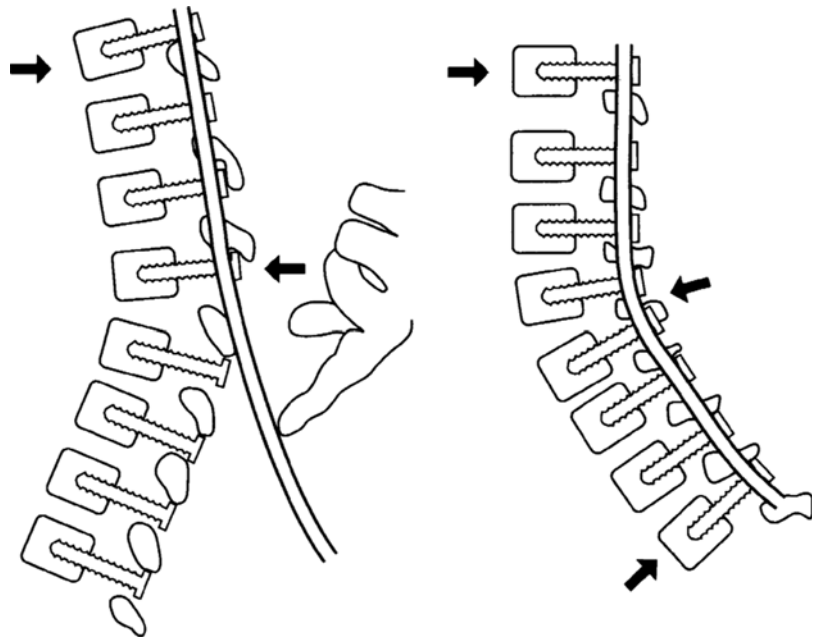

Fig. 35.17 Translation instrumentation in kyphosis. Translation instrumentation generates a three-point bending force on the apex of the kyphosis by exerting a posterior displacement force on the vertebra subject to translation

When the kyphosis is rigid, attempts at correction solely by the force of posterior instrumentation are always less than satisfactory due to mechanical failure at the bone-component interface. In this situation, an anterior release or an osteotomy to enhance the flexibility of the deformity is mandatory [31, 32]. Following the release osteotomy, dynamic or rigid translation instrumentation may be applied to yield satisfactory results (Fig. 35.18).

When the kyphosis is rigid and so severe as to call for a vertebral column resection, application of three-point bending forces with rigid translation instrumentation with a fixed moment arm cantilever beam construct is most suitable. Employing this type of construct allows compression over the resection site when an anterior structure support was reconstructed. When nonstructural cancellous chip graft was used to fill the resection gap, the construct, by resisting the axial load, protects the anterior column from collapsing (Fig. 35.19).

Spondylolisthesis

Reduction of spondylolisthesis may be achieved either by three-point bending or translation force. Though these two methods are very similar in look the force acting on the displaced vertebra is quite different. When the displaced segment is at the end of the instrumentation it becomes a terminal three-point bending construct the fulcrum being the segment just below. However when the displaced segment is intercalary the force for reduction becomes translation (Fig. 35.20). Both methods may be effectively carried out by a fixed moment arm cantilever beam construct. Some of the instruments offer screws of special design with elongated connectors for this purpose.

Tumors

The principle of reconstruction of the spinal column by posterior instrumentation in tumor surgery is similar to that for traumatic instabilities. When resection of the tumor results in significant compromise of the anterior column, reconstruction of the anterior column with posterior instrumentation is indicated. When the anterior column following resection is still quite competent of bearing axial loads, posterior compression instrumentation or neutral fixation with distraction instrumentation is sufficient (Fig. 35.21).

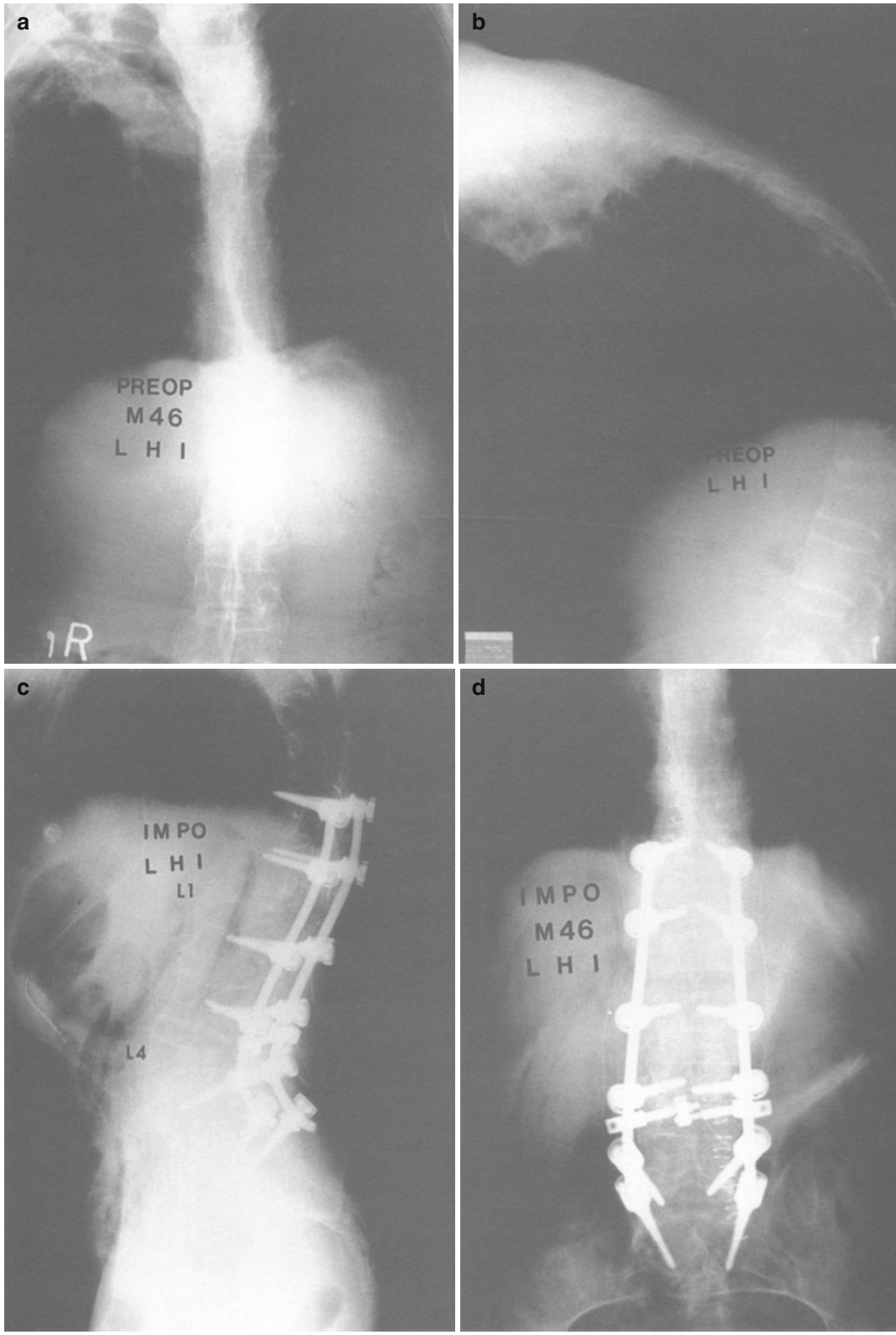

Fig. 35.18 (**a**, **b**) A 46-year-old male with ankylosing spondylitis.(**c**, **d**) He was treated by transpedicular decanceliization osteotomy of L 1 and L4 with posterior translation instrumentation

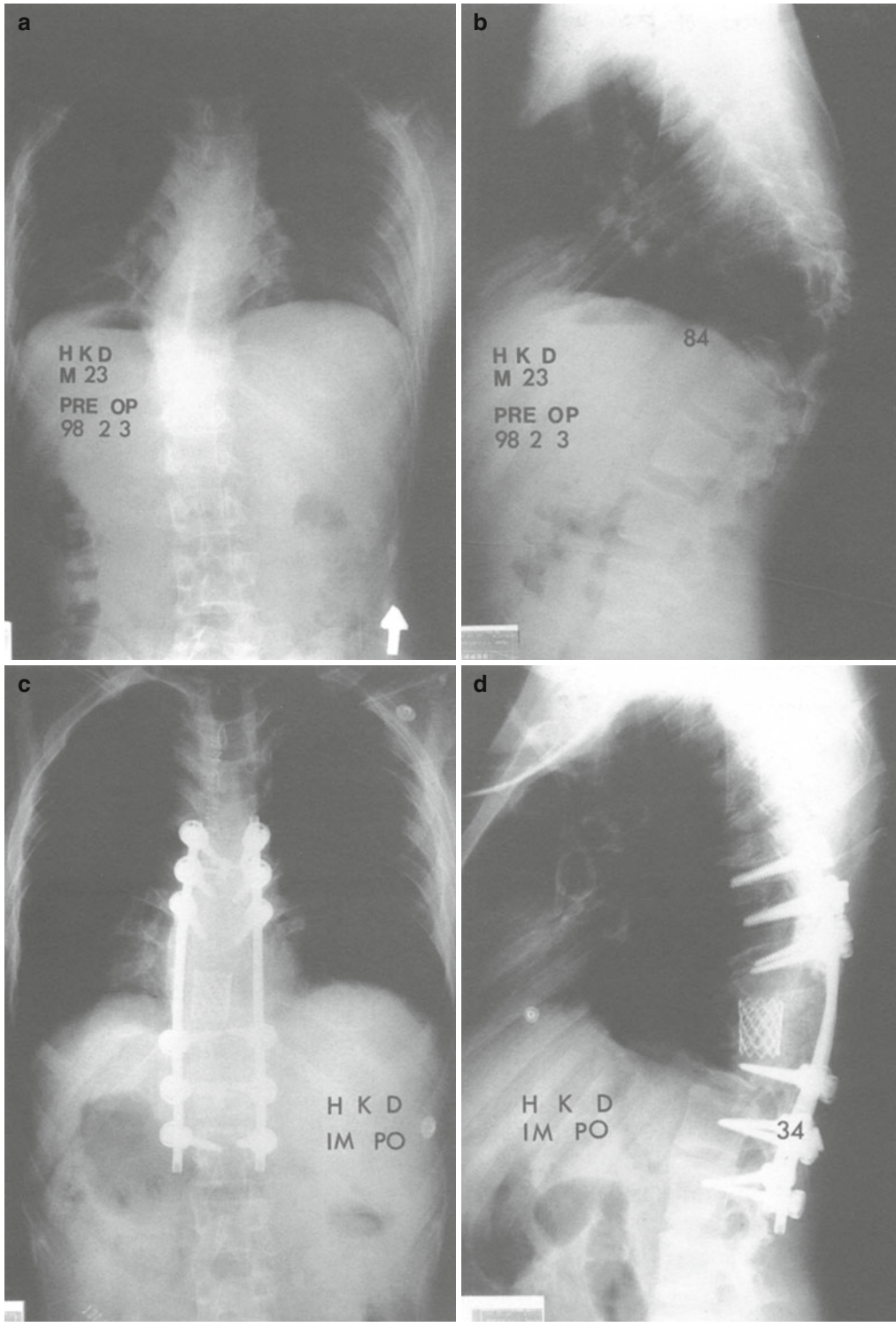

Fig. 35.19 (**a**, **b**) A 23-year-old male with congenital kyphosis. (**c**, **d**) He was treated by posterior vertebral column resection ofTl 0 and T11 with anterior column reconstruction using titanium mesh and posterior pedicle screw fixation. The posterior instrumentation functions as a translation instrumentation in the first stage of operation, but becomes a fixed moment arm cantilever beam fixation in compressive mode on insertion of ante-rior strut graft and posterior compression

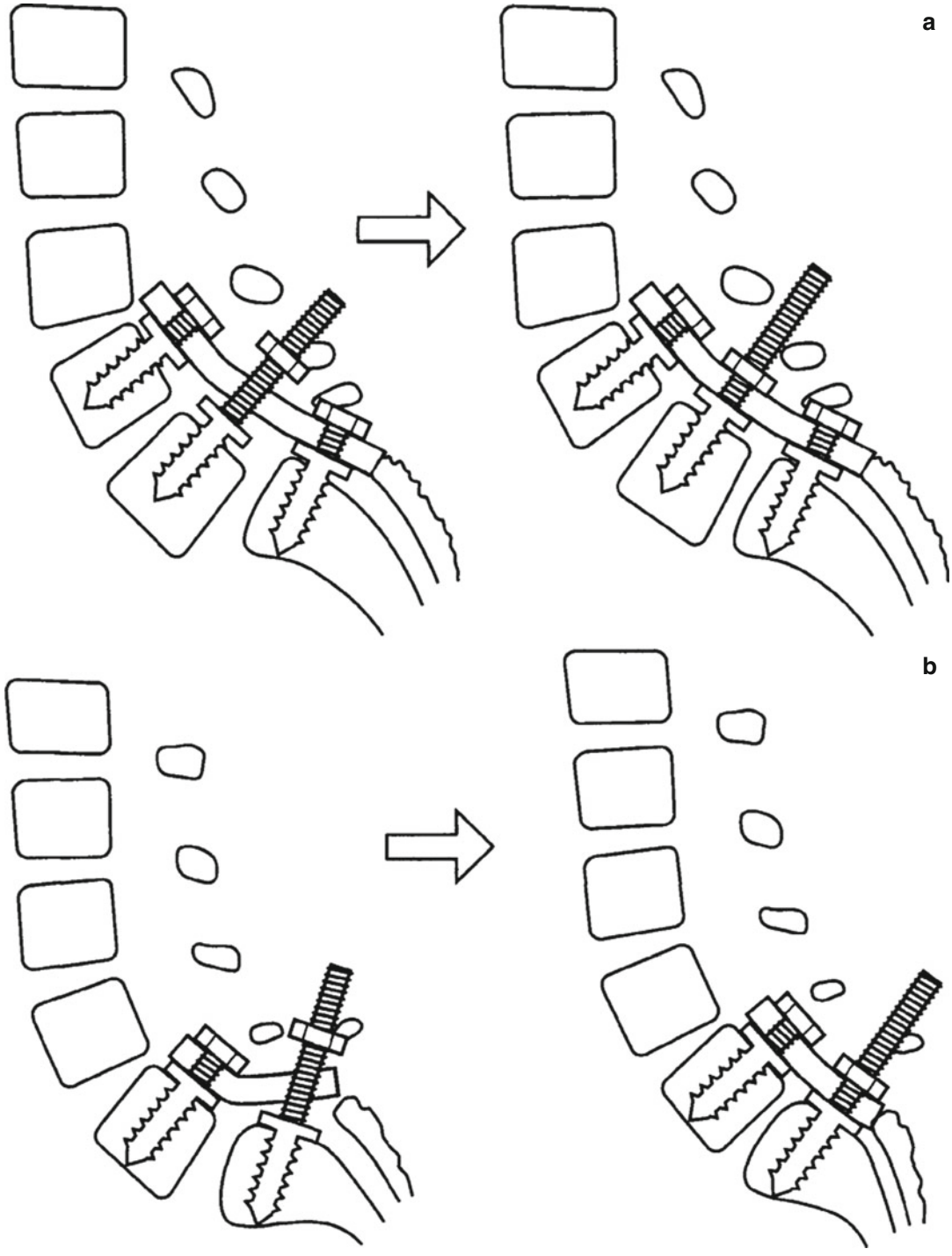

Fig. 35.20 (**a**) In spondylolisthesis, if the displaced segment is intercalary, the construct is a posterior translation construct. (**b**) In spondylolisthe-sis, if the displaced segment is at the end of the instrumentation, the construct is a terminal three-point bending construct and the fulcrum is the segment just below

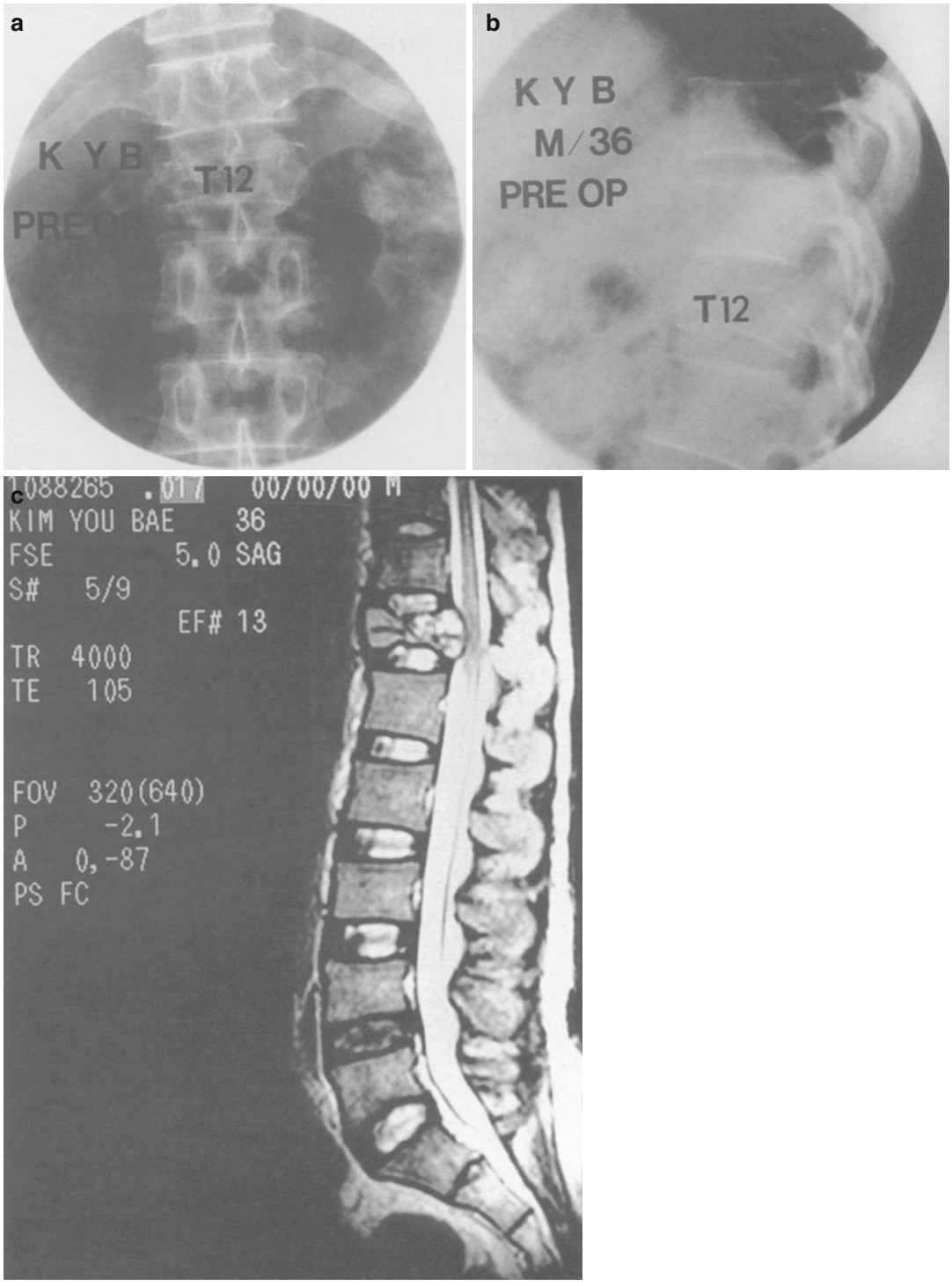

Fig. 35.21 (**a**, **b**) A 36-year-old male with hypernephroma and T12 metastasis. (**c**, **d**) Preoperative MRI. The sagittal and axial images show destruction of vertebral body and cord compression by tumor mass. (**d**, **e**) He was treated by total resection of the vertebral body with reconstruction of the anterior column using titanium mesh and posterior pedicle screw fixation. The posterior fixed moment arm cantilever instrumentation was applied in compressive mode over the anterior structural graft

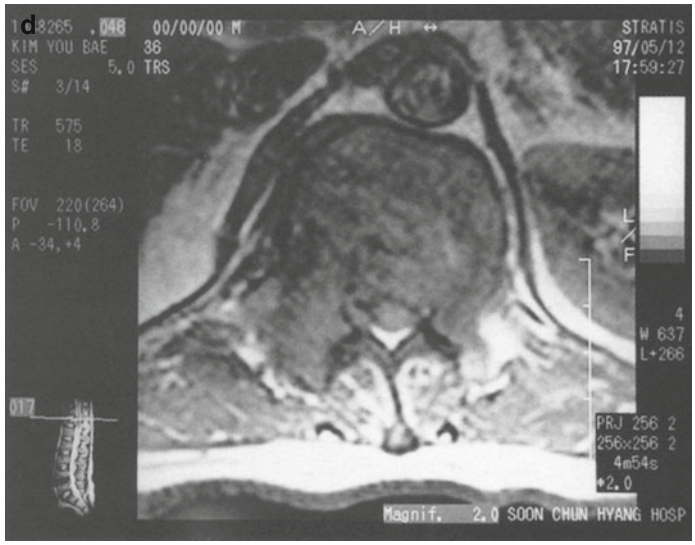

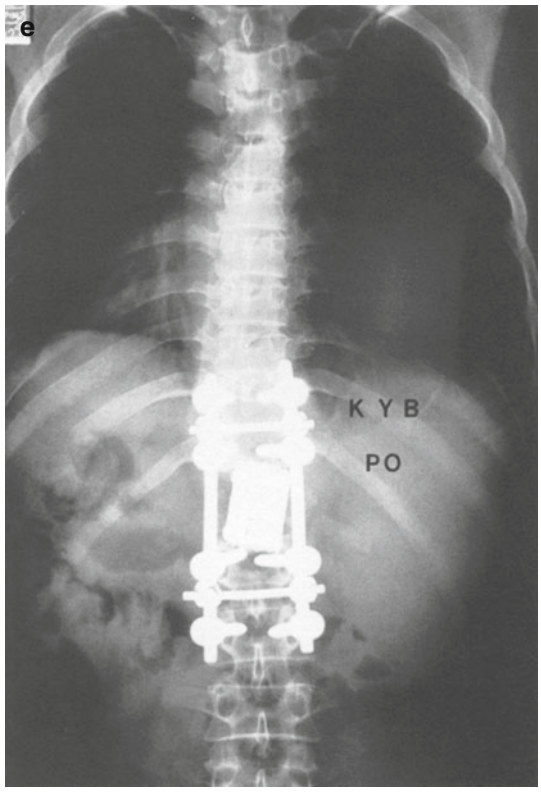

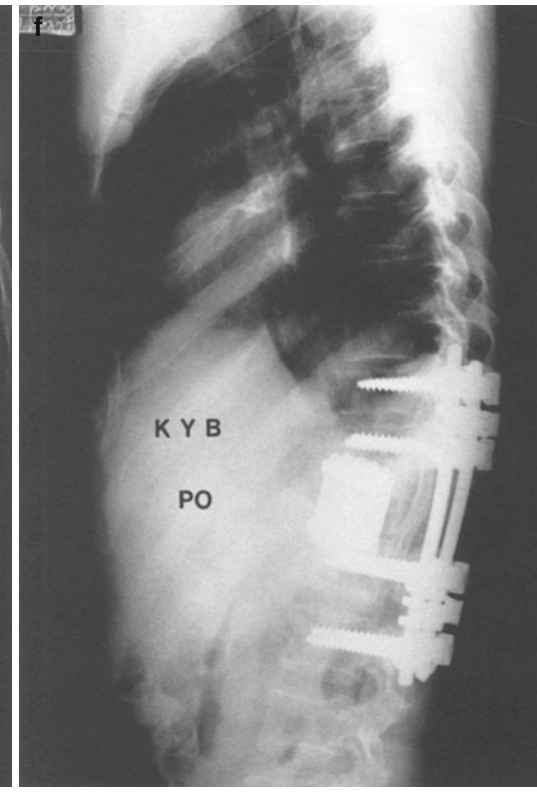

Fig. 35.21 (continued)

References

1. Abumi K, Panjabi MM, Duranceau J. Biomechanical evaluation of spinal fixation devices. Part III Stability provided by six spinal fixation devices and interbody bone graft. Spine. 1989;14:1249.
2. Ashman RB, Galpin RD, Corin JD, Johnston 2nd CE. Bio-mechanical analysis of pedicle screw instrumentation systems in a corpectomy model. Spine. 1989;14:l398.
3. Cotrel Y, Dubousset J, Guillaumat M. New universal instrumentation in spinal surgery. Clin Orthop. 1988;227:10.
4. Harrington PR. Treatment of scoliosis: correction and internal fixation by spine instrumentation. J Bone Joint Surg. 1962;44-A:591.
5. Luque ER. The anatomic basis and development of seg-mental spinal instrumentation. Spine. 1982;7:256.
6. Suk SI, Lee CK, Kim WJ, Chung YJ, Park YB. Segmental pedicle serew fixation in the treatment of thoracic idio-pathic scoliosis. Spine. 1995;20:l399.
7. Lenke LG. Posterior and posterolateral approaches to the spine. In: Bridwell KH, Dewald RL, editors. The textbook of spinal surgery. 2nd ed. Philadelphia: Lippincott-Raven; 1997. p. 193.
8. Benzel EC. Biomechanics of spine stabilization. New York: McGraw-Hill; 1995.
9. Rudisch A, Kremser C, Peer S, Kathrein A, Judmaier W, Daniaux H. Metallic artifacts in magnetic resonance imaging of patients with spinal fusion. A comparison of implant materials and imaging sequences. Spine. 1998;23:692.
10. Garfin SR. Spinal fusion: the use of bone screws in the vertebral pedicles. Summation. Spine. 1994;19: 2300S.
11. Zuk SI, Kim WJ, Lee SM, Kim JH, Chung ER. Thoracic pedicle screw fixation in spinal deformities: are they really safe? Spine. 2001;26:2049.
12. Nazarian SM, Louis RP. Posterior internal fixation with screw plates in traumatic lesions of the cervical spine. Spine. 1991;16:S64.
13. Licht NJ, Rowe DE, Ross LM. Pitfalls of pedicle screw fix-ation in the sacrum. A cadaver model. Spine. 1992;17:892.
14. Lonstein JE. The Galveston technique using Luque or Cotrel-Dubousset rods. Orthop Clin North Am. 1994;25:311.
15. Suk SI, Lee CK, Min HJ, Cho KH, Oh JH. Comparison of Cotrel-Dubousset pedicle screws and hooks in the treatment of idiopathic scoliosis. Int Orthop. 1994;18:341.
16. Skinner R, Maybee J, Transfeldt E, Venter R, Chalmers W. Experimental pull-out testing and comparison of variables in transpedicular screw fixation. A biome-chanical study. Spine. 1990;15:195.
17. Suk SI, Cha SI, Lee Ck, Kim WJ. A study on the pull-out strength of pedicle screws in relation to the size of drill 491 holes and inserted screws. Presented at the 30th annual meeting of the Scoliosis Research Society, Asheville, 13–16 Sept 1995.
18. Kwok AW, Finkelstein JA, Woodside T, Hearn TC, Hu RW. Insertional torque and pull-out strengths of conical and cylindrical pedicle screws in cadaveric bone. Spine. 1996;21:2429.
19. Yerby SA, Ehteshami JR, McLain RF. Loading of pedicle screws within the vertebra. J Biomech. 1997;30:951.
20. Schufflebarger HL. Moss Miami Instrumentation. In: Bridwell KH, Dewald RL, editors. The textbook of spinal surgery. 2nd ed. Philadelphia: Lippincott-Raven; 1997. p. 675.
21. Lim TH, Eck JC, An HS, Hong JH, Ahn JY, You JW. Bio-mechanics of transfixation in pedicle screw instrumen-tation. Spine. 1996;21:2224.
22. Ritterbusch JF, Ashman RB, Roach JW. Biomechanical comparison of spinal instrumentation systems. Orthop Trans. 1987;11:87.
23. Cunningham BW, Sefter JC, Shono Y, McAfee PC. Static and cyclical biomechanical analysis of pedicle screw spinal constructs. Spine. 1993;18:1677.
24. McCormack T, Karaikovic E, Gaines RW. The load-sharing classification of spine fractures. Spine. 1994;19:1741.
25. Zou D, Yoo JV, Edwards WT, Donovan DM, Chang KW, Bayley JC, et al. Mechanics of anatomic reduction of tho-racolumbar burst fractures. Comparison of distraction versus distraction plus lordosis in the anatomic reduc-tion of the thoracolumbar burst fracture. Spine. 1993;18:195.
26. Cotrel Y, Dubousset J. A new technique of spine fixation by a posterior approach in the treatment of scoliosis. Rev Chir Othop. 1987;70:489.
27. Denis F. Cotrel-Dubousset instrumentation in the treat-ment of idiopathic scoliosis. Orthop Clin North Am. 1988;19:291.
28. Sanders JO, Sanders AE, More R, Ashman RB. A preliminary investigation of shape memory alloys in the surgical correction of scoliosis. Spine. 1993;18:1640.
29. Denis F. The three-column spine and its significance in the classification of acute thoracolumbar spinal injuries. Spine. 1983;8:817.
30. Denis F. Spinal instability as defined by the three-column spine concept in acute spinal trauma. Clin Orthop. 1984;189:65.
31. Bradford DS, Tribus CB. Current concepts and manage-ment of patients with fixed decompensated spinal deformity. Clin Orthop. 1994;306:64.
32. Suk SI, Kim JH, Kim WJ, Lee SM, Chung ER, Nah KH. Posterior vertebral column resection for severe spinal deformities. Spine. 2002;27:2374.

Biomechanics of Sacral Fixation

36

J.C.Y. Leong, G.X. Ni, B. Yu, and W.W. Lu

Anatomic Considerations of Sacral Fixation

The wedge-shaped Sacrum not only gives support to the vertebral column, it also provides strength and stability to the pelvis. Recent renewed interest in sacral screw fixations together with advancements in mechanical understanding has resulted in increased attention being paid to the surgical anatomy of the sacrum [1–6]. Awareness of the anatomical structure, and the adjacent neurovascular and visceral structures and their configurations will minimize complications and contribute to a successful surgical outcome.

In the adult, the sacrum is composed of five vertebral bodies fused together by four ossified intervertebral disks. The sacrum articulates above with the fifth lumbar (L5) vertebra, below with the coccyx, and laterally from the auricular surfaces with the two iliac bones of the hip to form the sacroiliac joints. The projecting anterior edge of the first sacral vertebra is called the sacral promontory and the two sides are the sacrum alas. The sacral promontory is used as a landmark for making pelvic measurements.

Even though sacral screw fixation techniques vary, the anterior sacral anatomy is particularly important. Bicortical purchase to the sacrum is required to enhance the strength of fixation, but a complex interdigitation of neurovascular, visceral, and urogenital structures lies anterior to the sacrum. These are the common and internal iliac arteries, veins, the lumbosacral and obturator trunks, and the rectosigmoid portion of the large bowel. The common and internal iliac veins are located posterior and lateral to the corresponding arteries. It has been shown that the veins lie in the connective tissue immediately in front of the sacral ala [7]. At the level of the first and second sacral vertebrae, the internal iliac veins lie on the anterolateral sacral alar surface, more specifically, the extension of the srcuate line onto the sacrum, medial to the sacroiliac joints. Standard anatomic texts have placed the internal iliac veins directly anterior to the sacroiliac joints [6, 8–10]. Other studies [3, 7] also reported these vessels medial to that position on the anterolateral surfaces of the sacral ala medical to the sacroiliac joint. The internal iliac artery lies anterolaterally and does not come in contact with the bony sacrum.

J.C.Y. Leong, MD
Department of Orthpaedics,
The Open University of Hong Kong,
Hong Kong, China
e-mail: jcyleong@ouhk.edu.hk

G.X. Ni, MD, PhD • B. Yu, MD, PhD
Department of Orthopaedics and Traumatology,
Nanfang Hospital, Southern Medical University,
Guangzhou, Guangdong, China
e-mail: yubinol@163.com

W.W. Lu, PhD (✉)
Department of Orthopaedics and Traumatology,
The University of Hong Kong, Hong Kong, China
e-mail: wwlu@hkusua.hku.hk

D.G. Poitout (ed.), *Biomechanics and Biomaterials in Orthopedics*,
DOI 10.1007/978-1-84882-664-9_36

Studies have also found that the lumbosacral trunk enters the pelvis deep to the medial margin of the psoas major and descends over the pelvic brim. Within the pelvis itself, the trunk runs on the anterior surface of the sacral ala and rests on the sacral extension of the arcuate line medial to the SI joint. The obturator nerve courses far enough anterior to the sacrum, between the sacroiliac joint and the lumbosacral trunk, that it does not come in contact with the sacrum. Injury to any of these can lead to hemorrhage, neurologic deficit, infection, and chronic pain. Furthermore, Sacral osteomyelitis, peritonitis, and sepsis are potential sequelae of bowel perforation with possible life threatening consequences [7].

For S1 screws, the three structures most commonly at risk are the lumbosacral trunk, the internal iliac vein, and the sacroiliac joint. The internal iliac artery and the obturator nerve are considerably anterior to the sacrum and are not at risk. The descending colon, protected by its mesentery, is not prone to injury at the S1 level. Therefore, two safe zones for S1 screw placement have been identified (Fig. 36.1): The first is bordered laterally by the SI joint. Its medial border is delineated by the lumbosacral trunk. The second safe zone lies between the sacral promontory medially and the internal iliac vein laterally and is about 22–27 mm wide. There have also been some concerns about the best entry, direction and depth for sacral screw insertion. By dissecting the cadaveric specimen, Esses et al. [11] and Mirkovic and co-authors [7], found that anteromedial bicortical screw fixation had a larger safe zone compared to anterolateral fixation. It has been reported that screws placed anteromedially are stronger than screws inserted anterolaterally [12–14]. Clinically, the anteromedial pathway is more commonly used for sacral screw fixation.

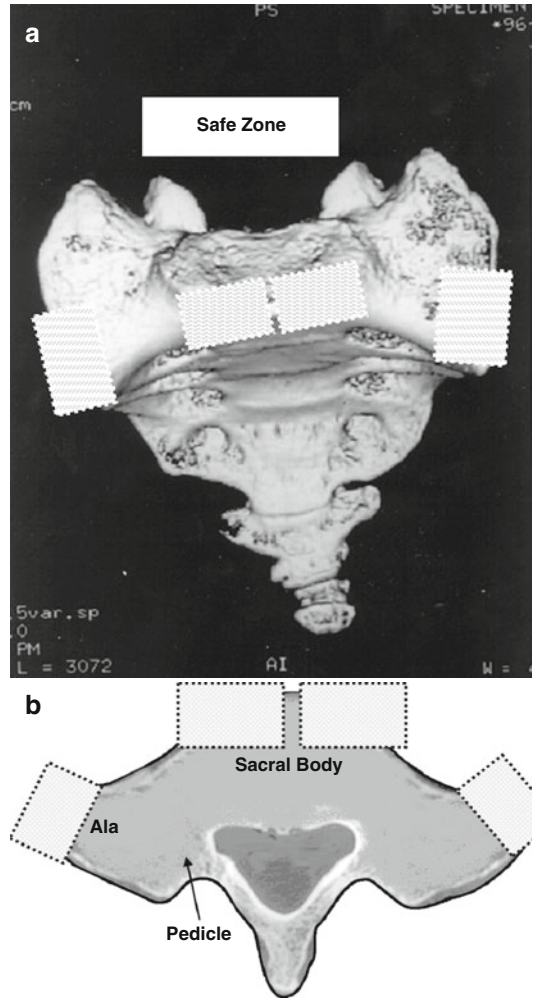

Fig. 36.1 Two safe zones identified on the sacrum for screw placements. (**a**) Viewed from CT reconstructed 3-D model. (**b**) Top view of the safe zones on the sacrum

Bone Mineral Considerations of the Sacral Fixation

Following the popularity of spinal pedicle screw instrumentation, much attention has been focused on the importance of bone mineral density (BMD) for instrumented spine fusion in clinical practice [15–20]. Clinical reports have shown that sacral screw fixation has a high failure rate. The failure of sacral screw fixation may be due to several factors such as inadequate sacral bone purchase, inappropriate direction or depth of the screw insertion, and bone mineral density variations within the sacrum [13, 21–23]. Previous studies [24–26] employed BMD measurements to obtain area density (g/cm^2) using dual energy X-ray absorptiometry (DEXA), or volumetric density (g/cm^3) using quantitative computed tomography (QCT) (Fig. 36.2). QCT is advantageous in that it can quantify BMD along the screw insertion

pathway, and is therefore a more accurate technique than DEXA for measuring the relationship between BMD and the strength of screw fixation [24, 27]. Most investigations into sacral BMD distributions have been carried out on aged specimens, with only a few studies on young cadaveric specimens. Since sacral fixations are commonly applied in patients of young to middle age, BMD measurements of young specimens provide clinically relevant data for the assessment and comparison of sacral fixation. In this text, we will focus on the BMD variations within the S1 body and ala of young patients.

Based on 13 young adult fresh cadaveric sacrum specimens, recent studies [27, 28] reported a mean BMD of the S1 vertebral body of 381.9 mg/cm^3, 31.9 % higher than that of the sacral ala (mean 296.9 mg/cm^3). Table 36.1 and Fig. 36.3 list the bone mineral density at different regions of the S1 body and ala. There are significant differences in BMD, with the regions near the lateral posterior and lateral anterior areas of the vertebral body having higher BMD. This again shows that these areas would provide better purchase for pedicle screw fixation. Furthermore, BMD of the posterior region closest to the spinal canal was lower than that of lateral and central areas. In the ala, the BMD of the internal anterior areas closest to the S1 body were the highest with a BMD of 326.8 mg/cm^3.

Fig. 36.2 The sacral specimen in the QCT device

The mean BMD at different layers (Fig. 36.4) of the S1 body and ala has also listed in Table 36.2. The BMD of the first layer in the S1 body, close to the superior end plate, was significantly higher than the others with a BMD of 516 mg/cm^3. The BMD was lowest in the central layer of the body, and increased again towards the inferior endplate. This suggests that sacral pedicle screws directed close to or cephalad penetrating the superior sacral end plate would achieve better purchase. In the ala, the BMD of the top layer was highest with a BMD of 329 mg/cm^3 and the BMD decreased caudally from the top layer.

Based on the principle that inserting the pedicle screws directly penetrating the superior endplate should increase the fixation strength, a novel sacral screw fixation technique has been developed recently with good clinical results. To support the clinical findings, the mechanical stability of this technique was conducted afterwards [29]. Following cyclic loading, the mean maximum insertion torque and mean pull-out force were significantly higher for bicortical fixation through the S1 endplate (mean 3.17 N·m and 1457N) than bicortical fixation through the anterior sacral cortex (mean 1.98 N·m and 1122N). By taking advantage of the density of the upper sacrum and the thick cortical endplate of the S1, the bicortical S1 endplate sacral pedicle screw

Table 36.1 The mean values (SD) of BMD at different columns of S1 body and ala

S1 body columns	Lateral posterior	Lateral anterior	Middle posterior	Middle middle	Middle anterior	
The mean values of BMD (SD)	381.6 (5)[a]	368.9 (64.8)[a]	297.6 (102.6)[a]	372 (93.9)[a]	351.1 (68.1)	
Ala columns	Internal anterior	Internal posterior	Middle anterior	Middle middle	Middle posterior	Lateral
The mean values of BMD (SD)	326.8 (12)[a]	226 (135)	205.4 (69.2)	185.1 (91.1)	182(83.9)	210.1(77)

[a]Significant difference found, Unit: mg./cm^3

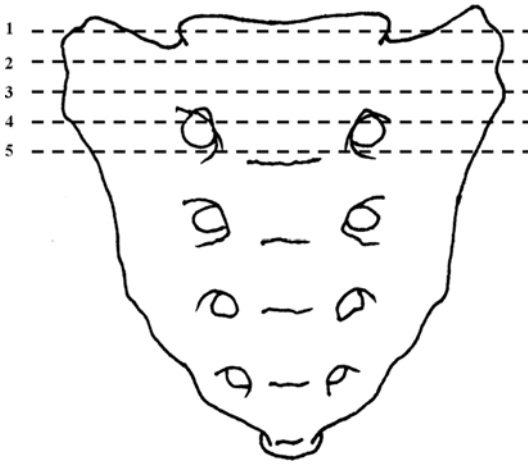

Fig. 36.3 Schematic diagram of the front of the sacrum showing the five transverse layers. (*1–5*) Transverse layers of the front of the sacrum with different resistances

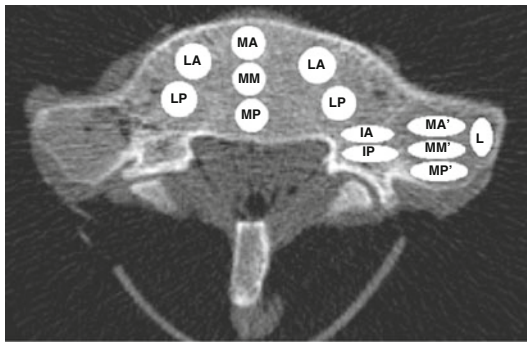

Fig. 36.4 Axial view of seven vertical columns in S1 body and six vertical columns in S1 ala. The IA and IP areas are also defined as sacral pedicle, *LA* Lateral Anterior, *LP* Lateral Posterior, *MA* Middle Anterior, *MM* Middle Middle, *IA* Internal Anterior, *IP* Internal Posterior, *L* Lateral

Table 36.2 The mean values (SD) of bone mineral density at different layers of S1 body and ala

Layers	1	2	3	4	5
S1 body	516.1 (72)[a]	376.9 (37)	342.4 (56)	365.6 (56)	397.5 (81)
Ala	N/A	329.1 (196)[a]	225.6 (128)	177.4 (8)	142.1 (63)

[a]Significant difference; Unit: mg./cm^3

fixation technique provided a greater screw insertion torque and a stronger screw fixation after cyclic loading than the conventional bicortical anterior cortex fixation technique. In addition, for both fixation techniques, the screw insertion torque was shown to correlate with the screw pull-out force following cyclic loading, indicating that insertion torque was a good intraoperative indicator of screw pull-out force.

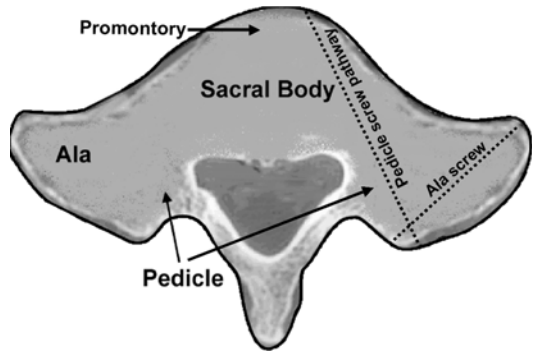

Fig. 36.5 Schematic diagram of the sacral body, ala and pedicle. The pedicle screw pathway and the ala screw pathway are defined based on BMD measurements

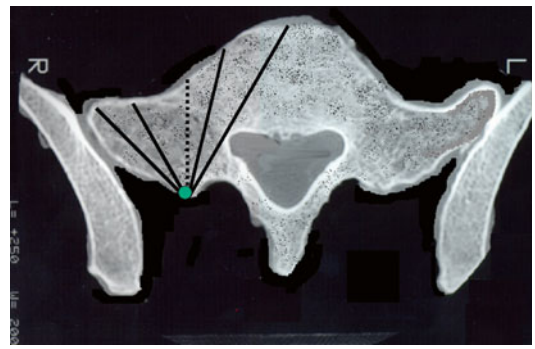

Fig. 36.6 CT showing the angles of screw insertion

Based on the BMD distribution within the sacrum [13, 27, 28], the recommended screw pathway is shown in Fig. 36.5. Further to radiographs, CT scans, and specimen observation, it is suggested that the S1 pedicle screw should be directed parallel to the S1 end plate in the sagittal plane, and the ala screw inserted to the tip of the ala along the ala slope. The insertion angle of the S1 pedicle screw in the transverse plane should be between 15° and 25° medially and the angle of the ala screw should be 30–40° laterally for better bone purchase (Fig. 36.6 from CT). If the insertion angle is less than 10° for S1 pedicle screws, the screw will not obtain good purchase on the S1 promontary, leading to a greatly reduced purchase of bone and less biomechanical stability. On the other hand, if the insertion angle for the S1 screw is larger than 25°, the potential

for injury to the spinal cord is higher [30]. With respect to ala screw insertion, Edwards and Louis preferred lateral placement into the sacral ala at 35–45° [31, 32], while Mirkovic and associates suggested the screw should be angled at 30–40° in order to obtain a better purchase [7]. If the angle of ala screw is greater than 45°, the potential for lumbosacral trunk injury is high [7].

The importance of vertebral bone mineral density for screw fixation has been the subject of several studies to determine screw stability and predict lumbar vertebrae strength [7, 11–13, 20, 33–35]. Some have suggested that pre-operative measurement of BMD is necessary for transpedicular screwing in osteoporotic cases [28, 36, 37]. Other studies [20, 38] found that vertebral bodies of human lumbosacral spines had a mean BMD of 92 mg/cm^3 and the mean BMD of the sacrum was 152 mg/cm^3 for the elderly of mean age of 78 years old. Studies also indicated that at a QCT BMD value of less than 90 mg/ml, early loosening of the screw may be expected, while it is less likely with an BMD of more than 120 mg/cm^3. The mean BMD from young adults with mean age of 31 years was approximately 2.5 times greater than that in the above mentioned group. Since the sacrum mainly consists of cancellous bone and the lumbosacral junction sustains more load than others above the sacrum, failure of sacral screw fixation can occur without significant osteoporosis.

Biomechanical Considerations of the Sacral Fixation

Strengths of Varieties of Fixations

The sacral screw can be placed either anteromedially through the S1 pedicle into the promontory or anterolaterally into the sacral ala. There are a few anatomical and biomechanical studies regarding the safety of the screw placement when bicortical inseertions are used [3, 7, 21, 39]. (see section above). A variety of fixation techniques and instruments have been designed to improve the strength of lumbosacral fixation [8, 33, 37, 40–46]. It is assumed that increasing the number of sacral screws and using a triangulated insertion technique may increase the strength of purchase for lumbosacral fixation. A technique with a sacral Chopin block using S1 pedicle and ala screws with modified CD instrumentation was introduced to clinical practice in the early 1990s [47–49]. This new technique can theoretically increase the strength of fixation due to the anteromedial screw and the added ala screw in divergent triangular orientation. However, a clinical study conducted by Devlin et al. [50] found that the CD system using sacral pedicle and ala screws in the deformity correction of adult patients did not appear to offer any advantages over alternative techniques in achieving arthrodesis.

A cadaveric study [13] using a sacral Chopin block with S1 pedicle and ala screws on sacra of different age groups evaluated the stiffnesses and failure strengths of fixation under different loading conditions. With bicortical screw purchase, the average stiffnesses of single screw and two divergent triangulated screw fixations (Fig. 36.7) were found to show statistically significant differences under compression, tension and torsion (see Table 36.3). With one S1 pedicle screw fixation, the average stiffness was 203 N/mm for compression, 147 N/mm for tension and 2 Nmm/deg. for torsion. With two-screw fixation, the average stiffness increased to 255 N/mm (126 %), 185 N/mm (126 %) and 2.4 Nm/deg (120 %) respectively, suggesting increasing the number of screws and using a triangulated insertion can increase the strength of fixation.

Biomechanical tests have also shown that triangulated double screws instrumented either anteriorly or posteriorly, can significantly increase the strength of fixation [30, 41, 51]. Ogon and associates [51] found that anterior double screw fixation can increase fixation strength in vitro by 73 %, while Ruland and co-authors [30] found that a doubled pull-out strength can be achieved by using posterior triangulated CD pedicle screws with a transverse plate. By applying the load along the screw axis instead of simulating in vivo loads perpendicular to the screw axis, Zindrick and co-authors [52] conducted a pullout test to compare the strength of screw fixation in different orientations. They found that the anterolaterally

directed screw sustained greater loads to failure. In contrast, other biomechanical studies reported that anteromedial screw fixation was significantly stronger than anterolateral screw insertion [3, 21, 37, 53]. This also correlated with the higher bone density of the S1 centrum, which provides a more rigid bone screw fixation [21].

A negative relation between the specimen age and the stiffnesses under different loading conditions has also been found [13]. Table 36.3 shows that the younger specimens had significantly higher stiffnesses than the aged ones. The average failure strength under tension load was found to be 1450 N in the younger specimens (<30 years), but 980 N in the aged specimens (>60 years). Studies have also revealed that the bone mineral density is closely related to the fixation strength of transpedicular screws [36, 38, 52–54]. Under the same test conditions, it was found that fixation stiffnesses of the aged specimens were lower than those of younger specimens.

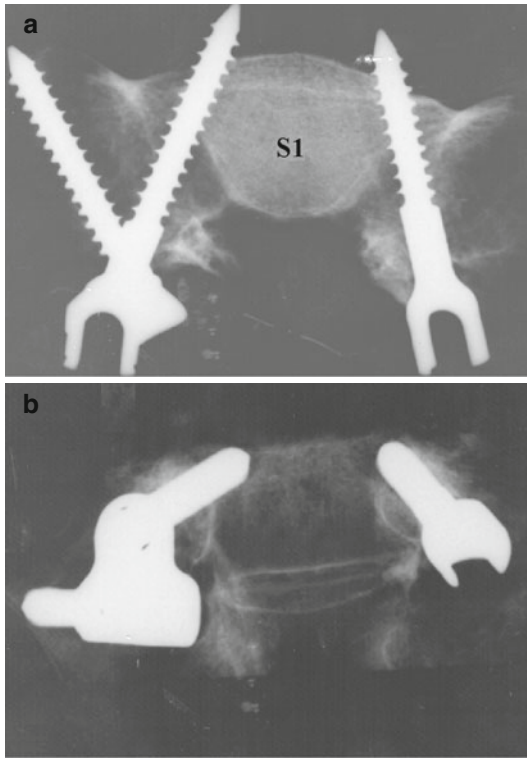

Fig. 36.7 (**a**, **b**) AP and top view of instrumented specimen. *Right side* was with one anteromedial S1 pedicle screw and left side was a Chopin Block with anteromedial and anterolateral (alar) screws

Loosening of Sacral Screw Fixation Under Fatigue Loading

In the early postoperative period, before bony fusion has taken place, the mechanical properties of the fixation will determine the stability of that part of the spine. In some cases, sacral screw fixation may not maintain sufficient stability, eventually resulting in loosening, pull-out, screw breakage, or migration. Cyclic loading is thought to be the main reason leading to change in the biomechanical properties of pedicle screw fixation [55–58] and the major failure mechanism appears to be screw pull-out at the bone-screw interface [50, 59, 60]. While a few studies have characterized the effects of cyclic loading on pull-out strength of sacral screw fixation, the majority of studies [21, 53, 61, 62] investigating the effects of insertion torque and bone mineral density have used single loading to failure by compression of the screw head perpendicular to the axis of the screw, rather than fatigue loading.

Table 36.3 The average stiffness of younger and aged specimens with one and two screw fixation to the sacrum

	One screw fixation			Two screw fixation		
	Compression (mean ± SD)	Tension (mean ± SD)	Torsion (mean ± SD)	Compression (mean ± SD)	Tension (mean ± S)	Torsion (mean ± SD)
<30 years	220 ± 34	169 ± 24	2.1 ± 0.8	296 ± 43	209 ± 23	2.7 ± 0.6
>60 years	179 ± 20	112 ± 19	1.9 ± 0.4	195 ± 23	150 ± 27	1.9 ± 0.3
P value	0.003	0.001	0.007	0.001	0.001	0.007
Total	203 ± 35	147 ± 35	2 ± 0.6	255 ± 62	185 ± 38	2.4 ± 0.6

Unit: Compression = N/mm; Tension = N/mm; Torsion = Nm/deg

Some studies [14, 63] have simulated cyclic loading of sacral screw fixations in young adult human specimens to investigate the effects of unicortical versus bicortical and medial versus lateral screw fixation on pull-out strength, and also the correlation between pull-out strength, bone density and insertion torque under fatigue condition. In these studies, human sacrums from young (24–36 year old) cadavers specimens were used. Bone mineral density was measured using a peripheral Quantitative Computed Tomography (pQCT) machine with a scan slice thickness of 5 mm. Seven-millimeter Compact CD sacral screws [47, 49] were then inserted, randomized into four groups according to the combinations of orientation (medial or lateral) and fixation (unicortical or bicortical). Screws were inserted according to the following depths: unicortically; up to but not engaging the cortex (2 mm short of the anterior cortex); or bicortically, with the threads at least 2 mm anterior to the cortex. The screw holes were not tapped, and the insertion torque was measured throughout screw insertion using a torque driver. The specimens were placed on a servo-hydraulic MTS 858 bionix testing machine and cyclic loading performed with the loading axis directed perpendicularly to the axis of the screw (Fig. 36.8). A rigid linkage was used at the screw head, using the CCD rod and linkage system. The cyclic loading ranged from –40 N to –400 N and was conducted at 2 Hz up to 20,000 cycles. Following cyclic loading, the specimen was re-oriented in the testing machine, and a pull-out test was performed along the axis of the screw at a loading rate of 10 N/s until the screw was completely pulled out of the sacrum. The results from these studies shown that the average pull-out force after cyclic loading was 1271N for the medial bicortical screw fixation and 778N for the medial unicortical screw fixation. The average pull-out force after cyclic loading was 570N for the lateral bicortical screw fixation and 368N for the lateral unicortical screw fixation. Table 36.4 lists the all the relevant data from this study. The difference between the pull-out force of bicortical and the unicortical fixation was highly significant for the medial screw fixation and significant for the lateral screw fixation, showing that depth of screw penetration significantly affects the pull-out force following fatigue loading. The average pull-out force was significantly greater for the medial bicortical screw fixation than for both bicortical and unicortical lateral (ala) screw fixation [13]. There was also a significant difference of pull-out force between the medial unicortical and the lateral unicortical screw fixation. The pull-out force following fatigue loading is therefore significantly affected by the screw orientation. The maximum mean insertion torque was 1.93 N.m for the medial bicortical screw fixation, which was 35 % higher than that for medial unicortical screw fixation (Table 36.4). The insertion torque for lateral bicortical screw fixation was 50 % lower than for medial bicortical, but there was no significant difference between the insertion torque for medial unicortical screw fixation and lateral unicortical screw fixation. For medial screw fixation, the pull-out force correlated significantly with insertion torque and BMD. The correlation and linear regression between insertion torque and pull-out force are shown in Figs. 36.9 and 36.10, respectively. In this study,

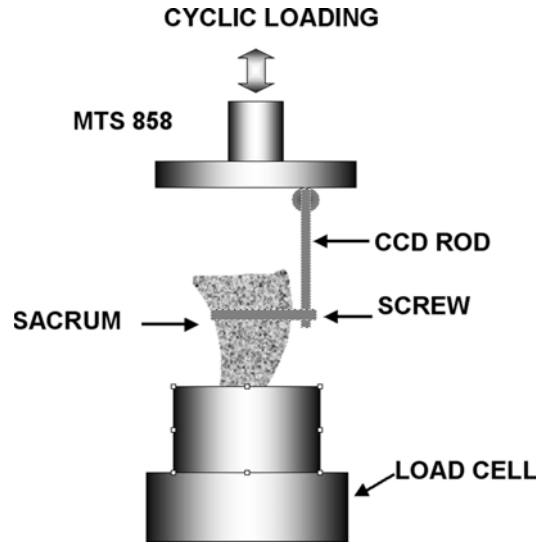

Fig. 36.8 Schematic of the specimen loaded in the cyclic loading testing apparatus. The lower part of the sacrum was embedded in a metal cup filled with Epoxy. Cyclic axial compressive force was applied to the screw via the CCD rod, allowing translation and rotation of the screw. Force was measured by the load cell, which was situated inferiorly

Table 36.4 Average BMD, insertion torque and pull-out force for the medial and lateral bicortical and unicortical screw insertions

Orientation	Depth	Number of specimens	Pullout force (N)		Insertion torque (N.m)		BMD of body (g/ml)	
Medial	Bicortical	11	1271	(449)	1.93	(0.67)	0.38	(0.08)
	Unicortical	11	778	(443)	1.26	(0.4)	0.4	(0.06)
Lateral(alar)	Bicortical	7	570	(194)	0.96	(0.24)	0.24	(0.05)
	Unicortical	6	368	(171)	0.88	(0.19)	0.26	(0.04)

Standard deviations are included in parentheses

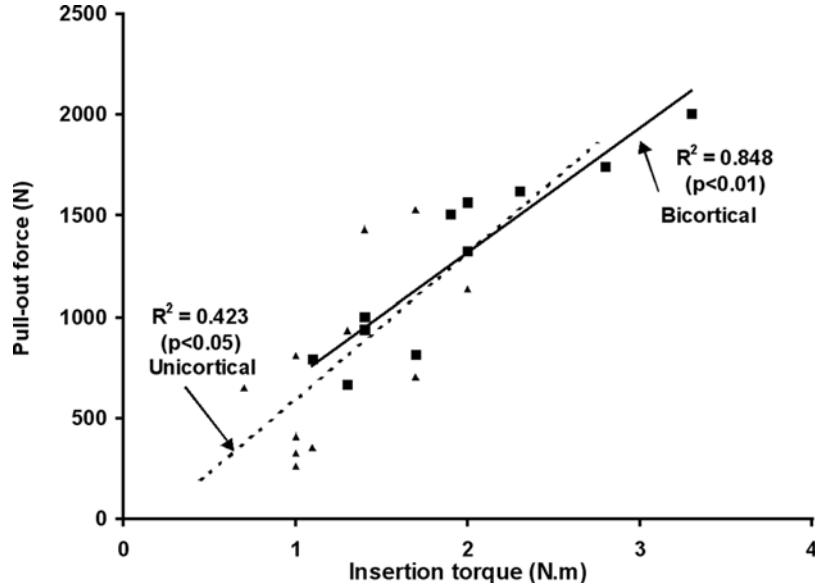

Fig. 36.9 A plot of pull-out force versus insertion torque for sacral screw insertions. Linear regression lines for both data sets are plotted

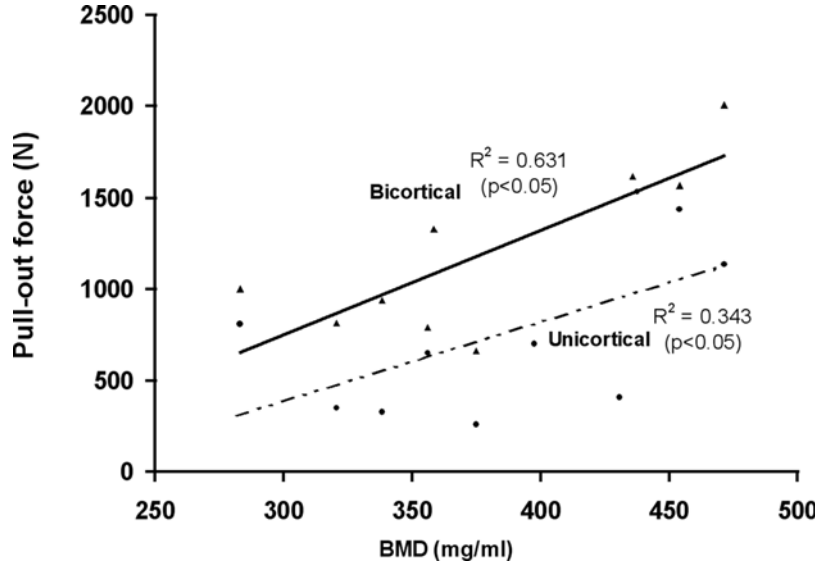

Fig. 36.10 A plot of pull-out force versus bone density (*BMD*) for medial sacral screw insertions. Linear regression lines for both data sets are also plotted

the insertion torque also showed a significant linear correlation with BMD. However, no significant linear correlation was seen between pull-out force, insertion torque or bone density for lateral screw fixation to the ala. Some authors [21, 53] also found the strength of medial screws to be stronger than lateral screws under compression, both for bicortical and unicortical fixation, and a similar result was found for the pull out strength of unicortical screws [12]. In contrast, however, other studies [52, 54] have shown that bicortical laterally-placed screws sustained higher pull-out loads than medial screws. Based on the anatomical evaluation [7], lateral screw placement, if it were to engage the anterior cortex (bicortical fixation), carries a risk of injury to either the lumbosacral trunk or the internal iliac vein. The potential for trunk injury with laterally bicortical screws is particularly high (55 %).

Intraspecimen bone densities and insertional torques may account for differences in screw fixation. An in vitro study found the bone mineral density in the S1 centrum region to be 56 % denser than in the S1 lateral alar region [53], and this is consistent with other results [14, 21]. A recent study [63] further showed the insertion torques for medial bicortical and unicortical screw fixation to be 101 % and 43 % higher than the insertion torques for lateral bicortical and unicortical screw fixation, respectively. The pull-out forces sustained by medial bicortical and unicortical screw fixation following cyclic loading were significantly higher than those placed laterally, where the BMD and insertion torques are lower.

A previous study of the depth of insertion of transpedicular vertebral screw [37] suggested that even a 5 mm difference in screw length can produce a significant increase in bone screw fixation strength in vertebral bone. However, it has been reported that in an older population, unicortical and bicortical sacral screw fixations sustained similar loads to failure [3, 5, 53]. The anterior cortex of the sacrum was found to be anatomically thin in the elderly sacrum, and as such has little mechanical effect on screw fixation. For young cadaveric specimens, bicortical screw fixation proved to be stronger than unicortical fixation for both medially and laterally placed screws, despite the overall screw lengths differing by less than 5 mm [14, 55]. Engagement of the anterior cortex therefore makes a significant contribution to the pull out strength of sacral screw fixation following fatigue loading in younger specimens [25, 64–66].

Biomechanical findings strengthen the clinical use of pre-operative bone density measurement in selecting patients who may be candidates for sacral screw fixation, and suggest intra-operative insertion torque, insertion depth, and orientation as indicators of the fixation strength.

References

1. Arman C, Naderi S, Kiray A, Aksu FT, Yilmaz HS, Tetik S, Korman E. The human sacrum and safe approaches for screw placement. J Clin Neurosci. 2009;16:1046–9.
2. Banta CJ, King AG, Dabezies EJ, Liljeberg RL. Measurement of the effective pedicle diameter in the human spine. Orthopaedics. 1989;12:939–42.
3. Dohring J, Krag MH, Johnson CC. Sacral screw fixation: a morphologic anatomic and mechanical study (abstract). Proc North Am Spine Soc. 1990.
4. Ergur I, Akcali O, Kiray A, Kosay C, Tayefi H. Neurovascular risks of sacral screws with bicortical purchase: an anatomical study. Eur Spine J. 2007;16:1519–23.
5. Farcy JPC, Rawlins BA, Glassman SD. Technique and results of fixation to the sacrum with iliosacral screws. Spine. 1992;17(Suppl):190–5.
6. Xu R, Ebraheim NA, Mohamed A, El-Gamal H, Yeasting RA. Anatomic considerations for dorsal sacral plate-screw fixation. J Spinal Disord. 1995;8(5):352–6.
7. Mirkovic S, Abitbol JJ, Steinman J, Edwards CC, Schaffler M, Massie J, Garfin SR. Anatomic consideration for sacral screw placement. Spine. 1991;16(Suppl):289–94.
8. Jackson RP. Insertion of intrasacral rods for sacral fixation and spinal correction with in situ rod contouring technique. In: Bridwell KH, Dewald RL, editors. The textbook of spinal surgery. 2nd ed. Philadelphia: Lippincott-Raven; 1997. p. 2187–209.
9. Morse BJ, Ebraheim NA, Jackson WT. Preoperative CT determination of angles for sacral screw placement. Spine. 1994;19:604–7.
10. Xu R, Ebraheim NA, Yeasting RA, Wong FY, Jackson WT. Morphometric evaluation of the first sacral vertebra and the projection of its pedicle on the posterior aspect of the sacrum. Spine. 1995;20(8):936–40.
11. Esses SI, Botsford DJ, Huler RJ, Rauschning W. Surgical anatomy of the sacrum. A guide for rational screw fixation. Spine. 1991;16(6 Suppl):S283–8.

12. Ashman RB, Bechtold JE, Edwards WT, Johnston CE, McAfee PC, Tencer AF. In vitro spinal arthrodesis implant mechanical testing protocols. J Spinal Disord. 1989;12:274–81.
13. Leong JCY, Lu WW, Zheng YG, Zhu QA, Zhong SZ. Comparison of the strengths of lumbosacral fixation achieved with techniques using one and two triangulated sacral screws. Spine. 1998;23(21):2289–94.
14. Qingan Z, Lu WW, Holmes AD, Zheng YG, Zhong S, Leong CY. The effects of cyclic loading on pull-out strength of sacral screw fixation: an *in vitro* biomechanical study. Spine. 2000;25:1065–9.
15. Granhed H, Johnson R, Hansson T. Mineral content and strength of lumbar vertebrae: a cadaver study. Acta Orthop Scand. 1989;52:105–9.
16. Hadjipavlou AG, Nicodemus CL, Al-Hamdan FA, Simmons JW, Pope MH. Correlation of bone equivalent mineral density to pull-out strength of triangulated pedicle screw construct. J Spinal Disord. 1997;10(1):12–9.
17. Okuyama K, Sato K, Abe E, Inaba H, Shimada Y, Murai H. Stability of transpedicle screwing for the osteoporotic spine: an in vitro study of the mechanical stability. Spine. 1993;18:2240–5.
18. Smit TH, Odgaard A, Schneider E. Structure and function of vertebral trabecular bone. Spine. 1997;22:2823–33.
19. Snyder BD, Zaltz I, Hall JE, Emans JB. Predicting the integrity of vertebral bone screw fixation in anterior spinal instrumentation. Spine. 1995;20:1568–74.
20. Wittenberg RH, Lee KS, Shea M, 3 White AA, Hayes WC. Effect of screw diameter, insertion technique, and bone cement augmentation of pedicular screw fixation strength. Clin Orthop. 1993;296:278–87.
21. Smith SA, Abitbol JJ, Carlson GD, Anderson DR, Taggart KW, Garfin SR. The effects of depth of penetration, screw orientation, and bone density on sacral screw fixation. Spine. 1993;18(8):1006–10.
22. Vesterby A, Mosekilde L, Gundersen H, Melsen F, Mosekilde L, Holm K, Sorensen S. Biologically meaningful determinants of the in vitro strength of lumbar vertebrae. Bone. 1991;12:219–24.
23. Weaver JK, Chalmers J. Cancellous bone: its strength and changes with aging and an evaluation of some methods for measuring its mineral content. J Bone Joint Surg. 1966;48A:289–9.
24. Ericksson S, Isberg BO, Lindgren JU. Prediction of vertebral strength by dual photon absorptiometry and quantitative computed tomography. Calcif Tissue Int. 1989;44:243–50.
25. Imai Y, Sone T, Tomomitsu T, Imai H, Mikawa Y, Watanabe R, Fukunaga M. Precision and accuracy for pheripheral quantitative computed tomography evaluated using radial specimens. J Bone Miner Res. 1997;12:263.
26. Rüeggsegger P. The use of peripheral QCT in the evaluation of bone remodelling. The Endocrinologist. 1994;4(3):167–76.
27. Zheng YG, Lu WW, Zhu Q, Qin L, Shizhen Z, Leong JCY. Bone mineral density variations of the sacrum in young adults and its significance for sacral fixation. Spine. 1999;25:353–7.
28. Lu WW, Zheng YG, Holmes AD, Zhu QA, Luk KDK, Leong JCY. Bone mineral density variations along the lumbosacral spine. Clin Orthop. 2000;378:255–63.
29. Luk KD, Chen L, Lu WW. A stronger bicortical sacral pedicle screw fixation through the s1 endplate: an in vitro cyclic loading and pull-out force evaluation. Spine (Phila Pa 1976). 2005;30:525–9.
30. Ruland CM, McAfee PC, Warden KE, Cunningham BW. Triangulation of pedicular instrumentation: a biomechanical analysis. Spine. 1991;16(Suppl):270–6.
31. Edwards CC. Spinal screw fixation of the lumbar and sacral spine. Early results treating the first 50 cases. Orthop Trans. 1987;11:99.
32. Louis R. Fusion of the lumbar and sacral spine by internal fixation with screw plates. Clin Orthop. 1986;203:18–33.
33. Allen Jr BL, Ferguson RL. The Galveston experience with L-rod instrumentation for adolescent idiopathic scoliosis. Clin Orthop. 1988;229:59–69.
34. Glazer PA, Colliou O, Lotz JC, Bradford DS. Biomechanical analysis of lumbosacral fixation. Spine. 1996;21:1211–22.
35. Wittenberg RH, Shea M, Swartz DE, Lee KS, White 3rd AA, Hayes WC. Importance of bone mineral density in instrumented spine fusions. Spine. 1991;16(6):647–52.
36. Halvorson TL, Kelley LA, Thomas KA, Whitecloud 3rd TS, Cook SD. Effects of bone mineral density on pedicle screw fixation. Spine. 1994;19:2415–20.
37. Krag MH, Beynnon BD, Pope MH, DeCoster TA. The depth of insertion of transpedicular vertebral screws into human vertebrae: effect upon screw-vertebra interface strength. J Spinal Disord. 1989;1:287–94.
38. Wittenberg RH, Shea M, Edwards WT, Swartz DE, White AA, Hayes WC. A biomechanical study of the fatigue characteristics of thoracolumbar fixation implants in a calf spine model. Spine. 1992;17(6S):S121–8.
39. Yoganandan N, Larson SJ, Cusick JF, Pintar F, Maiman DJ. Structural strength and kinematics of pedicle scrw/plate fixation of the lumbar spine. Presented at the annual meeting of the International Society for the Study of the Lumbar Spine. Boston; 1990.
40. Ashman RB, Birch JG, Bone LB. Mechanical testing of spinal instrumentation. Clin Orthop. 1988;227:113–25.
41. Bayley JC, Yuan HA, Fredrickson BR. The Syracuse I-plate. Spine. 1991;16:120–4.
42. Early S, Mahar A, Oka R, Newton P. Biomechanical comparison of lumbosacral fixation using Luque-Galveston and Colorado II sacropelvic fixation: advantage of using locked proximal fixation. Spine (Phila Pa 1976). 2005;30:1396–401.

43. Krag MH, Beynnon BD, Pope MH, Frymoyer JW, Haugh LD, Weaver DL. An internal fixation for posterior application to short segments of the thoracic, lumbar, or lumbosacral spine: design and testing. Clin Orthop. 1986;203:75–98.
44. Ngu BB, Belkoff SM, Gelb DE, Ludwig SC. A biomechanical comparison of sacral pedicle screw salvage techniques. Spine (Phila Pa 1976). 2006;31: E166–8.
45. Ogilvie JW, Schengel M. Comparison of lumbosacral fixation devices. Clin Orthop. 1986;203:120–5.
46. Tomlinson T, Chen J, Upasani V, Mahar A. Unilateral and bilateral sacropelvic fixation result in similar construct biomechanics. Spine (Phila Pa 1976). 2008;33(20):2127–33.
47. Chopin D. A new device for pelvic fixation for spinal surgery: the sacral block. Presented at 8th international congress on cotrel-dubousset instrumentation. Minneapolis; 1991.
48. Jackson RP, Hamilton AC. C-D screws with oblique canals for improved sacral fixation: a prospective clinical study of the first fifty patients. 7th proceeding of the international congress on cotrel-dubousset instrumentation. 1990, p. 75–86.
49. SOFAMOR. In vitro biomechanical evaluation report of the compact CD fixture in lumbo-sacral. Study done by the Biomechanical Laboratory of Paris-Pr Lavaste Department. 1990 (Unpublished data).
50. Devlin VJ, Oheneba BA, Bradford DS, Ogilvie JW, Transfeldt EE. Treatment of adult spinal deformity with fusion to the sacrum using CD instrumentation. J Spinal Disord. 1991;4(1):1–14.
51. Ogon M, Haid C, Krismer M, Sterzinger W, Bauer R. Comparison between single-screw and triangulated, double-screw fixation in anterior spine surgery. Spine. 1996;21:2728–34.
52. Zindrick MR, Wiltse LL, Widell EH, et al. A biomechanical study of intrapeduncular screw fixation in the lumbosacral spine. Clin Orthop. 1986;203:99–112.
53. Carlson GD, Abitbol JJ, Anderson DR, et al. Screw fixation in the human sacrum: an in vitro study of the biomechanics of fixation. Spine. 1992;17(6S): S197–203.
54. Zdeblick TA, Kunz DN, Cooke ME. Pedicle screw pull-out strength: correlation with insertional torque. Spine. 1993;18(12):1673–6.
55. Cunningham BW, Sefter JC, Shono Y, McAfee PC. Static and cyclical biomechanical analysis of pedicle screw spinal constructs. Spine. 1993;18(12):1677–88.
56. Lu WW, Luk KDK, Ruan DK, Fei ZQ, Leong JCY. Stability of the whole lumbar spine after multilevel fenestration and discectomy. Spine. 1999;24:1277–82.
57. Pfeiffer M, Hoffman H, Goel VK, Weinstein JN, Griss P. In vitro testing of a new transpedicular stabilization technique. Eur Spine J. 1997;6(4):249–55.
58. Yamagata M, Kitahara I, Minami S, et al. Mechanical stability of the pedicle screw fixation systems for the lumbar spine. Spine. 1992;17(3 Suppl):S51–4.
59. Perra JH. Techniques of instrumentation in long fusion to the sacrum. Clin Orthop North Am. 1994;25:287–99.
60. Shea M, Edwards WT, Clothiaux PL, Crowell RR, Nachemson AL, White AA, Hayes WC. Three-dimensional load displacement properties of posterior lumbar fixation. J Orthop Trauma. 1991;5:420–7.
61. McCalden RW, Mcgeough JA, Court-Brown CM. Age-related changes in the compressive strength of cancellous bone. J Bone Joint Surg. 1997;79A:421–7.
62. McCord DH, Cunningham BW, Shono Y, Myers JJ, McAfee PC. Biomechanical analysis of lumbosacral fixation. Spine. 1992;17:235–43.
63. Lu WW, Zhu QA, Holmes AD, Luk KDK, Zhong S, Leong JCY. Loosening of sacral screw fixation under in vitro fatigue loading. J Orthop Res. 2000;18:808–14.
64. Kornblatt MD, Casey MP, Jacobs RR. Internal fixation in lumbosacral spine fusion: a biomechanical and clinical study. Clin Orthop. 1986;203:141–50.
65. Lee CK, Langrana NA. Lumbosacral spinal fusion: a biomechanical study. Spine. 1984;9:574–81.
66. Myers BS, Belmont PJ, Richardson WJ, Yu JR, Harper KD, Nightingale RW. The role of imaging and in situ biomechanical testing in assessing pedicle screw pull-out strength. Spine. 1966;21(17):1962–8.

Current State of Management for Osteoporosis and Orthopaedic Related Spinal Problems

37

Ping-chung Leung

The Bone and Joint Decade in year 2000 reported that a survey done in the Scandinavian countries and New Zealand on the orthopaedic surgeons' awareness of osteoporosis revealed that less than 20 % of them were knowledgable about this common condition although they are actively dealing with bone and joint problems. One of the important tasks for the Bone and Joint Decade was therefore, to give priority to osteoporosis in the public and professional promotional programs [1].

The Bone and Joint Decade is coming to an end, there is no proper evaluation on the outcome of the decade's efforts. Nevertheless, from my personal observations, orthopaedic surgeons involved on the front line of osteoporosis management and prevention, are still the minority. Most if not all, of the major epidermiological studies and drug trials on osteoporosis, are still mastered by physicians and epidemiologists only [2, 3].

This chapter will be giving a comprehensive account of the therapeutic management of osteoporosis in its first half, then attempt to comment on the current management of the osteoporotic spine in the second half.

P.-c. Leung, MBBS, MS, DSc, Hon DSocSc
Professor Emeritus, Department of Orthopaedics and Traumatology, Faculty of Medicine,
Jockey Club Centre for Osteoporosis Care and Prevention, The Chinese University of Hong Kong,
5/F, School of Public Health Building, Shatin, N.T.,
Hong Kong, China
e-mail: pingcleung@cuhk.edu.hk

Therapeutic Management of Osteoporosis

Biological Basis

Under normal physiological conditions, the bone integrity is maintained through a delicate balance of bone formation and bone resorption. When nutrition is plentiful and mechanical stimulation adequate, osteoblast activities bring about new bone formation, while at the same time, osteoclasts are responsible for the breakdown of bone in bone resorption. There is a delicate balance between the build-up and break-down which is responsible for bone's healthy integrity. After the age of maximal physical activities bone resorption tends to become more active, leading to osteopenia and later osteoporosis in women after menopause and in men 5–10 years later. The increased fragility in osteoporotic bone increases the susceptibility to fractures. For every 10 % of bone lost, the risk of fracture doubles. It has been estimated in the United States that the life time risk for a woman over 50 years of age to suffer from fracture is 45 %, of which hip fractures would be around 50 %. Although men develop osteoporosis later and to a less severe degree, 30 % of all elderly hip fractures still happen in the male [4].

With regard to the hormonal and molecular biological background of osteoporosis, declining estrogen in paramenopausal women is certainly

D.G. Poitout (ed.), *Biomechanics and Biomaterials in Orthopedics*,
DOI 10.1007/978-1-84882-664-9_37

a major factor. On the molecular side, osteoclasts are generated through the activity of a cytokine RANK which receives a ligand RANKL, both of which are neutralised by another protein molecule osteoprotegrin (OPG). The relative concentrations of these protein molecules therefore, regulate the production of osteoclasts, hence the severity of osteoporosis. The regulation activities are monitored by mechanisms directly or indirectly related to estrogen, including those of androgen [5].

Pathological conditions causing bone loss include hyperparathyroidism, hyperthyroidism, Paget's disease and cancer. Orthopaedic practice is more concerned with cancer invasion of bones. The occurrence of cancers induces an increase in osteoclast formation either manifested as systematic hypercalcaemia or locally as bone metastases. Cancer cells probably promote osteoclast formation by producing parathyroid hormone-related protein (PTHrP). The experimental proof of the postulation has been obtained through the neutralizing effects of antibodies against PTHrP [6]. Cancer cells like those in prostatic cancer, metastasing to bone, have been demonstrated to possess an accompanying osteoclast component which facilitates their establishment and expansion [7].

Therapeutic Management

Estrogen has been the first agent used to improve bone quality after menopause. Evidence of its bone protection effects is revealed through its protection on bone density manifested in radiographs and bone mineral density (BMD) screenings. Various studies indicated that the improved bone quality reduces the fracture risk by over 50 % [8]. The value of estrogen, however, was out-weighted by its undesirable side-effects of cancer induction on the breast and uterus, as well as its tendency on thromboembolic promotion.

With the establishment of the knowledge on the molecular biology of osteoporosis, it is possible to develop, after estrogen replacement, other modalities of therapy. Inhibition of bone resorption can be achieved through osteoclasts reduction, and a control of osteoclast activities with therapeutic agents.

The search for therapeutic agents with estrogenic effects but free from adversely affecting target organs of oestrogen revealed a group of chemicals known as Surface Estrogen Receptor Modulators (SERMS). Such drugs, like tamoxifen and raloxifen, attach to estrogen receptors tightly so that the cells with the receptors are freed from being affected by estrogen. One disadvantage of the SERMS is that uterine cells might escape their influence and might even become more prone to cancer development [9].

After the SERMS, the bisphosphonates (BPs) are another group of drugs developed for the treatment of osteoporosis. BPs are analogs of pyrophosphates which concentrate in bones inducing effective inhibitions on bone resorption. BPs were discovered empirically during studies of bone mineralization. The mechanism of action depends on the inhibition of an enzyme farnesyl diphosphate synthase, which takes an active part in the osteoclast survival and activity. Alendronate was the first BP popular for the control of bone resorption, lowering of bone turnover, and achieving a positive bone balance shown in BMD screening. Clinical studies have shown that taking BPs achieves about 50 % reduction in fracture of the spine and hip. Since then, BPs were further developed by offering lower doses and less frequent administrations (weekly, monthly and yearly instead of daily) through refinement in the chemical structures. BPs enjoy rapidly rising popularities because of their safety and users' high compliance. For at least two decades, BPs are known to be safe: only mild stomach upset and occasional renal and cardiac problems are encountered [10]. However, since longer durations of consumption (over 5 years) and high doses are given in cancer patients, serious problems start to appear in the bones

themselves. Avascular necrosis of the jaw occurred frequently in cancer patients using large doses of BP's. In orthopaedic practices, cases of atypical bone fractures following minimal trauma and occurring at odd sites were reported after 5–10 years of BP administration for the prevention of osteoporosis. The explanations given to such unusual happenings include: over-suppression of bone resortpion which destroys the normal balance of bone formation and bone loss leading to abnormal thickening of bone cortices which fail to respond effectively to mechanical stresses [11, 12].

Another therapeutic agent that inhibits bone resorption by blocking osteoclast activities is calcitonin, a hormone from the parathyroid gland. This hormone could be extracted from the pig and salmon and has been used first in cases of Paget's disease. Calcitonin is available as an injection or nasal spray. In cases of osteoporotic spine fracture, calcitonin offers a most effective option for pain control. One disadvantage of calcitonin is its tendency to null its own receptors, thus making therapy useless in prolonged administration [13].

Although most popular therapeutic agents used for the control or prevention of osteoporosis work via an anti-resorptive pathway, bone forming agents are also available. Parathyroid hormone is used as an anabolic agent. Parathormone should normally causes bone resorption and elevation of serum calcium. However it is also found to stimulate bone formation provided it is intermittently administered. Clinically injections of parathormone increases the BMD of the spine and femoral necks in osteoporotic women and men [14] which could be maintained for about 18 months after which it must be stopped, otherwise bone resorption instead would result.

Floride treatment markedly increases spinal BMD but it unfortunately also inhibits bone mineralization and apparently, does not lower fracture rates. Approval is therefore not obtained in the USA for use of floride in osteoporosis. Strontium on the other hand, is not only supporting bone formation but also mildly suppressing osteoclast actvities [15]. Strontium is popular in Europe as a therapeutic agent for osteoporosis.

Newer therapeutic agents are being investigated and will probably be developed soon, basing on the understanding of OPG/RANKL molecular biology. The complicated balancing effects of enzyme actions will open up new pathways of therapeutic development which is not mature yet. Other targets for inhibiting osteoclast activities are also being investigated. Cathepsin K is a lysosomal cysteine proteinase expressed at high levels within osteoclasts. It therefore forms a good target of molecular attack in the attempt to block bone resorption [16].

Orthopaedic surgeons are serving the remedial end of osteoporotic complications, i.e., when osteoporotic bones fracture. They should be aware of the availability of therapeutic options. Since the World Health Organisation classified declining BMD levels as attritable to "osteopenia" and "osteoporosis" [1], the need to consider preventive measures to contain the deterioration of BMD loss becomes necessary. Orthopaedic surgeons might remain modest to leave the general preventive programs to clinicians, nevertheless, when fractures have already happened, they need to be actively responsible for the prevention of future fractures. In that regard, orthopaedic surgeons should have an update command on the treatment policy of osteoporosis treatment. The following sketch gives a simple protocol for osteoporosis treatment at different ages (Fig. 37.1).

Apart from the generally accepted policy of prevention and treatment, orthopaedic surgeons should be able to explain to their patients about the adverse effects of different options of therapy so as to allow them to evaluate advantages against risks.

A simple recommendation of the general information to be given to patients about the adverse effects of therapeutic agents used for osteoporosis is given in Table 37.1.

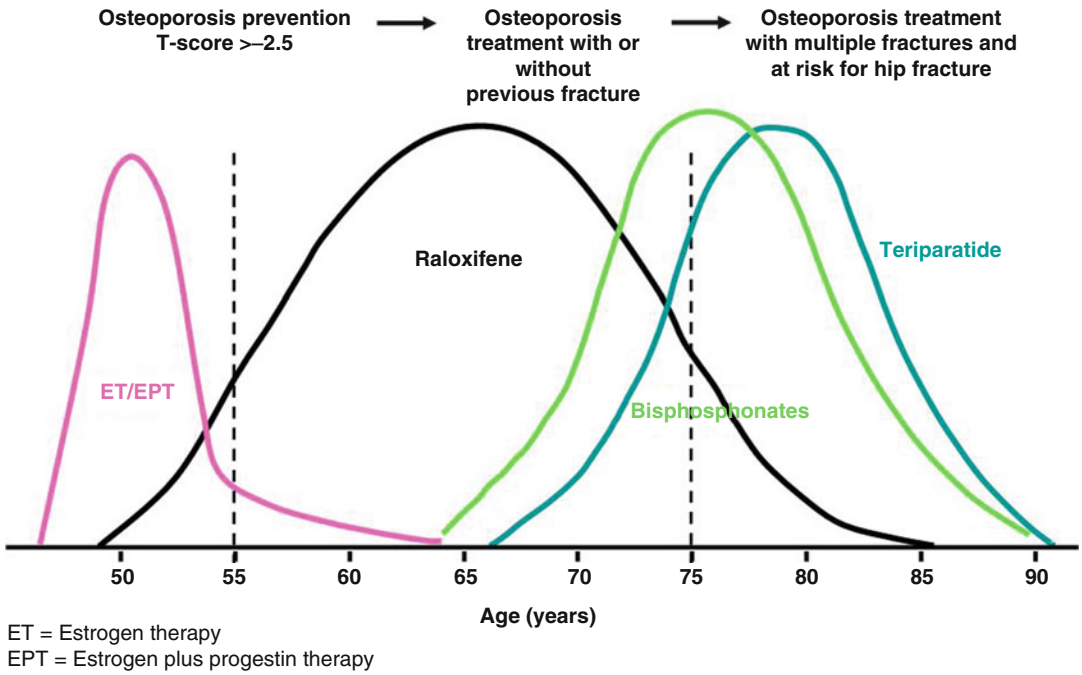

Fig. 37.1 A simple recommendation for the treatment of menopausal osteoporosis

Table 37.1 The adverse effects of therapeutic agents used for osteoporosis

Therapeutic agent	Serious adverse effects
Oestrogen	↑ Breast and uterine cancer incidence
SERMS	↑ Uterine cancer incidence
Bisphosphonates	Stomach upset, occasional cardiac and renal symptoms Prolonged use might disturb biomechanics of bone remodeling leading to odd fractures Avascular necrosis if the jaw happens when massive doses are used
Calcitonin	Develops receptor resistance, hence only indicated for short term treatment, particularly for pain control resulting from osteoporotic fracture of line spine
Parathormone	Only for short term use (18 months) (osteoblastic effects)
Strontium	In granule form, mild stomach upset
New therapy (OPG/RANKL target Growth factors, New Bone resortpion inhibition)	Not ready for recommandation

Osteoprosis and the Spine

Since Osteoporosis is a pathological feature of ageing, how is the spine being affected? What are the changes in the vertebral bodies and intervertebral discs? [17]

The morphological changes of the osteoporotic spine include a gradual loss of vertical height because of micro-fractures of the vertebral bodies, and deformities might occur if more severe fractures occur, particularly when multiple levels are involved. The osteoporotic spine would not respond uniformly to the decline of mechanical strength of the supporting vertebral bodies, as bone mineral density (BMD) decreases. Instead, a number of risk factors would be jointly affecting different patterns of behaviour [18, 19].

Degeneration is a fact of life. The spine, being the major weight bearing pillar of the human body, naturally would give prominent manifestations of degeneration with aging. Loss of bone minerals is another sign of advancing age and slowing of physical activities. Epidemiological studies in the past years have shown the prevalence of lumbar spondylosis with increasing age, affecting particularly those with a high working demand on mechanical stress. The intervertebral discs are structurally designed as shock-absorbing units to maintain the weight bearing function and in so doing, would be very much affected by degeneration [20]. It has long been known that intervertebral discs lose their central fluid contents with aging, resulting in shrinkage and loss of height [17].

In a study looking at the prevalence of osteoporotic vertebral fractures (loss of height) among Asians which included Chinese, Koreans, Indonesians and Japanese, it was found that the risk factors were low BMD, maternal history of osteoporosis, older age, defective physical ability and the presence of cataracts [21]. In that study the intervertebral discs were not assessed. One additional interest could have been: whether the elderly people being studied had shrinking discs like the degenerative spine.

A number of studies aiming at the identification of risk factors in relation to osteoporotic fractures of the spine were available in current literature. None of them took special interests at the intervertebral discs [22–25].

In fact, it has appeared to the orthopaedic surgeon for a long time that although spondylosis and osteoporosis of the spine are both degenerative pathologies, they do not co-exist together in the same patient. This practical observation has not been taken seriously by other experts on osteoporosis, although as early as 1991 and 1996, reports on such relationship between lumbar spondylosis and osteoporosis were already available. In the recent few years, more clinical studies were completed on the investigation of the relationship between the degenerative and osteoporotic spine, and the morphology of the intervertebral discs.

Verstraeten and Van Ermen observed that osteoarthritis retarded the development of osteoporosis in 1991 [25]. Margulies and Payzer made the similar observations on the lumbar spine [26]. In 2003, Dequeker and Miyakoshi both reported clinical and research evidences of the inverse relationship between degenerative and osteoporotic spine [27, 28]. The BMD changes (increases) of the spine in relation to degenerative changes in elderly women were studied by Muraki and Yamamoto in Japan in 2004 [29] and the reverse relationship was again observed. There should be little doubt today that degenerative changes in the spine slows down the development of osteoporosis and the BMD is also better maintained.

Osteoporosis and Intervertebral Discs

Orthopaedic surgeons, for many years, have also observed that for the severely collapsed vertebral bodies caused by osteoporosis, the intervertebral discs adjacent to the affected vertebral bodies, tend to occupy a wider space radiologically.

In 2001, we completed a survey on the morphological changes in the spine of elderly Chinese women and found that shortening of the vertebral bodies co-existed with widening of the intervertebral discs.

While enlarged intervertebral discs assumingly, could be due to breakage of the end plates of the vertebral bodies, leaving vacant spaces to be filled, but why should the disc, which normally dry up and shrink with age, expand instead [30, 31]? This phenomenon has not been explained but increasing interests are mounting. In 1998, Harada studied the relationship between BMD and intervertebral discs and observed decreasing heights with increasing BMD [17]. In 2005, Baron reported disc changes in treated and untreated overweight post-menopausal women [32]. Pye and Reid did the same study on men and women with different values of BMD. The observation was: wider disc spaces accompanied low BMD [33]. In 2007, we reported a modified grading system for

lumbar disc degeneration in elderly subjects [34]. We used this grading system to estimate, using MRI, the volume of vertebral bodies and discs, which were observed to decrease with decreasing BMD: the vertebral bodies strictly obeyed this principle while the intervertebral disc behaved less impressively. In fact, when marked decrease in vertebral heights occurred, the disc in-between would even expand [35].

We did another study using MRI to detect disc degeneration in relation to BMD in elderly subjects. Among 196 females and 163 males, females were found to have more severe disc degeneration than males; and lower BMD was associated with less severe disc degeneration [36].

Clinical Implications

Now that we are aware of the reverse relationship between osteoporosis and osteoarthritis of the spine, if the molecular causes leading to this reverse relationship were known, new treatment options for both conditions might emerge. Our earlier observations showed that decreasing spinal BMD could be related to a decline in the blood supply to the bone. Osteoporosis in the spine could be involving complex molecular changes [37]. The higher contents of fatty tissues within the vertebral bodies in the osteoporotic spine further supported the assumption and the need for further research [38].

With regard to the behaviour of the intervertebral disc in spinal osteoporosis, are there clinical implications? Firstly, to observe the progress of the osteoporotic spine, and to comment on the prognosis, it is important to include an analysis of the intervertebral discs. The more changes in the discs, the more collapses of the vertebral bodies may be expected. On the other hand, the expanded discs should have positive effects on the maintenance of the height of the individual and might also have symptom relieving effects.

Secondly, now that vertebroplasty and kyphoplasty are getting popular, surgeons should be aware that not only are the long-term effects of the minimally invasive procedures remain uncertain [39, 40] but the morphology of the intervertebral discs should have influences on the behaviour of the adjacent vertebral bodies which will be facing the stress-riser challenges of the hardened vertebrae after cement injection. This issue will be further discussed in the subsequent paragraphs.

Thirdly, surgeons attempting to perform open surgery on the osteoporotic spine should be aware of the bizarre morphology of the intervertebral discs: some of them undergoing the usual degenerative changes while other could be less affected and might be even expanded. Without the awareness, surgeons might not be able to put in implants accurately.

Treatment of Osteoporotic Fracture in the Spine

The vertebral bodies of the spine, because of their constant weight-bearing role, must be the most frequently affected skeletal units in osteoporosis associated with ageing. Fractures of the long bones resulting from bone loss have received a lot of attention because of the absolute need and sometimes, complexity of surgical management. When preventive treatment is administered for osteoporosis, the main justification lies on the reduction of fracture risks related to the hip region, while the fractures occurring in the vertebral bodies are not of equivalent concern [41]. As a matter of fact, both male and female, when reaching elderly age, commonly suffer from arthritic changes of the joints, of which the spine is also most frequently involved. Pain arising from degenerative changes of the spinal units cannot be differentiated from that initiated by the gradual collapse of the vertebral bodies as a result of loss of bone substance. Such back pain is usually taken as a fact of life among the elderlies, until an acute severe vertebral collapse initiates severe pain that demands an imaging investigation which will reveal the osteoporotic vertebral fracture.

An osteoporotic vertebral collapse might be the cause of severe back pain that would gradually

go away automatically or, at its worst, takes a week or two to subside. Hence for the usual cases, no specific treatment plan is required apart from bed rest and simple pain control measures [42]. It is only in recent years, when interventional radiography becomes the fashion, that advocates on active treatment for osteoporotic vertebral bodies develop special techniques to achieve more effective pain control and even preservation of the vertebral height of the affected vertebra in operative procedures of vertebroplasty and kyphoplasty.

The rationale of either vertebroplasty or kyphoplasty is simple. Since vertebral bodies do not have a rich supply of sensory nerve fibres, the pain resulting from a osteoporotic collapse is due to a variable degree of instability arising from the lost height. Therefore preserving the vertebral height by using acrylic to fill up the empty spaces would preserve the stability, thence control the pain. Since the procedures are gaining higher and higher popularities, we would discuss the indications, procedures, justifications and adverse effects in detail in the following paragraphs.

Indications

One has to be very clear about the indications of acryllic strengthening of the osteoporotic vertebral collapse before starting the special procedure of either vertebroplasty or kyphoplsty. The most straightforward indication is uncontrollable pain in an elderly person who cannot tolerate. Reports have indicated that pain control could be rapid in a high percentage of cases. Secondly, the number of vertebral bodies involved would affect the result of treatment. Single level gives the best results while more levels give uncertain outcome. Other factors affecting the results include the technique of instrumentation and whether the acryllic could stay in the desirable site, as leakage during injection tends to be unavoidable. The timing of the procedure is also important because late administration and chronic cases have been shown to be less effective [43].

Technique of Vertebroplasty/ Kyphoplasty

Perfect facilities of radio-imaging and spinal injection instrumentations should be available. The technical team should be experienced with minimally invasive procedures, procedures related to spinal biopsy or intervertebral disc manoevres. The site of entry into the osteoporotic vertebral body is the spinal pedicle which can be entered unilaterally or bilaterally. The appropriate canulla should be chosen to allow sufficient amount of acryllic injection. Since the adequate amount of acryllic is essential for the success of the procedure, the fluidity of the acrylic is cruxial. Insufficient amount of acryllic fails to satisfy the filling effects to maintain stability. Too much amount predisposes to leakage around the vertebral body leading to spinal canal obstruction or might be even direct invasion of the paraspinal venous plexuses. Special acryllic bone cement has been created to facilitate vertebroplasty injections.

The choice of Kyphoplasty is based on the assumption that spacing up the fractured space in the vertebral body with an inflatable balloon would allow the appropriate amount of acryllic to be injected so that the preservation of vertebral height could be better achieved. This procedure is naturally more invasive and technically more demanding apart from being more costly [44].

Outcome of Vertebroplasty/ Kyphoplasty

The expected achievements of vertebral augmentation include pain relief, vertebral height restoration, and better functional outcome. The results of various studies have demonstrated that in single vertebra augmentation, pain control tends to be quicker in at least 80 % of cases in the first 6 weeks, after which there is no difference with the unoperated patients. There is no obvious difference in pain control between the verterbroplasty and kyphoplasty groups. The efficacy on pain control cannot be correlated with age, sex, BMD, personal habits and medications.

Even when there is no height restoration, pain control is still achieved.

When the vertebral height is assessed for restoration after augmentation, it is found that the gain in height is limited to 2.9–8.4 mm only. Kyphoplasty is usually gaining more than vertebroplasty but the difference is not remarkable. Looking at the correction of angulations resulting from the compression fracture, very limited achievements are observed. For vertebroplasty, angle correction is 4.3–6°, whereas for kyphoplsty, 3.4–9°.

Other functional outcomes like ambulation ability and hospital stay, also show improvement. Over 90 % of patients become ambulatory in a shorter period and 40 % have shorter hospital stays [45–48].

Complications of Vertebroplasty/ Kyphoplasty

Percutaneous vertebral augmentation is not without danger if one only studies carefully the venous anatomy around the vertebral units. Intra-operatively, the leakage of acryllic through cracks in the fractured vertebral body may lead to invasion of the para vertebral venous plexuses or leakage into the spinal canal. In the former case, cerebral and pulmonary embolism have been reported. In the latter, early or late neurological damages may result. It has been estimated that 9–70 % of vertebroplasties and 2–33 % of kyphoplasties actually produce intraoperative leakage of acryllic outside the collapsed vertebral body [45].

Apart from complications of acryllic leakage during operation, other adverse events have been reported. They include: rib fracture, spinal pedicle fracture, dural tear, epidural haematoma, nerve injuries and misplacements.

Late complications are related to the change of the biomechanical state of the spine after the injection. The injected vertebral body is much denser and harder than its counterpart above and below, thus producing an abnormal state of stress-riser. With further decline of BMD in the vertebrae as osteoporosis develops further, the stress-riser effect is increasing all the time, putting extra-mechanical stresses above and below. Frankel reported that 12–50 % of vertebroplasties and 20–30 % of kyphoplasties develop compression fractures in the adjacent vertebrae within one year [49].

Selection Between Vertebroplasty and Kyphoplasty

Advacates on kyphoplasty expect better preservation of vertebral heights after Kyphoplasty which involves a forced expansion of the fracture space. Using a mechanical balloon to achieve the expansion is a sound concept. However, one could imagine that the limited space and the different natures of the vertebral compression fractures would be hindering the ideal achievement of the operative manoevre.

Many comparative studies have already shown the following:

(i) Both kyphoplasty and vertebroplasty show efficacy in pain control and improvement in quality of life.
(ii) Kyphoplasty creates larger space for acryllic filling, therefore requires less pressure and produces less leakage.
(iii) Kyphoplasty produces better height restoration.
(iv) Both kyphoplasty and vertebroplasty achieve little angulation correction.

However the difference between the two procedures are not impressive, neither are the long term results after 1 year [50, 51].

A Correct Attitude on Vertebral Augmentation

One controversial area still exists in spite of the growing popularity of vertebral augmentation. Osteoporosis affecting the BMD of the vertebral bodies is a slow continous process, that affects all levels although some of the more stress-bearing levels tend to be more affected than others. After

strengthening and stabilizing one fractured vertebral body, is the same procedure to be repeated when other levels suffer the same hazard? On the other hand, it is also well known that vertebral compression fractures do not cause too much instability and the most bothering symptom, viz, pain, generally disappear gradually with time. Is surgical intervention really necessary?

Two clinical studies have been started to investigate whether acryllic filling, i.e. vertebroplasty, has advantages over conservative treatment of active observation and symptomatic treatment. The final analysis will throw light on the available procedures of vertebral augmentation, which, though "non-invasive", is not without complications [39, 40].

Before the objective answer becomes clear, orthopaedic surgeons should not be overwhelmed with a "new" option for treatment of osteoporosis which is a continuous physiological process. At the present stage, they may carefully review the indications known to be giving the best outcome in the short term. Table 2 gives a summary of the recommendations. (Table 37.2)

Uncertainties related to vertebral augmentation need to be addressed. We are yet uncertain about the favourable age range, number of vertebral units, that can be safely injected, types of fracture and BMD levels that would do better with augmentation. Neither are we clear about the morbidities and even mortality related. Moreover, we remain skeptical about "prophylactic" augmentation.

On the other hand, we are aware that interesting research on bio-engineering, including special acryllics that would allow easy injection, firmer consolidation to bone texture is in progress. Results of vertebral augmentation may be improved with the better injection maternal, which might also be mixed with hydroxyapaptite and bone substitutes.

Table 37.2 Recommendations for vertebral augmentation

More favourable results are expected with the following:
Single unit, T11 – L2
Single Burst fracture, mild
Anterior wedging >30°
Progressive collapse
Conservative treatment failed badly
Essential requirements are:
Excellent fluoroscopy
Accurate cannula placement
Prevention of infection
Good cement contrast
Ba SO4 30 % Wt/val. to PMMA could be considered
Accurate volume of cement injection must be accomplished
Slow injection 6–8 min (sets in 20 min)
Low injection Pressure (90 % strength in 60 min)

Conclusion

Osteoporosis is a physiological process in the bones happening in aging. We worry about the complications which are the occurrence of fractures. We have, to date, means to slow down the physiological process which is losing its balance with aging. We do this by either slowing down the bone loss or increasing the bone regeneration. These artificial means, apart from fulfilling their specific mechanistic tasks, unfortunately also interfere with the normally active remodelling power of the bone, thus giving real worries when long term administration is required.

Fractures in the elderlies result from a variety of predisposing conditions of which the important ones like declining general physique and balancing power, medication, unfavourable physical environments, could be more important than a declining BMD. It is therefore in-correct to rely solely on the BMD level to consider drug treatment as the only means of fracture prevention. One must realize that what the reports refer to as reduced percentages of fracture risks are overall general statistical messages that might not apply to the individual who is under his/her own personal risks of fracture development. In the planning for prophylactic treatment therefore, one must weigh the general benefits of the therapy against the possible complications and avoid being over-energetic.

On the other hand, some orthopaedic surgeons receive osteoporotic fracture patients, give them adequate surgical treatment and yet hesitate to suggest therapeutic means to slow down the declining BMD with the aim of preventing another fracture. Under such circumstances, since the osteoporotic fracture already happened, one expects a rapid decline of the general physique which will be a real high risk predisposing to unexpected falls, thence bone fractures. Under such circumstances, hardening the bones should be a real logical consideration helpful to the prevention of another fracture.

When compression fractures in the vertebral bodies have occurred as a result of loss of bone substance, they frequently escape the attention of both the patient and attending physician unless pain becomes prominent. When the fracture becomes known, two opposing attitudes are prevalent: either staying conservative and keep waiting for spontaneous disappearance of pain, or hurrying to interventional surgical treatment. The responsible surgeon should not forget the analgesic effect of calcitonin for osteoporotic vertebral fractures. Only if pain control is unsatisfactory and interventional imaging facilities are available, the option of minimally invasive surgery, viz vertebroplasty/kyphoplasty, could be considered. Nevertheless, since the long term outcome of the augmentation procedures are yet uncertain, surgical intervention should be kept as a last resort, rather than a routine, practice.

References

1. WHO. Prevention and management of osteoporosis. World Health Organ Tech Rep Ser. 2003;921:1–164.
2. Reginster JY, Burlet N. Osteoporosis: a still increasing prevalence. Bone. 2006;38(2 Suppl 1):S4–9.
3. Bonura F. Prevention, screening and management of osteoporosis: an overall view of current strategies. Postgrad Med. 2009;121(4):5–17.
4. Kanis JA, Oden A, Johnell O, et al. The use of clinical risk factors enhances the performance of BMD in the prediction of hip and osteoporotic fractures in men and women. Osteoporos Int. 2007;18(8):1033–46.
5. Teitelbaum SL. Bone resorption by osteoclasts. Science. 2000;289:1504–10.
6. Southby J, Kissin MK, Danks JA, et al. Immunohistochemical localization of parathyroid hormone-related protein in human breast cancer. Cancer Res. 1990;50:7710–6.
7. Guise TA, Yin JJ, Taylor SD, et al. Evidence for a causal role of parathyroid hormone-related protein in the pathogenesis of human breast cancer-mediated osteolysis. J Clin Investig. 1996;98:1544–9.
8. Michaelsson K. Hormone replacement therapy and risk of hip fracture: population based case–control study. Br Med J. 1998;316:1858–63.
9. Sato M, Grese TA, Dodge JA, et al. Emerging therapies for the prevention or treatment of postmenopausal osteoporosis. J Med Chem. 1999;42:1–24.
10. Ensrud KE, Barrett-Cannor EL, Schwartz A, et al. Randomised trial of effect of alendronate continuation versus discontinuation in woman with low BMD. J Bone Miner Res. 2004;19:1259–69.
11. Schneider JP. Should bisphosphonates be continued indefinitely? An unusual fracture in a healthy woman on long-term alendronate. Geriatrics. 2006;61:31–3.
12. Cheng KH, Leung KK, Lee KC, et al. Sequential nontraumatic femoral shaft fractures in a patient on long term alendronate. Hong Kong Med J. 2007;13(6):485–9.
13. Wada S, Udagawa N, Nagata N, et al. Physiological levels of calcitonin regulate the mouse osteoclast calcitonin receptor by a protein kinase Alpha-mediated mechanism. Endocrinology. 1996;137:312–20.
14. Lindsay R, Nieves J, Formica C, et al. Randomised controlled study of effect of parathyroid hormone on vertebral-bone mass and fracture incidence among postmenopausal women on oestrogen with osteoporosis. Lancet. 1997;350:550–5.
15. Riggs BL, Hodgson SF, Ofallon WM, et al. Effect of fluoride treatment on the fracture rate in postmenopausal women with osteoporosis. N Engl J Med. 1990;322:802–9.
16. Rodan GA, Martin TJ. Therapeutic approaches to bone diseases. Science. 2000;289:1508–14.
17. Harada A, Okuizumi H. Correlation between BMD and intervertebral disc degeneration. Spine. 1998;23:857–67.
18. WHO. Assessment of fracture risk and application to screen for post-menopausal osteoporosis. WHO technical report series. Geneva: WHO; 1994. p. 1–129.
19. Lau EMC, Chan HL, Leung PC. Normal ranges for vertebral height ratio and prevalence of vertebral fracture in Hong Kong Chinese: a comparison with America Caucasians. J Bone Miner Res. 1996;11(9):1364–8.
20. Andersson GB. Epidemiological features of chronic low back pain. Lancet. 1999;354:581–3.
21. Lau EM, Chan YH, Leung PC. Vertebral deformity in Chinese men: prevalence, risk factors, BMD and body composition. Calcif Tissue Int. 2000;66(1):47–52.

22. Rowe SM, Sung ST, Lee JY. Epidemiology of osteoporosis in Korea. Osteoporosis Int. 1997;7 suppl 3:S88–90.
23. Xu L, Cummings SR, Qin M. Vertebral fractures in Beijing. China J Bone Miner Res. 2000;15(10): 2019–25.
24. Cooper C, Atkinson EJ. Incidence of clinically diagnosed vertebral fractures in Rochester, Minnesota, 1985–1989. J Bone Miner Res. 1992;7(2):221–7.
25. Verstraeten A, Van Ermen H. Osteoarthrosis retards the development of osteoporosis: observation of the co-existence of osteoarthrosis and osteoporosis. Clin Orthop. 1991;264:169–77.
26. Margulies JY, Payzer A. The relationship between degenerative changes and osteoporosis in the lumber spine. Clin Orthop. 1996;324:145–52.
27. Dequeker J, Aerssens J. Osteoarthritis and osteoporosis: clinical and research evidence of inverse relationship. Aging Clin Exp Res. 2003;15:426–39.
28. Miyakoshi N, Itoi E, Murai H. Inverse relationship between osteoporosis in post-menopausal women. Spine. 2003;28:492–5.
29. Muraki S, Yamamotos S, et al. Impact of degenerative spinal disease on BMD of the lumbar spine in elderly women. Osteoporosis Int. 2004;15:724–48.
30. Leung PC, Or A, Lau EMC. Morphological changes in the osteoporotic spine of elderly Chinese women. Hong Kong J Orth Surg. 2002;6(1):27–33.
31. Kellgren JH, Lawrence JS. Osteoarthrosis and disc degeneration in the urban population. Ann Rheum Dis. 1958;17:388–96.
32. Baron YM, Bincat MP, Galleja N. Inter vertebral disc height in treated and untreated over weight postmenopausal women. Hum Reprod. 2005;20:3566–70.
33. Pye SR, Reid DM, Adams JE. Radiographic features of lumbar disc degeneration and BMD in men and women. Ann Rheum Dis. 2006;65:234–8.
34. Griffith J, Wang YX, Leung PC. Modified Pfirrmann grading system for lumbar intervertebral disc degeneration in elderly subjects. Spine. 2007;32:E708–12.
35. Kwok AW, Griffith J, Leung PC. Estimated volume of both vertebral body and disc decreases as BMD decreases though this effect is seen more in the vertebral body than the disc. Bone. 2008;43 suppl 1:S66–7.
36. Wang YX, Griffith J, Leung PC. Relationship between gender, BMD and disc degeneration in the lumbar spine: a study in elderly subjects using an eight-level MRI based disc degeneration grading system. Osteoporos Int. 2011;22:91–6.
37. Griffith J, Yeung DKW, Leung PC. Vertebral BMD, marrow perfusion and fat content in healthy men and men with osteoporosis: dynamic contrast-enhanced MR imaging. Radiology. 2005;236:945–51.
38. Griffith J, Yeung DKW, Leung PC. Compromised bone marrow perfusion in osteoporosis. J Bone Miner Res. 2008;23(7):1068–74.
39. Klazen CA, Verhaar HJ, Lohle PNM, et al. VERTOS II: percutaneous vertebroplasty versus conservative therapy in patients with painful osteoporotic vertebral compression fractures; rationale, objectives and design of a multicenter randomized controlled trial. Trials. 2007;8(33):1–5.
40. Gray LA, Jarvik JG, Heagerty PJ, et al. Investigational vertebroplasty efficacy and safety trial a randomized controlled trial of percutaneous vertebroplasty. BMC Musculoskelet Disord. 2007;8(126):1–7.
41. Rotella DP. Osteoprosis: challenges and new opportunities for therapy. Curr Opin Drug Discov Devel. 2002;5(4):477–86.
42. Lau EMC, Leung PC. Osteoporosis and fractures. In: Obrant K, editor. Management of fractures in severely osteoporotic bone. London: Springer; 2000. p. 3–13.
43. Lewis G. Percutaneous vertebroplasty and kyphoplasty for the stand-alone augmentation of osteoporosis-induced vertebral compression fractures: present status and future directions. J Biomed Mater Res B Appl Biomater. 2007;81B(2):371–86. doi:10.1002/jbm.b.30674.
44. Groen RJM, Phillips FM, Hoogland PV, et al. Anatomical and pathological considerations in percutaneous vertebroplasty and kyphoplasty: a reappraisal of the vertebral venous system. Spine. 2004;29(13): 1465–71.
45. Shen MS, Kim YH. Vertebroplasty and kyphoplasty: treatment techniques for managing osteoporotic vertebral compression fractures. Bull NYU Hosp Jt Dis. 2006;64(3):106–13.
46. Mathis JM, Ortiz AO, Zoarski GH. Vertebroplasty versus kyphoplasty – a comparison and contrast. Am J Neuroradiol. 2004;25:840–5.
47. Phillips FM, Ho E, Gupta P. Early radiographic and clinical results of balloon kyphoplasty for treatment of osteoporotic vertebral compression fractures. Spine. 2003;28(19):2260–5.
48. Lavelle W, Carl A, Khaleel MA. Vertebroplasty and kyphoplasty. Anaesthesiol Clin. 2007;25(4):913–28.
49. Frankel MB, Monroe T, Wang C. Percutaneous vertebral augmentation: an elevation in adjacent level fracture risk in kyphoplasty as compared with vertebroplasty. Spine J. 2007;7:575–82.
50. Deramond H, Saliou G, Aveillan M, et al. Respecture contribution of vertebroplasty and kyphoplasty to the management of osteoporotic vertebral fractures. Joint Bone Spine. 2006;73:610–3.
51. Cloft HJ, Jensen ME. Kyphoplasty: an assessment of a new technology. Am J Neuroradiol. 2007;28: 200–3.

Optimised Treatment of Hip Fractures

38

Karl-Göran Thorngren

The Future Problem

Fractures of the proximal part of the femur, hip fractures, are common and costly. The number of hip fractures has increased in all western countries during recent decades. This has occurred mainly because of an increase in the number of elderly people and also due to an increase in the risk for hip fracture among the oldest persons [1–5]. Due to an increase in ageing population all over the world there will be a geographical shift in the occurrence of hip fractures. The incidence rates of hip fractures are higher in white populations than in others and vary by geographical region. Age adjusted incidence rates of hip fracture by gender are higher in Scandinavia than in North America and lower in countries of Southern Europe [6, 7]. The absolute number of hip fractures in each region is determined not only by ethnic composition, but also by the size of the population and its age distribution. In 1990 one third of all hip fractures in the world occurred in Asia despite lower incidence rates among Asians. Almost half of the fractures occurred in Europe, North America and Oceania. These populations are smaller but older. It was estimated in the beginning of the 1990s that 323 million people aged 65 years and over were living around the world. This has been estimated to increase to 1555 million by the year 2050 [8]. The increase will be especially high in Africa, Asia, South America and the Eastern Mediterranean regions. In USA demographic changes alone will more than double the number of hip fractures from 238,000 1986 to 512,000 in the year 2040 [8]. In another publication [9] the 340,000 hip fractures around year 2000 will increase to 650,000 in the year 2050. It has been calculated that the now close to two million hip fractures in the world could rise to over six million in the year 2050. Of these then 71 % is calculated to be in Africa, Asia, South America or the eastern Mediterranean region [10].

Already today hip fractures are highly resource consuming and strenuous for the organisation of medical care. Optimised methods for operation and rehabilitation along with preventive measures are necessary to cope with this increasing problem, otherwise it can become overwhelming.

Fracture Types

Hip fractures consist of different types in the proximal femur. It is very important whether the fracture is located in the femoral neck (cervical fracture, intracapsular) or through the parts of the proximal femur which constitute muscle insertions (trochanteric fractures, extracapsular) because both the treatment and the cause of

K.-G. Thorngren, MD, PhD, FRCSEd(Hon)
Department of Orthopedics,
Skane University Hospital, Lund, Sweden
e-mail: karl-goran.thorngren@med.lu.se

D.G. Poitout (ed.), *Biomechanics and Biomaterials in Orthopedics*,
DOI 10.1007/978-1-84882-664-9_38

healing are different [11]. Cervical fractures are best classified into undisplaced (Garden I and II) or displaced (Garden III and IV) [12]. Other subgrouping has proven difficult to reproduce [13]. The trochanteric fractures are for routine use best classified into two-fragmented fractures (stable) or multi-fragment fractures (unstable). The basocervical fractures are a transition form between cervical and trochanteric fractures. They are usually treated as trochanteric fractures, but can in some cases have healing complications similar to the cervical ones. Sub-trochanteric fractures are more comminuted and include the area down to 5 cm below the trochanter minor.

The blood supply to the femoral head is often damaged after cervical fractures, because the vessels either penetrate within the marrow cavity or are positioned sub-periosteally on the femoral neck. Varying degree of vascular damage caused at the fracture moment will give varying amount of healing complications. The extracapsular trochanteric fractures have good vascular supply and few healing complications. Some of them are however very shattered with stability problems. Different systems for a more detailed classification of the fractures exist, but these are best suited for specialised research projects, as the reproducibility has been a major problem. In the Swedish national registration of hip fractures (RIKSHÖFT) Table 38.1 shows the fracture types registered based on 170,000 cases.

The diagnosis of a hip fracture is made by ordinary x-ray. On these pictures also the fracture type is classified. It also gives information about circumstances that can influence the choice of operation method, i.e. earlier performed operations. It can also disclose a pelvic fracture, which is a common differential diagnosis for pain from the hip area in elderly patients after a fall. All patients with pain from the hip after a fall, who have a normal, ordinary x-ray should be furthering diagnosed with MRI. It can usually disclose undisplaced hip fractures with risk of displacement and potential functional problems. It is also good for diagnosing undisplaced pelvic fractures, which are not uncommon in the pelvic rami in these age groups. If there is no access to MRI also a CT can disclose fractures, but not totally dismiss the suspicion. Scintigraphy performed after a couple of days can strengthen the fracture suspicion if positive with a localised high uptake. In lack of all these facilities mobilisation with weight bearing under supervision is a possibility with repeated x-ray check-ups, but it is a rather costly way of treatment as the patient usually has to be put into a hospital ward. MRI has proven particularly valuable for acute diagnosing of undisplaced fractures, which are not possible on ordinary x-ray. On the STIR-sequence an increased signal in the bone marrow is seen and on T1-weighted pictures the fracture oedema is seen as a dark line against a light background of trabecular bone marrow.

Table 38.1 Fracture types registered based on 170,000 cases in the Swedish national registration of hip fractures

Type I	Undisplaced cervical fractures	16.1 %
Type II	Displaced cervical fractures	36.3 %
Type III	Baso-cervical fractures	3.6 %
Type IV	Trochanteric two-part fractures	22.6 %
Type V	Trochanteric multi-fragment fractures	14.6 %
Type VI	Sub-trochanteric fractures	6.8 %

Already in the pre-operative course increased attention should be given to the pain relief of the patient, prevention of pressure sores and an early handling for rapid operation. The treatment should aim at operation as soon as possible, immediate mobilisation on the next day with full weight bearing as much as can be tolerated from pain, but no limitations in weight bearing due to fear of instability in the osteosynthesis. Only in certain very comminuted pertrochanteric or subtrochanteric fractures non-weight bearing should be recommended. In the other cases, particularly the femoral neck fractures, an early weight bearing is a test of the stability of the osteosynthesis and a failure can then be rapidly followed with a re-osteosynthesis or with a hip arthroplasty.

For the fracture types listed above the two major controversial areas are the displaced femoral neck fractures and the trochanteric multifragment fractures in combination with subtrochanteric fractures. The cervical displaced fractures are a combined biological and biomechanical problem due to the influence of the blood supply to the

healing whereas the trochanteric/subtrochanteric fractures are predominantly a biomechanical stability problem due to the good vascularisation of the bone fragments. There are different philosophies for the treatment of these different fracture types, which will be further discussed below. It is possible to determine the circulation to the femoral head with high accuracy with the use of scintimetry, but this is resource consuming and also tends to delay the operation. MRI, probably with contrast, will possibly in the future become available, as a routine tool for the choice of operation method for femoral neck fractures, but these techniques are not yet developed.

Cervical Fractures

The blood supply to the femoral head after a cervical fracture has a decisive importance for the healing. The healing complications after a cervical fracture consist either of re-dislocation (early change of position) or pseudarthrosis (non-healing) or segmental collapse (femoral head necrosis after a healed fracture) [14–16]. A segmental collapse is thus re-building of the femoral head after vascular damage and needs a healed fracture for the vessels to grow in. At present there is no practical useful method to determine the blood circulation pre-operatively. The degree of dislocation of the fracture on an ordinary x-ray picture is not prognostically sufficiently accurate. Preoperative scintimetry is resource consuming, depending on the positioning of the leg and delays the operation. MRI is not yet developed for this purpose. The goal for the future and a very important area for research is to be able to prognosticate the healing complications already pre-operatively and based on that choose the primary method for operation. Patients with a good blood supply to the femoral head should then get a primary osteosynthesis and those with a clearly bad circulation instead a primary arthroplasty. In waiting for this diagnostic possibility the choice of operation method will be dependent on the grade of dislocation seen on the x-ray picture combined with the age of the patient, the patient's other medical conditions and her functional level pre-fracture.

Undisplaced Cervical Fractures

These have little or no displacement of the fracture and usually very little risk for vascular damage to the femoral head and thereby little healing complications. This group of cervical fractures contains the Garden groups I and II [12]. Primary operation with osteosynthesis is advocated all over the world. The most used methods are either two or more parallel screws or two hook pins. The screws mostly differ by modifications of the configuration of the screwing in the top part [11, 17]. A few centres have tried not to operate some undisplaced fractures [18]. This leads to increased risks of dislocation and thereby a prognostic deterioration for the healing. Non-operative treatment also demands non-weight bearing and increased check-ups, both clinically and with radiography. It is a much safer method to operate the fracture and allow the patient full immediate weight bearing [19].

Displaced Cervical Fractures

These fractures have been the area of continuous disagreement for the last half century. Slowly more agreement is reached. There is a geographical difference internationally concerning the treatment principles for the displaced cervical fractures. In Scandinavia, particularly in Sweden and Norway, primary osteosynthesis has been performed in all cases with displaced cervical fractures. The basic philosophy has been to perform a small, quick and for the patient less burdening operation first and in the case of a healing complication later as a secondary procedure do a well-planned arthoplasty. This is usually then performed as a total hip arthroplasty where both the femoral and the acetabular parts are exchanged. It is an undisputed fact that the best long-term result after a femoral neck fracture is a healed fracture and preservation of the patient's own femoral head provided no segmental collapse appears. This will give no future problems. An arthroplasty always has the risk of dislocation in the short time perspective and in the long run the risk of loosening and for the hemi-arthroplasties

also by the years deterioration of the acetabular cartilage. When a patient has been operated with an osteosynthesis and 2 years has passed since the fracture and this is healed without complications, there is little risk of further problems from this hip [11, 20]. Some patients however never regain the full functional level that they had before the fracture. The complications after an arthroplasty increase after 5–10 years and this risk has to be balanced against the expected remaining lifetime for the patient [21]. Therefore arthroplasty is used mainly in elderly patients with clearly displaced fractures.

Internationally in many western countries the primary choice for a displaced femoral neck fracture is to perform an arthroplasty. This basic principle has been to treat all patients with arthroplasty to avoid healing complications in some. The treatment philosophy is now modified and an increasing amount of primary osteosyntheses is performed above all in relatively younger patients and those with less severe dislocation. Many studies have shown somewhat increased mortality after primary arthroplasty compared to primary osteosynthesis [11, 21, 22]. At the same time studies have shown a higher need of re-operation after the primary osteosynthesis within the first 2 years after the fracture compared to after a primary arthroplasty. The complications after a primary arthroplasty develop later and also a re-arthroplasty is a bigger operation and has more inherited complications than a secondary arthroplasty after a failed primary osteosynthesis [17].

The international literature shows that healing problems due to vascular damage of the femoral head by the displaced cervical fracture leads to non-union in 10–30 % of the cases and segmental collapse in further 10–20 % of cases. With an optimised osteosynthesis technique the healing complications (both non-union and segmental collapse) has been limited to in total 20–25 % for the displaced cervical fractures [20, 23].

Primary arthroplasty results in dislocation in around 4 % of the cases with hemi-arthroplasty and in 10 % with total hip arthroplasty. Infection consists of 2–5 %. Following a hemi-arthroplasty around 20 % of the cases in the long run develop wear and deterioration of the acetabular cartilage. Loosening is expected in around 10 % of the cases. Fracture in connection with the arthroplasty amount to 2–4 %. Re-operation with arthroplasty after a primary osteosynthesis has been reported to 20–30 % of the displaced cervical fractures. A major re-operation within the first years after a primary arthroplasty is expected to be needed in around 10 % of the cases. These are then rather complicated operations [11, 17, 21].

Unipolar hemiarthroplasty or a total hip replacement give better functional results within the first 2 years than a primary osteosynthesis. A total hip arthroplasty or a bipolar hemiarthroplasty probably gives better functional results after 2 years than a unipolar hemiarthroplasty. Cemented stem gives better outcome than uncemented. Uncemented cup is not recommended to these osteoporotic patients [11, 16].

Randomised studies have been performed both in Sweden and abroad to improve the criteria for the choice between a primary osteosynthesis and a primary arthroplasty [24–27]. Most of these studies have shown relatively high number of complications for osteosynthesis when compared with previously published consecutive series during the last decades [20, 23]. A differentiated treatment protocol results in fewer re-operations [15, 16, 28–30].

Based on the results of these randomised studies the treatment policy in Sweden has changed during the last decade so the most displaced fractures in elderly patients now in increasing amount receive a primary arthroplasty. A primary arthroplasty is advocated if the cervical fracture is clearly displaced with lack of continuity both on the frontal and the side view, particularly in patients with high degree of osteoporosis. Also the patient should have been walking prior to the fracture. The age should be above 70–75 years, where biological age is more important than chronological. Irrespective of the patient's age the primary arthroplasty is recommended in cases with disease to the hip joint such as rheumatoid arthritis or a pathological fracture secondary to malignancy or other destruction of the hip joint; e.g. after infection. Also a lately diagnosed fracture is indicated for arthroplasty, particularly if the scintimetry has shown a low uptake. Arthrosis

in the fractured hip joint is also an indication for primary arthroplasty. The primary arthroplasty is however not recommended in patients with severe dementia, bedridden patients or patients with bad muscular function due to the increased risk of dislocation.

The tendency internationally now aims at a differentiated treatment protocol according to the principles given above. In waiting for better diagnostic possibilities of the circulation to the femoral head, the principles indicated will probably result in that two thirds of the displaced cervical fractures will be operated with primary osteosynthesis and the other third with a primary arthroplasty, then preferably a bipolar with cemented stem.

Timing of Operation

Hip fracture patients should be operated as soon as practically possible. Directly life threatening conditions must of course have priority before the hip fractures, but these elderly patients will have a prolonged rehabilitation and functional less optimal result if the time between arrival to hospital and operation is unnecessarily delayed. This in turn leads to more complications and inactivity in these elderly persons. It can also generate increased nursing needs with great economic consequences. The goal is to operate the patient on the day of arrival and at latest within 24 h. If the patient is operated with osteosynthesis within 6 h from the fracture it has been shown that the risk for blood circulation disturbance to the femoral head and thereby following healing complications diminish [31].

Apart from being strenuous for the patient due to pain and immobilisation a delay of the operation is associated with increased morbidity and mortality. A delay of more than 24 h between arrival to hospital and osteosynthesis of the fracture has shown association to increased mortality. Lower mortality has been shown when the operation was performed within 12 h. If a delay is unavoidable the time should be used to improve the general condition of the patient, particularly the fluid balance [16, 17, 21].

Practical Considerations at Operation

Osteosynthesis for cervical fractures is performed with the use of a fracture table allowing traction under the image intensifier. Preferably a biplanar image intensifier is used. It is wise to supervise the transferring of the patient to the fracture table, as the injured leg has to be treated with great care to prevent fracture displacement occurring or damage to the retinacular vessels. A manual traction on the leg straightening it out during transfer is advisable. Also to reduce the risk of pressure sores padding should be applied to any area of pressure such as around the feet, sacrum and groin. The uninjured leg should be flexed and abducted as much as possible. Positioning of the image intensifier is easier if the hip and knee are flexed to 90° on the uninjured side (Fig. 38.1). A displaced cervical fracture is reduced by longitudinal traction followed by inward rotation. A biplanar image intensifier has the advantage that after positioning of the equipment no further movements of the stand or tube are necessary, which thereby avoids jeopardising the draping and thereby the sterility. The shifting between the views is done on the monitor with a foot pedal, which considerably saves operation time. Also the easy rapid shifting between the positions increases the precision in the positioning of the osteosynthesis material. The importance for the circulation to the femoral head of a low traumatic operating technique has been proven [32]. The channel should be pre-drilled and hammering in of osteosynthesis material avoided. Also impaction of the fracture by hammering increases the damage of the circulation to the femoral head. The best way to achieve compression in the fracture is by the patient's own muscle forces at weight bearing. For undisplaced fractures early surgery will allow aspiration of any haematoma within the joint capsule. This may reduce the risk of avascular necrosis caused by ischaemia from a tamponade effect on the intracapsular vessels. Cervical fractures are operated with parallel pins or screws to allow axial compression along the axis of the femoral neck perpendicular to the fracture line when the patient is weight bearing. This is a physiological way of compressing the

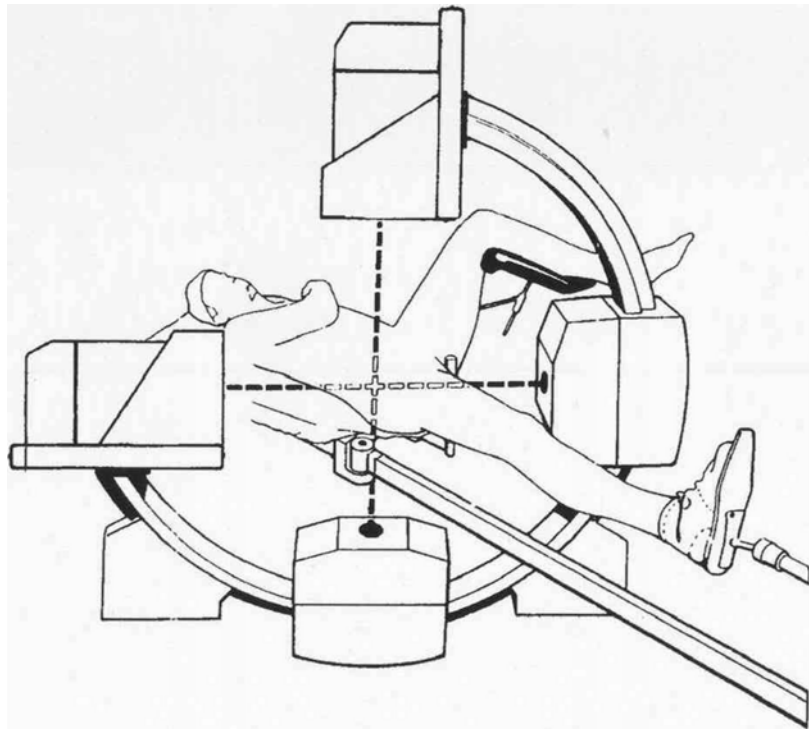

Fig. 38.1 Positioning of biplanar image intensifier. Patient supine on traction table

fracture. To prevent slipping out of the osteosynthesis material they are either threaded as screws or have a hook that can be pressed out through a central canal. To facilitate parallel positioning most devices are cannulated and have instruments to enable parallel placement. The most commonly used methods of fixation are two or three parallel cancellous screws, two parallel hook pins or a dynamic hip screw. The blood circulation to the femoral head via the capsule vessels along the femoral neck is vulnerable. Sudden forceful movements of the hip during reduction or excessive traction causing fracture diastasis may damage the femoral head circulation. The fracture is usually reduced by applying traction to the outstretched leg, followed by internal rotation. These manoeuvres should be checked throughout the procedure in both the lateral and the anterior-posterior radiograph using the image intensifier which should have a large field of view and a good resolution facility. The reduction manoeuvre is begun by using the fracture table to apply gentle traction to the leg, progressively while checking in the AP radiograph. Traction is applied until the medial parts of the femoral neck, the calcar region, are approximated with anatomical contact between the bone ends. Next, the lateral view is obtained and the foot is rotated inwards until the dorsal angulation of the femoral neck fracture has been counteracted. This part of the manoeuvre can be likened to closing an open book. The aim is to restore the alignment of the femoral neck such that a straight line can be drawn to bisect the femoral head, trochanteric region and shaft. It is essential that there is no residual fracture angulation, as this will increase the risk of re-displacement of the fracture. Quite frequently there is need to apply more than 90° of inward rotation to achieve reduction. Small corrections with ab-adduction and sometimes elevation of the leg may also be needed to obtain an anatomical reduction. Following the reduction maneuver it is advisable to slacken the traction somewhat. This allows some impaction to occur at the fracture site and reduces the risk of the femoral head rotating during drilling.

Open reduction is very seldom indicated. Only in very young patients it can be tried and then

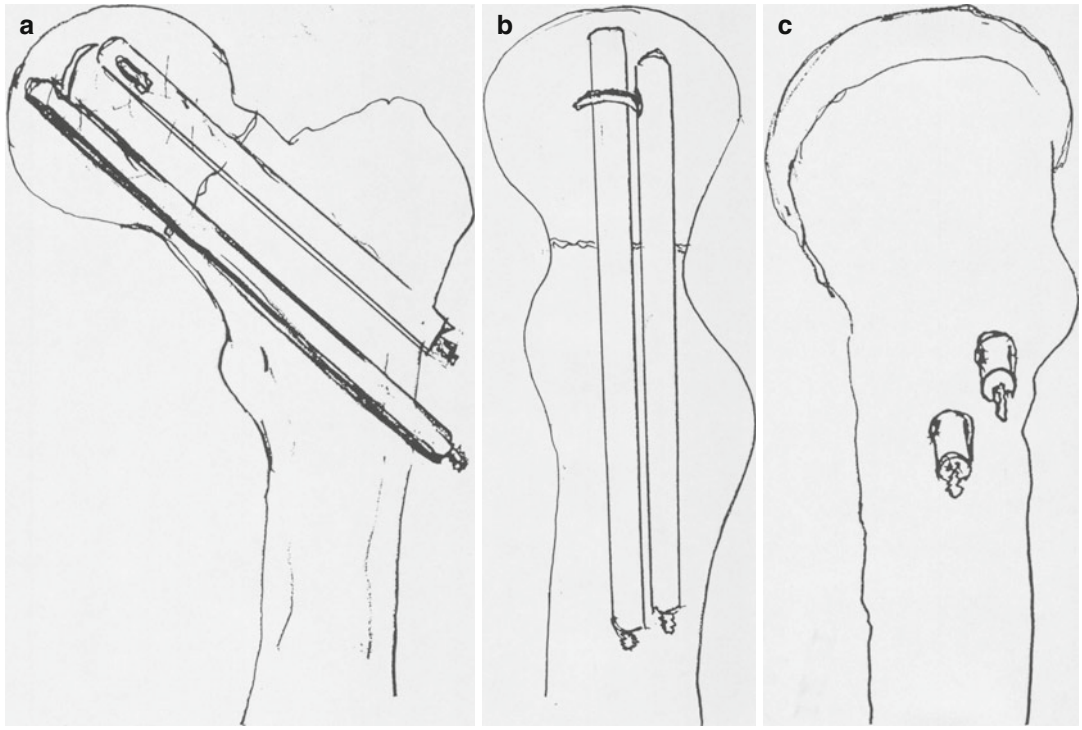

Fig. 38.2 Positioning of osteosynthesis material for hook pin osteosynthesis after anatomical position of femoral neck fracture. (**a**) Anterior/posterior view drawn as seen in image intensifier. (**b**) Lateral view as seen in image intensifier. (**c**) Lateral view as seen at the operation

combined with insertion of a pedicle graft consisting of a piece of bone with a muscle bridge which is implanted into the fracture site. In all middle aged and older patients the alternative is rather a total hip arthroplasty if there is inability to obtain an adequate closed reduction. This is also advisable if the fracture is more than 1 week old or if there is early re-displacement following internal fixation.

Positioning of Two Hook Pins or Screws

Commonly used screws are the Garden screws, Asnis screws, Uppsala screws and AO screws. In Sweden and Norway the Hansson hook pins are widely spread. The screws and pins usually are about 7 mm in diameter and inserted parallel to each other. The aim is to create a three point fixation, where the first point is the entry hole for the firm lateral cortical bone, the second point is the pin lying on the calcar inferiorly or posteriorly within the medullary cavity of the neck and the third at the subcondral bone plate (Fig. 38.2). The lateral skin incision should be extended distally from a point about 2 cm distal to the greater trochanter for a length of about 5 cm. The exact positioning of the incision is best located using a guide wire or other radiopaque object on the skin surface and screening with an image intensifier in the AP view. After skin incision a guide wire is introduced. The inferior pin should be inserted through a drill hole at the level of the middle/lower part of the lesser trochanter. If the drill hole is situated distal to this point there is increased risk of fracture of the femur through the distal hole. The distal pin should rest along the calcar femorale and go up into the femoral head until 2–3 mm from the joint line (Fig. 38.3). While introducing the Kirschner wire the position is repeatedly checked with an image intensifier in

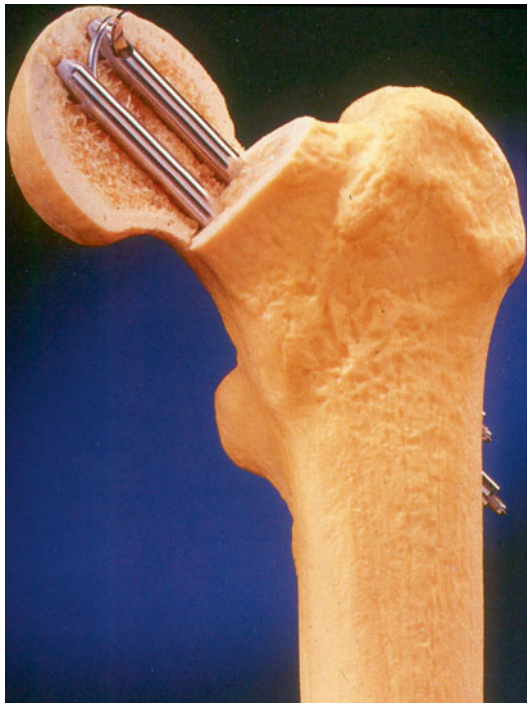

Fig. 38.3 Hook pin osteosynthesis

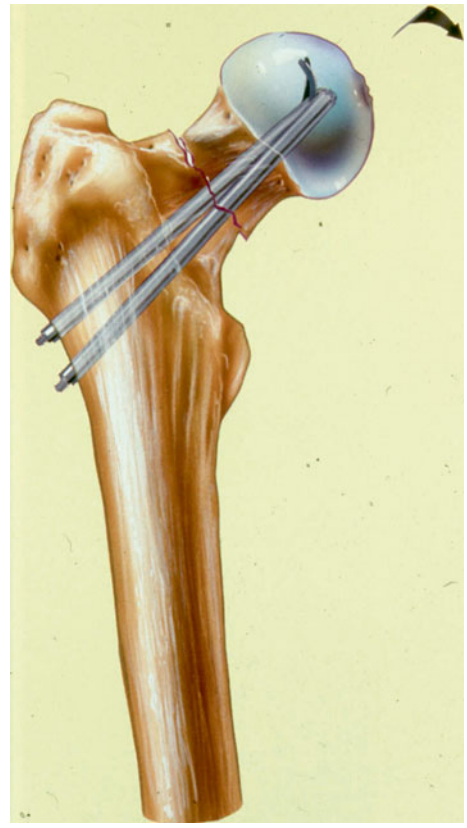

Fig. 38.4 Drawing of hook pin osteosynthesis after weight bearing. An axial somewhat rotational compression often occurs resulting in physiological impaction of the fracture and some angulation of the pins still allowing further axial compression

the AP and lateral planes. On the lateral view the guide wire should appear within the centre of the femoral head and neck. The second, proximal guide wire is then placed in a position parallel to the first one. It should be as spread apart as possible from the lower one in the femoral neck. When three screws are used, for example of Asnis type [33], a triangular pattern is recommended for undisplaced or impacted intracapsular fractures. For displaced fractures four screws in a diamond pattern is suggested. This is said to give better rotatory stability. Impaction along the femoral neck combined with a minor rotation gives somewhat angulation of the osteosynthesis material, but still allows further impaction when two pins are used (Fig. 38.4).

Considerations at Arthroplasty

The hip fracture patient is usually a woman with osteoporosis and short statue. Extra care should be taken not to cause perforation of the acetabulum by reaming for a total hip arthroplasty or by causing a femoral shaft fracture. Smaller sizes of the arthroplasty are usually needed. Postoperative direct weight bearing should be allowed and postoperative restriction should be kept to a minimum. Capsulectomy should be avoided to prevent postoperative dislocation and a posteriolateral exposure is usually favoured due to limited tissue dissection needed, which give shorter operation times and less blood loss. The abductors are not damaged by this approach and there is a lower risk of femoral penetration. This exposure has been said to have a somewhat higher risk of dislocation and the sciatic nerve must be carefully watched to prevent damage. Anteriolateral approach is possible to have a lower risk of dislocation, but has the disadvantage of a greater tissue dissection and a more restricted access for positioning of straight long stem arthroplasties. If a hemiarthroplasty is to be

used special care is necessary not to damage the acetabular cartilage. Forceful movements and hammering should be avoided and the femur is preferably prepared only by handheld reamers. Cementation of the femoral shaft gives better results than the uncemented classical Austin-Moore prosthesis. There is concern about less tolerance of these elderly patients to the cementation procedure so pulse and blood pressure should preferably be monitored and excessive pressure should be avoided even if modern cementing techniques are recommended. There is a risk of cardiac arythmia and low blood pressure during the insertion of the cement. To prevent this a venting catheter to allow air to escape from the femur during cementation and cortisone intravenously have been tried. There are no regular studies to approve this.

Depending on the patient's biological age and activity level before the fracture different types of arthroplasty are chosen. Usually an ordinary one block hemiartroplasty is chosen for the oldest and most disabled patients, whereas a bipolar hemiarthroplasty is used for somewhat younger and fit patients and a total hip arthroplasty is given to the youngest and healthiest patients [16, 34].

Trochanteric Fractures

In trochanteric fractures the circulation to both bone ends is undamaged and healing complications are much less usual than for the cervical fractures. Instead osteoporosis increases the risk of fragmentation in trochanteric fractures. A minor part of the trochanteric fractures can be so comminuted that early direct weight bearing is hindered. The most widely spread operation method is a sliding screw plate (Fig. 38.5). It is a method that is fairly easy to teach on a large scale and has few complications. Modern metal techniques withstands metal fatigue unless in cases with longstanding pseudarthrosis where a metal plate fracture can occur, usually after 6–12 months. During the last decade short intramedullary devices have been introduced as alternatives to the screw plate (Fig. 38.4). The postulated advantages are shorter operation time, less bleeding due to other exposure and a biomechanically shorter lever arm for weight bearing on the osteosynthesis material. Randomised studies have not shown any superior results of these intramedullary devices compared to the ordinary extramedullary screw plate. In some cases a significantly increased risk of femoral shaft fracture has been shown. Inadequate reaming of the femur is normally the cause, in conjunction with excessive force when inserting the nail. An alternative reason may be that the lateral cortical bone around the lag screw is not load protected by a barrel, as with the screw plate. A fissure in this area may more readily extend. The main indications for intramedullary fixation are low trochanteric fractures, hip fractures with associated femoral shaft fracture and pathological extracapsular fractures.

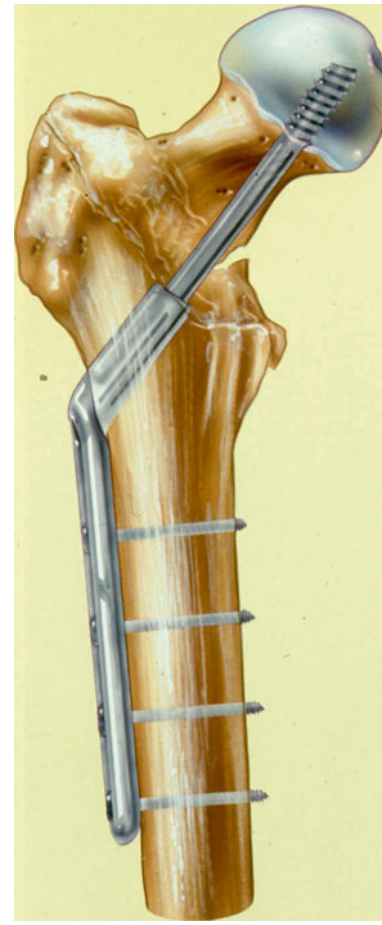

Fig. 38.5 Trochanteric fracture operated with screw plate

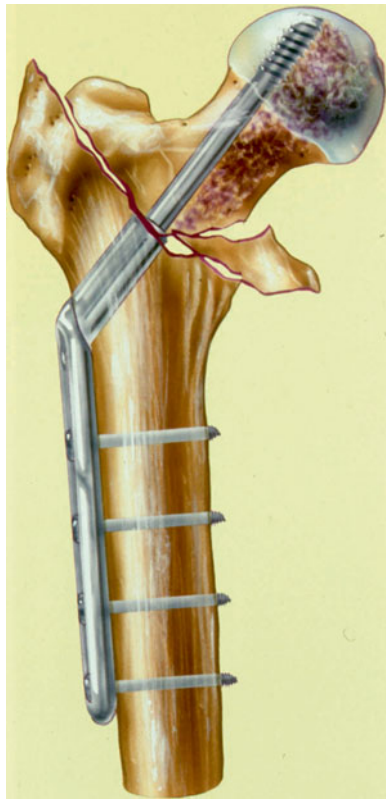

Fig. 38.6 Trochanteric fracture with screw plate after compression by weight bearing resulting in cutting through of the femoral head

There is also a modification of the side plate that allows sliding along the femoral shaft combined with that along the femoral neck to impact the fracture more anatomically [35]. The results on consecutive series seem promising with a lowered cut out of the screw in the femoral head (Fig. 38.6).

A basic biomechanical principle for good healing of trochanteric and subtrochanteric fractures is contact between the major weight bearing bone fragments. Rigid fixation systems counteract this and lead to pseudarthrosis and in the long run breakage of the plate due to metal fatigue. At reposition during operation and the following mobilisation and weight bearing good contact is aimed at in the major bone fragments, sometimes to the price of a certain shortening of the leg. The main goal is a rapid healing of the fracture. In some cases increasing pain and too much collapse of the fracture make non-weight bearing necessary. This is also the case if the screw through the femoral neck and head threatens to cut through the subcondral bone into the hip joint (Fig. 38.6). If the patient cannot support the weight bearing with some walking aid such as a walking table, rollator, quatra peds, sticks or crutches some weeks of sitting in a chair might be necessary. In the long run all trochanteric fractures heal, usually within 3–5 months. The development of femoral head necrosis is very rare, but there is some percentage of pseudarthrosis development which is higher if a more rigid fixation system has been used [16].

Dynamic extramedullary osteosynthesis (screw plate) is much better than rigid nail plates [36]. The Ender method, which was previously widely spread in Europe, has in several randomised studies shown inferior results compared to the screw plate [37]. The intramedullary type of osteosynthesis with a screw up through the femoral neck and a short intramedullary rod often with transverse screws through the femoral shaft (the first type was called Gamma nail) has in several randomised comparative studies shown the same risk cut out through the femoral head as the conventional screw plate whereas the intramedullary device has resulted in more re-operations, usually due to fracture at the distal end of the intramedullary nail. The technique is somewhat more demanding to perform [11]. It is however used as the only routine method in some centres in Europe. In the literature there are reports of a frequency of cut out of the femoral screw through the femoral head into the acetabulum with the use of a conventional screw plate in up to 10 % of the cases. This has been diminished to some percent only with the axial screw plate (Medoff plate). Reversed, oblique pertrochanteric fractures are especially suited for this type of osteosynthesis.

Subtrochanteric Fractures

The subtrochaneric fractures have a considerably higher frequency of healing complications compared to the trochanteric ones. This is due to the high mechanical forces acting in this area and that the fractures often are very comminuted which gives inferior stability to the osteosynthesis system. One problem with the conventional screw

plate for subtrochanteric fractures is that a distal fracture line transfers the dynamic screw plate to become a more static implant as the fracture is situated below the area for the gliding screw. This leads to complications associated with the static fixations such as delayed healing, pseudarthrosis, breakage of the plate and cutting through of the femoral head by the screw [11, 17]. This has led to an increased use of long intramedullary nails with transverse fixation screws in the distal part and a screw through the femoral head and neck in the proximal part. With this device also very long and comminuted femoral shaft fractures can be handled [16].

Weightbearing and Rehabilitation

The goal after a hip fracture is to rehabilitate the patient to the same functional level as before the fracture [5, 16]. A stable osteosynthesis system or a well-fixed arthroplasty is a pre-requisite for this. The operation should allow direct postoperative weight bearing to start immediately the day after the operation (Fig. 38.7). This is possible for the majority of patients operated with osteosynthesis for femoral neck fractures as well as for those receiving an arthroplasty. The weight bearing by walking gives a physiological impaction of the fracture and stimulates the bone healing process. The rule is immediate postoperative weight bearing. Furthermore elderly patients usually find it difficult to have restricted weight bearing and cannot handle crutches as young patients.

As mentioned above for trochanteric fractures the majority can have full weight bearing whereas a small part of the fractures need more care due to very comminuted fractures. During recent decades successful rehabilitation programs have spread consisting of direct mobilisation in the hospital and continued walking rehabilitation in the patient's own home [3, 28, 38–46].

Hip Fracture Audit

Due to the increasing burden on the health care system of the osteoporotic fractures in the elderly, particularly the hip fractures, it is very important to know the results of everyday treatment on a national basis of these fractures,. In Sweden, a national registration of hip fracture treatment called RIKSHÖFT was introduced in 1988 [16, 47]. This has spread internationally and in 1995 the Standardised Audit of Hip Fractures in Europe (SAHFE) was started based on the Swedish RIKSHÖFT experience [14].

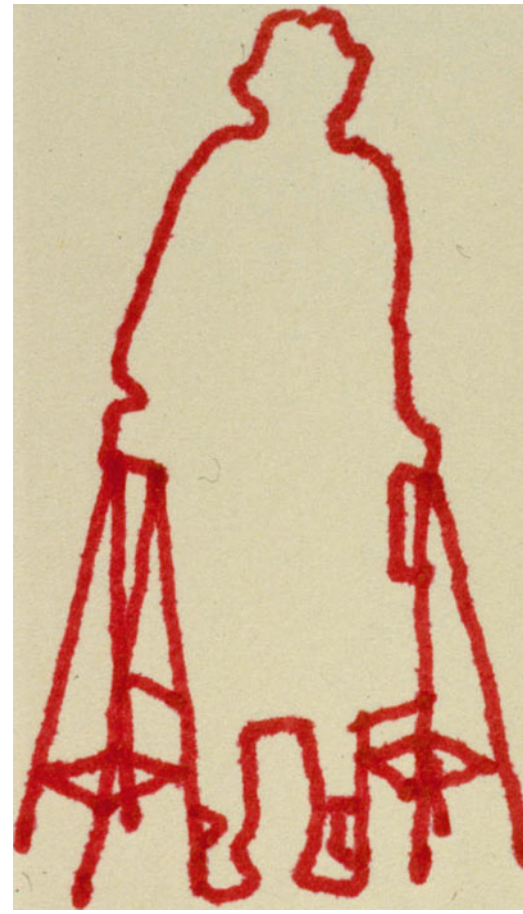

Fig. 38.7 Weight bearing with quatrapeds. Direct postoperative mobilisation and continued rehabilitation in the patients own home

The pattern of living before fracture and postoperatively up till 4 months after femoral neck (Fig. 38.8) or trochanteric fractures (Fig. 38.9) shows that of those patients coming from own home, the majority had returned there after 2–3 weeks of treatment at the orthopedic department. Actually, the mean hospitalisation time is now just below 10 days. The rest of the patients

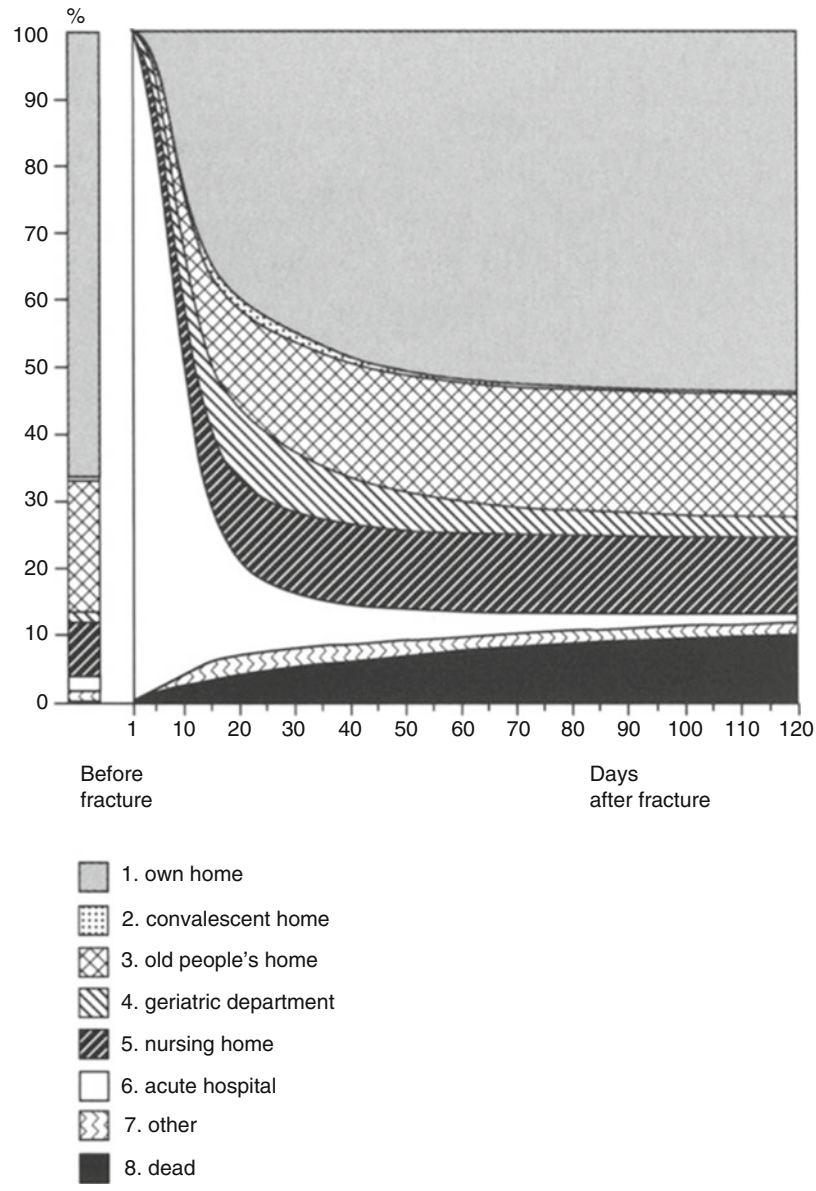

Fig. 38.8 Living pattern before and at different time periods after a femoral neck fracture in Sweden based on 30.000 patients

are rehabilitated through an institution. This is mainly due to other diseases existing before the fracture. Within a month from the fracture the majority of the patients from own home or service house have returned to their previous place of living. Already after 2 months a very stable pattern of rehabilitation is apparent from the graph and at 4 months after the fracture, the majority of the patients are back in their pre-fracture way of living.

Irrespective of the philosophy chosen for the treatment of hip fractures it is of utmost importance to be able to compare the results from the different treatment programs. Different countries have various traditions both socially and in medical treatment, but internationally comparisons will more rapidly bring out optimised ways of treatment that will be the solution to cope with the increasing amount of hip fractures during the coming decades (see www.rikshoft.se).

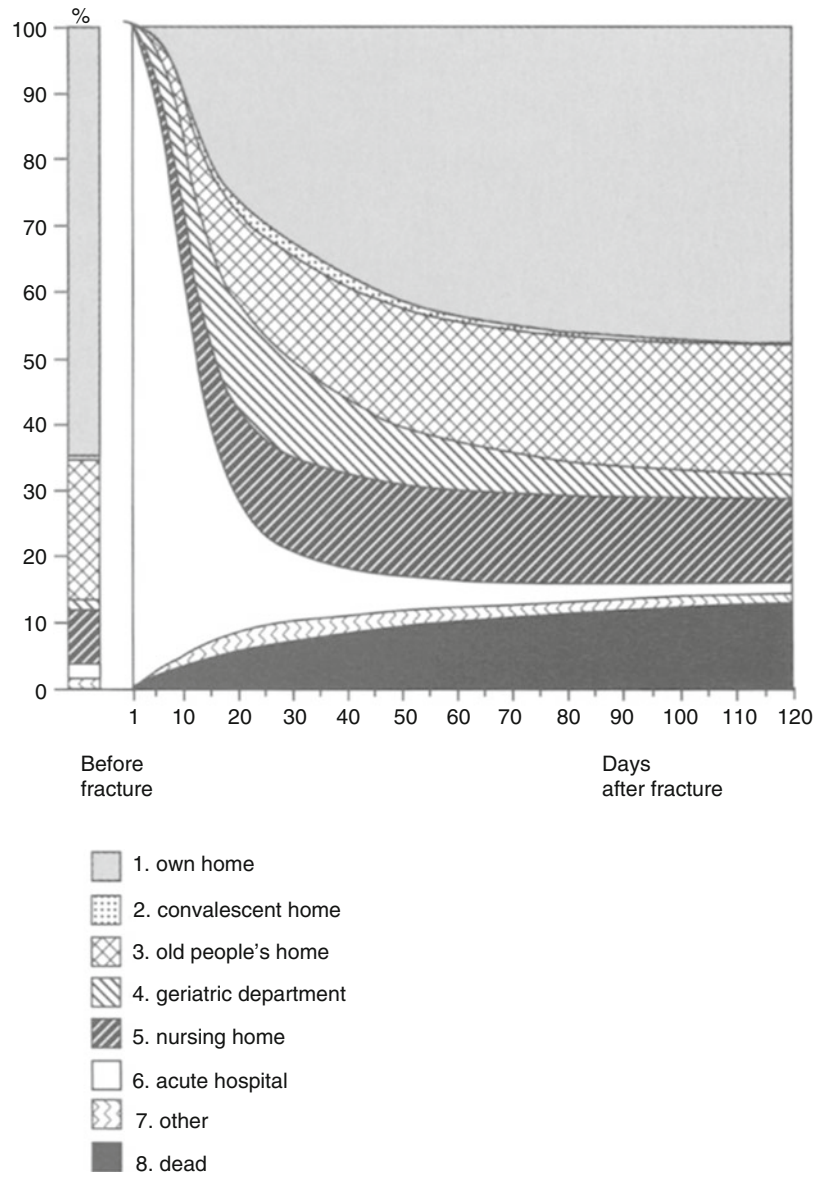

Fig. 38.9 Living pattern before and at different time periods after a trochanteric hip fracture in Sweden based on 30.000 patients

References

1. Jarnlo G-B, Jakobsson B, Ceder L, Thorngren K-G. Hip fracture incidence in Lund, Sweden, 1966-1986. Acta Orthop Scand. 1989;60:278–82. 1. Wallace WA. The increasing incidence of fractures of the proximal femur: an orthopaedic epidemic. Lancet. 1983;i:1413–4.
2. Zetterberg C, Elmersson S, Andersson GBJ. Epidemiology of hip fractures in Göteborg, Sweden 1940-1983. Clin Orthop Relat Res. 1984;191:278–82.
3. Jarnlo G-B, Ceder L, Thorngren K-G. Early rehabilitation at home of elderly patients with hip fractures and consumption of resources in primary care. Scand J Prim Health Care. 1984;2:105–12.
4. Obrant K, Bengnér U, Johnell O, Nilsson B, Sernbo I. Increasing age-adjusted risk of fragility fractures: a sign of increasing osteoporosis in successive generations? Editorial. Calcif Tissue Int. 1989;44: 157–67.
5. Thorngren K-G. Fractures in older persons. Disabil Rehabil. 1994;16:119–26.
6. Melton III LJ. Differing patterns of osteoporosis across the world. In: Chesnut III CH, editor. New

dimensions in osteoporosis in the 1990s. Hong Kong: Excerpta medica Asia; 1991. p. 13–8.
7. Johnell O, Gullberg B, Allander E, Kanis JA. The apparent incidence of hip fracture in Europé: a study of national register sources (MEDOS Study Group). Osteoporos Int. 1992;2:298–302.
8. WHO Study Group. Assessment of fracture risk and its application to screening for postmenopausal osteoporosis. WHO Technical Report Series No 843. 1994.
9. Brody JA. Prospects for an ageing population. Nature. 1985;315:463–6.
10. Cooper C, Campion G, Melton III J. Hip fractures in the elderly: a world-wide projection. Osteoporos Int. 1992;2:285–9.
11. Parker MJ, Pryor GA, Thorngren K-G. Handbook of hip fracture surgery. Oxford: Butterworth-Heinemann; 1997. p. 1–145.
12. Garden RS. Low-angle fixation in fractures of the femoral neck. J Bone Joint Surg. 1961;43-B:647–63.
13. Frandsen PA, Andersen E, Madsen F, Skjödt T. Garden's classification of femoral neck fractures: an assessment of inter-observer variation. J Bone Joint Surg. 1988;70-B:588–90.
14. Parker MJ, Currie CT, Mountain JA, Thorngren K-G. Standardised audit of hip fracture in Europé (SAHFE). Hip Int. 1998;8:10–5.
15. Thorngren K-G. Hip fractures in the geriatric patient. Natural history, therapeutic approach and rehabilitation potential. In: Stein H, editor. Scientific proceedings SIROT 97. Freund Publishing House Ltd; 1999, 161–70.
16. Thorngren K-G. Fractures of the femoral neck and proximal femur. In: Bentley G, editor. European surgical orthopaedics and traumatology. Heidelberg: Springer; 2014. p. 2203–68.
17. Koval KJ, Zuckerman JD. Hip fractures. A practical guide to management. New York: Springer; 2000.
18. Raaymakers ELFB, Marti RK. Non-operative treatment of impacted femoral neck fractures: a prospective study of 170 cases. J Bone Joint Surg. 1991;73-B:950–4.
19. Cserhati P, Kazár G, Manninger J, Fekete K, Frenyó S. Nonoperative or operative treatment for displaced femoral neck fractures: a comparative study of 122 non-operative and 125 operatively treated cases. Injury. 1996;27(8):583–8.
20. Strömqvist B, Nilsson LT, Thorngren K-G. Femoral neck fracture fixation with hook-pins, 2-year results and learning curve in 626 prospective cases. Acta Orthop Scand. 1992;63(3):282–7.
21. Parker MJ, Pryor GA. Hip fracture management. Boston: Blackwell Scientific Publications; 1993. p. 1–292.
22. Rodrigues J, Herrara A, Canales V, Serrano S. Epidemiologic factors, mortality and morbidity after femoral neck fractures in the elderly – a comparative study: internal fixation vs hemiarthroplasty. Acta Orthop Belg. 1987;53:472–9.
23. Rehnberg L, Olerud C. Subchondral screw fixation for femoral neck fractures. J Bone Joint Surg. 1989;71-B:178–80.
24. Rödén M, Schön M, Fredin H. Primary treatment of displaced femoral neck fractures. Acta Orthop Scand. 1999;70(Suppl 287).
25. Tidermark J, Ponzer S, Törnkvist H, Svensson O, et al. Internal fixation vs. 1999.
26. Rogmark C, Johnell O, Sernbo I and the NOA Study Group. Nail or arthroplasty – a randomized study of displaced cervical hip fractures with 1-year results. Acta Orthop Scand. 1999;70(Suppl 287).
27. Neander G, Dalén N. Osteosynthesis versus total hip arthroplasty for displaced femoral neck fractures – results after 4 years of a prospective randomized study. Acta Orthop Scand. 1999;70(Suppl 287).
28. Holmberg S, Thorngren K-G. Consumption of hospital resources for femoral neck fracture. Acta Orthop Scand. 1988;59:377–81.
29. Thorngren K-G. Optimal treatment of hip fractures. Acta Orthop Scand. 1991;62 Suppl 241:31–4.
30. Alberts KA, Isacson J, Sandgren B. Femoral neck fractures – fewer secondary hip arthroplasty procedures with a differentiated treatment protocol. Acta Orthop Scand. 1999;70(Suppl 287).
31. Manninger J, Kazar G, Fekete G, et al. Avoidance of avascular necrosis of the femoral head, following fractures of the femoral neck, by early reduction and internal fixation. Injury. 1985;16:437–48.
32. Strömqvist B. Femoral head vitality after intracapsular hip fracture: 490 cases studied by intravital tetracycline labeling and Tc-MDP radionuclide imaging. Acta Orthop Scand. 1983;Suppl 200.
33. Asnis S, Wanek-Sgaglione L. Intracapsular fractures of femoral neck: results of cannulated screw fixation. J Bone Joint Surg. 1994;76A:1793–803.
34. Kyle RF, Cabanela NE, Russel TA, et al. Fractures of the proximal part of the femur. Instruction course lecture. J Bone Joint Surg Am. 1994;76:924–52.
35. Medoff RJ, Maes K. A new device for the fixation of unstable pertrochanteric fractures of the hip. J Bone Joint Surg. 1991;73-A:1192–9.
36. Chinoy MA, Parker MJ. Fixed nail plates versus sliding hip systems for the treatment of trochanteric femoral fractures: a meta analysis of 14 studies. Injury Int J Care Injured. 1999;30:157–63.
37. Parker MJ, Handoll HHG, Bhonsle S, Gilespie WJ. Ender nails compared with nail or screw plate devices for trochanteric femoral fractures: a meta-analysis of randomised trials. Hip Int. 1999;9(1): 41–8.
38. Ceder L, Thorngren K-G, Wallden B. Prognostic indicators and early home rehabilitation in elderly patients with hip fractures. Clin Orthop. 1980;152: 173–84.

39. Ceder L, Thorngren K-G. Rehabilitation after hip repair (letter). Lancet. 1982;2(8307):1097–8.
40. Borgquist L, Nordell E, Lindelöw G, Wingstrand H, Thorngren K-G. Outcomed after hip fracture in different health care districts. Rehabilitation of 837 consecutive patients in primary care 1986-88. Scand J Prim Health Care. 1991;9:244–51.
41. Borgqvist L, Lindelöw G, Thorngren K-G. Costs of hip fractures. Rehabilitation of 180 patients in primary health care. Acta Orthop Scand. 1991;62:39–48.
42. Holmberg S, Thorngren K-G. Rehabilitation after femoral neck fracture: 3053 patients followed for 6 years. Acta Orthop Scand. 1985;56:305–8.
43. Snedal J, Thorngren M, Ceder L, Thorngren K-G. Outcome patients with a nailed hip fracture requiring rehabilitation on hospital for chronic care. Scand J Rehabil Med. 1984;16:171–6.
44. Thorngren M, Nilsson LT, Thorngren K-G. Prognostic-based rehabilitation of hip fractures. Compr Gerontol. 1988;2:12–7.
45. Jalovaara P, Berglund-Rödén M, Wingstrand H, Thorngren K-G. Treatment of hip fracture in Finland and Sweden. Prospective comparison of 788 cases in three hospitals. Acta Orthop Scand. 1992;63:531–5.
46. Berglund-Rödén M, Swierstra BA, Wingstrand H, Thorngren K-G. Prospective comparison of hip fracture treatment, 856 cases followed for 4 months in the Netherlands and Sweden. Acta Orthop Scand. 1994;65:287–94.
47. Thorngren K-G. Experience from Sweden. In: Medical audit. Rationale and practicalities. Cambridge University Press; 1993. p. 365–75.

Three-Dimensional Biomechanical Assessment of Knee Ligament Ruptures

39

D.R. Labbe, A. Fuentes, J.A. de Guise, R. Aissaoui, and N. Hagemeister

The complex biomechanics of the human knee joint are the result of an equilibrium of forces exerted by its surrounding soft tissue structures. When one of these forces is removed, as is the case when a ligament ruptures, a redistribution of forces occurs and the biomechanical properties of the knee are altered. One of the most frequently diagnosed knee ligament ruptures is that of the anterior cruciate ligament (ACL). Such a rupture causes increased laxity of the knee joint as well as a complex rotational and translational instability whereby many patients describe a feeling that their knee is slipping, or "giving way" [1].

The ACL has been one of the most studied structures of the musculoskeletal system. Despite the abundance of literature, there is little consensus amongst orthopaedic surgeons as to the specific biomechanical effect of an ACL rupture on knee joint function [2]. However, in order to provide effective treatment, it is important that the mechanisms of an injury and the resulting pathomechanics be identified [3]. As such, biomechanical studies of the impact of ACL injuries remain a hot topic and are the subject of much debate. They provide important information that cannot be obtained through current clinical evaluations.

In 2008, Chan et al. [4] proposed a new paradigm, « Orthopaedic sport biomechanics », where the role of biomechanics in orthopaedics is threefold: (1) it helps in the prevention of musculoskeletal sport-related injury and trauma, (2) it provides an objective quantitative assessment to evaluate the immediate outcome of treatment, either operative or conservative, (3) it acts as an objective tool to monitor the long-term rehabilitation progress, and to indicate if an athlete is adequately recovered to a satisfactory level for returning to sports.

Given the ACL's important role in the 3D stability of the knee joint [5], particularly in internal tibial rotation [6, 7], identifying the pathomechanics of an ACL rupture requires the ability to record knee bone movements in 3D [8, 9]. To do so, one must be able to follow the bones with sufficient precision despite skin movement artifacts, and to represent this movement in an anatomical coordinate system that is highly reproducible.

D.R. Labbe, MD
Research Laboratory, Imaging and Orthopedic Research Center Hospital of the University of Montreal, Montréal, QC, Canada

A. Fuentes, PhD
Research Laboratory, Imaging and Orthopedic Research, École Technologie Supérieure, Montreal, QC, Canada

J.A. de Guise, PhD • R. Aissaoui, PhD
N. Hagemeister, PhD (✉)
Génie de la Production Automatisée, École de Technologie Supérieure et CRCHUM, Montreal, QC, Canada
e-mail: nicola.hagemeister@etsmtl.ca

D.G. Poitout (ed.), *Biomechanics and Biomaterials in Orthopedics*,
DOI 10.1007/978-1-84882-664-9_39

For the past 20 years, our research group has been working on the precise recording and *in vivo* analysis of 3D kinematics of the knee, with an emphasis on the effect of an ACL rupture. This chapter presents the non-invasive methodology used to obtain precise and reliable recordings of knee bone movements as well as its use in establishing the biomechanical impact of an ACL rupture on regular paced gait. This is followed by an analysis of the kinematics of the pivot shift test, a clinical test that reproduces the functional instability of the knee. Finally, the implications of 3D biomechanical analyses of the knee are discussed.

Recording 3D Knee Kinematics

Marker Attachment

The recording of human movement is generally achieved by fixing motion capture devices or markers (active or passive) to different body segments. There are a number of technologies available that allow for high spatial and temporal precision when recording movement. As such, it is theoretically possible to quantify very subtle changes in knee joint kinematics. However, in practice, the skin displacement relative to the underlying bones introduces significant measurement errors. Many authors have raised this issue and quantified the effect of skin displacement artifacts [10–16]. For movements of smaller amplitude, e.g. axial rotation of the tibia, the error due to such artifacts has been shown to surpass the actual motion of the bones [12].

In order to limit these errors, different strategies have been proposed for the fixation of motion-capture devices or markers to the lower limb. These solutions can be separated into three categories: optimization of skin mounted markers, percutaneous fixations and external attachment systems. This section provides a brief summary of each of these categories and presents the solution used by our research group.

Skin Mounted Marker Optimization

The first category involves an optimization of the simplest method for attaching motion capture devices: fixing them directly to the skin. This is usually done using a double-sided tape and obviously does nothing to reduce skin displacement artifacts. The optimization consists in fixing a large number of markers over the thigh and shank. Algorithms are then used to approximate the true bone movements based on the fact that in the absence of skin displacement, there should be no relative movement between the different markers.

Many different methodologies and algorithms have been proposed. Some studies have shown significant reductions in skin displacement artifacts [11, 17, 18], while others found these artifacts to remain substantial after application of the algorithm [19–21]. Overall, this method has shown promise, but results vary widely from one study to the next. The main challenge for these algorithms stems from the fact that the source of movement of the skin is the same as that of the bones; frequencies are thus similar [14]. Furthermore, it is possible for all the skin-mounted markers to move without actual bone movement. Strategies relying on algorithms to reduce artifacts from skin-mounted markers are also ill suited for clinical evaluation because of the time and energy necessary to fix a large number of markers.

Percutaneous Fixation

Percutaneous pins, or intra-cortical pins, are generally stainless steel cylinders with diameters that vary from 2.5 to 3.6 mm [22]. They are screwed into the cortical bone at depths up to 20 mm. Electromagnetic sensors or reflective markers are mounted on the pins using a fixation device. The use of such pins is obviously the method that allows for the most precise measurement of bone movements. No study of their accuracy has been published, as this is the method that is considered to be the gold standard in evaluating knee joint kinematics. As such, many authors have conducted studies where knee joint kinematics were simultaneously recorded

by percutaneous pins and by another attachment system to evaluate to precision of the latter [12, 16].

Despite being considered the gold standard, the use of percutaneous pins does not guarantee 100 % accuracy. In addition to the error of the motion capture technology, the tendons and the skin surrounding the pins may, in some cases, cause the pins to bend or become dislodged. Some studies have reported the exclusion of up to 54 % of their subjects because of such dislodgement [12, 16, 22]. In the absence of such complications, percutaneous pins remain the most accurate method for measuring bone movements. However, their use brings obvious drawbacks related to their invasive nature. Local or general anesthesia must be administered to the subjects and the fixation of the pins can be time consuming. As such, their use is restricted to research or peri-operative evaluation.

External Attachment Systems

The final category for reduction of skin displacement artifacts is composed of several different non-invasive systems that attach to the lower limb and onto which reflective markers or electromagnetic sensors are mounted. They are said to be non-invasive because they contact the skin without penetrating it.

The most widespread amongst such systems consists of rigid plastic plates that are fixed to the shank and thigh, usually at mid-segment. This method is commonly referred to as the Cleveland Clinic method (Fig. 39.1). When one of the markers is fixed to a pin that is perpendicular to the rigid plate, it is called the Helen Hayes method [15].

Manal et al. [15] evaluated the accuracy of 6 variations of such attachments for measuring axial tibial rotations during gait. They found it to be about ±4° using the most accurate variation (Fig. 39.1b). Given that the range of axial tibial rotation averages approximately 9°, this is a significant error. Ferber et al. [23] later used this variation of the attachment system to evaluate the test-retest reliability of this attachment system to record knee joint kinematics during running. For many kinematic parameters, intra-class correlation coefficients (ICCs) were found to be below 0.75, which is considered to be the limit of acceptability [24].

Other research groups have developed their own, more elaborate attachment systems and used them in recording lower limb gait kinematics [25–27]. The system developed and used by our research group is now called the KneeKG™ (Emovi inc., Montreal, Canada). First described by Sati et al. [28] under the name of exoskeleton, this system includes a femoral and a tibial component (Fig. 39.2). The design of the femoral component was inspired by a fluoroscopic study that showed that the amplitude of skin displacement about the knee varies greatly depending on the exact location [10]. The study identified two locations where the displacement is minimal. The femoral component attaches to these anatomical locations. It is composed of a rigid arch with spring-loaded forms at each extremity, effectively forming a clamp. The medial extremity of this clamp inserts between the vast medialis and the sartorius muscle tendon; the lateral extremity inserts between the femoral biceps and the ilio-tibial band (ITB). Both extremities rest atop the femoral condyles. A medial condyle support pad and a stabilizing plaque that is attached to a Velcro strap, placed around the proximal thigh, prevent rotation of the system about the clamp's contact points.

The accuracy of the KneeKG™ was evaluated by a fluoroscopic study. Radio-opaque beads were fixed to the femoral component, which was installed on three different subjects who performed active flexion/extension under fluoroscopy. Average errors were found to be −0.4° in abduction/adduction and −2.3° in tibial rotation [28]. A subsequent study of five subjects, with a similar methodology, found that the quadratic error is diminished by a factor of 4.3 for abduction/adduction and by a factor of 6.2 for axial tibial rotation when compared with skin mounted markers [29]. Both these studies evaluated the accuracy of the KneeKG™ using non weight-bearing knee flexions.

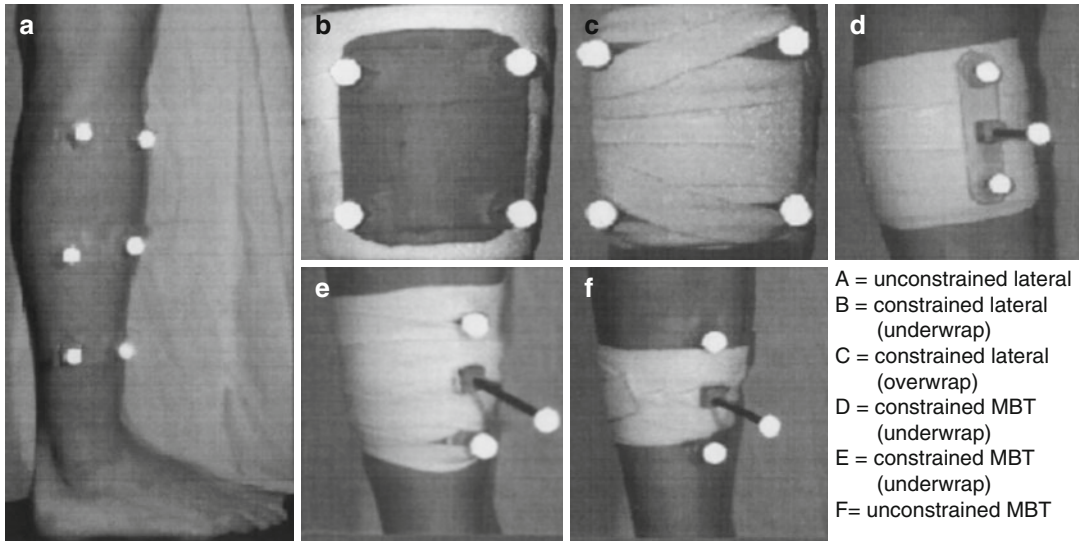

Fig. 39.1 Different variations of the Cleveland Clinic and Helen Hayes methods (From Manal et al. [15], with permission)

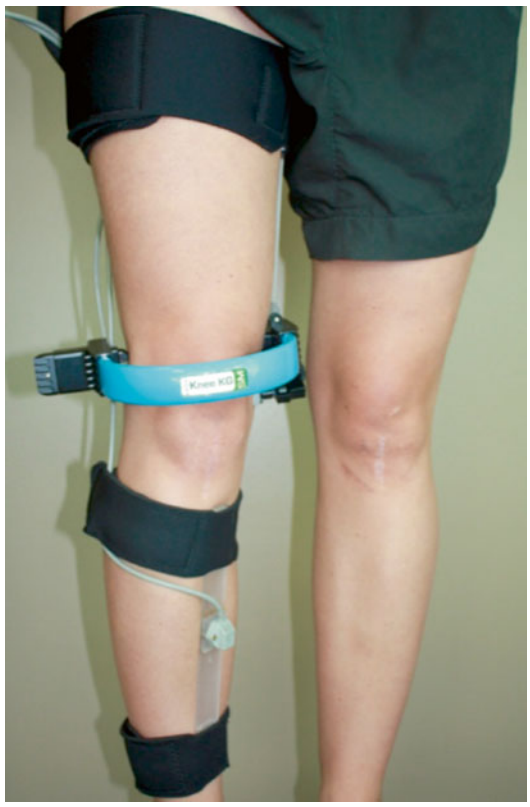

Fig. 39.2 The tibial and femoral components of the KneeKG™ attachment system

The intra- and inter-observer reliability of the KneeKG™ were evaluated to insure that when the system was removed and reinstalled, similar results were obtained regardless of the examiner who installed it [30]. In the intra-observer setting, a single observer installed the system and recorded the gait kinematics three times each for 12 different subjects. Reliability was found to be high, with intra-class correlation coefficients (ICC) between 0.88 and 0.94 for knee rotations. The average standard measurement error (SEM) was below 1° for rotations about all three axes. In the inter-observer setting, three observers each installed the system twice on all 12 subjects. Similar to the intra-observer data, the ICCs from the inter-observer measurements were between 0.89 and 0.94, with all SEMs below 1°.

Movement Representation

Euler Angles Versus Helical Axis Definition

After knee movement has been measured precisely and reliably, it is necessary to represent it in a meaningful way. It has been suggested that the unambiguous description of spatial motion is more difficult than its measurement [31]. Because

the knee is not a hinge and movement about that joint does not occur in a 2D plane, it is difficult to represent knee kinematics. Typically, 2 methods are used to study 3D kinematics of the knee: Euler angles [32] and helical axes [33].

Even though the knee is not gyroscopic, the Euler angle method is the most widely employed. With this method, it is possible to describe a 3D movement as 3 successive rotations about three different axes defined in space: flexion/extension, abduction/adduction and internal/external tibial rotation. These axes can be fixed or floating, and represented locally or globally. The major advantage of this method is that it is easier to interpret the results clinically with anatomical descriptions of movements. With this method, it is also possible to compute anteroposterior (AP), proximodistal (PD), and mediolateral (ML) translations.

However, the main disadvantage of the Euler angle method is that it is very sensitive to anatomical reference axes definition. Small errors (1–2 mm in the definition of points used to build the coordinate system) cause errors in orientation as well as in kinematic amplitude on the order of 2°. When coordinate systems are built on subjects, errors in landmark definition can be on the order of 30 mm. These large errors make it difficult, even impossible, to compare results [19]. Also, it is not clear if differences in bone geometry affect the kinematic patterns that are generated. For this reason, we do not know the 3D kinematics of the normal knee. Each knee has a kinematic representation associated with a given local coordinate system.

The helical axes method [33] uses the 3D position of each bone to describe the movement of the knee between 2 moments in time as a unique rotation and a unique translation about a finite rotation axis. Therefore, when employing this method to describe knee kinematics, we need to define the time period during which we want to express the rotation and translation of one bone with respect to the other. The main advantage of this method is that it is independent of an anatomical coordinate system definition. However, the use of helical axes to describe joint movements is not well understood by the clinical community [32]. Also, the method is sensitive to noise in the measurement and to the time period used for computation of the finite rotation axis.

We chose to follow the recommendation of the International Society of Biomechanics (ISB) by representing knee movements using Euler angles, which allow for better clinical interpretation. We therefore needed to define anatomical coordinate systems associated with the femur and tibia.

Anatomical Coordinate Systems

Anatomical landmarks need to be identified in order to establish the bone-embedded coordinate systems. These landmarks can be defined by a pointer or by fixing markers directly over them. This technique generates errors of many mm or even a few cm. To diminish imprecision when building coordinate systems, we have developed a method that uses fewer anatomical landmarks to define the reference coordinate system than other methods in the literature [34].

This coordinate system is called the Functional Postural (FP) method and was first described by Hagemeister et al. [35] The joint centers are defined as follows.

Ankle joint center (AJC):	The midpoint between the medial and lateral malleoli.
Hip joint center (HJC):	The center of the femoral head. It is identified from a recording of hip circumduction using a pivot algorithm, as proposed by Siston and Delph [36].
Knee joint center (KJC):	The midpoint between the medial and lateral epicondyles, projected onto the mean axis of knee flexion/extension

The PD axes of the tibia and femur are respectively defined by the vectors joining the KJC to

the AJC and the KJC to the HJC. The subject is then placed in a reference guide with his frontal plane aligned with that of the guide. The sagittal plane is then defined during a movement of slight flexion/extension, alternating between approximately 10° of flexion and maximum extension. It is defined as the plane whose normal vector is the cross product of the normal vector of the frontal plane with the vector joining the HJC and the AJC. The neutral position of the knee joint is defined at the moment when the PD axes of the tibia and femur are aligned in the sagittal plane. In this position, the AP axes of the tibia and femur are defined as perpendicular to the normal vector of the sagittal plane and their PD axes. Finally, the ML axes of each of the bones are the axes that complete the orthonormal sets (Fig. 39.3).

Inter- and Intra-tester Variability

To test inter- and intra-tester variability for the calibration procedure, the following protocol was performed. The attachment system was first installed on each subject, and three testers performed the above-described calibration procedure on four subjects. Each tester repeated the procedure 5 times. Then, the subjects walked on a treadmill at a comfortable speed for 3 min, and finally, 30 gait cycles were recorded. The mean of these 30 cycles was used to compute the kinematic parameters (flexion/extension, abduction/adduction and internal/external rotation of the tibia as well as A-P translation as a function of percentage of the gait cycle) in association with the 15 calibration procedures. The resulting 15 curves were compared for each subject using an adjusted coefficient of multiple determinations. Figure 39.4 presents an example of the kinematic parameters calculated with 5 calibration procedures performed by 1 tester on 1 subject.

The results show that the calibration method allows the measurement of 3D knee kinematics with good reproducibility. Mean errors generated by the calibration procedure are 1.1° in flexion/extension, 1.1° in abduction/adduction, 0.8° in internal/external tibial rotation, and 2.6 mm in A-P translation.

Gait Analysis

Following an ACL injury, gait analysis has been shown to provide beneficial information for assessing knee stability [37] and functional impairments [38] under dynamic conditions. Numerous studies have already reported that patients with an ACL deficiency present altered 3D knee kinematics [9, 38–43] and 3D knee joint moments [38, 44–46]during gait. In these studies, 3D biomechanical patterns of the knee are presented over a full gait cycle, which is divided into a stance phase and in a swing phase. These phases represent 60 % and 40 % of the total gait cycle (GC), respectively. During the stance phase, sub-phases occur as follow: the initial contact (1–2 % of the GC), the loading phase (1–10 % of the GC), the mid stance phase (10–30 % of the GC), the terminal stance phase (30–50 % of the GC) and the pre-swing phase (50–60 % of the GC) [47].

Gait Biomechanics

Kinematics

To identify knee biomechanical deficiencies following an injury, a good understanding of "normal" patterns is required, since they serve as a reference to compare the pathological patterns [48]. Numerous studies have published "normal" knee biomechanical patterns during gait. Typically, the knee arcs of motion during walking in the sagittal, frontal and transverse planes are approximately 70°, 5° and 9°, respectively [47]. However, a qualitative review of these studies unveils a lack of correspondence in normal 3D knee kinematic patterns. These discrepancies are generally found in the frontal and transverse plane. The variation in methodologies used to record 3D joint kinematics between studies is potentially responsible for these differences [49].

Kinetics

During gait, the knee joint is continuously submitted to important moments and forces that influence the joint kinematics in all three planes of movement. Since joint kinetics cannot be

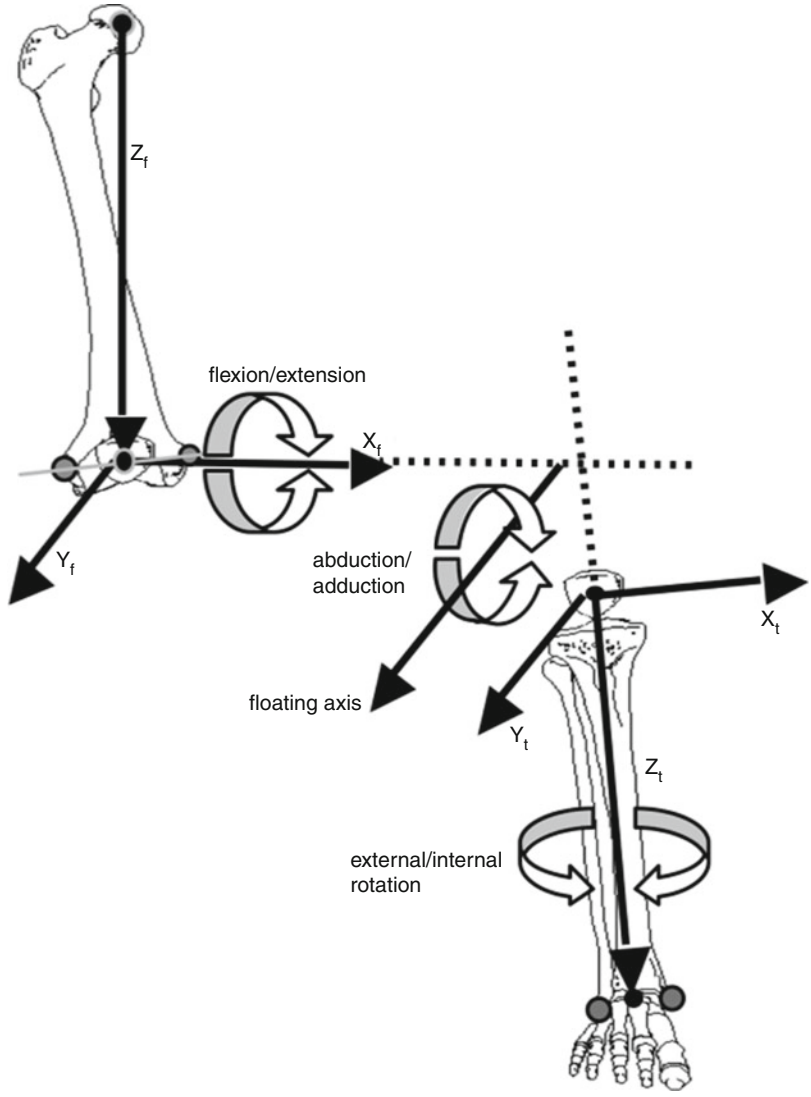

Fig. 39.3 Coordinate axes construction using femoral condyles, malleoli (*gray dots*) and a functional method for definition of the centre of the femoral head and the centre of the knee (*black dots*)

measured *in vivo*, we must first record the joint kinematics and the ground reaction forces to compute these forces and moments [50] using calculations of inverse dynamics. The internal joint forces and moments applied by the joint's soft tissue structures (muscles and ligaments) must constantly counteract the external forces and moments acting upon the knee. For example, during gait, the limb must alternately counterbalance moments that tend to extend and flex the knee joint. Quantifying knee joint kinetics allows a better understanding of functional adaptations following an injury such as an ACL tear [51].

ACL-Deficient Gait

The scientific literature relating to gait adaptations in ACL-deficient patients is abundant. However, a consensus on which gait compensatory mechanism is adopted by these patients remains to be established [52]. In fact, it was suggested that different biomechanical adaptations could be

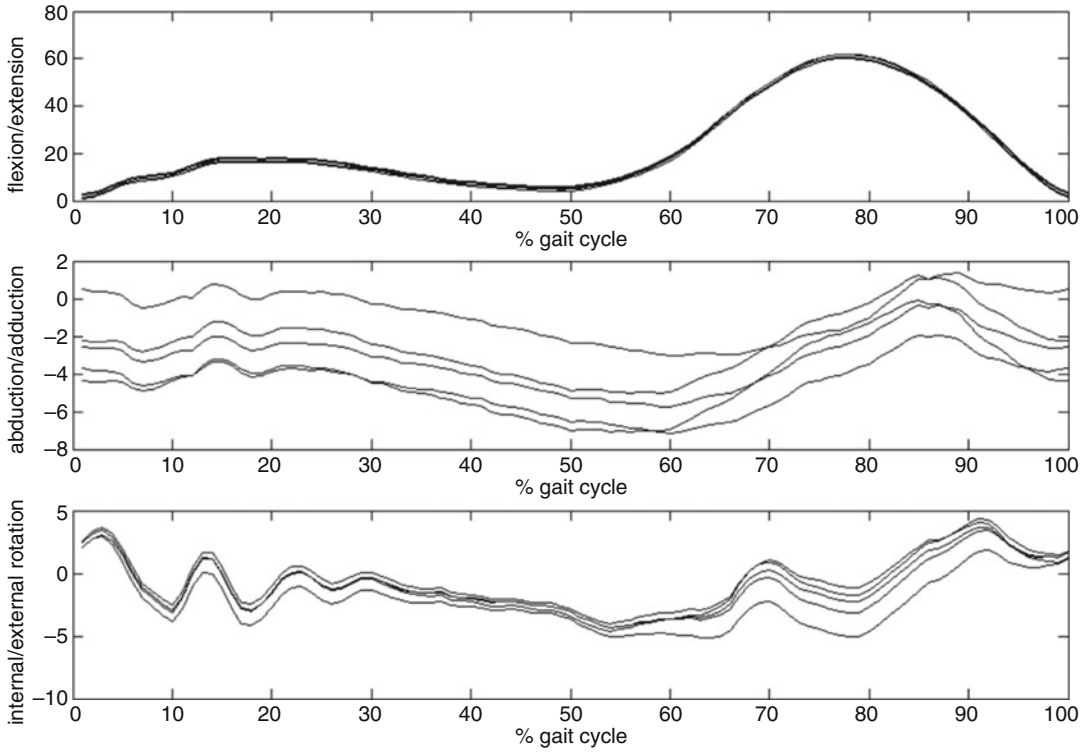

Fig. 39.4 Example of kinematic parameters calculated with 5 calibration procedures performed by 1 tester on 1 subject. Abduction is negative, internal rotation is negative, anterior translation of the femur is positive. Each curve corresponds to one trial

adopted within an ACLD population [43] and that gait adaptation changes over time [38]. To date, two main gait compensatory mechanisms have been proposed: (1) the quadriceps avoidance gait and (2) the hamstring facilitation strategy. Furthermore, only a restricted number of studies have looked at knee biomechanical patterns associated with the role of the ACL (i.e. anteroposterior translation and internal/external axial rotation). The following section will present a brief review of theses adaptations and biomechanical deficiencies and relate them to the results of our studies.

We conducted a 3D knee biomechanical assessment of 29 chronic ACLD patients and 15 healthy participants during treadmill walking. The 3D knee biomechanics were recorded using the KneeKG™ and a VICON optoelectronic system (Oxford Metrics, Oxford, UK). Joint centers and coordinate systems were defined using the FP method and the biomechanical patterns were computed using the ISB convention [32].

Quadriceps Avoidance Gait

Quadriceps avoidance gait is defined by the absence of the external knee flexor moment during the mid stance phase of the gait cycle [45]. Since this external joint moment tends to flex the knee while the body is progressing forward, an eccentric contraction of the quadriceps is typically required to counterbalance this moment. Berchuck et coll. 1990 [45] suggested that ACLD patients adopt this compensatory mechanism by reducing the quadriceps contraction. The rationale behind this hypothesis is that ACLD patients tend to avoid the anterior traction of the proximal tibia provoked by the quadriceps contraction, which could lead to AP instability. One study did show a decrease in quadriceps muscle activity during stance phase [53] and

several other studies [38, 51, 54, 55] identified a decrease in the external knee flexor moment in ACLD patient.

However, not all of the scientific community endorses this compensatory mechanism theory. In fact, recently published studies refute the very presence of these changes [42, 52, 56]. In our study, ACLD patients did not exhibit a quadriceps avoidance gait pattern (Fig. 39.5). This is supported by several studies demonstrating no EMG changes in the quadriceps muscle activity [52, 57–59]. In contrast with the quadriceps avoidance gait theory, some authors suggest that a reduction of the external knee flexor moment could be related to other biomechanical adaptations. Indeed, some believe that this gait adaptation could be associated with higher knee flexion angles [38, 45, 55]. Others suggest it could be linked to an increased external hip flexor moment [43, 55, 60], which would decrease the tension in the quadriceps. These controversial results underline the lack of consensus concerning this knee biomechanical adaptation [61].

Roberts et al. [52] suggested that the presence of the quadriceps avoidance gait pattern could be linked to methodological considerations since most of the studies reporting this strategy used a simpler linked segment model to compute knee joint moments. In our study, joint moments were computed using inverse dynamics with the wrench notation and quaternion algebra [62].

Hamstring Facilitation Strategy

In the past few years, several biomechanical studies have found that ACLD patients adopt a hamstring facilitation strategy. The rationale behind this compensatory mechanism theory is that higher hamstring muscle activity will act as an agonist to the injured ACL by generating a posterior traction of the proximal tibia. Numerous studies have shown a significant increase hamstring muscles activity [52, 53, 57, 59]. Furthermore, many studies have identified biomechanical changes that could be linked to this adaptation strategy. First, ACLD patients have been shown to walk with a higher knee flexion angle during the terminal stance phase [53, 58, 63–65]. Interestingly, the knee flexion angle during the stance phase was positively correlated with the duration of hamstring activity [57]. Additionally, ACLD patients have been found to display higher hamstring activity in the swing to stance transition [66]. The findings of our study are in agreement with these kinematic compensations. Indeed, Fig. 39.6 shows the knee flexion/extension pattern over a full gait cycle for the ACLD group and the control group. The ACLD group walked with significantly higher knee flexion angles at initial ground contact, during the terminal stance phase and at the end of the swing phase. The asterisks (*) show where statistical differences ($P<0.05$) were identified.

Biomechanical Deficiencies Associated with the Role of the ACL

Studies quantifying the AP translation and internal-external axial rotation of the knee are scarce. This is mainly due to the high level of error associated with the measurement of these small amplitude translations and rotations. Nevertheless, an increased anterior translation of the tibia in the transition between a non-weightbearing and weightbearing condition was reported in ACLD patients [67]. Furthermore, two studies using an electrogoniometer to quantify the kinematics of ACLD knees during gait showed an increase in anterior tibial translation [9, 68]. However, given the error associated with the measurement of proximal AP translation of the tibia [14], these results should be considered with caution.

Although only a few papers were published on the impact of an ACL tear on the knee axial rotation, contradictions emerge between studies. Some authors identified an increase in external tibial rotation with regards to the femur during gait [9, 52]. Others found a shift towards internal tibial rotation [40, 41]. Our study is in agreement with the latter. Whereas previous papers showed that this shift occurs throughout the gait cycle, our results only identified statistical differences in the swing to stance transition and during the beginning of the loading phase (Fig. 39.7).

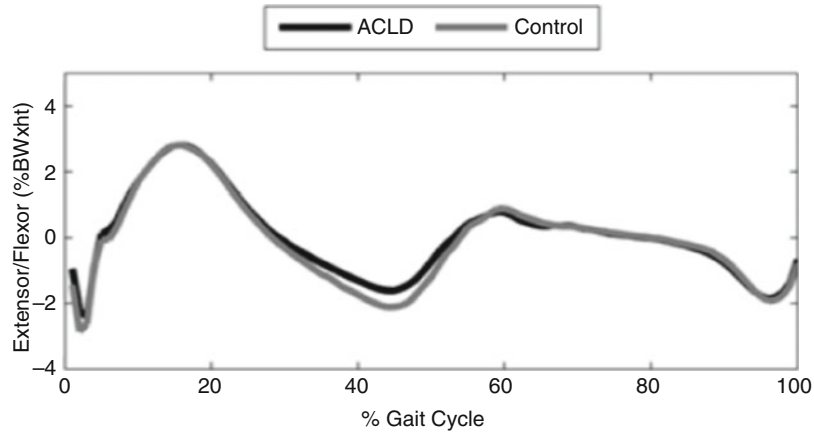

Fig. 39.5 Sagittal plane knee joint moments over a full gait cycle

The identified decrease in external tibial rotation in ACLD patients at the end of the swing phase, where the knee reaches near full extension, was also reported in previous studies [40, 68]. These results support previous findings that the screw home mechanism is altered after an ACL injury [69]. This altered axial tibial rotation could also be explained by the lack of knee extension at the end of the swing phase.

Three-dimensional biomechanical evaluations have allowed a better understanding of the impact of an ACL injury on the function of the knee joint. The large number of studies on this subject underlines the importance of such evaluations as complements to orthopaedic physical assessments in helping to improve current treatments for ACL injuries.

Analysis of the Pivot Shift Phenomenon

During a clinical evaluation, an ACL-deficient knee will generally present an increase in joint laxity, especially in the AP axis. This uniaxial laxity is relatively easy to evaluate using clinical examinations. The most sensitive of these examinations is the Lachman test, whereby the clinician applies an anterior force to the tibia while holding the femur in place. The amount of anterior displacement is very useful in diagnosing an ACL rupture [70–73] but it shows no correlation to subjective criteria of knee joint function [74–78]. The pivot shift test is a dynamic clinical test that reproduces the 3D rotational instability felt by patients who describe feeling

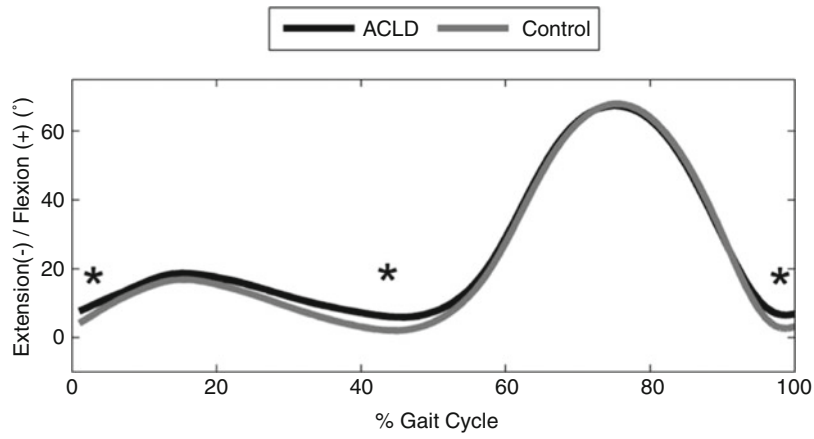

Fig. 39.6 Sagittal plane knee kinematic patterns during gait for ACL-deficient patients and healthy participants

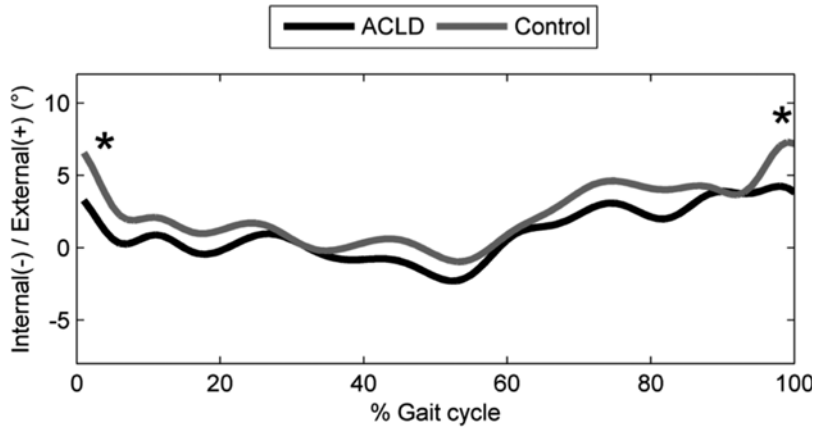

Fig. 39.7 Transverse knee kinematic patterns during gait for ACL-deficient patients and healthy participants

that their knee is giving way. The pivot shift grade correlates with reduced patient satisfaction, partial giving way, full giving way, difficulty cutting, difficulty twisting, activity limitation, reduced overall knee function, reduced sports participation, and Lysholm score [74]. Subjects with higher-grade pivot shift tests had less satisfaction, more limitations and lower knee function.

A meta-analysis found that the Lachman test is more sensitive but less specific than the pivot shift test [70]. In other words, a positive pivot shift test indicates an ACL rupture and a negative Lachman test rules it out.

Although it is obviously important to diagnose an ACL rupture, it is often the level of knee joint function that is of most interest and that clinicians aim to restore. Both tests are important parts of a clinical evaluation but serve different purposes. The pivot shift test's specificity makes it a valuable complement to the Lachman test in establishing a diagnosis, but more importantly, the pivot shift test is the only test which can be used to assess the level of knee joint function and predict long term outcome. As such, many studies conclude that the objective of reconstructive surgery should be to eliminate the presence of a pivot shift and not only to diminish AP laxity [39, 79–81].

Clinical Examination

The pivot shift test is performed with the patient supine and the examined leg lifted off the examining table by a clinician. A gentle valgus force is applied to the knee and the knee is flexed in a controlled manner with slight internal rotation of the tibia. In the ACL-deficient knee, as flexion occurs, the tibia translates anteriorly and rotates internally. The joint is subluxed at this point. As the knee is flexed past 30°, soft tissues and joint geometry cause the joint to reduce [82]. This is the pivot shift.

The clinician attributes the grade of the pivot shift relying on his interpretation and experience as being 0 (absent), 1 (glide), 2 (clunk) or 3 (gross) [83]. The nature of this grading scale renders it poorly repeatable [84]. Indeed, it has been shown that different clinicians frequently attribute different grades to a same patient [85]. No objective method for evaluating the pivot shift test currently exists, despite several attempts in the literature [86–91]. In the absence of an objective pivot shift measurement tool, it is difficult for less experienced clinicians to attribute a grade with a sufficiently high level of confidence for it to be used in determining the course of treatment.

Recording the Pivot Shift

The KneeKG™ attachment system, presented in Sect. 2.1.3, was designed for use on a standing subject. Its femoral component, which rests atop the femoral condyles, falls out of place when a subject is placed in a supine position. For this reason, an adapted version of this system was developed to record the kinematics of the pivot shift. The rigid arc of the femoral component is replaced by an elastic Velcro strap (Fig. 39.8a). This strap allows for inward pressure to be applied and it prevents the attachment from falling out of place when the subject is supine. The purpose of the rigid plates is to improve the attachment's stability and to allow for fixation of the motion capture sensors.

The tibial component is composed of a rigid plate that is held over the tibia with an elastic Velcro strap, immediately distal to the tibial tuberosity (Fig. 39.8b). It is short in length to allow a clinician to manipulate the lower limb without displacing it. A preliminary study conducted with three subjects wearing this attachment system showed it to be as reliable as the KneeKG™ for gait analysis.

The FP method, which is used to establish the anatomical axes, was also adapted to for the pivot shift test. The joint rotations were passively applied on the supine subject by the examiner.

Kinematics of the Pivot Shift

The reduction phase of the pivot shift occurs when the subluxed tibia returns to its normal position. This reduction has been described as a combination of posterior translation and external tibial rotation. With the development of methodologies to record the 3D kinematics of the pivot shift, many studies have investigated these features and how they relate to the grade of the pivot shift established by a clinician. One of the objectives of such studies is to develop an objective grading scale where, for example, some combination of both axial tibial rotation and posterior translation would be taken as a pivot shift score and the grade would be established from these scores.

Recent studies have found that the 3D kinematics of the pivot shift vary too much between subjects for such a simple score to be used. Although the amplitude of posterior translation correlates to the clinical grade, values are very different for two subjects of a same grade. The axial tibial rotation is even more variable: some subjects present significant external rotations during the reduction phase while others show none at all [88], leading authors to question its relevance in measuring the pivot shift.

In a recent study, we recorded the knee joint kinematics of 127 pivot shift tests and investigated the correlation with the clinical grade established by the clinician who performed the test [30, 92, 93]. Figure 39.9 presents a typical recording of a grade 3 pivot shift. A spike in linear velocity and acceleration is clearly visible during the reduction phase.

To further investigate the kinematic features of the pivot shift that are related to its clinical grade, we conducted a principal component analysis (PCA). The objective of PCA is to reduce the number of features while retaining as much of the variation present in the original dataset as possible. To do so, it transforms a large number of features into a smaller number of uncorrelated features, called principal components (PCs). The first PC accounts for the largest amount of variability in the data and each of the subsequent PC accounts for the largest amount of the remaining variability.

We applied PCA on our full set of features, which was composed of the amplitude, velocity and acceleration of AP, ML and total translations, abduction/adduction and axial tibial rotation. The first PC accounted for 38 % of the overall variability between the pivot shift recordings and the first four PCs accounted for a total of 69 %. To verify which PCs contained variability that is useful in grading the pivot shift, we calculated their correlation to the clinical grades. The first PC had a Spearman's rank correlation coefficient of 0.55 while the next three had coefficients of −0.09, 0.04 and 0.01, respectively [92]. These values show that only the first PC is related to the pivot shift grade.

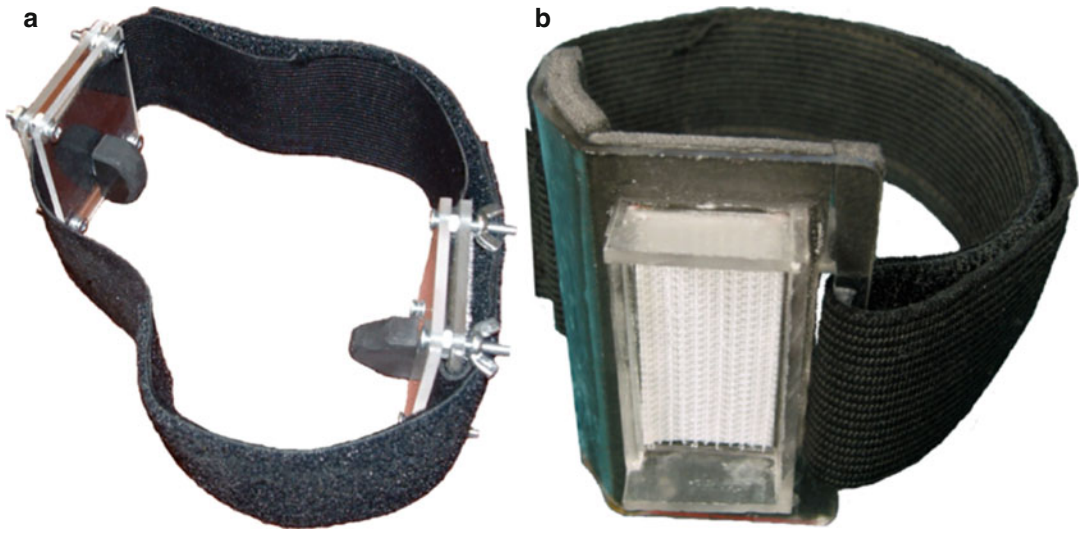

Fig. 39.8 The femoral (**a**) and tibial (**b**) components of the attachment system developed for data acquisition with the subject in a supine position

Next, we calculated the factor loadings of the original features on the first PC. Loading factors are correlations between the features and the PCs. Features with a high loading factor are rep-

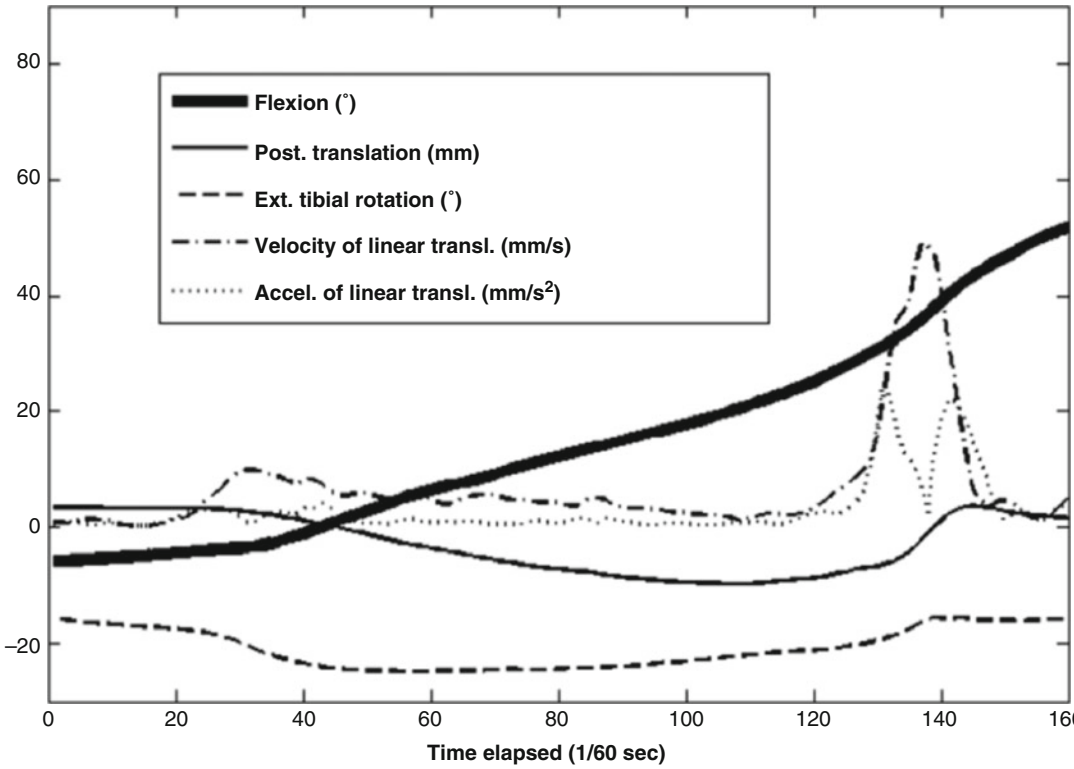

Fig. 39.9 Kinematics of a typical grade 3 pivot shift (Adapted from Labbe et al. [30], with permission.)

resentative of the component [94]. Table 39.1 shows the features with factor loadings that are superior to 0.5 on the first PC.

These results show that the translational component of the pivot shift is indeed more closely related to the grade than its rotational component. Moreover, the acceleration and velocity of the translations have a higher correlation to the grade than the actual amplitude of those translations. Other authors have also found the acceleration to be an important feature of the pivot shift [87, 89]. This makes sense since the existing subjective scale describes the pivot shift grades using terms such as "clunk" and "gross clunk", which infer a notion of suddenness rather than amplitude of displacement.

Recent studies in biomechanics have successfully classified kinematic data using machine learning methods [95–98]. We chose to use a support vector machine (SVM) approach using the grade established by the clinician as a gold standard. An SVM is a supervised learning method used for binary classification. To distinguish multiple classes, the method must be applied iteratively. This lends itself well to the grading of the pivot shift. In fact, the recordings can be first separated into that present a clunk (grade 2 and 3) and those that don't (grades 0 and 1). As a second step, the recordings with a glide (grade 1) can be distinguished from those with no glide (grade 0). Finally, those presenting a clunk (grade 2) can be distinguished from those presenting a more obvious, gross clunk (grade 3).

The features that load on the first principal component were added to the SVM classifier in descending order of their factor loadings (Table 39.1). All of these features were used to separate grades 0 and 1 from 2 and 3, and to separate grade 2 from grade 3 recordings with maximum sensitivity. For separating grades 0 and 1, maximum sensitivity was attained using only the amplitude of tibial translation and the velocity of axial tibial rotation. It makes sense that the acceleration and velocity of the translation are not useful for this step as we are distinguishing between the absence and presence of a glide. There is no notion of clunk in these grades [93].

The SVM classifier established the same grade as the evaluating clinician 66 % of the time and was within one grade for 95 % of recordings (Table 39.2). Agreement between the clinicians and the classifier, as defined by a Cohen's weighted Kappa, was $\kappa = 0.68$, which is considered to be substantial agreement [99]. Because of the subjective nature of the existing scale, which relies heavily on a clinician's interpretation, is it to be expected that there be some disagreement with classification method. Nonetheless, such a method offers an objective alternative to grading the pivot shift and sheds new light on the features that are felt and subjectively evaluated when a clinician grades a pivot shift. These features could be used to develop a quantitative measure of the pivot shift on a continuous scale.

The assessment of the 3D kinematics of the knee during the pivot shift test helps to further understand the effect of an ACL rupture on knee joint function. More importantly, such instrumented evaluations could eventually be used to help the clinician diagnose the severity of an injury, evaluate its impact on a specific patient and choose the appropriate treatment.

Table 39.1 The factor loadings of the pivot shift features on the first principal component

Pivot shift feature	PC_1
Total translation acceleration	0.840
AP translation velocity	0.809
Total translation velocity	0.799
ML translation acceleration	0.758
AP translation acceleration	0.693
Abduction acceleration	0.669

From Labbe et al. [92], with permission

Table 39.2 Grading of the pivot shift recordings by clinicians (lines) and a SVM-based classifier (columns)

Clinicians ↓ Classifier→	Grade 0	Grade 1	Grade 2	Grade 3
Grade 0	**22**	5	0	1
Grade 1	8	**12**	4	0
Grade 2	4	5	**23**	1
Grade 3	0	0	8	**14**

From Labbe et al. [93], with permission

General Discussion

In vivo measurement of small translations and rotations of the knee is a difficult task, especially in the frontal and transverse planes (abduction/adduction and internal/external tibial rotation). Precision is an important concern due to the fact that soft tissue movements introduce noise into the recordings of the underlying bone movements. Reinschmidt et al. [16] compared knee rotations in subjects whose kinematics were recorded via skin markers and bone pins inserted into the femur and tibia. They showed that average errors during running due to skin movements were about 21 % for flexion/extension, 63 % for internal/external tibial rotation, and 70 % for abduction/adduction. Since bone-embedded pins are not a solution that can be used in clinics on a routine basis, it is important to use a marker fixation method that limits skin displacement artifacts.

The method used to represent the movement in the anatomical axes of the knee is also of critical importance. In fact, small errors in the positioning of these axes generate large errors in rotation calculations [19]. One solution to improve reliability without the use of x-rays is to use a method that requires as few anatomical landmarks as possible to define the coordinate system. The method we used, the FP method, has been shown to yield reproducible data when repeated measures where performed by the same observer or by different observers. By using such a method, combined with a validated attachment system, we can record *in-vivo* knee biomechanics with maximum precision and reliability.

The resulting biomechanical assessments provide information on knee joint function that is not available through current clinical evaluations. This includes the normal joint kinematics, the kinematic impact of an injury and the extent to which different treatments restore normal joint kinematics. Such information allows healthcare professionals to evaluate the immediate and long-term outcome of treatment, establish the right time to return to sports participation and suggest injury prevention exercises. These are the three roles of biomechanics Chan's Orthopaedic Sport biomechanics paradigm [4].

The results presented in this chapter suggest that two other roles should be added to this paradigm. Gait analysis has shown its potential in evaluating the impact of an injury on knee joint function. As such, biomechanics has the potential to allow health professionals to better understand the functional impact that an injury has on a specific patient and to tailor his treatment plan accordingly. The relation between altered knee joint kinematics and degenerative changes in the knee has been shown [100, 101]. Personalized biomechanical evaluations can have a significant impact on the development of rehabilitation programs and surgical treatments aimed at restoring the dynamic stability of a knee and preventing secondary injuries.

The assessment of the kinematics of the pivot shift shows that biomechanics can also be an important tool as a diagnostic aid. Indeed, a recent study by Peeler et al. [102] showed the level of precision and validity of clinical exams for ACL ruptures performed by front line healthcare professionals (physiotherapists, sport therapists, general practitioners) to be much lower than had been previously reported. The authors speculate that this could be due to the difficulty in performing the manual clinical tests and the subjective bias related to grading such tests. This underlines the need for objective analytical methods that can aid in establishing a correct diagnosis.

Biomechanics already has the potential to be a useful tool in orthopaedics, as demonstrated by the examples in this chapter. With availability of improved methods for recording and analyzing bone movements, more and more studies are finding potential applications for prevention, diagnosis, impact assessment and evaluation of outcome of different joint injuries and ailments. The key to benefiting from the full potential of integrating 3D biomechanical assessments into orthopaedic practice is to have a multidisciplinary approach of dynamic interactivity and communication between specialists from different fields.

Acknowledgments The authors would like to acknowledge the participation of the clinicians in the different studies presented in this chapter: Dr Tim Heron and Dr Véronique Godbout, University hospital of University of Montreal, Dr Patrick Lavigne, Maisonneuve-Rosemont Hospital, Dr Guy Grimard, Ste-Justine Hospital, Dr Pierre Ranger and Dr Julio Fernandes, Sacré-Coeur Hospital and Dr David Baillargeon, Cité de la santé, Montréal.

References

1. Bull AMJ, Amis AA. The pivot-shift phenomenon: a clinical and biomechanical perspective. Knee. 1998;5:141–58.
2. Bicer EK, Lustig S, Servien E, Selmi TA, Neyret P. Current knowledge in the anatomy of the human anterior cruciate ligament. Knee Surg Sports Traumatol Arthrosc. 2010;18(8):1075–84.
3. Bahr R, Krosshaug T. Understanding injury mechanisms: a key component of preventing injuries in sport. Br J Sports Med. 2005;39:324–9.
4. Chan KM, Fong DT, Hong Y, Yung PS, Lui PP. Orthopaedic sport biomechanics - a new paradigm. Clin Biomech (Bristol, Avon). 2008;23 Suppl 1:S21–30.
5. Woo SL-Y, Adams D, Takai S. The human anterior-cruciate ligamentand its replacement: biomechanical considerations. In: Niwa S, Perren S, Hattori T, editors. Biomechanics in orthopedics. Tokyo: Springer; 1993. p. 13–30.
6. Girgis FG, Marshall JL, Monajem A. The cruciate ligaments of the knee joint. Anatomical, functional and experimental analysis. Clin Orthop. 1975:216–31.
7. Furman W, Marshall JL, Girgis FG. The anterior cruciate ligament. A functional analysis based on postmortem studies. J Bone Joint Surg Am. 1976;58:179–85.
8. Favre J, Luthi F, Jolles BM, Siegrist O, Najafi B, Aminian K. A new ambulatory system for comparative evaluation of thee-dimansional knee kinematics, applied to anterior cruciate ligament injuries. Knee Surg Sports Traumatol Arthrosc. 2006;14:592–604.
9. Zhang LQ, Shiavi RG, Limbird TJ, Minorik JM. Six degrees-of-freedom kinematics of ACL deficient knees during locomotion-compensatory mechanism. Gait Posture. 2003;17:34–42.
10. Sati M, de Guise JA, Larouche S, Drouin G. Quantitative assessment of skin-bone movement at the knee. Knee. 1996;3:121–38.
11. Alexander EJ, Andriacchi TP. Correcting for deformation in skin-based marker systems. J Biomech. 2001;34:355–61.
12. Benoit DL, Ramsey DK, Lamontagne M, Xu L, Wretenberg P, Renstrom P. Effect of skin movement artifact on knee kinematics during gait and cutting motions measured in vivo. Gait Posture. 2006;24(2):152–64.
13. Holden J, Orsini J, Siegel K, Kepple T, Gerber L, Stanhope S. Surface movement errors in shank kinematics and knee kinetics during gait. Gait Posture. 1997;5:217–27.
14. Manal K, McClay Davis I, Galinat B, Stanhope S. The accuracy of estimating proximal tibial translation during natural cadence walking: bone vs. skin mounted targets. Clin Biomech (Bristol, Avon). 2003;18:126–31.
15. Manal K, McClay I, Stanhope S, Richards J, Galinat B. Comparison of surface mounted markers and attachment methods in estimating tibial rotations during walking: an in vivo study. Gait Posture. 2000;11:38–45.
16. Reinschmidt C, van den Bogert AJ, Nigg BM, Lundberg A, Murphy N. Effect of skin movement on the analysis of skeletal knee joint motion during running. J Biomech. 1997;30:729–32.
17. Andriacchi TP, Alexander EJ, Toney MK, Dyrby C, Sum J. A point cluster method for in vivo motion analysis: applied to a study of knee kinematics. J Biomech Eng. 1998;120:743–9.
18. Waite JC, Beard DJ, Dodd CA, Murray DW, Gill HS. In vivo kinematics of the ACL-deficient limb during running and cutting. Knee Surg Sports Traumatol Arthrosc. 2005;13:377–84.
19. Kadaba MP, Ramakrishnan HK, Wootten ME. Measurement of lower extremity kinematics during level walking. J Orthop Res. 1990;8:383–92.
20. Cappozzo A, Catani F, Leardini A, Benedetti MG, Croce UD. Position and orientation in space of bones during movement: experimental artefacts. Clin Biomech (Bristol, Avon). 1996;11:90–100.
21. Cheze L, Fregly BJ, Dimnet J. A solidification procedure to facilitate kinematic analyses based on video system data. J Biomech. 1995;28:879–84.
22. Levens A, Inman V, Blosser J. Transverse rotation of the segments of the lower extremity in locomotion. J Bone Joint Surg. 1948;30:859–72.
23. Ferber R, McClay Davis I, Williams 3rd DS, Laughton C. A comparison of within- and between-day reliability of discrete 3D lower extremity variables in runners. J Orthop Res. 2002;20:1139–45.
24. Streiner DL, Norman GR. Health measurement scales : a practical guide to their development and use. New York: Oxford University Press; 2003.
25. Goujon H, Bonnet X, Sautreuil P, Maurisset M, Darmon L, Fode P, et al. A functional evaluation of prosthetic foot kinematics during lower-limb amputee gait. Prosthet Orthot Int. 2006;30:213–23.
26. Houck J, Yack HJ, Cuddeford T. Validity and comparisons of tibiofemoral orientations and displacement using a femoral tracking device during early to mid stance of walking. Gait Posture. 2004;19:76–84.

27. Marin F, Allain J, Diop A, Maurel N, Simondi M, Lavaste F. On the estimation of knee joint kinematics. Hum Mov Sci. 1999;18:613–26.
28. Sati M, de Guise JA, Larouche S, Drouin G. Improving in vivo knee kinematic measurements: application to prosthetic ligament analysis. Knee. 1996;3:179–90.
29. Ganjikia S, Duval N, Yahia LH, de Guise J. Three-dimensional knee analyzer validation by simple fluoroscopic study. Knee. 2000;7:221–31.
30. Labbe DR, de Guise JA, Godbout V, Grimard G, Baillargeon D, Lavigne P, et al. Accounting for velocity of the pivot shift test manoeuvre decreases kinematic variability. Knee. 2011;18(2):88–93.
31. Kinzel GL, Gutkowski LJ. Joint models, degrees of freedom, and anatomical motion measurement. J Biomech Eng. 1983;105:55–62.
32. Grood ES, Suntay WJ. A joint coordinate system for the clinical description of three-dimensional motions: application to the knee. J Biomech Eng. 1983;105:136–44.
33. Kinzel GL, Hall Jr AS, Hillberry BM. Measurement of the total motion between two body segments. I analytical development. J Biomech. 1972;5:93–105.
34. Cappozzo A. Gait analysis methodology. Hum Mov Sci. 1984;3:27–50.
35. Hagemeister N, Parent G, Van de Putte M, St-Onge N, Duval N, de Guise J. A reproducible method for studying three-dimensional knee kinematics. J Biomech. 2005;38:1926–31.
36. Siston RA, Delp SL. Evaluation of a new algorithm to determine the hip joint center. J Biomech. 2006;39:125–30.
37. Lam MH, Fong DT, Yung P, Ho EP, Chan WY, Chan KM. Knee stability assessment on anterior cruciate ligament injury: clinical and biomechanical approaches. Sports Med Arthrosc Rehabil Ther Technol. 2009;1:20.
38. Wexler G, Hurwitz DE, Bush-Joseph CA, Andriacchi TP, Bach BR Jr. Functional gait adaptations in patients with anterior cruciate ligament deficiency over time. Clin Orthop. 1998:166–75.
39. Andriacchi TP, Briant PL, Bevill SL, Koo S. Rotational changes at the knee after ACL injury cause cartilage thinning. Clin Orthop Relat Res. 2006;442:39–44.
40. Andriacchi TP, Dyrby CO. Interactions between kinematics and loading during walking for the normal and ACL deficient knee. J Biomech. 2005;38:293–8.
41. Georgoulis AD, Papadonikolakis A, Papageorgiou CD, Mitsou A, Stergiou N. Three-dimensional tibiofemoral kinematics of the anterior cruciate ligament-deficient and reconstructed knee during walking. Am J Sports Med. 2003;31:75–9.
42. Knoll Z, Kocsis L, Kiss RM. Gait patterns before and after anterior cruciate ligament reconstruction. Knee Surg Sports Traumatol Arthrosc. 2004;12:7–14.
43. Torry MR, Decker MJ, Ellis HB, Shelburne KB, Sterett WI, Steadman JR. Mechanisms of compensating for anterior cruciate ligament deficiency during gait. Med Sci Sports Exerc. 2004;36:1403–12.
44. Alkjaer T, Simonsen EB, Jorgensen U, Dyhre-Poulsen P. Evaluation of the walking pattern in two types of patients with anterior cruciate ligament deficiency: copers and non-copers. Eur J Appl Physiol. 2003;89:301–8.
45. Berchuck M, Andriacchi TP, Bach BR, Reider B. Gait adaptations by patients who have a deficient anterior cruciate ligament. J Bone Joint Surg Am. 1990;72:871–7.
46. Bulgheroni P, Bulgheroni MV, Andrini L, Guffanti P, Castelli C. Walking in anterior cruciate ligament injuries. Knee. 1997;4:159–65.
47. Perry J. Gait analysis: normal and pathological function. Thorofare: SLACK Incorporated; 1992.
48. Whittle MW. Gait analysis: an introduction. Edinburgh/Toronto: Butterworth Heinemann Elsevier; 2007.
49. Chau T, Young S, Redekop S. Managing variability in the summary and comparison of gait data. J Neuroeng Rehabil. 2005;2:22.
50. Vaughan CL. Are joint torques the Holy Grail of human gait analysis ? Hum Mov Sci. 1996;15: 423–43.
51. Andriacchi TP. Dynamics of pathological motion: applied to the anterior cruciate deficient knee. J Biomech. 1990;23 Suppl 1:99–105.
52. Roberts CS, Rash GS, Honaker JT, Wachowiak MP, Shaw JC. A deficient anterior cruciate ligament does not lead to quadriceps avoidance gait. Gait Posture. 1999;10:189–99.
53. Hurd WJ, Snyder-Mackler L. Knee instability after acute ACL rupture affects movement patterns during the mid-stance phase of gait. J Orthop Res. 2007;25:1369–77.
54. Noyes FR, Schipplein OD, Andriacchi TP, Saddemi SR, Weise M. The anterior cruciate ligament-deficient knee with varus alignment. An analysis of gait adaptations and dynamic joint loadings. Am J Sports Med. 1992;20:707–16.
55. Patel RR, Hurwitz DE, Bush-Joseph CA, Bach B, Andriacchi TP. Comparison of clinical and dynamic knee function in patients with anterior cruciate ligament deficiency. Am J Sports Med. 2003;31: 68–74.
56. Rudolph KS, Eastlack ME, Axe MJ, Snyder-Mackler L. Basmajian Student Award Paper: movement patterns after anterior cruciate ligament injury: a comparison of patients who compensate well for the injury and those who require operative stabilization. J Electromyogr Kinesiol. 1998;8:349–62.
57. Beard DJ, Soundarapandian RS, O'Connorc JJ, Dodd CA. Gait and electromyographic analysis of anterior cruciate ligament deficient subjects. Gait Posture. 1996;4:83–8.

58. Boerboom AL, Hof AL, Halbertsma JP, van Raaij JJ, Schenk W, Diercks RL, et al. Atypical hamstrings electromyographic activity as a compensatory mechanism in anterior cruciate ligament deficiency. Knee Surg Sports Traumatol Arthrosc. 2001;9:211–6.
59. Rudolph KS, Axe MJ, Buchanan TS, Scholz JP, Snyder-Mackler L. Dynamic stability in the anterior cruciate ligament deficient knee. Knee Surg Sports Traumatol Arthrosc. 2001;9:62–71.
60. Ferber R, Osternig LR, Woollacott MH, Wasielewski NJ, Lee JH. Gait mechanics in chronic ACL deficiency and subsequent repair. Clin Biomech (Bristol, Avon). 2002;17:274–85.
61. Hart JM, Ko JW, Konold T, Pietrosimione B. Sagittal plane knee joint moments following anterior cruciate ligament injury and reconstruction: a systematic review. Clin Biomech (Bristol, Avon). 2010;25(4):277–83.
62. Dumas R, Aissaoui R, de Guise JA. A 3D generic inverse dynamic method using wrench notation and quaternion algebra. Comput Methods Biomech Biomed Engin. 2004;7:159–66.
63. Bulgheroni P, Bulgheroni MV, Andrini L, Guffanti P, Giughello A. Gait patterns after anterior cruciate ligament reconstruction. Knee Surg Sports Traumatol Arthrosc. 1997;5:14–21.
64. Gao B, Zheng NN. Alterations in three-dimensional joint kinematics of anterior cruciate ligament-deficient and -reconstructed knees during walking. Clin Biomech (Bristol, Avon). 2010;25:222–9.
65. Lewek MD, Chmielewski TL, Risberg MA, Snyder-Mackler L. Dynamic knee stability after anterior cruciate ligament rupture. Exerc Sport Sci Rev. 2003;31:195–200.
66. Papadonikolakis A, Cooper L, Stergiou N, Georgoulis AD, Soucacos PN. Compensatory mechanisms in anterior cruciate ligament deficiency. Knee Surg Sports Traumatol Arthrosc. 2003;11:235–43.
67. Beynnon BD, Fleming BC, Labovitch R, Parsons B. Chronic anterior ligament deficiency is associated with increased anterior translation of tibia during the transition from non-weightbearing to weightbearing. J Orthop Res. 2002;20:332–7.
68. Marans HJ, Jackson RW, Glossop ND, Young C. Anterior cruciate ligament insufficiency: a dynamic three-dimensional motion analysis. Am J Sports Med. 1989;17:325–32.
69. Ellison AE. The pathogenesis and treatment of anterolateral rotatory instability. Clin Orthop Relat Res. 1980:51–5.
70. Scholten RJ, Opstelten W, van der Plas CG, Bijl D, Deville WL, Bouter LM. Accuracy of physical diagnostic tests for assessing ruptures of the anterior cruciate ligament: a meta-analysis. J Fam Pract. 2003;52:689–94.
71. Katz JW, Fingeroth RJ. The diagnostic accuracy of ruptures of the anterior cruciate ligament comparing the Lachman test, the anterior drawer sign, and the pivot shift test in acute and chronic knee injuries. Am J Sports Med. 1986;14:88–91.
72. Kim SJ, Kim HK. Reliability of the anterior drawer test, the pivot shift test, and the Lachman test. Clin Orthop Relat Res. 1995:237–42.
73. Liu SH, Osti L, Henry M, Bocchi L. The diagnosis of acute complete tears of the anterior cruciate ligament. Comparison of MRI, arthrometry and clinical examination. J Bone Joint Surg Br. 1995;77:586–8.
74. Kocher MS, Steadman JR, Briggs KK, Sterett WI, Hawkins RJ. Relationships between objective assessment of ligament stability and subjective assessment of symptoms and function after anterior cruciate ligament reconstruction. Am J Sports Med. 2004;32:629–34.
75. Eastlack ME, Axe MJ, Snyder-Mackler L. Laxity, instability, and functional outcome after ACL injury: copers versus noncopers. Med Sci Sports Exerc. 1999;31:210–5.
76. Lephart SM, Perrin DH, Fu FH, Gieck JH, McCue FC, Irrgang JJ. Relationship between selected physical characteristics and functional capacity in the anterior cruciate ligament-insufficient athlete. J Orthop Sports Phys Ther. 1992;16:174–81.
77. Engstrom B, Gornitzka J, Johansson C, Wredmark T. Knee function after anterior cruciate ligament ruptures treated conservatively. Int Orthop. 1993;17:208–13.
78. Pollet V, Barrat D, Meirhaeghe E, Vaes P, Handelberg F. The role of the Rolimeter in quantifying knee instability compared to the functional outcome of ACL-reconstructed versus conservatively-treated knees. Knee Surg Sports Traumatol Arthrosc. 2005;13:12–8.
79. Jonsson H, Riklund-Ahlstrom K, Lind J. Positive pivot shift after ACL reconstruction predicts later osteoarthrosis: 63 patients followed 5-9 years after surgery. Acta Orthop Scand. 2004;75:594–9.
80. Tamea Jr CD, Henning CE. Pathomechanics of the pivot shift maneuver. An instant center analysis. Am J Sports Med. 1981;9:31–7.
81. Leitze Z, Losee RE, Jokl P, Johnson TR, Feagin JA. Implications of the pivot shift in the ACL-deficient knee. Clin Orthop Relat Res. 2005: 229–36.
82. Galway HR, MacIntosh DL. The lateral pivot shift: a symptom and sign of anterior cruciate ligament insufficiency. Clin Orthop Relat Res. 1980:45–50.
83. Hefti E, Müller W, Jakob R, Stäubli H. Evaluation of knee ligament injuries with the IKDC form. Knee Surg Sports Traumatol Arthrosc. 1993;1:226–34.
84. Lane CG, Warren R, Pearle AD. The pivot shift. J Am Acad Orthop Surg. 2008;16:679–88.
85. Noyes FR, Grood ES, Cummings JF, Wroble RR. An analysis of the pivot shift phenomenon. The knee motions and subluxations induced by different examiners. Am J Sports Med. 1991;19:148–55.

86. Amis AA, Cuomo P, Siva Rama RB, Giron F, Bull AM, Thomas R, et al. Measurement of knee laxity and pivot-shift kinematics with magnetic sensors. Oper Techn Orthop. 2008;18:8.
87. Kubo S, Muratsu H, Yoshiya S, Mizuno K, Kurosaka M. Reliability and usefulness of a new in vivo measurement system of the pivot shift. Clin Orthop Relat Res. 2007;454:54–8.
88. Bull AM, Earnshaw PH, Smith A, Katchburian MV, Hassan AN, Amis AA. Intraoperative measurement of knee kinematics in reconstruction of the anterior cruciate ligament. J Bone Joint Surg Br. 2002;84:1075–81.
89. Hoshino Y, Kuroda R, Nagamune K, Yagi M, Mizuno K, Yamaguchi M, et al. In vivo measurement of the pivot-shift test in the anterior cruciate ligament-deficient knee using an electromagnetic device. Am J Sports Med. 2007;35:1098–104.
90. Lopomo N, Zaffagnini S, Bignozzi S, Visani A, Marcacci M. Pivot-shift test: Analysis and quantification of knee laxity parameters using a navigation system. J Orthop Res. 2010;28:164–9.
91. Lane CG, Warren RF, Stanford FC, Kendoff D, Pearle AD. In vivo analysis of the pivot shift phenomenon during computer navigated ACL reconstruction. Knee Surg Sports Traumatol Arthrosc. 2008;16:487–92.
92. Labbe DR, de Guise JA, Mezghani N, Godbout V, Grimard G, Baillargeon D, et al. Feature selection using a principal component analysis of the kinematics of the pivot shift phenomenon. J Biomech. 2010;43(16):3080–4.
93. Labbe DR, de Guise JA, Mezghani N, Godbout V, Grimard G, Baillargeon D, et al. Objective grading of the pivot shift phenomenon using a support vector machine approach. J Biomech. 2011;44(1):1–5.
94. Ho R. Handbook of univariate and multivariate data analysis and interpretation with SPSS. Chapman: Chapman & Hall/CRC; 2006.
95. Chan YY, Fong DT, Chung MM, Li WJ, Liao WH, Yung PS, et al. Identification of ankle sprain motion from common sporting activities by dorsal foot kinematics data. J Biomech. 2010;43:1965–9.
96. Lauer RT, Smith BT, Betz RR. Application of a neuro-fuzzy network for gait event detection using electromyography in the child with cerebral palsy. IEEE Trans Biomed Eng. 2005;52:1532–40.
97. Giansanti D, Macellari V, Maccioni G. New neural network classifier of fall-risk based on the Mahalanobis distance and kinematic parameters assessed by a wearable device. Physiol Meas. 2008;29:N11–9.
98. Lau HY, Tong KY, Zhu H. Support vector machine for classification of walking conditions of persons after stroke with dropped foot. Hum Mov Sci. 2009;28:504–14.
99. Landis JR, Koch GG. The measurement of observer agreement for categorical data. Biometrics. 1977;33:159–74.
100. Andriacchi TP, Mundermann A. The role of ambulatory mechanics in the initiation and progression of knee osteoarthritis. Curr Opin Rheumatol. 2006;18:514–8.
101. Scarvell JM, Smith PN, Refshauge KM, Galloway HR, Woods KR. Association between abnormal kinematics and degenerative change in knees of people with chronic anterior cruciate ligament deficiency: a magnetic resonance imaging study. Aust J Physiother. 2005;51:233–40.
102. Peeler J, Leiter J, MacDonald P. Accuracy and reliability of anterior cruciate ligament clinical examination in a multidisciplinary sports medicine setting. Clin J Sport Med. 2010;20:80–5.

Knee Ligamentoplasty: Prosthetic Ligament or Ligament Allograft?

40

Dominique G. Poitout and B. Ripoll

Lesions of the central pivot of the knee are responsible for chronic disabling instabilities which, in the long term, lead to irreversible arthrotic destruction of the articular surfaces. Since 1980, we have been using synthetic ligaments and, more recently, since 1986, preserved human ligaments. The principle of ligamentoplasty is quite simply to replace torn ligaments with a prosthesis, aiming to reproduce the anatomical course of the ligament and its functional properties as faithfully as possible.

The main advantages of these techniques are:

Shortening of the time under surgery,

The other anatomical structures of the knee are not damaged,

And the possibility of early rehabilitation.

D.G. Poitout, MD (✉)
Faculté de Médecine Nord, Sce Chirurgie Orthopédique et Traumatologie, Aix-Marseille Université, Centre Hospitalier et Universitaire Marseille North, Chemin des Bourrely, 13015 Marseille, France
e-mail: Dominique.POITOUT@ap-hm.fr

B. Ripoll, MD
Department of Orthopaedic Surgery and Trauma, Hopital Nord, Chemin des Bourrely, 13015 Marseille, France

General Biomechanics

Basic Properties

A mechanical evaluation of an artificial ligament is only useful if it is compared with the properties of the corresponding human ligament.

The Parameters

The parameters evolve along the usual tension–elongation curve which determines the behavior of the ligament. Extreme stresses are only encountered in traumatological circumstances.

The rigidity of the ligament directly affects the function of the joint because if it is too rigid, it requires an intense muscular effort to mobilize the knee and risks causing tearing of the ligament or its attachments; if it is too weak, it will prevent the ligament from playing its stabilizing role.

Apart from *rigidity*, the main parameters therefore seem to us to be the values of strength and elastic lengthening which, more than the maximum values, represent the true tolerance limit of the ligament as well as the time it takes for the initial length of the ligament to recover after single stretching.

Measuring Methods

Two main methods can be used:

A specimen involving the ligament and the bone consists of removing knees from cadavers, and dissecting them until only the anterior

D.G. Poitout (ed.), *Biomechanics and Biomaterials in Orthopedics*,
DOI 10.1007/978-1-84882-664-9_40

cruciate ligament connects the two articular surfaces.

Another way of testing ligaments consists of attaching them directly to the inside of traction machines, using grips.

The problem with this technique is that with grips there are always phenomena which crush and lacerate the tissue, which can alter its elasticity or its strength, hence the preparation of a cone-shaped device which surrounds the ends of the ligaments fixed in acrylic resin.

Mechanical Properties of the Human Anterior Cruciate Ligament and of Prosthetic Ligaments

As far as the mechanical properties of the anterior cruciate ligament of a cadaver is concerned, it would appear that there is no significant difference between the results obtained on a frozen specimen after being frozen for several months.

On the other hand, the age of the subject displays a difference in the maximum average strength between a group of subjects approximately 60 years of age and a group of subjects approximately 20 years of age with the strength being double.

As far as the rate of elongation is concerned, it seems that the maximum strength of the human anterior cruciate ligament increases with elongation and it is often seen that although a slow rate leads to tearing due to bone avulsion, a rapid rate is more likely to lead to the ligament tearing in its middle part.

The Life of a Ligament

Two series of tests can be used in practice:

Cyclical tensioning tests,

Cyclical deformation tests.

As far as cyclical tensioning is concerned, the variations in tension experienced by the ligament during flexion–extension of the knee are reproduced, at the end of which each ligament has its residual elongation measured and a maximum elongation test is performed to assess the changes in the strength and rigidity of this ligament, compared with a new ligament.

When a cyclical deformation test is used, the resistance to repeated flexion is analyzed, combining constant, fixed-angle flexion of the ligament and continuous axial rotation of this ligament. This test therefore varies the points where maximum tension and compression forces are applied in a homogeneous manner on the periphery. At the end of this test, the ligament is subjected to a maximum elongation test.

Implantation in vivo in animals is certainly the method most used in research on synthetic ligaments. However, the frequency with which premature tears occur in the implant is regrettable as are the problems associated with applying the observations made in animal studies to man.

Biocompatibility and Rehabilitation

Biocompatibility

The Risks

In the case of ligament prostheses, general tolerance at a distance from the implant can take several forms, whether it be problems associated with general cytotoxicity, allergic reactions, toxicity specific to an organ, or teratogenicity.

As for local tolerance, it has to be dissociated from the local inflammatory reaction connected with the introduction of any kind of foreign body into the system. This reaction does not affect biocompatibility, insofar as it ends after a few days or a few weeks to make way for stabilization of the interface.

Carcinogenicity can be linked either to the chemical structure of the implants, or to their physical structure.

Although most of the polymers used have proved to be carcinogenic in animal studies under certain conditions, these phenomena are very rare in man and are only present in a few rare cases of sarcomas seen near vascular prostheses made of Dacron.

The Tests

Tests in vitro, consisting of placing the material studied in a cell culture and observing the reciprocal interactions between these two

elements, are interesting because they are rapid (of the order of a few hours to a few days), reproducible, and specific.

In vivo tests make it possible to take into account the stresses connected with the functioning of the prosthesis and, in particular, involving the immune system of the host through the host's reaction to foreign bodies, the course of which, to a large extent, determines the tolerance of the implant.

Rehabilitation of the Artificial Ligament

Colonization of the prosthesis by the tissues of the host – or rehabilitation – is a phenomenon very much linked to its biotolerance. This idea of the prosthesis being a more or less temporary support for a biological new ligament is very debatable and many papers demonstrate that the mechanical role of this recolonization is extremely limited.

The chemical nature of the implant can become involved in this phenomenon as well as its physical nature and it seems to be an established fact that, far more than the diameter of the fibers or their direction, it is the porosity of the implant which is the decisive factor.

Finally, the mechanical stresses seem to be just as important in maintaining the functional properties of the ligaments. And, conversely, immobilization is responsible for considerable fragilization of the ligament tissue and its insertions.

The Ligaments Used

Artificial Ligaments

Carbon

Carbon ligament prostheses consist of elementary filaments 5–10 μm in diameter, grouped into unidirectional bundles or in plaited or twisted strands of several thousand elements. Endurance in traction is theoretically very high. However, when this strength is measured on a traction machine, the figures are often clearly lower than the theoretical value anticipated. Shear strength is poor, which leads to fragmentation of the fibers and, when histological slices are taken, many breaks in the filaments can be seen.

Plaiting the fibers considerably reduces the rigidity of the prostheses. It seems that the best results are obtained for a ligament consisting of 32 strands of 3000 filaments plaited at an angle of 43°.

As far as biocompatibility is concerned, taking account of the usual fragmentation of carbon fibers, this is seen to turn into a foreign body, rapidly developing into abundant and regular fibrosis, the mechanical properties of which are, however, insufficient to replace a prosthetic ligament. On the other hand, the possibility of lymphatic drainage is proven by the almost constant discovery of carbon in the regional ganglions.

Carbon ligaments also poses problems for the anchorage technique, because the fragility of the fibers makes it difficult to attach them.

To summarize, carbon fiber is a material which, mechanically, has great resistance to traction, very high rigidity, and poor resistance to shearing forces, in spite of the various plaiting and sheathing measures adopted. Used as a cruciate ligament prosthesis, it inevitably breaks with the stresses being relayed progressively to the fibrous new ligament which appears, the mechanical properties of which are inadequate to ensure that this function is effective.

Polyethylene

High-molecular-weight polyethylene is largely used by orthopedists for manufacturing total hip acetabula on account of its excellent resistance to abrasion. Several ligaments have been made since 1974, consisting of strands of plaited filaments, the shape of which varies according to the type of ligament used (polyflex of Cendis).

As far as the basic properties of this ligament are concerned, it appears that:

The elastic strength is very limited,

The recovery time after single tensioning is short,

And experiments performed at different tensions show the slowness with which the ligament returns to its initial length.

As far as its biocompatibility and rehabilitation are concerned, polyethylene displays no cytotoxic effects and is well tolerated by the host tissues.

In summary, high-molecular-weight polyethylene has good biological tolerance. The attachment methods of certain ligaments, such as Cendis, for example, make it easy to use, all the more so that their mechanical properties are wholly satisfactory.

Polypropylene

Polypropylene is a synthetic polymer which has been suggested as a strengthening prosthesis. An example is Kennedy Lad. This is a plait of twisted polypropylene which is used to strengthen ligamentoplasty and is sutured along the whole course of the transplant.

As far as the basic properties are concerned: the rigidity of the plait is linear, with the tension–elongation curve having a uniform slope up to break point. The maximum elastic strength values are, consequently, difficult to measure.

As far as the in vivo life of the plait itself is concerned, it would appear that the overall solidity of attachment increases with time and stabilizes as from the sixth month; the rigidity reaches values of the order of 100 kg Newton per meter and is therefore similar to that of normal ligaments.

As far as the biocompatibility of the product is concerned, using polypropylene as suture material has never posed major tolerance problems, even in the long term.

Polytetrafluoroethylene

Polytetrafluoroethylene, which is still called Teflon, is used as a biomaterial under the name of Gortex for vascular prostheses or cruciate ligament prostheses. As far as its basic properties are concerned: tearing always occurs suddenly by pulling an attachment eyelet hole, without previously modifying the slope of the curve.

The maximum resistance value is very high on isolated ligaments and its rigidity increases with the degree of elongation, but is close to that of the cruciate ligament for its area of physiological use.

Dacron

Dacron is certainly the most used of the synthetic polymers of the ethylene polyterephthalate family. It is a material with an essentially fibrous structure used in the form of a plaited or knitted strand still called Dacron Velvet. The large mesh of this latter type of ligament is intended to encourage good assimilation of the implant into the host tissue.

As far as its biocompatibility is concerned, tests on cell culture show the absence of any cytotoxic effect by Dacron but an analysis of the implantation phenomena in vivo is interesting because a gradual improvement can be seen in the signs of inflammation, as fibrous encapsulation of the ligament takes place. In the intra-articular position, dacron only seems to produce moderate and transitory synovial reactions where the implant remains intact. On the other hand, major inflammatory reactions with changes in the cartilage and in the synovial membrane can be seen if the prosthesis breaks.

As far as carcinogenicity is concerned; under certain conditions many synthetic polymers, including Dacron, have a carcinogenic effect in animals, almost exclusively in rodents. This phenomenon occurs very rarely in man for the materials currently used. Three cases of sarcoma have been published after a Dacron vascular prosthesis was implanted. This suggests that man is only slightly prone to these phenomena or at least that there are very long latency periods of the order of several decades.

To summarize, Dacron is generally fairly well tolerated biologically. The most worrying problem is not the solidity of the implants but the fairly common occurrence of reactional synovitis which sometimes makes it necessary to remove the synthetic material.

Tendon Allografts

Although ligament or tendon autografts are well tolerated, and widely used, they do, however, mean that a neighboring tendon or ligament has to be sacrificed, the removal of which prolongs the time of the operation and alters the bio-mechanical conditions of the functioning of the joint.

Xenografts of bovine origin are closer to the ligament prostheses treated with glutaraldehyde

for increasing the reticulation of the collagen fibers. They are currently rarely implanted in man because of their poor biocompatibility and their inadequate mechanical properties.

Ligament and tendon allografts make it possible to replace the anterior cruciate ligament as an autograft without sacrificing a neighboring tendon.

The specification for ligament and tendon allografts is as follows:

The allograft has to have a similar morphological structure and mechanical properties to those of the ligament replaced.

It has to be perfectly well tolerated.

In the long term, it has to be able to be recolonized by the cells of the host to which it will serve as directional support.

The way in which it is obtained has to be compatible with the legislation on organ removal.

It has to be able to be preserved and stored in a sterile manner without suffering major decomposition.

Its surgical implantation has to be easy, cause little trauma, and allow the graft to be firmly anchored.

Finally, the properties of the allograft have to be stable over time.

Different Allografts Which Can Be Used

Allografts have to be taken from young donors, so that the force and stress values at rupture are similar to those of a normal ligament (1725 Newtons). The allograft that would best meet the morphology and structure criteria would, of course, be an allograft of an anterior cruciate ligament, however, the choice of this ligament presents considerable technical problems. The patellar tendon, on the other hand, can be easily removed with two bone insertions on the patella and the tibia; it is sufficiently long and has mechanical properties which are clearly superior to those of the anterior cruciate ligaments, even if it is reduced to its middle third.

Preservation by Cryogenics Seems

In order to avoid transmitting any infectious, bacterial, viral, or mycotic pathologies to the host subject, it is necessary to have a sterile allograft. The allograft is removed in the operating theater from selected donors with all the usual asepsis-related surgical precautions. The graft is then packed in a sterile pack bathed in an antibiotic-containing solution and frozen to −198°C in the Blood Transfusion Center. Other methods for sterilizing the allograft by irradiation or exposure to ethylene oxide were found not to be satisfactory.

Tolerance in the Host Subject

Although the different cellular and protein components which the ligament allografts removed in isolation contain can trigger an immune response, the apatite contained in the bone as well as in the collagen of the tendon does not trigger a clinically perceptible immune response.

Allografts preserved by freezing do not trigger the appearance of the immune HLA group as has been proved by various immunological studies performed at the Blood Transfusion Center in Marseilles.

Mechanical Studies

The graft consisting of the central third of the patellar tendon together with its insertions has been studied mechanically. Creep tests as well as traction tests right up to rupture show that: freezing does not alter the appearance, the color, or the mechanical properties of the grafts; which is not the case for an irradiated tendon – which takes on a board-like appearance –, or an irradiated and freeze-dried tendon, the fibers of which come apart and have a fibrillary appearance.

The problem with these grafts is the mechanical behavior in situ in the long term during revascularization. Experimental studies are currently being conducted to see what the importance is of this revascularization and its effect on the mechanics of the joint in the months and years following implantation.

Conclusion

Apart from the unexpected gain in solidity, synthetic ligaments often also have the advantage of shortening the operating time and allowing early rehabilitation.

The design of a prosthesis of this kind should, in our view, most definitely be directed

towards an implant which is itself capable of bearing all the stresses to which the anterior cruciate ligament is subjected immediately after implantation and in the long term. However, the idea of new ligaments which a more or less biodegradable implant could produce or of a functional unit that combining synthetic material and newly formed tissue would produce, although a satisfying idea, seems to us to be illusory from a practical point of view. We have seen some of the models proposed and have shown the striking correlation which exists between the mechanical properties of the prosthetic ligaments and the quality of the results obtained when they are implanted in man.

As far as the use of preserved ligament allografts are concerned, according to the first clinical results, it would appear that there is a considerable percentage of joint laxity when these are used.

The solution, perhaps, is to combine a preserved allograft and a reinforcing prosthetic ligament, which would prevent stresses being exerted directly on the allograft during its rehabilitation period (2–3 years), with the prosthetic ligament being ruptured when the allograft has regained satisfactory mechanical behavior.

Only the test of time will, of course, be able to confirm whether such a choice is well founded.

Index

D.G. Poitout (ed.), *Biomechanics and Biomaterials in Orthopedics*,
DOI 10.1007/978-1-84882-664-9

D